130081, 130081A-130081D
Load and Resistance Factor Design (LRFD) for Highway Bridge Superstructures

Design Manual-US Units

NHi
NATIONAL HIGHWAY INSTITUTE

U.S. Department of Transportation
Federal Highway Administration

1. Report No. FHWA NHI 08-048	2. Government Accession No.	3. Recipient's Catalog No. FHWA NHI 08-048	
4. Title and Subtitle Load and Resistance Factor Design (LRFD) For Highway Bridge Superstructures - Design Manual		5. Report Date April 2007	
		6. Performing Organization Code FHWA/OPCD/NHI	
7. Author (s) Michael A. Grubb, P.E., John A. Corven, P.E., Kenneth E. Wilson, P.E. S.E., Justin W. Bouscher, P.E., Laura E. Volle, E.I.T.		8. Performing Organization Report No. MN105179	
9. Performing Organization Name and Address Michael Baker Jr., Inc. Airside Business Park, 100 Airside Drive Moon Township, PA 15108		10. Work Unit No. (TRAIS)	
		11. Contract or Grant No. DTFH61-02-D-63001	
12. Sponsoring Agency Name and Address Federal Highway Administration National Highway Institute (HNHI-10) 4600 N. Fairfax Drive, Suite 800 Arlington, Virginia 22203		13. Type of Report and Period Covered Final Submission December 2004 – April 2007	
		14. Sponsoring Agency Code FHWA	
15. Supplementary Notes Baker Principle Investigator: Raymond A. Hartle, P.E. Baker Project Manager: Scott D. Vannoy, P.E. FHWA Contracting Officer's Technical Representative: Louisa M. Ward FHWA Contracting Officer's Task Manager: Firas I. Sheikh Ibrahim, Ph.D., P.E. Review Team Members: Thomas K. Saad, P.E. and Jeff Smith		FHWA expresses thanks to the AASHTO Oversight Committee for co-funding this effort.	

16. **Abstract**

This document presents the theory, methodology, and application for the design and construction of both steel and concrete highway bridge superstructures. The manual is based on the *AASHTO LRFD Bridge Design Specifications* Fourth Edition, 2007. Design examples and commentary throughout the manual are intended to serve as a guide to aid bridge structural design engineers with the implementation of the *AASHTO LRFD Bridge Design Specifications*, and is presented in both US Customary Units and Standard International Units.

This manual is comprised of four volumes. Volume 1covers general steel and concrete superstructure design considerations including the history of bridge design, loads and load combinations, deck design, and bearing design. Volume 2 covers simple and continuous composite steel bridge superstructure design and construction with a focus on straight/skewed/curved girders, connections/splices, and bracing member design. Volume 3 covers the design and construction of simple and continuous composite concrete bridge superstructures concentrating on precast pretensioned girders, girder continuity by means of reinforced concrete joints and post-tenioning, and cast-in-place post-tensioned superstructures. Volume 4 provides detailed superstructure design examples which support the text in Volumes 1 through 3. The four design examples covered in Volume 4 include: a straight steel girder superstructure with no skew, a straight steel girder superstructure with a skew, a steel tub girder superstructure, and a concrete I-girder superstructure. AASHTO references are provided throughout each volume.

Key reference documents used in the development of this manual are given immediately following each section in each chapter (as applicable).

17. Key Words Bridge Design, Load and Resistance Factor Design, LRFD, Superstructure, Deck, Bearing, I-Girder, Fatigue, Splices, Bracing, Precast, Prestressed Concrete, Pretensioned, Post-tensioned		18. Distribution Statement This report is available to the public from the NHI Bookstore at http://www.nhi.fhwa.dot.gov/training/nhistore.aspx		
19. Security Classif. (of this report) Unclassified		20. Security Classif. (of this page) Unclassified	21. No. of Pages 1982	22. Price

Form DOT F 1700.7 (8-72)   Reproduction of completed page authorized

ACKNOWLEDGEMENTS

Table of Contents

Legend:

Normal Text - To Be Completed

Bold Text − Completed To Date

Italicized Text – Future Development

Volume I - General Design Considerations

Chapter 1 - History of Bridges in America

Chapter 2 - Preliminary Design Considerations

Chapter 3 - Life Cycle Cost Considerations

Chapter 7 - Deck Design

Chapter 8 - Bearing Selection and Design

Chapter 9 - Joint Selection and Design

<u>Volume II - Steel Bridge Superstructure Design</u>

Chapter 1 - Construction of Steel Bridges

Chapter 2 - Steel Bridge Design

Volume III - Concrete Bridge Superstructure Design

Chapter 1 - Construction of Concrete Bridges

Chapter 2 - Concrete Bridge Design

Volume IV - Superstructure Design Examples

Volume 1
General Design Considerations

Chapter 1
History of Bridges in America

Published by the
American Association of State
Highway and Transportation Officials

AASHTO LRFD Bridge Design Specifications

Customary U.S. Units
Third Edition • 2004

ISBN: 1-56051-250-4 • Publication Code: LRFDUS-3

1.1 Introduction

Bridges have helped shape our nation. Bridge design and construction methods have advanced significantly in America and have helped advance our people as well.

This chapter describes the history of bridges in America, tracing its early history, the demand for railroad bridges, the National Highway System, and mass transit. This chapter also describes the primary design philosophies and codes, including Allowable Stress Design (ASD), Load Factor Design (LFD), and Load and Resistance Factor Design (LRFD). A design example is also included for each of these three design philosophies.

1.2 Early History

Future Development

1.3 Railroad Demands

Future Development

1.4 Highways (National System)

Future Development

1.5 Mass Transit

Future Development

1.6 Design Philosophies and Codes

Simply stated, safety in any engineering design is assumed when the demands placed on components and materials are less than what is supplied, so that:

Demand < Supply

Another way of stating this same principle with respect to structural engineering is that the effect of the loads must be less than the resistance of the materials, so that:

Load < Resistance

When a particular loading or combination of loadings reaches the component or material capacity, safety margins approach zero and the potential for failure exists. The goal of the basic design equation is to limit the potential for failure to the lowest probability practical for a given situation.

When applying this principle to design, it is essential that both sides of the inequality be evaluated for the same conditions. For example, if the effect of applied loads produces tension in a concrete member, the load should be compared to the tensile resistance of the concrete and not some other aspect of the material such as the compressive resistance.

For bridge design, the left side of the inequality representing the loads is constantly changing due to live loads and other environmental loads. Under some circumstances, due to deterioration of the structure over time, the right side of the inequality representing the resistance also changes. These uncertainties throughout the life of the structure are almost impossible to predict but must be accounted for.

The way the uncertainties are considered is what separates different design philosophies. Presently, three design philosophies (or codes) for bridge design are in general use in the United States. In order of age, they are allowable (or working) stress design (ASD), load factor design (LFD), and load and resistance factor design (LRFD).

For ASD, a single factor of safety on the resistance side of the inequality accounts for the uncertainty. The use of LFD, on the other hand, applies load factors to each type of load depending on the combination and the material resistance is also modified by reduction factors. Hence, LFD accounts for uncertainty on both sides of the inequality.

LRFD is similar to LFD in the fact that the uncertainty is accounted for on both sides of the inequality. However, the major advantage LRFD has over LFD is that LRFD is probability-based. LRFD was developed based on a specific reliability index that targets a specific probability of failure. Each design philosophy is discussed in more detail in the following sections.

1.6.1 Allowable Stress Design (ASD)

Allowable stress design (ASD), also known as working stress design (or WSD), is the oldest design code in use for bridges in the United States today. Of the three philosophies, ASD is the most simplistic.

The ASD method of design utilizes unfactored loads (taken at unity), which are combined to produce a maximum effect in a member. The maximum load or combination of loads cannot exceed the allowable (or working) stress of the material. The allowable or working stress is found by taking the strength of the material and applying an appropriate factor of safety that is greater than unity.

The basic equation for allowable stress design is:

$$\sum DL + \sum LL = R_u / FS$$ Equation 1.1

where:
    DL = dead loads applied to the element under consideration
    LL = live loads applied to the element under consideration
    R_u = ultimate resistance or strength of the element under consideration
    FS = factor of safety, > 1.0

Note that loads other than dead and live load have been excluded from the above equation for simplicity.

A graphical representation of the ASD philosophy is shown in Figure 1.1. As can be seen in the figure, the assumption of ASD is that loads and resistances both have a probability of occurrence of 1.0. The load types include dead loads, live loads, and environmental loads, all of which in reality have different occurrence probabilities and different effects.

Therefore, it is evident that the factor of safety applied to the resistance side of the inequality dictates the width of the safety margin in the graphical representation and is the only aspect of ASD that accounts for uncertainty.
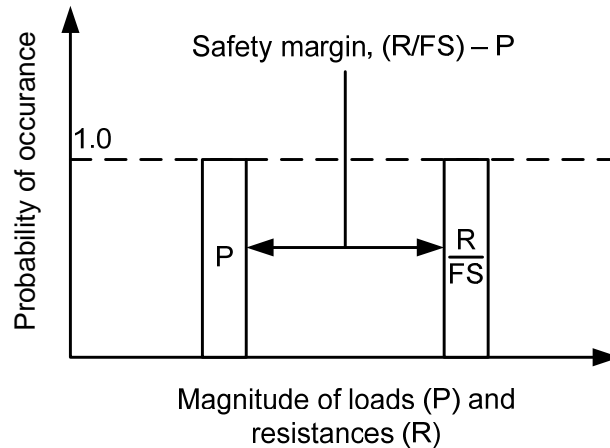
Figure 1.1 Allowable Stress Design

(adapted from NHI Course No. 132068, Pub. FHWA HI-98-032, May 2001, page 2-2)

The advantages of ASD are:

➢ ASD has an inherent simplicity. Because it does not involve the use of load or resistance factors, the computations are relatively simple.

The limitations of ASD are:

➢ In ASD, no consideration is given to the fact that various types of loads have different levels of uncertainty. For example, the dead load of a bridge can be estimated with a high degree of accuracy. However, earthquake loads acting on bridges cannot be estimated with the same degree of accuracy and confidence. Nevertheless, dead loads, live loads and environmental loads are all treated equally in ASD.

➢ Because the factor of safety applied to the resistance side of the inequality is based on experience and judgment, consistent measures of risk cannot be determined for ASD.

1.6.1.1 Allowable Stress Design Example

For this example, assume a dead load of 50 kips, a live load of 25 kips and an ultimate structural resistance of 150 kips. Use a factor of safety of 1.5 for this example.

$$\Sigma DL + \Sigma LL = 50 + 25 = 75 \text{ kips}$$

$$R_u / FS = 150 / 1.5 = 100 \text{ kips}$$

Since 75 < 100, the fundamental equation is satisfied and the design is acceptable for the given loadings at a factor of safety of 1.5.

1.6.2 Load Factor Design (LFD)

Load factor design (LFD) was introduced several decades ago in an effort to refine the ASD philosophy. LFD utilizes loads multiplied by load factors and load combination coefficients, which are generally greater than unity. The factored loads are combined to produce a maximum effect in a member. Load factors vary by type of load and reflect the uncertainty in estimating magnitudes of different load types. The combination of the factored loads cannot exceed the strength of the material multiplied by a reduction factor less than unity.

In LFD, uncertainty is also accounted for in the resistance side of the inequality. The resistance side is multiplied by a reduction factor, phi (ϕ), which is generally less than unity in order to account for variability of material properties, structural dimensions, and workmanship.

The following relationship represents LFD design. Note that loads other than dead and live load have been excluded from the equation for simplicity.

$$\gamma(\textstyle\sum \beta_{DL}DL + \sum \beta_{LL}LL) = \phi R_u \qquad\qquad \text{Equation 1.2}$$

where:
  DL = dead loads applied to the element under consideration
  LL = live loads applied to the element under consideration
  R_u = ultimate resistance or strength of the element under consideration
  γ = load factor applied to all loads
  β_{DL} = load combination coefficient for dead loads
  β_{LL} = load combination coefficient for live loads
  ϕ = reduction factor

The advantages of LFD are:

➢ In LFD, a load factor is applied to each load combination to account for the relative likelihood that a specific combination of loads would occur simultaneously.

➢ In LFD, consideration is given to the fact that various types of loads have different levels of uncertainty. For example, the dead load of a bridge can be estimated with a higher degree of accuracy than the live loads. Therefore, the load combination coefficient for live load is greater than that for dead load.

The limitations of LFD are:

➢ LFD is not as simple to use as ASD.

➢ LFD does not achieve relatively uniform levels of safety.

1.6.2.1 Load Factor Design Example

Using the same loads and ultimate structural resistance from the ASD example in
1.6.1.1, the design inequality for LFD Strength Load Combination I is listed below.
Note that a reduction factor of 0.9 has been assumed.

$$\gamma = 1.3$$
$$\beta_{DL} = 1.0$$
$$\beta_{LL} = 1.67$$
$$\phi = 0.9$$

$$\gamma \left(\Sigma\, \beta_{DL}\, DL + \Sigma\, \beta_{LL}\, LL \right) = 1.3\, (1.0 * 50 + 1.67 * 25) = 119.3 \text{ kips}$$

$$\phi\, R_u = 0.9 * 150 = 135 \text{ kips}$$

Since 119.3 < 135, the fundamental equation is satisfied and the design is
acceptable for this particular strength combination.

1.6.3 Load and Resistance Factor Design (LRFD)

The LRFD design method is the latest advancement in transportation structures
design practice. In the year 2000, AASHTO (in concurrence with FHWA) set a
transition date of October 1, 2007, after which all new bridges on which states initiate
preliminary engineering, shall be designed by the *AASHTO LRFD Bridge Design
Specifications* (*AASHTO LRFD*).

The LRFD design methodology is similar to LFD design. On the load side of the
inequality, LRFD utilizes load factors but not load combination coefficients.   In
addition to load factors, LRFD uses a load modifier, eta (η), which is applied to all
loads equally. The combination of the factored loads, termed "limit states" in LRFD,
cannot exceed the strength of the material multiplied by a resistance factor less than
unity.   Several limit states are included for service, strength, and extreme event
considerations. The different limit states will be discussed in future topics throughout
this course.

The resistance side of the LRFD inequality is similar to that of LFD, although
resistance factors differ from LFD.   The following relationship represents LRFD
design. Note that loads other than dead and live load have been excluded from the
equation for simplicity.

$$\eta\left(\Sigma\, \gamma_{DL}\, DL + \Sigma\, \gamma_{LL}\, LL \right) = \phi R_n \qquad\qquad \text{Equation 1.3}$$

where:
    DL = dead loads applied to the element under consideration
    LL = live loads applied to the element under consideration
    R_n = nominal resistance or strength of the element under consideration

η = load modifier applied to all loads
γ_{DL} = load factor for dead loads
γ_{LL} = load factor for live loads
ϕ = resistance factor

A graphical representation of the LRFD process is shown in Figure 1.2. As can be seen in the figure, the factored safety margin is small, but when the theoretical actual loads and nominal resistances are observed, the actual safety margin is actually much wider. LRFD also takes into account the different probabilities of occurrence for loads and resistances.
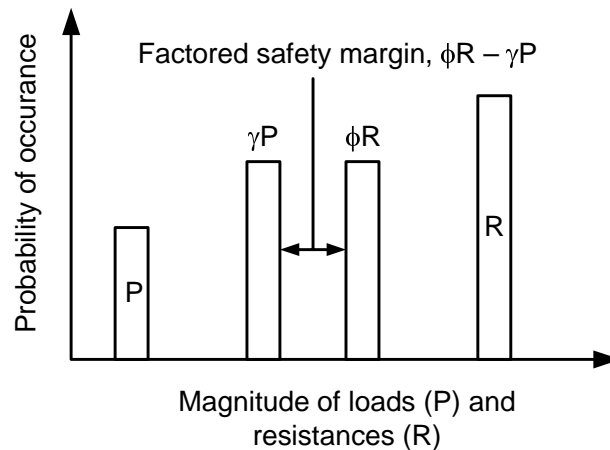
Figure 1.2 Load and Resistance Factor Design

(adapted from NHI Course No. 132068, Pub. FHWA HI-98-032, May 2001, page 2-3)

The differences in how load factors are applied in LFD and in LRFD are significant, but perhaps the greatest difference between LFD and LRFD is that reliability theory was used in LRFD to derive the load and resistance factors. The load and resistance factors were statistically "calibrated" in an effort to obtain a more uniform level of safety for different limit states and types of material.

These calibrations are based on a reliability index, β, which for the 1994 LRFD code was set at a target of $\beta = 3.5$. The reliability indices of previous *AASHTO LRFD* specifications ranged from as low as 2.0 to as high as 4.5. A target reliability of 3.5 was considered appropriate, as it was slightly higher than an average of previous specifications and design philosophies. Based on these calibrations and reliability indices, a higher load factor or lesser resistance factor is applied to loads and materials whose behavior is less-well known and cannot be as accurately predicted. In this manner, greater knowledge of some resistances and loadings can be accounted for, allowing more efficient designs while still applying appropriate levels of safety to those resistances and loads which are more ambiguous. As research is conducted and the knowledge base increases, load and resistance factors can be altered to account for the greater certainty, or in some cases, greater uncertainty of loads or resistances.

The advantages of LRFD are:

➢ LRFD accounts for variability in both resistance and loads.

➢ LRFD achieves relatively uniform levels of safety for different limit states and material types.

➢ LRFD provides more consistent levels of safety in the superstructure and substructure as both are designed using the same loads for predicted or target probabilities of failure.

The limitations of LRFD are:

➢ The most rigorous method for developing and adjusting resistance factors to meet individual situations requires availability of statistical data and probabilistic design algorithms.

➢ Implementation requires a change in design procedures for engineers accustomed to ASD or LFD.

As noted above, the LRFD specifications introduce a new term in the design equation which is a load modifier. *AASHTO LRFD* Article 1.3.2.1 defines the eta term, η, as a combination of factors due to the effects of ductility, redundancy and importance. At the time of this writing, the three factors, termed η_D, η_R and η_I, are all in development. The final combination of η factors depends on the desired loading condition.

For maximum values of γ_i:

$$\eta_i = \eta_D \eta_R \eta_I \geq 0.95$$

AASHTO LRFD Equation 1.3.2.1-2

For minimum values of γ_i:

$$\eta_i = (\eta_D \eta_R \eta_I)^{-1} \leq 1.0$$

AASHTO LRFD Equation 1.3.2.1-3

The ductility factor, η_D, can be modified for the strength limit state to reflect a bridge's ductility characteristics. A higher factor of 1.05 is applied to bridges or materials with lower ductility, and a factor of 0.95 is applied if a higher level of ductility is provided as per *AASHTO LRFD* Articles 1.3.3, and C1.3.3. For non-strength limit states, or for materials which are considered to comply with the *AASHTO LRFD* Articles 1.3.3 and C1.3.3 for ductility, a factor of 1.0 is used.

The redundancy factor, η_R, as the name implies, accounts for the redundant nature of the bridge or element. The preference is to design bridges with a suitable level of redundancy unless there is a specific reason not to do so. For strength limit states, a value of 1.05 is used for elements with lower redundancy, and a value of 0.95 is

used for elements with a higher level of redundancy, as defined in *AASHTO LRFD* Article C1.3.4. For bridges with normal redundancy, and for all limit states other than strength, a factor of 1.0 should be used.

The use of the importance factor, η_I, is somewhat more subjective than the ductility and redundancy factors. The importance of a bridge structure is the decision of the owner, although *AASHTO LRFD* Article C1.3.5 does give some guidance. For strength limit states, importance can range from 1.05 for important bridges to 0.95 for less important bridges. For typical bridges, and limit states other than strength, a factor of 1.0 should be used.

In summary, bridge designers that are accustomed to using the LFD design code will recognize many similarities when learning the LRFD design code. While load and resistance factors differ for LRFD as compared to LFD, many procedures for determining design loads and material strengths are the same.

1.6.3.1 Load and Resistance Factor Design Example

Using the same loads and ultimate resistance from the ASD example in 1.6.1.1, and the following factors corresponding to a strength limit state, the design is as follows:

$$\eta = 1.05 \ (\eta_D = 1.00, \ \eta_R = 1.00, \ \eta_I = 1.05)$$
$$\gamma_{DL} = 1.25$$
$$\gamma_{LL} = 1.75$$
$$\phi = 0.9$$

$$\eta \ (\Sigma \ \gamma_{DL} \ DL + \Sigma \ \gamma_{LL} \ LL) = 1.05 \ (1.25 * 50 + 1.75 * 25) = 111.6 \text{ kips}$$

$$\phi \ R_n = 0.9 * 150 = 135 \text{ kips}$$

Since 111.6 < 135, the fundamental equation is satisfied and the design is acceptable for this particular strength limit state.

Volume 1
General Design Considerations

Chapter 2
Preliminary Design Considerations

2.1 Introduction

During the preliminary phase of a bridge design, several critical decisions must be made which set the course for the final design phase. These decisions directly influence whether the bridge design and construction will be successful or burdened with problems.

Ill-conceived preliminary designs cannot be made efficient during final design, regardless of how well the individual bridge components are designed. This chapter describes some of those preliminary design considerations, highlighting the differences in efficient design requirements using concrete and steel.

2.2 General Design and Location Constraints

Some of the considerations and constraints that must be addressed during preliminary design include the alignment of the roadway and bridge, significant location features, vertical and horizontal clearance requirements, environmental considerations, and bridge aesthetics.

2.2.1 Alignment and Location Features

The alignment and location of the bridge must satisfy both the on-bridge and under-bridge requirements. The bridge must be designed for the alignment of the roadway or railway it is supporting. This can result in a tangent bridge if the alignment is straight or slightly curved, a curved bridge if the alignment has a significant curve, or a flared bridge to allow for a varying roadway width. A curved bridge, supporting a roadway with an alignment of significant horizontal curvature, is shown in Figure 2.1.
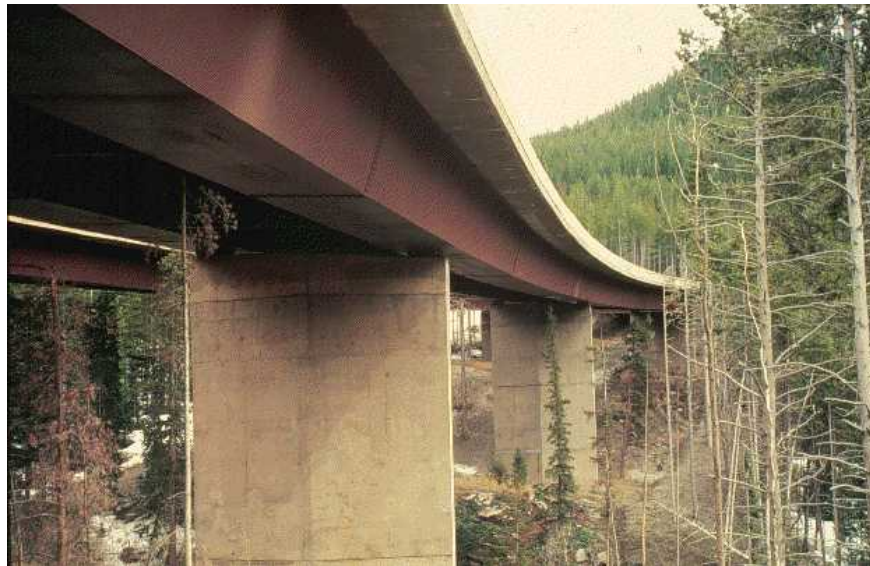
Figure 2.1 Bridge with Curved Alignment

The preliminary design must also consider the need for skewed substructure units. A skew may be necessary if the feature that is being crossed (such as a roadway, railway, or waterway) is not oriented perpendicular to the bridge.

When defining the alignment and location of a bridge, any possible future variations in the alignment or width of the waterway, highway, or railway spanned by the bridge must be considered. For example, if the roadway being crossed may be widened in the future, then consideration should be given to locating the bridge's substructure units to facilitate the future roadway width. In addition, the bridge width should be determined with consideration to future widening of the roadway supported by the bridge.

The route location for bridges must be established to facilitate a cost-effective design, construction, operation, inspection, and maintenance. It must also provide the desired level of traffic service and safety, and it must minimize adverse highway impacts.

Bridges over waterways or in floodplains must be aligned and located based on the following considerations:

> ➢ hydrologic and hydraulic characteristics of the waterway, including flood history, channel stability, and any tidal ranges and cycles
> ➢ effect of the proposed bridge on flood flow patterns
> ➢ scour potential at the bridge foundations
> ➢ potential for creating new flood hazards or worsening existing flood hazards
> ➢ consistency with the standards and criteria of the National Flood Insurance Program, where applicable
> ➢ long-term aggradation or degradation
> ➢ any environmental approval requirements

2.2.2 Clearance Requirements

In addition to alignment and location constraints, bridges must also be designed to satisfy all clearance requirements. The two basic types of clearance requirements are vertical clearance and horizontal clearance.

Vertical clearance requirements are established to prevent collision damage to the superstructure, such as that shown in Figure 2.2. Requirements for vertical clearance are defined in AASHTO, *A Policy on Geometric Design of Highways and Streets*. Vertical clearance is measured from the top of the roadway surface to the bottom of the lowest girder. For prestressed concrete girder bridges, the girder camber must be considered when computing the vertical clearance. For complex structures, it may be necessary to investigate the vertical clearance at several locations to ensure that the controlling value has been determined.

For many highway bridges, the required vertical clearance is 14'-6". The specified minimum clearance should include 6 inches for possible future overlays.

When evaluating whether or not to utilize wider girder spacings, a number of issues should be considered. Girder depth limitations based on vertical clearance requirements may limit how many girders can be removed from a cross section. Maintaining the required vertical clearance by raising the bridge profile is generally not economical.

Horizontal clearance requirements are established to prevent collision damage to the substructure. Requirements for horizontal clearances are defined in Chapter 3 of the AASHTO *Roadside Design Guide.* Horizontal clearance requirements can be used to determine the type of abutment selected. For example, stub abutments are often used when a wide opening is required under the superstructure, and they provide a larger scope of view for the driver. Full-height abutments restrict the opening under the superstructure, but they also allow shorter span lengths.

Figure 2.2 Violation of Vertical Clearance Requirement

In addition, railway bridges have clearance requirements that are set forth in American Railway Engineering and Maintenance-of-Way Association (AREMA), *Manual for Railway Engineering*. Clearances for railroad bridges must also satisfy local laws and any additional requirements of the railroad owner.

For bridges over navigable waterways, required navigational clearances, both vertical and horizontal, must be established and satisfied in cooperation with the U.S. Coast Guard. In addition, permits for construction must be obtained from the Coast Guard, as well as from any other agencies having jurisdiction over the waterway.

2.2.3 Environmental Considerations

During the preliminary stages of a bridge design, any environmental considerations unique to the bridge site and bridge type must also be addressed. For example, the impact of the bridge and its approaches on local communities, historic sites, wetlands, and any other aesthetically or environmentally sensitive regions must be considered.

The engineer must ensure that all laws and regulations are satisfied, including any state water laws, provisions of the National Flood Insurance Program, and any federal and state regulations concerning encroachment on floodplains, fish, and wildlife habitats.

For bridges crossing waterways, the stream forces, consequences of riverbed scour, removal of embankment stabilizing vegetation, and impacts to tidal dynamics must also be considered.

For bridges with concrete components, the design must provide protection of the reinforcing steel and/or prestressing steel against corrosion during the life of the structure. Such design considerations include concrete quality, protective coatings, minimum reinforcing steel cover, and protection for prestressing tendons. Aggregates from sources that are known to be excessively alkali-silica resistive should not be used in bridge design.

In addition, consideration should be given to portions of the structure where:

 ➢ air-entrainment of the concrete is required
 ➢ epoxy-coated or galvanized reinforcement is required
 ➢ special concrete additives are required
 ➢ the concrete is expected to be exposed to salt water or to sulfate soils or water
 ➢ special curing procedures are required

2.2.4 Aesthetics

Every bridge makes a visual impact within its unique setting, some favorable and others unfavorable. Although beauty can sometimes be in the eyes of the beholder, there are several qualities of beauty to which most people can attest. Just as people can generally agree on what makes a painting or a symphony a work of beauty, so it is with bridges. There are several guiding principles that generally lead to the design of an aesthetically pleasing bridge.

Some of the most basic characteristics of aesthetically pleasing bridges include the following:

 ➢ they are generally simple – that is, they have few individual elements, and its elements are similar in function, size, and shape
 ➢ they have relatively slender girders
 ➢ the lines of the bridge are continuous, or they appear to be continuous
 ➢ the shapes of the bridge's members reflect the forces acting on them – that is, they are largest where the forces are greatest and smallest where the forces are least

Since bridge engineering is a profession that serves the general public, engineers must take responsibility for the aesthetic impact of their bridges. Bridges generally last for a very long time, many for several centuries. The bridge engineer's responsibility to the public is not limited to designing safe, serviceable, and economical bridges. He or she is also obligated to design bridges that are pleasing for people to look at on a daily basis for many decades to come. The ability to design aesthetically pleasing bridges is a skill that can be developed by engineers by following a series of aesthetic principles. It is the engineer's responsibility to the traveling public to learn and master these skills.

Some of the most important determinants of a bridge's appearance are described below (as adapted from Frederick Gottemoeller's *Bridgescape: The Art of Designing*

Bridges, Second Edition, 2004, John Wiley & Sons, Inc.). These ten determinants are listed in order of importance to the aesthetic quality of the bridge.

2.2.4.1 Vertical and horizontal geometry

This first and most important determinant involves the basic geometry of the bridge relative to its surrounding topography and other nearby structures. While the bridge engineer usually is not able to define the vertical or horizontal geometry of the bridge, small adjustments in the bridge's alignment can lead to significant improvements to its appearance. Some of these adjustments include the following:

> ➤ Locate the bridge along an alignment that looks like the short distance between points.
> ➤ Provide a vertical and horizontal alignment that consists of long and continuous curves and tangents rather than a series of short and dissimilar segments.
> ➤ Whenever possible, provide curve lengths that are longer than the minimums set by AASHTO.
> ➤ Curve lengths should be as long as possible, preferably longer than the bridge itself
> ➤ Whenever possible, provide a crest vertical curve on overpasses.
> ➤ Adjust the horizontal alignment if needed to simplify column placement and provide consistent pier types.

2.2.4.2 Superstructure type

The superstructure type is the second most important determinant of bridge appearance. Superstructure type is generally a function of structural requirements and economic considerations. It is often governed by the unique bridge site and the corresponding span lengths. Some of the primary factors influencing the choice of superstructure type are as follows:

> ➤ If the bridge is curved or tapered, then the girders must be well suited to the required curve or taper.
> ➤ The span requirements and the required vertical clearances will affect the superstructure type and proportions.
> ➤ The nature of the bridge site and its surrounding topography may limit the choice of superstructure type (such as the unique bridge site requirements for arches, rigid frames, and cable-supported bridges).
> ➤ The superstructure type plays a major role in the establishment of a signature bridge.
> ➤ Relative slenderness is desirable in the selection of the superstructure type.
> ➤ Maintain continuity of structural form, material, and depth, and maintain continuity as much as possible between adjoining bridge types.

For girder bridges, several considerations can enhance the aesthetic quality of the bridge. Curved girders should be used for roadways with a significant horizontal curve. If the underside view of the bridge is especially important, box girders can provide an attractive solution. Integrally frame cross frames emphasize the visual

continuity of the superstructure and can minimize the pier size. If girders must be added to accommodate a flared bridge width, the girders should be added in a systematic and logical manner.

For arches and frames, the aesthetic quality of the bridge is enhanced by providing a visual thrust for the arch, either by the surrounding topography or by visual thrust blocks. For rigid frames, the legs should be approximately one-quarter to one-half of the span length.

For trusses, the design should incorporate a graceful and simple shape, a minimum number of members, a consistency of the angles, and small connection details.

Figure 2.3 Slenderness Improves the Aesthetic Quality of a Bridge

2.2.4.3 Pier placement

The next most important determinant of a bridge's appearance is the pier placement. The placement of the piers is affected by several factors, including the under-bridge clearance requirements, hydraulic requirements, navigational channels, foundation conditions, and span length requirements. In addition to satisfying each of these pier placement criteria, there are also several aesthetic principles for pier placement:

➢ For most bridges, there should be an odd number of spans.
➢ Piers should not be placed in the deepest part of a valley or cut.
➢ Whenever possible, piers should be placed on natural points of high ground.
➢ Piers should be placed as symmetrically as possible relative to shorelines.
➢ The span length should generally exceed the pier height.
➢ The ratio of the pier height to the span length should be similar from span to span.

Figure 2.4 Providing an Odd Number of Spans Enhances Bridge Aesthetics

2.2.4.4 Abutment placement and height

The visual function of an abutment is to get the bridge started, to connect the bridge with the earth. The placement, height, and appearance of the abutment can play a significant role in improving or detracting from the beauty of a bridge. As a general rule of thumb, the abutments should be placed to open up the view to the people traveling under the bridge. The following are some general guidelines for abutment placement and height:

  ➢ The abutment height should not be less than one-half of the girder depth.
  ➢ For three- or four-span bridges, use minimum height pedestal abutments.
  ➢ If both abutments are visible at the same time, provide the same height-to-clearance ratio at both ends of the bridge.
  ➢ Use abutment wingwalls that are parallel to the roadway crossing the bridge (U-wings).

For skewed bridges, it can be beneficial to place the abutment near the top of the embankment and to place it at right angles to the roadway crossing the bridge. This improves the aesthetics of the bridge, reduces the amount of required fill, and simplifies analysis and construction. While it may increase span lengths, it also reduces the required length and height of the abutments, which may provide a compensating savings.

Figure 2.5 Abutment Placement Providing an Open View

2.2.4.5 Superstructure shape, including parapet and railing details

After the superstructure type has been selected and the abutments and piers have been located, there are additional choices that can be made to enhance the superstructure shape and the parapet and railing details. As previously described, it is desirable to design the superstructure such that it appears to be slender, light, and continuous. In addition, the superstructure shape should accentuate the function of the superstructure and the flow of forces through the superstructure to the substructure. Slenderness, lightness, and continuity can be achieved using some of the following techniques:

- ➢ Maximize the girder spacing, and maximize the girder overhang.
- ➢ The overhang should not be less than the girder depth.
- ➢ Provide a structural depth that is either constant or that varies smoothly over the length of the bridge.
- ➢ Consider haunched girders where feasible.
- ➢ Make haunches long enough to be in proportion to the span length.
- ➢ Use pointed haunches at the piers to accentuate the flow of forces.
- ➢ Provide a haunched girder depth that is approximately 1.3 to 2.0 times the shallowest girder depth.

Figure 2.6 Haunched Girders Can Improve the Aesthetics of the Bridge

Railings and parapets also affect the aesthetic statement of a bridge. The height of the parapets should be between one-quarter and one-half of the exposed girder depth. In addition, it should also be no less than $1/80^{th}$ of the span length. Incisions, recesses, and sloped planes can break up the face of the parapet horizontally, enhancing the aesthetics of the superstructure.

2.2.4.6 Pier shape

Pier shape can play an important role in the visual impact of a bridge, especially for girder bridges. There is no correct pier shape for all bridges, but it important that a clear visual relationship is maintained for all substructure units.

For short piers, it is desirable to use piers which eliminate or minimize the pier cap. The taper of V-shaped and A-shaped piers should be limited, and hammerhead piers should have logical shapes.   The pier width should be proportional to the superstructure depth, the span lengths, and the visible pier heights.

For tall piers, no more than two columns should be used at each pier line, if possible. The vertical members should be tapered or flared such that they are wider at the based of the pier. In addition, the pier shaft and cap should be integrated as much as possible, rather than giving the appearance of two distinct elements.

For groups of piers, each pier should have the same basic shape, and the shapes and curves of adjoining piers should be consistent.

Figure 2.7 Aesthetically-Pleasing Tall Piers

2.2.4.7 Abutment shape

The abutment shape can also play a significant role in the aesthetic quality of a bridge, especially for bridges of four spans or less. The shapes and details of the abutments should be selected to complement and enhance the shapes and details of other bridge components.

To frame the opening and to create a sense of transition between the abutment and the superstructure, the face of the abutment can be sloped inward. However, to make the superstructure appear longer or to emphasize the separation between the abutment and the girders, the face of the abutment can be sloped outward.

As a general rule of thumb, the beam seat width should be at least one-half the girder depth. In addition, abutments should be designed such that the adjoining retaining walls blend into the abutment without an abrupt change in appearance.

2.2.4.8 Colors

Although the shapes and patterns of the superstructure and substructure play the most significant role in creating the visual statement of a bridge, the surfaces of those shapes can also add to that visual statement. The two most prominent qualities of the surface are its color and its textures and ornamentation.

The application of a specific color to a bridge is not necessary for the creation of an aesthetically-pleasing bridge. At the same time, however, the application of color can not compensate for poor decisions elsewhere in the aesthetics of the bridge.

2.2.4.9 Surface textures and ornamentation

Similar to color, surface textures and ornamentation can also enhance the shapes and patterns for the bridge, but they can not undo the visual impact of poor decisions concerning those shapes and patterns.

Concrete provides many opportunities for surface textures through the use of form liners and custom formwork. However, it is important to ensure that the pattern contributes to the overall design features and patterns of the structure itself. In addition, the pattern should be large enough to be recognizable to travelers on or beneath the bridge.

2.2.4.10 Signing, lighting, and landscaping

Finally, signing, lighting, and landscaping also influence the aesthetics of the bridge. Bridge-mounted signs should fit into the overall design of the bridge, and sign bridges on structures should be kept as simple as possible.

Light should be avoided on short bridges, if possible. However, if they are necessary on the bridge, they should be placed in some consistent relationship to the geometry of the bridge, and their poles should be mounted on a widened area in the parapet.

Landscaping can be used to emphasize continuity of the space through the bridge and to soften the hard edges of the bridge. The colors and shapes of the landscaping should complement those of the bridge itself.

After studying these ten determinants of the bridge's appearance, it is important to note that the most important determinants are those which affect the geometry and appearance of the entire bridge, and the least important determinants are those which affect smaller details of the bridge. It is also important to note that many of these ten determinants can be fully implemented at no additional cost to the bridge owner.

2.3 Construction and Constructibility Issues

Future Development

2.4 Steel Bridge Superstructures

2.4.1 Introduction

The sole purpose of a bridge is to transfer load from one side to the other side of an expanse. Thus, its design should present minimal conflicts. Although bridge design is not quite so simple, it does afford the designer significant latitude in developing the design to best satisfy this purpose.

2.4.2 Bridge Layout

2.4.2.1 Span Optimization

Steel has the versatility to be built in most any span arrangement. However, steel is most efficient when it is used in properly proportioned span arrangements, and not forced into a span arrangement set for prestressed concrete.   *While many factors may dictate where piers may and may not be placed, there are many cases where locating piers is the prerogative of the Engineer; carefully arranged spans can usually has a very positive impact on the cost of the bridge*. In the following, the relationship between substructure and superstructure costs will be examined, along with the importance of span length and relative span length of continuous-span bridges.

Figure 2.8 Continuous Span Steel Bridge

Continuous-span steel bridges are usually more efficient than simple-span bridges. Thus, where possible, a single multi-span unit should be employed in lieu of many simple spans or several continuous-span units. Elimination of as many end spans and associated joints as possible is desirable for both first-cost and maintenance considerations.   Modern design techniques and modern bearings permit much longer multi-span steel structures than commonly used in the past.   Thermal

considerations should lead to separate units only after careful consideration of thermal requirements.

2.4.2.2 Balanced Spans

For continuous-span units with more than two spans, span lengths preferably should be proportioned such to yield approximately equal maximum positive dead-load moments in the end and interior spans. Such arrangements are called "balanced span arrangements". Balanced span arrangements result in negative moments at piers somewhat larger than the concomitant positive moments. As a result, a constant girder depth may be optimally employed. ***A balanced span arrangement has end span lengths between 0.75 and 0.82 of the interior span lengths***.

The optimum girder depth is that depth that provides a minimum cost girder for the structural unit. The optimum depth distributes the steel area between the flanges and the web of a girder. Composite girders are actually designed for two conditions—the noncomposite load during construction and the combined noncomposite and composite load on the completed bridge. There is no known algorithm that correctly optimizes the depth of such girders. Factors including desired web slenderness, live load deflection limit, flange stability and web bend buckling all contribute to the mix in selecting a girder depth.

A compromise between that depth for the positive and negative moments is required. However, a balanced span arrangement provides a single optimum for all spans. If unbalanced spans are employed, it may be desirable to taper the depth of the girder so that different depths are employed in different spans. Frequently an average-depth girder in a poorly proportioned continuous-span unit is found to be neither optimum for the larger or the smaller spans. An average girder depth often leads to flanges that are too large and too small in the long and short spans, respectively. If the girder is too shallow in the longer spans, deflections may be problematic. The Engineer should be aware that the use of different depths in the same unit may draw load (moment) to the deeper (stiffer) portion of the unit, further exacerbating the imbalance of moments.

To illustrate the balanced span concept further, the unfactored moments in a tangent three-span continuous box girder caused by the dead load applied to the noncomposite section (DC_1) are shown in Figure 2.9. The span arrangement for this girder (190′-0″ − 236′-0″ − 190′-0″) is reasonably balanced with an end-to-center span ratio of approximately 0.81.

Also shown in Figure 2.9 are the moments assuming the same total length for the box girder, but with a different span arrangement (200′-0″ − 216′-0″ − 200′-0″). For this particular unbalanced span arrangement, the end-to-center span ratio is approximately 0.93. As shown in Figure 2.9, note that the ratio of the maximum positive DC_1 moment in the end span to the maximum positive DC_1 moment in the center span increases from 1.2 to 2.5 when going from the balanced to the unbalanced span arrangement. For a steel-girder design, the larger uneven distribution of the moments from span to span in the unbalanced arrangement − which is the case for both the dead and live load moments in this instance (live load

moments not shown) – will have a significant overall effect on the girder efficiency and economy. Assuming that the girder depth is optimized for either the interior or exterior spans, or else averaged, the chosen girder depth will be inefficient for the moments in either some or all spans.
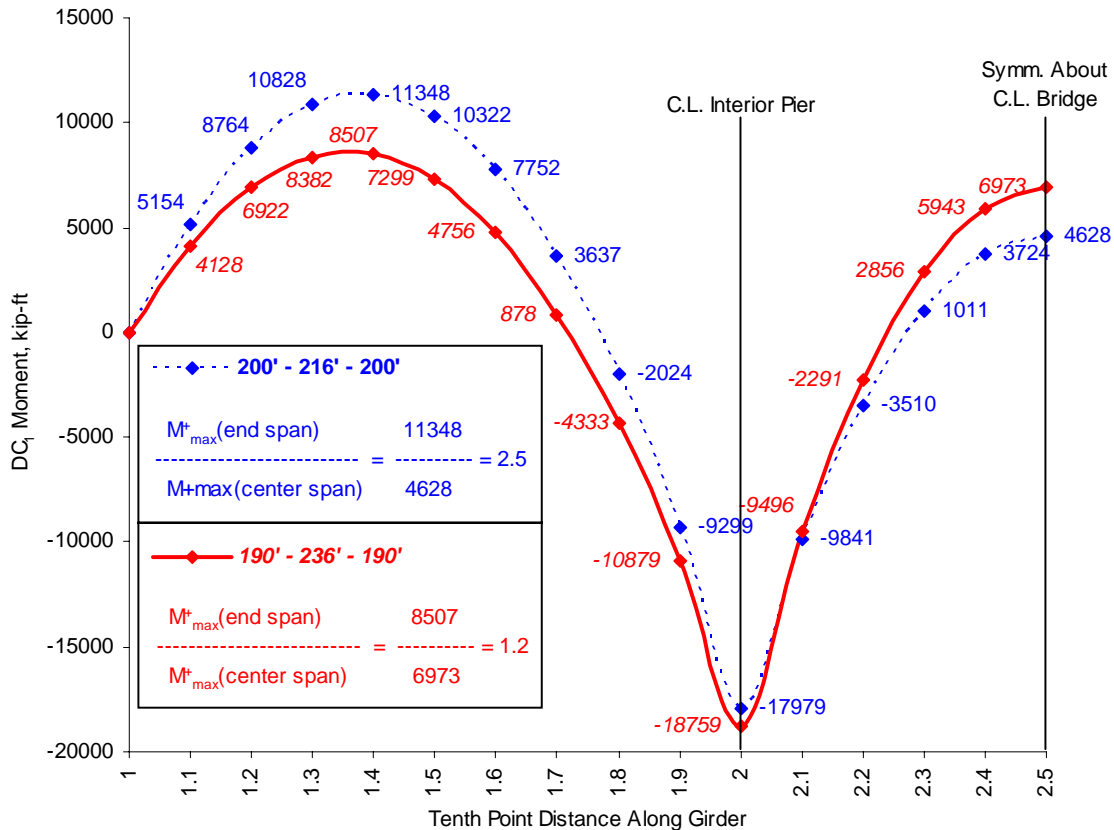
Figure 2.9 Component Dead Load (DC$_1$) Moments for Different Span Arrangements – Box Girder

Another disadvantage associated with the use of an unbalanced span arrangement for this particular box-girder design is that fact that the resulting moments will not likely permit the bottom-flange longitudinal stiffener in the box to be terminated at the field splices, as is the case for the balanced span arrangement. Termination of the stiffener at the field splice is desirable because the flange bending stress at the weld termination is zero; thus, fatigue of the base metal at the weld termination need not be checked. Otherwise, a special transition radius is required at the termination of the stiffener weld to avoid a fatigue detail in either Category E or E′. As the nominal fatigue resistance of Category E or E′ details is low, it therefore becomes difficult to terminate the stiffener in regions of net applied tensile stress. Thus, expensive termination details or lengthy extensions of the stiffener may have to be used to satisfy fatigue requirements. Similar considerations would apply to a longitudinal web stiffener for either a box- or an I-girder

In some situations, unbalanced span arrangements may be required. For example, where there are severe depth restrictions, or where it is desirable to eliminate center piers (e.g. for certain overpass-type structures), it may be necessary to consider ill-proportioned short end spans. One solution in these cases may be to extend the end spans to provide a balanced span ratio. Another option may be to shorten the bridge to a single span with higher abutments.   A third solution and less desirable solution may be to provide short end spans and tie down the end bearings. In the latter case, a shallower center span is possible when haunches are employed at the piers, which improves the appearance of the bridge and may reduce the steepness or length of the approach grades.   A fourth solution, which is less desirable aesthetically and from a maintenance point of view, would be to utilize simple spans.

2.4.2.3 Relation of Substructure to Superstructure

2.4.2.3.1 General

In determining the most economical spans, it is necessary to compare the relative cost of the superstructure and substructures since the cost of the substructure has a major impact on the optimum span length. If the substructure costs are relatively low, utilizing shorter spans is called for; if substructure costs are relatively high, longer spans are desirable. Other things being not considered, the cost of the substructure should approximately equal the cost of the superstructure steel on a multi-span bridge. An important corollary is that reduction of the pier cost has a double effect in that the savings in the piers justifies less costly (by an equal amount) shorter spans. It can be observed that the shape of the superstructure may affect pier cost, and thereby the span length, and finally the total bridge cost.

Figure 2.10 Full Height Abutment (Shorter Span)

Figure 2.11 Stub Abutment   (Longer Span)

Hence, when alternate designs are investigated, the substructure for the steel design must be evaluated and designed concurrently with the superstructure if efficiency is to be obtained. ***Since substructure costs have such a substantial impact on the most economical span arrangement, the proper steps must be taken if the Engineer is to ensure that the substructure design is the most efficient possible when combined with the steel superstructure***. Therefore, a few words are in order at this juncture regarding the selection of a substructure form to satisfy the demands of a particular site.

2.4.2.3.2 Substructure Type

As stated earlier, the substructure type is dictated in part by the superstructure type. For example, small footprint pier designs can be obtained by drawing the superstructure loads to a single column. One way to accomplish this objective is with a hammerhead pier. More desirably, a superstructure type consisting of a single girder that requires no pier cap leads to an even more economical pier design. Careful steps are often taken to optimize a steel superstructure design without giving due consideration to the substructure design. In fact, when pier caps are made integral with the girders, and/or integral abutments are employed, it is difficult to differentiate between the two parts from the whole. Since steel is an inherently versatile material that can be adapted to most any substructure and span arrangement, steel is often the material of choice when the site dictates unique span arrangements. Each of these situations presents unique challenges to the Engineer. To achieve a truly efficient steel design, the superstructure and substructure type must be compatible with respect to economic, structural and aesthetic demands. Modern bridge design calls for a unified approach to the design of superstructure and substructure.

Figure 2.12 Hammerhead Piers

The type of substructure is defined by considering its many functions and the existing soil conditions. The substructure is designed for various specified combinations of the resulting vertical and lateral load effects. Different load factors are applied to each force effect to account for the probability of the combination of individual design loads occurring simultaneously. Vertical loads are primarily dead and live loads plus impact. Lateral loads include wind on the structure and on the live loads; braking; bearing friction; thermal forces; ice; stream flow; earth pressure; ship impact; debris; and seismic forces. Lateral loads are resisted by overturning moments and shear in the piers and abutments. Overturning moments can cause an increase in the size of the foundation beyond that required for only vertical loads; however, an objective for an efficient foundation is one that requires minimal additional material beyond that required for vertical loads. This is particularly true for pile foundations where there is latitude in not only the pile-group size, but also the arrangement of the piles. A potentially inefficient design may occur if more piles are used than required to resist the vertical load. Sizing a spread footing presents a similar challenge.

Transferring the vertical loads to the ground through a minimum number of pier columns is usually desirable. For example, single-shaft piers carry the entire vertical load as well as resist lateral loads. The critical moment in the shaft is partially due to transversely and longitudinally eccentric vertical loads. Usually the maximum moment and maximum axial load are not coincident. Further, *AASHTO LRFD* Table 3.4.1-1 requires modified load factors. Load Combination Strength III applies 1.4 times the wind load, but no live load. Load Combination Strength V applies 1.35 times the live load, but only 0.40 times the wind load. Further, maximum live loads are reduced from the maximum vertical live load in order to cause the maximum

overturning moment; e.g. live load is applied in only one span or on only one half of the cross-section to obtain maximum overturning with concomitant reductions in the maximum vertical load. In multiple-column piers there are multiple or redundant paths for live loads. It is almost axiomatic that such a condition demands an uneconomical vertical load capacity in excess of the design vertical load.

When appropriate, single shaft piers that support multiple girders with a pier cap, or a single box girder without a pier cap, avoid the uneconomical redundant path dilemma. Hammerhead pier caps can be designed integral with the steel girders if underclearance is limited. It is common to employ an integral pier cap in conjunction with a single-shaft pier to avoid a skewed pier. Integral cap beams are frequently constructed of prestressed concrete to make them easily integral with the pier column. A disadvantage of this type of pier is the need to shore the girder sections while the cap is built. Since integral pier caps are often employed where a typical cap would be in the clearance envelope, shoring is often not an option.

Figure 2.13 Integral Pier Cap

In cases where shoring is not possible, an integral steel cap beam may be employed.   Usually, steel cap beams are employed with five or fewer I-girders or two tub girders. Steel cap beams present two concerns:

   1) a fracture-critical cap beam, and
   2) ensuring that the steel cap beam is stable on the pier shaft.

The shaft itself may support two or three of the I-girders while additional exterior girders are supported by what are essentially diaphragms. In the case of tub girders, two bearings may be used to support the diaphragm on the shaft. Steel box diaphragms are commonly employed.   Designers frequently employ bolted connections to provide redundancy via the use of multiple elements rather than single element welded members.

A broad section for the pier shaft helps reduce the overturning moments. However, if large volumes of concrete are required in the pier shaft, the cost is increased and the casting rate may be limited by constraints imposed by heat of hydration. The use of a hollow shaft may be desirable in this situation. In some cases, it may be most economical to precast sections of the pier shafts

For cases where a less costly spread footing might be applicable in lieu of a pile-supported foundation, the optimal arrangement of the cross-section of the footing is less critical and other considerations might take precedence. As discussed above, the use of less costly spread footings combined with shorter spans may lead to a more economical bridge.

In the case of long viaduct-type bridges, the length of bridge that can be built without expansion joints is not defined by specification. The elimination of joints, in addition to providing savings in the number of bearings, cross-frames and expansion devices, removes simple supports, which tend to require spans that are shorter than the adjacent spans in order to provide the necessary economy. Longitudinal forces can be distributed to several piers in proportion to their stiffnesses by attaching the superstructure to the pier with longitudinally fixed bearings, forcing the piers to flex. This allows less expensive elastomeric fixed bearings to be used. Steel bridges well over 2,000 ft in length have been successfully built in cold climates with expansion joints provided only at the ends.

From the above discussion, it is clear that it is sometimes difficult to separate the superstructure and substructure analysis, as well as the economic and aesthetic aspects of the design. The preceding discussion cites a few examples of some of the considerations that an Engineer will make when judiciously selecting a cost-effective substructure type for a steel-girder bridge. Again, substructure design demonstrates the uniqueness of each bridge and the requirement for an Engineer to address the substructure design with a unique thought process and ideas. The selection of the best substructure type for a given steel superstructure, in combination with the development of reasonably accurate cost data for the chosen substructure, will help to ensure the selection of a well-conceived span arrangement, which in turn will lead to an overall more desirable steel bridge.

2.4.2.3.3 Cost Curves

For projects in which spans may be varied, it is prudent to develop superstructure and substructure cost curves comparing cost to span length for a series of preliminary designs having different span lengths and arrangements. Since the concrete deck cost is independent of span length, that cost need not be considered in these curves. The most economical span arrangement is at the minimum point of the total cost curve, if the curve representing the sum of the variable superstructure and fixed substructure cost per unit over the span range is investigated, as shown in Figure 2.14. For the case illustrated in Figure 2.14, the optimum span length is approximately 165 feet. For multiple continuous-span units, this would be the span length chosen for the interior spans. The length of the end spans would then be selected to provide a balanced span arrangement.
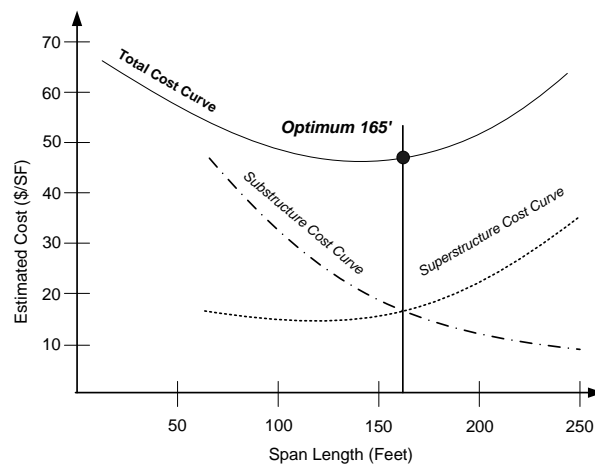
Figure 2.14 Sample Span Optimization

The validity of the preceding analysis is only as good as the accuracy of the costs. If rule-of-thumb estimates are applied for substructure costs, they can lead to improper conclusions about the most economical span lengths. As a minimum, pier costs should consider separately concrete reinforcement, concrete forming, concrete, and foundation costs. Simplicity and repetition of the formwork are the keys to economy. Changes to the unit costs that may result from an improved knowledge of specific site conditions should be incorporated in the analysis and the curves regenerated before selecting the final span arrangement.

2.4.3 Superstructure Types

2.4.3.1 Multi-Girder Systems

2.4.3.1.1 Girder Spacing and Deck Overhangs

The cost of steel multi-girder bridge superstructures depends in part on girder spacing and the deck overhang. It is desirable to take advantage of the new load distribution rules in the LRFD provisions that provide improved assignment of dead and live load to longitudinal stringers. Design of the deck itself is also important when investigating the cross-section. Generally it is desirable to balance the overhang and girder spacing so that interior and exterior girders are nearly the same size. Several of the factors that lead to an economical cross-section are examined below.

2.4.3.1.1.1 Girder Spacing

Where depth limitations are not an overriding factor, it is generally cost-effective to minimize the number of girder lines by using wider girder spacings for steel multi-girder bridges. Fewer girders provide these economic benefits:

1) fewer girders and cross-frames to fabricate, handle, inspect, coat, transport and erect,

2) fewer bearings to purchase, install and maintain,

3) fewer bolts and welded splices,

4) reduced fabrication and erection time, and

5) lower total structural steel weight.

Another intrinsic benefit of utilizing wider girder spacings is that because each individual girder must carry more load, deeper girders are often economical. The greater depth leads to an increased moment of inertia of each girder, which in turn makes for a stiffer structure with smaller deflections. This result is somewhat at odds with the provision for straight-girder bridges allowing live load deflection to be computed by assuming all lanes loaded and equally distributed to all girders, which leads to a reduced load assigned to each girder as the number of girders is increased.

When evaluating whether or not to utilize wider girder spacings, a number of issues deserve consideration. Girder depth limitations based on vertical clearance demands may limit how many girders can be removed from the cross-section. Maintaining the required vertical clearance by raising the bridge profile is often not economical

2.4.3.1.1.1.1 Effect on Deck Design

Larger girder spacing beyond some limit leads to a thicker concrete deck, which can translate to additional cost for concrete and reinforcing steel. The weight of a thicker deck on longer spans may lead to significant increase in girder sizes. However, in many instances, the additional costs of a thicker deck are more than offset by the savings realized from reducing the number of girders.

When cast-in-place decks are used, the weight of concrete in the troughs of stay-in-place deck forms must be considered. Much of this weight can be eliminated by placing styrofoam in the form flutes. When employing wider girder spacings, the method of forming the deck must be considered. Deeper galvanized metal permanent deck forms are extremely stiff and can clear span up to about 13.5 feet. Precast concrete deck panels are sometimes used as an alternative stay-in-place form system, but these forms can only be used for girder spacings up to approximately 10 feet.

Figure 2.15 Precast Concrete Deck Panels

Conventional removable forming can be used to span similar or greater girder spacings. Some form of intermediate support or shoring is required. However, such forming adds complexity and the expense of removal. Traditionally, the weight of wood forming has not been considered in the design because it is temporary. However, its weight acting on the noncomposite section might be considered in longer spans. The weight is removed from the composite dead load section. The form weight is applied to the noncomposite section, but removed from the composite section so it can have an effect on the determination of vertical cambers.

For very wide girder spacings, cast-in-place posttensioned prestressed decks have been used. Spans of thirty feet with overhangs half that amount have been successfully made. In these applications, a vaulted deck section (variable thickness) is economical. Such a shape permits posttensioning without draping to be used effectively in both positive and negative bending. Vaulted deck forming systems are rarely permanent. Transverse posttensioning of lesser spans also has been used without vaulting. Other precast decks using mild steel transversely with nominal longitudinal posttensioning have been used successfully. Precast decks augment the speed of steel erection by removing the set trades from much of the contract, thereby speeding completion of the bridge.

2.4.3.1.1.1.2 Redecking

Another consideration related to the use of fewer girders associated with wider girder spacings are the myriad issues associated with future redecking. These issues include girder capacity, stability, uplift, cross-frame forces, and several other factors such as geometric constraints. Future redecking is different from phased construction (discussed below) and may present different design considerations. It is advisable to check for the temporary conditions that may exist during redecking as part of the design to ensure that the bridge has adequate capacity for a redecking

plan. A number of Owners require such an analysis. Redecking of bridges that require more lanes to be carried by fewer girders than in the total cross-section are suspect. Skewed supports can experience uplift that is not found when the total cross-section is effective. Of course, horizontally curved bridges are frequently problematic structures during redecking.

When the deck is removed from some of the girders and temporary barriers are erected, the bridge undergoes significant structural changes. The unloaded girders tend to rise while the cross-frames tend to restrain them. This applies some upward, unloading force to the composite girders. The wet concrete is then placed on the bare girders as a noncomposite load. However, the adjacent composite girders are much stiffer and tend to draw additional load in excess of the unloading experienced by the earlier deck removal. This additional load is added to the live load and the load from the additional barriers. The empirical wheel-load distribution factors that may have been used for the design are no longer appropriate since the girders have varying stiffness at the time.

Figure 2.16 Conventional Deck Replacement Under Traffic

Of course, the original girder dead load moments and shears and cross-frame forces are added to the redecking analyses results to obtain the proper condition of the bridge during the various stages of redecking. Not infrequently, the cross-frames are found to be significantly overloaded compared to the original forces due to the unified construction and live load. One of the options available is to disconnect cross-frames, or at least the cross-frame diagonals, between the composite and noncomposite girders during the redecking. This simplifies the analysis situation, but not the field situation where cross-frames must be reconnected under the completed deck. Usually the old holes will not line up and new holes are required, or new diagonals can be made with one end blank (un-drilled).

The more flexible the bridge, the more redecking issues would be anticipated. Thus, if the dead load deflections are large, changes in deflections during redecking would be a certainty and problems would seem to be a corollary.

2.4.3.1.1.1.3 Phased Construction

Phased construction is defined as building a parallel portion of a bridge at a different time. For example, if a bridge is to be replaced by a wider new bridge, the old bridge may be left in service while a portion of the new bridge is built. The old bridge is then removed and the remainder of the new bridge is added. This situation is usually simpler than redecking under traffic, as described above.

Figure 2.17 Phased Construction

The simplest way to construct such a bridge is as two bridges and then to connect them with cross-frames in the closure bay followed by a closure pour. Cross-frames in the closure area can be left with the diagonals disconnected at one end (the top and bottom strut then maintain the lateral spacing without constraining the vertical deflection) until completion of the second stage; then, installation can be completed prior to the closure pour (after the closure pour only if the underbridge access allows). This permits the bridge to be built with none of the problematic issues associated with the connections between the composite and noncomposite girders. There is some reluctance to use closure pours by some Owners due to unfortunate experience with them. However, proper computation of cambers should give very compatible deflections. The deck pouring sequence needs to be considered, as does shrinkage. When constraint of the bridge abutments is planned, cambers are much more difficult to correctly determine.

2.4.3.1.1.2 Deck Overhangs

Deck overhangs in steel multi-girder bridges are often overlooked as insignificant. In fact, deck overhangs are an important factor in the overall economy of the bridge.

Overhangs should be established to provide a reasonable balance of the total factored dead and live load major-axis bending moments in the exterior and interior girders. Otherwise, the exterior and interior girders are designed for different loads leading to inefficient designs for the more lightly loaded girders if all girders are kept the same size, or to different size girders with differing stiffnesses. The wheel-load distribution factors in the LRFD Specifications are sometimes not applicable for bridges with cross-sections having girders with differing stiffnesses. If the stiffnesses are comparable, the wheel-load distribution factors in the specifications are adequate.

There are a number of factors that affect the design of exterior girders. The new wheel-load distribution factors for the exterior girder tend to more correctly apply a greater live load to those girders than did the older wheel load distribution factors in the Standard Specifications, which were developed for smaller overhangs on much shallower girders than are prevalent today (2006). As discussed below, deck weight can be assigned equally between all stringers in the cross section if the girders are of approximately equal stiffness at cross-frame/diaphragm connection points. Additionally, a larger portion of the barrier weight should also be assigned to the exterior girders. As a result, the exterior girders are often designed for significantly more load than the interior girders if the overhang is as large as 35 percent of the girder spacing (or larger).

The transverse bending moment in the deck over the exterior girders is a function of the vertical loads on the overhang and impact on the barrier. These vertical loads typically include the self-weight of the deck, weight of the parapet, sidewalk, sound barrier, light poles, sign supports and live load on the overhang.

Article 2.5.2.7.1 of the *AASHTO LRFD* Specifications states that unless future widening of the bridge is not plausible, the load carrying capacity of the exterior girders is not to be less than the load carrying capacity of the interior girders. This requirement can be used to establish the *lower limit* on the length of the deck overhangs. However, as mentioned above, if the overhang is of a typical size, the total factored major-axis bending moments will tend to be *larger* in the exterior girders than the interior girders. Hence, it is necessary to limit the length of the deck overhangs to ensure a reasonable balance between interior and exterior girder moments.

In general, if the overhang is too large, the exterior girders will be critical and will be required to be larger than the interior girders. As discussed elsewhere, this leads to uneconomical designs. Therefore, keeping a reasonably small overhang with a minimal number of girders yields the most economical steel I-girder cross-section in most cases.

As overhangs become larger, it becomes more difficult to control the twist and web deflection of the exterior noncomposite girder induced by loads on the cantilevered forming brackets. These brackets are typically spaced at three or four foot increments along the exterior girders. Vertical load on the bracket is usually resisted by a bolt and clip mechanism attached to the top flange. The vertical load is applied to the edge of the flange. The lateral load due to the eccentricity of the vertical load

with respect to the shear center of the girder is resisted by a couple at the top flange and in the web or bottom flange where the bottom of the bracket diagonal rests. This vertical load on the top flange is countered by the permanent deck form supports on the interior side of the exterior girder. The eccentric deck overhang loads include: deck forms, walkway, screed rail, a portion of the wet concrete in the overhang, and the ephemeral weight of the deck finishing machine. The lateral loads from the brackets create a non-uniform torsional moment in the girder that is resisted by the lateral bending in the flanges and the cross-frames. The torsional moments bend the exterior girder top flanges outward, causing lateral bending stresses in the girder flanges (note that in tub girders, these stresses are only significant in the exterior top flange). It should be noted, as discussed later, that the *AASHTO LRFD* Specifications permit cross frame spacings greater than the traditional 25-foot maximum limit, thus increasing the non-uniform torsional moment in the top flange. Also, the *AASHTO LRFD* Specifications do not permit nominal yielding in main load-carrying members during construction, except for localized yielding of the web in hybrid sections. The design of the girder for these effects is treated in more detail in DM Volume 2, Chapter 2, Section 2.2.3.4.2.

Figure 2.18 Cantilevered Forming Brackets

It is preferable to carry the forming brackets down the web to the bottom flange-to-web intersection. Since that may not be practical with very deep girders; it is possible to transmit the horizontal components of the reactions on the cantilever forming brackets directly onto the exterior girder web if the Engineer ensures that the web does not yield and that it does not deform such that the screed rail elevation is compromised. Excessive deformation of the web or top flange may lead to excessive deflection of the brackets resulting in a problematic deck finish.

Once the concrete deck is made composite, the deck and the cross-frames act in concert to provide the restoring forces that tend to make the girders deflect more equally under loads applied to the deck (i.e. the composite dead loads, DC_2 and DW, and the live loads). Again, this results in a larger portion of the loads applied over

the interior girders to be transferred to the exterior girders of steel multi-girder bridges. In deeper girders, full-depth cross frames become more effective and the horizontal shear force in the deck is better mobilized. For these reasons, more load is transferred from the interior of the deck to the exterior girders than was found in the 1940s by Newmark (*1*), who tested beams less than 30 inches deep with diaphragms less than half that depth. Article 4.6.2.2.2d of the *AASHTO LRFD* Specifications permits recognition of the effect of the exterior girders rigidly connected to the remainder of the bridge when live-load lateral distribution factors are employed to compute the live load effects in exterior girders.   This article states that for multi I-girder bridges with cross-frames or diaphragms, the distribution factor for the exterior girders is not to be taken less than that which would be obtained by assuming the cross-section deflects and rotates as a rigid cross-section. Equation C4.6.2.2.2d-1, which is reproduced below, satisfies this assumption and is analogous to the conventional approximation used for computing loads on pile groups.

$$R = \frac{N_L}{N_b} + \frac{X_{ext}\sum\limits^{N_L} e}{\sum\limits^{N_L} x^2}$$

Equation 2.1

AASHTO LRFD Equation C4.6.2.2.2d-1

where:
- R = reaction on exterior girder in terms of lanes
- N_L = number of loaded lanes under consideration
- *e* = eccentricity of a design truck or a design lane load from the center of gravity of the pattern of girders, ft
- x = horizontal distance from the center of gravity of the pattern of girders to each girder, ft (note: this is a signed quantity)
- X_{ext} = horizontal distance from the center of gravity of the pattern of girders to the exterior girder, ft
- N_b = number of girders in the cross-section

This special investigation is specified because the distribution factors given for bending moment in multi I-girder cross-sections in Tables 4.6.2.2.2b-1 and 4.6.2.2.2d-1 were determined without consideration of cross-frames or diaphragms; hence, while they are conservative for interior girders, they are generally unconservative for exterior girders in steel multi-girder bridges. Therefore, the distribution factor for the exterior girders determined from the special analysis (e.g. Equation C4.6.2.2.2d-1) will usually control.   The distribution factors for interior girders in multi-girder cross-sections given in Table 4.6.2.2.2b-1 provide a significant reduction in the distribution of live load to the interior girders over past methods. Therefore, overall, regardless of whether refined analysis methods or the live-load distribution factors currently given in the *AASHTO LRFD* Specifications are employed, the exterior girders will typically be assigned more live load moment and the interior girders will typically be assigned significantly less live load moment than

previously assumed using earlier AASHTO live-load distribution factors that did not recognize the behavior of deeper multi-girder bridges that are commonly used today.

In summary, for the reasons discussed above, experience shows that deck overhangs for cast-in-place concrete decks limited to between approximately 28 and 35 percent of the girder spacing tend to yield reasonable balance between the total interior and exterior girder moments.

2.4.3.1.1.3 Deflection Issues

2.4.3.1.1.3.1 Dead Load Distribution

Intermediate cross-frames or diaphragms act to equalize the girder deflections within a cross-section, and thus, nearly equalize the load in equal-stiffness noncomposite girders regardless of the amount of load applied to the individual girders. This equalization of deflections creates restoring forces in the cross-frames or diaphragms. *AASHTO LRFD* Article 4.6.2.2.1 recognizes this fact by stating that for multi-girder bridges satisfying certain conditions (e.g. width of the deck is constant, girders are parallel and have approximately the same stiffness, number of girders is not less than four, etc.), the permanent load of the wet concrete deck may be distributed equally to each of the girders in the cross-section. Although not currently stated, an additional condition of some importance in ensuring a reasonably equal distribution of these loads is that the bearing lines should not be significantly skewed (approximately 10 degrees from normal is a suggested limit) when the intermediate cross-frame/diaphragm lines are normal to the girders. (Note: as mentioned later on, where intermediate cross-frames/diaphragms are placed in collinear skewed lines parallel to the skewed supports, the assumption of equal distribution of dead loads may be extended to bridges having bearing lines skewed up to 20 degrees.). This assumption is particularly important when determining the noncomposite deflections used in determining girder cambers.
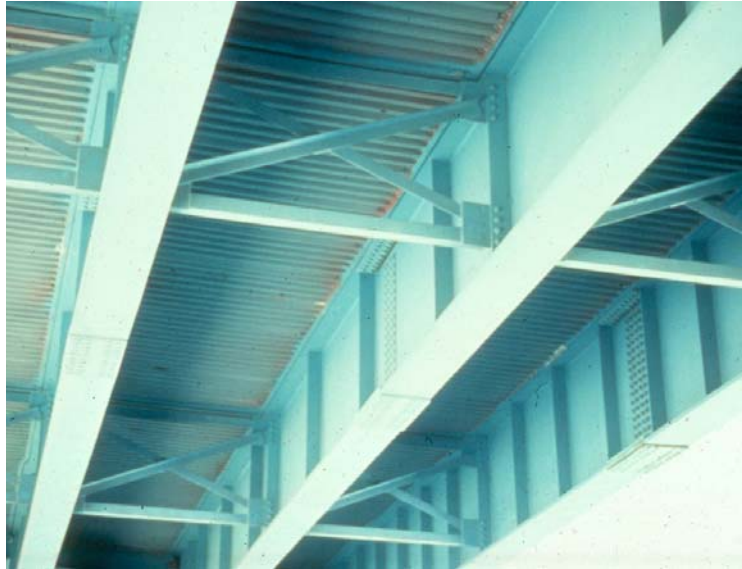
Figure 2.19 Cross Frames

AASHTO LRFD Article 4.6.2.2.1 also indicates that for bridges satisfying the stated conditions, permanent loads applied to the deck after the deck is made composite may also be distributed equally to each girder. For the wearing surface load, DW, this is a reasonable assumption and has been the customary practice. However, Engineers have often applied this assumption to the concrete barrier load as well. This provision dates back to the 1940s when concrete deck overhangs were much smaller and the provision was applied to much lighter curbs and railings, not barriers. When refined methods of analysis are employed, these loads may be applied at their true location, which usually results in the computed portion of the load resisted by the exterior girders to be significantly larger than an equal distribution assumption would indicate. To better simulate the actual distribution of these loads when line-girder analyses are employed, consideration should be given to performing a reasonable approximation of this effect. Assigning a percentage of the barrier loads to the exterior girders and to the adjacent interior girder is a better assumption based on refined analyses of several cases. At least one State DOT requires that the barrier load be equally distributed to an exterior girder and the adjacent interior girder. Other State DOTs assign 60 percent of the barrier weight to the exterior girder and 40 percent to the adjacent interior girder. The Engineer may choose to use the live load distribution lever rule to determine the effect of the dead load on the exterior of the deck if the overhang is particularly large. In these cases, the portion of dead load applied to the exterior girder may be larger than the load itself. The interior girders would then sense an uplift condition in those cases. Regardless of the analysis assumption, recognizing the concentrated effect of heavy edge loads is suggested.

2.4.3.1.1.3.2 Live Load Deflection

The live load deflection criteria in the LRFD specification are optional. No rational theoretical argument for a particular live load deflection limit has been presented and some believe that such a limit is unnecessary. It is probably best viewed as a

serviceability limit.   Traditionally, the averaging approach has been used most frequently to determine the appropriate live load assigned to a girder in a straight bridge to compute live load deflection. Unlike the Standard Specifications, which are ambiguous in this regard, LRFD specifies that a multiple presence factor shall be applied. Thus, the more traffic lanes on a bridge, the smaller the live load assigned to a girder. The fewer girders in the cross-section, the more live load assigned when computing deflection. However, if the wheel load distribution factor for moment or a refined analysis is used to compute live load deflections, the number of girders in the cross section has a much less significant effect on deflection and fewer girders may in fact be needed than when the averaging approach is used.

The LRFD live load deflection provisions also differ from the Standard Specifications in other ways. LRFD specifies that live load deflection be computed with a lighter live load than that specified for the strength limit states (refer to AASHTO LRFD Article 3.6.1.3.2). The LRFD Specifications permit the concrete to be considered fully effective in regions of negative flexure when computing live load deflections. They also permit continuous cast-in-place parapets to be considered in the computation of the stiffness resisting the deflection.

2.4.3.1.1.4 Varying Roadway Width

It is not uncommon for the roadway width to vary on a structure. In some cases, the girders may remain parallel with the width of the deck varying. In these cases, the dead and live load resisted by each girder varies along the structure length. In other cases, it is necessary to splay the girders in plan in order to accommodate the roadway, as shown in Figure 2.20. Keeping as many girders as parallel as possible is advisable to keep cross-frames and stay-in-place formwork similar, thereby keeping their cost minimal. Varying all of the cross-frames is an expensive and usually unnecessary option.
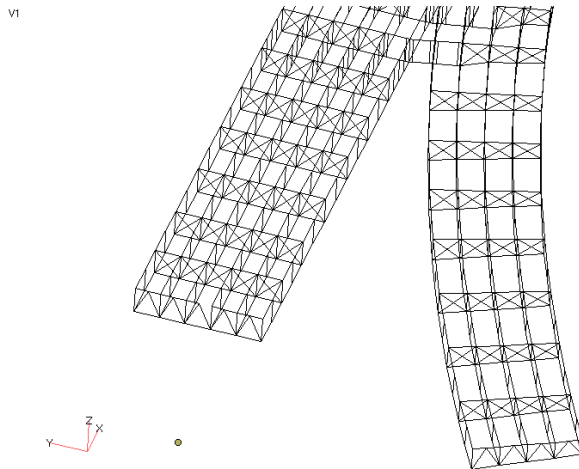
Figure 2.20 Splayed-Girder Framing Plan

Where moderate deviations from parallel beams or a constant deck width exist, the Engineer may find that the live-load lateral distribution factors are appropriate. For

more complex framing plans, the use of refined analysis methods is recommended to determine the distribution of the loads. In either case, it is advisable to check the deck design to ensure that its design is both adequate and economical. Varying the deck overhang is one of the least desirable options since it complicates forming, reinforcement detailing, and design. A variable overhang width also causes the design of the exterior girder to be particularly onerous.

In cases where distribution factors are employed, Article 4.6.2.2.1 of the *AASHTO LRFD* Specifications permits the distribution factor to either be varied at selected locations along the span, or else a single value of the distribution factor to be used in conjunction with a suitable value for the girder spacing (e.g. when the girder spacing varies, the average value of the girder spacing within the splay might be used).

Wheel load distribution factors for steel box girders are given in *AASHTO LRFD* Article 4.6.2.2.2b, which states that N_L be used in lieu of the girder spacing when determining a single value of the distribution factor for the case of varying roadway width, where N_L is the number of design lanes at the section under consideration determined as specified in *AASHTO LRFD* Article 3.6.1.1.1. Furthermore, it should be noted that for box girders, special geometric restrictions on the use of live-load distribution factors are specified in *AASHTO LRFD* Article 6.11.2.3 and are summarized in Figure 2.21. Included are some basic cross-sectional limitations and a requirement that the bearing lines not be skewed (refer to DM Volume 2, Chapter 2, Section 2.2.4.1.2). Also included is a requirement that where nonparallel box sections are used, the distance center-to-center of adjacent flanges at supports is not to exceed 135 percent nor be less than 65 percent of the distance center-to-center of the flanges of each adjacent box (refer to Figure 2.21). The reason for these limitations is the applicability of the wheel load distribution factors. For cases not satisfying these limitations, refined analysis methods are to be employed. As for I-girders, it has been found that widely spaced box girders are the most economical, and these configurations are often beyond the limitations of the empirical wheel load distribution factors.

c/a ≤ min. (0.6, 6ft)
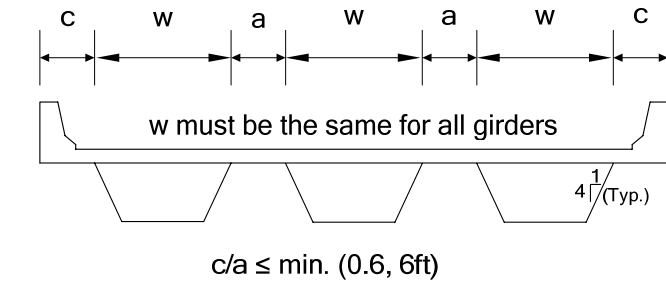
(a) Typical Bridge Cross Section
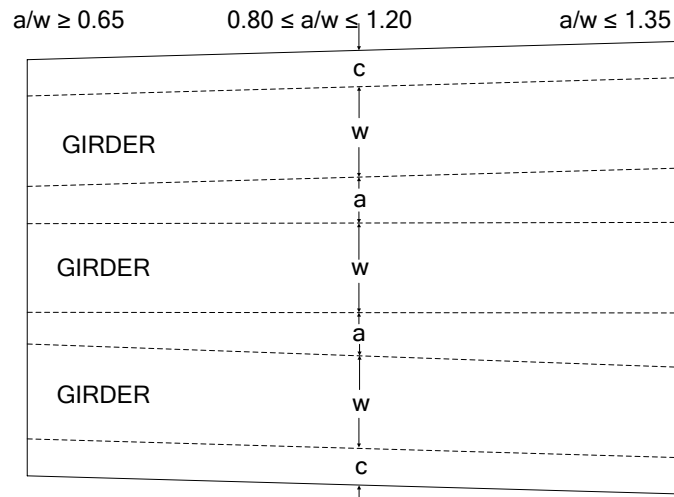
(b) Example of Possible Variation in Box Girder Bridge Width

Figure 2.21 Box Girder Geometric Restrictions on use of Live Load Distribution Factor

2.4.3.1.1.4.1 Discontinuous Girders

At gore areas and other areas where the roadway width varies greatly, it is economical to discontinue one or more girders. In such cases, the discontinuous girders are usually framed into a bulkhead between girders (refer to Figure 2.22). It is not advisable to discontinue an exterior girder because it complicates the overhang, creates an awkward connection detail, and certainly is not aesthetic. Discontinuing a girder adjacent to an exterior girder is also not desirable since it is likely to load additionally the already critical exterior girder. The Specifications have no provision to consider discontinuous girders other than by refined analysis methods. In these cases, as with splayed girders, it is advisable to keep girder spacing constant over as much of the bridge as practical in order to minimize the number of different cross-frames that must be detailed and fabricated.
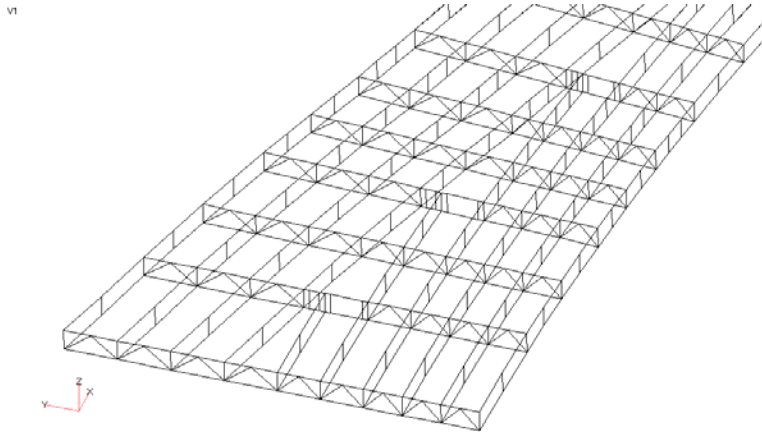
Figure 2.22 Discontinuous Girders

To moderate the effect of the discontinued girder(s) on bulkheads and on the deck, it is desirable to locate the discontinuity near the location(s) of lowest moment in the span; controlling the stiffness of the girders on either side of the discontinuity can further mitigate differential deflections. By attaching the bulkhead to the deck with shear studs, the question of whether or not it is a fracture-critical member should be silenced for in-service inspection purposes, but the bulkhead should be fabricated to more stringent fracture-critical member requirements.

2.4.3.1.1.5 Girder-Substringer Systems

For continuous-span bridges having spans ranging anywhere above 200 to 300 feet, a cost-effective alternative in some cases has been found to be a combined girder-substringer framing system, as illustrated in
Figure 2.23. This system consists of widely spaced composite main girders braced laterally by heavy K-shaped cross-frames. Main girder spacings from 16 feet to 28 feet have been used. Halfway in-between the main girders, rolled-beam substringers are used to span continuously between the cross-frames and provide support for the deck and live load. The cross-frames supporting the substringers are considered primary load-carrying members in this type of system.

1.   N. M. Newmark. 1948. "Design of I-Beam Bridges", Proceedings of the ASCE, American Society of Civil Engineers, New York, NY, 1948.
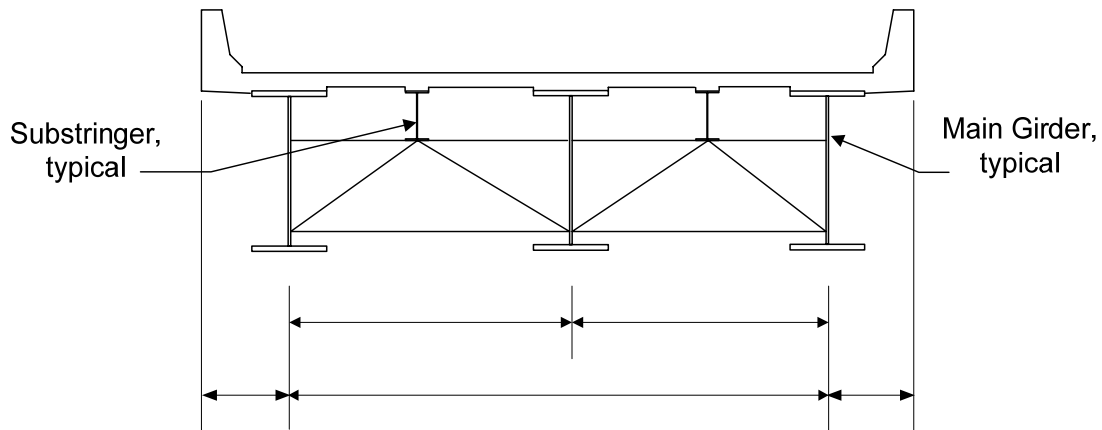
Figure 2.23 Girder-Substringer Framing Plan

2.4.3.1.2 Field Section Size

Field sections are girder sections fabricated and shipped to the bridge site, usually without bolted splices. The number of field sections and the location of splices have a significant effect on the efficiency of the design of steel girders. Fewer field splices obviously reduces the cost for splices, but total steel cost is affected by additional factors regarding the location and number of bolted splices. The choice of field splice locations is in many ways job specific. The weight and length of sections should be determined after consultation with fabricators who are expected to be bidding the work. For example, the crane capacity in the shop legally limits the weight the fabricator can lift with each crane. Sometimes a section can be made slightly lighter to accommodate that capacity relieving the fabricator of calling for an additional crane every time the section is to be moved, interrupting other production. Sections too long to fit in normal lay-down areas also interrupt normal operations. Flanges too wide to fit in blasting machines or girders too deep to clear overhead cranes are examples of the interrelated factors that affect the cost of fabricating girders. As discussed further below, material availability may also influence field-section size.

Figure 2.24 Bridge Fabricating Shop

Material availability from the mills and its cost is significant in some instances, but it is often difficult for the design Engineer to ascertain availability and cost.   For example, at this time (2006) plates are considered standard between 0.375 and 2 inches thick. Above two inches in thickness, there is an extra charged. There may be only one producer that produces bridge quality plates above three inches thick, introducing a substantial extra even though plates up to 4 inches thick are permitted by specification. A deep web plate may be available from one mill but its cost might lead the fabricator to choose to build the girder web up by splicing plates together. Another example is the issue of camber. Camber is typically cut into the web plate. If camber is large, the fabricator may choose to partially shape the web camber by sections of web plate rather than ordering a deep plate to burn out the camber with a large amount of waste.   Camber issues are beyond the Engineer to consider at design.

Shipping also affects the fabricator's cost. If the site is far from the fabrication shop and an escort(s) is required due to length and/or weight, it may be economical to use smaller sections to reduce or eliminate the number of escorts. To complicate things further, each state has its own regulations regarding shipping. Interstate shipments simply multiply the complexity. The manner that the girders are to be erected also affects the choice of field section size. Girders that are too long to be erected with a single crane may lead to erection issues that shorter sections might avoid.

Traditionally, bolted splices have been located in regions of lower moment. However, since splices are designed to resist shear as well as moment, a single splice in a simple-span girder might be located in the center of the span where shear is low rather than providing two field splices at points of lower moment. At the center of the span, shear is minimal and the bolted splice-design provisions may permit a reduction in web bolts. The flexural resistance of a composite simple-span straight girder at the strength limit state can be at or near the full plastic moment M_p. However, the flexural resistance of the girder at a bolted splice is limited to the

moment at first yield according to the specifications, which also has to be given some consideration when locating the splice in this case.

2.4.3.1.2.1 Transportation

The fabricator is responsible to deliver the steel to the bridge site, and therefore, is familiar with the issues related to transportation of field sections. Large field sections require determination of a specific route to determine the cost of transportation. The distance between the fabrication plant and bridge site is only one cost factor affecting transportation cost. But, there are factors that may be addressable by the Engineer that can materially affect transportation costs. The Engineer is encouraged to discuss any large steel bridge design projects in their early stages with the fabricators who are likely to bid on the project.   These fabricators will provide parameter information particular to their preferences.   An astutely designed steel girder bridge is one that more than one fabricator is likely to bid competitively.

Girders are preferably shipped in the vertical position, although they sometimes are shipped tilted or even horizontal. Shipping is perhaps the most nebulous of the issues involving steel girder bridges. The ability to ship a girder is dependent on the particular route, which means that the fabricator must inspect that route in order to give definitive information to the Engineer regarding practical girder size limits.

Figure 2.25 Transporting Bridge Girders by Truck

Examples of special transportation provisions include additional blocking and tie-downs, special multi-axle trailers, escort vehicles, restricted hours for highway use, and special types of railroad cars, etc. Although such special provisions result in additional costs along with added shop handling costs, these costs may be offset by the need to erect fewer sections with fewer field splices, which can result in significant savings.

2.4.3.1.2.1.1 Highway Transportation

The American highway system has matured to the point that it is the means of choice to ship the majority of steel-bridge components from the fabricator to the bridge site. Essentially all fabricators are capable of shipping by truck. Some fabricators have their own fleet of trucks so they keep trucking costs in-house. Having a personal fleet also permits control over delivery dates, even time of delivery. Since highways are generally publicly owned and used by the public, they are subject to strict regulation to ensure safety and equal use. Load weight, length, and width are controlled, usually by the state, and regulations differ between the states. There are discrete limits on size. Certain sizes may be shipped without an escort, others may require two escorts and so forth. There may also be limits on the time of day certain loads may be shipped and the number of shipments in a day.

For example, it would be nonsensical to design a field section that requires extra shop-crane capacity and an extra escort to ship 250 miles to the bridge site when shortening it by three feet and lightening it by five tons would eliminate both of these extra costs. Therefore, to know these limits is particularly useful.

For truck shipment, lengths up to 175 feet are possible depending on the location and most states will allow up to 80-foot lengths without restrictions. However, when lengths exceed about 140 feet, fabricators should be consulted. Loads up to approximately 40 tons in weight are typically accomplished without permits. Loads up to approximately 80 to 100 tons are possible, but require close cooperation with the state and route checks. When loads are in the 80 to 100 ton range, again fabricators should be consulted. The normal unrestricted limitation on load width is 8 feet. Above 12 feet in width, travel lane width restrictions become a factor and fabricators should once again be consulted. With the proper permits, escorts and limit on the day or time of travel, load widths up to 16 feet (or even larger depending on the circumstances) may be possible. Load height is generally restricted by clearances, or the overall stability of the piece during shipment. Generally, a guideline is to limit the height to approximately 10 feet. Above 10 feet, consult with fabricators as specialized shipping equipment may potentially be used, or I-girder pieces may possibly be shipped lying on their side. (Note: the preceding shipping recommendations in this paragraph are from the National Steel Bridge Alliance (NSBA) based on conversations with several fabricators).

Figure 2.26 Bridge Girder Transported on Side

2.4.3.1.2.1.2 Rail Transportation

The fabricator might choose rail transportation for particularly deep girders, and girders that are to be shipped a great distance. A typical railroad flat car is 53′-6″ long by 10′-8″ wide with an average capacity of 70 tons (*2*). Rail access at the bridge site is often not available, and pieces must usually be off-loaded and trucked to the bridge site. An interesting aspect of rail transportation is that it can change the competitive situation for a bridge. If the bridge cannot be shipped by truck and must be shipped by rail for whatever reason, the interest is opened for fabricators from greater distances since loading and unloading of the railcars, and demurrage are the largest factors in the cost of rail shipping, while mileage is a less significant cost than highway mileage.

Longer loads may be shipped in standard gondola cars, or supported on bolsters on two flat cars at opposite ends of the load and connected by an idler car. Since the bolsters can be up to 1′-6″ above the floor of the car, the net height available for the load is reduced by up to that amount. The bolsters must be able to accommodate relative movement. Truck/train "piggyback" cars, which vary in length up to 85 feet and can handle loads over 100 feet in length when idler cars are used to accommodate the overhang beyond the end of the car, have also been used. For restricted rail movements, load heights up to 16 feet and weights up to 100 tons may be possible depending on the available routing. Widths up to approximately 12 or 13 feet may also be possible depending on the route and the configuration of the load (*2*).

Again, it should be emphasized that the requirements for a particular project related to rail movement should be investigated with the likely fabricators on an individual project basis.

2.4.3.1.2.1.3 Waterway Transportation

There are no longer many steel bridge fabricators located on navigable water in the United States. For the appropriate structure, water transportation is very practical. A project practical for water shipment usually involves many field sections, and of course, the fabricator and the bridge site must be on or near the water. Water shipment is particularly beneficial when site conditions permit erection directly from the barge. The potential for transporting sub-assemblies or assembling entire bridge spans, floating them into position and erecting them onto their bearings directly from the barge may offer significant economies. Water shipment is most often used for crossings over navigable water.

2.4.3.1.2.2 Handling and Erection

Some fabricators also erect bridges and are therefore familiar with handling and erection of steel girders. Other fabricators do not erect steel. Horizontally curved girders present particular erection considerations that are not addressed herein. Some fabricators prefer less stringent tolerances, but the erector generally prefers tighter tolerances to ensure proper fit-up. Where practical, the erector prefers to erect steel and leave the site. However, there are numerous instances where staged erection is required.

Over the past forty years, steel-girder designs have led to relatively more slender girders for economic reasons. In composite construction, the structure that carries live load is composed in part of the concrete deck as well as the steel girders. Thus, the steel girders alone must be only strong enough to carry the noncomposite load. Therefore, there are at least two critical load cases in the design of such girders. This has led particularly to smaller top flanges in positive bending regions where the composite section assists in resisting the live load. The smaller top flange permits more of the web to be in compression in positive bending. The introduction of higher strength steel grades for use in girders also tends to increase their slenderness. Many of the old "rules" were based on steel with a minimum specified yield stress of 33 ksi. Today, yield stresses are sometimes twice that amount. Thus, flanges half the traditional size on girders designed for the same web depth are found economical. A third issue is the reduced factor of safety for dead load within the Load Factor Design and LRFD Specifications compared to traditional working stress design. Traditional working stress design specified the limiting dead load stress based on a safety factor of 1.82 against first yield or elastic buckling, whereas with the newer specifications, the factor of safety on dead load stress ranges from 1.25 to 1.5. The result is that a much lighter girder is permitted for the noncomposite condition than was required 50 years ago.

To take advantage of these improvements in the economics of steel-girder bridges, additional consideration must be made for handling, deflection and erection of the girders before the deck hardens. For bridges of unusual complexity, the LRFD Specifications require that the Engineer consider a means of constructing the bridge, while still leaving the responsibility for the actual construction of the bridge up to the Contractor. Since this provision is relatively new, the responsibilities of the Engineer are not well delineated and generally are left to the Owner to specify. The

discussion here does not define the legal responsibilities of the Engineer or the Contractor. Instead, it will narrate some of the issues that may be addressed in this regard.

There are three basic requirements for the steel frame to be erected safely and properly. First, the steel must be stable in all stages of erection. Second, the steel must be erected in such a condition that stresses match those computed in design. This is generally the case if the deflected steel structure under self-weight matches that assumed in determining self-weight cambers. Third, the steel must be able to resist the specified wind loads within reasonable levels of lateral deflection during erection and as erected.

Temporary support of the steel during erection historically has been the responsibility of the Erector. However, there have been cases where temporary supports were not called for on the design drawings and the Contractor claimed that they should have been called for. The design Engineer cannot take responsibility for the erection, which he/she will not supervise. However, the Owner may request that the design Engineer provide some indication on the Plans of the potential need for temporary supports, generally without designing them.

Figure 2.27 Bridge Girder Erection

The Erector will design temporary supports to support the girders at all stages so that additional steel can be erected and bolted up. The elevation of the steel during shop fit-up is at the cambered no-load elevation. The no-load elevation refers to the elevation at which the girders are erected under a theoretically zero-stress condition; that is, neglecting any stress due to the steel dead load acting between points of temporary support. If the steel is detailed for the no-load elevation, and the steel is approximately supported during field erection in that position, it will be possible to fit up the additional steel with little problem. Although the no-load condition cannot be

obtained precisely, it should be close enough to permit fit-up with drift pins and without reaming of bolt holes.

Transient thermal loads can change the shape of the steel and be a nuisance in erecting certain structures. For example, some box girders may be so sensitive to temperature that erection at night is desirable.

AASHTO LRFD Article 4.6.2.7.3 requires the Engineer to consider the need for temporary wind bracing during construction for I- and box girder bridges. Typically, a noncomposite I-girder bridge system without a concrete deck or lateral bracing between girders resists lateral wind load only based on the lateral stiffness and strength of the sum of the erected girder flanges. On larger spans, this situation can lead to excessive stresses and lateral deflections that are of concern. As discussed in more detail later, some form of lateral bracing between at least one pair of girders can often be found to mitigate excessive stresses and deflection due to wind before the deck hardens. The lateral bracing allows the girder flanges to act as truss chords.

Since the bracing is not effective until it is in-place, it behooves the Erector to erect the pair of laterally braced girders first. The Engineer needs to consider the erection sequence when locating the lateral bracing. The design Engineer usually does not know how the Erector will erect the bridge and should not require the use of a specific erection sequence. However, if in the judgement of the Engineer, lateral bracing is required for wind loads that may be encountered during the erection, the bracing should be called out on the design plans to avoid an "extra". As discussed in more detail later, top-flange bracing usually has less significant effect on the design and is more lightly loaded than is bottom-flange bracing. If, for example, a single line of bracing is employed, its location implies that the two girders forming that particular bay would be erected first. The plans should note that assumption. If the Erector chooses another option such as elimination of the bracing or a different erection sequence for the girders, then the Erector is responsible for a re-engineered scheme that is acceptable to the Owner's Engineer.

Lateral bracing may not be required over the entire length of the bridge. Calculations may indicate that partial length bracing is adequate. The bracing may be located in the top or bottom plane of the girders. Additional discussion on lateral bracing for wind is given below under the heading of Lateral Bracing.

Each field section as defined between field splices must be able to be handled without buckling and without yielding. Field splices should be located close enough to each other that the individual pieces will be stable for handling both in the shop and in the field and for erection without requiring any special stiffening trusses or falsework. The following guideline contained in Article C6.10.3.4 of the *AASHTO LRFD* Specifications may be used to help indicate relatively stable straight I-girder field sections:

$$b_{fc} \geq \frac{L}{85}$$
<div align="right">Equation 2.2</div>

AASHTO LRFD Equation C6.10.3.4-1

where:

b_{fc} = minimum width of the compression flange within the girder shipping piece (in.)

L   = length of the girder shipping piece (in.)

For tub sections, *AASHTO LRFD* Article C6.7.5.3 discusses cases where a full-length top lateral bracing system may not necessarily be employed. As discussed in *AASHTO LRFD* Article C6.11.3.2, in cases where a full-length top lateral bracing system is not employed within a tub section, L in the preceding equation should be taken as the larger of the distances along the field piece between panels of lateral bracing or between a panel of lateral bracing and the end of the piece. For cases where a full-length top lateral bracing system is employed, Equation 2.2 need not be considered for top flanges of tub sections.

Special site conditions may affect the options available for handling, erection and transportation of large field sections. Examples include sites located in difficult terrain, ecologically sensitive areas or areas where there might be industrial facilities or active rail lines or highways underneath the bridge. The Engineer should become familiar with the site and any special conditions that might affect the size of the field sections.

2.   NSBA. 1981. "Fabrication – Its Relation to Design, Shop Practices, Delivery and Costs", *Highway Structures Design Handbook*, available from the National Steel Bridge Alliance, Chicago, IL.

2.4.3.1.3 Constant vs. Variable Depth Girders

The decision to use a variable depth girder in a steel multi-girder bridge is usually driven by consideration of clearance requirements, economics, poor span arrangement, and/or aesthetics. Girder depth is typically varied utilizing either a straight-line taper or a parabolic haunch along the bottom flange. Both I-girder and box-girder members can be designed with a variable depth. Usually box girders are given parabolic haunches rather than tapers. If the webs of a box girder are inclined, the inclination is usually held constant with the bottom flange width reduced with an increase in the girder depth.

Generally, the deeper portion of the girder is stiffer than the shallower portion. Thus, moments are increased in the deeper section with a concomitant reduction in the shallower sections compared to a constant-depth girder. This phenomenon may provide some economy by reducing the flange demand in the longer positive moment regions. It also tends to reduce the vertical deflections in those regions. However, the typical haunched girder does not provide much of this benefit since the deeper portion is so short. The phenomenon is much more pronounced if a constant depth section is employed over the piers, with the section tapering to a shallower one on each side. The transition might occur within the pier field section or an adjacent one; however, changes in the slope should not be made right at a field

splice in either case. One might question the aesthetics of such girders, but usually not their efficiency in longer spans.

Figure 2.28 Variable Depth Girders

Application of higher strength (high-performance) steel permits smaller flanges for a given depth girder in a given application. However, the smaller flanges reduce the girder stiffness leading to larger dead and live load deflections for a given depth. Thus, if a 50-ksi design was controlled by deflection, the girder must be deeper if 70-ksi steel is employed. Fortunately, the LRFD live load specified for computing deflection (*AASHTO LRFD* Article 3.6.1.3.2) is smaller than HS25 loading (which is used by many State DOTs to compute live load deflection for designs by the AASHTO Standard Specifications), and parapet stiffness is now permitted to be included in computing live load deflections in the *AASHTO LRFD* Specifications (Article 2.5.2.6.2), as mentioned previously. The result is that many designs meet LRFD deflection requirements that might not meet the deflection limit when deflection is checked for HS25 loading. Constant web depth members utilizing Grade HPS 70W steel flanges (with Grade 50W steel typically utilized in the web) are sometimes economical for spans up to and even exceeding 500 feet in length when applied in the proper depth. Thus, a parametric study of these applications is usually justified.

In cases where there is an underclearance or deflection problem, it may be beneficial to haunch the girders at interior piers instead of using parallel flanges. Also, as discussed previously, if the proper span balance cannot be maintained and a constant depth girder is utilized, the depth of the girder in each span will not necessarily be at the most efficient or optimum depth. In such cases, it may be economical to go with a variable web depth member in certain spans to transition between optimum depths. A linear taper often proves to be more cost-effective than a parabolic haunch for this situation.

A variable web depth steel member is typically achieved by inclining the bottom flange utilizing either a linear taper, a parabolic haunch, or a so-called "fish belly" haunch, as demonstrated in Figure 2.29. The desired girder depth is cut into the web plate and then the bottom flange plate is pulled into place and welded to the web plate. In a tapered or haunched girder, a transition is typically made from the sloping part of the taper or haunch to a horizontal bottom flange near the bearing to accommodate the bearing sole plate. The transition is made by using either a welded joint or by bending the flange plate. Bending of the plate depends on the required radius and the length of plate available from the mill. Proportioning of the flange plate at the transition location should allow for the possibility that the fabricator may bend the plate. Bending of the flange plate into a "fish belly" type of transition can help to smooth out the transition, in lieu of a more abrupt transition which can result in an extremely sharp increase in the web stress as the vertical component of the flange force is transferred back into the web. The distance from the edge of the sole plate to the transition should be at least 12 inches in order to clear any distortion that may result from bending or welding of the flange plate and to accommodate any possible future jacking needs for bearing maintenance.
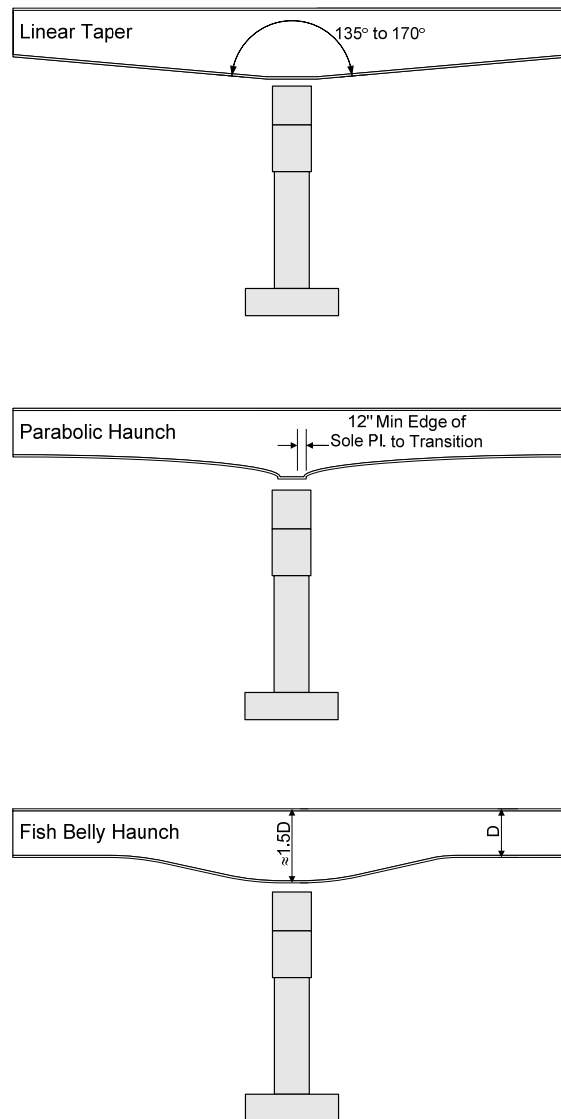
Figure 2.29 Variable Web Depth Members

Variable web depth members are important aesthetically because they visually demonstrate the flow of the forces in the bridge and make the bridge appear thinner. To ensure that the tapers or haunches are long enough in proportion to the span, they preferably should be brought out to the point of dead-load inflection in the span (i.e. where a field splice would typically be located in a continuous span). Parabolic haunches at interior piers typically offer a smoother transition to the rest of the girder and are generally more visually pleasing. Haunches should typically not be deeper than 1.5 times the midspan depth of the girder to prevent the haunch from appearing too heavy in proportion to the midspan section. Conversely, a haunch that is too shallow does not save enough material to justify the added fabrication cost and is not aesthetically pleasing. The total angle at the point of haunch (i.e. between the haunches on either side of the interior pier) preferably should be between approximately 135 and 160 degrees to prevent the appearance of too sharp a haunch at the bearing point.

Fabrication costs for variable web depth members are higher than for constant web depth members due to the additional cutting and fitting operations discussed previously. Straight tapers are less costly than parabolic haunches because it is easier to cut the webs, locate and fit web stiffeners, weld flange transitions and fit-up the member at the web-to-flange joint. For bridges with spans exceeding approximately 400 feet, the haunched section may be so deep as to require a longitudinal field splice in the section, which increases fabrication costs significantly. A horizontal field splice may be required because of the maximum plate width availability from the mill and/or because the depth of the haunched section may preclude shipping of the section without a longitudinal field splice (typically when the depth exceeds about 14 feet). Plates are generally available from many plate mills in maximum widths up to 150 inches. Generally, the maximum usable plate width from such a plate is about 144 inches. Larger plate widths may be available from select mills. Again, the Engineer is encouraged to contact the fabricator regarding maximum practical plate widths.   Longitudinal web splices may either be welded or field bolted. A field bolted splice can either be fabricated using a sub-flange on the bottom of the top section and the top of the bottom section of the web plates (which are then field bolted together), or using side plates similar to a conventional bolted web splice. Note that it may be easier to ship two I-sections than deep tee sections, which may need to be temporarily braced during shipment. Thus, when designing exceptionally deep, variable web-depth girders, consult with fabricators in the area regarding feasibility of shipping, field section size/depth and jobsite access.

In variable web depth tub girders with inclined webs, the inclination of the webs preferably should remain constant to simplify the analysis and fabrication. Assuming a constant distance between the webs at the top of the tub, which is also preferred, along with a varying web depth, the width of the bottom flange must also vary along the length and the web heights at a given cross-section must be kept equal in order to maintain constant web slopes. When a vertical curve must also be built into the web because of camber or roadway profile and camber, the establishment of the developed shape of the plate becomes more difficult; that is, the shape of the flat plate pattern from which the web must be cut. Experienced steel detailers and fabricators generally have software available though to establish the necessary pattern. It should be noted that a curved inclined web for a tub section can be cut from a flat plate as part of a cone shape. If, however, the slope varies, the webs are no longer developable and must be heated to conform to the desired shape.

Erection of variable web depth members is affected to some degree by their more complex geometry. However, these complications are generally considered minimal by most erectors. Therefore, erection considerations typically need not enter into the decision process as to whether or not variable web or constant web depth members should be used. An exception might be when the bridge is to be erected by incremental launching, in which case the use of constant web depth members is recommended.

Regarding the design of variable web depth members, the bottom flange carries a portion of the vertical shear in the region of the sloping web. Thus, the force in the bottom flange in this region is increased over the force resulting from the normal

flexural stress by the amount of the vertical shear component. The major-axis bending moment in this region is developed from the smaller horizontal component of the resultant bottom flange force. In negative-moment regions, the web shear is reduced by the vertical component of this force. Also, as mentioned previously, at the point where the bottom flange is made horizontal in the vicinity of the bearings, the shear component in the inclined flange is transferred back into the web. Extra web stiffening in this region may be necessary in some cases to prevent buckling caused by the concentration of force. The design of a variable web depth member to account for these effects is discussed in more detail in DM Volume 2, Chapter 2, Section 2.2.3.3.3.

Figure 2.30 Haunched Girder Web Stiffeners

2.4.3.1.4 I-Girders

2.4.3.1.4.1 Introduction

This section of the manual will discuss additional issues that are specific to the preliminary design of steel I-girder bridges; namely, the selection of the type of girder (rolled shape or welded girder), the layout of the framing plan including the cross-frame or diaphragm spacings and configurations and the potential need for lateral bracing. Proportioning of the flange and web plates for welded I-girders, including the determination of initial sizes, is discussed in DM Volume 2, Chapter 2, Section 2.2.3. Further information regarding the design of the bracing members and their connections may be found in DM Volume 2, Chapter 2, Sections 2.3 and 2.4.

2.4.3.1.4.2 Fundamental Behavior of Stringer Bridges

Steel stringer bridges appear to be relatively benign structures. Given the number of failures and early deterioration of this bridge type observed each year, this appearance is often deceiving. These bridges certainly obey the laws of structural

analysis, including statics and strength of materials. However, many design provisions are based on rules that have been developed over the past decades from experience that may not be applicable to modern efficient designs. Anticipating the correct load paths and hence participation of the various components can be somewhat demanding on the Engineer.

The LRFD provisions have advanced the art of bridge design by the inclusion of probabilistic design and many improved strength equations. Also, but less often addressed, is the introduction of revised assumptions regarding analysis, or translation of loads to load effects. It is important to understand the fundamental behavior of steel stringer bridges and the basis of the various load-to-load effect provisions and their derivation in the LRFD Specifications. In this section, the fundamental behavior of steel stringer bridges is discussed, followed by an examination of some of the load-to-load effect assumptions.

The components of typical steel stringer bridges include the stringers, cross-frames/diaphragms, concrete deck, bearings and substructure. Each of these components is interconnected to other components with welds, bolts, shear connectors, various types of bonds, and friction. Structural analysis is the art of determining the distribution of internal energy, or the load paths, resulting from the application of loads. The load paths extend from the loads to the ground. Thus, they generally include several elements and their connections. There are numerous and redundant load paths in stringer bridges; of course the amount of load that passes along any given path is a function of its stiffness relative to all available paths.

There are many simplifications provided in the LRFD Specifications to assist in determining the load to be assigned to a path. Some paths are only tacitly recognized because they are relatively minor and are typically not designed for computed loads. In fact, the term "distortion-induced fatigue" implies a load path that is not readily apparent and may not have been included in the analysis. It is the responsibility of the Engineer to ensure that the simplifications are appropriate for a particular design situation. When they are deemed inappropriate, proper remedial measures must be taken to ensure that the analysis is appropriate. These simplifications are discussed in the Specification Commentary; however, some may be in need of further elucidation.

2.4.3.1.4.2.1 Elements of Stringer Bridges

Stringers span between bearings; they transfer load to the bearings. The transfer is accomplished by a combination of bending, shear and thrust. Cross-frames transfer load between stringers by a combination of axial force, and, to a lesser degree, by bending. Bearings transfer load from the stringers to the substructure. Bearings frequently resist horizontal as well as vertical loads. Of course, the substructure resists the forces from the bearings.

Behavior of the concrete deck is complex. Live load is usually applied directly to the deck, which transfers the majority of the load into the stringers. The deck typically acts compositely with the stringers to create a much stiffer and stronger member

than if the steel stringer acts alone. The deck also acts compositely with the cross-frames to aid in the transfer of load between stringers. Further, the horizontal shear stiffness of the deck, which is the stiffest element in a stringer bridge, transfers the loads between stingers.

Lateral bracing between stringers may be located in the plane of the top flanges or the plane of the bottom flanges. Historically, the specifications have addressed bottom-flange bracing as resisting lateral wind loads. In earlier days, bridges were often built with two main girders and a floor system composed of floor beams and minor stringers. The floor beams were usually much shallower than the girders, leaving the lower portion of the main girders without lateral support. The bottom lateral bracing formed a truss with the bottom flanges and was assumed to help resist the lateral wind force in these cases.

The lateral bracing is not able to discern between wind and other loads so it acts to resist all loads. Once the deck is hardened, bottom-flange lateral bracing acts to form a pseudo box composed of the bracing, the two I girders and the deck between the girders.

In later years, it became evident that full-depth cross frames that are stiffer than any lateral bracing transferred the majority of the lateral wind load up to the deck. Therefore, the lateral bracing became superfluous in the final condition and, as discussed later in this chapter, the AASHTO Specifications allowed it to be removed in most cases. However, girders alone must resist lateral wind until the deck hardens when lateral bracing is absent. The result is that the girders are often not stiff enough nor strong enough to resist wind prior to the deck hardening without either permanent or temporary lateral bracing. There are three alternatives: temporary bracing supplied by the contractor; permanent top flange lateral bracing; or permanent bottom-flange lateral bracing. It may not be necessary for the bracing to extend over the entire bridge length; that issue is addressed elsewhere in this chapter.

Top-flange lateral bracing is generally not significant in redistribution of loads although it acts with the top flanges of the girders to which it is connected. However, it may be significant on longer spans. It participates with the top-flange in resisting moment. It may also introduce lateral bending into the top flange.

Bottom-flange lateral bracing may cause redistribution of the loads applied to the composite structure. In doing this, the bracing and its connections experience significant force. Inclusion of the lateral bracing members in the analysis is recommended to properly determine girder moments, shears, and deflections, as well as forces in the lateral bracing and its connections.

2.4.3.1.4.2.2 Loads and Load Paths

Bridge loads are of the utmost importance since the sole purpose of a bridge is to permit load to traverse a span. Hence, a bridge can be thought of as a pure structure that only has to support load and perhaps be aesthetically pleasing at the same time. Bridge gravity loads can be separated into dead load and live load.

Dead load can be further divided into loads applied to the non-composite structure and loads applied after the structure becomes composite. Live load is usually applied to the completed structure; however, some live loads, such as the deck-finishing machine, are applied to the unfinished bridge. Environmental loads including thermal changes, wind, ice, earthquake, and stream flow may be applied to the non-composite or composite bridge. The Specification provides for a number of load combinations with different load factors to account for the likelihood that they will occur at once. The probability factors also tacitly adjust for the likelihood of the full magnitude of the loads being applied in combination. The provisions permit modification of the load factors if the Engineer expects that the likelihood of some load combination is outside of that considered in the Specification. The LRFD Specification has explicitly included the consideration of loads applied during construction that traditionally have not been considered in the AASHTO Specifications. These new considerations are discussed elsewhere.

Loads paths for wheel loads are perhaps the most important of any of the load paths in steel stringer bridge design. Wheel loads are transferred through the deck directly to the stringers. The deck is typically acting compositely with all the stringers in the cross-section. If a composite stringer shortens as it is put into flexure, the concrete deck is compressed. The deck attached to the adjacent stringer must also shorten the same amount less the shear deformation that occurs between stringers. Hence, horizontal shear in the deck is a second load path for distributing the wheel loads that will transfer load to adjacent stringers in proportion to the relative stiffness of the two paths.

Transverse load paths are also created by the cross-frames or diaphragms. The cross-frames/ diaphragms act somewhat similarly to the horizontal deck shear in transferring the load. Cross-frames/diaphragms cause adjacent stringers to deflect an equal amount less the deflection caused by any elastic shortening of the cross-frame/diaphragm members and by any rotation of the adjacent stringers. These transverse members transfer load by a combination of shear and bending, and also act compositely with the deck. The amount of load transferred in the cross-frames/diaphragms is proportional to their stiffness compared to the stiffness of the other available load paths.

Wheel-load distribution factors (WLDFs) have been used in the AASHTO Specifications since the earliest days. These factors are assumed to consider the various load paths available to distribute live load to and away from the stringer being designed. Their application gives the portion of the live load moment or shear to be employed in the design of an individual stringer. Implicit is the assumption that the design at hand is similar to that assumed in the development of the WLDFs. The WLDFs given in *AASHTO LRFD* Article 4.6.2.2 have been derived from studies of analytical models of stringer bridges composed of typical members with typical relative stiffnesses. The WLDFs for interior stringers are based on analyses that recognize the bending and horizontal shear stiffness of the deck, but without cross-frames/diaphragms considered (*3*). Hence, these WLDFs are slightly conservative for interior stingers.

The WLDFs for exterior stringers developed from analytical models without cross-frames/diaphragms were found to give unconservative results for steel stringer bridges with these members included. Hence, the code writers developed a special WLDF for exterior girders in such bridges based on the assumption that the bridge cross-section deflects and rotates as a rigid cross-section (discussed previously – refer to Equation 2.1). Implicit is a further assumption that the stringers all have approximately the same stiffness. The WLDFs for girders with skewed supports were developed from analyses that considered cross-frames/diaphragms and the horizontal shear stiffness of the deck. If the stringers in the cross-section have different sizes, then the accuracy of all the WLDFs can be called into question. Other inaccuracies can occur for a number of reasons, particularly in some continuous spans. Unparallel skews also are problematic.

All of the analyses made to develop the WLDFs were elastic, as are all known design-based computer software analyses at this time. Many computer programs employ the influence line principle for live load analysis. The influence line method applies only to linearly elastic structures. For example, if a bearing lifts off during loading, the structural behavior is non-linear and the influence line method is incorrect. Likewise, if a stringer behaves inelastically, strictly speaking, the influence line method is incorrect.

Inherent in strength of materials theory is the assumption that plane sections remain plane under load. This assumption is not critically held in stringer bridges. As discussed previously, flexure in a composite stringer deviates from this theory slightly. Assuming that the stringer is in positive flexure, the compression in the concrete is distributed across the width by shear. Due to shear lag, the compressive stress is reduced at increasing distance from the stringer. There are rules given in *AASHTO LRFD* Article 4.6.2.6 that define the amount of concrete that is to be considered effective. Generally, these rules are conservative and much more deck is effective than the current rules allow. However, this is not always the case. An extreme but common example when the rule is unconservative is at the point where a concrete deck is discontinued during the deck-casting process. The stringer continues to resist moment beyond the end of the deck while the stress in the concrete at its terminus must be zero. However, all of the force in the concrete does not leave the deck at a point. A similar narrowing of the effective width of deck occurs at piers when the reaction is introduced into the composite stringer.

Deck design is often based on the assumption that the stringers are rigid. Although this is never the case, often it is an adequate assumption for the design of the deck. The empirical deck design method permitted in the LRFD Specifications (*AASHTO LRFD* Article 9.7.2) is based on the assumption that the deck supports do not deflect and the deck is restrained against rotation at the stringers. As reality deviates from these assumptions, the accuracy of this design approach could perhaps be called into question. The deck on stringers often is "dished" due to live load. The curvature of the deck can be translated back to a moment by differentiation of the shape. For decks on very flexible stringers, this additional moment probably should be investigated to ascertain that the empirical deck design approach is adequate in such cases.

3.   Zokaie, T., T.A. Osterkamp, and R.A. Imbsen. 1991. "Distribution of Wheel Loads on Highway Bridges." Final Report for NCHRP Project 12-26, Transportation Research Board, National Research Council, Washington, D.C.

2.4.3.1.4.3 Rolled Beams vs. Welded Girders

For spans less than about 120 feet in steel I-girder bridge superstructures, the Engineer has the option to choose rolled shapes over welded girders for the main stringers.

Wide-flange (I) shapes are hot rolled from billets by repeatedly passing the blooms through rolls to form the final shape. Wide-flange shapes differ from standard sections in that they are made on a mill with extra rolls having a vertical axis in addition to the rolls with horizontal axes. Such rolls permit rolling sections with wider flanges; hence the name. Wide-flange shapes are designated by the nominal depth and weight per foot; e.g. a W36 X 182 is nominally 36 inches deep (with an actual depth of 36.33 inches) and weighs 182 pounds per foot. The available domestic shapes are listed in the AISC *Manual of Steel Construction* (4) and also in the literature available from the domestic shape producers. The wide-flange sections used for bridge stringers typically range between 24-inch (W24) and the deepest shapes available domestically, which have a 40-inch (W40) nominal depth. (Note: the Engineer is alerted to the special requirements contained in *AASHTO LRFD* Article A3.1 of Reference 5 related to welded joints in rolled heavy wide-flange shapes subjected to tensile forces and having a flange thicker than 2 inches).

Figure 2.31 Rolled Beam Superstructure

Figure 2.32 Fabricated Girder Superstructure

Wide-flange sections are doubly symmetric and have relatively thick webs compared to most welded I-shape sections. The rolling process imposes a maximum web depth-to-thickness ratio of approximately 60. In the past, partial length cover plates were often welded to the flanges of rolled wide-flange shapes used in bridges in order to increase their bending capacity. However, research has shown that cover-plate weld termination must be assigned a very low permissible stress range (Category E or E′), which has essentially limited the current use of welded partial length cover plates on highway bridges to in-kind replacements.

A common application of rolled beams is as stringers between welded girders in larger bridges (e.g. Figure 2.23). In these structures, the rolled beams usually span between 20 and 30 feet and are supported on cross-frames that are bolted to the welded girders. Rolled shapes for this application are often between 18 and 24 inches deep.

Table 2.5.2.6.3-1 of the *AASHTO LRFD* Specifications provides suggested minimum depths for constant depth superstructures. A 40-inch deep rolled beam will meet the suggested minimum depth for a 120-foot composite continuous span. For a composite simple span, the same table suggests the maximum span for a 40-inch deep beam to be approximately 100 feet. The size of the rolled beam must also meet critical stress or live load deflection criteria. Before designing a rolled-beam bridge, the Engineer should consider consulting with shape producers to ascertain the availability of a specific section size and length. The maximum available length of rolled wide-flange shapes is approximately 120 feet and varies by section size (again, consult with the shape producers for maximum length availability for a specific section). Stock lengths are typically available from steel service centers in 5-foot increments between 30 and 60 feet, but they may not meet toughness requirements and may not be domestically produced.

Rolled shapes for use in bridges should typically be ordered as ASTM A 709 Grade 50S (or AASHTO M 270 Grade 50S), which is the equivalent grade to ASTM A 992 for structural shapes. ***Note that uncoated weathering steel Grade 50W wide-flange shapes are available under the ASTM A 709 specification. However,***

rolled wide-flange shapes are not available in any of the high-performance steel grades (i.e. Grades HPS 50W, HPS 70W or HPS 100W).

A shape equivalent to a rolled wide-flange shape can be fabricated from plate stock to form an I-shape. It can be shown for a given web depth-to-thickness ratio that the minimum cross-sectional area of a doubly symmetric noncomposite I-shape that is required to support a given moment can be computed as follows (6):

$$A_{min} = \left(\frac{18S^2}{\alpha}\right)^{\frac{1}{3}}$$ Equation 2.3

where:
   α = web depth-to-thickness ratio (D/t_w)
   S = section modulus (in^3)

This relationship shows, for example, that using an optimized welded girder having a web with a slenderness D/t_w of 150 saves almost 30 percent of the steel required in an optimal shape having a D/t_w of 55 that is typical of a wide-flange shape. Therefore, significant material savings can obviously be obtained by fabricating I-shaped girders with larger web depth-to-thickness ratios. Whereas rolled beams are practically limited to a maximum web depth-to-thickness ratio of approximately 60, welded I-shapes of much more slender web proportions can be fabricated. However, if the web depth-to-thickness is too thin, vertical stiffeners are required to prevent shear buckling and longitudinal stiffeners may be required to prevent web bend buckling.

The use of a singly symmetric girder section with a smaller flange in a composite section provides additional economy over the doubly symmetric rolled shape without a cover plate. The potential to use deeper welded sections also reduces live-load deflections, which can lead to the use of uneconomical rolled beam sections or to required depths that may not be available.

2.4.3.1.4.3.1 Vertical Camber

Vertical camber is cut into welded plate girder webs to counteract the effect of the self-weight deflection and to impose the vertical curvature of the roadway alignment. When the dead load has been applied, the girder will deflect to the alignment of the profile of the roadway. One of the advantages of steel girders is that they can be cambered accurately so that the final roadway elevation is very close to theoretical. A camber diagram is provided on the design plans with the appropriate camber shown for use in grading of the deck, and also with the total camber shown for use in fabricating the steel girders. The camber supplied to account for the deflection due to the weight added to the steel is provided. A survey of the erected steel is made to determine the height of the deck haunches to account for the deflection due to the deck and the superimposed dead load.

Figure 2.33 Surveying Erected Steel Prior to Deck Placement

Rolled beams, however, are rarely cambered to account for dead load deflection. The web of the beam may distort when the camber exceeds 7 to 8 inches.   For bridges utilizing rolled beams, a deflection diagram, which is the mirror image of a camber diagram, is typically shown on the plans instead. Rolled beams have a natural camber due to the effects of uneven cooling during the rolling process, but this camber is rarely large enough to offset the effects of the dead load deflections. Where natural camber exists, it is usually oriented such that the beam is cambered down over interior piers and cambered up at midspan sections. However, most of the deflection will still have to be accounted for primarily by varying the thickness of the deck haunch over the beams along the length in order to achieve the desired profile grade. The minimum thickness of the deck haunch will typically occur at the interior piers and abutments or perhaps at the field splice locations. Usually, the Engineer will detail the minimum deck haunch at the piers and abutments and then vary it elsewhere along the span. For a welded girder, the thickness of the deck haunch will generally vary much less than for a rolled beam. The haunch thickness will vary with the thickness of the top flange and any differences between the actual and theoretical steel deflections.

For all the apparent economic advantages of the welded I-shape in terms of savings in material, rolled shapes generally require less fabrication. For situations where rolled beams are adequate and available, fabricators often prefer them. However, fabricators like to have the option to substitute an equivalent welded girder in case availability, delivery or other specific requirements (e.g. maximum available length or camber) become problematic. Some Owners consider rolled beams to be more economical than welded girders in situations where a choice can be made. ***Therefore, for bridges with spans where a choice between a rolled beam or a welded shape is possible and where significant camber is not required, consider specifying rolled beams, ensure that the selected sections are available, and allow the fabricator to substitute an equivalent welded girder should the situation warrant. However, since differences in the preferences of***

some fabricators and Owners do occur and market conditions are forever changing, it is considered prudent to check with the Owner and/or the fabricators who may be potential bidders on the job prior to making a final decision.

4.   AISC. 2001. *Manual of Steel Construction – Load and Resistance Factor Design.* 3rd Ed. American Institute of Steel Construction, Chicago, IL.
5.   AISC. 2005. *Specification for Structural Steel Buildings.* ANSI/ASCE 360.5, American Institute of Steel Construction, Chicago, IL, March 9.
6.   Haaijer, G. 1961. "Economy of High Strength Steel Structural Members." *Journal of the Structural Division*, American Society of Civil Engineers, New York, NY, Vol. 87, No. ST 8.

2.4.3.1.4.4 Cross-Frame or Diaphragm Spacing and Configuration

Cross-frames and diaphragms perform many important functions in steel composite I-girder stringer bridges. Cross-frames and diaphragms:

- ➢ provide stability to top flanges in compression prior to hardening of the deck
- ➢ provide stability to bottom flanges in compression
- ➢ help distribute dead and live loads between stringers
- ➢ transfer lateral wind loads from the bottom of the girder to the deck and from the deck to the bearings
- ➢ resist flange lateral bending effects
- ➢ resist girder torsion causing non-uniform torsion in the girders
- ➢ work with the deck to reduce transverse deck stresses
- ➢ provide lateral support to exterior girders when resisting eccentric loads from deck overhang brackets
- ➢ provide end support for deck expansion dams
- ➢ provide opportunities to jack bridges during bearing replacement
- ➢ provide support for utilities and walkways
- ➢ provide geometric control during erection (girder spacing and alignment)

As discussed previously, cross-frames and diaphragms, along with the concrete deck, provide the restoring forces that minimize internal energy in the bridge by resisting the differential deflections between girders, which tends to equalize the load the girders carry regardless of how localized the loads are applied. During erection and prior to the hardening of the deck, the cross-frames/diaphragms are often the only element available to provide the necessary restoring forces to resist the independent deflections of the girders.

Figure 2.34 Cross Bracing During Construction

Restoring forces between girders will often be small for bridges with moderate deck overhangs and approximately equal girder stiffnesses at points of connection of the cross frames/ diaphragms; e.g. straight bridges with approximately equal-size girders and bearing lines skewed not more than approximately 10 degrees from normal where intermediate cross-frames/ diaphragms are placed in collinear lines normal to the girders. Where intermediate cross-frames/diaphragms are placed in collinear skewed lines parallel to the skewed supports, which is permitted for support skew angles up to 20 degrees (see *AASHTO LRFD* Article 6.7.4.2), this assumption may be extended to bridges having bearing lines skewed up to 20 degrees. ***In fact, in all such cases, it is reasonable to assume that all girders in the cross-section will resist the component dead loads acting on the noncomposite section (i.e. the DC$_1$ loads) equally,*** neglecting any effects of elastic shortening in the cross-frame members. The assumption of equal vertical girder deflections under the DC$_1$ loads in these cases has been borne out in the field. However, assuming that the girders deflect due to the loads applied to each often leads to problems in the field when the deflections are actually nearly equal, e.g. equal deflections when unequal cambers were specified leads to problems when screeding the deck.

In other cases, the differential deflections of the points on a pair of girders connected by a cross-frame may be very significant. In girder bridges with skews larger than 20 degrees, cross-frames are not permitted to be skewed parallel to the supports, but must be perpendicular to the girders. Obviously, the points on the two girders cannot deflect equally. For example, the bearing at the oblique angle on the exterior girder is perpendicular to a relatively flexile point on the opposite girders. Vertical loads applied to the girders opposite the oblique bearing are resisted by the girders to which they are applied and by the oblique bearing, which receives some portion of the load via the cross-frames in the path between the bearing and the loaded point. The minimum energy theorem requires that the portion of the load transferred to the oblique bearing be related to the relative stiffnesses of the paths to the bearings supporting the loaded girders and the paths to the other bearings, particularly the

oblique bearing. The elements that develop this system of minimum energy are the cross-frame elements.   The cross-frame forces in this case can become very significant making connections problematic and expensive.   If diaphragms are employed instead of cross-frames, the load is transferred by the diaphragm end moments and shears.   In either case, the connections to the girders must be designed to resist these forces. History has shown that when these restoring forces are not considered, even in right bridges, fatigue cracks can materialize in the girders and elsewhere. Options to be considered to reduce these restoring forces are discussed in the next section of this chapter on Cross-Frame/Diaphragm Spacing.

Figure 2.35 Diaphragms on Skewed Bridge

Load is drawn to the girder(s) with the greatest stiffness when there are girders of differing stiffness within a cross-section. For example, staged construction creates a case where some girders are composite when adjacent girders are being decked. When the wet concrete deck is placed on the noncomposite steel, a disproportionate portion of this new load is drawn to the stiffer composite girders. To avoid this effect, the cross-frames/diaphragms connected to the two stages might be disconnected and a closure pour used after the cross-frames/diaphragms are made effective.

In heavily skewed bridges (i.e. bridges with supports skewed more than 20 degrees from normal), the cross-frames/diaphragms are subjected to larger forces. The cross frames/diaphragms at skewed supports contribute an additional effect to the bridge not present in perpendicular or radial cross-frames/diaphragms. As discussed in more detail later on, forces in these skewed cross-frames/diaphragms have a longitudinal (i.e. tangent to the girders) component of force that causes moments at the ends of girders at simple supports to be other than zero; usually these moments are negative. The lateral constraint of the bearings in these cases can cause significant increases in the cross-frame/diaphragm forces and consequent girder end moments.

Cross-frames/diaphragms must help provide the necessary restoring forces to resist the significant differential deflections of the girders that typically occur in heavily skewed bridges. This is especially true near supports where at one cross-frame connection point, a girder will have zero deflection because it is located right at the support, whereas at the other cross-frame connection point on the adjacent girder, which may be located several feet from the support, the girder may be undergoing significant vertical deflection. That is, there is a difference in the stiffness of the two girders at the points where the cross-frames are connected. Obviously, the assumption of equal girder deflections under the DC_1 loads is not accurate in this case. As discussed later, the differential deflections of the girders in skewed bridges also result in the girders rotating out-of-plumb with respect to the longitudinal axis of the girders; in particular, at the end supports. Additional discussion on specific design considerations for I-girder bridges with skewed supports is provided in DM Volume 2, Chapter 2, Section 2.2.3.8.

It is also important to ensure that where the cross-frame chords or diaphragm flanges are not attached directly to the girder flanges that provisions be made to transfer the calculated horizontal force in the cross-frames to the flanges through the connection plates, which must be positively attached to both girder flanges. This is particularly significant when large restoring forces are developed in the transverse bracing members. The term connection plate is given to a transverse stiffener plate attached to the girder to which a cross-frame or diaphragm is connected. The eccentricity between the cross-frame chords or diaphragm flanges and the girder flanges should be recognized in the design of the connection plates and their connection to the web and flanges of the girders. Additional more detailed information related to the design of cross-frame and diaphragm members and their connections is also given in DM Volume 2, Chapter 2, Sections 2.3 and 2.4.

Figure 2.36 Cross-Frame Connection to Girder

The discussion that immediately follows relates to the process of laying out the spacing of the cross-frame or diaphragm members in an I-girder bridge to arrive at a reasonable initial framing plan for further investigation during the preliminary design

stages. Additional discussion is also provided later on the use of cross-frames versus diaphragms for an I-girder bridge and when the use of each type may be more appropriate, the different possible configurations for cross-frame members, and the preliminary sizing of cross-frames and diaphragm members where needed to perform the analysis.

2.4.3.1.4.4.1 Spacing

Since 1949, the AASHTO Standard Specifications for steel design have specified a limit of 25 feet on the longitudinal cross-frame or diaphragm spacing. While this limit has ensured satisfactory performance of steel-bridge superstructures over the years, it is essentially an arbitrary limit that was based on the experience and knowledge that existed at that time. In particular, the limit was targeted at much shorter spans than achieved with modern stringer bridges. It was also developed for stringers designed for much lower stress levels. The preceding discussion references restoring forces that create forces in cross-frame members and moments and shears in diaphragms. The total restoring force within a bay of a span is a function of the relative stiffnesses of the pair of girders and the difference in the applied loading to each. Thus, the fewer the cross-frames/diaphragms, the larger the cross-frame/diaphragms forces per member. In fact, the forces are nearly proportional to the number of cross-frames/diaphragms in the bay of a span. Thus, too few cross-frames/diaphragms will result in higher cross-frame/diaphragm forces and are more likely to lead to fatigue damage at some future time.

In the LRFD Specifications (*AASHTO LRFD* Article 6.7.4.1), this long-standing requirement limiting the maximum spacing to 25 feet has been removed. Instead, the need for cross-frames or diaphragms at all stages of construction and the final condition is to be established by rational analysis. This requirement implies that cross-frames and diaphragms may be spaced at distances exceeding 25 feet where rational analysis and investigation indicates that such spacings are acceptable (note however that an upper limit on the cross-frame or diaphragm spacing in horizontally curved I-girder bridges is specified in *AASHTO LRFD* Article 6.7.4.2). The investigation should consider all the issues related to the primary functions of cross-frames and diaphragms that were discussed in the preceding section of this chapter. Removing the arbitrary 25-foot maximum spacing limit can allow cross-frames and diaphragms to be located more efficiently, and in certain instances, may even prevent having to add an additional cross-frame or diaphragm line in a span just to satisfy this limit, whereas an additional line may not have been required otherwise in order to satisfy the design criteria. Cross-frames and diaphragms should be spaced at nearly uniform spacing in most cases, for efficiency of the design, for constructibility and to allow for the use of simplified methods of analysis for calculation of flange lateral bending stresses. As discussed later, closer spacings may be necessary adjacent to interior supports, in the vicinity of skewed supports and perhaps near midspan. Also, as specified in *AASHTO LRFD* Article 6.7.4.2, where supports are not skewed, the cross-frames or diaphragms should be placed in contiguous lines normal to the girders.

The Engineer should exercise some restraint when extending cross-frame or diaphragm spacings beyond 25 feet. Interestingly, removal of the 25-foot spacing

limit leads to the need to consider the cross-frames/diaphragms in the design of the girders, as well as to potentially treat them more like primary members in more cases than in the past. For example, the transfer of the noncomposite load from a heavily loaded stringer to a lightly load one is accomplished via the cross-frames/diaphragms. Theoretically, only one cross-frame/diaphragm at mid-span will be sufficient to transfer the load assuming that it has adequate capacity. However, the same magnitude of load will be transferred through the single cross-frame/diaphragm as through several; as a result the force in that single cross-frame/diaphragm is several times larger than if several cross-frames/diaphragms spaced at the traditional 25 feet were employed. A simple check on the magnitude of this restoring force can be made by finding the average load assuming all girders to be loaded equally. The amount of load in the single cross-frame/diaphragm is equal to the difference between the applied load and the average load. If the span is such that traditional spacing would require four cross-frames/diaphragms, the single cross-frame/diaphragm would carry approximately four times the load carried by each cross-frame/diaphragm in the traditional arrangement. A primitive assumption might be that the live load forces in the single cross-frame/diaphragm would also be about four times those in the cross frames/diaphragms provided in the traditional arrangement. It should be pointed out that stresses in the concrete deck will also increase with fewer cross-frames/diaphragms. The Engineer should at least be cognizant of these effects when fewer cross-frame/diaphragm lines are provided, especially during construction when the bridge is noncomposite and/or when the bridge is heavily skewed or has an irregular framing plan.

As discussed below, greater spacing of cross-frames/diaphragms has obvious effects on the design of discretely braced compression flanges; in particular, on the design of exterior-girder flanges where the cross-frames/diaphragms act as reactions resisting the lateral force from the overhang brackets. Although more uniform spacing is generally preferred, one option often overlooked is to vary the spacing of cross-frames/diaphragms along the span in certain critical regions. For example, tighter spacing near continuous supports, and perhaps near midspan, may be desirable, with much wider spacings provided elsewhere. This obviously permits a reduction in critical spacing without increasing the total number of cross frames.

One of the primary functions of cross-frames and diaphragms is to provide stability to top flanges in compression prior to hardening of the deck. Cross-frame/diaphragm spacings in simple spans and in the positive-moment regions of continuous spans are typically controlled by constructibility criteria. For these cases, the spacings must be adequate to ensure that the top compression flange of the noncomposite girder has adequate lateral-torsional buckling resistance under the self-weight of the steel and the weight of any metal stay-in-place deck forms, plus the maximum moments generated during the deck-casting sequence. As discussed previously, exterior girder flanges are also subject to flange lateral bending stresses due to the torsion resulting from loads applied to deck overhang brackets during construction. Therefore, for exterior girders, the cross-frame/diaphragm spacings must be sufficient to ensure that the compression flange has adequate lateral-torsional buckling resistance under the combination of the major-axis bending stresses due to the self-weight of the steel, the weight of the deck forms (if applicable) and the deck-casting sequence, and the flange lateral bending stresses

resulting from the effects of the deck overhang loads. The specific design checks that must be made to ensure that the spacings provide adequate lateral-torsional buckling resistance under these conditions are described in detail under Constructibility Verifications in DM Volume 2, Chapter 2.

Figure 2.37 Cross-Frame Connections to Girder Top Flange

In the negative-moment regions of continuous spans, another of the primary functions of cross-frames/diaphragms is to provide stability to bottom flanges in compression, both during construction prior to hardening of the deck and under the total dead plus live load after the bridge is open to traffic. In this case, the spacings must be adequate to ensure that the bottom compression flange of the noncomposite girder has adequate lateral-torsional buckling resistance under the maximum moments generated during the deck-casting sequence (including the moments due to the self-weight of the steel and any stay-in-place deck forms). Also, for exterior girders, lateral flange bending stresses due to the effects of deck overhang brackets loads should be considered as discussed above.   However, since the maximum accumulated negative moments from the sequential deck-placement analysis typically do not differ significantly from the calculated DC_1 moments assuming the deck is placed all at once, this constructibility condition normally does not control the cross-frame/diaphragm spacings, or bottom-flange sizes, in the negative-moment regions.   Instead, the cross-frame/diaphragm spacings, and bottom-flange sizes, in these regions are normally governed by the sum of the factored dead and live load stresses at the strength limit state (i.e. the design condition after the bridge has been completed and is open to traffic).   The specific design checks that must be made to ensure that the cross-frame/diaphragm spacings in negative-moment regions provide adequate lateral-torsional buckling resistance to the bottom flange under this strength limit state condition are described in detail under Strength Limit State Verifications for Flexure in DM Volume 2, Chapter 2.

A third primary function of cross-frames/diaphragms is to help limit flange lateral bending stresses due to wind load, both during construction and in the final condition. When wind load is applied to the noncomposite structure during construction, there is no deck to provide horizontal diaphragm action. Therefore, the cross-frames/diaphragms in I-girder bridges act as struts in distributing the total wind force on the structure to the flanges of all girders in the cross-section. The force is then transmitted to the ends of the span or to the closest point(s) of lateral wind bracing through lateral bending of the flanges, which is restrained by the cross-frames or diaphragms at discrete points along the span. Normally, the resulting lateral flange bending stresses for this condition do not control the cross-frame/diaphragm spacings based on the load combinations that must be investigated for this case. Further discussion on checking for the effects of wind load during construction may be found under Constructibility Verifications in DM Volume 2, Chapter 2.

For I-girder bridges in the final condition with composite concrete decks, wind load on the upper half of the exterior girders, the deck, the barriers and the vehicles may be assumed transmitted directly to the deck, which acts as a lateral diaphragm to carry the load to the supports. Lateral bending in the top flanges does not need to be considered because the flange is continuously supported by the deck. Wind load on the lower half of the exterior girders may be assumed applied laterally to the bottom flange, which transmits the load to the adjacent cross-frames/diaphragms through lateral bending of the flange. The frame action of the cross-frames/diaphragms then transmits the wind forces up to the deck, which in turn transmits them to the supports through horizontal diaphragm action. It can be shown that in the majority of cases, only a small portion of the wind force on the lower half of a composite structure is resisted through lateral bending of the bottom flanges; most all the wind force is transmitted directly to the deck through the cross-frames/diaphragms. As a result, the cross-frame/diaphragm spacings are normally not controlled by the lateral flange bending stresses resulting from wind loads applied to the composite structure in the final condition for the load combinations that must be investigated for this case. Further discussion on checking for the effects of wind load on the composite structure in the final condition may be found under Strength Limit State Verifications for Flexure in DM Volume 2, Chapter 2.

I-girder bridges with skewed supports present several issues related to the layout of cross-frames and diaphragms. It is important to note that AASHTO defines the skew angle as the angle between the axis of support relative to a line normal to the longitudinal axis of the bridge, i.e. a 0° skew denotes a rectangular bridge. As specified in Article 6.7.4.2 of the *AASHTO LRFD* Specifications, where supports are not skewed more than 20 degrees from normal, cross-frames or diaphragms may be placed in contiguous skewed lines parallel to the skewed supports, as shown in Figure 2.38. This requirement is consistent with past practice and is based on welding access to the acute corner between the connection plate and web. Where supports are skewed more than 20 degrees from normal, the cross-frames or diaphragms must be normal to the girders and may be placed in either a contiguous line or in staggered patterns. Figure 2.39 shows a layout where the cross-frames are placed in a contiguous line and Figure 2.40 shows a layout where the cross-frames are placed in a staggered pattern.
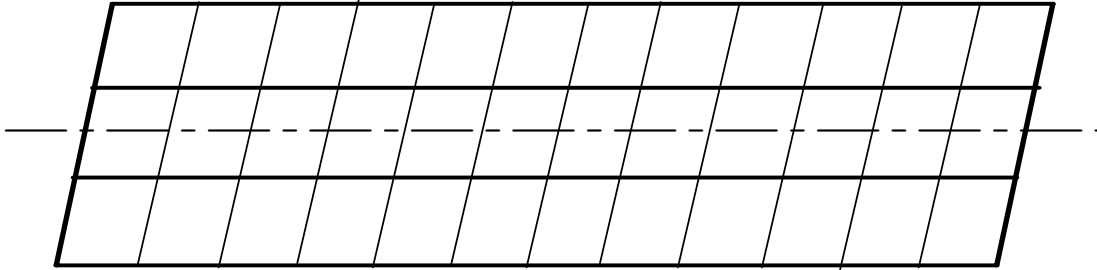
Figure 2.38 Contiguous Cross-Frame/Diaphragm Lines Parallel to Skew (for skew ≤ 20°)
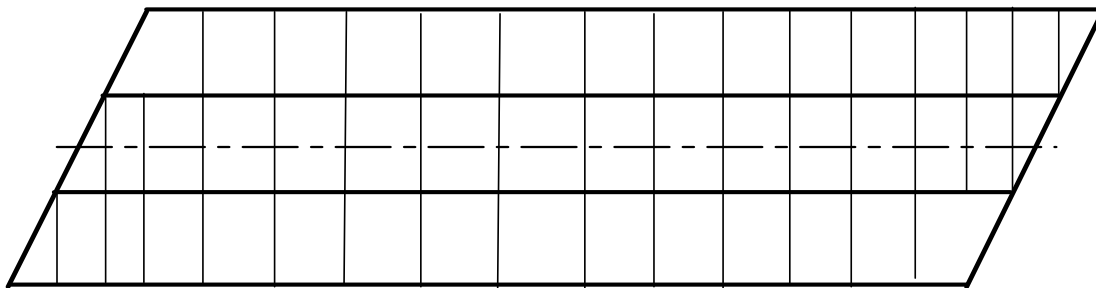
Figure 2.39 Contiguous Cross-Frame/Diaphragm Lines Normal to Girders (for skew > 20°)
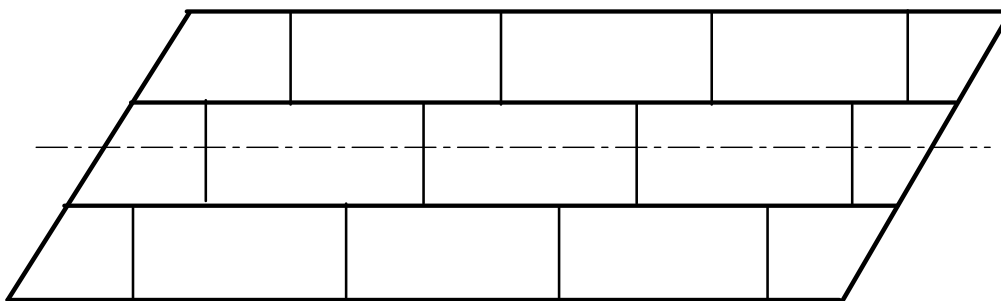
Figure 2.40 Staggered Cross-Frame/Diaphragm Lines Normal to Girders (for skew > 20°)

In some cases, where supports are skewed more than 20 degrees, it may be advantageous to stagger the cross-frames/diaphragms, particularly in the vicinity of the supports, to reduce the transverse stiffness of the bridge. By staggering the cross-frames/diaphragms, the transverse stiffness of the superstructure is reduced because the flanges are able to flex laterally and relieve some of the force in the cross-frames/diaphragms. Although the forces in the transverse bracing members

are decreased, staggering the cross-frames/diaphragms also has the effect of increasing the lateral bending stresses in the girder flanges.

As discussed previously, in heavily skewed bridges, significant differential vertical deflections of the girders occur at the cross-frame/diaphragm connection points. As the girders deflect and rotate by different amounts, the cross-frames/diaphragms, which are of fixed dimension and deflect and rotate along with the girders, develop restoring forces in an attempt to equalize the adjacent girder deformations. However, because the bracing members are of fixed dimension, the girders must also twist about their longitudinal axes in order to maintain compatibility of deformations. As a result, the girders are subject to torsion. The twist, which occurs along the entire girder, is generally largest at the end supports where the differential deflections and rotations are typically the highest. An I-girder section, which is an open section, resists torsion through a combination of St. Venant and warping torsional stiffness. However, the warping torsional stiffness generally predominates and manifests itself primarily through the development of lateral bending stresses in the girder flanges (7). The lateral bending stresses are exacerbated when cross-frames/diaphragms are staggered due to the fact that there is transverse bracing, carrying significant restoring forces, on only one side of the girder at a given cross-frame/diaphragm connection point. Closed-form solutions to estimate the restoring forces in the bracing members and the flange lateral bending stresses in skewed bridges, with or without staggered cross-frames/diaphragms, do not currently exist so a special investigation is generally advisable. The consideration of lateral flange bending in skewed I-girder bridges is discussed further under Design Considerations for Skewed Supports in DM Volume 2, Chapter 2.

Another option to consider where supports are skewed more than 20 degrees is to remove highly stressed cross-frames/diaphragms, which typically results in discontinuous cross-frame/ diaphragm lines. A discontinuous cross-frame/diaphragm line is defined as one that does not form a continuous line between multiple girders. Removal of highly stressed cross-frames/ diaphragms, particularly near obtuse corners at supports (Figure 2.39) releases the girders torsionally. This is often beneficial in reducing the overall transverse stiffness of the bridge superstructure, along with the restoring forces in the remaining transverse bracing members, as long as the girder twist is not excessive. Highly stressed cross-frame/diaphragm removal also aids in erection by making the installation of the remaining transverse bracing less difficult. Depending on the severity of the skew, it may be necessary to remove other cross-frame/diaphragm members along the span in addition to those near the supports. A preliminary refined analysis of the entire bridge superstructure is useful in indicating which cross-frames/diaphragms are potential candidates for removal. As with staggered lines, discontinuous cross-frame/diaphragm lines can also exacerbate the flange lateral bending stresses in the girders, particularly near locations where the lines are discontinued. Further investigation of these stresses is desirable. However, even with staggered or discontinuous cross-frame lines, often the lateral bending is not critical and the net result is a desirable reduction in cross-frame/diaphragm forces.

Figure 2.41 Discontinuous Cross Frame

Other issues to consider relate to the cross-frames/diaphragms along the skewed support lines. At skewed interior support lines in continuous spans, *AASHTO LRFD* Article 6.7.4.2 states that cross-frames/diaphragms are not needed along the skewed support line if cross-frames/diaphragms normal to the girders are provided at bearings that resist lateral forces. The cross-frames/ diaphragms normal to the girders must be proportioned to transmit all the lateral components of force from the superstructure to the bearings that provide lateral restraint. Otherwise, the lateral bending in the bottom flange near the restrained bearings may be excessive. At severely skewed interior supports, e.g. with skews exceeding 20 degrees from the normal, placement of cross-frames/diaphragms along the skewed support line is not recommended. The detailing of the intersections with the cross-frames/diaphragms oriented normal to the girders is complex and those members should be sufficient to resist any lateral components of force that develop at the bearings. For skews not exceeding 20 degrees from the normal, cross-frames/diaphragms along the skewed support line alone may be sufficient. In this case, if cross-frames/diaphragms are also provided normal to the girders, they may be spaced too close together along the girders introducing significant lateral flange bending stresses into the girders. Whatever the case, consideration should always be given to providing a means to allow jacking of the girders to replace bearings.

A row of cross-frames/diaphragms is always required at abutments (simple supports) to support the free edge of the deck. End rotations of the girders create forces in these cross-frames/diaphragms. As mentioned previously, at cross-frames/diaphragms along skewed end support lines, tangential components of the skewed end support cross-frame/diaphragm forces act along each girder. In order to maintain static equilibrium, vertical bending moments and shears must develop in the girders at the end supports. Since these end moments are usually negative, they can potentially introduce tensile stresses in the deck or subject the bottom flange to compression adjacent to the supports. *AASHTO LRFD* Article 6.7.4.2 requires that the effect of the tangential components of force transmitted by the

skewed end support members be considered. The net components of the skewed end support cross-frame/diaphragm forces *transverse* to the girders introduce a torque at the girder ends, which can contribute further to the twisting at the girder ends. This effect may also need to be considered when the end cross-frame/diaphragm forces are large. The effect of these transverse forces may need to be considered in the design of the transverse deck reinforcement. Further discussion of these effects is provided under Design Considerations for Skewed Supports in DM Volume 2, Chapter 2.

In order for the connection plates for a skewed cross-frame/diaphragm to transfer the force between the bracing members without undue distortion, the connection plates should be oriented in the plane of the transverse bracing. Two options for this detail are most commonly used; either a skewed connection plate (Figure 2.42), or a bent gusset plate (Figure 2.43). The skewed connection plate should be limited to a maximum angle of 20 degrees from normal, as precise fitting of the connection plates becomes more difficult and the welding of the connection plates to the web within the acute corners becomes more problematic at larger angles. For angles not exceeding 20 degrees from normal, it is desirable to give the fabricator the option to use either detail.
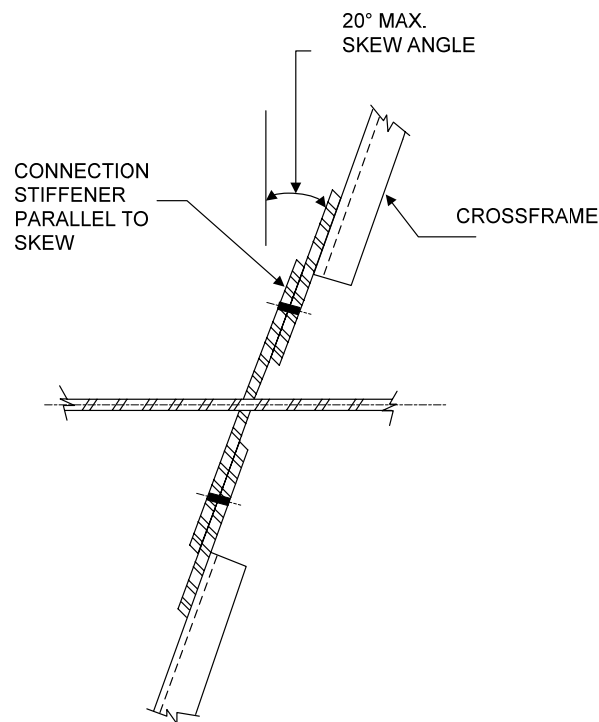
Figure 2.42 Skewed Connection Stiffener

CROSSFRAME

WEB ℄
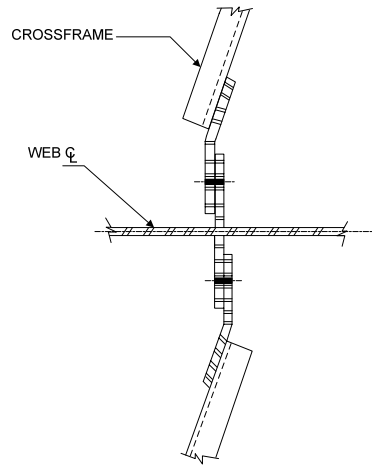
Figure 2.43 Bent Gusset Plate

In summary, based on the issues raised in the preceding discussion, for simple spans and the positive-moment regions *in the end spans* of straight continuous-span I-girder units, a cross-frame/diaphragm spacing between 18 and 25 feet would be reasonable to assume for preliminary investigation. For the positive-moment regions *in the interior spans* of straight continuous-span I-girder units, a preliminary cross-frame/diaphragm spacing between 24 and 30 feet would be reasonable to assume. For the negative-moment regions of straight continuous-span I-girder units, a preliminary cross-frame/diaphragm spacing between 18 and 24 feet would be reasonable to assume, with the lower end of this range used for the first cross-frame adjacent to the interior piers. Obviously, upon further more detailed investigation of the specific design criteria related to the issues discussed above, adjustments to these initial spacings may need to be made. Adjustments will also likely need to be made in the regions of skewed supports. Additional discussion on cross-frames/diaphragms and their spacing may be found in Reference 8.

7.   Salmon, C.G., and J.E. Johnson. 1996. *Steel Structures – Design and Behavior*. 4th Ed. Emphasizing Load and Resistance Factor Design, HarperCollins Publishers, Inc., New York, NY.
8.   Mertz D.R.. 2000. *Bridge Designer's Guide to Intermediate Cross-Frame Diaphragms*, American Iron and Steel Institute, Washington, D.C.

2.4.3.1.4.4.2 Type, Configuration and Preliminary Sizing

Development of cost-effective cross frames/diaphragms requires careful attention to their design and their detailing. Although these members account for only a small percentage of the total structure weight, they account for a significant percentage of the total erected cost of a steel stringer superstructure.

As specified in Article 6.7.4.2 of the *AASHTO LRFD* Specifications, cross-frames/diaphragms for rolled beams and plate girders should be as deep as practicable, but as a minimum should be at least 0.5 of the beam depth for rolled beams and 0.75 of the girder depth for plate girders. This will help to ensure that the

cross-frames/diaphragms provide adequate torsional resistance to prevent twisting of the beam or girder cross-section at the brace points.

Cross-frames/diaphragms have been the indirect cause of fatigue cracking in a number of bridges. However, changes in the AASHTO bridge specifications over the past twenty years have tended to address these historical problems. As specified in *AASHTO LRFD* Article 6.6.1.3.1, transverse connection plates for cross-frames/diaphragms must be welded or bolted to both flanges of the cross-section in order to provide rigid load paths that preclude the development of significant distortional bending stresses in web gaps that could potentially induce fatigue crack growth (see DM Volume 2, Chapter 2 under Fatigue and Fracture Limit State Verifications for further discussion on distortion induced fatigue).   In addition, transverse connection plates attached to both flanges contribute to the overall torsional resistance of the cross-section at the brace points, which is particularly important when more shallow diaphragm sections are used. Previously, welding to tension flanges was forbidden, but such welds on connection plates have been shown to provide Category C' fatigue resistance. Some states still prefer attaching end angles to diaphragm sections in the shop for field bolting directly to the longitudinal stringers, which eliminates the need for transverse connection plates. In this case, it is recommended that the end connection angles conform to the minimum depth recommendations given above.

Figure 2.44 Shop Welding of Diaphragm Connection Plate

Regarding when the use of diaphragms is more appropriate than cross-frames for an I-girder bridge, there are no hard and fast rules. Diaphragms are used most often in rolled beam bridges or in plate-girder bridges when the girders are less than about 48 inches deep. Channel sections or rolled I-shapes are most commonly used for diaphragms in I-girder bridges; solid-plate diaphragms are rarely used unless needed as special jacking diaphragms to accommodate bearing replacement. Channel sections can either be rolled channels or bent plate channels (i.e. a plate

bent into the shape of a channel by the fabricator) attached directly to the connection plates or attached directly to the stringers using end angles. The Engineer is encouraged to consult with local fabricators regarding their preference. Rolled I-shapes can either be attached to connection plates using gusset plates, attached directly to the stringers using end angles, or attached directly to the connection plates. However, if attached directly to the connection plates, rolled I-shapes have to be coped at the top and bottom at the connection plates to avoid interference, which obviously increases cost. As specified in *AASHTO LRFD* Article 6.7.4.2, end moments in diaphragms should be considered in the design of the connection between the beam or girder and the diaphragm. Also, diaphragms with length-to-depth ratios greater than 4.0 may be designed as beams. Otherwise, shear deformations must be considered in the design of the diaphragm.

Figure 2.45 Rolled Shape Used as Diaphragm

The two most commonly used cross-frame configurations in an I-girder bridge are the K-type configuration and the X-type configuration. The X-type configuration is typically the preferred configuration for intermediate cross-frames (i.e. cross-frames not located at end supports), in particular for deeper girders, but preferences can vary between and within states. The K-type configuration is preferable for end cross-frames and for intermediate cross-frames when the angle of the diagonals with respect to the horizontal is less than about 30 degrees. When this angle becomes too shallow in an X-type configuration, the unsupported length of the diagonals can become too large and these members may also be subject to vibrations. In a K-type configuration, the K formed by the diagonals and one of the chords can either be pointed up (i.e. diagonals intersecting the mid-length of the bottom chord), or pointed down (i.e. diagonals intersecting the mid-length of the top chord). The former configuration is preferred for intermediate cross-frames to reduce the unsupported length of the more heavily loaded bottom chord. The latter configuration is preferred for end cross-frames to provide support to the top chord. At the ends of bridges, the edges of the concrete deck must be supported in order to support the wheel loads coming onto the deck (refer to *AASHTO LRFD* Articles 6.7.4.1 and 9.4.4). In an I-

girder bridge, a rolled I-shape or a rolled or bent plate channel is typically used as the top chord of the end cross-frames in order to provide the necessary support. Pointing the diagonals up in a K-type configuration provides some additional support to this heavier top-chord member in the end cross-frames. One state includes a Z-type intermediate cross-frame configuration in their standard details to be used on plate-girder bridges only with girder depths exceeding 42 inches. This configuration includes a top and bottom strut and a single diagonal sloping toward the bottom flange of the outside girder in the exterior bay.

Figure 2.46 X-Type Cross Frame Configuration

Cross Frame Configuration

Some standard details for I-girder bridges have shown intermediate cross-frames without a top chord. The top chord provides support to the top flange and additional geometry control to the girders during construction. It is recommended here that the use of intermediate cross-frames without top chords preferably be limited to straight bridges with regular framing plans and shorter spans (less than or equal to approximately 150 feet) where dead load does not predominate. The use of intermediate cross-frames without top chords is not recommended for bridges for which geometry control and stability during the erection is especially critical; e.g.

skewed bridges, horizontally curved bridges or bridges that are constructed by incremental launching.

Cross-frames should be configured and detailed to allow the fabrication of as many identical frames as possible. Cross-frames that be assembled in a jig and brought to the site assembled minimizes the chances of errors and field misfits. Knocked down cross-frames require more shop and field handling and are more difficult to erect due to the large number of different pieces that need to be tracked, handled and hoisted. Cross-frame configurations that can be welded from one side only are preferred to prevent having to turn the cross-frame assembly over in the shop. Differences in elevations of the girders should be accounted for with the cross-frame members and not in the connection or gusset plates. That is, configuring the cross-frames as parallelograms rather than rectangles will often increase the number of identical connection plates that can be used. Where used, all gusset plates should be rectangular to minimize fabrication. Further information on the design of cross-frames/diaphragms and their connections is given in DM Volume 2, Chapter 2, Sections 2.3 and 2.4. Additional information on recommended cross-frame/diaphragm configurations and details is given in Reference 9.

At this point, a few words are in order regarding the preliminary sizing of cross-frame and diaphragm members. As specified in *AASHTO LRFD* Article 6.7.4.1, if permanent cross-frames/diaphragms are included in the structural model used to determine force effects, they are to be designed for all applicable limit states for the calculated force effects. But as a minimum, the cross-frame/ diaphragm members are to be designed to transfer wind loads and to meet all applicable slenderness requirements (*AASHTO LRFD* Articles 6.8.4 or 6.9.3, as applicable), and minimum thickness requirements (*AASHTO LRFD* Article 6.7.3). Unlike line-girder analyses, when refined analysis methods are employed, the cross-frames/diaphragms are typically included in the structural model. As a result, preliminary sizes must be entered for these members in order to perform the analysis. The methods used to input there sizes vary with the analysis approach and the specific software that is used. Regardless, it is important that reasonable initial sizes be entered as the stiffness of these members does influence the distribution of the forces within the superstructure. Disproportionately large cross-frame/diaphragm members will draw larger forces, which may result in having to increase the sizes of these members even further. It is best to start with smaller member sizes and then increase the sizes from there as necessary.

Preliminary sizes for cross-frame members can be obtained based on the permitted slenderness ratios specified for tension and compression members specified in *AASHTO LRFD* Articles 6.8.4 and 6.9.3, respectively. In general, single angles, or when necessary, structural tees, are preferred for cross-frame members. Double angles are more expensive to fabricate and painting the backs of the angles can cause problems. Reasonable preliminary sizes for cross-frame/diaphragm members can also be obtained based on past experience with similar designs. Should cross-frame or diaphragm member sizes need to be changed significantly based on the results of an initial analysis cycle, these changes should be reflected in the next analysis cycle. As small changes in size (e.g. one or two shapes in the shape tables) are unlikely to have a dramatic effect on the overall analysis results, some

amount of engineering judgment and experience is required to determine when changes should be made.

9.   AASHTO/NSBA Steel Bridge Collaboration. 2006. "Guidelines for Design Details, G1.4" National Steel Bridge Alliance, Chicago, IL.

2.4.3.1.4.5 Lateral Bracing

According to Article 6.7.5.1 of the *AASHTO LRFD* Specifications, the need for lateral bracing is to be investigated for all stages of assumed construction procedures and the final condition. For steel I-girder bridges with multiple girders, lateral bracing may be placed in the plane of either the top or bottom flanges, or in both planes. The investigation of the need for lateral bracing in an I-girder bridge is primarily related to control of deformations and the cross-section geometry during construction; that is, during the erection and the placement of the concrete deck. It may be found to be particularly useful during construction in resisting lateral wind loads prior to the hardening of the deck. *AASHTO LRFD* Article 6.7.5.1 points out that lateral bracing may also be utilized for the transfer of lateral wind and seismic loads to the bearings, presumably in the final condition.

Figure 2.47 Lateral Bracing

Lateral bracing has been sometimes placed in the plane of the bottom flanges of multiple I-girder bridges, typically in the outer bays, and designed to act as a truss between girder flanges to resist wind load and to transfer lateral wind loads to the bearings when the bridge is in its final condition. In fact, up until 1979, the AASHTO Standard Specifications required that for all plate-girder bridges with spans of 125 feet or longer, some lateral wind bracing must be provided at the bottom-flange level.

This requirement was replaced by an empirical procedure to determine the need for bottom lateral bracing to resist the wind loads. It was observed that the lateral wind force is resisted primarily by the cross frames/diaphragms, which transfer the force to the deck. The deck, in turn, resists the wind forces mainly in diaphragm action. At the bearings, the force is then removed from the deck via the cross frames/diaphragms to the laterally restrained bearings. This design procedure permits elimination of the costly bottom lateral bracing in many I-girder bridges for that reason. However, lateral bracing is sometimes useful for additional purposes, as discussed below.

The 1979 empirical procedure for lateral bracing design was not brought forward to the LRFD Specifications. Instead, the provisions require that the Engineer investigate rationally the potential need for lateral bracing in I-girder bridges for the stated conditions. In longer continuous-span bridges, lateral bracing may be used to stabilize girders during erection and to provide truss-type stiffness to resist wind during erection stages. In some instances, the contractor may choose to use a type of temporary lateral bracing for these purposes. Often the temporary bracing is made of tensioned cables configured in an X-pattern.
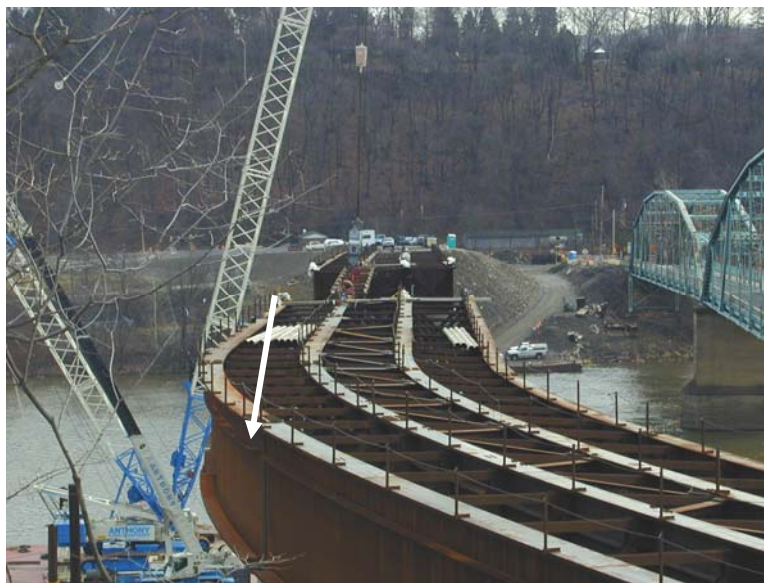
Figure 2.48 Top Flange Lateral Bracing

It has been observed that a single plane of top flange lateral bracing contributes little to the behavior of the bridge after the deck has hardened. In fact, removal of top lateral bracing members may be expensive and problematic if bolted to the top flange. One-inch (±) thick fill plates (between the gusset plates and the underside of the top flange) may be used to keep clear of stay-in-place form installation. However, if top plane lateral bracing members are left in place, they may be difficult to maintain, which may be one reason to consider a system of more easily removable temporary lateral bracing in some cases.

In a finished composite structure, top flange lateral bracing is subject to much lower live load forces and the effect of top lateral bracing members on the

overall behavior of the composite structure can generally be ignored should the bracing be left in place after construction of the bridge is completed. However, top flange lateral bracing may have an effect on the noncomposite girder behavior by causing significant lateral flange moments in the top flanges depending on the configuration of the bracing pattern, as discussed in more detail below.

Bottom flange lateral bracing creates a pseudo-closed section formed by the I-girders connected with the bracing and the hardened concrete deck. As a result, the lateral bracing members connecting the bottom flanges generally are subject to significant live load forces and should be considered primary members. For this reason *AASHTO LRFD* Article 6.7.5.1 states that if permanent lateral bracing members are included in the structural model used to determine live load force effects, they must be designed for all applicable limit states and be considered primary members. The addition of bottom flange lateral bracing usually causes increases in cross-frame/diaphragm forces in straight girders since the cross-frames/diaphragms are acting to retain the shape of the pseudo-box section. By retaining the shape, de facto, the girders with the lateral bracing tend to deflect the same amount. This leads to a reduction in the difference in moments. Thus, the exterior girder, which is usually the higher stressed girder, experiences a lesser moment (and lesser deflections) when bottom-flange lateral bracing is employed. This modified behavior is not recognized by the live-load distribution factors provided in the LRFD Specifications. Also, depending on the configuration of the bracing pattern, as discussed below, the bracing may induce significant lateral bending moments in the bottom flanges in some cases. Since bottom flange lateral bracing carries significant live load, it must also be detailed very carefully with respect to fatigue if it is left in the finished structure.

The lateral bracing configuration and connection details deserve considerable attention. Arrangement of the bracing is important. A single member per bay is usually adequate. A bay is typically defined as the distance between cross-frames where wide cross-frame spacing leads to long bracing members. Arranging the lateral bracing members in a Pratt truss pattern is usually desirable over the Warren truss pattern. The reason being that only one Pratt truss member applies force against the flange at a cross-frame. The top chord of the cross-frame and the lateral flange bending resist the force in the lateral bracing member. The Warren Truss pattern applies the force from two lateral bracing members at the intersection increasing lateral flange moments and top chord forces.
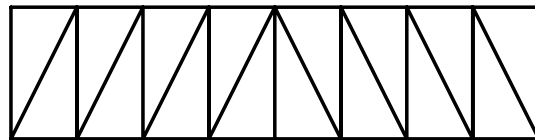
Figure 2.49 Pratt Truss Lateral Bracing Pattern
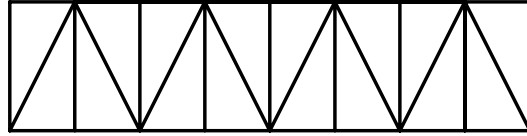
Figure 2.50   Warren Truss Lateral Bracing Pattern

The most desirable connection of lateral bracing members to the girders is to bolt the gusset plates to the flanges. Welding of the connection plates to the flanges or the web typically results in a fatigue Category E detail with a very low fatigue resistance. Also, as discussed in *AASHTO LRFD* Article 6.6.1.3.2, to minimize the effect of out-of-plane distortion stresses on the fatigue resistance of the base metal adjacent to the welds when the connection plates are attached to the web, the connections must be carefully detailed, as the lateral bracing members can be subjected to significant design forces.   As a result, bolting the gusset plates directly to the flanges is the highly preferred alternative.   Further discussion on the design of lateral bracing members and their connections is given in DM Volume 2, Chapter 2, Sections 2.2.3.6.1.2, 2.3, and 2.4.   Additional information on recommended lateral bracing connections and details is given in Reference 9.

Figure 2.51 Bolted Gusset Plate

AASHTO LRFD Article 6.7.5.2 deals specifically with lateral bracing requirements for I-section members. The only requirements in this article are that continuously braced flanges, such as those encased in concrete or anchored to the deck by shear connectors, do not require lateral bracing, and the need for lateral bracing adjacent to supports of I-girder bridges to provide stability during construction should be considered.

The primary function of lateral bracing in multiple I-girder bridges is to control the geometry and provide stability to the bridge superstructure during erection and placement of the concrete deck. The application of composite design to girders has

in effect created at least two structures. The first is the noncomposite structure that supports its own weight and at least some of the weight of the wet concrete deck prior to its hardening. Hardening of the concrete adds another very stiff element to the bridge, i.e. the deck. The deck acts with the steel in resisting longitudinal bending moments applied subsequently. However, the deck also acts as a very stiff diaphragm that ensures that the top flanges of the girders act nearly in unison (except for shear lag). Of course, this has always been the case, but before composite design was employed, the steel girders were designed to resist all loads without the assistance of the deck in longitudinal bending. Thus, the girders were usually stronger and stiffer than their composite counterparts. Prior to the wide acceptance of welding for bridges, stringer bridges were usually rolled shapes. Longer spans were designed as girder-stringer bridges. The girders were riveted and the stringers between the girders were rolled shapes. Welded beams worked well as composite girders and came into common usage in much longer-span multi-girder bridges that replaced the girder-stringer noncomposite bridges.

Figure 2.52 Riveted Girder and Floorbeam with Rolled Stringers

Early American bridges were designed and built by bridge companies. After World War II, the bridge consulting engineering firms completely took over the design function from the builders. However, contractors generally maintained an engineering function and performed what today is generically referred to as construction engineering. The consulting firm designed the completed bridge and the contractor dealt with the construction issues. Soon, the design and construction functions were completely separated as owners contracted for the design and construction separately. Today, the more elaborate structures, such as trusses, arches, and cable-stayed bridges are constructed by contractors who retain a consulting engineering firm to perform the construction engineering for the project. The more routine girder bridges are often built with little construction engineering.

The use of high-performance (higher-strength) steels, wider girder spacings, longer girder spans, and complex geometry has subtly led to the need for the application of

construction engineering in the building of many stringer bridges. The tradition of consulting firms not employing construction engineering during design, combined with the trend of contracting firms to ignore it in the building of modern steel stringer bridges, has led to a litigious no-man's land in many cases. At some point the Owner, Engineer, and contractor need concurrence with regard to responsibility for temporary conditions during construction. Often, it is nearly impossible for the designer to anticipate construction conditions and to control the building of the bridge. The LRFD provisions do assign certain responsibilities, however, to the Engineer (refer to *AASHTO LRFD* Article 2.5.3).

In a steel I-girder bridge, the presence of cross-frames or diaphragms alone does not necessarily ensure that the girders are adequately braced against lateral-torsional buckling. Unlike building columns, which are restrained against the ground by gravity and cannot translate longitudinally with respect to each other, girders in steel I-girder bridges are often free to translate longitudinally with respect to adjacent girders when the deck is not present. This negates one of the requirements for girder stability, i.e., girder planes remain in a plane. Longitudinal restraint provided by the bearings provides some restraint against both twist and longitudinal deflection of the girders. However, often the cross-bracing alone is inadequate to restrain the girders longitudinally and failure of the entire cross-section of girders in lateral-torsional buckling can result.

Figure 2.53 Failure of Girders During Construction

Lateral flange bracing is a sure means of preventing such a failure of the girders prior to hardening of the concrete deck. Lateral bracing between at least one pair of girders in one or more panels adjacent to the supports can provide the necessary shear restraint to prevent the rectangle formed by the girders and cross-bracing from changing shape into a dangerous parallelogram as the girders translate with respect to each other. For continuous-span bridges, such bracing might only be necessary

adjacent to interior supports. In other cases, provision of adequate lateral bracing at other locations is often warranted.

Should the bridge be constructed by incremental launching, lateral bracing will likely be required in one or more bays along significant portions of each span in order to provide the necessary geometry control of the bridge cross-section during the launch.

For smaller-span straight bridges, cross-frames or diaphragms acting alone in plan with the girders through Vierendeel truss action may be sufficient to prevent longitudinal translation of the girders. As mentioned above, locking girders against longitudinal movement during erection is typically employed to accomplish the same objective.

AASHTO LRFD Article C6.7.5.2 suggests that lateral bracing be considered to prevent significant relative horizontal movement of the girders in spans greater than 200 feet and to control wind induced girder stresses. However, individual circumstances, such as horizontal curvature, skew, or high wind loads acting on the noncomposite structure, may warrant the inclusion of some lateral bracing for smaller spans. Removing the lateral bracing at some point during (or after) the construction at the Owner's discretion is an option. If added by the contractor, it is usually required that it be removed. However, even if temporary lateral bracing is used, the method used to analyze the bridge system regarding design and removal of the lateral bracing must properly recognize it.

Although flange lateral bracing is not particularly effective for transferring lateral wind loads in the final condition when the bridge is composite with the deck, lateral bracing can provide a significantly stiffer load path for wind loads acting on the noncomposite structure during construction. Lateral bracing markedly reduces the lateral deflections and flange lateral bending stresses due to wind load acting on the noncomposite bridge system. One or two panels of lateral bracing adjacent to a support (preferably in the plane of the top flanges) can provide an effective line of support at the cross-frame or diaphragm line within the span where the lateral bracing terminates, thereby reducing the effective span length resisting the lateral wind loads. Large lateral deflections are undesirable during construction and could potentially result in damage to the bearings. At least one state DOT limits the maximum lateral wind load deflections in the final erected noncomposite structure during construction under an assumed design wind pressure. An approximate approach to determine how many panels of lateral bracing, if any, might be necessary to reduce lateral wind load deflections during construction to an acceptable level is presented under Constructibility Verifications in DM Volume 2, Chapter 2.

2.4.3.1.5 Box Girders

2.4.3.1.5.1 Introduction

This section of the manual will discuss additional issues that are specific to the preliminary design of steel box-girder bridges; namely, the selection of the type of

girder (tub girder or closed box) and girder cross-section (multi-box or single box), and the layout of the framing plan -- including the spacing and configuration of internal and external cross-frames/diaphragms. Also discussed will be issues related to the design of the top-flange lateral bracing for tub girders, and issues related to the selection of bearing arrangements and the type of deck. Proportioning of the flange and web plates for box girders is discussed in DM Volume 2, Chapter 2, Section 2.2.4. Further information regarding the design of the bracing members and their connections may be found in DM Volume 2, Chapter 2, Sections 2.3 and 2.4.

Box girders provide a more efficient cross-section for resisting torsion than I-girders, and are particularly advantageous for horizontally curved superstructures because of this high torsional resistance. The main advantage this torsional resistance provides is that each box section is more able to carry the load applied to it rather than shifting load to the girder on the outside of the curve, as is the case for torsionally weak I-girders. The tendency to more uniformly share gravity loads reduces the relatively large and often troubling deflection of the girder on the outside of the curve. Box girders are able to resist the applied loads often without the extensive use of permanent cross-frames/diaphragms between the girders. These members are required in I-girder bridges to shift load between the girders. Erection costs of box girders are often less because the erection of one box girder in a single lift is equivalent to the placement and connection of two I-girders. Box girders are also inherently more stable during erection and may often be erected with fewer cranes than I-girders, which often require more cranes to provide stability to the girders until they can be braced by their neighbors. Because of their smooth uninterrupted profile, steel box girders are also aesthetically pleasing and are often employed because of their aesthetic qualities. When a single box girder is used, there is of course no visible bracing.

Steel box bridge members have been used in large trusses and straddle beams since at least the 1930s. Early box members were built up of four plates riveted to four hot-rolled angles. Access holes were provided for riveting. More recently, however, welded steel box girders, which were not practical until welding became acceptable for connecting major bridge elements, replaced riveted members. The first welded box girder bridges in America were probably constructed in Massachusetts in the 1950s. They were made up of four plates welded into a rectangular box. The two bridges that were constructed had rather severe horizontal curves, which was most likely the reason that the torsionally stiff box sections were used. At that time, behavior of open curved sections was not well understood. Analysis of curved closed-box sections could be done more confidently, although warping behavior was often not explicitly considered. Closely spaced internal cross frames were used in the early box girders to control and minimize warping. Inspection of the Massachusetts box-girder structures in the late 1980s showed the interiors of the boxes to be in pristine condition after more than 30 years of service in the relatively harsh New England environment.

It was likely observed that the amount of steel required for these bridges was excessive. New York State designed two box-girder bridges in the western tier of the state in the early 1960s. The designs employed lateral bracing between the top flanges of the individual boxes in the positive-moment regions. Hence, the boxes in

these regions were actually tubs with top flanges. The torsional shear was resisted by a pseudo-box section created by the addition of top-flange lateral bracing members. The lateral bracing was simply designed by resolving the force due to the torsional shear flow into the individual lateral bracing members.   Interestingly, the portions of the girders in the dead load negative-moment regions of these continuous-span bridges over the interior supports were closed-box sections built up from four plates. Perhaps the large torsion at the supports was believed better handled with a solid top plate, or perhaps the non-composite behavior in those regions was of concern. One of the bridges was field tested at the time of construction to confirm its behavior. In the 1990s, the bridge was field tested again and a refined analysis was performed; both confirmed that the original design was appropriate.

All of these early bridges were designed having radial supports. They used either two bearings or a wide rubber bearing at each support so that it could be assumed that most of the torsion would be resisted at supports by the bearings rather than by the diaphragms between the girders. Adequate internal bracing was used to ensure that the boxes did not distort to such a degree that the adequacy of the closed-section analysis could be disputed.

The smooth appearance of tub girders fabricated from welded plates soon became popular with both the public and Engineers. As with I-girders and other bridge types, tub girders were found susceptible to fatigue cracking when not properly detailed. For example, some longitudinal tub girders were welded to transverse box members without fully appreciating the implications of fatigue. As with many technological advances, the application preceded full investigation and improper detailing led to early fatigue cracking in some of these bridges. The result was that the zeal for steel tub-girder bridges cooled substantially.

In the early 1960s, Vlasov solved the problem of warping in a closed box subject to non-uniform torsion (10). The solution showed the relation between the transverse bending in the box webs and flanges and the internal bracing spacing. Similarly, the relation between internal bracing and longitudinal warping stresses and distortional shears was also presented. Dabrowski followed by developing equations to predict the distortional shears and stresses (11). In 1968, Wright et al wrote a paper describing how the Vlasov solution for the box-girder problem was analogous to the Beam-on-Elastic-Foundation (BEF) problem (12). This meant that cross frame forces and through-thickness bending stresses in the box plates could be computed using well-established equations. A series of charts permitted semi-graphical solutions. The work was given wider distribution via a Bethlehem Steel publication authored by Heins and Hall (13). This work provided more confidence in predicting the behavior the design of box-section members. A further advance was the application of finite-element analyses to box girders that addressed their distortion as a whole structural unit. As a result, the fatigue life of weldments could be better quantified. One result of these efforts has been identification of fatigue-critical areas where bolting rather than welding is usually employed on box sections.

Design provisions for straight composite steel tub girders were first introduced in the 10th Edition of the AASHO Bridge Specifications dated 1969. These provisions,

developed as part of a joint effort between the American Iron and Steel Institute (AISI) and the University of Washington, were based on analytical work as well as some model tests. The provisions applied solely to tangent multi-box cross-sections. By implication, skewed supports were not considered. Torsion was implicitly considered and recognized in the distribution of live loads, but was thought to be insignificant in the design of tub girders based on the parameters covered by the research and limited in the specifications. The capacity of the bottom plate in compression was based on classical plate buckling equations (14). Special wheel-load distribution factors were developed to assign live load to the tub girders (15). To ensure that the wheel-load distribution factors were applied within the limits of the research study from which they were developed, limits were placed on the cross-section within the provisions.

Design provisions for horizontally curved box girders were included in the first edition of the AASHTO Guide Specifications for Horizontally Curved Bridges dated 1980. These provisions considered more general design parameters. Torsion was explicitly considered. However, skewed supports were not specifically addressed, although clearly skewed supports create more torsion than does curvature in many typical bridges. This does not imply that skewed supports could not be considered within these provisions, but they clearly did not recognize the criticalness of skews. The original allowable stress design provisions were developed under the Consortium of University Research Team (CURT) Project, which was under the direction of the FHWA, a group of state DOTs, and industry representatives (16). The Guide Specifications also included Load Factor Design provisions, which were developed separately under AISI Project 190 (17). The bridge cross-section was not limited in the curved-girder provisions; instead, a rational analysis was required to distribute the loads. Box flange plate capacity was again based on classical plate buckling equations, only including the effect of shear stress (18). (Note: a box flange is explicitly defined in AASHTO LRFD Article 6.2 as a flange that is connected to two webs). The consideration of torsion implied consideration of forces developed in internal cross frames and lateral bracing, as well as bracing between adjacent girders. Since consideration of distortional stresses was also required by these provisions, the computation of the distorsional warping stiffness of the box sections became necessary. This could be determined directly by finite-element analysis or by using the BEF analogy. Torsional moments resulting from the superstructure analysis could be used in conjunction with the BEF analogy to compute cross-frame forces as well as through-thickness bending stresses due to cross-section distortion.

There were several failures of major steel box bridges around the world, generally during construction, which demonstrated that these bridges were not without their concerns. The British formed a special commission called the Merrison Commission to investigate these failures. From the work of that commission came the Rules by the same name. These new rules were extremely conservative in their attempt to ensure that no additional failures of box- girder bridges would occur. When applied literally, the rules ensured that no such bridges would fail because they would be too expensive to build. This conundrum prompted a major research project in Britain, which included both analytical studies and supportive testing. The research, completed in about 1980, resulted in the development of the modern BS54 box-girder design provisions.

In the late 1970s, the FHWA formed a task force to develop a new American design specification, specifically for steel box-girder bridges. The firm of Wolchuk and Mayrbaurl developed the Proposed Design Specifications for Steel Box Girder Bridges in 1980 (19). The vast majority of this work was derived from the British research. Although the proposed specifications were mainly directed toward larger box girder bridges than were typically built in the United States, it has been employed in the design of several bridges in the U.S.

The 2003 AASHTO Guide Specifications for Horizontally Curved Steel Girder Highway Bridges employed much of the earlier work from the 1980 AASHTO Guide Specifications. These specifications were developed by BSDI, Ltd. and Auburn University under the direction and sponsorship of the National Cooperative Highway Research Program (NCHRP), and include Load Factor Design provisions only (20). Several refinements were introduced in these provisions related specifically to tub girders. Shear connectors were required to be designed for torsional shear as well as vertical bending. The connectors were also to be designed for transverse shear forces. These provisions also included special considerations for box girders during construction.   Single-box and composite closed-box cross-sections were also covered more extensively than in any previous AASHTO provisions.

The design provisions for straight and horizontally curved box girders were unified for the first time in the Third Edition of the AASHTO LRFD Specifications. The specific provisions are covered below and in DM Volume 2, Chapter 2, Section 2.2.4.

2.4.3.1.5.2 Fundamental Behavior of Box Girder Bridges

Figure 2.54 shows qualitatively the deformations of a box section due to vertical (bending) and torsional loads. The deformations include vertical deflection due to flexure (Figure 2.54a), rotation or twist due to torsion (Figure 2.54b) and cross-section distortion due to torsion (Figure 2.54c).

(a) Vertical deflection due to flexure

(b) Rotation due to torsion

(c) Distortion due to torsion
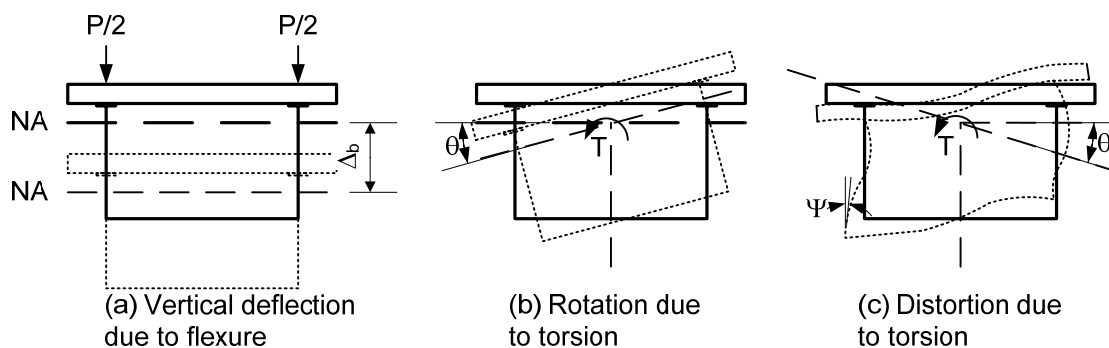
Figure 2.54 Box-Section Deformations due to Vertical and Torsional Loads

Figure 2.55 shows in simplistic fashion how a vertical load applied away from the shear center of the box can be separated into bending (Figure 2.55a) and torsional (Figure 2.55b) components based on the principle of superposition.
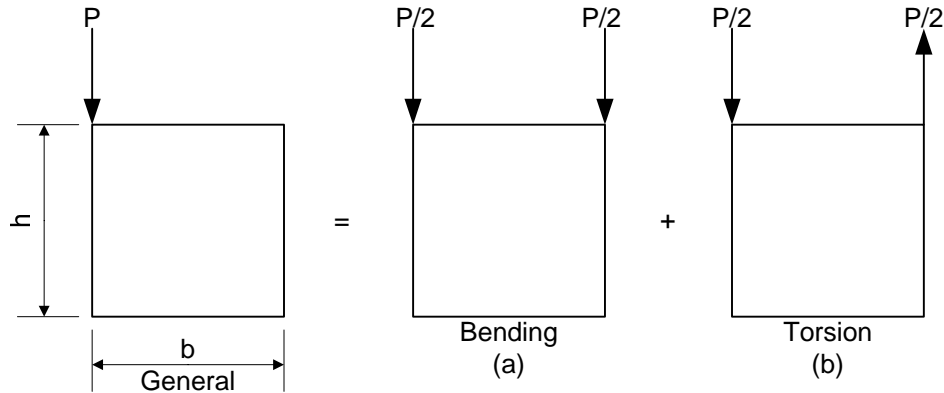
Figure 2.55 Separation of Vertical Load into Bending and Torsional Components

Figure 2.56 shows how the torsional load can be further separated into pure torsional (Figure 2.56a) and distortional (Figure 2.56b) components.
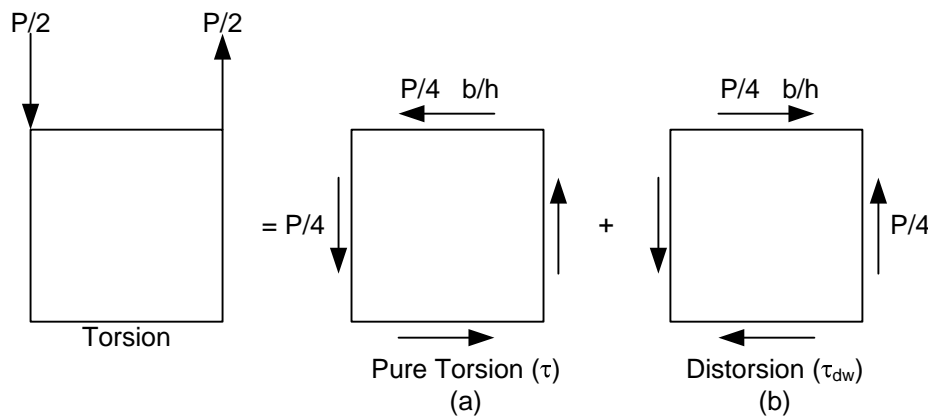
Figure 2.56 Separation of Torsional Load into Pure Torsion and Distortion Components

The bending and torsional components result in three normal stresses, four shear stresses and one through-thickness bending stress, as illustrated in Figure 2.57.
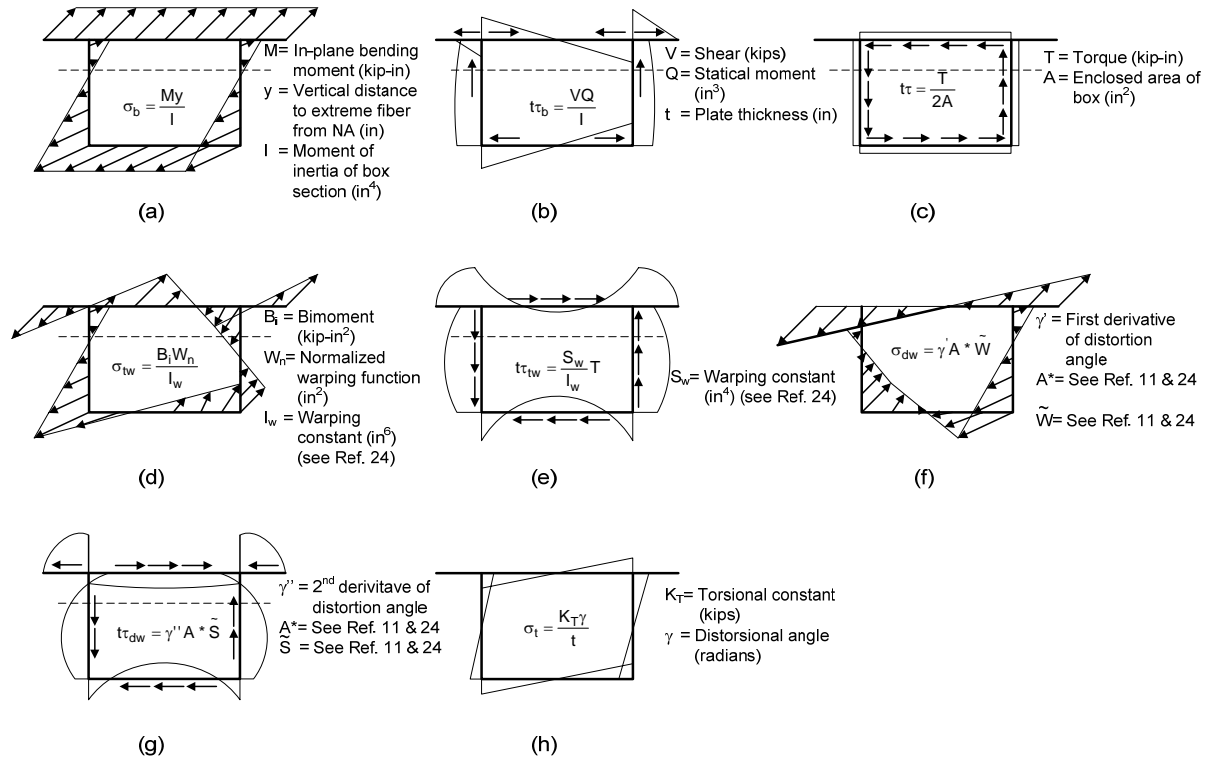
Figure 2.57 Box-Section Stresses due to Bending and Torsional Components

Figure 2.57a and Figure 2.57b show the normal stress and shear flow, respectively, due to bending of the box section about the major axis. Figure 2.57c shows the pure torsional or St. Venant torsional shear flow, which is a function of the box wall thickness and the reciprocal of the enclosed area of the box (see Equation 2.6 below). Figure 2.57d and Figure 2.57e show the normal stress and shear flow, respectively, due to warping torsion (see DM Volume 2, Chapter 2, Section 2.2.3.1.2 for a further discussion of St. Venant and warping torsion). The warping torsional constant for closed-box sections is approximately equal to zero; therefore, shear and normal stresses due to warping torsion are typically quite small and are usually neglected for closed-box sections (i.e. box sections composed of four steel plates, pseudo-box sections composed of tub sections closed at the top by a system of lateral bracing members or tub sections with top lateral bracing and a composite concrete deck). Thus, the primary torsional resistance mechanism in box sections consists of the St. Venant torisonal shear flow around the closed section. Figure 2.57f, Figure 2.57g, and Figure 2.57h show the stresses associated with distortion of the box cross-section; that is, normal distortional warping stress, distortional warping shear flow and distortion transverse bending (i.e. through-thickness) bending stress, respectively, resulting from the torsion. The stress diagram shown in Figure 2.57h shows the transverse bending stresses in the outside fiber of the box components. These distortional stresses basically occur because the section is not perfectly round. The shear flow must change direction at the corners, which tends to warp the section. If the section were round, the distortional stresses would be zero.

The amount of the warping is related primarily to the amount of distortion in the cross-section of the box. Warping due to distortion of the cross-section creates normal (longitudinal) stresses and associated shearing stresses termed distortional warping stresses (Figure 2.57f and Figure 2.57g). In addition to the warping stresses, transverse bending stresses through the thickness of the flanges and webs also occur (Figure 2.57h). The transverse bending stresses are associated with the shear flow vector changing direction. Since torsion is not mitigated along the section, the section tends to continue to distort and warp until interrupted. In closed-box and tub girders, this interruption is accomplished with intermediate internal cross-frames or diaphragms. These members provide quite rigid restraint against movement of the four corners of the box with respect to each other; hence, restoring the box to its original shape. Astute location of these braces controls the distortion and associated warping actions.

The work required of the cross-frame or diaphragm members is a function of the applied torque, cross-frame spacing, and the torsional stiffness of the box. The warping stresses are a function of the same parameters. The longitudinal warping stresses are largest at the corners of the box section where critical welded details are often located, and according to the specification, must be considered when checking fatigue (*12*). *AASHTO LRFD* Article 6.11.5 requires that these stresses be considered for fatigue in certain specific cases by adding the magnitude of the range of live load longitudinal warping stresses to the magnitude of the range of the live load major-axis bending stresses. Adequate internal cross bracing usually controls the magnitude of these stresses in boxes of typical proportion such that they are not critical to the ultimate resistance of the box section at the strength limit state. *AASHTO LRFD* Article 6.11.5 also requires that the range of transverse bending stresses be considered in these same cases when evaluating the fatigue resistance of the base metal adjacent to flange-to-web welds and adjacent to the termination of fillet welds connecting transverse elements to webs and box flanges. The calculation of distortional stresses and stress ranges, along with the specific cases for which these stresses must be considered for fatigue, are discussed in greater detail in DM Volume 2, Chapter 2, Section 2.2.4.6.1.1.1.

Composite box girder bridges are actually designed as two different constructions; noncomposite and composite. The noncomposite case may be separated into two different cases; cross-sections composed of girders that are not connected to adjacent girders, and cross-sections composed of girders that are connected to adjacent girders via cross-frames or diaphragms. The composite bridge can also be separated into similar cases.

Torsion is generally introduced into bridge girders by three different means. The first is application of vertical or lateral loads not passing through the shear center of the cross-section. This includes essentially all dead, live, and wind loads. The second is through horizontal curvature of the girders. The third is through the bearings or supports. A single bearing will resist little torsion and stability must be obtained at other bearing points with more than one bearing or by cross-frames or diaphragms attaching the girder to adjacent girders. Conversely, a pair of bearings on a skewed support can introduce substantial torsion into a box girder. The bearing nearest the span receives greater load than does the rear bearing; hence, a torque is introduced

by the presence of unbalanced loads with respect to the shear center of the section. Connections between the boxes tend to restore the girder to its original position. As a result, the forces in these cross frames/diaphragms are often referred to as restoring forces.

The composite box girder is subjected to torsion by similar means. However, it resists torsion in a much different manner than a torsionally weak I-girder. The concrete deck acts to restore the box girder by distributing torsion as well as flexural loads to adjacent girders. The deck of a multi-box-girder bridge acts similar to the deck of a multi-I-girder bridge in that load is transferred by horizontal shear as well as by flexure in the deck. However, the deck of a box-girder bridge is also subjected to the horizontal shear due to the shear flow in the box. Hence, it is particularly important to check the deck reinforcement for these additional shear forces.

2.4.3.1.5.3 Type

Although the design of composite closed-box sections used as primary longitudinal flexural members is covered in the AASHTO LRFD Specifications, there are few such closed steel box girder bridges built in the U.S. today due to the cost of the necessary safety requirements for a welder to be inside of a closed box. Therefore, the configuration of steel boxes has migrated toward the tub girder. Early tests and experience have shown that the corrosion of the inside surfaces of closed steel box sections caused by the limited oxygen and water present in the entrapped air is of little consequence. The sections need not be hermetically sealed to prevent corrosion of the interior if provision is made for drainage and air circulation to reduce the likelihood of condensation. Tub girders cannot be completely sealed because moisture may enter through inevitable cracks in the concrete deck. However, corrosion of the interior has been shown to be minimized when provisions are made for adequate drainage and ventilation of the interior.

Another reason that tub girders tend to dominate the scene in the U.S. is their inherent economy. The wide spacing between the webs at the top of economical tubs would be very expensive to close with a steel plate. Tub girders with inclined webs also allow for the use of a narrower more economical bottom flange plate while enjoying the advantage of a wider spacing of the webs supporting the deck.

An exception to tub girders is a steel box straddle beam often employed to provide support, while also providing the necessary underclearance. In these cases, closed steel box girders are found to be very economical. Usually straddle-beam boxes are relatively narrow; typically less than four feet wide. If there is adequate vertical clearance, the longitudinal girders can be supported on the box with traditional bearings. If adequate vertical clearance is not available, the girders are designed to abut or penetrate the box straddle-beam. Steel straddle beams provide an advantage over concrete straddle beams in that they may be erected quickly with minimal traffic interruption, as is commonly associated with a concrete straddle beam. However, if the girders abut or penetrate the box, they are even more quickly erected than a similar detail with a concrete straddle beam. To maintain the advantage of avoidance of shoring provided by utilizing a steel straddle beam, it is necessary to plan for the erection of the girders. Possible alternative fabrication

procedures for the closed boxes are discussed in Reference 40. The design of such straddle beams is assumed covered by the AASHTO LRFD Specifications.

Multi-cell single steel boxes are rarely employed and are not covered in the AASHTO LRFD Specifications. One of the few such structures in the U.S. is the ramp structure on the western side of the Fort Duquesne Bridge in Pittsburgh, Pennsylvania, which was constructed in the late 1960s. There have been few, if any, of these structures built since that time. Analysis of the multi-cell single box requires consideration of the torques in adjacent cells and the complex addition of torsional and flexural shears. Fabrication, shipping and erection of these structures are also difficult. The use of a nearly full-width bottom flange required by these structures is almost never economical. As a corollary, the fewer the number of boxes and the narrower the boxes, the more economical the cross-section.

Single box cross-sections are often chosen for prestressed concrete bridges for the simple reason that they are economical. A number of single-box steel bridges have also been built in the U.S. As with prestressed concrete, they have been generally found to be very economical when compared with cross-sections composed of two or more boxes. In some situations, they can be competitive with multi-stringer I-girder bridges. One of the drawbacks to their wider use may have been the lack of their treatment in the AASHTO Standard Specifications. The work that led to these provisions was intended to limit design to box girders that did not require consideration of torsion in their design. These Specifications state specifically that the wheel-load distribution factors given are only applicable to cross-sections with two or more single-cell composite box sections. Fortunately, the 1993 and 2003 AASHTO Guide Specifications for horizontally curved steel bridges have no such specific cross-sectional limitations. These curved-girder provisions require a rational analysis that is capable of addressing curved or tangent bridges. Thus, a single-box cross section that inherently must resist torsion is acceptable. The AASHTO LRFD Specifications permit the use of single box cross-sections with no limitations. These provisions require that shear due to St. Venant torsion and transverse or through-thickness bending and longitudinal warping stresses due to cross-section distortion must be considered for single-box sections. The economy of a single box comes from several facts: There are fewer pieces to fabricate and erect; there are two fewer webs for each box girder eliminated; a single box resisting all of the dead load is less affected by fatigue considerations than would be the case with more boxes, each with less dead load; and the substructure supporting a single box is more economical than a wider redundant pier and foundation required for more than one box girder.

As with prestressed concrete box-girder bridges, a transversely post-tensioned concrete deck may be used when large deck overhangs or girder spacings are employed. A bridge width too great to be built with a single box can be designed with more box girders, again, as would be the case with prestressed concrete box girders. Such a bridge was built in Canada (Macmillan Yard, Toronto) having a deck nearly 100-feet wide supported on two steel boxes, with a clear span between the boxes of about 30 feet and 15-foot overhangs. This vaulted deck was transversely post-tensioned. Vaulting, again as with prestressed concrete box girders, permits straight (undeviated) transverse strands to work in both positive and negative

bending. This particular bridge was bid successfully against a similar post-tensioned segmental concrete design. If the cross-section configurations of competing concrete and steel box girder bridges are similar, then properly designed steel is competitive with concrete. The converse is also true: A two-box steel bridge cannot compete with a single-box concrete bridge. A recent example is the Four Bears Bridge across the Missouri River in North Dakota. There are no examples of a two-box concrete bridge competing with a single-box steel bridge. The Storrow Drive Bridge across the Charles River in Boston is a good example of a recent steel single-box bridge carrying a wide deck (approximately 80 feet in width). The deck on this bridge is supported on transverse beams and is not post-tensioned.

The issue of redundancy of single box bridges has been raised. If some longitudinal strands in a concrete single-box bridge fail due to the bridge being struck, or due to corrosion, failure could possibly occur due to the unbalanced prestressing force in combination with gravity. If a steel single-box bridge is struck, its ductility is likely to prevent failure. If a brittle fracture should occur in the steel of a single box bridge, failure could possibly occur due to overstressing of the section at the piers. However, modern bridge steels have proven to be quite ductile and no brittle fractures have been reported in these modern materials that are twenty years or less in age.

2.4.3.1.5.4 Bearing Arrangement

The arrangement of bearings can have a significant influence on the design of box girders. A single bearing centered over the shear center at a support minimizes the torque resisted by that support. The torsion due to vertical load is removed from the box at such a support via the cross-frame(s) or diaphragm(s) connecting the box to its neighboring box(es). As specified in AASHTO LRFD Article 6.11.1.2, if single bearings narrower than the bottom flange are used, they are to be aligned with the center of the box and all other supports must have adequate resistance against overturning under any design load combination. As specified in AASHTO LRFD Article 6.11.1.2, double bearings may be placed between or outboard of the webs. Placing the bearings outboard of the box reduces overturning loads on the bearings and reduces uplift reactions. Wide box spacing, large overhangs, and curvature all can create large uplift forces in addition to the uplift issue related to skewed supports. Uplift should generally be checked ignoring the effect of any future wearing surface to ensure that parapet loads on the overhang do not cause uplift that would only be resisted by a future wearing surface.

If a support has a pair of bearings, the torque resisted by the pair may be rather large. If a two-bearing support is skewed, the lead bearing is loaded heavier than the rear bearing, thus introducing torque. In single-box sections, significant torsional loads may occur during construction as well as under live loads. Live loads positioned near the extremes of the deck can cause critical torsional loads without causing critical flexural moments. Therefore, live load positioning must be investigated for both flexure and torsion. It is important to recognize the position and configuration of the bearings in such analyses in sufficient completeness to permit direct computation of the reactions.

Orientation of guided bearings can usually be addressed in a manner similar to I-girder bearings. Note that in lieu of bearings, integral cap beams of steel or concrete are often used with box sections.

2.4.3.1.5.5 Spacing and Configuration of Internal and External Cross-Frames and Diaphragms

2.4.3.1.5.5.1 Internal Cross-Frames/Diaphragms

This discussion is based on the assumption that the top of the box or tub is closed by either a steel plate or adequate lateral bracing. Hence, the box girder is treated as a closed section since shear can flow around the section. The shear center is located within the closed section. Torsion is the main load effect controlling the spacing and stiffness of internal diaphragms or cross-frames. Unlike moment that varies along the girder, torque remains relatively constant over the girder length until the girder is torsionally restrained. The magnitude of torsional warping is related to the magnitude of the torque and the amount of distortion in the cross-section of the box; i.e., warping increases as the box becomes more susceptible to cross-sectional distortion. Internal cross-frames are the usual means of controlling the distortion.

As specified in AASHTO LRFD Article 6.7.4.3, intermediate internal cross-frames/diaphragms are required in box-section members if there is much torsion. A simple X-brace will restrain the relative position of the four corners of the box minus the elastic shortening of the bracing members. However, the webs and flanges distort due to transverse bending introduced by the torque and the cross-bracing. Wright et al (12) showed that the equations for the cross-section distortion and restraining cross-frame members are analogous to those for a beam on an elastic foundation. The bending in the webs and flanges is analogous to the flex in the beam so supported, while the cross-frame members are analogous to the supports. The cross-frame is typically attached to transverse stiffeners serving as connection plates that are attached to the web and to the top and bottom flanges. Hence, the web at the cross-frame is stiffer than the web alone. The bottom flange is not typically stiffened transversely unless a bottom transverse member is provided within the internal cross-frames. These transverse elements would be typically welded to the flange or attached to the longitudinal flange stiffeners (if present) by bolting. Without such stiffening, the bottom flange plate is more flexible that the web and will distort more. In certain situations, this sharp discontinuity in stiffness can cause significant through-thickness transverse bending fatigue stresses (due to cross-section distortion) at the end of the vertical connection plates. Through-thickness transverse bending stresses are most critical in cases where the applied torques are significant; e.g. boxes resting on skewed supports.   Steps that can taken to ameliorate this situation, and the specific cases for which this situation must be considered, are discussed in more detail under Fatigue Limit State Verifications for Box Girders in DM Volume 2, Chapter 2, Section 2.2.4.6.

Spacing of the internal cross-frames/diaphragms is primarily determined based on control of distortion of the box. Forces in the cross-frames also should not cause awkward, expensive connections.   Distortion is most easily monitored by the magnitude of the longitudinal warping stresses at the cross-frames. This action is

the result of restoring the shape of the box to its original shape. On straight bridges without skew, most of the distortion is due to live load. If skew is present, dead load and live load are both important sources of torque. Boxes with or without skew on which the deck is unsymmetrically placed can also be subject to significant torque. The required cross-frame spacing is roughly inversely proportional to torque that the box must resist. As specified in AASHTO LRFD Article 6.11.1.1, for all single box sections, horizontally curved sections, and multiple box sections not meeting the requirements of AASHTO LRFD Article 6.11.2.3 (discussed further in DM Volume 2, Chapter 2, Section 2.2.4.1.2) or with box flanges that are not fully effective according to the provisions of AASHTO LRFD Article 6.11.1.1 (refer to DM Volume 2, Chapter 2, Section 2.2.4.1.1), transverse bending stresses due to cross-section distortion are limited to 20 ksi at the strength limit state. Longitudinal warping stresses are to be added to the bending stresses for fatigue in all the aforementioned cases, but are to be ignored at the strength limit state. However, AASHTO LRFD Article C6.7.4.3 does recommend spacing the internal cross-frames/diaphragms to limit the longitudinal warping stresses due to the critical factored torsional loads to 10 percent of the stresses due to major-axis bending at the strength limit state. The spacing of the internal cross-frames/diaphragms is limited to 30 ft in these specific cases (AASHTO LRFD Article 6.7.4.3 – note that it has recently been proposed to AASHTO to raise this limit from 30 ft to 40 ft to reflect the additional torsional stiffness provided by box sections in relation to I-sections). Again, the calculation of the distortional stresses is discussed further in DM Volume 2, Chapter 2, Section 2.2.4.6.1.1.1. AASHTO LRFD Article C6.7.4.3 further states that where distortion of the section is adequately controlled by internal cross-frames or diaphragms, acting in conjunction with a top lateral bracing system in the case of tub sections, the St. Venant torsional stiffness constant J for the box section may be determined as:

$$J = 4\,\frac{A_o^2}{\Sigma\dfrac{b}{t}}$$

Equation 2.4
AASHTO LRFD Equation C6.7.4.3-1

where:

A_o = area enclosed by the box section (in.^{2})
b = width of rectangular plate element (in.)
t = thickness of the plate element (in.)

For tub sections where top lateral bracing forms a pseudo-box section, formulas are available (*11*, *21*) to calculate the thickness of an equivalent plate for different possible configurations of top lateral bracing for use in Equation 2.4.

For all other cases not mentioned in the preceding paragraph, transverse bending stresses and longitudinal warping stresses due to cross-section distortion have been shown to be small (*15*). Therefore, it may be possible to consider reducing the number of permanent internal cross-frames/diaphragms in such cases taking into account that as a minimum, internal cross-frames/diaphragms should be placed at points of maximum moment within the span and at points adjacent to field splices. Additional permanent or temporary internal cross-bracing members may also be

required for transportation, construction and at the lifting points of each shipping piece. It is also important to note that for *all* tub sections, internal cross-bracing in combination with lateral top flange bracing (discussed below) is required to stabilize the shape of the tub section prior to hardening of the concrete deck. Thus, caution is advised when considering any significant reduction in the amount of internal cross-bracing.

If at least two intermediate internal cross-frames/diaphragms are not provided in each span, *AASHTO LRFD* Article 6.11.1.3 requires that the total effective thickness of the flange-to-web welds not be less than the smaller of the web or flange thickness of the box section in order to develop the smaller of the full web or flange section. Full-thickness welds should be provided in this case due to secondary flexural stresses that may develop in the box section as a result of vibrations and/or cross-section distortion.   Where two or more intermediate internal cross-frames/diaphragms are provided in each span, *AASHTO LRFD* Article 6.11.1.3 permits the use of fillet welds for the flange-to-web connections. The welds must be placed on both sides of the connecting flange or web plate to minimize the potential for a fatigue failure resulting from transverse bending stresses, and the welds must meet the minimum and maximum size requirements specified in *AASHTO LRFD* Article 6.13.3.4 (see the section on the design of Welded Connections in DM Volume 2, Chapter 2).   The provision of at least two internal intermediate cross-frames/diaphragms per span can significantly reduce the distortional stress range at the web-to-flange welded joints such that fillet welds meeting the size requirements of *AASHTO LRFD* Article 6.13.3.4 and other appropriate design requirements may be assumed adequate (*22*).

As indicated in *AASHTO LRFD* Article C6.11.3.2, in tub sections with inclined webs with a slope exceeding 1 to 4 (which is permitted when outside the special restrictions specified in *AASHTO LRFD* Article 6.11.2.3 and discussed in DM Volume 2, Chapter 2, Section 2.2.4.1.2), and/or where the unbraced length of the top flanges exceeds 30 feet, additional intermediate cross-frames, diaphragms or struts may be required to reduce the lateral bending in discretely braced top flanges of tub sections resulting from a uniformly distributed transverse load acting on the flanges. This load results from the change in the horizontal component of the web dead load shear plus the change in the St. Venant torsional dead load shear per unit length along the member. In lieu of a refined analysis, the maximum lateral flange bending moments M_ℓ due to the transverse load can be estimated as follows:

$$M_\ell = \frac{F_\ell L_b^2}{12}$$

Equation 2
AASHTO LRFD Equation C6.10.3.4-2

where:
   F_ℓ = magnitude of the factored uniformly distributed transverse load (kip/in.)
   L_b = unbraced length (in.)

This simple equation is based on the assumption that the flange is continuous at both brace points. At simple supports, the equation is unconservative. The entire transverse load at the top is assumed applied to the top flanges (23).

Overhang construction can cause significant lateral bending of the outer top flange of tubs that otherwise is rather lightly loaded.   Overhang brackets are generally attached to the top flange and apply an outward lateral pull of the exterior flange. This pull is equilibrated by a similar force on the lower portion of the tub. Preferably, the lower force is applied at the level of the bottom flange. If the force is applied to the web, some manner of restraining the web is required.   The cross-frame/diaphragm or strut can be assumed to act as a reaction supporting the top flange as a beam within the panel under consideration.   Wind loads during construction may also create moment in the top flanges.

One of the most challenging issues with box girders is access for inspection. The use of internal K-frames with the K-node at the top seems to provide the best access while providing the required stiffness to prevent box distortion. At supports, internal plate diaphragms are generally employed.   Access through the diaphragms at interior supports is provided with access holes at least 18 inches wide and 24 inches high.   In addition to restraining distortion of the box section, the diaphragms at supports also transfer load from the girder webs to the bearing(s).   If a single centered bearing is used, the diaphragm must be stout enough to resist the reaction and transfer the load around any access hole.   Reinforcement around the hole may be required, particularly if the access hole requires a large portion of the diaphragm or if a single bearing is located under the diaphragm. Auxiliary stiffeners on the diaphragm or webs may be employed to spread out the reaction. In such cases, it may be desirable to perform a refined analysis of the diaphragm. Torsion causes a different magnitude of shear in the webs of the box on the two sides of the diaphragm. AASHTO LRFD Article 6.7.4.3 requires that an internal plate diaphragm provided for continuity or to resist torsional forces be connected to the flanges and webs of the box section. External plate diaphragms with aspect ratios, or ratios of length to depth, less than 4.0 and internal plate diaphragms act as deep beams (AASHTO LRFD Article C6.7.4.3) and should be evaluated by considering principal stresses rather than by simple beam theory. Fatigue-sensitive details on these diaphragms and at the connection of the diaphragms to the flanges should be investigated by considering the principal tensile stresses. Further information on the design of solid-plate diaphragms may be found in DM Volume 2, Chapter 2, Section 2.4.4.

The attachment of internal cross-frame connection plates to box flanges is discussed in DM Volume 2, Chapter 2, Section 2.2.4.6.1.2.

2.4.3.1.5.5.2 External Cross-Frames/Diaphragms

Cross-frames or diaphragms between the boxes attempt to restore the relative position of the adjacent sides of two tub or closed-box girders. In addition to vertical load, these members resist and/or introduce torsion in the boxes. To resist the action of these members, AASHTO LRFD Article 6.7.4.3 requires that an interior cross-frame/diaphragm be used in-line with each exterior cross-frame/diaphragm.

At end supports, both external and internal members are required to support the deck and the wheel loads coming onto the deck. External bracing also acts to restrain the rotation of the boxes at the end supports. If single bearings are used, the distance that the deck and its supporting members span may effectively be as large as the distance between the bearings, and not the distance between the inner top flanges, depending on the rotation permitted by the external bracing in conjunction with the torsional stiffness of the box. Deck stresses and the demand on the external diaphragm increase with increased end rotation of the boxes.

The uncluttered appearance of box girders is lost with too many external cross-frames. External cross-frames or diaphragms must be provided between girder lines at interior supports, particularly during erection, unless analysis indicates that the boxes are torsionally stable without these members. This is especially true when a box or tub girder has only one bearing per support. External bracing is sometimes needed before the deck hardens to control the relative deflection and rotation of adjacent boxes. Many times these members are removed after the deck has hardened. Removal is awkward; particularly if the released members have large built-up forces in them after the deck hardens. A partially connected member might fail or remaining bolts may fail. Removal of members with large forces due to earlier loads introduces restoring forces into the bridge. Depending on the magnitude of these forces, it may be necessary to analytically re-introduce the opposite forces as a superimposed load condition to evaluate the effect of the release of the bracing forces on the bridge. For example, a member having a force of 100 kips tension introduces a reversed force of 100 kips when removed. Removal of temporary bracing with large forces may lead to increased deck stresses.

2.4.3.1.5.6 Lateral Bracing

The shear center of an open tub section is located below the bottom flange (24). The addition of top lateral bracing raises the shear center to the inside of the tub resulting in a pseudo-box section significantly increasing the torsional stiffness. Lateral bracing between common top flanges of a tub is therefore required to ensure proper shear flow in individual tub girders. Without lateral bracing, the section acts as an open section and is very unstable under torsion. Top-flange bracing also helps in retention of the tub shape due to lateral forces induced by inclined webs in cases where the web slope exceeds 1 to 4 (as discussed previously in Section 2.4.3.1.5.5.1). Limiting the inclination of the webs to a slope of 1 to 4 minimizes the lateral component to a magnitude that the flange can resist.

AASHTO LRFD Article 6.7.5.3 permits the use of lateral bracing system over less than the entire girder in straight tub girders if torsion is small such that it can be resisted without excessive deformation. Particular attention should be paid in such cases to torsional loadings that might be induced during shipping, erection and placement of the concrete deck. Whenever a partial-length lateral bracing system is considered, AASHTO LRFD Article 6.7.5.3 requires that the local stability of the top flanges and the global stability of the individual tub sections be investigated for the Engineer's assumed construction sequence. It is suggested that at least one panel of lateral bracing be provided on each side of an anticipated lifting point. The need

for additional lateral bracing to resist the shear flow resulting from any net torque on the steel section due to unequal factored deck weight loads acting on each side of the top flanges, or any other eccentric loads acting on the non-composite steel section during shipping or construction, should also be considered. When a straight tub with a partial-length lateral bracing system is subject to a net torque, top-flange lateral bending stresses and cross-section distortional stresses must be considered.

Full-length lateral bracing is desirable even with straight girders when the torques on the non-composite section are particularly large, e.g. tub-section members on which the deck weight is applied unsymmetrically, or members resting on skewed supports. A full-length lateral bracing system can help limit distortions that may result from temperature changes occurring prior to deck placement, and resist the torsion and twist resulting from any eccentric loads that may act on the steel section during construction, including the effects of deck overhang brackets. AASHTO LRFD Article C6.7.5.3 recommends that a full-length lateral bracing system be provided within straight tub sections utilized on spans greater than about 150 feet. For horizontally curved tub girders, a full-length lateral bracing system must always be provided according to AASHTO LRFD Article 6.7.5.3. Top lateral bracing should always be continuous across field splice locations. Otherwise, large lateral flange bending stresses might occur in the top flanges of the tub where the bracing is discontinued.

Although not required by code, it is desirable to attach lateral bracing to the top flanges of the tub rather than to the webs (and preferably by bolting). When these members are attached to the webs, forces in the lateral bracing are transferred to the web or connection plates before the forces can be resisted by the top flanges. This creates a circuitous load path and potential fatigue prone details; both which must be considered in the design. In such cases, the connections to the web must be made according to the requirements of AASHTO LRFD Article 6.6.1.3.2 to prevent potential problems resulting from distortion-induced fatigue (refer to the section on Fatigue and Fracture Limit State Verifications in DM Volume 2, Chapter 2, Section 2.2.3.6.1.2). Also, as specified in AASHTO LRFD Article 6.7.5.3, if the bracing is attached to the webs, the cross-sectional area of the tub for shear flow Ao (see below) must be reduced to reflect the actual location of the bracing, and a means of transferring the forces from the bracing to the top flange must be provided; that is, an adequate load path, with fatigue considered, must be provided between the bracing-to-web connections and the top flanges. Some Owners specify removable deck forms, even within the tub. These forms are very difficult to remove when lateral bracing is attached to the flanges. To avoid connections of the bracing to the web, it is recommended that the requirement for removable forms be rescinded wherever possible in favor of using permanent metal deck forms within the tub(s). One-inch ( ) thick fill plates between the gusset plates and the underside of the top flanges can be used to stay clear of the stay-in-place form installation.

The top lateral bracing must be designed to resist the shear flow in the pseudo-box section resulting from any torsion acting on the steel section due to the factored loads before the deck has hardened.   These members also act with the tub in flexure. Hence, forces in the bracing due to flexure of the tub during construction must also be considered (based on the assumed construction sequence). Top

lateral bracing members are also subject to wind load forces acting on the noncomposite tub section during construction.

When the forces in the bracing members are not computed directly with a refined analysis, the shear flow f across the top of the pseudo box section (in units of kips/in.) can be computed as follows:

$$f = \frac{T}{2A_o}$$

Equation 2.6

AASHTO LRFD Equation C6.11.1.1-1

where:
A_o = enclosed area within the box section (in.^{2})
T = internal torque due to the factored loads (kip-in.)

In calculating A_o, it is assumed that the top lateral bracing acts as an equivalent plate, effectively closing the tub to form a box. The torsional shear (in kips) across the top of the tub equals the resulting shear flow times the center-to-center distance *w* between the top flanges. That force is then resolved into the vector along the diagonal bracing member. There is also a compatibility force due to flexure that must be resolved into the same vector. Bracing member forces due to flexure of the noncomposite tub can be estimated by an approach presented in Reference 23 in the absence of a more refined analysis. Note that since top lateral bracing contributes to the flexural stiffness of the tub section, the bracing member should be resolved into the section properties when determining stiffness for analysis and for section properties when computing stresses (refer to the last paragraph of *AASHTO LRFD* Article C6.11.1.1 – see also Equations 2.3b and 2.3c in DM Volume 2, Chapter 2, Section 2.2.1.4.1.2).

When torques are large and a dominate torque direction occurs, it is possible to orient the lateral bracing members such that they are in tension for shear flow, although they may be in compression due to flexure, and vice versa. By configuring the lateral bracing as a Pratt Truss (Figure 2.49) with the directions of the diagonals determined from the sign of the torque, significant economy can often be realized with the Pratt Truss configuration over the more typical Warren Truss configuration (Figure 2.50) that leads to half of the diagonal members in compression. As discussed previously for I-sections, in the Pratt Truss orientation, only one member applies lateral force against the flange at a cross-frame or strut. The force is resisted mainly by the strut or the top chord of the cross-frame, and to some degree by lateral bending of the top flange. In the Warren Truss orientation, two lateral bracing members apply force at the intersection with the flange and the cross-frame or strut. This has the effect of substantially increasing the lateral flange bending moments and the forces in the top chord or strut. Note that an approach for estimating the flange lateral bending stresses due to these forces when a Warren Truss configuration is utilized (in lieu of a refined analysis) is presented in Reference 23. Single-diagonal lateral bracing configurations such as the Pratt Truss or Warren

Truss configurations are preferred over X-type configurations because there are fewer pieces to fabricate and erect and fewer connections to detail.

AASHTO LRFD Article C6.7.5.3 recommends that the following requirement be satisfied to ensure that a reasonable minimum area is provided for the diagonal members of the top lateral bracing for tub sections:

$$A_d \geq 0.03w$$

<div align="right">

Equation 2.7
AASHTO LRFD Equation C6.7.5.3-1

</div>

where:

A_d = minimum required cross-sectional area of one diagonal (in.^{2})
w = center-to-center distance between the top flanges (in.)

This requirement was included in the 1993 AASHTO Guide Specifications for horizontally curved girders and was intended to ensure that top lateral bracing would be sized to that the tub would act as a pseudo-box section with normal stresses due to warping torsion less than or equal to 10 percent of the major-axis bending stresses and with minimal warping torsional displacements. The criterion was originally developed based on tub sections with vertical webs, with ratios of section width-to-depth between 0.5 and 2.0, and with X-type lateral bracing configurations with the diagonal members at an angle of 45 degrees to the longitudinal centerline of the girder flanges (25). Although most tub-girder configurations will likely differ from the configurations for which the above criterion was developed, the criterion at least ensures that some reasonable minimum area will be provided for these members regardless of the configuration. In many cases, larger members will likely be required to resist the applied member forces.

When selecting the bracing arrangement, the angle the bracing is to make with the flanges must be determined. As the angle is increased, the bracing force due to both torsion and flexure is reduced. Also, a larger angle between bracing and flange reduces the length of the brace, which is important for bracing that must resist compression. Opposing these facts is that a flatter angle reduces the number of elements required in the bracing system. It is for this reason that a Pratt Truss arrangement that allows tension bracing is economical. It should be noted that usually the direction of the Pratt Truss configuration changes over a span. At the central location, it may be desirable to introduce one bay of X-bracing.

One of the commonly asked questions is whether lateral bracing members attached to the top flange midway between cross-frames/diaphragms act as a brace point for the top flange in compression. There probably is no concrete answer, but it is conservative to not assume a brace point at these connections, unless a buckling analysis of the structure based on a refined model of the tub(s) is performed. AASHTO LRFD Article 6.11.3.2 takes the conservative position when it states that the unbraced length of the top flanges of tub sections should be taken as the distance between interior cross-frames or diaphragms. If the lateral bracing member can be oriented so that it is in tension for the shear flow in regions where the same member is in compression due to flexure, there is less need to control its length and spanning from cross-frame to cross-frame is obviously the most economical

arrangement.   At locations where only struts exist between the top flanges, top lateral bracing attached to the flanges at these points may be considered to act as brace points at the discretion of the Engineer according to AASHTO LRFD Article C6.11.3.2.

2.4.3.1.5.7 Concrete Deck Options

The cross-section of the deck may be a traditional flat soffit deck or vaulted.   If moderate spacings of the boxes are employed, a deck with a flat soffit (inside and between the girders) and mild reinforcing is best.   However, if bolder spacings and/or overhangs are used, a vaulted deck with transverse post-tensioning may be the most economical choice.

In a limited number of cases, a precast concrete deck has been employed with steel tub girders.   Typically such decks are not economical.   However, when speed of construction is important, precasting has been found to be practical.   Deck panels may be placed on one or two tubs and spliced together on a longitudinal joint.   This splice can be accomplished with mild reinforcing and a field-cast joint.   Deck units may be joined together with epoxy as the units are installed and post-tensioned. The post-tensioning force should be adequate to prevent transverse cracking due to thermal changes in the steel

As mentioned above, if a single-bearing design is used, the transverse bending moment in the deck is usually much larger than that determined by the free span between webs due to the rotation of the boxes when vertical load is placed on the deck between the webs of adjacent boxes.   Cross-frames/diaphragms between the boxes can reduce the rotation and associated deck stresses.   Large skews and other extreme torques can cause large shear flow in the deck.   Even with top lateral bracing, the stiffer deck resists most of the shear flow once it hardens.   AASHTO LRFD Article C6.11.1.1 states that for tub sections, the deck should be assumed to resist all the torsional shear acting on top of the composite box section.   The deck reinforcement should be designed for this horizontal shear.

Precast decks have been designed for tub girders.   The first such application was the steel alternate design of the Wallace Viaduct in Idaho (not built).   This bridge had precast vaulted deck units ten feet long.   The deck was post-tensioned in both the longitudinal and transverse directions. In this design, prestressing to overcome thermal stresses was required.   This requirement was found to be too severe in that the ducts could not be practically located and the cost was excessive. The ramps on this project employed single box cross-sections.   The mainline unit required more boxes. However, they were widely spaced with deck spans up to 30 feet. Separate deck sections were designed for placement on each tub and subsequent post-tensioning both transversely and longitudinally.   Some deck sections were over 40 feet wide.

Another vaulted deck design was utilized on the MacMillan Yard Bridge near Toronto, Ontario (alluded to previously).   The advantage of a vaulted deck, of course, is that undeviated post-tensioning can act at the top of the deck in negative bending and at the bottom of the deck in positive bending.   The MacMillan Yard

Bridge had two boxes in the cross-section with deck overhangs of 15 feet and a free deck span between box webs of approximately 30 feet for a total deck width approaching 100 feet. This deck was cast-in-place, but post-tensioned transversely, with only mild reinforcement provided longitudinally. This design was bid successfully against a segmental concrete design.

A precast deck design was also utilized on the box girder bridges on the Westchester Parkway in New York State. These box-girder bridges were designed originally with a cast-in-place deck, but the contractor opted for a precast deck that was post-tensioned longitudinally in order to speed construction and take advantage of a per diem payment for early completion. Transverse joints were grouted and tensioned. Shear connectors were welded through pockets in the deck and grouted. The bridges were built in phases with longitudinal joints. Adjacent phases were connected with small closure pours containing mild reinforcing only. The transverse length of the deck sections traversed two tub girders, or a width of about 40 feet. Again, this project was satisfactorily completed and is functioning well.

10.   Vlasov, V.Z. 1961. *Thin Walled Beam Theory*. NSF, Washington, D.C.
11.   Dabrowski, R. 1968. *Curved Thin-Walled Girders*. Translation No. 144, Cement and Concrete Association, London, England.
12.   Wright, R.N., and S.R. Abdel-Samad. 1968 "Analysis of Box Girders with Diaphragms." *Journal of the Structural Division*, American Society of Civil Engineers, New York, NY, Vol. 94, No. ST10, October.
13.   Heins, C.P., and D.H. Hall. 1981. "Designers Guide to Steel Box Girder Bridges." *Booklet No. 3500*, Bethlehem Steel Corporation, Bethlehem, PA, February.
14.   Timoshenko, S.P., and J.M. Gere. 1961. *Theory of Elastic Stability*. McGraw-Hill, New York, NY.
15.   Johnston, S.B., and A.H. Mattock. 1967. "Lateral Distribution of Load in Composite Box Girder Bridges." *Highway Research Record*, No. 167, Bridges and Structures, Transportation Research Board, Washington, D.C.
16.   Consortium of University Research Teams. 1975.   "Tentative Design Specifications for Horizontally Curved Highway Bridges." CURT Report, Part of Final Report, Research Project HPR2-(111), March.
17.   Galambos, T.V. 1978. "Tentative Load Factor Design Criteria for Curved Steel Bridges." Research Report No. 50, Department of Civil Engineering, Washington University, St. Louis, MO, May.
18.   Culver, C.G., and J. Mozer. 1971. "Horizontally Curved Highway Bridges, Stability of Box Girders." Department of Civil Engineering, Carnegie Mellon University, Pittsburgh, PA, Report No. B2 submitted to the FHWA, Contract No. FH-11-7389, July.
19.   FHWA. 1980. "Proposed Design Specifications for Steel Box Girder Bridges." *FHWA-TS-80-205*, Federal Highway Administration, Washington, D.C.
20.   Hall, D.H., Grubb, M.A., and C.H. Yoo. 1999. "Improved Design Specifications for Horizontally Curved Steel Girder Highway Bridges." *NCHRP Report 424*. Transportation21.
21.   Kolbrunner, C., and K. Basler. 1966. *Torsion in Structures*. Springer-Verlag, New York, NY.

22.   Haaijer, G. 1981. "Simple Modeling Technique for Distortional Analysis for Steel Box Girders." *Proceedings of the MSC/NASTRAN Conference on Finite Element Methods and Technology*, MacNeal/Schwendler Corporation, Los Angeles, CA.
23.   Fan, Z., and T.A. Helwig. 1999. "Behavior of Steel Box Girders with Top Flange Bracing." *Journal of Structural Engineering*, American Society of Civil Engineers, Reston, VA, Vol. 125, No. 8, August.
24.   Heins, C.P. 1975. *Bending and Torsional Design in Structural Members*. Lexington Books, D.C. Heath and Company, Lexington, MA.
25.   Heins, C.P. 1978. "Box Girder Bridge Design – State of the Art." *AISC Engineering Journal*, American Institute of Steel Construction, Chicago, IL, 4th Qtr.

2.4.3.1.6 Redundancy Considerations

The term redundancy implies the exceeding of what is considered necessary or normal. Hence, the implication in structural redundancy is the inclusion of something that is not necessary for the normal functioning of the structure. In order to design structures with the least cost, that style of structural redundancy is a type the Engineer tries best to avoid.

Structural redundancy became a matter of some discussion when several structures suffered major fractures. It was observed that a fracture failure in bridges such as the Silver Bridge, which had no redundancy, led to the loss of life. On the other hand, fracture failures experienced by other bridges, such as the I-79 Bridge over Neville Island, which was structurally redundant, only led to minimal inconvenience. Since those days, much effort has been spent defining structural redundancy, when it exists, and how it can best be obtained. This approach falls under the rubric of designing for failure, since if the bridge does not fail, structural redundancy is not called upon. But the importance of bridges and the human lives they carry seems to call out for at least some level of redundancy in every structure.

Structural redundancy is typically defined as the ability of the structure to continue to carry loads after a member fails. The implication is that the failure of a single member will be identified before a second member fails. Structural redundancy exists in most highway bridges. However, it is not always simple to determine the presence or absence of adequate redundancy as defined herein. For example, it may not exist in a single box girder cross-section of either steel or posttensioned concrete; it may or may not exist in a horizontally curved multi-girder bridge.

Therefore, it becomes necessary to consider a methodology for the determination of whether redundancy exists. A bridge would be expected to support its design load after a fracture occurs. Assume that it will not be expected to support more than the design live load. The bridge must also support its dead load. A load factor of 1.3 is suggested for both of these loads based approximately on the dead-load factor applied in the LFD and LRFD methodologies. The lower factor applied to the live load is based on expected overloading. The method of loading must be considered in a fracture investigation. Much of the load (i.e. the dead load) is applied to a

noncomposite structure, but the fracture effect acts entirely on the composite structure. The live load is applied to the composite structure in both cases.

The dead load is applied as in design.   However, the fracture introduces a redistribution of internal actions and external reactions as a result of the fracture. In a steel structure, introduction of the fracture is rather straightforward. The stress at the fracture face must be zero. Thus, forces are applied to the fractured structure at the location of the assumed fracture in a reverse sense to those applied under dead load, forcing the net resultant stresses at the fracture face to be zero. The resulting load case is additive to the dead load cases originally employed during the design.

Ensuring that adequate reinforcing within the deck and adequate shear connection of the deck to the girders are provided to resist the effects of the fracture are important factors in determining the redundancy of composite steel bridges.

In a posttensioned concrete structure, the process is similar but more complex. The typical case would be a segmental box girder with a portion of the bottom flange destroyed. The force in the broken strands would be reversed and applied to the remaining structure. Grouting of the strands must be considered. The multiple strands provide some redundancy against failure of a strand.

The same concept can be employed in steel structures by using multiple elements to from a member. Typically, this type of redundancy occurs with riveted members. Modern truss members and arch ties have been made of built-up bolted members to provide redundancy, as have girder bridges that were considered non-redundant. In these structures, the remaining elements in the member need to be examined to ensure that they are adequate. Additional bolt shear forces are encountered should an element fail when the force in the failed element is redistributed through the bolts in the vicinity of the failure to the functioning elements.

Perhaps the best approach is to design and build the structure such that it does not fail; hence avoiding the need for providing structural redundancy as defined herein. This approach also has been investigated intensely since the 1960s—and with great success. It was observed that most all of the steel bridges that failed were either welded using the older technologies that existed at the time, as in the case of Neville Island girder-bridge, or of old material and/or out-of-date design practice, as in the case of the Silver Bridge. Investigations showed that tougher steel, better design of details, and more intense inspection makes steel bridges much tougher and extremely resistant to fracture. This research is borne out as is evidenced in the paucity of fractures of newer bridges in the United States. In structures that are not considered structurally redundant, *AASHTO LRFD* requires that the critical elements be built according to the Owner's Fracture Control Plan (typically based on the fracture control plan specified in the AASHTO/AWS *Bridge Welding Code* – see DM Volume 2, Chapter 2 under Fatigue and Fracture Limit State Verifications). This plan includes stringent steel and welding consumable specifications and strict welding procedures with close inspection. Generally, the additional costs associated with this work and material specification is not great and can usually be more than offset by the increased efficiency of the structural form. Cross-sections having a single tub or widely-spaced tubs are a good example of such economy. Single tubs save not

only on steel and fabrication costs; they permit significantly reduced-cost substructures. A number of these bridges have been built across the nation and are functioning safely. These structures are discussed in more detail in Section 2.4.3.1.5.3 of this chapter.

2.4.3.2 Two-Girder Systems

Two-girder systems have fallen into disuse in the United States due to their perceived lack of redundancy. Historically, two-girder systems were very common and many are still in use. Two-girder systems may be divided into two categories; deck-type and through-type systems.

Figure 2.58 Deck-Type Two-Girder System

Figure 2.59 Through-Type Two-Girder System

One significant advantage of the through-type system is the increased clearance that this system provides. Railroads found this particularly advantageous since elevating the rail grade is even more expensive than doing the same for a highway. The compression flange of the girders in a through-girder system must receive its bracing

from stiffening brackets. One disadvantage of the through-type system is that the girders must be spaced wider apart than the roadway width, forcing a relatively heavy floor system. The deck-type system has less clearance than the through-type system. However, the deck overhangs permit a girder spacing less than the deck width. Hence, a relatively lighter floor system can be used. The deck-type system also provides a more traditional appearance.

Many of the older bridges were built of riveted girders with rolled shapes for the floor system. The multiple elements in the riveted flanges provided redundancy. One reason that these bridges were so common was their economy. The cost of labor for riveting and the cost of material for the two-girder cross-section were reduced with this system compared to those costs for a comparable multi-girder cross-section.

Most existing two-girder bridges in the United States are noncomposite since they were built prior to composite design being widely employed in bridge construction. Most are simple-span construction for the same reason; continuous-span construction was uncommon in the days of riveted construction.

Another issue related to the early two-girder bridges is the tendency of the floor-beam ends to create end moments at the girders. These moments were rarely accounted for in the design and have led to fatigue cracking of the girder webs in some cases. The fatigue cracks usually occur at the flange-web juncture. Often the floor beams are attached to wide plates or brackets that extend into the floor-beam span. These types of attachments tend to increase the end moments in the floor beams and these moments must be removed by couples in the girder through the development of lateral moments in the girder flanges. Often the connection plates are not attached to the flanges, forcing the load through the flange-to-web welds.

Two-girder bridges often are found to have bottom flange lateral bracing. These members resist lateral wind force since the bottom portion of the girders may be unsupported by the floor beams. The lateral bracing members also may act with the sway bracing in the vicinity of the supports. In addition, these members act in resisting torsional loads by converting the cross-section of the structure into a pseudo-box section. Dead loads that are not applied symmetrically to the deck cause torsion, and subsequently, forces in the lateral bracing system. Live loads are usually unsymmetrical with respect to the cross-section and cause torsion in a similar fashion.   Live load forces in the lateral bracing system need to be investigated for fatigue. Removal of the lateral bracing usually leads to an increase in the live load girder moments and wind forces in the girder flanges.

Decks of two-girder bridges behave somewhat differently than decks on typical multi-girder bridges. The full width of the deck is often not fully effective near bearings due to shear-lag effects. The result is slightly higher horizontal shear stresses in the deck. If the floor beam deflects significantly, stresses transverse to the girders are generated in the deck since the deflection of the deck varies across its width. If the floor beams and the stringers (if necessary) are at the level of the bottom of the deck and the stringers are bolted to the floor beams, the stringers are likely not acting as continuous beams and there may be excessive longitudinal stresses in the top of the deck.

There are a few bridges of this type recently built in the United States. Most are composite with the main girders and often are composite with the floor beams (and stringers where provided). More bridges of this type have been built in Switzerland, where the deck is often precast and attached to the girders with shear studs welded through pockets in the deck. The deck sections are then posttensioned and the stud pockets grouted.

The advantages of two-girder cross sections are the same as in earlier days. They provide a minimum number of webs, which introduces significant economy. The amount of welding is substantially reduced with only two main girders in the cross-section and by utilizing rolled shapes for the floor beams/stringers. Fatigue is less critical in the main girders since they are usually proportioned to carry a number of traffic lanes, hence they are heavier than girders in multi-girder bridges and the effect of a single truck is much less. Two-girder bridges also require fewer bearings and can be erected in less time.

The main girders may be built-up using angles and plates bolted together (much as a riveted girder) in order to provide the desired redundancy via the multiple-element technique discussed previously. The only two-girder bridges that are known to have experienced fractures continued to carry live loads after fracture occurred. A refined analysis with assumed hypothetical cracked components (described elsewhere in this manual – see the preceding section of this chapter on Redundancy Considerations and DM Volume 2, Chapter 2 under Fatigue and Fracture Limit State Verifications) can demonstrate that many of these bridges are redundant in their own right.

2.5 Prestressed Concrete Bridge Superstructures

The objective of this topic is to introduce various types of prestressed concrete structures, their typical spans and applications. Different types of construction, using precast and cast-in-place techniques are introduced. The intent is to familiarize the reader with basic concepts, terminology and techniques to be addressed in greater detail in subsequent Chapters.

2.5.1 Introduction

Prestressed concrete bridges are defined by their type of superstructure – for example, precast girder, cast-in-place or precast box girder, cable-stay, etc. It is customary when describing a bridge, to quote the typical or maximum span length, overall bridge length or number of spans to indicate the scale of the structure.

The typical or maximum span length depends very much upon the type of superstructure. Different types of superstructure, their application and span ranges are presented below as a guide for selecting a bridge solution. They are presented in approximate order of increasing span length and complexity.

2.5.2 Superstructure Types

The following is a summary of the main types of prestressed concrete bridge construction. It is not necessarily an exhaustive treatment of all types and applications. Some projects may incorporate combinations of types and construction techniques.

2.5.2.1 Slab Bridges (Cast-in-Place)

Slab construction is often used for small superstructures generally in the span range of 20 to 40 feet. For spans in the lower half of this range, the slab superstructure is usually solid concrete. In the upper half of this range, it may be voided to save weight. Alternatively, if a slab is structurally continuous, it may be solid but haunched, being shallower at mid-span and deeper over interior supports. The structural capacity of both solid and voided slabs may be provided by mild steel reinforcing or by post-tensioning.

Slab type superstructures, whether solid, voided or haunched, are constructed cast-in-place on site using temporary formwork and falsework.

2.5.2.2 Precast Prestressed Plank

Being produced off-site at a factory, precast prestressed concrete planks offer a means of constructing a small span solid or voided slab superstructure requiring little on-site cast-in-place concrete and formwork (Figure 2.60). The main structural capacity is provided by longitudinal pre-tensioning strands installed in the factory.

Precast planks have small bottom flanges and are placed side-by side, almost in contact, leaving only a narrow erection tolerance gap between the flanges (Figure 2.60). Above the small bottom flange, there is a wider gap or sometimes a block-out about 6 to 9 inches wide to facilitate connection of transverse post-tensioning ducts. After the wider gaps and blockouts have been filled with a cast-in-place concrete, transverse post-tensioning of either strand or bars is installed through ducts in each plank to make them function structurally as a monolithic slab. It is very important to give special care and attention to design details, fabrication, erection and installation in order to ensure tendon ducts align transversely and are properly sealed to protect tendons from corrosion.

Typically, precast prestressed planks are suitable for simply-supported structures with spans up to about 40 feet. It is possible to make spans continuous for traffic loads by means of suitable details for reinforced connections over interior supports.

Figure 2.60 Precast Prestressed Plank (spans 20 to 40 feet)

2.5.2.3 Inverted Tee Beams

Inverted T-beams are usually based upon the bottom portion of a standard AASHTO I-beam (below) comprising the bottom flange and a portion of the web (Figure 2.61). They are erected side-by-side with their bottom flanges almost in contact – leaving only a small gap for erection tolerance. After sealing the small gaps with a suitable permanent material or tape and placing transverse reinforcement, the spaces between the webs them are completely filled with cast-in-place concrete to the elevation of the top of the deck. In this manner, inverted T girders are both the primary structural member and permanent formwork. This type of superstructure is usually suitable for simply-supported spans in the range of about 25 to 40 feet and offers an alternative to cast-in-place slabs or precast prestressed planks.

2.5.2.4 Double-T Girders

Double-T girders are widely used by the building industry. However, for bridges, the top flange must be thickened to carry highway traffic loads or an additional

reinforced concrete slab must be placed on site, using the thin top flange only as a permanent form (Figure 2.61)
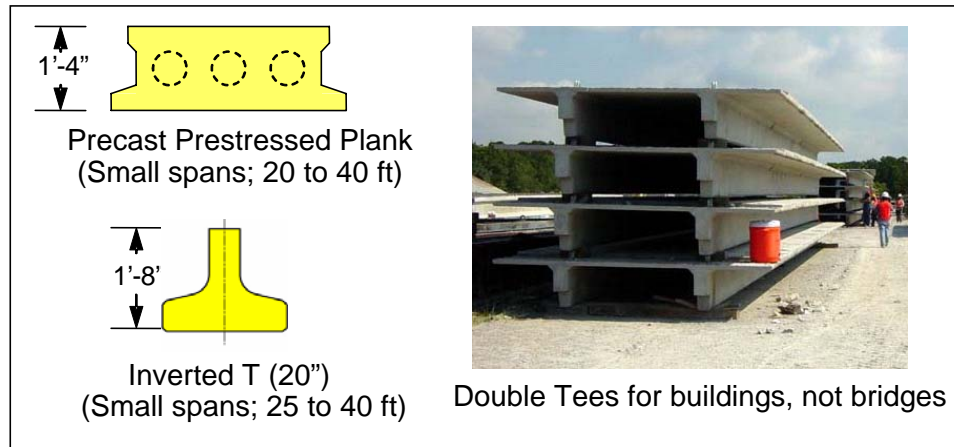
Figure 2.61 Precast Sections for Short Spans

2.5.2.5 Box Beams

Precast prestressed concrete box beams are of a hollow rectangular section and may be placed against each other, similar to precast planks, or may be spaced apart. A reinforced concrete deck slab is cast on top. Close contact eliminates or minimizes the need for deck slab formwork. Span ranges are similar to those of standard I-girders (below) but, in comparison to I-girders, the section itself utilizes more material and requires more complex forms.

2.5.2.6 I-Girders

Precast prestressed concrete I-girder construction has become a familiar feature of the Interstate landscape over the last few decades. A typical superstructure comprises several I-girders with a reinforced concrete deck slab. The span length depends upon the type and size of the girder section, the spacing between girders and thickness of the deck slab. A deeper section girder spans a greater length and, for the same section, closer spacing (i.e. more girders) facilitates a longer span. However, widely spaced girders require a thicker and heavier deck slab. An economical design strives for an overall balance between the thickness of the deck slab, girder spacing and span length.

Many different I-girder sections have been developed. Perhaps the most familiar is the standard AASHTO beam. This has been adapted and modified over time – morphing into the "Bulb-T" and similar deep sections with wide top flanges (Figure 2.62).

The decision to use a particular I-girder section or size depends much upon the industrial availability of precast components within a given region, transportation, permits, accessibility of the site and crane capacity.

Spans for simply-supported I-girder bridges range from about 40 feet for an AASHTO Type II beam, to about 140 feet for a 78" deep Bulb-T.

Figure 2.62 Precast Pretensioned I-Girders (spans from 40 to 140 feet)

When I-girders are made structurally continuous over interior piers by installing post-tensioning tendons through specially detailed cast-in-placed splice joints, it is possible to gain an extra 10 to 15% span length. This method, often referred to as "spliced I-girder construction", is generally, though not exclusively, more suitable for larger scale projects (Figure 2.63).
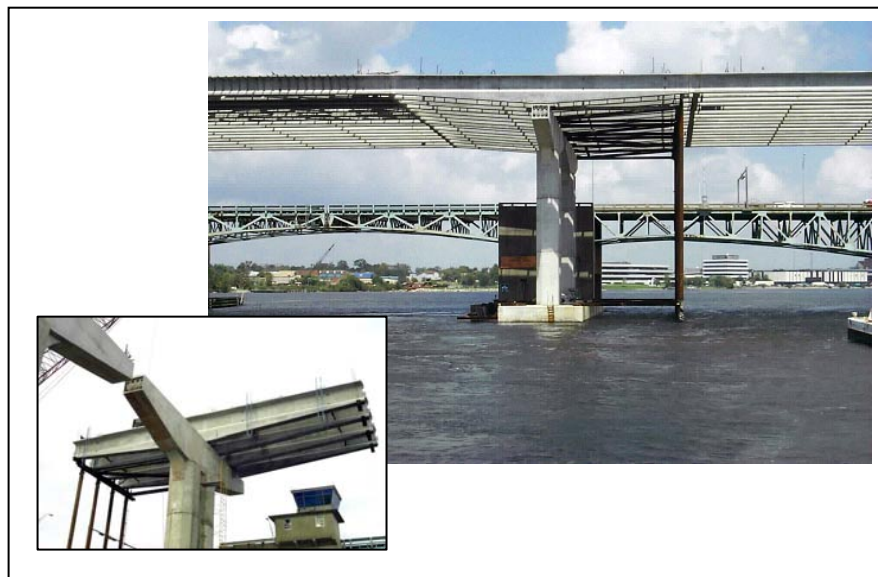
Figure 2.63 Spliced I-Girder Construction (spans 100 to 250 feet)

2.5.2.7 U-Beams

In regions with a strong precast concrete industry, precast prestressed U-beam sections have been developed primarily to address needs such as bridge aesthetics (Figure 2.64). Available in depths from 48" to 72", spans range from about 50 to 125ft.

Figure 2.64 U-Beam (spans 50 to 125 feet)

2.5.2.8 Box Girder Cast-in-Place on Falsework

In some cases, it is economical or practical to construct a bridge entirely on-site using formwork and cast-in-place construction. This is often influenced by regional construction practice, for example, in California (Figure 2.65).

Figure 2.65 Box Girder Cast-in-Place on Falsework (spans 100 to 250 feet)

In regions or remote sites with no convenient precast concrete girder industry, cast-in-place construction may be more feasible than precast construction, especially for smaller bridges or individual projects as it requires only modest sized construction equipment and practices familiar to the building industry.

Typically, construction of box-girders on falsework facilitates spans of approximately 100 to 250ft – thereafter, for cast-in-place work it is usually more economical to adopt balanced cantilever construction utilizing form-travelers (below). Cast-in-place closed box girder sections usually have multiple webs. The torsional rigidity of closed box sections makes this type of construction well suited to sharply curved viaducts and interchange ramp structures.

2.5.2.9 Precast Segmental Span-by-Span Box Girders

Spans of precast segmental span-by-span bridges are made up of a number of precast box-section, match cast, segments placed on an erection truss or support system spanning from pier to pier (Figure 2.66). Longitudinal post-tensioning tendons, usually external to the concrete but inside the box, extending from pier to pier provide prestress to compress the segments into a monolithic span. The bridge alignment needs to be straight or only very slightly curved so that segments can be supported on straight erection trusses. Usually it is possible to erect an entire span in a matter of a day or two depending upon the size, number and weight of segments. The rapid rate of erection is a major advantage for some projects.

Figure 2.66 Precast Segmental Span-by-Span Box Girder (spans 80 to 160 feet)

Segment depths usually range from 6 to 10 feet for spans from about 80 to 160ft. The maximum span is governed by the capacity, weight and ease (or lack thereof) of advancing the erection trusses. For normal highway structures carrying two lanes and shoulders, the practical limit is about 160 feet; above this, erection trusses tend to become extremely heavy and awkward to handle – as was the case with the few

bridges with spans up to 180ft. Consequently, for spans over about 150 ft, balanced cantilever construction is usually more appropriate.

2.5.2.10 Precast Segmental Balanced Cantilever Box Girder

Precast segmental balanced cantilever construction is suitable for spans ranging from about 150 to 500ft (Figure 2.67). Precast, match-cast, segments are erected sequentially on each side of a pier in an approximately symmetrical (balanced) manner until two cantilevers meet at mid-span where they are made continuous using a cast-in-place joint.

When segments are erected, first on one end of the cantilever and then the other, there is an out-of-balance effect that must be carried by a temporary support system. This might be a system of stability towers and jacks at each pier or an erection gantry. Erection gantries not only stabilize the cantilever, but also facilitate overhead delivery and erection of segments from the already completed portion of the structure. Erection by overhead gantry must proceed in a sequential manner form one end of the bridge to the other. On the other hand, erection using sets of stability towers at the piers facilitate the erection of more than one cantilever at a time.

As segments are erected in cantilever, post-tensioning tendons, usually internal to the top slab are installed, extending from one segment on one end of the cantilever to its counterpart on the other. Additional tendons are installed through the mid-span closure to provide continuity. Typically, it is possible to erect one or two segments on each end of a cantilever per day (i.e. 2 to 4 total per balanced cantilever per day) and to complete a cantilever cycle – connecting two cantilevers – in two to three weeks.

Figure 2.67 Precast Segmental Balanced Cantilever (spans 150 to 500 feet)

In a continuous structure, interior span lengths may be varied to some extent by including more or fewer segments. This feature makes precast segmental cantilever construction very adaptable to variable spans often controlled by available clearances and locations for piers. End span lengths of a continuous balanced

cantilever unit are usually 60% to 75% of a typical span so as to maintain a positive reaction at the abutment or expansion joint pier.

Precast segments for balanced cantilever construction for spans up to about 200 feet or thereabouts are usually of a constant depth – typically about 1/20th of the span length. For spans over about 200 feet, segments are usually of variable depth – typically L/20 at the pier to about L/40 at midspan. These are approximate ranges – there are no hard and fast rules – and there are many other factors to consider. The upper end of the span range (about 500 ft) is limited by the size and weight of the precast segments and the ability to cast, transport and erect them. There is no limit to the lower end of the span range and many highway ramp and viaduct structures contain spans, particularly end spans, much shorter than 100 feet. The torsional rigidity of the large box section is ideally suited to sharply curved viaducts and interchange ramps.

2.5.2.11 Cast-in-Place Balanced Cantilever

Cast-in-place balanced cantilever construction is appropriate for continuous structures with spans in the range of about 200 to 800 ft. Segments are cast-in-place, first on one side of a pier and then on the other, using form travelers (Figure 2.68).

Form travelers are adjustable frames that support the bottom soffit, inside and outside web, and top slab soffit formwork for a new segment from the already completed portion of the cantilever. Segments are typically 16 to 20 feet long. In order to commence construction with travelers, a pier table must be built first over each pier using ordinary formwork. The pier table itself may be up to 40 feet long. The depth of the superstructure usually varies from about L/20 at the pier to L/40 at midspan. Depending upon the width of the deck, there may be two or three webs.

In order to minimize out-of-balance effects as segments are cast first on one end of a cantilever and then on the other, it is usual to offset the pier table to give a maximum of only a half-segment out-of-balance. Out of balance construction effects are carried by stability towers or ties at the piers. The weight and effects of the form travelers must be considered in the cantilever design.

As segments are cast, longitudinal internal tendons are installed in the top slab extending from a new segment on one end of the cantilever to the previously cast segment on the other. A closure segment connects cantilevers at midspan and further longitudinal tendons are installed to develop continuity. By offsetting work crew cycles, it is usual to be able to complete a segment on one end of a cantilever in a week – for a total of 2 segments per balanced cantilever per week.

Form Travelers and
Stability Towers

Acosta Bridge, Jacksonville, 630ft main
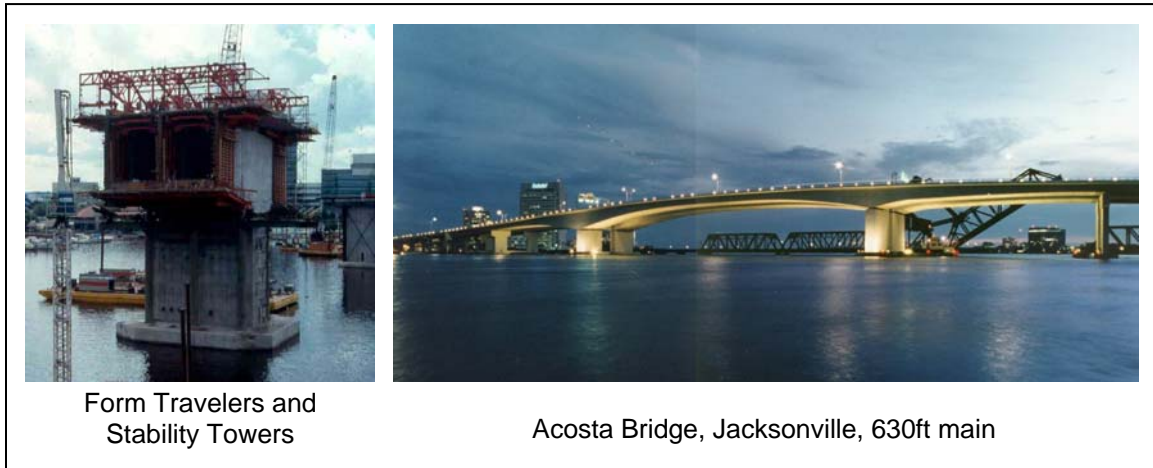
Figure 2.68 Cast-in-Place Balanced Cantilever (spans 200 to 800 feet)

Interior span lengths may be varied to some extent by including more or fewer segments or by carefully adjusting the length of cast-in-place segments within the capabilities of the form traveler system. This allows for adaptability to variable spans that may be governed by available clearances and locations for piers. End span lengths of a continuous balanced cantilever unit are usually 60% to 75% of a typical span so as to maintain a positive reaction at the abutment or expansion joint pier.

Although individual form travelers may weigh many tons and the stability towers must be capable of resisting heavy temporary loads, the overall size and scale of the equipment is relatively lightweight for the range of spans that can be built. This makes cast-in-place balanced cantilever ideally suited to spans up to about 800 feet. Thereafter, the maximum depth and segment sizes become significant that it is usually more economical to consider an alternative type of construction – namely cable stay.

2.5.2.12 Cable Stay

Cable stay construction (Figure 2.69) becomes very cost effective for highway bridge spans over about 600 feet, although some smaller span structures have occasionally been built. For concrete, the upper span limit for cable stay construction is currently about 1,500 feet. Spans of 2,000 feet are possible using a combination of concrete and more lightweight steel construction for the central portion of the main span. The cable stay portion may be part of a longer continuous series of superstructure spans. The back-spans on either side of the main span may range from about 0.45 to 0.65 of the main span depending upon the overall configuration and continuity. The back-span cables are arranged and anchored so as to provide support to the main span.

Concrete cable stay bridges are built using either cast-in-place or precast segmental construction. Cast-in-place techniques utilize form travelers supported by the completed deck and the new leading cable stays or a system of temporary stays. Precast segments are erected using cranes or temporary winch devices supported on the previously completed deck and the new leading cable stay.

Cast-in-place superstructure cross sections comprising edge girders, transverse beams and a deck slab require two planes of stays – one at each edge. The natural, large torsional rigidity of a closed precast segmental box facilitates the use of a single plane of stays along the center of the deck.

Figure 2.69 New Sunshine Skyway, Precast Segmental Cable Stay (1,200 foot span)

Although the main load carrying capacity is provided by the cable stays, it is necessary to incorporate both longitudinal and transverse post-tensioning to provide continuity and cater for localized load effects. Cable stay bridges are generally, although not exclusively, suitable only for major projects – but smaller span structures are feasible.

2.5.2.13 Other Prestressed Concrete Structures

Reinforced concrete arches have been used for many years, mostly to carry reinforced concrete or pretensioned I-girder decks on spandrel walls. In recent years, precast segmental construction was used to build the arch ribs of the Natchez Trace Parkway Arch Bridge (Figure 2.70). Precast segmental cantilever construction was used to construct the spans resting upon the ribs and main pier columns.

Figure 2.70 Precast Segmental Arch (600 foot span)

Precast segmental construction has been used in a one-directional manner to erect segments progressively in continuous cantilever over a series of piers (Figure 2.71). Temporary intermediate piers were used to reduce cantilever moments. The alignment features radii as tight as 250 feet for which the torsional rigidity of the large closed cell box section is ideally suited.
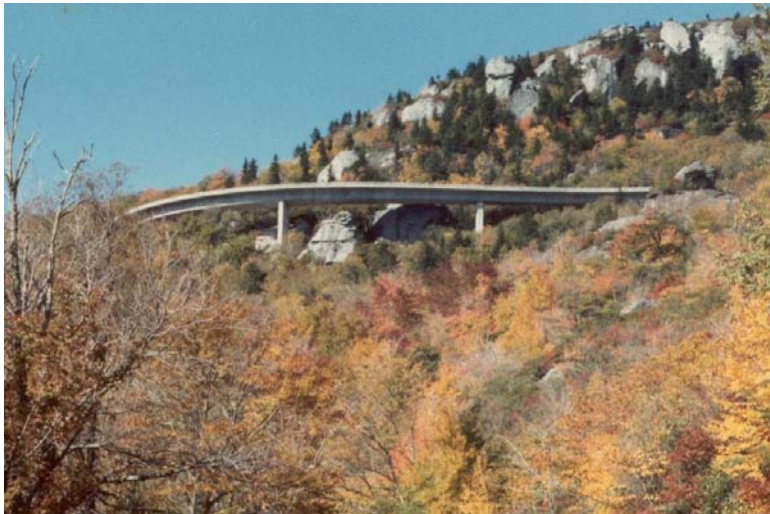
Figure 2.71 Progressive Cantilever (180 foot span)

A combination of span-by-span and cantilever construction has often been used to create a long main-span for a navigation channel in bridges of otherwise shorter constant spans.

2.5.2.14 Summary of Types and Span Lengths

Prestressed concrete is very adaptable for bridges of all types of construction and span lengths. The above offers only a summary of the main types and techniques.

The use of a particular type for a given project depends upon many factors such as; availability of precast concrete plants, regional construction practices, transport and access to site, size of cranes, use of special erection equipment or falsework in addition to the more obvious constraints like available clearances, locations for piers and necessary span lengths. When it comes to the necessary span lengths and bridge types, there is much overlap. For many applications, there is a choice of different types of construction. This is summarized and illustrated in Figure 2.72.
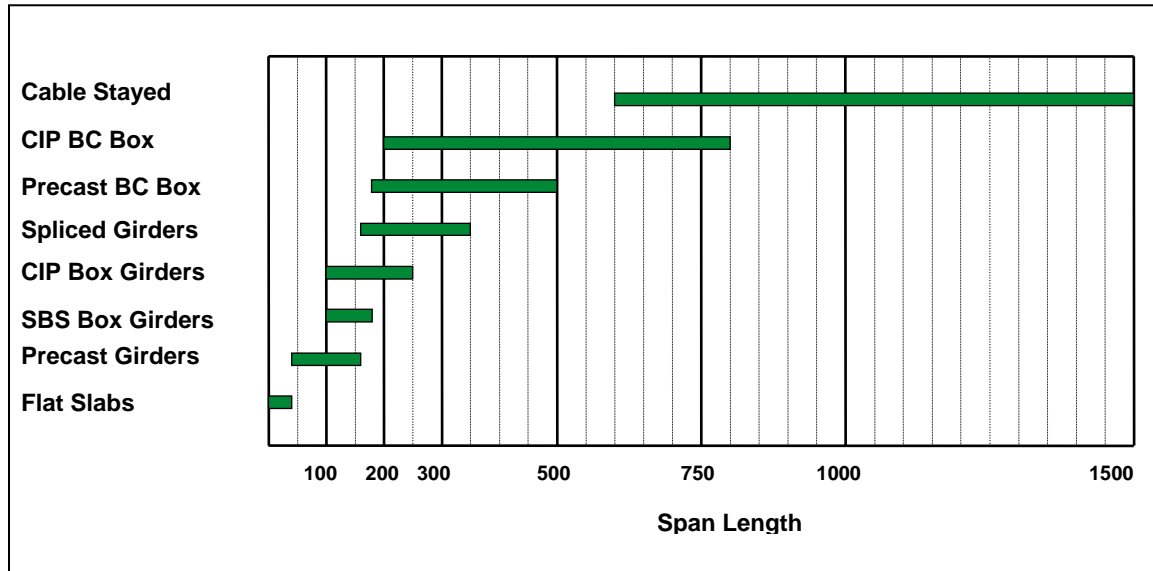
Figure 2.72 Summary of Prestressed Bridge Type and Span Length

In this chart, cast-in-place slabs, precast prestressed planks, inverted T's and double-T type structures have been generically combined under the heading "flat slabs". The term "CIP" means "Cast-in-Place", "BC" means "Balanced Cantilever" and "SBS" means "Span-by-Span". "Spliced-girders" refers to bridges of I-girders which may be of constant depth or have variable depth haunched sections that are made continuous. "Precast girders" is intended to include all types and sizes of AASHTO, Bulb-T, U-Beam and Box-Beam bridges. For more information on I-girders refer to DM Volume 3, Chapter 1, Section 1.3.

The span ranges are general guides and are in no way intended to limit choice to a particular type of construction for any given project.

2.5.3 Span Length Optimization

When making the choice of bridge type, it is important to take into account the fact that certain types of construction are more suited to some applications than others. It should never be assumed that the comparison of bridge type and cost can be based solely upon span length.

It is appropriate to optimize the span length within a given bridge type: for example, the choice of using different depth standard AASHTO I-girder with different span

lengths and numbers of piers – or similarly, between the larger standard AASHTO girders and Bulb-T's.

When it comes to longer spans where for example the choice may lie between precast or cast-in-place balanced cantilever, the span optimization exercise should consider the difference in construction techniques, schedules and times, in addition to the locations and numbers of piers for different span lengths.

It is far less simple and sometimes can be misleading to compare span length and cost across different bridge types – for example; I-girders versus precast segmental. In such cases, a comprehensive examination of all viable, applicable scenarios should be made to obtain realistic construction costs, schedules and times.

In cases where significant lateral loads may need to be sustained by bridge piers, for example for vessel impact, span lengths should be chosen to optimize the balance between permanent vertical loads and foundation size. For instance, it may be better to adopt a long span to take advantage of the large foundations required for the infrequent high lateral loads or to arrange the span lengths so as to place piers in a lower vessel impact zone, as opposed to using shorter spans and more piers, each of which must carry a higher vessel impact but less vertical load.

For short span structures such as "flat slabs", the choice of an appropriate span length may depend more on the availability of precast prestressed components or preference of the local construction industry to use cast-in-place construction on falsework.

2.6 Cost Comparisons

Cost comparison is one of the important parts of preliminary design and selection between alternative types of bridge structures, but it is not necessarily the most important part. Many other factors go into the selection of the appropriate bridge type, span length and arrangement, superstructure type, substructure type, and all other design elements of a bridge. Cost can be the most obvious comparison method, but aesthetics, local environmental concerns, and owner preferences can all factor into the final bridge selection. Public involvement can also help to determine the outcome, which may or may not be the least cost alternative under consideration.

2.6.1 Alternative Bridge Types

Alternative bridge types were discussed earlier, but each bridge type has a typical associated cost, which is based on previous design experience, and is usually expressed in dollars per square foot. Typical costs based on previous experience at an engineering design firm located in Southwestern Pennsylvania for various bridge types are shown in Table 2.1

Table 2.1 Comparison of Bridge Type Costs as of 2005 for Southwestern Pennsylvania

Superstructure Type	_Cost per Sq. Ft._
Concrete box beam	$100 - 105
Steel I-girder (120' - 180' span range)	$125 - 130
Segmental girders (150' - 600' span range)	$125 - 250
Cable-stayed bridge (500 - 800' span range)	$250 - 350

These costs can be used for preliminary cost estimates, although they represent a cost only at a point in time at a specific location and under specific economic conditions. These costs can vary greatly depending on the cost of materials at the time of construction, the location of the final construction concerning local labor rates, proximity to access routes, fabricators, and raw materials. Before using these costs as a guide for selecting a low-cost alternative, local conditions should be analyzed and the costs per square foot adjusted to reflect the local conditions at the time of the construction of the bridge.

2.6.2 Span Length

One of the biggest drivers of cost and a valuable comparison method for alternative bridge types is the consideration of the effects of span length on the cost of a

structure.   This comparison involves the cost of both the superstructure and substructure, as varying span length affects the cost of both components. As can be seen in Figure 2.73, a greater span length will cost much more in superstructure, but much less in substructure, and the opposite is true of short span lengths over the same length of bridge. For example, a thousand-foot steel superstructure with no piers will require massive beams that can increase costs dramatically, while one hundred ten-foot spans, the same length of structure, will require a much smaller superstructure, decreasing those costs, but greatly increase substructure costs. To select the most appropriate span arrangement to achieve a low-cost alternative, plotting span length versus cost will produce a parabolic curve, with the low point being the optimum number of spans. As with other cost comparison methods, using the least-cost span arrangement may not be the most appropriate due to aesthetic, environmental, and owner considerations.
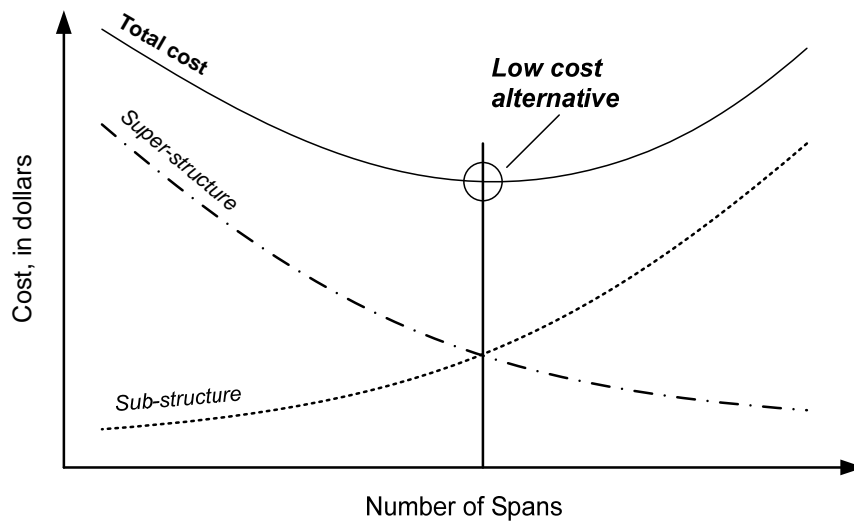
Figure 2.73 Span versus Cost

A graph similar to Figure 2.73 can be generated for each material type, and if the axes are lined up, cost comparisons considering not only span arrangement but also structural material and any other differences in alternatives can be considered. Again with an overlapping comparison, selection of the lowest point of the total cost parabolic curves will be the most cost-effective span arrangement and superstructure type. An example of this type of comparison is shown in Figure 2.74.
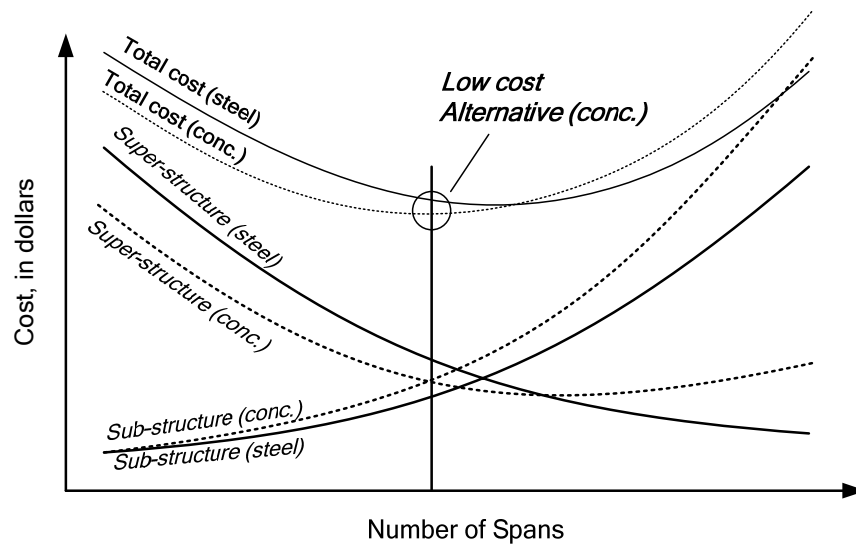
Figure 2.74 Span and Materials versus Cost

2.6.3 Alternative Superstructure Materials

While owner preference, aesthetics, and environmental concerns may govern the selection of superstructure materials, cost comparison can also be a deciding factor. Prestressed concrete beam cost typically includes all of the materials that go into the girders. Reinforcing steel, prestressing steel, and concrete all contribute to the cost of prestressed concrete beams which are usually expressed in a unit cost of dollars per beam. Steel girder costs include the manufacturing and fabrication of plate, rolled, and box girders and are typically expressed in a unit cost of dollars per pound of steel.

When selecting alternatives, the best options can be selected before any design is performed based on typical costs of superstructure materials and the expected span length. In shorter span bridges, the cost of concrete superstructures is typically the lesser of the two, while in longer span bridges, steel beams are typically the less costly option. Prestressed concrete superstructures also have a maximum span length which can limit their use in longer span bridges. Other considerations for alternative materials should include long-term effects of maintenance costs, and other complete life cycle costs which are discussed further in DM Volume 1, Chapter 3, Life Cycle Cost Considerations.

2.6.4 Preliminary Cost Estimates

Cost comparison of bridge alternatives in the preliminary design stage typically involves the creation of an itemized cost estimate for each different superstructure type, span arrangement, and any other major differentiating factors between alternatives. These cost estimates are variable based on the final construction location of the bridge structure; therefore, using previous cost estimates for future jobs should be done with caution to ensure that the proper material categories, unit costs, and contingencies are included.

Itemized cost estimates involve the creation of a material take-off. The material take-off is created using the preliminary bridge structure plans, and estimating the amount of various construction materials for the bridge. Typical categories include girders, deck concrete, pier concrete, abutment concrete, guiderails, lighting structures, concrete coatings and sealers, and structural paint. These categories typically correspond to the local bidding cost structures, and can vary from state to state. Once the material take-off has been tabulated, each category of construction material has an associated cost per unit. These unit costs are also tied to local conditions, and will vary greatly from state to state, even within states. The measurement units can also vary, and designers need to be sure that the right amounts of material are being costed with the proper unit cost. The unit cost includes provisions for material and labor. Unit costs can be obtained from many sources, including previous jobs in similar areas, ASCE publications, AASHTO publications, and state DOT publications. The application of the correct unit cost is imperative to providing a quality cost comparison and should be as exact as possible in the preliminary stages.

Finally, itemized cost estimates are summed and a contingency factor is applied. This contingency factor can range from ten to thirty-five percent depending on the design engineer's confidence in the bridge design, the variability of unit costs, and local typical practices. The contingency is intended to account for changes in the bridge design which may occur between preliminary and final design, as well as changes in unit costs between preliminary and final design.

Another method of generating the preliminary cost estimate for comparison purposes is to apply a typical cost per square foot for that bridge type based on the area of the deck surface. The costs that are presented above in Table 2.1 are just a guideline, and the actual cost per square foot for a bridge structure will vary greatly depending on location, time of construction, distance from fabrication facilities, access to main roads, and many other factors. Because of all of the variables in a cost estimate, the cost per square foot, which is typically based solely on previous construction projects which may or may not match the conditions of the project being evaluated, will give a less accurate estimate than an itemized material take-off.

In conclusion, preliminary cost comparisons can be a useful tool in the selection of the optimum alternative bridge design for a location, but the design engineer should work with the owner to consider other factors, such as aesthetics, environmental concerns, and owner preferences. There should also be a distinction made between the initial cost of a bridge project and the life-cycle cost. In some cases, due to maintenance, expected rehabilitation, and other long-term factors, life-cycle costs of a bridge alternative could be higher for a structure with a lower initial cost. Selection based on individual cost alone could prove to be more costly in long-term maintenance of the structure, therefore life-cycle cost analysis and comparison should be carried out before making a final decision on a bridge alternative.

This page intentionally left blank.

Volume 1
General Design Considerations

Chapter 4
Limit States

4.1 Introduction

This chapter presents the general principles of limit states in bridge design, and it describes the primary limit states used in LRFD – service, fatigue and fracture, strength, and extreme event.

For each limit state, this chapter describes the various load combinations and load factors, it presents the primary applications, and it provides some of the basic equations.

4.2 Limit States in LRFD

Load and resistance factor design utilizes load combinations called limit states which represent the various loading conditions which structural materials should be able to withstand. They are broken into four major categories, strength, service, fatigue, and extreme. Different load combinations are intended to analyze a structure for certain responses, such as deflections, permanent deformations, ultimate strength, and inelastic responses without failure. Not all limit states have to be checked for all structures, and the applicable limit states should be determined by the designing engineer. When all applicable limit states and combinations are satisfied, a structure is deemed acceptable under the LRFD design philosophy.

The service limit state contains load combinations which reflect loadings intended to control stresses, deformations, and crack widths in structural materials. Loads in service limit states are taken at regular service conditions, and load factors are typically closer to 1.00.

Strength limit state combinations are intended to create conditions of maximum loading on a bridge structure. These combinations bring the structure under considerable loading which will cause possible overstresses and structural deformations, but the structural integrity should be maintained.

The fatigue and fracture limit state is intended to analyze the stress range of a structural material. The loading conditions represent a single truck, occurring over a specific number of cycles. The material toughness requirements that should be tested should match that of the AASHTO Material Specifications.

Extreme limit states are load combinations that are intended to analyze the ability to withstand an event of extreme loading with a recurrence period that is greater than the design life of the structure. Such events as earthquakes, major floods, vehicular collisions, or ice flow impact would all be considered an extreme limit state. Much like strength limit states, members are intended to deform and deflect, but not fail under extreme limit state conditions.

Each type of limit state contains more than one load combination, numbered with roman numerals. These combinations reflect different load types, and different load factors based on the intended loading condition that is to be reflected.

For reference, the load factors table presented in *AASHTO LRFD* Table 3.4.1-1 is presented below in Table 4.1. Note that in strength and extreme limit states, permanent loads are factored individually as presented in *AASHTO LRFD* Table 3.4.1-2, and as shown in Table 4.2.

Table 4.1 *AASHTO LRFD* Load Combinations and Load Factors

Load Combination Limit State	DC DD DW EH EV ES EL	LL IM CE BR PL LS	WA	WS	WL	FR	TU CR SH	TG	SE	Use one of these at a time			
										EQ	IC	CT	CV
Strength I (unless noted)	γ_p	1.75	1.00	--	--	1.00	0.50/1.20	γ_{TG}	γ_{SE}	--	--	--	--
Strength II	γ_p	1.35	1.00	--	--	1.00	0.50/1.20	γ_{TG}	γ_{SE}	--	--	--	--
Strength III	γ_p	--	1.00	1.40	--	1.00	0.50/1.20	γ_{TG}	γ_{SE}	--	--	--	--
Strength IV *EH, EV, ES, DW* *DC only*	γ_p 1.5	--	1.00	--	--	1.00	0.50/1.20	--	--	--	--	--	--
Strength V	γ_p	1.35	1.00	0.40	1.00	1.00	0.50/1.20	γ_{TG}	γ_{SE}	--	--	--	--
Extreme Event I	γ_p	γ_{EQ}	1.00	--	--	1.00	--	--	--	1.00	--	--	--
Extreme Event II	γ_p	0.50	1.00	--	--	1.00	--	--	--	--	1.00	1.00	1.00
Service I	1.00	1.00	1.00	0.30	1.00	1.00	1.00/1.20	γ_{TG}	γ_{SE}	--	--	--	--
Service II	1.00	1.30	1.00	--	--	1.00	1.00/1.20	--	--	--	--	--	--
Service III	1.00	0.80	1.00	--	--	1.00	1.00/1.20	γ_{TG}	γ_{SE}	--	--	--	--
Service IV	1.00	--	1.00	0.70	--	1.00	1.00/1.20	--	1.00	--	--	--	--
Fatigue *LL, IM, CE only*	--	0.75	--	--	--	--	--	--	--	--	--	--	--

Table 4.2 Load Factors for Permanent Loads, γ_p

Type of Load	Load Factor	
	Maximum	Minimum
DC: Component and attachments	1.25	0.90
DD: Downdrag	1.80	0.45
DW: Wearing surfaces and utilities	1.50	0.65
EH: Horizontal earth pressure		
• Active	1.50	0.90
• At-rest	1.35	0.90
EL: Locked-in erection stresses	1.00	1.00
EV: Vertical earth pressure		
• Overall stability	1.00	N/A
• Retaining walls and abutments	1.35	1.00
• Rigid buried structure	1.30	0.90
• Rigid frames	1.35	0.90
• Flexible buried structures other than metal box culverts	1.95	0.90
• Flexible metal box culverts	1.50	0.90
ES: Earth surcharge	1.50	0.75

4.3 Service Limit States

Within the service limit states, there are four load combinations that are designed to test various aspects of the structure being analyzed under nominal loading conditions which could easily be expected during normal operation, and will occur many times over the design life of the structure. The service limit states are intended to control deflections in superstructures and cracks in prestressed concrete structures. These limit states are numbered Service I – Service IV. The basic function of each limit state is as follows:

➢ Service I

This limit state contains load factors for loads that could be expected under normal operating conditions with a fifty-five mile per hour wind. Most loads are taken at a 1.00 load factor, only some wind loads and some temperature loads are factored by other values. The results of this load combination can be used to control deflection in a structure, control crack widths in reinforced concrete members, and analyze slope stability in geotechnical situations. For prestressed concrete, the Service I limit state should be used to investigate compression, while tension should be investigated with the Service III limit state.

➢ Service II

The Service II limit state contains load factors combined to produce maximum effects on steel structure yielding, as well as slip of slip-critical connections within the structure. Vehicular live load is the focus of this Service limit state, as the load factor for live load is 1.30, where most other load factors are 1.00. The Service II limit state corresponds to the overload provisions for steel structures that appeared in past AASHTO specifications for WSD and LFD designs.

➢ Service III

Within the Service III limit state, loads are factored and combined to produce the greatest effect on prestressed concrete superstructure elements. Crack control is the goal of this load combination, which focuses on a modified live load, applying only a 0.80 factor to live loads, while most other loads maintain a 1.00 load factor.

➢ Service IV

The Service IV limit state is another limit state that is intended to control cracking in prestressed concrete structure elements. The load factors in this case focus on wind loading, with a 0.70 factor on wind, equating to a high wind load over eighty miles per hour.

4.3.1 Live Load Deflection

One of the objectives of the Service limit states is to determine if the applied loads and factored resistance of the structural materials is able to control deflections under normal live load conditions. According to *AASHTO LRFD* Article 2.5.2.6.2, acceptable deflections for bridge elements are related to the length of the element. When no other guidance exists, the AASHTO deflection guidelines for steel or concrete superstructures are as follows:

➢ Vehicular live load, general....................................... Span Length / 800

➢ Vehicular and pedestrian live loads .... Span Length / 1000

➢ Vehicular live load on cantilever .... Span Length / 300

➢ Vehicular and pedestrian live loads on cantilever..... Span Length / 375

If factored live loads do not produce deflections greater than these criteria in Service limit states, the design is acceptable.

4.3.1.1 Permanent Deformations

Using the Service II limit state load combination, steel structures which are exposed to this load pattern and combination should be checked for the effects of permanent deformations. The provisions for permanent deformations apply to design live loads as presented in *AASHTO LRFD* Article 3.6.1.1. If other live loads, such as permit loads and overloads, as specified by the Owner, are to be checked, the live load factor shown in Table 4.1 should be reduced for the Service II limit state.

For reinforced concrete deck sections, if tensile stresses due to Service II loads or factored construction loads exceed the factored modulus of rupture for the concrete deck section, then a minimum of one percent reinforcing must be present in the deck. Controlling cracks in the deck section will also assist in providing adequate resistance for Service II tensile stresses.

Under flexure, to limit the effects of permanent deformations of steel girder flanges, both composite and non-composite steel members shall not exceed the following flange stress conditions, as presented in *AASHTO LRFD* Article 6.10.4.2.2.

➢ Top steel flange, composite sections:

$$f_f = 0.95R_hF_{yf}$$

AASHTO LRFD Equation 6.10.4.2.2-1

➢ Bottom steel flange, composite sections:

$$f_f + \frac{f_l}{2} \leq 0.95R_hF_{yf}$$

AASHTO LRFD Equation 6.10.4.2.2-2

> ➤ Both steel flanges, non-composite sections:

$$f_f + \frac{f_l}{2} \leq 0.80 R_h F_{yf}$$

AASHTO LRFD Equation 6.10.4.2.2-3

where:

f_f =   flange stresses at section for Service II limit state without consideration of flange lateral bending (ksi)

f_l =   flange lateral bending stress for Service II limit state (*AASHTO LRFD* Article 6.10.1.6) (ksi)

R_h =   hybrid factor determined by *AASHTO LRFD* Article 6.10.1.10.1

Bridges comprised of continuous span flexure members may redistribute some negative moment at pier sections under the Service II limit state as long as the section in question meets the requirements of *AASHTO LRFD* Article B6.2. Redistribution of these negative moments must follow the procedures outlined in *AASHTO LRFD* Article B6.3 or B6.6, as appropriate as determined by the design engineer.

Other considerations for controlling the effects of permanent deflections include keeping Service II limit state loads for longitudinal compressive stresses in shored-construction decks below 0.6f'$_c$.

In addition, all sections except those in positive flexure which meet AASHTO requirements outlined in *AASHTO LRFD* Article 6.10.2.1.1, the following condition must be satisfied:

$$f_c = F_{crw}$$

AASHTO LRFD Equation 6.10.4.2.2-4

where:

f_c =   compression flange stresses under Service II limit state loads without considering flange lateral bending (ksi)

F_{crw} =   nominal bend-buckling resistance in steel girder webs without longitudinal bracing, see *AASHTO LRFD* Article 6.10.1.9. (ksi)

4.3.2 Crack Control

The Service limit states are used to evaluate and control the cracking of reinforced and prestressed concrete structural elements, as well as the deflections. Under these two service conditions, cracking stress in concrete sections shall be taken as the modulus of rupture, per *AASHTO LRFD* Article 5.5.2. The modulus of rupture, as presented in *AASHTO LRFD* Article 5.4.2.6 can be determined either by testing procedures, or without solid experimental information, the following guidelines can be used.

> ➤ For normal weight concrete .... $0.24 \sqrt{f'_c}$

➢ For sand-lightweight concrete................. $0.20 \sqrt{f'_c}$

➢ For all-lightweight concrete.................... $0.17 \sqrt{f'_c}$

Note that these values are considered unconservative for any tensile forces in concrete sections that are not a result of flexure. For tensile forces not a result of flexure, the direct tensile stress should be used for the modulus of rupture to check for crack control.

4.4 Fatigue and Fracture Limit States

The fatigue and fracture limit states comprise a single load combination intended to produce the greatest effect of a stress range on a structural element which tests the facture-critical and fatigue properties against a single truck loading as specific in *AASHTO LRFD* Article 3.6.1.4.1. This limit state is not applicable to all bridge designs, and the use of this limit state is left to the design engineer to determine if the effects of fatigue and fracture could be a problem for their structure. Specifically, AASHTO does not require fatigue limit state checks for some concrete decks, or wooden decks, as specified in *AASHTO LRFD* Article 9.5.3.

Fatigue in reinforced, prestressed, and partially-prestressed concrete components should assume the following according to *AASHTO LRFD* Article 5.7.1.

- ➢ Prestressed concrete resists tension at uncracked sections
- ➢ Strain in concrete varies linearly
- ➢ The modular ratio, *n*, is rounded to the nearest integer, not less than 6.0
- ➢ An effective modular ratio of *2n* is applicable to permanent loads and prestress

Fatigue in concrete sections is evaluated for fatigue in reinforcing bars and any present prestressing tendons. For prestressing tendons, the stress range for fatigue is dependant on radii of curvature.

- ➢ 18.0 ksi for radii of curvature in excess of 30.0 feet
- ➢ 10.0 ksi for radii of curvature less than 12.0 feet
- ➢ All other lengths linearly interpolated

Reinforcing bars in concrete sections are checked against the following equation for the fatigue limit state. Bar bends in areas of high stress should be avoided to ensure that reinforcing bars are sufficient in fatigue.

$$f_f \leq 21 - 0.33 f_{min} + 8 \left(r/h \right)$$ Equation 4.1

AASHTO LRFD Equation 5.5.3.2-1

where:
f_f =   stress range (ksi)
f_{min} =   minimum live load stress from fatigue limit state combined with the more severe stress from either permanent loads, or permanent loads, shrinkage, and creep-induced external loads. This value is positive if in tension, negative if in compression.
r/h =   ratio of base radius to height of rolled-on transverse deformations; if the actual value is not known, 0.3 may be used.

Fatigue in steel structures is categorized as either load- or distortion-induced, as described below. The rest of the provisions of this section apply to steel superstructure elements unless otherwise noted.

The fatigue limit state includes only live loads, impact loads, and the loads from centrifugal forces in the case of curved or superelevated structures. No permanent loads, water loads, time or temperature dependant loads are included in the fatigue checks. The stress range that is produced from the analysis with this limit state should be compared against the allowable stress ranges for the structure materials, as shown in AASHTO. If appropriate shear connectors are provided on steel beams with concrete decks, the short-term composite section may be used to compute the fatigue stress. Only sections in tension should be considered for fatigue effects, unless the compression stresses are less than twice the maximum tensile stresses.

The material resistance factor, ϕ, is 1.00 for fatigue limit states, as the resistance is dependant on detail categories which are well documented. The overall load factor, η, is also 1.00 for fatigue limit states, although specific load factors, γ, still apply per the load factor table.

To reflect the cyclic nature of fatigue limit state load patterns, the design equation for LRFD can be modified for the fatigue limit state to:

.

$$\gamma(\Delta f) = (\Delta F)_n$$

<div align="right">Equation 4.2
AASHTO LRFD Equation 6.6.1.2.2-1</div>

where:

γ	=	load factor from Table 4.1
(Δf)	=	live load stress range due to fatigue load
$(\Delta F)_n$	=	nominal fatigue resistance, specific to detail category

4.4.1 Fatigue Resistance

Fatigue resistance for steel structural members is determined by detail categories, which are based on connection types, and member shape. Detail categories A, B, and B' have shown through experience to rarely govern, therefore fatigue limit state considerations are less imperative for these detail categories. In general, most steel superstructure elements fall into detail categories A, B, or B'. A few selected detail descriptions are presented in Table 4.3. The detail categories are more extensively described in *AASHTO LRFD* Article 6.6.1.2.2.

Table 4.3 Detail Categories for Load-Induced Fatigue (excerpt from *AASHTO LRFD* Table 6.6.1.2.3-1)

GENERAL CONDITION	SITUATION	DETAIL CATEGORY	ILLUSTRATIVE EXAMPLE (*AASHTO LRFD* FIG. 6.6.1.2.3-1)
Plain Members	Base metal: • With rolled or cleaned surfaces; flame-cut edges • Of unpainted weathering steel, all grades • At net section of eyebar heads and pin plates	A B E	1, 2
Built-up Members	Base metal and weld metal in components, without attachments, connected by: • Continuous full-penetration groove welds with backing bars removed, or • Continuous fillet welds parallel to direction of applied stress • Continuous full-penetration groove welds with backing bars in place, or • Continuous partial-penetration groove welds parallel to the direction of applied stress	B B B' B'	3, 4, 5, 7

AASHTO presents illustrations depicting a typical fatigue detail for each condition that is referenced. An excerpt from that illustration, *AASHTO LRFD* Figure 6.6.1.2.3-1, is shown below in Figure 4.1. The excerpts shown match the number that is referenced in the excerpt from the fatigue detail table, Table 4.4.
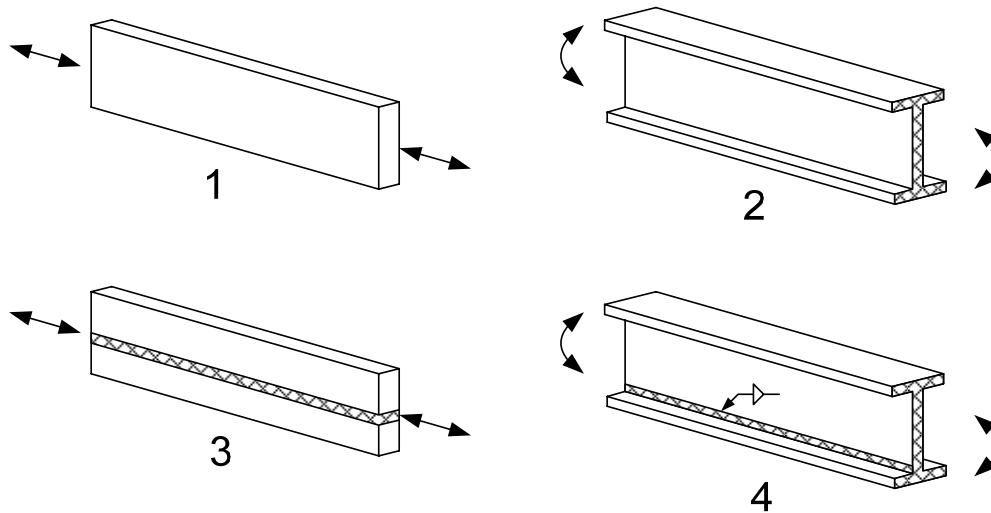
Figure 4.1 Illustrative Examples of Fatigue Details

The following table shows the resistances for the various detail categories that are presented in *AASHTO LRFD* Table 6.6.1.2.5-3. These fatigue thresholds should then be applied to the formula given below to obtain the true fatigue resistance for a section. Also included in this table are the ADTT values over a 75-year design life, with only one cycle per truck. An infinite life check will govern in most high traffic situations, except for detail categories E and E'. Finally, the detail category constant, A, is presented in Table 4.4. This value is used in the calculation of the nominal fatigue resistance.

Table 4.4 Fatigue Resistance Detail Category Specific Properties

Detail Category	Constant-Amplitude Fatigue Threshold (ksi)	75-year $(ADTT)_{SL}$ Equivalent to Infinite Life (trucks per day)	Detail Category Constant, A $(\times 10^8, ksi^3)$
A	24.0	535	250.0
B	16.0	865	120.0
B'	12.0	1035	61.0
C	10.0	1290	44.0
C'	12.0	745	44.0
D	7.0	1875	22.0
E	4.5	3545	11.0
E'	2.6	6525	3.9

In addition to the properties shown in Table 4.5 for the different detail categories, a factor applies related to the cycles per truck passage, depending on the span length of the member in question, the type of structure, and location of the load, as well as the direction of the force in the member.

Table 4.5 Cycles per Truck Passage

Longitudinal Members	Span Length	
	> 40.0 ft.	≤ 40.0 ft.
Simple span girders	1.0	2.0
Continuous girders		
1) near interior support	1.5	2.0
2) elsewhere	1.0	2.0
Cantilever girders	5.0	
Trusses	1.0	
Transverse Members	Spacing	
	> 20.0 ft.	≤ 20.0 ft.
	1.0	2.0

To calculate the nominal fatigue resistance, $(\Delta F)_n$, for a steel member, the following equation must be applied.

$$(\Delta F)_n = \left(\frac{A}{N}\right)^{\frac{1}{3}} \geq \frac{1}{2}(\Delta F)_{TH}$$

AASHTO LRFD Equation 6.6.1.2.5-1

where:

N	=	(365) (75) n $(ADTT)_{SL}$
A	=	constant from Table 4.4
N	=	number of stress range cycles from Table 4.5
$(ADTT)_{SL}$	=	single lane ADTT from Table 4.4
$(\Delta F)_{TH}$	=	constant-amplitude fatigue threshold, Table 4.4

In the case of details connected with transversely loaded fillet welds, and a loaded discontinuous plate, the equation for determining the nominal fatigue resistance is altered per *AASHTO LRFD* Eq. 6.6.1.2.5-3.

4.4.2 Distortion-Induced Fatigue

Distortion-induced fatigue effects are cracks and other structural deficiencies that result from secondary stresses. These secondary stresses are a result of a lack of rigidity from insufficient load paths between transverse members and longitudinal

members making up the cross section being analyzed. Distortion-induced fatigue is an observed problem that has appeared recently in steel bridge structures across the country. Much research has been done on this problem which usually involves the separation of web stiffeners from flanges at sections of negative moment. Rotation due to live loading causes cross-frames to transfer load to stiffeners which rotate girder webs. The embedment of the top flange of a girder in the deck causes it to resist this rotation, which causes distortion-induced fatigue cracking. This problem is more prevalent in exterior girders as they typically have only a single stiffener to resist this fatigue cracking. An example of this separation can be seen in Figure 4.2.

Distortion-induced
fatigue crack
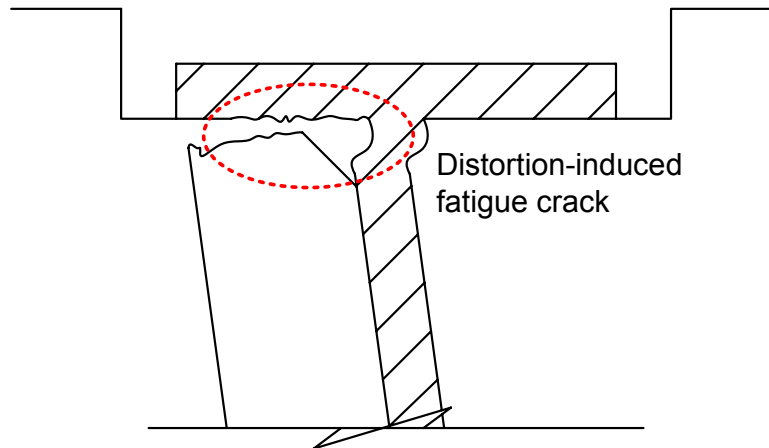
Figure 4.2 Distortion-Induced Fatigue

To reduce the effects of these fatigue loads, connection plates should be provided, and the provisions of *AASHTO LRFD* Article 6.10.5.3 should be followed to ensure that steel girder webs do no buckle, and elastic flexure in the web is controlled.

Transverse connections should be achieved through cross-frames, diaphragms or floorbeams which are welded or bolted to the main girders of the cross section. Unless better information is available on lateral loads, a 20.0 kip force for straight, non-skewed bridges has been found through experience to be adequate for design of transverse connection elements.

Lateral connection plates should also be provided to aid in reducing distortion-induced fatigue. The guidelines for these connections are presented in *AASHTO LRFD* Article 6.6.1.3.2.

4.5 Strength Limit States

The strength limit state load combinations are sets of loads and load factors to analyze structural elements for ultimate failure strength conditions under various live load and wind load conditions. These load combinations are intended to be combinations that would not occur during normal operation of the structure, but could occur during the design life of the structure. The load combinations may cause permanent deformations or overstresses in structural elements, but will not cause failure.

Strength limit states are the load combinations which are primarily used to test a bridge structure for ultimate resistance capacity. Not all Strength limit states are applicable to all bridge structures, and the designer should use their engineering judgment to decide which combinations to use and which to discount for their design.

➢ Strength I

The Strength I limit state is the primary load combination for evaluating the capacity of structural members under full live load conditions without wind effects. While temperature load factors are still under development, the load factors for time-dependant effects are reduced for the Strength I case, as some inelastic deformation is expected in the structure which would relieve some of these stresses. Most checks against failure will occur with this limit state which applies to almost all bridge structure designs.

➢ Strength II

This limit state can be tailored to each specific bridge project to allow owners to specify an overload, or permit vehicle that should be allowed on the bridge under specific circumstances. Conservatively, permit vehicles are assumed to be unescorted, therefore vehicular live load is applied in lanes other than the lane occupied by the permit vehicle. In the event of a permit vehicle that is not as long as the entire bridge span, lane load should be considered prior to and after the permit vehicle loading. Other live loads are slightly reduced from the effects that are in the Strength I limit state to reflect the conservatism of the assumptions presented above. Wind loads are not included in this limit state, similar to the Strength I state, and a similar release on time-dependant effects is allowed.

➢ Strength III

This limit state reflects a high wind condition which would normally prevent live load from using the bridge. While some live load may be present, it would be considered statistically insignificant, and therefore the load factor on live load for this limit state is zero. The wind loads on the structure are increased through higher load factors to account for the focus of this limit state.

➢   Strength IV

The Strength IV limit state is designed more for longer-span bridges, as a modification to the Strength I limit state. For most bridges in the short to medium span range (up to 200 feet), the Strength I limit state controls. But, for spans greater than 200 feet, the dead load to live load ratio begins to increase. The load factors for the Strength IV case reflect this increased ratio and in most cases, Strength IV will control for longer span bridges. According to *AASHTO LRFD* Article C3.4.1, tests have verified this for spans up to 600 feet in length.

➢   Strength V

This limit state is a combination of the Strength I and Strength III conditions where high winds and significant live load both affect the bridge. Live loads are reduced somewhat to reflect the idea that high winds will discourage some live load, and wind loads are not increased as much as in the Strength III case. Wind on live load effects enter into the load combination only in this limit state out of all the Strength cases.

The strength limit states will typically allow loads to deform and stress a structure into an inelastic response. The resistance factors that are applied to the structure for the strength limit state differs by material type, desired response, and analysis type. An example of steel resistance factors is shown in Table 4.6. For all primary steel connections, *AASHTO LRFD* Article 6.13.1 specifies that the strength limit state must govern the design of these connections.

Table 4.6 Steel Resistance Factors for Strength Limit States

For flexure;	$\phi_f = 1.00$
For axial compression, steel only;	$\phi_c = 0.90$
For shear connectors;	$\phi_{sc} = 0.80$
For A 307 bolts in shear;	$\phi_s = 0.65$

For concrete structures, the strength and stability of structural members should be evaluated at the strength limit state. The provisions of *AASHTO LRFD* Article 5 provide guidance on the determination of the nominal resistance of concrete members, and the resistance factors again vary based on reinforcement, prestressing, desired response, analysis method, and other factors. An example of concrete resistance factors is shown in Table 4.7.

Table 4.7 Concrete Resistance Factors for Strength Limit States

For flexure and torsion of reinforced concrete;	$\phi = 0.90$
For flexure and torsion of prestressed concrete;	$\phi = 1.00$
For shear and torsion, light weight concrete;	$\phi = 0.70$
For bearing on concrete;	$\phi = 0.70$
Segmented lightweight concrete shear, unbonded tendons;	$\phi = 0.65$

Other construction materials have different resistance factors based on the research performed on those materials and the level of knowledge about their response to various loading conditions. It is the design engineer's responsibility to choose the appropriate resistance factor when performing strength limit state checks, based on the structural material, response being analyzed, and load type.

4.5.1 Fracture Toughness Requirements

For members and any connections with tensile forces in the Strength I limit state load combination, project plans shall specify that Charpy V-notch fracture toughness tests must be conducted on samples of the structural material. The required fracture toughness for a structural material is dependant on the temperature zone the final project is to be constructed in, according to *AASHTO LRFD* Article 6.6.2. It is the responsibility of the design engineer to note which members of a structure are fracture critical, as these members have different fabrication specifications, per *AASHTO LRFD* Article C6.6.2.   Fracture-critical members will include all attachments with a length greater than 4.0 inches in the direction of the tensile force.

4.6 Extreme Event Limit State

The extreme event limit state represents loadings that are those that would occur only once over the design life of a structure. Typically, supporting information is available on local conditions which are considered for extreme event analysis. Areas that are at risk for earthquakes, especially the west coast of the United States, will need to be checked for extreme limit states for earthquake loadings. Areas that experience sub-freezing temperatures in the winter, or which are downstream from an area that does, may include ice floes as extreme event limit state checks. Human error which causes collision is also considered an effect which is analyzed in the extreme limit state. Collisions can be with either the bridge superstructure or substructure. The effects of a collision on either part of the bridge can have an effect on both, therefore if collisions are possible, they should be analyzed for both parts of a bridge structure. Not all extreme limit states apply to all areas of the country and all types of bridge construction, therefore it is the design engineer's responsibility to choose which extreme limit states are applicable. All four load types that are included as extreme events are analyzed separately.

Two extreme event limit state combinations are presented in the *AASHTO LRFD* specification. These limit states differentiate between the live loads that would most likely be present during the different extreme events, and the extreme event which is being considered in each limit state.

$\triangleright$ Extreme I

The Extreme I limit state is the load combination that is used to analyze a structure for earthquake loading. In this load case, the live load factor is considered under development. The AASHTO specifications direct that the $_{EQ}$ load factor should be determined on a project-specific basis. This would lead to a differing $_{EQ}$ between various projects depending on the engineer's judgment, and experience, something that the LRFD design philosophy is working to eliminate. Previous AASHTO specifications have set this value equal to zero, but current research shows that setting this value to $\gamma_{EQ} < 1.0$, or more specifically 0.50 may be applicable for most average daily truck traffic (ADTT) conditions. (*AASHTO LRFD* Articles 3.4.1, C3.4.1)

$\triangleright$ Extreme II

This limit state includes the effects of ice flows, vehicular collisions, and vessel collisions. The effects of these three events are not to be combined at the same time; each is supposed to be checked individually. The load factors for live load in this limit state reflect the fact that if one of the extreme events does occur, the likelihood of full live load being on the bridge is small. Time and temperature dependant effects are not included in this load combination as extensive inelastic deformations are expected under this loading condition.

The effects of an extreme event limit state are allowed to cause damage to a structure. Stresses and deformations well into the inelastic range are allowed and, in some cases, expected. Prevention of full loss of structural integrity and collapse is the goal of analysis of the extreme event limit states.

The load factors on extreme event loads, as well as their applicability to a structure design, are left to the bridge design engineer. The load factors presented in the AASHTO specifications are meant as a guideline, as the extreme event limit states are still under development. These load factors may be updated and extreme limit states added or eliminated as research continues in this area.

Volume 1
General Design Considerations

Chapter 5
Loads and Load Combinations

5.1 Introduction

The limit state design which governs the *AASHTO LRFD* bridge design specification utilizes certain specific load types which include loadings to account for dead loads, live loads, wind loads, construction loads, time-dependant loads, temperature-dependant loads, and collision loads. The load types presented in this chapter apply only to tangent-construction bridges using the *AASHTO LRFD* specification. The loads which are presented in this chapter pertain only to the design of bridge superstructures. In some sections, other loads do exist, but these loads have little to no effect on the design of superstructure components, and are not mentioned.

.

5.2 Load Factors and Combinations

Load and resistance factor design is primarily concerned with limit states, which are load combinations which modify both the magnitude of loads, and the resistance of structural materials, to represent certain worst-case effects. These limit states include:

➢ Those for design against cracking and deflection, or *Service* conditions

➢ Those for design against failure under increased loading, or *Strength* conditions

➢ Those for design against fatigue failures, or *Fatigue* conditions

➢ Those for design against events of large loading which have a recurrence period longer than the design life of the bridge, or *Extreme* conditions.

These limit states involve a number of load factors and resistance factors which are applied to the basic LRFD equation,

$$\eta(\sum \gamma_{DL} DL + \sum \gamma_{LL} LL) = \phi R_n \qquad \text{Equation 5.1}$$

where:

η	=	load modifier applied to all loads
γ_{DL}	=	load factor for dead loads
γ_{LL}	=	load factor for live loads
DL	=	dead loads applied to structure element
LL	=	live loads applied to structure element
ϕ	=	resistance factor
R_n	=	nominal resistance (strength) of structure element

The load factors for each of these limit states, and the sub-limit states which exist in each category differ based on the desired loading condition. Some load combinations reflect instances of high wind, where live load would not typically be present on a bridge, but wind loads are very high. Others reflect instances of normal operating conditions, while some represent earthquake conditions, or vehicular collisions with bridge structures. Resistance factors affecting the resistance of structural materials also vary based on the limit state being investigated. More information on load factors and load combinations is presented in DM Volume 1, Chapter 4, Limit States.

5.3 Dead Loads

5.3.1 Component Dead Loads

Component dead loads include those loads, induced by gravitational forces, on a bridge structure due to its structural parts. All steel and concrete members, reinforcing within concrete sections, and future attachments later in the erection procedure produce dead loads. The *AASHTO LRFD* specifications refer to dead loads as permanent loads, which is an appropriate description. These loads are present from the time a structural member is erected and will not decrease or vary with time, temperature, or any other outside factor.

Component dead loads are typically divided into two categories, labeled DC1 and DC2. DC1 loads are typically those loads which are added and present during the erection of the main spans of a bridge. Typical inclusions in DC1 are the self-weight of girders, deck sections, and cross-frames. DC2 loads include permanent loads that are placed later in the erection procedure and could be moved later in the service life of the bridge. Raised sidewalks, roadway barriers, lighting structures, and other attachments to a structure make up the DC2 loads. The section properties that are used to calculate the effects of DC1 and DC2 loads may be different depending on the materials and construction sequence of a structure. DC1 loads may only affect a non-composite section for a bridge with a steel superstructure, but DC2 loads would affect a composite section, producing different deflections and reactions. Both DC1 and DC2 loads are considered one load type, DC, for purposes of calculating a load factor for load combinations.

In the Service limit states, DC loads are given a load factor of 1.0 to show the certainty of these loads, and to reflect normal operating conditions for Service limit states. In Strength limit states, DC load factors can vary between 0.90 and 1.50 depending on the effect desired, and the combination being used. Extreme limit state dead loads are evaluated much like Strength limit states to account for possible variability of these permanent loads under abnormal, and possibly extreme loading conditions. Fatigue limit state evaluation does not account for the effects of DC dead loads.

Typically, component dead loads are expressed in kips per cubic foot, and the geometric properties of the various bridge components are used to calculate the expected gravitational effects to be used as component dead loads. The design engineer is encouraged to investigate local conditions, specific bridge construction specifications or methods, and advances in materials technology to obtain the most appropriate unit weight for determination of permanent component dead loads. In the absence of more precise information, *AASHTO LRFD* provides some guidance for typical unit weights in Table 3.5.1-1. An excerpt of that table for some of the most common structural materials is presented in Table 5.1.

Table 5.1 Unit Weights of Typical Components, DC

Material		Unit Weight (kcf)
Concrete	Lightweight	0.110
	Sand-lightweight	0.120
	Normal weight with f'$_c$ ≤ 5.0 ksi	0.145
	Normal weight with 5.0 < f'$_c$ ≤ 15.0 ksi	0.140 + 0.001f'$_c$
Steel		0.490
Wood	Hard	0.060
	Soft	0.050

(from AASHTO LRFD Table 3.5.1-1)

5.3.2 Component Dead Loads Design Example

Calculate the component dead load (DC1) for the steel girder and tributary area of normal weight concrete (f'$_c$ = 4.0 ksi) as shown:
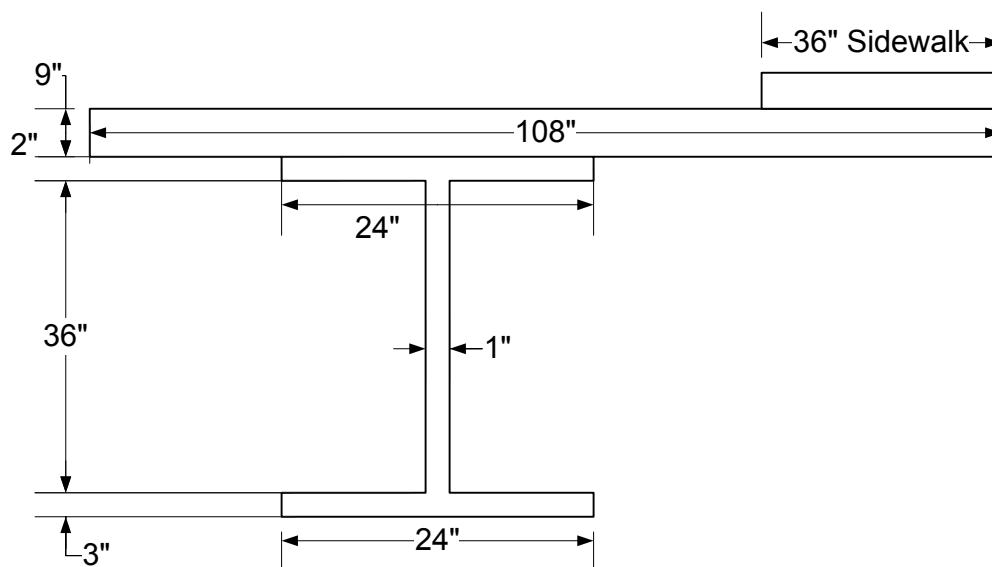
Figure 5.1 Steel Girder and Tributary Area

First, calculate area of concrete contributing to DC1. Since sidewalks are placed after the deck and girders, they are a DC2 load, and therefore will not factor into this calculation.

Deck width = 108", Deck height = 9"
Deck area (normal weight concrete, f'$_c$ = 4.0 ksi) = 108 x 9 = 972 in^2

Next, the area of the girder should be calculated.

Flange width = 24", Top Flange thickness = 2", Bottom Flange thickness = 3", Web thickness = 1", Web height = 36"

Girder area (steel) = 24 x 2 + 24 x 3 + 36 x 1 = 156 in^2

The unit weight of normal weight concrete, f'c = 4.0 ksi from Table 5.1 is 145 pounds per cubic foot. The unit weight of steel from Table 5.1 is 490 pounds per cubic foot. Applying these unit weights to the areas already calculated gives:

[972 in^2 / 144 in^2/ft^2] x 145 pcf = 978.75 lb/ft
[156 in^2 / 144 in^2/ft^2] x 490 pcf = 530.83 lb/ft

These two loads are added together to produce the final DC1 load per foot on the girder shown as:

978.75 + 530.83 = 1509.58 lb/ft, approximately **1.51 kip/ft**

5.3.3 Wearing Surface and Utility Loads

Wearing surfaces and utility loads are considered semi-permanent loads, and are grouped within the DW load type. Wearing surfaces can be those applied at initial construction, or anticipated future wearing surfaces for maintenance of the bridge. Utility loads include the weight of conduits and attachments for not only bridge components, but also those using the bridge as a method of crossing. These loads are slightly more variable than those for component dead loads. The wearing surface that is used in the future may end up being heavier or lighter than anticipated, depending on advances in technology and common practice by the time a resurfacing is needed. Utilities may also be added or removed, and the weight of conduits and connectors in the future may change. To reflect this variability, in Strength and Extreme limit states, the load factors for wearing surface and utility loads ranges from 0.65 for minimum effects to 1.50 for maximum effects.

5.3.4 Sequence of Application

The sequence of erection of a bridge structure determines the classification of some dead loads which are applied to the structure. Beams, decks and any other basic structural components are typically classified as DC1 loads, permanent component dead loads. When the composite action of a bridge structure is variable over the construction sequence, these DC1 loads are typically applied to a non-composite section.

Secondary permanent load applications fall into either the DC2 or DW load categories. DC2 loads include sidewalks, barriers, parapets, and other structural attachments which are considered bridge components, but do not contribute to the structural stability of a bridge. DW loads include any wearing surfaces that are applied either initially, or anticipated in the future, and utility loads are also included in the DW load category. In structures in which composite action is variable, DC2 and DW loads are typically applied to the composite section for reactions, stresses, and deflections.

Other dead loads are specified by the *AASHTO LRFD* specifications, and are included specifically in some Strength limit states. These dead loads are due to the effects of earth pressure, vertically and horizontally, earth pressure surcharge, and other geotechnical effects. These loads are not discussed in this section, as they rarely, if ever, influence the design of a bridge superstructure.

5.4 Construction Loads

Construction loads include those loads which are a direct effect of erection procedures, casting of deck sections, and other sequential activities which can introduce additional forces outside the normal range of service forces that the bridge would see in its design life. Some of these forces remain a consideration for the structure after construction is complete, such as in cable-stayed bridges, and other construction forces represent equipment and pedestrian loads which will be eliminated after the structure opens for service.

General load factors for these construction loads are described in *AASHTO LRFD* Article 3.4.2. The weight of the structure and attachments, or the DC load as described above, is assigned a load factor of 1.25 or greater. As the actual construction loads can vary from contractor to contractor, state to state, and even with the time of year and location of construction, the estimation of the loads due to mounted equipment, mobile equipment, and construction workers is less certain than the load due to the gravitational self-weight of bridge structural components. The load factor for the construction forces themselves in combination should be greater than 1.50. Wind forces can greatly affect a bridge under construction, as the surfaces that wind can affect are greater and more random, therefore a factor of 1.25 or higher on all wind loads should be applied in combination for construction loads. All other loads which are present during the construction sequence shall have a load factor of 1.00.

5.4.1 Construction Loads on Concrete Structures

Construction loads on concrete superstructures are presented in detail in *AASHTO LRFD* Article 5. *AASHTO LRFD* Article 5.5.4.2 presents the criteria for selecting an appropriate resistance factor, dependant on the type of reaction being analyzed and the type of concrete making up the superstructure in question. An excerpt from this table showing some example resistance factors is presented in Table 5.2.

Table 5.2 Resistance Factors for Construction Loads on Concrete Structures

Flexure and tension of reinforced concrete	0.90
Flexure and tension of prestressed concrete	1.00
For bearing on concrete	0.70
For tension in steel in anchorage zones	1.00

The construction loads that are incorporated into the design of concrete structures should be noted on contract drawings and documents, to make the owner and bidding contractors aware of the maximum construction loads for which a structure has been evaluated. Construction loads for concrete structures can include;

➢ Erection loads

➢ Temporary supports and restraints

➢ Closure forces due to misalignment

➢ Residual forces and deformations from removal of temporary loads and supports

➢ Residual strain-induced effects from removal of temporary loads and supports

The load types which are to be considered for concrete bridge construction loads include the following load types which are then combined for Strength and Service limit states.

➢ *DIFF* – differential loads which are applied to balanced cantilever construction bridges. These loads are taken as two percent of the DC dead load which is applied to one cantilever arm

➢ *CLL* – distributed construction live load which accounts for the major equipment, aside from specialized erection equipment, which may be present on a bridge structure during the construction process. In the absence of more precise information, a load of 0.005 to 0.010 ksf should be used, per *AASHTO LRFD* Article 5.14.2.3.2

➢ *CE* – load to represent specialized construction equipment ranging from delivery trucks, to formtraveler launching gantries and other auxiliary structures, and the loads that this equipment introduces to the structure during the lifting and placing of bridge segments

➢ *IE* – dynamic load from construction equipment

➢ *CLE* – longitudinal load from construction equipment

➢ *U* – segmental unbalance load, usually used on structures with a balanced cantilever type construction sequence

➢ *WE* – wind load on construction equipment surfaces, taken as 0.1 ksf over all exposed surfaces

➢ *WUP* – wind load uplift, applicable to cantilevered construction structures, unless specific conditions and analysis dictate otherwise. Typical loading is 0.005 ksf of deck area on one side of cantilever only.

➢ *A* – static weight of next segment being placed

➢ *AI* – dynamic load due to accidental release of segment being described in *A*, typically 100% of *A*

➢ *CR* – creep load, see *AASHTO LRFD* Article 5.14.2.3.6

➢ *SH* – shrinkage load, see *AASHTO LRFD* Article 5.14.2.3.6

> ➤ *T* – thermal load resulting from both temperature variation (*TU*) and temperature gradient (*TG*)

It is recommended that design engineers consult with contractors experienced in the erection procedure that is being recommended to obtain the most accurate construction loading information. Segmental construction concrete bridge structures are very susceptible to being controlled by construction loads, although all bridge types should be checked for construction loads to ensure that structural damage does not occur during the construction process.

Concrete structure construction loads must then be combined into Service and Strength load combinations. For Service load combinations, Table 5.3, taken from *AASHTO LRFD* Table 5.14.2.3.3-1, no cracking should occur from construction loads, stress limits for other limit states shall apply, compressive stresses shall not exceed 0.50 f'$_c$, and tensile forces shall be limited depending on the joint types present in the structure, per *AASHTO LRFD* Article 5.14.2.3.3.

Strength limit states for construction loads should be evaluated using the resistance factors as described above and using the following equations to determine the factored force effects:

For maximum force effects:

$$\sum \gamma Q = 1.1(DL + DIFF) + 1.3CE + A + AI$$

<div align="right">AASHTO LRFD Equation 5.14.2.3.4-1</div>

For minimum force effects:

$$\sum \gamma Q = DC + CE + A + AI$$

<div align="right">AASHTO LRFD Equation 5.14.2.3.4-2</div>

5.4.2 Construction Loads on Steel Structures

For steel superstructure elements, factored construction loads are typically compared with Service II limit state conditions and are not specifically determined in the same manner as for concrete superstructure elements.

5.4.3 Other Construction Load Considerations

Further construction load provisions in the *AASHTO LRFD* specifications call for stay-in-place formwork for concrete structure elements to be designed for construction loads.

Table 5.3 Service Load Combinations for Construction Loads in Concrete Superstructure Members

Load Combination	Dead Load			Live Load				Wind Load			Other Loads					Earth Loads EH EV ES	Tensile Limit State		See Note
	DC	DIFF	U	CLL	CE	IE	CLE	WS	WUP	WE	CR	SH	TU	TG	WA		Excluding "other loads"	Including "other loads"	
a	1.0	1.0	0.0	1.0	1.0	1.0	0.0	0.0	0.0	0.0	1.0	1.0	1.0	γ_{TG}	1.0	1.0	$0.190\sqrt{f'_c}$	$0.220\sqrt{f'_c}$	-
b	1.0	0.0	1.0	1.0	1.0	1.0	0.0	0.0	0.0	0.0	1.0	1.0	1.0	γ_{TG}	1.0	1.0	$0.190\sqrt{f'_c}$	$0.220\sqrt{f'_c}$	-
c	1.0	1.0	0.0	0.0	0.0	0.0	0.0	0.7	0.7	0.0	1.0	1.0	1.0	γ_{TG}	1.0	1.0	$0.190\sqrt{f'_c}$	$0.220\sqrt{f'_c}$	-
d	1.0	1.0	0.0	1.0	1.0	0.0	0.0	0.7	1.0	0.7	1.0	1.0	1.0	γ_{TG}	1.0	1.0	$0.190\sqrt{f'_c}$	$0.220\sqrt{f'_c}$	1
e	1.0	0.0	1.0	1.0	1.0	1.0	0.0	0.3	0.0	0.3	1.0	1.0	1.0	γ_{TG}	1.0	1.0	$0.190\sqrt{f'_c}$	$0.220\sqrt{f'_c}$	2
f	1.0	0.0	0.0	1.0	1.0	1.0	1.0	0.3	0.0	0.3	1.0	1.0	1.0	γ_{TG}	1.0	1.0	$0.190\sqrt{f'_c}$	$0.220\sqrt{f'_c}$	3

(AASHTO LRFD Table 3.4.2.3.3-1)

Notes:
1 = equipment not working
2 = normal erection procedure
3 = moving equipment

5.5 Live Loads

In addition to dead loads, which are continually acting on a bridge, and construction loads, which act on a bridge only during its construction, a bridge must also be designed to resist live loads. The primary difference between dead loads and live loads is that dead loads are permanent but live loads are transient. That is, dead loads act on the bridge at all times, but lives loads are not necessarily present at all times. In addition, dead loads are stationary loads, but live loads are moving loads. Two common forms of live loads are vehicular loads and pedestrian loads.

5.5.1 Design Vehicular Load

Vehicles crossing a bridge come in various shapes, sizes, and weights, such as cars, motorcycles, tractors, buses, and trucks. A bridge must be designed to resist all of the live loads that may legally pass across the bridge. However, the vehicles that most significantly affect a bridge are trucks. When compared with the effects of trucks on a bridge, the effects of cars and other vehicles are negligible. Therefore, the live loads used to design a bridge are based on truck loads.

There are many different types of trucks acting on our bridges today. Trucks come in many different configurations, varying in the following ways:

- ➢ Number of axles
- ➢ Spacing of axles
- ➢ Weight on each axle
- ➢ Total truck length
- ➢ Total truck weight

Since today's bridges must be able to resist a wide variety of trucks, bridges must be designed to resist all of those trucks. However, for the bridge engineer to consider every possible truck configuration that may act on a bridge would be excessively time consuming and unfeasible. Therefore, bridge engineers have developed what is called a notional vehicular load. A notional vehicular load is a theoretical or imaginary load that does not actually exist but that conservatively represents the load affects of vehicles that may legally act on the bridge. The design vehicular loads currently used by AASHTO are notional vehicular loads.

5.5.1.1 Number of Design Lanes

When designing a bridge for live load, the bridge engineer must determine the number of design lanes acting on the bridge. The number of design lanes is directly related the roadway width.

There are two terms used when considering the placement of live load across the width of the bridge:

- ➢ Design lane

> ➤ Loaded width within the design lane

A design lane generally has a width of 12 feet. The number of design lanes is simply computed as the roadway width divided by the 12-foot design lane width, rounded down to the nearest integer. For example, if the distance between the curbs is 70 feet, then the number of design lanes is five. When computing the number of design lanes, possible future adjustments to the roadway should be considered. For example, if a median is currently present on the bridge but may be removed in the future, then the number of design lanes should be computed assuming that the median is not present.

There are a few exceptions to the 12-foot design lane width. First, if the actual traffic lanes on a bridge have a width of less than 12 feet, then the design lane width should equal the actual traffic lane width. Second, for a roadway width between 20 and 24 feet, the bridge should be designed for two lanes, with the design lane width equal to one-half the roadway width.

The design lanes can be positioned anywhere across the width of the roadway, but they can not overlap one another. In designing a bridge, the design lanes should be positioned such that the effect being considered is maximized. For example, when computing the maximum moment in an exterior girder, the lanes should be positioned as close as possible to that exterior girder. This is illustrated in Figure 5.2.
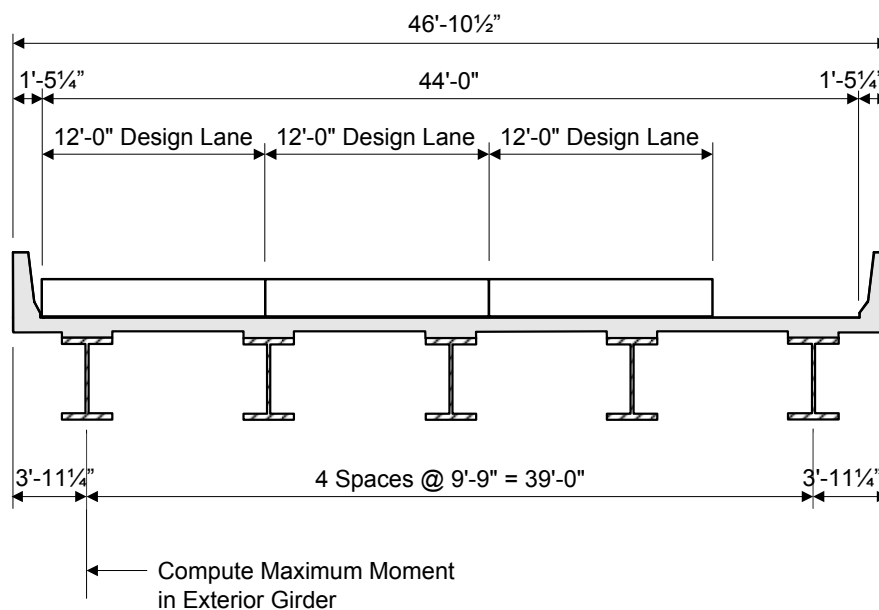
Figure 5.2 Position of Design Lanes

While the design lane generally has a width of 12 feet, the loaded width within the design lane is only 10 feet. The design truck, the design tandem, and the design lane must be located entirely within the 10-foot loaded width. The 10-foot loaded width can be located anywhere within the 12-foot design lane, as long as the entire

10-foot loaded width is entirely within the 12-foot design lane. Similar to the placement of the design lane, the loaded width within the design lane is positioned such that the effect being considered is maximized. For example, for the exterior girder from the previous example, the loaded widths would be positioned as illustrated in Figure 5.3.
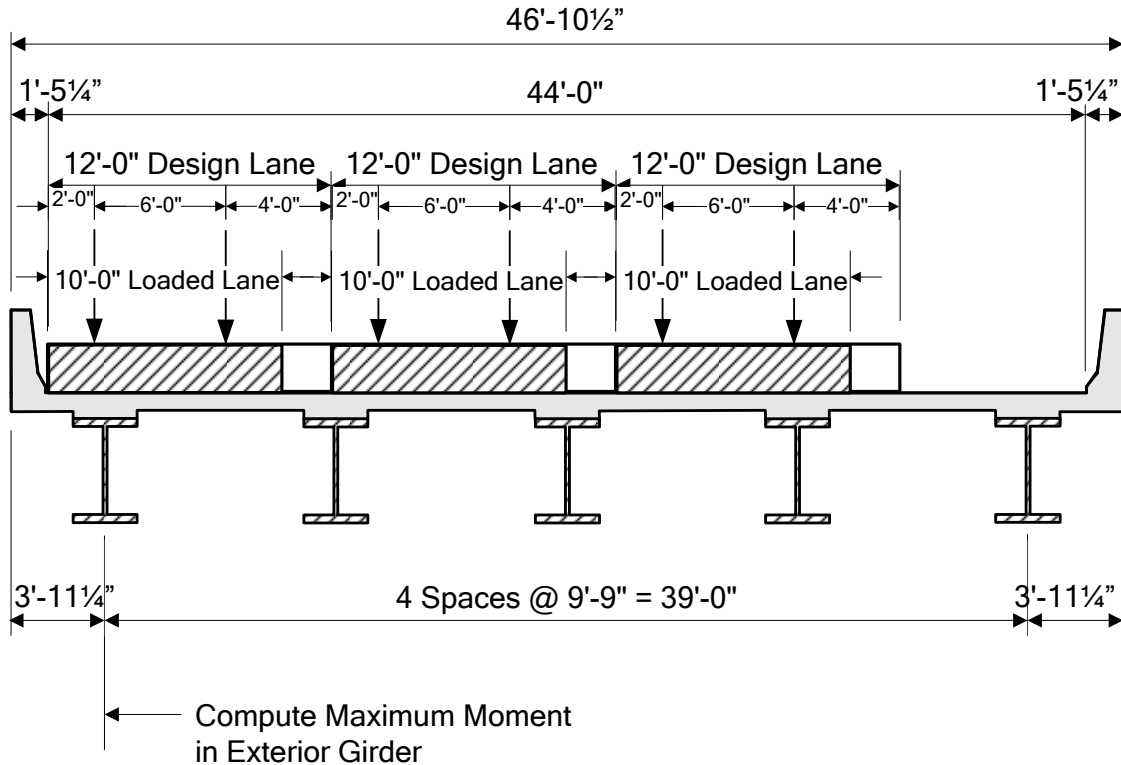
Figure 5.3 Position of Loaded Width within Design Lanes

As another example, if the maximum moment in the second girder from the left were being computed, then the 10-foot loaded width within the leftmost design lane should be shifted to the right side of that design lane.

5.5.1.2 HL-93

The design vehicular load currently used by AASHTO is designated as HL-93, in which "HL" is an abbreviation for highway loading and "93" represents the year of 1993 in which the loading was accepted by AASHTO. The HL-93 live load is based on a 1990 study by the Transportation Research Board (TRB), and it consists of three different load types:

- ➢ Design truck
- ➢ Design tandem
- ➢ Design lane

The following describes how these three different load types are configured in the longitudinal direction, how they are configured in the transverse direction, and how they are combined to form the HL-93 loading.

In the longitudinal direction, the design truck has three axles. The first axle has a loading of 8 kips, and the second and third axles have loadings of 32 kips each. The spacing between the first and second axles is 14 feet, but the spacing between the second and third axles varies between 14 and 30 feet. The axle spacing is selected such that the maximum effect is achieved. The minimum axle spacing of 14 feet usually controls. However, a situation in which an axle spacing greater than 14 feet may control is for a continuous short-span bridge in which the maximum negative moment at the pier is being computed and the second and third axles are positioned in different spans. The design truck is illustrated in Figure 5.4.

8 Kips   32 Kips   32 Kips

14'-0"   Varies (14'-0" to 30'-0")
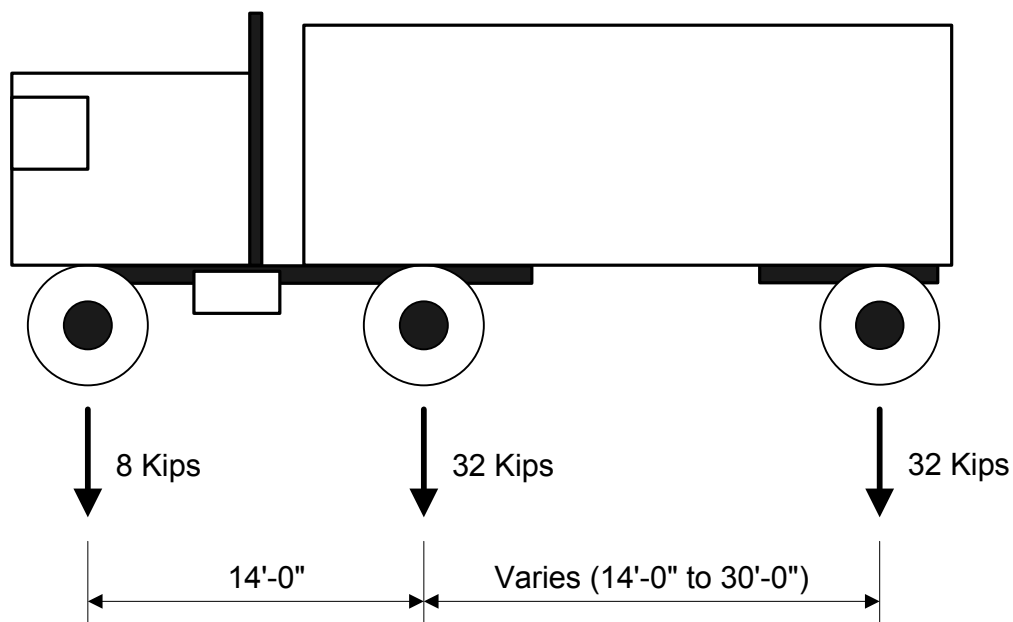
Figure 5.4 Design Truck

The design tandem has two axles, each with a loading of 25 kips. The axle spacing for the design tandem is 4 feet. The design tandem is illustrated in Figure 5.5.
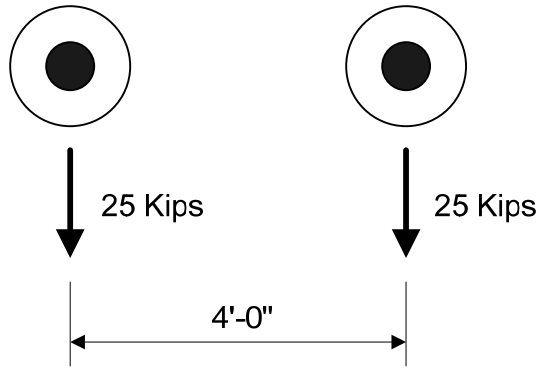
Figure 5.5 Design Tandem

The design lane has a uniform load of 0.64 kips per linear foot, distributed in the longitudinal direction. The design lane is illustrated in Figure 5.6.
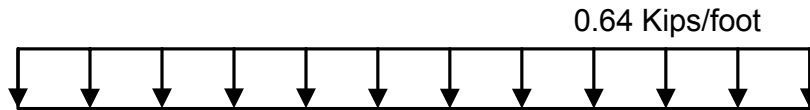
Figure 5.6 Design Lane

In the transverse direction, the design truck and design tandem should be located in such a way that the effect being considered is maximized. However, the center of any wheel load must not be closer than 2 feet from the edge of the design lane. (The single exception is for the design of a deck overhang, in which case the center of the wheel load can be as close as 1 foot from the face of the curb or railing.) The transverse live load configuration for a design truck or design tandem is illustrated in Figure 5.7.
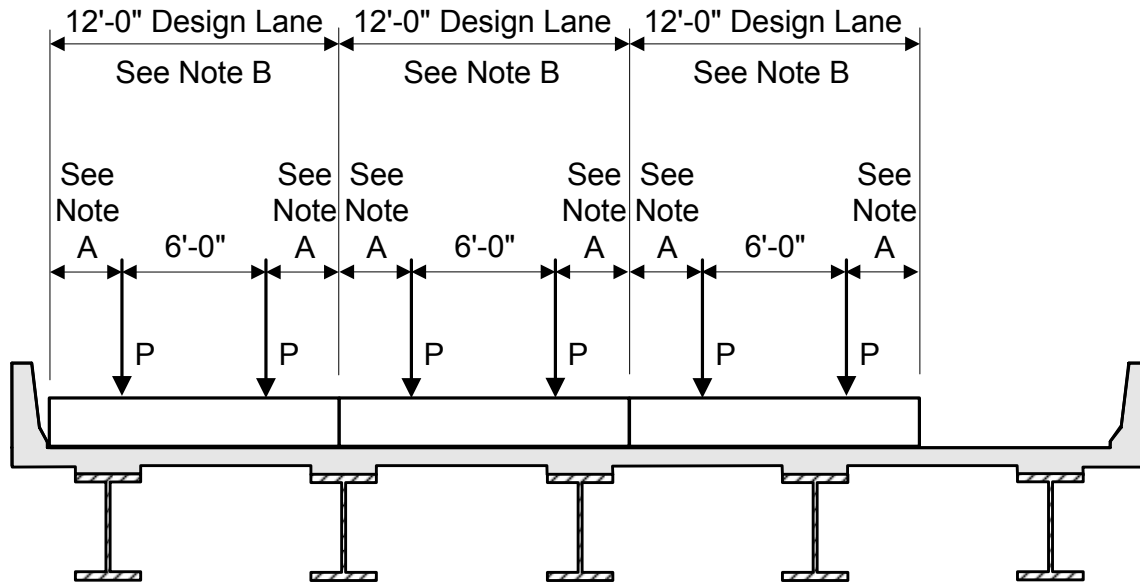
P = Wheel Load

Note A: Position wheel loads within the design lane such that the effect being considered is maximized; minimum = 2'-0".

Note B: Position design lanes across the roadway such that the effect being considered is maximized.

Figure 5.7 Transverse Configuration for a Design Truck or Design Tandem

Similarly, the design lane is distributed uniformly over the 10-foot loaded width. Since the design lane is 0.64 kips per linear foot in the longitudinal direction and it acts over a 10-foot width, the design lane load is equivalent to 64 pounds per square foot. The transverse live load configuration for a design lane is illustrated in Figure 5.8.
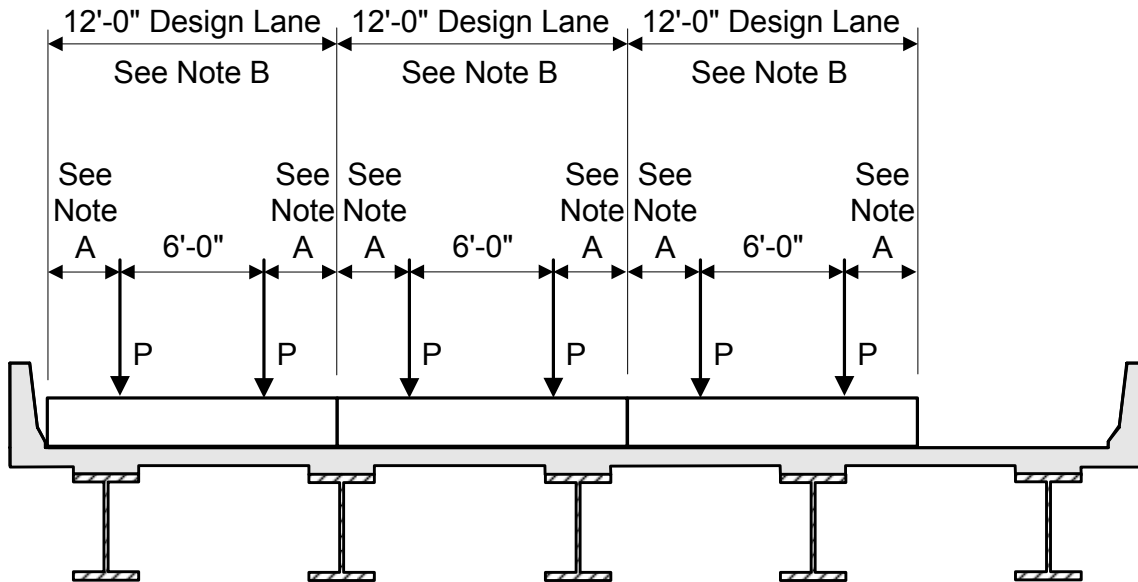
P = Wheel Load

Note A: Position wheel loads within the design lane such that the effect being
considered is maximized; minimum = 2'-0".

Note B: Position design lanes across the roadway such that the effect being
considered is maximized.

Figure 5.8 Transverse Configuration for a Design Lane

The HL-93 loading consists of various combinations of the design truck, design
tandem, and design lane. Specifically, the HL-93 loading is taken as the maximum
of the following two conditions:

> ➢ The effect of the design tandem plus the design lane (see Figure 5.9)
> ➢ The effect of the design truck plus the design lane (see Figure 5.10)

In addition, for negative moment and reaction at interior piers, a third condition is
also considered. A second truck is added with a minimum headway between the
front and rear axles of the two trucks equal to 50 feet, the rear axle spacing of the
two trucks is set at a constant 14 feet, and all loads are reduced by 10 percent.

25 Kips   25 Kips

4'-0"

Plus

0.64 Kips/foot
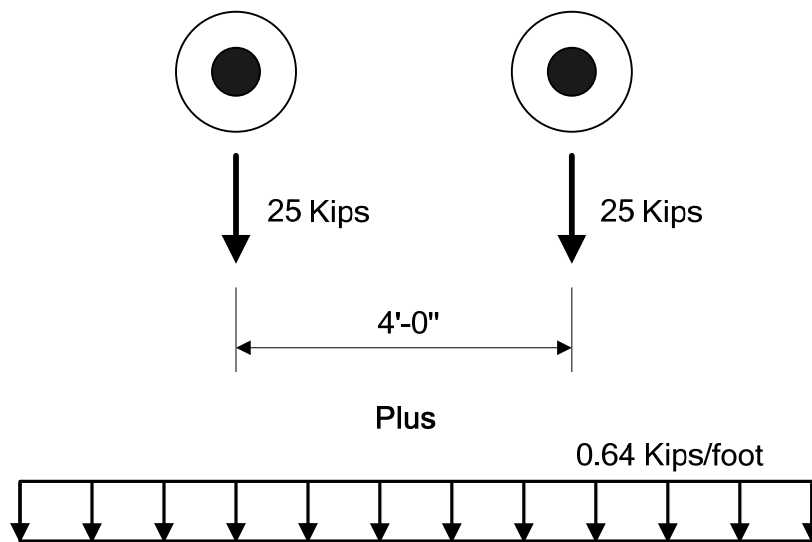
Figure 5.9 Effect of Design Tandem Plus Design Lane

8 Kips   32 Kips   32 Kips

14'-0"   Varies (14'-0" to 30'-0")

Plus

0.64 Kips/foot
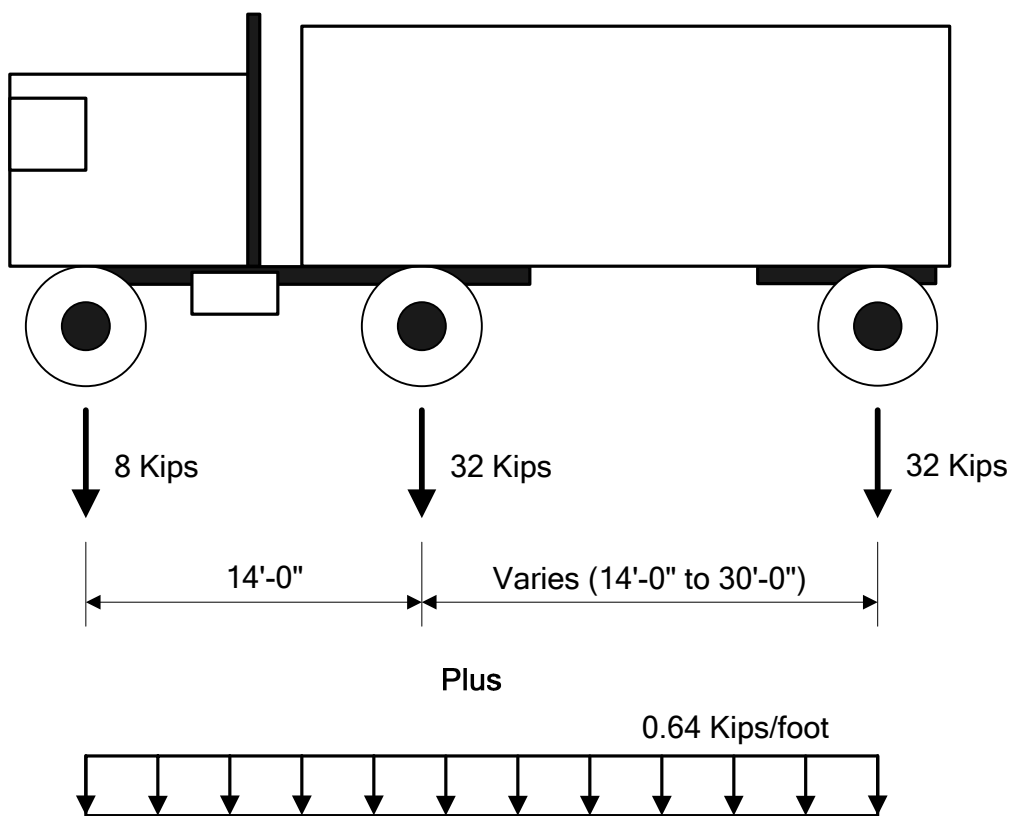
Figure 5.10 Effect of Design Truck Plus Design Lane

The design truck and the design lane are similar to those used in the AASHTO *Standard Specifications for Highway Bridges*, which preceded the *AASHTO LRFD Bridge Design Specifications*. However, in the AASHTO *Standard Specifications for*

Highway Bridges, the design truck and design lane are considered separately and are not combined, whereas they are combined for the HL-93 live load in the *AASHTO LRFD Bridge Design Specifications.*

5.5.2 Fatigue Load

In addition to the live loading described above, fatigue live load must also be considered. Fatigue is a phenomenon of material failure caused by repeated applications of a load. When applied infrequently, these loads would cause no undesirable effects, but when applied repeatedly, they can lead to failure. When the load is cyclic, the stress level that leads to failure can be significantly less than the material yield stress. The effects of fatigue are based on the following considerations:

- ➢ The type and quality of the structural detail
- ➢ The magnitude of the stress range
- ➢ The number of applications (or cycles) of this stress range

Since most trucks have a weight less than the design vehicular load, it would be excessively conservative to use the HL-93 loading described above for fatigue load. Therefore for fatigue load, AASHTO uses the design truck with the following adjustments:

- ➢ The axle spacing between the two 32-kip axles is a constant 30 feet.
- ➢ The fatigue truck is placed in only one lane.
- ➢ The load factor for fatigue is 0.75 (based on calibration studies).

The fatigue load is illustrated in Figure 5.11.

8 Kips   32 Kips   32 Kips

14'-0"   30'-0"
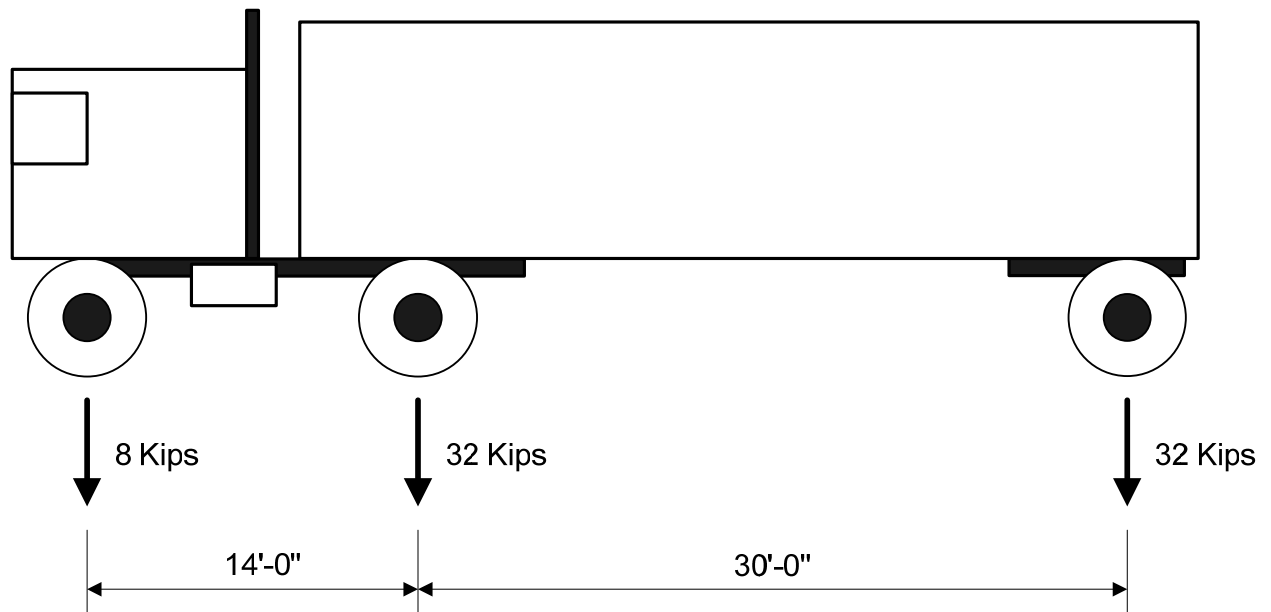
Figure 5.11 Fatigue Load

In addition to the actual loading, the number of cycles also influences the fatigue design of a bridge. In the absence of more accurate traffic data, the average daily truck traffic (ADTT) for a single lane may be computed as:

$$ADTT_{SL} = p(ADTT)$$

Equation 5.2

AASHTO LRFD Equation 3.6.1.4.2-1

where:

$ADTT_{SL}$	=	number of trucks per day in a single lane averaged over the design life
p	=	fraction of truck traffic in a single lane (see Table 5.4)
ADTT	=	number of trucks per day in one direction averaged over the design life

Table 5.4 Fraction of Truck Traffic in a Single Lane, p
(Based on *AASHTO LRFD* Table 3.6.1.4.2-1)

Number of Lanes Available to Trucks	p
1	1.00
2	0.85
3 or more	0.80

In the above equation, the ADTT can usually be obtained from the bridge owner. If ADTT data is not available, then the ADTT can be estimated based on the average daily traffic (ADT) and the percentage of truck traffic to total traffic. This percentage can vary widely, depending on the type of roadway crossing the bridge and the

location of the bridge, but if more accurate data is not available, the percentages presented in Table 5.5 can be used. The ADTT can be estimated by multiplying the ADT times the percentage presented in Table 5.5. It should be noted that the number of stress cycles does not affect the fatigue load but rather the fatigue resistance.

Table 5.5 Percentage of Trucks in Traffic
(Based on *AASHTO LRFD* Table C3.6.1.4.2-1)

Class of Highway	Percentage of Trucks in Traffic
Rural Interstate	20%
Urban Interstate	15%
Other Rural	15%
Other Urban	10%

5.5.3 Pedestrian Load

For bridges designed for both vehicular and pedestrian load and with a sidewalk width exceeding 2 feet, a pedestrian load of 75 pounds per square foot is used. However, for bridges designed exclusively for pedestrian and/or bicycle traffic, a live load of 85 pounds per square foot is used.

The actual magnitude of pedestrian load is highly unpredictable, which increases in significance for bridges in which pedestrian load is the only live load. Therefore, for bridges designed exclusively for pedestrian and/or bicycle traffic, AASHTO specifies a greater pedestrian load than for bridges with both vehicular and pedestrian load.

5.5.4 Vehicular Collision Force (Barrier and Deck Design Only)

In the design of barriers and decks, a vehicular collision force must be considered. AASHTO specifies six different test levels for use in the design of bridge railings for vehicular collision force. These six text levels are based on NCHRP Report 350, "Recommended Procedures for the Safety Performance Evaluation of Highway Features." They are summarized in Table 5.6.

Table 5.6 Bridge Railing Test levels
(Adapted from *AASHTO LRFD* Article 13.7.2)

Name	Abbreviation	Description
Test Level One	TL-1	Generally acceptable for work zones with low posted speeds and very low volume, low speed local streets
Test Level Two	TL-2	Generally acceptable for work zones and most local and collector roads with favorable site conditions as well as where a small number of heavy vehicles is expected and posted speeds are reduced
Test Level Three	TL-3	Generally acceptable for a wide range of high-speed arterial highway with very low mixtures of heavy vehicles and with favorable site conditions
Test Level Four	TL-4	Generally acceptable for the majority of applications on high speed highways, freeways, expressways, and interstate highways with a mixture of trucks and heavy vehicles
Test Level Five	TL-5	Generally acceptable for the same applications as TL-4 and where larger trucks make up a significant portion of the average daily traffic or when unfavorable site conditions justify a higher level of rail resistance
Test Level Six	TL-6	Generally acceptable for applications where tanker-type trucks or similar high center-of-gravity vehicles are anticipated, particularly along with unfavorable site conditions

The user agency is responsible to determine which of the above test levels is most appropriate for the bridge site. For most interstates, TL-4 generally satisfies the design requirements. For each test level, AASHTO specifies vehicular collision force requirements that the bridge railing must satisfy. These vehicular collision force requirements include the following:

> ➢ Weight of vehicle, W
> ➢ Out-to-out wheel spacing on an axle, B
> ➢ Height of vehicle center-of-gravity above the bridge deck, G
> ➢ Angle of vehicular impact (as measured from the face of the railing), θ

The first three variables are illustrated in Figure 5.12. The testing criteria for the various test levels are presented in Table 5.7.
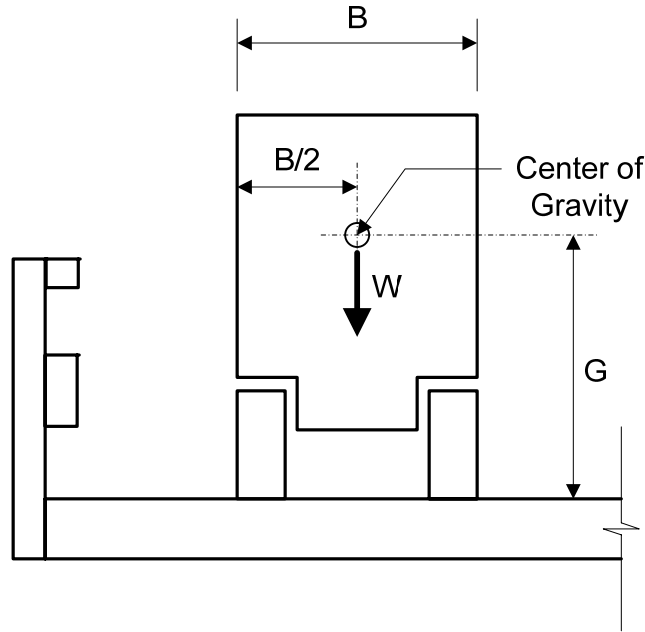
Figure 5.12 Vehicular Collision Force

Table 5.7 Bridge Railing Test levels
(Adapted from *AASHTO LRFD* Article 13.7.2)

Vehicle Characteristics	Small Automobiles		Pickup Trucks	Single-Unit Van Truck	Van-Type Tractor-Trailer		Tractor-Tanker Trailer
W (Kips)	1.55	1.8	4.5	18.0	50.0	80.0	80.0
B (Feet)	5.5	5.5	6.5	7.5	8.0	8.0	8.0
G (Inches)	22	22	27	49	64	73	81
Crash Angle, θ	20°	20°	25°	15°	15°	15°	15°
Test Level	Test Speeds (mph)						
TL-1	30	30	30	N/A	N/A	N/A	N/A
TL-2	45	45	45	N/A	N/A	N/A	N/A
TL-3	60	60	60	N/A	N/A	N/A	N/A
TL-4	60	60	60	50	N/A	N/A	N/A
TL-5	60	60	60	N/A	N/A	50	N/A
TL-6	60	60	60	N/A	N/A	N/A	50

For each test level, barriers are available that have been tested to verify their conformance with the above requirements. Additional information about vehicular collision forces and bridge railings is presented in *AASHTO LRFD* Article 13.

5.5.5 Multiple Presence of Live Load

As previously described, a bridge must be designed for the number of design lanes that can be placed on the roadway and it must be designed for the HL-93 live load, which conservatively represents the maximum load affects of vehicles that may legally act on the bridge. For a bridge design with more than one design lane, the controlling HL-93 live load configuration must be placed in each design lane simultaneously.

However, for a bridge with several design lanes, it is unlikely that each lane will be fully loaded with trucks simultaneously. To account for this improbability, AASHTO applies multiple presence factors. The bridge engineer must consider each possible combination of number of loaded lanes, multiplied by the corresponding multiple presence factor, and then use the loading condition for which the effect being considered is maximized. Multiple presence factors are presented in Table 5.8.

<div align="center">

Table 5.8 Multiple Presence Factors
(Based on *AASHTO LRFD* Table 3.6.1.1.2-1)

</div>

Number of Loaded Lanes	Multiple Presence Factor
1	1.20
2	1.00
3	0.85
>3	0.65

Since the probability that all lanes will be fully loaded decreases as the number of loaded lanes increases, the multiple presence factor also decreases as the number of loaded lanes increases. For the purposes of determining the number of loaded lanes, pedestrian loads may be taken to be one loaded lane.

It is important to note the applications for which multiple presence factors should and should not be used. Multiple presence factors should be applied in the following cases:

  ➤ For use with refined analysis methods
  ➤ For use with the lever rule
  ➤ For use whenever a sketch is required to compute the live load distribution
  ➤ For use with braking forces

However, multiple presence factors should not be applied in the following cases:

  ➤ For the approximate live load distribution factors presented in *AASHTO LRFD* Article 4.6.2
  ➤ For the fatigue limit state in which one design truck is used

The multiple presence factors have already been included in the approximate equations presented in *AASHTO LRFD* Article 4.6.2. Therefore, for the fatigue limit

state, the force effects must be divided by the multiple presence factor for a single lane, which is 1.20.

5.5.6 Dynamic Load Allowance

The HL-93 loading is based on a static live load applied to the bridge. However, in reality, the live load is not static but is moving across the bridge. Since the roadway surface on a bridge is usually not perfectly smooth and the suspension systems of most trucks react to roadway roughness with oscillations, a dynamic load is applied to the bridge and must also be considered with the live load. In previous specifications, AASHTO referred to this dynamic effect as *impact*, but it now refers to it as *dynamic load allowance*.

Dynamic load allowance is defined in *AASHTO LRFD* Article 3.2 as "an increase in the applied static force effects to account for the dynamic interaction between the bridge and moving vehicles." This additional dynamic force effect is illustrated in the generic live load response curve presented in Figure 5.13.
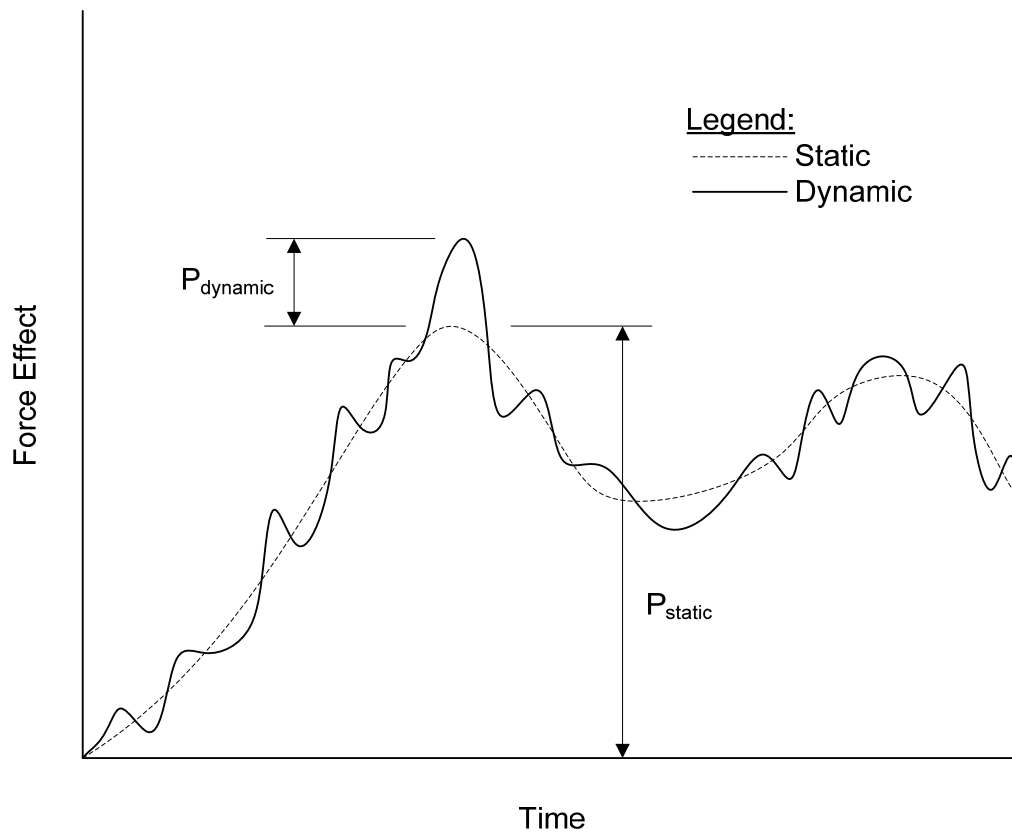
P_{static} = Maximum static force effect

$P_{dynamic}$ = Maximum additional dynamic force effect

Figure 5.13 Static and Dynamic Live Load Response

Referring to Figure 5.13, the dynamic load allowance is equal to:

$$IM = \frac{P_{dynamic}}{P_{static}}$$
Equation 5.3

To compute the total live load effect, including both static and dynamic effects, the following equation is used:

$$P_{LL+I} = P_{LL}(1+IM)$$
Equation 5.4

where:
P_{LL+I}	=	force effect due to both live load and dynamic load allowance
P_{LL}	=	force effect due to live load only (without dynamic load allowance)
IM	=	dynamic load allowance (previously referred to as impact)

In previous specifications, AASHTO defined impact such that its value increased to a maximum value of 30% as the span length decreased. However, in the *AASHTO LRFD Bridge Design Specifications*, dynamic load allowance is no longer a function of span length, and its value depends only on the component and the limit state. AASHTO currently assigns values to dynamic load allowance as presented in Table 5.9.

Table 5.9 Dynamic Load Allowance, IM
(Based on *AASHTO LRFD* Table 3.6.2.1-1)

Component	Limit State	Dynamic Load Allowance, IM
Deck Joints	All Limit States	75%
All Other Components	Fatigue and Fracture Limit States	15%
	All Other Limit States	33%

Deck joints have a greater dynamic load allowance because the hammering effect of the passing vehicles is more significant for deck joints than for other components, such as girders, beams, bearings, and columns.

Dynamic load allowance should not be applied to the following loads:

➢ Centrifugal force
➢ Braking force
➢ Pedestrian load
➢ Design lane (dynamic load allowance is applied to the design truck and design tandem but not to the design lane)

In addition, there are several bridge components for which dynamic load allowance should not be applied, including the following:

➢ Retaining walls not subject to vertical reactions from the superstructure
➢ Foundation components that are entirely below ground level
➢ Wood components
➢ Any other components identified by the specific agency governing the bridge design

5.5.7 Braking Force

When a truck decelerates or stops on a bridge, a longitudinal force is transmitted to the bridge deck, which is also transmitted to the substructure units with fixed bearings. This longitudinal force is known as the braking force.

The braking force is specified by AASHTO as the greater of either:

➢ 25 percent of the axle weights of the design truck or design tandem

➢ 5 percent of the design truck plus lane load, or 5 percent of the design tandem plus lane load

The 25% factor is derived using the following kinetic energy formula:

$$F_B = \left(\frac{v^2}{2ga}\right)W = bW$$ Equation 5.5

where:

F_B	=	braking force
v	=	initial truck velocity (assumed to be 55 mph)
g	=	gravitational acceleration
a	=	length of uniform deceleration (assumed to be 400 feet)
W	=	truck weight
b	=	braking value

Substituting the assumed values into the above equation leads to a value for b of approximately 25%.

AASHTO specifies that the braking force is to be based on all lanes which are considered to be loaded and which are carrying traffic in the same direction. For bridges which may become one-directional in the future, all lanes should be loaded. In addition, the appropriate multiple presence factor should be applied in the braking force computations.

The braking force is applied 6.0 feet above the roadway surface, and it acts longitudinally in whichever direction causes the maximum force effects.

5.6 Wind Loads

Wind loads represent the typical wind conditions of the local area where the bridge is being constructed. Only exposed surfaces are subject to direct application of wind loads, and different wind load cases exist for wind on structure, wind on live load, wind on construction equipment, and wind in the vertical direction. The limit states vary in their load factors for application of wind loads, the desired wind speed, and its effects on live load. In general, smaller structures are not controlled by wind effects, but larger structures with more exposed surfaces can be controlled by wind load.

5.6.1 Horizontal Wind Pressure

The base design wind velocity as specified by AASHTO is 100 miles per hour. This represents a conservative estimate of the highest wind speeds that a structure will experience over the design life of the structure. The wind pressure load from this horizontal wind is applied to all exposed surfaces when the structure is looked at in elevation, perpendicular to the direction of the wind. All girders, decks, attachments, and other structural components which are exposed in elevation are subject to the same uniform wind pressure. Any analysis of wind loads should include multiple attack angles to determine from which direction wind causes the greatest force effect.

For structures in various environments, or over 30.0 feet in height, the base wind velocity is modified per the following equation from *AASHTO LRFD* Article 3.8.1.1.

$$V_{DZ} = 2.5V_0 \left(\frac{V_{30}}{V_B} \right) \ln \left(\frac{Z}{Z_0} \right)$$

AASHTO LRFD Equation 3.8.1.1-1

where:
- V_{DZ} = design wind velocity at a design elevation, Z (mph)
- V_0 = friction velocity, see Table 5.10
- V_{30} = wind velocity at 30.0 ft. above low ground or design water level (mph)
- V_B = base wind velocity, 100 mph
- Z = height of structure at which wind loads are being calculated, > 30.0 ft.
- Z_0 = friction length, see Table 5.10

The values of V_0 and Z_0 are terms which are determined from meteorological effects based on the surrounding land conditions of the bridge. The descriptions of these land features are paraphrased from *ASCE 7-93* in the *AASHTO LRFD* specification and are as follows;

> ➢ Open country – open terrain with only scattered obstructions with heights generally less than 30.0 feet. This category includes flat, open plains and grasslands.

> ➢ Suburban – urban and suburban areas, wooded areas, or other terrain with many closely spaced obstructions with the size of a single-family dwelling, or larger. The suburban category shall only be used if the terrain type extends for 1,500 feet or greater in the prevailing upwind direction from the bridge structure.

> ➢ City – large city centers with at least half the buildings having a height in excess of 70.0 feet. The city category shall only be used if the terrain type extends for one half mile or greater in the prevailing upwind direction from the bridge structure. In addition to typical wind loads, possible channeling effects and increased wind velocities due to the bridge being located in the wake of larger structures should be considered in the analysis of wind loads.

Once the terrain type is determined, V_0 and Z_0 are selected from *AASHTO LRFD* Table 3.8.1.1-1, shown here as Table 5.10.

Table 5.10 Values of V_0 and Z_0 for Various Upstream Surface Conditions

Condition	Open Country	Suburban	City
V_0 (mph)	8.20	10.90	12.00
Z_0 (ft.)	0.23	3.28	8.20

The value of the V_{30} term may be established by the following criteria, as presented in *AASHTO LRFD* Article 3.8.1.1.

> ➢ Fastest-mile-of-wind charts available in *ASCE 7-88* for various recurrence intervals.
> ➢ Site-specific wind surveys
> ➢ In the absence of better criterion, the assumption that $V_{30} = V_B = 100$ mph

5.6.2 Calculation of Design Wind Velocity Design Example

For this example, assume a bridge structure 40.0 ft. in height over the design water level. The structure is located in an area where wooded terrain prevails for at least two miles in all directions. From *ASCE 7-88*, the fastest-mile-of-wind is 115 mph for the area the bridge is located.

$$V_{DZ} = 2.5V_0\left(\frac{V_{30}}{V_B}\right)\ln\left(\frac{Z}{Z_0}\right)$$

Equation 5.6

AASHTO LRFD Equation 3.8.1.1-1

$$V_{DZ} = 2.5(10.90)\left(\frac{115}{100}\right)\ln\left(\frac{40.0}{3.28}\right)$$

Therefore, V_{DZ} = **78.4 mph**

5.6.3 Horizontal Wind Pressure on Structures

The load case for horizontal wind on structures, WS, is based on the design wind speed, and given base wind pressures in the absence of more precise local information.   The information shown in Table 5.11 is taken from *AASHTO LRFD* Table 3.8.1.2.1-1 and is used to determine the horizontal wind pressure force.

Table 5.11 Base Pressures, P_B corresponding to V_B = 100 mph

Superstructure Component	Windward Load, ksf	Leeward Load, ksf
Trusses, Columns, and Arches	0.050	0.025
Beams	0.050	N/A
Large flat surfaces	0.040	N/A

The wind pressure can then be calculated using the following equation.

$$P_D = P_B\left(\frac{V_{DZ}}{V_B}\right)^2 = P_B\frac{V_{DZ}^{\,2}}{10,000}$$

AASHTO LRFD Equation 3.8.1.2.1-1

As a limit, the wind load on windward chords of trusses and arches, and beams and girders cannot be less than 0.30 klf. The leeward load on chords of trusses and arches cannot be less than 0.15 klf.

Various angles of attack for wind direction should be investigated to determine which gives the worst case response in the bridge structure. The angle of attack shall be determined as the skew angle from a perpendicular to the longitudinal axis of the member in question. For various standard angles of attack, the value of base pressure, P_B, will vary as shown in Table 5.12, taken from *AASHTO LRFD* Table 3.8.1.2.2-1. The pressures for lateral loads and longitudinal loads are to be applied simultaneously.

Table 5.12 Base Pressures, P_B for Various Angles of Attack, V_B = 100 mph

Skew Angle of Wind	Trusses, Columns and Arches		Girders	
	Lateral Load	Longitudinal Load	Lateral Load	Longitudinal Load
Degrees	ksf	ksf	ksf	ksf
0	0.075	0.000	0.050	0.000
15	0.070	0.012	0.044	0.006
30	0.065	0.028	0.041	0.012
45	0.047	0.041	0.033	0.016
60	0.024	0.050	0.017	0.019

5.6.4 Horizontal Wind Pressure on Live Load

In addition to the wind loads that are applied to all exposed surfaces of bridge superstructures, wind also affects the exposed surfaces of live load traffic passing over the bridge, introducing additional forces in the load type WL. The pressure exerted on a superstructure due to the wind on live load is consistent with the assumptions made in the determination of limit states and load combinations that at wind speeds in excess of 55 miles per hour, the amount of traffic that would be present on the structure at one time is significantly reduced.

For all structures where the WL load type is used, an uninterruptible, moving force of 0.10 klf acting normal to the roadway, located 6.0 feet above the roadway, should be applied and transmitted to the structure. For any situation where an attack angle other than normal to the lane has been found to be the controlling wind direction, the forces for WL will change per Table 5.13, which is transcribed from *AASHTO LRFD* Table 3.8.1.3-1.

Table 5.13 Wind Components on Live Load

Skew Angle	Normal Component	Parallel Component
Degrees	klf	klf
0	0.100	0.000
15	0.088	0.012
30	0.082	0.024
45	0.066	0.032
60	0.034	0.038

5.6.5 Vertical Wind Pressure on Structure

For load combinations where wind on live load is not considered, and uplift of the structure is potentially a problem, vertical wind pressure may generate loads that need to be considered. This load type is considered to be a 0.020 ksf upward force for all wind speeds, but only at an attack angle perpendicular to the bridge structure. The area of effect for vertical wind pressure includes the width of all deck surfaces,

parapets and sidewalks, and is considered to be a longitudinal line load. The windward side of the bridge is the only that should see the effects of vertical wind pressure.

5.7 Thermal Loads

In addition to forces caused by applied loads, a bridge must also be designed to resist forces due to deformation. An example is thermal loads, which are caused by deformations due to changes in temperature. Two types of thermal loads must be considered in bridge design – uniform temperature change and temperature gradient.

5.7.1 Uniform Temperature Change

The first type of thermal load that must be considered in bridge design is uniform temperature change, in which the entire superstructure changes temperature by a constant amount. Uniform temperature change causes the entire superstructure to lengthen due to temperature rise or shorten due to temperature fall. In addition, if the supports are constrained, uniform temperature change induces reactions at the bearings and forces in the corresponding substructure units. Uniform temperature change is illustrated in Figure 5.14.
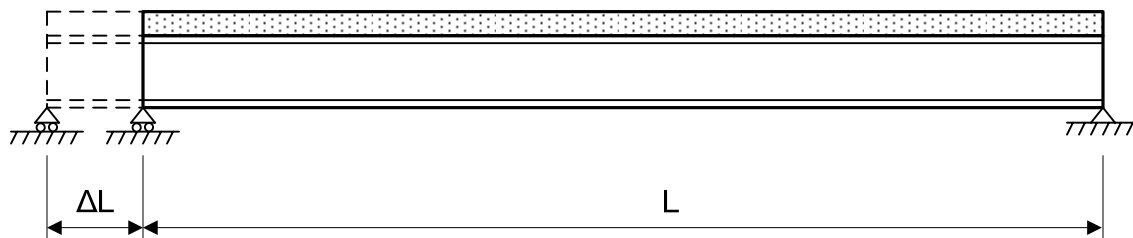
Figure 5.14 Uniform Temperature Change

As depicted in Figure 5.14, the entire superstructure changes in length when subjected to a uniform temperature change. The magnitude of the change in length, ΔL, is a function of:

➤ Material properties
➤ Temperature change
➤ Expansion length

This relationship is expressed mathematically as follows:

$$\Delta L = \alpha \, \Delta T \, L \qquad\qquad \text{Equation 5.7}$$

where:
ΔL	=	change in length
α	=	coefficient of thermal expansion
ΔT	=	change in temperature
L	=	expansion length

To compute the design movement in an elastomeric bearing which will not be reset after erection, an additional factor of 1.3 must be included in the above formula. The values for ∆L and L are illustrated in Figure 5.14. It is important to note that the expansion length is measured to a point of fixity.   The coefficient of thermal expansion is approximately 0.0000065/˚F for steel, 0.0000060/˚F for normal weight concrete, and 0.0000050/˚F for lightweight concrete. The change in temperature is based on the construction temperature, the minimum design temperature, and the maximum design temperature.

AASHTO provides two methods for determining the minimum and maximum design temperatures.   Procedure A, which has traditionally been used by AASHTO, is based on the temperature ranges presented in Table 5.14.

Table 5.14 Temperature Ranges
(Based on *AASHTO LRFD* Table 3.12.2.1.1-1)

Climate	Steel or Aluminum	Concrete	Wood
Moderate	0˚F to 120˚F	10˚F to 80˚F	10˚F to 75˚F
Cold	-30˚F to 120˚F	0˚F to 80˚F	0˚F to 75˚F

As used in the above table, moderate climate is defined as climate in which less than 14 days have an average temperature of less than 32˚F, and cold climate is defined as climate in which 14 or more days have an average temperature of less than 32˚F. The temperature range to concrete is less than that for steel or aluminum because concrete generally has more thermal inertia than does steel or aluminum, which makes concrete more resistant to changes in temperature.

To illustrate the application of the above table, for a steel girder in cold climate which was constructed at 68˚F, the design temperature rise is 120˚F - 68˚F = 52˚F, and the design temperature fall is 68˚F – (-30˚F) = 98˚F.

Procedure B is based on contour maps which present contour lines for the maximum and minimum design temperatures for both concrete girder bridges and steel girder bridges. The bridge engineer can locate the bridge site on the contour maps and determine the maximum and minimum design temperatures to within about 10˚F, either by interpolating between contour lines or by using the most conservative adjacent contour line.

Uniform temperature change must be considered in the design of many bridge components, including the following:

  ➢ Deck joints
  ➢ Bearings
  ➢ Piers at which the bearings are constrained against thermal movement

5.7.2 Temperature Gradient

Another type of thermal load that may need to be considered in bridge design is temperature gradient. Past experience, owner input, and bridge type are all factors that should be used in determining whether temperature gradient should be considered. When subjected to heat from the sun, the bridge deck usually heats more than the underlying girders. Since heat causes expansion, this causes the deck to expand more than the girders, which results in upward bending. Temperature gradient is illustrated in Figure 5.15.
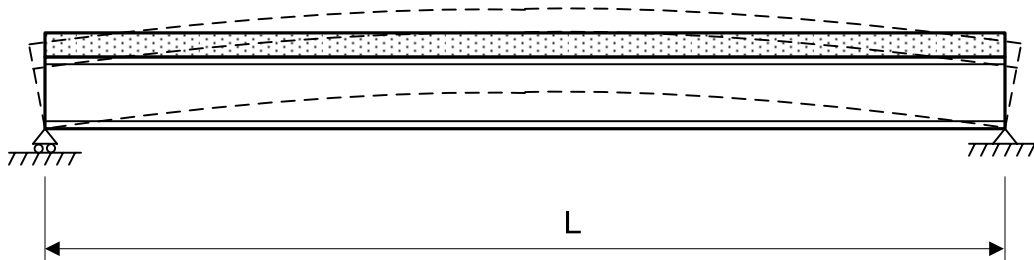
Figure 5.15 Temperature Gradient

Bridge location plays a more significant role in temperature gradient than in uniform temperature change. Bridges located in western states are generally more sensitive to temperature gradient than bridges located in eastern states. To assist the bridge engineer in computing temperature gradient, AASHTO has divided the nation into four solar radiation zones, identified as Zones 1, 2, 3, and 4. Zone 1 has the highest gradient temperatures.

The variation in temperature throughout the depth of the superstructure is illustrated in Figure 5.16.
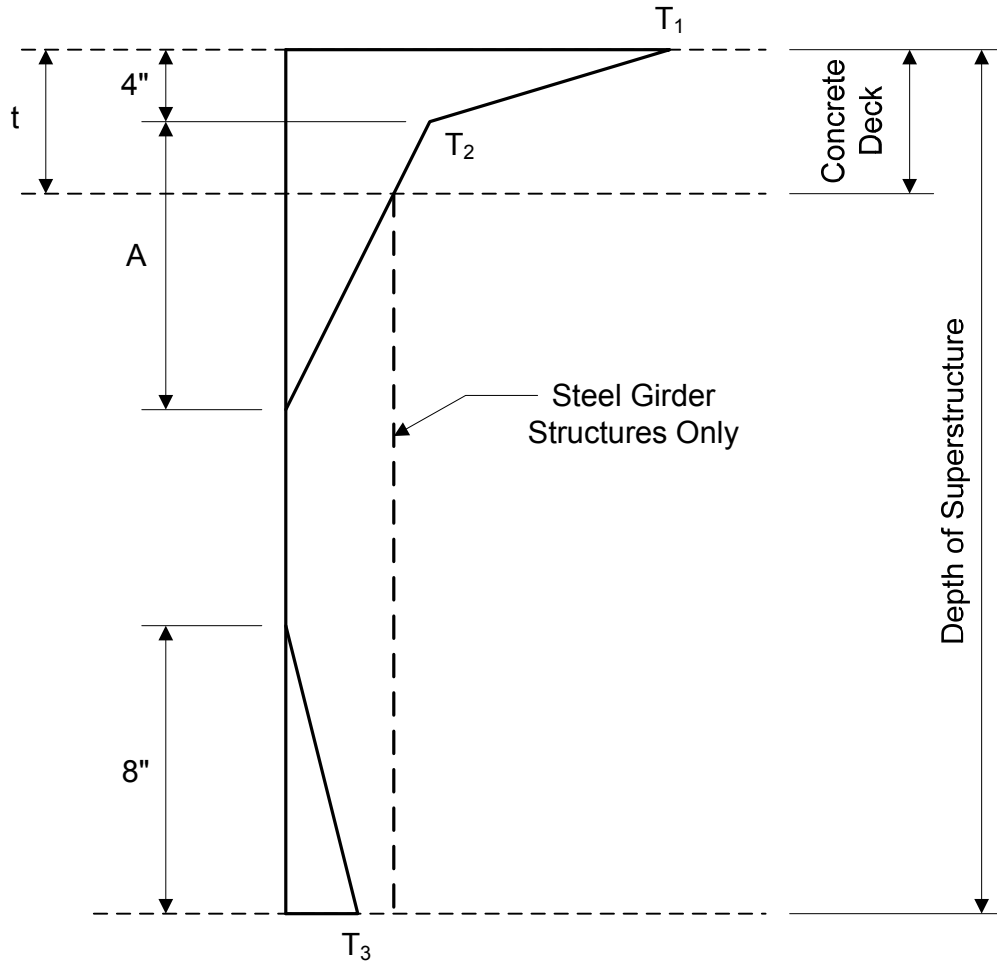
Figure 5.16 Positive Vertical Temperature Gradient

The value for A, as shown in Figure 5.16, depends on the superstructure material and depth, and the values for the temperatures (T_1, T_2, and T_3) are a function of the solar radiation zone in which the bridge is located.

When analyzing a bridge for temperature gradient, the following structure responses must be considered:

- ➢ Axial extension
- ➢ Flexural deformation
- ➢ Internal stresses

5.8 Creep and Shrinkage

Another force effect due to deformation is creep and shrinkage. Creep is a material property in which the member continues to deform with time under sustained loads at unit stresses within the elastic range. Shrinkage is a material property in which the volume changes independently of the loads it sustains. Both creep and shrinkage are time-dependent deformations. They may occur concurrently, and they generally cannot be separated from each other.

Concrete is the most common material that experiences creep and shrinkage. To a lesser degree, wood can also experience creep, such as in transversely prestressed wood bridges. Some of the parameters in concrete that most significantly influence creep and shrinkage are the following:

- ➢ Water-cement ratio
- ➢ Curing method
- ➢ Ambient humidity
- ➢ Aggregates
- ➢ Air content
- ➢ Age at load application

Creep and shrinkage influences both the internal stresses and the deformations of a bridge.

5.8.1 Stresses

In segmental bridges, the creep and shrinkage effects on the internal stresses can be significant, and their contribution to the final stresses must be included in the design process. As an illustration, consider a three-span segmental bridge constructed by the cantilever method. Moment diagrams for various conditions are presented in Figure 5.17.
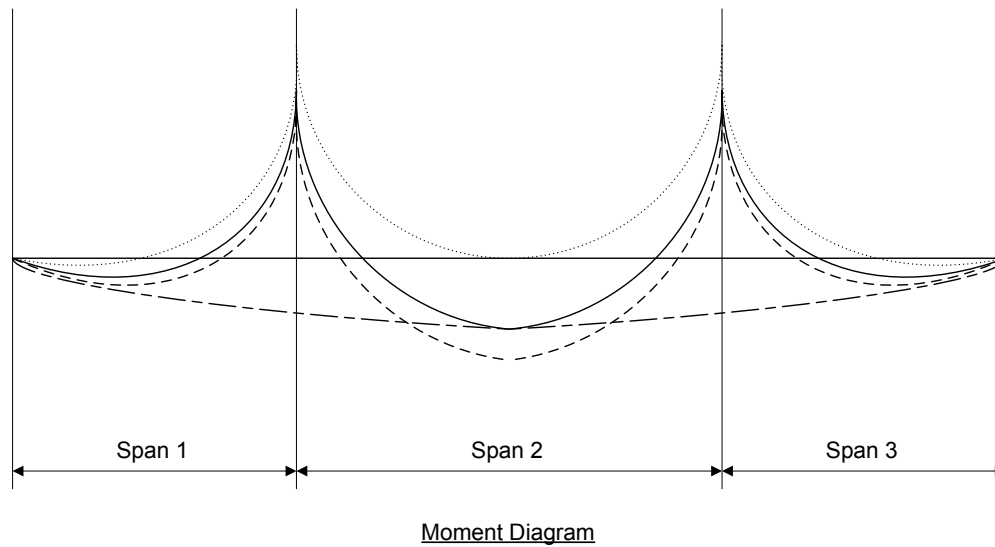
Moment Diagram

Legend:

.... Moment diagram as constructed by the cantilever method (without creep and shrinkage effects)

————— Moment diagram at time infinity (with creep and shrinkage effects)

– – – – – – Moment diagram as constructed on falsework (without creep and shrinkage effects)

— – — – — Approximate representation of creep and shrinkage effects

Figure 5.17 Moment Diagrams for Three-span Segmental Bridge

It can be seen from Figure 5.17 that the forces induced by applied loads are affected not only by the construction method but also by creep and shrinkage. The moment diagram with forces at time infinity (with creep and shrinkage effects) is somewhere between the moment diagrams as constructed by the cantilever method (without creep and shrinkage effects) and as constructed on falsework (also without creep and shrinkage effects). In other words, the final forces in the structure are somewhere between the "cantilever-method" constructed forces and the "falsework" constructed forces.

5.8.2 Deflections

In segmental bridges, the creep and shrinkage effects on the deflections can also be significant. Their contribution to deformations must be considered when:

  ➢ Computing deformations
  ➢ Computing casting curves
  ➢ Computing camber data
  ➢ Computing internal stresses due to deformations

Creep and shrinkage effects induce both stresses and deformations that affect the internal forces on the structural system. For prestressed concrete bridges, cable-

stayed bridges, composite structures, and many other indeterminate structures, creep and shrinkage effects can govern the design of the structural members.

5.9 Accumulated Locked-in Force Effects

Another loading condition that must be considered in bridge design is accumulated locked-in force effects. These force effects can result from the construction process, and they include such effects as secondary forces from post-tensioning. Accumulated locked-in force effects vary both in magnitude and in nature, depending on the bridge type and the erection method.

AASHTO considers accumulated locked-in force effects as a permanent load. It is the only permanent load for which AASHTO assigns a maximum load factor of 1.00 and a minimum load factor of 1.00.

This page intentionally left blank.

Volume 1
General Design Considerations

Chapter 7
Deck Design
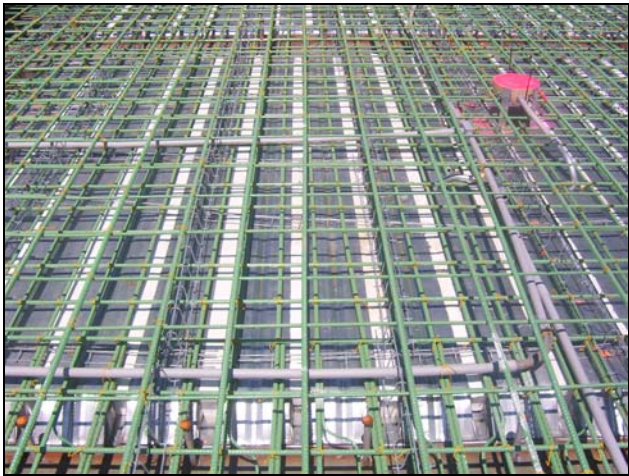
7.1 Introduction

A bridge deck provides a smooth and safe riding surface for the traffic utilizing the bridge, and it transfers the live load and dead load of the deck to the underlying bridge components. During deck design, the engineer must consider the most suitable deck material, overhang design and construction, formwork, and deck staging.

7.2 General Design Considerations

The most common materials used for decks are concrete, metal, and wood. However, several general design considerations are common to all deck materials.

7.2.1 Composite Action

AASHTO LRFD Article 9.4.1 specifies that all decks, with the exception of wood and open grid decks, must be made composite with the supporting components, unless there are compelling reasons not to do so. Composite action is beneficial for several reasons. It enhances the stiffness of the superstructure, it improves the economy of the bridge, and it prevents vertical separation between the deck and its supporting components.

Composite action is made possible by providing shear connectors at the interface between the deck and its supporting components. Shear connectors can be in the form of studs or angles, and they must be designed for both strength and fatigue limit states. Shear connectors must be designed for force effects computed on the basis of full composite action, regardless of whether composite action was considered in the design and proportioning of the primary members. This requirement ensures the integrity of the connection under all possible load cases.

7.2.2 Deck Drainage

Since a primary function of the deck is to provide a safe riding surface, deck drainage must be considered during the deck design. Computations can be performed to determine the allowable length of the bridge without scuppers. This length is a function of the roughness coefficient of the deck surface, the deck cross slope, the grade as a function of the location on the bridge, the design speed, the rate of rainfall, and the width of deck to be drained. If this computation shows that deck drainage is required, then scuppers or other forms of drainage are designed and detailed to meet the drainage requirements of the bridge.

Based on past experience, the deck joint regions are particularly affected by poor deck drainage and are commonly susceptible to deterioration from excessive water. Therefore, special care should be given to the design and detailing of deck drainage near deck joints.

7.2.3 Deck Appurtenances

To safely direct traffic on the bridge, appurtenances are provided along the edges of the bridge. They are also sometimes provided between directions of traffic. Deck appurtenances are usually concrete, and they can be provided in the form of curbs, parapets, barriers, and dividers. Deck appurtenances should generally be made structurally continuous. Since the deck appurtenances may be damaged due to vehicular collision, their structural contribution should not be considered for strength or extreme event limit states. However, their structural contribution may be considered for service and fatigue limit states.

7.2.4 Edge Supports

Edge supports must be provided along the edges of the deck, unless the deck is designed to support wheel loads in extreme positions with respect to its edges. The edge support may be either an edge beam or an integral part of the deck. Expansion joint hardware may be considered to be a structural element of the edge support if it is integrated with the deck.

7.2.5 Stay-in-place Formwork

Stay-in-place formwork can be used to support the uncured deck concrete during construction. Stay-in-place formwork should not be used in the overhang of concrete decks. Additional information about stay-in-place formwork is provided in Section 7.3.6 of this topic.

7.2.6 Limit States

For decks designed using the traditional design method, the deck must be designed to satisfy requirements for service, strength, fatigue, and extreme event limit states. For the service limit state, deflections caused by live load plus dynamic load allowance must be limited as specified in *AASHTO LRFD* Article 9.5.2. For the strength limit state, the deck must be designed to meet the structural requirements of *AASHTO LRFD* pertaining to the deck type and material selected. For the fatigue limit state, design requirements are provided for metal grid, filled grid, partially filled grid, steel grid, and steel orthotropic decks, but there are no fatigue requirements for concrete decks and wood decks. For the extreme event limit state, force effects transmitted by traffic and by combination railings must be considered during deck design.

7.3 Concrete Decks

7.3.1 General

Reinforced concrete is the most common material used for deck design. The primary advantages of concrete decks are their strength and their ability to provide a smooth riding surface. In recent years, automation of deck concrete placement and finishing has improved the cost-effectiveness of this deck type. However, cast-in-place concrete decks can experience excessive differential shrinkage with the supporting beams, and they can lead to slow construction.

Recent research into concrete mixes and curing methods has enhanced performance characteristics such as freeze-thaw resistance, high abrasion resistance, and low shrinkage. To improve the durability of concrete decks against environmental factors, additives and wearing surfaces are frequently used. Additives can potentially increase the life and lower the long-term costs of concrete bridge decks by enhancing resistance to water, corrosion, and deicing salt.

Concrete decks can be designed using several methods, including the traditional design method and the empirical design method. The following sections provide background information, equations, and design examples for each of these two methods.

7.3.2 Traditional Design Method

The traditional design method of deck design is based on flexure and has been included in many previous editions of AASHTO's bridge specifications. The reinforcing steel normal to the supporting girders is considered the primary reinforcement and is computed based on the design moments. The reinforcing steel in the other direction is distribution reinforcement and is computed based on a specified percentage of the primary reinforcement area.

7.3.2.1 Primary Reinforcement Requirements

The design of the primary deck reinforcement by the traditional design method involves the following steps:

1. Obtain design criteria.
2. Determine minimum slab thickness.
3. Determine minimum overhang thickness.
4. Select slab and overhang thickness.
5. Compute dead load effects.
6. Compute live load effects.
7. Compute factored positive and negative design moments.
8. Design for positive flexure in deck.
9. Check for positive flexure cracking under service limit state.

10. Design for negative flexure in deck.
11. Check for negative flexure cracking under service limit state.

These design steps are presented and illustrated through the following design example.

1. Obtain design criteria

The design requirements for this deck design example are as follows:

Girder spacing = 9.75 feet
Number of girders = 5
Deck top cover = 2.5 inches (*AASHTO LRFD* Table 5.12.3-1)
Deck bottom cover = 1 inch (*AASHTO LRFD* Table 5.12.3-1)
Deck reinforced concrete unit weight = 150 pcf (*AASHTO LRFD* Article 3.5.1)
Deck concrete strength, f'$_c$ = 4.0 ksi (*AASHTO LRFD* Article 5.4.2.1)
Reinforcement strength, f$_y$ = 60 ksi (*AASHTO LRFD* Article 5.4.3)
Future wearing surface unit weight = 140 pcf (*AASHTO LRFD* Table 3.5.1-1)

The superstructure cross section is presented in Figure 7.1.
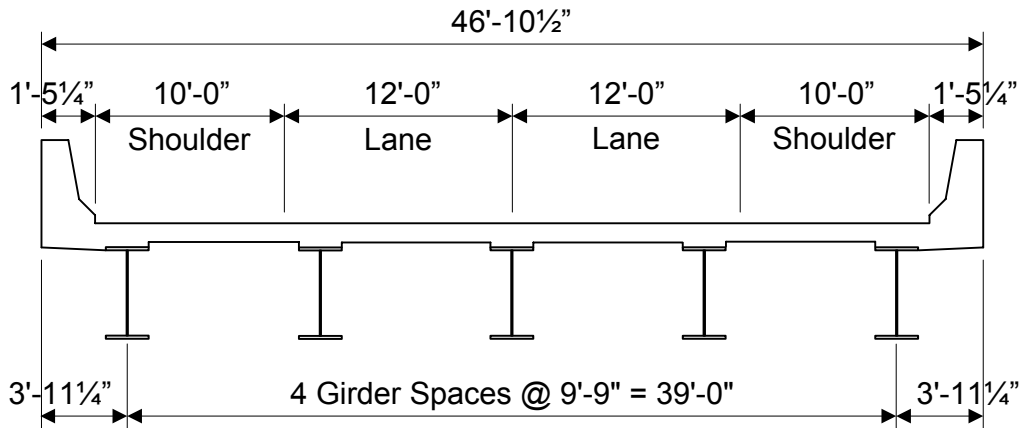
Figure 7.1 Superstructure Cross Section for Design Example

It should be noted that the ratio between the overhang and the girder spacing in this design example is as follows:

$$\frac{\text{Overhang}}{\text{Girder Spacing}} = \frac{3'-11\ 1/4"}{9'-9"} = 0.40$$

The overhang width is generally determined such that the moments and shears in the exterior girder are similar to those in the interior girder. In addition, the overhang is set such that the positive and negative moments in the deck slab are balanced. A

common rule of thumb is to make the overhang approximately 30% to 50% of the girder spacing.

2. *Determine minimum slab thickness*

Based on *AASHTO LRFD* Article 9.7.1.1, the concrete deck thickness cannot be less than 7.0 inches, excluding any provision for grinding, grooving, and sacrificial surface.

3. *Determine minimum overhang thickness*

Similarly, based on *AASHTO LRFD* Article 13.7.3.1.2, the deck overhang thickness for concrete deck overhangs supporting concrete parapets or barriers cannot be less than 8.0 inches.

4. *Select slab and overhang thickness*

After the minimum slab and overhang thicknesses are determined, they can be increased as needed based on client standards and design computations. For this design example, an 8.5 inch deck thickness and a 9.0 inch overhang thickness will be used.

5. *Compute dead load effects*

The dead load moments in the deck must be computed, generally using structural analysis software. For this design example, an analysis produces the dead load moments presented in Table 7.1. These design moments are based on a 1-foot strip running across the width of the deck.

Table 7.1 Unfactored Dead Load Moments (K-ft/ft)

Dead Load	Bay	Location in Bay										
		0.0	0.1	0.2	0.3	0.4	0.5	0.6	0.7	0.8	0.9	1.0
Slab	Bay 1	-0.74	-0.33	-0.01	0.22	0.36	0.41	0.37	0.24	0.01	-0.30	-0.71
	Bay 2	-0.71	-0.30	0.02	0.24	0.38	0.42	0.38	0.24	0.01	-0.31	-0.72
	Bay 3	-0.72	-0.31	0.01	0.24	0.38	0.42	0.38	0.24	0.02	-0.30	-0.71
	Bay 4	-0.71	-0.30	0.01	0.24	0.37	0.41	0.36	0.22	-0.01	-0.33	-0.74
Barrier	Bay 1	-1.66	-1.45	-1.24	-1.03	-0.82	-0.61	-0.40	-0.19	0.02	0.22	0.43
	Bay 2	0.47	0.40	0.33	0.26	0.19	0.12	0.05	-0.02	-0.09	-0.16	-0.23
	Bay 3	-0.23	-0.16	-0.09	-0.02	0.05	0.12	0.19	0.26	0.33	0.40	0.47
	Bay 4	0.43	0.22	0.02	-0.19	-0.40	-0.61	-0.82	-1.03	-1.24	-1.45	-1.66
FWS	Bay 1	-0.06	0.04	0.11	0.15	0.17	0.17	0.14	0.08	0.00	-0.11	-0.24
	Bay 2	-0.24	-0.12	-0.02	0.05	0.09	0.11	0.10	0.07	0.01	-0.07	-0.18
	Bay 3	-0.18	-0.07	0.01	0.07	0.10	0.11	0.09	0.05	-0.02	-0.12	-0.24
	Bay 4	-0.24	-0.11	0.00	0.08	0.14	0.17	0.17	0.15	0.11	0.04	-0.06

The controlling dead load moments from Table 7.1 are presented in Table 7.2.

Table 7.2 Controlling Dead Load Moments

Dead Load	Controlling Positive Moment	Controlling Negative Moment
DC_1 (slab)	0.42 K-ft/ft	-0.74 K-ft/ft
DC_2 (barrier)	0.47 K-ft/ft	-1.66 K-ft/ft
DW (future wearing surface)	0.17 K-ft/ft	-0.24 K-ft/ft

It is assumed for the sake of simplicity that all controlling positive moments are coincident and all controlling negative moments are also coincident.

6. Compute live load effects

Similarly, the live load moments in the deck must also be computed. Again, an analysis program is frequently used to compute the live load moments. These design moments are based on the following live load design requirements:

➢ Minimum distance from the center of the design vehicle wheel to the inside face of the barrier = 1 foot (*AASHTO LRFD* Article 3.6.1.3.1)

➢ Dynamic load allowance, IM = 0.33 (*AASHTO LRFD* Table 3.6.2.1-1)

➢ Multiple presence factor, m, with one lane loaded = 1.20 (*AASHTO LRFD* Table 3.6.1.1.2-1)

➢ Multiple presence factor, m, with two lanes loaded = 1.00 (*AASHTO LRFD* Table 3.6.1.1.2-1)

➢ Multiple presence factor, m, with three lanes loaded = 0.85 (*AASHTO LRFD* Table 3.6.1.1.2-1)

The controlling live load moments for this design example are presented in Table 7.3. Multiple presence factors are included in the values in Table 7.3, but dynamic load allowance is excluded.

Table 7.3 Controlling Live Load Moments

Live Load	Controlling Positive Moment	Controlling Negative Moment
One truck (with m = 1.20)	36.76 K-ft	-28.51 K-ft
Two trucks (with m = 1.00)	26.46 K-ft	-29.40 K-ft

Using the values presented in Table 7.3, the maximum controlling positive moment is 36.76 K-ft, which is based on one truck and an m value of 1.20. The maximum controlling negative moment is -29.40 K-ft, which is based on two trucks and an m value of 1.00.

The dead load moments in Table 7.1 and Table 7.2 are in units of K-ft/ft, while the live load moments in Table 7.3 are in units of K-ft. To compute the live load moments in units of K-ft/ft, the values in Table 7.3 must be divided by an equivalent

strip width. Based on *AASHTO LRFD* Table 4.6.2.1.3-1, the equivalent strip widths are presented in Figure 7.2.

Overhang Moment
= 45.0 + 10.0X

Positive Moment =
26.0 + 6.6S

Negative Moment
= 48.0 + 3.0S
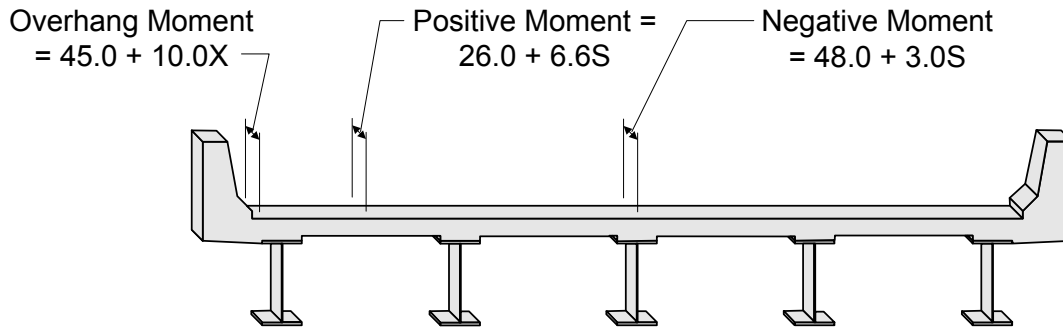
Figure 7.2 Equivalent Strip Widths

In Figure 7.2, X represents the distance from the load to the point of support and S represents the spacing of the supporting components, each measured in units of feet. The equivalent strip width is then computed in units of inches.

For negative moment, the live load moment is based on the distance from the centerline of the girder to the design section for negative moment. The design section for negative moment is as shown in Figure 7.3.

b_f

$b_f /4$

Design Section for
Negative Moment
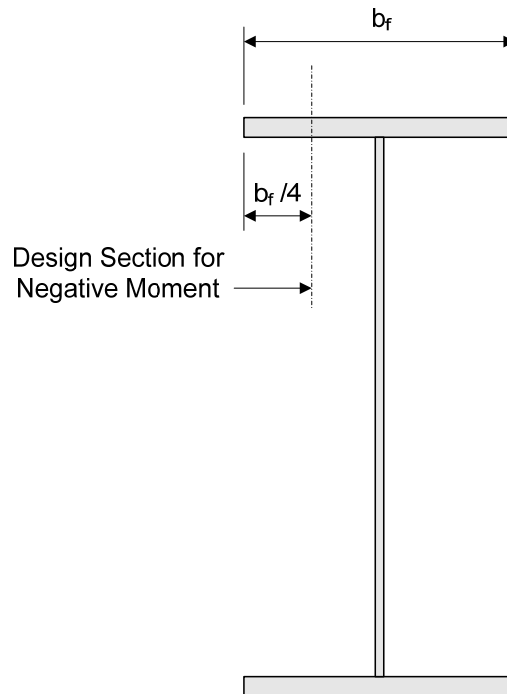
Figure 7.3 Design Section for Negative Moment

Assuming a top flange width of 12 inches, the design section for negative moment is 3 inches from the centerline of the girder. Therefore, for this design example, X and S can be computed as follows:

$$X = 2.25 \text{ ft} - 1.0 \text{ ft} = 1.25 \text{ ft} \qquad \text{and} \qquad S = 9.75 \text{ ft}$$

For positive moment, the equivalent strip width and the resulting live load plus dynamic load allowance moment are computed as follows:

$$\text{Equivalent Strip Width} = 26.0 + 6.6S = 26.0 + 6.6(9.75) = 90.35 \text{ inches} = 7.53 \text{ ft}$$

$$M_{LL+I} = \frac{1.33(36.76 \text{ K} - \text{ft})}{7.53 \text{ ft}} = 6.49 \frac{\text{K} - \text{ft}}{\text{ft}}$$

For negative moment, the equivalent strip width and the resulting live load plus dynamic load allowance moment are computed as follows:

$$\text{Equivalent Strip Width} = 48.0 + 3.0S = 48.0 + 3.0(9.75) = 77.25 \text{ inches} = 6.44 \text{ ft}$$

$$M_{LL+I} = \frac{1.33(-29.40 \text{ K} - \text{ft})}{6.44 \text{ ft}} = -6.07 \frac{\text{K} - \text{ft}}{\text{ft}}$$

Similarly, for the overhang moment, the equivalent strip width is computed as follows:

$$\text{Equivalent Strip Width} = 45.0 + 10.0X = 45.0 + 10.0(1.25) = 57.5 \text{ inches} = 4.79 \text{ ft}$$

The overhang moment will be computed in a subsequent section of this chapter.

### *AASHTO Deck Slab Design Table (*AASHTO LRFD *Article A4):*

The above live load moment computations are based on a finite element analysis program. As an alternative or as an independent check, AASHTO provides a deck slab design table in the appendix to *AASHTO LRFD* Article 4. This table may be used to determine the live load design moments for different girder arrangements. The table is based on a set of assumptions and limitations which were used to develop the table and which are presented in *AASHTO LRFD* Article A4. These assumptions include the following:

➢ The moments are computed using the equivalent strip method.
➢ The moments apply to concrete slabs supported on parallel girders.
➢ Multiple presence factors are included in the tabulated live load values.
➢ Dynamic load allowance is included in the tabulated live load values.
➢ The moments are applicable for decks supported by at least three girders.

For positive moment, the tabulated live load plus dynamic load allowance moment for a girder spacing, S, of 9'-9" is 6.74 K-ft/ft. This value is approximately 4% greater than the value of 6.49 K-ft/ft computed above using an analysis program.

For negative moment, the tabulated live load plus dynamic load allowance moment for a girder spacing, S, of 9'-9" and for a distance of 3 inches from the centerline of girder to the design section for negative moment is -6.65 K-ft/ft. This value is approximately 10% greater than the value of -6.07 K-ft/ft computed above using an analysis program.

It can be seen that the values from *AASHTO LRFD* Table A4-1 are slightly greater than the live load values computed using a finite element analysis program. Generally, using the values presented in *AASHTO LRFD* Table A4-1 may be beneficial due to time savings by not having to develop a finite element model. However, since the time was spent to develop the finite element model for this deck design, the values obtained from the analysis program will be used for this design example.

Based on *AASHTO LRFD* Articles 5.5.3.1 and 9.5.3, fatigue does not need to be investigated for concrete deck design in multi-girder applications.

7. *Compute factored positive and negative design moments*

After the dead load and live load moments have been computed, they must be factored and combined. The load factors for the Strength I limit state, as presented in *AASHTO LRFD* Tables 3.4.1-1 and 3.4.1-2, are as shown in Table 7.4.

Table 7.4 Load Factors for Strength I Limit State

Load	Maximum Load Factor	Minimum Load Factor
DC$_1$ (slab)	1.25	0.90
DC$_2$ (barrier)	1.25	0.90
DW (future wearing surface)	1.50	0.65
LL (live load)	1.75	1.75
IM (dynamic load allowance)	1.75	1.75

Therefore, the maximum factored positive moment can be computed as follows:

$$M_{pos} = 1.25\left(0.38\ \frac{K-ft}{ft}\right) + 1.25\left(0.19\ \frac{K-ft}{ft}\right) + 1.50\left(0.09\ \frac{K-ft}{ft}\right)$$

$$+ 1.75\left(6.49\ \frac{K\text{-}ft}{ft}\right) = 12.21\ \frac{K-ft}{ft}$$

Similarly, the maximum factored negative moment can be computed as follows:

$$M_{neg} = 1.25\left(-0.74\ \frac{K-ft}{ft}\right) + 1.25\left(-1.66\ \frac{K-ft}{ft}\right) + 1.50\left(-0.06\ \frac{K-ft}{ft}\right)$$

$$+ 1.75\left(-6.07\ \frac{k\text{-}ft}{ft}\right) = -13.72\ \frac{K-ft}{ft}$$

8. *Design for positive flexure in deck*

Since positive flexure produces compression in the top fiber and tension in the bottom fiber, sufficient reinforcement must be provided in the bottom layer of the deck to resist the factored positive moment. The first step in designing the positive flexure reinforcement is to assume a bar size. From the bar size, the effective depth can be computed, then the required reinforcement area, and then the required reinforcement spacing.

For this design example, assume the use of #5 bars to resist positive flexure in the deck. Therefore, the effective depth is computed as follows:

$$d_s = \text{Slab Thickness} - \text{Bottom Cover} - \frac{\text{Bar Diameter}}{2} - \text{Top Integral Wearing Surface}$$

$$= 8.5 \text{ inches} - 1.0 \text{ inches} - \frac{0.625 \text{ inches}}{2} - 0.5 \text{ inches} = 6.69 \text{ inches}$$

Then the required reinforcement area is computed using the basic reinforcing steel equations that can be found and derived in most reinforced concrete textbooks.

$$M_r = \phi M_n = \phi A_s F_y \left(d_s - \frac{a}{2} \right) \qquad\qquad \text{Equation 7.1}$$

where: $$a = \frac{A_s F_y}{0.85 f'_c\, b} \qquad\qquad \text{Equation 7.2}$$

For this design example:

$$a = \frac{A_s F_y}{0.85 f'_c\, b} = \frac{A_s (60 \text{ ksi})}{0.85(4.0 \text{ ksi})\left(\dfrac{12 \text{ inches}}{1 \text{ ft}} \right)} = \left(1.47\, \frac{\text{ft}}{\text{inch}} \right) A_s$$

$$M_r = \phi M_n = \phi A_s F_y \left(d_s - \frac{a}{2} \right) = 0.90 A_s (60 \text{ ksi}) \left[6.69 \text{ inches} - \frac{\left(1.47\, \dfrac{\text{ft}}{\text{inch}} \right) A_s}{2} \right]$$

Setting M_r equal to the factored design moment of 12.21 K-ft/ft produces the following required reinforcement area:

$$A_s = 0.43\, \frac{\text{inches}^2}{\text{ft}}$$

The required reinforcement spacing can then be computed as follows:

$$\text{Required Spacing} = \frac{0.31\frac{\text{inches}^2}{\text{bar}}}{0.43\frac{\text{inches}^2}{\text{ft}}} = 0.72 \text{ ft} = 8.7 \text{ inches}$$

Therefore, use #5 at 8 inches for the positive flexural reinforcement. Computing the provided flexural resistance serves as an independent check:

$$A_s = \frac{0.31\,\text{inches}^2}{(8\,\text{inches})\left(\dfrac{1\,\text{ft}}{12\,\text{inches}}\right)} = 0.465\,\frac{\text{inches}^2}{\text{ft}}$$

$$a = \frac{\left(0.465\,\dfrac{\text{inches}^2}{\text{ft}}\right)(60\,\text{ksi})}{0.85(4.0\,\text{ksi})\left(\dfrac{12\,\text{inches}}{1\,\text{ft}}\right)} = 0.684\,\text{inches}$$

$$M_r = 0.90\left(0.465\,\frac{\text{inches}^2}{\text{ft}}\right)(60\,\text{ksi})\left[6.69\,\text{inches} - \frac{0.684\,\text{inches}}{2}\right]$$

$$= 13.28\,\frac{\text{K}-\text{ft}}{\text{ft}} > 12.21\,\frac{\text{K}-\text{ft}}{\text{ft}} \qquad \therefore \text{OK}$$

After the bar size and spacing have been determined, the maximum reinforcement limit must also be checked based on the requirements of *AASHTO LRFD* Article 5.7.3.3.1, as follows:

$$\frac{c}{d_e} \leq 0.42 \qquad\qquad\qquad \text{Equation 7.3}$$

AASHTO LRFD Equation 5.7.3.3.1-1

where:

$$c = \frac{a}{\beta_1} \qquad\qquad\qquad \text{Equation 7.4}$$

$$c = \frac{0.684\,\text{inches}}{0.85} = 0.80\,\text{inches}$$

$$d_e = d_s = 6.69\,\text{inches}$$

Therefore,

$$\frac{c}{d_e} = \frac{0.80\,\text{inches}}{6.69\,\text{inches}} = 0.12 \leq 0.42 \qquad \therefore \text{OK}$$

9. Check for positive flexure cracking under service limit state

After the required reinforcing steel has been computed and the maximum reinforcement limit has been checked, the control of cracking by distribution of the reinforcement must be checked in accordance with *AASHTO LRFD* Article 5.7.3.4. The basic equations for this design check are as follows:

$$s \le \frac{700\gamma_e}{\beta_s f_s} - 2d_c \qquad\qquad \text{Equation 7.5}$$

AASHTO LRFD Equation 5.7.3.4-1

$$\beta_s = 1 + \frac{d_c}{0.7(h - d_c)} \qquad\qquad \text{Equation 7.6}$$

where:

γ_e	=	exposure factor
d_c	=	thickness of the concrete cover measured from the extreme tension fiber to the center of the closest flexural reinforcement, in inches
f_s	=	tensile stress in steel reinforcement at the service limit state, in ksi
h	=	overall thickness of the component, in inches

These equations are based on a physical crack model rather than the statistically-based model used in previous editions of the AASHTO specifications.

Since the Class 2 exposure condition applies to concrete decks, the exposure factor equals 0.75. The values of d_c and h are illustrated in Figure 7.4.
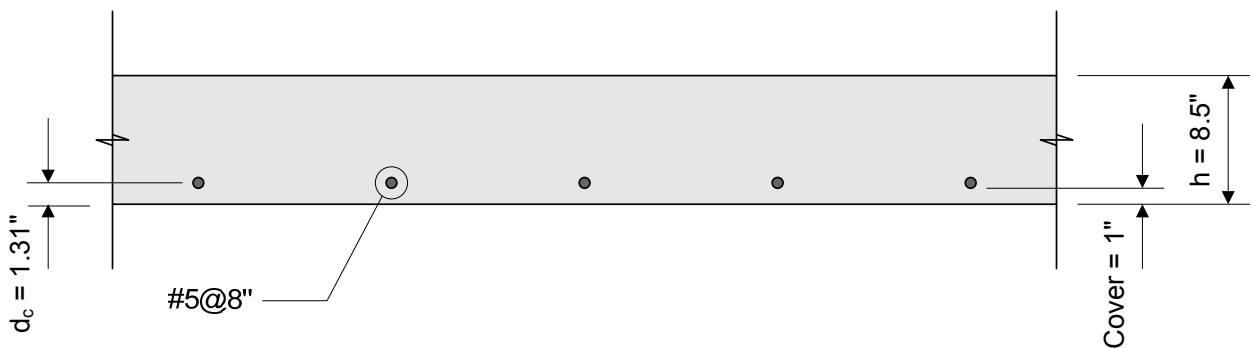
Figure 7.4 Crack Control by Distribution of Reinforcement

For this design example:

$$d_c = 1\,\text{inch} + \frac{0.625\,\text{inches}}{2} = 1.31\,\text{inches}$$

$$\beta_s = 1 + \frac{1.31\,\text{inches}}{0.7(8.5\,\text{inches} - 1.31\,\text{inches})} = 1.26$$

The tensile stress in the steel reinforcement at the service limit state, f_s, is computed using load factors of 1.00, as follows:

$$M_{service} = 1.00\left(0.38\,\frac{K-ft}{ft}\right) + 1.00\left(0.19\,\frac{K-ft}{ft}\right) + 1.00\left(0.09\,\frac{K-ft}{ft}\right)$$
$$+ 1.00\left(6.49\,\frac{K-ft}{ft}\right) = 7.15\,\frac{K-ft}{ft}$$

The computation of the service limit state stress is then computed using the following equations. It should be noted that other methods are also available in reinforced concrete textbooks, all of which produce similar results.

$$n = 8$$

$$\rho = \frac{A_s}{bd_s} \qquad\qquad\qquad \text{Equation 7.7}$$

$$\rho = \frac{0.465\,\text{inches}^2}{(12\,\text{inches})(6.69\,\text{inches})} = 0.00579$$

$$k = \sqrt{(\rho n)^2 + (2\rho n)} - \rho n \qquad\qquad\qquad \text{Equation 7.8}$$

$$k = \sqrt{[(8)(0.00579)]^2 + [2(8)(0.00579)]} - [(8)(0.00579)] = 0.262$$

$$j = 1 - \frac{k}{3} \qquad\qquad\qquad \text{Equation 7.9}$$

$$j = 1 - \frac{0.262}{3} = 0.913$$

$$f_s = \frac{M}{A_s jd} \qquad\qquad\qquad \text{Equation 7.10}$$

$$f_s = \frac{\left(7.15\,\dfrac{K-ft}{ft}\right)\left(\dfrac{12\,\text{inches}}{1\,ft}\right)}{\left(0.465\,\dfrac{\text{inches}^2}{ft}\right)(0.913)(6.69\,\text{inches})} = 30.2\,\text{ksi}$$

The spacing of the steel reinforcement is then checked as follows:

$$\frac{700\gamma_e}{\beta_s f_s} - 2d_c = \frac{700(0.75)}{(1.26)(30.2)} - 2\,(1.31) = 15.8 \text{ inches} > 8 \text{ inches} \qquad \therefore \text{ OK}$$

<div align="right">Equation 7.11</div>

Therefore, the distribution of the positive flexure reinforcement meets the crack control requirements of *AASHTO LRFD* Article 5.7.3.4. The primary reinforcement in the bottom layer of the deck is as shown in Figure 7.5.
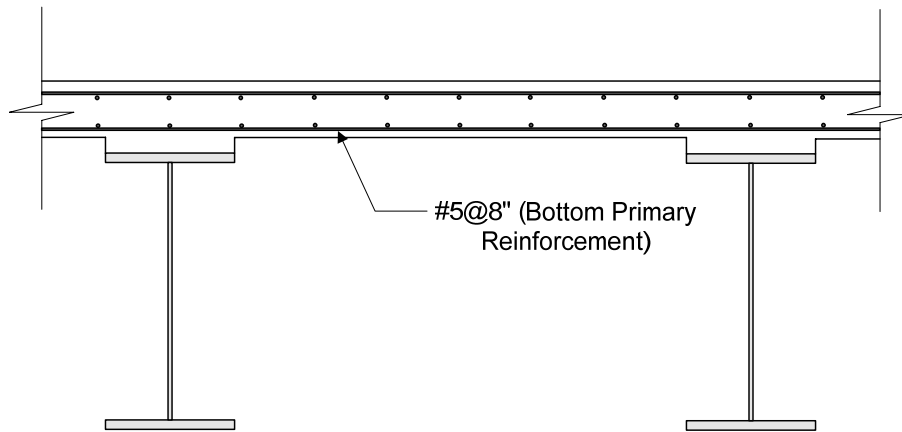
Figure 7.5 Primary Reinforcement in Bottom of Deck

10. Design for negative flexure in deck

After the positive flexure reinforcement has been designed, the negative flexure reinforcement must also be designed. Negative flexure produces compression in the bottom fiber and tension in the top fiber of the deck. Therefore, sufficient reinforcement must be provided in the top layer of the deck to resist the factored negative moment. Similar to the positive flexure reinforcement, the first step in designing the negative flexure reinforcement is to assume a bar size. For this design example, assume the use of #5 bars to resist negative flexure in the deck. Therefore, the effective depth is computed as follows:

$$d_s = \text{Slab Thickness} - \text{Top Cover} - \frac{\text{Bar Diameter}}{2}$$

$$= 8.5 \text{ inches} - 2.5 \text{ inches} - \frac{0.625 \text{ inches}}{2} = 5.69 \text{ inches}$$

Then the required reinforcement for negative flexure is computed similar to the procedure for the positive flexure reinforcement. For this design example:

$$a = \frac{A_s F_y}{0.85 f'_c b} = \frac{A_s(60 \text{ ksi})}{0.85(4.0 \text{ ksi})\left(\dfrac{12 \text{ inches}}{1 \text{ ft}}\right)} = \left(1.47 \frac{\text{ft}}{\text{inch}}\right) A_s$$

$$M_r = \phi M_n = \phi A_s F_y \left(d_s - \frac{a}{2}\right) = 0.90 A_s (60 \text{ ksi})\left[5.69 \text{ inches} - \frac{\left(1.47 \dfrac{\text{ft}}{\text{inch}}\right) A_s}{2}\right]$$

For negative flexure, the absolute value of the negative moment is used as the design moment in the required reinforcement computations. Setting M_r equal to the factored design moment of 13.72 K-ft/ft produces the following required reinforcement area:

$$A_s = 0.58 \frac{\text{inches}^2}{\text{ft}}$$

The required reinforcement spacing can then be computed as follows:

$$\text{Required Spacing} = \frac{0.31 \dfrac{\text{inches}^2}{\text{bar}}}{0.58 \dfrac{\text{inches}^2}{\text{ft}}} = 0.53 \text{ ft} = 6.4 \text{ inches}$$

Therefore, use #5 at 6 inches for the negative flexural reinforcement. Computing the provided flexural resistance serves as an independent check:

$$A_s = \frac{0.31 \text{ inches}^2}{(6 \text{ inches})\left(\dfrac{1 \text{ ft}}{12 \text{ inches}}\right)} = 0.62 \frac{\text{inches}^2}{\text{ft}}$$

$$a = \frac{\left(0.62 \dfrac{\text{inches}^2}{\text{ft}}\right)(60 \text{ ksi})}{0.85(4.0 \text{ ksi})\left(\dfrac{12 \text{ inches}}{1 \text{ ft}}\right)} = 0.91 \text{ inches}$$

$$M_r = 0.90\left(0.62 \frac{\text{inches}^2}{\text{ft}}\right)(60 \text{ ksi})\left[5.69 \text{ inches} - \frac{0.91 \text{ inches}}{2}\right]$$

$$= 14.60 \frac{\text{K} - \text{ft}}{\text{ft}} > 13.72 \frac{\text{K} - \text{ft}}{\text{ft}} \quad \therefore \text{OK}$$

After the bar size and spacing have been determined, the maximum reinforcement limit must be also checked, as follows:

$$\frac{c}{d_e} \leq 0.42$$

<div align="right">*AASHTO LRFD* Equation 5.7.3.3.1-1</div>

where:

$$c = \frac{a}{\beta_1} = \frac{0.91 \text{ inches}}{0.85} = 1.07 \text{ inches}$$

$$d_e = d_s = 5.69 \text{ inches}$$

Therefore,
$$\frac{c}{d_e} = \frac{1.07 \text{ inches}}{5.69 \text{ inches}} = 0.19 < 0.42 \qquad \therefore \text{ OK}$$

11. *Check for negative flexure cracking under service limit state*

Control of cracking by distribution of the reinforcement is then checked in accordance with *AASHTO LRFD* Article 5.7.3.4. For this design example:

$$d_c = 2 \text{ inch} + \frac{0.625 \text{ inches}}{2} = 2.31 \text{ inches}$$

$$\beta_s = 1 + \frac{2.31 \text{ inches}}{0.7(8.5 \text{ inches} - 2.31 \text{ inches})} = 1.53$$

The tensile stress in the steel reinforcement at the service limit state, f_s, is computed using load factors of 1.00, as follows:

$$M_{service} = 1.00\left(-0.74 \frac{K-ft}{ft}\right) + 1.00\left(-1.66 \frac{K-ft}{ft}\right) + 1.00\left(-0.06 \frac{K-ft}{ft}\right)$$
$$+ 1.00\left(-6.07 \frac{K-ft}{ft}\right) = -8.53 \frac{K-ft}{ft}$$

The service limit state stress for negative flexure is computed similar to the procedure for computing the service limit state stress for positive flexure.

$$n = 8$$

$$\rho = \frac{A_s}{bd_s} = \frac{0.62 \text{ inches}^2}{(12 \text{ inches})(5.69 \text{ inches})} = 0.00908$$

$$k = \sqrt{(\rho n)^2 + (2\rho n)} - \rho n = \sqrt{[(8)(0.00908)]^2 + [2(8)(0.00908)]} - [(8)(0.00908)] = 0.315$$

$$j = 1 - \frac{k}{3} = 1 - \frac{0.315}{3} = 0.895$$

$$f_s = \frac{M}{A_s jd} = \frac{\left(8.53\frac{K-ft}{ft}\right)\left(\frac{12\ inches}{1\ ft}\right)}{\left(0.62\frac{inches^2}{ft}\right)(0.895)(5.69\ inches)} = 32.4\ ksi$$

The spacing of the steel reinforcement is then checked as follows:

$$\frac{700\gamma_e}{\beta_s f_s} - 2d_c = \frac{700(0.75)}{(1.53)(32.4)} - 2(2.31) = 6.0\ inches \approx 6\ inches \qquad \therefore OK$$

Therefore, the distribution of the negative flexure reinforcement meets the crack control requirements of *AASHTO LRFD* Article 5.7.3.4. The primary reinforcement in the top layer of the deck is as shown in Figure 7.6.

#5@6" (Top Primary Reinforcement)
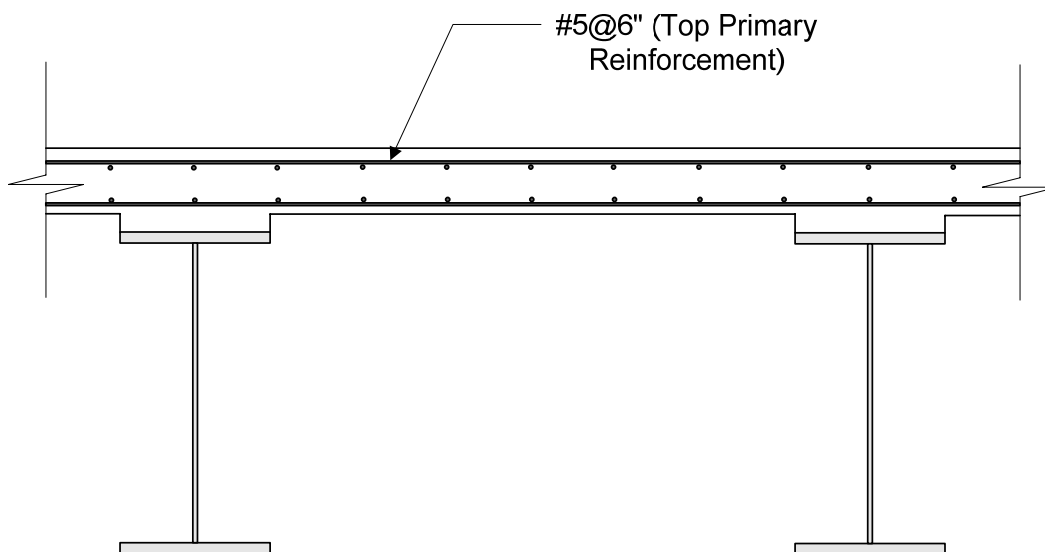
Figure 7.6 Primary Reinforcement in Top of Deck

7.3.2.2 Distribution Reinforcement Requirements

In addition to the primary reinforcement, which is placed normal to the supporting girders, distribution reinforcement must also be provided, which is placed in the opposite direction. According to *AASHTO LRFD* Article 9.7.3.2, the distribution reinforcement is placed in the bottom of the deck and is computed as a percentage of the primary reinforcement for positive moment. When the primary reinforcement is parallel to the traffic, the distribution reinforcement is computed as follows:

$$\frac{100}{\sqrt{S}} \le 50 \text{ percent} \qquad\qquad \text{Equation 7.12}$$

When the primary reinforcement is perpendicular to traffic, the distribution reinforcement is computed as follows:

$$\frac{200}{\sqrt{S}} \le 67 \text{ percent} \qquad\qquad \text{Equation 7.13}$$

As used in the above equations, S is defined as the effective span length, as described for the empirical design method (see Figure 7.11). For this design example, assume a top flange width of 12 inches and a web thickness of 7/16 inches. Therefore, the effective span length is computed as follows:

$$S = \text{Spacing}_{\text{girder}} - b_f + \left(\frac{b_f - t_w}{2}\right) \qquad\qquad \text{Equation 7.14}$$

$$S = 117 \text{ inches} - 12 \text{ inches} + \left(\frac{12 \text{ inches} - 0.4375 \text{ inches}}{2}\right) = 110.78 \text{ inches} = 9.23 \text{ ft}$$

Since the primary reinforcement is perpendicular to traffic for this design example, the distribution reinforcement is computed as follows:

$$\frac{200}{\sqrt{9.23}} = 72.4 > 67 \text{ percent} \qquad \therefore \text{Use 67 percent}$$

$$67\% \text{ of } A_s = (0.67)\left(0.465 \frac{\text{inches}^2}{\text{ft}}\right) = 0.312 \frac{\text{inches}^2}{\text{ft}}$$

Therefore, use #5 at 10 inches. The provided distribution reinforcement is as follows:

$$A_s = \frac{0.31 \text{ inches}^2}{(10 \text{ inches})\left(\dfrac{1 \text{ ft}}{12 \text{ inches}}\right)} = 0.372 \frac{\text{inches}^2}{\text{ft}} > 0.312 \frac{\text{inches}^2}{\text{ft}} \quad \therefore \text{OK}$$

The distribution reinforcement in the bottom layer of the deck is as shown in Figure 7.7.
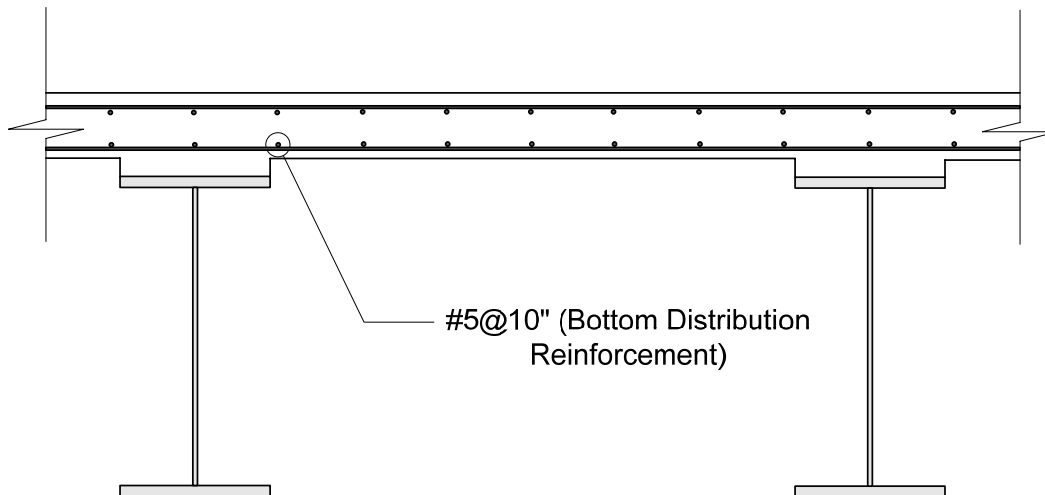
Figure 7.7 Distribution Reinforcement in Bottom of Deck

Since no specific requirements are provided in *AASHTO LRFD* for the distribution reinforcement in the top of the deck, the temperature and shrinkage requirement of *AASHTO LRFD* Article 5.10.8.2 must be satisfied, as follows:

$$A_s \geq 0.11 \frac{A_g}{f_y}$$ Equation 7.15

AASHTO LRFD Equation 5.10.8.2-1

$$0.11 \frac{(8.5 \text{ inches}) \left(12 \frac{\text{inches}}{\text{ft}} \right)}{60 \text{ ksi}} = 0.187 \frac{\text{inches}^2}{\text{ft}}$$

When using the above equation, the calculated area of reinforcing steel must be equally distributed on both concrete faces. In addition, the maximum spacing of the temperature and shrinkage reinforcement must be smaller than 3.0 times the deck thickness or 18.0 inches. Therefore, the amount of steel required for the top longitudinal reinforcement is:

$$A_s = \frac{0.187 \frac{\text{inches}^2}{\text{ft}}}{2} = 0.094 \frac{\text{inches}^2}{\text{ft}}$$

Use #4 at 10 inches. The provided temperature and shrinkage reinforcement is as follows:

$$A_s = \frac{0.20 \text{ inches}^2}{(10 \text{ inches}) \left(\frac{1 \text{ ft}}{12 \text{ inches}} \right)} = 0.24 \frac{\text{inches}^2}{\text{ft}} > 0.094 \frac{\text{inches}^2}{\text{ft}} \quad \therefore \text{ OK}$$

Therefore, #4 at 10 inches satisfies both the area and spacing requirements for the temperature and shrinkage reinforcement. The reinforcement in the top layer of the deck is as shown in Figure 7.8.
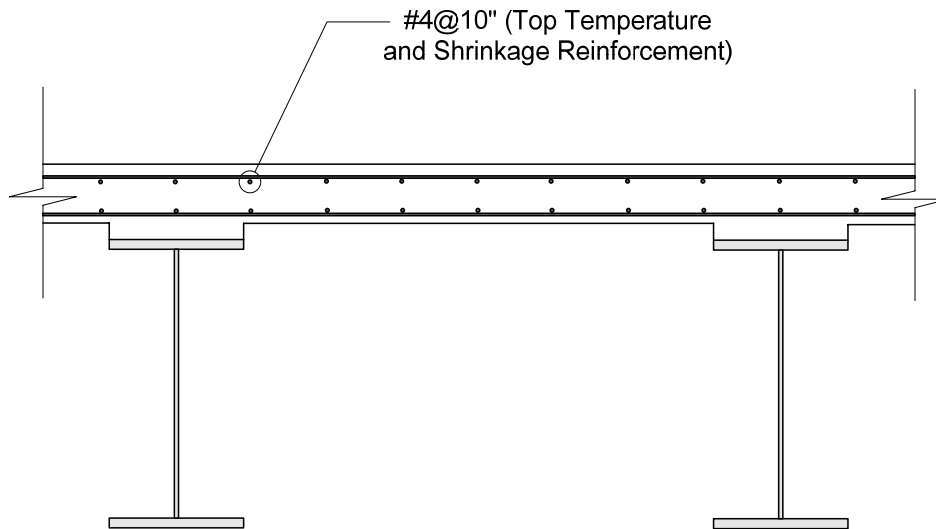
Figure 7.8 Temperature and Shrinkage Reinforcement in Top of Deck

7.3.2.3 Reinforcement Requirements over Piers

If the superstructure is comprised of simple span precast girders made continuous for live load, the top longitudinal reinforcement should be designed according to *AASHTO LRFD* Article 5.14.1.2.7. For continuous steel girder superstructures, the top longitudinal reinforcement should be designed according to *AASHTO LRFD* Article 6.10.1.7.

For this design example, continuous steel girders are used to span the piers of a multi-span bridge. Based on *AASHTO LRFD* Article 6.10.1.7, the total cross-sectional area of the longitudinal reinforcement over the piers should not be less than 1 percent of the total slab cross-sectional area. These bars must have a specified minimum yield strength of at least 60 ksi, the bar size cannot exceed #6 bars, and the bar spacing cannot exceed 12 inches. For this design example:

$$\text{1\% of } A_g = (0.01)(8.5 \text{ inches})\left(12\frac{\text{inches}}{\text{ft}}\right) = 1.02\frac{\text{inches}^2}{\text{ft}}$$

AASHTO specifies that two-thirds of the required longitudinal reinforcement should be placed in the top layer of the deck. Therefore, for this design example, the following reinforcement is required for the top layer over the piers:

$$\left(\frac{2}{3}\right)\left(1.02\frac{\text{inches}^2}{\text{ft}}\right) = 0.68\frac{\text{inches}^2}{\text{ft}}$$

Use #5 at 5 inches in the top layer over the piers. The provided reinforcement is as follows:

$$A_s = \frac{0.31\,\text{inches}^2}{(5\,\text{inches})\left(\dfrac{1\,\text{ft}}{12\,\text{inches}}\right)} = 0.74\,\frac{\text{inches}^2}{\text{ft}} > 0.68\,\frac{\text{inches}^2}{\text{ft}} \quad \therefore \text{OK}$$

The remaining one-third of the required longitudinal reinforcement should be placed in the bottom layer of the deck. Therefore, for this design example, the following reinforcement is required for the bottom layer over the piers:

$$\left(\frac{1}{3}\right)\left(1.02\,\frac{\text{inches}^2}{\text{ft}}\right) = 0.34\,\frac{\text{inches}^2}{\text{ft}}$$

Use #5 at 10 inches in the bottom layer over the piers. The provided reinforcement is as follows:

$$A_s = \frac{0.31\,\text{inches}^2}{(10\,\text{inches})\left(\dfrac{1\,\text{ft}}{12\,\text{inches}}\right)} = 0.37\,\frac{\text{inches}^2}{\text{ft}} > 0.34\,\frac{\text{inches}^2}{\text{ft}} \quad \therefore \text{OK}$$

The required longitudinal reinforcement over the piers is as shown in Figure 7.9.
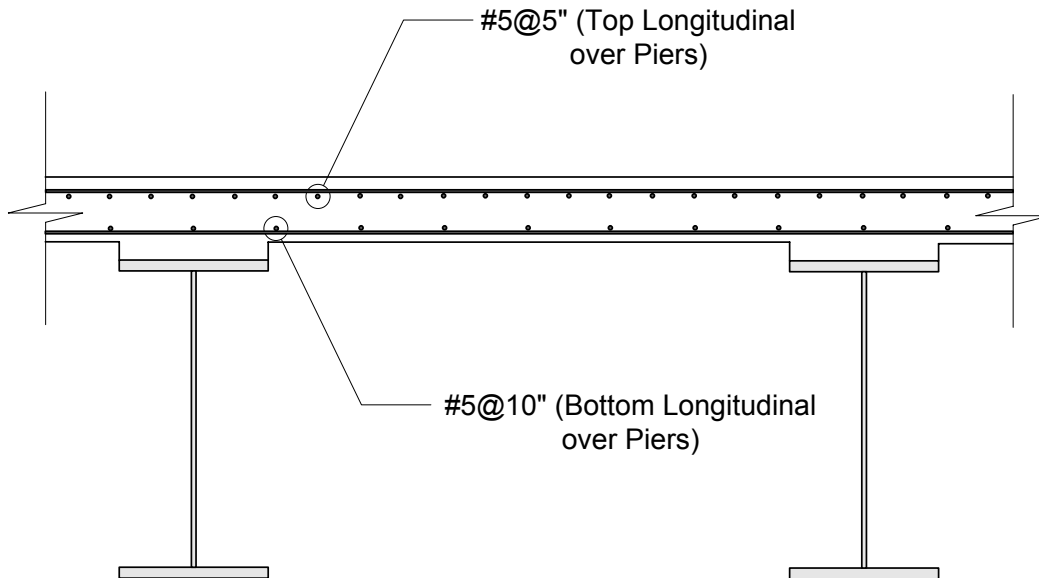
Figure 7.9 Longitudinal Reinforcement over Piers

After designing the primary reinforcement, the distribution reinforcement, and the longitudinal reinforcement over the piers, it is valuable to provide a schematic showing all of the reinforcement and identifying the bar size and spacing for each one. For this design example, a schematic of the final deck design based on the

traditional design method is provided in Figure 7.10. A comparison with the deck design based on the empirical design method is provided in Table 7.6.

#5@5" (Top Reinforcement *)

#4@10" (Top Temperature and Shrinkage Reinforcement **)

#5@6" (Top Primary Reinforcement)

#5@8" (Bottom Primary Reinforcement)

#5@10" (Bottom Distribution Reinforcement)
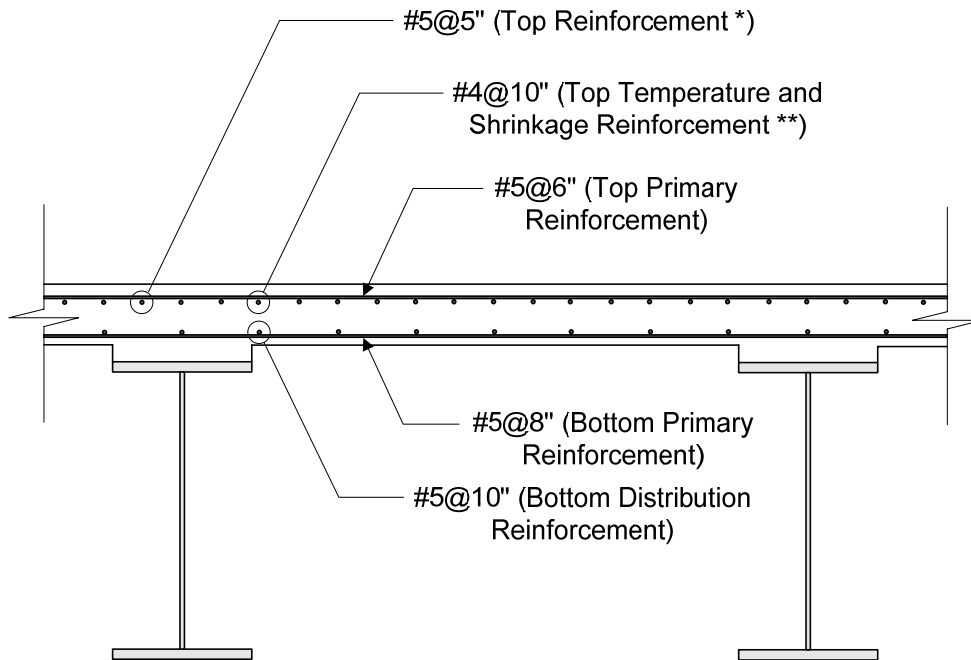
* Provide only in negative moment regions over piers

** Provide wherever negative moment reinforcement over piers is not present

Note: All other reinforcement is provided throughout the entire deck

Figure 7.10 Bridge Deck Based on Traditional Design Method

7.3.3 Empirical Design Method

In addition to the traditional design method, AASHTO also provides specifications for an empirical design method. This method, which is new to the *AASHTO LRFD Bridge Design Specifications*, does not require the computation of design moments and is simpler to apply than the traditional design method. However, it is applicable only under specified design conditions. The empirical design method is described in *AASHTO LRFD* Article 9.7.2.

7.3.3.1 Design Theory

While the traditional design method is based on flexural behavior with the girders acting as supports, the empirical design method is based on internal arching behavior with a complex internal membrane stress state.

Extensive research has shown that concrete bridge decks behave similar to an internal compressive dome. This behavior is made possible by the cracking of the concrete in the positive moment region of the deck, which causes the neutral axis to move upward in that portion of the deck. This results in structural behavior similar to that of a compressive dome. The arching behavior is also made possible by the

lateral confinement provided by the surrounding concrete deck, nearby rigid appurtenances, and supporting components acting compositely with the deck. While the failure mode for the traditional design method is flexural failure, the failure mode for the empirical design method is punching shear.

The reinforcing steel provided using the empirical design method serves two purposes:

➢ It provides for local flexural resistance.
➢ It provides global confinement required to develop arching effects.

The primary differences between the traditional design method and the empirical design method are summarized in Table 7.5.

Table 7.5 Traditional and Empirical Design Methods

Characteristic	Traditional Design Method	Empirical Design Method
Structural behavior	Flexural behavior with girders acting as supports	Internal membrane stress state, referred to as internal arching
AASHTO LRFD reference	*AASHTO LRFD* Article 9.7.3	*AASHTO LRFD* Article 9.7.2
Previous AASHTO bridge specifications	Included in previous AASHTO specifications	New to the *AASHTO LRFD Bridge Design Specifications*
Application	Slab must have four layers of reinforcing steel, two in each direction, and must satisfy minimum slab thickness requirements	Slab must satisfy a more extensive set of design conditions presented in *AASHTO LRFD* Article 9.7.2.4 and in the following section of this chapter
Deck overhang	May be used for the design of the deck overhang	May not be used for the design of the deck overhang
Purpose of reinforcing steel	Provide for flexural resistance	Provide for flexural resistance and provide global confinement required to develop arching effects
Mode of failure	Flexural failure	Punching shear failure
Factor of safety against failure	At least 10.0	Approximately 8.0
Basis of design	Computation of design moments using flexural design theory	Extensive research and experiments; no design moments are computed
Simplicity of design computations	More design computations are required than with the Empirical Design Method	Fewer design computations are required than with the Traditional Design Method

7.3.3.2 Design Conditions

Although the empirical design method is simpler than the traditional design method, the empirical design method may be used only if a set of design conditions are satisfied, as specified in *AASHTO LRFD* Article 9.7.2.4. These design conditions include the following:

➢ Diaphragms must be used at lines of support.
➢ Supporting components must be made of steel and/or concrete.
➢ Deck must be fully cast-in-place and must be water cured.
➢ Deck must have a uniform depth.
➢ 6.0 ≤ effective length to design depth ratio ≤ 18.0.
➢ Core depth of the deck ≥ 4.0 inches.
➢ Effective length ≤ 13.5 feet.
➢ Minimum depth of the deck ≥ 7.0 inches.
➢ Overhang ≥ 5 x deck depth (without a continuous barrier), or overhang ≥ 3 x deck depth (with a continuous barrier).
➢ Deck concrete strength, f'_c ≥ 4.0 ksi.
➢ Deck is composite with the supporting structural components.
➢ Minimum of two shear connectors at 24-inch spacing in negative moment region.

As used with the empirical design method, the effective length for slabs supported on steel or concrete girders is defined as the distance between flange tips, plus the flange overhang, taken as the distance from the extreme flange tip to the face of the web, disregarding any fillets (see *AASHTO LRFD* Article 9.7.2.3). The effective slab length is illustrated in Figure 7.11.
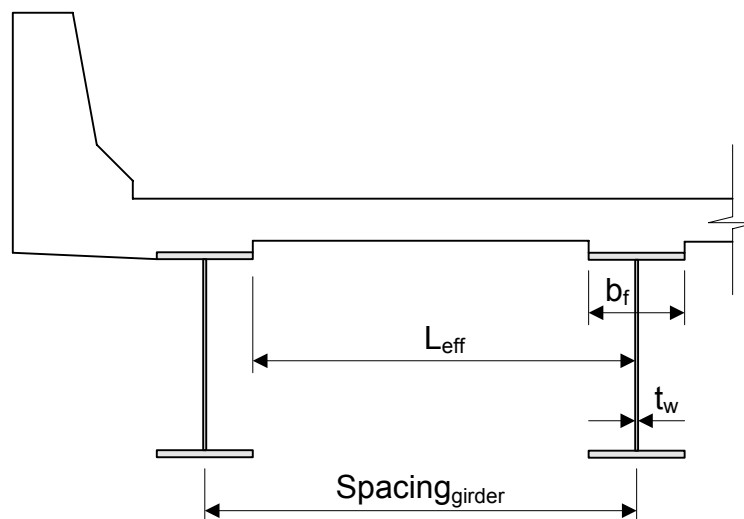
Figure 7.11 Effective Slab Length

$$\text{Effective Slab Length, } L_{\text{eff}} = \text{Spacing}_{\text{girder}} - b_f + \left(\frac{b_f - t_w}{2} \right)$$

Equation 7.16

The empirical design method is based on extensive non-linear finite element analysis and extensive experimentation, and the above design conditions reflect the current scope of analysis and experimentation using this design method. Failure to meet the above design conditions does not necessarily mean that the empirical design method will result in deck failure. Rather, it simply means that sufficient testing has not yet been performed to verify a safe design, and it therefore should not be used for that application.

In addition to the design conditions previously presented, it should be noted that the empirical design method does not apply if the unit being designed is not "monolithic." The use of stay-in-place forms is not consistent with the empirical design method.

In addition, if there is a second course wearing surface (that is, two-stage deck construction), the second stage should not be considered when evaluating the design conditions for the empirical design method. The first stage alone must satisfy the design conditions for empirical design.

7.3.3.3 Reinforcement Requirements

For bridges satisfying each of the above design conditions, the reinforcement requirements of the empirical design method are specified in *AASHTO LRFD* Article 9.7.2.5. These reinforcement requirements are as follows:

> ➢ Four layers of reinforcement (top in each direction and bottom in each direction).
> ➢ Area of each bottom layer of reinforcement ≥ 0.27 inches^2/foot.
> ➢ Area of each top layer of reinforcement ≥ 0.18 inches^2/foot.
> ➢ Spacing of reinforcement ≤ 18 inches.
> ➢ Grade 60 reinforcement or better.

The above reinforcement requirements demonstrate that neither dead load nor live load moments are required using the empirical design method. The minimum area of reinforcing steel is specified, regardless of the design moments or the girder spacing. This reflects the fact that the empirical design method is based on research showing that the above reinforcement requirements satisfy all AASHTO design requirements for any bridge which satisfies the specified design conditions.

An example of a bridge deck reinforcing pattern based on the empirical design method is presented in Figure 7.12.
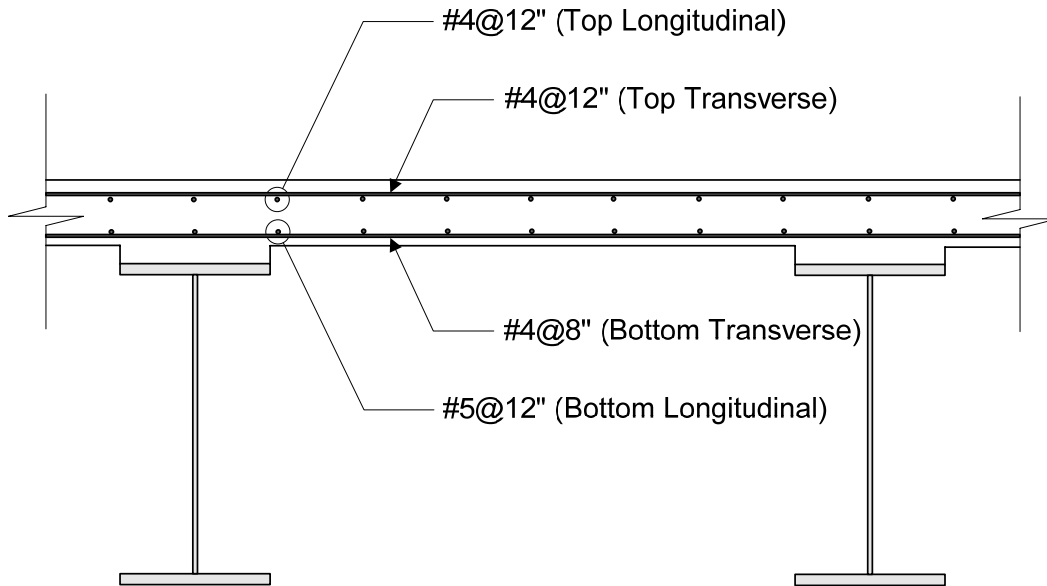
Figure 7.12 Bridge Deck Based on Empirical Design Method

The sufficiency of the reinforcing steel shown in Figure 7.12 can be checked as follows:

Top Transverse:

$$A_s = \frac{0.20 \text{ inches}^2}{(12 \text{ inches})\left(\dfrac{1 \text{ foot}}{12 \text{ inches}}\right)} = 0.20 \frac{\text{inches}^2}{\text{foot}} > 0.18 \frac{\text{inches}^2}{\text{foot}} \qquad \therefore \text{ OK}$$

Top Longitudinal:

$$A_s = \frac{0.20 \text{ inches}^2}{(12 \text{ inches})\left(\dfrac{1 \text{ foot}}{12 \text{ inches}}\right)} = 0.20 \frac{\text{inches}^2}{\text{foot}} > 0.18 \frac{\text{inches}^2}{\text{foot}} \qquad \therefore \text{ OK}$$

Bottom Longitudinal:

$$A_s = \frac{0.31 \text{ inches}^2}{(12 \text{ inches})\left(\dfrac{1 \text{ foot}}{12 \text{ inches}}\right)} = 0.31 \frac{\text{inches}^2}{\text{foot}} > 0.27 \frac{\text{inches}^2}{\text{foot}} \qquad \therefore \text{ OK}$$

Bottom Transverse:

$$A_s = \frac{0.20 \text{ inches}^2}{(8 \text{ inches})\left(\dfrac{1 \text{ foot}}{12 \text{ inches}}\right)} = 0.30 \frac{\text{inches}^2}{\text{foot}} > 0.27 \frac{\text{inches}^2}{\text{foot}} \qquad \therefore \text{ OK}$$

It should be noted that reinforcement must be provided in each face of the slab with the outermost layers placed in the direction of the effective slab length and placed as close to the concrete surfaces as permitted by the cover requirements.

The reinforcing steel in the deck overhang must be designed based on the traditional design method. Additional reinforcing steel required in the negative flexure region (over piers) is as presented with the traditional design method.

A comparison between the deck design example using the traditional design method and that using the empirical design method is presented in Table 7.6.

Table 7.6 Comparison of Design Methods for Deck Design Example

Reinforcement	Traditional Design Method	Empirical Design Method
Top Transverse	#5@6"	#4@12"
Bottom Transverse	#5@8"	#4@8"
Top Longitudinal	#4@10"	#4@12"
Bottom Longitudinal	#5@10"	#5@12"

It is clear from Table 7.6 that, for this particular design example, the transverse reinforcement requirements are greater using the traditional design method than using the empirical design method. For this design example, the longitudinal reinforcement requirements are similar using both methods.

7.3.4 Deck Overhang Design and Construction

Design of the deck overhang involves the following steps:

1. Design for flexure in deck overhang.
2. Check for cracking in overhang under service limit state.
3. Compute overhang cut-off length requirement.
4. Compute overhang development length.

These design steps are presented and illustrated through a continuation of the previous design example. The deck overhang dimensions from that design example, as well as the locations of the design sections and the live load on the overhang, are presented in Figure 7.13.
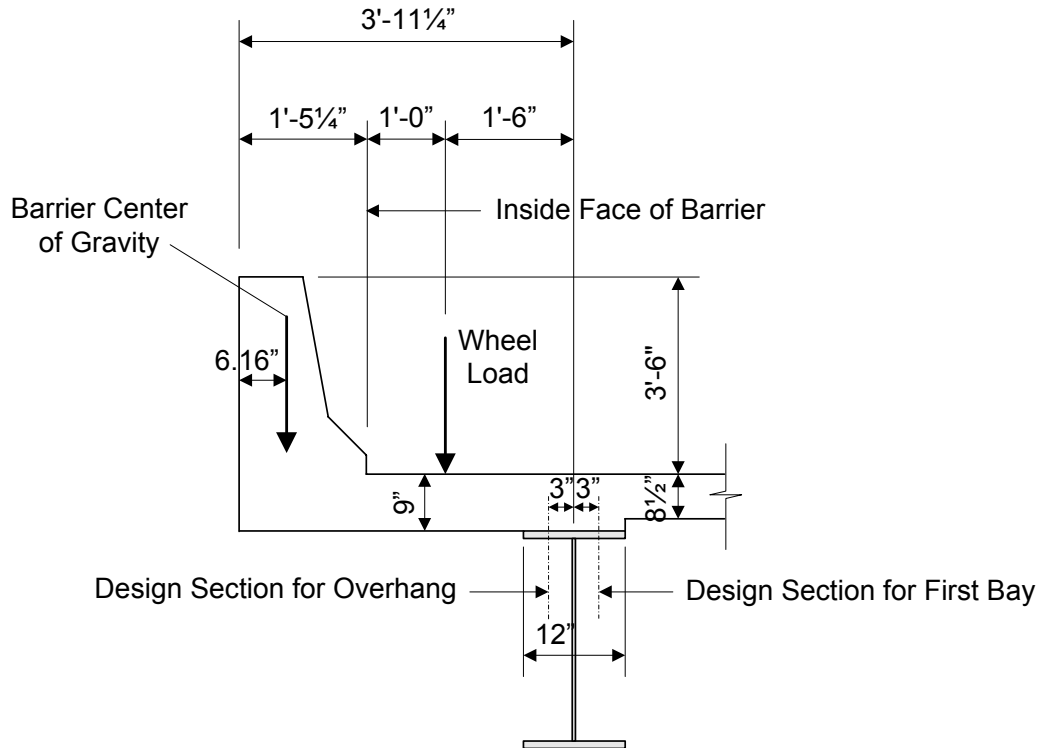
Figure 7.13 Deck Overhang Dimensions and Live Load

1. *Design for flexure in deck overhang*

As described in Appendix A to *AASHTO LRFD* Article 13, deck overhangs must be designed to satisfy three different design cases. These three design cases are summarized in Table 7.7.

Table 7.7 Deck Overhang Design Cases

Design Case	Applied Loads	Limit State	Design Locations
Design Case 1	Horizontal (transverse and longitudinal) vehicular collision force	Extreme event limit state	At inside face of barrier
			At design section for overhang
			At design section for first bay
Design Case 2	Vertical vehicular collision force	Extreme event limit state	Usually does not control
Design Case 3	Dead and live loads	Strength limit state	At design section for overhang
			At design section for first bay

In addition, the deck overhang must be designed to provide a resistance greater than the resistance of the concrete barrier.

Design Case 1: Design overhang for horizontal vehicular collision force

The overhang must be designed for the vehicular collision moment plus the dead load moment, acting concurrently with the axial tension force from vehicular collision, in accordance with *AASHTO LRFD* Article A13.4.1. The barrier that has been selected for use with this design example is approved for Test Level TL-3 and is shown in Figure 7.14.
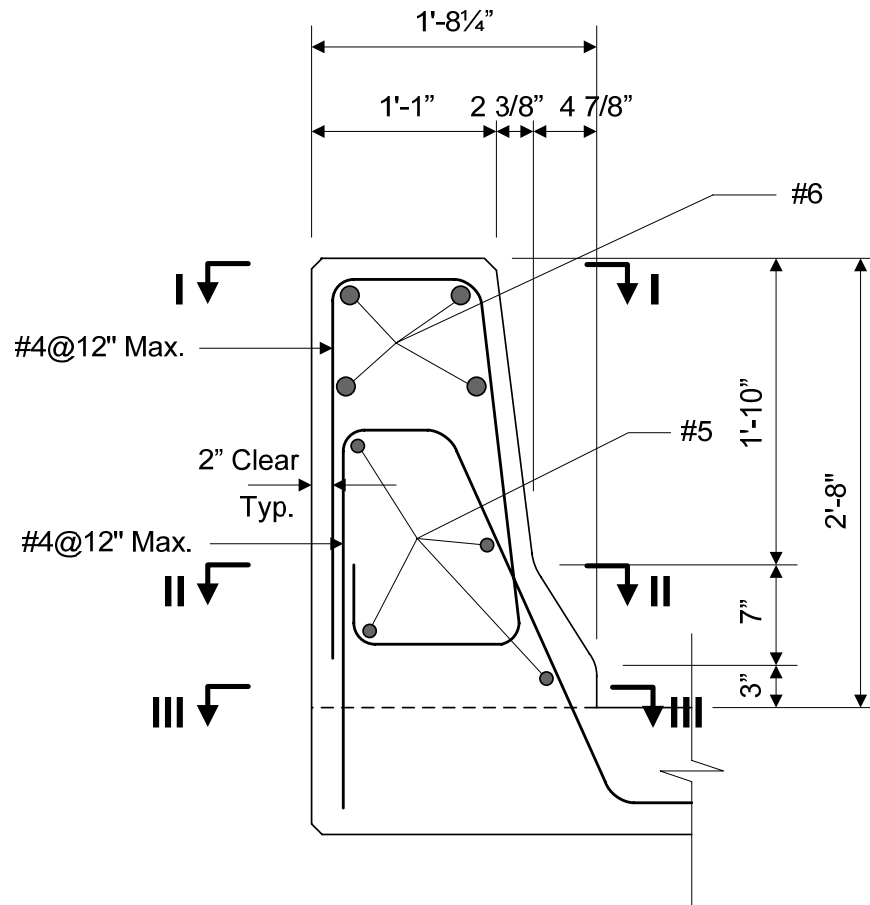
Figure 7.14 Barrier Configuration

Based on the dimensions shown in Figure 7.14, the cross-sectional area and weight of the barrier are:

$$\text{Area} = (13")(32") + \frac{1}{2}(2.375")(22") + \frac{1}{2}(4.875")(7") + (2.375")(7") + (7.25")(3") =$$

$$= 497.6 \text{ inches}^2 = 3.46 \text{ ft}^2$$

$$\text{Weight} = (3.46 \text{ ft}^2)(0.150 \text{ kcf}) = 0.52 \text{ kips/ft}$$

The moment capacity of the barrier is computed based on the formation of yield lines at the limit state. The fundamentals of yield line analysis can be found in many structural analysis textbooks. For an assumed yield line pattern that is consistent

with the geometry of the barrier, a solution is obtained by equating the internal work along the yield lines with the external work due to the applied loads. While a full explanation of the barrier design equations and their derivation is beyond the scope of this manual, Figure 7.15 illustrates the assumed yield line pattern for a barrier wall.
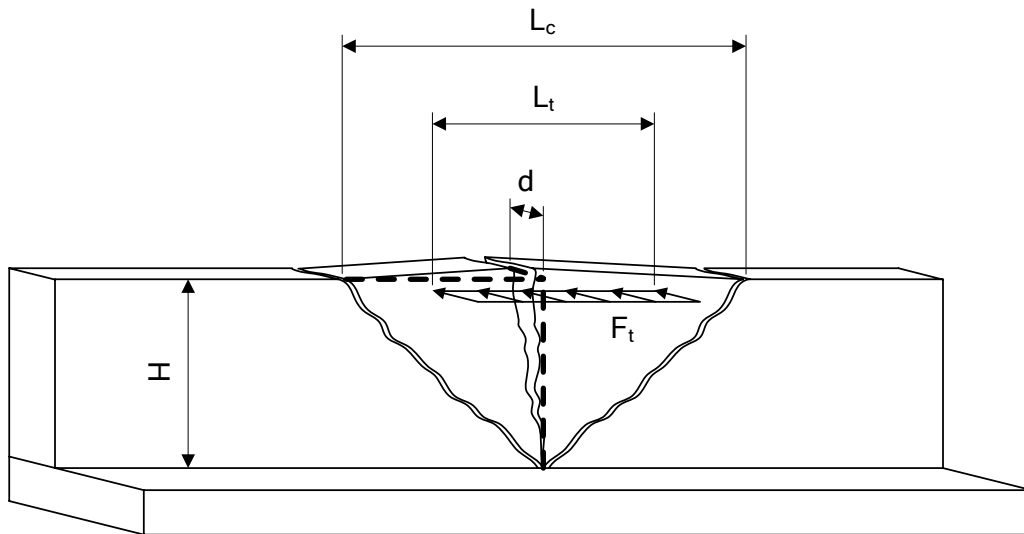
Figure 7.15 Assumed Yield Line Pattern for Barrier Wall

As used in Figure 7.15:

F_t = transverse vehicle impact force
L_t = longitudinal length of distribution of impact force, F_t
L_c = critical length of wall failure
H = height of wall
δ = lateral displacement of wall due to transverse force

If relatively thick parapets are used, then using a thicker deck can be beneficial to develop yield lines in the parapets. As an alternative, the deck can be designed for the forces, without the need to develop the parapet load since the parapet could be thicker than required.

The ultimate flexural capacity of the barrier about its horizontal axis, M_c, at Sections I, II, and III (see Figure 7.14) can be calculated as follows, assuming a constant thickness for each section:

At Section I:

$$a = \frac{A_s F_y}{0.85 f'_c b} = \frac{(0.20 \text{ inches}^2)(60 \text{ ksi})}{0.85(4.0 \text{ ksi})(12 \text{ inches})} = 0.29 \text{ inches}$$

$$d = 13 \text{ inches} - 2 \text{ inches} - \frac{1}{2}(0.50 \text{ inches}) = 10.75 \text{ inches}$$

$$M_c = \phi A_s F_y \left(d_s - \frac{a}{2} \right) \qquad\qquad \text{Equation 7.17}$$

$$M_c = \phi A_s F_y \left(d_s - \frac{a}{2} \right) = 1.0 \left(0.20 \frac{in^2}{ft} \right) (60\ ksi) \left[10.75\ in - \frac{0.29\ in}{2} \right] = 10.61 \frac{K - ft}{ft}$$

Similarly, at Section II, using an increased barrier thickness:

$$d = 15.375\ \text{inches} - 2\ \text{inches} - \frac{1}{2}(0.50\ \text{inches}) = 13.125\ \text{inches}$$

$$M_c = \phi A_s F_y \left(d_s - \frac{a}{2} \right) = 1.0 \left(0.20 \frac{in^2}{ft} \right) (60\ ksi) \left[13.125\ in - \frac{0.29\ in}{2} \right] = 12.98 \frac{K - ft}{ft}$$

Finally, at Section III:

$$d = 20.25\ \text{inches} - 2\ \text{inches} - \frac{1}{2}(0.50\ \text{inches}) = 18\ \text{inches}$$

$$M_c = \phi A_s F_y \left(d_s - \frac{a}{2} \right) = 1.0 \left(0.20 \frac{in^2}{ft} \right) (60\ ksi) \left[18\ in - \frac{0.29\ in}{2} \right] = 17.86 \frac{K - ft}{ft}$$

Assuming that the failure mechanism includes the entire height of the barrier, the moment capacity, M_c, is computed by averaging the above components over their respective heights:

$$M_c = \frac{\left[\left(\dfrac{10.61\dfrac{K-ft}{ft} + 12.98\dfrac{K-ft}{ft}}{2} \right)(22\ in) + \left(\dfrac{12.98\dfrac{K-ft}{ft} + 17.86\dfrac{K-ft}{ft}}{2} \right)(10\ in) \right]}{32\ in} =$$

$$12.93 \frac{K-ft}{ft}$$

Similarly, assuming that the failure mechanism includes only between Section I and II (the top 22 inches of the barrier), the moment capacity, M_c, is computed as follows:

$$M_c = \frac{10.61\dfrac{K-ft}{ft} + 12.98\dfrac{K-ft}{ft}}{2} = 11.80 \frac{K-ft}{ft}$$

For this design example, there is no top beam included on the barrier. Therefore, the ultimate moment capacity of the beam at the top of the wall, M_b, is zero.

To compute the ultimate flexural resistance of the barrier about its vertical axis, M_w, the barrier must be divided into three portions, as illustrated in Figure 7.16. The moment capacity is then computed for each portion about its vertical axis.
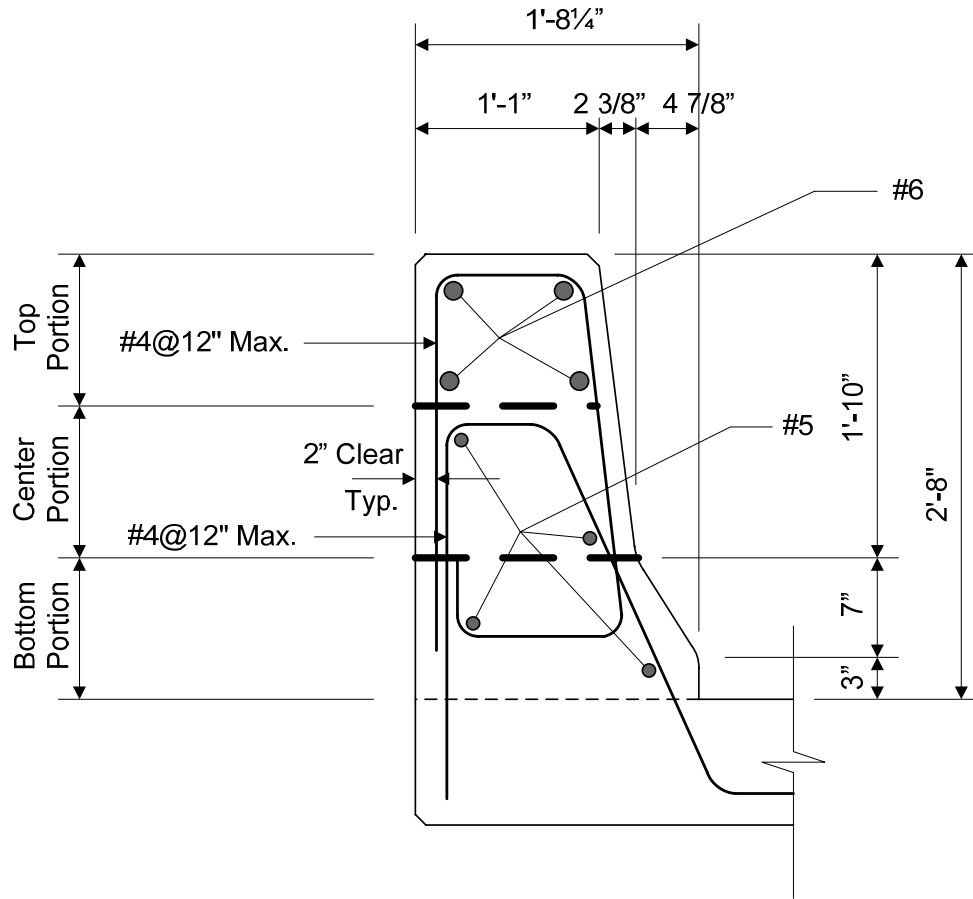
Figure 7.16 Three Portions of Barrier for Computation of M_w

For the top portion of the barrier, there are four #6 bars. To compute the ultimate flexural resistance of the barrier about its vertical axis, it can be assumed that two #6 bars are for positive flexure and two are for negative flexure. The effective depth can be computed based on an average of the structural depth of that portion.

$$a = \frac{A_s F_y}{0.85 f'_c b} = \frac{\left(0.88 \text{ inches}^2\right)\left(60 \text{ ksi}\right)}{0.85\left(4.0 \text{ ksi}\right)\left(11 \text{ inches}\right)} = 1.41 \text{ inches}$$

$$d = 13.59 \text{ inches} - 2 \text{ inches} - \frac{1}{2}\left(0.75 \text{ inches}\right) = 11.22 \text{ inches}$$

$$M_w = \phi A_s F_y \left(d_s - \frac{a}{2}\right) \qquad\qquad \text{Equation 7.18}$$

$$M_w = 1.0(0.88 \text{ inches}^2)(60 \text{ ksi})\left[11.22 \text{ in} - \frac{1.41 \text{ in}}{2}\right] = 46.27 \text{ K} - \text{ft}$$

For the center portion of the barrier, there are two #5 bars. Similar to the top portion, it can be assumed that one #5 bar is for positive flexure and one is for negative flexure.

$$a = \frac{A_s F_y}{0.85 f'_c b} = \frac{(0.31 \text{ inches}^2)(60 \text{ ksi})}{0.85(4.0 \text{ ksi})(11 \text{ inches})} = 0.50 \text{ inches}$$

$$d = 14.78 \text{ inches} - 2 \text{ inches} - \frac{1}{2}(0.625 \text{ inches}) = 12.47 \text{ inches}$$

$$M_w = \phi A_s F_y\left(d_s - \frac{a}{2}\right) = 1.0(0.31 \text{ inches}^2)(60 \text{ ksi})\left[12.47 \text{ in} - \frac{0.50 \text{ in}}{2}\right] = 18.94 \text{ K} - \text{ft}$$

Similarly, for the bottom portion of the barrier, there are two #5 bars.

$$a = \frac{A_s F_y}{0.85 f'_c b} = \frac{(0.31 \text{ inches}^2)(60 \text{ ksi})}{0.85(4.0 \text{ ksi})(10 \text{ inches})} = 0.55 \text{ inches}$$

$$d = 17.81 \text{ inches} - 2 \text{ inches} - \frac{1}{2}(0.625 \text{ inches}) = 15.50 \text{ inches}$$

$$M_w = \phi A_s F_y\left(d_s - \frac{a}{2}\right) = 1.0(0.31 \text{ inches}^2)(60 \text{ ksi})\left[15.50 \text{ in} - \frac{0.55 \text{ in}}{2}\right] = 23.59 \text{ K} - \text{ft}$$

For the case in which different reinforcement steel area is used for positive and negative flexure, the moments for both should be computed and then the average should be used. This is acceptable because the yield line mechanism for this case will have some positive moment hinges and some negative moment hinges.

However, for collision near the expansion joint, the flexural resistance for positive moment should be used. Positive moment will cause tension along the inside face of the barrier, and the only yield line to form is caused by a moment causing tension along the inside face.

Assuming that the failure mechanism includes the entire height of the barrier, the ultimate flexural resistance of the barrier about its vertical axis, M_w, is computed by adding each of the three components:

$$M_w = 46.27 \text{ K} - \text{ft} + 18.94 \text{ K} - \text{ft} + 23.59 \text{ K} - \text{ft} = 88.80 \text{ K} - \text{ft}$$

Similarly, assuming that the failure mechanism includes only the top two portions of the barrier (the top 22 inches of the barrier), the ultimate flexural resistance of the barrier about its vertical axis, M_w, is computed as follows:

$$M_w = 46.27 \, K - ft + 18.94 \, K - ft = 65.21 \, K - ft$$

For impacts within a wall segment, the barrier resistance, R_w, and the critical length of yield line failure pattern, L_c, are computed based on *AASHTO LRFD* Article A13.3.1, as follows:

$$R_w = \left(\frac{2}{2L_c - L_t} \right) \left(8M_b + 8M_w + \frac{M_c L_c^{\,2}}{H} \right) \qquad \text{Equation 7.19}$$

<div align="right">*AASHTO LRFD* Equation A13.3.1-1</div>

$$L_c = \frac{L_t}{2} + \sqrt{\left(\frac{L_t}{2} \right)^2 + \frac{8H(M_b + M_w)}{M_c}} \qquad \text{Equation 7.20}$$

<div align="right">*AASHTO LRFD* Equation A13.3.1-2</div>

where:
- L_t = longitudinal length of distribution of impact force (see *AASHTO LRFD* Table A13.2-1)
- M_b = additional flexural resistance of beam in addition to M_w, if any, at top of wall
- M_w = flexural resistance of the wall about its vertical axis
- M_c = flexural resistance of cantilevered walls about an axis parallel to the longitudinal axis of the bridge

Assuming that the failure mechanism includes the entire height of the barrier and using the previously computed values for M_b, M_w, and M_c, the values for R_w and L_c are computed as follows:

$$L_c = \frac{4 \, ft}{2} + \sqrt{\left(\frac{4 \, ft}{2} \right)^2 + \frac{8(3.5 \, ft)(0 \, K \text{-} ft + 88.80 \, K - ft)}{12.93 \, \dfrac{k \text{-} ft}{ft}}} = 16.01 \, ft$$

$$R_w = \left(\frac{2}{2(16.01 \, ft) - 4 \, ft} \right) \left(8(0 \, K \text{-} ft) + 8(88.80 \, K - ft) + \frac{\left(12.93 \, \dfrac{K \text{-} ft}{ft} \right)(16.01 \, ft)^2}{3.5 \, ft} \right)$$

$$= 118.3 \, kips$$

Similarly, assuming that the failure mechanism is only the top portion (the top 22 inches of the barrier) and using the previously computed values for M_b, M_w, and M_c, the values for R_w and L_c are computed as follows:

$$L_c = \frac{4 \text{ ft}}{2} + \sqrt{\left(\frac{4 \text{ ft}}{2}\right)^2 + \frac{8(1.83 \text{ ft})(0 \text{ K-ft} + 65.21 \text{ K} - \text{ft})}{11.80 \frac{\text{k-ft}}{\text{ft}}}} = 11.22 \text{ ft}$$

$$R_w = \left(\frac{2}{2(11.22 \text{ ft}) - 4 \text{ ft}}\right)\left[8(0 \text{ K-ft}) + 8(65.21 \text{ K} - \text{ft}) + \frac{\left(11.80 \frac{\text{K-ft}}{\text{ft}}\right)(11.22 \text{ ft})^2}{1.83 \text{ ft}}\right]$$

$$= 144.4 \text{ kips}$$

The barrier load capacity is then taken as the minimum for the investigated failure mechanisms, or 118.3 kips. The barrier that has been selected for use with this design example is assumed to be approved for Test Level TL-3. Therefore, based on *AASHTO LRFD* Table A13.2-1, the transverse design force, F_t, is 54.0 kips.

$$R_w = 118.3 \text{ kips} > 54.0 \text{ kips} = F_t \qquad \therefore \text{ OK}$$

For impacts at the end of a wall or at a joint, the barrier resistance, R_w, and the critical length of yield line failure pattern, L_c, are computed based on *AASHTO LRFD* Article A13.3.1, as follows:

$$R_w = \left(\frac{2}{2L_c - L_t}\right)\left(M_b + M_w + \frac{M_c L_c^2}{H}\right) \qquad \qquad \text{Equation 7.21}$$

AASHTO LRFD Equation A13.3.1-3

$$L_c = \frac{L_t}{2} + \sqrt{\left(\frac{L_t}{2}\right)^2 + H\left(\frac{M_b + M_w}{M_c}\right)} \qquad \qquad \text{Equation 7.22}$$

AASHTO LRFD Equation A13.3.1-4

Assuming that the failure mechanism includes the entire height of the barrier and using the previously computed values for M_b, M_w, and M_c, the values for R_w and L_c are computed as follows:

$$L_c = \frac{4 \text{ ft}}{2} + \sqrt{\left(\frac{4 \text{ ft}}{2}\right)^2 + (3.5 \text{ ft})\left[\frac{0 \text{ K-ft} + 88.80 \text{ K} - \text{ft}}{12.93 \frac{\text{k-ft}}{\text{ft}}}\right]} = 7.30 \text{ ft}$$

$$R_w = \left(\frac{2}{2(7.30\ \text{ft})-4\ \text{ft}}\right)\left(0\ \text{K-ft} + 88.80\ \text{K} - \text{ft} + \frac{\left(12.93\ \dfrac{\text{K-ft}}{\text{ft}}\right)(7.30\ \text{ft})^2}{3.5\ \text{ft}}\right)$$

$$= 54.0\ \text{kips}$$

Similarly, assuming that the failure mechanism is only the top portion (the top 22 inches of the barrier) and using the previously computed values for M_b, M_w, and M_c, the values for R_w and L_c are computed as follows:

$$L_c = \frac{4\ \text{ft}}{2} + \sqrt{\left(\frac{4\ \text{ft}}{2}\right)^2 + (1.83\ \text{ft})\left(\frac{0\ \text{K-ft} + 65.21\ \text{K} - \text{ft}}{11.80\ \dfrac{\text{k-ft}}{\text{ft}}}\right)} = 5.76\ \text{ft}$$

$$R_w = \left(\frac{2}{2(5.76\ \text{ft})-4\ \text{ft}}\right)\left(0\ \text{K-ft} + 65.21\ \text{K} - \text{ft} + \frac{\left(11.80\ \dfrac{\text{K-ft}}{\text{ft}}\right)(5.76\ \text{ft})^2}{1.83\ \text{ft}}\right)$$

$$= 74.2\ \text{kips}$$

The barrier load capacity is then taken as the minimum for the investigated failure mechanisms, or 54.0 kips. The barrier that has been selected for use with this design example is assumed to be approved for Test Level TL-3. Therefore, based on *AASHTO LRFD* Table A13.2-1, the transverse design force, F_t, is 54.0 kips.

$$R_w = 54.0\ \text{kips} \approx 54.0\ \text{kips} = F_t \qquad \therefore\ \text{OK}$$

After computing the barrier load capacity, the horizontal vehicular collision force must be checked at the inside face of the barrier, at the design section for the overhang, and at the design section for the first girder bay. These design locations are presented in Figure 7.13. As shown in Table 7.7, these design checks are for the extreme event limit state.

Check at inside face of barrier:

The dead load moment at the inside face of the barrier is computed as follows:

$$M_{deck} = \frac{(0.150\ \text{kcf})(9\ \text{inches})\left(\dfrac{1\ \text{ft}}{12\ \text{inches}}\right)(1.4375\ \text{ft})^2}{2} = 0.116\ \frac{\text{K} - \text{ft}}{\text{ft}}$$

$$M_{barrier} = \left(0.53 \, \frac{kips}{ft} \right) \left(1.4375 \, ft - \frac{6.16 \, inches}{\left(\dfrac{12 \, inches}{1 \, ft} \right)} \right) = 0.490 \, \frac{K-ft}{ft}$$

Therefore, the total factored design moment for the extreme event limit state is:

$$M_u = (1.25) \left[0.116 \, \frac{K-ft}{ft} + 0.490 \, \frac{k-ft}{ft} \right] + 17.86 \, \frac{K-ft}{ft} = 18.62 \, \frac{K-ft}{ft}$$

Based on *AASHTO LRFD* Article A13.4.2, the axial tensile force, T, is computed as follows:

$$T = \frac{R_w}{L_c + 2H} \qquad\qquad \text{Equation 7.23}$$

AASHTO LRFD Equation A13.4.2-1

where:
  R_w = total transverse resistance of the barrier
  L_c = critical length of yield line failure pattern
  H   = height of wall

Using the previously computed values for R_w, L_c, and H for the controlling failure mechanism:

$$T = \frac{54.0 \, kips}{7.30 \, ft + 2(3.5 \, ft)} = 3.78 \, \frac{kips}{ft}$$

After these values have been computed, the required area of reinforcing steel is computed similar to the procedure for the deck. Based on the traditional design method, #5 at 6 inches was used for the top primary reinforcement. For the overhang reinforcement, assume the use of #5 bars to resist the negative flexure in the deck. Therefore, the effective depth is computed as follows:

$$d_s = \text{Slab Thickness} - \text{Top Cover} - \frac{\text{Bar Diameter}}{2}$$

$$= 9.0 \, inches - 2.5 \, inches - \frac{0.625 \, inches}{2} = 6.19 \, inches$$

$$a = \frac{A_s F_y}{0.85 f'_c b} = \frac{A_s (60 \, ksi)}{0.85(4.0 \, ksi) \left(\dfrac{12 \, inches}{1 \, ft} \right)} = \left(1.47 \, \frac{ft}{inch} \right) A_s$$

$$M_r = \phi M_n = \phi A_s F_y \left(d_s - \frac{a}{2} \right) = 0.90 A_s (60 \text{ ksi}) \left[6.19 \text{ inches} - \frac{\left(1.47 \frac{\text{ft}}{\text{inch}} \right) A_s}{2} \right]$$

Setting M_r equal to the factored design moment of 28.97 K-ft/ft produces the following required reinforcement area:

$$A_s = 1.22 \frac{\text{inches}^2}{\text{ft}}$$

The required reinforcement spacing can then be computed as follows:

$$\text{Required Spacing} = \frac{0.31 \frac{\text{inches}^2}{\text{bar}}}{1.22 \frac{\text{inches}^2}{\text{ft}}} = 0.25 \text{ ft} = 3.0 \text{ inches}$$

Therefore, use two #5 bars bundled at 6 inches for the overhang reinforcement. Taking into account the axial tension force, the provided flexural resistance is computed as follows:

$$A_s = \frac{2(0.31 \text{ inches}^2)}{(6 \text{ inches}) \left(\frac{1 \text{ ft}}{12 \text{ inches}} \right)} = 1.24 \frac{\text{inches}^2}{\text{ft}}$$

$$T_a = A_s F_y \qquad\qquad \text{Equation 7.24}$$

$$T_a = \left(1.24 \frac{\text{inches}^2}{\text{ft}} \right) (60 \text{ ksi}) = 74.40 \frac{\text{kips}}{\text{ft}}$$

$$C = T_a - T \qquad\qquad \text{Equation 7.25}$$

$$C = 74.40 \frac{\text{kips}}{\text{ft}} - 3.78 \frac{\text{kips}}{\text{ft}} = 70.62 \frac{\text{kips}}{\text{ft}}$$

$$a = \frac{C}{0.85 f'_c b} \qquad\qquad \text{Equation 7.26}$$

$$a = \frac{70.62 \frac{\text{kips}}{\text{ft}}}{0.85(4.0 \text{ ksi}) \left(\frac{12 \text{ inches}}{1 \text{ ft}} \right)} = 1.73 \text{ inches}$$

$$M_r = \phi\left[T_a\left(d_s - \frac{a}{2}\right) + T\left(\frac{d_s}{2} - \frac{a}{2}\right)\right] \qquad \text{Equation 7.27}$$

$$M_r = 0.90\left[\begin{array}{l}\left(74.40\,\frac{\text{kips}}{\text{ft}}\right)\left(6.19\text{ inches} - \dfrac{1.73\text{ inches}}{2}\right) \\ +\left(3.78\,\frac{\text{kips}}{\text{ft}}\right)\left(\dfrac{6.19\text{ inches}}{2} - \dfrac{1.73\text{ inches}}{2}\right)\end{array}\right]$$

$$= 30.35\,\frac{K-ft}{ft} > 28.97\,\frac{K-ft}{ft} \qquad \therefore \text{ OK}$$

After the bar size and spacing have been determined, the maximum reinforcement limit must also be checked based on the requirements of *AASHTO LRFD* Article 5.7.3.3.1, as follows:

$$\frac{c}{d_e} \le 0.42 \qquad \text{Equation 7.28}$$

AASHTO LRFD Equation 5.7.3.3.1-1

where: $\qquad c = \dfrac{a}{\beta_1} = \dfrac{1.73\text{ inches}}{0.85} = 2.04\text{ inches}$

$$d_e = d_s = 6.19\text{ inches}$$

Therefore, $\qquad \dfrac{c}{d_e} = \dfrac{2.04\text{ inches}}{6.19\text{ inches}} = 0.33 \le 0.42 \qquad \therefore \text{ OK}$

Check at design section for overhang:

The overhang must also be checked at the design section for the overhang, as illustrated in Figure 7.13. The collision forces are distributed over a distance L_c for moment and L_c+2H for axial force. Since the design section is moved away from the face of the barrier, the distribution length will increase. This design example assumes a distribution length increase based on a 30° angle from the face of the barrier, as illustrated in Figure 7.17.
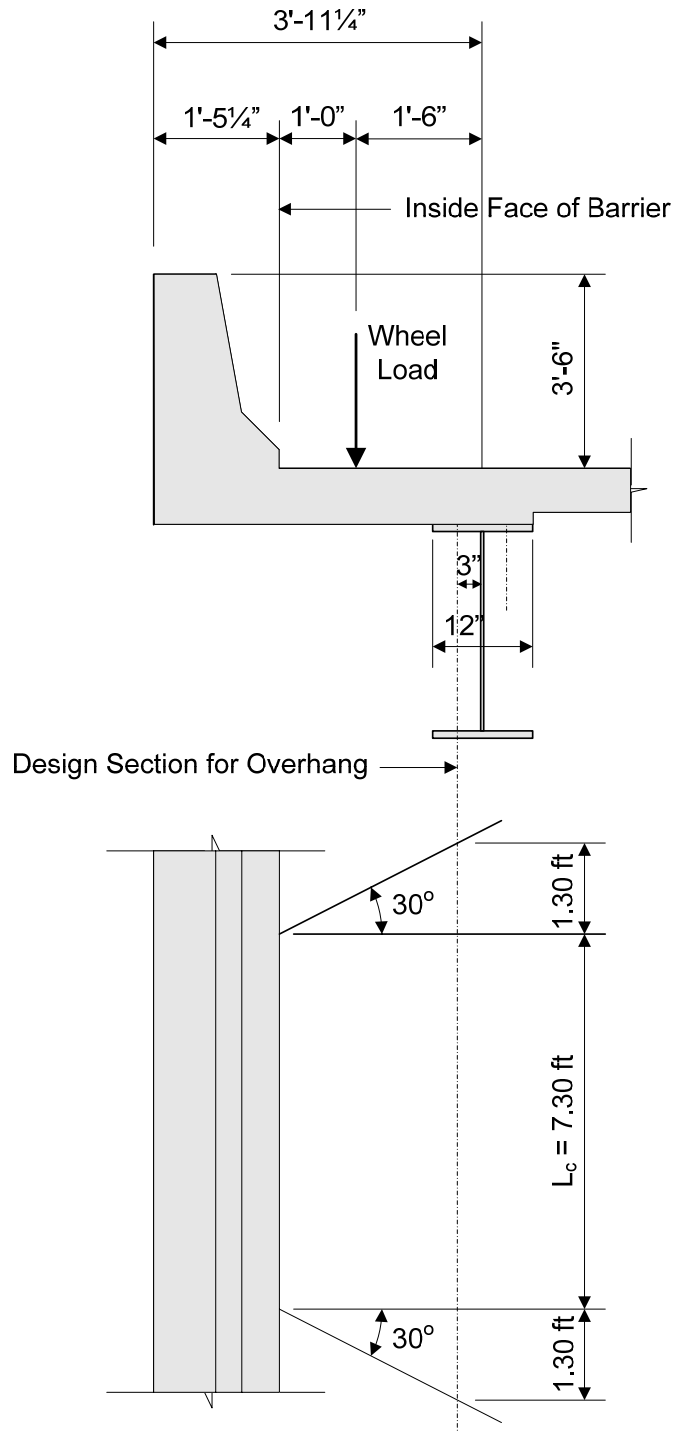
Figure 7.17 Assumed Distribution of Collision Moment Load in the Overhang

Using the same general procedures used for the check at the inside face of the barrier, the dead load moment at the design section in the overhang is computed as follows:

$$M_{deck} = \frac{(0.150 \text{ kcf})(9 \text{ inches})\left(\frac{1 \text{ ft}}{12 \text{ inches}}\right)(3.6875 \text{ ft})^2}{2} = 0.77 \frac{K-ft}{ft}$$

$$M_{barrier} = \left(0.53 \frac{kips}{ft}\right)\left(3.6875 \text{ ft} - \frac{6.16 \text{ inches}}{\left(\frac{12 \text{ inches}}{1 \text{ ft}}\right)}\right) = 1.68 \frac{K-ft}{ft}$$

$$M_{FWS} = \frac{(0.140 \text{ kcf})(2.5 \text{ inches})\left(\frac{1 \text{ ft}}{12 \text{ inches}}\right)(2.25 \text{ ft})^2}{2} = 0.07 \frac{K-ft}{ft}$$

The barrier moment capacity is adjusted as follows, based on the distribution shown in Figure 7.17:

$$M_{barrier\ capacity} = \frac{\left(17.86 \frac{K-ft}{ft}\right)(7.30 \text{ ft})}{7.30 \text{ ft} + 2(1.30 \text{ ft})} = 13.17 \frac{K-ft}{ft}$$

Therefore, the total factored design moment for the extreme event limit state is:

$$M_u = 1.25\left[0.77 \frac{K-ft}{ft} + 1.68 \frac{k-ft}{ft}\right] + 1.50\left(0.07 \frac{K-ft}{ft}\right) + 13.17 \frac{K-ft}{ft}$$

$$= 16.34 \frac{K-ft}{ft}$$

The axial tensile force, T, is computed as follows:

$$T = \frac{R_w}{L_c + 2(1.30 \text{ ft}) + 2H} = \frac{54.0 \text{ kips}}{7.30 \text{ ft} + 2(1.30 \text{ ft}) + 2(3.5 \text{ ft})} = 3.20 \frac{kips}{ft}$$

After these values have been computed, the required area of reinforcing steel is computed similar to the procedure for the deck. Similar to the face of the barrier, the effective depth and required reinforcement are computed as follows:

$$d_s = \text{Slab Thickness} - \text{Top Cover} - \frac{\text{Bar Diameter}}{2}$$

$$= 9.0 \text{ inches} - 2.5 \text{ inches} - \frac{0.625 \text{ inches}}{2} = 6.19 \text{ inches}$$

$$a = \frac{A_s F_y}{0.85 f'_c b} = \frac{A_s (60 \text{ ksi})}{0.85(4.0 \text{ ksi}) \left(\frac{12 \text{ inches}}{1 \text{ ft}} \right)} = \left(1.47 \frac{\text{ft}}{\text{inches}} \right) A_s$$

$$M_r = \phi M_n = \phi A_s F_y \left(d_s - \frac{a}{2} \right) = 0.90 A_s (60 \text{ ksi}) \left[6.19 \text{ inches} - \frac{\left(1.47 \frac{\text{ft}}{\text{inches}} \right) A_s}{2} \right]$$

Setting M_r equal to the factored design moment of 24.48 K-ft/ft produces the following required reinforcement area:

$$A_s = 1.00 \frac{\text{inches}^2}{\text{ft}}$$

Therefore, the required reinforcing steel at the design section for the overhang is less than that at the inside face of the barrier.

Check at design section for first bay:

To design for flexure at the design section for the first bay, the distribution of the collision moment across the width of the deck is assumed to be similar to the distribution of the moment due to the barrier weight, as shown in Figure 7.18. The ratio, M_1/M_2, for the moment due to the barrier weight is assumed to equal the ratio, M_1/M_2, for the collision moment. The collision moment can then be computed by using the increased distribution length based on the 30˚ angle from the face of the barrier, as illustrated in Figure 7.17.
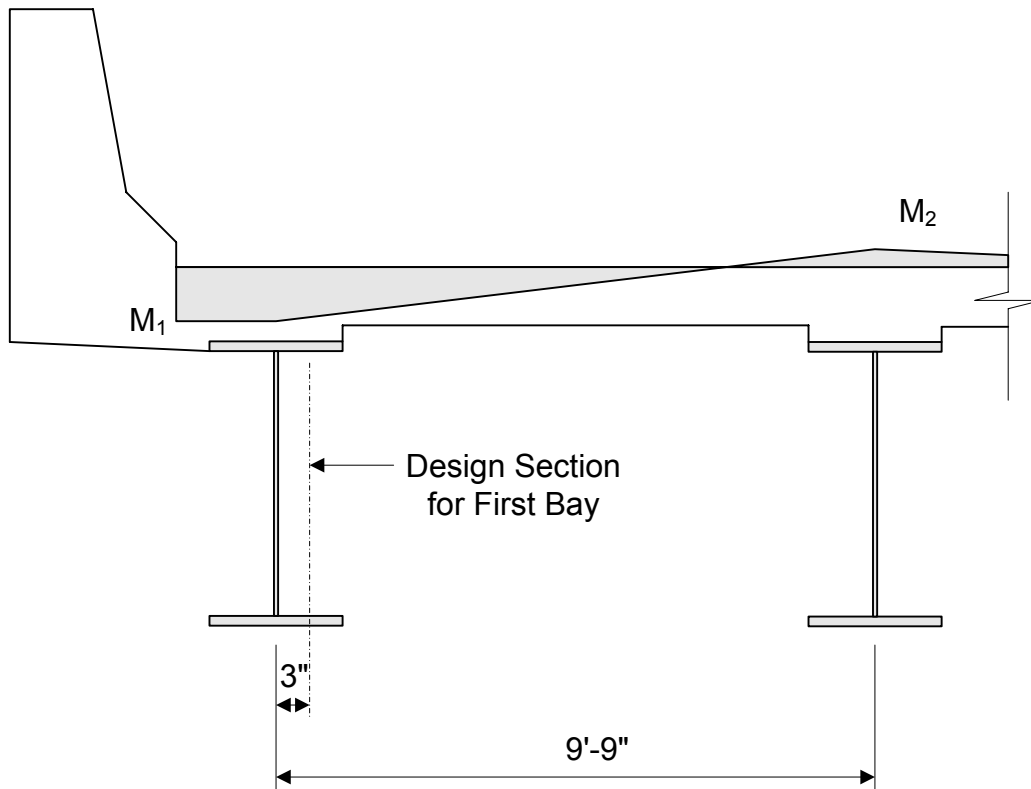
Figure 7.18 Assumed Distribution of Collision Moment

As described in previous sections of this chapter, the dead load moments in the deck can be computed using structural analysis software, based on a 1-foot strip running across the width of the deck. For this design example, the dead load moments are presented in Table 7.1, and the moments at the girders due to barrier weight are as follows:

$$M_{barrier\ 1} = -1.66 \frac{K-ft}{ft} \quad \text{and} \quad M_{barrier\ 2} = 0.47 \frac{K-ft}{ft}$$

Since the collision moment at the inside face of the barrier is -28.21 K-ft/ft, the collision moment at the design section for the first bay can be computed as follows:

$$M_{collision\ 2} = M_{collision\ 1} \frac{M_{barrier\ 2}}{M_{barrier\ 1}} = -17.86 \frac{K-ft}{ft} \left(\frac{0.47 \frac{K-ft}{ft}}{-1.66 \frac{K-ft}{ft}} \right) = 5.06 \frac{K-ft}{ft}$$

Based on interpolation, the collision moment at the design section for the first bay is:

$$M_{collision} = -17.86 \frac{K-ft}{ft} + \left[\left(5.06 \frac{K-ft}{ft} + 17.86 \frac{K-ft}{ft} \right) \left(\frac{0.25\ ft}{9.75\ ft} \right) \right]$$

$$= -17.27 \frac{K-ft}{ft}$$

Applying the 30° angle distribution, similar to the procedure used at the design section for the overhang, the barrier moment capacity is adjusted as follows:

$$M_{barrier\ capacity} = \frac{\left(-17.27 \frac{K-ft}{ft} \right) (7.30\ ft)}{7.30\ ft + 2(1.59\ ft)} = -12.03 \frac{K-ft}{ft}$$

Using the unfactored dead load moments presented in Table 7.1, the total factored design moment for the extreme event limit state is:

$$M_u = 1.25 \left[-0.74 \frac{K-ft}{ft} - 1.66 \frac{k-ft}{ft} \right] + 1.50 \left(-0.06 \frac{K-ft}{ft} \right) - 12.03 \frac{K-ft}{ft}$$

$$= -15.12 \frac{K-ft}{ft}$$

The axial tensile force, T, is computed as follows:

$$T = \frac{R_w}{L_c + 2(1.59\ ft) + 2H} = \frac{54.0\ kips}{7.30\ ft + 2(1.59\ ft) + 2(3.5\ ft)} = 3.09 \frac{kips}{ft}$$

After these values have been computed, the required area of reinforcing steel is computed:

$$d_s = \text{Slab Thickness} - \text{Top Cover} - \frac{\text{Bar Diameter}}{2}$$

$$= 8.5\ \text{inches} - 2.5\ \text{inches} - \frac{0.625\ \text{inches}}{2} = 5.69\ \text{inches}$$

$$a = \frac{A_s F_y}{0.85 f'_c b} = \frac{A_s (60\ ksi)}{0.85(4.0\ ksi)\left(\frac{12\ inches}{1\ ft} \right)} = \left(1.47 \frac{ft}{inch} \right) A_s$$

$$M_r = \phi M_n = \phi A_s F_y \left(d_s - \frac{a}{2} \right)$$

$$= 0.90 A_s (60\ ksi) \left[5.69\ \text{inches} - \frac{\left(1.47 \frac{ft}{inch} \right) A_s}{2} \right]$$

Setting M_r equal to the factored design moment of 22.63 K-ft/ft produces the following required reinforcement area:

$$A_s = 1.02 \frac{\text{inches}^2}{\text{ft}}$$

Therefore, the required reinforcing steel at the design section for the first bay is also less than that at the inside face of the barrier.

Design Case 2: Design overhang for vertical collision force

The overhang is also designed for the vertical forces specified in *AASHTO LRFD* Article A13.4.1. As shown in Table 7.7, these design checks are also for the extreme event limit state. However, for concrete barriers, the case of vertical collision force never controls.

Design Case 3: Design overhang for dead load and live load

Finally, the overhang must be designed for dead load and live load. The dead load and live load must be checked at the design section for the overhang and at the design section for the first girder bay. These design locations are presented in Figure 7.13. As shown in Table 7.7, these design checks are for the strength limit state.

Check at design section for overhang:

As presented in Figure 7.2, the equivalent strip for live load on an overhang is:

$$\text{Equivalent Strip Width} = 45.0 + 10.0SX$$
$$= 45.0 + 10.0(1.25) = 57.5 \text{ inches} = 4.79 \text{ ft}$$

Applying a multiple presence factor of 1.20 for one lane loaded and a dynamic load allowance of 0.33, the moment due to live load and dynamic load allowance is computed as follows:

$$M_{LL+I} = \frac{(1.20)(1.33)(16 \text{ kips})(1.25 \text{ ft})}{4.79 \text{ ft}} = 6.66 \frac{K - ft}{ft}$$

Using the same dead load moments that were previously computed, the total factored design moment for the strength limit state is:

$$M_u = 1.25\left[0.77\frac{K-ft}{ft} + 1.68\frac{k-ft}{ft}\right] + 1.50\left(0.07\frac{K\text{-}ft}{ft}\right)$$

$$+ 1.75\left(6.66\frac{K\text{-}ft}{ft}\right) = 16.82\frac{K-ft}{ft}$$

Since the total factored design moment for Design Case 3 is less than that computed for Design Case 1 at the design section for the overhang, Design Case 3 does not control at this design section.

Check at design section for first bay:

The dead load and live load moments are taken from Table 7.1, Table 7.2, and Table 7.3. The maximum negative live load moment occurs in Bay 4. Since the negative live load moment is produced by a load on the overhang, the equivalent strip is computed based on a moment arm to the centerline of the girder. As presented in Figure 7.2, the equivalent strip is:

$$\text{Equivalent Strip Width} = 45.0 + 10.0SX$$
$$= 45.0 + 10.0(1.50) = 60.0 \text{ inches} = 5.00 \text{ ft}$$

Therefore, the moment due to live load and dynamic load allowance is computed as follows:

$$M_{LL+I} = \frac{1.33\left(\text{-}29.40\frac{K\text{-}ft}{ft}\right)}{5.00 \text{ ft}} = -7.82\frac{K-ft}{ft}$$

Using the same dead load moments that were previously computed, the total factored design moment for the strength limit state is:

$$M_u = 1.25\left[\text{-}0.74\frac{K-ft}{ft} - 1.66\frac{k-ft}{ft}\right] + 1.50\left(\text{-}0.06\frac{K\text{-}ft}{ft}\right)$$

$$+ 1.75\left(\text{-}7.82\frac{K\text{-}ft}{ft}\right) = -16.78\frac{K-ft}{ft}$$

Since the total factored design moment for Design Case 3 is less than that computed for Design Case 1 at the design section for the first girder bay, Design Case 3 does not control at this design section.

Based on the computations for the three design cases, it is clear that the design of the deck overhang is controlled by Design Case 1 (horizontal vehicular collision force) at the inside face of the barrier for the extreme event limit state. As previously computed, the factored design moment is 28.97 K-ft/ft and the required reinforcing steel is 1.22 inches^2/foot. Also as previously computed, the required negative

flexural reinforcement is #5 at 6 inches. Therefore the provided reinforcement due to negative flexure is:

$$A_s = \frac{0.31 \text{ inches}^2}{(6 \text{ inches})\left(\dfrac{1 \text{ ft}}{12 \text{ inches}}\right)} = 0.62 \frac{\text{inches}^2}{\text{ft}} < 1.22 \frac{\text{inches}^2}{\text{ft}}$$

Since the area of reinforcing steel required in the overhang is greater than the area of reinforcing steel provided for the negative moment regions, reinforcement must be added in the overhang area to satisfy the design requirements. The design requirements can be satisfied by bundling one #5 bar to each negative flexure reinforcing bar in the overhang area. Therefore, the provided reinforcement in the overhang is:

$$A_s = \frac{2(0.31 \text{ inches}^2)}{(6 \text{ inches})\left(\dfrac{1 \text{ ft}}{12 \text{ inches}}\right)} = 1.24 \frac{\text{inches}^2}{\text{ft}} > 1.22 \frac{\text{inches}^2}{\text{ft}} \qquad \therefore \text{ OK}$$

Once the required area of reinforcing steel is known, the maximum reinforcement limit must be checked in accordance with *AASHTO LRFD* Article 5.7.3.3.1. The ratio of c/d_e is more critical at the minimum deck thickness, so the compression block will be checked in Bay 1 where the deck thickness is 8.5 inches.

$$a = \frac{\left(1.24 \dfrac{\text{inches}^2}{\text{ft}}\right)(60 \text{ ksi})}{0.85(4.0 \text{ ksi})\left(\dfrac{12 \text{ inches}}{1 \text{ ft}}\right)} = 1.82 \text{ inches}$$

$$\frac{c}{d_e} \leq 0.42$$

where: $$c = \frac{a}{\beta_1} = \frac{1.82 \text{ inches}}{0.85} = 2.15 \text{ inches}$$

$$d_e = d_s = 5.69 \text{ inches}$$

Therefore, $$\frac{c}{d_e} = \frac{2.15 \text{ inches}}{5.69 \text{ inches}} = 0.38 < 0.42 \qquad \therefore \text{ OK}$$

2. *Check for cracking in overhang under service limit state*

Cracking in the overhang must be checked for the service limit state in accordance with *AASHTO LRFD* Article 5.7.3.4. However, since this design check is presented in previous sections of this chapter and since it does not control most deck overhang

designs, the cracking check computations are not shown in this deck overhang design example.

3. *Compute overhang cut-off length requirement*

The next step is to compute the cut-off location of the additional, bundled #5 bar in the first bay. This is done by determining the location where the total design moment (including dead load, live load, and collision load) is less than or equal to the resistance provided by #5 bars at 6 inches (negative design reinforcement).

The factored negative flexural resistance provided by #5 at 6 inch spacing is computed as follows:

$$A_s = \frac{0.31\,\text{inches}^2}{(6\,\text{inches})\left(\dfrac{1\,\text{ft}}{12\,\text{inches}}\right)} = 0.62\,\frac{\text{inches}^2}{\text{ft}}$$

$$a = \frac{\left(0.62\,\dfrac{\text{inches}^2}{\text{ft}}\right)(60\,\text{ksi})}{0.85(4.0\,\text{ksi})\left(\dfrac{12\,\text{inches}}{1\,\text{ft}}\right)} = 0.91\,\text{inches}$$

$$M_r = 0.90\left(0.62\,\frac{\text{inches}^2}{\text{ft}}\right)(60\,\text{ksi})\left[5.69\,\text{inches} - \frac{0.91\,\text{inches}}{2}\right]$$
$$= 14.60\,\frac{\text{K} - \text{ft}}{\text{ft}}$$

Based on the factored flexural resistance and an interpolation of the factored design moments, the theoretical cut-off point for the additional #5 bar is approximately 3.75 feet from the centerline of the fascia girder.

Then, based on *AASHTO LRFD* Article 5.11.1.2, the additional cut-off length required beyond the theoretical cut-off point is the maximum of the following three values:

$$d_e = 5.69\,\text{inches}$$

$$15(\text{nominal bar diameter}) = 15(0.625\,\text{inches}) = 9.375\,\text{inches}$$

$$\frac{1}{20}(\text{clear span}) = \frac{1}{20}(9.75\,\text{ft})\left(12\,\frac{\text{inches}}{\text{ft}}\right) = 5.85\,\text{inches}$$

Therefore, using 9.5 inches as the additional cut-off length, the total required length past the centerline of the fascia girder into the first bay is:

Total cut-off length = 45 inches + 9.5 inches = 54.5 inches

The location of the cut-off length is shown in Figure 7.19.

4. Compute overhang development length

In addition to the cutoff length, the overhang development length must also be computed. The basic development length is the larger of the following three values:

$$\frac{1.25A_b f_y}{\sqrt{f'_c}} = \frac{1.25(0.31)(60)}{\sqrt{4}} = 11.63 \text{ inches}$$

$$0.4d_b f_y = 0.4(0.625)(60) = 15 \text{ inches}$$

12 inches

Therefore, the basic development length for the overhang reinforcement is 15 inches. However, the following modification factors must also be applied:

Epoxy coated bars: 1.2
Bundled bars: 1.2
Spacing > 6 inches with more than 3 inches of
clear cover in direction of spacing: 0.8

Applying these modification factors to the basic development length:

$$L_d = (15 \text{ inches})(1.2)(1.2)(0.8) = 17.3 \text{ inches} \qquad \text{Use 18 inches}$$

Since the 18-inch development length must extend beyond the design section, which is located 3 inches beyond the centerline of the girder, the required development distance beyond the centerline of the fascia girder is 21 inches.

Development distance = 21 inches < 54.5 inches = Cut-off distance   ∴ OK

The development length is shown in Figure 7.19.

#5 @ 6" (Bundled bars for overhang)

21"

3"   18"   Development length
(beyond design section)

Design Section

12"

45"   9½" Cut-off length

54.5"

9'-9"
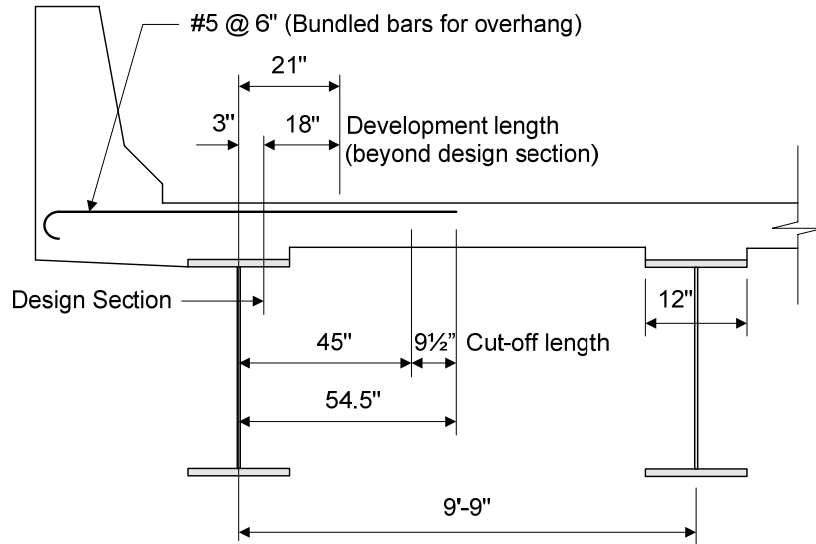
Figure 7.19 Length of Overhang Negative Moment Reinforcement

7.3.5 Precast Decks

Precast concrete decks have been used on bridges since the 1950s. The primary benefit of precast decks is that they expedite bridge construction, thereby reducing construction-related traffic delays. Conventional cast-in-place deck construction with its associated curing requirements can consume more than one month on a typical bridge construction project. However, forming, casting, and curing operations of precast decks can be carried out at a remote location with reduced on-site impact to motorists. Precast decks are applicable to a wide variety of common bridge types and are applicable to deck replacement projects as well as new construction.

When constructing a precast concrete deck, the precast elements are brought to the construction site ready to be set in place and can be joined together quickly. A subsequent cast-in-place concrete pour can seal the joints and tie individual units together, forming a uniform homogenous bridge deck with improved ride quality. Deck joints can be oriented either transversely across the width of the bridge or longitudinally along the length of the bridge. The typical panel distance between joints is greater than 5 feet, sometimes exceeding 20 feet.

Several different systems of precast decks have been used. One system for full-depth concrete slab span bridges speeds construction by eliminating the need for deck forming. This system consists of precast inverted T-beam units with looped reinforcement extending from the sides of each unit. The inverted beams are installed adjacent to each other in a manner that interlocks the looped reinforcement. The beams are made composite with cast-in-place concrete that seals the joints and fills the voids between the T's to form a solid full-depth concrete slab span structure.

Another system consists of precast deck sections that are installed on girders, with each panel extending the full width of the bridge. No on-site deck forming is needed, thereby reducing the required construction time. Similar to the previously described system, the units of this system are connected together with a series of looped

reinforcement extending from the sides of the panels. They are then sealed with cast-in-place concrete.

A third system seals the joints between adjacent precast beams with a cast-in-place concrete pour. This system is applicable for box girders, as well as bulb-T girders and double-T beams.

Research on precast decks has resulted in the implementation of post-tensioning for connection durability and overlaid systems for ride quality. Other issues that have been addressed include panel casting and placement tolerances, shear connections, vertical alignment, final grade adjustment, drainage, and barrier connections.

7.3.6 Stay-in-place Formwork

Stay-in-place forms can be used to span the distance between bridge girders, providing formwork for cast-in-place concrete decks. Stay-in-place forms serve to support the uncured deck concrete during construction, and as the name suggests, they remain a part of the bridge after construction is completed.

Stay-in-place formwork is designed to behave elastically during construction. The forms are designed to support the self-weight of the form, the deck reinforcement, the deck concrete, including the concrete in the valleys of the form, as well as a construction load of 50 pounds per square foot. They are also designed to limit deflection to a specified maximum value, such as 1/180 of the form span or ½ inch. The flexural stress and elastic deformation requirements for stay-in-place forms are presented in *AASHTO LRFD* Article 9.7.4.1.

Stay-in-place formwork can be either steel or concrete. A typical steel stay-in-place form is illustrated in Figure 7.20. As shown in Figure 7.20, the stay-in-place forms often bear on angles welded to the girders. Due to their corrugated cross section, they can support dead load of the deck while the concrete cures. The corrugations of the form are oriented perpendicular to the girder length. Stay-in-place forms generally have closed tapered ends and are used for the interior girder bays only, where the forms can be supported on both sides by the girders. Welding is generally not permitted either to flanges in tension or to bridge elements fabricated with non-weldable grades of steel.

Section A-A
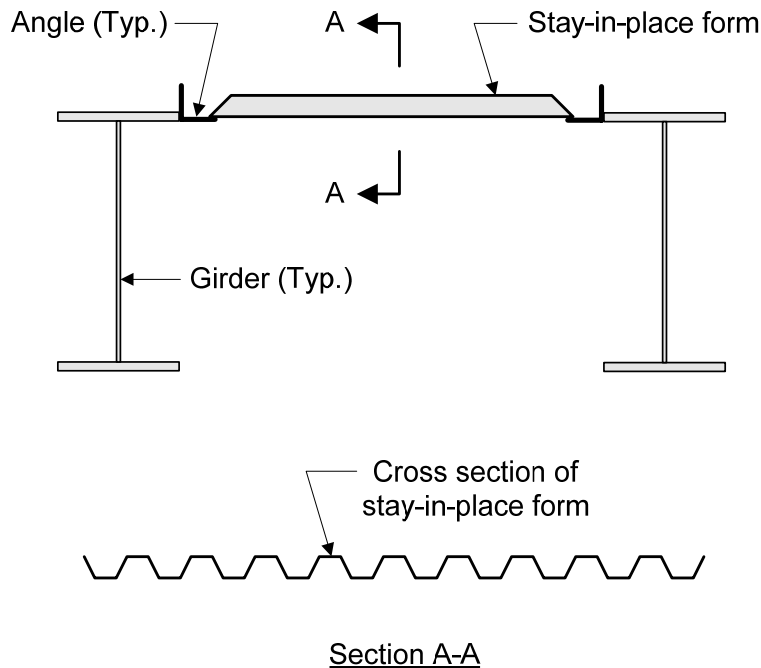
Figure 7.20 Steel Stay-in-place Formwork

In addition to steel formwork, concrete formwork can also be used. Concrete formwork must satisfy the depth, reinforcement, creep and shrinkage control, and bedding requirements presented in *AASHTO LRFD* Article 9.7.4.3.

Some of the benefits of stay-in-place forms are:

➢ Ease of installation, since they are installed from the top rather than the bottom
➢ Reduced labor cost compared with traditional formwork which must be removed
➢ Reduced construction time compared with traditional formwork which must be removed
➢ Facilitates a uniform slab thickness

However, some disadvantages of stay-in-place forms include:

➢ Water than passes through the porous concrete deck is trapped in the forms and can cause corrosion of the reinforcement
➢ Underside inspection of the bridge deck is not possible, and therefore any cracks and corrosion in the underside of the deck are not visible

7.3.7 Deck Staging

Deck staging must be considered to provide an acceptable deck placement sequence during construction. An analysis of the proposed deck sequence must address (but is not limited to) the following considerations:

- ➢ Stability and strength of the girder throughout deck construction.
- ➢ Change in the stiffness in the girder as different portions of the deck are placed.
- ➢ Temporary stresses and "locked-in" erection stresses in the girders.
- ➢ Bracing of the compression flange of the girders and its effect on the stability and strength of the girder.
- ➢ Bracing of the overhang deck forms
- ➢ Potential for uplift at bearings

The analysis of the deck staging is performed in an incremental manner using a concrete modulus of elasticity equal to 70% of the concrete modulus of elasticity at 28 days for concrete which is at least 24 days old. Therefore, the stiffnesses used in the model will change with each deck stage.

It is common practice to leave a block-out in the deck to facilitate proper placement and alignment of the deck joints after the dead load deflections have occurred.

The deck in the positive moment regions are generally placed before the deck in the negative moment regions. This sequence minimizes the potential for tensile stresses and cracking in the deck in the negative moment regions.

For prestressed concrete bridges made continuous for live load, the deck staging is frequently as follows:

1. Place intermediate diaphragms and shear blocks between beams, and place end diaphragms at abutments.
2. Place slab in positive moment regions.
3. Place continuity diaphragms at piers.
4. Place slab in negative moment regions.
5. Place barriers in the positive moment region and then in the negative moment region (unless continuous placement can be maintained).

A sample deck placement sequence plan is presented in Figure 7.21.
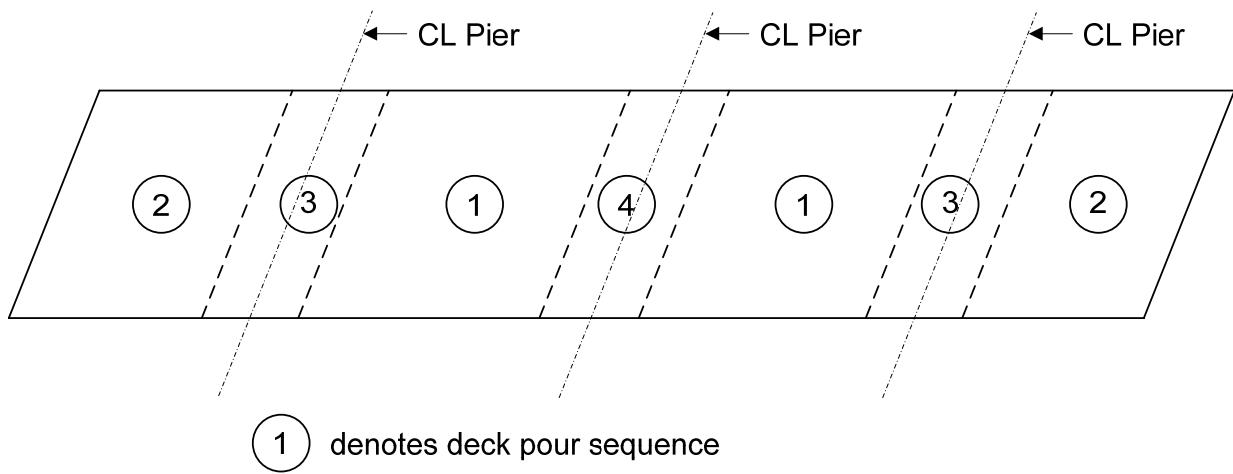
Figure 7.21 Sample Deck Placement Sequence Plan

7.4 Design of Bridge Railing

Many different railings are used on our nation's bridges today. The bridge engineer usually does not need to design the railings for a bridge. Instead the railings are selected from a set of crashed-tested and approved railings.

NCHRP Report 350, "Recommended Procedures for the Safety Performance Evaluation of Highway Features," was published in 1993 and presents uniform guidelines for the crash testing of both permanent and temporary highway safety features and recommended evaluation criteria to assess the test results. Performance is evaluated in terms of several parameters:

> ➤ Degree of hazard to which occupants of the impacting vehicle would be exposed
> ➤ Degree of hazard to workers and pedestrians who may be behind the barrier
> ➤ Structural adequacy of the barrier
> ➤ Behavior of the vehicle after impact

With the guidelines provided in NCHRP 350, a given railing or barrier may be tested to one of six test levels. A test level is defined by the impact speed, the impact angle of approach, and the type of test vehicle. Bridge barriers designed and tested to satisfy Test Level 1 are generally used on low service level roadways, such as rural connectors, local roads, or restricted work zones. Barriers designed and tested to satisfy Test Level 6, however, are usually used on high service level roadways, such as freeways and major highways. To illustrate the six test levels, Table 7.8 contains testing information used for each level.

Table 7.8 Test Matrix for Barriers

Test Level	Impact Conditions		
	Heaviest Vehicle Used	Nominal Speed	Nominal Impact Angle
TL-1	2000P (Pickup Truck)	50 km/hr	25°
TL-2	2000P (Pickup Truck)	70 km/hr	25°
TL-3	2000P (Pickup Truck)	100 km/hr	25°
TL-4	8000S (Single-unit Van Truck)	80 km/hr	15°
TL-5	36000V (Tractor/Van Trailor)	80 km/hr	15°
TL-6	36000T (Tractor/Tank Trailor)	80 km/hr	25°

Table 7.8 shows that, as the test level increases, either the heaviest test vehicle size increases or the nominal impact speed increases if the same vehicle is being used.

To be approved for use on a bridge, a barrier must satisfy three phases:

1. Research and development – the design evolves and is eventually subjected to a set of crash tests, which are assessed based on a set of evaluation criteria.
2. Experimental – the in-service performance of the experimental barrier is closely monitored.
3. Operational – the in-service performance of the approved barrier continues to be monitored.

When a barrier satisfies these three phases, it is approved to resist a set of design forces, as presented in Table 7.9. Just as Table 7.8 shows that a higher test level can resist a heavier test vehicle or a greater impact speed, Table 7.9 shows that a higher test level can resist greater design forces. The variables and designations used in Table 7.9 are defined in *AASHTO LRFD* Article 13.3 and are illustrated in *AASHTO LRFD* Figure A13.2-1.

Table 7.9 Design Forces for Traffic Railings
(Based on *AASHTO LRFD* Table A13.2-1)

Design Forces and Designations	Railing Test Level					
	TL-1	TL-2	TL-3	TL-4	TL-5	TL-6
F_t Transverse (kips)	13.5	27.0	54.0	54.0	124.0	175.0
F_L Longitudinal (kips)	4.5	9.0	18.0	18.0	41.0	58.0
F_v Vertical (kips) Down	4.5	4.5	4.5	18.0	80.0	80.0
L_t and L_L (feet)	4.0	4.0	4.0	3.5	8.0	8.0
L_v (feet)	18.0	18.0	18.0	18.0	40.0	40.0
H_e (min.) (inches)	18.0	20.0	24.0	32.0	42.0	56.0
Minimum H Height of Rail (inches)	27.0	27.0	27.0	32.0	42.0	90.0

Example:

The Typical Concrete Barrier, shown in Figure 7.22, has been tested and approved for Test Level 5.

Concrete strength, f'$_c$ = 4 ksi
Reinforcing steel strength, f$_y$ = 60 ksi
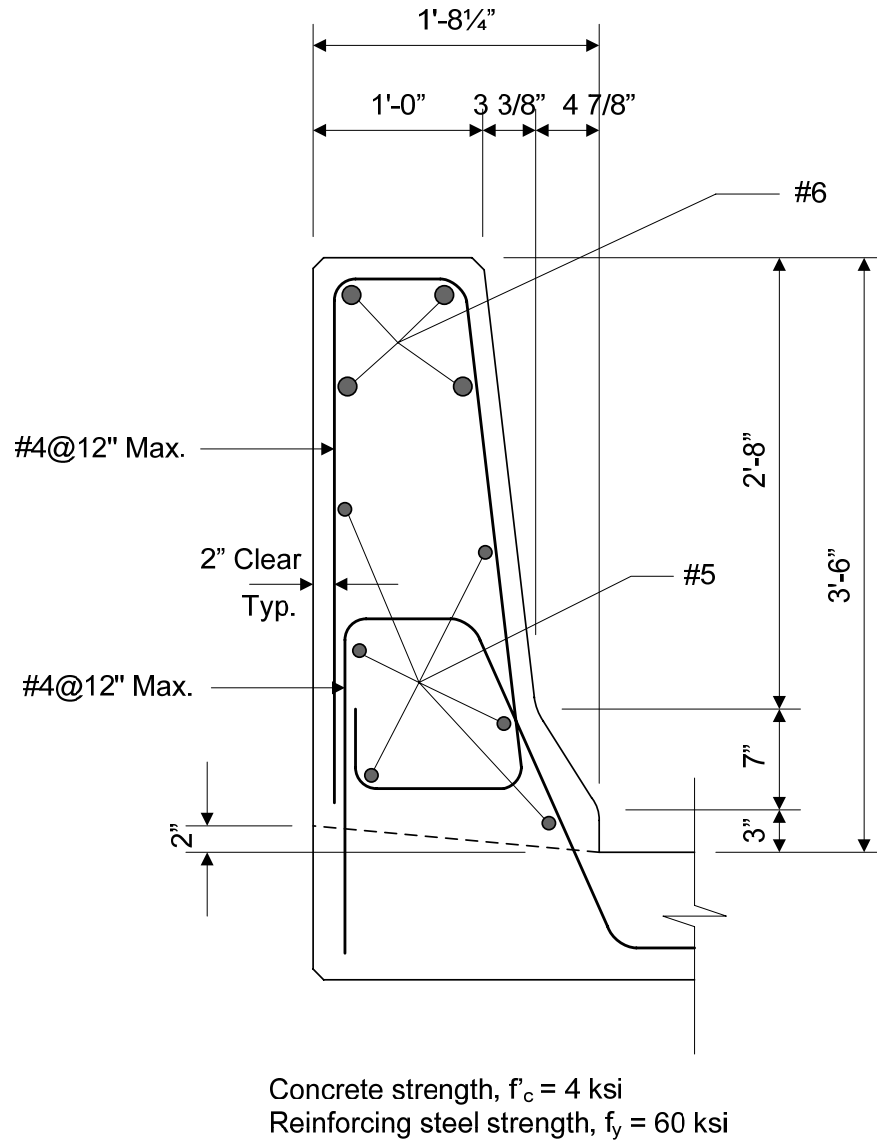
Figure 7.22 Typical Concrete Barrier, Approved for Test Level 5

Similarly, the Alternate Concrete Barrier, shown in Figure 7.23, has been tested and approved for Test Level 4.

Concrete strength, f'$_c$ = 4 ksi
Reinforcing steel strength, f$_y$ = 60 ksi
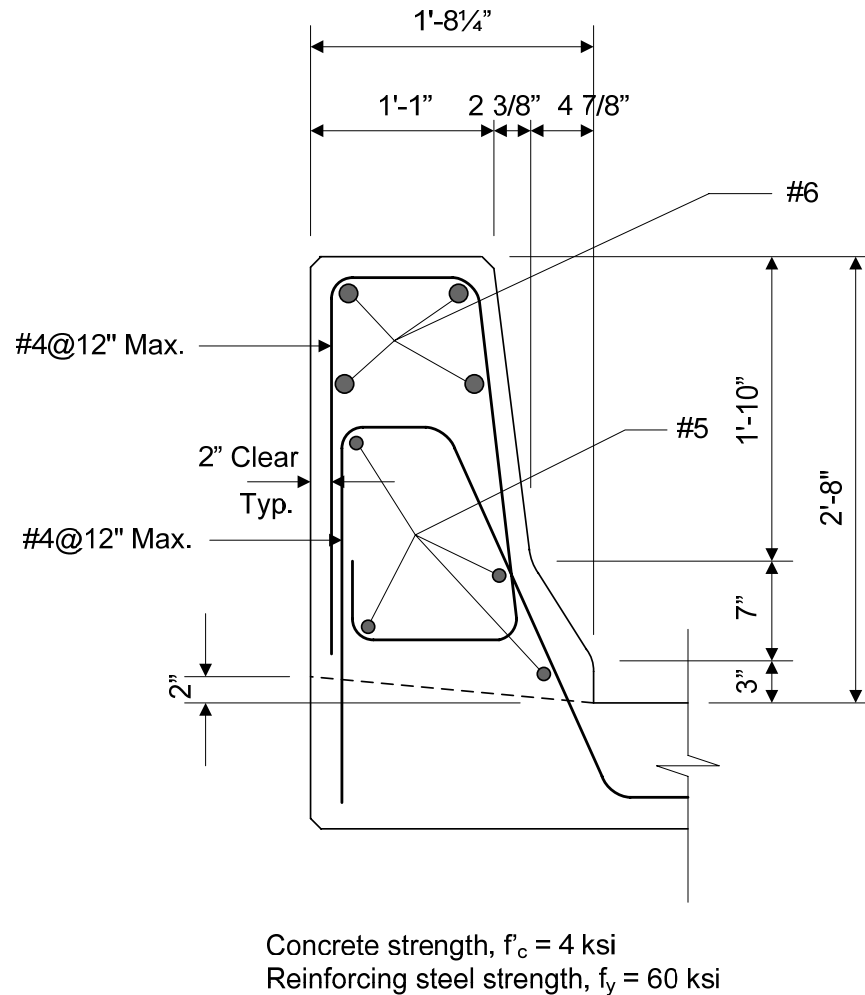
Figure 7.23 Alternate Concrete Barrier, Approved for Test Level 4

Several observations can be made from these two barrier examples. First, the two barriers are similar, but the Typical Concrete Barrier, which is 3'-6" high, is approved for Test Level 5, while the Alternate Concrete Barrier, which is only 2'-8" high, is only approved for Test Level 4. It is intuitive that for similar barriers, the taller barrier can be utilized for higher service level roadways.

Second, the approved barrier details define more than just the barrier shape. They also define all dimensions of the barrier, all reinforcing steel required in the barrier, the required reinforcement clear distance, and the required concrete and reinforcing steel strengths. If these barriers are utilized on a bridge, each of these requirements must be fully satisfied.

Third, the barrier has been approved for a specific test level and therefore satisfies specific performance characteristics. However, the test level does not necessarily define a specific barrier application. That determination rests with the appropriate transportation agency responsible for the bridge.

Finally, the engineer does not necessarily need to perform any barrier design. Instead, they select a barrier that has been tested and approved for the specific test level required by the governing agency for that particular bridge location. However, for a concrete barrier, sample design computations are presented in Section 7.3.4 of this chapter. The values computed in Section 7.3.4 are required for the design of the overhang portion of the deck.

7.5 Metal Decks

Future Development

7.6 Other Decks (Timber, Aluminum, FRP, etc.)

Future Development

7.7 Deck Connections to the Superstructure

Future Development

7.8 Deck Detailing

Future Development

Volume 1
General Design Considerations

Chapter 8
Bearing Selection and Design

8.1 Introduction

Bearings are located between the superstructure and the substructure of a bridge. They transmit loads from the superstructure to the substructure while also facilitating translations and/or rotations. This topic describes the process for selecting the optimum bearing, as well as the design process for the selected bearing.

8.2 Design Criteria

Bearing selection and design generally involves three basic steps:

1. Obtain the required design input.
2. Select the most feasible bearing type.
3. Design the most feasible bearing type.

The first step is to obtain the required design input. The bearing design input generally depends on whether the bearing is fixed or expansion. The function and capabilities of fixed and expansion bearings are illustrated in Figure 8.1 and summarized in Table 8.1.

Figure 8.1 Fixed and Expansion Bearings

Table 8.1 Capabilities of Fixed and Expansion Bearings

Capabilities	Fixed Bearing	Expansion Bearing
Resists vertical force	Yes	Yes
Resists horizontal force	Yes	No
Facilitates vertical movement	No	No
Facilitates horizontal movement	No	Yes
Facilitates rotation	Yes	Yes

Bearings can be fixed in both the longitudinal and transverse directions, fixed in one direction and expansion in the other, or expansion in both directions.

When deciding which bearings are fixed and which are expansion on a bridge, several guidelines are commonly considered:

➢ The bearing layout for a bridge must be developed as a consistent system. Vertical movements are resisted by all bearings, horizontal movements are resisted by fixed bearings and facilitated in expansion bearings, and rotations are generally allowed to occur as freely as possible.

➢ For maintenance purposes, it is generally desirable to minimize the number of deck joints on a bridge, which can in turn affect the bearing layout.

➢ The bearing layout must facilitate the anticipated thermal movements, primarily in the longitudinal direction but also in the transverse direction for wide bridges.

- ➢ It is generally desirable for the superstructure to expand in the uphill direction wherever possible.
- ➢ If more than one substructure unit is fixed within a single superstructure unit, then forces will be induced into the fixed substructure units and must be considered during design.
- ➢ For curved bridges, the bearing layout can induce additional stresses into the superstructure, which must be considered during design.
- ➢ Forces are distributed to the bearings based on the superstructure analysis.

8.2.1 Loads

Bearings must be designed to resist the loads transferred from the superstructure to the substructure. The primary load is generally the vertical load, which is caused by dead load, vehicular live load, dynamic load allowance, pedestrian live load, and any other vertical loads which may be present. For some bearings, a minimum vertical load is specified in addition to a maximum vertical load.

In addition, fixed bearings must also resist horizontal loads in the direction of fixity. Horizontal loads can be caused by wind load on structure, wind on live load, uniform temperature, vehicular braking force, vehicular centrifugal force, earthquake, and any other horizontal loads which may be present.

It is important to note that expansion bearings do not resist horizontal loads in the direction of expansion. For example, if a bearing facilitates expansion in the longitudinal direction, then that bearing will not resist longitudinal loads. Similarly, if a bearing facilitates expansion in the transverse direction, then it will not resist transverse loads. Horizontal loads are generally applied only to fixed bearings.

A schematic showing the various loads acting on a bearing is presented in Figure 8.2.
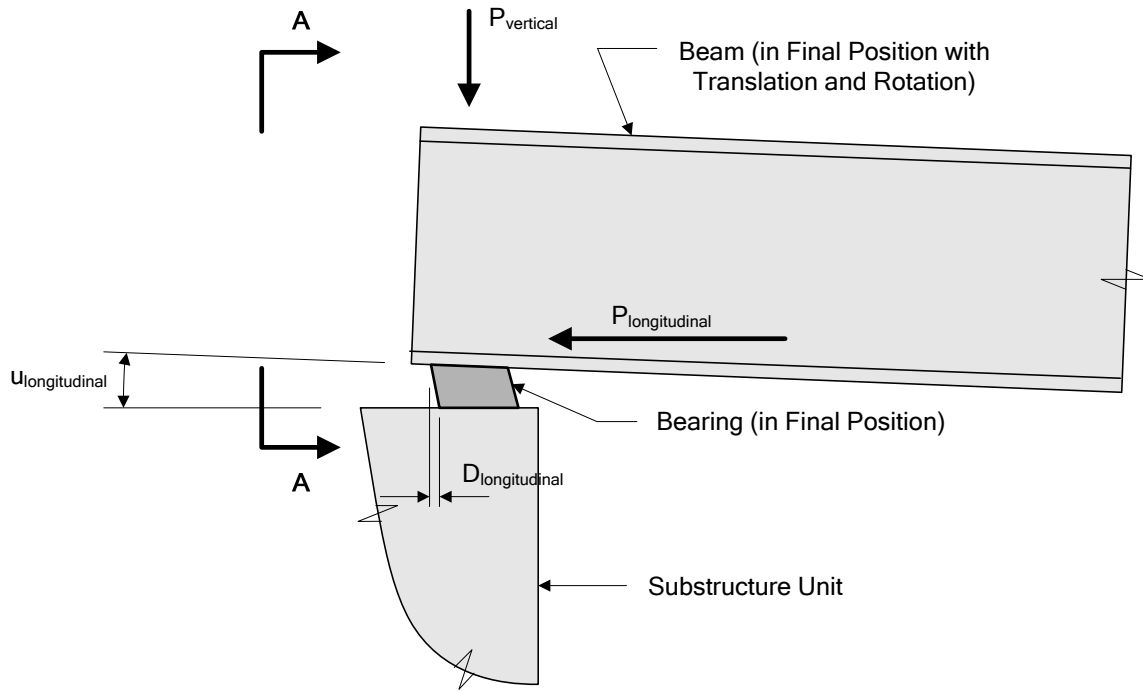
Elevation
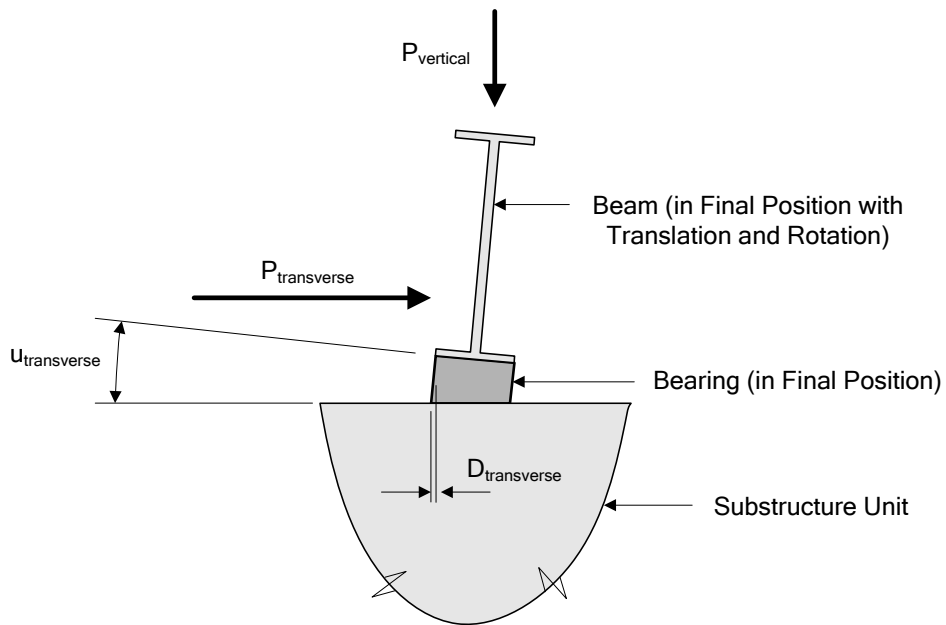
View A-A

Figure 8.2 Bearing Loads and Moments

8.2.2 Translation

In addition to resisting loads, a bearing must also facilitate translation in the girders or beams that are being supported. For example, if the superstructure lengthens due to temperature rise or shortens due to temperature fall, then the bearings must be designed to facilitate this longitudinal translation. Although translation is usually greatest in the longitudinal direction, translation in the transverse direction can also be significant, especially on wide, curved, or skewed bridges.

Fixed bearings are designed such that no translation is permitted in the direction of fixity. Expansion bearings are designed to facilitate the anticipated translation in the direction of expansion.

Bearing translation is illustrated in Figure 8.2.

8.2.3 Rotation

A bearing must also facilitate rotation in the girders or beams that are being supported. For example, if a girder deflects due to dead load or live load, then this deflection will cause the end of the girder to rotate in the longitudinal direction (about the transverse axis of the bridge). Similarly, for a curved bridge, the torsional effects in the girders may cause the end of the girder to rotate in the transverse direction (about the longitudinal axis of the bridge). The bearing must be designed to facilitate these anticipated rotations.

Bearing rotation is also illustrated in Figure 8.2.

8.3 Types of Bearings

There are many different types of bearings, and each one has its own unique applications, based on the magnitude of the loads, translations, and rotations about the various axes of the bridge. Some of the most common bearing types are presented in Table 8.2, along with a general description of the bearing.

Table 8.2 Bearing Type Descriptions

Bearing Type	General Description
Bronze bearing	A bearing in which displacements or rotations take place by the sliding of a bronze surface against a mating surface.
Cotton-duck-reinforced pad (CDP)	A pad made from closely spaced layers of elastomer and cotton-duck, bonded together during vulcanization.
Disc bearing	A bearing that accommodates rotation by deformation of a single elastomeric disc molded from a urethane compound. It may be movable, guided, unguided, or fixed. Movement is accommodated by sliding of polished stainless steel on PTFE.
Double cylindrical bearing	A bearing made from two cylindrical bearings placed on top of each other with their axes at right angles to facilitate rotation about any horizontal axis.
Fiberglass-reinforced pad (FGP)	A pad made from discrete layers of elastomer and woven fiberglass bonded together during vulcanization.
Knuckle bearing	A bearing in which a concave metal surface rocks on a convex metal surface to provide rotation capability about any horizontal axis.
Metal rocker or roller bearing	A bearing that carries vertical load by direct contact between two metal surfaces and that accommodates movement by rocking or rolling of one surface with respect to the other.
Plain elastomeric pad (PEP)	A pad made exclusively of elastomer, which provides limited translation and rotation.
Pot bearing	A bearing that carries vertical load by compression of an elastomeric disc confined in a steel cylinder and that accommodates rotation by deformation of the disc.
PTFE sliding bearing	A bearing that carries vertical load through contact stresses between a PTFE sheet or woven fabric and its mating surface, and that permits movements by sliding of the PTFE over the mating surface.
Steel-reinforced elastomeric bearing	A bearing made from alternate laminates of steel and elastomer bonded together during vulcanization. Vertical loads are carried by compression of the elastomer. Movements parallel to the reinforcing layers and rotations are accommodated by deformation of the elastomer.

Five common bearing types are illustrated in Figure 8.3.

Low Friction
Sliding Surface

Cylindrical Bearing

Low Friction
Sliding Surface
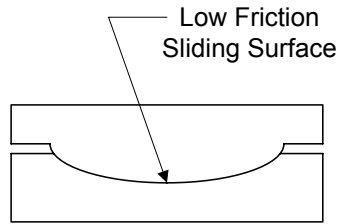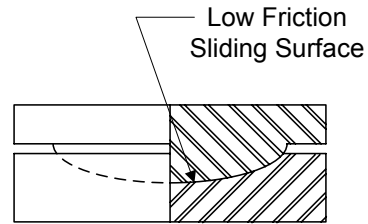
Spherical Bearing

Rocker Bearing

Elastomeric Disk — Piston

Pot

Pot Bearing

Rubber
Cover

Rubber Interior Layer — Reinforcement
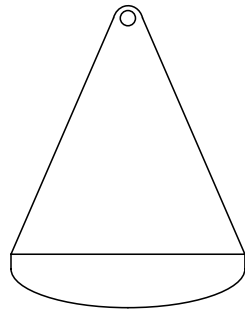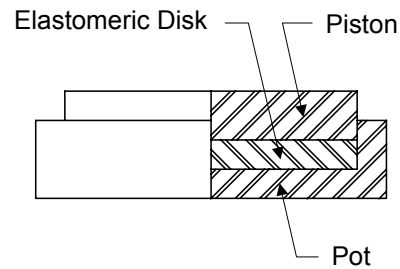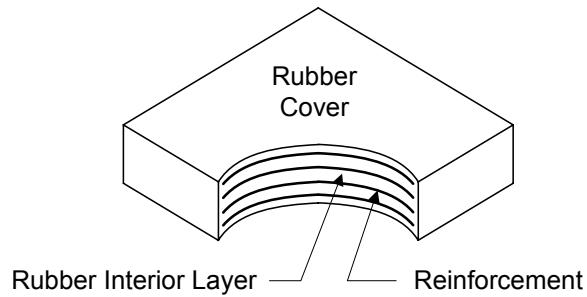
Elastomeric Bearing

Figure 8.3 Common Bearing Types
(Based on *AASHTO LRFD* Figure 14.6.2-1)

After the bearing layout for the entire bridge has been established and the bearing
design requirements have been defined, the second step is to select the most
feasible bearing type. Several tools are available to the bridge engineer to assist in
selecting feasible bearing types.

One such tool is presented in *AASHTO LRFD* Table 14.6.2-1, in which the suitability of various bearing types is presented in terms of movement, rotation, and resistance to loads. This information is presented in Table 8.3.

Table 8.3 Bearing Suitability
(Based on *AASHTO LRFD* Table 14.6.2-1)

Type of Bearing	Movement		Rotation about Bridge Axis Indicated			Resistance to Loads		
	Long.	Trans.	Long.	Trans.	Vert.	Long.	Trans.	Vert.
Plain elastomeric pad	S	S	S	S	L	L	L	L
Fiberglass-reinforced pad	S	S	S	S	L	L	L	L
Cotton-duck-reinforced pad	U	U	U	U	U	L	L	S
Steel-reinforced elastomeric bearing	S	S	S	S	L	L	L	S
Plane sliding bearing	S	S	U	U	S	R	R	S
Curved sliding spherical bearing	R	R	S	S	S	R	R	S
Curved sliding cylindrical bearing	R	R	U	S	U	R	R	S
Disc bearing	R	R	S	S	L	S	S	S
Double cylindrical bearing	R	R	S	S	U	R	R	S
Pot bearing	R	R	S	S	L	S	S	S
Rocker bearing	S	U	U	S	U	R	R	S
Knuckle pinned bearing	U	U	U	S	U	S	R	S
Single roller bearing	S	U	U	S	U	U	R	S
Multiple roller bearing	S	U	U	U	U	U	U	S

In the above table:

 ➢ S represents suitable
 ➢ U represents unsuitable
 ➢ L represents suitable for limited applications
 ➢ R represents may be suitable but requires special considerations or additional elements such as sliders or guideways

8.3.1 Bearing Suitability Design Example:

Consider a bearing in which large vertical loads (approximately 1750 kips) must be resisted and rotation must be facilitated about all three axes. According to Table 8.3, only four bearing types may be suitable – steel-reinforced elastomeric bearings, curved sliding spherical bearings, disc bearings, and pot bearings. For this design example, these four bearing types would need to be evaluated further.

Another valuable tool is presented in the American Iron and Steel Institute's (AISI) *Steel Bridge Bearing Selection and Design Guide*, Table I-A. This table not only

presents load, translation, and rotation capabilities of each bearing type, but it also presents information about initial costs and maintenance costs. This information is presented in Table 8.4.

Table 8.4 Summary of Bearing Capabilities
(Based on AISI's *Steel Bridge Bearing Selection and Design Guide*, Table I-A)

Bearing Type	Load (Kips)		Translation (Inches)		Rotation (Radians)	Costs	
	Min.	Max.	Min.	Max.	Limit	Initial	Maintenance
Plain elastomeric pads	0	100	0	0.6	0.01	Low	Low
Cotton duck elastomeric pads	0	315	0	0.2	0.003	Low	Low
Fiberglass elastomeric pads	0	135	0	1	0.015	Low	Low
Steel-reinforced elastomeric pads	50	780	0	4	0.04	Low	Low
Flat PTFE slider	0	>2250	1	>4	0	Low	Moderate
Curved lubricated bronze	0	1570	0	0	>0.04	Moderate	Moderate
Pot bearing	270	2250	0	0	0.02	Moderate	High
Pin bearing	270	1000	0	0	>0.04	Moderate	High
Rocker bearing	0	400	0	4	>0.04	Moderate	High
Single roller	0	100	1	>4	>0.04	Moderate	High
Curved PTFE	270	1570	0	0	>0.04	High	Moderate
Multiple rollers	110	2250	4	>4	>0.04	High	High

8.3.2 Bearing Capabilities Design Example:

Referring to the bearing requirements from the previous design example, in which vertical loads of approximately 1750 kips must be resisted and rotation must be facilitated, Table 8.4 provides two bearings types which may be suitable – pot bearings and multiple rollers. However, according to Table 8.4, pot bearings have a moderate initial cost and a high maintenance cost, whereas multiple rollers have a high initial cost and a high maintenance cost. In addition, multiple rollers may not facilitate rotation about all three axes. Therefore, based on Table 8.4, pot bearings may be the most feasible bearing type for this specific design application.

Another valuable tool from AISI's *Steel Bridge Bearing Selection and Design Guide* is a set of three preliminary bearing selection diagrams. Separate diagrams are presented for each of the following rotation requirements:

➢ Minimal design rotation (rotation ≤ 0.005 radians)
➢ Moderate design rotation (rotation ≤ 0.015 radians)
➢ Large design rotation (rotation > 0.015 radians)

These three diagrams are presented below in Figure 8.4, Figure 8.5, and Figure 8.6. In each diagram, the limit lines which define the regions are approximate and could be moved approximately 5% in either direction. Therefore, if a specific bearing application falls near a limit line, the engineer should investigate both bearing types.
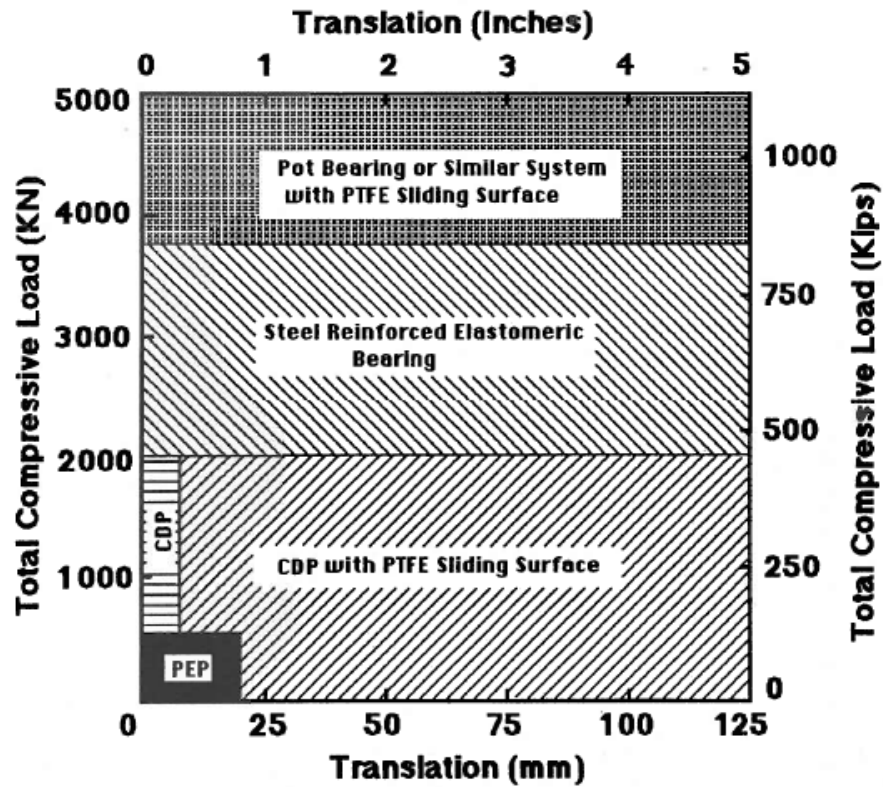
Figure 8.4 Preliminary Bearing Selection Diagram for Minimal Design Rotation (Rotation ≤ 0.005 Radians)
(From AISI's *Steel Bridge Bearing Selection and Design Guide*, Figure I-1)
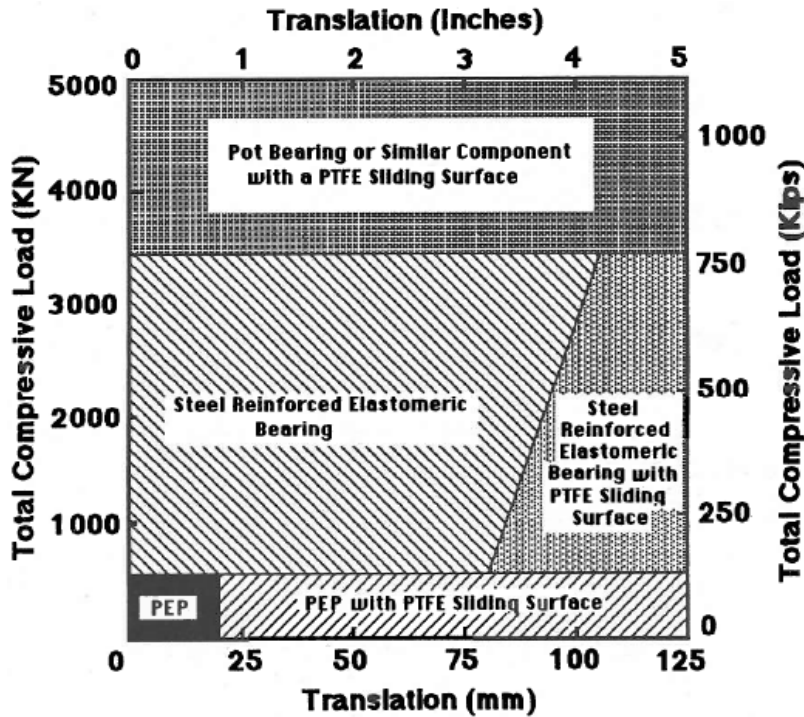
**Figure 8.5 Preliminary Bearing Selection Diagram for Moderate Design
Rotation (Rotation ≤ 0.015 Radians)
(From AISI's *Steel Bridge Bearing Selection and Design Guide*, Figure I-2)**
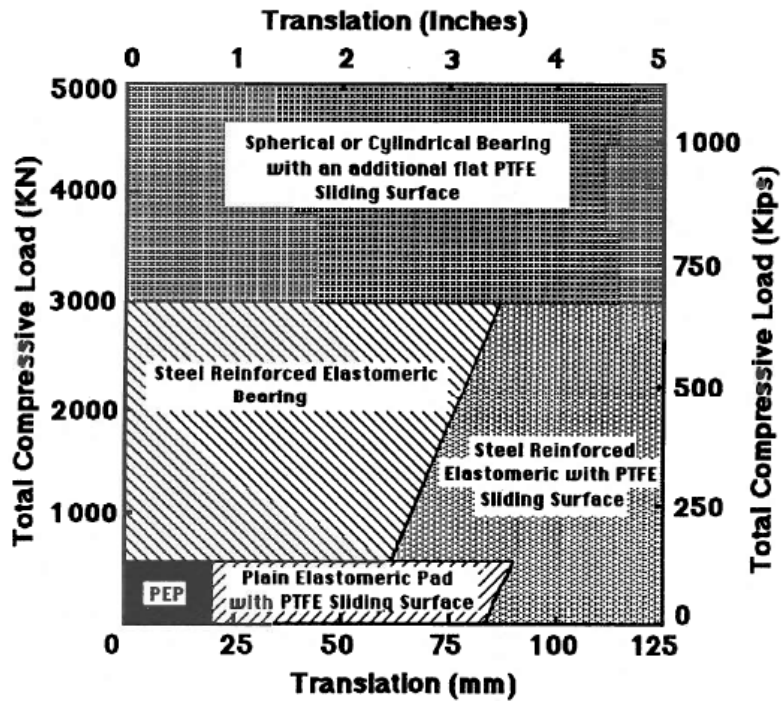
**Figure 8.6 Preliminary Bearing Selection Diagram for Large Design Rotation
(Rotation > 0.015 Radians)
(From AISI's *Steel Bridge Bearing Selection and Design Guide*, Figure I-3)**

8.3.3 Preliminary Bearing Selection Design Example:

Consider a bearing which must resist a vertical load of 740 kips, a translation of 1.25 inches, and a rotation of 0.010 radians. Since the rotation is less than 0.015 radians but greater than 0.005 radians, the diagram in Figure 8.5 applies to this bearing application. According the Figure 8.5, for a total compressive load of 740 kips and a translation of 1.25 inches, the preliminary bearing selection is steel reinforced elastomeric bearings. However, since the application falls near the limit line, pot bearings or similar components with a PTFE sliding surface should also be considered.

After defining the bearing design requirements and evaluating the feasible bearing types, the third basic step is to design the most feasible bearing type. There are several general design requirements that apply to all bearing types. Bearing movements and loads from the following sources must be considered during the design of virtually all bearing types:

➢ **Bridge skew** – skewed bridges move both longitudinally and transversely, with the transverse movement becoming more significant as the skew angle increases.

➢ **Bridge curvature** – curved bridges move both tangentially and radially, with the radial movement becoming more significant as the radius of curvature decreases.

➢ **Beam camber or curvature** – initial camber may cause a large initial bearing rotation, but this rotation may decrease as the bridge construction progresses.

➢ **Construction** – construction movements must be considered, although they have a short duration.

➢ **Misalignment or construction procedures** – construction loads and movements due to tolerances must also be considered.

➢ **Traffic loading** – bearing movements caused by traffic loading have not yet been well defined, but they can cause considerable wear to the bearing and are receiving increased recognition.

➢ **Thermal effects** – the magnitude of the thermal change in length, ΔL, is a function of the material properties, the temperature change, and the expansion length, as expressed in the following equation:

$$\Delta L = \alpha \, \Delta T \, L \qquad\qquad\qquad \text{Equation 8.1}$$

where:
ΔL	=	thermal change in length
α	=	coefficient of thermal expansion
ΔT	=	change in temperature
L	=	expansion length

Some general rules that should be followed during the design of virtually all bearing types are presented in Table 8.5.

Table 8.5 General Rules for Bearing Design

Observation	General Rule	Consequence of Ignoring Rule
LOAD COMBINATIONS – Some combinations of loads and movements are not possible.	Consider only feasible load and movement combinations, as specified in *AASHTO LRFD* Article 3.4.1.	Using unrealistic load combinations may result in a costly bearing which performs poorly.
LOAD DIRECTIONS – Loads do not necessarily all act in the same direction, and movements do not necessarily take place in the same direction.	Consider the directions of each loading component when computing load and movement combinations.	Adding the absolute values of all loads and movements may result in unrealistic conditions and uneconomical bearings.
INITIAL CONDITIONS – Temporary initial conditions can adversely affect the design of some bearings.	Consider adjusting the position of the bearing during the final stages of construction.	Designing the bearing to resist temporary initial conditions may result in an unnecessarily large and costly bearing.
PROTECTION – Bearings are typically located where dirt, debris, and moisture can collect.	Design and install the bearings to provide protection against the environment and to allow easy access for inspection.	Collection of dirt, debris, and moisture can lead to corrosion and deterioration of the bearing.
SERVICE LIFE – Due to severe demands on a bridge bearing, its service life is often less than that of other bridge components.	Provide allowances for bearing replacement (including space for lifting jacks and employment of appropriate details, such as jacking stiffeners).	Failure to provide jacking details may require expensive retrofits to provide sufficient jacking space and resistance.

The following descriptions and design requirements apply to specific bearing types. For additional details, refer to the appropriate sections of *AASHTO LRFD* Article 14.7.

8.3.4 Steel Bearings

Steel bearings come in a variety of shapes and sizes. For example sliding bearings consist of two surfaces, frequently one steel and one bronze, with lubrication between them, sliding against each other. Polytetrafluorethylene (PTFE) is often used for lubrication, and it provides favorable chemical resistance and a low coefficient of friction. Steel sliding bearings can be fabricated with flat surfaces to facilitate horizontal movement, or they can be fabricated with curved surfaces to facilitate both horizontal movement and rotation.

Rocker bearings are another type of steel bearings. In rocker bearings, a curved surface is generally placed on top of a flat surface. The two steel parts are

constrained by a dowel pin to prevent horizontal movement. Therefore, rocker bearings are generally used at fixed supports.

Another type of steel bearings is roller bearings, in which one or more steel cylinders is placed between two parallel steel plates. Since the rollers facilitate horizontal movement, roller bearings are generally used at expansion supports.

These steel bearing types are described in further detail in various sections of *AASHTO LRFD* Article 14.7.

8.3.5 Pot Bearings

Pot bearings are commonly used for moderate to large bridges. They carry vertical load by compression of an elastomeric disc contained in a steel cylinder and accommodate rotation by deformation of the disc. Pot bearings are generally used for applications requiring a multidirectional rotational capacity and a medium to large range of load.

The primary components of a pot bearing are illustrated in Figure 8.7. The schematic in Figure 8.7 shows a sample pot bearing, but it does not necessarily represent the exact configuration of all pot bearings.
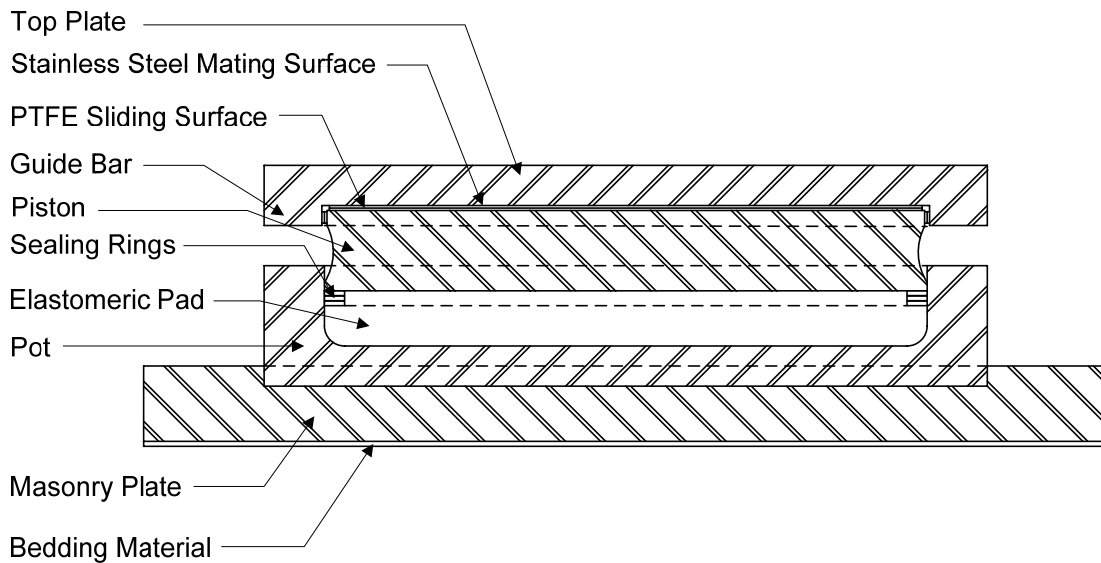
Figure 8.7 Components of a Pot Bearing

Pot bearings resist vertical load primarily through compressive stress in the elastomeric pad. The pad can deform and it has some shear stiffness, but it has very limited compressibility. Pot bearings generally have a large reserve of strength against vertical load.

Pot bearings facilitate rotation through deformation of the elastomeric pad. During rotation, one side of the pad compresses and the other side expands. Pot bearings can sustain many cycles of small rotations with little or no damage. However, pot

bearings can experience significant damage when subjected to relatively few cycles of large rotations.

Pot bearings can also resist horizontal loads. Pot bearings can either be fixed, guided, or non-guided. Fixed pot bearings can not translate in any direction, and they resist horizontal load primarily through contact between the rim of the piston and the wall of the pot. Guided pot bearings can translate in only one direction, and they resist horizontal load in the other direction through the use of guide bars. Non-guided bearings can translate in any direction, and they do not resist horizontal loads in any direction.

Although a pot bearing consists of many components (see Figure 8.7), only the elastomeric pad, sealing rings, pot, and piston require design computations. Therefore, there are a limited number of design steps:

1. Obtain required design input.
2. Select a feasible bearing type.
3. Select preliminary bearing properties.
4. Design the elastomeric pad.
5. Design the sealing rings.
6. Design the pot.
7. Design the piston.
8. Check the concrete or grout support.

These design steps are presented and illustrated through the following design example.

8.3.5.1 Pot Bearing Design Example

1. Obtain required design input

The required design input for this bearing design example is as follows:

Service limit state:
Total vertical load = 830 kips

Strength limit state:
Total vertical load = 1250 kips
Design rotation = 0.014 radians

Strength and extreme event limit states:
Total horizontal load = 70 kips

The minimum vertical load on a pot bearing should not be less than 20 percent of the vertical design load.

2. Select a feasible bearing type

To select a feasible bearing type, Figure 8.4, Figure 8.5, and Figure 8.6 may be used. Since the required service rotation is less than 0.014 radians, Figure 8.5 is applicable. For a total compressive load of 830 kips and a translation of 0 inches, the preliminary bearing selection diagram in Figure 8.5 shows that a pot bearing is a feasible bearing type for this application.

3. *Select preliminary bearing properties*

The next step is to select the preliminary bearing properties. These are obtained from the *AASHTO LRFD Bridge Design Specifications*, as well as from past experience. For this design, the following preliminary pot bearing properties were selected:

Maximum compressive stress on elastomer at service limit state = 3.5 ksi
Structural weathering steel: AASHTO M270 Grade 50
Pier cap concrete strength, f'_c = 4.0 ksi

4. *Design the elastomeric pad*

Pot bearings are generally designed for a compressive stress of 3.5 ksi on the elastomeric pad under total service load. The area of the elastomeric pad, as well as the pot, is controlled by this compressive stress requirement.

$$A_{pad} = \frac{830 \text{ kips}}{3.5 \text{ ksi}} = 237 \text{ inches}^2$$

$$D_p = \sqrt{\frac{4 \ A_{pad}}{\pi}} = \sqrt{\frac{4\left(237 \text{ inches}^2\right)}{\pi}} = 17.4 \text{ inches}$$

Therefore, use an 18-inch diameter elastomeric pad.

$$\sigma_s = \frac{830 \text{ kips}}{\left[\dfrac{\pi\left(18 \text{ inches}\right)^2}{4}\right]} = 3.26 \text{ ksi} < 3.5 \text{ ksi} \qquad \therefore \text{ OK}$$

Based on *AASHTO LRFD* Article 14.7.4.3, the depth of the elastomeric pad, h_r, must satisfy the following strain requirement:

$$h_r \geq 3.33 \ D_p \ \theta_u \qquad\qquad\qquad \text{Equation 8.2}$$

$$\textit{AASHTO LRFD} \text{ Equation 14.7.4.3-1}$$

where:
    D_p =   internal diameter of pot
    θ_u =   design rotation in radians

This equation limits the edge deflections due to rotation in the elastomeric pad to 15 percent of the nominal pad thickness. For this design example:

$$h_r \geq 3.33(18 \text{ inches})(0.014 \text{ radians}) = 0.84 \text{ inches}$$

Therefore, use an elastomeric pad depth, h_r, of 0.875 inches. In addition, the elastomeric pad should have a hardness between 50 and 60 Durometer, it should be lubricated (preferably with silicone grease), and it should provide a snug fit into the pot.

5. *Design the sealing rings*

Sealing rings provide a seal between the pot and the piston and can be provided in one of two configurations:

- ➢ Three rings with rectangular cross-sections
- ➢ One ring with circular cross-section

For three rings with rectangular cross-sections, the following geometric constraints are required:

$$\text{Width} \geq 0.02\,D_p \quad \text{and} \quad \text{Width} \geq 0.25 \text{ inches}$$

$$\text{Width} \leq 0.75 \text{ inches}$$

$$\text{Depth} \geq 0.2\,\text{Width}$$

For one ring with a circular cross-section, the cross-sectional diameter must satisfy the following equation:

$$\text{Diameter} \geq 0.0175\,D_p \quad \text{and} \quad \text{Diameter} \geq 0.15625 \text{ inches}$$

For this design example, three rings with rectangular cross-sections are being used. The width and depth of each ring are computed as follows:

$$\text{Width} \geq 0.02\,D_p = 0.02(18 \text{ inches}) = 0.36 \text{ inches}$$
$$\text{and} \quad \text{Width} \geq 0.25 \text{ inches}$$

$$\text{Width} \leq 0.75 \text{ inches}$$

Therefore, use a ring width of 0.4 inches.

$$\text{Depth} \geq 0.2\,\text{Width} = 0.2(0.4 \text{ inches}) = 0.08 \text{ inches}$$

Using a ring width of 0.4 inches and a ring depth of 0.08 inches, the total thickness of the three rings is 0.24 inches. This is less than one-third of the pad thickness

(0.875 inches / 3 = 0.292 inches), satisfying a common rule-of-thumb to control the concentration of elastomer strain at the rings.

6. *Design the pot*

The pot walls must be thick enough to resist both the internal hydrostatic pressure of the elastomeric pad and the pressure from any lateral loads. These two requirements are satisfied using the following two equations:

$$t_w \geq \frac{D_p\,\sigma_s}{1.25\,F_y} \quad \text{and} \quad t_w \geq 0.75 \text{ inches} \qquad \text{Equation 8.3}$$

AASHTO LRFD Equations 14.7.4.6-5 and 14.7.4.6-6

$$t_w \geq \sqrt{\frac{25\,H_u\,\theta_u}{F_y}} \qquad \text{Equation 8.4}$$

AASHTO LRFD Equation 14.7.4.7-1

where:

σ_s	=	service average compressive stress due to total load
F_y	=	yield strength of the steel
H_u	=	lateral load from applicable strength and extreme event load combinations
θ_u	=	design strength limit state rotation

For this design example,

$$t_w \geq \frac{D_p\,\sigma_s}{1.25\,F_y} = \frac{(18 \text{ inches})(3.26 \text{ ksi})}{1.25\,(50 \text{ ksi})} = 0.94 \text{ inches}$$

$$\text{and} \quad t_w \geq 0.75 \text{ inches}$$

$$t_w \geq \sqrt{\frac{25\,H_u\,\theta_u}{F_y}} = \sqrt{\frac{25\,(70 \text{ kips})\,(0.014 \text{ radians})}{50 \text{ ksi}}} = 0.70 \text{ inches}$$

Therefore, for this design example, use a pot wall thickness of 1 inch.

Since the pot base must be thick enough to resist the moments from the cantilever bending of the walls, the lateral load equation for the pot wall also applies to the pot base:

$$t_b \geq \sqrt{\frac{25\,H_u\,\theta_u}{F_y}}$$

In addition, for a pot base that bears directly against concrete or grout:

$$t_b \geq 0.06 \, D_p \quad \text{and} \quad t_b \geq 0.75 \text{ inches}$$

For a pot base that bears directly on steel girders or load distribution plates:

$$t_b \geq 0.04 \, D_p \quad \text{and} \quad t_b \geq 0.50 \text{ inches}$$

For this design example, assuming that the pot base bears directly on load distribution plates:

$$t_b \geq \sqrt{\frac{25 \, H_u \, \theta_u}{F_y}} = \sqrt{\frac{25 \, (70 \text{ kips}) \, (0.014 \text{ radians})}{50 \text{ ksi}}} = 0.70 \text{ inches}$$

$$t_b \geq 0.04 \, D_p = 0.04 \, (18 \text{ inches}) = 0.72 \text{ inches}$$
$$\text{and} \quad t_b \geq 0.50 \text{ inches}$$

Therefore, for this design example, the pot wall thickness is 1 inch and the pot base thickness is 0.75 inches.

7. Design the piston

The piston must be thick enough to provide sufficient rigidity and strength. Therefore, the piston thickness must satisfy the following minimum requirement:

$$t_{piston} \geq 0.06 \, D_p$$

The height from the top of the rim to the underside of the piston, h_w, must satisfy all three of the following requirements:

$$h_w \geq \frac{1.5 \, H_u}{D_p \, F_y} \quad \text{and} \quad h_w \geq 0.125 \text{ inches} \quad \text{and} \quad h_w \geq 0.03 \, D_p \qquad \text{Equation 8.5}$$
AASHTO LRFD Equations 14.7.4.7-2 and 14.7.4.7-3 and 14.7.4.7-4

Finally, the clearance, c, between the inside diameter of the pot and the diameter of the piston rim must satisfy the following requirements:

$$c \geq \theta_u \left(h_w - \frac{D_p \, \theta_u}{2} \right) \quad \text{and} \quad c \geq 0.02 \text{ inches} \qquad \text{Equation 8.6}$$

AASHTO LRFD Equation 14.7.4.7-5

For this design example:

$$t_{piston} \geq 0.06 \, D_p = 0.06(18 \text{ inches}) = 1.08 \text{ inches}$$
$$\therefore \text{Use } t_{piston} = 1.25 \text{ inches}$$

$$\frac{1.5\, H_u}{D_p\, F_y} = \frac{1.5(70\text{ kips})}{(18\text{ inches})(50\text{ ksi})} = 0.12 \text{ inches}$$

$$\text{and} \quad 0.03\, D_p = 0.03(18\text{ inches}) = 0.54 \text{ inches}$$

$$\therefore \text{Use } h_w = 0.54 \text{ inches}$$

$$c \geq \theta_u\left(h_w - \frac{D_p\, \theta_u}{2}\right)$$

$$= (0.014\text{ radians})\left[0.54\text{ inches} - \frac{(18\text{ inches})(0.014\text{ radians})}{2}\right]$$

$$= 0.0058 \text{ inches} \qquad \therefore \text{Use } c = 0.02 \text{ inches}$$

The PTFE must be designed and recessed based on the PTFE design criteria, and the piston thickness must take into account the PTFE recess requirements.

8.   *Check the concrete or grout support*

The masonry plate of a pot bearing is designed similarly to masonry plates for other applications. Assuming that confinement reinforcement is absent in the concrete, the concrete bearing must satisfy the following requirement:

$$P_r = \phi P_n = \phi\left[0.85 f'_c\, A_1 m\right] \qquad\qquad \text{Equation 8.7}$$
$$\textit{AASHTO LRFD} \text{ Equations 5.7.5-1 and 5.7.5-2}$$

For this design example, assuming a masonry plate measuring 28 inches by 28 inches and assuming that the modification factor, m, equals 1:

$$P_r = \phi P_n = \phi\left[0.85 f'_c\, A_1 m\right] = 0.70\left[0.85(4.0\text{ ksi})(28\text{ inches})^2(1)\right]$$
$$= 1866 \text{ kips} > 1250 \text{ kips} \qquad \therefore \text{OK}$$

The final pot bearing configuration for this design example is presented in Figure 8.8.
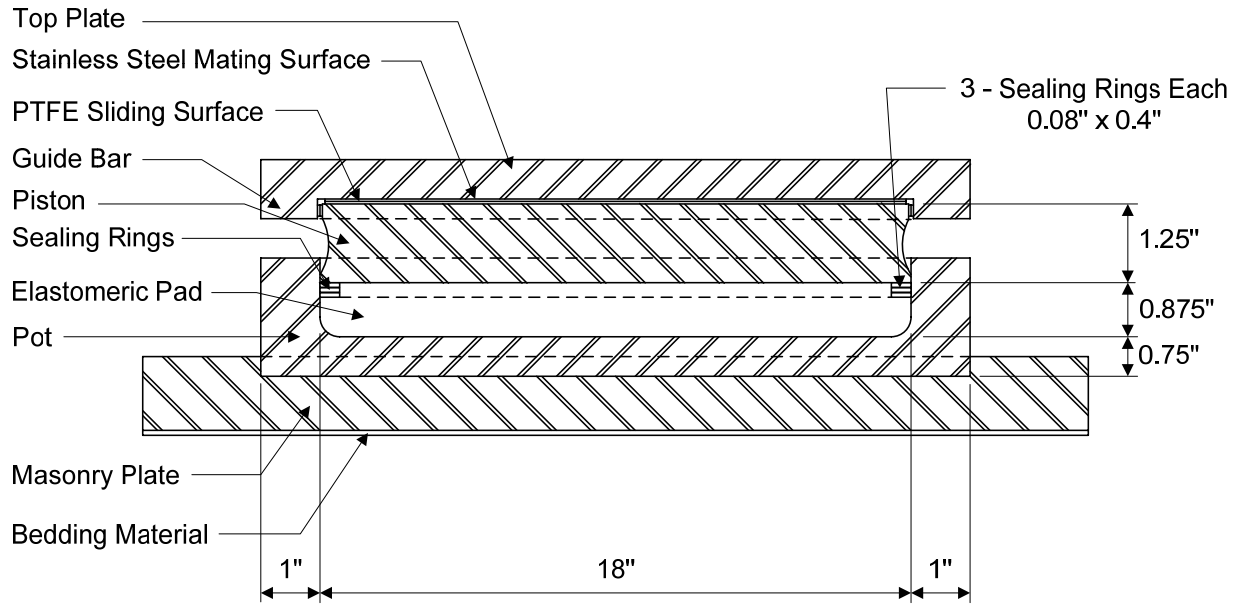
Figure 8.8 Final Configuration of Pot Bearing Design Example

8.3.6 Elastomeric Bearings

Elastomeric bearings are commonly used on small to moderate sized bridges. There are two general types of elastomeric bearings – plain and reinforced. As the name suggests, plain elastomeric pads consist entirely of elastomer, and they are usually rectangular in shape. Plain elastomeric pads can be used for small bridges, in which the vertical loads, translations, and rotations are relatively small.

Reinforced elastomeric pads are often used for larger bridges with more sizable vertical loads, translations, and rotations. Reinforced elastomeric pads consist of multiple layers of elastomer bonded to layers of reinforcing material, such as steel plate, fiberglass, or cotton-duck. A sample reinforced elastomeric pad is illustrated in Figure 8.9.

Plan

Section A-A
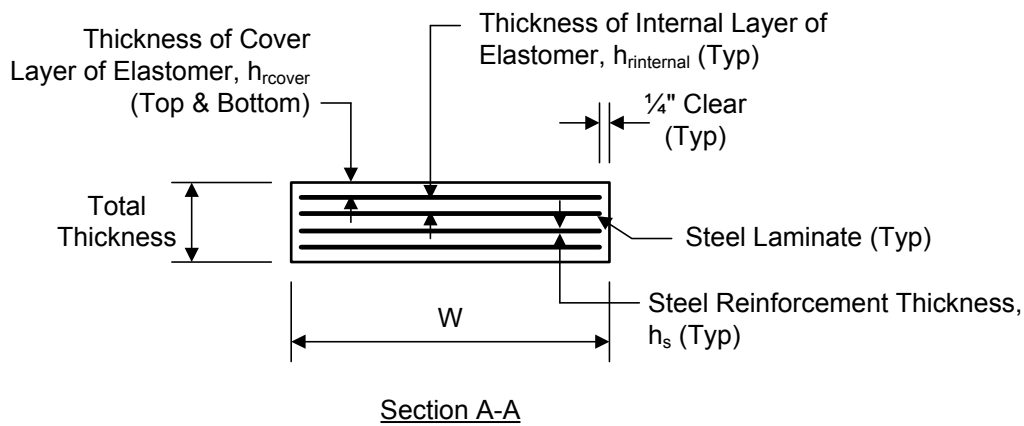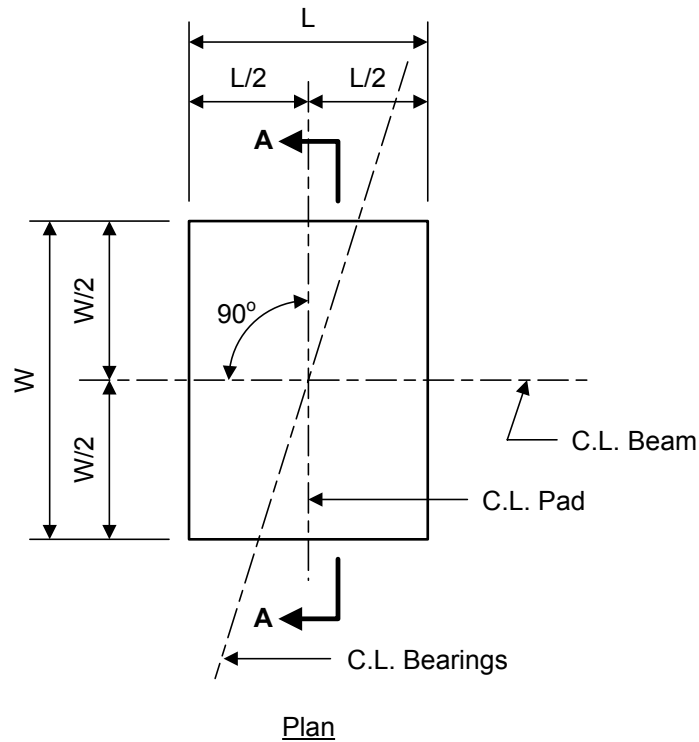
Figure 8.9 Reinforced Elastomeric Pad

There are two methods available for designing elastomeric bearings – Design Method A and Design Method B. Design Method A usually results in a bearing with a lower capacity than a bearing designed with Method B. However, Method B requires additional testing and quality control.

The design of an elastomeric bearing generally involves the following steps:

1.   Obtain required design input.
2.   Select a feasible bearing type.

3. Select preliminary bearing properties.
4. Select design method (Design Method A or B).
5. Compute shape factor.
6. Check compressive stress.
7. Check compressive deflection.
8. Check shear deformation.
9. Check rotation (Design Method A) or combined compression and rotation (Design Method B).
10. Check stability.
11. Check reinforcement.
12. Check anchorage (Design Method A) or design for seismic provisions (Design Method B).

8.3.6.1 Design Method A

For Design Method A, these design steps are presented and illustrated through the following design example for a steel-reinforced elastomeric pad at an abutment. The bearings are expansion only in the longitudinal direction; they are fixed in the transverse direction. The following requirements for Design Method A are further described in *AASHTO LRFD* Article 14.7.6.

1. Obtain required design input

The required design input for this bearing for the service limit state is as follows:

DL = 78.4 kips
LL+I = 110.4 kips
Design rotation = 0.007 radians
Design longitudinal translation = 0.76 inches
Minimum vertical force due to permanent load, P_{sd} = 67.8 kips

Therefore, the total service limit state vertical load is as follows:

DL + LL+I = 78.4 kips + 110.4 kips = 188.8 kips

The design requirements for the strength limit state are as follows:

Factored shear force = 8.6 kips

2. Select a feasible bearing type

To select a feasible bearing type, Figure 8.4, Figure 8.5, and Figure 8.6 may be used. Since the required rotation is 0.007 radians, Figure 8.5 is applicable. For a total compressive load of 188.8 kips and a translation of 0.76 inches, the preliminary bearing selection diagram in Figure 8.5 shows that steel-reinforced elastomeric bearings are a feasible bearing type.

3. *Select preliminary bearing properties*

The next step is to select the preliminary bearing properties. These are obtained from the *AASHTO LRFD Bridge Design Specifications*, as well as from past experience. For this design, the following preliminary bearing pad configuration was selected (see Figure 8.9 for illustration of terminology):

Pad length, L = 14 inches
Pad width, W = 15 inches
Elastomer cover thickness, h_{rcover} = 0.25 inches
Elastomer internal layer thickness, $h_{rinternal}$ = 0.375 inches
Number of steel reinforcement layers = 9
Steel reinforcement thickness, h_s = 0.1196 inches

In addition, the following material properties were selected:

Elastomer hardness = 50 (*AASHTO LRFD* Article 14.7.6.2)
Elastomer shear modulus, G = 0.095 ksi (*AASHTO LRFD* Table 14.7.5.2-1)
Elastomer creep deflection at 25 years divided by instantaneous deflection = 0.25 (*AASHTO LRFD* Table 14.7.5.2-1)
Steel reinforcement yield strength, F_y = 50 ksi
Steel reinforcement constant-amplitude fatigue threshold for Detail Category A, ΔF_{TH} = 24.0 ksi (*AASHTO LRFD* Table 6.6.1.2.5-3)

4. *Select design method (Design Method A or B)*

Since additional testing and quality control is not desired for this bridge, Design Method A is selected.

5. *Compute shape factor*

The next step is to compute the shape factor. The shape factor for individual elastomer layers is the plan area divided by the area of the perimeter free to bulge. For steel-reinforced elastomeric bearings, the following requirements must be satisfied before calculating the shape factor:

1. All internal layers of elastomer must be the same thickness.
2. The thickness of the cover layers cannot exceed 70 percent of the thickness of the internal layers.

For this design example, all internal layers are 0.375 inches thick. The thickness of the cover layers (0.25 inches) is 66.7 percent of the thickness of the internal layers (0.375 inches). Therefore, both of these requirements are satisfied.

For rectangular bearings without holes, the shape factor for the ith layer is:

$$S_i = \frac{L\ W}{2\ h_{ri}\ (L + W)} \qquad \text{Equation 8.8}$$

AASHTO LRFD Equation 14.7.5.1-1

For the internal layers of elastomer, the shape factor is computed as follows:

$$S_{internal} = \frac{(14 \text{ inches}) (15 \text{ inches})}{2 (0.375 \text{ inches}) (14 \text{ inches} + 15 \text{ inches})} = 9.66$$

For the cover layers of elastomer, the shape factor is computed as follows:

$$S_{cover} = \frac{(14 \text{ inches}) (15 \text{ inches})}{2 (0.25 \text{ inches}) (14 \text{ inches} + 15 \text{ inches})} = 14.48$$

6. *Check compressive stress*

For steel-reinforced elastomeric bearings, the compressive stress in the elastomer at the service limit state is limited by each of the following two equations, in which S is based on the thickest layer of the bearing:

$$\sigma_s \leq 1.0 \text{ ksi} \quad \text{and} \quad \sigma_s \leq 1.0 \, G \, S \qquad \qquad \text{Equation 8.9}$$
AASHTO LRFD Equation 14.7.5.3.2-4

For this bearing design,

$$\sigma_s = \frac{188.8 \text{ kips}}{(14 \text{ inches})(15 \text{ inches})} = 0.899 \text{ ksi} < 1.0 \text{ ksi} \qquad \therefore \text{ OK}$$

$$\sigma_s = 0.899 \text{ ksi} < 0.917 \text{ ksi} = 1.0(0.095 \text{ ksi})(9.66) = 1.0 \, G \, S \qquad \therefore \text{ OK}$$

Therefore, the compressive stress requirements are satisfied for this bearing.

7. *Check compressive deflection*

The instantaneous compressive deflection is obtained from the following equation:

$$\delta = \sum \varepsilon_i \, h_{ri} \qquad \qquad \text{Equation 8.10}$$
AASHTO LRFD Equation 14.7.5.3.3-1

where:
ε_i = instantaneous compressive strain in the ith elastomer layer
h_{ri} = thickness of the ith elastomeric layer

Since test results are not available for this design example, the instantaneous compressive strain can be approximated from *AASHTO LRFD* Figure C14.7.5.3.3-1. For 50 durometer reinforced bearings with a compressive stress of 0.899 ksi and shape factor of 9.66, the compressive strain is approximately 4.0%. For the cover layers, with a shape factor of 14.48, the compressive strain is approximately 3.3%. Therefore, the instantaneous deflection is computed as follows:

$$\delta = [2(0.25 \text{ inches})(0.033)] + [8(0.375 \text{ inches})(0.040)] = 0.137 \text{ inches}$$

In addition, the effects of creep should also be considered. For this design example, material-specific data is not available. As presented in the material properties, the elastomer creep deflection at 25 years divided by the instantaneous deflection equals 0.25 (*AASHTO LRFD* Table 14.7.5.2-1). Therefore, the total deflection value, which includes both the instantaneous deflection and the effects of creep, can be computed as follows:

$$\delta_{total} = \delta_{instantaneous} + \delta_{creep} = (0.137 \text{ inches})(1 + 0.25) = 0.171 \text{ inches}$$

The initial compressive deflection in any layer of a steel-reinforced elastomeric bearing at the service limit state without dynamic load allowance can not exceed $0.07 h_{ri}$. For this design example:

$$\delta_{internal} = \varepsilon_{internal} \, h_{rinternal} = (0.040)(0.375 \text{ inches}) = 0.015 \text{ inches}$$

$$0.07 \, h_{rinternal} = (0.07)(0.375 \text{ inches}) = 0.026 \text{ inches} > 0.015 \text{ inches} \qquad \therefore \text{ OK}$$

8. Check shear deformation

The shear deformation is checked to ensure that the bearing can facilitate the anticipated horizontal bridge movement. Also, the shear deformation is limited to avoid rollover at the edges and delamination due to fatigue. The total horizontal movement for this bridge design example is based on thermal effects only and is presented in the design requirements as 0.76 inches. Other criteria that could add to the shear deformation include construction tolerances, braking force, and longitudinal wind, if applicable. One factor that can reduce the amount of shear deformation is pier flexibility. For a steel-reinforced elastomeric bearing, the smaller of the total elastomer thickness or the bearing thickness must satisfy the following equation:

$$h_{rt} \geq 2 \, \Delta_s \qquad\qquad \text{Equation 8.11}$$
$$\text{AASHTO LRFD Equation 14.7.6.3.4-1}$$

In this example, this requirement is checked as follows:

$$h_{rt} = 2(0.25 \text{ inches}) + 8(0.375 \text{ inches}) = 3.50 \text{ inches}$$

$$2\Delta_s = 2(0.76 \text{ inches}) = 1.52 \text{ inches} < 3.50 \text{ inches} \qquad \therefore \text{ OK}$$

9. Check rotation

Rotation is checked to ensure that no point in the bearing experiences net uplift. The rotation about the transverse axis is checked as follows:

$$\sigma_s \geq 0.5\, G\, S \left(\frac{L}{h_{ri}} \right)^2 \left(\frac{\theta_{s,x}}{n} \right) \qquad\qquad \text{Equation 8.12}$$

AASHTO LRFD Equation 14.7.6.3.5d-1

Similarly, the rotation about the longitudinal axis is checked as follows:

$$\sigma_s \geq 0.5\, G\, S \left(\frac{W}{h_{ri}} \right)^2 \left(\frac{\theta_{s,z}}{n} \right) \qquad\qquad \text{Equation}$$

8.13
AASHTO LRFD Equation 14.7.6.3.5d-2

where:
   n   =   number of interior layers of elastomer that are bonded on each face

If the thickness of the elastomer cover layers is greater than one-half the thickness of the interior layers, then the value of n may be increased by ½ for each such cover layer. Therefore, for this design example:

$$n = ½ + 8 + ½ = 9$$

For this design example, the service rotation due to total load is about the transverse axis and is presented in the design requirements as 0.007 radians. For elastomeric pads and steel-reinforced elastomeric bearings, an additional rotation of 0.005 radians must be included as an allowance for uncertainties unless an approved quality control plan justifies a smaller value (as specified in *AASHTO LRFD* Article 14.4.2). Since this additional rotation of 0.005 radians must be added to the service rotation of 0.007 radians, the total rotation for this design example is 0.012 radians.

$$0.5\, G\, S \left(\frac{L}{h_{ri}} \right)^2 \left(\frac{\theta_{s,x}}{n} \right) = 0.5(0.095 \text{ ksi})(9.66) \left(\frac{14 \text{ inches}}{0.375 \text{ inches}} \right)^2 \left(\frac{0.012}{9} \right) = 0.853 \text{ ksi}$$

$$\sigma_s = 0.899 \text{ ksi} > 0.853 \text{ ksi} \qquad \therefore \text{ OK}$$

The service rotation due to the total load about the longitudinal axis is negligible compared to the service rotation about the transverse axis. Therefore, the rotation check about the longitudinal axis is not computed in this bearing design example.

10. *Check stability*

The total thickness of the rectangular pad must not exceed one-third of the pad length or one-third of the pad width, or expressed mathematically:

$$h_{total} \leq \frac{L}{3} \qquad \text{and} \qquad h_{total} \leq \frac{W}{3} \qquad\qquad \text{Equation 8.14}$$

AASHTO LRFD Article 14.7.6.3.6

For this design example:

$$h_{total} = 2(0.25 \text{ inches}) + 8(0.375 \text{ inches}) + 9(0.1196 \text{ inches})$$
$$= 4.5764 \text{ inches}$$

$$\frac{L}{3} = \frac{14 \text{ inches}}{3} = 4.67 \text{ inches} > 4.5764 \text{ inches} \qquad \therefore \text{OK}$$

$$\frac{W}{3} = \frac{15 \text{ inches}}{3} = 5.0 \text{ inches} > 4.5764 \text{ inches} \qquad \therefore \text{OK}$$

Therefore, the bearing pad satisfies the stability requirements.

11.   Check reinforcement

The steel reinforcement thickness must be able to sustain the tensile stresses induced by compression in the bearing.   The reinforcement thickness must also satisfy the requirements of the *AASHTO LRFD Bridge Construction Specifications*. For this design example, the thickness of the steel reinforcement, h_s, is 0.1196 inches.

For the service limit state:

$$h_s \geq \frac{3\, h_{max}\, \sigma_s}{F_y} \qquad\qquad \text{Equation 8.15}$$

$$\text{\textit{AASHTO LRFD} Equation 14.7.5.3.7-1}$$

$$h_s \geq \frac{3\, h_{max}\, \sigma_s}{F_y} = \frac{3(0.375 \text{ inches})(0.899 \text{ ksi})}{50 \text{ ksi}} = 0.0202 \text{ inches} \qquad \therefore \text{OK}$$

For the fatigue limit state:

$$h_s \geq \frac{2.0\, h_{max}\, \sigma_L}{\Delta F_{TH}} \qquad\qquad \text{Equation 8.16}$$

$$\text{\textit{AASHTO LRFD} Equation 14.7.5.3.7-2}$$

$$\sigma_L = \frac{110.4 \text{ kips}}{(14 \text{ inches})(15 \text{ inches})} = 0.526 \text{ ksi}$$

As presented in the material properties, the steel reinforcement constant-amplitude fatigue threshold for Detail Category A, ΔF_{TH}, is 24.0 ksi.

$$h_s \geq \frac{2.0\, h_{max}\, \sigma_L}{\Delta F_{TH}} = \frac{2.0(0.375 \text{ inches})(0.526 \text{ ksi})}{24.0 \text{ ksi}} = 0.0164 \text{ inches} \qquad \therefore \text{OK}$$

Therefore, the steel reinforcement thickness satisfies both the service limit state and fatigue limit state requirements.

12. Check anchorage

The bearing pad must be secured against horizontal movement if the factored shear force sustained by the deformed pad at the strength limit state exceeds one-fifth of the minimum vertical force due to permanent load, P_{sd}.

As previously defined, the minimum vertical force due to permanent load, P_{sd}, is 67.8 kips and the factored shear force at the strength limit state is 8.6 kips. The need for anchorage is checked as follows:

$$\frac{P_{sd}}{5} > V_{strength} \hspace{2cm} \text{Equation 8.17}$$

AASHTO LRFD Article 14.7.6.3.7

$$\frac{P_{sd}}{5} = \frac{67.8 \text{ kips}}{5} = 13.6 \text{ kips} > 8.6 \text{ kips} = V_{strength}$$

Therefore, for this design example, the bearing pad does not need to be secured against horizontal movement.

The abutment bearings are expansion in the longitudinal direction but fixed in the transverse direction. Therefore, the bearings must be restrained in the transverse direction. Based on the previous computation, the expansion bearing pad does not need to be secured against horizontal movement. However, the horizontal connection must satisfy the seismic requirements of *AASHTO LRFD* Article 3.10.9. This check will be described in a later section of this chapter.

A schematic showing a plan view and sectional view of the final elastomeric bearing configuration is presented in Figure 8.10.

Plan

Section A-A
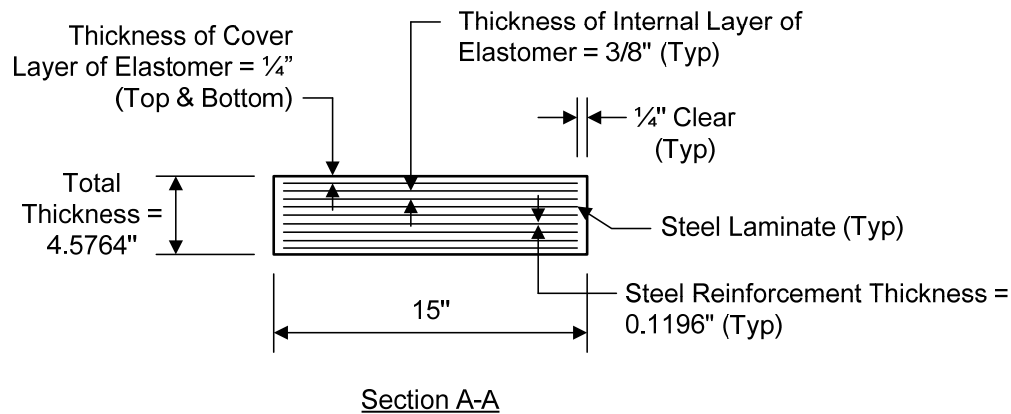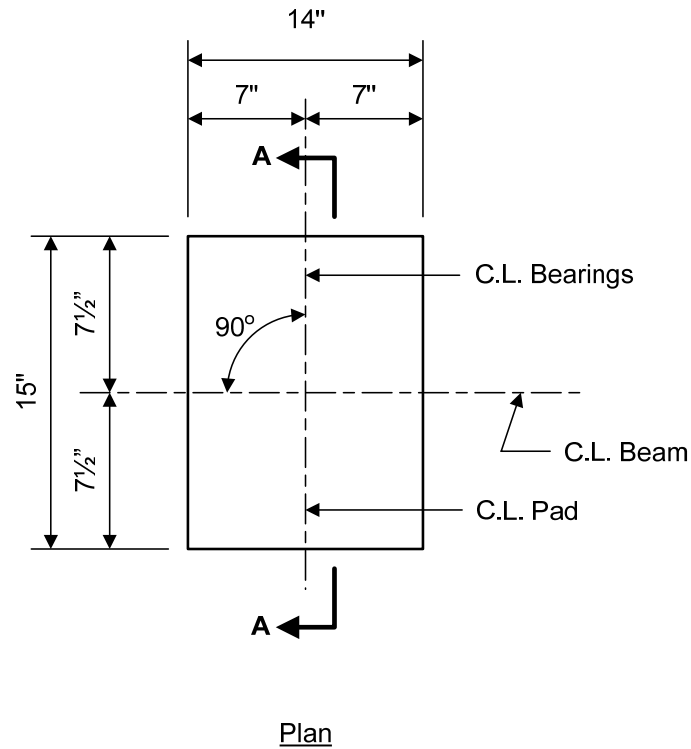
Figure 8.10 Final Configuration of Elastomeric Bearing Design Example

8.3.6.2 Design Method B

Many of the design procedures for Design Method B are similar to those of Design Method A. However, some primary differences between the two methods are summarized in Table 8.6.

Table 8.6 Elastomeric Bearing Design Methods A and B

Characteristic	Design Method A	Design Method B
Application	Applicable for plain elastomeric pads and steel-reinforced elastomeric bearings	Applicable for steel-reinforced elastomeric bearings only
AASHTO LRFD reference	*AASHTO LRFD* Article 14.7.6	*AASHTO LRFD* Article 14.7.5
Bearing capacity	Stress limits for Design Method A usually result in a bearing with a lower capacity than with Method B	Stress limits for Design Method B usually result in a bearing with a higher capacity than with Method A
Additional testing and quality control	Does not require additional testing and quality control	Requires additional testing and quality control
Design steps unique to that method	• Check rotation • Check anchorage	• Check combined compression and rotation • Design for seismic provisions

8.3.7 Disc Bearings

Disc bearings consist of an unconfined elastomeric disc. Disc bearings are more economical than many other steel bearing types, and they are frequently used when smaller load capacity is required. Disc bearings may be movable, guided, unguided, or fixed. Movement is accommodated by sliding of polished stainless steel on PTFE.

8.4 Bearing Anchorage

Bearings which are intended to be fixed in either the longitudinal or transverse direction must be designed for restraint in the direction of fixity. That is, if a bridge is designed such that the bearings at a specific substructure unit are fixed in one or both directions, then those bearings must be designed to provide restraint in those directions.

In addition to the requirements presented in previous sections of this chapter, *AASHTO LRFD* Article 3.10.9 provides additional bearing anchorage requirements. For example, assuming that the bridge in the previous elastomeric bearing design example is located in Seismic Zone 1, *AASHTO LRFD* Article 3.10.9.2 specifies that the horizontal design connection force in the restrained directions must be at least equal to 0.2 times the vertical reaction due to the tributary permanent load and the tributary live loads assumed to exist during an earthquake. This minimum design value is intended to relieve the engineer from a more rigorous analysis for bridges in parts of the country with very low seismicity.

For the previous elastomeric bearing design example, since all abutment bearings are restrained in the transverse direction, the tributary permanent load can be taken as the reaction at the bearing. Assuming that γ_{EQ} equals zero (see *AASHTO LRFD* Article 3.4.1), no tributary live load will be considered.

$$H_{EQ} = 0.2 \, DL \qquad\qquad \text{Equation 8.18}$$
$$H_{EQ} = 0.2 \, (78.4 \text{ kips}) = 15.7 \text{ kips}$$

For two 7/8" diameter A 307 bolts with a minimum tensile strength of 60 ksi, the factored shear resistance for threads excluded from the shear plane is computed as follows in accordance with *AASHTO LRFD* Article 6.13.2.7:

$$R_n = 0.48 A_b F_{ub} N_s \qquad\qquad \text{Equation 8.19}$$
$$\text{\textit{AASHTO LRFD} Equation 6.13.2.7-1}$$

$$R_n = 0.48 (2 \text{ bolts})(0.60 \text{ inches}^2/\text{bolt})(60 \text{ ksi})(1 \text{ shear plane/bolt})$$
$$= 34.6 \text{ kips}$$

$$R_r = \phi_s R_n \qquad\qquad \text{Equation 8.20}$$
$$\text{\textit{AASHTO LRFD} Equation 6.13.2.2-2}$$

$$R_r = (0.65)(34.6 \text{ kips}) = 22.5 \text{ kips} > 15.7 \text{ kips} \qquad \therefore \text{ OK}$$

After the anchor bolt size and quantity have been determined, the anchor bolt length must also be computed. As an approximation, the bearing stress may be assumed to vary linearly from zero at the end of the embedded length to its maximum value at the top surface of the concrete, in accordance with *AASHTO LRFD* Article 14.8.3.1. The bearing resistance of the concrete is based on *AASHTO LRFD* Article 5.7.5.

Assuming that the modification factor, m, equals 1, the bearing stress is computed as follows:

$$P_r = \phi_b P_n = \phi_b 0.85f'_c A_1 m \qquad\qquad \text{Equation 8.21}$$
$$\textit{AASHTO LRFD} \text{ Equations 5.7.5-1 and 5.7.5-2}$$

$$f_{brg} = \frac{P_r}{A_1} = \frac{\phi_b 0.85f'_c A_1 m}{A_1} = \phi_b 0.85f'_c m \qquad\qquad \text{Equation 8.22}$$

$$f_{brg} = (0.70)(0.85)(4.0 \text{ ksi})(1) = 2.38 \text{ ksi}$$

The total transverse horizontal force acting on each bolt is:

$$H_{EQ} / \text{bolt} = \frac{15.7 \text{ kips}}{2 \text{ bolts}} = 7.9 \text{ kips/bolt}$$

Using the linear bearing stress approximation from above, the required anchor bolt area resisting the transverse horizontal load can be calculated:

$$A_1 = \frac{H_{EQ}/\text{bolt}}{\dfrac{0 + f_{brg}}{2}} = \frac{7.9 \text{ kips/bolt}}{\dfrac{0 + 2.38 \text{ ksi}}{2}} = 6.6 \text{ inches}^2$$

A_1 is the product of the anchor bolt diameter and the anchor bolt length of embedment into the concrete pedestal or beam seat. Since the anchor bolt diameter is known, the required anchor bolt length can be computed as follows:

$$A_1 = (\text{Length}_{bolt})(\text{Diameter}_{bolt}) \qquad\qquad \text{Equation 8.23}$$

$$\text{Length}_{bolt} = \frac{A_1}{\text{Diameter}_{bolt}} = \frac{6.6 \text{ inches}^2}{0.875 \text{ inches}} = 7.6 \text{ inches} \qquad \text{Use 8 inches}$$

In addition to the above calculations, individual states and agencies may have their own bearing design and anchor bolt requirements.

This page intentionally left blank.

Volume 2
Steel Bridge Superstructure Design

Chapter 2
Steel Bridge Design

2.1 Introduction

This chapter provides an overview of the design process for steel-bridge superstructure components according to the *AASHTO LRFD* Specifications. Basic fundamental concepts related to the structural behavior of steel are reviewed to complement and expand on the specification commentary, and to aid in the understanding and implementation of the specification provisions in the design of various steel-bridge superstructure components at each limit state. Although the *AASHTO LRFD* design specifications are generally member and component based, the behavior of the entire steel-bridge system must also be considered in certain instances to ensure proper performance and overall stability, particularly during the various stages of construction, and proper behavior under the assumed loading.

2.2 Girder/Beam/Stringer Design

2.2.1 Composite Construction

2.2.1.1 Introduction

In general, the term composite construction refers to structural systems in which there is a structural interaction between materials having diverse engineering properties, such as steel and concrete or steel and timber. Technically, reinforced concrete, prestressed concrete and fiber-reinforced plastics are composites, but are not included under the rubric of composite construction.

In this treatise, composite construction means two components, steel and concrete, that are structurally connected. The earliest patents related to composite construction date to the 1880s and relate generally to what are called "concrete encased beams". The bond between the concrete and steel was realized to create the composite action. Engineers were aware of the composite behavior, particularly its increased stiffness, but generally did not take full advantage of its additional strength. Steel beams fully encased in concrete were widely used in building design from the early 1900s until the development of lightweight materials for fire protection after WWII.

Viest et al (*1*) site the first patent relating to composite highway bridges to J. Kahn in 1926. In Australia, a paper by Knight (*2*) on composite slab and steel-girder bridges dating to 1934 discusses the design of shear connectors, the effect of varying the modular ratio on the composite section properties, the propping of main girders and the prestressing of steel girders by upward cambering. The Germans expressed an interest in composite construction and even published a code of standard practice due to the pressures of a steel shortage immediately following World War II, which forced engineers to use the most economical design methods available to cope with the large number of structures that had to be reconstructed following the war. Interestingly, the German bridges built by propping were not found to be successful. The concrete crept to such an extent that after a few months, the negative moment applied to the composite section by releasing the props was resisted almost entirely by the steel section.

In the U.S., the first AASHO bridge-design code in 1944 contained an approved method for the design of composite girders. With its publication, official recognition was given to this method of construction for highway bridges and an increasing number of composite highway bridges were built in the U.S. However, only simple spans were addressed in the AASHO code for a number of years and concurrent research indicated that there were a number of issues that needed to be addressed. Modern procedures for the design of composite steel bridges can be traced back to the 1957 edition of the AASHO Bridge Specifications. Viest (*3*) in a 1960 review of research on composite girders noted that that a critical factor in ensuring composite action is that the bond between the concrete and steel remain unbroken. As investigators began to perform additional research on the behavior of mechanical shear connectors during the decade of the 1960s and the specifications continued to

evolve, the use of composite construction for steel bridges began to accelerate until it is now the dominant form of construction used for steel-girder bridges in the U.S.

Unshored composite construction means that two separate load-carrying conditions, noncomposite and composite, are encountered in the design. The noncomposite case involves the steel skeletal frame supporting itself and the weight of the wet concrete. After the concrete hardens, it works with the steel girder forming a much stronger and stiffer composite girder. Alternatively, the concrete deck may be precast and attached to the steel girders. Other materials such as fiber-reinforced plastics and aluminum have been employed as bridge decks with limited success as of this writing (2006).

The composite action between the deck and steel girders is ensured by the use of welded mechanical shear connectors between the girder and the deck. The function of the shear connectors is to transfer the horizontal shear between the deck and the girder forcing the steel girder and the concrete deck to act together as a structural unit by preventing slip along the concrete-steel interface. By ensuring a linear strain from the top of the concrete deck to the bottom of the girder, the planes of the composite girder remain essentially plane under load in the elastic realm, at least through the depth of the steel girder.

Figure 2.1 Steel Girder with Stud Shear Connectors

Although composite action was understood and composite action was recognized as present in girder bridges, composite design was not permitted by AASHO until the mid-1940s. At that time, most girder bridges were simple-span construction. Some cantilever girder bridges were built with hinges, but early composite behavior was generally limited to simple spans. Mechanical shear connection of various shapes was employed to augment the present, but undependable, bond between the deck and the top flange. It was observed that flexible shear connectors were best to accommodate the strain that occurred in the concrete between the shear connector rows.   By making the deck composite, the neutral axis shifts upward. This makes the doubly symmetric steel section uneconomical. To better balance the section,

partial length cover plates were often welded to the bottom flange. These cover plates increased the economy of composite rolled beams. However, because the cover plates were terminated, this required the force in the cover plates to be transferred to the base flange. This, in turn, created stress raisers in the fillet welds connecting the plates to the flanges and subsequent fatigue cracks in the heat-affected regions of the base flange.

In the 1960s, continuous girder spans became commonplace. The negative bending regions near piers permitted some differences of opinion. *AASHTO LRFD* Specifications provided for the elimination of shear connectors in the region between dead-load contraflexure points. Sometimes the longitudinal reinforcement in that region was made composite in the same regions with minimal shear connection. This thinking had been adopted from the building industry where specifications regarding composite construction were adopted earlier. In building design, the live load is applied much as the dead load and there are actual regions where continuous spans see no negative moment for the design loading. Discontinuing the shear connectors near the dead load point of contraflexure in a bridge, however, effectively causes the deck slab to act as a partial length cover plate. Where this is done, the provisions should allow for the design to place enough additional shear connectors to transfer the force in the slab back into the steel girder. However, this has two negative effects. First, in regions of negative flexure, the tensile stress in the deck may become large enough to cause unwanted cracking just past the location where the shear connectors end. Second, the shear connectors at the discontinuity may be overloaded similar to the welds at the termination of a partial length cover plate, particularly if the appropriate slab forces are not considered in the design. Thus, as discussed further below, it is strongly recommended in the current specifications that shear connectors be provided throughout the length of the bridge.

At other points along the girder, shear connectors were spaced according to the absolute value of the composite shear and stud spacing became tighter near abutment bearings. Subsequent research has demonstrated that shear connectors can be placed more uniformly according to the fatigue requirements related to the shear range acting on the stud. Ultimate shear capacity is then checked by assuming that the studs between the point of maximum moment and the end of the region will deform until they are all engaged up to their full static capacity.

As defined in *AASHTO LRFD* Article 6.10.1.2, a noncomposite section is a section where the concrete deck is not connected to the steel section by shear connectors. Although permitted by the *AASHTO LRFD* Specifications, noncomposite sections are not recommended because they are uneconomical and there is no positive attachment of the deck to the girder. For the purposes of this discussion, continuous members in which noncomposite sections are utilized in negative flexure regions only will still be referred to as composite girders. However, *AASHTO LRFD* Article 6.10.10.1 strongly recommends that shear connectors be employed throughout the span of composite girders. The commentary states that shear connectors help control deck cracking in regions of negative flexure where the deck is subject to tensile stress and has longitudinal reinforcement. It further states that this practice is conservative, which is certainly the case. A cursory review of moment influence lines will show that when the live load is placed for critical shear range, it will

produce positive moment in the girder. Thus, there are actually no critical negative moments for shear connector design in continuous spans with regard to a moving fatigue truck load. Hence, there is no reason to treat the location between points of dead-load contraflexure solely as a negative moment region in a highway bridge.

AASHTO LRFD Article 6.6.1.2 permits the recognition of continuous shear connectors by allowing the use of the uncracked section to compute fatigue stresses and stress ranges in the girder, and of course, in the shear connectors. This not only simplifies design calculations, it properly recognizes behavior of the composite girder.   An additional requirement of extending the one percent longitudinal reinforcement to the regions where the deck is in tension under factored construction loads and overloads is certainly logical.

In a noncomposite girder, or a girder in which there are no shear connectors along the entire length of the member, if friction between the deck and girder is neglected, the girder and deck are each assumed to separately carry a part of the load. In this case, there are two neutral axes; one at the centroid of the deck and one at the centroid of the girder.   Under vertical load causing positive moment, the lower surface of the deck will theoretically be in tension and elongate while the top surface of the girder will be in compression and shorten. With friction neglected, only vertical internal forces will act between the deck and the girder and slip will occur between the two components. In other words, a plane section does not remain plane under load. Although numerous field tests have shown that considerable bond develops on the concrete-steel faying surface such that unintended composite action occurs, this bond is conservatively ignored and the stiffness of the deck is not included when calculating the section properties for design.

Composite design offers a number of inherent advantages. Significant weight savings along with shallower sections can be achieved utilizing composite sections. When plate girders are used, composite design typically allows for the use of a smaller top flange. Stiffer composite sections allow for the use of longer spans and reduced live load and composite dead load deflections.   The nominal flexural resistance of a composite section, particularly in regions of positive flexure, greatly exceeds the resistance of the steel girder and concrete deck considered separately, which provides a significant overload capacity. A composite concrete deck also provides positive lateral support to top flanges.

There are many advantages of composite construction but there are some construction concerns that the Engineer needs to be aware of during the design of a composite bridge superstructure. Although shallower sections are achieved from composite design, they yield larger deflections due to the steel self-weight and wet concrete.   The deck placement sequence is also of concern.   Certain deck placement sequences may induce temporary moments in the girders that are considerably higher than the final noncomposite dead load moments after the entire deck is placed. The smaller top flanges due to composite design typically places more than half the web depth in compression during the deck placement in regions of positive flexure. This can lead to out-of-plane distortions of the small girder compression flange and web if not accounted for in the design. Redecking is also

more difficult since the concrete around the shear connectors must be removed along the entire length of each girder.

1.   Viest, I. M., R.S. Fountain, and R.C. Singleton. 1958. "Composite Construction in Steel and Concrete for Bridges and Buildings", McGraw-Hill, New York.
2.   Knight, A.W. 1934. "The Design and Construction of Composite Slab and Girder Bridges", *J. Instn Engrs Aust.*, Vol. 6, No. 1.
3.   Viest, I.M. 1960. "Review of Research on Composite Steel-Concrete Construction", *Journal of the Structural Division*, American Society of Civil Engineers, Vol. 86, No. ST6, June 1960.

2.2.1.2 Unshored vs. Shored Composite Construction

Composite bridge construction can either be designed unshored or shored. Construction where the bare steel girders are shored along their length until the concrete deck is acting compositely with the steel girders is called shored composite construction and is permitted according to *AASHTO LRFD* Article 6.10.1.1.1a. Construction where the bare steel girder resists load applied before it is made composite with the concrete deck is called unshored composite construction and is the recommended approach. Permanent loads and transient loads applied after the concrete deck hardens or is made composite are assumed resisted by the composite girder. According to previous specifications, a concrete deck may be considered sufficiently hardened after attaining 75 percent of its specified 28-day compressive strength f'_c. *AASHTO LRFD* Article C6.10.1.1.1a states that other indicators may now be used in the judgment of the Engineer.

In unshored composite construction, the dead load of the steel and the concrete and other loads are placed on the steel section in its final erected condition. This means that there are no temporary supports used during construction. For example, if a composite steel six-girder multi-girder bridge is erected using a temporary tower under three of the girders while the remaining three girders are erected, and then the shoring tower is removed, the stresses in the steel may be different from the case of all girders erected without shoring. The difference depends on the detailing. If the girders are cambered and the cross frames are detailed assuming that all girders are erected under zero gravity and connections are made without reaming of the bolt holes, there is little difference in girder stresses. If, however, the girders are cambered and the cross-frames are detailed to be erected with the first three girders shored, and the others erected without shoring and then connected, the stress state may be different than in the first instance.

Shoring of girders until the deck is cast and has hardened creates similar situations. In this case, the girders are composite for the deck weight and for the steel weight if the shoring is in place to keep the steel in the no-load condition. If the shoring is added after the steel is erected, only the deck weight is applied to the shored condition. A similar situation exists when a bridge is redecked under traffic as described in DM Volume 1, Chapter 2, Section 2.4.3.1.1.1.2. Some of the girders are composite when deck load is added to the adjacent girders. When cross-frames are connecting the composite and noncomposite girders, the bridge acts in some

ways as shored. Much of the noncomposite load is transferred to the composite girders because of their greater stiffness. This transfer increases the forces in the connecting cross-frames and changes the dead load deflections of the girders.

The major disadvantage of shored composite construction is that most of the dead load is carried by the composite section, which puts large forces in the shear connectors and the concrete deck increasing deflections due to creep of the concrete. This affects the rideability of the bridge over time and tends to put much of the stress saved in the original design back into the steel girders. For this reason, shored composite construction is not popular in bridges. However, it is important to recognize when the design becomes effectively a shored bridge and take appropriate action to ensure proper consideration of loads and deflections.

When shored construction is used, it must be indicated as such in the contract documents. One of the reasons that shored construction is rarely used for bridges is the effect of the concrete creep. It is difficult to predict the amount of creep. If the girders are cambered for final elevation, they are often very high at the time of construction. If they are not cambered properly for creep, the roadway may deflect too much as the structure ages. Although shored construction is permitted according to the *AASHTO LRFD* Specifications, its use is not recommended.

There have been no known demonstration bridges built with shored construction in the U.S. There has been limited research on the effects of concrete creep on composite steel girders under significant dead loads. Shored composite bridges constructed in Germany are known not to have retained composite action. In addition, when shored construction is used, there is an increased likelihood of large tensile stresses occurring in the concrete deck at permanent support points. Also, close tolerances on girder cambers may be difficult to achieve. Therefore, all subsequent discussion in this section will refer to unshored composite construction.

Unshored construction is the common practice for composite bridge construction because it better utilizes the advantages of steel in that shoring is not required and dead load deflections are much better predicted.

2.2.1.3 Effective Flange Width

When a composite girder is subjected to flexure, plane sections do not remain plane. It can be demonstrated with simple mechanics that the shear force in the web is distributed from the web to the extreme edges of the flanges and shear deformation occurs as the shear is so distributed. This distortion is the result of what is called shear lag. Since the concrete deck is wider and less efficient than steel in distributing the shear, there can be significant distortion of the concrete deck, as illustrated in Figure 2.2 (a). Of course with this distortion there is a non-uniform longitudinal stress distribution across the concrete slab, as shown in Figure 2.2 (b).
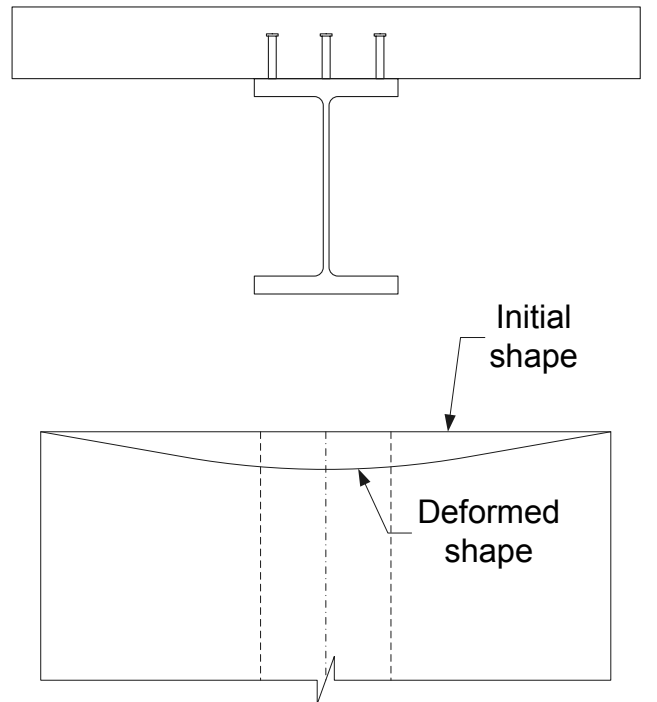
a) Deformed shape of concrete deck after bending –
plan view
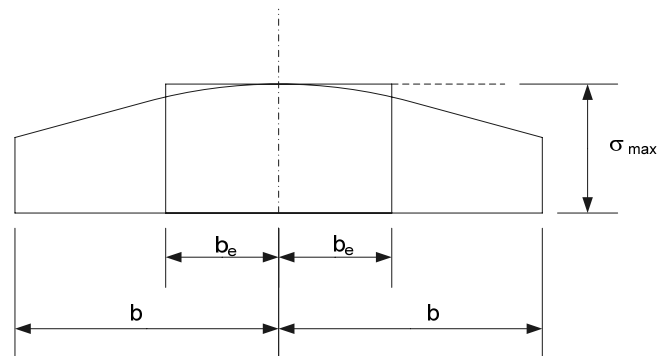
b) Shear lag and effective flange width

Figure 2.2 Shear Lag

Theoretical solutions for the true longitudinal stress distribution across the section can be determined from the theory of elasticity as applied to plates, but the solutions are not amenable for design use as they are complex and depend on the relative dimensions and stiffness of the system, as well as on the applied loading. Concentrated loads and reactions introduce a sharp discontinuity in shear, which creates a most significant shear lag effect. For example, the effective width of the composite deck near a reaction is less than in the center of a long span with a uniform load applied. It is rather intuitive that the full width of the deck would not be effective at an interior support of a continuous span. It becomes effective over some distance away from the reaction.

The question arises as to how much of the deck can be safely assumed in the design of composite girders. To address this question in a simple manner the concept of an effective flange width was introduced. The effective flange width [$2b_e$ in Figure 2.2 (b)] is the width of concrete deck which can be assumed to be uniformly stressed. This width should give the same result as the actual non-uniform stress distribution if integrated over the entire width.   Various theoretical solutions have been proposed for the effective concrete flange width, which ignore the effect of any transverse deck cracking and inelastic behavior. These solutions have generally tended to give a smaller effective width than experimentally determined values (*4*).

The effective flange width for composite girders is specified in *AASHTO LRFD* Article 4.6.2.6.1. In the absence of a more refined analysis, the effective flange width may be taken as follows:

For interior girders, the least of:

  ➢ One-quarter of the effective span length;
  ➢ 12.0 times the average depth (thickness) of the deck, plus the greater of the web thickness or one-half the width of the top flange of the girder; or
  ➢ The average spacing of adjacent girders.

For exterior girders, one-half the effective flange width of the adjacent interior girder plus the least of:

  ➢ One-eighth of the effective span length;
  ➢ 6.0 times the average depth of the deck, plus the greater of one-half the web thickness or one-quarter of the width of the top flange of the girder; or
  ➢ The width of the deck overhang.

In the above, the effective span length is to be taken as the actual span length for simply supported spans, and the distance between points of permanent load contraflexure for continuous spans, as appropriate for either positive or negative moments. For tub girders, the effective flange width of each web is to be determined as though each web is an individual supporting element. For closed box sections, the distance between the outside of the webs at the tops is to be used in lieu of the web thickness in the above requirements. For closed box and tub sections, the spacing should be taken as the spacing between the centerlines of the box or tub sections. The average depth of the deck should be based on the *structural* deck thickness; that is, the total thickness of the deck minus the thickness of any integral wearing surface.

The effective flange width, determined as specified above, is generally to be used to determine the resistance of the composite section at all limit states. However, *AASHTO LRFD* Article 4.6.2.6.1 does recommend that for the calculation of deflections of the composite section, the full flange width be used in lieu of the effective flange width in determining the composite stiffness of the section for the analysis. This recommendation also implicitly applies to the calculation of live load

deflections according to *AASHTO LRFD* Article 2.5.2.6.2, where it is stated that the entire roadway width be included in determining the composite stiffness of the design cross-section for the computation of live load deflections at the service limit state. *AASHTO LRFD* Article 2.5.2.6.2 also recommends that the structurally continuous portion of barriers, sidewalks and railings be included in determining the composite stiffness when a structurally continuous concrete barrier is present and included in the models used for the analysis as permitted. Although there is currently no specific requirement given in the specification for attachment of the barrier or its reinforcement to the deck, such attachment is understood to satisfy barrier crash testing requirements and may be satisfactory to ensure composite behavior with the deck. *AASHTO LRFD* Article C4.6.2.6.1 permits the width of the deck overhang for this analysis to be extended by the following amount:

$$\Delta w = \frac{A_b}{2t_s} \qquad\qquad \text{Equation 2.1}$$

AASHTO LRFD Equation C4.6.2.6.1-1

where:
   A_b =   cross-sectional area of the barrier (in.^{2})
   t_s =   structural thickness of the concrete deck (in.)

For straight girder systems in which a line-girder analysis is employed, the composite bending stiffness of an individual girder for the calculation of live-load deflections may be taken as the total composite stiffness, determined as outlined above, divided by the number of girders.

4.   Chapman, J.C., and J.S. Teraskiewicz. 1968. "Research on Composite Construction at Imperial College", *Proc. Conf. On Steel Bridges*, British Constructional Steelwork Association, London, England.

EXAMPLE:

Calculate the effective flange width for the composite section shown in Figure 2.3, which is assumed to be the section for an exterior girder located in the positive-moment region in the end span of a three-span continuous steel-girder bridge. The effective span length is taken as the distance from the abutment to the point of permanent load contraflexure, which is assumed to be 100.0 ft (the total span length is 140 ft). The girder spacing is 12.0 ft and the width of the deck overhang is 3 ft – 6 in. The *structural* deck thickness is 9.0 in.
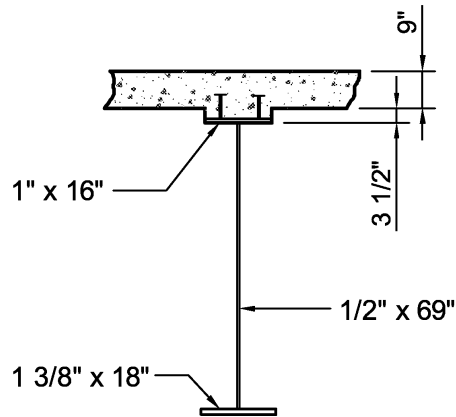
Figure 2.3 Example Composite Cross-Section – Exterior Girder – Positive Flexure Region

First, calculate the effective flange width for an interior girder, which is taken as the least of:

$$\frac{L}{4} = \frac{100.0 \times 12}{4} = 300.0 \text{ in.}$$

or

$$12.0t_s + \frac{b_{tf}}{2} = 12.0(9.0) + \frac{16.0}{2} = 116.0 \text{ in. (governs)}$$

or

$$\text{average spacing of girders} = 144.0 \text{ in.}$$

Based on the calculated effective flange width of 116.0 inches for the interior girder, the effective flange width for the exterior girder is then taken as the least of:

$$\frac{116.0}{2} + \frac{L}{8} = 58.0 + \frac{100.0 \times 12}{8} = 208.0 \text{ in.}$$

or

$$\frac{116.0}{2} + 6.0t_s + \frac{b_{tf}}{4} = 58.0 + 6.0(9.0) + \frac{16.0}{4} = 116.0 \text{ in.}$$

or

$$\frac{116.0}{2} + \text{ width of the overhang} = 58.0 + 42.0 \text{ in.} = 100.0 \text{ in. (governs)}$$

Should the top flange widths of the exterior and adjacent interior girder be different, it is recommended that the top flange width of the exterior girder be used in calculating the portion of the interior girder effective flange width to be combined with the exterior girder.

2.2.1.4 Elastic Section Properties

The following discussion relates to the calculation of the basic elastic section properties for composite sections in regions of positive and negative flexure for use in the design calculations. The calculation of the yield moment and plastic moment for a composite section is covered in the next section of this chapter under Miscellaneous Fundamental Calculations.

Composite girders must be treated specially with regard to section properties. This discussion will be limited to unshored composite construction. Unshored composite construction essentially is the design of two girders—the noncomposite girder and the composite girder. Of course, separate analyses are required for each case. The steel girders do not need to have capacity to carry both dead and live load, particularly in positive bending with respect to the compression flange and web. Hence, stability of these girders during erection is more critical than erection of steel that is capable of carrying all the load. Since most steel-girder bridges today have continuous spans, the issue of how to deal with negative bending must also be addressed since the concrete deck is placed in tension. There has not been a great deal of research on this basic issue because composite construction was originally developed for simple spans and the specifications were developed for buildings. Where continuous spans existed, the design provisions simply assumed they were noncomposite.

The situation with bridges with moving live loads is quite different. Instead of a moment or shear diagram, the designer must deal with moment and shear envelopes. Thus, the term negative moment region has little meaning in bridge design. Chapter 6 of the *AASHTO LRFD* Specifications provides an improved treatment of this issue compared to past *AASHTO LRFD* specifications. Live load can often produce approximately equal positive and negative moments in the regions near points of dead load contraflexure. Thus, much of a girder may be either in positive or negative bending. The live load is applied to the composite section, while much of the dead load is applied to the noncomposite section. Superimposed dead load, however, is applied to the composite section.

To determine which section properties to use depends on the condition.   For analysis, it has been shown that the stiffness properties of the full composite section in positive and negative moment gives the best results when compared to field measurements for composite dead and live loads. As discussed later, *AASHTO LRFD* Article 6.10.1.5 permits this assumption. Field measurements indicate that the full composite section assumption gives the best correlation with service stresses. Thus, as also discussed later, *AASHTO LRFD* Articles 6.6.1.2.1 and 6.10.4.2.1 permit the use of the full composite section to determine flexural stresses for both positive and negative moment at the fatigue and service limit states, respectively, when certain conditions are met.

For strength, the section assuming the concrete is cracked and ineffective is best used for negative moment acting on the composite section in order to be conservative. The issue with regard to section properties is when to use the cracked section. In regions where the moments due to the transient and permanent loads

applied to the composite section are of opposite sign at the strength limit state (i.e. in potential regions of stress reversal), the appropriate composite section to apply to each moment depends on the net stress in the concrete deck due to these loads. According to *AASHTO LRFD* Article 6.10.1.1.1b, if the net stress in the concrete deck due to the sum of the factored moments caused by these loads is compressive, the associated composite section may be used with each of the moments. That is, positive moments should be applied to the appropriate composite section including the transformed area of the concrete deck, and negative moments should be applied to the composite section consisting of the steel girder plus the longitudinal reinforcement only.   If the net stress in the concrete deck is tensile, then the concrete deck is assumed cracked and ineffective. In this case, the moments due to these loads (both positive and negative moments) must be applied to the composite section consisting of the steel girder plus the longitudinal reinforcement only.   The computation of concrete deck stresses is discussed further below.   Since bolted splices are often made in regions of low moment where the transient and permanent load moments are often opposite in sign, the use of proper section properties near points of zero dead load moment is important.

Computation of deflections of composite girders is also dependent on section properties. Best correlation between measured and computed deflections has been obtained when the full composite section is assumed. Deflections at the time of construction are closest to those computed with a modular ratio of *n* and deflections are closest to those computed with a modular ratio of 3*n* about three years after the deck is cast (the modular ratio is discussed in the next section).

2.2.1.4.1 Sections in Positive Flexure

The elastic behavior of a composite steel/concrete girder subject to positive flexure is similar to the behavior of an equivalent homogenous steel girder composed of the actual steel girder and a transformed area of the concrete deck. As opposed to reinforced concrete design, in which the reinforcing steel is transformed to an equivalent concrete area, the concrete deck in a composite steel section is transformed into equivalent steel. The deck area is typically transformed by using a deck width equal to b_{eff}/n, where b_{eff} is the effective flange width and n is the modular ratio. In relatively rare cases where the steel girder is relatively small in relation to the concrete deck, the elastic neutral axis of the transformed composite section may fall within the deck. The concrete below the neutral axis is then assumed cracked in tension and therefore ineffective. In such cases, the effective transformed area of the concrete becomes a function of the neutral axis position (see example below). Since the transformed area approach assumes a linear variation of stress with strain, it is not applicable to the computation of the ultimate strength of a composite section.

As specified in *AASHTO LRFD* Article 6.10.1.1.1b, the modular ratio should be taken as:

$$n = \frac{E}{E_c}$$

Equation 2.2

AASHTO LRFD Equation 6.10.1.1.1b-1

where:
    E   =   modulus of elasticity of the steel = 29,000 ksi
    E_c =   modulus of elasticity of the concrete determined as specified in
                         AASHTO LRFD Article 5.4.2.4 (ksi)

According to *AASHTO LRFD* Article 5.4.2.4, the modulus of elasticity, E_c, for concrete with a unit weight between 0.090 and 0.155 kcf may be taken as:

$$E_c = 33,000 w_c^{1.5} \sqrt{f_c'}$$

<div align="right">Equation 2.3</div>
<div align="right">*AASHTO LRFD* Equation 5.4.2.4-1</div>

where:
    w_c =   unit weight of the concrete (kcf)
    f_c' =   minimum specified 28-day compressive strength of the concrete (ksi)

For normal weight concrete, w_c should usually be assumed to be 0.145 kcf for the calculation of E_c. An additional 0.005 kcf is often included in w_c to account for the weight of the rebars, but this weight should not be included when calculating E_c.

EXAMPLE

Calculate the modular ratio, n, assuming normal weight concrete and a specified minimum 28-day compressive strength for the concrete, f'_c, equal to 4.0 ksi.

$$E_c = 33,000 w_c^{1.5} \sqrt{f_c'}$$

$$E_c = 33,000(0.145)^{1.5} \sqrt{4.0} = 3,644 \text{ ksi}$$

$$n = \frac{E}{E_c}$$

$$n = \frac{29,000}{3,644} = 7.96$$

Note that *AASHTO LRFD* Article C6.10.1.1.1b permits rounding of the modular ratio values for normal weight concrete as follows in lieu of using the exact calculated value:

$$2.4 \leq f_c^{'} < 2.9 \ \ n = 10$$
$$2.9 \leq f_c^{'} < 3.6 \ \ n = 9$$
$$3.6 \leq f_c^{'} < 4.6 \ \ n = 8$$
$$4.6 \leq f_c^{'} < 6.0 \ \ n = 7$$
$$6.0 \leq f_c^{'} \qquad n = 6$$

EXAMPLE

Locate the elastic neutral axis of the transformed composite section for the composite rolled beam substringer shown below (W24 x 68), which is assumed to be located in a region of positive flexure. In this case, the elastic neutral axis is located in the deck so the portion of the concrete below the neutral axis is assumed cracked in tension and ineffective. Assume a 10-inch-thick structural concrete deck and that the effective flange width of the deck is equal to 124.5 inches. The deck haunch from the top of the web to the bottom of the deck is 4.0 inches. The modular ratio *n* is equal to 8.
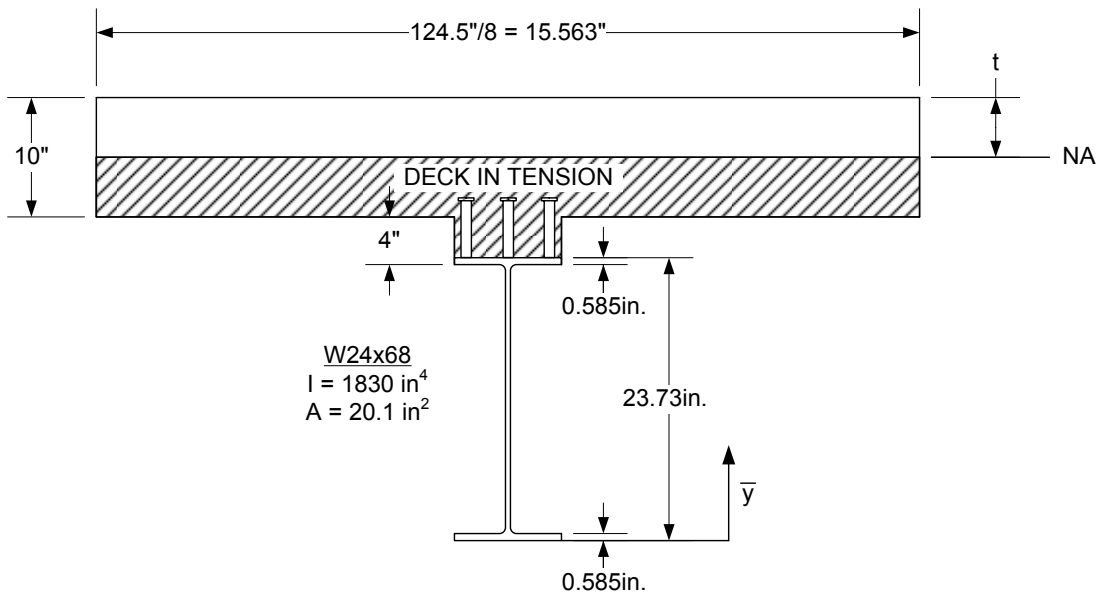
$$\frac{\Sigma y\bar{A}}{A} = \frac{20.1(11.865) + (15.563t)(23.145 + 4.0 + 10.0 - \frac{t}{2})}{20.1 + 15.563t}$$

$$= \frac{238.5 + 578.14t - 7.78t^2}{20.1 + 15.563t}$$

The neutral axis is located at the following location measured from the bottom of the beam:

$$\text{N.A.} = 23.145 + 4.0 + 10.0 - t$$
$$= 37.145 - t$$

Therefore: $37.145 - t = \dfrac{238.5 + 578.14t - 7.78t^2}{20.1 + 15.563t}$

Rearranging: $0 = 7.783t^2 + 20.15t - 508.1$

$$t = \frac{-20.15 + \sqrt{406.02 + 15818.2}}{15.566} = 6.89''$$

Calculate the moment of inertia of the transformed composite section about the neutral axis:

$$I = 1830 + \frac{1}{3}(15.563)(6.89)^3 + 20.1(10.0 - 6.89 + 4.0 + 11.28)^2 = 10{,}324 \text{ in.}^4$$

2.2.1.4.1.1 Effects of Concrete Creep and Shrinkage

When concrete is placed under a sustained long-term stress, there is an instantaneous elastic strain, followed by a time-dependent increase in strain known as creep. Theoretical and experimental studies of concrete creep have been widely reported in the literature and the reader is referred elsewhere, including to DM Volume 3 of this Manual on concrete bridge superstructure design, for more detailed discussions on the phenomenon of concrete creep. Suffice it to say, when a composite steel girder is subject to a constant sustained loading, such as permanent loads applied to the composite section (e.g. barriers, railings, wearing surface, etc.), the concrete deck stress is not constant. As time passes, the concrete creeps. The strain in the steel girder increases and the steel stresses become larger, while the strains and concomitant stresses in the concrete deck are reduced. The reduction of stress in the concrete is a function of the relative stiffness of the girder and the concrete deck.

The actual calculation of creep stresses in composite girders is theoretically complex and not necessary for the design of composite girders. Instead, a simple approach has been adopted for design in which a modular ratio appropriate to the duration of the load is used to compute the corresponding elastic section properties. As specified in *AASHTO LRFD* Article 6.10.1.1.1b, for transient loads applied to the composite section, the so-called "short-term" modular ratio n is used. For permanent loads applied to the composite section, the so-called "long-term" modular ratio of $3n$ is used. The short-term modular ratio is based on the initial tangent modulus, E_c, of the concrete, while the long-term modular ratio is based on an effective apparent modulus, E_c/k, to account for the effects of creep. In U.S. practice, a value of k equal to 3 has been accepted as a reasonable value.

As concrete cures, it will contract or shrink with time. Although shrinkage is included in most of the basic load combinations given in *AASHTO LRFD* Table 3.4.1-1, the

effects of shrinkage on the behavior of composite steel girders are less well understood than creep and are often ignored in U.S. design practice as of this writing. However, some state DOTs require that shrinkage be included as part of the camber considerations. As the concrete deck shrinks, it introduces compression in the flange attached to it while corresponding tensile stresses are introduced in the concrete deck as long as there is no loss of bond between the two materials. The effect of the shortening of both the concrete deck and top flange is to generate a positive moment in the composite girder with its concomitant increase in deflection. The amount of deflection is a function of a number of parameters including the distance of the deck-flange interface from the neutral axis and the stiffness of both the deck and the girder. Shrinkage stresses cannot exceed the modulus of rupture of the deck concrete.

Although shrinkage increases the stresses in the girder, it does not appreciably diminish its capacity in the positive moment region because added load will reverse the shrinkage stresses in the deck, which will release its pull on the girder. In the negative moment regions of a girder, the deck is considered ineffective by the fact that it is assumed cracked.

2.2.1.4.1.2 Section Property Calculations

The calculation of the elastic section properties for the composite section shown in Figure 2.3 is given below. These properties would be used for design calculations in regions designed for positive flexure. As specified in *AASHTO LRFD* Articles 6.10.1.1.1a and 6.10.1.1.1b, for the calculation of the stresses in the composite girder, the properties of the bare steel section would be used for permanent loads applied before the concrete deck has hardened or is made composite. The properties of the long-term 3*n* composite section would be used for permanent loads applied after the concrete deck has hardened or is made composite. The properties of the short-term *n* composite section would be used for transient loads applied after the concrete deck is made composite. *AASHTO LRFD* Article 6.10.1.1.1d requires that *n* be used to compute concrete deck stresses for permanent loads, whereas 3*n* is to be used for calculating the stresses in the steel girder due to permanent loads. The reason for this is to check concrete stresses at the time of construction prior to creep when such stresses are highest, and to check steel stresses after creep has occurred when such stresses are the highest.   For the calculation of the longitudinal stresses in the concrete deck due to transient loads in regions of positive flexure, again the properties of the short-term *n* composite section are to be used (refer to *AASHTO LRFD* Article 6.10.1.1.1d).

In the calculation of the long-term and short-term composite properties, the appropriate transformed area of the concrete deck is used. Note that it is permitted to include the longitudinal reinforcement lying within the effective flange width in the computation of the long-term and short-term composite section properties. However, this reinforcement usually is not considered effective in compression at the strength limit state because it is not tied; therefore, its contribution is typically neglected in positive bending regions for strength limit state checks. Typically, the area of the concrete deck haunch is not considered in the computation of the composite section properties; the haunch depth is considered, however.

Consideration may be given to including the longitudinal reinforcement when computing stresses at the service and fatigue limit states.

Obviously the moment of inertia is greater when creep is ignored so the girder tends to sag under creep. The question of camber for this condition is addressed in a later section.

EXAMPLE

Calculate the elastic section properties for the composite section shown in Figure 2.3. Calculate the properties of the bare steel section, the long-term composite section and the short-term composite section.

<div align="center">Steel Section</div>

Component	A	d	Ad	Ad^2	I_o	I
Top Flange 1" x 16"	16.00	35.00	560.0	19,600	1.33	19,601
Web ½" x 69"	34.50				13,688	13,688
Bottom Flange $1\frac{3}{8}$" x 18"	24.75	−35.19	−871.0	30,649	3.90	30,653
	75.25		−311.0			63,942

$$-4.13(311.0) = \quad -1,284$$
$$I_{NA} = \quad 62,658 \quad \text{in.}^4$$

$d_s = \dfrac{-311.0}{75.25} = -4.13 \text{ in.}$

$d_{TOP\,OF\,STEEL} = 35.50 + 4.13 = 39.63 \text{ in.}$ $d_{BOT\,OF\,STEEL} = 35.88 - 4.13 = 31.75 \text{ in.}$

$S_{TOP\,OF\,STEEL} = \dfrac{62,658}{39.63} = 1,581 \text{ in.}^3$ $S_{BOT\,OF\,STEEL} = \dfrac{62,658}{31.75} = 1,973 \text{ in.}^3$

<div align="center">Composite Section; 3n = 24</div>

Component	A	d	Ad	Ad^2	I_o	I
Steel Section	75.25		−311.0			63,942
Concrete Slab 9" x 100"/ 24	37.50	42.50	1,594	67,734	253.1	67,987
	112.8		1,283			131,929

$$-11.37(1,283) = \quad -14,588$$
$$I_{NA} = \quad 117,341 \quad \text{in.}^4$$

$d_{3n} = \dfrac{1,283}{112.8} = 11.37 \text{ in.}$

$d_{TOP\,OF\,STEEL} = 35.50 - 11.37 = 24.13 \text{ in.}$ $d_{BOT\,OF\,STEEL} = 35.88 + 11.37 = 47.25 \text{ in.}$

$S_{TOP\,OF\,STEEL} = \dfrac{117,341}{24.13} = 4,863 \text{ in.}^3$ $S_{BOT\,OF\,STEEL} = \dfrac{117,341}{47.25} = 2,483 \text{ in.}^3$

Composite Section; $n = 8$

Component	A	d	Ad	Ad^2	I_0	I
Steel Section	75.25		−311.0			63,942
Concrete Slab 9" x 100"/ 8	112.5	42.50	4,781	203,203	759.4	203,962
	187.8		4,470			267,904
				−23. 80(4,470) =		−106,386
				I_{NA} =		161,518 in.⁴

$$d_n = \frac{4,470}{187.8} = 23.80 \text{ in.}$$

$$d_{TOP\,OF\,STEEL} = 35.50 - 23.80 = 11.70 \text{ in.} \qquad d_{BOT\,OF\,STEEL} = 35.88 + 23.80 = 59.68 \text{ in.}$$

$$S_{TOP\,OF\,STEEL} = \frac{161,518}{11.70} = 13,805 \text{ in.}^3 \qquad S_{BOT\,OF\,STEEL} = \frac{161,518}{59.68} = 2,706 \text{ in.}^3$$

As an aside, for tub and closed-box sections with inclined webs, the area of the inclined webs should be used in computing all section properties. The moment of inertia of *each* inclined web I_{ow} with respect to a horizontal axis at mid-depth of the web may be taken as follows:

$$I_{ow} = I_w \left(\frac{S^2}{S^2 + 1} \right)$$

Equation 2.3a

where:

I_w = moment of inertia of each inclined web with respect to an axis normal to the web (in.⁴)

S = web slope with respect to the horizontal (typically equal to 4.0)

Also, inspection manholes are often inserted in the bottom flanges of tub and closed-box sections near supports. These manholes should be subtracted from the bottom-flange area when computing the elastic section properties for use in the region of the access hole. Finally, as discussed in *AASHTO LRFD* Article C6.11.1.1, consideration should be given to including the longitudinal component of the top lateral bracing area when computing the section properties of tub sections (for determining the stiffness for the analysis and for determining flexural stresses) since the top lateral bracing contributes to the flexural stiffness of these sections. The longitudinal component of the top-flange bracing area A_d may be computed as follows:

For single-diagonal lateral bracing systems:

$$A_d = A \cos\theta$$

Equation 2.3b

For X-type lateral bracing systems:

$$A_d = 2A\cos\theta$$

<div align="right">Equation 2.3c</div>

where:

A   =   area of a single top-flange bracing diagonal member (in.^{2})

θ =   angle of the top-flange bracing member(s) with respect to a tangent to the girder (degrees)

When the lateral bracing members are attached directly to the top flanges (which is preferred), A_d can simply be included with the top-flange areas in computing the section properties.

Figure 2.4 Inspection Access in Box girder Bottom Flange

2.2.1.4.2 Sections in Negative Flexure

For a composite steel/concrete girder subject to negative flexure in continuous spans, *AASHTO LRFD* Article 6.10.1.1.1c states that the short-term and long-term sections are to generally consist of the steel section and the longitudinal reinforcement within the effective width of the concrete deck. That is, the concrete deck in tension is typically assumed cracked and not participating in the resistance of moment at the strength limit state. An exception is permitted for design calculations at the service and fatigue limit states and for the computation of tensile stresses in the concrete deck, as discussed below.

2.2.1.4.2.1 Minimum Negative Flexure Concrete Deck Reinforcement

To control concrete deck cracking in regions of negative flexure, *AASHTO LRFD* Article 6.10.1.7 specifies that the total cross-sectional area of the longitudinal reinforcement that is provided in these regions shall be not less than 1 percent of the total cross-sectional area of the deck. The reinforcement is to have a specified minimum yield strength not less than 60 ksi and a size not exceeding No. 6 bars. It is further stated that the required reinforcement should be placed in two layers uniformly distributed across the deck width, with two-thirds of the reinforcement placed in the top layer. As mentioned in *AASHTO LRFD* Article C6.10.1.7, when

precast deck panels are used as deck forms, it may not be possible to place the required reinforcement in two layers, in which case this placement requirement may be waived at the discretion of the Engineer. The individual bars are to be spaced at intervals not exceeding 12.0 in. The use of small bars at relatively close spacing is intended to ensure closely spaced cracks of small width.

It is of interest to examine the effect of the deck reinforcing. One No. 6 bar has an area of 0.44 square inches. Thus, assuming an area of reinforcement exactly equal to 1 percent of the total cross-sectional area of the deck has been provided, it is effective for 44 square inches of deck cross section. If the deck is 8 inches thick, the bars are spaced at approximately 5 inches. If the concrete is stressed to its modulus of rupture of 0.5 ksi at the time it cracks, it will introduce 22 kips or 50 ksi into the reinforcing bar. Since the bar has a yield stress of 60 ksi, it will not yield and a full-depth crack should be arrested when it is about 0.001 inches wide. If the deck tensile stress is larger, more reinforcing bars will be required to resist the crack progression and possible yield or debonding of the reinforcing. The use of steels with higher yield stress in negative moment regions tends to cause higher deck stresses.

The effective width of concrete deck is actually close to the entire deck width in most girder bridges; that is the reason the reinforcement is distributed across the entire concrete section. Thus, the longitudinal deck stresses are somewhat lower than traditionally computed using the effective width specified. Nonetheless, tensile stresses are significant and should be considered in designing longitudinal deck reinforcement. In addition to the deck stresses due to flexure, the deck is subjected to additional tensile stresses due to temperature and shrinkage. Sequential casting of the deck further complicates the design of longitudinal deck reinforcement. Locating the proper point to terminate longitudinal deck reinforcement will be examined in later sections; the point is generally further from the point of critical negative moment than the point of dead-load contraflexure.

Precast deck panels may be advantageous over a cast-in-place concrete deck due to the speed of construction and better quality control. Design of a precast concrete deck with respect to longitudinal stresses in the deck is similar to design of the longitudinal reinforcement. Tensile stresses in the deck need to be overcome by pretensioning. This is done before the deck is attached to the steel girders with grouted shear connectors.

As illustrated in the example below, the total cross-sectional area of the deck is to be used to satisfy the minimum 1 percent area requirement. Note in the example that the deck overhang tapers are included in calculating the total cross-sectional area of the deck. As specified in *AASHTO LRFD* Article 6.10.1.1.1c, only the reinforcement within the appropriate effective flange width is to be considered acting with each girder. In the example, the effective flange width for the exterior girder in regions of negative flexure is computed to be 100.5 inches (from separate calculations similar to those shown previously).

EXAMPLE

Assume the following cross-section for a steel I-girder bridge. Calculate the minimum required negative longitudinal reinforcement over the exterior girder.
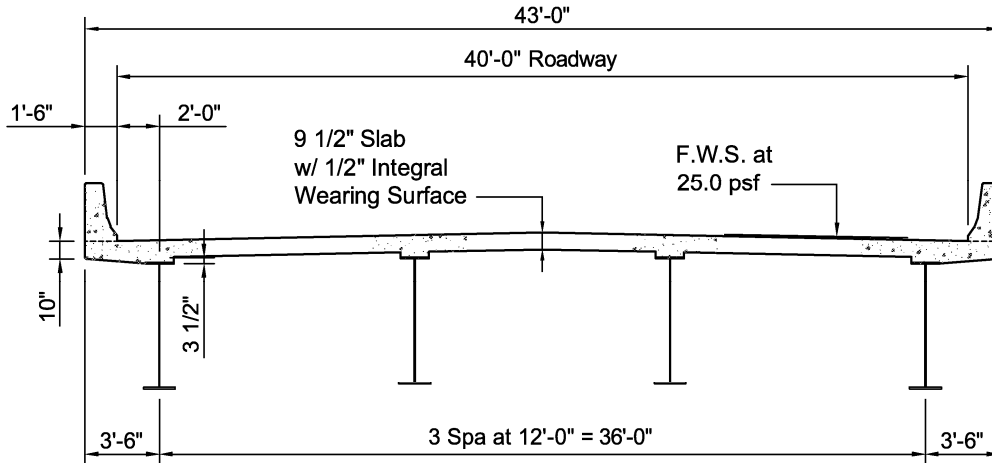
$$A_{deck} = \frac{9.0}{12}(43.0) + 2\left[\frac{1}{12}\left(\frac{3.0}{2} + 0.5\right)\left(3.5 - \frac{18/2}{12}\right)\right] = 33.17 \text{ ft}^2 = 4{,}776 \text{ in.}^2$$

$$0.01(4{,}776) = 47.76 \text{ in.}^2$$

$$\frac{47.76}{43.0} = 1.11 \text{ in.}^2/\text{ft} = 0.0926 \text{ in.}^2/\text{in.}$$

$$0.0926(100.5) = 9.30 \text{ in.}^2$$

The location of the point of termination of the longitudinal reinforcement is specified in *AASHTO LRFD* Article 6.10.1.7, which requires that this reinforcement be provided wherever the longitudinal tensile stress in the concrete deck due to either the factored construction loads or Load Combination Service II given in *AASHTO LRFD* Table 3.4.1-1 (see DM Volume 1, Chapter 5 for a further discussion of the Service II Load Combination) exceeds ϕf_r. f_r is the modulus of rupture of the concrete specified in *AASHTO LRFD* Article 5.4.2.6 and ϕ is the appropriate resistance factor for concrete in tension specified in *AASHTO LRFD* Article 5.5.4.2.1. Previous specifications limited the placement of longitudinal deck reinforcement to regions of negative flexure only, which were taken as between points of permanent load contraflexure. However, the deck on steel girder bridges can often experience significant tensile stresses outside the points of permanent load contraflexure. This can occur under moving live loads and during the placement of the concrete deck in stages, in which case regions of the deck that have already been placed may be subject to negative flexure during subsequent casts, even though these regions may be subjected primarily to positive flexure in the final condition. Tensile stresses in the deck due to thermal and shrinkage strains can also occur in regions where these

stresses otherwise might not be anticipated. The conditions cited above are particularly prevalent in highly skewed continuous girder bridges.

Terminating the longitudinal deck reinforcement based on the requirement to prevent the calculated tensile stresses in the deck from exceeding the modulus of rupture during construction and under design overload (Service II) conditions is a rational approach. The prior assumption in this regard often permitted large tensile deck stresses in underreinforced regions that led to premature deck cracking.

Examples illustrating how to locate the minimum longitudinal reinforcement based on the calculated level of deck stress are given in later sections of this chapter under Constructibility and Service Limit State Verifications (Sections 2.2.3.4.1 and 2.2.3.5.2).

Calculations of composite sections properties are based on the first-order assumption that plane sections remain plane.   Stresses in the longitudinal reinforcement and the deck, be it in tension or compression, are based on this assumption. For this assumption to be valid, the deck-steel interface may not slip. Slip is prevented by the introduction of adequate shear connectors. Prior *AASHTO LRFD* provisions in this regard required shear connectors in the negative moment regions be provided based on the first moment of only the longitudinal reinforcement used in the design of the composite section. Of course, the first moment of the entire effective deck is much larger and would require closer spacing of shear studs. The deck in these negative moment regions generally remains effective as a result of the significant bond that normally exists between the concrete and steel. If shear connectors are present when the bond is broken, they are heavily loaded and may cause fatigue cracks in the top flange. If they are not present and the bond should fail, the shear connectors at the contraflexure points must carry all of the shear and are generally overloaded. *AASHTO LRFD* Article 6.10.10.1 recommends that shear connectors be provided along the entire length of continuous composite bridges, including the negative moment regions. When shear connectors are provided along the entire length, satisfaction of the requirements of *AASHTO LRFD* Article 6.10.1.7 regarding the provision and placement of minimum negative flexure longitudinal reinforcement can then be used to an advantage in the design calculations at the fatigue and service limit states. As permitted in *AASHTO LRFD* Article 6.6.1.2.1 when the preceding requirements are satisfied, fatigue live load stresses and stress ranges may be computed assuming the concrete deck to be fully effective for both positive and negative flexure.   Also, as permitted in *AASHTO LRFD* Article 6.10.4.2.1, flexural stresses on the composite section due to Load Combination Service II can be determined assuming the concrete deck to be fully effective for both positive and negative flexure.

Concrete provides significant resistance to tensile stress at service load levels. By providing the minimum negative flexure longitudinal reinforcement according to the provisions of *AASHTO LRFD* Article 6.10.1.7, in conjunction with shear connectors along the entire length of the member, crack length and width can be controlled so that full-depth cracks should not occur. These practices are common in reinforced concrete design. Where cracks occur, the stress in the longitudinal reinforcement increases until the cracked concrete and reinforcement ultimately reach equilibrium.

As a result, the deck may experience staggered transverse cracking that is prevented from coalescence to damaging size by the proper design of the longitudinal reinforcement. Recognizing that the concrete is effective in tension has a significant beneficial effect on the computation of fatigue stress ranges *in top flanges* subject to tensile stresses. It can also significantly reduce the Service II flexural stresses in these regions. However, when the concrete deck is assumed effective in negative flexure, more than half of the web may be in compression increasing the susceptibility of the web to bend buckling under the Service II Load Combination. This issue is explored in greater depth in the later sections of this chapter under Web Bend-Buckling Resistance and Service Limit State Verifications (Sections 2.2.2.4 and 2.2.3.5.2.2).

When shear connectors are omitted in so-called negative moment regions, additional shear connectors are required at points of permanent load contraflexure according to the provisions of *AASHTO LRFD* Article 6.10.10.3. The commentary explains that the extra shear connectors are determined for the maximum force in the longitudinal reinforcement. The force in the concrete deck on the positive moment region is also removed at this point if the deck is uncracked. However, the additional shear connectors are not investigated for this force. The design of these additional connectors, and the design of shear connectors in general, is discussed in more detail in a later section of this chapter under Shear Connector Design (Section 2.2.5). According to *AASHTO LRFD* Article 6.10.1.7, under this condition, the negative flexure longitudinal reinforcement is to be extended into the positive flexure regions beyond these additional connectors by a distance not less than the reinforcement development length specified in Section 5 of the *AASHTO LRFD* Specifications.

To further control concrete deck cracking, *AASHTO LRFD* Article C6.10.1.7 discusses the importance of preventing nominal yielding of the 1 percent longitudinal reinforcement, and suggests that nominal yielding of this reinforcement be prevented under Load Combination Service II. Since the minimum longitudinal reinforcement must have a specified minimum yield strength not less than 60 ksi according to *AASHTO LRFD* Article 6.10.1.7, any nominal yielding of this reinforcement is judged to be insignificant under the Service II Load Combination for the following conditions: 1) unshored construction where the steel section utilizes steel with a specified minimum yield stress less than or equal to 70 ksi in either flange, and 2) shored construction where the steel section utilizes steel with a specified minimum yield strength less than or equal to 50 ksi in either flange. For all other cases, it is recommended that the Engineer perform an explicit check for nominal yielding of the longitudinal reinforcement under the Service II Load Combination. This check would be made only for the permanent loads and transient loads applied after the concrete deck has been made composite.

Figure 2.5 Reinforcement and Shear Connectors

2.2.1.4.2.2 Section Property Calculations

The calculation of the elastic section properties for the composite section shown in Figure 2.6 is given below, which represents a section from an exterior girder in a region of negative flexure. These properties would be used for design calculations in regions of negative flexure. As specified in *AASHTO LRFD* Articles 6.10.1.1.1a and 6.10.1.1.1c, the properties of the bare steel section would be used for permanent loads applied before the concrete deck has hardened or is made composite. The properties of the steel section plus the longitudinal reinforcement would always be used at the strength limit state for permanent loads and transient loads applied after the concrete deck has hardened or is made composite. The properties of the steel section plus the longitudinal reinforcement would also be used for these loads at the fatigue and service limit states in regions of negative flexure, unless the Engineer invokes the provisions of *AASHTO LRFD* Articles 6.6.1.2.1 and/or 6.10.4.2.1 permitting the concrete to be considered effective in tension for negative flexure at the fatigue and/or service limit states, respectively (as discussed previously).   In that case, the properties of the long-term $3n$ composite section (including the transformed area of the concrete deck) would be used for permanent loads applied after the concrete deck has hardened or is made composite. The properties of the short-term n composite section (including the transformed area of the concrete deck) would be used for transient (live) loads applied after the concrete deck has hardened or is made composite. These properties would be computed exactly as illustrated above for sections in positive flexure; again, the longitudinal reinforcement may be conservatively neglected in these computations.

Although not shown here or required by the *AASHTO LRFD* Specifications, for stress calculations involving the application of permanent loads to the long-term composite section in regions of negative flexure, consideration might be given to conservatively adjusting the area of the longitudinal reinforcement for the effects of concrete creep by dividing the rebar area by 3. The concrete is assumed to transfer the force from the longitudinal deck steel to the rest of the cross-section and

concrete creep acts to reduce that force over time effectively increasing the stress in the steel section.

For the calculation of the longitudinal stresses in the concrete deck due to both permanent and transient loads in regions of negative flexure, the properties of the short-term *n* composite section are to be used, as discussed later (refer also to *AASHTO LRFD* Article 6.10.1.1.1d).

EXAMPLE

Calculate the elastic section properties for the composite section shown in Figure 2.6. Calculate the properties of the bare steel section and the steel section plus the longitudinal reinforcement (Note: longitudinal reinforcement not shown in Figure 2.6).

For the purpose of the example calculations given below, the previously calculated minimum 1 percent longitudinal reinforcement, which would typically be placed in two layers, is assumed combined into a single layer placed at the centroid of the two layers (with each layer also including the assumed transverse deck reinforcement). From separate calculations, the centroid of the two layers is computed to be 4.63 in. from the bottom of the deck. Also, although a larger reinforcement area may be provided in the actual deck design, the calculated minimum required area is used in the subsequent calculations.
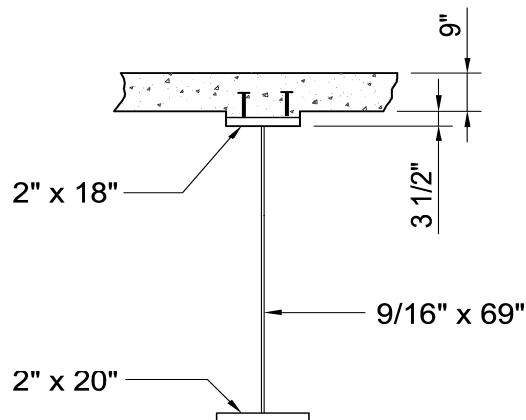
Figure 2.6 Example Composite Cross-Section – Exterior Girder – Negative Flexure Region

Steel Section

Component	A	d	Ad	Ad^2	I_o	I
Top Flange 2" x 18"	36.00	35.50	1,278	45,369	12.00	45,381
Web 9⁄16" x 69"	38.81				15,399	15,399
Bottom Flange 2" x 20"	40.00	−35.50	−1,420	50,410	13.33	50,423
	114.8		−142.0			111,203

$$-1.24(142.0) = \quad -176.1$$
$$I_{NA} = \quad 111,027 \quad \text{in.}^4$$

$$d_s = \frac{-142.0}{114.8} = -1.24 \text{ in.}$$

$$d_{TOP\ OF\ STEEL} = 36.50 + 1.24 = 37.74 \text{ in.} \qquad d_{BOT\ OF\ STEEL} = 36.50 - 1.24 = 35.26 \text{ in.}$$

$$S_{TOP\ OF\ STEEL} = \frac{111,027}{37.74} = 2,942 \text{ in.}^3 \qquad S_{BOT\ OF\ STEEL} = \frac{111,027}{35.26} = 3,149 \text{ in.}^3$$

Steel Section + Long. Reinforcement

Component	A	d	Ad	Ad^2	I_o	I
Steel Section	114.8		−142.0			111,203
Long. Reinforcement	9.30	42.63	396.5	16,901		16,901
	124.1		254.5			128,104

$$-2.05(254.5) = \quad -521.7$$
$$I_{NA} = \quad 127,582 \quad \text{in.}^4$$

$$d_{reinf} = \frac{254.5}{124.1} = 2.05 \text{ in.}$$

$$d_{TOP\ OF\ STEEL} = 36.50 - 2.05 = 34.45 \text{ in.} \qquad d_{BOT\ OF\ STEEL} = 36.50 + 2.05 = 38.55 \text{ in.}$$

$$S_{TOP\ OF\ STEEL} = \frac{127,582}{34.45} = 3,703 \text{ in.}^3 \qquad S_{BOT\ OF\ STEEL} = \frac{127,582}{38.55} = 3,310 \text{ in.}^3$$

Note that for tub or closed-box sections, longitudinal flange stiffeners, if present, are often included when computing the elastic section properties. The longitudinal component of the top lateral bracing area may also be included in the top flange area when computing the section properties for tub sections and the properties of the inclined webs should also be considered, as discussed previously in Section 2.2.1.4.1.2 of this chapter.

2.2.1.5 Stress Calculations

2.2.1.5.1 Steel Girder

The elastic bending stresses in the steel girder of a composite section are dependent on the manner of construction. For unshored construction, the steel girders are erected first and must support their own weight, the weight of the deck forms and wet concrete, or the weight of precast deck panels. Once the concrete

deck has hardened or is made composite, bending stresses in the steel girder due to all permanent and transient loads are computed based on the appropriate transformed composite section properties; that is, the long-term composite section properties are applied to permanent loads and the short-term composite section properties are applied to transient loads. For shored construction, in which the steel girders are supported on temporary shoring along their length, all bending stresses in the steel girder due to all permanent and transient loads are computed based on the appropriate transformed composite section properties.

Regardless of the method of construction, since plane sections are assumed to remain plane, the calculated elastic stresses due to the various loadings acting on the composite section may be summed. However, at elastic stress levels, the principle of superposition does not apply to the bending moments due to the various loadings, as these moments are each applied to different sections; that is, the girder stiffness is changing as each of the moments are applied. Therefore, at elastic stress levels, the individual bending moments may not be summed.

EXAMPLE

Calculate the bending stress in the bottom flange of the girder shown in under the Strength I Load Combination (see DM Volume 1, Chapter 5 for a discussion of the Strength I Load Combination). The load modifier η is assumed to be 1.0. Assume unshored construction. The section is located in a region of positive flexure. Use the section properties computed earlier for this section. Assume the following unfactored bending moments:

M_{DC1} = +2,202 kip-ft
M_{DC2} = +335 kip-ft
M_{DW} = +322 kip-ft
M_{LL+IM} = +3,510 kip-ft

DC1 represents the permanent loads applied before the concrete deck has hardened or is made composite, DC2 represents the permanent loads (other than wearing surface and utility loads) applied after the concrete deck has hardened or is made composite, DW represents the wearing surface and utility loads, and LL+IM represents the live load plus impact loads. Both DW and LL+IM are assumed applied after the concrete deck has hardened or is made composite.

Bot. flange:

$$f = 1.0 \left[\frac{1.25(+2,202)}{1,973} + \frac{1.25(+335)}{2,483} + \frac{1.5(+322)}{2,483} + \frac{1.75(+3,510)}{2,706} \right] 12 = +48.26 \text{ ksi}$$

Calculate the bending stress in the bottom flange of the girder shown in under the Strength I Load Combination. The load modifier η is assumed to be 1.0. Assume unshored construction. The section is located in a region of negative flexure. Use the section properties computed earlier for this section. Note that the

section is a hybrid section utilizing Grade HPS 70W steel flanges and a Grade 50W web. Assume the following unfactored bending moments:

M_{DC1} = -4,840 kip-ft
M_{DC2} = -690 kip-ft
M_{DW} = -664 kip-ft
M_{LL+IM} = -4,040 kip-ft

Bot. flange:

$$f = 1.0 \left[\frac{1.25(-4,840)}{3,149} + \frac{1.25(-690)}{3,310} + \frac{1.5(-664)}{3,310} + \frac{1.75(-4,040)}{3,310} \right] 12 = -55.42 \text{ ksi}$$

2.2.1.5.2 Concrete Deck

For calculating longitudinal flexural stresses in a transformed concrete deck of a composite section, the calculated stress in the deck must be *divided by the modular ratio*. In a composite girder, longitudinal flexural stresses in the deck are assumed to result only from the permanent loads and transient loads applied after the concrete deck has hardened or is made composite.

According to *AASHTO LRFD* Article 6.10.1.1.1d, the short-term modular ratio *n* is to always be used to calculate the deck stresses. Previous specifications required that the longitudinal flexural stresses in the concrete deck due to permanent loads be calculated using either the *n* or 3*n* section, whichever gave the more critical stress in the deck. The *n* composite section generally governs the deck stress calculation when the deck stresses due to the permanent and transient loads are of the same sign. However, for example, in situations where smaller compressive permanent load stresses can result in larger net tensile stresses in the deck in the vicinity of points of contraflexure (i.e. in potential regions of stress reversal), the use of the 3*n* composite section when calculating the permanent load stresses will produce a more critical tension stress in the deck.   It was felt, however, that such a level of refinement in the calculation of longitudinal deck stresses was no longer warranted.

EXAMPLE

Calculate the maximum bending stress in the concrete deck for the composite girder shown in Figure 2.3 under the Service II Load Combination. Assume unshored construction. The section is assumed to be located in a region of positive flexure. Use the section properties computed earlier for this section, and the unfactored bending moments given in the preceding example at this section. Assume *n* = 8.

Conc. deck:

$$f = \frac{1}{8} \left[\frac{1.0(+335)}{161,518} + \frac{1.0(+322)}{161,518} + \frac{1.3(+3,510)}{161,518} \right] (23.20)(12) = +1.125 \text{ ksi}$$

2.2.1.6 Stiffness Assumptions for Analysis

AASHTO LRFD Article 6.10.1.5 states that for loads applied to noncomposite sections, the stiffness properties of the steel beam alone are to be used in the analysis of flexural members for reasons discussed previously. This requirement applies to all loads applied to a noncomposite girder, and to all loads applied to the bare steel section of a composite girder before the deck has hardened or is made composite.

In continuous spans, as described above, the composite section in negative moment regions will typically have a different stiffness for design calculations at the strength limit state because the concrete deck in tension is assumed cracked and not participating. However, in computing the stiffness properties to be used in the analysis of composite flexural members at all limit states, *AASHTO LRFD* Article 6.10.1.5 states that the stiffness properties of the full composite section are to be used over the entire bridge length for permanent loads and transient loads applied to the composite section. This assumption is to be employed even when shear connectors are omitted from the negative flexure regions of continuous composite girders resulting in noncomposite sections in those regions. For permanent loads applied to the composite section, the stiffness properties of the long-term 3n composite section should be used and for transient loads applied to the composite section, the stiffness properties of the short-term n composite section should be used.

Several field tests of continuous composite bridges have shown that there is considerable composite action in regions of negative flexure, even in cases where shear connectors are omitted in those regions. Consideration of the concrete deck in tension tends to increase the negative moments acting on the composite section by up to approximately 10 percent and reduce the positive moments by less than approximately three percent.

2.2.2 Miscellaneous Fundamental Calculations

This section will cover the calculation of some other important miscellaneous parameters that are often utilized in steel-bridge-girder design. These parameters include the plastic moment M_p, the yield moment M_y, the depth of the web in compression in the elastic range D_c and at the plastic moment D_{cp}, the web bend-buckling resistance F_{crw}, and the flange-stress reduction factors – namely the web load-shedding factor R_b and the hybrid factor R_h.

2.2.2.1 Plastic Moment

The plastic moment M_p is defined in the *AASHTO LRFD* Specifications as the resisting moment of a fully yielded cross-section (about the major axis). M_p is calculated as the moment of the plastic forces acting on the cross-section about the plastic neutral axis (Note: for sections subject to flexure only, M_p may be calculated as the moment of the plastic forces about any axis parallel to the plastic neutral axis). Plastic forces in steel portions of the cross-section are calculated using the yield strengths of the flanges, web and longitudinal reinforcing steel, as appropriate.

Plastic forces in concrete portions of the cross-section (in compression only) are based on a rectangular stress block, with the magnitude of the compressive stress taken equal to $0.85f'_c$. Concrete in tension is neglected. The position of the plastic neutral axis is calculated based on the equilibrium condition that there is no net axial force acting on the cross-section.

The plastic moment is used as a theoretical measure of the maximum potential resistance of noncomposite or composite sections satisfying specific steel grade, flange and web slenderness, compression-flange bracing and ductility requirements, as applicable. In the *AASHTO LRFD* Specifications, such sections in straight bridges that are composite in regions of positive flexure are termed compact sections. Noncomposite sections or composite sections in regions of negative flexure in straight bridges satisfying these requirements are termed compact web sections, which are less commonly used. For sections that can achieve the full plastic-moment resistance, it is assumed that the section is completely elastic up to M_p and then rotates inelastically at M_p with no increase in the moment resistance. The effects of strain hardening are conservatively ignored. This idealized moment-rotation behavior is termed elastic-perfectly plastic behavior (refer to Figure 2.15).

For homogenous noncomposite sections, M_p may simply be calculated as follows:

$$M_p = F_y Z \qquad \qquad \text{Equation 2.4}$$

where:
  Z   =   plastic section modulus (in^3)

Z is calculated as the sum of the first moments of the flange and web areas about the plastic neutral axis. For rolled wide-flange sections, values of Z are tabulated in the AISC *Manual of Steel Construction* (*5*). For hybrid noncomposite sections, the products of the yield strength and Z value for each individual component would be summed to calculate M_p.

For composite sections, the stress distribution in the cross-section at M_p is assumed independent of the manner in which the stresses are induced into the beam. Thus, M_p is computed in the same manner for both unshored and shored construction even though the elastic stress distribution differs for each method of construction. Also, creep and shrinkage are assumed to have no effect on the internal stress distribution at M_p. Thus, when checking the flexural resistance of a composite section against M_p, the moments acting on the noncomposite, long-term composite and short-term composite sections may be directly summed for comparison to M_p. The effect of the sequence of application of the different types of loads on the stress states and partial yielding within the cross-section on the resistance is not considered.

For composite sections in positive flexure, the attainment of M_p is possible only if the steel girder is provided with an adequate number of shear connectors so that the horizontal shear force from the concrete deck is effectively transmitted to the steel girder. The natural bond between the steel and concrete is not sufficient by itself. The design of shear connectors for ultimate strength is covered in a later section of

this chapter under Shear Connector Design (Section 2.2.5.3). M_p for a composite section in positive flexure can be determined as follows:

1) calculate the plastic forces of each individual component in the cross-section and use them to determine whether the plastic neutral axis is in the web, top flange or concrete deck,
2) calculate the location of the plastic neutral axis within the element determined in Step 1, and
3) calculate M_p. AASHTO LRFD Article D6.1 in Appendix D to Section 6 provides equations for seven possible cases in AASHTO LRFD Table D6.1-1 (Table 2.1).

In the table, d is the distance from the element plastic force to the plastic neutral axis. The element forces are assumed to act at the mid-thickness of the flanges and concrete deck, at the mid-depth of the web and at the center of the longitudinal reinforcement.

The element forces in the table are to be computed as follows:

$$P_{rt} = F_{yrt}A_{rt}$$

$$P_s = 0.85f'_c b_s t_s$$

$$P_{rb} = F_{yrb}A_{rb}$$

$$P_c = F_{yc}b_c t_c$$

$$P_w = F_{yw}Dt_w$$

$$P_t = F_{yt}b_t t_t$$

All element forces, dimensions and distances are to be taken as positive. The conditions should be checked in the order listed in the table. The forces in the longitudinal reinforcement may be conservatively neglected by setting the terms P_{rb} and P_{rt} equal to zero in the equations given in the table. Application of the table to the composite cross-section given in Figure 2.3 is illustrated below.

EXAMPLE

Calculate the plastic moment M_p for the composite section shown in Figure 2.3, which is in a region of positive flexure, using the equations given in AASHTO LRFD Table D6.1-1 (Table 2.1). The longitudinal reinforcement will be conservatively neglected. Assume the web and flange steel is Grade 50W steel and that f'_c for the concrete deck is 4.0 ksi. The effective flange width of the concrete deck b_{eff} was computed earlier to be 100.0 inches.

$$P_t + P_w + P_c = A_{steel}F_y = 75.25(50) = 3{,}763 \text{ kips}$$

$$P_s = 0.85f_c' \, b_{eff} t_s = 0.85(4.0)(100.0)(9.0) = 3{,}060 \text{ kips}$$

$$3{,}060 \text{ kips} < 3{,}763 \text{ kips}$$

$\therefore$ PNA is in the top flange, use Case II in *AASHTO LRFD* Table D6.1-1 (Table 2.1)

$$\bar{y} = \frac{t_c}{2}\left[\frac{P_w + P_t - P_s}{P_c} + 1\right]$$

$$\bar{y} = \frac{1.0}{2}\left[\frac{50(69.0)(0.5) + 50(1.375)(18.0) - 3{,}060}{50(1.0)(16.0)} + 1\right]$$

$$= 0.44 \text{ in. from the top of the top flange}$$

Check equilibrium by calculating and comparing the total plastic forces acting on the compression and tension sides of the plastic neutral axis:

Compression side:

$$3{,}060 + (0.44)(16.0)(50) = 3{,}412 \text{ kips}$$

Tension side:

$$(1.0 - 0.44)(16.0)(50) + (69.0)(0.5)(50) + (18.0)(1.375)(50) = 3{,}411 \text{ kips} \quad \text{ok}$$

$$M_p = \frac{P_c}{2t_c}\left[\bar{y}^2 + (t_c - \bar{y})^2\right] + \left[P_s d_s + P_w d_w + P_t d_t\right]$$

Calculate the distances from the PNA to the centroid of each element:

$$d_s = \frac{9.0}{2} + 3.5 + 0.44 - 1.0 = 7.44 \text{ in.}$$

$$d_w = 1.0 + \frac{69.0}{2} - 0.44 = 35.06 \text{ in.}$$

$$d_t = 1.0 + 69.0 + \frac{1.375}{2} - 0.44 = 70.25 \text{ in.}$$

$$M_p = \left[\frac{50(1.0)(16.0)}{2(1.0)}\right]\left[(0.44)^2 + (1.0 - 0.44)^2\right] +$$
$$\left[(3{,}060)(7.44) + 69.0(0.5)(50)(35.06) + 1.375(18.0)(50)(70.25)\right]$$

$$M_p = 170{,}382 \text{ kip} - \text{in.} = 14{,}199 \text{ kip} - \text{ft}$$

For composite sections in negative flexure, a similar procedure can be used. In this case, however, the tensile strength of the concrete is ignored and the contribution of the longitudinal reinforcement should be included. *AASHTO LRFD* Table D6.1-2 (Table 2.2) contains the equations for the two cases most likely to occur in practice. Again, the conditions should be checked in the order listed in the table.

AASHTO LRFD Tables D6.1-1 and D6.1-2 (Table 2.1 and Table 2.2) can also be used to compute M_p for a noncomposite section as well, if desired, by eliminating the terms pertaining to the longitudinal reinforcement and the concrete deck from the equations. The tables can also be applied to compute M_p for a closed-box or tub section by applying the equations to calculate M_p for one-half of the box section. For sections with inclined webs, the web depth D should be measured along the web slope.

5.   AISC. 2001. *Manual of Steel Construction – Load and Resistance Factor Design*. 3rd Ed. American Institute of Steel Construction, Chicago, IL, November 2001.

Table 2.1 Calculation of $\overline{Y}$ and M_p for Sections in Positive Flexure

CASE	PNA	CONDITION	$\overline{Y}$ AND M_p
I	In Web	$P_t + P_w \geq P_c + P_s + P_{rb} + P_{rt}$	$\overline{Y} = \left(\dfrac{D}{2}\right)\left[\dfrac{P_t - P_c - P_s - P_{rt} - P_{rb}}{P_w} + 1\right]$ $M_p = \dfrac{P_w}{2D}\left[\overline{Y}^2 + (D - \overline{Y})^2\right] + \left[P_s d_s + P_{rt} d_{rt} + P_{rb} d_{rb} + P_c d_c + P_t d_t\right]$
II	In Top Flange	$P_t + P_w + P_c \geq P_s + P_{rb} + P_{rt}$	$\overline{Y} = \left(\dfrac{t_c}{2}\right)\left[\dfrac{P_w - P_t - P_s - P_{rt} - P_{rb}}{P_c} + 1\right]$ $M_p = \dfrac{P_c}{2t_c}\left[\overline{Y}^2 + (t_c - \overline{Y})^2\right] + \left[P_s d_s + P_{rt} d_{rt} + P_{rb} d_{rb} + P_c d_c + P_t d_t\right]$
III	Concrete Deck, Below P_{rb}	$P_t + P_w + P_c \geq \left(\dfrac{c_{rb}}{t_s}\right)P_s + P_{rb} + P_{rt}$	$\overline{Y} = (t_s)\left[\dfrac{P_c + P_w + P_t - P_{rt} - P_{rb}}{P_s}\right]$ $M_p = \left(\dfrac{\overline{Y}^2 P_s}{2t_s}\right) + \left[P_{rt} d_{rt} + P_{rb} d_{rb} + P_c d_c + P_w d_w + P_t d_t\right]$
IV	Concrete Deck, at P_{rb}	$P_t + P_w + P_c + P_{rb} \geq \left(\dfrac{c_{rb}}{t_s}\right)P_s + P_{rt}$	$\overline{Y} = c_{rb}$ $M_p = \left(\dfrac{\overline{Y}^2 P_s}{2t_s}\right) + \left[P_{rt} d_{rt} + P_c d_c + P_w d_w + P_t d_t\right]$
V	Concrete Deck, Above P_{rb} Below P_{rt}	$P_t + P_w + P_c + P_{rb} \geq \left(\dfrac{c_{rt}}{t_s}\right)P_s + P_{rt}$	$\overline{Y} = (t_s)\left[\dfrac{P_{rb} + P_c + P_w + P_t - P_{rt}}{P_s}\right]$ $M_p = \left(\dfrac{\overline{Y}^2 P_s}{2t_s}\right) + \left[P_{rt} d_{rt} + P_{rb} d_{rb} + P_c d_c + P_w d_w + P_t d_t\right]$
VI	Concrete Deck, at P_{rt}	$P_t + P_w + P_c + P_{rb} + P_{rt} \geq \left(\dfrac{c_{rt}}{t_s}\right)P_s$	$\overline{Y} = c_{rt}$ $M_p = \left(\dfrac{\overline{Y}^2 P_s}{2t_s}\right) + \left[P_{rb} d_{rb} + P_c d_c + P_w d_w + P_t d_t\right]$
VII	Concrete Deck, Above P_{rt}	$P_t + P_w + P_c + P_{rb} + P_{rt} \geq \left(\dfrac{c_{rt}}{t_s}\right)P_s$	$\overline{Y} = (t_s)\left[\dfrac{P_{rb} + P_c + P_w + P_t + P_{rt}}{P_s}\right]$ $M_p = \left(\dfrac{\overline{Y}^2 P_s}{2t_s}\right) + \left[P_{rt} d_{rt} + P_{rb} d_{rb} + P_c d_c + P_w d_w + P_t d_t\right]$
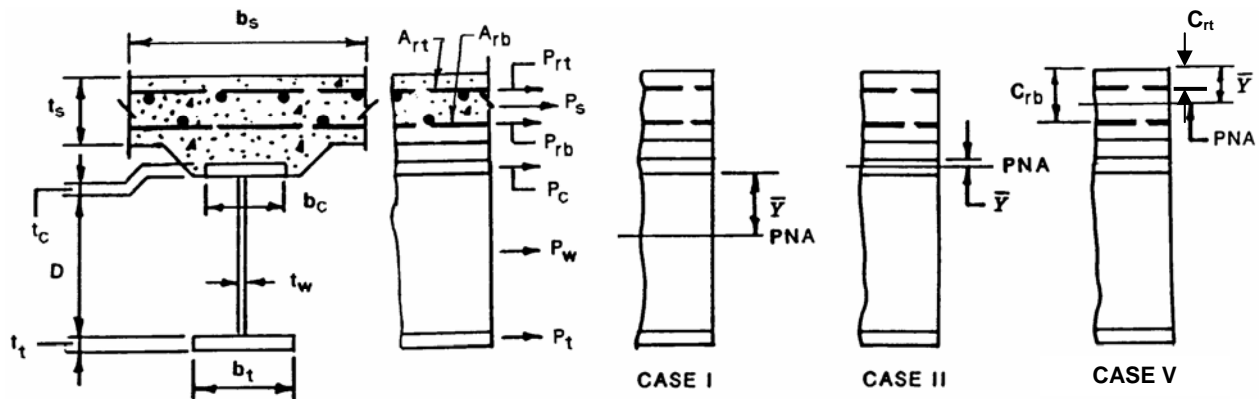
Table 2.2 Calculation of $\overline{Y}$ and M_p for Sections in Negative Flexure

CASE	PNA	CONDITION	$\overline{Y}$ AND M_p
I	In Web	$P_c + P_w \geq P_t + P_{rb} + P_{rt}$	$\overline{Y} = \left(\dfrac{D}{2}\right)\left[\dfrac{P_c - P_t - P_{rt} - P_{rb}}{P_w} + 1\right]$ $M_p = \dfrac{P_w}{2D}\left[\overline{Y}^2 + (D - \overline{Y})^2\right] + \left[P_{rt}d_{rt} + P_{rb}d_{rb} + P_t d_t + P_c d_c\right]$
II	In Top Flange	$P_c + P_w + P_t \geq P_{rb} + P_{rt}$	$\overline{Y} = \left(\dfrac{t_t}{2}\right)\left[\dfrac{P_w + P_c - P_{rt} - P_{rb}}{P_t} + 1\right]$ $M_p = \dfrac{P_t}{2t_t}\left[\overline{Y}^2 + (t_t - \overline{Y})^2\right] + \left[P_{rt}d_{rt} + P_{rb}d_{rb} + P_w d_w + P_c d_c\right]$
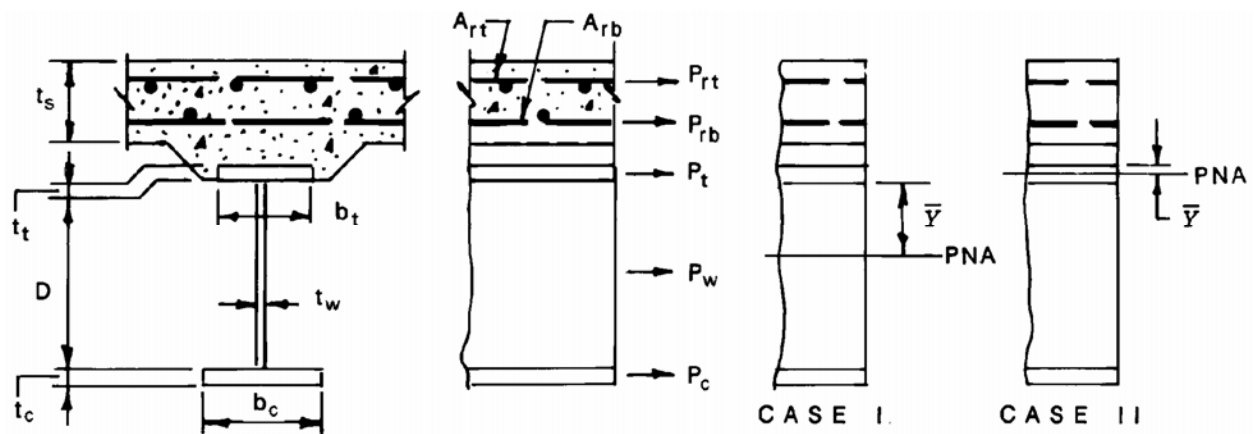
2.2.2.2 Yield Moment

The yield moment M_y is defined in the *AASHTO LRFD* Specifications as the moment at which an outer fiber, in a member subjected to flexure about the major-axis, attains the nominal yield stress neglecting the effect of any residual stresses. In the *AASHTO LRFD* Specifications, M_y is used in the resistance calculations for certain types of sections – primarily compact composite sections in regions of positive flexure in straight continuous-span bridges.

AASHTO LRFD Article D6.2 in Appendix D to Section 6 discusses the yield moment. For a noncomposite section, *AASHTO LRFD* Article D6.2.1 states that M_y is to be taken as the smaller of the moment required to cause nominal first yielding in the compression flange (M_{yc}), or the moment required to cause nominal first yielding in the tension flange (M_{yt}) at the strength limit state.

AASHTO LRFD Article D6.2.2 states that for composite sections in positive flexure, M_y is to be taken as the sum of the moments applied separately to the steel, short-term and long-term composite sections to cause nominal first yielding in either flange at the strength limit state. M_y is taken as the lesser of either M_{yc} or M_{yt}. As discussed in the previous section, in a composite girder, moments are applied to different sections and this fact must be appropriately accounted for in the computation of M_y. M_y for a composite section in positive flexure can therefore be determined as follows: 1) calculate the moment M_{D1} caused by the factored permanent load applied before the concrete deck has hardened or is made composite and apply this moment to the steel section, 2) calculate the moment M_{D2} caused by the remainder of the factored permanent load and apply this moment to the long-term composite section, 3) calculate the additional moment M_{AD} that must be applied to the short-term composite section to cause nominal yielding in either steel flange, and 4) calculate M_y as the sum of the total permanent load moment and M_{AD}. This procedure can be represented in equation form as follows:

> ➢ Solve for M_{AD} from the following equation:

$$F_{yf} = \frac{M_{D1}}{S_{NC}} + \frac{M_{D2}}{S_{LT}} + \frac{M_{AD}}{S_{ST}}$$

Equation 2.5

AASHTO LRFD Equation D6.2.2-1

> ➢ Calculate:

$$M_y = M_{D1} + M_{D2} + M_{AD}$$

Equation 2.6

AASHTO LRFD Equation D6.2.2-2

where:
S_{NC} = section modulus for the steel section (in.^{3})
S_{ST} = section modulus for the long-term composite section (in.^{3})

S_{LT} = section modulus for the short-term composite section (in.^{3})

In regions of positive flexure, the longitudinal reinforcement may be neglected in the calculation of S_{ST} and S_{LT}.

For a composite section in negative flexure, *AASHTO LRFD* Article D6.2.3 states that a procedure similar to the above is to be used to compute M_y, only in this case, both S_{ST} and S_{LT} are to be taken for the section consisting of the steel girder plus the longitudinal reinforcement within the effective flange width of the concrete deck. Also, M_{yt} is to be taken with respect to either the tension flange or the longitudinal reinforcement, whichever is the smallest value. *AASHTO LRFD* Article D6.2.4 addresses the procedure to be used for sections with cover plates.

In all cases, the calculations are to disregard the effects of any flange lateral bending or local web yielding in hybrid sections.

EXAMPLE

Calculate the yield moment M_y for the composite section shown in Figure 2.3, which is in a region of positive flexure, using the equations given in *AASHTO LRFD* Article D6.2.2. For a composite section in positive flexure, M_{yt}, or the yield moment calculated for the tension flange, typically controls. From earlier calculations, the section moduli to the bottom flange were calculated as follows: S_{NC} = 1,973 in.^{3}; S_{LT} = 2,483 in.^{3}; S_{ST} = 2,706 in.^{3}. Use the unfactored bending moments at this section given in a previous example. Assume the calculation is to be done for Load Combination Strength I and that the load modifier η is to be taken equal to 1.0 (see DM Volume 1, Chapter 5 for a further discussion of the Strength I Load Combination and the load modifier η).

$$F_{yf} = \frac{M_{D1}}{S_{NC}} + \frac{M_{D2}}{S_{LT}} + \frac{M_{AD}}{S_{ST}}$$

AASHTO LRFD Equation D6.2.2-1

$$50 = 1.0\left[\frac{1.25(2,202)(12)}{1,973} + \frac{1.25(335)(12) + 1.50(322)(12)}{2,483} + \frac{M_{AD}}{2,706}\right]$$

$$M_{AD} = 78,206 \text{ kip-in.} = 6,517 \text{ kip-ft}$$

$$M_y = M_{D1} + M_{D2} + M_{AD}$$

AASHTO LRFD Equation D6.2.2-2

$$M_y = 1.0\left[1.25(2,202) + 1.25(335) + 1.50(322) + 6,517\right]$$
$$M_y = 10,171 \text{ kip-ft}$$

The ratio of M_p/M_y is a property of the cross-sectional shape known as the shape factor. For doubly symmetric noncomposite I-shapes bent about their major axis, the shape factor is approximately 1.12. For singly symmetric composite girders in regions of positive flexure, the shape factor is much larger. Values on the order of 1.4 to 1.6 are quite common.

2.2.2.3 Depth of the Web in Compression

2.2.2.3.1 In the Elastic Range (D$_c$)

In the *AASHTO LRFD* Specifications, the depth of the web in compression in the elastic range D_c is used primarily in computing the web bend-buckling resistance F_{crw} and the web load-shedding factor R_b, both of which are described in more detail below. For composite sections in negative flexure and noncomposite sections, D_c is also used to determine whether the section qualifies as a slender or a non-slender web section for determining the nominal flexural resistance. Slender and non-slender web sections are discussed later on in this chapter as well.

In the elastic range of stress at the service, fatigue and strength limit states, D$_c$ for composite sections is a function of the dead-to-live load stress ratio. This is because in a composite girder, the dead and live loads are applied to different sections, as discussed previously. For composite sections in positive flexure, this is an especially important consideration as the dead-load stress has a significant effect on the location of the elastic neutral axis. Note that when checking the section for web bend-buckling during construction, however, while the girder is still in the noncomposite condition before the concrete deck hardens or is made composite, D_c of the steel section alone (which is a section property independent of the stress) is used in the calculations.

At sections in positive flexure, D_c of the composite section (refer to Figure 2.7 – the terms shown in the figure are described below) increases with increasing span length because of the increasing dead-to-live load ratio. With increasing spans, the larger noncomposite dead load stresses acting on the steel section alone effectively cause the neutral axis to be much lower than it would if all loads were applied to the composite section, which obviously increases the depth of the web in compression. Therefore, in general, it is important in certain cases to recognize the effect of the dead load stress on the location of the neutral axis at these sections.

AASHTO LRFD Article D6.3.1 in Appendix D to Section 6 states that D_c for composite sections in positive flexure is to be taken as the depth over which the algebraic sum of the stresses acting on the steel, long-term composite and short-term composite sections due to the dead and live loads, plus impact, is compressive. The following equation, which can simply be derived from an examination of the stress diagram and cross-section given in Figure 2.7, is provided in this article to compute D_c in lieu of calculating D_c utilizing the individual stress diagrams:
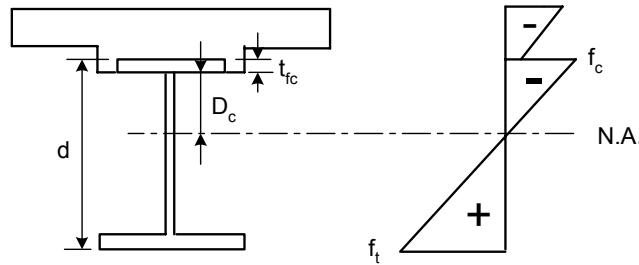
Figure 2.7 D_c for a Composite Section in Positive Flexure

$$D_c = \left(\frac{-f_c}{|f_c| + f_t} \right) d - t_{fc} \geq 0 \qquad \qquad \text{Equation 2.7}$$

AASHTO LRFD Equation D6.3.1-1

where:
d	=	total depth of the steel section (in.)
f_c	=	sum of the compression-flange stresses caused by the different loads, i.e. DC1, the permanent load acting on the noncomposite section; DC2, the permanent load acting on the long-term composite section; DW, the wearing surface load acting on the long-term composite section; and LL+IM, live load plus impact acting on the short-term composite section (ksi). For stresses in compression, f_c is to be taken as negative.
f_t	=	sum of the tension-flange stresses caused by the different loads (ksi) – see above.
t_{fc}	=	thickness of the compression flange (in.)

Flange lateral bending stresses are to be ignored in the computation of f_c and f_t.

EXAMPLE

Calculate the depth of the web in compression D_c for the composite section shown in Figure 2.3, which is in a region of positive flexure, using Equation 2.7.   Assume the calculation is to be done for Load Combination Strength I and that the load modifier η is to be taken equal to 1.0 (see DM Volume I, Chapter 5 for a further discussion of the Strength I Load Combination and the load modifier η). From earlier calculations, the sum of the factored stresses in the tension flange f_t was computed to be +48.26 ksi. From separate calculations similar to those illustrated previously, the sum of the factored stresses in the compression flange f_c is computed to be –28.46 ksi.

$$D_c = \left(\frac{-f_c}{|f_c| + f_t} \right) d - t_{fc} \geq 0$$

AASHTO LRFD Equation D6.3.1-1

$$d = 1.375 + 69.0 + 1.0 = 71.375 \text{ in.}$$

$$t_{fc} = 1.0 \text{ in.}$$

$$D_c = \left(\frac{-(-28.46)}{|-28.46| + 48.26} \right) 71.375 - 1.0 = 25.48 \text{ in.}$$

Note from the previous elastic section property calculations that D_c for the short-term ($n = 8$) composite section is (11.70 in. − 1.0 in.) = 10.70 in. Therefore, the noncomposite dead load stress has a significant effect on the actual value of D_c for this composite section.

According to the AASHTO LRFD Specifications, for composite sections in positive flexure at the fatigue, service and strength limit states, D_c only needs to be employed in the computation of the nominal flexural resistance for sections in which longitudinal web stiffeners are required based on AASHTO LRFD Article 6.10.2.1.1.

For composite sections in positive flexure *without* longitudinal web stiffeners that meet the section proportioning limits of *AASHTO LRFD* Article 6.10.2, and also the ductility requirement of *AASHTO LRFD* Article 6.10.7.3 to prevent premature crushing of the concrete deck, the web bend-buckling resistance F_{crw} is generally close to or larger than the yield stress of the compression flange F_{yc} at the strength limit state. Also, for loads applied at the service and fatigue limit states after the deck has hardened or is made composite, the increased compressive stresses in the web tend to be compensated for by the increase in F_{crw} resulting from the corresponding decrease in D_c after the section becomes composite. These compensating effects simply continue at the strength limit state. As a result, since theoretical web bend-buckling of these sections is essentially prevented at all elastic stress levels, the web load-shedding factor R_b (discussed below) is specified to be 1.0 for composite sections in positive flexure without longitudinal web stiffeners. Since computations of F_{crw} and R_b are not required for these sections, it follows that a computation of D_c is also not required. For sections with longitudinal web stiffeners, the section proportioning requirements of *AASHTO LRFD* Article 6.10.2.1.2 are not generally sufficient to ensure that web bend-buckling will not occur. As a result, the specifications require the calculation of F_{crw} and R_b, and consequently D_c, for these sections. The calculation of D_c for composite sections in positive flexure can potentially complicate bridge load rating calculations because of the dependency of the flexural resistance on the applied load. Therefore, avoiding the computation of D_c is desirable where practical.

Figure 2.8 Continuous Steel Girder Bridge

For composite sections in negative flexure, the concrete deck is typically not considered to be effective in tension, except perhaps at the fatigue and service limit states as permitted by the Specifications (and discussed previously). When the concrete deck is not considered effective, the distance between the neutral-axis locations for the steel and composite sections is small, as the composite section only consists of the steel section plus the longitudinal reinforcement. As a result, the location of the neutral axis for the composite section is essentially unaffected by the dead load stress. In fact, accounting for the effect of the dead load stress actually results in a smaller value of D_c in regions of negative flexure.

Therefore, for the majority of situations involving composite sections in negative flexure, AASHTO LRFD Article D6.3.1 of the Specifications conservatively specifies the use of D_c computed for the section consisting of the steel girder plus the longitudinal reinforcement, without considering the algebraic sum of the stresses acting on the noncomposite and composite sections. Again, this avoids potential difficulties in bridge load rating calculations since the resulting value of D_c is independent of the applied loading.

A single exception to the preceding requirement is specified; that is, if the concrete deck is assumed effective in tension in regions of negative flexure at the service limit state, as permitted for composite girders that have shear connectors throughout their entire length and minimum longitudinal reinforcement satisfying the provisions of *AASHTO LRFD* Article 6.10.4.2.1, Equation 2.7 must be used to compute D_c. When calculating the web bend-buckling resistance F_{crw} at the service limit state, a more precise calculation of D_c, accounting for the *beneficial* effect of the dead load stress in this case, is required when the concrete deck is considered effective in tension. Otherwise, the reduction in F_{crw} will be too large and not reflective of the actual potential web bend-buckling resistance at this limit state.

EXAMPLE

Calculate the depth of the web in compression D_c for the composite section shown in Figure 2.6, which is in a region of negative flexure, using Equation 2.7.   Assume the calculation is to be done for Load Combination Service II (see DM Volume 1, Chapter 5 for a further discussion of the Service II Load Combination) and that the appropriate conditions specified in *AASHTO LRFD* Article 6.10.4.2.1 are met to allow the concrete deck to be considered effective in tension for this load combination. From separate calculations similar to those illustrated previously, the composite elastic section moduli for the long-term (3n) and short-term (n) composite sections for the section shown in Figure 2.6, including the concrete deck, are as follows:

Composite Section; 3n = 24: $S_{TOP\ OF\ STEEL}$ = 6,148 in^3 $S_{BOT\ OF\ STEEL}$ = 3,594 in^3

Composite Section; n = 8: $S_{TOP\ OF\ STEEL}$ = 13,772 in^3 $S_{BOT\ OF\ STEEL}$ = 3,875 in^3

Using section properties for the steel section (computed earlier) along with the section properties given above and the unfactored moments given earlier in a previous example for this section, calculate the factored Service II stresses f_t in the top flange and f_c in the bottom flange:

Top flange:

$$f_t = \left[\frac{1.0(-4,840)}{2,942} + \frac{1.0(-690 + -664)}{6,148} + \frac{1.3(-4,040)}{13,772} \right] 12 = 26.96 \text{ ksi}$$

Bottom flange:

$$f_c = \left[\frac{1.0(-4,840)}{3,149} + \frac{1.0(-690 + -664)}{3,594} + \frac{1.3(-4,040)}{3,875} \right] 12 = -39.23 \text{ ksi}$$

Calculate D_c using Equation 2.7:

$$D_c = \left(\frac{-f_c}{|f_c| + f_t} \right) d - t_{fc} \geq 0$$

AASHTO LRFD Equation D6.3.1-1

$$d = 2.0 + 69.0 + 2.0 = 73.0 \text{ in.}$$

$$t_{fc} = 2.0 \text{ in.}$$

$$D_c = \left(\frac{-(-39.23)}{|-39.23| + 26.96} \right) 73.0 - 2.0 = 41.27 \text{ in.}$$

Note from separate calculations that D_c for the short-term (n = 8) composite section is equal to 54.97 in. Therefore, this example clearly illustrates the substantial benefit

of calculating D_c taking into account the effect of the dead load stress when the concrete is considered effective in tension in regions of negative flexure at the service limit state.

2.2.2.3.2 At the Plastic Moment (D_{cp})

In the *AASHTO LRFD* Specifications, the depth of the web in compression at the plastic moment D_{cp} is used primarily in one of the criteria to determine if a composite section in positive flexure qualifies as a compact section at the strength limit state, and to determine if a non-slender composite section in negative flexure or a non-slender noncomposite section qualifies as either a compact web or a noncompact web section at the strength limit state. All the preceding section classifications for determining the nominal flexural resistance are discussed in more detail later on in this chapter.

At sections in positive flexure, the depth of the web in compression typically reduces (i.e. from D_c) as plastic strains associated with moments larger than R_hM_y are incurred. R_h is the hybrid factor discussed in more detail below. In fact, for composite sections in positive flexure, the neutral axis at the plastic moment M_p will often be located either in the concrete deck or in the top flange of the steel girder, as illustrated in the example M_p calculation given above. In such cases, the entire web of the girder is in tension and D_{cp} is to be taken as zero according to *AASHTO LRFD* Article D6.3.2. When D_{cp} is equal to zero, all web-slenderness requirements in the Specifications based on D_{cp} are assumed automatically satisfied. The location of the plastic neutral axis for composite sections in positive flexure can be determined from the conditions listed in *AASHTO LRFD* Table D6.1-1 (Table 2.1). Again, the position of the plastic neutral axis is calculated based on the equilibrium condition that there be no net axial force acting on the assumed fully yielded cross-section. For deeper girders (e.g. with longitudinal web stiffeners), it is possible that the conditions in *AASHTO LRFD* Table D6.1-1 (Table 2.1) may indicate that the plastic neutral axis is located in the web. In this case, D_{cp} may be calculated from the following equation given in *AASHTO LRFD* Article D6.3.2:

$$D_{cp} = \frac{D}{2}\left(\frac{F_{yt}A_t - F_{yc}A_c - 0.85f'_cA_s - F_{yrs}A_{rs}}{F_{yw}A_w} + 1\right) \qquad \text{Equation 2.8}$$

AASHTO LRFD Equation D6.3.2-1

where:
- A_c = area of the compression flange (in^2)
- A_{rs} = total area of the longitudinal reinforcement within the effective concrete deck width (in^2)
- A_s = area of the concrete deck (in^2)
- A_t = area of the tension flange (in^2)
- A_w = area of the web (in^2)
- $F_{yc}, F_{yt}, F_{yw}, F_{yrs}$ = specified minimum yield strength of the compression flange, tension flange, web and longitudinal reinforcement, respectively (ksi)

At sections in negative flexure, the depth of the web in compression typically increases (i.e. from D_c) as plastic strains associated with moments larger than $R_h M_y$ are incurred. The location of the plastic neutral axis for composite sections in negative flexure and for noncomposite sections can be determined from the conditions listed in *AASHTO LRFD* Table D6.1-2 (Table 2.2 – note that for noncomposite sections, all terms related to the longitudinal reinforcement in *AASHTO LRFD* Table D6.1-2 (Table 2.2) should be set equal to zero). In calculating D_{cp} in regions of negative flexure, the concrete deck is assumed not to be effective in tension. Therefore, in most all cases, the plastic neutral axis will be located in the web. For rare cases in which the plastic neutral axis is located in the top flange and the entire web is in compression, D_{cp} is to be taken equal to the web depth D according to *AASHTO LRFD* Article D6.3.2.   For composite sections in negative flexure where the plastic neutral axis is located in the web, D_{cp} may be computed as follows (all terms are defined above):

$$D_{cp} = \frac{D}{2A_w F_{yw}} \left[F_{yt} A_t + F_{yw} A_w + F_{yrs} A_{rs} - F_{yc} A_c \right] \qquad \text{Equation 2.9}$$

AASHTO LRFD Equation D6.3.2-2

EXAMPLE

Calculate the depth of the web in compression D_{cp} for the composite section shown in Figure 2.6, which is in a region of negative flexure, using Equation 2.9. Recall that this section is assumed to be a hybrid section utilizing Grade HPS 70W steel flanges and a Grade 50W web. The area of longitudinal reinforcement A_{rs} was determined previously to be 9.30 in^2 with a specified minimum yield strength F_{yrs} = 60 ksi.

$$A_t = (2.0)(18.0) = 36.0 \text{ in}^2$$
$$A_w = (0.5625)(69.0) = 38.8 \text{ in}^2$$
$$A_c = (2.0)(20.0) = 40.0 \text{ in}^2$$

$$D_{cp} = \frac{D}{2A_w F_{yw}} \left[F_{yt} A_t + F_{yw} A_w + F_{yrs} A_{rs} - F_{yc} A_c \right]$$

AASHTO LRFD Equation D6.3.2-2

$$D_{cp} = \frac{69.0}{2(38.8)(50)} \left[(70)(36.0) + (50)(38.8) + (60)(9.30) - (70)(40.0) \right] = 39.44 \text{ in.}$$

Check equilibrium by calculating and comparing the total plastic forces acting on the tension and compression sides of the plastic neutral axis:

Tension side:

$$(69.0 - 39.44)(0.5625)(50) + (36.0)(70) + (9.30)(60) = 3,909 \text{ kips}$$

Compression side:

$$(39.44)(0.5625)(50) + (40.0)(70) = 3,909 \text{ kips} \quad \text{ok}$$

Note that for the section consisting of the steel girder plus the longitudinal reinforcement, the elastic depth of the web in compression D_c is (38.55 in. − 2.0 in.) = 36.55 in., which is smaller than D_{cp} as expected.

2.2.2.4 Web Bend-Buckling Resistance F_{crw}

The buckling behavior of a slender web plate subject to pure bending is similar to the buckling behavior of a flat plate. A perfectly flat plate with no initial imperfections would not deflect laterally from its initial flat position until its theoretical buckling load is reached. However, in many experimental tests, bending deformations and associated transverse displacements of web plates occur from the onset of load application due to initial web out-of-flatness, and increase progressively throughout the entire range of applied bending moment. As expected, these deformations are largest in the compression zone of the web. Because of the stable postbuckling behavior of the web, however, a significant change in the rate of increase of the transverse displacements of the web as a function of the applied loads is not observed as the theoretical web bend-buckling stress is exceeded (*6*). Therefore, web bend-buckling behavior is essentially a load-deflection rather than a bifurcation phenomenon; that is, a distinct buckling load is not observed.

Since web plates in bending do not collapse when the theoretical buckling load is reached, the available postbuckling strength can be considered in determining the nominal flexural resistance of sections with slender webs at the strength limit state, as discussed in the next section under the topic of the Web Load-Shedding Factor. However, in certain situations, it is desirable to limit the bending deformations and transverse displacements of the web. This is particularly true during the construction condition and at the service and fatigue limit states.

The advent of composite design has led to a significant reduction in the size of compression flanges in regions of positive flexure. As a result, more than half of the web of the noncomposite section will be in compression in these regions during the construction condition before the concrete deck has hardened or is made composite. As a result, the web is more susceptible to bend-buckling in this condition.

Control of transverse web displacements at the fatigue limit state is also desirable to prevent significant elastic out-of-plane flexing of the web under repeated live loading, which could potentially lead to fatigue cracks at the web-to-flange junctions.

And finally, at the service limit state, a significant structural performance requirement is to prevent objectionable permanent deflections of the girders due to expected severe traffic loadings that could impair the riding quality of the bridge. Therefore, a control on the amount of transverse web displacement is again desirable. In a composite girder at the service limit state, regions in negative flexure are most

susceptible to web bend-buckling, especially when the concrete deck is assumed effective in tension as permitted for composite sections satisfying the provisions of *AASHTO LRFD* Article 6.10.4.2.1. In this case, more than half the web is likely to be in compression, again increasing the susceptibility of the web to bend-buckling.

To control the web plate bending strains and transverse displacements during construction and at the fatigue and service limit states, the *AASHTO LRFD* Specifications use the theoretical web bend-buckling load as a simple index. The web bend-buckling resistance is specified in *AASHTO LRFD* Article 6.10.1.9. The equation for the web bend-buckling resistance F_{crw} (in units of ksi) is provided in *AASHTO LRFD* Article 6.10.1.9.1. This equation is derived from the equation for the elastic buckling stress of a flat plate subject to pure bending (*7*):

$$F_{cr} = \frac{k\pi^2 E}{12(1-\mu^2)(b/h)^2}$$

Equation 2.10

AASHTO LRFD Article C6.9.4.2

where:

b	=	width of the plate along the edge subject to bending (in.)
E	=	Young's modulus (29,000 ksi for steel)
h	=	thickness of the plate (in.)
k	=	bend-buckling coefficient (discussed below)
μ	=	Poisson's ratio (0.3 for steel)

Substituting the slenderness ratio D/t_w of the web for *b/h*, and the values of *E,* π and μ in Equation 2.10 yields Equation 2.11 as follows:

$$F_{crw} = \frac{0.9Ek}{\left(\dfrac{D}{t_w}\right)^2}$$

Equation 2.11

AASHTO LRFD Equation 6.10.1.9.1-1

F_{crw} is not to exceed the smaller of $R_h F_{yc}$ and $F_{yw}/0.7$, where F_{yc} and F_{yw} are the specified minimum yield strengths of the compression flange and web, respectively, and R_h is the hybrid factor (discussed below). Since the web carries only a relatively small portion of the total bending moment, the transition zone resulting from inelastic buckling is not considered significant and only an elastic buckling equation is provided.

F_{crw} is to be checked against the maximum compression-flange bending stress due to the factored loads, calculated without considering flange lateral bending. Utilizing the maximum compressive stress in the web rather than the stress in the compression flange in order to obtain greater precision is not warranted for this check. In hybrid sections with a lower yield-strength web, the longitudinal and plate bending strains in the inelastic web at the web-flange juncture are constrained by a stable nominally elastic compression flange (*8*). Since the flange will tend to restrain the longitudinal strains resulting from web bend-buckling at compression-flange stress levels up to $R_h F_{yc}$, the use of an F_{crw} value that is potentially greater than F_{yw}

in hybrid sections is felt to be justified. The upper limit of $F_{yw}/0.7$ is a conservative limit to cover hybrid sections with F_{yw}/F_{yc} less than 0.7, which are permitted according to *AASHTO LRFD* Article 6.10.1.3, but are not recommended.

According to *AASHTO LRFD* Article 6.10.3.2, the maximum compression-flange stress in a noncomposite I-section due to the factored loads, calculated without consideration of flange lateral bending, must not exceed the resistance factor for flexure ϕ_f times F_{crw} for all critical stages of construction. This requirement also applies at sections where top flanges of tub girders are subject to compression during construction. For closed-box sections, *AASHTO LRFD* Article 6.11.3.2 states that the maximum longitudinal flange stress due to the factored loads, calculated without consideration of longitudinal warping, must not exceed $\phi_f F_{crw}$ at sections where noncomposite box flanges are subject to compression during construction (note: a box flange is defined in the *AASHTO LRFD* Specifications as a flange connected to two webs). For tub or closed-box sections with inclined webs, D_c should be taken as the depth of the web in compression measured along the slope (i.e. D_c divided by the cosine of the angle of inclination of the web plate with respect to the vertical) when computing F_{crw}. Should F_{crw} be exceeded for the construction condition, the Engineer has several options to consider:

1) provide a larger compression flange or a smaller tension flange to reduce D_c,
2) adjust the deck-placement sequence to reduce the compressive stress in the web,
3) provide a thicker web, or
4) as a last resort should the previous options not prove practical or cost-effective, provide a longitudinal web stiffener.

According to *AASHTO LRFD* Articles 6.10.4.2.2 and 6.11.4, at the service limit state, the compression-flange stress in I- and box (i.e. closed box or tub) sections due to the Service II loads, calculated without consideration of flange lateral bending or longitudinal warping, as applicable, is also not to exceed F_{crw}. A resistance factor is not specified because the resistance factor is defined to be 1.0 for all serviceability checks. For reasons discussed previously (under the topic of D_c), this check is waived for composite sections in positive flexure without longitudinal web stiffeners. Again, for tub or closed-box sections with inclined webs, D_c should be taken as the depth of the web in compression measured along the slope in computing F_{crw}. The options to consider should F_{crw} be exceeded are similar to those discussed in the preceding paragraph related to the construction condition, except obviously for adjustment of the deck-placement sequence.

Figure 2.9 Interior of Box Girder with Inclined Webs

An explicit check on web bend-buckling is not specified at the fatigue limit state in the *AASHTO LRFD* Specifications.   *AASHTO LRFD* Article 6.10.5.3 does provide a check for shear buckling of the web, however, under the shear due to unfactored permanent load plus the factored fatigue load. The factored fatigue load for this particular check is specified to be twice that calculated using the Fatigue Load Combination, which is based on the fatigue live load given in *AASHTO LRFD* Article 3.6.1.4 (see DM Volume 1, Chapter 5 for further discussion on the fatigue live load and the Fatigue Load Combination). The factored fatigue load specified for this check is intended to represent the live loading causing the maximum stress range for fatigue over the assumed 75-year design life of the bridge. This check is discussed in more detail under a later section of this chapter on Fatigue Limit State Verifications (Section 2.2.3.6.1.1.2). A check is not specified for bend-buckling under this load condition because the bend-buckling check under the Service II load combination (discussed in the preceding paragraph) will always control. This includes composite sections in positive flexure with longitudinal web stiffeners that do not satisfy *AASHTO LRFD* Article 6.10.2.1.1. In this case, the smaller value of F_{crw} resulting from the larger value of D_c at the fatigue limit state (i.e. larger than the value at the service limit state) tends to be compensated for by the lower web compressive stress due to the load condition specified for the fatigue limit state check given in *AASHTO LRFD* Article 6.10.5.3.

2.2.2.4.1 Bend-Buckling Coefficient

2.2.2.4.1.1 Webs Without Longitudinal Stiffeners

For webs without longitudinal stiffeners, the bend-buckling coefficient *k* to be substituted in Equation 2.11 is given by *AASHTO LRFD* Equation 6.10.1.9.1-2 as follows:

$$k = \frac{9}{(D_c /D)^2}$$ Equation 2.12

AASHTO LRFD Equation 6.10.1.9.1-2

For a doubly symmetric I-girder (i.e. D_c = 0.5D), Equation 2.12 yields a k value of 36.0. This value is approximately equal to k_{ss} + 0.8(k_{sf} − k_{ss}), where k_{ss} = 23.9 and k_{sf} = 39.6 are the bend-buckling coefficients for simply supported and fully restrained longitudinal edge conditions, respectively, along the flanges (*7*). For singly symmetric I-girders, the use of the k value from Equation 2.12 has been found to provide a reasonable approximation of the theoretical bend-buckling resistance.

To ensure that the above boundary conditions at the web-flange juncture are satisfied, *AASHTO LRFD* Article 6.10.2.2 provides minimum flange proportioning requirements. Specifically, the requirement given by *AASHTO LRFD* Equation 6.10.2.2-3 that the thickness of the flanges be greater than or equal to 1.1 times the thickness of the web, and the requirement given by *AASHTO LRFD* Equation 6.10.2.2-2 that the flange widths equal or exceed 1/6 of the web depth help ensure that the boundary conditions assumed in the web bend-buckling formulation are sufficiently accurate.

Substituting k = 36.0 and the effective web slenderness for a singly symmetric section $2D_c/t_w$ for D/t_w in Equation 2.11 and rearranging yields the web-slenderness limit λ_{rw} for a noncompact-web section given in *AASHTO LRFD* Article 6.10.6.2.3 as follows:

$$\frac{2D_c}{t_w} \le \lambda_{rw} = 5.7\sqrt{\frac{E}{F_{yc}}}$$ Equation 2.13

AASHTO LRFD Equation 6.10.6.2.3-1

This important limit applies to composite sections in negative flexure and noncomposite sections and distinguishes a non-slender versus a slender web section. For sections with webs satisfying this limit (i.e. non-slender web sections), theoretical web bend-buckling will not occur for elastic stress levels, computed according to beam theory, at or below F_{yc}. Therefore, for these sections, the web load-shedding factor R_b (discussed below) will always equal 1.0 and the web bend-buckling checks described above need not be made. Both compact-web and noncompact-web sections (discussed later) fall into this category. Sections not satisfying this limit are termed slender-web sections, which rely on significant post bend-buckling resistance at the strength limit state. For different grades of steel, the slenderness limit λ_{rw} from Equation 2.13 is as follows:

Table 2.3 Slenderness Limit for Different Grades of Steel

F_{yc} (ksi)	λ_{rw}
36.0	162
50.0	137
70.0	116
90.0	102
100.0	97

Although relatively rare, in certain cases, near points of permanent-load contraflexure, both edges of the web (top and bottom) may be in compression when the stresses in the steel and composite sections due to the moments of opposite sign are accumulated. This is particularly true when the concrete is considered to be effective in tension at the service limit state, as permitted in *AASHTO LRFD* Article 6.10.4.2.2. In such cases, the neutral axis lies above the web and Equation 2.12 cannot be used to compute *k*. Therefore, *AASHTO LRFD* Article 6.10.1.9.1 states that when both edges of the web are in compression, *k* for use in Equation 2.11 is to be taken equal to 7.2. This value is approximately equal to the theoretical bend-buckling coefficient for a web plate under *uniform* compression assuming fully restrained longitudinal edge conditions along the flanges (*7*). Although such cases are infrequent and the accumulated web compressive stresses are usually small and unlikely to be critical when this occurs, a *k* value is still provided in the specification to allow these cases to be considered in computer software.

EXAMPLE

Calculate the web bend-buckling resistance F_{crw} for the composite section shown in Figure 2.3, which is in a region of positive flexure, using Equations 2.11 and 2.12. Grade 50W steel is assumed for the flanges and web (i.e. R_h = 1.0). Perform the calculation for the noncomposite section for the constructibility check; i.e. check *AASHTO LRFD* Equation 6.10.3.2.1-3. The maximum accumulated unfactored positive moment at this section due to the deck-casting sequence plus the steel weight, which is assumed to be +2,889 kip-ft, is used in this check. By inspection, the Strength IV Load Combination governs for this particular check (see the later section of this chapter on Constructibility Verifications and DM Volume 1, Chapter 5 for a further discussion of the Strength IV load combination). From separate calculations, the stress in the top (compression) flange due to the factored loads is computed to be f_{bu} = 1.5(-21.93) = -32.89 ksi. From earlier section property calculations, D_c for the steel section is computed to be (39.63 in. – 1.0 in.) = 38.63 in. Since the web slenderness $2D_c/t_w$ of 154.5 exceeds λ_{rw} = 137 for 50-ksi steel from Equation 2.13 (Table 2.3), the steel section is a slender-web section and web bend-buckling must be checked. The resistance factor for flexure ϕ_f is equal to 1.0 (*AASHTO LRFD* Article 6.5.4.2).

$$k = \frac{9}{(D_c/D)^2}$$

AASHTO LRFD Equation 6.10.1.9.1-2

$$k = \frac{9}{(38.63/69.0)^2} = 28.7$$

$$F_{crw} = \frac{0.9Ek}{\left(\dfrac{D}{t_w}\right)^2}$$

<div align="right">AASHTO LRFD Equation 6.10.1.9.1-1</div>

$$F_{crw} = \frac{0.9(29,000)(28.7)}{\left(\dfrac{69.0}{0.5}\right)^2} = 39.33 \text{ ksi}$$

$F_{yw}/0.7 = 50/0.7 = 71.43 \text{ ksi}$

$R_hF_{yc} = (1.0)(50) = 50.00 \text{ ksi (controls)} > 39.33 \text{ ksi} \quad \text{ok}$

$$f_{bu} \le \phi_f F_{crw}$$

<div align="right">*AASHTO LRFD* Equation 6.10.3.2.1-3</div>

$f_{bu} = \left|-32.89 \text{ ksi}\right| < \phi_f F_{crw} = (1.0)(39.33) = 39.33 \text{ ksi} \quad \text{ok}$

As specified in *AASHTO LRFD* Article 6.10.4.2.2, for composite sections in positive flexure without longitudinal stiffeners (i.e. satisfying the web slenderness requirement of *AASHTO LRFD* Article 6.10.2.1.1), a web bend-buckling check is not required at the service limit state.

EXAMPLE

Calculate the web bend-buckling resistance F_{crw} for the hybrid composite section shown in Figure 2.6, which is in a region of negative flexure, using Equations 2.11 and 2.12.   First, perform the calculation for the noncomposite section for the constructibility check; i.e. check *AASHTO LRFD* Equation 6.10.3.2.1-3.   The maximum accumulated unfactored negative moment at this section due to the deck-casting sequence plus the steel weight, which is assumed to be -4,918 kip-ft, is used in this check.   By inspection, the Strength IV Load Combination governs for this particular check. From separate calculations, the stress in the bottom (compression) flange due to the factored loads is computed to be f_{bu} = 1.5(-18.74) = -28.11 ksi. From earlier section property calculations, D_c for the steel section is computed to be (35.26 in. – 2.0 in.) = 33.26 in. Since the web slenderness $2D_c/t_w$ of 118.3 exceeds λ_{rw} = 116 for 70-ksi steel from Equation 2.13 (Table 2.3), the steel section is a slender-web section and web bend-buckling must be checked. The resistance factor for flexure ϕ_f is equal to 1.0 (*AASHTO LRFD* Article 6.5.4.2).   From separate calculations, the hybrid factor R_h (discussed later) for the steel section alone is computed to be 0.983.

$$k = \frac{9}{(D_c/D)^2}$$

<div align="right">AASHTO LRFD Equation 6.10.1.9.1-2</div>

$$k = \frac{9}{(33.26/69.0)^2} = 38.7$$

$$F_{crw} = \frac{0.9Ek}{\left(\dfrac{D}{t_w}\right)^2}$$

<div align="right">AASHTO LRFD Equation 6.10.1.9.1-1</div>

$$F_{crw} = \frac{0.9(29,000)(38.7)}{\left(\dfrac{69.0}{0.5625}\right)^2} = 67.13 \text{ ksi}$$

$F_{yw}/0.7 = 50/0.7 = 71.43 \text{ ksi}$

$R_h F_{yc} = (0.983)(70) = 68.81 \text{ ksi (controls)} > 67.13 \text{ ksi}$ ok

$$f_{bu} \le \phi_f F_{crw}$$

<div align="right">AASHTO LRFD Equation 6.10.3.2.1-3</div>

$f_{bu} = \left|-28.11 \text{ ksi}\right| < \phi_f F_{crw} = (1.0)(67.13) = 67.13 \text{ ksi}$ ok

For sections in negative flexure, a web bend-buckling check is also required at the service limit state according to *AASHTO LRFD* Article 6.10.4.2.2. Therefore, perform the calculation for Load Combination Service II (see DM Volume 1, Chapter 5 for a further discussion of the Service II Load Combination) and assume that the appropriate conditions specified in *AASHTO LRFD* Article 6.10.4.2.1 are met to allow the concrete deck to be considered effective in tension for this load combination. Check *AASHTO LRFD* Equation 6.10.4.2.2-4 for this condition. From earlier computations, D_c for this case, which is a function of the accumulated stresses, was calculated to be 41.27 in. and the Service II stress in the compression flange due to the factored loads f_c was calculated to be 39.23 ksi. From separate calculations, the hybrid factor R_h (discussed later) for the composite section is computed to be 0.977.

$$k = \frac{9}{(41.27/69.0)^2} = 25.2$$

$$F_{crw} = \frac{0.9(29,000)(25.2)}{\left(\dfrac{69.0}{0.5625}\right)^2} = 43.71 \text{ ksi}$$

$F_{yw}/0.7 = 50/0.7 = 71.43 \text{ ksi}$

$R_h F_{yc} = (0.977)(70) = 68.39 \text{ ksi (controls)} > 43.71 \text{ ksi}$ ok

$$f_c \leq F_{crw}$$

AASHTO LRFD Equation 6.10.4.2.2-4

$$f_c = \left| -39.23 \text{ ksi} \right| < F_{crw} = 43.71 \text{ ksi ok}$$

2.2.2.4.1.2 Webs With Longitudinal Stiffeners

For webs with longitudinal stiffeners, the bend-buckling coefficient *k* depends on the distance from the centerline of the closest longitudinal stiffener to the inner surface of compression flange, d_s, with respect to the optimum location of the stiffener, which is at d_s/D_c = 0.4, where D_c is the elastic depth of the web in compression.   The value of *k* to be substituted in Equation 2.11 is therefore given by *AASHTO LRFD* Equation 6.10.1.9.2-1 or *AASHTO LRFD* Equation 6.10.1.9.2-2 as follows:

➤ If $\dfrac{d_s}{D_c} \geq 0.4$, then:

$$k = \frac{5.17}{(d_s/D)^2} \geq \frac{9}{(D_c/D)^2}$$

Equation 2.14

AASHTO LRFD Equation 6.10.1.9.2-1

➤ If $\dfrac{d_s}{D_c} < 0.4$, then:

$$k = \frac{11.64}{\left(\dfrac{D_c - d_s}{D}\right)^2}$$

Equation 2.15

AASHTO LRFD Equation 6.10.1.9.2-2

For existing riveted girders, d_s should be taken between the gage line of the closest angle longitudinal stiffener to the inner leg of the compression-flange element. The development of these equations is discussed in Reference 9.   In cases where Equation 2.14 controls, the longitudinal stiffener is below its optimum location and web bend-buckling occurs in the panel between the stiffener and the compression flange. In cases where Equation 2.15 controls, the stiffener is above its optimum location and web bend-buckling occurs in the panel between the stiffener and the tension flange. In cases where d_s is equal to $0.4D_c$ (i.e. the stiffener is located at its optimum position), web bend-buckling theoretically occurs simultaneously in both panels, in which case, both equations yield a *k* value of 129.3 for the case of a doubly symmetric girder.   Note that both equations for *k* assume simply supported longitudinal edge conditions along the flanges.

Figure 2.10 Girder with Longitudinal Stiffeners

Studies on noncomposite girders have indicated that the optimum location of one longitudinal stiffener is $0.4D_c$ for bending and $0.5D$ for shear. The distance $0.4D_c$ is recommended as the optimum location because shear is almost always accompanied by moment and because a properly proportioned longitudinal stiffener can effectively control lateral web deflections under both bending (*10*) and shear.

Changes in flange size can cause D_c to vary along the girder length. Also, as discussed previously, D_c in a composite girder is a function of the applied load. Because D_c may vary along the span, it is suggested that the longitudinal stiffener be located based on D_c computed at the section with the largest compressive flexural stress. Since the longitudinal stiffener is normally located a fixed distance from the compression flange, the stiffener cannot be at its optimum location at other sections along the girder length with a lower stress and a different D_c. These sections must also be examined to ensure that they satisfy the specified limit states. *AASHTO LRFD* Article 6.10.11.3.1 requires that longitudinal stiffeners be located at a vertical position on the web such that Equation 2.11 is satisfied to prevent web bend-buckling when checking constructibility (refer to *AASHTO LRFD* Equation 6.10.3.2.1-3), and at the service limit state (refer to *AASHTO LRFD* Equation 6.10.4.2.2-4). In addition, the stiffener must be located to satisfy all other appropriate design requirements at the strength limit state. Several trial locations of the stiffener may need to be investigated to determine an appropriate location, particularly for composite sections in regions of positive flexure.

For composite sections in positive flexure, the calculated web bend-buckling resistance is different before and after placement of the deck and is a function of the applied loading. For noncomposite loadings during construction, D_c of the steel section is typically large and web bend-buckling must be checked. In a longitudinally stiffened girder, D_c for the composite girder can also be large enough at the service limit state in regions of positive flexure that web bend-buckling may still be of concern. In this case, D_c must be calculated based on the accumulated flexural stresses due to the factored loads using Equation 2.7. For composite sections in negative flexure, it is suggested that the longitudinal stiffener initially be located at

$0.4D_c$ from the inner surface of the compression flange at the section with the maximum flexural compressive stress due to the factored loads at the strength limit state, with D_c calculated for the section consisting of the steel girder plus the longitudinal reinforcement. For noncomposite sections, D_c would be based on the section consisting of the steel girder alone. Based on the required bend-buckling checks and other strength limit state checks, the stiffener may have to be moved up or down from this initial trial position, especially in cases where the concrete deck is assumed effective in tension in regions of negative flexure at the service limit state as permitted in *AASHTO LRFD* Article 6.10.4.2.1 (and discussed previously). In this case, D_c must be calculated based on the accumulated stresses using Equation 2.7.

Because simply supported boundary conditions were assumed in the development of Equations 2.14 and 2.15, it is possible at locations where the longitudinal stiffener might be located at an inefficient position for a particular condition, for the web bend-buckling resistance of the longitudinally stiffened web to be less than that computed for a web of the same dimensions without longitudinal stiffeners. This anomaly is due to the fact that Equation 2.12 for the bend-buckling coefficient for webs without longitudinal stiffeners was derived assuming partial rotational restraint of the web panel by the flanges. Therefore, the k value from Equation 2.12 serves as a lower limit on the k value for a longitudinally stiffened web panel computed from Equation 2.14. This lower limit is not applied to Equation 2.15 because it would never control in this case. Also, as discussed previously for webs without longitudinal stiffeners, k is to be taken equal to 7.2 for the rare case in which both edges of the longitudinally stiffened web are in compression.

In regions where the web undergoes stress reversal, it may be necessary, or desirable, to use two longitudinal stiffeners on the web. Equations 2.14 and 2.15 conservatively neglect any benefit of placing more than one longitudinal stiffener on the web. However, *AASHTO LRFD* Article 6.10.1.9.2 does permit the Engineer to perform a direct buckling analysis of a web panel with multiple longitudinal stiffeners, if desired, to determine F_{crw} or k for this case. Simply supported boundary conditions should be assumed at the flanges and at the longitudinal stiffener locations in such an analysis. If F_{crw} determined from the bucking analysis is greater than or equal to F_{yc}, then the girder may be proportioned using a web load-shedding factor R_b (discussed later) equal to 1.0. The termination of longitudinal stiffeners in these regions is problematic in that a punitive Category E or E' detail exists at the end of the stiffener-to-web welds. One way to address this issue is to continue a single longitudinal stiffener from the positive moment region to the negative moment region. A single longitudinal stiffener can be extended over both regions by bending the stiffener from the top portion of the web in the positive moment region to the bottom portion in the negative moment region. Hence, in the contraflexure region, the stiffener will pass through the mid-height of the web. As noted above, the current specification provisions permit the computation of the web bend-buckling resistance with the longitudinal stiffener located at any position on the web.

Rearranging Equation 2.11 yields the web slenderness D/t_w at or below which theoretical web bend-buckling will not occur for elastic stress levels, computed according to beam theory, at or below F_{yc}:

$$\frac{D}{t_w} \leq 0.95 \sqrt{\frac{Ek}{F_{yc}}}$$

Equation 2.16

AASHTO LRFD Equation 6.10.1.10.2-1

For sections satisfying this limit, the web load-shedding factor R_b will always equal 1.0. Based on the k value of 129.3 for the case of a doubly symmetric girder, i.e. D_c = 0.5D, with a single longitudinal stiffener located at the optimum position on the web, i.e. d_s = 0.4D_c, the slenderness limit from Equation 2.16 is as follows for different grades of steel:

Table 2.4 Slenderness Limit for Different Grades of Steel

F_{yc} (ksi)	$0.95\sqrt{Ek/F_{yc}}$
36.0	300
50.0	260
70.0	220
90.0	194
100.0	184

For singly symmetric girders with D_c/D > 0.5 and/or where a single longitudinal stiffener is not located at its optimum position, the limiting D/t_w will generally be less than the value shown in the preceding table.

EXAMPLE

Calculate the web bend-buckling resistance F_{crw} for the longitudinally stiffened section shown in Figure 2.11, which is in a region of positive flexure, using Equation 2.11 and Equation 2.14 or 2.15, as applicable. Grade 50W steel is assumed for the flanges and web (i.e. R_h = 1.0). First, calculate F_{crw} for the noncomposite section for the constructibility check; i.e. check *AASHTO LRFD* Equation 6.10.3.2.1-3. The maximum accumulated unfactored positive moment at this section due to the deck-casting sequence, which is assumed to be +11,750 kip-ft, is used in this check. The unfactored moment due to the steel weight at this section is assumed to be +6,480 kip-ft. By inspection, the Strength IV Load Combination governs for this particular check (see the later section of this chapter on Constructibility Verifications and DM Volume 1, Chapter 5 for a further discussion of the Strength IV load combination). From separate calculations, the stress in the top (compression) flange due to the factored loads is computed to be f_{bu} = 1.5(-24.24) = -36.36 ksi. D_c for the steel section is computed to be 85.29 in. The resistance factor for flexure ϕ_f is equal to 1.0 (*AASHTO LRFD* Article 6.5.4.2).
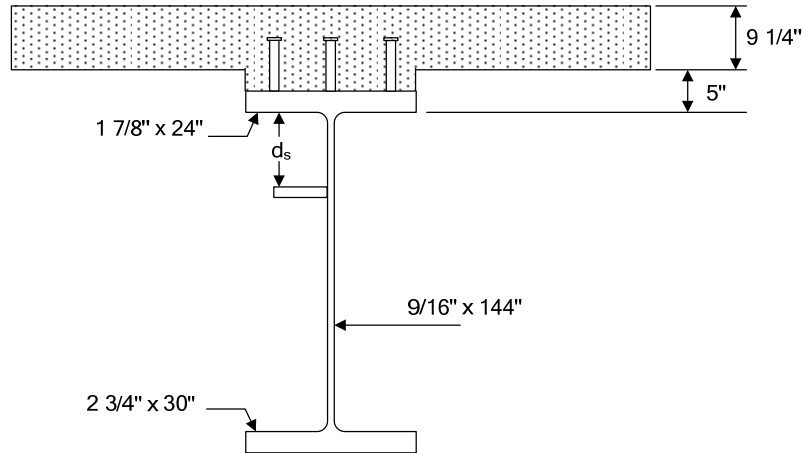
Figure 2.11 Longitudinally Stiffened Girder Section – Positive Flexure Region

Try locating the stiffener initially at the theoretical optimum location:

$$d_s = 0.4D_c = 0.4(85.29) = 34.12 \text{ in.}$$

Therefore, use Equation 2.14 to calculate the bend-buckling coefficient k.

$$k = \frac{5.17}{(d_s/D)^2} \geq \frac{9}{(D_c/D)^2}$$

AASHTO LRFD Equation 6.10.1.9.2-1

$$k = \frac{5.17}{(34.12/144.0)^2} = 92.09$$

$$\frac{9}{(85.29/144.0)^2} = 25.65 < 92.09 \quad \text{ok}$$

$$F_{crw} = \frac{0.9Ek}{\left(\dfrac{D}{t_w}\right)^2}$$

AASHTO LRFD Equation 6.10.1.9.1-1

$$F_{crw} = \frac{0.9(29,000)(92.09)}{\left(\dfrac{144.0}{0.5625}\right)^2} = 36.68 \text{ ksi}$$

$$F_{yw}/0.7 = 50/0.7 = 71.43 \text{ ksi}$$

$$R_h F_{yc} = (1.0)(50) = 50.00 \text{ ksi (controls)} > 36.68 \text{ ksi} \quad \text{ok}$$

$$f_{bu} \leq \phi_f F_{crw}$$

<div align="right">*AASHTO LRFD* Equation 6.10.3.2.1-3</div>

$$f_{bu} = \left|-36.36 \text{ ksi}\right| < \phi_f F_{crw} = (1.0)(36.68) = 36.68 \text{ ksi ok}$$

For sections with longitudinal stiffeners, a web bend-buckling check is also required at the service limit state for composite sections in positive flexure; i.e. check *AASHTO LRFD* Equation 6.10.4.2.2-4. From separate computations, under Load Combination Service II (see DM Volume 1, Chapter 5 for a further discussion of the Service II Load Combination), the stress in the compression flange f_c is –32.36 ksi, and the stress in the tension flange f_t is +37.66 ksi. Since D_c for the composite section in this case is a function of the accumulated factored stresses, use Equation 2.7 as follows:

$$D_c = \left(\frac{-f_c}{\left|f_c\right| + f_t}\right)d - t_{fc} \geq 0$$

<div align="right">*AASHTO LRFD* Equation D6.3.1-1</div>

$$d = 2.75 + 144.0 + 1.875 = 148.63 \text{ in.}$$

$$t_{fc} = 1.875 \text{ in.}$$

$$D_c = \left(\frac{-(-32.36)}{\left|-32.36\right| + 37.66}\right)148.63 - 1.875 = 66.81 \text{ in.}$$

Since d_s = 34.12 in. is also greater than $0.4D_c$ = 0.4(66.81) = 26.72 in. in this case, again use Equation 2.14 to compute k:

$$k = \frac{5.17}{(34.12/144.0)^2} = 92.09$$

$$\frac{9}{(66.81/144.0)^2} = 41.81 < 92.09 \text{ ok}$$

$$F_{crw} = 36.68 \text{ ksi}$$

$$f_c \leq F_{crw}$$

<div align="right">*AASHTO LRFD* Equation 6.10.4.2.2-4</div>

$$f_c = \left|-32.36 \text{ ksi}\right| < F_{crw} = 36.68 \text{ ksi ok}$$

Separate checks are also necessary to ensure that the section has adequate nominal flexural resistance at the strength limit state with the longitudinal stiffener in this position. In this particular instance, using the theoretical optimum location of the stiffener as the initial trail location worked well. However, this may not always be the case. Checks at other sections in the positive flexure region (where the stiffener may not be located at the optimum position) could also potentially require the stiffener to be moved to a different position.

Checks for sections in negative flexure are similar to those illustrated above for webs without longitudinal stiffeners, except that the appropriate *k* value from Equation 2.14 or 2.15 is used to compute F_{crw}. As recommended above, it is suggested that the longitudinal stiffener initially be located at $0.4D_c$ from the inner surface of the compression flange at the section with the maximum flexural compressive stress due to the factored loads at the strength limit state, with D_c calculated for the section consisting of the steel girder plus the longitudinal reinforcement for composite sections and the steel girder alone for noncomposite sections.

6.   Basler K., B.T. Yen, J.A. Mueller, and B. Thurlimann. 1960. "Web Buckling Tests on Welded Plate Girders.", *WRC Bulletin No. 64*, Welding Research Council, New York, NY.
7.   Timoshenko, S.P., and J.M. Gere. 1961. *Theory of Elastic Stability*. Mc-Graw-Hill, New York, NY.
8.   ASCE. 1968. "Design of Hybrid Steel Beams." Joint ASCE-AASHO Subcommittee on Hybrid Beams and Girders, *Journal of the Structural Division*, American Society of Civil Engineers, Vol. 94, No. ST6, New York, NY.
9.   Frank, K.H., and T.A. Helwig. 1995. "Buckling of Webs in Unsymmetric Plate Girders." *AISC Engineering Journal*, American Institute of Steel Construction, Chicago, IL, Vol. 32, 2nd Qtr.
10.   Cooper, P.B. 1967. "Strength of Longitudinally Stiffened Plate Girders." *Journal of the Structural Division*, American Society of Civil Engineers, New York, NY, Vol. 93, No. ST2, April.

2.2.2.5 Web Load-Shedding Factor R_b

As discussed in the preceding section, once the theoretical web bend-buckling load is reached, a slender-web girder does not collapse but has significant postbuckling resistance. As buckling of the compression zone of the web increases, the ability of the web to carry its portion of the load, as computed by ordinary beam theory, decreases. However, this does not mean failure. Instead, a redistribution of stress to the stiffer longitudinal elements results; that is, to the compression flange and the immediately adjacent portion of the web. The tension flange stress is not increased significantly by the shedding of the web compressive stresses. As a result, for a given moment, the stress in the compression portion of the web that is deflecting laterally is less than that calculated for a linear distribution and the stress in the compression flange is greater, as illustrated in Figure 2.12. Therefore, yielding may occur in the compression flange before the yield moment calculated from ordinary beam theory is attained.

Tension
Flange
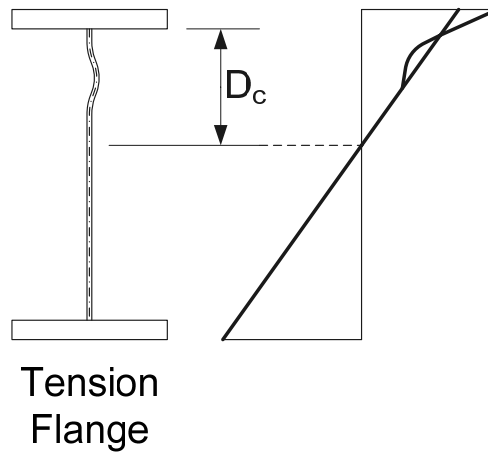
Figure 2.12 Load Shedding from the Web to the Compression Flange

To account for this postbuckling resistance in the design of a slender-web girder, or a girder with a web slenderness exceeding λ_{rw} given by Equation 2.13, an approximate method is needed to account for the extra load the compression flange must carry after the web becomes partially ineffective.   Basler and Thurlimann (*11*) developed such an approach by assuming a linear distribution of stress acting on an effective cross-section, with the nominal flexural resistance M_n reached when the extreme fiber of this effective section in compression reaches either the yield stress or a critical buckling stress, as applicable.   The effective section assumes that a portion of the web in which the buckling (or out-of-plane deformation) occurs becomes ineffective (Figure 2.13). They assumed an effective width b_e equal to $30t_w$ for a web with a slenderness D/t_w of about 345.   This value was the limiting slenderness to preclude the failure mode of vertical flange buckling, or buckling of the compression flange into the web, for 33,000-psi yield strength steel at an assumed web-to-flange area ratio A_w/A_f of 2 (where A_f is the area of each flange) and an assumed residual tension stress level of 16.5 ksi (note: the vertical flange buckling limit state is discussed in more detail in Section 2.2.3.3.2 of this chapter under Web Sizing). The nominal flexural resistance was then assumed to increase linearly from the resistance of this effective section up to a value of M_y at a web slenderness of λ_{rw}. A more general linear equation containing A_w/A_f as a parameter was then developed as follows:

$$\frac{M_n}{M_y} = 1 - 0.0005 \frac{A_w}{A_f} \left(\frac{D}{t_w} - \lambda_{rw} \right)$$

Equation 2.17

The expression on the right-hand side of the preceding equation has come to be known as the web load-shedding factor R_b.   The load-shedding factor, which is less than or equal to 1.0, can be used to either reduce the section modulus to the compression flange effectively increasing the compression-flange stress, or to reduce the nominal flexural resistance of the compression flange. Design specifications, including the *AASHTO LRFD* Specifications, have traditionally followed the latter course.   In the *AASHTO LRFD* Specifications, the web load-

shedding factor to be applied to the nominal flexural resistance of the compression flange at the strength limit state is specified in *AASHTO LRFD* Article 6.10.1.10.2. Note that the effect of load shedding to the compression flange is not considered significant and is ignored whenever the nominal flexural resistance exceeds the yield moment M_y.
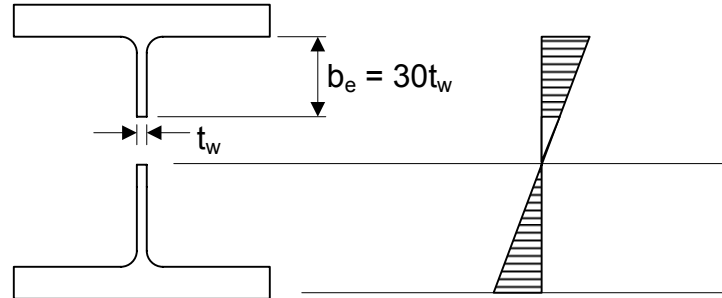
Figure 2.13 Effective Cross-Section

The preceding equation assumes that the ratio of A_w/A_f does not exceed approximately 3. To accommodate larger ratios up to 10, the *AASHTO LRFD* Specifications utilize a form of the more general equation developed by Basler (*10*) in which the coefficient of 0.0005 in Equation 2.17 is replaced by the following coefficient:

$$\frac{a_r}{1200 + 300a_r} \qquad \text{Equation 2.18}$$

where:
a_r = A_w/A_{fc}
A_{fc} = area of the compression flange (in^2)

For sections with flanges satisfying the minimum flange proportioning requirements given by *AASHTO LRFD* Equations 6.10.2.2-2 and 6.10.2.2-3 in the *AASHTO LRFD* Specifications (i.e. $b_f \geq D/6$ and $t_f \geq 1.1t_w$, respectively), the ratio of the web area to the compression-flange area will always be less than or equal to 5.45. Hence, even though the modified coefficient given by Equation 2.18 is used, it is not necessary to specify the limiting ratio of 10.

Furthermore, to better accommodate singly symmetric sections, the *AASHTO LRFD* Specifications have replaced a_r in Equation 2.18 with a_{wc}, where a_{wc} is typically equal to the ratio of two times the web area in compression to the area of the compression flange. In addition, D/t_w in Equation 2.17 is replaced by the effective web slenderness ratio $2D_c/t_w$ resulting in the following equation for R_b given as Equation 6.10.1.10.2-3 in the *AASHTO LRFD* Specifications:

$$R_b = 1 - \left(\frac{a_{wc}}{1200 + 300a_{wc}}\right)\left(\frac{2D_c}{t_w} - \lambda_{rw}\right) \leq 1.0 \qquad \text{Equation 2.19}$$

AASHTO LRFD Equation 6.10.1.10.2-3

where:

a_{wc} = $2D_c t_w / b_{fc} t_{fc}$

b_{fc} =   width of the compression flange (in.)

t_{fc} =   thickness of the compression flange (in.)

For compression flanges that have cover plates, the cover-plate area may be added to the compression-flange area in the denominator of the equation for a_{wc}.

In previous specifications, the denominator (under the radical) of λ_{rw} in Equation 2.19 was the actual compression-flange bending stress due to the factored loads rather than F_{yc}. While this refinement can lead to an increase in the value of R_b in some cases, the increase is not likely to be overly significant. Also, using the actual flange stress to compute the nominal flexural resistance can lead to difficulties in load rating since the flexural resistance is a function of the applied load. Therefore, F_{yc} is now conservatively utilized in the equation for λ_{rw}. *AASHTO LRFD* Article C6.10.1.10.2 suggests a preferred alternative should a larger value of R_b be desired at a section where the nominal flexural resistance of the compression flange is significantly below F_{yc}. The suggested alternative is to substitute the *smaller* of the following values for F_{yc} when determining λ_{rw} for use in Equation 2.19, and also in Equations 2.16 and 2.20, as applicable:

> ➢ The nominal flexural resistance of the compression flange F_{nc} calculated assuming R_b and R_h are equal to 1.0 (see the next section for a discussion on the hybrid factor R_h);
> ➢ The compression-flange bending stress due to the factored loads when the tension-flange bending stress due to the factored loads reaches a value of $R_h F_{yt}$.

For composite sections subject to positive flexure, the concrete deck acting as a compression-flange element typically contributes a large fraction of the flexural resistance. To account for this in an approximate fashion in a longitudinally stiffened composite section in these regions, which may be subject to web bend-buckling at the strength limit state, a fraction of the transformed concrete deck area based conservatively on the long-term 3n composite section may be included with the steel compression-flange area in computing the a_{wc} term in Equation 2.19 as follows:

$$a_{wc} = \frac{2D_c t_w}{b_{fc} t_{fc} + b_s t_s \left(1 - f_{DC1} / F_{yc}\right) / 3n} \qquad \text{Equation 2.20}$$

AASHTO LRFD Equation 6.10.1.10.2-6

where:

b_s = effective flange width of the concrete deck (in.)

f_{DC1} = compression flange stress caused by the factored permanent load applied before the concrete deck has hardened or is made composite, calculated without consideration of flange lateral bending (ksi)

t_s = thickness of the concrete deck (in.)

For these sections, D_c in Equation 2.20 is a function of the accumulated stresses and must therefore be calculated using Equation 2.7.

As discussed previously, for composite sections in positive flexure *without* longitudinal stiffeners, web bend-buckling is not considered a concern, and therefore, the R_b factor is always taken equal to 1.0 for these sections according to *AASHTO LRFD* Article 6.10.1.10.2. Even if this were not specified to be the case, including the transformed concrete area in the a_{wc} term for these sections as shown in Equation 2.20, would likely ensure a value of R_b equal to 1.0 in most every case.

For composite sections in negative flexure, D_c in Equation 2.19 should conservatively be computed using the section consisting of the steel girder plus the longitudinal deck reinforcement.

As indicated in *AASHTO LRFD* Article C6.11.8.2.2, in calculating R_b for a tub section, one-half of the effective box flange width should be used in conjunction with one top flange and a single web. The effective box flange width is defined in *AASHTO LRFD* Article 6.11.1.1. For a closed-box section, one-half of the effective top and bottom box flange width should be used in conjunction with a single web.

AASHTO LRFD Article 6.10.1.10.2 lists the four specific conditions for which the R_b factor may be explicitly taken equal to 1.0 as follows:

- ➤ When the section is composite and in a region of positive flexure and the web slenderness D/t_w does not exceed 150 (i.e. longitudinal web stiffeners are not required);
- ➤ When checking constructibility according to the provisions of *AASHTO LRFD* Article 6.10.3.2 (since the web bend-buckling resistance F_{crw} must not be exceeded during construction as discussed previously);
- ➤ When one or more longitudinal web stiffeners are provided and Equation 2.16 is satisfied (i.e. whenever the web slenderness D/t_w does not exceed the slenderness at or below which theoretical web bend-buckling will not occur for elastic stress levels at or below F_{yc} at the strength limit state);
- ➤ When Equation 2.13 is satisfied for webs without longitudinal web stiffeners (i.e. whenever the web slenderness $2D_c/t_w$ does not exceed the noncompact-web slenderness limit λ_{rw} at or below which theoretical web bend-buckling will not occur for elastic stress levels at or below F_{yc} at the strength limit state).

Otherwise, R_b must be calculated from Equation 2.19.

Bend-buckling of longitudinally stiffened webs is prevented up through the service limit state in the *AASHTO LRFD* Specifications, but is permitted at the strength limit state as discussed previously. It should be noted, however, that the current longitudinal stiffener proportioning requirements given in *AASHTO LRFD* Article 6.10.11.3 do not ensure that a horizontal line of near zero lateral deflection will be maintained throughout the post-buckling response of the web. As a result, when computing R_b from Equation 2.19 at the strength limit state for longitudinally stiffened webs in regions of positive or negative flexure, the presence of the longitudinal

stiffeners is conservatively ignored (i.e. the noncompact-web slenderness limit λ_{rw} is used in Equation 2.19 rather than the limiting slenderness to prevent theoretical web bend buckling in longitudinally stiffened webs given by Equation 2.16).

EXAMPLE

Calculate the web load-shedding factor at the strength limit state for the hybrid composite section (without longitudinal web stiffeners) shown in Figure 2.6, which is in a region of negative flexure. First, determine if R_b is indeed less than 1.0 by checking Equation 2.13. For sections in negative flexure at the strength limit state, use D_c for the section consisting of the steel girder plus the longitudinal reinforcement (*AASHTO LRFD* Article D6.3.1).

$$\frac{2D_c}{t_w} = \frac{2(36.55)}{0.5625} = 130.0$$

$$\frac{2D_c}{t_w} > \lambda_{rw} = 5.7\sqrt{\frac{E}{F_{yc}}} = 5.7\sqrt{\frac{29,000}{70}} = 116.0$$

AASHTO LRFD Equation 6.10.6.2.3-1

Therefore, the section is a slender-web section subject to web bend-buckling at elastic stress levels at the strength limit state and R_b is less than 1.0. Calculate R_b from Equation 2.19:

$$R_b = 1 - \left(\frac{a_{wc}}{1200 + 300a_{wc}}\right)\left(\frac{2D_c}{t_w} - \lambda_{rw}\right) \leq 1.0$$

AASHTO LRFD Equation 6.10.1.10.2-3

where:

$$a_{wc} = \frac{2D_c t_w}{b_{fc} t_{fc}}$$

AASHTO LRFD Equation 6.10.1.10.2-5

$$a_{wc} = \frac{2(36.55)(0.5625)}{20(2)} = 1.028$$

$$R_b = 1 - \left(\frac{1.028}{1200 + 300(1.028)}\right)(130.0 - 116.0) = 0.990$$

EXAMPLE

Calculate the web load-shedding factor R_b for the longitudinally stiffened section shown in Figure 2.11, which is in a region of positive flexure. Grade 50W steel is assumed for the flanges and web. The web bend-buckling coefficient was calculated in an earlier example to be $k = 92.09$ for this section. First, determine if R_b is potentially less than 1.0 by checking Equation 2.16.

$$\frac{D}{t_w} = \frac{144}{0.5625} = 256.0$$

$$\frac{D}{t_w} > 0.95\sqrt{\frac{Ek}{F_{yc}}} = 0.95\sqrt{\frac{29,000(92.09)}{50}} = 219.6$$

AASHTO LRFD Equation 6.10.1.10.2-1

Therefore, the section is subject to web bend-buckling at elastic stress levels at the strength limit state. Calculate R_b from Equation 2.19:

$$R_b = 1 - \left(\frac{a_{wc}}{1200 + 300a_{wc}}\right)\left(\frac{2D_c}{t_w} - \lambda_{rw}\right) \le 1.0$$

AASHTO LRFD Equation 6.10.1.10.2-3

For composite longitudinally stiffened sections in positive flexure, the term a_{wc} is calculated from Equation 2.20 as follows, which includes a fraction of the transformed concrete deck along with the steel compression-flange area:

$$a_{wc} = \frac{2D_c t_w}{b_{fc}t_{fc} + b_s t_s \left(1 - f_{DC1}/F_{yc}\right)/3n}$$

AASHTO LRFD Equation 6.10.1.10.2-6

From separate computations, under Load Combination Strength I (see DM Volume 1, Chapter 5 for a further discussion of the Strength I Load Combination), the stress in the compression flange f_c is –41.63 ksi, and the stress in the tension flange f_t is +49.34 ksi. Since D_c for the composite section in this case is a function of the accumulated factored stresses, use Equation 2.7 as follows:

$$D_c = \left(\frac{-f_c}{|f_c| + f_t}\right)d - t_{fc} \ge 0$$

AASHTO LRFD Equation D6.3.1-1

$$d = 2.75 + 144.0 + 1.875 = 148.63 \text{ in.}$$

$$t_{fc} = 1.875 \text{ in.}$$

$$D_c = \left(\frac{-(-41.63)}{|-41.63| + 49.34}\right)148.63 - 1.875 = 66.14 \text{ in.}$$

$$\frac{2D_c}{t_w} = \frac{2(66.14)}{0.5625} = 235.2$$

$$\lambda_{rw} = 5.7\sqrt{\frac{E}{F_{yc}}} = 5.7\sqrt{\frac{29,000}{50}} = 137.3$$

AASHTO LRFD Equation 6.10.6.2.3-1

From separate calculations, the compression-flange stress at the strength limit state (Strength I) caused by the factored permanent load applied before the concrete deck has hardened is f_{DC1} = -25.52 ksi. The modular ratio n is equal to 8. The effective flange width of the concrete deck is b_s = 123.0 in.   Therefore:

$$a_{wc} = \frac{2(66.14)(0.5625)}{(24.0)(1.875)+(123.0)(9.25)\left(1-\left|-25.52\right|/50\right)/24} = 1.091$$

AASHTO LRFD Equation 6.10.1.10.2-6

$$R_b = 1-\left(\frac{1.091}{1200+300(1.091)}\right)(235.2-137.3) = 0.930$$

11. Basler, K., and B. Thurlimann. 1961. "Strength of Plate Girders in Bending." *Journal of the Structural Division*, American Society of Civil Engineers, New York, NY, Vol. 87, ST6, August.

2.2.2.6 Hybrid Factor R_h

A hybrid girder is defined as a fabricated steel girder with a web that has a specified minimum yield strength less than one or both flanges. As a result, yielding of the lower strength web will occur before the maximum flange strength has been reached.   Therefore, the web will participate to a lesser extent than in a homogeneous girder when the moment capacity of the hybrid girder is attained.
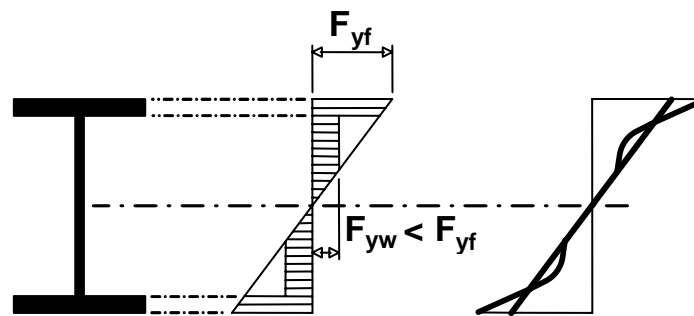
$$R_h = \frac{12+\beta\left(3\rho-\rho^3\right)}{12+2\beta}$$

$$\beta = \frac{2D_n t_w}{A_{fn}}$$

ρ = the smaller of F_{yw}/f_n and 1.0

Figure 2.14 Hybrid Factor, R_h

Hybrid girders are covered in general in *AASHTO LRFD* Article 6.10.1.3. Although the specifications can be applied safely to all types of hybrid girders, for greater design efficiency, it is recommended in *AASHTO LRFD* Article 6.10.1.3 that the difference in the specified minimum yield strengths of the web and the higher strength flange be limited to one steel grade. That is, the specified minimum yield strength of the web should not be less than the larger of 70 percent of the specified minimum yield strength of the higher strength flange and 36.0 ksi.

As for a homogeneous girder, a hybrid girder unloads elastically. If the yield stress in the web was exceeded during the initial loading, a small residual curvature will remain in the girder after unloading. However, under all subsequent loading and unloading cycles, the girder will behave elastically if the moment upon reloading does not exceed the previously applied maximum moment. Also, as in a homogeneous girder, residual stresses will cause inelastic behavior in a hybrid girder during the initial application of the load, but the ultimate resistance of the girder will generally not be affected by the presence of residual stresses. Additional more detailed information on the overall behavior of hybrid girders, along with initial design recommendations, may be found in Reference 8 and in References 12 through 16.

Hybrid girders utilizing HPS 70W steel for the flanges and Grade 50W steel for the web have recently proven to be a popular and economical option, primarily in regions of negative flexure (*16a*, *16b*). Hybrid girders utilizing a tension flange with a higher yield stress than the web and a compression flange with the same yield stress as the web may also prove economical, particularly for composite sections in positive flexure. Because of stability issues before the concrete deck cures, it is often necessary to use a top flange that is not fully stressed at the strength limit state in regions of positive flexure. Test data for hybrid sections with nominally larger yield strengths in the web than in one or both flanges are limited. Therefore, in such cases, *AASHTO LRFD* Article 6.10.1.3 limits the nominal yield strength that may be used for the web in determining the flexural and shear resistance of the section to 120 percent or less of the specified minimum yield strength of the lower strength flange. This is felt to be a range that is supported by the limited available test data. An exception is permitted for composite sections in positive flexure with a higher strength steel in the web than in the compression flange, in which case the full web strength may be used in determining the flexural and shear resistance.

The preceding section of this chapter discussed the redistribution of stress that occurs in slender-web girders from the compression zone of the web to the compression flange as a result of localized bend buckling of the web. A similar redistribution of stress from the web to the flanges occurs in hybrid girders as a result of the early localized yielding of the lower strength web; the primary difference being that in the case of the hybrid girder, the redistribution occurs to both the compression and tension flanges (Figure 2.14). In the first case, the web load-shedding factor R_b is used to account for the reduced contribution of the web to the nominal flexural resistance resulting from web bend buckling. In the case of the hybrid girder, the hybrid factor R_h is used to account for the effect of earlier yielding of the lower strength steel in the web.

As is the case with the load-shedding factor, the hybrid factor, which is less than or equal to 1.0, can be used to either reduce the section modulus to each flange effectively increasing the flange stresses, or to reduce the nominal flexural resistance of each flange. Again, design specifications, including the *AASHTO LRFD* Specifications, have traditionally followed the latter course. In the *AASHTO LRFD* Specifications, the hybrid factor to be applied to the nominal flexural resistance of each flange of a hybrid girder is specified in *AASHTO LRFD* Article 6.10.1.10.1. Note that the redistribution of the stress to the flanges resulting from local yielding of the web is not considered significant and is ignored whenever the nominal flexural resistance exceeds the yield moment M_y. Also, for rolled shapes, which are obviously homogeneous sections based on the nominal yield strength, homogeneous built-up sections and built-up sections with a higher-strength steel in the web than in both flanges, R_h is to be explicitly taken equal to 1.0 according to *AASHTO LRFD* Article 6.10.1.10.1.

For all other cases, the specification allows the Engineer to compute R_h based on a direct iterative strain compatibility analysis. In lieu of such an analysis, the R_h factor is to be determined as follows:

$$R_h = \frac{12 + \beta(3\rho - \rho^3)}{12 + 2\beta}$$

Equation 2.21

AASHTO LRFD Equation 6.10.1.10.1-1

where:

$\beta \quad = \quad \dfrac{2D_n t_w}{A_{fn}}$

$\rho \quad = \quad$ the smaller of F_{yw}/f_n and 1.0

$A_{fn} \quad =$ sum of the flange area and the area of any cover plates on the side of the neutral axis corresponding to D_n (in.^{2}). For composite sections in negative flexure, the area of the longitudinal reinforcement may be included in calculating A_{fn} for the top flange.

$D_n \quad =$ larger of the distances from the elastic neutral axis of the cross-section to the inside face of either flange (in.). For sections where the neutral axis is at the mid-depth of the web, the distance from the neutral axis to the inside face of the flange on the side of the neutral axis where yielding occurs first.

$f_n \quad =$ for sections where yielding occurs first in the flange, a cover plate or the longitudinal reinforcement on the side of the neutral axis corresponding to D_n, the largest of the specified minimum yield strengths of each component in the calculation of A_{fn} (ksi). Otherwise, the largest of the elastic stresses in the flange, cover plate or longitudinal reinforcement on the side of the neutral axis corresponding to D_n at first yield on the opposite side of the neutral axis.

Equation 2.21 is the basic fundamental equation for R_h originally derived for doubly symmetric I-sections (*12, 14*) (or for sections where the elastic neutral axis is reasonably close to the mid-depth of the web), and included for such sections in

previous *AASHTO LRFD Specifications*.   Previous specifications also included a separate more complex R_h equation for singly symmetric composite sections subject to positive flexure (*14*).   The more complex equation for composite sections has been eliminated in the *AASHTO LRFD* Specifications in lieu of the basic Equation 2.21, which has been generalized to consider all possible combinations associated with different positions of the elastic neutral axis and different yield strengths of the top and bottom flange elements in a non-iterative fashion. In this context, a flange element is considered to be a flange, a cover plate or plates attached to that flange or the longitudinal reinforcement (associated with the top flange only). Singly symmetric sections (both noncomposite and composite) are handled using the base equation by focusing on the side of the neutral axis where nominal yielding occurs first, or the side of the neutral axis subject to the most extensive web yielding prior to first yielding of any flange element. All flange elements on the side of the neutral axis where nominal yielding occurs first are conservatively assumed to be located at the edge of the web in the calculation of R_h. In addition, any shift in the neutral axis caused by the effect of web yielding is considered negligible. These assumptions are similar to the assumptions made originally in the development of the R_h equation for singly symmetric composite sections (*14*), and are not considered overly punitive since computed R_h values are typically close to 1.0.

As illustrated in the examples given below, the first step in computing R_h using Equation 2.21 is to determine D_n. According to the definition, D_n is to be taken as the larger of the distances from the elastic neutral axis of the cross-section to the inside face of either flange.   The following suggestions are made regarding the calculation of D_n for composite sections:

> ➢ For composite sections in positive flexure, D_n may conservatively be taken as the distance from the neutral axis of the short-term *n* composite section to the inside face of the bottom flange.
> ➢ Except as noted in the next bullet item, for composite sections in negative flexure, it is recommended that the elastic neutral axis based on the section consisting of the steel girder plus the longitudinal reinforcement be used in determining D_n.
> ➢ For composite sections in negative flexure at the service limit state in which the concrete deck is considered to be effective as permitted in *AASHTO LRFD* Article 6.10.4.2.1, D_n may conservatively be taken as the distance from the neutral axis of the short-term *n* composite section to the inside face of the bottom flange. Note that when the concrete deck is *not* considered to be effective in negative flexure, the same value of R_h is used at the strength and service limit states.

In all of the above cases, a more accurate solution can be obtained by calculating the neutral axis location based on the sum of the accumulated factored stresses at the appropriate limit state.   However, using the above suggested neutral axes locations for the computation in each case will prevent the flexural resistance from being a function of D_n with D_n being a function of the applied load, which can result in potential complications in load rating. Also, significant differences in the calculated values of R_h, which are generally close to 1.0 in most cases as mentioned above, as

a function of the neutral-axis location are not anticipated nor deemed worthy of introducing any additional complexity into the calculation.

In cases where the neutral axis is located at the mid-depth of the web, D_n is to be taken as the distance from the neutral axis to the inside face of the flange on the side of the neutral axis where yielding occurs first. Should yielding occur simultaneously on both sides of the neutral axis, D_n should be taken as the distance to the flange element with the smaller value of A_{fn}.

Once the value of D_n has been established, the next step is to calculate A_{fn}. A_{fn} is defined as the sum of the areas of the flange elements on the side of the neutral axis corresponding to D_n. This would include the flange area, the area of any cover plates, and for composite sections in negative flexure, the area of the longitudinal reinforcement if D_n happens to be measured to the top flange. With D_n and A_{fn} established, the constant β used in Equation 2.21 can then be calculated.

In order to calculate the constant ρ used in Equation 2.21, the stress f_n must first be calculated. According to the stated definition of f_n, for sections where nominal yielding occurs first in a flange element on the side of the neutral axis corresponding to D_n, which is the case in most instances, f_n is to be taken as the largest of the specified minimum yield strengths of each flange element included in the calculation of A_{fn}. Should yielding occur first on the other side of the neutral axis, f_n is to be taken as the largest of the calculated elastic stresses in the various flange elements on the side of the neutral axis corresponding to D_n when nominal first yielding occurs on the opposite side. f_n is then divided into the specified minimum yield strength of the web F_{yw} in order to determine ρ, which cannot exceed 1.0.

As indicated in *AASHTO LRFD* Article C6.11.8.2.2, in calculating R_h for a tub section, one-half of the effective box flange width should be used in conjunction with one top flange and a single web. The effective box flange width is defined in *AASHTO LRFD* Article 6.11.1.1. For a closed-box section, one-half of the effective top and bottom box flange width should be used in conjunction with a single web.

Finally, as discussed in *AASHTO LRFD* Article C6.10.3.2.1, for hybrid sections that are composite in the final condition but noncomposite during construction (i.e. sections in bridges built using unshored composite construction), R_h must be calculated separately for the noncomposite and composite sections. For the constructibility design checks, R_h for the noncomposite section would be applied, and for all subsequent checks in which the member is composite, R_h for the composite section would be applied.

EXAMPLE

Calculate the hybrid factor for the composite section shown in Figure 2.6, which is in a region of negative flexure. The flanges are Grade HPS 70W steel and the web is Grade 50W steel.

First, calculate D_n or the larger of the distances from the elastic neutral axis of the cross-section to the inside face of either flange. As recommended above, in most

cases for composite sections in negative flexure, use the section consisting of the steel girder plus the longitudinal reinforcement to calculate D_n. From earlier calculations for this section, the distance from the neutral axis to the inside face of the top flange is 32.45 in. and to the inside face of the bottom flange is 36.55 in. Therefore, D_n is 36.55 in.

Next, calculate A_{fn} or the sum of the area of the flange elements on the side of the neutral axis corresponding to D_n. Since there are no cover plates and D_n is measured to the bottom flange, the only flange element contributing to A_{fn} is the bottom flange. Therefore, A_{fn} = 20(2) = 40.0 in^2.

$$\beta = \frac{2D_n t_w}{A_{fn}}$$

AASHTO LRFD Equation 6.10.1.10.1-2

$$\beta = \frac{2(36.55)(0.5625)}{40.0} = 1.028$$

Since the flanges are the same yield strength, nominal yielding will occur first on the side of the neutral axis corresponding to D_n (separate calculations show that the 60-ksi longitudinal reinforcement does not yield first). For sections where nominal yielding occurs first in a flange element on the side of the neutral axis corresponding to D_n, f_n is taken as the largest of the specified minimum yield strengths of each flange element included in the calculation of A_{fn}. Therefore, f_n = 70.0 ksi.

$$\rho = \frac{F_{yw}}{f_n} = \frac{50.0}{70.0} = 0.714 \le 1.0$$

$$R_h = \frac{12 + \beta(3\rho - \rho^3)}{12 + 2\beta}$$

AASHTO LRFD Equation 6.10.1.10.1-1

$$R_h = \frac{12 + 1.028[3(0.714) - (0.714)^3]}{12 + 2(1.028)} = 0.984$$

Assuming the concrete deck is *not* considered to be effective in negative flexure at the service limit state, this same value of R_h would be used for this section at the strength and service limit states.

If the concrete deck is considered to be effective in negative flexure at the service limit state, as permitted in *AASHTO LRFD* Article 6.10.4.2.1, a different value of R_h should be calculated for use in the service limit state design checks. As recommended above, in this case, D_n may conservatively be taken as the distance from the neutral axis of the short-term *n* composite section to the inside face of the bottom flange. From separate calculations, this value is computed to be D_n = 54.97

in. Since D_n is measured to the bottom flange, $A_{fn} = 20(2.0) = 40.0$ in² and $f_n = 70.0$ ksi. Therefore:

$$\beta = \frac{2(54.97)(0.5625)}{40.0} = 1.546$$

$$\rho = 50.0/70.0 = 0.714$$

$$R_h = \frac{12 + 1.546\left[3(0.714) - (0.714)^3\right]}{12 + 2(1.546)} = 0.977$$

From earlier calculations, the neutral axis location for this section (assuming the concrete is effective in negative flexure) was determined based on the sum of the accumulated factored stresses at the service limit state. Based on these calculations, D_n would be taken equal to 41.27 in. (versus 54.97 in. when based on the short-term composite section). Performing calculations similar to the above based on this smaller value of D_n would result in a value of R_h equal to 0.982. Although a slightly larger value of R_h is obtained in this case using the more accurate neutral axis location, the R_h factor is now a function of the applied load, which can potentially complicate rating calculations.

EXAMPLE

Calculate the hybrid factor for the section shown in Figure 2.3, which is in a region of positive flexure. Assume the top flange and web are Grade 50W steel and the bottom flange is Grade HPS 70W steel.

First, calculate R_h for the noncomposite girder, which would be used in all the constructibility design checks for this section. From earlier calculations for the steel girder at this section, the distance from the neutral axis to the inside face of the top flange is 38.63 in. and to the inside face of the bottom flange is 30.38 in. Therefore, D_n is 38.63 in.

Next, calculate A_{fn} or the sum of the area of the flange elements on the side of the neutral axis corresponding to D_n. Since there are no cover plates and D_n is measured to the top flange, the only flange element contributing to A_{fn} is the top flange. Therefore, $A_{fn} = 16(1) = 16.0$ in.²

$$\beta = \frac{2D_n t_w}{A_{fn}}$$

AASHTO LRFD Equation 6.10.1.10.1-2

$$\beta = \frac{2(38.63)(0.5)}{16.0} = 2.414$$

Separate calculations indicate that nominal first yielding will occur in the Grade 50W top flange. For sections where nominal yielding occurs first in a flange element on

the side of the neutral axis corresponding to D_n, f_n is taken as the largest of the specified minimum yield strengths of each flange element included in the calculation of A_{fn}. Therefore, $f_n = 50.0$ ksi.

$$\rho = \frac{F_{yw}}{f_n} = \frac{50.0}{50.0} = 1.0$$

$$R_h = \frac{12 + \beta(3\rho - \rho^3)}{12 + 2\beta}$$

AASHTO LRFD Equation 6.10.1.10.1-1

$$R_h = \frac{12 + 2.414[3(1.0) - (1.0)^3]}{12 + 2(2.414)} = 1.0$$

Now, calculate R_h for the composite girder, which would be used in all the service and strength limit state design checks. As recommended above, in this case, D_n may conservatively be taken as the distance from the neutral axis of the short-term n composite section to the inside face of the bottom flange. From earlier calculations, this value is computed to be $D_n = 58.31$ in. Since D_n is measured to the bottom flange, $A_{fn} = 18(1.375) = 24.75$ in.[2]

$$\beta = \frac{2(58.31)(0.5)}{24.75} = 2.356$$

Separate calculations indicate that nominal first yielding will occur in the Grade HPS 70W bottom flange. Therefore, $f_n = 70.0$ ksi.

$$\rho = \frac{F_{yw}}{f_n} = \frac{50.0}{70.0} = 0.714$$

$$R_h = \frac{12 + 2.356[3(0.714) - (0.714)^3]}{12 + 2(2.356)} = 0.969$$

12. Frost, R.W., and C.G. Schilling. 1964. "Behavior of Hybrid Beams Subjected to Static Loads." *Journal of the Structural Division*, American Society of Civil Engineers, New York, NY, Vol. 90, ST3, June.
13. Schilling, C.G. 1967. "Web Crippling Tests on Hybrid Girders." *Journal of the Structural Division*, American Society of Civil Engineers, New York, NY, Vol. 93, ST1, February.
14. Schilling, C.G. 1968. "Bending Behavior of Composite Hybrid Beams." *Journal of the Structural Division*, American Society of Civil Engineers, New York, NY, Vol. 94, ST8, August.
15. Carskaddan, P.S. 1968. "Shear Buckling of Unstiffened Hybrid Beams." *Journal of the Structural Division*, American Society of Civil Engineers, New York, NY, Vol. 94, ST8, August.

16.   Toprac, A.A., and M. Natarajan. 1971. "Fatigue Strength of Hybrid Plate Girders." *Journal of the Structural Division*, American Society of Civil Engineers, New York, NY, Vol. 97, ST4, April.

16a.   Lwin, M. M. 2002. *High Performance Steel Designer's Guide.* Federal Highway Administration, Western Resource Center, San Francisco, CA, April.

16b.   Horton, R., E. Power, K. V. Ooyen, and A. Azizinamini. 2000. "High Performance Steel Cost Comparison Study." Conference Proceedings, Steel Bridge Design and Construction for the New Millenium with Emphasis on High Performance Steel, November 30 - December 1, Federal Highway Administration, Washington, D. C.

2.2.3 I-Girders

Section 2.4.2 of DM Volume 1, Chapter 2 discussed important issues related to general bridge layout, including span optimization; the relationship of the substructure to the superstructure; the selection of girder spacing and deck overhangs; the determination of field section sizes; and the use of constant versus variable depth girders. Section 2.4.3.1.4 of DM Volume 1, Chapter 2 covered additional issues specific to the preliminary design of steel I-girder bridges. These issues included the selection of the type of girder (rolled shape or welded girder), the layout of the framing plan including the cross-frame/diaphragm spacings and configurations and the potential need for lateral bracing. The fundamental behavior of steel stringer (i.e. multi I-girder) bridges was also discussed. This section of the Manual covers the proportioning of the flange and web plates for welded I-girders, including the determination of initial sizes; the specific *AASHTO LRFD* design provisions for checking I-girders for the service, fatigue and fracture, and strength limit states and for constructibility; design considerations for skewed I-girder bridges; and bearing considerations for I-girder bridges. But before covering these items, some important fundamental concepts related to the behavior of I-girders are reviewed in the following section.

2.2.3.1 Fundamental Concepts

This section covers the basic fundamental concepts related to the behavior of I-girder sections under flexure, torsion and shear. Only the basic fundamentals will be covered in this discussion as necessary to aid in further understanding of the specific design provisions for I-sections presented in subsequent sections of this chapter. Some rudimentary understanding of strength of materials and stability principles is assumed in this discussion. The reader is referred to the numerous available structural engineering textbooks and literature for further more detailed information on the fundamental behavior of these sections.

2.2.3.1.1 Flexure

2.2.3.1.1.1 Noncomposite Members with Full Lateral Support

This section will cover the behavior of noncomposite I-section members subject to flexure (note that the behavior of composite I-section members in negative flexure is similar and is assumed also covered by the subsequent discussions). It is assumed

in this discussion that the member is subject to transverse loads perpendicular to one principal axis (i.e. no biaxial bending); that the loads all pass through the shear center of the cross-section and thus, the member is not subject to torsion; that the member has sufficient lateral support along its length to prevent lateral-torsional buckling; and that the member has been proportioned to prevent local buckling of the compression flange prior to reaching its maximum potential flexural resistance F_{max} or M_{max}. Biaxial bending and the shear center will not be covered in detail in this discussion, but additional information on these topics can be found in any strength of materials textbook.

A qualitative bending moment versus rotation relationship for a homogeneous *compact web section* under the preceding conditions is shown in Figure 2.15. A homogeneous section is a considered to be a section in which the flanges and web have the same nominal yield strength. In the *AASHTO LRFD* Specifications, a compact web section is defined as a noncomposite section (or a composite section in negative flexure) that has a web with a slenderness at or below which the section can achieve a maximum flexural resistance M_{max} equal to the plastic moment M_p prior to web bend buckling having a statistically significant influence on the response. This assumes that specific steel grade, ductility, flange slenderness and lateral bracing requirements are satisfied (these specific requirements will be discussed in more detail in subsequent sections of this chapter). M_p was discussed in detail in a preceding section of this chapter (Section 2.2.2.1). Compact web sections are typically shallower sections with thicker webs; that is, rolled beams and welded girder sections with proportions similar to rolled beams.
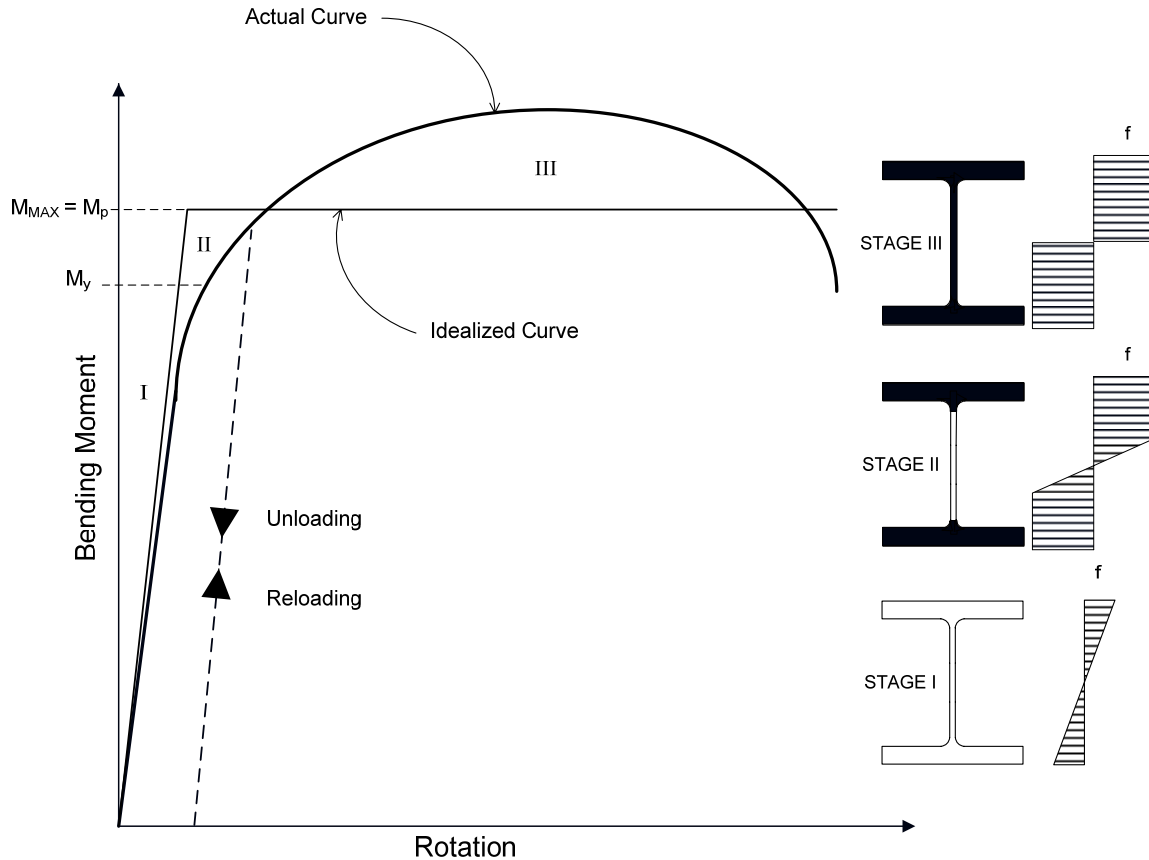
Figure 2.15 Bending Moment versus Rotation for Homogenous Compact Web Section

Proceeding along the actual curve shown in Figure 2.15, the initial Stage I behavior represents completely elastic behavior. As the section approaches the theoretical yield moment M_y (discussed previously in Section 2.2.2.2), the presence of residual stresses will result in some inelastic behavior in the outer fibers of the cross-section before the calculated M_y is reached. At Stage II, yielding continues and begins to progress throughout the section as the section approaches M_p. The actual curve shown in Figure 2.15 assumes the presence of a moment gradient along the length of the member with peak moments occurring at individual cross-sections. Under moment gradient conditions, the formation of a local buckle causing a decline in the flexural resistance requires yielding of the flange over a portion of the length of the member. Before such a local buckle can form, there may be significant strain hardening in the region of maximum moment. In such cases, as illustrated in the figure, compact web sections are actually able to exceed M_p due to the strain hardening before eventually unloading due to local buckling of the compression flange. However, because this excess flexural resistance is difficult to accurately predict, it is ignored in design. Also, under uniform moment conditions, local buckling will invariably occur before there is any significant increase in the flexural resistance attributable to strain hardening. Under these conditions, the resistance essentially plateaus at M_p before unloading eventually occurs.

Therefore, the idealized curve shown in Figure 2.15 is assumed for design. Because the residual stresses do not reduce the plastic moment, the section is assumed elastic up to M_p, and is then assumed to rotate inelastically at a constant moment equal to M_p. At this stage (Stage III in Figure 2.15), the entire cross-section has yielded; that is, each component of the cross-section is assumed to be at F_y. In some cases, if certain requirements are met, the available inelastic rotation capacity in these sections (i.e. the difference between the elastic rotation at M_p and the rotation where the moment drops below M_p) can be utilized to allow a redistribution of the bending moments from interior piers to more lightly loaded sections in positive flexure prior to making the design verifications at the service and strength limit states. In addition, composite sections in positive flexure may be able to achieve a nominal flexural resistance at or just below M_p in certain cases when these sections are used at interior piers.

In a hybrid section (discussed previously in Section 2.2.2.6), an additional stage between Stage I and Stage II occurs in which yielding develops in the lower-strength web while the flanges remain elastic (assuming both flanges have a yield strength higher than the web). Then at Stage II (in Figure 2.15), yielding will progress through the flanges while the web remains partially elastic. Otherwise, the behavior is similar. Again, the presence of residual stresses does not reduce $M_{max} = M_p$. Also, as discussed above, the redistribution of the stress to the flanges resulting from the local yielding of the web is ignored whenever the nominal flexural resistance exceeds the yield moment M_y. Therefore, the hybrid factor R_h is not applied to M_p for compact web sections.

The dotted line shown in Figure 2.15 illustrates the behavior of a member that is loaded with a moment greater than M_y and then unloaded. Note that elastic behavior is observed both during the unloading and subsequent reloading and a small residual curvature will remain in the member. Also, because the member behaves elastically during unloading and subsequent reloading, the effect of residual stresses is only observed during the initial application of the load as long as the moment due to any subsequent loads does not exceed the previously applied moment.

Figure 2.16 shows a qualitative moment versus rotation relationship for a homogeneous *slender web section* under the previously stated conditions. In the *AASHTO LRFD* Specifications, a slender web section is defined as a noncomposite section (or a composite section in negative flexure) that has a web with a slenderness at or above which the theoretical bend-buckling stress is reached in the web prior to reaching M_y. Because web bend-buckling is assumed to occur in such sections, the web load-shedding factor R_b (discussed previously in Section 2.2.2.5) must be introduced to account for the effect of the post bend buckling resistance or redistribution of the web compressive stresses to the compression flange resulting from the bend buckling of the web. Therefore, the maximum flexural resistance M_{max} is taken as the smaller of $R_b M_{yc}$ and M_{yt} for a homogeneous slender-web section, where M_{yc} and M_{yt} are the yield moments with respect to the compression and tension flanges, respectively (Figure 2.16 assumes yielding with respect to the compression flange controls). For a hybrid slender-web section, the hybrid factor R_h

is also introduced to account for the redistribution of the stress to both flanges resulting from the local yielding of the web. As for a compact web section, residual stresses will contribute to yielding and some inelastic behavior will occur prior to reaching M_{max}, as shown in Figure 2.16. However, unlike a compact web section, a slender web section has little or no available inelastic rotation capacity after reaching M_{max}.   Therefore, the flexural resistance drops off quite rapidly after reaching M_{max}, and redistribution of moments is obviously not permitted when these sections are used at interior piers.
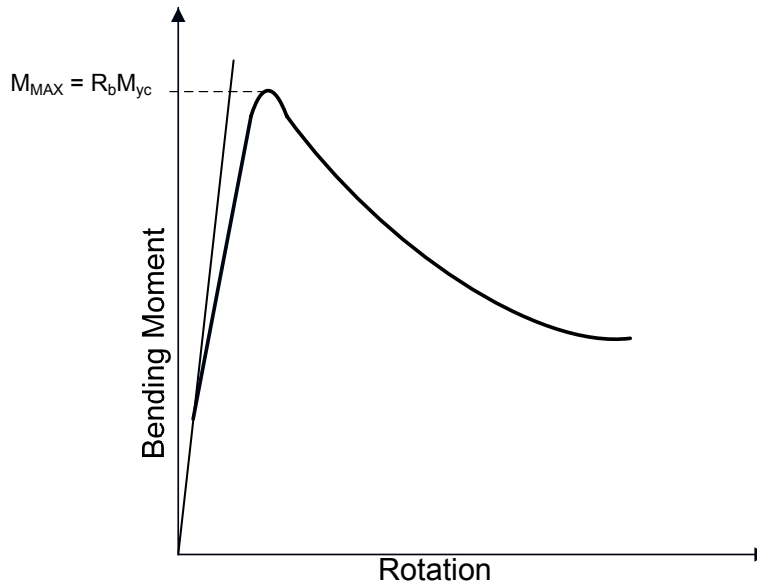
Figure 2.16 Moment versus Curvature for Homogenous Slender Web Section

Sections with a web slenderness in-between the slenderness limits for a compact web and a slender web section are termed *noncompact web sections*. This represents a change from previous Specifications, which defined *sections* as either compact or noncompact and did not distinguish between a noncompact and a slender web. In the *AASHTO LRFD* Specifications, a noncompact web section is defined as a noncomposite section (or a composite section in negative flexure) that has a web satisfying specific steel grade requirements and with a slenderness at or below which theoretical web bend-buckling does not occur at elastic stress levels, computed according to beam theory, smaller than M_{max}.   Because web bend buckling is not assumed to occur, R_b is taken equal to 1.0 for these sections. The maximum flexural resistance of a noncompact web section M_{max} is taken as the smaller of $R_{pc}M_{yc}$ and $R_{pt}M_{yt}$, and falls in-between M_{max} for a compact web and a slender web section as a linear function of the web slenderness ratio. R_{pc} and R_{pt} are termed web plastification factors for the compression and tension flange, respectively. The web plastification factors are essentially effective shape factors that define a smooth linear transition in the maximum flexural resistance between M_y and M_p. The specific expressions defining the web plastification factors will be given later on in this chapter (Section 2.2.3.7.1.2.2).

The basic relationship between M_{max} and the web slenderness $2D_c/t_w$ given in the *AASHTO LRFD* Specifications is shown in Figure 2.17. Figure 2.17 assumes that yielding with respect to the compression flange controls and that lateral-torsional buckling and local buckling (discussed later) are prevented. The relationship is defined for in terms of all three types of sections; compact web, noncompact web and slender web. The specific web slenderness limits $\lambda_{pw(Dc)}$ and λ_{rw} that delineate the different types of sections in Figure 2.17 will be defined later in Section 2.2.3.7.1.2 of this chapter (note that λ_{rw} was previously presented as Equation 2.13 as part of the discussion on web bend buckling). Note that at the slenderness limit $\lambda_{pw(Dc)}$ delineating a compact web and an noncompact web section, R_{pc} is taken equal to the cross-section shape factor M_p/M_{yc} corresponding to the compression flange. At the slenderness limit λ_{rw} delineating a noncompact web and a slender web section, R_{pc} is equal to the hybrid factor R_h.
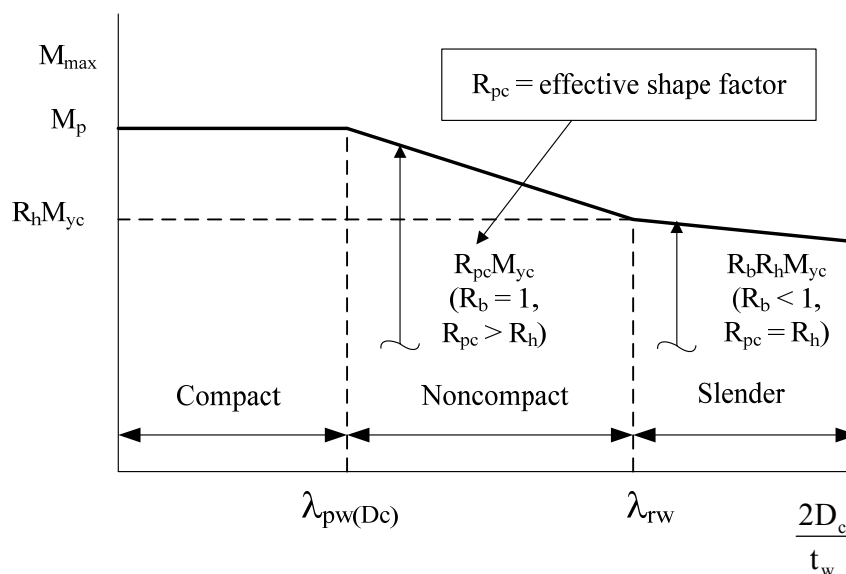
Figure 2.17 M_{max} versus Web Slenderness

Although the maximum flexural resistance of slender web sections has been expressed in terms of moment in the preceding discussion for convenience, it is considered more appropriate to express the maximum resistance in terms of stress for sections in which the maximum resistance is always less than or equal to M_y. Therefore, in the *AASHTO LRFD* Specifications, the flexural resistance for slender web sections is expressed in terms of stress (with the maximum flexural resistance given the moniker F_{max}). As discussed previously, in composite construction, the combined effects of the loadings acting on different states of the member cross-section (i.e. noncomposite, long-term composite and short-term composite) are better handled by working with flange stresses rather than moments. Bridge engineers are also generally more accustomed to working with stresses and analysis software can typically obtain stresses more directly than moments.

For compact web and noncompact web sections in which the maximum potential flexural resistance equals or exceeds M_y, expressing the flexural resistance in terms

of stress would generally result in stress limits greater than the yield stress for cases where the resistance exceeds M_y. Therefore, the resistance equations are more conveniently written in terms of bending moment for these sections. Also, as mentioned previously, for sections in which the flexural resistance is expressed in terms of moment, moments acting on the noncomposite, long-term composite and short-term composite sections may be directly summed for comparison to the nominal resistance. Effects of partial yielding within the cross-section and the sequence of application of loads acting on the different sections need not be considered.

The provisions provided in the main body of the *AASHTO LRFD* Specifications for noncomposite sections and composite sections in negative flexure (specifically the provisions of *AASHTO LRFD* Article 6.10.1.8) assume slender web behavior; that is, the nominal flexural resistance equations for these sections in the main body of the specification are expressed in terms of stress and the nominal flexural resistance does not exceed the yield stress of the flange times the appropriate flange-stress reduction factors. The provisions were couched in this way because the majority of steel-bridge I-sections utilize either slender webs or noncompact webs that approach the noncompact web slenderness limit λ_{rw}. The provisions in the main body of the specifications may be applied to sections with compact webs or noncompact webs that are nearly compact, which are typically used on bridges with shorter spans. However, this is done at the expense of some economy with the potential loss in economy increasing with decreasing web slenderness. In such cases, the Engineer is encouraged to utilize the optional provisions of Appendix A to Section 6 of the *AASHTO LRFD* Specifications, which apply directly to compact web and noncompact web sections satisfying specific steel grade and web and flange proportioning requirements. These provisions should especially be employed for sections utilizing compact webs. In Appendix A, the nominal flexural resistance equations are expressed in terms of bending moment and the nominal flexural resistance is permitted to exceed the nominal moment at first yield. The provisions of Appendix A are discussed further in Section 2.2.3.7.1.2.2 of this chapter.

2.2.3.1.1.2 Lateral-Torsional Buckling

This section will cover the basics of lateral-torsional buckling of noncomposite I-section flexural members (and composite I-section members in negative flexure). As the subject of lateral-torsional buckling is a relatively complex subject, only the basics will be covered here. There is much additional information available on this subject in the literature. It will be assumed in this discussion that the compression flanges are sturdy enough that they will not buckle locally and that the cross-section will not distort prior to buckling of the entire member between points of lateral support of the compression flange. The principal variable affecting the lateral-torsional buckling resistance is the distance between the points of lateral support. However, other variables affect the resistance as well including, but not limited to, the end restraints, type and position of the loads, material properties, residual stresses, initial imperfections and cross-section distortion.

If the compression flange of an I-section member does not have adequate lateral support, the member may deflect laterally in a torsional mode before the

compressive bending stress reaches the yield stress. For a compression flange to be adequately braced, the bracing must be sufficient to restrain lateral deflection of the flange and twisting of the entire cross-section at the brace points. The *AASHTO LRFD* Specifications refer to such flanges as *discretely braced compression flanges*. Figure 2.18 shows a doubly symmetric I-section member in pure bending, simply supported and held against twisting at both ends.   Under uniform compression, the top flange would buckle downward in its weak direction if this motion were not prevented by the web. Instead, if the force in the compression flange is large enough, the flange will tend to buckle horizontally, or in the only direction that it is free to move. The bottom flange, which is in tension, tends to remain straight. Therefore, the top flange tending to buckle, bends further than the bottom flange, which tends to remain straight. As a result, the entire cross-section rotates as one rigid unit, as shown in Figure 2.18. For an ideal straight and centered member, there is no tendency for this lateral-torsional motion until the moment reaches a critical magnitude M_{cr} at which the member becomes unstable and can undergo lateral deflections and rotations leading to collapse. For an I-section member, the tendency of the member to twist is resisted by a combination of St. Venant torsion and warping torsion (discussed in more detail below in the section on Torsion).   The general equation for the *elastic* lateral-torsional buckling resistance M_{cr} for a doubly symmetric I-section bent about the strong axis is given as (*17*):

$$M_{cr} = \frac{C_b \pi}{kL} \sqrt{EI_y GJ} \sqrt{1 + \frac{\pi^2 C_w E}{GJ(kL)^2}(C^2 + 1)} \pm \left(\frac{C\pi}{kL}\right)\sqrt{\frac{C_w E}{GJ}} \qquad \text{Equation 2.22}$$

where:
C	=	coefficient to account for load height effect
C_b	=	moment-gradient modifier
C_w	=	warping constant = $I_y h^2/4$ (in.^{6})
E	=	Young's modulus
G	=	shear modulus
h	=	vertical distance between flanges
I_y	=	moment of inertia about the vertical axis in the plane of the web (in.^{4})
J	=	St. Venant torsion constant (in.^{4})
k	=	effective length factor
L	=	unbraced length

Other more complex formulations have been developed for singly symmetric sections (*18-20*). The resistance to the differential bending of the flanges in their own plane increases with the bending rigidity of each flange in its own plane and with the distance between the flanges, as reflected in the warping constant C_w.
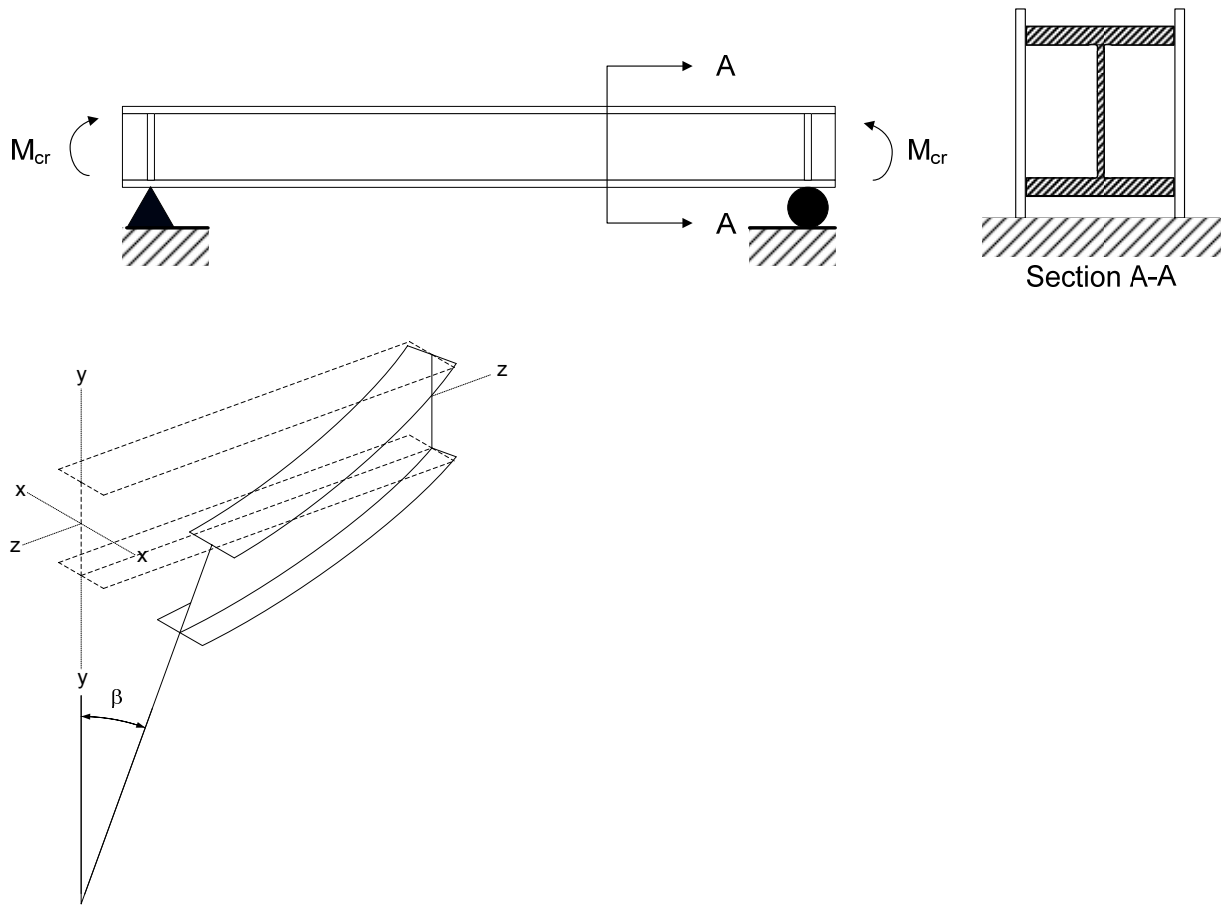
Figure 2.18 Doubly Symmetric I-section Member

In the development of Equation 2.22, it is assumed that the end supports for the member are torsionally simple, which means the end sections are prevented from twisting about the z-axis (Figure 2.18), but are free to warp out of plane. The effect of any warping restraint can be accounted for with the effective length factor k. For the case of no warping restraint, k = 1.0, and for full warping restraint, k = 0.5 (*21*). The base lateral-torsional buckling equations in the *AASHTO LRFD* Specifications conservatively assume k = 1.0. *AASHTO LRFD* Article C6.10.8.2.3 makes reference to a procedure (*18,22*) that can be used to calculate a reduced effective length factor for lateral torsional buckling that accounts for the restraint from adjacent unbraced lengths that are less critically loaded than the unbraced length under consideration. The resulting lower value of k can be used to appropriately increase the elastic lateral-torsional buckling resistance and to modify the unbraced length L_b in special situations. This use of this procedure is demonstrated in Reference 23.

The beneficial effect of a variation in the moment gradient along the length between brace points is accounted for by using the moment gradient modifier C_b, which can take a value between 1.0 and 2.3 depending on the ratio and relative sign of the end moments. The C_b factor will be discussed in greater detail in a subsequent section of this chapter on Strength Limit State Verifications (Section 2.2.3.7.1.2).

The coefficient *C* accounts for the tipping or stabilizing effect that occurs if transverse loads are applied at the top or bottom flange of the member. Top flange loading aggravates the tendency toward lateral bucking and therefore the last term in the brackets of Equation 2.22 should be subtracted if the load is applied through the top flange. Bottom flange loading has a stabilizing effect and therefore the last term should be added if load is applied through the bottom flange. For a simple span, *C* = 0.45 for a uniformly distributed load and 0.55 for a concentrated load. If the load is applied through the centroid or if the beam is loaded by end moments, *C* is taken equal to zero. Most specifications, including the *AASHTO LRFD* Specifications, neglect the effect of load height. The neglect of this effect is believed justified because of the conservative approximations made in simplifying the theoretical formulas for use in design and also by the relative severity of the loading condition on which the provisions are based. Also, when loads are applied to the top flange, the members transmitting the load typically provide restraint to the twisting (e.g. the concrete deck). More recent formulations have accounted for the effect of the load height instead through the C_b factor (*18*). Although not done in the *AASHTO LRFD* Specifications, *AASHTO LRFD* Article C6.10.8.2.3, points out that for unusual situations with no intermediate cross-bracing and for unbraced cantilevers with significant loading applied to the top flange, load-height effects should be considered in the calculation of C_b. In such cases, C_b can actually be less than 1.0. Solutions for unbraced cantilevers are given in Reference 24.

In the *AASHTO LRFD* Specifications, Equation 2.22 (minus the load height effect) is simplified and extended to cover singly symmetric sections by introducing an effective radius of gyration for lateral-torsional buckling r_t, which is essentially the radius of gyration of the compression flange plus 1/3 of the depth of the web in compression. Also, within the main provisions of the specification, the St. Venant torsional constant *J* is assumed equal to zero in Equation 2.22. As discussed previously, the main provisions of the specification are assumed to apply to slender web sections. For very slender web sections, such as deep longitudinally stiffened girders, the contribution of *J* to the elastic lateral-torsional buckling resistance is generally small. Distortion of the web into an S shape and the corresponding raking of the flanges relative to each other is likely to reduce the buckling resistance further. For less slender sections approaching the noncompact web section slenderness limit λ_{rw} (refer to Equation 2.13), ignoring *J* tends to be conservative, but the resulting simplification of the equation leads to greater overall design convenience. For compact web and noncompact web sections designed according to the optional provisions of Appendix A, *J* is included in the elastic buckling equation since these stockier sections are not subject to significant web distortion. Both forms of the elastic lateral-torsional buckling equations given in the *AASHTO LRFD* Specifications will be presented later on in Section 2.2.3.7.1.2 of this chapter under the topic of Strength Limit State Verifications.

Lateral-torsional buckling in the elastic range is of primary importance for relatively slender girders braced at longer than normal intervals. Therefore, the elastic lateral-torsional buckling resistance is most useful when considering the resistance of such girders during the construction phase. In most cases, girders will be braced at intervals such that the girder will buckle laterally and torsionally only after some portions of the girder have exceeded the yield strain. This phenomenon is referred

to as inelastic lateral-torsional buckling. Inelastic lateral-torsional buckling is complex, as it is influenced by the magnitude and distribution of residual stresses, initial geometric imperfections, and the reduction in various stiffness properties (i.e. Young's modulus, shear modulus, minor-axis bending stiffness, St. Venant torsional stiffness and warping torsional stiffness) as a result of yielding due to in-plane flexure prior to buckling. Many researchers have employed a tangent-modulus approach to investigate the effect of inelastic lateral-torsional buckling. As shown in Figure 2.19, the *AASHTO LRFD* Specifications have adopted a simple linear expression to approximate the lateral-torsional buckling resistance of discretely braced compression flanges in the inelastic range (note that Figure 2.19 also shows the basic form of the flange local buckling equations in the *AASHTO LRFD* Specifications, which is similar to the form of the lateral-torsional buckling equations). Flange local buckling will be discussed in the next section of this chapter).
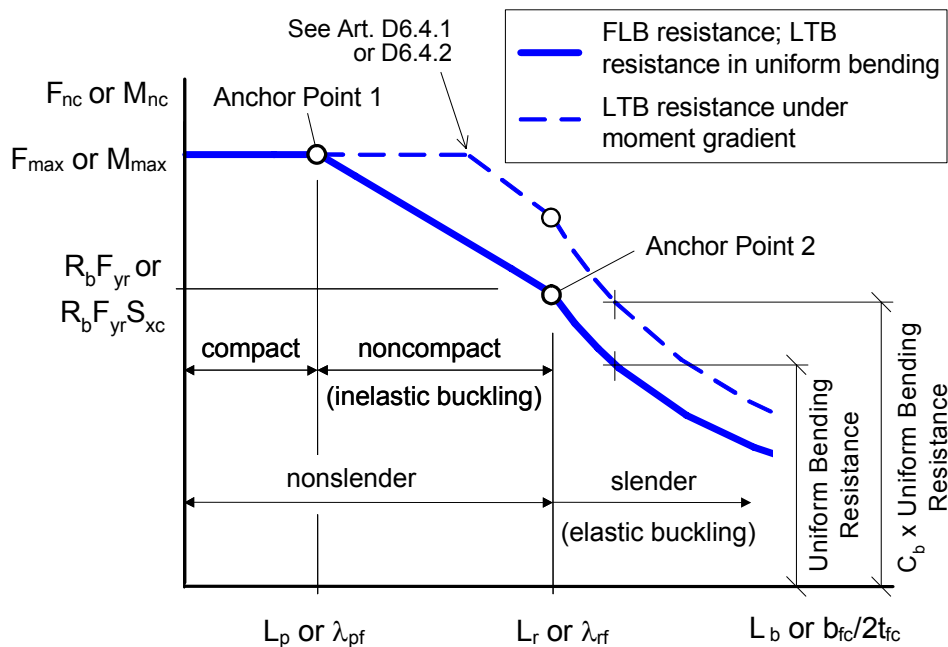
Figure 2.19 Form of the Compression-Flange Resistance Equations in the *AASHTO LRFD* Specifications

Looking at the solid curve in Figure 2.19, which represents the lateral-torsional buckling resistance for the case of uniform major-axis bending, the inelastic buckling resistance falls in-between Anchor Points 1 and 2. Anchor Point 1 is located at the unbraced length $L_b = L_p$ for lateral-torsional buckling under uniform bending corresponding to development of the maximum potential flexural resistance, labeled as F_{max} or M_{max} in the figure, as applicable (discussed previously). L_p is also referred to as the limiting *compact unbraced length*.

Note that in many cases, particularly under uniform bending, it will not be economical to brace the girder at a distance equal to L_p or below in order to reach F_{max} or M_{max}.

Anchor Point 2 is located at the unbraced length $L_b = L_r$ for which the inelastic and elastic lateral-torsional buckling resistances are the same. In the main provisions, this resistance is taken as $R_b F_{yr}$, where F_{yr} is taken as the smaller of $0.7F_{yc}$ and F_{yw}, but not less than $0.5F_{yc}$. With the exception of hybrid sections with F_{yw} significantly smaller than F_{yc}, $F_{yr} = 0.7F_{yc}$. This limit corresponds to an assumed nominal compression flange residual stress effect of $0.3F_{yc}$. As pointed out in *AASHTO LRFD* Article C6.10.8.2.3, the $0.5F_{yc}$ limit on F_{yr} avoids anomalous situations for some types of cross-sections in which the inelastic buckling equation gives a larger resistance than the corresponding elastic buckling curve. In the optional Appendix A, in which nominal flexural resistances are expressed in terms of bending moment, this resistance is taken as $R_b F_{yr} S_{xc}$, where S_{xc} is the elastic section modulus to the compression flange.   An additional limit of $R_h F_{yt} S_{xt}/S_{xc}$ is also placed on F_{yr} in Appendix A, where S_{xt} is the section modulus to the tension flange, in order to preclude the effects of early tension-flange yielding on the elastic lateral-torsional buckling resistance in unusual cases where the depth of the web in compression is small. L_r is also referred to as the limiting *noncompact unbraced length*.   For L_b greater than L_r, the lateral-torsional buckling resistance is governed by elastic buckling.   The specific expressions given for L_p and L_r in the *AASHTO LRFD* Specifications will be discussed later on in Section 2.2.3.7.1.2 of this chapter.

For unbraced lengths subject to a moment gradient, the lateral-torsional buckling resistances for the case of uniform major-axis bending are simply scaled by the moment gradient modifier C_b, with the exception that the inelastic lateral-torsional buckling resistance is capped at F_{max} or M_{max}, as illustrated by the dashed line in Figure 2.19. The maximum unbraced length at which the lateral-torsional buckling resistance is equal to F_{max} or M_{max} under a moment gradient may be determined from *AASHTO LRFD* Article D6.4.1 or D6.4.2 (in Appendix D to Section 6 of the *AASHTO LRFD* Specifications), as applicable.

2.2.3.1.1.3 Compression-Flange Local Buckling

This section will cover the basics of compression-flange local buckling in noncomposite I-section flexural members (and composite I-section members in negative flexure).   In the *AASHTO LRFD* Specifications, local buckling is only to be considered for discretely braced compression flanges, which typically occur on these types of members. Local bend buckling of webs was covered in an earlier section of this chapter. Local buckling of uniformly compressed components of compression members will be discussed in a later section of this chapter on Compression Member Design (i.e. Section 2.4.3.2.1.3.1).

Figure 2.20 Local Buckling of Compression Flange

Both rolled and built-up steel sections are composed of flat plate elements. When these elements are compressed, they may buckle locally out of their original planes, as illustrated in Figure 2.20. In a flexural member, the width-to-thickness ratio of the compression flange is the controlling parameter for local buckling.   The critical elastic buckling stress for a perfectly flat plate with no residual stress subjected to a uniform uniaxial compressive stress is given as follows (*7*):

$$F_{cr} = \frac{k_c \pi^2 E}{12(1-\mu^2)(b_{fc}/t_{fc})^2}$$ Equation 2.23

where:
  b_{fc} =   width of the plate along the edge subject to compression (in.)
  E   =   Young's modulus (29,000 ksi for steel)
  t_{fc} =   thickness of the plate (in.)
  k_c =   plate buckling coefficient (discussed below)
  μ =   Poisson's ratio (0.3 for steel)

The plate buckling coefficient k_c depends on the boundary conditions of the plate element. For one-half of a girder compression flange (i.e. substitute $b_{fc}/2$ for b_{fc} in Equation 2.23), the longitudinal edge representing the flange-web juncture may be assumed pinned or restrained against rotation. The other longitudinal edge of the flange is free. For idealized pinned conditions at one edge and the other edge free, k_c is equal to 0.425 for a long plate typical of practical structural members; for fully-restrained conditions along one edge, k_c increases to 1.277 (*7*).   If an objective is to reach F_{yc} prior to elastic local buckling of the flange, substituting F_{yc} for F_{cr} in Equation 2.23 and rearranging yields:

$$\frac{b_{fc}}{2t_{fc}} \leq 0.95 \sqrt{\frac{Ek_c}{F_{yc}}}$$ Equation 2.24

In Appendix A to Section 6, the following expression is given for k_c for built-up sections:

$$k_c = \frac{4}{\sqrt{\dfrac{D}{t_w}}}$$
<div align="right">Equation 2.25</div>

<div align="right">*AASHTO LRFD* Equation A6.3.2-6</div>

This expression, which results from research by Johnson (*25*), accounts for the fact that thinner webs in built-up sections tend to offer less rotational restraint to prevent flange local buckling. The calculated value of k_c from Equation 2.25 must fall between the range of 0.35 and 0.76. The lower-bound value of 0.35 (which controls at D/t_w values greater than approximately 130) is back-calculated by equating the local buckling resistances given in the *AASHTO LRFD* Specifications to measured resistances from tests conducted by Johnson and others with D/t_w values ranging from 72 to 245. The fact that the lower-bound value is less than 0.425 (which assumes idealized simply supported boundary conditions along the web-flange juncture) is indicative of the fact that web local buckling in more slender webs tends to destabilize the compression flange. The upper-bound value of 0.76 corresponds to the traditional value that has been assumed for rolled shapes (*26*). In fact, k_c is explicitly specified to be 0.76 for rolled shapes in Appendix A, as web-flange interaction effects on the local buckling resistance of compression flanges of rolled shapes are considered to be negligible. In the Main Provisions of the specifications, which are assumed to apply only to slender-web sections, a k_c value of 0.35 is conservatively assumed for all sections resulting in *AASHTO LRFD* Equation 6.10.8.2.2-5 (when k_c is taken equal to 0.35 and F_{yr} is substituted for F_{yc} in Equation 2.24).

A $b_{fc}/2t_{fc}$ limit based on Equation 2.24 is not rational, however, as elastic local buckling typically does not control for practical bridge-girder sections. The flange-proportioning limit specified in *AASHTO LRFD* Article 6.10.2.2 (discussed below under Flange Sizing), which limits $b_{fc}/2t_{fc}$ to a practical maximum value of 12.0, precludes elastic flange local buckling for specified minimum yield strengths of the compression flange F_{yc} up to and including 90 ksi. In fact, because of this, elastic flange local buckling resistance equations are not provided in either Appendix A or the Main Provisions of the *AASHTO LRFD* Specifications in order to streamline the specifications. The use of the inelastic flange local buckling resistance equation (discussed below) is permitted for the rare case in which $b_{fc}/2t_{fc}$ may be in the elastic buckling range for F_{yc} greater than 90 ksi.

In previous Specifications, limits on the width-to-thickness ratio of compression flanges were typically specified as a function of the yield strength of the flange and were taken to be an indirect check on the local buckling resistance of the flange. As discussed below, in the *AASHTO LRFD* Specifications, the compression-flange local buckling resistance as a function of $b_{fc}/2t_{fc}$ and the yield strength of the flange is now explicitly calculated, with $b_{fc}/2t_{fc}$ capped at the specified upper limit of 12.0.

For intermediate values of $b_{fc}/2t_{fc}$, residual stresses and initial imperfections give rise to inelastic local buckling, represented in the *AASHTO LRFD* Specifications by a linear transition curve (the specific equation representing this curve will be presented later on in the chapter). As shown by the solid curve in Figure 2.19, which also represents the compression-flange local buckling resistance (note that the flange local buckling resistance for moment gradient cases is the same as that for the case of uniform major-axis bending; that is, the relatively minor influence of moment gradient effects is neglected), the inelastic buckling resistance falls in-between Anchor Points 1 and 2.

Anchor Point 2 is located at the compression-flange slenderness $b_{fc}/2t_{fc} = \lambda_{rf}$ for which the inelastic and elastic flange local buckling resistances are the same. Note that the resistance F_{yr} at this anchor point is taken to be the same resistance as described earlier for lateral-torsional buckling. λ_{rf} is given by Equation 2.24, with F_{yr} appropriately substituted for F_{yc} (and with k_c taken as 0.35 in the Main Provisions only). λ_{rf} is referred to as the limiting slenderness ratio for a *noncompact flange.* In the *AASHTO LRFD* Specifications, a noncompact flange is defined as a discretely braced compression flange with a slenderness at or below which localized yielding within the cross-section associated with a hybrid web, residual stresses and/or cross-section monosymmetry has a statistically significant effect on the nominal flexural resistance. For $b_{fc}/2t_{fc}$ greater than λ_{rf}, the local buckling resistance is governed by elastic buckling.

Anchor Point 1 is located at the compression-flange slenderness $b_{fc}/2t_{fc} = \lambda_{pf}$ corresponding to development of the maximum potential flexural resistance, labeled as F_{max} or M_{max} in the figure, as applicable (discussed previously). λ_{pf} is referred to as the limiting slenderness ratio for a *compact flange*. A compact flange is defined in the *AASHTO LRFD* Specifications as a discretely braced compression flange with a slenderness at or below which the flange can sustain sufficient strains such that the maximum potential flexural resistance is achieved prior to flange local buckling having a statistically significant influence on the response (assuming bracing requirements are also satisfied to develop the maximum potential resistance).

In order to achieve the maximum potential flexural resistance, flanges may be required to undergo significant plastic compressive strain without having local buckling occur. For plastic design, a girder will have adequate rotation capacity at a plastic hinge if its flanges are capable of straining to the point of incipient strain hardening prior to buckling, which is typically at a point approximately 15 to 20 times the yield strain.   To achieve this condition, the compression-flange slenderness should not exceed the following limit:

$$\frac{b_{fc}}{2t_{fc}} \leq 0.30\sqrt{\frac{E}{F_{yc}}}$$

Equation 2.26

The development of this limit is beyond the scope of this document, but is described in detail elsewhere (*21, 27*).   Because residual stress effects and material imperfections have less effect in the plastic range, and because compressive plastic strains only about one-half the strain necessary to reach strain hardening are

required to simply reach maximum flexural resistance equal to the plastic moment, this limit was felt to be too severe for λ_{pf} (28).   Therefore, the limit for λ_{pf} was increased to the following:

$$\frac{b_{fc}}{2t_{fc}} \leq 0.38\sqrt{\frac{E}{F_{yc}}}$$ Equation 2.27

AASHTO LRFD Equation 6.10.8.2.2-4

Note that Equation 2.27 is equivalent to *AASHTO LRFD* Equation 6.9.4.2-2 (Equation 2.334) with k_c taken as the lower-bound value of 0.35.

The nominal flexural resistance of the compression flange for noncomposite sections and composite sections in negative flexure is taken as the smaller of the calculated local buckling and lateral-torsional buckling resistances.

2.2.3.1.1.4 Composite Sections in Positive Flexure

Basic fundamentals regarding composite sections (e.g. unshored versus shored construction, modular ratio, effective deck width, elastic section properties, stiffness assumptions for analysis, yield moment and plastic moment) were reviewed in a preceding section of this chapter. Some additional fundamental issues related specifically to the behavior of composite sections subject to positive flexure will be reviewed in this section.

In the *AASHTO LRFD* Specifications, the nominal flexural resistance of composite sections *in straight girders* subject to positive flexure that satisfy specific steel grade, web slenderness and ductility requirements is permitted to exceed the moment at first yield at the strength limit state.   Sections meeting these requirements are termed *compact sections*. The nominal flexural resistance of sections not meeting one or more of these requirements, termed *noncompact sections*, is not permitted to exceed the moment at first yield. The terms compact and noncompact sections are retained from previous Specifications. For compact sections, the nominal flexural resistance is most appropriately expressed in terms of moment and for noncompact sections, the nominal flexural resistance is most appropriately expressed in terms of the elastically computed flange stress (for reasons discussed previously).

In order to qualify as a compact section, the section must be in a straight girder and the specified minimum yield strengths of the flanges must not exceed 70 ksi. The use of larger yield strengths may result in significant nonlinearity and potential crushing of the concrete deck prior to reaching nominal flexural resistance values above the moment at first yield. Also, the section must not have any longitudinal web stiffeners (i.e. D/t_w must not exceed 150 as discussed in the next section of this chapter on Web Sizing).   There are insufficient test data to support designing sections with longitudinal stiffeners for moments above $R_h M_y$. Composite sections with longitudinal stiffeners are deeper sections that tend to be used on longer spans and thus, are subject to larger noncomposite dead load stresses. Therefore, the depth of the web in compression D_c is likely to be such that substantial inelastic strains would not be able to develop in the web prior to bend buckling of the web

occurring at moment levels close to R_hM_y. Finally, the section must also satisfy the following web slenderness limit:

$$\frac{2D_{cp}}{t_w} \le 3.76\sqrt{\frac{E}{F_{yc}}}$$

Equation 2.28

AASHTO LRFD Equation 6.10.6.2.2-1

where:

D_{cp} =   depth of the web in compression at the plastic moment (discussed previously)

Equation 2.28 is a web slenderness limit for compact sections retained from previous Specifications. In a composite girder subject to positive flexure, the concrete deck causes an upward shift in the neutral axis, which reduces the depth of the web in compression. This reduction continues as plastic strains associated with moments larger than R_hM_y are incurred. As a result, most composite sections in positive flexure without longitudinal stiffeners in straight bridges will qualify as compact according to Equation 2.28. Since the majority of the web is in tension in these sections, there is typically significant available reserve capacity. Compact composite sections in positive flexure must also satisfy a ductility requirement (discussed below) to prevent premature crushing of the concrete deck prior to achieving the calculated nominal flexural resistance, which will ensure a ductile mode of failure.

The nominal flexural resistance of compact composite sections in positive flexure depends on the ratio of the depth of the plastic neutral axis below the top of the deck D_p to the total depth of the composite section D_t. Sections with a ratio of D_p/D_t less than or equal to 0.1 can reach the plastic moment M_p of the composite section as a minimum without any ductility concerns. When the ratio of D_p/D_t exceeds 0.1, the nominal flexural resistance is reduced from M_p as a linear function of D_p/D_t to provide an additional margin of safety against premature crushing of the concrete deck, which follows a general philosophy espoused by Wittry (*29*). The linear equation, which is simpler in form than the equation given in previous Specifications, depends only on M_p and the ratio of D_p/D_t, as also suggested in Reference 30.   This equation will be presented later on in this chapter in Section 2.2.3.7.1.1.1 of this chapter under Strength Limit State Verifications.

The nominal flexural resistance of these sections in straight continuous spans is subject to an additional limitation, unless the span and all adjacent interior-pier sections have sufficient ductility and robustness to ensure that the redistribution of moments caused by partial yielding within the positive flexure regions is insignificant. Composite I-sections in positive flexure can have a shape factor, or ratio of M_p/M_y, exceeding 1.5 in certain cases (note: as a point of comparison, the shape factor of a doubly symmetric noncomposite I-section is typically around 1.12). As a result, a considerable amount of yielding and inelastic curvature is required to reach M_p, which reduces the stiffness of the composite section. The resulting reduction in stiffness can shift moment from the positive to the negative flexure regions in continuous spans. The shedding of moment to adjacent interior-pier sections could potentially result in incremental collapse under repeated live loads if the interior-pier sections do not have the additional capacity needed to sustain these larger

moments; for example, interior-pier sections with slender webs and moment-rotation curves similar to the curve shown in Figure 2.16 that unload rapidly once the peak moment resistance is exceeded. Therefore, in such situations, the amount of additional moment allowed above $R_h M_y$ at compact composite sections in positive flexure in continuous spans is limited to 30 percent of $R_h M_y$. To ensure adequate strength and ductility of the composite section, the resulting nominal flexural resistance of $1.3 R_h M_y$ must not exceed either M_p or the nominal flexural resistance determined from the linear relationship discussed above, as applicable. In most cases, unless D_p/D_t is relatively large or M_p/M_y is relatively small, the limiting value of $1.3 R_h M_y$ will control. As discussed below under Tips on Flange Sizing, additional flexural resistance beyond this limit is usually not needed at the strength limit state as the size of the bottom flange of these sections will most often be controlled by fatigue or service limit state design criteria. In fact, because other limit state criteria will likely control in this instance, treating these sections conservatively as noncompact sections (discussed below) simplifies the calculations somewhat and should not result in a significant loss of economy in most cases.

As alluded to previously, the limiting value of $1.3 R_h M_y$ may be waived if special steps outlined in *AASHTO LRFD* Article 6.10.7.1.2 are taken to ensure that the span and all adjacent interior-pier sections have adequate ductility to absorb the effects of potential moment shifting. The specific steps, which will be reviewed in more detail later on, involve restrictions on the skew and cross-frame alignment, and on the steel grade, compression-flange slenderness and bracing, web slenderness, shear and minimum available plastic rotation capacity of the adjacent pier sections. As an example, most rolled shapes or welded shapes of comparable proportions will satisfy the restrictions related specifically to the cross-section.

For noncompact composite sections in positive flexure, the nominal flexural resistance of the top (compression) flange is limited to the specified minimum yield strength of the flange times the flange-stress reduction factors R_b and R_h. The nominal flexural resistance of the bottom (tension) flange is limited to the specified minimum yield strength of the flange times R_h. Noncompact sections must also satisfy the ductility requirement discussed in the next paragraph to ensure a ductile failure. An additional limitation is specified for extremely rare cases when a noncompact composite section may be utilized in shored construction. In such cases, the longitudinal stress in the concrete deck is limited to $0.6f'_c$ to ensure linear behavior of the concrete, which is assumed in the calculation of the flange stresses. This limitation is not required for the more common case of unshored construction, as the stress in the concrete deck is typically significantly less than f'_c at first yield of either flange.

As discussed previously, both compact and noncompact composite sections in positive flexure must satisfy a ductility requirement to prevent premature crushing of the concrete deck prior to reaching the specified nominal flexural resistance. In the *AASHTO LRFD* Specifications, the ductility requirement for composite steel sections has been made equivalent to the maximum reinforcement requirement for concrete structures specified in *AASHTO LRFD* Article 5.7.3.3.1. That is, the ratio of D_p/D_t must be less than or equal to 0.42. Although noncompact sections are not permitted to exceed the moment at first yield, it is required that the ductility requirement still be

satisfied to ensure a ductile failure, and to prevent premature crushing of the deck for sections that may utilize up to 100-ksi steel and/or that are utilized in shored construction. In calculating D_t, the thickness of the concrete deck haunch over the girder may be conservatively neglected. Otherwise, a lower-bound estimate of this thickness should be used. Satisfying this requirement also helps permit the web bend buckling check to be neglected for composite sections in positive flexure without longitudinal stiffeners after the deck hardens or is made composite, as discussed previously.

Top (compression) flanges of composite sections in positive flexure are referred to in the *AASHTO LRFD* Specifications as *continuously braced flanges.* A continuously braced flange is defined as a flange encased in concrete or anchored by shear connectors (note that top flanges of sections in negative flexure will also often qualify as continuously braced flanges at the strength limit state under this definition). For a continuously braced compression flange, one side of the flange is effectively prevented from local buckling, or else both sides of the flange must buckle in the direction away from the concrete deck, resulting in highly restrained boundary conditions at the web-flange juncture. The concrete deck also helps restrain lateral deflections of the flange associated with local and lateral-torsional buckling. As a result, continuously braced compression flanges need not be checked for local or lateral-torsional buckling according to the *AASHTO LRFD* Specifications. Lateral flange bending stresses (discussed below) also need not be considered for continuously braced flanges, including any lateral flange bending stresses induced in the flange before it becomes continuously braced. The lateral resistance of the composite concrete deck is generally sufficient to compensate for the neglect of any initial lateral bending stresses in the flange, as well as any additional lateral bending stresses that may be induced after the deck has been placed.

2.2.3.1.2 Torsion

A torsional moment applied to the opposite ends of a member causes each cross-section of the member to twist or rotate, as shown in Figure 2.21(a). If the member is a round member or a solid tube, the resistance to the torsion is provided solely by shear stresses, which are proportional to the distance from the centroid; there is no warping as each cross-section rotates in its own plane. The resistance resulting from the distribution of shear stresses is known as pure torsion or St. Venant torsion.
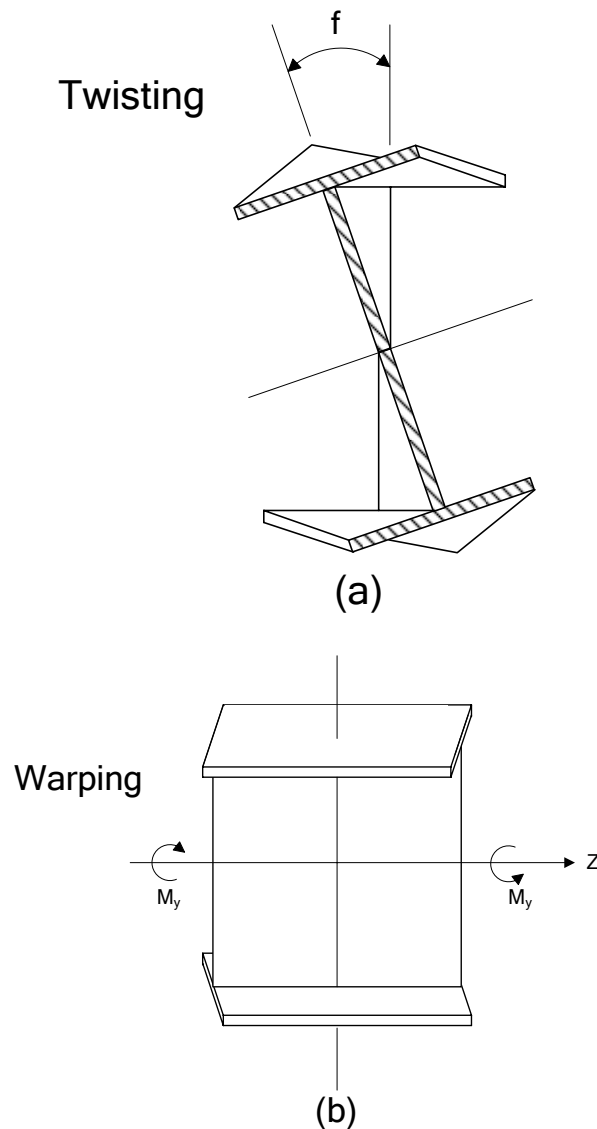
Figure 2.21 (a) Rotated Cross Section, (b) Warped Section

If a non-circular cross-section, such as an I-section, is subjected to a torsional moment, the cross-section will deform non-uniformly in the longitudinal direction so that plane sections do not remain plane after twisting occurs. This cross-sectional deformation is referred to as warping, as shown in Figure 2.21 (b). If the warping is not restrained, the torsional moment is resisted as St. Venant torsion. If warping is restrained, additional torsional resistance results from transverse shears that develop in the girder flanges due to the flexural resistance of the flanges.   The resisting torque is equal to the transverse force in the flange times the distance between the flange centers. This additional component of the torsional resistance resulting from restraint of warping is known as non-uniform or warping torsion. The transverse shears bend each flange as a rectangular beam about its own major axis resulting in lateral flange bending moments and normal warping stresses in each flange (Figure 2.22(a)).   These normal warping stresses are more commonly referred to as lateral flange bending stresses, which are additive to the major-axis

flexural stresses acting on the member. The lateral flange bending moment times the distance between flange centers is often referred to as the bimoment, which is most commonly used in the computation of certain fundamental torsional section properties (*32*).

$$\sigma = \frac{M_x y}{I_x} + \text{WARPING NORMAL STRESS}$$

(a)

$$\tau = \frac{V_y Q_x}{I_x t} + \text{ST. VENANT TORSION} + \text{WARPING TORSION}$$

(b)
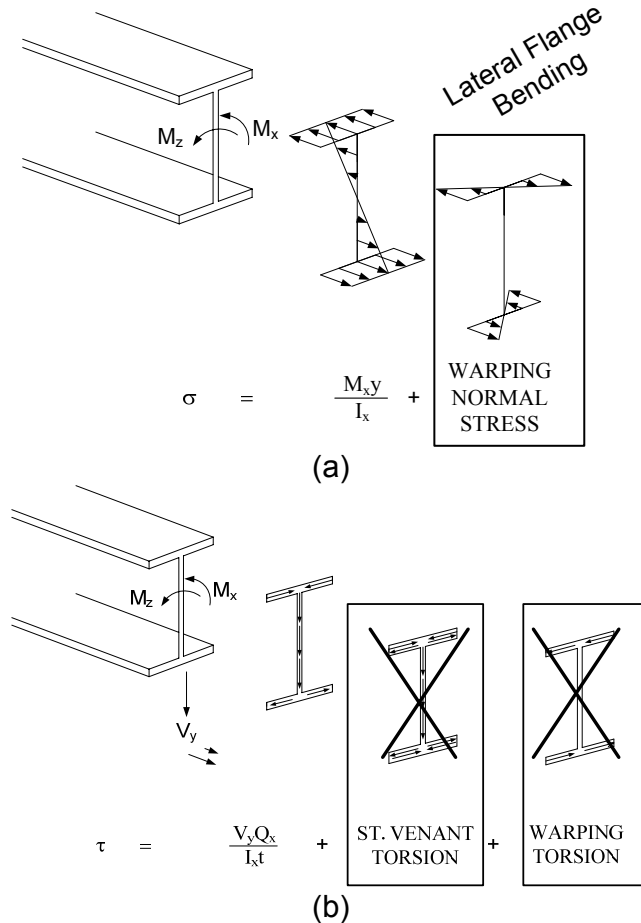
Figure 2.22 (a) Normal Stresses, (b) Shear Stresses

Torsion is generally resisted through a combination of St. Venant torsion and warping torsion. For closed cross-sections, such as box girders or tubular members, and for relatively compact open sections, such as rolled channels, tees or angles, St. Venant torsion generally dominates. For large open cross-sections, such as many rolled shapes and fabricated I-sections, warping torsion is generally predominant. In design, it is often convenient and always conservative to base the design on the dominant type of torsion for the section under consideration and neglect the effect of the other type of torsion. As discussed previously, this was done in neglecting the contribution of the St. Venant torsion in the development of the elastic lateral-torsional buckling resistance equation for slender-web I-sections in the Main Provisions of the *AASHTO LRFD* Specifications (note, however, that both St. Venant and warping torsion are considered in the development of the LTB resistance equation for stockier compact web and noncompact web I-sections given in Appendix A to *AASHTO LRFD* Section 6). Also, as shown in Figure 2.22 (b), in an I-section subject to torsion, the shears due to St. Venant torsion are typically

neglected. As an aside, the transverse shears due to warping torsion are also typically neglected, leaving only the bending shears as a consideration in the design. For an I-section subject to torsion, the lateral flange bending moments and stresses due to warping torsion are the primary consideration.

2.2.3.1.2.1 St. Venant Torsion

Assume an I-section is subjected to equal and opposite torques on otherwise free ends, as shown in Figure 2.23(a); that is, the section is theoretically free to warp out-of-plane at each end (i.e. there is no restraint to warping). Also, assume that the cross-section does not distort so that the rate of twist ϕ per unit length is constant. Therefore, the section may be thought of as three interconnected rectangular elements (flanges and web) twisting through the same angle. As a result, the torsional shear distribution will be almost identical to that in the three separate narrow rectangles. For a narrow rectangle subject to pure torsion, the following relationship between the resisting torque T_s and the twist per unit length can be derived (21):

$$T_s = G\left(bt^3/3\right)\frac{d\phi}{dz}$$

Equation 2.29

where:

    b   =   width of the rectangle (in.)
    G   =   shear modulus (ksi)
    t   =   thickness of the rectangle (in.)

For an I-section, the total resisting torque consists of the individual contributions from the flanges and from the web or:

$$T_s = G\sum\frac{bt^3}{3}\frac{d\phi}{dz} = GJ\frac{d\phi}{dz}$$

Equation 2.30

where:
    J   =   St. Venant torsional constant $= \sum bt^3/3 \,(\text{in.}^3)$

where b and t are the individual width and thickness of each of the individual flange and web elements. In Appendix A to *AASHTO LRFD* Section 6, a more accurate approximation of *J* for an I-section, neglecting the effect of web-to-flange fillets, is given as follows (33):

$$J = \frac{Dt_w^3}{3} + \frac{b_{fc}t_{fc}^3}{3}\left(1-0.63\frac{t_{fc}}{b_{fc}}\right) + \frac{b_{ft}t_{ft}^3}{3}\left(1-0.63\frac{t_{ft}}{b_{ft}}\right)$$

Equation 2.31

AASHTO LRFD Equation A6.3.3-9

where:
    b_{fc} =   width of the compression flange (in.)

b_{ft} = width of the tension flange (in.)
D = depth of the web (in.)
t_{fc} = thickness of the compression flange (in.)
t_{ft} = thickness of the tension flange (in.)
t_w = thickness of the web (in.)

For flanges with $b_f/2t_f$ greater than 7.5, the term in parentheses for that flange in Equation 2.31 may be taken equal to one. More accurate values of J for rolled W-shapes, including the effect of the web-to-flange fillets, are tabulated in Reference 128a.
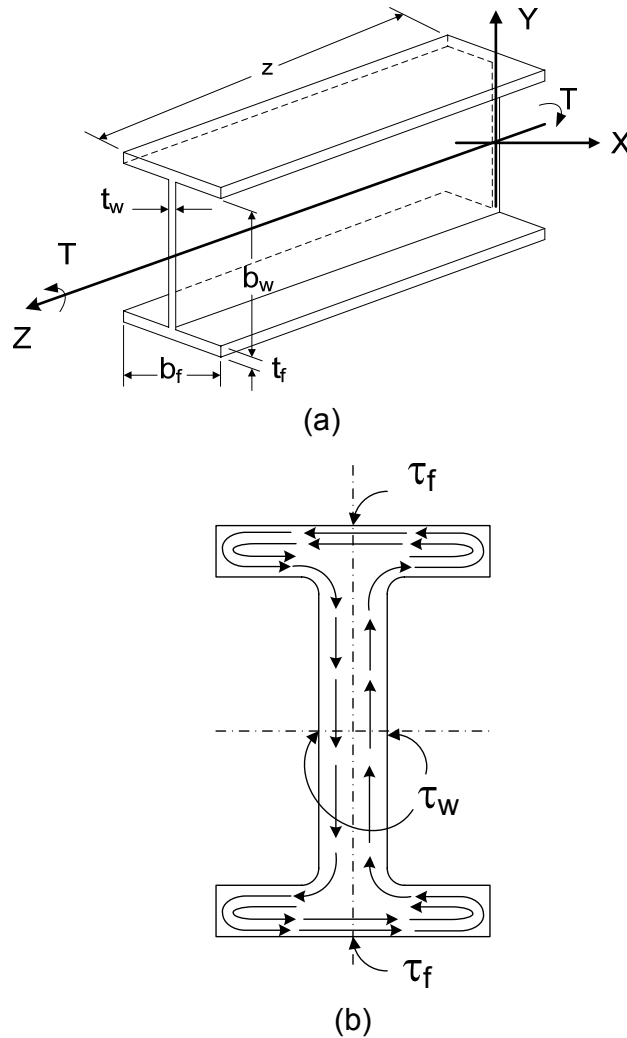

(a)

(b)

Figure 2.23 (a) I-Section Subject to Equal and Opposite Torques, (b) Peaks of Shear Stress

Although typically neglected, as discussed above, the St. Venant torsional shears in the flanges (τ_f) and web (τ_w) of the I-section can be approximated from the formula for a narrow rectangle, again summing the contribution from the separate components:

$$\tau_f = \frac{T_s t_f}{J} \qquad \tau_w = \frac{T_s t_w}{J}$$

Equation 2.32

As shown in Figure 2.23 (b), peaks of shear stress occur on the outer fibers at the center of the flange and on the outer fibers at mid-height of the web.

The St. Venant torsional stiffness is reduced by distortion of the cross-section. The resistance of the flanges to twisting and the interaction between the flanges and web will cause the section to distort. When web distortion becomes significant, the two flanges plus the adjacent portions of the web act as semi-independent beams bent in the transverse direction. As a result, a greater portion of the total torque will be resisted by warping torque than indicated by strength of materials theory (assuming there is warping restraint). It is for this reason that the contribution of the St. Venant torsional stiffness is conservatively neglected in determining the elastic lateral-torsional buckling resistance of slender-web sections in the *AASHTO LRFD* Specifications. For compact web and noncompact web sections, an additional safeguard is specified to allow the use of the full St. Venant torsional stiffness in determining the elastic lateral-torsional buckling resistance in Appendix A to *AASHTO LRFD* Section 6 as follows:

$$\frac{I_{yc}}{I_{yt}} \geq 0.3$$

Equation 2.33

AASHTO LRFD Equation A6.1-2

where:

I_{yc} = moment of inertia of the compression flange of the steel section about the vertical axis in the plane of the web (in.^{4})

I_{yt} = moment of inertia of the tension flange of the steel section the vertical axis in the plane of the web (in.^{4})

This limit guards against the use of extremely monosymmetric noncomposite I-sections. Cross-section distortion can significantly reduce the influence of the St. Venant torsional stiffness on the lateral-torsional buckling resistance of these sections.

2.2.3.1.2.2 Warping Torsion

The warping component of the total torque T_w for an I-section is given as follows (*21, 28*):

$$T_w = -EC_w \frac{d^3\phi}{dz^3}$$

Equation 2.34

where:

C_w = warping torsional constant = $I_y h^2/4$ (in.^{6})

h = distance between the centerlines of the flanges (in.)

I_y = moment of inertia of the I-section about a vertical axis in the plane of the web (in.^{4})

Therefore, the following differential equation results for the total torsional moment *T*:

$$T = T_s + T_w = GJ\frac{d\phi}{dz} - EC_w\frac{d^3\phi}{dz^3}$$

Equation 2.35

Knowing the boundary conditions, the differential equation can be solved for ϕ and its various derivatives leading to exact theoretical solutions for the various torsional stresses and lateral flange bending moments.

However, as mentioned previously, in I-girder design, the St. Venant torsional component is typically ignored and all torsion is assumed carried by warping torsion. The magnitude of the warping torque is typically not needed in design. Also, the shears in the flanges due to warping torsion are generally ignored. The main components of interest are the lateral flange bending moments and associated lateral flange bending stresses. Therefore, rather than solving the more complex differential equation to obtain these quantities, reasonable engineering approximations are typically made in design in order to obtain these values (unless they are obtained directly from a refined analysis of the structure).

In straight I-girder bridges, significant flange lateral bending may be caused by wind, by torsion from eccentric concrete deck overhang loads acting on cantilever forming brackets placed along exterior girders, and by the use of discontinuous cross-frame/diaphragm lines in conjunction with skews exceeding 20°. As will be seen and demonstrated later on in this chapter, with the exception of lateral flange bending due to the effects of skew, the most common approximation used to obtain the flange lateral bending moments (in lieu of a refined analysis) is based on the assumption of interior unbraced lengths in which the flange is continuous with approximately equal adjacent unbraced lengths such that, due to approximate symmetry boundary conditions, the ends of the unbraced lengths are effectively torsionally fixed. In addition, the major-axis bending moment is generally assumed constant between the brace points. These are generally conservative approximations, which are also often used to determine lateral flange bending effects due to curvature in horizontally curved I-girder bridges. Once the lateral flange bending moments have been determined, the first-order flange lateral bending stresses can simply be determined by dividing the lateral moment by the section modulus of the flange about a vertical axis in the plane of the web.

After the lateral flange bending stresses have been determined, the issue then becomes how to effectively and rationally combine these stresses with the flange major-axis bending stresses in order to check the capacity of the flange (or section). In the Third Edition *AASHTO LRFD* Specifications, the following basic form is introduced for all the resistance equations in which the combined effects of major-axis and flange lateral bending must be considered for members in which the major-axis bending resistance is expressed in terms of flange stress:

$$f_{bu} + \frac{1}{3}f_\ell \le \phi_f F_n \qquad\qquad \text{Equation 2.36}$$

where:

f_{bu} = flange major-axis bending stress determined as specified in *AASHTO LRFD* Article 6.10.1.6 (ksi)

f_ℓ = flange lateral bending stress (ksi)

F_n = nominal flexural resistance in terms of flange major-axis bending stress (ksi)

ϕ_f = resistance factor for flexure

and as follows for members in which the bending resistance is expressed in terms of moment:

$$M_u + \frac{1}{3}f_\ell S_x \le \phi_f M_n \qquad\qquad \text{Equation 2.37}$$

where:

M_n = nominal flexural resistance in terms of the major-axis bending moment (kip-in.)

M_u = member major-axis bending moment determined as specified in *AASHTO LRFD* Article 6.10.1.6 (kip-in.)

S_x = elastic section modulus about the major-axis of the section to the flange under consideration generally taken as M_y/F_y (in.^{3})

Equations 2.36 and 2.37 are referred to as the one-third rule equations. A detailed discussion of the derivation and validation of the one-third rule equations is provided in Reference 34. Basically, the one-third rule equations address the combined effects of major-axis bending and lateral bending by handling discretely braced compression flanges as equivalent beam-columns. For discretely braced tension flanges, the one-third rule equations approximate the full plastic strength of a rectangular cross-section subjected to combined major-axis and lateral bending. The resistance equations are written in an interaction format in which the left-hand side of the equations pertains to the applied load effects, and the right-hand side of the equations is the appropriate member resistance in major-axis bending. The stress f_{bu} in Equation 2.36 and the moment M_u in Equation 2.37 are analogous to the axial loading within a beam-column, and the stress f_ℓ is analogous to the beam-column bending moment. Note that M_u is considered analogous to axial loading since it produces axial stresses in the flanges. The factor of 1/3 in front of f_ℓ provides an accurate linear approximation of the beam-column resistance or the flange plastic strength (as applicable), at least up to the specified limit on f_ℓ of $0.6F_{yf}$ given in the Specifications (Figure 2.24). In both forms of the equations, all terms are to be taken as positive in sign (with an exception discussed in *AASHTO LRFD* Article C6.10.1.6). The application of the various forms of the one-third rule equations at different limit states will be discussed in greater detail in later sections of this chapter.
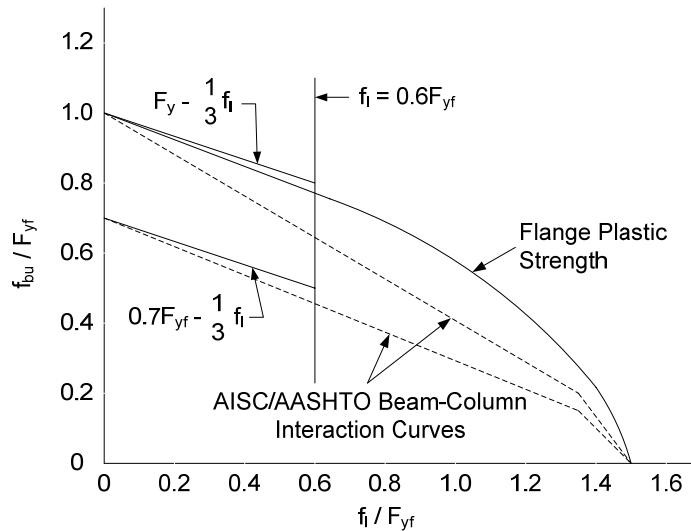
Figure 2.24 One-Third Rule Equations – Conceptual Basis

In beam-column members subject to axial compression, secondary bending moments arise equal to the compressive force times the lateral deflection of the member. As a result, the internal bending moments in the beam-column members are amplified. Taking the equivalent beam-column analogy one step further, as applied to girder flanges in the one-third rule equation development, consideration must therefore be given to amplifying the compression-flange lateral bending stresses in certain situations. Amplification of tension-flange stresses is not required since the effects tend to be relatively minor compared to the effects on compression flanges. In bridge members, it is generally impractical to calculate second-order flange lateral bending stresses directly for the case of moving live loads. Therefore, in the *AASHTO LRFD* Specifications, a simpler approach is provided in *AASHTO LRFD* Article 6.10.1.6 to account for the second-order effects in an approximate fashion. That is, whenever Equation 2.36 is applied to check a discretely braced compression flange, second-order lateral bending stresses in the flange may be approximated by amplifying first-order values as follows:

$$f_\ell = \left(\frac{0.85}{1 - \dfrac{f_{bu}}{F_{cr}}} \right) f_{\ell 1} \geq f_{\ell 1} \qquad \text{Equation 2.38}$$

AASHTO LRFD Equation 6.10.1.6-4

where:

f_{bu} = largest value of the compressive stress due to the factored loads throughout the unbraced length in the flange under consideration, calculated without consideration of flange lateral bending (ksi)

$f_{\ell 1}$ = first-order compression-flange lateral bending stress (ksi)

F_{cr} = elastic lateral-torsional bucking stress determined from *AASHTO LRFD* Equation 6.10.8.2.3-8 or *AASHTO LRFD* Equation A6.3.3-8, as applicable (ksi). *AASHTO LRFD* Equation A6.3.3-8 may only be

applied for unbraced lengths in which the web is compact or noncompact

An equivalent expression is used whenever Equation 2.37 is employed:

$$f_\ell = \left(\frac{0.85}{1 - \dfrac{M_u}{F_{cr}S_{xc}}} \right) f_{\ell 1} \geq f_{\ell 1}$$

                    Equation 2.39

AASHTO LRFD Equation 6.10.1.6-5

where:

M_u =   largest value of the major-axis bending moment due to the factored loads throughout the unbraced length causing compression in the flange under consideration (kip-in.)

S_{xc} =   elastic section modulus about the major-axis of the section to the compression flange taken as M_{yc}/F_{yc} (in.^{3})

Equations 2.38 and 2.39 represent an established form of the amplification equation used to estimate maximum second-order elastic moments in braced beam-column members whose ends are restrained by other framing. The purpose of these equations is to guard conservatively against large unbraced lengths in which second-order flange lateral bending effects are significant; for example, in certain construction situations such as when determining the effective of eccentric concrete deck overhang loads acting on exterior-girder flanges. As shown in Reference 35, these equations give accurate to conservative estimates of flange second-order lateral bending stresses. The equations tend to be significantly conservative for larger unbraced lengths in which f_{bu} also approaches F_{cr} or M_u approaches $F_{cr}S_{xc}$. In most cases, F_{cr} will be computed from *AASHTO LRFD* Equation 6.10.8.2.3-8. However, for sections with compact or noncompact webs, *AASHTO LRFD* Equation A6.3.3-8, which includes the contribution of the St. Venant torsional stiffness in determining F_{cr}, may optionally be used.

In cases where the amplification resulting from these equations is large, consideration may be given to using an effective length factor k less than 1 in the calculation of the elastic lateral-torsional buckling resistance to appropriately increase F_{cr} (the procedure for calculating k was discussed previously under Lateral-Torsional Buckling). *It should be noted that F_{cr} for use in Equation 2.38 is not limited to $R_bR_hF_{yc}$ and $F_{cr}S_{xc}$ for use in Equation 2.39 is not limited to $R_{pc}M_{yc}$, as these quantities would be when calculating the elastic lateral-torsional buckling resistance in the design of the compression flange.* For cases where the amplification of construction dead-load stresses is large, an additional alternative would be to consider conducting a direct geometric nonlinear analysis to more accurately determine the second-order effects. In the final constructed condition, the amplification factor would only need be considered for the bottom flange in negative-flexure regions in continuous spans. In these cases, however, F_{cr} is increased significantly due to the moment gradient that exists in these regions, through the moment-gradient modifier C_b.

AASHTO LRFD Article 6.10.1.6 indicates when first-order flange lateral bending stresses in discretely braced compression flanges, determined from an elastic analysis, need to be amplified. That is, whenever the unbraced length L_b exceeds the limiting value of L_b for which f_ℓ equals $f_{\ell 1}$ in Equation 2.38, which is given as:

$$\left(L_b\right)_{lim} = 1.2L_p \sqrt{\frac{C_b R_b}{f_{bu}/F_{yc}}}$$

Equation 2.40

AASHTO LRFD Equation 6.10.1.6-2

or equivalently, the limiting value of L_b for which f_ℓ equals $f_{\ell 1}$ in Equation 2.39, which is given as:

$$\left(L_b\right)_{lim} = 1.2L_p \sqrt{\frac{C_b R_b}{M_u/M_{yc}}}$$

Equation 2.41

AASHTO LRFD Equation 6.10.1.6-3

where:

C_b = moment-gradient modifier specified in *AASHTO LRFD* Article 6.10.8.2.3 or *AASHTO LRFD* Article A6.3.3, as applicable

L_p = limiting unbraced length to reach a lateral-torsional buckling resistance equal to F_{max} or M_{max}, as applicable, specified in *AASHTO LRFD* Article 6.10.8.2.3 (in.)

R_b = web load-shedding factor specified in *AASHTO LRFD* Article 6.10.1.10.2

The application of Equations 2.38 through 2.41 will be demonstrated later on in this chapter.

2.2.3.1.3 Shear

2.2.3.1.3.1 General

The algebraic sum of the applied loads and reactions on either side of the transverse cross-section of a girder is the shear force *V* at that section. Shear can only occur in the presence of bending, but is usually considered independent of bending in design practice (note that this discussion only deals with shear due to bending and not shear caused by torsion which was discussed in the previous section). *V* is resisted by internal shear stresses that are maximum on horizontal and vertical planes passing through the neutral axis of the section. The elastic shear stress f_v is given by the following fundamental equation:

$$f_v = \frac{VQ}{It}$$

Equation 2.42

where:

I   =   moment of inertia of the section about the strong axis (in.[4])
Q   =   first statical moment of the cross-sectional area above the point where the shear stress is calculated taken about the neutral axis of the cross-section (in.[3])
t   =   thickness of the girder where the shear stress is calculated (in.)

For an I-girder, the distribution of elastic shear stresses through the depth of the section is shown in Figure 2.25. Note that the shear stress in the flanges is generally small and is typically ignored. The variation in the shear stress in the web is also small so the shear stress in the web is typically approximated as an average shear stress equal to the shear force divided by the web area or V/Dt_w. Shear forces resisted in this manner are typically referred to as shears carried by beam action.
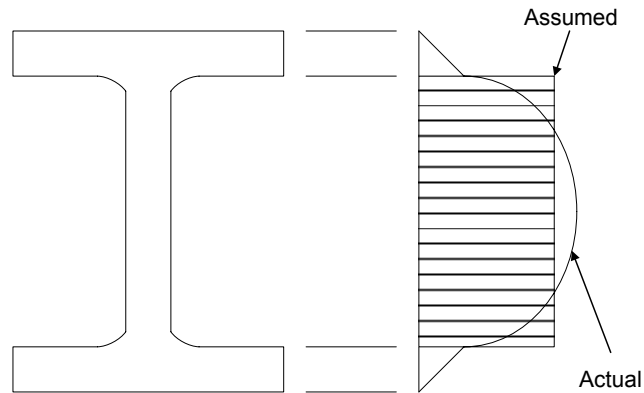
Figure 2.25 Distribution of Elastic Shear Stresses

The shear force causing yielding in shear is known as the plastic shear force V_p. The shear yield stress τ_y is equal to $F_{yw}/\sqrt{3}$. Therefore, V_p is calculated as follows:

$$V_p = \frac{F_{yw}}{\sqrt{3}}Dt_w = 0.58F_{yw}Dt_w \qquad\qquad \text{Equation 2.43}$$

AASHTO LRFD Equation 6.10.9.2-2

Deflections due to shear are typically much smaller than bending deflections and usually do not need to be considered, except for beams with large depth-to-length ratios.

In composite girders, the vertical shear force is assumed resisted by the web of the steel girder. The horizontal shear force per unit length VQ/I, where I is the moment of inertia of the transformed composite section, that develops during bending of the girder (sometimes referred to as shear flow) must be transferred between the deck and girder by shear connectors to prevent slip along the concrete/steel interface in order to facilitate composite action between the girder and the deck. The design of shear connectors for this horizontal shear force is discussed in Section 2.2.5 of this chapter.   Flange-to-web welds are also typically designed for the horizontal shear flow.

2.2.3.1.3.2 Shear Buckling Resistance

To investigate the shear buckling resistance, consider a theoretically flat web panel hypothetically subjected to pure shear, as shown in Figure 2.26(a). The length of the panel between transverse stiffeners is d_o, and the clear height of the panel between flanges is D. As shown in Figure 2.25(b) and Figure 2.25(c), an element in pure shear is equivalent to an element rotated 45 degrees and acted upon by a principal tensile stress and an equal principal compressive stress acting in the perpendicular direction. Assume then that the web will buckle in shear perpendicular to the direction of the principal compressive stress. The panel, if properly supported around the edges, does not fail at this point unless the stress is well above the proportional limit. The buckled plate is able to support the diagonal compression through beam shear since unrestrained out-of-plane deflection of the panel is prevented by the diagonal tension. For web panels with significant post-buckling resistance (discussed below), it is assumed that the diagonal compression retains the value of beam shear resistance it had when the plate buckled all the way up to complete failure.

(a)

(b)

(c)
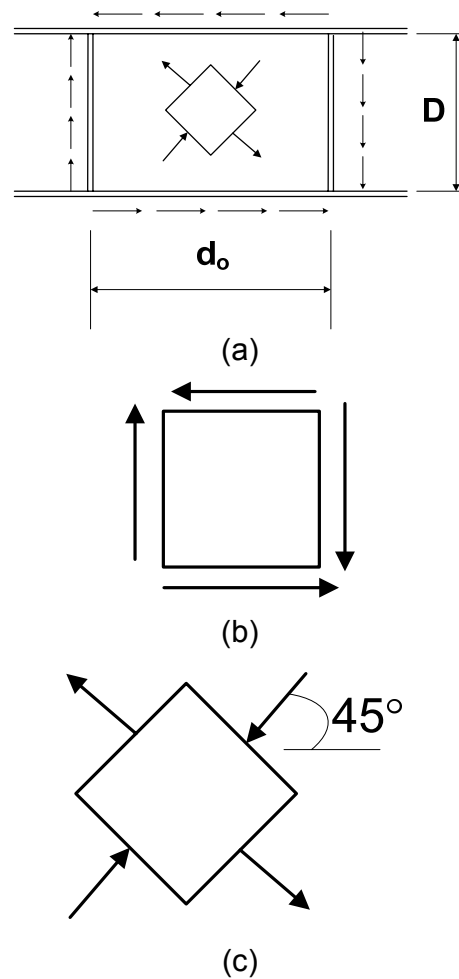
Figure 2.26 (a) Web Panel Subjected to Pure Shear, (b) Pure Shear, (c) Shear Equivalent

The elastic buckling stress of a flat plate subject to pure shear is given as follows (*7*):

$$\tau_{cr} = \frac{k\pi^2 E}{12(1-\mu^2)(D/t_w)^2}$$

Equation 2.44

Assuming simply supported boundary conditions along the edges, which is the typical assumption used in design practice, the shear buckling coefficient *k* is given as (*7*):

$$\text{For } \frac{d_o}{D} \le 1: \quad k = 4.0 + \frac{5.34}{\left(\dfrac{d_o}{D}\right)^2}$$

Equation 2.45

$$\text{For } \frac{d_o}{D} > 1: \quad k = \frac{4.0}{\left(\dfrac{d_o}{D}\right)^2} + 5.34 \qquad \text{Equation 2.46}$$

where d_o is the transverse stiffener spacing.

In the *AASHTO LRFD* Specifications, Equations 2.45 and 2.46 have been consolidated into a single simplified expression for *k*, which is independent of the panel aspect ratio, as follows:

$$k = 5 + \frac{5}{\left(\dfrac{d_o}{D}\right)^2} \qquad \text{Equation 2.47}$$

AASHTO LRFD Equation 6.10.9.3.2-7

For an unstiffened web, *k* is taken equal to 5.0, which is a conservative approximation of the exact value of *k* = 5.34 for an infinitely long strip with simply supported edges (*7*).

For design, Equation 2.44 is expressed in nondimensional form by introducing the constant *C*, which is defined as the ratio of the shear buckling stress τ_{cr} to the shear yield stress τ_y. Therefore, substituting ν = 0.3 in Equation 2.44:

$$C = \frac{\tau_{cr}}{\tau_y} = \frac{k\pi^2 E\sqrt{3}}{F_{yw}(12)(1-0.91)(D/t_w)^2} = \frac{1.57}{\left(\dfrac{D}{t_w}\right)^2}\left(\frac{Ek}{F_{yw}}\right) \qquad \text{Equation 2.48}$$

AASHTO LRFD Equation 6.10.9.3.2-6

which is given as *AASHTO LRFD* Equation 6.10.9.3.2-6.

As is the case for lateral-torsional buckling and flange local buckling, residual stresses and geometric imperfections can cause inelastic buckling in shear as the critical stress approaches the yield stress. A transition curve for inelastic buckling was developed by Basler (*36*) based on the assumption that $\tau_{cr} = \sqrt{0.8\tau_y\tau_{cr}}$. That is, it was assumed that the proportional limit for shear is $0.8\tau_y$, which is higher than for flanges in compression because the effect of residual stresses is less for shear. Therefore, dividing τ_{cr} under the preceding radical by τ_y to obtain *C*, and substituting the value of *C* from Equation 2.48 gives:

$$C = \sqrt{0.8C} = \sqrt{0.8\frac{1.57}{\left(\dfrac{D}{t_w}\right)^2}\left(\frac{Ek}{F_{yw}}\right)} = \frac{1.12}{\dfrac{D}{t_w}}\sqrt{\frac{Ek}{F_{yw}}} \qquad \text{Equation 2.49}$$

AASHTO LRFD Equation 6.10.9.3.2-5

which is given as *AASHTO LRFD* Equation 6.10.9.3.2-5. When *C* exceeds 0.8, *C* is taken from Equation 2.49. Therefore, substituting a *C* value of 0.8 in Equation 2.48 and solving for D/t_w gives $D/t_w = 1.40\sqrt{Ek/F_{yw}}$ above which *C* is calculated from Equation 2.49 and at or below which *C* is calculated from Equation 2.48. When C is equal to 1.0, the shear resistance is equal to the shear yield stress. Therefore, substituting a C value of 1.0 into Equation 2.49 and solving for D/t_w gives $D/t_w = 1.12\sqrt{Ek/F_{yw}}$ below which *C* is taken equal to 1.0 and shear yielding controls. The relationship between the buckling strength in shear and the web slenderness ratio D/t_w, based on the preceding equations, is shown graphically in Figure 2.27.
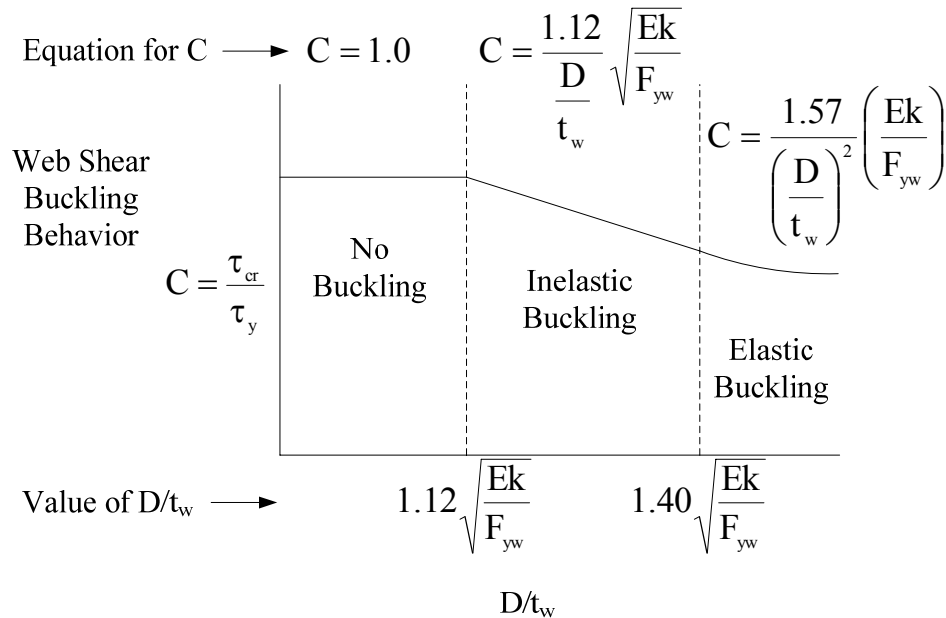
Figure 2.27 Web Shear Buckling Behavior

The nominal shear resistance of the girder based on shear buckling (elastic or inelastic) or shear yielding can be computed as:

$$V_n = V_{cr} = \tau_{cr}Dt_w \qquad\qquad \text{Equation 2.50}$$

Substituting C = τ_{cr}/τ_y gives:

$$V_n = V_{cr} = C\tau_yDt_w = CV_p \qquad\qquad \text{Equation 2.51}$$
$$\textit{AASHTO LRFD} \text{ Equation 6.10.9.2-1}$$

2.2.3.1.3.3 Post-Buckling Shear Resistance

A web plate stiffened by flanges and transverse stiffeners can carry shear forces considerably greater than its shear buckling resistance; that is, the panel has

considerable post-buckling shear resistance. After the web buckles, the girder acts in a manner similar to a Pratt truss with part of each web panel acting as a diagonal tension member carrying the tension forces by membrane action of the web (so-called tension-field action), with the compression forces carried by the transverse stiffeners in conjunction with the adjacent portions of the web (Figure 2.28). The ability of a plate girder to carry shear in the post-buckling range by truss action was recognized as early as 1898 (*36*). Early applications of the diagonal tension-field theory were primarily in the aircraft industry where strength-to-weight ratios are critical factors and thin metal construction is employed.
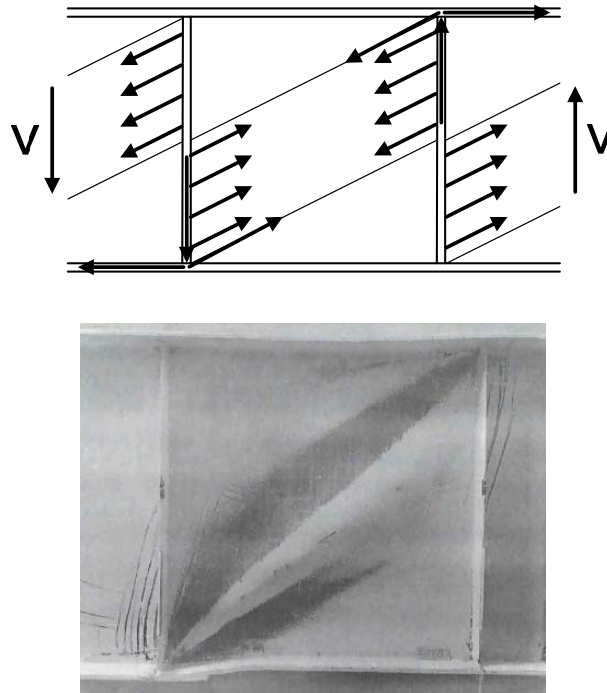
Figure 2.28 Web Shear Buckling Behavior

As mentioned above, it is assumed that the diagonal compression retains the value of beam shear resistance it had when the plate first buckles all the way up to complete failure. Therefore, the nominal shear resistance for post buckling can be computed by summing the contributions of beam action V_{cr} and tension-field action $V_{tf.}$ The development of $V_{tf.}$ has been the subject of numerous research studies worldwide and many different theories have been espoused. An in-depth discussion of all these theories or even the development of the classical value of V_{tf} as developed by Basler (*21, 28, 36*), which is still used in many design specifications including the *AASHTO LRFD* Specifications, is beyond the scope of this document. The Basler formulation, which neglects any contribution of the flanges in resisting the diagonal tensile stresses, and conservatively assumes that the angle of the diagonal tension field is at 45 degrees from the horizontal, results in the following expression for V_{tf}:

$$V_{tf} = \frac{0.87 V_p (1-C)}{\sqrt{1 + \left(\dfrac{d_o}{D}\right)^2}}$$

Equation 2.52

Therefore, the total nominal shear resistance can be written as:

$$V_n = V_p \left[C + \frac{0.87(1-C)}{\sqrt{1 + \left(\dfrac{d_o}{D}\right)^2}} \right]$$

Equation 2.53

AASHTO LRFD Equation 6.10.9.3.2-2

Previous Specifications included a moment-shear interaction relationship for web panels subject to tension-field action. According to this relationship, the bending and shear resistance of web panels subject simultaneously to both high shear and bending stresses was reduced due to the yielding that could potentially occur under the action of the combined stresses. Recent research (*37*) has led to the removal of this relationship in the *AASHTO LRFD* Specifications. Instead, web panels with the entire section along the panel proportioned to satisfy the following criterion:

$$\frac{2Dt_w}{\left(b_{fc} t_{fc} + b_{ft} t_{ft}\right)} \leq 2.5$$

Equation 2.54

AASHTO LRFD Equation 6.10.9.3.2-1

are assumed able to develop the full post-buckling shear resistance due to tension-field action given by Equation 2.53. If Equation 2.54 is satisfied, along with the requirement on the cross-section aspect ratio given by Equation 2.56 (discussed below), and if the maximum moment within the web panel is used to check the flexural resistance, then it is felt that the shear resistance equations given in the specification adequately reflect the majority of the available experimental test results without the need to consider moment-shear interaction effects. The moment-shear interaction relationship was not originally developed to handle the effect of moving loads. Although maximum moment and shear envelope values were typically used to check this relationship, these values generally were not caused by concurrent loadings, which added a level of conservatism. Determining the most critical combination of concurrent moment and shear to check this relationship was not practical. In addition, the anchorage of the tension field and additional shear resistance provided by the composite concrete deck is conservatively neglected in all the shear resistance equations.

If Equation 2.54 is not satisfied, the total area of the flanges within the panel is small relative to the area of the web and the full post-buckling resistance generally cannot be developed. Rather than reducing the shear resistance to V_{cr}, it was felt to be conservative to use a lesser level of the post-buckling shear resistance given by the following equation (*28*):

$$V_n = V_p \left[C + \frac{0.87(1-C)}{\sqrt{1 + \left(\dfrac{d_o}{D}\right)^2} + \dfrac{d_o}{D}} \right]$$

Equation 2.55

AASHTO LRFD Equation 6.10.9.3.2-8

which is given as *AASHTO LRFD* Equation 6.10.9.3.2-8. The extra d_o/D term in the denominator reflects the solution that neglects the shear contribution within the wedges outside of the tension band that was implicitly included by Basler in the development of Equation 2.53.

A recent development also incorporated in the *AASHTO LRFD* Specifications is the extension of the post-buckling shear resistance due to tension-field action to webs of hybrid girders (37, *38, 38a*). In previous Specifications, the shear resistance of hybrid girder webs was conservatively limited to V_{cr} given by Equation 2.51.

Equations 2.53 and 2.55 are applied to stiffened interior web panels. End panels, adjacent to abutments, are not permitted to develop any post-buckling resistance. Instead, the shear resistance of these panels is limited to V_{cr} (Equation 2.51) in order to provide a sufficient anchor for the development of the tension field in the immediately adjacent interior panels; that is, to absorb any imbalance of the computed horizontal component of the diagonal tension stress in the adjacent panels. In determining V_{cr} for the end panel, the shear buckling coefficient k is to be calculated based on the spacing from the support to the first transverse stiffener adjacent to the support, which cannot exceed 1.5D.

The maximum spacing of transverse stiffeners in interior panels without longitudinal stiffeners is limited to 3D and in interior panels with longitudinal stiffeners is limited to 1.5D. Should the spacing exceed these values, the web is considered to be unstiffened. The shear resistance of unstiffened webs is limited to V_{cr}.

Since longitudinal stiffeners divide a web panel into subpanels, the shear resistance of the entire panel could potentially be taken as the sum of the shear resistances of the subpanels. Although a longitudinal stiffener located at its optimum position on the web for flexure also increases the buckling resistance of the web in shear, the increase is relatively small compared to the increase in the bend buckling resistance resulting from the stiffener. Therefore, the specifications conservatively neglect the influence of the longitudinal stiffener in computing the nominal shear resistance of the web; that is, the total web depth D is used in computing the shear resistance.

17.   Brockenbrough, R.L., and B.G. Johnston. 1981. *USS Steel Design Manual.* United States Steel Corporation, ADUSS 27-3400-04, Pittsburgh, PA, January.
18.   Galambos, T.V., ed. 1998. *Guide to Stability Design Criteria for Metal Structures.* 5th Edition, Structural Stability Research Council. John Wiley and Sons, Inc., New York, NY.

19.   Kitipornchai, S., and N.S. Trahair. 1980. "Buckling Properties of Monosymmetric I-Beams." *Journal of the Structural Division*, American Society of Civil Engineers, New York, NY. Vol. 106, No. ST5, May.

20.   Kitipornchai, S., and N.S. Trahair. 1986. "Buckling Properties of Monosymmetric I-Beams Under Moment Gradient." *Journal of the Structural Division*, American Society of Civil Engineers, New York, NY. Vol. 112, No. ST4.

21.   McGuire, W. 1968. *Steel Structures*. Prentice-Hall, Inc., Englewood Cliffs, NJ.

22.   Nethercot, D.A., and N.S. Trahair. 1976. "Lateral Buckling Approximations for Elastic Beams." *The Structural Engineer*. Vol. 54, No. 6.

23.   NSBA. 2006. "Example 1: Three-Span Continuous Straight Composite I-Girder." NSBA *Steel Bridge Design Handbook*, available from the National Steel Bridge Alliance (www.steelbridges.org), Chicago, IL.

24.   Doswell, B. 2002. "Lateral-Torsional Buckling of Wide Flange Cantilever Beams." *Proceedings of the 2002 Annual Stability Conference*. Structural Stability Research Council, University of Missouri, Rolla, MO.

25.   Johnson, D.L. 1985. "An Investigation into the Interaction of Flanges and Webs in Wide Flange Shapes." *Proceedings SSRC Annual Technical Session*, Cleveland, OH, Structural Stability Research Council, University of Missouri, Rolla, MO.

26.   AISC. 2005. *Specification for Structural Steel Buildings*. ANSI/AISC 360-05, American Institute of Steel Construction, Chicago, IL, March 9.

27.   Hall, D.H. 2000. "The Effect of Material Properties on the Stability of Steel Girder Bridges." *Proceedings SSRC Annual Technical Session*, Memphis, TN, Structural Stability Research Council, University of Missouri, Rolla, MO.

28.   Salmon, C.G., and J.E. Johnson. 1996. *Steel Structures – Design and Behavior*. Fourth Edition, HarperCollins College Publishers, New York, NY.

29.   Wittry, D.M. 1993. "An Analytical Study of the Ductility of Steel Concrete Composite Sections." Masters thesis. University of Texas, Austin, TX. December.

30.   Wittry, D.M. 1993. "An Analytical Study of the Ductility of Steel Concrete Composite Sections." Masters thesis. University of Texas, Austin, TX. December.

31.   Yakel, A., and A. Azizinamini. 2005. "Improved Moment Strength Prediction of Composite Steel Plate Girders in Positive Bending." *Journal of Bridge Engineering*, American Society of Civil Engineers, Reston, VA, January/February.

32.   Heins, C.P. 1975. *Bending and Torsional Design in Structural Members*. Lexington Books, Lexington, MA.

33.   El Darwish, I.A., and B.G. Johnston. 1965. "Torsion of Structural Shapes." *Journal of the Structural Division*, American Society of Civil Engineers, New York, NY, Vol. 91, No. ST1, February.

34.   White, D.W., and M.A. Grubb. 2005. "Unified Resistance Equations for Design of Curved and Tangent Steel Bridge I-Girders." *Proceedings of the Transportation Research Board Sixth International Bridge Engineering Conference*. Boston, MA, July.

35.   White, D.W., A.H. Zureick, N. Phoawanich, and S.K. Jung. 2001. "Development of Unified Equations for Design of Curved and Straight Steel

Bridge I-Girders." Final Report to the American Iron and Steel Institute Transportation and Infrastructure Committee, Professional Service Industries, Inc. and the Federal Highway Administration. School of Civil and Environmental Engineering, Georgia Institute of Technology, Atlanta, GA.

36. Basler, K. 1961. "Strength of Plate Girders in Shear." *Journal of the Structural Division*. American Society of Civil Engineers, Vol. 87, No. ST7, October.

37. White, D.W., M. Barker, and A. Azizinamini. 2004. "Shear Strength and Moment Shear Interaction in Transversely-Stiffened Steel I-Girders." Structural Engineering, Mechanics and Materials Report No. 27, School of Civil and Environmental Engineering, Georgia Institute of Technology, Atlanta, GA.

38. White, D.W., and M. Barker. 2004. "Shear Resistance of Transversely Stiffened Steel I-Girders." Structural Engineering, Mechanics and Materials Report No. 26, School of Civil and Environmental Engineering, Georgia Institute of Technology, Atlanta, GA.

38a. Jung, S.-K., and D.W. White. 2006. "Shear Strength of Horizontally Curved Steel I-Girders – Finite Element Studies." *Journal of Constructional Steel Research*, 62(4).

2.2.3.2 Flange Sizing

2.2.3.2.1 Flange Width

Basic cross-section proportion limits for flanges of steel I-girders are specified in *AASHTO LRFD* Article 6.10.2.2. The limits apply to both tension and compression flanges.

The minimum width of flanges is specified as:

$$b_f \geq D/6$$

<div align="right">Equation 2.56
AASHTO LRFD Equation 6.10.2.2-2</div>

where b_f is the width of the flange and D is the web depth. It has been established that the cross-section aspect ratio D/b_f has a significant effect on the strength and moment-rotation characteristics of I-girders (*39*). Limited tests have been conducted on I-sections with very narrow flanges, or D/b_f ratios greater than 6. Those tests that have been conducted have indicated nominal flexural and shear resistances below those given by the current and previous Specifications. Limiting the aspect ratio to a maximum value of 6 also helps to ensure that stiffened interior web panels can develop post-buckling shear resistance due to tension-field action. *The limit given by Equation 2.56 is a lower limit and flange widths should not be set based on this limit*. Practical size flanges should easily satisfy this limitation based on satisfaction of other design criteria.

Fabricators prefer that flange widths never be less than 12 inches to prevent distortion and cupping of the flanges during welding, which sets a practical lower limit.

Composite design has led to a significant reduction in the size of compression flanges in regions of positive flexure as economical composite girders normally have smaller top flanges than bottom flanges. In regions of positive flexure during deck placement, more than half the web is typically in compression. As a result, maximum moments generated during the deck-casting sequence, coupled with top compression flanges that are too narrow, can lead to out-of-plane distortions of the compression flanges and web during construction. The following relationship from *AASHTO LRFD* Article C6.10.3.4 is a suggested guideline on the minimum top compression flange width b_{fc} that should be provided in these regions to help minimize potential problems in these cases:

$$b_{fc} \geq \frac{L}{85}$$

Equation 2.57

AASHTO LRFD Equation C6.10.3.4-1

where *L* is the length of the girder shipping piece. This same guideline was discussed previously in DM Volume 1, Chapter 2, Section 2.4.3.1.2.2. As discussed there, satisfaction of this simple guideline can also help ensure that individual field sections will be stable for handling both in the fabrication shop and in the field, and also for erection without requiring any special stiffening trusses or falsework. It is strongly recommended that Equation 2.57 be used in conjunction with Equation 2.56 to establish a *minimum* required top-flange width in regions of positive flexure in composite girders.

As a practical matter, fabricators order flange material from wide plate, typically between 72 and 96 inches wide, and either weld the shop splices in the individual flanges after cutting them to width, or weld the different thickness plates together to form one wide plate and then strip the individual flanges. In the latter case, the individual flange widths must be kept constant within an individual shipping piece, which is preferred. Changing of flange widths at shop splices should be avoided if at all possible. Stripping the individual flanges from a single wide plate allows for fewer weld starts and stops and results in only one set of run-on and run-off tabs. It is estimated that up to 35% of the labor required to join the flanges can be saved by specifying changes in thickness rather than width within a field section (*40*).

A fabricator will generally order plate with additional width and length for cutting tolerance, sweep tolerance and waste. Waste is a particular concern when horizontally curved flanges are cut curved. The Engineer should give some consideration as to how the material might be ordered and spliced; a fabricator can always be consulted for assistance. Flanges should be sized (i.e. width, thickness and length) so that plates can be ordered and spliced with minimal waste. Reference 40, which is a free publication available from the NSBA (www.steelbridges.org), contains some specific recommendations and illustrative examples related to this issue.

Plate width and length availability is another important consideration when it comes to sizing girder flanges. The availability of plate material varies from mill to mill. Generally, plates are available in minimum widths ranging from 48 to 60 inches, and maximum widths ranging from 150 to 190 inches. Reference 40 contains some

example plate length and width availability information from a single mill.   A fabricator and/or producer should be consulted regarding the most up-to-date plate availability information. The maximum available plate length is generally a function of the plate width and thickness, steel grade and production process. For example, high performance steel (HPS) is currently produced by either quenching and tempering (Q&T) or by thermo-mechanical-controlled-processing (TMCP) (*41*). TMCP HPS is currently available in plate thicknesses up to 2 inches and in maximum plate lengths from approximately 600 to 1500 inches depending on weights. Q&T HPS is available in plate thicknesses from 2 to 4 inches (or less for larger plate widths), but because of the furnaces that are used in the tempering process, is subject to a maximum plate-length limitation of 600 inches (50 feet) or less depending on weights. Therefore, whenever Q&T HPS is used (i.e. generally when HPS plates over 2 inches in thickness are specified), the maximum plate-length limitation should be considered when laying out flange (and web) transitions in a girder.

EXAMPLE

Determine a preliminary top-flange width for the exterior girder in the positive-flexure region of the end span of a three-span continuous composite bridge with spans of 140 ft – 175 ft – 140 ft. The field section running from the abutment to the field splice is 100 ft in length. As illustrated below in the section on Web Sizing, the web depth D chosen for this girder is 69 in.

Use the following guideline provided in *AASHTO LRFD* Article C6.10.3.4:

$$b_{fc} \geq \frac{L}{85}$$

<div align="right">AASHTO LRFD Equation C6.10.3.4-1</div>

where L is the length of the girder shipping piece = 100 feet. Therefore:

$$\left(b_{fc}\right)_{min} = \frac{100(12)}{85} = 14.1 \text{ in.}$$

Check the minimum flange width requirement given in *AASHTO LRFD* Article 6.10.2.2:

$$b_f \geq D/6$$

<div align="right">AASHTO LRFD Equation 6.10.2.2-2</div>

$$\left(b_f\right)_{min} = \frac{69.0}{6} = 11.5 \text{ in.} < 12.0 \text{ in.}$$

$$14.1 \text{ in.} > 12.0 \text{ in.} \quad ok$$

Because the top flange of the exterior girders will be subject to flange lateral bending due to the effect of the eccentric deck overhang loads, and also due to wind loads

during construction, a top-flange width larger than the above-calculated minimum width will be used. A flange width of 16 inches is chosen.

2.2.3.2.2 Flange Thickness

The minimum thickness of flanges (both tension and compression flanges) is specified in *AASHTO LRFD* Article 6.10.2.2 as follows:

$$t_f \geq 1.1t_w$$ Equation 2.58

AASHTO LRFD Equation 6.10.2.2-3

Equation 2.58 ensures that the boundary conditions assumed at the web-flange juncture in the compression-flange local buckling and web bend buckling formulations within the *AASHTO LRFD* Specifications are reasonably accurate. This relationship also ensures that the flanges will provide some level of restraint against web shear buckling. *The limit given by Equation 2.58 is a lower limit and flange thicknesses should not be set based on this limit.* Practical size flanges should easily satisfy this limitation based on satisfaction of other design criteria. **Fabricators prefer that flange thicknesses never be less than ¾ inches (40).** It is best to limit the number of different flange plate thicknesses specified for a given project. Flange sizes should be grouped if possible to minimize the number of thicknesses of plate that must be ordered. Larger order quantities of plate cost less and minimizing the number of different flange plate thicknesses simplifies fabrication and inspection and reduces mill quantity extras.

Reference 40 recommends that flange thicknesses should be selected in 1/8-inch increments for plates up to 2½ inches in thickness, and in ¼-inch increments for plates over 2½ inches in thickness. That is, flange thicknesses should not be specified in 1/16-inch increments.

Flange thickness transitions (i.e. shop-welded splices), which are preferred over flange width transitions as discussed previously, are located based on design considerations, plate length availability and the economics of welding and inspecting a splice compared to the cost of extending a thicker plate. In typical cases, no more than two shop splices, or three different flange thicknesses, should be necessary in any one field section, unless the girders are very heavy or long, or there are specific mill length availability limits as described above. Reference 40 contains a table (Table 1.5.2.A) for A 709 Grade 50 steel that gives a suggested weight savings per inch of flange width that can be used to evaluate whether or not it might be economical to introduce a shop splice at a given location. Usually, somewhere between 800 and 1,200 pounds of material must be saved in order to justify the introduction of a welded shop splice. However, this number can often vary between different fabrication shops so it is best to consult with a fabricator, if possible, regarding this issue. In certain cases, the fabricator would like to have the option to eliminate a shop splice by extending the thicker flange plate. Therefore, the design plans should consider allowing this option subject to the approval of the Engineer, who should evaluate the resulting changes in the deflections and stresses to determine if they are acceptable. Note that flange transitions in the top and bottom

flanges do not necessarily have to be made at the same cross-section, and in some cases, it may not be economical to do so.

As a final consideration, at flange shop splices, the area of the thinner plate should not be less than one-half the area of the thicker plate to reduce the stress concentration and ensure a smooth transition of stress across the splice.

2.2.3.2.3 Other Proportioning Requirements

Another requirement related to flange proportioning specified in *AASHTO LRFD* Article 6.10.2.2 relates to the flange width-to-thickness ratio (of both compression and tension flanges) as follows:

$$\frac{b_f}{2t_f} \leq 12.0 \hspace{3cm} \text{Equation 2.59}$$

AASHTO LRFD Equation 6.10.2.2-1

Equation 2.59 is essentially carried over from Allowable Stress Design provisions as a practical upper limit to ensure that the flange will not distort excessively when welded to the web.

The final requirement related to proportioning of the flanges is specified in *AASHTO LRFD* Article 6.10.2.2 as follows:

$$0.1 \leq \frac{I_{yc}}{I_{yt}} \leq 10 \hspace{3cm} \text{Equation 2.60}$$

AASHTO LRFD Equation 6.10.2.2-4

where I_{yc} is the moment of inertia of the compression flange of the steel section about the vertical axis in the plane of the web (in.[4]), and I_{yt} is the moment of inertia of the tension flange of the steel section about the vertical axis in the plane of the web (in.[4]). Previous Specifications checked the ratio of I_{yc} to I_y, or the moment of inertia of the entire steel section about the vertical axis in the plane of the web. Replacing I_y with I_{yt} represents a simplification of this requirement. Equation 2.60 ensures more efficient flange proportions and prevents the use of unusual singly symmetric sections in which the yield moment M_y may in fact be larger than the plastic moment M_p. Sections with an I_{yc}/I_{yt} ratio outside the specified limits behave more like tee sections with the shear center located at the intersection of the larger flange and the web. Such sections may be particularly difficult to handle during construction. The satisfaction of Equation 2.60 also ensures the validity of the lateral-torsional buckling equations (discussed later) for cases involving moment gradients.

2.2.3.2.4 Tips on Flange Sizing

In straight bridges, flange sizes are typically controlled by certain limit states. Knowing this in advance can save some time and effort in the proportioning of the flanges.

As discussed above, the sizes of top flanges in regions of positive flexure are most always governed by constructibility verifications. Recommendations were made above on establishing a preliminary top-flange width in these regions. The establishment of a reasonable preliminary design thickness for the flange is primarily an educated guess based on experience. Use the guidelines given above to establish the minimum flange thickness, which is a reasonable starting point for shorter spans (say approximately 120 feet or less), and increase the thickness from there in reasonable increments for longer spans. Recommendations on preliminary cross-frame/diaphragm spacings to assume in these regions were made in DM Volume 1, Chapter 2, Section 2.4.3.1.4.4.1. The final size of the top flange and/or the spacing of the cross-frames/diaphragms in these regions will typically be controlled by either the calculated local buckling or lateral torsional buckling resistance under the critical construction condition. For exterior girders, which usually control, the critical construction condition will most often be the combined major-axis and lateral bending stress in the top flange due to the effect of the deck-casting sequence plus the deck overhang loads. Therefore, it is recommended that the final top-flange size and cross-frame/diaphragm spacing in these regions be determined based on this condition, and then subsequent design verifications be made at the strength, fatigue and service limit states, as applicable. All these design verifications at the various limit states are discussed in greater detail in succeeding sections of this chapter.

For straight bridges, the sizes of the bottom flanges for compact composite sections in regions of positive flexure are most always governed by the service or fatigue limit state verifications under the load combinations specified in *AASHTO LRFD* Table 3.4.1-1 and in the absence of flange lateral bending. It is recommended that preliminary sizes for the bottom flanges in these regions be determined based on the relatively simple flange stress check at the service limit state described in *AASHTO LRFD* Article 6.10.4.2.2 (and in Section 2.2.3.5.2.1 of this chapter under Service Limit State Verifications). Typically, for composite construction, the bottom flange will be somewhat wider than the top flange. In certain cases, the size of the bottom flange may have to be increased from this level in some areas due to stress-range limitations at the fatigue limit state at certain critical welded details (e.g. cross-frame/diaphragm connection plate welds to the bottom flange near points of permanent load contraflexure). Design verifications on the flanges at the strength limit state should be made last. Constructibility verifications on the bottom flanges will typically not control in these regions.

Top-flange sizes in regions of negative flexure are typically controlled by tension-flange yielding at the strength limit state. For girders that are composite throughout their length, the longitudinal deck reinforcement (which must satisfy the minimum one-percent longitudinal reinforcement requirement specified in *AASHTO LRFD* Article 6.10.1.7) within the effective deck width can be included when calculating the composite section properties in these regions. As a result, a top flange with an area slightly smaller than the area of the bottom flange can be assumed. For girders that are noncomposite in these regions, the area of the top flange will be the same as the area of the bottom flange. The bottom-flange sizes in these regions are typically controlled by either the flange local buckling or lateral-torsional buckling resistance

at the strength limit state. Initial trial flange sizes in these regions are primarily educated guesses based on experience. Often, depending on the span arrangement and other factors, the flanges may be somewhat wider than the corresponding flanges in regions of positive flexure. As discussed above, the width transitions should be made at the field splices. Changes in the top-flange width can lead to some inconveniences with respect to the deck forming, but these problems are not insurmountable and are relatively minor when compared to the overall economy of the girder design.   Other limit state verifications typically do not control in these regions and should be checked last.   Finally, recommendations on preliminary cross-frame/diaphragm spacings to assume in these regions were also made in DM Volume 1, Chapter 2, Section 2.4.3.1.4.4.1.

39.   White, D.W., and K.E. Barth. 1998. "Strength and Ductility of Compact-Flange I Girders in Negative Bending." *Journal of Constructional Steel Research*, Vol. 45, No. 3.

40.   AASHTO/NSBA Steel Bridge Collaboration. 2003. "Guidelines for Design for Constructibility, G12.1."   American Highway of State Highway and Transportation Officials, Washington, D.C., Publication No. GDC-1.

41.   Wilson, A.D.   2002.   "Availability and Future Development of High Performance Steel."   Proceedings of the 2002 NABRO/FHWA HPS Conference, Salt Lake City, UT.

2.2.3.3 Web Sizing

2.2.3.3.1 Web Depth

The first step in sizing the web plates of a fabricated steel I girder is to establish the web depth. The proper web depth is an extremely important consideration affecting not only the economy, but also the constructibility and performance of steel-girder bridges. The web depth obviously dictates the flange sizes for a given design. Since there are limits on the flange width-to-thickness ratio, and also on the flange width based on the web depth (discussed previously in Section 2.2.3.2 of this chapter under Flange Sizing), the web depth cannot be selected indiscriminately. As the strength of the steel increases, the flange size is typically reduced and the web thickness is typically increased to prevent buckling. Hence, there is a tendency to employ ever-shallower girders employing higher strength steels, such as ASTM A 709 Grade HPS 70W steel.   The result is a tendency to infringe on the recommended span-to-depth ratio.

AASHTO LRFD Article 2.5.2.6.3 provides suggested minimum depths for steel I-girders in simple and continuous spans based on traditional maximum recommended span-to-depth ratios (the recommended minimum web depths are discussed in more detail in Section 2.2.3.5.1.1 of this chapter). Limiting span-to-depth ratios are evident back to at least 1908 (*42*). Deflection is inextricably related to web depth.   In the absence of geometric restrictions on depth, these recommended limits on web depths should be held, particularly when higher strength steels -- which typically result in smaller flanges -- are used.

In cases, where there girder depth in not restricted, a section deeper than the recommended minimum depth may be desired to provide greater stiffness to the girders in their noncomposite condition during construction. Steel-girder bridges with skewed supports may have large cross-frame forces that are related to girder deflections; increasing the girder depth, hence the girder stiffness, may mitigate the cross-frame forces. As discussed in DM Volume I, Chapter 2 under the heading of Girder Spacing and Deck Overhangs (Section 2.4.3.1.1), girders deeper than the minimum recommended depth may be economical when girder spacing is large because each girder receives more load. From a standpoint of girder weight, the actual span-to-depth ratio should not be excessively high or low. However, it should be noted that in general, the relative efficiency of the steel decreases at a more rapid rate as the span-to-depth ratio increases (i.e. depth decreases) than when that ratio decreases (i.e. depth increases) (*43*).

There are many instances where clearances demand a depth less than the suggested minimum depth. Raising the bridge profile in order to maintain the required vertical clearance is often not practical. Steel is very adaptable in such situations. However, girders shallower than the suggested minimum depth are prone to issues related to deflection. The effect on cross-frame forces and bridge constructibility, including the girder rotations, may demand special attention. Also, as discussed in greater detail in DM Volume I, Chapter 2, Section 2.4.3.1.3 on Constant vs. Variable Depth Girders, variable depth girders may be desirable where clearance or awkward span arrangements exist. In these cases the most economical means of varying depth is by utilizing a straight-line taper, usually starting near the field-section splice off an interior support. Aesthetic considerations are also another reason to vary girder depth. A parabolic haunch is usually considered the most aesthetic, although not the most economical, means of varying the depth. These webs are not economical. The greater depth extends over such a short distance it gives little structural advantage. At the same time, there is significant cost associated with lost web material and the fabrication of the haunched flange.

The recommended depth rules are not directly applicable to variable depth girders. Obviously, a conservative approach is to use the table of recommended minimum depths (i.e. *AASHTO LRFD* Table 2.5.2.6.3-1 discussed subsequently in Section 2.2.3.5.1.1 of this chapter) to set the minimum depth. But the depth of the deeper portion should be greater than the depth determined from the table for the span between bearings. A suggested more reasonable approach for tapered-depth girders is to apply the value from the table to the depth at a point on the girder approximately 10 percent of the span away from the bearing. In the limit, the deflections of a tapered girder should not be less than the deflections of a constant-depth girder would be if the constant-depth girder met the recommended depth from the table. Such a limit (i.e. based on deflections) is also suggested for application to girders with parabolic haunches. Additional information and discussion on variable web depth members may be found in DM Volume 1, Chapter 2, Section 2.4.3.1.3 and in Section 2.2.3.3.3 of this chapter.

In most cases, the optimum web depth will be greater than the minimum depth based on the traditional span-to-depth ratios. Note that the optimum web depth can

be established by preparing a series of designs with different web depths to arrive at an optimum cost-effective depth based on weight and/or cost.

As discussed in more detail in Section 2.2.3.5.1.1 of this chapter, the suggested minimum depths in *AASHTO LRFD* Table 2.5.2.6.3-1 are based on historical values. For simple spans, the requirement in the *AASHTO* Standard Specifications is that the span divided by the steel girder depth should not exceed 30. This value has been employed by *AASHO/AASHTO* since the 1970s. The reciprocal of this value is the constant of 0.033 applied to the span length in the table. For continuous spans, the constant of 0.027 applied to the span length is obtained by reducing the constant 0.033 by 80 percent to account for the effect of end restraint. The suggested minimum overall depth of the composite I-girder for simple spans, i.e. including the deck, is based on applying a constant of 0.040 to the span length. The constant 0.040 is the reciprocal of the traditional maximum span-to-depth ratio of 25 suggested for the overall depth of simple-span composite girders in the Standard Specifications. Similarly, the constant of 0.032 for continuous spans in this case is 80 percent of the simple-span value. Note that an end depth-to-span ratio of 90 percent of the simple-span ratio might be considered in either case to better account for only one end of the span being restrained by continuity.

Generally, the greatest depth determined from the above values found for each span in a continuous girder would be used for the bridge. If the span lengths vary greatly, a tapered girder might be optimal. If a depth far greater than the suggested minimum depth is employed, the flanges will be too small to meet the recommended minimum sizes discussed previously (see Section 2.2.3.2 of this chapter on Flange Sizing).

EXAMPLE

Select a trial constant web depth for a three-span continuous I-girder bridge having spans of 140–175–140 feet. Assume there are no depth restrictions. From *AASHTO LRFD* Table 2.5.2.6.3-1 (refer to Section 2.2.3.5.1.1 of this chapter – Table 2.8), the suggested minimum depth of the steel section in a composite I-section in a continuous span is given as 0.027L, where L is the span length between bearings. Using the longest span of 175 feet, the depth of the steel section is:

$$0.027(175) = 4.725 \text{ ft} = 56.7 \text{ in.}$$

A check of the end span using 90 percent of the simple span value 0.033 gives a depth of

$$0.033(0.90)(140) = 4.16 \text{ ft} = 50.0 \text{ in.}$$

A deeper web will provide greater stiffness, hence less deflection. Improved constructibility is usually obtained with girders deeper than Span/30. Hence, where practical, a web depth greater than that suggested in the table is suggested. Since there are no depth restrictions in this case, a depth of girder based on the recommended total composite section depth from the table [i.e. *AASHTO LRFD*

Table 2.5.2.6.3-1 (Table 2.8)] is suggested. Therefore, compute the suggested girder depth of the composite continuous span based on the value 0.032*L*:

$$0.032(175.0) = 5.60 \text{ ft} = 67.2 \text{ in.}$$

A web depth of 69 inches is chosen.

2.2.3.3.2 Web Thickness

Cross-section proportion limits for webs of I-sections are specified in *AASHTO LRFD* Article 6.10.2.1. As specified in *AASHTO LRFD* Article 6.10.2.1.1, for webs without longitudinal stiffeners, the webs must be proportioned such that:

$$\frac{D}{t_w} \leq 150 \qquad\qquad \text{Equation 2.61}$$

AASHTO LRFD Equation 6.10.2.1.1-1

where D is the web depth and t_w is the web thickness. This limit is a practical upper limit on the web slenderness expressed as a function of D, which served as an upper limit on the slenderness of unstiffened webs in previous versions of the *AASHTO LRFD Specifications* and in the *Standard Specifications*. In these Specifications, the slenderness limit for webs without longitudinal stiffeners is generally expressed as a function of the specified minimum yield strength of the steel and the elastic depth of the web in compression D_c (to accommodate singly symmetric sections). The limit exceeded 150 for girders with a specified minimum yield strength of 50 ksi or below. This limit was established as an upper bound below which fatigue due to excessive transverse web deflections was deemed not to be a consideration (*44, 45*). However, expressing the limit in this fashion makes the initial proportioning of the web more difficult as D_c is not known until the entire cross-section has been defined. Expressing the limit as a function of D allows for easier proportioning of the web in preliminary design, once the web depth has been established, relative to previous Specifications. To control transverse web displacements in slender-web girders (i.e. girders with larger values of $2D_c/t_w$) at critical limit states, including the fatigue limit state, separate web bend-buckling and shear buckling checks are now specified in the *AASHTO LRFD* Specifications, as discussed previously.

There are other significant advantages to expressing the slenderness limit in this fashion. First, by limiting the slenderness of transversely stiffened webs to 150, maximum transverse stiffener spacings up to 3D are permitted. In previous Specifications, where the slenderness of a transversely stiffened web is permitted to exceed 150 (i.e. the established limit for unstiffened webs), additional transverse stiffeners beyond those needed for shear are required for handling during fabrication and erection in these girders with more slender webs. The maximum permitted spacing of these extra stiffeners is limited to $D[260/(D/t_w)]^2$ (*36*). That is, as the web slenderness of the girder exceeds 150, the maximum permitted spacing of the stiffeners is reduced to less than 3D according to the preceding relationship. By limiting the web slenderness to 150, the need for additional transverse stiffeners for handling is eliminated; stiffeners need only be provided for shear and can potentially

be spaced up to the maximum limit of 3D.   Second, by satisfying Equation 2.61, the web bend-buckling check can be disregarded in the design of composite sections in positive flexure (without longitudinal stiffeners) after the section is in its final composite condition. As discussed earlier, the web bend-buckling resistance F_{crw} for such sections is generally close to or larger than F_{yc} at the strength limit state.

Equation 2.61 is considered valid for sections with specified minimum yield strengths up to and including 100 ksi. The 2005 AISC LRFD Specification (*26*) provides the following limits on the web slenderness of slender-web girders to prevent theoretical elastic buckling of the web as a column subjected to radial transverse compression due to the curvature of the flanges. This phenomenon is referred to as vertical flange buckling (*8*):

$$\text{For } \frac{a}{h} \leq 1.5: \quad \frac{h}{t_w} \leq 11.7 \sqrt{\frac{E}{F_y}} \qquad \text{Equation 2.62}$$

$$\text{For } \frac{a}{h} > 1.5: \quad \frac{h}{t_w} \leq \frac{0.42E}{F_y} \qquad \text{Equation 2.63}$$

where h is the clear distance between flanges and a is the clear distance between transverse stiffeners. For unstiffened webs, the slenderness h/t_w is limited to 260. Equation 2.63 is slightly modified from the original version of the equation proposed by Basler and Thurlimann (*46*):

$$\frac{h}{t_w} \leq \frac{0.48E}{\sqrt{F_y (F_y + 16.5)}} \qquad \text{Equation 2.64}$$

As discussed previously, this equation was utilized to establish an upper web slenderness limit in the original development of the web load-shedding factor R_b. The equation assumes a flat residual stress level of 16.5 ksi. Replacing the value of 16.5 ksi in Equation 2.64 with the more general residual stress level of $0.3F_y$ assumed in the 2005 AISC Specification results in Equation 2.63.   The preceding vertical flange buckling limits are not considered in the *AASHTO LRFD Specifications*. For girders that satisfy Equation 2.61, the vertical flange buckling limits do not control unless F_y is greater than 85.0 ksi. Also, tests (*10, 47*) have indicated that the influence of the vertical flange buckling mode, or folding of the compression flange vertically into the web, on the nominal flexural resistance of the girder is small even when the web slenderness significantly violates the vertical flange buckling limits.

For webs that do not satisfy Equation 2.61, longitudinal web stiffeners are required. As specified in *AASHTO LRFD* Article 6.10.2.1.2, for webs with longitudinal stiffeners, the webs must be proportioned such that:

$$\frac{D}{t_w} \leq 300 \qquad\qquad \text{Equation 2.65}$$

AASHTO LRFD Equation 6.10.2.1.2-1

Again, the limit is independent of the yield strength and D_c to allow for easier proportioning of the web for preliminary design. Even for longitudinally stiffened girders with webs that significantly exceed the limit given by Equation 2.65, tests (*10,48*) have demonstrated that the nominal flexural resistance is not significantly affected by the vertical flange buckling failure mode. Extensive yielding of the compression flange in flexure preceded the vertical flange buckling failure. However, it should be noted that webs that have larger D/t_w values than permitted by Equation 2.65 are relatively inefficient, are likely to be more susceptible to distortion induced fatigue and are more susceptible to the limit states of web crippling and web local yielding discussed in *AASHTO LRFD* Article D6.5 (Appendix D to Section 6).

To reduce the deformation of the web and the potential for weld defects during fabrication, fabricators prefer a minimum web thickness of 7/16 inches, with a ½-inch minimum web thickness preferred (40). A minimum web thickness of 9/16 inches should prevent shadowing of the transverse stiffeners on the girder web.

Changes in the web thickness along the girder preferably should be made at field splices. In field sections over interior piers in continuous spans, the web thickness may have be increased (typically in 1/16-inch increments) over the thickness provided in adjacent regions of positive flexure, particularly if the concrete deck is considered to be effective in negative flexure at the service limit state as permitted in *AASHTO LRFD* Article 6.10.4.2.1. Should this be the case, the web bend-buckling check at the service limit state specified in *AASHTO LRFD* Article 6.10.4.2.2 (and discussed in more detail in Section 2.2.2.4 of this chapter on the Web Bend Buckling Resistance) will likely control the thickness of the web in these regions. Girders utilizing the preferred minimum web thickness (or greater) will usually have so-called "partially stiffened" webs, in which transverse stiffeners typically only need be provided in a few web panels near the abutments and over the interior piers, up to the point where the web thickness is such that transverse stiffeners are no longer required.

A useful guideline for determining the trade-off between adding more stiffeners versus increasing the thickness of web material is that approximately 10 pounds of web material should be saved for every 1 pound of stiffener material added.

2.2.3.3.3 Variable Web Depth Members

As discussed previously in this chapter and in DM Volume 1, Chapter 2, Section 2.4.3.1.3, clearance requirements, a poor span arrangement, economics and/or aesthetics may lead to the decision to use a variable web depth member. The design of variable web depth I-section members is covered in *AASHTO LRFD* Article

6.10.1.4. Further discussion on variable web depth members may be found in DM Volume 1, Chapter 2, Section 2.4.3.1.3.

The bottom flange of variable web depth members carries a portion of the vertical shear in the region of the sloping web. Thus, the force in the bottom flange in this region is increased due to the vertical shear component. The major-axis bending moment in this region is developed from the smaller horizontal component of the resultant bottom-flange force. Therefore, if the normal stress in an inclined bottom flange (without considering flange lateral bending) is determined by simply dividing the major-axis bending moment by the elastic section modulus, the bending stress in the flange will generally be underestimated. According to *AASHTO LRFD* Article C6.10.1.4, the horizontal component of the flange force can be determined as:

$$P_h = MA_f/S_x$$

<div align="right">Equation 2.66
AASHTO LRFD Equation C6.10.1.4-1</div>

where:
  A_f = area of the inclined bottom flange (in.^{2})
  M = major-axis bending moment at the section under consideration (kip-in.)
  S_x = elastic section modulus to the inclined bottom flange (in.^{3})

According to Reference 49, the normal stress in the inclined flange may then be determined as:

$$f_n = P_h/A_f \cos\theta$$

<div align="right">Equation 2.67
AASHTO LRFD Equation C6.10.1.4-2</div>

where θ is the angle of inclination of the bottom flange with respect to the horizontal.

The vertical component of the flange force affects the vertical web shear. According to *AASHTO LRFD* Article C6.10.1.4, the vertical component of the flange force may be determined as:

$$P_v = P_h \tan\theta$$

<div align="right">Equation 2.68
AASHTO LRFD Equation C6.10.1.4-3</div>

As pointed out in Reference 49, for fish-belly haunches, P_v is equal to zero near the supports. In regions of positive flexure with tapered or parabolic haunches sloping downward toward the supports, the vertical web shear is *increased* by P_v. For all other cases, the vertical web shear is *reduced* by P_v. The specification allows the Engineer to reduce the web dead-load shear by the vertical component of the flange force where desired and permitted by static equilibrium. Reduction of the live-load shear is not recommended in these cases because many combinations of concurrent shear and moment must be evaluated in order to determine the critical (or smallest) shear reduction.

In parabolic haunches, the downward slope of the bottom flange is larger at positions closer to supports. At interior supports, this change in the inclination of the bottom flange along with the compressive stress in the flange introduces a compressive distributed transverse force on the web (*49*). Therefore, *AASHTO LRFD* Article C6.10.1.4 recommends that transverse stiffeners be provided within these types of haunches with a spacing d_o not to exceed approximately 1.5*D*. Otherwise, the Engineer should check the stability of the web under this force.

The bottom flange of a variable web depth member is usually made horizontal in the vicinity of the bearings. Where this transition occurs, the vertical component of the inclined flange force is transferred back into the web as a concentrated load, which causes additional stress in the web and the web-to-bottom flange welds. Thus, additional local stiffening may be required in this area. According to *AASHTO LRFD* Article C6.10.1.4, additional stiffening is not required if the web local yielding provisions of *AASHTO LRFD* Article D6.5.2 (Appendix D to Section 6) are satisfied using a length of bearing *N* equal to zero. For compressive concentrated loads, the provisions of *AASHTO LRFD* Article D6.5.2 generally govern relative to the web crippling provisions of *AASHTO LRFD* Article D6.5.3 when *N* is taken equal to zero. Smoothing out the transition with a fish-belly flange rather than providing a sharp transition can help to reduce the increase in web stress at these locations.

42.   Ketchum, M.S. 1908. *The Design of Highway Bridges*. First Edition, McGraw-Hill, New York, NY.
43.   Fountain, R.S., and C.E. Thunman, Jr. 1987. "Deflection Criteria for Steel Highway Bridges." Proceedings of the AISC National Engineering Conference, New Orleans, LA, April 29 – May 7.
44.   Yen, B.T., and J.A. Mueller. 1966. "Fatigue Tests of Large Size Welded Plate Girders." *WRC Bulletin No. 118*, November.
45.   Mueller, J.A., and B.T. Yen. 1968. "Girder Web Boundary Stresses and Fatigue." *WRC Bulletin No. 127*, January.
46.   Basler, K., and B. Thurlimann. 1963. "Strength of Plate Girders in Bending." Transactions of the American Society of Civil Engineers, Vol. 128, Part II.
47.   Lew, H.S., and A.A. Toprac. 1968. "Static Strength of Hybrid Plate Girders." *SFRL Technical Report*, University of Texas, Austin, TX.
48.   Owen, D.R.J., K.C. Rockey, and M. Skaloud. 1970. "Ultimate Load Behavior of Longitudinally Reinforced Webplates Subjected to Pure Bending." IABSE Publications, Vol. 30-I.
49.   Blodgett, O.W. 1982. *Design of Welded Structures*. The James F. Lincoln Arc Welding Foundation, Cleveland, OH.

2.2.3.4 Constructibility Verifications

Although not identified as a formal limit state, the *AASHTO LRFD* Specifications provide significant emphasis on constructibility and specify it as a primary objective of bridge design in *AASHTO LRFD* Article 1.3.1. *AASHTO LRFD* Article 2.5.3 states that bridges should be designed such that fabrication and erection can be performed without undue difficulty or distress, and so that locked-in construction force effects are within tolerable limits. If a particular sequence of construction has been assumed by the Engineer in order to induce a particular set of dead load stresses

(e.g. a particular deck-placement sequence), that sequence must be identified in the contract documents. Also, for bridges considered to be of unusual complexity, at least one means of constructing the bridge must be provided by the Engineer in the contract documents to assist the Contractor in preparing a reasonable bid. Responsibility for the actual construction of the bridge is left to the Contractor, who may still use a more innovative or custom construction sequence in order to gain an advantage over the competitors, if desired. The actual responsibilities of the Engineer in this regard are not well defined and are generally left up to the Owner to specify. In addition, according to *AASHTO LRFD* Article 2.5.3, if the design requires temporary bracing, strengthening or support (e.g. falsework) during the erection by the specified sequence, this must be also be identified in the contract documents.

For steel structures, *AASHTO LRFD* Article 6.5.1 requires that the bridge be investigated for each stage that may be critical during construction, handling, transportation and erection. This is particularly important with respect to modern steel-girder designs, which are typically more slender than in the past due to the advent of composite construction, the introduction of higher-strength steels, and the increased use of limit-states design approaches. In composite construction, the steel girders alone must be strong enough to carry the full noncomposite dead loads. Since the composite section assists in resisting the live loads, smaller top flanges can be used in regions of positive flexure. Thus, more than half the depth of the web is in compression in these regions during construction. Also, the use of higher-strength steels and limit-states design approaches, with their smaller factor of safety on dead load than traditional working stress design, have resulted in much lighter girders overall for the noncomposite condition than were required prior to these advancements.

For steel I-section flexural members, the provisions for design for constructibility are given in *AASHTO LRFD* Article 6.10.3. The provisions are intended to provide adequate strength and stability of the main load-carrying members during construction, to properly account for dead load deflections, and to control the slip in load-resisting bolted connections at each critical construction stage to ensure that the proper geometry of the structure is maintained. As stated in *AASHTO LRFD* Article 6.10.3.1, nominal yielding or reliance on post-buckling resistance is not to be permitted for main load-carrying members during the critical stages of construction. An exception is permitted for the localized yielding of the web that may occur in hybrid members.

All design checks for strength are to be made using the appropriate factored loads specified in *AASHTO LRFD* Articles 3.4.1 and 3.4.2. ***Note that although the Strength IV load combination will typically only control where the dead to live load force effect ratio exceeds about 7.0 for the bridge in its final condition, this load combination can control during the investigation of critical construction stages and should be considered in all constructibility design checks for strength.*** For the calculation of deflections, all load factors are to be taken as 1.0. Slip of bolted connections is to be checked using the appropriate factored loads, with the slip resistance of the connection to be determined as specified in *AASHTO LRFD* Article 6.13.2.8 (see Section 2.3.2.4.1.1 of this chapter).

As specified in *AASHTO LRFD* Article 6.10.3.4, girder sections in positive flexure that are composite in the final condition, but noncomposite during construction, are to be investigated during the various stages of the deck placement. For fascia girders, the effects of the forces resulting from the deck overhang loads are also to be considered. Design checks are to be made for flexure (*AASHTO LRFD* Article 6.10.3.2) and shear (*AASHTO LRFD* Article 6.10.3.3), as appropriate, to ensure adequate strength. Checks on the concrete deck stresses during the deck placement must also be made (*AASHTO LRFD* Article 6.10.3.2.4). Wind-load effects on the noncomposite structure prior to casting of the deck are also an important consideration. As specified in *AASHTO LRFD* Article 4.6.2.7.3, the need for temporary wind bracing to control lateral bending and lateral deflections during construction must be investigated. Potential uplift at bearings is also an important consideration and must be investigated at each critical construction stage according to *AASHTO LRFD* Article 6.10.3.1. Should concentrated loads not be applied to the web through a deck or deck system, and bearing stiffeners also not be provided at such locations, the web must satisfy the provisions of *AASHTO LRFD* Article D6.5 (Appendix D to Section 6) to prevent web crippling and web local yielding.

AASHTO LRFD Article 6.10.3.5 refers to the provisions of *AASHTO LRFD* Article 6.7.2, which state that vertical camber must be specified to account for the dead-load deflections. The deflections due to the steel weight, concrete weight, future wearing surface or other loads not applied at the time of construction are to be reported separately. When staged or phased construction is specified, i.e. when the superstructure is built in separate longitudinal units with a longitudinal joint, the sequence of the load application should be recognized in determining the stresses and the required cambers.

2.2.3.4.1 Deck Placement Analysis

Depending on the length of the bridge, the construction of the deck may require placement in sequential stages. Thus, certain sections of the steel girders will become composite before other sections. If certain placement sequences are followed, temporary moments induced in the girders during the deck placement can be significantly higher than the final noncomposite dead load moments after the sequential placement is complete. Therefore, *AASHTO LRFD* Article 6.10.3.4 requires that sections in positive flexure that are noncomposite during construction (and composite in the final condition) be investigated for flexure according to the provisions of *AASHTO LRFD* Article 6.10.3.2 during the various stages of the deck placement. Furthermore, changes in the load, stiffness and bracing during the various stages are to be considered in the analysis.

EXAMPLE

Consider the sample deck placement shown in Figure 2.29 for a three-span continuous bridge. For this bridge, it is assumed that the positive moment regions are placed first with each of the casts in the end spans (from the abutment to the field splice) placed simultaneously. Then, the positive moment region of the interior span is assumed placed. After the positive moment regions have been placed, the negative moment regions over the piers are assumed placed simultaneously.
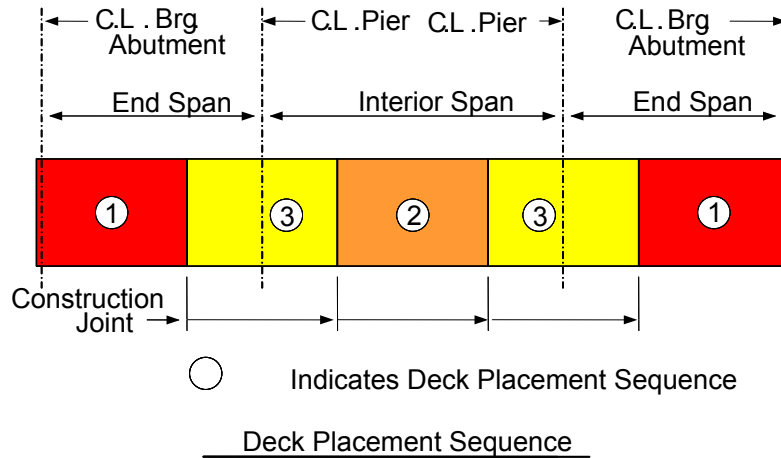
Figure 2.29 Deck Placement Sequence

Although simultaneous placement in the end spans followed later by simultaneous placement over the piers is shown in this example for simplicity, it is often more desirable to cast the deck from one end of the bridge. Simultaneous placement in the end spans, as assumed here, would require two finishing machines. Also, for this case, a more critical situation in actuality would be where the concrete would be assumed cast in only one end span since it would be practically impossible to ensure simultaneous placement of the two end casts. If the deck were cast from one end for the case shown in Figure 2.29, the second cast would likely extend from the end of the first cast in one end span over the adjacent pier to either the first or second construction joint shown in the center span (depending on how much concrete could be cast in a single day). Casting would then continue on from there accordingly in appropriate stages.   In this case, a retarder admixture may be required in the concrete mix for the casts over the piers to reduce the potential for early cracking caused by tensile stresses induced by subsequent casts. Should the bridge be short and narrow enough that the deck could be cast from one end of the bridge to the other in a single day (instead of in stages), the end span would still have to be checked for the critical instantaneous unbalanced case where wet concrete exists over the entire end span, with no concrete yet on the remaining spans.

Figure 2.30 (and all subsequent figures for this example) shows an elevation view of an exterior girder, which will be used to show the results for each stage of the deck placement sequence assumed for this example in Figure 2.29. In Figure 2.30, the girders are in place but no deck concrete has yet been placed. The entire girder length is noncomposite at this stage. Before the deck is placed, the noncomposite girder must resist the moments due to the girder self-weight and the weight of any stay-in-place (SIP) forms (if present). The moments due to these effects are shown at Location A, which is the location of maximum positive moment in the first end span.
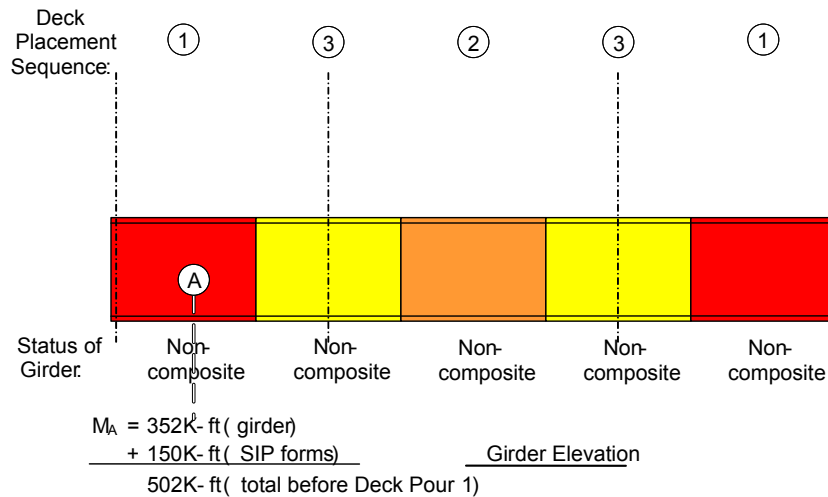
Deck Placement Sequence: ① ③ ② ③ ①

Status of Girder: Non-composite | Non-composite | Non-composite | Non-composite | Non-composite

M_A = 352 K-ft (girder)
+ 150 K-ft (SIP forms)
502 K-ft (total before Deck Pour 1)

Girder Elevation

Figure 2.30 Girder Elevation View

Figure 2.31 shows the first deck placement (Cast 1), which is located in the positive moment regions of the end spans.   The moment due to the wet concrete load, which consists of the weight of the deck and deck haunches, is added to the moments due to the girder self-weight and SIP forms.   Since the concrete in this first placement has not yet hardened, the moment due to the first deck placement is resisted by the noncomposite girder. The cumulative positive moment in the exterior girder at Location A after the first deck placement is +2,889 kip-ft, which is the maximum positive moment this section will experience during the assumed placement sequence. This moment is significantly larger than the moment of +2,202 kip-ft that would be computed at this location assuming a simultaneous placement of the entire deck (i.e. ignoring the sequential stages).

Deck Placement Sequence: ① ③ ② ③ ①

Status of Deck: Deck Placed But Not Yet Hardened ... Deck Placed But Not Yet Hardened

Status of Girder: Non-composite | Non-composite | Non-composite | Non-composite | Non-composite

M_A = 352 K-ft (girder)
+ 150 K-ft (SIP forms)
+ 2387 K-ft (Deck Pour 1)
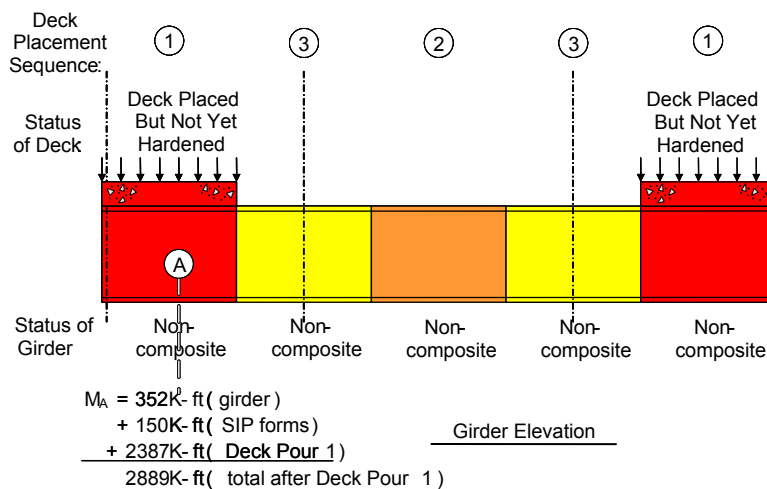2889 K-ft (total after Deck Pour 1)

Girder Elevation

Figure 2.31 Deck Placement Analysis 1

The next deck placement (Cast 2) is located in the positive moment region of the interior span, as shown in Figure 2.32. The concrete in the first placement is now

assumed hardened so that those portions of the girder are now composite. Therefore, as required in *AASHTO LRFD* Article 6.10.3.4, those portions of the girder are assumed composite in the analysis for this particular deck placement. The remainder of the girder is noncomposite. Since the deck casts are relatively short-term loadings, the short-term modular ratio *n* is used to compute the composite stiffness. The previous casts are assumed fully hardened in this case, but adjustments to the composite stiffness to reflect the actual strength of the concrete in the previous casts at the time of this particular placement could be made, if desired. The cumulative moment at Location A has decreased from +2,889 kip-ft after Cast 1 to +2,103 kip-ft after Cast 2 because the placement in the middle span causes a negative moment in the end spans.

Figure 2.32 Deck Placement Analysis 2
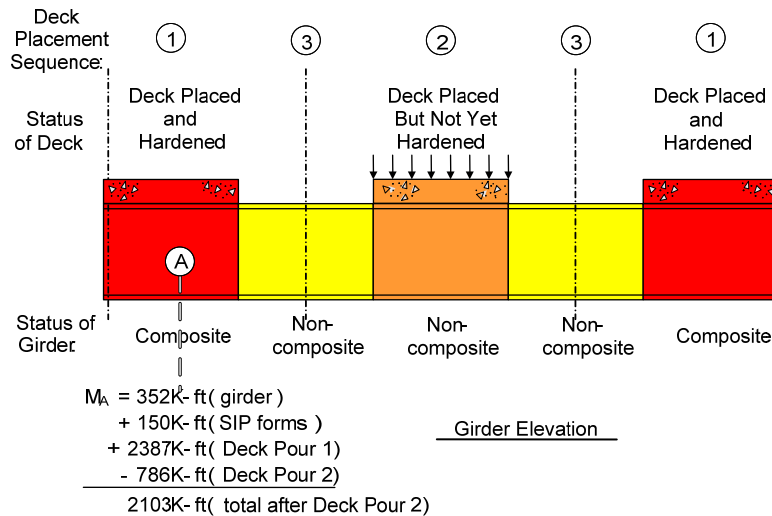
The last deck placement (Cast 3) is located in the negative moment regions over the piers (Figure 2.33). Again, the concrete in Casts 1 and 2 is assumed fully hardened in the analysis for Cast 3. The cumulative moment at Location A has increased slightly from +2,103 kip-ft to +2,170 kip-ft, which is less than the moment of +2,889 kip-ft experienced at Location A after Cast 1.
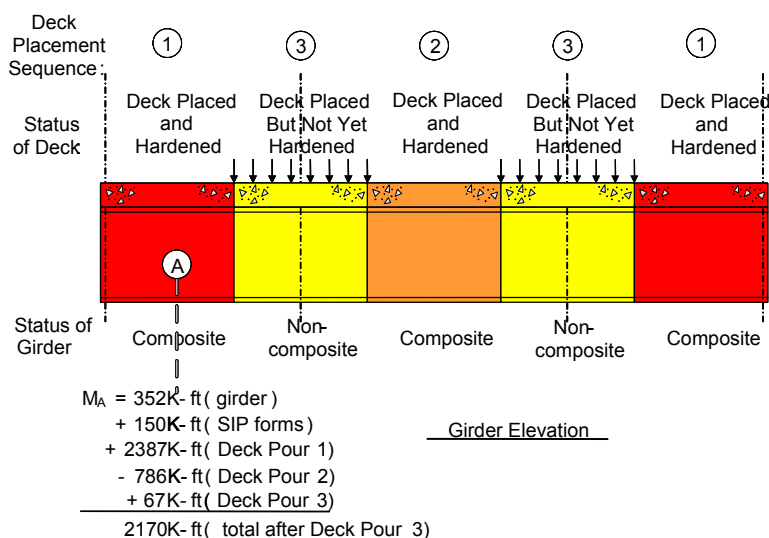
Figure 2.33 Deck Placement Analysis 3

Table 2.5 shows a more complete set of the unfactored dead-load moments in the end span (Span 1) from the abutment to the end of Cast 1 computed from the example deck placement analysis. Data are given at 12.0-ft increments along the span measured from the abutment. The end of Cast 1 is at the field splice, which is located 100.0 feet from the abutment. Location A is 56.0 feet from the abutment. Cross-frames are spaced at 24.0 feet along the girder and the length to each cross-frame from the abutment is indicated in bold in the table. In addition to the moments due to each of the individual casts, Table 2.5 gives the moments due to the steel weight, the moments due to the weight of the SIP forms, the sum of the moments due to the three casts plus the weight of the SIP forms, the maximum accumulated positive moments during the sequential deck casts (*not including the steel weight*), the sum of the moments due to the dead loads DC_2 and DW applied to the final composite structure, and the moments due to the weight of the concrete deck, haunches and SIP forms assuming that the concrete is placed simultaneously on the noncomposite girders instead of in sequential steps. The assumed weight of the SIP forms includes the weight of the concrete in the form flutes. Although the forms are initially empty, the weight of the deck reinforcement is essentially equivalent to the weight of the concrete in the form flutes.

The slight differences in the moments on the last line of Table 2.5 and the sum of the moments due to the three casts plus the weight of the SIP forms are due to the changes in the girder stiffness with each sequential cast.   The principle of superposition does not apply directly in the deck-placement analyses since the girder stiffness changes at each step of the analysis.   However, note the significant differences between the moments on the last line of Table 2.5 (which assumes a simultaneous placement of these loads along the entire girder) and the maximum accumulated positive moments (i.e. Max. +M) during the sequential deck casts. In regions of positive flexure, the noncomposite girder should be checked for the effect of this larger maximum accumulated deck-placement moment.   This moment at Location A is shown in bold in Table 2.5, along with the moment due to the steel weight. The sum of these moments is computed as:

$$M = 352 + 2{,}537 = 2{,}889 \text{ kip-ft}$$

which agrees with the moment at this location shown in Figure 2.31.

Table 2.5 Moments from Deck-Placement Analysis

Span -> 1	Unfactored Dead-Load Moments (kip-ft)									
Length (ft)	**0.00**	12.00	**24.00**	42.00	**48.00**	56.00	**72.00**	84.00	**96.00**	100.0
Steel Weight	0	143	250	341	353	**352**	296	206	74	21
SIP Forms (SIP)	0	63	110	147	151	150	124	84	27	4
Cast										
1	0	870	1544	2189	2306	2387	2286	1983	1484	1275
2	0	-168	-336	-589	-673	-786	-1010	-1179	-1347	-1403
3	0	14	28	50	57	67	86	101	115	120
Sum of Casts + SIP	0	779	1346	1797	1841	1818	1486	989	279	-4
Max +M	0	933	1654	2336	2457	**2537**	2410	2067	1511	1279
DC_2 + DW	0	275	477	643	661	657	551	386	148	52
Deck, haunches + SIP	0	786	1360	1822	1870	1850	1528	1038	335	53

The unfactored vertical dead-load deflections in Span 1 from the abutment to the end of Cast 1 for the example problem, including the deflections resulting from the assumed deck-placement sequence, are summarized in Table 2.6. The format of the data in Table 2.6 is similar to the format used in Table 2.5. Negative values are downward deflections and positive values are upward deflections. Again, since the deck casts are relatively short-term loadings, the *n*-composite stiffness is used for all preceding casts in computing the moments and deflections shown for Casts 2 and 3 in Table 2.5 and Table 2.6. Note that the moments and deflections on the final composite structure due to the sum of the DC_2 and DW loads shown in Table 2.5 and Table 2.6 are computed using the 3*n*-composite stiffness to account for the long-term effects of concrete creep. Also, the entire cross-sectional area of the deck associated with the exterior girder was assumed effective in the analysis in determining the stiffness of the composite sections.

Table 2.6 Vertical Deflections from Deck-Placement Analysis

Span -> 1	Unfactored Vertical Dead-Load Deflections (in.)									
Length (ft)	**0.00**	12.00	**24.00**	42.00	**48.00**	56.00	**72.00**	84.00	**96.00**	100.0
Steel Weight	0	-.17	-.32	-.47	-.50	-.51	-.47	-.39	-.29	-.25
SIP Forms (SIP)	0	-.07	-.14	-.20	-.21	-.21	-.20	-.16	-.12	-.10
Cast										
1	0	-1.32	-2.50	-3.78	-4.04	-4.27	-4.30	-3.95	-3.33	-3.08
2	0	.27	.52	.86	.96	1.08	1.25	1.32	1.32	1.31
3	0	-.01	-.03	-.04	-.04	-.05	-.05	-.05	-.04	-.03
Sum of Casts + SIP	0	-1.14	-2.14	-3.16	-3.34	-3.46	-3.30	-2.84	-2.17	-1.91
DC_2 + DW	0	-.17	-.32	-.46	-.48	-.49	-.45	-.38	-.28	-.24
Total	0	-1.48	-2.78	-4.09	-4.32	-4.46	-4.22	-3.61	-2.74	-2.40
Deck, haunches + SIP	0	-.92	-1.71	-2.47	-2.59	-2.64	-2.43	-2.02	-1.47	-1.27

Note the differences in the calculated deflections on the last line of Table 2.6 (assuming the deck is cast simultaneously on the noncomposite structure) and the

sum of the accumulated deflections during the sequential deck casts. In many cases, the deflections shown on the last line can be used to estimate the girder cambers, as required in *AASHTO LRFD* Article 6.10.3.5 to account for the dead-load deflections. When the differences in these deflections are not significant, the deflections due to the accumulated deck casts will eventually converge toward the deflections shown on the last line as concrete creep occurs. However, if the differences in the deflections are deemed significant, the Engineer may need to evaluate which set of deflections should be used, or else estimate deflections somewhere in-between to compute the girder cambers and avoid potential errors in the final girder elevations.

It is interesting to note that a refined 3D analysis of the example bridge yielded a maximum vertical deflection in Span 1 (at Location A) due to the weight of the concrete deck, haunches and SIP forms (assuming that the concrete is placed simultaneously on the noncomposite girders) of 2.61 inches in the exterior girders and 2.65 inches in the interior girders. From Table 2.5, the comparable maximum vertical deflection from a line-girder analysis is 2.64 inches, which indicates the assumption of equal distribution of the DC_1 loads to all the girders (which was assumed for this analysis) is the proper assumption in this case (see DM Volume 1, Chapter 2, Section 2.4.3.1.4.4 for further discussion on this issue).

AASHTO LRFD Article 6.10.3.1 requires that potential uplift at bearings be investigated at each critical construction stage. The unfactored vertical dead-load reactions resulting from the deck-placement analysis for the example problem are given in Table 2.7. Negative reactions represent upward reactions that resist the maximum downward force at the support under consideration. Conversely, positive reactions represent downward reactions that resist the maximum uplift force at the support.

Table 2.7 Unfactored Vertical Dead-Load Reactions from Deck-Placement Analysis (kips)

	Abut 1		Pier 1		Pier 2		Abut 2	
Steel Weight	-13		-53		-53		-13	
Sum		-13		-53		-53		-13
SIP Forms (SIP)	-6		-21		-21		-6	
Sum		-19		-74		-74		-19
Cast 1	-80		-55		-55		-80	
Sum		-99		-129		-129		-99
Cast 2	13		-75		-75		14	
Sum		-85		-204		-204		-85
Cast 3	-1		-110		-110		-1	
Sum		-86		-314		-314		-86
Sum of Casts + SIP		-73		-261		-261		-73
DC_2+DW		-26		-90		-90		-26
Total		-112		-404		-404		-112
Deck, haunches + SIP		-74		-261		-261		-74

Shown in Table 2.7 (under 'sum') are the accumulated reactions for the steel weight plus the individual deck casts, which should be used to check for uplift under the

deck placement. A net positive reaction indicates that the girder may lift-off at the support. Lift-off does not occur in this particular example; lift-off is most common when end spans of continuous units are skewed or relatively short. If the girder is permitted to lift-off its bearing seat, the staging analysis is incorrect unless a hold-down of the girder is provided at the location of a positive reaction.

Options to consider when uplift occurs include: 1) rearranging the concrete casts, 2) specifying a temporary load over that support, 3) specifying a tie-down bearing, or 4) if the uplift can be tolerated, performing another staging analysis with zero bearing stiffness at the support experiencing lift-off to determine the correct moments, deflections, and reactions. Note that the sum of the reactions from the analysis of the staged deck casts may differ somewhat from the reactions assuming the deck is cast simultaneously on the noncomposite structure (as given on the last line of Table 2.7); however, in most cases, the reactions should not differ greatly.

The maximum flexural stresses in the flanges of the steel section due to the factored loads resulting from the deck-placement sequence will next be calculated. Strength I and Strength IV are the applicable load combinations that will be considered (see DM Volume 1, Chapter 5 for further discussion on these load combinations). The cross-section of the girder at Location A is shown in Figure 2.3. The elastic section properties for this section were computed earlier. As specified in *AASHTO LRFD* Article 6.10.1.6 (and discussed further below in Section 2.2.3.7.1.2 under Strength Limit State Design Verifications), for design checks where the flexural resistance is based on lateral torsional buckling, the bending stress f_{bu} is to be determined as the largest value of the compressive stress throughout the unbraced length in the flange under consideration, calculated without consideration of flange lateral bending. For design checks where the flexural resistance is based on yielding, flange local buckling or web bend buckling, f_{bu} may be determined as the stress at the section under consideration. Cross-frames adjacent to Location A are located 48 ft and 72 ft from the abutment.   From inspection of Table 2.5, since the girder is prismatic between the two cross-frames, the largest stress within the unbraced length occurs right at Location A. The load modifier η factor will be assumed equal to 1.0 in this example. Therefore:

For Strength I:

$$\text{Top flange:}\quad f_{bu} = \frac{1.0(1.25)(2,889)(12)}{1,581} = -27.41\,\text{ksi}$$

$$\text{Bot. flange:}\quad f_{bu} = \frac{1.0(1.25)(2,889)(12)}{1,973} = 21.96\,\text{ksi}$$

For Strength IV:

$$\text{Top flange:}\quad f_{bu} = \frac{1.0(1.5)(2,889)(12)}{1,581} = -32.89\,\text{ksi}$$

$$\text{Bot. flange:} \quad f_{bu} = \frac{1.0(1.5)(2,889)(12)}{1,973} = 26.36 \text{ ksi}$$

AASHTO LRFD Article 6.10.3.2.4 requires that the longitudinal tensile stress in a composite concrete deck due to the factored loads not exceed ϕf_r during critical stages of construction, unless longitudinal reinforcement is provided according to the provisions of *AASHTO LRFD* Article 6.10.1.7. Assume normal weight concrete used with a 28-day compressive strength f'_c equal to 4.0 ksi. f_r is the modulus of rupture of the concrete determined as follows for normal weight concrete (*AASHTO LRFD* Article 5.4.2.6):

$$f_r = 0.24\sqrt{f'_c} = 0.24\sqrt{4.0} = 0.480 \text{ ksi}$$

ϕ is the appropriate resistance factor for concrete in tension specified in *AASHTO LRFD* Article 5.5.4.2.1. For reinforced concrete in tension, ϕ is equal to 0.90. Therefore:

$$\phi f_r = 0.90(0.480) = 0.432 \text{ ksi}$$

Check the tensile stress in the concrete deck at the end of Cast 1 in Span 1 (100.0 feet from the abutment) caused by the negative moment due to Cast 2. From Table 2.5, the negative moment at the end of Cast 1 due to Cast 2 is –1,403 kip-feet. The longitudinal concrete deck stress is to be determined as specified in *AASHTO LRFD* Article 6.10.1.1.1d; that is, using the short-term modular ratio *n* = 8. The Strength IV load combination controls by inspection.

$$f_{deck} = \frac{1.0(1.5)(-1,403)(23.20)(12)}{161,518(8)} = 0.453 \text{ ksi} > 0.432 \text{ ksi}$$

Therefore, the minimum one percent longitudinal reinforcement is required at this section (refer to *AASHTO LRFD* Article 6.10.1.7). The reinforcement is to be No. 6 bars or smaller spaced at not more than 12 inches. Separate calculations similar to those shown above indicate that the minimum longitudinal reinforcement in Span 1 must extend from the interior-pier section to a section approximately 95.0 feet from the abutment in order to satisfy this requirement for the construction condition. *Although not done in this example, a more accurate estimate of the concrete strength at the time Cast 2 is made, and the resulting modular ratio, can be used in this check.*

The effective width of the deck is 100.0 in. and the structural deck thickness is 9.0 in. Therefore, the total tensile force in the concrete deck at the end of Cast 1 is (0.453)(100.0)(9.0) = 408 kips. This force will be transferred from the deck through the shear connectors to the top flange. Sufficient shear connectors should be present at this location to resist this force and prevent potential crushing of the concrete around the studs or fracturing of the studs. To estimate the length over which this force must be transmitted, assume a 45-degree angle from the end of the cast to where the concrete deck is assumed effective. Therefore, the length in this particular case is estimated to be 50.0 inches (< 100.0 - 95.0 = 5.0 feet). The pitch of the studs is 12.0 inches in this region and that there are three studs per row. The

factored shear resistance of an individual 7/8-inch stud is computed to be 30.6 kips for f_c' equal to 4.0 ksi (see Section 2.2.5.3 of this chapter). Thus, the force resisted by the 15 studs within the 50-inch length is 15(30.6) = 459 kips > 408 kips. If necessary, the tensile force in the deck can be lowered by modifying the placement sequence.

2.2.3.4.2 Deck Overhang Loads

AASHTO LRFD Article 6.10.3.4 requires that the effects of the forces from deck overhang brackets acting on the fascia girders be considered. As shown in Figure 2.34, during the construction of steel girder bridges, concrete deck overhang loads are typically supported by cantilever forming brackets placed at approximately 3.0 to 4.0 ft spacings along the exterior (fascia) girders. Applied torsional moments act on the exterior girders due to the eccentricity of the deck weight and other loads acting on the brackets.   The torsional moments bend the top flanges of the exterior girders outward resulting in lateral bending stresses that should be considered in the design of the flanges. As will be seen below, the equations given in *AASHTO LRFD* Article 6.10.3.2 allow the Engineer to consider the effect of these lateral bending stresses in the design of the exterior-girder flanges.

Figure 2.34 Deck Overhang

The brackets may either bear directly on the web or be carried to the intersection of the bottom flange and the web, which is preferred (Figure 2.35). The horizontal components of the bracket reactions transmitted directly onto the exterior girder web may cause the web to exhibit significant plate deformations. Excessive deformations of the web or top flange resulting from the bracket support forces may cause the deck finish to be problematic. Therefore, if the brackets bear on the girder web, a means should be provided to ensure that the web is not damaged and that the associated deformations permit proper placement of the concrete deck.
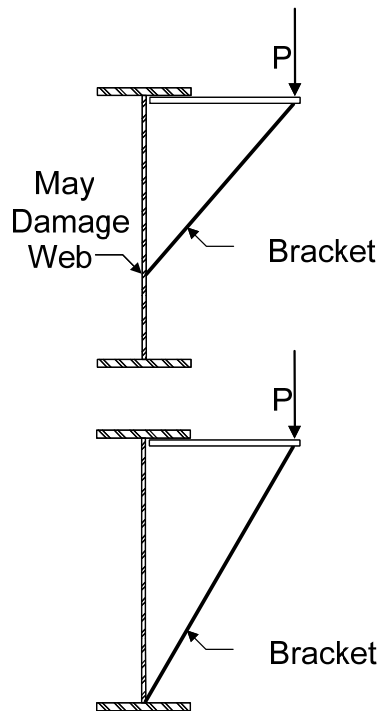
Figure 2.35 Forming Brackets

Figure 2.36 shows a bracket bearing at the intersection of the bottom flange and web. The lateral force on the flanges *F* resulting from the vertical deck overhang loads *P* is dependent on the angle the brackets make with respect to the vertical. In addition to the weight of the deck overhang, construction loads -- or dead loads and temporary loads that act on the overhang only during construction -- include the overhang deck forms, screed rail, railings, walkway and finishing machine. The Engineer should consider talking with local Contractors to obtain reasonable values for these loads. Load factors to be applied to construction loads are specified in *AASHTO LRFD* Article 3.4.2. Both the magnitude and application (i.e. assumed angle of the brackets) of the overhang loads should be indicated in the contract documents. Should the Contractor deviate significantly form the assumed angle and/or loads, an additional investigation by the Contractor may be necessary.

Typically, the major-axis bending moments due to the deck overhang construction loads are not considered in the design of the girders because these loads are usually much smaller in magnitude relative to other design loads on the bridge (e.g. permanent loads and design live loads). Also, the construction loads are temporary loads that are eventually removed. These loads are typically applied to the noncomposite steel section and the removal of these loads would need to be based on the composite section stiffness, which complicates the analysis. Such an analysis may be desirable in special situations involving large deck overhangs in order to obtain more accurate determinations of the required girder cambers. The lateral bending moments due to these loads are usually much more critical.
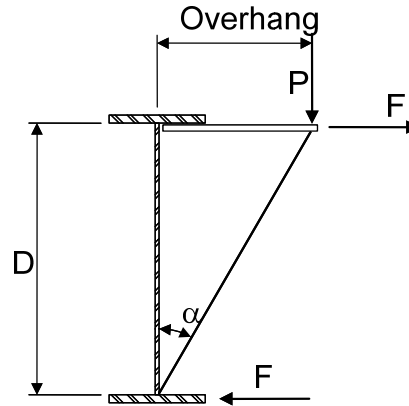
Figure 2.36 Bracket Bearing Directly on the Bottom Flange

AASHTO LRFD Article C6.10.3.4 gives approximate equations that may be used to estimate the maximum lateral bending moments M_ℓ in the flanges due to the lateral bracket forces in lieu of a more refined analysis. The equation to use depends on how the lateral bracket forces are assumed applied to the top flange. If a statically equivalent uniformly distributed bracket force F_ℓ is assumed, then M_ℓ may be determined as:

$$M_\ell = \frac{F_\ell L_b^2}{12}$$

Equation 2.69

AASHTO LRFD Equation C6.10.3.4-2

where L_b is the unbraced length. If a statically equivalent concentrated lateral bracket force P_ℓ is assumed at the middle of the unbraced length, then M_ℓ may be determined as:

$$M_\ell = \frac{P_\ell L_b}{8}$$

Equation 2.70

AASHTO LRFD Equation C6.10.3.4-3

Both equations assume reasonably equal continuous adjacent unbraced lengths such that the ends of the unbraced length under consideration are effectively torsionally fixed. Other approximate idealizations may need to be considered when the actual conditions do not match these assumptions. The lateral bending stress may then be computed as M_ℓ divided by the lateral section modulus of the flange ($t_f b_f^2/6$), and is limited to $0.6F_{yf}$ according to *AASHTO LRFD* Article 6.10.1.6. Furthermore, according to *AASHTO LRFD* Article 6.10.1.6, amplification of the first-order flange lateral bending stresses may be required in discretely braced compression flanges. Amplification of tension-flange lateral bending stresses is not required. Amplification of these stresses is discussed in more detail in Section 2.2.3.1.2.2 of this chapter under Fundamental Concepts (Equations 2.38 and 2.40 apply), and is demonstrated in the following example.

EXAMPLE

Calculate the lateral flange bending stresses due to the deck overhang loads within the 24-foot unbraced length of an exterior girder in the end span of a three-span continuous I-girder bridge encompassing Location A from the preceding example. The cross-section of the girder within this unbraced length is shown in Figure 2.3. The elastic section properties for this section were computed earlier. The girder is homogeneous with the yield strength of the flanges and web equal to 50 ksi. Assume the deck overhang bracket configuration shown in Figure 2.37 with the brackets extending to the bottom flange, which is preferred.
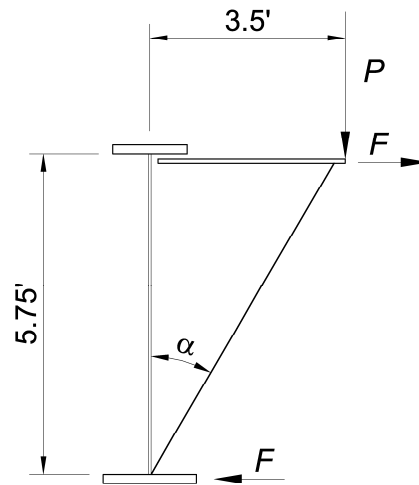
Figure 2.37 Deck Overhang Bracket

Although the brackets are typically spaced at 3 to 4 feet along the exterior girder, all bracket loads except for the finishing machine load are assumed applied uniformly. Calculate the vertical loads acting on the overhang brackets. Because in this case the bracket is assumed to extend near the edge of the deck overhang, assume that half the deck overhang weight is placed on the exterior girder and half the weight is placed on the overhang brackets. Conservatively include one-half the deck haunch weight in the total overhang weight. Assume the following bridge cross-section:

The top flange of the girder within the unbraced length under consideration is ¾" x 16" (Figure 2.3). The ½" integral wearing surface is not included in the indicated 10" dimension at the edge of the overhang. Therefore, the deck overhang weight assumed to be acting on the bracket is computed as:

$$P = 0.5*150\left[\frac{9.5}{12}(3.5)+\left[\frac{1}{12}\left(\frac{3.0}{2}+0.5\right)\left(3.5-\frac{16/2}{12}\right)\right]+\frac{2.75}{12}\left(\frac{16/2}{12}\right)\right] = 255 \text{ lbs/ft}$$

The other half of the overhang weight can be assumed to act at the edge of the top flange (at a distance of 8.0 inches from the shear center of the girder in this case). The effective deck weight acting on the other side of the girder can be assumed applied at the other edge of the top flange. The net torque can be resolved into flange lateral moments that generally act in the opposite direction to the lateral moments caused by the overhang loads. This effect is conservatively neglected in this example.

Construction loads, or dead loads and temporary loads that act on the overhang only during construction, are assumed as follows:

Overhang deck forms:	P = 40 lbs/ft
Screed rail:	P = 85 lbs/ft
Railing:	P = 25 lbs/ft
Walkway:	P = 125 lbs/ft
Finishing machine:	P = 3000 lbs

The finishing machine load is estimated as one-half of the total finishing machine truss weight, plus some additional load to account for the weight of the engine, drum and operator assumed to be located on one side of the truss. Note that the above loads are estimated loads used here for illustration purposes only. Again, it is recommended that the Engineer consider talking to local Contractors to obtain more accurate values for these construction loads.

The lateral force on the top flange due to the vertical load on the overhang brackets is computed as:

$$F = P \tan \alpha$$

where:
$$\alpha = \tan^{-1}\left(\frac{3.5 \text{ ft}}{5.75 \text{ ft}}\right) = 31.3°$$

Alternatively, *F* could simply be approximated as *P*(3.5 ft / 5.75 ft), but it will be computed as shown above in this example to more clearly illustrate how the lateral force is derived.

Assuming the flanges are continuous with the adjacent unbraced lengths and that the adjacent unbraced lengths are approximately equal, the lateral bending moment due to a statically equivalent uniformly distributed lateral bracket force may be estimated as:

$$M_\ell = \frac{F_\ell L_b^2}{12}$$

AASHTO LRFD Equation C6.10.3.4-2

The lateral bending moment due to a statically equivalent concentrated lateral bracket force assumed placed at the middle of the unbraced length may be estimated as:

$$M_\ell = \frac{P_\ell L_b}{8}$$

AASHTO LRFD Equation C6.10.3.4-3

According to *AASHTO LRFD* Article 6.10.1.6, lateral bending stresses determined from a first-order analysis may be used in discretely braced compression flanges for which:

$$L_b \leq 1.2 L_p \sqrt{\frac{C_b R_b}{f_{bu}/F_{yc}}}$$

AASHTO LRFD Equation 6.10.1.6-2

L_p is the limiting unbraced length specified in *AASHTO LRFD* Article 6.10.8.2.3 (see Section 2.2.3.7.1.2.1 of this chapter under Strength Limit State Verifications) determined as:

$$L_p = 1.0 r_t \sqrt{\frac{E}{F_{yc}}}$$

AASHTO LRFD Equation 6.10.8.2.3-4

where r_t is the effective radius of gyration for lateral torsional buckling specified in *AASHTO LRFD* Article 6.10.8.2.3 determined as:

$$r_t = \frac{b_{fc}}{\sqrt{12\left(1 + \frac{1}{3}\frac{D_c t_w}{b_{fc} t_{fc}}\right)}}$$

AASHTO LRFD Equation 6.10.8.2.3-9

For the steel section within the unbraced length under consideration, the depth of the web in compression in the elastic range D_c is 38.63 inches. Therefore,

$$r_t = \frac{16}{\sqrt{12\left(1 + \frac{1}{3}\frac{38.63(0.5)}{16(1)}\right)}} = 3.90 \text{ in.}$$

$$L_p = \frac{1.0(3.90)}{12}\sqrt{\frac{29,000}{50}} = 7.83 \text{ ft}$$

C_b is the moment gradient modifier specified in *AASHTO LRFD* Article 6.10.8.2.3. Separate calculations show that $f_{mid}/f_2 > 1$ in the unbraced length under consideration. Therefore, C_b must be taken equal to 1.0 (see Section 2.2.3.7.1.2 of this chapter under Strength Limit State Verifications for further information on the calculation of C_b). According to *AASHTO LRFD* Article 6.10.1.10.2, the web load-shedding factor R_b is to be taken equal to 1.0 when checking constructibility since web bend buckling is prevented during construction by a separate limit state check (see the next section of this chapter on Design Verifications for Flexure and Shear). Finally, f_{bu} is the largest value of the compressive stress due to the factored loads throughout the unbraced length in the flange under consideration, calculated without consideration of flange lateral bending. In this case, use f_{bu} = -32.89 ksi due to the deck-placement sequence, as computed earlier for the Strength IV load combination (which controls in this particular computation). Therefore:

$$1.2(7.83)\sqrt{\frac{1.0(1.0)}{|-32.89|/50}} = 11.59 \text{ ft} < L_b = 24.0 \text{ ft}$$

Because the preceding equation is not satisfied, *AASHTO LRFD* Article 6.10.1.6 requires that second-order elastic compression-flange lateral bending stresses be determined. The second-order compression-flange lateral bending stresses may be determined by amplifying first-order values (i.e. $f_{\ell 1}$) as follows:

$$f_\ell = \left|\frac{0.85}{1 - \frac{f_{bu}}{F_{cr}}}\right| f_{\ell 1} \geq f_{\ell 1}$$

AASHTO LRFD Equation 6.10.1.6-4

or:
$$f_\ell = (AF)f_{\ell 1} \geq f_{\ell 1}$$

where *AF* is the amplification factor and F_{cr} is the elastic lateral torsional buckling stress for the flange under consideration specified in *AASHTO LRFD* Article 6.10.8.2.3 determined as:

$$F_{cr} = \frac{C_b R_b \pi^2 E}{\left(\dfrac{L_b}{r_t}\right)^2}$$

AASHTO LRFD Equation 6.10.8.2.3-8

$$F_{cr} = \frac{1.0(1.0)\pi^2(29{,}000)}{\left(\dfrac{24(12)}{3.90}\right)^2} = 52.49 \text{ ksi}$$

As indicated in *AASHTO LRFD* Article C6.10.1.6, note that the calculated value of F_{cr} for use in *AASHTO LRFD* Equation 6.10.1.6-4 is not limited to $R_b R_h F_{yc}$ as specified in *AASHTO LRFD* Article 6.10.8.2.3.

The amplification factor is then determined as follows:

For Strength I:

$$AF = \frac{0.85}{\left(1 - \dfrac{|-27.41|}{52.49}\right)} = 1.78 > 1.0 \quad \text{ok}$$

For Strength IV:

$$AF = \frac{0.85}{\left(1 - \dfrac{|-32.89|}{52.49}\right)} = 2.28 > 1.0 \quad \text{ok}$$

AF is taken equal to 1.0 for tension flanges. The above equation for the amplification factor conservatively assumes an elastic effective length factor for lateral-torsional buckling equal to 1.0 (see Section 2.2.3.1.1.2 of this chapter under Fundamental Concepts for further discussion on the effective length factor for lateral-torsional buckling).

Note that first- or second-order flange lateral bending stresses, as applicable, are limited to a maximum value of $0.6F_{yf}$ according to *AASHTO LRFD* Equation 6.10.1.6-1.

In the Strength I load combination, a load factor of 1.5 is applied to all construction loads (refer to *AASHTO LRFD* Article 3.4.2).

For Strength I:

Dead loads: $P = 1.0[1.25(255) + 1.5(40 + 85 + 25 + 125)] = 731.3 \text{ lbs/ft}$

$F = F_\ell = P \tan \alpha = 731.3 \tan(31.3°) = 444.6 \text{ lbs/ft}$

$$M_\ell = \frac{F_\ell L_b^2}{12} = \frac{0.4446(24)^2}{12} = 21.34 \text{ kip} - \text{ft}$$

Top flange: $f_\ell = \dfrac{M_\ell}{S_\ell} = \dfrac{21.34(12)}{1(16)^2/6} = 6.00 \text{ ksi}$

Bot. flange: $f_\ell = \dfrac{M_\ell}{S_\ell} = \dfrac{21.34(12)}{1.375(18)^2/6} = 3.45 \text{ ksi}$

Finishing machine: $P = 1.0[1.5(3000)] = 4{,}500 \text{ lbs}$

$F = P_\ell = P \tan \alpha = 4{,}500 \tan(31.3°) = 2{,}736 \text{ lbs}$

$$M_\ell = \frac{P_\ell L_b}{8} = \frac{2.736(24)}{8} = 8.21 \text{ kip} - \text{ft}$$

Top flange: $f_\ell = \dfrac{M_\ell}{S_\ell} = \dfrac{8.21(12)}{1(16)^2/6} = 2.31 \text{ ksi}$

Bot. flange: $f_\ell = \dfrac{M_\ell}{S_\ell} = \dfrac{8.21(12)}{1.375(18)^2/6} = 1.33 \text{ ksi}$

Top flange:

f_ℓ total $= 6.00 + 2.31 = 8.31 \text{ ksi}$ * AF = (8.31)(1.78) = 14.79 ksi < $0.6F_{yf}$ = 30 ksi   ok

Bot. flange:

f_ℓ total $= 3.45 + 1.33 = 4.78 \text{ ksi}$ * AF = (4.78)(1.0) = 4.78 ksi < $0.6F_{yf}$ = 30 ksi   ok

For Strength IV:

Dead loads: $P = 1.0[1.5(255 + 40 + 85 + 25 + 125)] = 795 \text{ lbs/ft}$

$$F = F_\ell = P\tan\alpha = 795\tan(31.3°) = 483.4 \text{ lbs}/\text{ft}$$

$$M_\ell = \frac{F_\ell L_b^2}{12} = \frac{0.4834(24)^2}{12} = 23.20 \text{ kip} - \text{ft}$$

$$\text{Top flange: } f_\ell = \frac{M_\ell}{S_\ell} = \frac{23.20(12)}{1(16)^2/6} = 6.52 \text{ ksi}$$

$$\text{Bot. flange: } f_\ell = \frac{M_\ell}{S_\ell} = \frac{23.20(12)}{1.375(18)^2/6} = 3.75 \text{ ksi}$$

Finishing machine: Not considered

Top flange: f_ℓ total $= 6.52$ ksi $*$ AF $= 6.52(2.28) = 14.87$ ksi $< 0.6F_{yf} = 30$ ksi   ok
Bot. flange: f_ℓ total $= 3.75$ ksi $*$ AF $= 3.75(1.0) = 3.75$ ksi $< 0.6F_{yf} = 30$ ksi   ok

2.2.3.4.3 Design Verifications for Flexure and Shear

2.2.3.4.3.1 General

To ensure the goal of providing adequate strength and stability of I-section flexural members during construction, without permitting nominal yielding (except for localized web yielding in hybrid sections) or relying on post-buckling resistance, the requirements of *AASHTO LRFD* Articles 6.10.3.2 (Flexure) and 6.10.3.3 (Shear) must be satisfied at each critical construction stage. The applicable strength load combinations for these design checks include Strength I, Strength III and Strength IV (see DM Volume 1, Chapter 5 for additional information on these load combinations). As mentioned previously, when considering construction loads, the provisions of *AASHTO LRFD* Article 3.4.2 apply for determining the appropriate load factor to be applied to these loads in each strength combination.

A helpful flowchart detailing the constructibility design checks to be made for flexure and shear is provided in Appendix C to Section 6 of the *AASHTO LRFD* Specifications – Figure C6.4.1-1.

2.2.3.4.3.2 Flexure

In the constructibility design provisions for flexure given in *AASHTO LRFD* Article 6.10.3.2, an important distinction is made between discretely braced and continuously braced flanges. As discussed earlier, a discretely braced flange is braced at discrete intervals by bracing sufficient to restrain lateral deflection of the flange and twisting of the entire cross-section at the brace points. For the noncomposite steel girder during construction, both flanges along the entire length of the girder are considered to be discretely braced flanges. A continuously braced flange is encased in hardened concrete or anchored by shear connectors. Lateral flange bending need not be considered for a continuously braced flange. A

continuously braced compression flange is also assumed not to be subject to local or lateral-torsional buckling.

For discretely braced compression flanges, each of the following three equations must be satisfied during critical stages of construction according to *AASHTO LRFD* Article 6.10.3.2.1:

$$f_{bu} + f_\ell \le \phi_f R_h F_{yf}$$

Equation 2.71

AASHTO LRFD Equation 6.10.3.2.1-1

$$f_{bu} + \frac{1}{3} f_\ell \le \phi_f F_{nc}$$

Equation 2.72

AASHTO LRFD Equation 6.10.3.2.1-2

$$f_{bu} \le \phi_f F_{crw}$$

Equation 2.73

AASHTO LRFD Equation 6.10.3.2.1-3

where:

ϕ_f = resistance factor for flexure specified in *AASHTO LRFD* Article 6.5.4.2 = 1.0

f_{bu} = compression-flange stress calculated without consideration of flange lateral bending determined as specified in *AASHTO LRFD* Article 6.10.1.6 (ksi). f_{bu} is always taken as positive.

f_ℓ = flange lateral bending stress determined as specified in *AASHTO LRFD* Article 6.10.1.6 (ksi). f_ℓ is always taken as positive.

F_{crw} = nominal bend-buckling resistance for webs determined as specified in *AASHTO LRFD* Article 6.10.1.9 (Equation 2.11)(ksi)

F_{nc} = nominal flexural resistance of the compression flange determined as specified in *AASHTO LRFD* Article 6.10.8.2 (ksi).

R_h = hybrid factor specified in *AASHTO LRFD* Article 6.10.1.10.1 (Equation 2.21)

Equation 2.71 ensures that the maximum combined factored major-axis and lateral bending stress in the compression flange during construction will not exceed the specified minimum yield strength of the flange times the hybrid factor R_h. As such, Equation 2.71 is a yielding limit state check. For girders subject to significant lateral bending stresses f_ℓ and for members with compact or noncompact webs, Equation 2.71 will often control. For sections with slender webs, Equation 2.71 will not control and need not be checked when f_ℓ is equal to zero (see Section 2.2.3.1.1.1 of this chapter under Fundamental Concepts for definitions of compact, noncompact and slender webs). In categorizing the web as compact, noncompact or slender for these checks, the properties of the noncomposite steel section are used.   Note that for sections that are composite in the final condition, but noncomposite during construction, different values of R_h must be computed for the checks in which the member is noncomposite (i.e. Equation 2.71) and for the checks in which the member is composite.

Equation 2.72 ensures that the member has sufficient strength with respect to flange local buckling and lateral-torsional buckling under the maximum combined factored major-axis and lateral bending stress in the compression flange during construction. Equation 2.72 is based on the stress-based form of the one-third rule equation (i.e. Equation 2.36) since the nominal flexural resistance for constructibility is always expressed in terms of the flange stress (see Section 2.2.3.1.2.2 of this chapter under Fundamental Concepts for additional discussion on the one-third rule equation). The basics of the flange local buckling and lateral-torsional buckling limit states were discussed previously in the section on Fundamental Concepts. The calculation of the flange local buckling (FLB) resistance and lateral-torsional buckling (LTB) resistance F_{nc} according to the *AASHTO LRFD* Specification provisions is discussed in detail in Section 2.2.3.7.1.2 of this chapter under Strength Limit State Verifications. Note that for sections in *straight* I-girder bridges with compact or noncompact webs, *AASHTO LRFD* Article 6.10.3.2.1 permits the LTB resistance to be determined from the provisions of *AASHTO LRFD* Article A6.3.3 (Appendix A to Section 6), which include the beneficial effect of the St. Venant torsional constant *J*. For straight members having larger unbraced lengths that utilize such sections, the additional LTB resistance obtained by including the contribution of *J* may be beneficial. The LTB resistance M_{nc} computed from the provisions of Appendix A is expressed in terms of moment because, in general, Appendix A permits flexural resistances to exceed the yield moment resistance M_{yt} or M_{yc}, as applicable (see Section 2.2.3.7.1.2.2 of this chapter under Strength Limit State Verifications for further discussion on the provisions of Appendix A). Therefore, if the LTB resistance is computed from Appendix A in such cases, the resulting LTB resistance M_{nc} must be divided by S_{xc} (taken equal to M_{yc}/F_{yc}) to express the resistance in terms of stress for application in Equation 2.72. The calculated resistance F_{nc} may exceed F_{yc} in some cases, however Equation 2.71 will control ensuring that the combined factored stress in the flange will not exceed F_{yc} during construction. Equation 2.72 will generally control for members with noncompact flanges having large unsupported lengths during construction in combination with zero or small values of f_ℓ (see Section 2.2.3.1.1.3 of this chapter under Fundamental Concepts for the definition of a noncompact flange).

As specified in *AASHTO LRFD* Article 6.10.1.6, for design checks involving lateral-torsional buckling, the major-axis bending compressive stress f_{bu} and flange lateral bending stress f_ℓ are to be taken as the largest values throughout the unbraced length in the flange under consideration, which is consistent with established practice in applying beam-column interaction equations involving member stability checks. For design checks involving flange local buckling, f_{bu} and f_ℓ may be taken as the corresponding values at the section under consideration. However, when maximum values of these stresses occur at different locations within the unbraced length, which is often the case, it is conservative to use the maximum values in the local buckling check.

Sources of lateral flange bending during construction include curvature, eccentric concrete deck overhang loads acting on exterior girders, wind loading and the effect of staggered cross-frames/diaphragms and/or support skew. The determination of flange lateral bending moments due to curvature is addressed in *AASHTO LRFD*

Article 4.6.1.2.4b. The determination of lateral flange bending moments due to the effect of deck overhang loads was discussed in the preceding section of this chapter. Determination of flange lateral bending moments due to wind is discussed in the next section of this chapter. Lateral flange bending due to staggered cross-frames/diaphragms and/or support skew is discussed in *AASHTO LRFD* Article C6.10.1 and is preferably handled by a direct structural analysis of the bridge superstructure. Additional discussion on lateral flange bending in skewed bridges may be found in Section 2.2.3.8 of this chapter. As specified in *AASHTO LRFD* Article 6.10.1.6, the sum of the flange lateral bending stresses due to all sources cannot exceed 0.6F_{yf}. As demonstrated in the example given in the preceding section of this chapter, amplification of the flange lateral bending stresses in discretely braced compression flanges may be required in some cases (*AASHTO LRFD* Article 6.10.1.6). *Note that in all the one-third rule equations within the specification, when the effects of flange lateral bending are judged to be insignificant or incidental, the flange lateral bending term, f_ℓ, is simply set equal to zero in the appropriate equations.*

Equation 2.73 ensures that theoretical web bend-buckling will not occur during construction. The web bend-buckling resistance F_{crw} is discussed in a previous section of this chapter. Because the compression-flange stress is limited to F_{crw} during construction according to Equation 2.73, *the web load-shedding factor R_b is always taken equal to 1.0 when computing the nominal flexural resistance of the compression flange for the constructibility checks* (the web load-shedding factor R_b is also discussed in a previous section of this chapter). As a result, the R_b factor is not included in Equations 2.71 and 2.72. Note also that the web slenderness of compact and noncompact web sections is limited such that theoretical web bend-buckling will not occur for elastic stress levels, computed according to beam theory, at or below F_{yc}. Therefore, the specification indicates that Equation 2.73 need not be checked for these sections. Options to consider should Equation 2.73 be violated under the construction condition are given at the end of *AASHTO LRFD* Article C6.10.3.2.1 and are reiterated in the previous section of this chapter on the web bend-buckling resistance.   According to *AASHTO LRFD* Article 6.10.1.6, for design checks involving web bend-buckling or yielding (see below), f_{bu} and f_ℓ may be taken as the corresponding values at the section under consideration. As discussed above, it is conservative to use the maximum values of these stresses within the unbraced length in this check.

For a discretely braced tension flange, *AASHTO LRFD* Article 6.10.3.2.2 requires that the flange satisfy the following relationship during critical stages of construction under the combined factored major-axis bending and lateral bending stresses:

$$f_{bu} + f_\ell \leq \phi_f R_h F_{yt}$$

<div align="right">Equation 2.74</div>
<div align="right">*AASHTO LRFD* Equation 6.10.3.2.2-1</div>

For continuously braced flanges in compression or tension, *AASHTO LRFD* Article 6.10.3.2.3 requires that the following relationship be satisfied during critical stages of construction:

$$f_{bu} \leq \phi_f R_h F_{yf}$$

<div align="right">Equation 2.75</div>

<div align="right">*AASHTO LRFD* Equation 6.10.3.2.3-1</div>

Lateral bending does not need to be considered in Equation 2.75 because the flanges in these cases are continuously supported by the concrete deck.

Finally, *AASHTO LRFD* Article 6.10.3.2.4 limits the longitudinal tensile stress in a composite concrete deck due to the factored loads during critical stages of construction to ϕf_r, unless the minimum one-percent longitudinal reinforcement is provided according to the provisions of *AASHTO LRFD* Article 6.10.1.7. f_r is the modulus of rupture of the concrete (*AASHTO LRFD* Article 5.4.2.6) and ϕ is the resistance factor for concrete in tension equal to 0.9 (*AASHTO LRFD* Article 5.5.4.2.1). The stresses in the concrete deck are to be determined using the short-term modular ratio *n*, as specified in *AASHTO LRFD* Article 6.10.1.1.1d. The intent of this check is primarily to control concrete deck cracking during the deck placement when portions of the deck are placed in a span adjacent to a span where the concrete has already been placed. Negative moment in the adjacent span resulting from this placement causes tensile stresses in the previously placed concrete. Or in situations where long placements are made such that a negative flexure region is included in the initial placement, it is possible for the concrete in this region to be subject to tensile stresses during the remainder of the deck placement, which could potentially lead to early cracking of the deck. To help control the cracking, the minimum one-percent longitudinal reinforcement should be included in these regions wherever the tensile stresses in the deck due to the factored loads exceed the stated limit. This particular check is demonstrated in the previous example given under the topic of the deck placement analysis. As demonstrated at the end of that example, sufficient shear connectors should be present at the end of each cast to transfer the force from the deck to the top flange and prevent potential crushing of the concrete around the studs or fracturing of the studs.

EXAMPLE

Given the deck placement analysis results and the flange lateral bending stresses due to the deck overhang loads calculated in the preceding two examples, check the exterior-girder section at Location A within the end span of a three-span continuous bridge for flexure according to the *AASHTO LRFD* Specification provisions (refer to the first of the two preceding examples to determine Location A). The cross-section of the girder at this location (and within the entire 24-foot unbraced length encompassing this location) is shown in Figure 2.3. The elastic section properties for this section were computed earlier. The girder is homogeneous with the yield strength of the flanges and web equal to 50 ksi. Again, the reader is referred to Section 2.2.3.7.1.2 of this chapter under Strength Limit State Verifications for additional information on the procedures and formulas used in the subsequent calculations.

First, determine if the noncomposite section at Location A is a compact or noncompact web section according to *AASHTO LRFD* Equation 6.10.6.2.3-1 (or

alternatively, see *AASHTO LRFD* Table C6.10.1.10.2-2 (Table 2.3) or Equation 2.13):

$$\frac{2D_c}{t_w} \le 5.7\sqrt{\frac{E}{F_{yc}}}$$

AASHTO LRFD Equation 6.10.6.2.3-1

$$\frac{2D_c}{t_w} = \frac{2(38.63)}{0.5} = 154.5$$

$$5.7\sqrt{\frac{E}{F_{yc}}} = 5.7\sqrt{\frac{29,000}{50}} = 137.3 < 154.5$$

Therefore, the section at Location A is a slender-web section. As a result, for the top flange, *AASHTO LRFD* Equation 6.10.3.2.1-1 must be checked since f_ℓ is not zero. *AASHTO LRFD* Equation 6.10.3.2.1-3 must also be checked, and the optional provisions of Appendix A (to *AASHTO LRFD* Section 6 -- Article A6.3.3) cannot be used to determine the LTB resistance of the top (compression) flange.

Top Flange

The top flange at this location is a discretely braced compression flange. Therefore, calculate the FLB and LTB resistances. Since the member is prismatic between brace points, the nominal flexural resistance of the flange is taken as the lesser of the FLB and LTB resistances:

Local Buckling Resistance (AASHTO LRFD Article 6.10.8.2.2)

Determine the slenderness ratio of the top flange:

$$\lambda_f = \frac{b_{fc}}{2t_{fc}}$$

AASHTO LRFD Equation 6.10.8.2.2-3

$$\lambda_f = \frac{16}{2(1)} = 8.0$$

Determine the limiting slenderness ratio for a compact flange (alternatively, see *AASHTO LRFD* Table C6.10.8.2.2-1):

$$\lambda_{pf} = 0.38\sqrt{\frac{E}{F_{yc}}}$$

AASHTO LRFD Equation 6.10.8.2.2-4

$$\lambda_{pf} = 0.38\sqrt{\frac{29{,}000}{50}} = 9.2$$

Since $\lambda_f < \lambda_{pf}$,

$$\left(F_{nc}\right)_{FLB} = R_b R_h F_{yc}$$

AASHTO LRFD Equation 6.10.8.2.2-1

As specified in *AASHTO LRFD* Article 6.10.3.2.1, in computing F_{nc} for constructibility, the web load-shedding factor R_b is to be taken equal to 1.0 because the flange stress is always limited to the web bend-buckling stress according to *AASHTO LRFD* Equation 6.10.3.2.1-3. Therefore,

$$\left(F_{nc}\right)_{FLB} = 1.0(1.0)(50) = 50.0 \text{ ksi}$$

Lateral Torsional Buckling Resistance (AASHTO LRFD Article 6.10.8.2.3)

The limiting unbraced length L_p was computed earlier to be 7.83 feet. The effective radius of gyration for lateral torsional buckling r_t for the noncomposite section at Location A was also computed earlier to be 3.90 inches (refer to the preceding example under the topic of Deck Overhang Loads).

Determine the limiting unbraced length, L_r:

$$L_r = \pi r_t \sqrt{\frac{E}{F_{yr}}}$$

AASHTO LRFD Equation 6.10.8.2.3-5

where:
$$F_{yr} = 0.7 F_{yc} \le F_{yw}$$

$$F_{yr} = 0.7(50) = 35.0 \text{ ksi} < 50 \text{ ksi} \qquad \text{ok}$$

F_{yr} must also not be less than $0.5F_{yc} = 0.5(50) = 25.0$ ksi ok.

Therefore:
$$L_r = \frac{\pi(3.90)}{12}\sqrt{\frac{29{,}000}{35.0}} = 29.39 \text{ ft}$$

Since L_p = 7.83 feet < L_b = 24.0 feet < L_r = 29.39 feet,

$$\left(F_{nc}\right)_{LTB} = C_b\left[1-\left(1-\frac{F_{yr}}{R_h F_{yc}}\right)\left(\frac{L_b - L_p}{L_r - L_p}\right)\right]R_b R_h F_{yc} \le R_b R_h F_{yc}$$

AASHTO LRFD Equation 6.10.8.2.3-2

As discussed previously (refer to the preceding example under the topic of Deck Overhang Loads), since $f_{mid}/f_2 > 1$ in the unbraced length under consideration, the moment-gradient modifier, C_b must be taken equal to 1.0. Therefore,

$$\left(F_{nc}\right)_{LTB} = 1.0\left[1 - \left(1 - \frac{35.0}{1.0(50)}\right)\left(\frac{24.0 - 7.83}{29.39 - 7.83}\right)\right](1.0)(1.0)(50) = 38.75 \text{ ksi} < 1.0(1.0)(50) = 50 \text{ ksi}$$

ok

F_{nc} is governed by the lateral torsional buckling resistance, which is less than the local buckling resistance of 50.0 ksi computed earlier. Therefore, $F_{nc} = 38.75$ ksi.

Web Bend-Buckling Resistance (AASHTO LRFD Article 6.10.1.9)

Determine the nominal elastic web bend-buckling resistance at Location A according to the provisions of *AASHTO LRFD* Article 6.10.1.9.1 as follows:

$$F_{crw} = \frac{0.9Ek}{\left(\dfrac{D}{t_w}\right)^2}$$

AASHTO LRFD Equation 6.10.1.9.1-1

but not to exceed the smaller of $R_h F_{yc}$ and $F_{yw}/0.7$,

where: $$k = \frac{9}{\left(D_c/D\right)^2}$$

AASHTO LRFD Equation 6.10.1.9.1-2

$$k = \frac{9}{\left(38.63/69.0\right)^2} = 28.7$$

Therefore,

$$F_{crw} = \frac{0.9(29,000)(28.7)}{\left(\dfrac{69.0}{0.5}\right)^2} = 39.33 \text{ ksi} < \min\left(R_h F_{yc}, F_{yw}/0.7\right) = R_h F_{yc} = 1.0(50) = 50 \text{ ksi}$$

ok

Now that all the required information has been assembled, check the requirements of *AASHTO LRFD* Article 6.10.3.2.1:

For Strength I:

$$f_{bu} + f_\ell \leq \phi_f R_h F_{yc}$$

AASHTO LRFD Equation 6.10.3.2.1-1

$$f_{bu} + f_{\ell} = \left|-27.41\right| \text{ ksi} + 14.79 \text{ ksi} = 42.20 \text{ ksi}$$

$$\phi_f R_h F_{yc} = 1.0(1.0)(50) = 50.0 \text{ ksi}$$

$$42.20 \text{ ksi} < 50.0 \text{ ksi} \quad \text{ok}$$

$$f_{bu} + \frac{1}{3} f_{\ell} \leq \phi_f F_{nc}$$

AASHTO LRFD Equation 6.10.3.2.1-2

$$f_{bu} + \frac{1}{3} f_{\ell} = \left|-27.41\right| \text{ ksi} + \frac{14.79}{3} \text{ ksi} = 32.34 \text{ ksi}$$

$$\phi_f F_{nc} = 1.0(38.75) = 38.75 \text{ ksi}$$

$$32.34 \text{ ksi} < 38.75 \text{ ksi} \quad \text{ok}$$

$$f_{bu} \leq \phi_f F_{crw}$$

AASHTO LRFD Equation 6.10.3.2.1-3

$$\phi_f F_{crw} = 1.0(39.33) = 39.33 \text{ ksi}$$

$$\left|-27.41\right| \text{ ksi} < 39.33 \text{ ksi} \quad \text{ok}$$

For Strength IV:

$$f_{bu} + f_{\ell} \leq \phi_f R_h F_{yc}$$

AASHTO LRFD Equation 6.10.3.2.1-1

$$f_{bu} + f_{\ell} = \left|-32.89\right| \text{ ksi} + 14.87 \text{ ksi} = 47.76 \text{ ksi}$$

$$\phi_f R_h F_{yc} = 1.0(1.0)(50) = 50.0 \text{ ksi}$$

$$47.76 \text{ ksi} < 50.0 \text{ ksi} \quad \text{ok}$$

$$f_{bu} + \frac{1}{3} f_{\ell} \leq \phi_f F_{nc}$$

AASHTO LRFD Equation 6.10.3.2.1-2

$$f_{bu} + \frac{1}{3} f_{\ell} = \left|-32.89\right| \text{ ksi} + \frac{14.87}{3} \text{ ksi} = 37.85 \text{ ksi}$$

$$\phi_f F_{nc} = 1.0(38.75) = 38.75 \text{ ksi}$$

$$37.85 \text{ ksi} < 38.75 \text{ ksi} \quad \text{ok}$$

$$f_{bu} \le \phi_f F_{crw}$$

AASHTO LRFD Equation 6.10.3.2.1-3

$$\phi_f F_{crw} = 1.0(39.33) = 39.33 \text{ ksi}$$
$$\left| -32.89 \right| \text{ksi} < 39.33 \text{ ksi} \quad \text{ok}$$

Bottom Flange

For Strength I:

$$f_{bu} + f_\ell \le \phi_f R_h F_{yt}$$

AASHTO LRFD Equation 6.10.3.2.2-1

$$f_{bu} + f_\ell = 21.96 \text{ ksi} + 4.78 \text{ ksi} = 26.74 \text{ ksi}$$
$$\phi_f R_h F_{yc} = 1.0(1.0)(50) = 50.0 \text{ ksi}$$
$$26.74 \text{ ksi} < 50.0 \text{ ksi} \quad \text{ok}$$

For Strength IV:

$$f_{bu} + f_\ell \le \phi_f R_h F_{yt}$$

AASHTO LRFD Equation 6.10.3.2.2-1

$$f_{bu} + f_\ell = 26.36 \text{ ksi} + 3.75 \text{ ksi} = 30.11 \text{ ksi}$$
$$\phi_f R_h F_{yc} = 1.0(1.0)(50) = 50.0 \text{ ksi}$$
$$30.11 \text{ ksi} < 50.0 \text{ ksi} \quad \text{ok}$$

Although the checks are illustrated here for completeness, the bottom flange will typically not control in this region.

2.2.3.4.3.3 Shear

For critical stages of construction, *AASHTO LRFD* Article 6.10.3.3 requires that interior panels of stiffened webs satisfy the following requirement:

$$V_u \le \phi_v V_{cr} \qquad \text{Equation 2.76}$$

AASHTO LRFD Equation 6.10.3.3-1

where:

ϕ_v = resistance factor for shear = 1.0 (*AASHTO LRFD* Article 6.5.4.2)

V_u = shear in the web at the section under consideration due to the factored permanent loads and factored construction loads applied to the noncomposite section (kips)

V_{cr} = shear-buckling resistance determined from *AASHTO LRFD* Equation 6.10.9.3.3-1 (Equation 2.51)(kips)

The use of tension-field action (i.e. post-buckling shear resistance) per Equation 2.53 or 2.55 is not permitted during construction, but is permitted after the deck has hardened or is made composite and if the section along the entire panel satisfies Equation 2.54. Instead, the nominal shear resistance during construction is limited to the shear-buckling resistance V_{cr}. The calculation of V_{cr} was discussed earlier under the section on Fundamental Concepts, and is also discussed below under the section on Strength Limit State Verifications. As will be discussed in the section on Strength Limit State Verifications, the shear in unstiffened webs and in the end panels of stiffened webs is already limited to V_{cr} at the strength limit state. Therefore, Equation 2.76 need not be checked for unstiffened webs and end panels of stiffened webs because it would not control.

EXAMPLE

Check the shear during construction in the critical interior panel of the first 100-foot-long field section in the 140-foot end span of a three-span continuous I-girder bridge. The web plate in this field section is ½" x 69". The yield strength of the web F_{yw} is 50 ksi. The critical panel for this check is assumed to be the panel immediately to the left of the fourth intermediate cross-frame from the abutment, which is located 96.0 feet from the abutment (assuming cross-frames spaced longitudinally along the girder at 24.0 feet). The transverse stiffener in this panel is assumed to be located at the maximum permitted spacing of d_o = 3D = 3(69.0) = 207.0 inches to the left of this cross-frame. Since shear is rarely increased significantly due to deck staging, the factored DC$_1$ shear at the cross-frame will be used in this check (the Strength IV load combination governs by inspection). The load modifier η is assumed equal to 1.0:

$$\left(V_u\right)_{DC_1} = 1.0(1.5)(-79) = -119 \text{ kips at } 96'\text{-}0'' \text{ from the abutment}$$

The shear buckling resistance of the 207-inch-long panel is determined as:

$$V_n = V_{cr} = CV_p$$

AASHTO LRFD Equation 6.10.9.3.3-1

C is the ratio of the shear buckling resistance to the shear yield strength determined from *AASHTO LRFD* Equation 6.10.9.3.2-4, 6.10.9.3.2-5 or 6.10.9.3.2-6, as applicable. First, compute the shear buckling coefficient, k

$$k = 5 + \frac{5}{\left(\dfrac{d_o}{D}\right)^2}$$

AASHTO LRFD Equation 6.10.9.3.2-7

$$k = 5 + \frac{5}{\left(\dfrac{207.0}{69.0}\right)^2} = 5.56$$

Since,

$$1.40\sqrt{\frac{Ek}{F_{yw}}} = 1.40\sqrt{\frac{29{,}000(5.56)}{50}} = 79.5 < \frac{D}{t_w} = \frac{69.0}{0.5} = 138.0$$

$$C = \frac{1.57}{\left(\dfrac{D}{t_w}\right)^2}\left(\frac{Ek}{F_{yw}}\right)$$

AASHTO LRFD Equation 6.10.9.3.2-6

$$C = \frac{1.57}{(138.0)^2}\left(\frac{29{,}000(5.56)}{50}\right) = 0.266$$

V_p is the plastic shear force determined as follows:

$$V_p = 0.58F_{yw}Dt_w$$

AASHTO LRFD Equation 6.10.9.3.3-2

$$V_p = 0.58(50)(69.0)(0.5) = 1{,}001\,\text{kips}$$

Therefore,

$$V_{cr} = 0.266(1{,}001) = 266\,\text{kips}$$

$$\phi_v V_{cr} = 1.0(266) = 266\,\text{kips}$$

$$\left|-119\right|\,\text{kips} < 266\,\text{kips} \qquad \text{ok}$$

2.2.3.4.4 Wind Loads

AASHTO LRFD Article 4.6.2.7.3 requires that the need for wind bracing to resist wind loads acting on the noncomposite structure prior to placing the concrete deck be investigated. Although the AASHTO design specifications are generally member or component based, in some cases it becomes necessary to consider the overall behavior of the entire bridge system. As will be demonstrated in the following example, for resisting wind loads during construction, the entire noncomposite bridge structure acts as a system. In certain cases, the addition of lateral bracing can help provide a stiffer load path for wind loads acting on the noncomposite structure to help reduce lateral deflections and lateral flange bending stresses. For checking stresses due to wind load during construction, the Strength III load combination is

used (dead load plus wind load with no live load on the structure -- see DM Volume 1, Chapter 5 for additional information on the Strength III load combination). According to *AASHTO LRFD* Article 3.4.2, the load factor applied to wind acting on the structure (WS) during construction is not to be taken less than 1.25, which is reduced from the load factor of 1.4 applied to WS in the base Strength III load combination. For checking deflections due to wind load during construction, all load factors are taken equal to 1.0 according to *AASHTO LRFD* Article 6.10.3.1.

EXAMPLE

Wind load acting on Span 1 of the following noncomposite structure prior to casting of the concrete deck will be investigated (see the framing plan shown in Figure 2.38). A rational approximate approach will be illustrated to help the Engineer evaluate how many panels of lateral wind bracing (if any) might be necessary to reduce the lateral deflections and lateral flange bending stresses due to the wind loads to a level deemed acceptable for the construction situation under consideration.
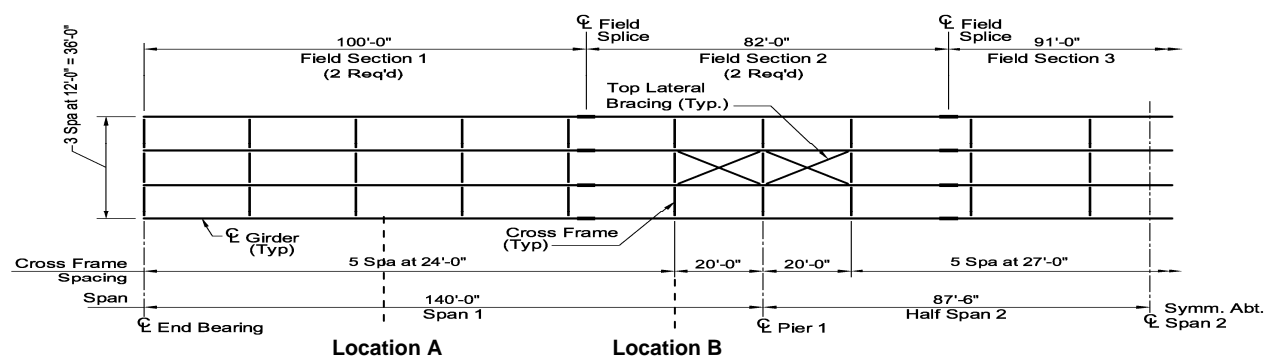

Figure 2.38 Framing Plan

The design horizontal wind pressure P_D used to compute the wind load acting on the structure WS is determined as specified in *AASHTO LRFD* Article 3.8.1. It will be assumed that the example bridge superstructure is 35 feet above the low ground and that it is located in open country.

In the absence of more precise data, the design horizontal wind pressure is to be determined as follows:

$$P_D = P_B \left(\frac{V_{DZ}}{V_B} \right)^2 = P_B \frac{V_{DZ}^2}{10,000}$$

AASHTO LRFD Equation 3.8.1.2.1-1

where:

P_B = base wind pressure = 0.050 ksf for beams (*AASHTO LRFD* Table 3.8.1.2.1-1)

V_{DZ} = design wind velocity at design elevation, Z (mph)

V_B = base wind velocity at 30 ft height = 100 mph

For bridges or parts of bridges more than 30 feet above low ground, V_{DZ} is to be adjusted as follows:

$$V_{DZ} = 2.5V_o\left(\frac{V_{30}}{V_B}\right)\ln\left(\frac{Z}{Z_o}\right)$$

AASHTO LRFD Equation 3.8.1.1-1

where:

V_o	=	friction velocity = 8.20 mph for open country (*AASHTO LRFD* Table 3.8.1.1-1)
V_{30}	=	wind velocity at 30 feet above low ground = V_B = 100 mph in the absence of better information
Z	=	height of the structure measured from low ground (> 30 feet)
Z_o	=	friction length of upstream fetch = 0.23 feet for open country (*AASHTO LRFD* Table 3.8.1.1-1)

Therefore,

$$V_{DZ} = 2.5(8.20)\left(\frac{100}{100}\right)\ln\left(\frac{35}{0.23}\right) = 103.0 \text{ mph}$$

$$P_D = 0.050\left[\frac{(103.0)^2}{10,000}\right] = 0.053 \text{ ksf}$$

The full design base wind velocity V_B = 100 mph is used in the above calculation for illustration purposes only. *For an actual temporary construction condition, however, strong consideration might be given to using a smaller design wind pressure depending on the specific situation and the anticipated maximum wind velocity at the site.*

P_D is to be assumed uniformly distributed on the area exposed to the wind. The exposed area is to be the sum of the area of all components as seen in elevation taken perpendicular to the assumed wind direction. The direction of the wind is to be varied to determine the extreme force effect in the structure or its components. As specified in *AASHTO LRFD* Article 3.8.1.2.1, the total wind load WS *acting on girder spans* is not to be taken less than 0.3 klf. Again, consideration might be given to waiving this requirement for the temporary construction condition. Conservatively using the smallest steel section in Span 1 (7/8" x 18" bottom flange; ½" x 69" web; 1" x 16" top flange), the total wind load per unit length *w* for the case of wind applied normal to the structure assuming no superelevation is computed as:

$$w = P_D h_{exp.} = 0.053[(0.875 + 69.0 + 1.0)/12] = 0.313 \text{ kips / ft} > 0.3 \text{ kips / ft} \quad \text{ok}$$

Determine the maximum major-axis bending stress f_{bu} in the top and bottom flanges due to the factored steel weight within the unbraced length encompassing Location A in Span 1 (refer to the first of the three preceding examples to determine Location A). The cross-section of the girder at this location (and within the entire 24-foot unbraced length encompassing this location) is shown in Figure 2.3. The elastic

section properties for this section were computed earlier. The girder is homogeneous with the yield strength of the flanges and web equal to 50 ksi. The largest moment due to the steel weight within the unbraced length is equal to 352 kip-feet right at Location A (Table 2.5). Therefore, since the member is assumed prismatic in-between these two cross-frames, the largest stress in both flanges also occurs at Location A. The Strength III load case applies to the case of dead plus wind load with no live load on the structure. The load modifier η is taken equal to 1.0 in this example. Therefore,

For Strength III:

Top flange:

$$f_{bu} = \frac{1.0(1.25)(352)(12)}{1,581} = -3.34 \text{ ksi}$$

Bot. flange:

$$f_{bu} = \frac{1.0(1.25)(352)(12)}{1,973} = 2.68 \text{ ksi}$$

Since there is no deck at this stage to provide horizontal diaphragm action, assume the cross-frames act as struts in distributing the total wind force on the structure to the flanges on all girders in the cross-section. The force is then assumed transmitted through lateral bending of the flanges to the ends of the span or to the closest point(s) of lateral wind bracing. Determine the total factored wind force on the structure assuming the wind is applied to the deepest steel section within Span 1 (i.e. the section over the interior pier -- 2" x 20" bottom flange; 9/16" x 69" web; 2" x 18" top flange -- Figure 2.6) and normal to the structure (with no superelevation). For the Strength III load combination, the load factor for wind during construction is not to be taken less than 1.25 (*AASHTO LRFD* Article 3.4.2).

$$W = \frac{1.0(1.25)(0.053)(2.0 + 69.0 + 2.0)}{12} = 0.403 \text{ kips / ft}$$

To illustrate the effect that a couple of panels of top lateral bracing can have in providing a stiffer load path for wind loads acting on the noncomposite structure during construction, assume the system of top lateral bracing shown in Figure 2.38; that is, top lateral bracing in the interior bays on each side of each interior-pier section. Bottom lateral bracing would serve a similar function, but unlike top bracing, would be subject to significant live-load forces in the finished structure that would have to be considered should the bracing be left in place. Again, it should be emphasized that this example is used only to demonstrate the suggested approximate procedure. It is unlikely that a 140-foot span would require lateral wind bracing under a reduced (and more reasonable) assumed design wind pressure during construction.

Assume that Span 1 of the structure (acting as a system) resists the lateral wind force as a propped cantilever, with an effective span length L_e of 120.0 feet. That is, the top lateral bracing is assumed to provide an effective line of fixity at the cross-

frame 20.0 feet from the pier for resisting the lateral force. Calculate the moment on the propped cantilever at Location A (Note: the following formula actually gives the moment at $0.375L_e$ = 45 feet from the abutment, but is used here to give a conservative approximation of the moment at Location A):

$$M_A = \frac{9}{128} WL_e^2 = \frac{9}{128}(0.403)(120.0)^2 = 408.0 \text{ kip} - \text{ft}$$

Calculate the moment on the propped cantilever at the assumed line of fixity (call it Location B -- 20.0 feet from the pier into Span 1):

$$M_B = \frac{1}{8} WL_e^2 = \frac{1}{8}(0.403)(120.0)^2 = 725.4 \text{ kip} - \text{ft}$$

The lateral wind moments are proportional to the square of the effective length L_e. Note that a refined 3D analysis of the example noncomposite structure subjected to the factored wind load yielded a total lateral moment in the top and bottom flanges of all four girders of 405 kip-ft at Location A and 659 kip-ft at Location B.

Proportion the total lateral moment to the top and bottom flanges at Location A according to the relative lateral stiffness of each flange (refer to Figure 2.3). Assume that the total flange lateral moment is then divided equally to each girder. The single bay of top bracing along with the line of cross frames adjacent to that bay (acting as an effective line of fixity) permits all the girders to work together as a system to resist the lateral wind force along the entire span.

Location A:

Top flange

$$I_\ell = \frac{1(16)^3}{12} = 341.3 \text{ in.}^4$$

Bottom flange

$$I_\ell = \frac{1.375(18)^3}{12} = 668.3 \text{ in.}^4$$

Top flange

$$M_\ell = \frac{408.0(341.3)}{(341.3 + 668.3)4} = 34.48 \text{ kip} - \text{ft}$$

Bottom flange

$$M_\ell = \frac{408.0(668.3)}{(341.3 + 668.3)4} = 67.52 \text{ kip} - \text{ft}$$

A similar computation can be made at Location B (however, this section is not checked for this condition in this example).

According to *AASHTO LRFD* Article 6.10.1.6, lateral bending stresses determined from a first-order analysis may be used in discretely braced compression flanges for which:

$$L_b \leq 1.2L_p \sqrt{\frac{C_b R_b}{f_{bu}/F_{yc}}}$$

AASHTO LRFD Equation 6.10.1.6-2

Again, f_{bu} is the largest value of the compressive stress due to the factored loads throughout the unbraced length in the flange under consideration, calculated without consideration of flange lateral bending. In this case, $f_{bu} = -3.34$ ksi. Earlier, it was determined that the moment gradient modifier C_b and the web load-shedding factor R_b within the unbraced length encompassing Location A are both equal to 1.0. The limiting unbraced length L_p was also determined earlier to be 7.83 feet. Therefore,

$$1.2(7.83)\sqrt{\frac{1.0(1.0)}{|-3.34|/50}} = 36.35 \text{ ft} > L_b = 24.0 \text{ ft}$$

Therefore, lateral bending stresses determined from a first-order analysis may be used. First- or second-order flange lateral bending stresses, as applicable, are limited to a maximum value of $0.6F_{yf}$ according to *AASHTO LRFD* Equation 6.10.1.6-1.

Location A:

Top flange:

$$f_\ell = \frac{34.48(12)}{1(16)^2/6} = 9.70 \text{ ksi} < 0.6F_{yf} = 30.0 \text{ ksi ok}$$

Bottom flange:

$$f_\ell = \frac{67.52(12)}{1.375(18)^2/6} = 10.91 \text{ ksi} < 0.6F_{yf} = 30.0 \text{ ksi ok}$$

Calculate the shear in the propped cantilever at Location B:

$$V_B = \frac{5}{8}WL_e = \frac{5}{8}(0.403)(120.0) = 30.23 \text{ kips}$$

Resolve the shear into a compressive force in the diagonal of the top bracing:

$$P = 30.23\left(\frac{\sqrt{(20.0)^2 + (12.0)^2}}{12.0}\right) = -58.76 \text{ kips}$$

In addition, the member carries a force due to the steel weight. Calculate the average stress in the top flange adjacent to the braced bay using the average

moment due to the factored steel weight along the 20-foot unbraced length adjacent to the pier section assumed applied to the larger section within this unbraced length (i.e. the interior-pier section; S_{tf} = 2,942 in^3). The unfactored major-axis bending moment due to the steel weight at the section 20 feet from the interior pier into Span 1 (i.e. at Location B) is –312 kip-ft. The unfactored major-axis bending moment due to the steel weight at the interior pier is –777 kip-ft. Therefore,

$$f_{tf_{avg.}} = \frac{1.0(1.25)(12)(-312 + -777)/2}{2,942} = 2.78 \text{ ksi}$$

Resolve this stress into the diagonal:

$$f_{diag.} = 2.78\left(\frac{20.0}{\sqrt{(20.0)^2 + (12.0)^2}}\right) = 2.38 \text{ ksi}$$

Assuming an area of 8.0 in.^{2} for the diagonal yields a compressive force due to the steel weight of –19.04 kips resulting in a total estimated compressive force of (-58.76) + (-19.04) = -77.80 kips. The diagonal must be designed to carry this force. Note that the refined 3D analysis, mentioned previously, yielded a total compressive force in the diagonal bracing member of approximately -67.0 kips.

Finally, estimate the maximum lateral deflection of Span 1 of the structure (i.e. the propped cantilever) due to the *unfactored* wind load using the total of the lateral moments of inertia of the top and bottom flanges of all four girders at Location A. For simplicity, this section is assumed to be an average section for the span (a weighted average section would likely yield greater accuracy):

$$\Delta_{\ell max.} = \frac{WL_e^4}{185EI} = \frac{(0.403/1.25)(120.0)^4(1,728)}{185(29,000)(341.3 + 668.3)4} = 5.3 \text{ in.}$$

Note that the refined 3D analysis yielded a maximum lateral deflection of approximately 5.6 inches in Span 1. If the top bracing were not present, L_e would increase to 140.0 feet and the estimated maximum lateral deflection calculated from the above equation would increase to 9.9 inches. Large lateral deflections may potentially result in damage to the bearings. Therefore, such an approach may be helpful to determine how many panels of top lateral bracing, if any, might be necessary to reduce the lateral deflection to a level deemed acceptable for the particular situation under consideration.

To analyze the center span for this condition, a similar approach can be taken using the actions of an assumed fixed-fixed beam rather than a propped cantilever.

2.2.3.5 Service Limit State Verifications

As specified in *AASHTO LRFD* Article 1.3.2.2, the service limit state is taken as restrictions on stress, deformation and crack width under regular service conditions.

As mentioned in the Commentary to this article, service limit state criteria are more experience-based and somewhat less scientifically oriented.

For steel structures, *AASHTO LRFD* Article 6.5.2 specifies that the provisions of *AASHTO LRFD* Article 2.5.2.6, dealing primarily with the control of elastic live-load deformations and the consideration of span-to-depth ratios, apply as applicable. For I-section flexural members in particular, the provisions of *AASHTO LRFD* Article 6.10.4.2 dealing with control of permanent deformations must also be checked. The intent of these provisions is to prevent objectionable permanent deformations due to localized yielding of the steel girder that would impair rideability under repeated severe traffic loadings. *AASHTO LRFD* Article 6.10.4 deals with the specific service limit state checks that are to be made for I-section flexural members, as discussed in more detail below.

A helpful flowchart detailing the design checks to be made at the service limit state (discussed below) is provided in Appendix C to Section 6 of the *AASHTO LRFD Specifications – AASHTO LRFD* Figure C6.4.2-1.

2.2.3.5.1 Elastic Deformations

AASHTO LRFD Article 6.10.4.1 deals with checks related to the control of elastic deformations in steel I-girder bridges under normal service conditions. Specifically, this article refers back to the applicable provisions of *AASHTO LRFD* Article 2.5.2.6 dealing with optional live-load deflection criteria and the criteria for span-to-depth ratios.

2.2.3.5.1.1 Span-to-Depth Ratios

To help control elastic deformations at the service limit state, the optional span-to-depth ratios suggested in *AASHTO LRFD* Article 2.5.2.6.3 should be considered to establish a reasonable minimum web depth for the design in the absence of specific depth restrictions (refer also to the previous Section 2.2.3.3.1 of this chapter on Web Depth).

The recommended minimum depths in *AASHTO LRFD* Article 2.5.2.6.3 are based on traditional maximum span-to-depth ratios. Span-to-depth ratios for highway bridges date back at least to 1908 when Milo S. Ketchum published "*The Design of Highway Bridges*"; the first such book of its kind (*42*). In this book, Ketchum presented "General Specifications for Steel Highway Bridges". Article 54, Depth Limits, from those Specifications indicated that the depth of steel beams preferably should not be less than one-twentieth of the span. This article went on to require that when that limit was not met, the beam must be designed to limit the deflections as if the limiting depth had been met. This stringent depth limit was most likely derived from earlier railroad bridge design provisions. Railroad loads tended to be heavier than highway loads. Further, most railroad bridges had no concrete deck and were not ballasted. The precise reasoning for the requirement is probably lost in antiquity. However, it is believed related to a desire to provide adequate stiffness.

Design stresses for the steel in 1908 were less than 20 ksi. Live loads were roughly equivalent to HS20. The deepest available rolled section at that time was the 21-inch

standard beam (wide-flange shapes had not yet been invented). Ketchum gives examples of multi-girder bridges using rolled shapes with spans up to 45 feet. Longer span girder bridges in that era were typically two-girder deck-type or through-type bridges with a floor system spanning between girders. The girders were built-up riveted I-sections. Frequently the girders were not composite with the deck and the two-girder bridges assigned more load to the girders than would occur in a multi-girder bridge.

In 1908, the specified minimum ultimate tensile strength of the steel was about 60 ksi and the minimum specified yield stress was about 30 ksi. Modern bridge steels are designed at twice the design stresses used in 1908. Hence, an efficiently proportioned girder today tends to provide less stiffness and be relatively shallower than would have been the case a century ago. Although Engineers were aware of composite action, they rarely took advantage of it in computation of strength or deflections.

In the First Edition of the AASHO Specifications for Bridges and Structures, 1931, the preferred maximum span-to-depth ratio of steel beams was set at 20. The provisions permitted shallower sections if deflections were limited to those that would have been computed if the girder were designed with a depth of Span/20. This limit was probably taken from Ketchum, although it was the same as the limit given in the AREA Specifications (for railroads) at that time. After about 1910, Universal Mill rolled shapes were available with depths of three feet. The maximum span-to-depth ratio of 20 limited the use of these shapes to spans of about 60 feet in simple-span bridges (most early steel bridges were simple-span bridges). In the Second Edition AASHO Specifications for Bridges and Structures, 1935, the span-to-depth ratio was relaxed from 20 to 25, presumably in recognition of the much deeper wide-flange shapes with much larger and more efficient flanges that had become available after about 1910. The AASHO Specifications required that If the steel beams were shallower than Span/25, they had to be designed such that the deflection would be the same as if they were designed for Span/25. Increasing the ratio to 25 increased the effective span of the available rolled shapes to about 75 feet. The change was not as dramatic as it appeared since the limit was generally applied to many beams rather than only two, and it was also generally applied to bridges with de facto composite decks. In the Third Edition AASHO Specification, dated 1941, a live load deflection limit of Span/800 was also introduced (see the next section of this chapter). The span-to-depth and live load deflection limits were relatively consistent with each other for the typical girder bridges constructed of the traditional steel grades. ASTM A 7 steel, having a specified minimum yield strength of 33.0 ksi, was the most commonly used steel for bridge design at that time, although the use of other grades was not forbidden. The Span/800 deflection limit obviously would have had a greater effect on the designs of that era had the design stresses been higher.

The advent of composite design eventually led to shallower girders being economical. Recognition of composite action in design implied a stiffer bridge. In earlier times, many bridges were built with decks not integral with the top flange so the depth limits were based on the assumption that no structural interaction existed between the deck and girders; composite design recognized this interaction when it existed. In the early 1950s, it became evident that composite wide flange beams with span-to-depth ratios greater than 25 could be economical. As a result, the preferred maximum span-to-depth ratio was relaxed to Span/30 for the steel beam, and left at Span/25 for the composite beam. As shown below, these preferred ratios remain to the present day.

The enabling use of digital computers for the analysis and design of bridges in the 1960s led to wider use of more economical continuous span steel-girder bridges. Continuous spans complicated the application of the relatively straightforward span-to-depth ratios. Questions arose with regard to the span length to be used in determining the limiting span-to-depth ratio and live load deflection. Since these were recommended (as opposed to specified) limits, the determination of the appropriate span length in each case was left up to the Owner and the Engineer. This resulted in a variety of approaches. A common approach was to liberally define the span length as the distance between points of permanent load contraflexure for determining the maximum span-to-depth ratio, and as the span between supports in determining the Span/800 live load deflection limit.

In the *AASHTO LRFD* Specifications, suggested minimum depths for steel I-girders in simple spans and in continuous spans are given in *AASHTO LRFD* Table 2.5.2.6.3-1 (Table 2.8 below). The suggested minimum depths are given as follows:

Table 2.8 Suggested Minimum Depths for Steel I-Girders in Simple and Continuous Spans

	Simple Spans	Continuous Spans
Overall Depth of Composite I-Beam	0.040L (L/25)	0.032L (L/32)
Depth of I-Beam Portion of Composite I-Beam	0.033L (L/30)	0.027L (L/37)

L is the span length between bearings. For simple spans, the suggested lower limit on the overall depth of the composite I-beam corresponds to Span/25 and the suggested lower limit on the I-beam portion of the composite I-beam corresponds to Span/30. For continuous spans, a built-in factor of 0.8 is included to reflect an effective span length based on an approximate distance within the span between points of permanent load contraflexure (note that as suggested previously in Section 2.2.3.3.1 of this chapter, an end depth-to-span ratio of 90 percent of the simple-span ratio might be considered in either case to better account for only one end of the span being restrained by continuity). Typically, the longest span length should be used to establish the girder depth. Although the limits are taken to apply to the overall depth of the girder, it is suggested that they be applied to the web depth for simplicity.

Note again that as mentioned previously in Section 2.2.3.3.1 of this chapter, in most cases, the optimum web depth (assuming no depth restrictions) will be greater than these suggested minimum depths based on the traditional span-to-depth ratios. Refer also to Section 2.2.3.3.1 for suggestions on how to apply these suggested minimum depths to variable web depth members.

2.2.3.5.1.2 Live Load Deflection

Limitation of live load deflection is a service limit state; such criteria are specified in *AASHTO LRFD* Article 2.5.2.6.2 and limit the computed elastic live-load vertical deflections. Although the criteria are optional, most states require their application.

The obvious reason for these provisions is to provide a level of stiffness. However, the reason(s) for a required stiffness is less clear.

Until the 1960s, bridges were designed to a working level; i.e., they were designed for a desired service level. Live load deflection has been a service design consideration from early times in the design of steel highway bridges in the U.S. Limits on live load deflection can be traced back to the railway specifications of the late 1800s, which gave limitations similar to those now given in the *AASHTO LRFD* Specifications (*43*). The requirement to limit deflection of a railroad bridge seems rather self-evident when one considers the rocking forces that could lead to catastrophe on a bridge that was too flexible. Large deflections could also lead to secondary stresses that might cause fatigue cracking that was not well understood in the early days of iron and steel bridges. As mentioned above, the first specified live load deflection limit for steel highway bridges in the U.S. was in the Third Edition *AASHO Specification,* 1941. The suggested limit of Span/800 under vehicular load, which remains in the specification today (*AASHTO LRFD* Article 2.5.2.6.2), is thought to have been recommended by the Bureau of Public Roads after studying several steel-beam bridges that were reportedly subjected to objectionable vibrations (*43*). This limit, in addition to the maximum span-to-depth ratio of 25 that was recommended at that time, was the first attempt to control service load deformations. This was only reasonable since the entire philosophy of working stress design was based on serviceability and not strength.

The advent of higher strength steels and concomitant increases in design stresses led to concern about the effect of live load deflection on economics. As early as the 1950s, ASCE began an investigation of the basis for these limits and found numerous shortcomings, including no clear basis for their use, and no evidence of structural damage that could be attributed to excessive deflections (*50*). Competition with prestressed concrete bridges in the 1960s led to further investigations as to the need for this serviceability limit. Field investigations at that time, again, showed no direct correlation.

Not only did the limitation remain, but In the early 1960s an additional limit was introduced; the live load deflection limit on steel bridges with both pedestrian and vehicular loads was set at Span/1000 as a result of isolated concerns related to human response. The criteria remained optional. One legend has it that this limit arose when a mother and wife of a political figure who was pushing her baby in a carriage across a bridge attributing her baby awakening to vibration of the bridge (*43*). This complaint prompted the state's governor to chastise the State Bridge Engineer. The issue of human comfort becomes a serviceability issue when people who might use a bridge find its motion objectionable. This is a departure from the other structural criteria provided in the Specification.

The complex issue of the human response of occupants of moving vehicles and of pedestrians to motion has been extensively studied. However, there still are no definitive guidelines on the tolerable limits of dynamic motion or static deflection to ensure creature comfort. Guidelines for limiting the natural frequency of bridges to provide tolerable motion are contained in the *Ontario Highway Bridge Design Code* (*51*), in which the deflection limits are tied to the first fundamental frequency of the

superstructure. These limits are provided in the form of graphs and are separated in conjunction with the anticipated pedestrian use. These provisions require that the designer compute the natural frequency of the composite bridge. Wright and Walker found a tenuous theoretical relationship between deflection and natural frequency (*52*). They observed that user comfort was an important factor. They reported that psychologists had found that humans think that vertical deflection they sense is about ten times the actual deflection. Wright and Walker postulated that human discomfort is due to acceleration, not deflection alone. They proposed a parameter, defined as the dynamic component of acceleration in the fundamental mode of vibration, be limited to 100 in^2/sec. The authors suggest that such acceleration is within the tolerable range experienced in building elevators contemporary with the writing of the paper (1960s). They further suggested that only bridges designed for pedestrian traffic or stationary vehicles be limited in motion by such a serviceability criterion. The issue of bridge vibrations and their relation to human response, along with the development of a reasonable means of controlling bridge vibrations to ensure adequate creature comfort, remains a complex and subjective issue in need of further study.

Other suggested live load deflection limits contained in *AASHTO LRFD* Article 2.5.2.6.2 include a limit of Span/300 for vehicular loads on cantilever arms, and a limit of Span/375 for combined vehicular and pedestrian loads on cantilever arms.

In checking all the deflection limits, the 'Span' is typically taken as the full span length of the girder. As mentioned previously, the limit on span-to-depth ratio for continuous spans was often determined by defining the span as the length between points of permanent load contraflexure. This led to shallower bridges with an increased flexibility when the limiting live load deflection was defined based on the actual span. Some states conservatively limited deflection by using the distance between points of permanent load contraflexure in computing the permissible deflection. Field tests have confirmed that decks of continuous composite girders in negative moment regions actually behave compositely. Tradition has assumed those regions to be non-composite. Use of the entire deck obviously reduces the computed deflections and brings them closer to actual with regard to the behavior of the deck.

The live load used to compute live load deflection has traditionally been the same as the design live load. This made sense for design based on service loads only. However, for strength-based design, a different and lighter load for service limit state checks is logical since the criteria are based on a different philosophy. In strength design, the capacity of the structure is challenged. Serviceability relates to the structure response to likely loads; these likely loads are reasonably less than the load used to check structural strength. However, even in service load design, live load application has often been different from application for design of the elements. For example, the 1941 AASHO Bridge Specifications permitted the Engineer to compute the moment in a stringer for deflection purposes by assuming that all of the lanes are loaded with the design load and that the resulting load is uniformly distributed equally to all stringers where adequate depth diaphragms or cross-frames exist. Some have since interpreted this provision to allow a reduction in load based on the multiple presence factor provision. The practice of loading all lanes appears

to be at odds, at least in some cases, with the provision in the 1935 Edition (Art. 3.2.11), which states: "In calculating stresses in structures which support cantilevered sidewalks, the sidewalk shall be considered as fully loaded on only one side of the structure if this condition produces maximum stress." This provision reveals an understanding that loading on the far side of a multi-stringer bridge unloads the near side; this understanding has been borne out in refined analyses. If one visualizes the entire cross-section rotating as a rigid body under each of the above load cases, as assumed in the development of the live-load distribution factor Equation 2.1 for exterior girders given in DM Volume 1, Chapter 2, it is apparent that the opposite side of the bridge rises when one side is loaded. Hence, from the time it was introduced, the assumption of uniform loading of girders for computation of deflection was known to be a very blunt instrument to simply require less stiffness.

With the adoption of Load Factor Design (LFD), many states increased live load to HS25 for strength. Some used the HS25 design live load to compute live load deflection; however, others departed from using the same live load for strength and service as discussed above and used the HS20 live load for checking deflection. The use of a 25-percent larger live load eliminated some of the economy possible with the lower factor applied to dead load in LFD. Since the same factors were not used for deflection, it was logical to keep the same traditional live load.

The combination of moving from 33- to 70-ksi yield-stress steel, along with the introduction of composite design, LFD and then LRFD, and the increase of the span-to-depth ratio for steel girders from 25 to 30 had a net effect of roughly increasing the permitted live load deflection by about threefold. Field experience of bridges built has provided scant evidence that the increased flexibility of steel bridges had led to any reduced functionality. Projection of this trend into the future would imply that the limit on live load deflection should be infinity. However, the First Tacoma Narrows Bridge and common sense intervene. It seems that some logical limit exists, but such a limit has proved elusive. It has also been shown that computation of live load deflection as specified in AASHO and AASHTO is not likely to predict the actual deflection. And so, as the live load deflection limit has become an increasingly critical factor in the design of steel bridges utilizing the higher-strength high performance steels (HPS), an additional investigation has recently been launched into the potential need for improved live load deflection criteria for steel bridges (*53*).

When applying the current live load deflection criteria, *AASHTO LRFD* Article 3.6.1.3.2 requires that the deflection be taken as the larger of the deflection resulting from: 1) the design truck alone (including the 33 percent dynamic load allowance), or 2) the design lane load in conjunction with 25 percent of the design truck (including the 33 percent dynamic load allowance). As specified in *AASHTO LRFD* Article 2.5.2.6.2, a load factor of 1.0 is applied according to the Service I load combination (see DM Volume 1, Chapter 5 for further information on the Service I load combination). This special loading is intended to produce deflections similar to those due to HS20. It was decided by the specification writers that it was unnecessary to check live load deflections for the heavier HL-93 design live load used for strength checks. The HL-93 design truck has the same weight as an HS20 truck. The HL-93 design lane load also has the same weight as that specified for HS20. The use of 25

percent of the design truck (0.25 * 72 kips = 18 kips) is similar to the HS20 single concentrated load of 18 kips used in combination with the HS20 lane load for determining bending moments and deflections in longer spans. Of course, the resulting deflections are less than those computed for HS25; hence, the *AASHTO LRFD* live load for deflection is more lenient in this case.

The provisions of *AASHTO LRFD* Article 2.5.2.6.2 for straight-girder bridges allow all integer 12-foot wide design lanes to be loaded with all girders assumed to deflect equally. This clause should only be applied when the longitudinal stiffness of the individual girders at all cross-sections is the same. Cases where the clause should not be applied include cases with skewed supports, different girder depths, or girders with different flange sizes. The assumption of equal live load deflection is not applicable to horizontally curved bridges. The *AASHTO LRFD* specifications are silent with regard to the application of this assumption to bridges with skewed supports. The live load deflection of individual girders is to be computed for curved girders (*AASHTO LRFD* Article 2.5.2.6.2) based on analysis of the superstructure as a structural system with live loads applied according the loading provisions of the Specifications.

There are other bridges where the equal deflection assumption is not rational. Loading of all lanes simultaneously of relatively wide bridges may not give a rational deflection. This is clearly the case if one visualizes the bridge cross-section rotating as a rigid body under load, much as assumed in the special analysis for determining the wheel-load distribution factor for exterior girders (see Equation 2.1 in DM Volume 1, Chapter 2).

An example can best demonstrate the fallacy of assuming equal deflection of girders in a wide bridge. Consider a 518-foot span made continuous by adjoining spans of slightly less length. The bridge has seven design lanes and seven girders in the cross-section. All girders have the same longitudinal stiffness and are connected with cross-frames and a composite concrete deck. The design live load is HS20; although not designed for HL-93 loading, as discussed above, the special *AASHTO LRFD* live load for live load deflection is intended to give deflections similar to HS20. The live load deflection limit is Span/800, where Span is the distance between bearings. In this case, the limit is 7.77 inches.

For this case, the live load distribution factor for deflection may be computed as follows by assuming all lanes are loaded and all girders are deflecting equally. *AASHTO LRFD* Article 2.5.2.6.3 specifies that the multiple presence factors *m* given in *AASHTO LRFD* Article 3.6.1.1.2 should be applied in calculating live load deflections. These factors are given in *AASHTO LRFD* Table 3.6.1.1.2-1 as follows: for one lane loaded, *m* = 1.2; for two lanes loaded, *m* = 1.0; for three lanes loaded, *m* = 0.85; for more than three lanes loaded, *m* = 0.65. Therefore:

$$(DF)_{LLdef} = m\left(\frac{N_L}{N_b}\right)$$ Equation 2.77

where:
    DF   =   distribution factor (lanes)

m = multiple presence factor specified in *AASHTO LRFD* Article 3.6.1.1.2

N_L = number of design lanes (roadway width/12 with fractions dismissed)

N_b = number of girders in the cross-section

$$(DF)_{LLdef} = 0.65\left(\frac{7}{7}\right) = 0.65 \text{ lanes}$$

Analysis of a single girder with this distribution factor gives a live load deflection of 6.8 inches, which is well below the deflection limit.

As shown below, a refined analysis of this bridge using the BSDI 3D System$_{SM}$ gives a live load deflection of 8.30 inches in one exterior girder (Girder 1) for four lanes loaded using an impact factor of 10 percent and a multiple presence factor of 0.65.

	Number of lanes loaded	Multiple presence factor	Live load deflection (in.)
	1	1.2	-5.70
	2	1.0	-8.18
	3	0.85	-7.26
	4	0.65	-8.30
Opposite side	2	1.0	1.30

Evidently, for this particular bridge, four lanes loaded results in the largest deflection (it should be noted that the center lanes were loaded two spans away from the span investigated to compute this deflection). When the multiple presence factors are considered, two lanes loaded gives almost the same live load deflection as does four lanes loaded in this case. Clearly, it does not appear reasonable to assume seven lanes loaded to calculate a live load deflection that meets the deflection limit, while the loading of only two lanes fails the same criteria. An argument can be made that deflection is only a relative issue and no hard rules are available as to the true deflection that should be permitted. However, it appears to be unreasonable to compute a smaller deflection on a bridge because it is wider than another bridge with the same span and girder spacing.

Also, as noted above, when the live load is restrained to the two lanes on the far (opposite) side of the deck in the area of the other exterior girder (i.e. Girder 7), the computed live load deflection in Girder 1 in an upward deflection of 1.3 inches (downward deflections are negative and upward deflections are positive in the above table). This deflection was the result of loading in the same span; loading in adjacent spans on the opposite side of the bridge was inconsequential. Thus, the addition of live load on the opposite side of the span of interest would actually unload Girder 1. This phenomenon is the reason that the 1935 AASHO Specification disallowed loading sidewalks on both sides in order to reduce the effect of a single sidewalk, as discussed previously.

Some State DOTs specify that the distribution factor used for moment is to be used to calculate live load deflections. When the distribution factor for moment is used, the lanes are implicitly located in the critical position. The width of the bridge and the
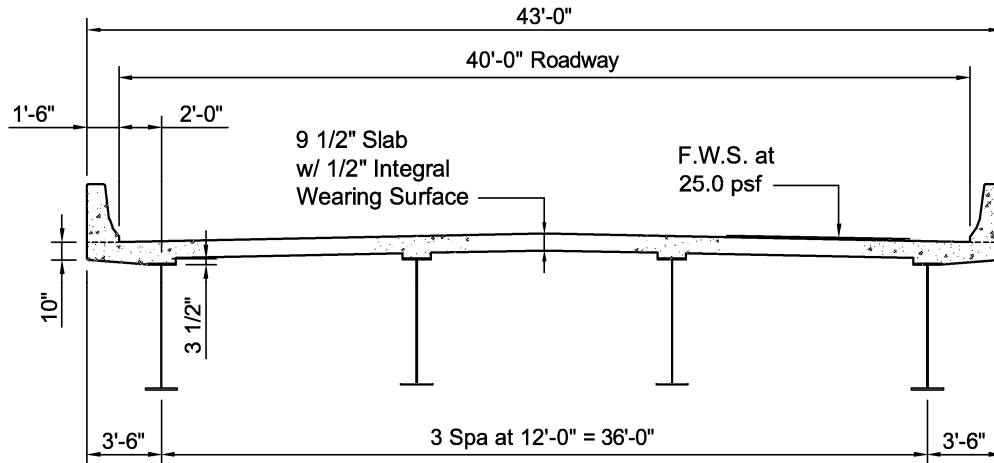
number of girders are less significant since the wheel load distribution factors are based on two lanes of traffic regardless of the bridge width. When a refined analysis is used or when the exterior girder is investigated, it is possible to place the live load in the striped lane(s) rather than in the critical transverse position. Such analyses would represent a more realistic service condition than the hypothetical situation that would be employed for a strength check.

AASHTO LRFD Article 4.6.2.6 on effective flange width states that the calculation of deflections should be based on the full flange width rather than the computed effective flange width. Again, as explained above, the assumption of the full deck width, as provided in *AASHTO LRFD* Article 6.10.1.5 for determining the composite cross-section stiffness for the analysis, gives more functionally correct results. For analysis of straight-girder bridges, the stiffness of an individual girder can be determined by dividing the stiffness of the entire bridge cross section by the number of girders.

Concrete barriers and sidewalks, and even railings, often contribute to the stiffness of composite superstructures at service load levels. Therefore, *AASHTO LRFD* Article 2.5.2.6.2 permits the entire width of the roadway and the *structurally continuous* portions of railings, sidewalks and barriers (i.e. continuous cast-in-place barriers) to be included in determining the composite stiffness for deflection calculations. Because the inclusion of the concrete items other than the deck can cause complications in the calculation of the composite stiffness (and in modeling with regard to their inclusion in refined analyses), it is suggested that these items be ignored. If the parapets are on the exterior of the deck, they tend to stiffen the exterior girders drawing load to those girders. Hence, computation of the deflections of the critical exterior based on refined analysis methods show that the computed deflections are not materially reduced by the consideration of the parapets.

EXAMPLE

Determine the distribution factor for live load deflection for the following cross-section of a straight steel I-girder bridge with equal stiffness girders based on the permitted assumption that all design lanes are loaded and that all girders are assumed to deflect equally:

The 40-ft wide roadway can support up to three 12-foot-wide design traffic lanes. For three traffic lanes, the multiple presence factor *m* is equal to 0.85. Therefore, from Equation 2.77:

$$(DF)_{LLdef} = m\left(\frac{N_L}{N_b}\right) = 0.85\left(\frac{3}{4}\right) = 0.638 \text{ lanes}$$

The bridge is a three-span continuous composite bridge with spans of 140 ft – 175 ft – 140 ft. The web depth of the girders is 69 in. Using this distribution factor, a separate line-girder analysis is performed for the two separate live load conditions to be used to calculate live load deflections according to *AASHTO LRFD* Article 3.6.1.3.2. The maximum live-load deflections in the end span and center span of the exterior girder due to the design truck plus the dynamic load allowance are computed to be:

(Δ_{LL+IM}) end span $\quad = \quad$ 0.91 in. (governs)
(Δ_{LL+IM}) center span $\quad = \quad$ 1.23 in. (governs)

The maximum live-load deflections in the end span and center span of the exterior girder due to the design lane load plus 25 percent of the design truck plus the dynamic load allowance are computed to be:

(Δ_{LL+IM}) end span $\quad = \quad$ 0.60 + 0.25(0.91) = 0.83 in.
(Δ_{LL+IM}) center span $\quad = \quad$ 0.85 + 0.25(1.23) = 1.16 in.

The dynamic load allowance of 33 percent was applied to the design truck in each case. A load factor of 1.0 was applied to the live load. The actual *n*-composite moments of inertia along the entire length of the girder were used in the analysis. The stiffness of the barriers was not included in the composite stiffness. However, the full width of the concrete deck associated with the exterior girder (versus the effective flange width) was used in determining the composite stiffness, as recommended in *AASHTO LRFD* Article 4.6.2.6 for the calculation of live-load

deflections. Check the suggested limit of Span/800 given in *AASHTO LRFD* Article 2.5.2.6.2:

$$\text{End Spans:} \qquad \Delta_{\text{ALLOW}} = \frac{140.0(12)}{800} = 2.10 \text{ in.} > 0.91 \text{ in.}$$

$$\text{Center Span:} \quad \Delta_{\text{ALLOW}} = \frac{175.0(12)}{800} = 2.63 \text{ in.} > 1.23 \text{ in.}$$

Application of the live load deflection provisions shown above results in deflection not being critical; that is, other limit states controlled the design. Infringement on the recommended girder depth might be possible in this case, while still meeting the live load deflection provisions. Of course, larger flanges would likely be required to meet the strength or perhaps the fatigue limit states.

Separate calculations indicate that the live load distribution factor for bending moment in the exterior girder of this example bridge (to be used for live load stress calculations) is 0.950 lanes, or approximately 1.5 times larger than the factor computed above. If this factor were used instead, the computed live load deflection in the center span would be 1.83 in. versus 1.23 in. If the live load deflection were computed based on the traditional live load distribution factor of *S*/11 used to compute live load bending stresses according to the Standard Specifications (i.e. *S*/5.5 converted to lanes), the live load deflection would be 2.10 in. The deflection limit would still be satisfied in both cases for this particular bridge.

It is probably well accepted that live load deflection cannot be accurately predicted using the assumption of uniform deflection of all girders due to all girders loaded (i.e. using the distribution factor given by Equation 2.77). The argument might be made that the actual live load deflection is not important; it is the relative deflection that is important. The assumption of uniform deflection yields widely varying accuracies depending on the particular bridge cross-section, and can potentially lead to significant design errors in certain situations. Generally, it is not prudent to add steel girders to a cross-section to reduce live load deflection. When this is done, the actually live load deflection may not be affected much, but the bridge cost is substantially increased. It is usually preferred to increase the stiffness of the girders while optimizing the number of girders for an economical cross section without consideration of live load deflection.

To investigate this issue further, a straight simple-span I-girder bridge with right supports having a span of 161 feet is investigated. Live load deflections computed from a refined analysis, such as would be used to calculate the deflections in a curved-girder bridge, are compared to the deflections computed for the same bridge from a line girder analysis utilizing the distribution factor given by Equation 2.77. The width of the bridge deck is 60.5 feet out-to-out; the roadway is 57.5 feet; the overhangs are 4.25 feet. Four 12-foot design traffic lanes can be placed on this roadway. Five-girder and seven-girder cross sections are examined. The overhang is held constant for both cross sections. The girder spacing for the 5-girder case is 13'-0". The girder spacing for the 7-girder case is 8'-8".

The girders are sized for the strength limit state based on *AASHTO LRFD* design criteria and the results of refined 3D finite element analyses using the BSDI 3D System.   The design live load is HL-93. These analyses show the exterior girder is critical with respect to both strength and live load deflection.   Therefore, only an exterior girder is sized; interior girders are assumed to be the same size. The bridge designs are then analyzed for HS25 live load with the 3D System. The girder sizes were checked and found, coincidentally, to meet the Load Factor Design (LFD) requirements given in the *AASHTO* Standard Specifications with almost precisely the same efficiency ratios. Hence, LRFD and LFD happen to give the same girder size based on strength for these particular cases. The LRFD live load factor is 1.75; the equivalent factor for LFD is 2.17 or 24 percent greater. This means that the HL-93 live load moment is roughly 24 percent larger than the HS25 moment in these cases.

The 5-girder homogeneous 50-ksi case consists of five 69-inch deep I-girders. The 7-girder homogeneous 50-ksi case consists of seven 69-inch deep I-girders. This depth gives a span-to-depth ratio of 28; thus, the girders are slightly deeper than the suggested span-to-depth ratio of 30, or depth-to-span ratio of 0.033 as given in *AASHTO LRFD* Article 2.5.2.6.3. A further comparison was made with similar deck cross-sections and hybrid girders having 70 ksi bottom flanges and 50 ksi webs and top flanges; the girder depths were decreased to 64 inches, which is the minimum depth that meets the optional span-to-depth ratio of 30.

As indicated previously, in the *AASHTO LRFD* Specifications, a special loading is used for the calculation of live load deflections, which is a lighter load than the HL-93 design live load. Either the design lane load in combination with one-fourth of the design truck or the design truck alone – whichever gives the greater deflection – is used.   Impact of 33% is applied only to the truck.   In the *AASHTO* Standard Specifications, the same live load is used for strength and live load deflection. For HS25, live load deflection is the larger of the deflection due to the lane load or the HS25 truck by itself.   Impact is computed by the traditional equation, 50/(125 + Span). Since live load deflection is a service criterion, the load factor applied to the live load in both specifications is 1.0.   The suggested live load deflection limit of Span/800 is 2.4 inches according to both specifications.

As discussed previously, the *AASHTO LRFD* specifications permit the application of the multiple presence factors (MPF) prescribed in *AASHTO LRFD* Article 3.6.1.1.2 in computing live load deflections. These factors also exist in the *AASHTO* Standard Specifications, although the values differ somewhat.   The MPFs in both specifications are summarized below.

No. of Lanes	*AASHTO LRFD* Specifications	*AASHTO* Standard Specifications
1	1.2	1.0
2	1.0	1.0
3	0.85	0.90
4	0.65	0.75

Therefore, according to the *AASHTO LRFD* Specification, for the 5-girder case, the lane load distribution factor (DF) for live load deflection is computed from Equation 2.77 as follows:

DF = 0.65 x (4 lanes/5 girders) = 0.52 lanes per girder

The similar computation for the 7-girder case is as follows:

DF = 0.65 x (4 lanes/7 girders) = 0.37 lanes per girder

According to the *AASHTO* Standard Specification, DF is computed as follows for the 5-girder case:

DF = 0.75 x (4 lanes/5 girders) = 0.60 lanes per girder

The similar computation for the 7-girder case is as follows:

DF = 0.75 x (4 lanes/7 girders) = 0.43 lanes per girder

The assumption of uniform participation indicates that an increase in the number of girders reduces significantly the live load deflection. If the computed deflection exceeds the suggested allowable deflection, additional girders are often added. In this example, the increase from 5 to 7 girders reduces the LRFD DF by:

[(0.52 – 0.37)/0.52] x 100% = 29 %.

Although live load deflection limits are subjective, addition of girders lines is not; it adds significantly to the cost of the bridge. The addition of two girder lines reduces the girder spacing and hence reduces the required size of each girder based on the strength limit state.

The computed maximum live load deflections from the analyses described above are summarized below. All deflections are in units of inches.

No. girders	Live load	All 50 ksi		Hybrid	
		3D	Line Girder	3D	Line Girder
5	Special LRFD	1.46	0.815	2.01	1.16
7	Special LRFD	1.47	0.758	1.97	1.04
5	HS25	2.02	1.22	2.81	1.74
7	HS25	2.02	1.15	2.73	1.58

The reported live load deflections for the refined 3D analysis are the maximum of the computed deflections for one, two, three and four lanes loaded including impact and multiplied by the appropriate MPF. The line girder columns give the live load deflections computed by assuming all lanes (4 lanes) are loaded and uniform participation of all girders. The appropriate MPFs are again applied for each case.

The 3D column under 'Hybrid' shows that the 5- and 7-girder hybrid sections are over deflected for HS25, while the maximum live load deflection for the special LRFD deflection loading meets the Span/800 limit for the hybrid cases.

Note in particular that the addition of two girder lines had no benefit whatsoever on the accurately computed live load deflections from the refined 3D analysis.

A comparison of the girder weights for the four cases given in the table is instructive.

Design	Girder Weight (lbs)	Total Weight (lbs)	Weight (psf)	Weight Efficiency Ratio
5-girder Hybrid	58,150	290,750	29.8	1.00
5-girder All 50 ksi	66,402	332,010	34.1	1.14
7-girder Hybrid	46,939	328,573	33.7	1.13
7-girder All 50 ksi	54,467	381,269	39.1	1.31

The girder weight does not reflect the additional two bays of cross frames, four additional bearings, additional erection and deck forming costs associated with the 7-girder options. Note that these additional costs did not provide any measurable reduction in actual live load deflections.

It is also instructive to examine the composite moments of inertia of the individual girders and of the total cross-sections. The table below gives the moment of inertia for a single girder and for the sum of the girders in each cross-section.

No. Girders MOI (in^4)	All 50 ksi	Hybrid
	69" Web	64" Web
5 Total MOI	303,303 in^4/gir 1,516,515 in^4	217,104 in^4/gir 1,085,520 in^4
7 Total MOI	219,532 in^4/gir 1,536,724 in^4	176,824 in^4/gir 1,237,768 in^4
% Increase in total stiffness	1.3	3.9

The 5-girder all 50-ksi cross-section girder has 38% greater stiffness than the comparable girder in the 7-girder cross-section. A similar comparison for the hybrid designs shows a 23% greater stiffness. The larger girder spacing for the 5-girder cross section results in more load to the exterior girder. However, the larger load is resisted by the greater stiffness resulting in nearly identical live load deflections for the 5- and 7-girder cross-sections under the same live loads.

The concept of uniform deflection may be examined by comparing the total stiffness of the composite cross-sections. The 5-girder cross-section in the all 50-ksi case is 99% as stiff as the comparable 7-girder cross-section. The 5-girder cross-section in the hybrid case is 88% as stiff as the comparable 7-girder cross-section.

As anticipated, the live load deflections computed from the refined 3D analysis are directly related to the inverse of the moment of inertia for all cases. For example, the ratio of the girder moments of inertia for the 5-girder all 50-ksi design to the 5-girder hybrid design (303,303/217,104 = 1.40) is inversely proportional to the ratio of the corresponding maximum live load deflections (2.01/1.46 = 1.38).

Although each case is different, the essence of this study probably remains true for all cases. It is incorrect to add girders to reduce the live load deflection of a multi-girder steel bridge. One might argue that the girder spacing could have been increased beneficially in the 7-girder case. That is true, but so could it have been increased in the 5-girder case.

This is not to say that flexibility should not be controlled. Wherever possible, it is best to meet or preferably exceed the minimum girder depths recommended in the specifications. Of course, there are situations such as curved girder bridges and bridges with differing girder stiffnesses where the uniform deflection assumption is not permitted. In these cases, specific loading is required for computation of live load deflections. It would likely be more consistent to consider the same assumption for all bridges.

2.2.3.5.1.3 Dead Load Deflection

All versions of the AASHTO Specifications, including the *AASHTO LRFD* Specification, are essentially silent regarding dead load deflections (as mentioned previously, *AASHTO LRFD* Article 6.7.2 does state that vertical camber be provided to account for the dead load deflections). Prior to composite design, the steel bridge girder was designed to support both dead and live load. With the advent of composite design, much of the dead load is applied on the non-composite structure while the live load is applied to the composite one. This has led to the reduction of the recommended depth of the steel section from $1/25^{th}$ of the span to $1/30^{th}$ of the span. This combined with higher strength steels and a smaller factor applied to dead load for design has, in many cases, results in very slender steel sections. Although there are no provisions for limiting of dead load deflection, the Engineer is wise to consider vertical deflection of the steel and its potential effects during the various stages of construction of the bridge.

2.2.3.5.2 Permanent Deformations

AASHTO LRFD Article 6.10.4.2 deals with checks related to the control of permanent deformations in steel I-girder bridges under repeated severe traffic loadings. Control of permanent deformations is important to ensure good riding quality.

To control permanent deformations according to *AASHTO LRFD* Article 6.10.4.2, checks are to be made on the flange stresses and for potential web bend buckling under the Service II load combination (see DM Volume 1, Chapter 5 for additional information on the Service II load combination). The standard design Service II loading is defined as 1.0*DC* + 1.0*DW* + 1.3(*LL+IM*), where *DC* represents the component dead loads, *DW* represents the wearing surface and utility loads and (*LL+IM*) represents the design live load plus the dynamic load allowance placed in multiple lanes. As will be discussed later on in the chapter, checks are also to be made to prevent slip in slip-critical bolted connections under the Service II loading.

The Service II load combination is intended to be equivalent to the Overload given in the *AASHTO Standard Specifications*. In the *AASHTO Standard Specifications*, the Overload is intended to represent live loads that can be allowed on the structure on infrequent occasions without causing permanent damage. The standard design Overload (i.e. for loadings of H20 or above) is defined as *D* + 5/3(*L+I*), where *D* represents the dead load and (*L+I*) represents the design live load plus impact placed in multiple lanes. Although the live load is to be placed in multiple lanes for design purposes, it can be shown that the live load factor of 5/3 essentially makes the loading equivalent to two times the design live load placed in a single lane (*54*). In both the *AASHTO LRFD Specifications* and the *Standard Specifications*, when these checks are to be applied to a design permit load, consideration should be given to reducing the load factor on the live load from 1.3 and 5/3, respectively, to 1.0 since the load is known.

As discussed previously, under certain conditions, *AASHTO LRFD* Article 6.10.4.2.1 permits flexural stresses caused by Service II loads applied to the composite section to be computed assuming the concrete deck is effective for both positive and negative flexure for the permanent deflection design checks. As specified in *AASHTO LRFD* Article 6.10.1.7, those conditions are that shear connectors must be provided along the entire length of the girder and that the minimum one percent longitudinal deck reinforcement must be placed wherever the tensile stress in the concrete deck due to either load combination Service II or due to the factored construction loads exceeds the factored modulus of rupture of the concrete. Under these conditions, the crack size is felt to be controlled to a degree such that the concrete deck may be considered effective in tension for computing the flexural stresses acting on the composite section at the service limit state. *When the above conditions are satisfied, the Engineer is strongly encouraged to consider the concrete deck to be fully effective in calculating all Service II flexural stresses, as this assumption better reflects the actual conditions in the bridge.*

EXAMPLE

AASHTO LRFD Article 6.10.1.7 requires that the minimum one percent longitudinal deck reinforcement be placed wherever the tensile stress in the concrete deck due to the factored construction loads and due to the Service II loads exceeds ϕf_r, where ϕ equals the resistance factor for reinforced concrete in tension equal to 0.90 (*AASHTO LRFD* Article 5.5.4.2.1) and f_r is the modulus of rupture of the concrete (*AASHTO LRFD* Article 5.4.2.6). For the three-span continuous I-girder bridge shown in the preceding example, an earlier example (in Section 2.2.3.4.1 under

Constructibility Verifications) showed that the longitudinal reinforcement in the 140-ft end span must extend from the interior-pier section to a section approximately 95.0 feet from the abutment in order to satisfy this requirement under the factored construction loads. The factored modulus of rupture was computed to be $\phi f_r = 0.432$ ksi in that particular example. Check the tensile stress in the deck to the Service II load combination at the section 95.0 feet from the abutment in the end span. The Service II moments are this section are as follows:

M_{DC2} = +87.0 kip-ft
M_{DW} = +83.0 kip-ft
M_{LL+IM} = -1,701 kip-ft

Note that only the DC2, DW and LL+IM loads are assumed to cause stress in the concrete deck. As discussed earlier, stresses in the concrete deck are determined as specified in *AASHTO LRFD* Article 6.10.1.1.1d. The short-term modular ratio *n* = 8. The short-term composite moment of inertia at this section is I = 161,518 in.^{4} The distance from the short-term composite elastic neutral axis to the top of the deck is 23.20 in.

$$f_{deck} = \frac{1.0[1.0(87) + 1.0(83) + 1.3(-1,701)](23.20)(12)}{161,518(8)} = 0.440 \text{ ksi} > 0.90 f_r = 0.432 \text{ ksi}$$

Therefore, extend the longitudinal reinforcement one foot further to a section 94.0 feet from the abutment. Using the moments at that section:

$$f_{deck} = \frac{1.0[1.0(98) + 1.0(94) + 1.3(-1,683)](23.20)(12)}{161,518(8)} = 0.430 \text{ ksi} < 0.432 \text{ ksi} \quad \text{ok}$$

The Engineer should ensure that the longitudinal reinforcement is adequately developed at this point.

2.2.3.5.2.1 Flange Stress Check

As specified in *AASHTO LRFD* Article 6.10.4.2.2, flange stresses due to the Service II loads are limited as follows to control permanent deflections in the steel girder at the service limit state:

➢ For the top steel flange of composite sections:

$$f_f \leq 0.95 R_h F_{yf}$$ Equation 2.78

AASHTO LRFD Equation 6.10.4.2.2-1

➢ For the bottom steel flange of composite sections:

$$f_f + \frac{f_\ell}{2} \leq 0.95 R_h F_{yf}$$ Equation 2.79

AASHTO LRFD Equation 6.10.4.2.2-2

➢ For both steel flanges of noncomposite sections:

$$f_f + \frac{f_\ell}{2} \le 0.80 R_h F_{yf}$$

Equation 2.80

AASHTO LRFD Equation 6.10.4.2.2-3

where:

f_f = flange stress at the section under consideration due to the Service II loads calculated without consideration of flange lateral bending (ksi). f_f is always taken as positive in these equations.

f_ℓ = flange lateral bending stress at the section under consideration due to the Service II loads (ksi). f_ℓ is always as positive in these equations.

R_h = hybrid factor determined as specified in *AASHTO LRFD* Article 6.10.1.10.1 (Equation 2.21)

Recall that continuous members in which noncomposite sections are utilized in negative flexure regions only should still be considered composite girders. Therefore, Equations 2.78 and 2.79 preferably should be applied in these regions, as applicable.

The base stress limits of $0.95F_{yf}$ for composite sections and $0.80F_{yf}$ for noncomposite sections have been retained from the *AASHTO Standard Specifications.* As discussed in References 53 and 54, these limits arose from bridge experiments conducted as part of the AASHO Road Test at Ottawa, Illinois in the early 1960s (*56*). The six steel bridges in the Road Test were subjected to more than 390,000 vehicle passages, which is roughly equivalent to 20 overload crossings every day for more than 50 years. Two of the bridges were composite and four were noncomposite. Each bridge had a span of 50 feet. The total accumulated permanent sets measured at the end of the test traffic are plotted in Figure 2.39. The differences in the magnitudes of the measured permanent sets in the composite and noncomposite bridges are evident in the figure. At stresses approaching 90 percent of F_{yf}, the permanent set was relatively low in composite bridge 2B compared to the permanent set in noncomposite bridge 3A. On the basis of this data, the limits were set as shown. Note that at these two limiting conditions, the measured permanent sets were of comparable magnitude.
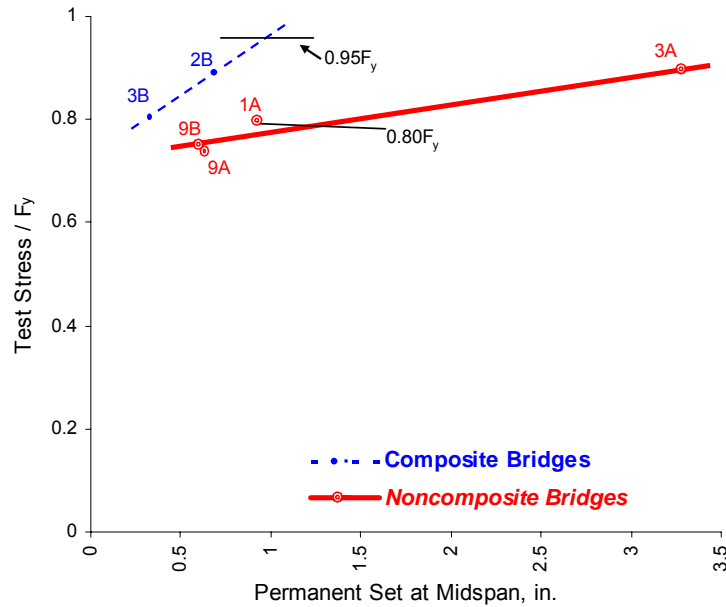
Figure 2.39 Permanent Set of AASHO Road Test Bridges

In the *AASHTO LRFD Specifications*, the hybrid factor R_h has been conservatively added to the stress limits to account for the increase in flange stress caused by early web yielding in hybrid sections. Note that a resistance factor ϕ is not included because the check is considered to be a serviceability check for which the resistance factor is always implicitly taken equal to 1.0.

The *AASHTO LRFD Specifications* have added a lateral flange bending term f_ℓ to the check. This term is not included in the check for the top flange of composite sections because the top flange in this case is continuously braced by the concrete deck. Therefore, the flange lateral bending stresses are small and can be neglected. *AASHTO LRFD* Article C6.10.4.2.2 indicates that for continuously braced top flanges of noncomposite sections, the f_ℓ term may also be neglected. In many cases, the f_ℓ term in the bottom flange can also be taken equal to zero. At the service limit state, lateral bending in the bottom flange is only a consideration for all horizontally curved I-girder bridges and for straight I-girder bridges with discontinuous cross-frame/diaphragm lines in conjunction with skews exceeding 20 degrees. Further discussion on lateral flange bending in skewed bridges may be found in Section 2.2.3.8 of this chapter. Other significant sources of lateral flange bending, such as concrete deck overhang loads and wind loads, are not a consideration at the service limit state. A factor of ½ is conservatively included in front of the f_ℓ term. When this factor is included, the equations approximate more rigorous yield interaction equations corresponding to a load at the onset of yielding at the web-flange juncture under combined major-axis and lateral bending (*57*). The effect of any minor yielding that occurs at the flange tips prior to this stage is comprehended. By controlling the yielding in this fashion under the combined effects of major-axis and lateral bending (with the lateral flange bending stresses not exceeding the

permissible upper limit of $0.6F_{yf}$ given in *AASHTO LRFD* Article 6.10.1.6), the resulting permanent deflections will be small. According to *AASHTO LRFD* Article 6.10.1.6, amplification of the first-order flange lateral bending stresses may be required in discretely braced compression flanges. Amplification of tension-flange lateral bending stresses is not required. Amplification of these stresses is discussed in more detail in Section 2.2.3.1.2.2 of this chapter under Fundamental Concepts.

AASHTO LRFD Article C6.10.4.2.2 lists sections for which Equations 2.78 through 2.80 do not control the design under the load combinations specified in *AASHTO LRFD* Table 3.4.1-1 and need not be checked. These sections include:

1) composite sections in negative flexure for which the main provisions of *AASHTO LRFD* Article 6.10.8 (assuming slender-web behavior) are applied to determine the nominal flexural resistance at the strength limit state,

2) noncomposite sections with f_ℓ equal to zero for which the main provisions of *AASHTO LRFD* Article 6.10.8 (assuming slender-web behavior) are applied to determine the nominal flexural resistance at the strength limit state, and

3) noncompact composite sections in positive flexure.

On the other hand, as mentioned previously in Section 2.2.3.2.4 of this chapter under Tips on Flange Sizing, Equation 2.79 (or else the fatigue limit state verifications discussed below) will often control the size of the bottom flange for compact composite sections in regions of positive flexure.

AASHTO LRFD Article 6.10.4.2.2 permits moment redistribution at the service limit state for continuous-span members in straight I-girder bridges that satisfy specific limitations spelled out in *AASHTO LRFD* Article B6.2 (in Appendix B to *AASHTO LRFD* Section 6). These limitations are discussed in more detail in Section 2.2.3.11 of this chapter under Moment Redistribution. Localized yielding at the service limit state at interior-pier sections results in redistribution of elastic moments to more lightly loaded sections in positive flexure. When the limitations of *AASHTO LRFD* Article B6.2 are satisfied, the procedures in *AASHTO LRFD* Appendix B may optionally be used to calculate the redistribution moments, which are in effect permanent moments that remain in the structure and cause the member to shakedown or behave elastically under subsequent passages of overload vehicles. As a result, should the redistribution moments be calculated according to these procedures, Equations 2.78 through 2.80, as applicable, need not be checked within the regions extending from the pier section from which moments were redistributed to the nearest flange transition or point of permanent-load contraflexure, whichever is closest, in each adjacent span. Outside of these regions, the applicable equations must still be satisfied after redistribution.   Again, more details on the procedures given in Appendix B are presented below in Section 2.2.3.11 under Moment Redistribution.

One final requirement in *AASHTO LRFD* Article 6.10.4.2.2 relates to the rare case of compact composite sections in positive flexure utilized in shored construction. In this case, longitudinal compressive stresses in the concrete deck due to the Service II loads are limited to $0.6f'_c$ to ensure linear behavior of the concrete. As discussed in

AASHTO LRFD Article C6.10.1.1.1a, the use of shored construction is not recommended (see also Section 2.2.1.2 of this chapter).

EXAMPLE

Check the flange stresses due to the Service II loads in the composite section shown in Figure 2.3. The load modifier η is specified to always equal 1.0 at the service limit state (*AASHTO LRFD* Article 1.3.2). Assume unshored construction. The section is located in a region of positive flexure. Use the section properties computed earlier for this section. Since the girder is homogeneous, R_h is equal to 1.0. The girder is straight and the supports are not skewed; therefore, f_ℓ in the bottom flange is equal to zero. Assume the following unfactored bending moments:

$$
\begin{aligned}
M_{DC1} &= &+2{,}202 \text{ kip-ft} \\
M_{DC2} &= &+335 \text{ kip-ft} \\
M_{DW} &= &+322 \text{ kip-ft} \\
M_{LL+IM} &= &+3{,}510 \text{ kip-ft}
\end{aligned}
$$

$$0.95 R_h F_{yf} = 0.95(1.0)(50) = 47.50 \text{ ksi}$$

Top flange:
$$f_f \le 0.95 R_h F_{yf}$$

AASHTO LRFD Equation 6.10.4.2.2-1

$$f_f = 1.0\left[\frac{1.0(2{,}202)}{1{,}581} + \frac{1.0(335 + 322)}{4{,}863} + \frac{1.3(3{,}510)}{13{,}805}\right]12 = -22.30 \text{ ksi}$$

$$\left|-22.30\right| \text{ ksi} < 47.50 \text{ ksi} \qquad \text{ok}$$

Bot. flange:
$$f_f + \frac{f_\ell}{2} \le 0.95 R_h F_{yf}$$

AASHTO LRFD Equation 6.10.4.2.2-2

$$f_f = 1.0\left[\frac{1.0(2{,}202)}{1{,}973} + \frac{1.0(335 + 322)}{2{,}483} + \frac{1.3(3{,}510)}{2{,}706}\right]12 = 36.80 \text{ ksi}$$

$$36.80 \text{ ksi} + 0 < 47.50 \text{ ksi} \qquad \text{ok}$$

EXAMPLE

Check the flange stresses due to the Service II loads in the composite section shown in Figure 2.6, which is in a region of negative flexure. The flanges are Grade HPS 70W steel and the web is Grade 50W steel. Assume unshored construction and that the appropriate conditions specified in *AASHTO LRFD* Article 6.10.4.2.1 are met such that the concrete deck can be considered effective in negative flexure at the

service limit state. The hybrid factor R_h for this section at the service limit state based on this assumption was computed earlier to be 0.977 (see the earlier section of this chapter on the Hybrid Factor). Use the section properties computed earlier for this section. Again, the girder is straight and the supports are not skewed; therefore, f_ℓ in the bottom flange is equal to zero. Assume the following unfactored bending moments:

$$
\begin{aligned}
M_{DC1} &= \quad -4{,}840 \text{ kip-ft} \\
M_{DC2} &= \quad -690 \text{ kip-ft} \\
M_{DW} &= \quad -664 \text{ kip-ft} \\
M_{LL+IM} &= \quad -4{,}040 \text{ kip-ft}
\end{aligned}
$$

$$0.95 R_h F_{yf} = 0.95(0.977)(70) = 64.97 \text{ ksi}$$

Top flange:

$$f_f \le 0.95 R_h F_{yf}$$

AASHTO LRFD Equation 6.10.4.2.2-1

$$f_f = 1.0 \left[\frac{1.0(-4{,}840)}{2{,}942} + \frac{1.0(-690 + -664)}{6{,}148} + \frac{1.3(-4{,}040)}{13{,}772} \right] 12 = 26.96 \text{ ksi}$$

$$26.96 \text{ ksi} < 64.97 \text{ ksi} \quad \text{ok}$$

Bot. Flange:

$$f_f + \frac{f_\ell}{2} \le 0.95 R_h F_{yf}$$

AASHTO LRFD Equation 6.10.4.2.2-2

$$f_f = 1.0 \left[\frac{1.0(-4{,}840)}{3{,}149} + \frac{1.0(-690 + -664)}{3{,}594} + \frac{1.3(-4{,}040)}{3{,}875} \right] 12 = -39.23 \text{ ksi}$$

$$\left| -39.23 \right| \text{ ksi} + 0 < 64.97 \text{ ksi} \quad \text{ok}$$

2.2.3.5.2.2 Web Bend Buckling Check

As specified in *AASHTO LRFD* Article 6.10.4.2.2, except for composite sections in positive flexure in which the web satisfies the requirement of *AASHTO LRFD* Article 6.10.2.1.1 (i.e. $D/t_w \le 150$ – no longitudinal web stiffeners), all sections must also satisfy the following check at the service limit state:

$$f_c \le F_{crw} \qquad \qquad \text{Equation 2.81}$$

AASHTO LRFD Equation 6.10.4.2.2-4

where:

f_c = compression-flange stress due to the Service II loads calculated without consideration of flange lateral bending (ksi)

F_{crw} = nominal bend-buckling resistance for webs determined as specified in *AASHTO LRFD* Article 6.10.1.9 (Equation 2.11)(ksi)

Again, a resistance factor is not specified (i.e. it is implicitly assumed equal to 1.0) because this is a serviceability check.

A web bend buckling check is specified at the service limit state to control bending deformations and transverse displacements of the web. Regions in negative flexure are particularly susceptible to web bend buckling in composite girders at the service limit state, especially when the concrete deck is considered to be effective in tension as permitted for composite sections in *AASHTO LRFD* Article 6.10.4.2.1 when certain conditions are satisfied. When the concrete deck is considered effective in tension, more than half of the web is likely to be in compression increasing the susceptibility of the web to bend buckling. As a result, the check in this case may often end up governing the web thickness of the girder in these regions when the concrete is assumed effective (as recommended when the appropriate conditions are satisfied). Because an explicit web bend buckling check is specified, the web load-shedding factor R_b is not included in Equations 2.78 through 2.80.

The reader is referred to Section 2.2.2.4 of this chapter on the Web Bend Buckling Resistance for further discussion on the particulars of this check. Example calculations illustrating this check are also given for a web of a composite section without longitudinal stiffeners subject to negative flexure (in which the concrete deck is assumed to be effective in tension), and for a web of a composite section with longitudinal stiffeners subject to positive flexure.

50.   ASCE. 1958. "Deflection Limitations of Bridges. Progress Report of the Committee on Deflection Limitations of Bridges of the Structural Division." *Journal of the Structural Division*, American Society of Civil Engineers, New York, NY, Vol. 84, No. ST3, May.

51.   Ontario Ministry of Transportation. 1991. *Ontario Highway Bridge Design Code – 3rd Edition*. Quality and Standards Division, Structural Office, Toronto, Canada.

52.   Wright, R.N., and W.H. Walker. 1971. "Criteria for Deflection of Steel Bridges." *AISI Bulletin No. 19*, American Iron and Steel Institute, Washington, D.C., November.

53.   Roeder, C.W., K. Barth, and A. Bergman. 2002. "Improved Live Load Deflection Criteria for Steel Bridges." Final Report for NCHRP Project 20-7[133], National Cooperative Highway Research Program, Transportation Research Board, Washington, D.C., November.

54.   Vincent, G.S. 1969. "Tentative Criteria for Load Factor Design of Steel Highway Bridges." *AISI Bulletin No. 15*, American Iron and Steel Institute, Washington, D.C., March.

55.   Hansell, W.C., and I.M. Viest. 1971. "Load Factor Design for Steel Highway Bridges." *AISC Engineering Journal.* American Institute of Steel Construction, Chicago, IL. October.

56.   The AASHO Road Test. 1962. "Report No. 4, Bridge Research, Highway Research Board Special Report 61D." Publication No. 953, National Academy of Sciences, National Research Council, Washington, D.C.

57.   Schilling, C.G. 1996. "Yield-Interaction Relationships for Curved I-Girders." Journal of Bridge Engineering, American Society of Civil Engineers, New York, NY, Vol. 1, No. 1

2.2.3.6 Fatigue and Fracture Limit State Verifications

As specified in *AASHTO LRFD* Article 1.3.2.3, the fatigue limit state is taken as restrictions on the stress range resulting from a single design truck occurring at an expected number of stress range cycles, which are intended to limit crack growth under repetitive loads to prevent fracture during the design life of the bridge. The fracture limit state is taken as a set of material toughness requirements intended to ensure that the steel has the ability to absorb energy without fracture at minimum specified service temperatures.

For steel structures, *AASHTO LRFD* Article 6.5.3 states that components and details are to be investigated for fatigue as specified in *AASHTO LRFD* Article 6.6. The investigations are to be made for the Fatigue load combination specified in *AASHTO LRFD* Table 3.4.1-1 using the fatigue live load given in *AASHTO LRFD* Article 3.6.1.4.   The Fatigue load combination and fatigue live load are discussed in DM Volume 1, Chapter 5. Fracture toughness requirements are to be in conformance with *AASHTO LRFD* Article 6.6.2. For I-section flexural members, the preceding requirements are reiterated in *AASHTO LRFD* Articles 6.10.5.1 and 6.10.5.2. In addition, a special fatigue requirement for webs is specified in *AASHTO LRFD* Article 6.10.5.3. Requirements for fatigue design of shear connectors and for bolts subject to tensile fatigue will be covered in later sections of this chapter.

2.2.3.6.1 Fatigue Limit State

In the *AASHTO LRFD* Specifications, fatigue is defined as the initiation and/or propagation of cracks due to repeated variation of normal stress with a tensile component. The fatigue life of a detail is defined as the number of repeated stress cycles that results in fatigue failure of a detail, and the fatigue design life is defined as the number of years that a detail is expected to resist the assumed traffic loads without fatigue cracking. In the *AASHTO LRFD* Specifications, the fatigue design life is taken to be 75 years.

As specified in *AASHTO LRFD* Article 6.6.1.1, fatigue is categorized as either "load-induced fatigue" (*AASHTO LRFD* Article 6.6.1.2) or "distortion-induced fatigue" (*AASHTO LRFD* Article 6.6.1.3). Load-induced fatigue is defined as fatigue effects due to in-plane stresses for which components and details are explicitly designed. For load-induced fatigue, specific design verifications are required for both flexure and shear to ensure adequate fatigue resistance for the expected number of stress range cycles, and to control web buckling and the resulting elastic flexing of the web under repeated loading. Distortion-induced fatigue is defined as fatigue effects due to secondary stresses not normally quantified in the typical analysis and design of a bridge. Distortion-induced fatigue is typically controlled by providing rigid load paths to preclude the development of significant secondary stresses that could induce fatigue crack growth.

A helpful flowchart detailing the design checks to be made at the fatigue and fracture limit state (discussed below) is provided in Appendix C to Section 6 of the *AASHTO LRFD* Specifications – Figure C6.4.3-1.

2.2.3.6.1.1 Load-Induced Fatigue

2.2.3.6.1.1.1 Flexure

Early attempts to quantify the fatigue resistance of a particular structural joint were based on tests on relatively small-scale specimens that simulated a prototype connection (*58*, *59*). The experiments contained a limited number of specimens and many variables were introduced which made it difficult to establish the significance of details, type of steels, stress conditions and the quality of fabrication. Because of the limitations of the test data, only approximate design relationships could be developed. Prior to the Ninth Edition of the AASHTO Specifications, 1965, welded bridges were checked for fatigue by limiting alternating stresses using American Welding Society (AWS) specifications. The Ninth Edition specifications introduced the concept of cycles of maximum stress combined with the modified Goodman diagram to limit maximum fatigue stresses for nine different conditions. These provisions were based primarily on the tests mentioned above. However, fatigue cracks were still being found in some beams with partial length cover plates after as little as 13 years of service. Fatigue cracks were also found at the ends of web-stiffener welds in stiffeners cut short of the beam flange.

Additional experimental data were therefore developed starting in 1968 under National Cooperative Highway Research Program (NCHRP) Project 12-7, which involved the fatigue testing of approximately 500 test beams and girders under constant amplitude loading (*60*, *61*). Large-scale rolled and welded beam specimens were tested both with and without attachments, such as cover plates and transverse stiffeners. The use of large-scale specimens overcame some of the difficulties associated with the previous data, including the effects of residual stresses, defect size and distribution and shear lag. The test data demonstrated that all fatigue cracks commence at an initial discontinuity in the weldment, or at the periphery of the weld, and grow perpendicular to the applied stresses. Such discontinuities are always present regardless of the welding process or techniques used during the fabrication. The data also showed that the termination of groove and fillet welds provides an even more critical crack growth condition than initial discontinuities in the weld due to high stress concentrations resulting from the geometrical conditions.

Analysis of the data from the NCHRP Project showed that the most important factors governing the fatigue resistance are the stress range and type of detail. Other parameters such as the minimum stress, maximum stress, type of steel and stress ratio (i.e. the ratio of minimum stress to maximum stress) did not play an important role. The stress range is the algebraic difference between the maximum stress and minimum stress at a detail. Stress range means that only the live load plus impact stresses need to be considered; dead load does not contribute to the stress range (Figure 2.40). The fact that stress range is the only significant design parameter is due to the existence of residual stresses in welded steel structures. The welding

process results in high tensile residual stresses due to shrinkage of the weld upon cooling, which are at or near the yield point of the weldment and the adjacent base metal. Tensile residual stresses of this magnitude occur regardless of the steel type, which is why the fatigue resistance is independent of the type of steel. Most of the fatigue life occurs in these regions of high tensile residual stress and is exhausted by the time the fatigue crack propagates out of this zone.
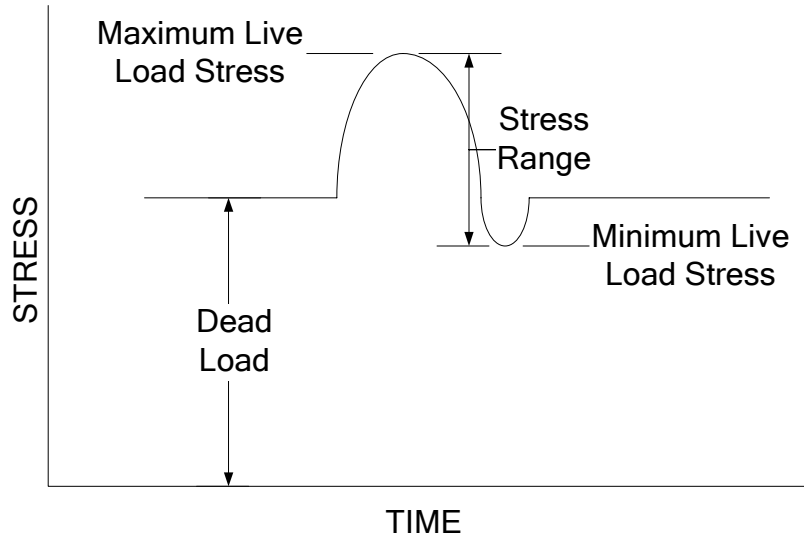
Figure 2.40 Components of a Stress Cycle

The tensile portion of a stress cycle propagates a fatigue crack. Therefore, material subjected to a cyclic loading at or near an initial discontinuity will be subject to a fully effective stress cycle in tension, even in cases of stress reversal, because the superposition of the tensile residual stress will elevate the entire cycle into the tensile stress region (Figure 2.41). The test data even showed an effective stress cycle in tension in cover-plated beams subjected to cyclic compression alone. Fatigue cracks occurred in the tensile residual stress zone at the cover plate weld terminations, but were arrested as they propagated into the adjacent compressive residual stress regions. No loss in load-carrying capacity was observed. This concept of considering only stress range has also been extended to rolled beam, bolted and riveted details where much different residual stress fields exist; the application of this concept to nonwelded details is conservative.
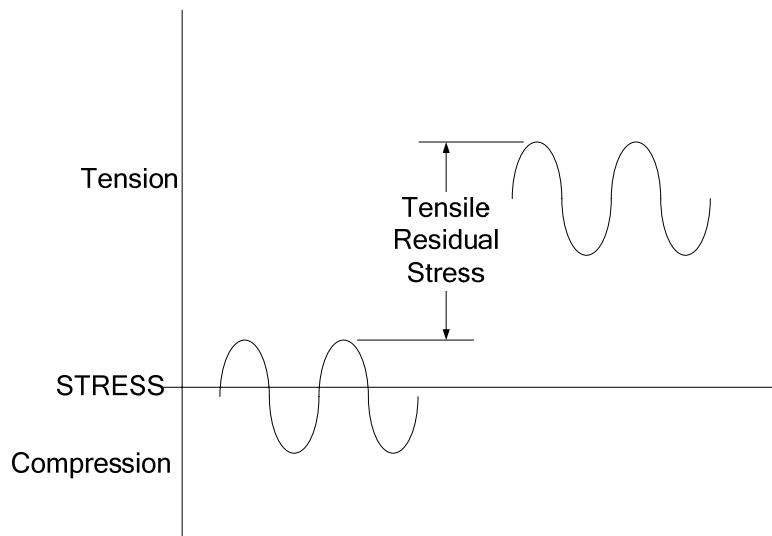
Figure 2.41 Effect of Residual Stress on a Stress Cycle

As a result of the observed behavior, fatigue design criteria need only be considered for details subject to effective stress cycles in tension and/or stress reversal. If a detail is subject to stress reversal, fatigue must be considered no matter how small the tension component of the stress cycle since a crack generated in the tensile residual stress zone could still be propagated to failure by the small tensile component of stress. Of course, the detail also must be subject to a net applied tensile stress to begin with when considering the maximum anticipated fatigue live load stress occurring over the fatigue design life acting in conjunction with the stress due to the unfactored permanent loads.

Once it was established that the stress range was the critical parameter defining the fatigue life, a relationship between the nominal fatigue resistance expressed in terms of stress range $(\Delta F)_n$ and the number of stress cycles to failure N, or S-N curve, could be established. Regression analyses showed that such a relationship could be developed with a constant slope in log-log space as follows:

$$\log N = \log A - B \log(\Delta F)_n \qquad \text{or} \qquad N = A(\Delta F)_n^{-B} \qquad \text{Equation 2.82}$$

where *log A* is the *log N*-axis intercept of the *S-N* curve and *B* is the slope constant of the curve. Failure in this case is defined as the growth of a crack large enough in size to result in the inability of a member to carry the load, but does not include brittle fracture where there is limited crack growth.

For each type of detail, a least squares linear regression analysis was performed to obtain a curve defining the estimated mean life for that particular detail group; i.e., where half the test data failed prior to reaching the estimated fatigue life and half the data failed after reaching this estimated life. A parallel curve was then drawn two standard deviations below this mean curve, which represented the 95 percent lower confidence limit. This lower bound curve defined a 97.5 percent probability of survival, or conversely, a 2.5 percent probability of failure. A set of such curves was

developed for five different detail categories ranging from A to E, with Category A representing details with the highest fatigue resistance and Category E representing details with the lowest fatigue resistance for the details tested as part of the NCHRP research program. Each curve had a slope constant *B* of approximately 3. These curves first appeared in the 1973 AASHTO Interim Specifications. Additional fatigue research conducted in the U.S. and abroad between 1973 and 1986 led to minor adjustments to the fatigue design curves and the inclusion of two additional curves for Categories B′ and E′. The slope constant of each curve was also set equal to 3. The complete set of current AASHTO *S-N* curves given in the *AASHTO LRFD* Specification is shown in Figure 2.42.
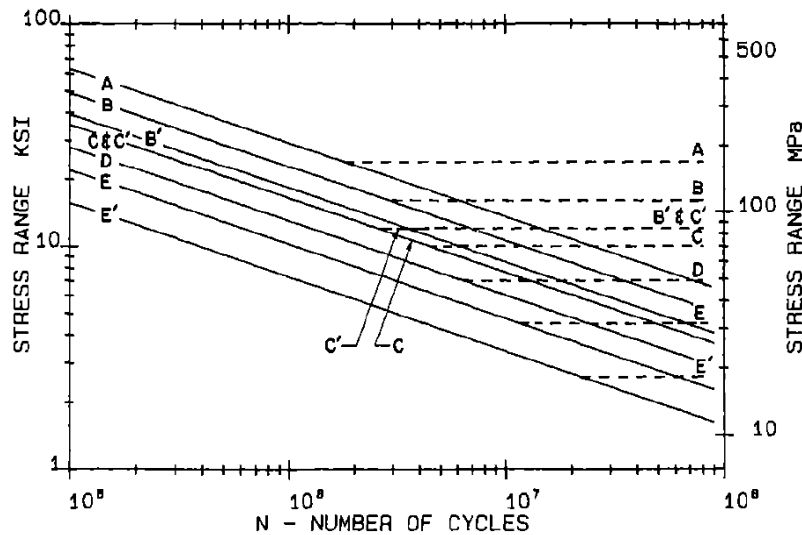

Figure 2.42 *AASHTO LRFD* S-N Curves

It was also observed from the test data that as the stress range decreased in magnitude, there was a level at which no fatigue cracking was observed in the test specimens.   The maximum stress range at which no fatigue crack growth will occur under constant amplitude loading is termed the constant-amplitude fatigue threshold $(\Delta F)_{TH}$ and is indicated by the dashed horizontal line in Figure 2.42 for each detail category.   Note that $(\Delta F)_{TH}$ decreases as the severity of the detail category increases.   For higher traffic-volume bridges, if the maximum stress range experienced by a detail due to the heaviest truck expected to cross the bridge over the fatigue design life is less than $(\Delta F)_{TH}$, then that detail has a theoretically infinite fatigue life. Therefore, the dashed-line portion of the *S-N* curves will be referred to here as the "infinite-life region". Values for $(\Delta F)_{TH}$ for each detail category are given in *AASHTO LRFD* Table 6.6.1.2.5-3 as follows:

Table 2.9 Values for (ΔF)$_{TH}$ for Each Detail Category

Detail Category	(ΔF)$_{TH}$ (ksi)
A	24.0
B	16.0
B′	12.0
C	10.0
C′	12.0
D	7.0
E	4.5
E′	2.6

With an identical slope constant of 3 for each curve in Figure 2.42, the equation for the sloping portion of the *S-N* curves can be written as follows:

$$(\Delta F)_n = \left(\frac{A}{N}\right)^{\frac{1}{3}}$$ Equation 2.83

Values of the *Log N*-axis intercept coefficient *A,* or as referred to in the *AASHTO LRFD* Specification, Detail Category Constant, are given in *AASHTO LRFD* Table 6.6.1.2.5-1 as follows:

Table 2.10 Detail Category Constants

Detail Category	Constant A times 10^8 (ksi^3)
A	250.0
B	120.0
B′	61.0
C	44.0
C′	44.0
D	22.0
E	11.0
E′	3.9

Equation 2.83 controls for lower traffic-volume bridges. The sloping portion of the S-N curves will be referred to here as the "finite-life region".

Category A defines the fatigue resistance of rolled plates and shapes without welded or bolted details or attachments and provides the maximum possible fatigue resistance of any detail. Category B applies to the majority of welded details, including longitudinal fillet and full penetration groove welds, transverse groove welds ground flush and transitioned flange splices. Bolted details are classified as Category B (including end-bolted cover plates). The nominal fatigue resistance of uncoated weathering steel base metal designed and detailed in accordance with

Reference 62 is also classified as Category B. Category B′, introduced in 1988, applies to longitudinal partial penetration groove welds, full penetration groove welds with backing bars left in place, and straight flange transition splices made with A 709 Grade 100/100W steel. Detail Categories A through B′ rarely control the design. Therefore, *AASHTO LRFD* Article 6.6.1.2.3 only requires that components and details with fatigue resistances less than or equal to Category C be designed to satisfy the specified fatigue requirements.

Category C applies to short attachments, unimproved transverse groove welds, welded shear studs and certain attachments with specified radius transitions. Category C marks the transition where geometrical stress concentrations begin to influence the fatigue resistance more than initial discontinuities in the weldment (*63*). Category C′ applies specifically to the toe of transverse stiffener-to-flange and transverse stiffener-to-web welds. Category D represents a transition between high and low fatigue strength details. The fatigue resistance of Category D details is influenced by any improvements to reduce the geometrical stress concentration and the attachment length.

Category E applies to base metal at the ends of partial length welded cover plates, base metal at the ends of welded longitudinal web stiffeners without specified radius transitions, gusset plate welds, long attachments and small radius transitions. Also included are fillet welds normal or parallel to the direction of applied stress subject to shear stress on the weld throat in order to prevent fatigue cracking in the weld metal initiating at the weld root (Note: this detail was classified as Category F in previous Specifications, but is now conservatively checked as a Category E detail in the *AASHTO LRFD* Specifications. As of this writing (2006), consideration is being given to reinstating Category F for checking shear on the throat of a fillet weld or potentially eliminating this category altogether). Normally, for the case of welds oriented normal to the direction of applied stress, the fatigue check for the base metal at the weld toe (Category C or less) will control unless the weld is required to carry a relatively large shear through the throat. The check for shear on the weld throat may be significant in the design of fillet-welded gusset-plate connections for heavily loaded cross-frame or lateral bracing members, particularly when checked as a Category E detail.

Category E′ details are the lowest fatigue-strength details and are similar to Category E details, but exhibit a reduced fatigue resistance due to a plate thickness effect, which results in a higher geometrical stress concentration. Category E′ details include longitudinal attachments with a thickness greater than 1.0 in., cover plate ends on flanges with a thickness greater than 0.8 in. and the ends of cover plates wider than the flange with no transverse end welds.

AASHTO LRFD Table 6.6.1.2.3-1 lists the detail categories for different details. Included in the table is a description of the general condition, a description of the specific situation, the corresponding detail category and the corresponding illustrative example number from Figure 6.6.1.2.3-1. The illustrative examples in Figure 6.6.1.2.3-1 are all keyed to the descriptions. For example, Figure 2.43 shows illustrative Example 7, which includes several details. Included are the base metal at the ends of a welded partial-length cover plate and the base metal at the ends of

welded longitudinal stiffeners (without a transition radius). As shown in the example, these are classified as either Category E or E′ details. Also included in this example are the base metal and weld metal for continuous fillet welds parallel to the direction of the applied stress, such as longitudinal stiffener-to-web welds, which are classified as a Category B detail. As shown in Figure 2.44, the examples are all keyed to *AASHTO LRFD* Table 6.6.1.2.3-1, which confirms for the cases shown in the photograph that the detail category for the ends of a welded partial-length cover plate is Category E′ (since the cover plate is narrower than the flange and the flange thickness is greater than 0.8 inches), and that the detail category for the base metal and weld metal for the continuous fillet weld connecting the longitudinal stiffener to the web is Category B. The illustrative examples are not intended to serve as standard details or necessarily as examples of good detailing practice.
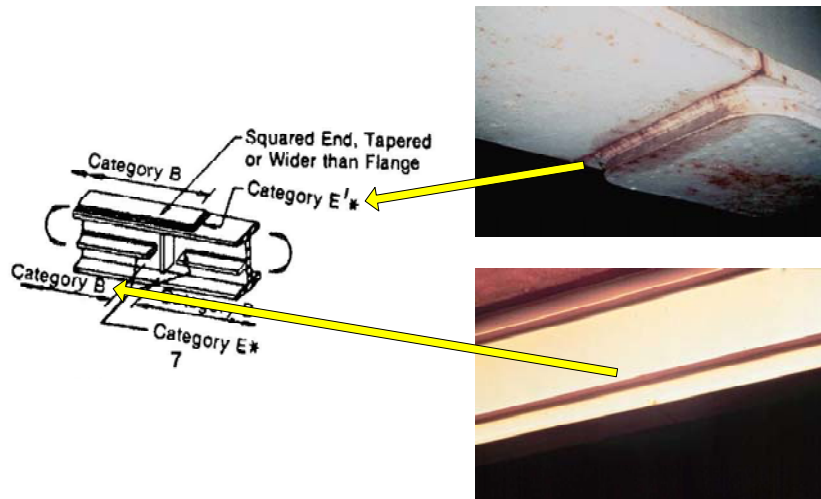

Figure 2.43 Illustrative Example 7

Figure 2.44 Category B and E'

Examples of design details to optimize the fatigue resistance can be found in References 63 through 65. The following basic general principles of good fatigue design taken from Reference 63 are restated as follows:

1. Design the bridge and its assemblage of members as a whole so as to provide easy paths for stress flow. Avoid gross discontinuities by providing gradual changes in cross-section. Put material at the points at which loads are to be resisted and avoid sudden changes in stiffness.
2. Select the individual connections on the basis of providing the easiest possible stress path through the connections.
3. Although all connections produce stress concentrations, their number and severity should be minimized.
4. If possible, position connections near points of low fatigue stress. For example, field splices in continuous girders should preferably be positioned near points of permanent-load contraflexure.
5. Avoid the introduction of unnecessary stresses, such as those associated with unnecessary eccentricities.

Details with a fatigue resistance less than Category C should be avoided if possible, but should not necessarily be precluded from use if they can be used in regions of low stress range. A Category C detail that is overstressed provides less safety than an understressed Category E detail. Note, however, that *AASHTO LRFD* Article 6.6.1.2.4 specifies some restricted use details (or details that should not be considered for use), including transversely loaded partial penetration groove welds and gusset plates attached to girder flanges with only transverse fillet welds.

Intersecting welds at details should always be avoided. Such details are possible, for example, at the intersection of transverse and longitudinal web stiffeners and at the intersection of gusset plates and transverse stiffeners. The restraining effect of the intersecting welds on the plate elements can result in the development of large restraint stresses during cooling, which can potentially result in cracking and low fatigue resistance. In most cases, it is desirable for the longitudinal weld, or the weld parallel to the applied stress, to be continuous to avoid a Category E detail at the weld termination if it is interrupted. End terminations of transverse welds are typically classified as Category C details.
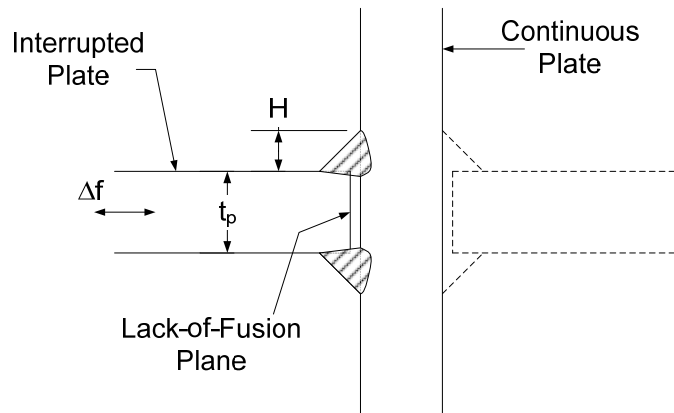
Figure 2.45 Cruciform Joint Detail

Fillet welds providing continuity between intersecting plate members (e.g. at transverse and longitudinal stiffener intersections and at transversely loaded web attachments) are often referred to as cruciform joints (Figure 2.45). Such joints are typically fabricated with one plate continuous while the other plate is interrupted, with fillet welds provided at the corners. As shown in Figure 2.45, a lack-of-fusion plane (or penetration at the weld root) may result depending on the thickness of the interrupted plate, weld size and depth of penetration. When only the continuous plate is loaded, the lack of fusion plane is parallel with the stress field and the fatigue resistance of the base metal at the weld is Category C. If the interrupted plate is loaded, the lack-of-fusion plane is perpendicular to the stress field (i.e. the fillet welds are transversely loaded) and the fatigue resistance of the base metal at the weld must be taken from the following equation given in *AASHTO LRFD* Article 6.6.1.2.5:

$$\left(\Delta F\right)_n = \left(\Delta F\right)_n^C \left(\frac{0.06 + 0.79\dfrac{H}{t_p}}{1.1t_p^{1/6}}\right) \le \left(\Delta F\right)_n^C \qquad \text{Equation 2.84}$$

AASHTO LRFD Equation 6.6.1.2.5-3

where:

$\left(\Delta F\right)_n^C$ = nominal fatigue resistance for Detail Category C (ksi)

H = effective throat of the fillet weld (in.)

t_p = thickness of the loaded plate (in.)

Equation 2.84 conservatively assumes no penetration at the weld root (*66*). The severity of the cruciform joint can be reduced by the proper selection of the continuous plate element. For example, at intersections of longitudinal and transverse stiffeners, the longitudinal stiffener (i.e. the loaded element) should be continuous while the transverse stiffener (i.e. the unloaded element) is interrupted. It should be emphasized that Equation 2.84 does *not* apply to the base metal at the toe of transversely loaded transverse stiffener-to-flange or transverse stiffener-to-web fillet welds, which are classified as Category C′.

Reference 63 discusses the need to provide a sufficient minimum length for the web gap between the end termination of the transverse weld and the weld toe of the longitudinal weld.   For example, where transverse stiffeners are welded to the flange, the end of the transverse weld should be terminated at least one inch from the web-to-flange weld toe to prevent intersecting welds and the formation of significant restraint stresses (Figure 2.46).   The stiffener plate should be coped to avoid interference with the web-to-flange weld. The weld should also be terminated approximately ¼ inch from the plate edges, as wrapping the weld around the plate could result in undercutting of the stiffener plate.   As shown in Figure 2.46, the minimum distance between the end of the web-to-stiffener weld and the near edge of the web-to-flange fillet weld, or a longitudinal stiffener-to-web weld as applicable, is limited to four times the web thickness, as specified in *AASHTO LRFD* Article 6.10.11.1.1. This limit is specified to eliminate the possibility of a weld intersection and the concomitant high restraint stresses resulting from weld shrinkage.   In addition, this limit helps to relieve flexing of the unsupported portion of the web in the gap to avoid fatigue-induced cracking of the stiffener-to-web welds, particularly during handling and shipping of the girders when the stiffeners are cut short from the tension flange (the web gaps should be blocked during shipment in this case). An upper limit on this distance equal to the lesser of six times the web thickness and 4.0 inches in also specified. The $6t_w$ limit is specified to avoid vertical buckling of the unsupported portion of the web. The 4.0-inch limit was arbitrarily selected to avoid large unsupported web segments in cases where the web thickness has been selected for reasons other than stability; an example being the webs of bascule girders at trunions. Additional information regarding the detailing of stiffeners (transverse, longitudinal and bearing) is provided in a later section of this chapter on Stiffener Design.   Further information regarding the detailing of gusset plates for lateral bracing members is provided below under Distortion-Induced Fatigue.
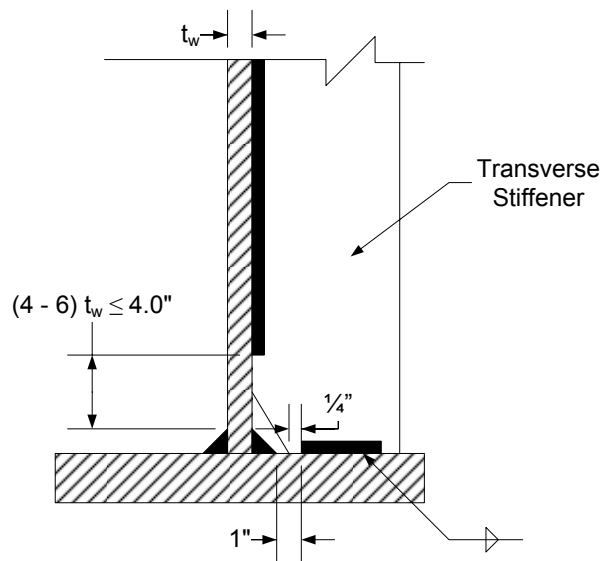

Figure 2.46 Transverse Stiffener Detail

Most of the early laboratory fatigue tests were based on constant-amplitude loading, which consists of a series of identical load cycles or a constant applied stress range. However, bridges are actually subject to variable-amplitude loading because of the variation of vehicle weights and different possible loading combinations. Variable-amplitude loading consists of a series of cycles of different magnitudes, usually applied in a random sequence. The effects of variable-amplitude loading are typically accounted for using a cumulative damage rule. The most widely used method to account for the effects of cumulative damage is the linear rule proposed by Miner (*67*). According to Miner's rule, fatigue damage occurs when the sum of the cumulative stress cycle ratios for the various stress cycles equals unity, or $\Sigma n_i / N_i = 1.0$, where n_i is the number of cycles applied at a stress range S_{ri} and N_i is the number of constant amplitude cycles to failure at S_{ri}. To evaluate the effectiveness of Miner's linear damage hypothesis in relating variable stress cycles to constant cycle data, variable-amplitude fatigue tests were carried out on large-scale beams under NCHRP Project 12-12 (*68*). The beams were identical to those tested under the original NCHRP Project 12-7. From the results of this study, it was determined that an equivalent constant-amplitude stress range, or an *effective stress range S_{re}*, that causes the same fatigue damage as an equal number of variable-amplitude cycles could be developed by combining Miner's linear damage rule with Equation 2.83 as follows:

$$S_{re} = \left(\sum \gamma_i S_{ri}^3 \right)^{1/3} \qquad\qquad \text{Equation 2.85}$$

where γ_i is equal to the frequency of occurrence of the stress range S_{ri}. Using an effective stress range allows constant-amplitude fatigue data and resistance curves to be used to define variable-amplitude conditions and also allows the fatigue damage resulting from an arbitrary load spectrum to be related to a single stress range.

Similarly, the gross weight of a fatigue design truck selected so that the fatigue damage caused by a given number of passages of this truck is the same as the damage caused by an equal number of passages of different-sized trucks in actual traffic can be computed as follows:

$$W_F = \left(\sum \alpha_i W_i^3 \right)^{1/3} \qquad\qquad \text{Equation 2.86}$$

where α_i is the fraction of trucks with a gross weight of W_i. The stress range caused by the passage of such a truck would be representative of the effective stress range given by Equation 2.85. To use Equation 2.86, a histogram of truck-weight data for a particular site would be required to arrive at the weight of the fatigue design truck. Since such data are generally not available, a gross weight of 54 kips was originally proposed for the fatigue design truck in Reference 69, which was calculated from Equation 2.86 based on weigh-in-motion data and the results of several nationwide traffic surveys (*65*). A constant rear-axle spacing of 30 feet was also proposed for the fatigue design truck in Reference 69 since that spacing was assumed to approximate the spacing for the 4- and 5-axle semitrailers that do most of the fatigue damage to bridges. Further, an impact factor of 1.15 was proposed for fatigue design since the impact factor in this case is for stress range rather than peak stress.

Also, it was felt by the Guide Specification writers that an average impact factor rather than a maximum factor would be more appropriate for fatigue design.

These concepts were carried forward to the *AASHTO LRFD* Specifications, with some slight modification. The fatigue design truck is specified to be a single HS20 truck, weighing 72 kips, with a constant rear-axle spacing of 30 feet (*AASHTO LRFD* Article 3.6.1.4.1). Then, a load factor of 0.75 is to be applied to the fatigue design truck, as specified for the Fatigue load combination in *AASHTO LRFD* Table 3.4.1-1, which results in a factored fatigue design truck weighing 54 kips. A dynamic load allowance (impact factor) of 1.15 is to be applied to the factored truck (*AASHTO LRFD* Article 3.6.2). As specified in *AASHTO LRFD* Article 3.6.1.4.3a, when the bridge is analyzed by a refined analysis method, the truck is to be positioned transversely and longitudinally to maximize the stress range at the detail under consideration regardless of the position of the actual traffic lanes on the deck. As specified in *AASHTO LRFD* Article 3.6.1.4.3b, when wheel-load distribution factors are used for the analysis, the appropriate factor specified for one-lane loaded in *AASHTO LRFD* Article 4.6.2.2 is to be used. Further, as specified in *AASHTO LRFD* Article 3.6.1.1.2, the multiple presence factor of 1.2 for one-lane loaded (*AASHTO LRFD* Table 3.6.1.1.2-1) is not to be applied for the fatigue limit state check. Therefore, when using the tabularized equation for the distribution factor for one-lane loaded for the interior girders, the 1.2 multiple presence factor must be divided out of the calculated factor. Or, when using the lever rule or the special analysis equation to compute the factor for one-lane loaded for the exterior girders, the 1.2 factor must not be applied.

The factored fatigue load produces a lower calculated stress range than the design loads used to check for fatigue in the AASHTO Standard Specifications. In the Standard Specifications, fatigue is checked for multiple lanes of truck loading (using the design truck with a variable rear-axle spacing) and multiple lanes of lane loading. In addition, for high-volume roadways, an additional check must be made for a single design truck. A reduced impact factor is not applied.   The reduction in the calculated stress range in the *AASHTO LRFD* Specifications is offset by an increase in the number of cycles of loading to be considered. In the Standard Specifications, fatigue checks are to be made for: over 2,000,000 cycles; 2,000,000 cycles; 500,000 cycles and/or 100,000 cycles depending on the case of the roadway (i.e. volume of average daily truck traffic) and the category of loading (truck or lane).   In the *AASHTO LRFD* Specifications, fatigue must be checked for a much higher number of cycles N in order to achieve a nearly equivalent fatigue design. The lower stress range and increased number of cycles are believed to be more reflective of actual conditions experienced by many bridges. As such, the fatigue provisions given in the *AASHTO LRFD* Specifications can be used more easily for both design and evaluation, whereas the fatigue provisions given in the Standard Specifications, which are based on a much lower number of design cycles than are actually experienced by most bridges, cannot easily be used for evaluation.

The preceding discussion on the effective stress range leads to the first principle of fatigue resistance, which applies in the finite-life region, and states that for lower traffic volumes, the fatigue resistance $(\Delta F)_n$ is inversely proportional to the cube of the effective stress range. This principle is reflected by Equation 2.83, which

represents the equation for the sloping portion of the *S-N* curve. **In the AASHTO LRFD Specifications, the effective stress range is represented by the factored fatigue design truck weighing 54 kips (plus impact).**

In the extreme life (or infinite life) region, for which many details on bridges located on high-volume routes are designed, most of the stress cycles in a spectrum will be below the constant-amplitude fatigue threshold $(\varDelta F)_{TH}$. These cycles do not cause fatigue damage under constant-amplitude loading. However, under variable-amplitude loading, larger stress cycles that exceed $(\varDelta F)_{TH}$ will contribute to fatigue crack growth, which will cause the threshold to decrease in magnitude until all stress cycles will eventually contribute to crack growth. Therefore, in the infinite-life region, fatigue design of welded details subject to variable-amplitude loading requires that the *maximum stress range* be considered in addition to the effective stress range. As a result, three different cases related to fatigue life are possible depending on the relative values of the effective stress range, maximum stress range and $(\varDelta F)_{TH}$: 1) effective stress range greater than $(\varDelta F)_{TH}$, 2) effective stress range less than $(\varDelta F)_{TH}$ and maximum stress range greater than $(\varDelta F)_{TH}$, or 3) effective and maximum stress ranges both less than $(\varDelta F)_{TH}$. These three cases are illustrated in Figure 2.47. For the first two cases, the fatigue life is defined by the S-N curve and its straight-line extension below $(\varDelta F)_{TH}$. Only for the third case will no fatigue crack growth be assured; that is, the detail will have a theoretically infinite fatigue life.
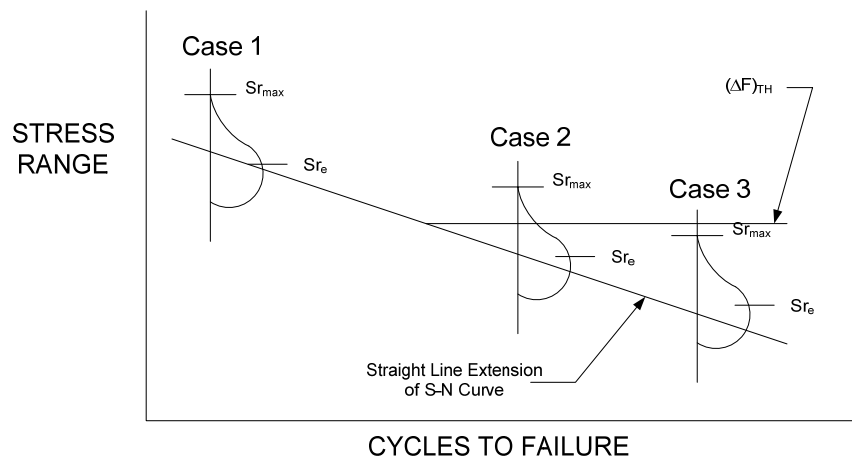

Figure 2.47 Three Cases of Variable Amplitude Stress Spectrum

The preceding discussion leads to the second principle of fatigue resistance, which applies in the infinite-life region, and states that for higher traffic volumes, the fatigue resistance $(\varDelta F)_n$ is infinite if the maximum stress range is less than $(\varDelta F)_{TH}$. **In the AASHTO LRFD Specifications, the maximum stress range is assumed to be twice the effective stress range, or twice the live load stress range due to the passage of the factored fatigue design truck (plus impact).** That is, the maximum stress range for fatigue design is assumed to be the stress range due to a 108-kip truck (plus impact) with a constant rear-axle spacing of 30 feet. This represents the heaviest truck expected to cross the bridge over its 75-year fatigue design life.

In the *AASHTO LRFD* Specifications, the two principles of fatigue resistance are combined into the following single equation for the nominal fatigue resistance *(ΔF)ₙ* given in *AASHTO LRFD* Article 6.6.1.2.5:

$$\left(\Delta F\right)_n = \left(\frac{A}{N}\right)^{\frac{1}{3}} \geq \frac{1}{2}\left(\Delta F\right)_{TH}$$
<div align="right">Equation 2.87</div>

<div align="right">*AASHTO LRFD* Equation 6.6.1.2.5-1</div>

The factor of ½ in front of $(\Delta F)_{TH}$ in Equation 2.87 relates to the assumption that the maximum stress range *(Δf)ₘₐₓ* is equal to twice the effective stress range *(Δf)ₑ*. If *(Δf)ₘₐₓ* must not exceed $(\Delta F)_{TH}$ and *(Δf)ₘₐₓ* is assumed equal to 2.0*(Δf)ₑ*, then *(Δf)ₑ* must not exceed ½$(\Delta F)_{TH}$ in order for the detail to have a theoretically infinite fatigue life. The inclusion of the ½ factor in Equation 2.87 allows the effective stress range (or the stress range due to the factored fatigue design truck of 54 kips) to be used in the design checks in both the finite-life and infinite-life regions, which simplifies the design.

The number of stress cycles *N* in Equation 2.87, or the required fatigue life as defined in the *AASHTO LRFD* Specifications, is to be computed from the following equation:

$$N = (365)(75)n(ADTT)_{SL}$$
<div align="right">Equation 2.88</div>
<div align="right">*AASHTO LRFD* Equation 6.6.1.2.5-2</div>

The number *365* represents the number of days in a year, the number *75* represents the fatigue design life of 75 years (a number other than 75 should be substituted if a fatigue design life other than 75 years is desired), *n* is the number of stress cycles per truck passage taken from *AASHTO LRFD* Table 6.6.1.2.5-2, and *(ADTT)ₛₗ* is the single-lane *ADTT* (Average Daily Truck Traffic) specified in *AASHTO LRFD* Article 3.6.1.4.2.

Short-span longitudinal members (with spans less than or equal to 40 feet in length according to *AASHTO LRFD* Table 6.6.1.2.5-2), transverse members loaded directly by a wheel (with a span less than or equal to 20 feet according to *AASHTO LRFD* Table 6.6.1.2.5-2), and areas near interior supports of continuous spans (with 'near' defined in *AASHTO LRFD* Article C6.6.1.2.5 as a distance equal to one-tenth of the span on each side of an interior support) will be subject to more than one stress cycle *n* per truck passage. As span length increases, the effect of the axle loads is attenuated. For cantilever girders, *n* is to be taken equal to 5.0 because these members are susceptible to large vibrations, which cause additional cycles after the truck leaves the bridge.

As specified in *AASHTO LRFD* Article 3.6.1.4.2, in the absence of better information, *(ADTT)ₛₗ* may be taken as follows:

$$\left(ADTT\right)_{SL} = p * ADTT$$
<div align="right">Equation 2.89</div>
<div align="right">*AASHTO LRFD* Equation 3.6.1.4.2-1</div>

where *ADTT* is the number of trucks per day *in one direction* averaged over the fatigue design life in the traffic lane carrying the majority of the truck traffic, and *p* is the fraction of truck traffic in a single lane taken from *AASHTO LRFD* Table 3.6.1.4.2-1. *AASHTO LRFD* Article C3.6.1.4.2 contains recommendations on how to compute the *ADTT* based on the average daily traffic (*ADT*) in the absence of site-specific data. The value of *p* depends on the number of lanes available to trucks on the bridge traveling in one direction. For one lane, *p* is equal to 1.0; for two lanes, *p* is equal to 0.85; and for three or more lanes, *p* is equal to 0.80.

As mentioned previously, for higher traffic volumes, the fatigue design for most details (except potentially for Categories E and E′) will be governed by the infinite life check; that is, the right-hand side of Equation 2.87. The following table (*AASHTO LRFD* Table C6.6.1.2.5-1) shows the values of $(ADTT)_{SL}$ for each detail category *above* which the nominal fatigue resistance is governed by one-half of $(\Delta F)_{TH}$ (or the infinite-life check):

Table 2.11 $(ADTT)_{SL}$ for each detail category *above* which the nominal fatigue resistance is governed by one-half of $(\Delta F)_{TH}$

Detail Category	75-Year $(ADTT)_{SL}$ Equivalent to Infinite Life (trucks per day)
A	535
B	865
B′	1035
C	1290
C′	745
D	1875
E	3545
E′	6525

The values in the table are computed from Equation 2.87 assuming a 75-year fatigue design life and *n* equal to one. For other values of *n*, the values in the table should be modified by dividing them by *n*. The use of this table can significantly simplify the fatigue design in many instances by eliminating the need to determine the values of *A* and *N* in Equation 2.87. The use of this table will be illustrated in the example to follow.

For load-induced fatigue considerations, each detail must satisfy the following design verification for flexure given in *AASHTO LRFD* Article 6.6.1.2.2:

$$\gamma(\Delta f) \le (\Delta F)_n \qquad\qquad \text{Equation 2.90}$$
$$\textit{AASHTO LRFD} \text{ Equation 6.6.1.2.2-1}$$

where γ is the load factor of 0.75 specified in *AASHTO LRFD* Table 3.4.1-1 for the Fatigue load combination and *(Δf)* is the stress range due to the passage of the HS20 (72 kip) fatigue design load (plus impact) specified in *AASHTO LRFD* Article

3.6.1.4. For the fatigue limit state, the load modifier η and resistance factor ϕ are both implicitly assumed equal to 1.0.

As specified in *AASHTO LRFD* Article 6.6.1.2.1 and discussed previously, Equation 2.90 need only be checked for details subject to a net applied tensile stress. That is, in regions where the unfactored permanent loads produce compression, fatigue need only be considered at a particular detail if the compressive stress at that detail is less than *twice* the maximum tensile live load stress caused by the factored fatigue design truck (i.e. the 54-kip truck). Again, according to the specification, two times the factored fatigue design truck represents the heaviest truck expected to cross the bridge over its 75-year fatigue design life. The effect of any future wearing surface may be conservatively ignored when making this check.

As discussed previously for the service limit state, under certain conditions, *AASHTO LRFD* Article 6.6.1.2.1 permits live load stresses and stress ranges for the fatigue limit state checks to be computed using the short-term composite section assuming the concrete deck is effective for both positive and negative flexure. As specified in *AASHTO LRFD* Article 6.10.1.7, those conditions are that shear connectors must be provided along the entire length of the girder and that the minimum one percent longitudinal deck reinforcement must be placed wherever the tensile stress in the concrete deck due to either the factored construction loads or load combination Service II exceeds the factored modulus of rupture of the concrete. Under these conditions, the crack size is felt to be controlled to such a degree that full-depth cracks will not occur. Where cracks do occur, the stress in the longitudinal reinforcement will increase until the crack is arrested and the cracked concrete and reinforcement reach equilibrium. Under these conditions, with a small number of staggered cracks that do not coalesce at any given section, the concrete can provide significant resistance to tensile stress at service load levels. *Using the short-term composite section to compute the factored fatigue load stresses due to both positive and negative flexure results in a significant reduction in the computed stress range at and near the top flange.* The stress range at or near the bottom flange is largely unaffected because the increase in stiffness for negative flexure is essentially offset by the increase in the distance from the *n*-composite neutral axis to the flange.

EXAMPLE

Check fatigue of the base metal at the cross-frame connection-plate welds to the flanges at the connection plate located 72.0 feet from the abutment in the 140-ft end span of a three-span continuous (140 ft – 175 ft – 140 ft) I-girder bridge. The cross-section of the composite girder at this section is shown in Figure 2.3. The elastic section properties for this section were calculated earlier in this chapter. The bridge has a 40-ft roadway width capable of handling three (3) design lanes. The average daily truck traffic *ADTT* in one direction averaged over the 75-year fatigue design life is assumed to be 2,000 trucks per day. Assume that the appropriate conditions specified in *AASHTO LRFD* Article 6.10.1.2.1 are met such that the concrete deck can be considered effective in positive and negative flexure for computing the live load stresses and stress ranges at the fatigue limit state. The unfactored permanent load moments at this section are as follows:

M_{DC1} = +1,824 kip-ft
M_{DC2} = +281 kip-ft
M_{DW} = +270 kip-ft

The unfactored moments at this section due to the fatigue load specified in *AASHTO LRFD* Article 3.6.1.4 (i.e. a 72-kip HS20 truck with a constant rear-axle spacing of 30 ft) placed in a single lane, including the 15 percent dynamic load allowance, are as follows:

$+M_{LL+IM}$ = +1,337 kip-ft
$-M_{LL+IM}$ = -496 kip-ft

First, check the top-flange connection-plate weld. Since the unfactored permanent loads produce compression at the top flange, determine if the top flange is subject to a net applied tensile stress according to the provisions of AASHTO LRFD Article 6.6.1.2.1. The total unfactored permanent-load compressive stress at the top-flange weld at this location (conservatively neglecting the future wearing surface) is computed as:

$$f_{DC_1} = \frac{1,824(12)(38.63)}{62,658} = -13.49 \text{ ksi}$$

$$f_{DC_2} = \frac{281(12)(23.13)}{117,341} = \underline{-0.665 \text{ ksi}}$$

$$-14.16 \text{ ksi}$$

Twice the maximum tensile stress at the top-flange weld at this location due to the negative moment caused by the factored fatigue load (i.e. factored by the 0.75 load factor specified for the Fatigue load combination) is:

$$f_{LL+IM} = \frac{2(0.75)|-496|(12)(10.70)}{161,518} = 0.591 \text{ksi}$$

$$|-14.16| \text{ ksi} > 0.591 \text{ksi}$$

Therefore, fatigue of the base metal at the connection-plate weld to the top flange at this location need not be checked.

Next, check the bottom-flange connection-plate weld. By inspection, it is determined that the base metal at the connection-plate weld to the bottom flange at this location is subject to a net applied tensile stress. Thus, the stress range $\gamma(\Delta f)$ at the connection-plate weld due to the factored fatigue load (i.e. factored by the specified 0.75 load factor) is computed using the properties of the short-term composite section as follows:

$$\gamma(\Delta f) = \frac{0.75(1,337)(12)(58.31)}{161,518} + \frac{0.75|-496|(12)(58.31)}{161,518}$$

$$= 5.96 \, \text{ksi}$$

Determine the fatigue detail category from *AASHTO LRFD* Table 6.6.1.2.3-1.

Under the condition of fillet-welded connections with welds normal to the direction of stress, the fatigue detail category for base metal at transverse stiffener-to-flange welds is Category C′.

According to *AASHTO LRFD* Equation 6.6.1.2.2-1, $\gamma(\Delta f)$ must not exceed the nominal fatigue resistance $(\Delta F)_n$. From *AASHTO LRFD* Equation 6.6.1.2.5-1, the nominal fatigue resistance is determined as:

$$(\Delta F)_n = \left(\frac{A}{N}\right)^{\frac{1}{3}} \geq \frac{1}{2}(\Delta F)_{TH}$$

AASHTO LRFD Equation 6.6.1.2.5-1

For a Category C′ detail, *AASHTO LRFD* Table 6.6.1.2.5-1 gives a Detail Category Constant A equal to $44.0 * 10^8$ ksi^3, and *AASHTO LRFD* Table 6.6.1.2.5-3 gives a constant-amplitude fatigue threshold $(\Delta F)_{TH}$ equal to 12.0 ksi. From *AASHTO LRFD* Article 3.6.1.4.2, the single-lane average daily truck traffic $(ADTT)_{SL}$ is computed as:

$$(ADTT)_{SL} = p * ADTT$$

AASHTO LRFD Equation 3.6.1.4.2-1

where *p* is the fraction of truck traffic in a single lane taken from *AASHTO LRFD* Table 3.6.1.4.2-1. For a 3-lane bridge, *p* is equal to 0.80. Therefore:

$$(ADTT)_{SL} = 0.80(2,000) = 1,600 \, \text{trucks per day}$$

The number of stress cycles *N* is computed as follows:

$$N = (365)(75)n(ADTT)_{SL}$$

AASHTO LRFD Equation 6.6.1.2.5-2

For continuous spans with span lengths greater than 40.0 feet, the number of stress cycles per truck passage *n* is equal to 1.0 at sections away from the pier (*AASHTO LRFD* Table 6.6.1.2.5-2). Sections ′away from the pier′ are defined as sections greater than a distance of one-tenth the span on each side of the interior support. Therefore:

$$N = (365)(75)(1.0)(1,600) = 43.8 * 10^6 \, \text{cycles}$$

$$\left(\frac{A}{N}\right)^{\frac{1}{3}} = \left(\frac{44.0 * 10^8}{43.8 * 10^6}\right)^{\frac{1}{3}} = 4.65 \text{ ksi} < \frac{1}{2}(12.0) = 6.00 \text{ ksi}$$

$$\therefore (\Delta F)_n = 6.00 \text{ ksi}$$

As a simpler alternative, *AASHTO LRFD* Table C6.6.1.2.5-1 (Table 2.11) shows the values of $(ADTT)_{SL}$ for each fatigue detail category *above which* the fatigue resistance is governed by one-half of $(\Delta F)_{TH}$ (such that the detail will theoretically provide infinite fatigue life). By using this table, it will usually not be necessary to determine the values of *A* and *N*. The values in the table assume a 75-year design life and one stress cycle *n* per truck passage. For other values of *n*, *AASHTO LRFD* Table C6.6.1.2.5-1 should be modified by dividing the values in the table by *n*. Therefore, from *AASHTO LRFD* Table C6.6.1.2.5-1, the 75-year $(ADTT)_{SL}$ equivalent to infinite fatigue life for a Category C′ detail is 745 trucks per day < 1,600 trucks per day. Therefore:

$$(\Delta F)_n = \frac{1}{2}(\Delta F)_{TH} = 6.00 \text{ ksi}$$

$$\gamma(\Delta f) \le (\Delta F)_n$$

AASHTO LRFD Equation 6.6.1.2.2-1

$$5.96 \text{ ksi} < 6.00 \text{ ksi} \quad \text{ok}$$

An alternative is to bolt the connection plates to the bottom flange, only in this region of high stress range, to raise the nominal fatigue resistance to that for a Category B detail. Bolting these particular connection plates to the tension flange will raise the nominal fatigue resistance to 8.00 ksi and may allow the designer to use a smaller bottom-flange plate in this region. However, the designer is cautioned that a Category C′ detail still exists at the termination of the connection-plate weld to the web just above the bottom flange. Also, the bolted connections must be detailed properly to ensure a positive attachment to the flange that offers rotational fixity to prevent distortion-induced fatigue caused by out-of-plane deformations (*AASHTO LRFD* Article 6.6.1.3). Reference 63 contains further discussion on these connections and provides examples of bolted connection details that provide the desired positive attachment. In most instances, bolting the connection plates to the flange is more expensive than welding the connection plates to the flange; thus, it is prudent for the Engineer to consult a fabricator to determine the most overall cost-effective solution.

EXAMPLE

Check fatigue of the base metal at the stud shear-connector weld to the top flange at the section located 100.0 feet from the abutment in the 140-ft end span of the three-span continuous I-girder bridge from the preceding example. The cross-section of the composite girder at this section is again shown in Figure 2.3. Other design

conditions are the same as in the preceding example. The unfactored permanent load moments at this section are as follows:

M_{DC1} = +74 kip-ft
M_{DC2} = +27 kip-ft
M_{DW} = +28 kip-ft

The unfactored moments at this section due to the fatigue load specified in *AASHTO LRFD* Article 3.6.1.4 (i.e. a 72-kip HS20 truck with a constant rear-axle spacing of 30 ft) placed in a single lane, including the 15 percent dynamic load allowance, are as follows:

$+M_{LL+IM}$ = +912 kip-ft
$-M_{LL+IM}$ = -688 kip-ft

Since the unfactored permanent loads produce compression at the top flange, determine if the top flange is subject to a net applied tensile stress according to the provisions of *AASHTO LRFD* Article 6.6.1.2.1. The total unfactored permanent-load compressive stress in the top flange at this location (neglecting the future wearing surface) is computed as:

$$f_{DC_1} = \frac{74(12)}{1,581} = -0.56 \text{ ksi}$$

$$f_{DC_2} = \frac{27(12)}{4,863} = \underline{-0.067 \text{ ksi}}$$

$$-0.627 \text{ ksi}$$

Twice the maximum tensile stress at the top-flange weld at this location due to the negative moment caused by the factored fatigue load (factored by the 0.75 load factor specified for the Fatigue load combination) is:

$$f_{LL+IM} = \frac{2(0.75)|-688|(12)}{13,805} = 0.897 \text{ ksi}$$

$$|-0.627| \text{ ksi} < 0.897 \text{ ksi}$$

Therefore, fatigue of the base metal at the stud shear-connector weld to the top flange at this location must be checked.

The stress range $\gamma(\Delta f)$ at the connection-plate weld due to the factored fatigue load (factored by the specified 0.75 load factor) is computed using the properties of the short-term composite section as:

$$\gamma(\Delta f) = \frac{0.75(912)(12)}{13,805} + \frac{0.75|-688|(12)}{13,805} = 1.04 \text{ ksi}$$

Determine the fatigue detail category from *AASHTO LRFD* Table 6.6.1.2.3-1.

Under the condition of longitudinally loaded fillet-welded attachments, the fatigue detail category for base metal adjacent to welded stud-type shear connectors is Category C.

From *AASHTO LRFD* Table C6.6.1.2.5-1, the 75-year $(ADTT)_{SL}$ equivalent to infinite fatigue life for a Category C detail for *n* equal to 1.0 is 1,290 trucks per day < 1,600 trucks per day. Therefore,

$$(\Delta F)_n = \frac{1}{2}(\Delta F)_{TH}$$

For a Category C detail, $(\Delta F)_{TH}$ = 10.0 ksi (*AASHTO LRFD* Table 6.6.1.2.5-3). Therefore:

$$(\Delta F)_n = \frac{1}{2}(10.0) = 5.00 \text{ ksi}$$

$$\gamma(\Delta f) \le (\Delta F)_n$$

<div align="right">*AASHTO LRFD* Equation 6.6.1.2.2-1</div>

$$1.04 \text{ ksi} < 5.00 \text{ ksi} \quad\quad \text{ok}$$

2.2.3.6.1.1.2 Shear

AASHTO LRFD Article 6.10.5.3 contains a special fatigue requirement for webs of flexural members. The check is intended to prevent shear buckling of the web under the heaviest truck expected to cross the bridge over its 75-year fatigue design life. In doing so, significant elastic flexing of the web under repeated live loading is not expected to occur and the member is thus assumed able to resist an infinite number of smaller loadings without fatigue cracking due to this effect.

In this check, interior panels of webs with transverse stiffeners, with or without longitudinal stiffeners, must satisfy the following requirement:

$$V_u \le V_{cr} \quad\quad\quad\quad\quad\quad \text{Equation 2.91}$$

<div align="right">*AASHTO LRFD* Equation 6.10.5.3-1</div>

where:
  V_u =   shear in the web at the section under consideration due to the unfactored permanent load plus *two times* the factored fatigue design truck (i.e. the 54-kip truck plus the 15 percent dynamic load allowance) (kips)
  V_{cr} =   shear-buckling resistance determined from *AASHTO LRFD* Equation 6.10.9.3.3-1 (Equation 2.51)(kips)

The calculation of V_{cr} was discussed earlier under the section on Fundamental Concepts, and is also discussed below under the section on Strength Limit State

Verifications. As will be discussed in the section on Strength Limit State Verifications, the shear in unstiffened webs and in the end panels of stiffened webs is already limited to V_{cr} at the strength limit state. Therefore, Equation 2.91 need not be checked for unstiffened webs and end panels of stiffened webs because it would not control.

A check for bend-buckling of the web under this condition is not required for reasons discussed previously in Section 2.2.2.4 of this chapter.

EXAMPLE

Check the special fatigue requirement for webs specified in *AASHTO LRFD* Article 6.10.5.3 at the first interior-pier section of the three-span continuous I-girder bridge from the preceding two examples. The cross-section of the composite girder at this section is shown in Figure 2.6. The girder is hybrid at this section with the flanges having a yield strength of 70 ksi and the web having a yield strength of 50 ksi. The transverse-stiffener spacing adjacent in the panel adjacent to the interior-pier section is d_o = 10.0 feet. The unfactored permanent load shears at the interior-pier section are as follows:

$$V_{DC1} = \text{-159 kips}$$
$$V_{DC2} = \text{-23 kips}$$
$$V_{DW} = \text{-22 kips}$$

The unfactored shear at this section due to the fatigue load specified in *AASHTO LRFD* Article 3.6.1.4 (i.e. a 72-kip HS20 truck with a constant rear-axle spacing of 30 ft) placed in a single lane, including the 15 percent dynamic load allowance, is as follows:

$$V_{LL+IM} = \text{-56 kips}$$

In this check, interior panels of webs with transverse stiffeners must satisfy the following requirement to control elastic flexing of the web under repeated live loading:

$$V_u \leq V_{cr}$$

AASHTO LRFD Equation 6.10.5.3-1

V_u is to be taken as the shear due to the unfactored permanent load plus the shear due to twice the factored fatigue load (factored by the 0.75 load factor specified for the Fatigue load combination), which is assumed to represent the heaviest truck expected to the cross the bridge over its 75-year fatigue design life. Therefore:

$$V_u = -159 + -23 + -22 + 2(0.75)(-56) = -288 \text{ kips}$$

The shear buckling resistance V_{cr} of the 10-foot web panel is determined as follows:

$$V_n = V_{cr} = CV_p$$

AASHTO LRFD Equation 6.10.9.3.3-1

C is the ratio of the shear buckling resistance to the shear yield strength determined from *AASHTO LRFD* Equation 6.10.9.3.2-4, 6.10.9.3.2-5 or 6.10.9.3.2-6, as applicable. First, compute the shear buckling coefficient, k

$$k = 5 + \frac{5}{\left(\dfrac{d_o}{D}\right)^2}$$

AASHTO LRFD Equation 6.10.9.3.2-7

$$k = 5 + \frac{5}{\left(\dfrac{10(12)}{69.0}\right)^2} = 6.65$$

Since, $1.40\sqrt{\dfrac{Ek}{F_{yw}}} = 1.40\sqrt{\dfrac{29,000(6.65)}{50}} = 86.9 < \dfrac{D}{t_w} = \dfrac{69.0}{0.5625} = 122.7$

$$C = \frac{1.57}{\left(\dfrac{D}{t_w}\right)^2}\left(\frac{Ek}{F_{yw}}\right)$$

AASHTO LRFD Equation 6.10.9.3.2-6

$$C = \frac{1.57}{(122.7)^2}\left(\frac{29,000(6.65)}{50}\right) = 0.402$$

V_p is the plastic shear force determined as follows:

$$V_p = 0.58F_{yw}Dt_w$$

AASHTO LRFD Equation 6.10.9.3.3-2

$$V_p = 0.58(50)(69.0)(0.5625) = 1,126 \text{ kips}$$

Therefore, $V_{cr} = 0.402(1,126) = 453 \text{ kips} > V_u = \left|-288\right| \text{ kips}$ ok

2.2.3.6.1.2 Distortion-Induced Fatigue

Distortion-induced fatigue is defined in the *AASHTO LRFD* Specifications as fatigue effects due to secondary stresses not normally quantified in the typical analysis and design of a bridge. These secondary stresses are typically caused by out-of-plane distortions generated by forces resulting from the three-dimensional interaction of bridge members. The resulting localized stresses can be significant in magnitude and generally are not explicitly considered in the design process.

For a bridge detail and/or weldment to be susceptible to distortion-induced fatigue, there must be an unstiffened gap, constraints at boundaries of the unstiffened gap and out-of-plane distortion. In the past, short unstiffened gaps were often intentionally designed into bridge structures to avoid a fatigue sensitive weldment on the tension flange. In fact, transverse welds on tension flanges were prohibited by AASHTO up until 1974. As a result, welded cross-frame/diaphragm connection plates and transverse stiffeners often had web gaps introduced above the tension flange. Web gaps were also introduced when gusset plates for lateral bracing were coped and not connected to transverse stiffeners. Bolted connections resulted in the introduction of additional web gaps. Intersecting components of a bridge at such details will result in small displacements perpendicular to the web plate that cause bending stresses within the gaps (Figure 2.48), which can result in fatigue crack propagation in the web plate, and in some cases when left unarrested, further propagation into the flange producing failure of the member. For the bending stresses to develop, sufficient constraint must exist at the ends of the web gap.
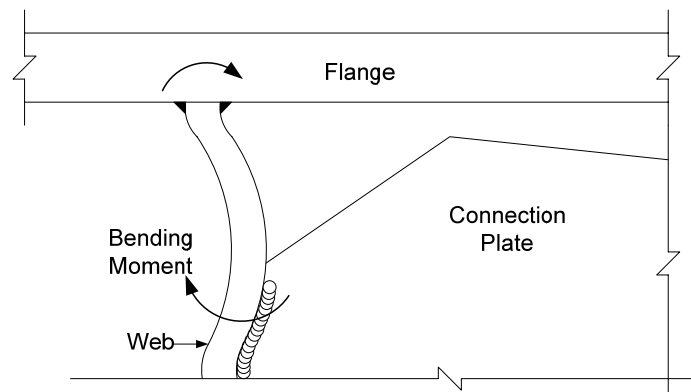

Figure 2.48 Web Gap Distortion

Some cases of web gap cracking have been attributed to high frequency vibration of plate elements. For example, vertical vibrations of relatively flexible lateral bracing members have resulted in out-of-plane movements of gusset plates attached to either the web or the flange (*63*). Even with small amounts of vibration, a very small gap between the lateral bracing member and the flange connection can lead to large out-of-plane bending stresses. Suggested lateral bracing details to limit the effects of out-of-plane distortion are discussed below.

In multiple-girder bridges, out-of-plane distortions of web gaps result from differential displacements between adjacent longitudinal members under eccentric loading causing forces to develop at the intersections between transverse and longitudinal members (Reference 63 details conditions resulting in out-of-plane distortions in other types of bridge structures). The magnitude of the resulting secondary stresses that develop in the web gap is difficult to estimate and the fatigue resistance of the details under these conditions is also difficult to quantify.   As a result, the design approach taken is to avoid such details and to provide rigid load paths to preclude the development of significant secondary stresses. *AASHTO LRFD* Article 6.6.1.3 requires that sufficient load paths be provided by connecting all transverse members

to the appropriate components comprising the cross-section of the longitudinal member, with the load paths provided by attaching the components through either welding or bolting.

AASHTO LRFD Article 6.6.1.3.1 deals with the detailing of transverse connection plates to prevent distortion-induced fatigue. Transverse connection plates (or transverse stiffeners serving as connection plates) attached to cross-frames, diaphragms or floorbeams are to be bolted or welded to both the compression and tension flanges of the cross-section in order to eliminate any web gaps. To ensure that the connection is not undersized, particularly at locations where larger out-of-plane forces may develop, it is recommended in *AASHTO LRFD* Article 6.6.1.3.1 that in the absence of better information, the welded or bolted connection in straight, nonskewed bridges be designed for a minimum of a 20.0 kip lateral force (*63*). For straight, skewed bridges and horizontally curved bridges, it is recommended in *AASHTO LRFD* Article C6.6.1.3.1 that the force be determined by analysis.

AASHTO LRFD Article 6.6.1.3.2 deals with the detailing of lateral connection plates. Connection plates for lateral bracing preferably should be attached directly to the flanges, and preferably by bolting. Bolting improves the fatigue resistance of the connection plate (Category B) and eliminates the need to provide an expensive radiused transition at the ends of a welded connection plate to improve the fatigue resistance above Category E. When the gusset plate is bolted to the flange, a minimum gusset gap of approximately 4.0 inches should exist between the edge of the flange and the first bolt line in the bracing member (Figure 2.49) to reduce stresses produced by vibration movement of the lateral bracing (*63*).

Should it not be practical to attached the connection plate directly to the flange, *AASHTO LRFD* Article 6.6.1.3.2 recommends that the connection plate be located a vertical distance not less than one-half the flange width above or below the flange, as applicable, to ensure adequate electrode access and to move the connection plate closer to the neutral axis of the girder to reduce the impact of the weld termination on the fatigue resistance. However, even if this is done, a welded Category E detail will not likely suffice at most locations requiring the connection plate to either be cut with a radius or bolted to the web. Should the connection plate be located on the opposite side of the web from a transverse stiffener, the connection plate should be centered on the stiffener and the stiffener should be rigidly attached to both the compression and tension flanges (Figure 2.50).

The same recommendations apply when the connection plate is located on the same side of the web as a transverse stiffener. The line of action of the laterals should intersect at the transverse stiffener. The connection plate should be welded to the stiffener (Figure 2.51) with sufficient copes provided to avoid intersecting welds, or else the bracing member can be extended and bolted to the stiffener with the connection plate coped around the stiffener (Figure 2.52). The ends of the bracing members must be kept a minimum of 4.0 in. from the web and any transverse stiffener to reduce distortion-induced gap stresses resulting from vibrations of the bracing members.

Should the web be unstiffened opposite the connection plate, the connection plate should be located a minimum of 6.0 inches above or below the flange, as applicable, but not less than one-half the flange width (Figure 2.53) in order to prevent large distortion-induced stresses from forming in the web between the connection plate and the flange.
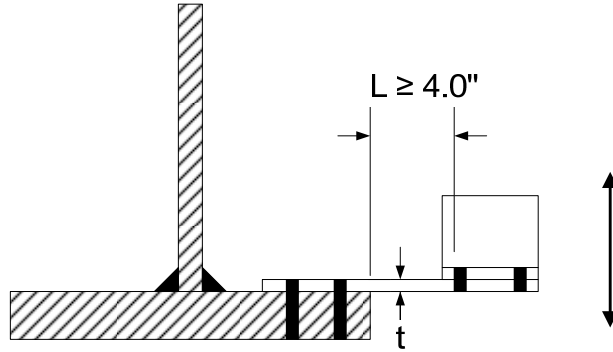

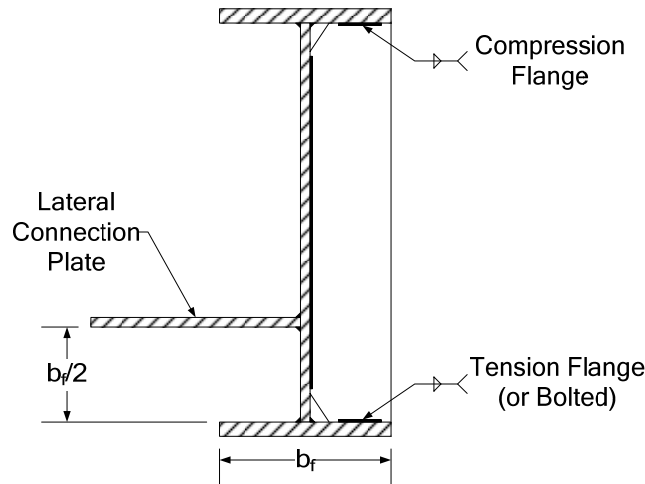**Figure 2.49 Schematic of Vibration at Lateral Gusset Bolted to the Flange**

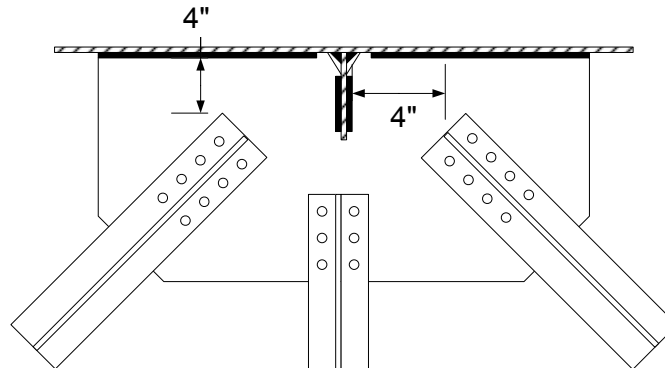**Figure 2.50 Acceptable Lateral Connection Plate Detail**

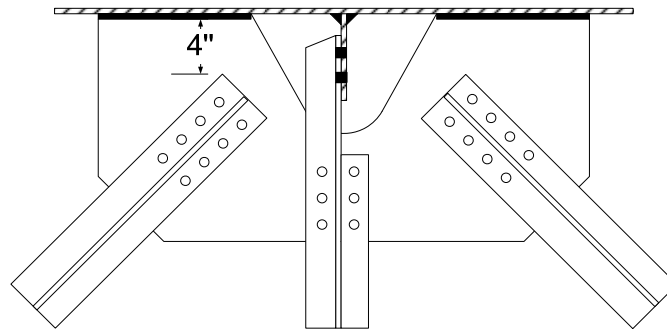**Figure 2.51 Lateral Connection Plate Welded to the Transverse Stiffener**

Figure 2.52 Lateral Bracing Member Bolted to the Transverse Stiffener
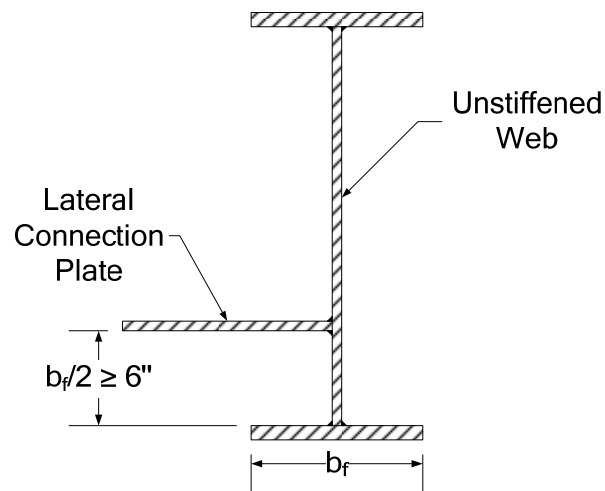

Figure 2.53 Lateral Connection Plate Attached to Unstiffened Web

2.2.3.6.2 Fracture Limit State

Fracture is defined as a tensile failure mode in which a member or component separates into two parts resulting in the loss of its load carrying capacity and potential collapse of the structure. In a steel bridge member, fracture can either be a ductile fracture, brittle fracture or a combination of the two modes.

Ductile fracture is characterized by plastic deformation prior to separation of the member or component. Ductile fracture is preferable over brittle fracture because there is generally a warning in the form of excessive deformations or deflection prior to failure. The existence of large plastic deformations is indicative that the material has basically followed its stress-strain curve through yielding until the ultimate strength is reached, as shown qualitatively in Figure 2.54 for a typical mild steel. Ductile failures generally occur at connections where there is cross-section loss due to plastic deformation in the vicinity of holes and/or concentrations of stress. The design of members or components for ductile fracture is based on the net section.
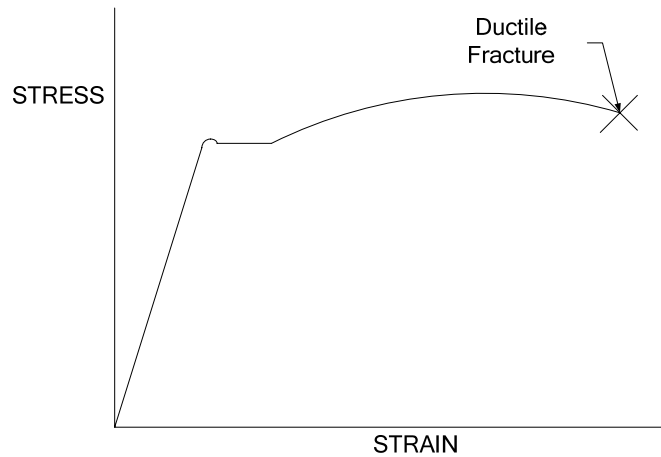
Figure 2.54 Typical Stress-Strain Curve for Mild Steel

Brittle fracture is sudden and without warning. With brittle fracture, there is little or no plastic deformation or yielding prior to separation of the member or component. Thus, the ultimate strength of the member is typically not reached (Figure 2.55). Since the average stress level at the time of brittle fracture is usually below the yield stress, there is less internal energy and the strength of the member or component is reduced. Brittle fracture typically initiates at an initial flaw or discontinuity in the steel. When a critical stress level is reached at a flaw, crack growth will continue in an unstable fashion at a nearly instantaneous rate until complete separation occurs. Thus, there is an interaction between the crack size and the tensile stress level. As crack size increases, the tensile stress level at which brittle fracture occurs decreases, while smaller cracks can tolerate higher tensile stress levels prior to failure. Hence, it is obviously important to control the size of any discontinuities during the fabrication process.
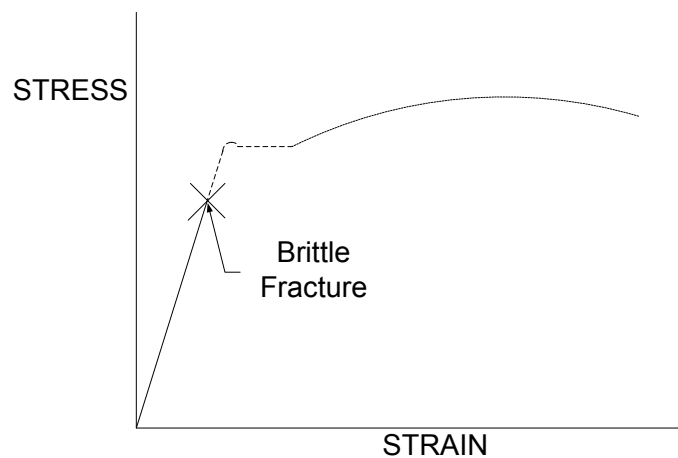

Figure 2.55 Stress-Strain Curve Indicative of a Brittle Fracture

Fracture toughness is a material property that is defined in the *AASHTO LRFD* Specifications as a measure of the ability of a structural material or element to absorb energy without fracture. As the fracture toughness of steel increases, its

ability to tolerate combinations of higher tensile stress and larger cracks prior to unstable crack growth also increases. The fracture toughness of the steel is ideally defined as the area under the stress-strain curve. Thus, a material experiencing a ductile fracture has a much larger area under the stress-strain curve (Figure 2.54), and thus, a larger fracture toughness (versus a material experiencing a brittle fracture). Materials such as steel, aluminum and copper have relatively high fracture toughness versus materials such as concrete, cast iron and stone.

The fracture toughness of steel is a function of the material properties, temperature, load rate and degree of constraint. As the yield strength of the steel increases, the ductility of the steel and its ability to plastically deform generally decreases. Alloying and heat treatment of these steels during manufacture is used to increase the fracture toughness. Fracture toughness decreases with temperature. At a certain temperature, called the transition temperature, bridge steels change from ductile to brittle. Slow static load rates result in a higher fracture toughness than rapid dynamic load rates. Truck loading on bridges generally results in an intermediate load rate. Highly constrained details, such as those utilizing thick plates, large welds and/or complex geometries, will also exhibit a lower fracture toughness because of the reduced ability of the steel to deform around a crack. As plate thickness increases, the ability of the plate to plastically deform also decreases.

During the fabrication process, preexisting cracks are introduced during the welding process and cannot be avoided. Quality control procedures during fabrication are intended to minimize the size of the initial flaws to increase both the fatigue and fracture resistance of welded details. The intent of the fatigue-design provisions in AASHTO is to prevent or limit stable crack growth, or small incremental crack growth (i.e. fatigue crack propagation) under cyclic loading over the service life of the structure, as continued fatigue crack growth will eventually result in brittle fracture if it not detected and arrested. Using a detail with a higher fatigue resistance or lowering the stress range at the detail can increase the fatigue design life or number of cycles required for failure. The inherent fracture toughness of the steel will limit the fatigue design life due to the maximum crack size that can be tolerated prior to brittle fracture (i.e. unstable crack growth).

Previous AASHTO Specifications specified separate permissible stress ranges for redundant and nonredundant members, with the limiting values for nonredundant members arbitrarily specified to be 80 percent of the limiting values specified for redundant members. However, as discussed below, larger fracture toughness is demanded in the AASHTO Specifications for members used in nonredundant applications. Since the reduction in permissible stress range in combination with the requirements for greater fracture toughness were considered by the specification writers to be an unnecessary double penalty for nonredundant members, only the permissible stress ranges for redundant members were carried forward to the *AASHTO LRFD* Specifications and are to be applied to both redundant and nonredundant members.

AASHTO has adopted a fracture control plan to ensure that bridge details do not fail due to brittle fracture. The fracture control plan, which was originally issued as an AASHTO Guide Specification in 1978 and is now instead given in Section 12 of

Reference 70, places controls on material properties and initial flaw sizes to provide adequate performance. The fracture control plan specifies: design and review responsibilities; welding inspector, fabricator and NDT personnel qualification and certification; welding requirements; welding procedures; welding repair procedures and required fracture toughness of the steel and weld metal. Stringent preheat and interpass temperature requirements are included to minimize the potential for hydrogen-induced cracking, which results from the presence of hydrogen (moisture) in the molten weld metal. As the weld cools and solidifies, the hydrogen migrates to the grain boundaries of the metal resulting in a weakened plane in the weld, which eventually cracks due to the presence of restraint and tensile residual stresses. The crack reduces the strength of the weld and may potentially lead to fatigue crack growth.

The fracture control plan utilizes the Charpy V-Notch impact test to determine the fracture toughness requirements for various bridge steels. Small, notched steel specimens are loaded at very high strain rates as the specimen absorbs the impact from a pendulum (Figure 2.56).   The maximum height the pendulum rises after impact measures the amount of energy absorbed in foot-pounds. When sets of specimens are tested at different temperatures, there is a shift or transition in energy absorption with temperature, as shown in Figure 2.57. It is obviously desirable for bridge steels to be operating in the area to the right of the transition zone.

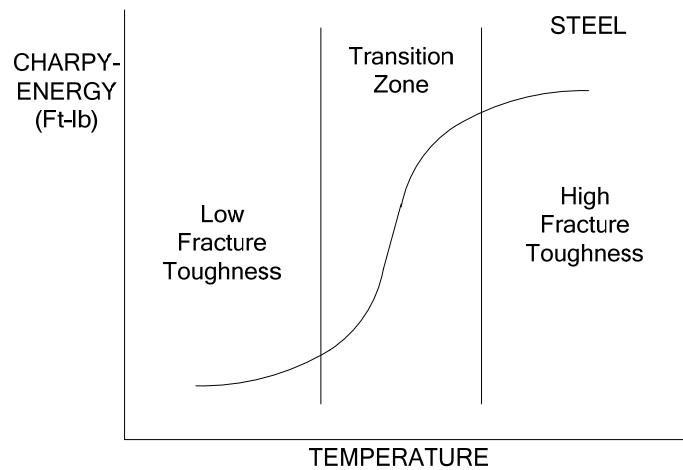**Figure 2.56 Charpy V Notch Testing Machine**

Figure 2.57 Typical Plot of Charpy Energy Versus Temperature for a Steel

The Charpy V-Notch impact test is a relatively severe test of fracture toughness and does not define the conditions under which bridge steels actually operate. The load rate that a Charpy impact specimen is subject to in the transition zone is approximately five times that expected during bridge loading. The fracture toughness decreases as the load rate increases at a given temperature. The constraint around the fracture zone of the Charpy specimen is typically more severe than found in bridges. Although plates thicker than the thickness of a Charpy specimen are used in bridges, a minimum level of fracture toughness is reached in the Charpy test, as the test represents a plane-strain condition. No further reduction in fracture toughness than the level attained in the Charpy test is realized with increasing plate thickness. The temperatures at which the impact tests are performed are also generally higher than the bridge is subject to.

The AASHTO fracture control plan uses three different temperature zones (designated Zones 1, 2 and 3) to qualify the fracture toughness of bridge steels. The three zones are differentiated by their minimum operating (or service) temperatures, which are given in *AASHTO LRFD* Table 6.6.2-1. The required fracture toughness increases as the minimum expected service temperature for the bridge decreases. The fracture toughness requirements (*AASHTO LRFD* Table 6.6.2-2) for various bridge steels are given in terms of the energy (in foot-pounds) absorbed by the Charpy specimens at specified test temperatures for the three different temperature zones. The requirements vary depending on whether the member is welded or mechanically fastened. The Charpy test temperatures are on average 70 degrees higher than the minimum service temperature for each zone to compensate for the higher load rates experienced by the test specimens (*71*). For higher strength steels, the requirements are generally more stringent for thicker plates. For the newer high performance steels (HPS), which provide significant improvements in fracture toughness, it was decided that these steels would be required to meet more stringent Zone 3 requirements in all three temperature zones (*41*).

Separate fracture toughness requirements are given in *AASHTO LRFD* Table 6.6.2-2 for nonfracture-critical and fracture-critical members (or components). A fracture-critical member (FCM) is defined as a component in tension whose failure is

expected to result in the collapse of the bridge or the inability of the bridge to perform its function. FCMs are subject to more stringent Charpy V-Notch fracture toughness requirements than nonfracture-critical members. FCMs must also be fabricated in accordance with the fracture control plan given in Reference 70. According to *AASHTO LRFD* Article 6.6.2, the Engineer has the responsibility to identify all bridge members or components that are fracture critical and clearly delineate their location on the contract plans. Examples of FCMs in bridges include certain truss members in tension, suspension cables, tension components of girders in two-girder systems, pin and link systems in suspended spans, cross girders and welded tie girders in tied-arches. In addition, any attachment having a length in the direction of the tension stress greater than 4 inches and welded to the tension area of a component of a FCM is also to be considered fracture critical.

Wherever possible, bridge details and concepts should be developed to provide some level of redundancy. In the *AASHTO LRFD* Specifications, redundancy is defined as the quality of a bridge that enables it to perform its design function in a damaged state. A redundant member is defined as a member whose failure does not cause failure of the bridge. At least three types of redundancy can be defined: 1) multiple load path redundancy, usually as seen in a cross-section; 2) statical redundancy or continuity of the load path from span to span (i.e. statical indeterminacy); and 3) internal member redundancy (i.e. providing multiple unwelded or mechanically fastened components of a beam, truss or arch member to act as crack arrestors). In identifying FCMs, the type(s) of redundancy that must be demonstrated is often dependent on the Owner; in some cases, only the first type of redundancy is accepted. Specific redundancy considerations related to composite steel bridges are discussed further in DM Volume 1, Chapter 2, Section 2.4.3.1.6.

AASHTO LRFD Article 6.6.2 does permit the use of refined analyses with assumed hypothetical cracked components to demonstrate redundancy, or to confirm that part of a hypothetically damaged structure is not fracture critical. Owners are becoming more receptive to such analyses. However, as discussed in *AASHTO LRFD* Article C6.6.2, the criteria for these analyses have not yet been codified so that items such as the loading cases to be considered, the location of the potential cracks, the degree of the dynamic effects to be included, the software to be used along with the degree of refinement of the model should all be agreed upon by the Owner and the Engineer. Relief from the full factored loads in the applicable strength limit state load combinations should be considered. The number of loaded design lanes versus the number of striped traffic lanes should also be given some consideration in the analysis.

As mentioned above, material for nonfracture-critical members and components sustaining tensile force effects is also subject to Charpy V-Notch testing to demonstrate adequate fracture toughness. *AASHTO LRFD* Article 6.6.2 requires that all primary *longitudinal* superstructure components and connections, except as noted, sustaining tensile force effects due to the Strength I load combination, along with transverse floorbeams subject to such effects, be subject to mandatory Charpy V-Notch fracture toughness testing. The components and connections requiring such testing (e.g. flange and web material subject to tension) must be so designated on the contract plans. The exceptions are noted as follows (unless designated

otherwise on the contract plans): splice plates and filler plates in double shear in bolted splices; intermediate transverse web stiffeners not serving as connection plates; bearings, sole plates and masonry plates; expansion dams; and drainage material. The specification of mandatory fracture toughness testing for other primary components and connections sustaining tensile force effects under the specified load combination, e.g. primary connections and components other than floorbeams that are *transverse* to the primary longitudinal components, is left to the discretion of the Owner.

58.   Munse, W.H., and L.H. Grover. 1964. "Fatigue of Welded Steel Structures." Welding Research Council, New York, NY.

59.   Gurney, T.R. 1968. "Fatigue of Welded Structures." *Cambridge University Press.*

60.   Fisher, J.W., K.H. Frank, M.A. Hirt, and B.M. McNamee. 1970. "Effect of Weldments on the Fatigue Strength of Steel Beams." NCHRP Report 102, Highway Research Board, Washington, D.C.

61.   Fisher, J.W., P.A. Albrecht, B.T. Yen, D.J. Klingerman, and B.M. McNamee. 1974. "Fatigue Strength of Steel Beams With Transverse Stiffeners and Attachments." NCHRP Report 147, Highway Research Board, Washington, D.C.

62.   FHWA. 1989. *Technical Advisory on Uncoated Weathering Steel in Structures.* Federal Highway Administration, U.S. Department of Transportation, Washington, D.C., October.

63.   National Highway Institute. 1990. "Economical and Fatigue Resistant Steel Bridge Details – Participant Notebook." National Highway Institute Course No. 13049, Federal Highway Administration, Publication No. FHWA-1-11-90-043, June.

64.   Fisher, J.W. 1977. "Bridge Fatigue Guide – Design and Details." American Institute of Steel Construction, Chicago, IL.

65.   Schilling, C.G. 1986. "Fatigue." Chapter I/6. *Highway Structures Design Handbook.* Available from the National Steel Bridge Alliance, Chicago, IL, February.

66.   Frank, K.H., and J.W. Fisher. 1979. "Fatigue Strength of Fillet Welded Cruciform Joints." *Journal of the Structural Division*, American Society of Civil Engineers, New York, NY, Vol. 105, No. ST9, September.

67.   Miner, M.A. 1945. "Cumulative Damage in Fatigue." *Journal of Applied Mechanics.* Volume 12, September.

68.   Schilling, C.G., K.H. Klippstein, J.M. Barsom, and G.T. Blake. 1975. "Fatigue of Welded Steel Bridge Members Under Variable-Amplitude Loadings." Final Report – NCHRP Project 12-12, Transportation Research Board, Washington, D.C., August.

69.   AASHTO. 1989. *Guide Specifications for Fatigue Design of Steel Bridges.* American Association of State Highway and Transportation Officials, Inc., Washington, D.C.

70.   AASHTO/AWS D1.5M/D1.5. 2002. *Bridge Welding Code.* American National Standard/American Association of State Highway and Transportation Officials/American Welding Society, Washington, D.C.

71.   AISI. 1975. *The Development of AASHTO Fracture-Toughness Requirements for Bridge Steels.*   American Iron and Steel Institute, Washington, D.C., February.

2.2.3.7 Strength Limit State Verifications

As specified in *AASHTO LRFD* Article 1.3.2.4, the strength limit state is taken to ensure that strength, as well as both global and local stability, are provided to resist the statistically significant load combinations that a bridge is expected to experience over its design life.   As mentioned in the Commentary to this article, structural damage and distress may be expected to occur at the strength limit state, but overall structural integrity should be maintained.

For steel structures, *AASHTO LRFD* Article 6.5.4 states that the strength load combinations specified in *AASHTO LRFD* Table 3.4.1-1 in combination with the resistance factors specified in *AASHTO LRFD* Article 6.5.4.2 are to be used to check the strength limit state. *AASHTO LRFD* Article 6.10.6 provides a "roadmap" to direct the Engineer to the appropriate articles giving the specific strength limit state checks that are to be made for composite or noncomposite I-section flexural members in regions of positive or negative flexure, as discussed in more detail below.

Helpful flowcharts detailing the design checks for flexure to be made at the strength limit state (discussed below) are provided in Appendix C to Section 6 of the *AASHTO LRFD Specifications*. A flowchart summarizing the basic "roadmap" presented in *AASHTO LRFD* Article 6.10.6 is given in *AASHTO LRFD* Figure C6.4.4-1.   The design checks for composite sections in positive flexure are summarized in the flowchart given in *AASHTO LRFD* Figure C6.4.5-1. The design checks for noncomposite sections and composite sections in negative flexure (according to the slender-web provisions given in *AASHTO LRFD* Article 6.10.8) are summarized in the flowchart given in *AASHTO LRFD* Figure C6.4.6-1.   Related flowcharts for the optional design provisions in *AASHTO LRFD* Appendix A to Section 6 (to be discussed below) and for determining unbraced length requirements to develop the maximum potential lateral-torsional buckling resistance in the presence of a moment gradient (see *AASHTO LRFD* Article D6.4 in Appendix D to Section 6) are given in *AASHTO LRFD* Figure C6.4.7-1 and in *AASHTO LRFD* Figures C6.4.8-1 and C6.4.9-1, respectively.   A flowchart for shear design is presented in *AASHTO LRFD* Article C6.10.9.1 (*AASHTO LRFD* Figure C6.10.9.1-1).

2.2.3.7.1 Flexure

In all the subsequent discussions below, the resistance factor for flexure ϕ_f is to be taken as 1.0, as specified in *AASHTO LRFD* Article 6.5.4.2.

As discussed in *AASHTO LRFD* Article C6.10.6.2.1, the flexural design provisions in the *AASHTO LRFD Specifications* assume low or zero levels of axial force in the member. Should a concentrically applied axial force due to the factored loads P_u in excess of ten percent of the factored axial resistance of the member P_r be applied at the strength limit state, the section should instead be checked according to the beam-column interaction equations given in *AASHTO LRFD* Article 6.8.2.3 or

6.9.2.2, as applicable (see Section 2.4.2.2.2 and 2.4.3.2.2 of this chapter). According to the beam-column interaction equations in these articles, when P_u is ten percent of P_r, the flexural resistance of the member is reduced by five percent. The specification writers felt that it would be reasonable to ignore the effect of the axial force in the design below this level. For a more-in-depth discussion regarding the design of composite steel bridge girders subjected to combined axial compression and flexure, such as might occur in a cable-stayed system with a composite I-girder deck system, the reader is referred to Reference 154.

As specified in *AASHTO LRFD* Article 6.10.6.2.1, if there are holes in the tension flange of a flexural member at the section under consideration, the tension flange must satisfy the following requirement at the strength limit state (*AASHTO LRFD* Article 6.10.1.8):

$$f_t \leq 0.84 \left(\frac{A_n}{A_g} \right) F_u \leq F_{yt}$$

<div align="right">Equation 2.92</div>

<div align="right">*AASHTO LRFD* Equation 6.10.1.8-1</div>

where:

A_n = net area of the tension flange determined as specified in *AASHTO LRFD* Article 6.8.3 (in.^{2})

A_g = gross area of the tension flange (in.^{2})

f_t = stress on the gross area of the tension flange due to the factored loads calculated without consideration of flange lateral bending (ksi)

F_u = specified minimum tensile strength of the tension flange determined as specified in *AASHTO LRFD* Table 6.4.1-1 (ksi)

It is assumed that the holes are the size of those typically used for connectors, such as bolts. For larger holes, the provisions of *AASHTO LRFD* Article 6.8.1 should be applied instead. If Equation 2.92 is satisfied, fracture on the net section of the tension flange is theoretically prevented and need not be explicitly checked. The factor of 0.84 in Equation 2.92 is approximately equivalent to the ratio of the resistance factor for fracture of tension members ϕ_u = 0.80 to the resistance factor for yielding of tension members ϕ_y = 0.95 (*AASHTO LRFD* Article 6.5.4.2). As will be discussed below, at compact composite sections in positive flexure and at composite sections in negative flexure and noncomposite sections designed according to the optional provisions of Appendix A, with no holes in the tension flange, the nominal flexural resistance is permitted to exceed the moment at first yield at the strength limit state. However, pending further research, the specification currently requires that Equation 2.92 still be checked at such sections where there are holes in the tension flange, which will likely prevent holes from being located in these sections at or near points of maximum applied moment where significant yielding of the web may occur.

2.2.3.7.1.1 Composite Sections in Positive Flexure

Fundamental issues related specifically to the behavior of composite sections subject to positive flexure were reviewed in a previous section of this chapter under Fundamental Concepts (Section 2.2.3.1.1.4). The specific *AASHTO LRFD* design requirements for these sections will now be discussed here.

Compact sections were defined previously as composite sections *in straight girders* subject to positive flexure that satisfy specific steel grade, web slenderness and ductility requirements such that the nominal flexural resistance is permitted to exceed the moment at first yield at the strength limit state. Sections in horizontally curved bridges, or sections not meeting one or more of these requirements, are termed noncompact sections. The design requirements for each of these types of sections are discussed below.

2.2.3.7.1.1.1 Compact Sections

AASHTO LRFD Article 6.10.6.2.2 defines the specific requirements that must be met in order for a composite section in positive flexure in a straight bridge to qualify as compact. These requirements are restated as follows:

- ➢ The specified minimum yield strengths of the flanges must not exceed 70.0 ksi;
- ➢ The web must satisfy the requirement of *AASHTO LRFD* Article 6.10.2.1.1 (i.e. $D/t_w \leq 150$ or no longitudinal stiffeners); and
- ➢ The web must satisfy the following web slenderness limit:

$$\frac{2D_{cp}}{t_w} \leq 3.76\sqrt{\frac{E}{F_{yc}}}$$

Equation 2.93

AASHTO LRFD Equation 6.10.6.2.2-1

where:
D_{cp} =   depth of the web in compression at the plastic moment determined as specified in *AASHTO LRFD* Article D6.3.2 (see Section 2.2.2.3.2 of this chapter)(in.)

The reasoning behind each of these requirements was discussed previously (see Section 2.2.3.1.1.4 under Fundamental Concepts).

The nominal flexural resistance of compact sections is given in *AASHTO LRFD* Article 6.10.7.1. As specified in *AASHTO LRFD* Article 6.10.7.1.1, at the strength limit state, these sections must satisfy the one-third rule equation (discussed previously) expressed in terms of bending moment as follows:

$$M_u + \frac{1}{3}f_\ell S_{xt} \leq \phi_f M_n$$

Equation 2.94

AASHTO LRFD Equation 6.10.7.1.1-1

where:

f_ℓ = lateral bending stress in the tension flange (ksi). f_ℓ is always taken as positive.

M_n = nominal flexural resistance of the section determined as specified in *AASHTO LRFD* Article 6.10.7.1.2 (see below)(kip-in.)

M_u = member major-axis bending moment due to the factored loads at the section under consideration (kip-in.). M_u is always taken as positive.

S_x = elastic section modulus about the major-axis of the section to the tension flange taken as M_{yt}/F_{yt}

The moment format is used because for these types of sections, the major-axis bending moment is physically a more meaningful quantity than the elastically computed flange bending stress. Also, the nominal flexural resistance of these sections is generally greater than the yield moment with respect to the tension flange M_{yt}. If desired, the equation could be considered in a stress format by dividing both sides of the equation by S_{xt}. Equation 2.94 is a conservative but accurate representation of a section analysis in which a pair of fully-yielded widths are discounted from the tension flange to accommodate flange lateral bending, with the remainder of the flange assumed to resist the vertical loads.

Note that only lateral bending in the bottom (tension) flange is considered in Equation 2.94. Lateral bending does not need to be considered in the top (compression) flange of these sections at the strength limit state because that flange is continuously supported by the concrete deck. Sources of lateral bending in the bottom flange of these sections at the strength limit state include curvature, wind loading and the effect of staggered cross-frames/diaphragms and/or support skew. The determination of flange lateral bending moments due to curvature is addressed in *AASHTO LRFD* Article 4.6.1.2.4b. Determination of flange lateral bending moments due to wind is discussed in *AASHTO LRFD* Article C4.6.2.7.1. Lateral flange bending due to staggered cross-frames/diaphragms and/or support skew is discussed in *AASHTO LRFD* Article C6.10.1 and is preferably handled by a direct structural analysis of the bridge superstructure. *AASHTO LRFD* Article C6.10.1 does contain a suggested value of f_ℓ to use for the preceding case in lieu of a direct structural analysis, if desired. Additional discussion on lateral flange bending in skewed bridges may be found in Section 2.2.3.8 of this chapter. As specified in *AASHTO LRFD* Article 6.10.1.6, the sum of the flange lateral bending stresses due to all sources cannot exceed $0.6F_{yf}$. Amplification of the flange lateral bending stresses is not required in this case since the bottom flange is in tension.

Note that in all the one-third rule equations within the specification, when the effects of flange lateral bending are judged to be insignificant or incidental, the flange lateral bending term, f_ℓ, is simply set equal to zero in the appropriate equations. The format of the equations then reduces to the more conventional and familiar format for checking the nominal flexural resistance of I-sections in the absence of flange lateral bending.

As specified in *AASHTO LRFD* Article 6.10.7.1.2, the nominal flexural resistance M_n of compact composite sections in positive flexure is given as follows:

> ➢ If $D_p \leq 0.1D_t$, then:

$$M_n = M_p$$

<div align="right">Equation 2.95</div>

<div align="right">*AASHTO LRFD* Equation 6.10.7.1.2-1</div>

> ➢ Otherwise:

$$M_n = M_p \left(1.07 - 0.7 \frac{D_p}{D_t} \right)$$

<div align="right">Equation 2.96</div>

<div align="right">*AASHTO LRFD* Equation 6.10.7.1.2-2</div>

where:
- D_p = distance from the top of the concrete deck to the neutral axis of the composite section at the plastic moment (in.)
- D_t = total depth of the composite section (in.)
- M_p = plastic moment of the composite section determined as specified in *AASHTO LRFD* Article D6.2 (see Section 2.2.2.1 of this chapter)(kip-in.)

In Equation 2.96, the nominal flexural resistance is reduced from M_p as a linear function of D_p/D_t when D_p exceeds $0.1D_t$ to provide an additional margin of safety against premature crushing of the concrete deck. Equation 2.96 is a simplified form of the equation given in previous Specifications.

For sections in continuous spans, the nominal flexural resistance is also given by Equation 2.95 or 2.96, as applicable, but the section must also satisfy the following:

$$M_n \leq 1.3R_hM_y$$

<div align="right">Equation 2.97</div>

<div align="right">*AASHTO LRFD* Equation 6.10.7.1.2-3</div>

where:
- M_y = yield moment determined as specified in *AASHTO LRFD* Article D6.2 (see Section 2.2.2.2 of this chapter)(kip-in.)
- R_h = hybrid factor determined as specified in *AASHTO LRFD* Article 6.10.1.10.1 (see Equation 2.21)

The reason for this limitation is discussed at some length in Section 2.2.3.1.1.4 under Fundamental Concepts.   The nominal flexural resistance need not be subject to this limitation when:

> ➢ The span under consideration and all adjacent interior-pier sections satisfy the requirements of *AASHTO LRFD* Article B6.2, and:
> ➢ The appropriate value of θ_{RL} from *AASHTO LRFD* Article B6.6.2 exceeds 0.009 radians at all adjacent interior-pier sections.

Sections meeting the above requirements are assumed to have sufficient ductility and robustness such that the redistribution of moments to adjacent pier sections caused by partial yielding within the positive flexure regions is inconsequential. The specific requirements of *AASHTO LRFD* Article B6.2 are discussed in more detail in Section 2.2.3.11 of this chapter on Moment Redistribution.   Basically, these requirements spell out necessary restrictions on skew and cross-frame alignment, and on steel grade, compression-flange slenderness and bracing, web slenderness, shear and minimum available plastic rotation capacity at the adjacent pier sections. θ_{RL} is defined in *AASHTO LRFD* Article B6.6.2 as the plastic rotation at which the interior-pier section moment begins to decrease with increasing plastic rotation. The specified value of 0.009 radians for θ_{RL} is assumed to be an upper bound value of the potential increase in the plastic rotations at adjacent interior-pier sections caused by any positive-moment yielding. *AASHTO LRFD* Article C6.10.7.1.2 indicates the types of interior-pier sections that meet these restrictions. Included in this list are most rolled shapes or welded shapes of comparable proportions.

In addition, compact composite sections in positive flexure must satisfy the ductility requirement specified in *AASHTO LRFD* Article 6.10.7.3 as follows:

$$D_p \leq 0.42 D_t$$

<div align="right">Equation 2.98

AASHTO LRFD Equation 6.10.7.3-1</div>

to prevent premature crushing of the concrete deck. This requirement is equivalent to the maximum reinforcement requirement for concrete structures specified in *AASHTO LRFD* Article 5.7.3.3.1. The thickness of the concrete deck haunch over the girder may be conservatively neglected in the calculation of D_t. Otherwise, a lower-bound estimate of this thickness should be used.

2.2.3.7.1.1.2 Noncompact Sections

The nominal flexural resistance of noncompact sections is given in *AASHTO LRFD* Article 6.10.7.2. As specified in *AASHTO LRFD* Article 6.10.7.2.1, at the strength limit state, the compression flange of these sections must satisfy the following:

$$f_{bu} \leq \phi_f F_{nc}$$

<div align="right">Equation 2.99

AASHTO LRFD Equation 6.10.7.2.1-1</div>

where:
f_{bu}	=	flange stress at the section under consideration calculated without consideration of flange lateral bending (ksi). f_{bu} is always taken as positive
F_{nc}	=	nominal flexural resistance of the compression flange determined as specified in *AASHTO LRFD* Article 6.10.7.2.2 (ksi)

The tension flange of these sections must satisfy the one-third rule equation (discussed previously) expressed in terms of stress as follows:

$$f_{bu} + \frac{1}{3}f_\ell \le \phi_f F_{nt} \qquad\qquad \text{Equation 2.100}$$

<div align="right">*AASHTO LRFD* Equation 6.10.7.2.1-2</div>

where:

F_{nt} =   nominal flexural resistance of the tension flange determined as specified in *AASHTO LRFD* Article 6.10.7.2.2 (ksi)

The stress format is more appropriate in members for which the maximum resistance is always less than or equal to the yield moment in major-axis bending. Again, flange lateral bending is not considered for the compression flange in Equation 2.99 because at the strength limit state, the flange is continuously supported by the concrete deck.

As specified in *AASHTO LRFD* Article 6.10.7.2.2, the nominal flexural resistance of the compression flange F_{nc} of a noncompact composite section in positive flexure is taken as:

$$F_{nc} = R_b R_h F_{yc} \qquad\qquad \text{Equation 2.101}$$

<div align="right">*AASHTO LRFD* Equation 6.10.7.2.2-1</div>

where:

R_b =   web load-shedding factor determined as specified in *AASHTO LRFD* Article 6.10.1.10.2 (Equation 2.19)

R_h =   hybrid factor determined as specified in *AASHTO LRFD* Article 6.10.1.10.1 (Equation 2.21)

The nominal flexural resistance of the tension flange F_{nt} is taken as:

$$F_{nt} = R_h F_{yt} \qquad\qquad \text{Equation 2.102}$$

<div align="right">*AASHTO LRFD* Equation 6.10.7.2.2-2</div>

Load shedding of the web compressive stresses to the tension flange as a result of bend buckling of the web is considered insignificant; therefore, the R_b factor is not included in Equation 2.102.

In addition, noncompact composite sections in positive flexure must satisfy the ductility requirement specified in *AASHTO LRFD* Article 6.10.7.3 (Equation 2.98) to ensure a ductile failure, and to prevent premature crushing of the deck for sections that may utilize up to 100-ksi steel and/or that are utilized in shored construction. Should shored construction be used, the maximum longitudinal compressive stress in the deck is also limited to 0.6f′$_c$ at the strength limit state to ensure linear behavior of the concrete according to *AASHTO LRFD* Article 6.10.7.2.1. As discussed in *AASHTO LRFD* Article C6.10.1.1.1a, the use of shored construction is not recommended (see also Section 2.2.1.2 of this chapter).

EXAMPLE

Check the composite section shown in Figure 2.3, which is from an exterior girder in a continuous-span bridge in a region of positive flexure, for the Strength V load combination (see DM Volume 1, Chapter 5 for more information on the Strength V load combination). The girder is homogeneous with the flanges and web having a yield strength of 50 ksi. The load modifier η is assumed to be 1.0. Assume unshored construction. Use the section properties computed earlier for this section. Assume the following unfactored bending moments:

M_{DC1} = +2,202 kip-ft
M_{DC2} = +335 kip-ft
M_{DW} = +322 kip-ft
M_{LL+IM} = +3,510 kip-ft

Determine first if the section qualifies as a compact section. According to *AASHTO LRFD* Article 6.10.6.2.2, composite sections in positive flexure in straight bridges qualify as compact when: 1) the specified minimum yield strengths of the flanges do not exceed 70 ksi (ok), 2) the web satisfies the requirement of *AASHTO LRFD* Article 6.10.2.1.1 such that longitudinal stiffeners are not required; i.e. $D/t_w \leq 150$ (D/t_w = 69.0/0.5 = 138.0 < 150 ok), and 3) the section satisfies the web-slenderness limit given by Equation 2.93 (earlier computations indicated that the plastic neutral axis of the composite section is located in the top flange. Therefore, according to *AASHTO LRFD* Article D6.3.2, D_{cp} is taken equal to zero for this case, and thus, Equation 2.93 is considered to be automatically satisfied). Therefore, the section qualifies as a compact section.

Compact composite sections in positive flexure must satisfy the ductility requirement given by Equation 2.98 to protect the concrete deck from premature crushing. At this section:

$$D_p = 9.0 + 3.5 - 1.0 + 0.44 = 11.94 \text{ in.}$$

$$D_t = 1.375 + 69.0 + 3.5 + 9.0 = 82.88 \text{ in.}$$

$$0.42D_t = 0.42(82.88) = 34.81 \text{ in.} > 11.94 \text{ in.} \qquad \text{ok}$$

In I-girder bridges with composite concrete decks, wind load on the upper half of the exterior girder, the deck, the barriers and the vehicles may be assumed transmitted directly to the deck, which acts as a lateral diaphragm to carry the load to the supports. Wind load on the lower half of the exterior girder may be assumed applied laterally to the bottom flange, which transmits the load to the adjacent cross-frames or diaphragms by flexural action. The frame action of the cross-frames or diaphragms then transmits the forces to the deck, which in turn transmits them to the supports through diaphragm action.

AASHTO LRFD Article C4.6.2.7.1 provides the following formula for the factored wind force per unit length applied to the bottom flange of composite or noncomposite exterior members with cast-in-place concrete or orthotropic steel decks:

$$W = \frac{\eta \gamma P_D d}{2}$$

AASHTO LRFD Equation C4.6.2.7.1-1

where P_D is the design horizontal wind pressure specified in *AASHTO LRFD* Article 3.8.1 and d is the depth of the girder. Assume for this example that P_D is calculated to be 0.053 ksf. (see the wind-load example in Section 2.2.3.4.4 of this chapter under Constructibility Verifications for the procedures used to calculate P_D).

P_D is to be assumed uniformly distributed on the area exposed to the wind. The exposed area is to be the sum of the area of all components as seen in elevation taken perpendicular to the assumed wind direction. The direction of the wind is to be varied to determine the extreme force effect in the structure or its components. For cases where the wind is not taken as normal to the structure, lateral and longitudinal components of the base wind pressure P_B for various angles of wind direction (assuming a base wind velocity V_B = 100 mph) are given in *AASHTO LRFD* Table 3.8.1.2.2-1. The angles are assumed measured from a perpendicular to the longitudinal axis. As specified in *AASHTO LRFD* Article 3.8.1.2.1, the total wind load WS per unit length *acting on girder spans* is not to be taken less than 0.3 klf.

Assuming no superelevation for the example bridge and a barrier height of 42 inches above the concrete deck, the minimum exposed height of the composite superstructure is computed as:

$$h_{exp.} = (0.875 + 69.0 + 3.5 + 9.5 + 42.0)/12 = 10.41\,\text{ft}$$

The total wind load per unit length w for the case of wind applied normal to the structure is computed as:

$$w = P_D h_{exp.} = 0.053(10.41) = 0.55\,\text{kips/ft} > 0.3\,\text{kips/ft} \qquad \text{ok}$$

For the wind-load path identified above, *AASHTO LRFD* Article C4.6.2.7.1 also provides the following approximate equation for computing the maximum flange lateral bending moment due to the factored wind load M_w within the unbraced length under consideration:

$$M_w = \frac{WL_b^2}{10}$$

AASHTO LRFD Equation C4.6.2.7.1-2

The unbraced length L_b at this section is 24.0 feet. Assemble the factored actions needed to check Equation 2.94 at this section.

Wind pressure on live load (WL) is specified in *AASHTO LRFD* Article 3.8.1.3. Wind pressure on live load is to be represented by a moving force of 0.1 klf acting normal to and 6 feet above the roadway, which results in an overturning force on the vehicle similar to the effect of centrifugal force on vehicles traversing horizontally curved bridges. The horizontal line load is to be applied to the same tributary area as the design lane load for the force effect under consideration. When wind on live load is

not taken normal to the structure, the normal and parallel components of the force applied to the live load may be taken from *AASHTO LRFD* Table 3.8.1.3-1. In this example, WL is assumed transmitted directly to the deck and is therefore not considered in the Strength V load combination. For simplicity, the effect of the overturning force due to WL on the vehicle wheel loads is also not considered in this example. It should be mentioned that for load cases where the direction of the wind is taken perpendicular to the bridge and there is no wind on live load considered, a vertical wind pressure of 0.020 ksf applied to the entire width of the deck is to be applied in combination with the horizontal wind loads to investigate potential overturning of the bridge (*AASHTO LRFD* Article 3.8.3). This load case is not investigated in this example.

The amplification factor, AF, for f_ℓ (*AASHTO LRFD* Article 6.10.1.6) is taken equal to 1.0 for flanges in tension. Note again that first- or second-order flange lateral bending stresses, as applicable, are limited to a maximum value of $0.6F_{yf}$ according to Equation 6.10.1.6-1. Therefore,

For Strength V:

Dead and live loads:

$$M_u = 1.0[1.25(2,202 + 335) + 1.5(322) + 1.35(3,510)] = 8,393 \text{ kip} - \text{ft}$$

Wind loads:

$$W = \frac{1.0(0.4)(0.053)(1.375 + 69.0 + 1.0)/12}{2} = 0.063 \text{ kips / ft}$$

$$M_w = \frac{0.063(24.0)^2}{10} = 3.63 \text{ kip} - \text{ft}$$

$$f_\ell = \frac{M_w}{S_\ell} = \frac{3.63(12)}{1.375(18)^2/6} = 0.587 \text{ ksi} * AF = 0.587(1.0) = 0.587 \text{ ksi} < 0.6F_{yf} = 30.0 \text{ ksi ok}$$

From an examination of the above flange lateral bending stress, it is apparent that for typical cross-frame spacings, the majority of the wind force on the lower half of a composite structure is transmitted directly to the deck through the cross-frames and only a small portion of the force is resisted through lateral bending of the bottom flange.

Determine the nominal flexural resistance of the section according to the provisions of *AASHTO LRFD* Article 6.10.7.1.2. For this section, M_p and M_y were computed earlier to be 14,199 kip-ft and 10,171 kip-ft, respectively (see Section 2.2.2.1 and Section 2.2.2.2 of this chapter).

$$0.1D_t = 0.1(82.88) = 8.29 \text{ in.} < D_p = 11.94 \text{ in.}$$

Therefore,

$$M_n = M_p\left(1.07 - 0.7\frac{D_p}{D_t}\right)$$

AASHTO LRFD Equation 6.10.7.1.2-2

$$M_n = 14{,}199\left[1.07 - 0.7\left(\frac{11.94}{82.88}\right)\right] = 13{,}761\,\text{kip} - \text{ft}$$

However, in a continuous span, the nominal flexural resistance of the section is limited to the following:

$$M_n = 1.3R_h M_y$$

AASHTO LRFD Equation 6.10.7.1.2-3

Or,

$$M_n = 1.3(1.0)(10{,}171) = 13{,}222\,\text{kip} - \text{ft} \quad \text{(governs)}$$

$$\therefore \qquad M_n = 13{,}222\ \text{kip} - \text{ft}$$

Calculate S_{xt}. The yield moment, M_y, was calculated with respect to the tension flange; therefore, $M_{yt} = M_y$:

$$S_{xt} = \frac{M_{yt}}{F_{yt}} = \frac{10{,}171(12)}{50} = 2{,}441\,\text{in}^3$$

Check Equation 2.94 now that all the required information has been assembled:

$$M_u + \frac{1}{3}f_\ell S_{xt} \le \phi_f M_n$$

AASHTO LRFD Equation 6.10.7.1.1-1

For Strength V:

$$M_u + \frac{1}{3}f_\ell S_{xt} = 8{,}393\ \text{kip} - \text{ft} + \frac{1}{3}\frac{(0.587)(2{,}441)}{12} = 8{,}433\ \text{kip} - \text{ft}$$

$$\phi_f M_n = 1.0(13{,}222) = 13{,}222\ \text{kip} - \text{ft}$$

$$8{,}433\ \text{kip} - \text{ft} < 13{,}222\ \text{kip} - \text{ft} \quad \text{ok}$$

The section has significant excess flexural resistance under this load combination at the strength limit state. Other limit-state criteria (e.g. service limit state or fatigue limit state criteria) are likely to control the design of the section in this case. As a result, consideration could be given to treating this section conservatively as a noncompact section, which simplifies the calculations somewhat and should not result in a significant loss of economy.

2.2.3.7.1.2 Composite Sections in Negative Flexure and Noncomposite Sections

Fundamental issues related specifically to the behavior of composite sections in negative flexure and noncomposite sections – specifically, noncomposite members with full lateral support, lateral-torsional buckling and compression-flange local buckling -- were reviewed in a previous section of this chapter entitled Fundamental Concepts. The specific *AASHTO LRFD* design requirements for these sections will now be discussed here.

As discussed in the preceding section, composite sections in positive flexure are classified as either compact or noncompact sections in the *AASHTO LRFD Specifications.* Previous Specifications also applied similar classifications to composite sections in negative flexure and noncomposite sections. However, in the *AASHTO LRFD Specifications*, new classifications were introduced for these latter types of sections. These new classifications were discussed previously in the section on Fundamental Concepts. However, they will be restated here, as it is important for the Engineer to understand these new classifications as they apply to composite sections in negative flexure and noncomposite sections in order to distinguish them from previous classifications and the extant classifications for composite sections in positive flexure. The new classifications are:

> ➢ *Compact Web Sections*: a noncomposite section or a composite section in negative flexure that has a web with a slenderness at or below which the section can achieve a maximum flexural resistance M_{max} equal to the plastic moment M_p prior to web bend buckling having a statistically significant influence on the response;
> ➢ *Noncompact Web Sections*: a noncomposite section or a composite section in negative flexure that has a web satisfying specific steel grade requirements and with a slenderness at or below which theoretical web bend-buckling does not occur at elastic stress levels, computed according to beam theory, smaller than F_{max} or M_{max}, as applicable;
> ➢ *Slender Web Sections*: a noncomposite section or a composite section in negative flexure that has a web with a slenderness at or above which the theoretical bend-buckling stress is reached in the web prior to reaching M_y.

Again, Figure 2.17 illustrates the basic relationship between the maximum potential flexural resistance M_{max} (or equivalently F_{max}) and the web slenderness $2D_c/t_w$ for all three types of sections; compact web, noncompact web and slender web (assuming yielding with respect to the compression flange controls and that lateral-torsional buckling and local buckling are prevented).

As mentioned previously, compact web sections are typically shallower sections with thicker webs; that is, rolled beams and welded girder sections with proportions similar to rolled beams. Sections with compact webs are potentially able to develop their full plastic moment capacity M_p provided that specific steel grade, ductility, flange and web slenderness and lateral bracing requirements are satisfied. The web slenderness requirement for a compact web section is stated in *AASHTO LRFD* Article A6.2.1 (Appendix A) as follows:

$$\frac{2D_{cp}}{t_w} \le \lambda_{pw(D_{cp})} \qquad\qquad \text{Equation 2.103}$$

AASHTO LRFD Equation A6.2.1-1

where D_{cp} is the depth of the web in compression at the plastic moment (discussed previously) determined as specified in *AASHTO LRFD* Article D6.3.2 (Appendix D to *AASHTO LRFD* Section 6), and $\lambda_{pw(D_{cp})}$ is the limiting slenderness ratio for a compact web section given as follows:

$$\lambda_{pw(D_{cp})} = \frac{\sqrt{\dfrac{E}{F_{yc}}}}{\left(0.54\dfrac{M_p}{R_h M_y} - 0.09\right)^2} \le \lambda_{rw}\left(\frac{D_{cp}}{D_c}\right) \qquad\qquad \text{Equation 2.104}$$

AASHTO LRFD Equation A6.2.1-2

where D_c is the depth of the web in compression in the elastic range. Equation 2.104 is modified relative to the slenderness limit given in previous Specifications for these sections. The modified limit accounts for the higher demands on the web placed on singly symmetric I-sections with larger shape factors M_p/M_y (*39*, *57*). The modified limit also eliminates the need for the interaction equation between the web and compression-flange compactness requirements that was provided in previous Specifications. When M_p/M_y is equal to 1.12, which is the typical shape factor for a doubly symmetric noncomposite I-section, the slenderness limit from Equation 2.104 reduces approximately to the slenderness limit given in previous Specifications for these sections as follows (assuming a homogeneous section; i.e. R_h = 1.0):

Table 2.12

M_p/M_y = 1.12

F_{yc} (ksi)	$\lambda_{pw(D_{cp})}$
36.0	107
50.0	91
70.0	77
90.0	68
100.0	64

For a shape factor M_p/M_y equal to 1.30, which is representative of the shape factor for a composite I-section in negative flexure, the limit is as follows:

Table 2.13

$M_p/M_y = 1.30$

F_{yc} (ksi)	$\lambda_{pw(D_{cp})}$
36.0	76
50.0	64
70.0	54
90.0	48
100.0	45

The upper limit of $\lambda_{rw}(D_{cp}/D_c)$ in Equation 2.104 (see below for a discussion of the slenderness limit λ_{rw}) is to protect against extreme cases where D_c/D is significantly less than 0.5. In such cases, D_{cp}/D is typically smaller than D_c/D. As such, in certain situations, the web slenderness associated with the elastic cross-section $2D_c/t_w$ may be larger than λ_{rw} while the slenderness associated with the plastic cross-section $2D_{cp}/t_w$ may be smaller than $\lambda_{pw(D_{cp})}$. In other words, the elastic web would be classified as slender at the same time the plastic web would be classified as compact. To guard against such situations and the possibility of theoretical bend buckling of the web prior to reaching M_p, the upper limit of $\lambda_{rw}(D_{cp}/D_c)$ is placed on $\lambda_{pw(D_{cp})}$.

Other requirements for compact web sections to achieve the maximum potential flexural resistance (e.g. flange slenderness and lateral bracing requirements) will be discussed later on.

Noncompact web sections are sections of intermediate web depth that satisfy the following web slenderness requirement given in *AASHTO LRFD* Article A6.2.2 (Appendix A):

$$\frac{2D_c}{t_w} \leq \lambda_{rw} = 5.7\sqrt{\frac{E}{F_{yc}}}$$

Equation 2.105

AASHTO LRFD Equation A6.2.2-1

The limiting value of λ_{rw}, which defines the limit below which theoretical web bend buckling does not occur for elastic stress values smaller than F_{yc}, is given as follows for different grades of steel:

Table 2.14

F_{yc} (ksi)	λ_{rw}
36.0	162
50.0	137
70.0	116
90.0	102
100.0	97

Noncompact web sections that also satisfy specific steel grade, compression-flange slenderness and lateral bracing requirements (to be discussed later on) can achieve a maximum potential flexural resistance anywhere from M_y up to M_p as a linear function of the web slenderness $2D_c/t_w$ with respect to the limits $\lambda_{pw(D_{cp})}$ and λ_{rw}.

Sections having a web with a slenderness exceeding λ_{rw} are termed slender web sections. Sections with slender webs rely upon significant web post bend buckling resistance at the strength limit state. The maximum potential flexural resistance of the compression flange of such sections, satisfying specific compression-flange slenderness and lateral bracing requirements (to be discussed later on), is $R_bR_hF_{yc}$. The nominal flexural resistance of the tension flange of such sections is R_hF_{yt}.

The majority of steel-bridge I-sections utilize either slender webs or noncompact webs that approach the slenderness limit λ_{rw}. Therefore, for the design of these sections, the simpler and more streamlined provisions of *AASHTO LRFD* Article 6.10.8 (hereafter referred to as the 'Main Provisions') are the most appropriate for determining the nominal flexural resistance at the strength limit state. These provisions presume slender-web behavior, and therefore, limit the nominal flexural resistance to be less than or equal to the moment at first yield. Thus, as discussed previously, the nominal flexural resistance equations in the Main Provisions are expressed in terms of the elastically computed flange stress.

For convenience, the Main Provisions may also be applied to sections with compact webs or with noncompact webs that are nearly compact, but at the loss of some economy. Therefore, as specified in *AASHTO LRFD* Article 6.10.6.2.3, sections *in straight bridges* meeting the following requirements:

➢ The specified minimum yield strengths of the flanges do not exceed 70 ksi;
➢ The web satisfies the noncompact slenderness limit λ_{rw} given by Equation 2.105, and;
➢ The flanges satisfy the following ratio:

$$\frac{I_{yc}}{I_{yt}} \geq 0.3 \qquad\qquad \text{Equation 2.106}$$

AASHTO LRFD Equation 6.10.6.2.3-2

can optionally be proportioned according to the provisions for compact web and noncompact web sections given in *AASHTO LRFD* Appendix A to Section 6. In *AASHTO LRFD* Appendix A, the nominal flexural resistance is expressed in terms of moment and may exceed the moment at first yield. *It is strongly recommended that compact web sections be designed according to the provisions of Appendix A to minimize the potential loss in economy*. Since the types of sections that would qualify for the use of *AASHTO LRFD* Appendix A are less commonly used, these somewhat more complex provisions for their design have been placed in an appendix in order to streamline and simplify the Main Provisions. The reason for the

limiting ratio given by Equation 2.106 was discussed previously in Section 2.2.3.1.2.1 of this chapter under the topic of St. Venant torsion.

As permitted at the service limit state (as discussed previously), moment redistribution for continuous-span members in straight I-girder bridges that satisfy specific limitations spelled out in *AASHTO LRFD* Article B6.2 (in *AASHTO LRFD* Appendix B to Section 6) is also permitted at the strength limit state according to *AASHTO LRFD* Article 6.10.6.2.3. These limitations are discussed in more detail in Section 2.2.3.11 of this chapter under Moment Redistribution. Localized yielding at the strength limit state at interior-pier sections results in redistribution of elastic moments to more lightly loaded sections in positive flexure. When the limitations of *AASHTO LRFD* Article B6.2 are satisfied, the procedures in *AASHTO LRFD* Appendix B may optionally be used to calculate the redistribution moments. Should the redistribution moments be calculated according to these procedures, the nominal flexural resistance equations (to be discussed below) need not be checked within the unbraced lengths immediately adjacent to the pier sections satisfying the requirements of *AASHTO LRFD* Article B6.2. Outside of these regions, all applicable flexural resistance equations must still be satisfied after redistribution. Again, more details on the procedures given in *AASHTO LRFD* Appendix B are presented below in Section 2.2.3.11 under Moment Redistribution.

The nominal flexural resistance equations for the design of composite sections in negative flexure and noncomposite sections at the strength limit state, that are contained in the Main Provisions (i.e. *AASHTO LRFD* Article 6.10.8) and in *AASHTO LRFD* Appendix A, will next be separately discussed.

2.2.3.7.1.2.1 Main Provisions (*AASHTO LRFD* Article 6.10.8)

General

As specified in *AASHTO LRFD* Article 6.10.8.1.1, at the strength limit state, discretely braced compression flanges must satisfy the one-third rule equation (discussed previously) expressed in terms of stress as follows:

$$f_{bu} + \frac{1}{3}f_\ell \le \phi_f F_{nc}$$ Equation 2.107

AASHTO LRFD Equation 6.10.8.1.1-1

where:
f_{bu} =   compression-flange stress calculated without consideration of
               flange lateral bending determined as specified in *AASHTO LRFD*
               Article 6.10.1.6 (ksi). f_{bu} is always taken as positive.
f_ℓ =   flange lateral bending stress determined as specified in *AASHTO*
               LRFD Article 6.10.1.6 (ksi). f_ℓ is always taken as positive.
F_{nc} =   nominal flexural resistance of the compression flange determined
               as specified in *AASHTO LRFD* Article 6.10.8.2 (ksi)

At the strength limit state, discretely braced compression flanges would typically be the bottom flanges in regions of negative flexure in continuous-span composite members and all compression flanges in noncomposite members. The nominal flexural resistance of the flange F_{nc} is to be taken as the smaller of the local buckling and lateral-torsional buckling resistance of the flange (discussed below). As specified in *AASHTO LRFD* Article 6.10.1.6, for design checks involving lateral-torsional buckling, the major-axis bending compressive stress f_{bu} and flange lateral bending stress f_ℓ are to be taken as the largest values throughout the unbraced length in the flange under consideration. This is consistent with established practice in applying beam-column interaction equations involving member stability checks. For design checks involving flange local buckling, f_{bu} and f_ℓ may be taken as the corresponding values at the section under consideration. However, when maximum values of these stresses occur at different locations within the unbraced length, which is often the case, it is conservative to use the maximum values in the local buckling check.

Discretely braced tension flanges must satisfy the following relationship at the strength limit state (*AASHTO LRFD* Article 6.10.8.1.2):

$$f_{bu} + \frac{1}{3} f_\ell \leq \phi_f F_{nt}$$

<div align="right">Equation 2.108</div>

<div align="right">*AASHTO LRFD* Equation 6.10.8.1.2-1</div>

where:
f_{bu} = tension-flange stress calculated without consideration of flange lateral bending determined as specified in *AASHTO LRFD* Article 6.10.1.6 (ksi). f_{bu} is always taken as positive

F_{nt} = nominal flexural resistance of the tension flange determined as specified in *AASHTO LRFD* Article 6.10.8.3 (ksi)

At the strength limit state, discretely braced tension flanges would typically be the bottom flanges in regions of positive flexure in continuous-span composite members, the bottom flanges of simple-span composite members and all tension flanges in noncomposite members. The nominal flexural resistance of the flange F_{nt} is based on yielding. According to *AASHTO LRFD* Article 6.10.1.6, for design checks involving yielding, f_{bu} and f_ℓ may be taken as the corresponding values at the section under consideration. As discussed in the preceding paragraph, it is conservative to use the maximum values of these stresses within the unbraced length in this check.

Sources of lateral flange bending in discretely braced flanges at the strength limit state include curvature, wind loading and the effect of staggered cross-frames/diaphragms and/or support skew (refer to the preceding section on Composite Sections in Positive Flexure for additional information). As specified in *AASHTO LRFD* Article 6.10.1.6, the sum of the flange lateral bending stresses due to all sources cannot exceed $0.6F_{yf}$. Further, according to *AASHTO LRFD* Article 6.10.1.6, amplification of the first-order flange lateral bending stresses may be required in discretely braced compression flanges. Amplification of tension-flange lateral bending stresses is not required. Amplification of these stresses is discussed

in more detail in Section 2.2.3.1.2.2 of this chapter under Fundamental Concepts (Equations 2.38 and 2.40 apply).

Continuously braced flanges in tension or compression must satisfy the following relationship at the strength limit state (*AASHTO LRFD* Article 6.10.8.1.3):

$$f_{bu} \le \phi_f R_h F_{yf}$$

Equation 2.109

AASHTO LRFD Equation 6.10.8.1.3-1

In this case, continuously braced tension flanges would typically be the top flanges in regions of negative flexure in continuous-span composite members. Continuously braced compression flanges would typically be the top flanges in regions of positive flexure in continuous-span noncomposite members, or the top flanges of simple-span noncomposite members, in which the flanges are considered continuously braced. For such cases, the specification considers the effects of any potential web bend buckling to be negligible, and therefore, the web load-shedding factor R_b is not included in Equation 2.109. Lateral bending does not need to be considered in Equation 2.109 because the flanges in these cases are continuously supported by the concrete deck.

Compression-Flange Flexural Resistance

As specified in *AASHTO LRFD* Article 6.10.8.2.1, the nominal flexural resistance of the compression flange F_{nc} is to be taken as the lesser of the local buckling resistance (*AASHTO LRFD* Article 6.10.8.2.2) and the lateral-torsional buckling resistance (*AASHTO LRFD* Article 6.10.8.2.3). This current language assumes the member is considered to be prismatic between brace points or the flange lateral bending stress is zero. If not, local buckling and lateral-torsional buckling should be checked separately according to Equation 2.107. The equations for the local and lateral-torsional buckling resistance are reviewed below. The reader is referred back to Figure 2.19, which illustrates the basic form of these equations as a function of the compression-flange slenderness and unbraced length, respectively.

Local Buckling Resistance

According to *AASHTO LRFD* Article 6.10.8.2.2, the local buckling resistance of the compression flange F_{nc} is to be taken as follows:

If $\lambda_f \le \lambda_{pf}$, then

$$F_{nc} = R_b R_h F_{yc}$$

Equation 2.110

AASHTO LRFD Equation 6.10.8.2.2-1

Otherwise:

$$F_{nc} = \left[1 - \left(1 - \frac{F_{yr}}{R_h F_{yc}} \right) \left(\frac{\lambda_f - \lambda_{pf}}{\lambda_{rf} - \lambda_{pf}} \right) \right] R_b R_h F_{yc}$$

Equation 2.111

AASHTO LRFD Equation 6.10.8.2.2-2

where:

λ_f = slenderness ratio for the compression flange = $b_{fc}/2t_{fc}$

λ_{pf} = limiting slenderness ratio for a compact flange

= $0.38\sqrt{\dfrac{E}{F_{yc}}}$ *AASHTO LRFD* Equation 6.10.8.2.2-4

λ_{rf} = limiting slenderness ratio for a noncompact flange

= $0.56\sqrt{\dfrac{E}{F_{yr}}}$ *AASHTO LRFD* Equation 6.10.8.2.2-5

F_{yr} = compression-flange stress at the onset of nominal yielding within the cross-section, including residual stress effects, but not including compression-flange lateral bending, taken as the smaller of $0.7F_{yc}$ and F_{yw}, but not less than $0.5F_{yc}$ (ksi)

R_b = web load-shedding factor determined as specified in *AASHTO LRFD* Article 6.10.1.10.2 (Equation 2.19)

R_h = hybrid factor determined as specified in *AASHTO LRFD* Article 6.10.1.10.1 (Equation 2.21)

λ_{pf} and λ_{rf} are Anchor Points 1 and 2, respectively, as shown on Figure 2.19. The derivation of these Anchor Points was discussed previously in the section on Fundamental Concepts. λ_{pf} defines the limiting slenderness ratio for a *compact flange*. A compact flange is able to achieve the maximum potential local buckling resistance (F_{max} in Figure 2.19) of $R_bR_hF_{yc}$, which is independent of the flange slenderness. For different grades of steel, the limiting ratio is as follows:

Table 2.15

F_{yc} (ksi)	λ_{pf}
36.0	10.8
50.0	9.2
70.0	7.7
90.0	6.8
100.0	6.5

λ_{rf} defines the limiting slenderness ratio for a *noncompact flange*. The local buckling resistance of a noncompact flange is expressed in Equation 2.111 as a linear function of the flange slenderness, as illustrated in Figure 2.19, which represents the inelastic local buckling resistance. λ_{rf} is the compression-flange slenderness at which the inelastic and elastic local buckling resistances are the same. The resistance at this point is assumed to be R_bF_{yr}. F_{yr} (and its associated limits) is discussed in more detail in the section on Fundamental Concepts (Section 2.2.3.1.1.2).

Compression flanges with a slenderness greater than λ_{rf} are termed *slender flanges* and their resistance is controlled by elastic local buckling. However, as pointed out previously, because $b_{fc}/2t_{fc}$ is limited to a practical maximum value of 12.0 in

AASHTO LRFD Article 6.10.2.2, elastic flange local buckling typically does not control for specified minimum yield strengths of the compression flange F_{yc} up to and including 90 ksi. Therefore, an elastic flange local buckling resistance equation is not provided. Instead, the use of Equation 2.111 is permitted for the rare case in which $b_{fc}/2t_{fc}$ may be in the elastic buckling range for F_{yc} greater than 90 ksi.

Lateral-Torsional Buckling Resistance

According to *AASHTO LRFD* Article 6.10.8.2.3, the lateral-torsional buckling resistance of the compression flange F_{nc} is to be taken as follows:

➢ If $L_b \leq L_p$, then

$$F_{nc} = R_b R_h F_{yc} \qquad\qquad\qquad \text{Equation 2.112}$$

$$\text{\textit{AASHTO LRFD} Equation 6.10.8.2.3-1}$$

➢ If $L_p < L_b \leq L_r$, then

$$F_{nc} = C_b \left[1 - \left(1 - \frac{F_{yr}}{R_h F_{yc}} \right) \left(\frac{L_b - L_p}{L_r - L_p} \right) \right] R_b R_h F_{yc} \leq R_b R_h F_{yc} \qquad \text{Equation 2.113}$$

$$\text{\textit{AASHTO LRFD} Equation 6.10.8.2.3-2}$$

➢ If $L_b > L_r$, then

$$F_{nc} = F_{cr} \leq R_b R_h F_{yc} \qquad\qquad\qquad \text{Equation 2.114}$$

$$\text{\textit{AASHTO LRFD} Equation 6.10.8.2.3-3}$$

where:
L_b	=	unbraced length (in.)
L_p	=	limiting unbraced length to achieve the nominal flexural resistance
F_{max}	=	$R_b R_h F_{yc}$ under uniform bending (in.)
	=	$1.0 r_t \sqrt{\dfrac{E}{F_{yc}}}$ *AASHTO LRFD* Equation 6.10.8.2.3-4
L_r	=	limiting unbraced length to achieve the onset of nominal yielding in either flange under uniform bending with consideration of compression-flange residual stress effects (in.)
	=	$\pi r_t \sqrt{\dfrac{E}{F_{yr}}}$ *AASHTO LRFD* Equation 6.10.8.2.3-5
C_b	=	moment gradient modifier (discussed below)
F_{cr}	=	elastic lateral-torsional buckling stress (ksi)
	=	$\dfrac{C_b R_b \pi^2 E}{\left(\dfrac{L_b}{r_t} \right)^2}$ *AASHTO LRFD* Equation 6.10.8.2.3-8

F_{yr} = compression-flange stress at the onset of nominal yielding within the cross-section, including residual stress effects, but not including compression-flange lateral bending, taken as the smaller of $0.7F_{yc}$ and F_{yw}, but not less than $0.5F_{yc}$ (ksi)

R_b = web load-shedding factor determined as specified in *AASHTO LRFD* Article 6.10.1.10.2 (Equation 2.19)

R_h = hybrid factor determined as specified in *AASHTO LRFD* Article 6.10.1.10.1 (Equation 2.21)

r_t = effective radius of gyration for lateral torsional buckling (in.)

$$= \frac{b_{fc}}{\sqrt{12\left(1+\dfrac{1}{3}\dfrac{D_c t_w}{b_{fc} t_{fc}}\right)}} \qquad \text{\textit{AASHTO LRFD} Equation 6.10.8.2.3-9}$$

Brace points defining the unbraced length L_b of the compression flange are considered to be points where lateral deflection of the girder flange and twisting of the entire cross-section are restrained. In the past, points of contraflexure have sometimes been considered to act as brace points. Since this practice can lead to significantly unconservative estimates of the lateral-torsional buckling resistance, the *AASHTO LRFD Specifications* do not imply that points of contraflexure should be considered as brace points. Instead, the effects of moment gradient are to be handled directly through the use of the moment gradient modifier C_b (discussed below).

L_p and L_r are Anchor Points 1 and 2, respectively, as shown on Figure 2.19. L_p defines the *compact unbraced length* limit. A member braced at or below the compact unbraced length limit is able to achieve the maximum potential lateral-torsional buckling resistance (F_{max} in Figure 2.19) of $R_b R_h F_{yc}$ under uniform bending, which is independent of the unbraced length. The limit is more restrictive than the limit given in previous Specifications. It was developed based on a linear regression analysis for a wide range of data from experimental tests under uniform major-axis bending (with an effective length factor k for lateral-torsional buckling effectively equal to 1.0) that fell within the inelastic lateral-torsional buckling region (73). **Note again that in many cases, it will not be economical to brace the girder at a distance equal to L_p or below in order to reach F_{max}, particularly under uniform bending conditions for which C_b is equal to 1.0.**

L_r defines the *noncompact unbraced length* limit. The lateral-torsional buckling resistance of a member braced at or below the noncompact unbraced length limit is expressed in Equation 2.113 as a linear function of the unbraced length, as illustrated in Figure 2.19, which represents the inelastic lateral-torsional buckling resistance. L_r is the unbraced length at which the inelastic and elastic lateral-torsional buckling resistances are the same. The resistance at this point is assumed to be $R_b F_{yr}$. F_{yr} (and its associated limits) is discussed in more detail in the section on Fundamental Concepts (Section 2.2.3.1.1.2).

Unbraced lengths greater than L_r are termed *slender unbraced lengths* and their resistance is controlled by elastic lateral-torsional buckling. As mentioned previously, lateral-torsional buckling in the elastic range is of primary importance for relatively

slender girders braced at longer than normal intervals, which most typically occurs during a temporary construction condition. The equation for the elastic lateral-torsional buckling stress F_{cr}, given above, is a conservative approximation of Equation 2.22 (assuming load-height effects are not considered), which is the exact beam-theory solution for the elastic lateral-torsional buckling resistance of a doubly symmetric I-section under uniform bending, when an effective radius of gyration r_t is introduced as follows:

$$r_t = \frac{b_{fc}}{\sqrt{12\left(\frac{h}{d} + \frac{1}{3}\frac{D_c t_w}{b_{fc} t_{fc}}\frac{D^2}{hd}\right)}}$$

Equation 2.115

AASHTO LRFD Equation C6.10.8.2.3-1

where d is the overall depth of the steel section and h is the depth between the flange centerlines. The expression for r_t given in the specifications, as shown above, is a simplification of Equation 2.115 obtained by assuming that $D = h = d$. However, Equation 2.115 is still provided in the Commentary (*AASHTO LRFD* Article C6.10.8.2.3) should the Engineer require a more precise calculation of the elastic lateral-torsional buckling stress. The web term $D_c t_w$ in both expressions for r_t accounts for the destabilizing effects of the flexural compression in the web on the lateral-torsional buckling resistance, and also extends the equation to cover singly symmetric I-section members. Previous Specifications used the radius of gyration of the compression flange only, which has been found to lead to some significant unconservative predictions relative to experimental and refined analytical results (73).

The equations for F_{cr} and L_r in the Main Provisions also assume that the St. Venant torsional constant J (in Equation 2.22) is equal to zero. Again, the LTB equations in the Main Provisions assume slender web behavior, and for very slender web sections (such as longitudinally stiffened girders), the effects of cross-section distortion essentially negate the contribution of J to the elastic LTB resistance. Although this assumption becomes more conservative as the web slenderness approaches the noncompact web slenderness limit λ_{rw} given by Equation 2.105, the simplicity and convenience of neglecting J generally outweighs the relative conservatism of this assumption. For composite I-sections in negative flexure, the equations are also conservative since they neglect the restraint provided to the bottom (compression) flange by the lateral and torsional stiffness of the concrete deck. However, for very slender web sections, the effect of this restraint is reduced by cross-section distortion and the fact that the deck may not provide an effectively fixed torsional restraint to such relatively large girders.

The above LTB equations assume an effective length factor k for lateral-torsional buckling equal to 1.0. As discussed in the previous section on Fundamental Concepts, warping restraint exists from adjacent unbraced lengths that are less critically loaded than the unbraced length under consideration, which can result in a reduced effective length factor for lateral-torsional buckling. A reduced effective length factor can be used to modify L_b (i.e., kL_b) and to increase the elastic lateral-

torsional buckling stress F_{cr} by a factor of $\left(1/k^2\right)$(*23*). *AASHTO LRFD* Article C6.10.8.2.3 makes reference to a procedure (*18, 22, 23*) that can be used to calculate a reduced effective length factor for lateral torsional buckling in special circumstances (e.g., when it becomes necessary to reduce the amplification of first-order flange lateral bending stresses).

The effect of a variation in the major-axis bending moment along the length between brace points, or a moment gradient, is accounted for by applying the moment gradient modifier C_b to the base inelastic and elastic LTB equations. When the moment and corresponding flange compressive major-axis bending stress are constant along the unbraced length, C_b has a base value of 1.0. Under moment gradient conditions, C_b may be taken greater than 1.0, which effectively increases the LTB resistance with the increase capped at F_{max} = $R_b R_h F_{yc}$ (refer to the dashed curves in Figure 2.19). C_b may conservatively be taken equal to 1.0 in all cases, except for some rare cases involving no cross-bracing within the span, as discussed below. In the Main Provisions, C_b is specified as follows:

➢   For unbraced cantilevers and for members when $f_{mid}/f_2 > 1$ or $f_2 = 0$:

$$C_b = 1.0$$

<div align="right">Equation 2.116</div>
<div align="right">*AASHTO LRFD* Equation 6.10.8.2.3-6</div>

➢   For all other cases:

$$C_b = 1.75 - 1.05\left(\frac{f_1}{f_2}\right) + 0.3\left(\frac{f_1}{f_2}\right)^2 \le 2.3$$

<div align="right">Equation 2.117</div>
<div align="right">*AASHTO LRFD* Equation 6.10.8.2.3-7</div>

where:
f_2 =   except as noted below, largest compressive stress without consideration of lateral bending at either end of the unbraced length of the flange under consideration, calculated from the critical moment envelope value (ksi). f_2 shall be due to the factored loads and shall be taken as positive. If the stress is zero or tensile in the flange under consideration at both ends of the unbraced length, f_2 shall be taken as zero.

f_0 =   stress without consideration of lateral bending at the brace point opposite to the one corresponding to f_2, calculated from the moment envelope value that produces the largest compression at this point in the flange under consideration, or the smallest tension if this point is never in compression (ksi). f_0 shall be due to the factored loads and shall be taken as positive in compression and negative in tension.

f_1 =   stress without consideration of lateral bending at the brace point opposite to the one corresponding to f_2, calculated as the intercept of the most critical assumed linear stress variation passing through

f_2 and either f_{mid} or f_0, whichever produces the smaller value of C_b (ksi). f_1 may be determined as follows:

➢ When the variation in the moment along the entire length between brace points is concave in shape:

$$f_1 = f_0$$

<div align="right">Equation 2.118

AASHTO LRFD Equation 6.10.8.2.3-10</div>

➢ Otherwise:

$$f_1 = 2f_{mid} - f_2 \geq f_0$$

<div align="right">Equation 2.119

AASHTO LRFD Equation 6.10.8.2.3-11</div>

where:
f_{mid} = stress without consideration of lateral bending at the middle of the unbraced length under consideration, calculated from the moment envelope value that produces the largest compression at this point, or the smallest tension if the point is never in compression (ksi). f_{mid} shall be due to the factored loads and shall be taken as positive in compression and negative in tension.

The basic form of the equation for C_b given by Equation 2.117 has been retained from previous Specifications. However, the definition of the cases where C_b must be taken equal to 1.0, and the calculation of the stresses f_1 and f_2 in Equation 2.117, have each been modified to remove ambiguities and to address specific cases where Equation 2.117 was previously unconservative.

Major-axis bending stresses are used in Equation 2.117 in the Main Provisions since dead and live load bending moments are applied to different sections in composite girders, which is significant when the nominal flexural resistance is not permitted to exceed the moment at first yield. However, as pointed out in *AASHTO LRFD* Article C6.10.8.2.3, the ratio of the major-axis bending moments at the brace points may be used in lieu of the bending stresses for convenience, if the Engineer feels that the use of the moment ratios does not have a significant effect on the calculated value of C_b.

It is convenient and always conservative to use the critical moment envelope values to compute the above stresses, particularly since concurrent moment values at the brace points are not normally tracked in the analysis. It can be shown that the use of the critical moment envelope values to compute f_2, f_{mid} and f_o is always conservative since a more critical stress distribution along the unbraced length, in terms of computing C_b, cannot exist for all possible concurrent loadings.

The application of the C_b equation to different cases will be illustrated through the examples given in Figure 2.58. In examining these cases, recall that according to the definitions given above, in the calculation of C_b, compressive stresses are to be taken as positive and tensile stresses are to be taken as negative. The first two

cases will illustrate when C_b must be taken equal to 1.0. In Case I shown in Figure 2.58a, the compressive stress at the middle of the unbraced length f_{mid} is greater than the largest compressive stress at either end of the unbraced length f_2. Therefore, C_b must be taken equal to 1.0. This is a common situation in regions of positive flexure when investigating the lateral-torsional buckling resistance of the top flange of the noncomposite girder in critical unbraced lengths during construction. In Case II shown in Figure 2.58b, the stress in the top flange at one end of the unbraced length is zero and the stress in the top flange at the other end of the unbraced length is tensile. As stated in the above definition of the stress f_2, when this situation occurs, f_2 is to be taken as zero. And further, when f_2 is equal to zero, C_b must be taken equal to 1.0. The situation shown in Figure 2.58b represents the rare case of a continuous span with no cross-bracing within the span. A case (not shown) where the stress would be zero at both ends of the unbraced length (and f_2 must then also be taken equal to zero according to the definition) would be a simply supported span with no cross-bracing within the span.   The last case (also not shown) for which C_b must be taken equal to 1.0 is for an unbraced cantilever, which is carried over from previous Specifications. As discussed previously in the section on Fundamental Concepts, for situations involving no cross-bracing within the span or unbraced cantilevers with significant loading applied to the top flange, consideration should be given to including load-height effects in the calculation of C_b (18, 24). In such situations, the calculated C_b values may actually be less than 1.0. As pointed out in *AASHTO LRFD* Article C6.10.8.2.3, when C_b is less than 1.0, F_{nc} may be smaller than F_{max} even when L_b is less than L_p. Therefore, in these cases, it is recommended that F_{nc} be calculated from Equation 2.113 whenever L_b is less than or equal to L_r.

In order to address other cases for which the previous calculation of C_b according to Equation 2.117 was significantly unconservative, Equation 2.117 now requires in certain situations the approximation of the stress variation along the unbraced length as the most critical of: 1) a line that passes through f_2 and f_{mid}, or 2) a line that passes between f_2 and f_0, whichever produces the smaller value of C_b. The intercept of the most critical line at the opposite end from f_2 is denoted as f_1.   The preceding approximation is represented by Equation 2.119. For example, Case III shown in Figure 2.58c represents a simply-supported member braced only at its ends and at midspan (only one-half of the member is shown in the figure).   In previous Specifications, using the compressive stresses at each end of the unbraced length would have given a C_b value of 1.75 according to Equation 2.117.   However, more accurate equations yield a C_b value of 1.3 for this case (26) since the flange compression is significantly larger within the unbraced length than the linear variation implicitly assumed by Equation 2.117 due to the parabolic shape of the moment diagram. As shown in Figure 2.58c, a line passing through f_2 and f_{mid} will produce a smaller value of C_b for this case than a line passing between f_2 and f_0 since the slope of a line through f_2 and f_{mid} is flatter and closer to that produced by a uniform moment. This fact is reflected when using Equation 2.119, which yields f_1 = $2(0.75f_2) - f_2 = 0.5f_2 > f_0$. Substituting $f_1/f_2 = 0.5$ into Equation 2.117 yields C_b = 1.3.

It should be noted, however, that in most cases, Equation 2.119 will not need to be employed.   The most common application of Equation 2.117 in design is for unbraced lengths in continuous spans in regions of negative flexure adjacent to

interior piers, which are typically subject to significant moment gradients. As shown in Case IV in Figure 2.58d, in these cases, where f_{mid} is smaller in magnitude than the average of f_0 and f_2 (or where the moment diagram is concave in shape along the entire length between brace points, which is the case in these regions), f_1 will always equal f_0. Therefore, the specification indicates that for cases where the moment diagram is concave in shape along the entire length between brace points, f_1 in Equation 2.117 may simply be taken equal to f_0, or the stress at the brace point opposite to the one corresponding to f_2, and Equation 2.119 need not be employed. This of course assumes that the section within the unbraced length is prismatic, or if a flange transition is present, that it is located a relatively short distance (i.e. $0.2L_b$) from the brace point with the smaller moment. As discussed further below, when this is not the case, C_b should be taken equal to 1.0. Sample illustrations of the calculation of the C_b factor for other cases, including cases of reverse curvature bending, are provided at the end of Appendix C to *AASHTO LRFD* Section 6. Further more detailed discussion on the derivation and calculation of the C_b factor may also be found in Reference 154.

a) Case I: f_{mid} & $f_2 > 1$

$f_{mid} > f_2$
$C_b = 1.0$

b) Case II: $f_2 = 0$

$f_2 = 0$
$C_b = 1.0$

c) Case III

$f_{mid}/f_2 = 0.75$
$f_1/f_2 = 0.5$
$C_b = 1.3$
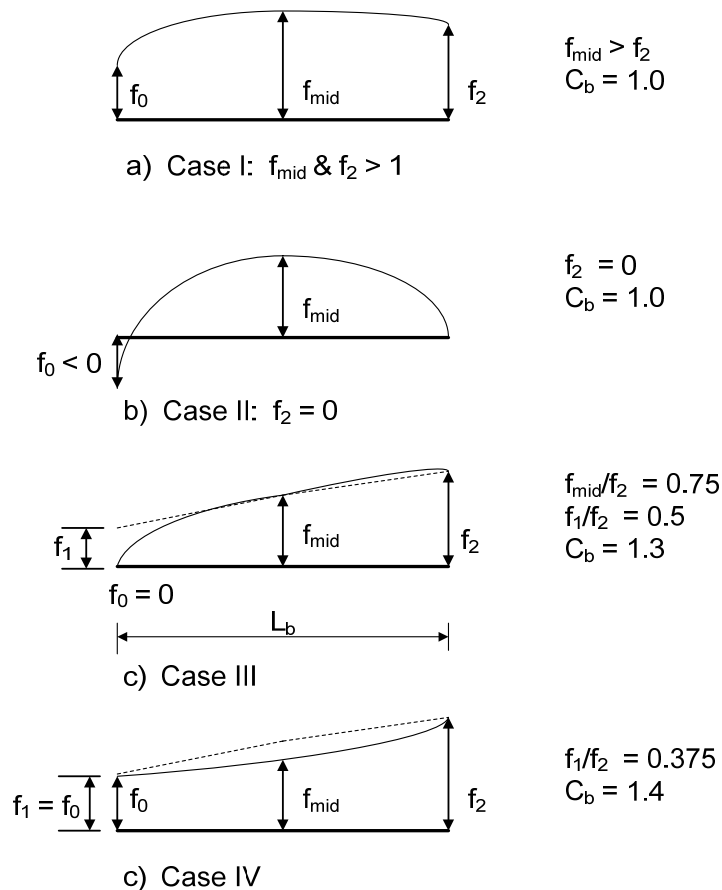
c) Case IV

$f_1/f_2 = 0.375$
$C_b = 1.4$

Figure 2.58 Moment Gradient Modifier C_b – Example Cases

As shown in Figure 2.19, under moment gradient conditions (i.e., $C_b > 1.0$), in addition to an increase in the base LTB resistance, the maximum potential LTB resistance $F_{max} = R_b R_h F_{yc}$ can be reached at larger unbraced lengths. The

provisions of *AASHTO LRFD* Article D6.4.1 (Appendix D to *AASHTO LRFD* Section 6) can be used to calculate the maximum unbraced lengths to achieve F_{max} under moment gradient conditions, and are recommended for use whenever C_b is greater than 1.0. The modifications to Anchor Points 1 and 2 to account for the effect of the moment gradient are given as follows in *AASHTO LRFD* Article D6.4.1:

> ➢ If $L_b \leq L_p$, then:

$$F_{nc} = R_b R_h F_{yc}$$

<div align="right">Equation 2.120</div>
<div align="right">*AASHTO LRFD* Equation D6.4.1-1</div>

> ➢ If $L_p < L_b \leq L_r$, then:

> • If $L_b \leq L_p + \dfrac{\left(1 - \dfrac{1}{C_b}\right)}{\left(1 - \dfrac{F_{yr}}{R_h F_{yc}}\right)}(L_r - L_p)$, then:

$$F_{nc} = R_b R_h F_{yc}$$

<div align="right">Equation 2.121</div>
<div align="right">*AASHTO LRFD* Equation D6.4.1-2</div>

> • Otherwise:

$$F_{nc} = C_b \left[1 - \left(1 - \frac{F_{yr}}{R_h F_{yc}}\right)\left(\frac{L_b - L_p}{L_r - L_p}\right)\right] R_b R_h F_{yc} \leq R_b R_h F_{yc}$$

<div align="right">Equation 2.122</div>
<div align="right">*AASHTO LRFD* Equation D6.4.1-3</div>

> ➢ If $L_b > L_r$, then:

> • If $L_b \leq \pi r_t \sqrt{\dfrac{C_b E}{R_h F_{yc}}}$, then:

$$F_{nc} = R_b R_h F_{yc}$$

<div align="right">Equation 2.123</div>
<div align="right">*AASHTO LRFD* Equation D6.4.1-4</div>

> • Otherwise:

$$F_{nc} = F_{cr} \leq R_b R_h F_{yc}$$

<div align="right">Equation 2.124</div>
<div align="right">*AASHTO LRFD* Equation D6.4.1-5</div>

The base LTB equations in the Specifications assume that the member is prismatic within the unbraced length. According to Reference 74, under uniform bending, the

reduction in the elastic LTB resistance due to a transition to a smaller section is approximately 5 percent when the transition is placed at 20 percent of the unbraced length from one of the brace points and the lateral moment of inertia of the flange in the smaller section is equal to one-half the corresponding value in the larger section. The reduction is less under moment gradient conditions as long as the larger bending moment occurs within the larger section, the lateral moment of inertia of the flange in the smaller section is greater than one-half the corresponding value in the larger section, and/or the section transition is placed closer to the brace point. Therefore, *AASHTO LRFD* Article 6.10.8.2.3 permits the effect of the section transition on the LTB resistance to be ignored when the stated conditions above are satisfied.   If there is more than one transition within the unbraced length, any transition within 20 percent of the unbraced length from the brace point with the smaller moment may be ignored and the LTB resistance based on the remaining sections may then be computed as described in the next paragraph.

For unbraced lengths containing a transition to a smaller section at a distance greater than 20 percent of the unbraced length from the brace point with the smaller moment, the LTB resistance F_{nc} at each section within the unbraced length may be taken as the smallest resistance within the unbraced length according to *AASHTO LRFD* Article 6.10.8.2.3 (note that the transition can either be in the compression or tension flange). The resulting LTB resistance must then not be exceeded at any section within the unbraced length. In addition, the C_b factor must be taken equal to 1.0 and the unbraced length must not be modified by an effective length factor. Essentially, the nonprismatic member is being replaced with an equivalent prismatic member. The cross-section of the equivalent member that gives the correct LTB resistance is generally some weighted average of all the cross-sections along the unbraced length.   If the cross-section that gives the smallest uniform bending resistance is used (i.e., calculated assuming C_b is equal to 1.0) and the calculated resistance based on that cross-section is not exceeded anywhere along the unbraced length, a conservative solution is obtained. A suggested procedure to obtain a more refined estimate of the LTB resistance for this case is given in Reference 23.

To avoid a significant reduction in the LTB resistance in such cases according to the above criteria, consider locating flange transitions within 20 percent of the unbraced length from the brace point with the smaller moment and ensure that the lateral moment of inertia of the flange (or flanges) of the smaller section is equal to or larger than one-half the corresponding value(s) for the flange(s) of the larger section at the transition.

Finally, for unbraced lengths consisting of singly symmetric noncomposite I-sections subject to reverse curvature bending, the LTB resistance must be checked for both flanges, unless the top flange is considered to be continuously braced. Because the flanges of these sections are different sizes, the LTB resistance may be governed by compression in the smaller flange, even though the compressive stress may be smaller than the maximum compressive stress in the larger flange.

Tension-Flange Flexural Resistance

For composite sections in negative flexure and noncomposite sections, the nominal flexural resistance of the tension flange is controlled by yielding. According to *AASHTO LRFD* Article 6.10.8.3, the nominal flexural resistance of the tension flange F_{nt} is to be taken as:

$$F_{nt} = R_h F_{yt}$$

<div align="right">Equation 2.125</div>

<div align="right">*AASHTO LRFD* Equation 6.10.8.3-1</div>

EXAMPLE

Check the composite section shown in Figure 2.6, which is the interior-pier section for an exterior girder in a straight continuous-span bridge (without skew), for the Strength I load combination (see DM Volume 1, Chapter 5 for more information on the Strength I load combination). The girder is hybrid with the flanges having a yield strength of 70 ksi and the web having a yield strength of 50 ksi. The load modifier η is assumed to be 1.0. Assume unshored construction. Use the section properties computed earlier for this section. The web load-shedding factor R_b for this section was computed earlier to be 0.990. The hybrid factor R_h for this section was computed earlier to be 0.984. Assume the following unfactored bending moments:

M_{DC1} = -4,840 kip-ft
M_{DC2} = -690 kip-ft
M_{DW} = -664 kip-ft
M_{LL+IM} = -4,040 kip-ft

First, determine if the section satisfies the noncompact web section slenderness limit given as follows:

$$\frac{2D_c}{t_w} < 5.7\sqrt{\frac{E}{F_{yc}}}$$

<div align="right">*AASHTO LRFD* Equation 6.10.6.2.3-1</div>

where D_c is the depth of the web in compression in the elastic range. For composite sections, D_c is to be determined as specified in *AASHTO LRFD* Article D6.3.1. According to *AASHTO LRFD* Article D6.3.1 (Appendix D to *AASHTO* LRFD Section 6), for composite sections in negative flexure at the strength limit state, D_c is to be computed for the section consisting of the steel girder plus the longitudinal reinforcement. For this section, D_c is equal to 36.55 inches. Therefore,

$$5.7\sqrt{\frac{29,000}{70}} = 116.0$$

$$\frac{2(36.55)}{0.5625} = 130.0 > 116.0$$

Since the section does not satisfy the noncompact web section slenderness limit, the section is classified as a slender-web section and the provisions of *AASHTO LRFD* Article 6.10.8 must be used to compute the nominal flexural resistance (i.e., the optional provisions of *AASHTO LRFD* Appendix A, which permit the nominal flexural resistance to exceed the moment at first yield, cannot be used).

Calculate the local buckling resistance of the bottom (compression) flange. Determine the slenderness ratio of the flange:

$$\lambda_f = \frac{b_{fc}}{2t_{fc}}$$

AASHTO LRFD Equation 6.10.8.2.2-3

$$\lambda_f = \frac{20}{2(2)} = 5.0$$

Determine the limiting slenderness ratio for a compact flange (alternatively, see *AASHTO LRFD* Table C6.10.8.2.2-1 or Table 2.15):

$$\lambda_{pf} = 0.38\sqrt{\frac{E}{F_{yc}}}$$

AASHTO LRFD Equation 6.10.8.2.2-4

$$\lambda_{pf} = 0.38\sqrt{\frac{29,000}{70}} = 7.73$$

Since $\lambda_f < \lambda_{pf}$ the flange is compact. Therefore,

$$F_{nc} = R_b R_h F_{yc}$$

AASHTO LRFD Equation 6.10.8.2.2-1

$$F_{nc} = (0.990)(0.984)(70.0) = 68.19 \text{ ksi}$$

Calculate the lateral-torsional buckling resistance of the bottom flange. The unbraced length L_b on either side of the interior-pier is 20.0 feet. A flange transition is located 15.0 feet from each side of the interior pier. At the transition, the top flange steps down to a 1" x 18" plate and the bottom flange steps down to a 1" x 20" plate. The web remains at 9/16" x 69". Since the flange transition is located at a distance greater than 20 percent of the unbraced length from the brace point with the smaller moment, the LTB resistance is to be taken as the smallest resistance within the unbraced length under consideration according to *AASHTO LRFD* Article 6.10.8.2.3. The moment gradient modifier C_b is also to be taken equal to 1.0 and L_b is not to be modified by an effective length factor. Calculate F_{nc} based on the smaller section at the flange transition. From separate calculations, D_c for the section consisting of the steel girder plus the longitudinal reinforcement is computed to be 38.29 inches for the smaller section at the transition. Therefore:

$$r_t = \frac{b_{fc}}{\sqrt{12\left(1 + \frac{1}{3}\frac{D_c t_w}{b_{fc} t_{fc}}\right)}}$$

AASHTO LRFD Equation 6.10.8.2.3-9

$$r_t = \frac{20}{\sqrt{12\left(1 + \frac{1}{3}\frac{38.29(0.5625)}{20(1)}\right)}} = 4.95 \text{ in.}$$

$$L_p = 1.0 r_t \sqrt{\frac{E}{F_{yc}}}$$

AASHTO LRFD Equation 6.10.8.2.3-4

$$L_p = \frac{1.0(4.95)}{12}\sqrt{\frac{29{,}000}{70}} = 8.40 \text{ ft}$$

$$L_r = \pi r_t \sqrt{\frac{E}{F_{yr}}}$$

AASHTO LRFD Equation 6.10.8.2.3-5

$$F_{yr} = 0.7 F_{yc} \le F_{yw}$$

$$F_{yr} = 0.7(70) = 49.0 \text{ ksi} < 50 \text{ ksi} \qquad \text{ok}$$

F_{yr} must also not be less than $0.5F_{yc}$ = 0.5(70) = 35.0 ksi ok.

$$L_r = \frac{\pi(4.95)}{12}\sqrt{\frac{29{,}000}{49.0}} = 31.53 \text{ ft}$$

Since L_p = 8.40 feet < L_b = 20.0 feet < L_r = 31.53 feet,

$$F_{nc} = C_b\left[1 - \left(1 - \frac{F_{yr}}{R_h F_{yc}}\right)\left(\frac{L_b - L_p}{L_r - L_p}\right)\right]R_b R_h F_{yc} \le R_b R_h F_{yc}$$

AASHTO LRFD Equation 6.10.8.2.3-2

From separate calculations similar to those illustrated previously, R_b and R_h for the smaller section at the flange transition are computed to be 0.977 and 0.971, respectively. Therefore,

$$F_{nc} = 1.0\left[1-\left(1-\frac{49.0}{0.971(70.0)}\right)\left(\frac{20.0-8.40}{31.53-8.40}\right)\right](0.977)(0.971)(70)$$

$$= 57.11\,\text{ksi} < 0.977(0.971)(70) = 66.41\,\text{ksi}$$

$$\therefore \quad (F_{nc})_{LTB} = 57.11\ \text{ksi}$$

The calculated lateral torsional buckling resistance must not be exceeded anywhere along the unbraced length. The major-axis bending stress in the bottom flange due to the factored loads at the interior-pier section for the Strength I load combination is computed to be:

Bot. flange:

$$f = 1.0\left[\frac{1.25(-4,840)}{3,149}+\frac{1.25(-690)}{3,310}+\frac{1.5(-664)}{3,310}+\frac{1.75(-4,040)}{3,310}\right]12 = -55.42\,\text{ksi}$$

Assume the following unfactored bending moments at the flange transition:

M_{DC1} = -2,656 kip-ft
M_{DC2} = -373 kip-ft
M_{DW} = -358 kip-ft
M_{LL+IM} = -2,709 kip-ft

Using the elastic section properties for the smaller section at the flange transition (from separate calculations), the major-axis bending stress in the bottom flange due to the factored loads at this section for the Strength I load combination is computed to be:

Bot. flange:

$$f = 1.0\left[\frac{1.25(-2,656)}{1,789}+\frac{1.25(-373)}{1,975}+\frac{1.5(-358)}{1,975}+\frac{1.75(-2,709)}{1,975}\right]12 = -57.17\,\text{ksi}$$

As specified in *AASHTO LRFD* Article 6.10.1.6, for design checks where the flexural resistance is based on lateral torsional buckling, f_{bu} is to be determined as the largest value of the compressive stress throughout the unbraced length in the flange under consideration, calculated without consideration of flange lateral bending. Therefore, f_{bu} = -57.17 ksi. As specified for discretely braced compression flanges at the strength limit state in *AASHTO LRFD* Article 6.10.8.1.1:

$$f_{bu} + \frac{1}{3}f_{\ell} \le \phi_f F_{nc}$$

AASHTO LRFD Equation 6.10.8.1.1-1

Since the bridge is straight and not skewed and wind load is not considered for the Strength I load combination, there are no sources of flange lateral bending.

Therefore, f_ℓ is equal to zero. Since $f_\ell = 0$, F_{nc} may be taken as the smaller of the local buckling and lateral-torsional buckling resistance. Therefore, F_{nc} is equal to $(F_{nc})_{LTB} = 57.11$ ksi.

$$f_{bu} + \frac{1}{3}f_\ell = |-57.17|\,\text{ksi} + \frac{1}{3}(0) = 57.17\,\text{ksi}$$

$$\phi_f F_{nc} = 1.0(57.11) = 57.11\,\text{ksi}$$

$$57.17\,\text{ksi} > 57.11\,\text{ksi} \qquad \text{say ok}$$

There is a slight overstress, but the suggested procedure for calculating the LTB resistance of a nonprismatic member within the unbraced length provides a conservative solution so the overstress will be permitted in this case.

For illustration, assume that the flange transition in this case is instead located 17.0 feet from each side of the interior pier. Since the flange transition is now located at a distance less than or equal to 20 percent of the unbraced length from the brace point with the smaller moment, *AASHTO LRFD* Article 6.10.8.2.3 permits the effect of the section transition on the LTB resistance to be ignored.   Therefore, the LTB resistance may be computed based on the larger section at the interior pier.

$$r_t = \frac{20}{\sqrt{12\left(1 + \dfrac{1}{3}\dfrac{36.55(0.5625)}{20(2)}\right)}} = 5.33\,\text{in.}$$

$$L_p = \frac{1.0(5.33)}{12}\sqrt{\frac{29{,}000}{70}} = 9.04\,\text{ft}$$

$$L_r = \frac{\pi(5.33)}{12}\sqrt{\frac{29{,}000}{49.0}} = 33.95\,\text{ft}$$

Since the effect of the transition is ignored, the moment gradient modifier C_b may also now be applied.

$$C_b = 1.75 - 1.05\left(\frac{f_1}{f_2}\right) + 0.3\left(\frac{f_1}{f_2}\right)^2 \le 2.3$$

<div align="right">

AASHTO LRFD Equation 6.10.8.2.3-7
</div>

f_2 is generally taken as the largest compressive stress without consideration of lateral bending due to the factored loads at either end of the unbraced length of the flange under consideration, calculated from the critical moment envelope value. Since the stress at both ends of the unbraced length is not zero or tensile, f_2 in this case is equal to the compressive stress in the bottom flange at the interior-pier section due to the factored loads, which was computed earlier to be 55.42 ksi (f_2 is

always taken as positive in this calculation). As stated in *AASHTO LRFD* Article 6.10.8.2.3, when the variation in the moment along the entire length between brace points is concave in shape (which is the case here), f_1 may simply be taken equal to f_0, where f_0 is the stress without consideration of lateral bending due to the factored loads at the brace point opposite to the one corresponding to f_2. f_0 is to be calculated from the moment envelope value that produces the largest compression, or the smallest tension if the point is never in compression. Assume the following unfactored bending moments at the first brace point located 20.0 feet from the interior pier:

$$M_{DC1} = \text{-2,390 kip-ft}$$
$$M_{DC2} = \text{-334 kip-ft}$$
$$M_{DW} = \text{-321 kip-ft}$$
$$M_{LL+IM} = \text{-2,615 kip-ft}$$

Since it is assumed that the flange transition does not exist in this case, calculate the major-axis bending stress in the bottom flange due to the factored loads at this brace point for the Strength I load combination using the section properties of the (larger) interior-pier section:

Bot. flange:

$$f_1 = f_o = 1.0\left[\frac{1.25(-2,390)}{3,149} + \frac{1.25(-334)}{3,310} + \frac{1.5(-321)}{3,310} + \frac{1.75(-2,615)}{3,310}\right]12 = -31.23 \text{ ksi}$$

f_0 is to be taken as positive in compression in the calculation of C_b. Therefore, $f_1 = f_0$ = 31.23 ksi.

$$C_b = 1.75 - 1.05\left(\frac{31.23}{55.42}\right) + 0.3\left(\frac{31.23}{55.42}\right)^2 = 1.25 < 2.3$$

Since L_p = 9.04 feet < L_b = 17.0 feet < L_r = 33.95 feet,

$$F_{nc} = C_b\left[1 - \left(1 - \frac{F_{yr}}{R_h F_{yc}}\right)\left(\frac{L_b - L_p}{L_r - L_p}\right)\right]R_b R_h F_{yc} \leq R_b R_h F_{yc}$$

AASHTO LRFD Equation 6.10.8.2.3-2

$$F_{nc} = 1.25\left[1 - \left(1 - \frac{49.0}{0.984(70.0)}\right)\left(\frac{17.0 - 9.04}{33.95 - 9.04}\right)\right](0.990)(0.984)(70)$$

$$= 77.38 \text{ ksi} > 0.990(0.984)(70) = 68.19 \text{ ksi}$$

$$\therefore \ (F_{nc})_{LTB} = 68.19 \text{ ksi}$$

For values of C_b greater than 1.0, *AASHTO LRFD* Article D6.4.1 allows the maximum lateral torsional buckling resistance, $(F_{nc})_{LTB} = F_{max} = R_b R_h F_{yc}$, to be

reached at larger unbraced lengths. However, since F_{max} is already reached at L_b = 17.0 feet in this case, it is not necessary to utilize these provisions.

By locating the flange transition within 20 percent of the unbraced length from the brace point with the smaller moment, the LTB resistance increased by 19.4 percent in this case.

Check the top (tension) flange. The nominal flexural resistance of the tension flange is based on yielding. As specified in *AASHTO LRFD* Article 6.10.1.6, for design checks where the flexural resistance is based on yielding, the major-axis bending stress f_{bu} may be determined as the corresponding stress at the section under consideration. The major-axis bending stress in the top flange due to the factored loads at the interior-pier section for the Strength I load combination is computed to be:

Top flange:

$$f_{bu} = 1.0\left[\frac{1.25(-4,840)}{2,942} + \frac{1.25(-690)}{3,703} + \frac{1.5(-664)}{3,703} + \frac{1.75(-4,040)}{3,703}\right]12 = 53.61\,\text{ksi}$$

As specified for continuously braced tension flanges at the strength limit state in *AASHTO LRFD* Article 6.10.8.1.3:

$$f_{bu} \le \phi_f R_h F_{yf}$$

AASHTO LRFD Equation 6.10.8.1.3-1

$$\phi_f R_h F_{yf} = 1.0(0.984)(70) = 68.88\,\text{ksi}$$

$$53.61\,\text{ksi} < 68.88\,\text{ksi} \quad \text{ok}$$

2.2.3.7.1.2.2 Appendix A

General

The conditions under which the optional provisions of Appendix A may be applied were discussed previously and are spelled out again in *AASHTO LRFD* Article A6.1. Sections designed according to the provisions of Appendix A must qualify as either compact web or noncompact web I-sections. Basically, the provisions of Appendix A account for the ability of certain compact and noncompact web I-sections to develop flexural resistances significantly greater than M_y. As a result, the equations giving the nominal flexural resistance in Appendix A are all more appropriately expressed in terms of bending moment. The provisions also account for the contribution of the St. Venant torsional resistance to the LTB resistance of these sections, which may be useful for compact and noncompact web sections with larger unbraced lengths, particularly under certain construction conditions. Example applications of the Appendix A provisions are demonstrated in References 74a and 74b.

As specified in *AASHTO LRFD* Article A6.1.1, at the strength limit state, discretely braced compression flanges must satisfy the one-third rule equation (discussed previously) expressed in terms of bending moment as follows:

$$M_u + \frac{1}{3}f_\ell S_{xc} \le \phi_f M_{nc}$$
<div align="right">Equation 2.126</div>

<div align="right">*AASHTO LRFD* Equation A6.1.1-1</div>

where:

M_u	=	bending moment about the major axis of the cross-section determined as specified in *AASHTO LRFD* Article 6.10.1.6 (kip-in.). M_u is always taken as positive.
f_ℓ	=	flange lateral bending stress determined as specified in *AASHTO LRFD* Article 6.10.1.6 (ksi). f_ℓ is always taken as positive.
M_{nc}	=	nominal flexural resistance based on the compression flange determined as specified in *AASHTO LRFD* Article A6.3 (kip-in.)
S_{xc}	=	elastic section modulus about the major axis of the section to the compression flange taken as M_{yc}/F_{yc} (in.^{3})

The nominal flexural resistance based on the compression flange M_{nc} is to be taken as the smaller of the local buckling and lateral-torsional buckling resistance (discussed below). As specified in *AASHTO LRFD* Article 6.10.1.6, for design checks involving lateral-torsional buckling, the major-axis bending moment M_u is to be taken as the largest value throughout the unbraced length under consideration causing compression in the flange under consideration. The flange lateral bending stress f_ℓ is also to be taken as the largest value throughout the unbraced length in the flange under consideration. For design checks involving flange local buckling, M_u and f_ℓ may be taken as the corresponding values at the section under consideration. However, when maximum values of these stresses occur at different locations within the unbraced length, which is often the case, it is conservative to use the maximum values in the local buckling check.

Discretely braced tension flanges must satisfy the following relationship at the strength limit state (*AASHTO LRFD* Article A6.1.2):

$$M_u + \frac{1}{3}f_\ell S_{xt} \le \phi_f M_{nt}$$
<div align="right">Equation 2.127</div>

<div align="right">*AASHTO LRFD* Equation A6.1.2-1</div>

where:

M_{nt}	=	nominal flexural resistance based on tension yielding determined as specified in *AASHTO LRFD* Article A6.4 (kip-in.)
S_{xt}	=	elastic section modulus about the major axis of the section to the tension flange taken as M_{yt}/F_{yt} (in.^{3})

The nominal flexural resistance M_{nt} is based on yielding. According to *AASHTO LRFD* Article 6.10.1.6, for design checks involving yielding, M_u and f_ℓ may be taken

as the corresponding values at the section under consideration. As discussed in the preceding paragraph, it is conservative to use the maximum values of these stresses within the unbraced length in this check. Note that when M_{yc} is less than or equal to M_{yt} and f_ℓ is equal to zero, the flexural resistance based on the tension flange does not control and Equation 2.127 need not be checked.

The elastic section moduli S_{xc} and S_{xt} in Equations 2.126 and 2.127 are defined as M_{yc}/F_{yc} and M_{yt}/F_{yt}, respectively, so that for a composite section with a web proportioned exactly at the noncompact web slenderness limit given in Equation 2.105, the flexural resistance given by Appendix A will be approximately the same as the flexural resistance given by the Main Provisions (*AASHTO LRFD* Article 6.10.8). Slight differences between the resistance predictions may occur for reasons pointed out in *AASHTO LRFD* Article CA6.1.1.

Sources of lateral flange bending in discretely braced flanges at the strength limit were discussed previously (refer to the preceding sections on Composite Sections in Positive Flexure and the Main Provisions for additional information). As specified in *AASHTO LRFD* Article 6.10.1.6, the sum of the flange lateral bending stresses due to all sources cannot exceed $0.6F_{yf}$. Further, according to *AASHTO LRFD* Article 6.10.1.6, amplification of the first-order flange lateral bending stresses may be required in discretely braced compression flanges. Amplification of tension-flange lateral bending stresses is not required. Amplification of these stresses is discussed in more detail in Section 2.2.3.1.2.2 of this chapter under Fundamental Concepts (Equations 2.39 and 2.41 apply).

According to *AASHTO LRFD* Article A6.1.3, continuously braced flanges in compression must satisfy the following relationship at the strength limit state:

$$M_u \leq \phi_f R_{pc} M_{yc} \qquad \text{Equation 2.128}$$
<div align="right">*AASHTO LRFD* Equation A6.1.3-1</div>

and according to *AASHTO LRFD* Article A6.1.4, continuously braced flanges in tension must satisfy the following relationship at the strength limit state:

$$M_u \leq \phi_f R_{pt} M_{yt} \qquad \text{Equation 2.129}$$
<div align="right">*AASHTO LRFD* Equation A6.1.4-1</div>

R_{pc} and R_{pt} are web plastification factors for the compression and tension flanges, respectively, which are discussed in more detail below. Lateral bending does not need to be considered in Equations 2.128 and 2.129 because the flanges in these cases are continuously supported by the concrete deck.

Web Plastification Factors

AASHTO LRFD Article A6.2 defines the web plastification factors R_{pc} and R_{pt} for the compression and tension flange, respectively. The web plastification factors are essentially effective shape factors that define a smooth linear transition in the maximum flexural resistance between M_y and M_p.

For a compact web section, or a section with a web satisfying Equation 2.103, the web plastification factors are equivalent to the cross-section shape factors as follows (*AASHTO LRFD* Article A6.2.1):

$$R_{pc} = \frac{M_p}{M_{yc}}$$

<div align="right">Equation 2.130</div>

<div align="right">*AASHTO LRFD* Equation A6.2.1-4</div>

$$R_{pt} = \frac{M_p}{M_{yt}}$$

<div align="right">Equation 2.131</div>

<div align="right">*AASHTO LRFD* Equation A6.2.1-5</div>

Thus, whenever R_{pc} and R_{pt} given by the preceding equations are used in the appropriate flexural resistance equations, the maximum flexural resistance of a compact web section M_{max} will equal the plastic moment M_p. By using R_{pc} and R_{pt} in the flexural resistance equations rather the simply expressing the maximum resistance as M_p for these types of sections, separate flexural resistance equations are not required for compact and noncompact web sections.

For a noncompact web section, or a section with a web not satisfying Equation 2.103 but satisfying Equation 2.105, the web plastification factors are given as follows (*AASHTO LRFD* Article A6.2.2):

$$R_{pc} = \left[1 - \left(1 - \frac{R_h M_{yc}}{M_p}\right)\left(\frac{\lambda_w - \lambda_{pw(D_c)}}{\lambda_{rw} - \lambda_{pw(D_c)}}\right)\right]\frac{M_p}{M_{yc}} \le \frac{M_p}{M_{yc}}$$

<div align="right">Equation 2.132</div>

<div align="right">*AASHTO LRFD* Equation A6.2.2-4</div>

$$R_{pt} = \left[1 - \left(1 - \frac{R_h M_{yt}}{M_p}\right)\left(\frac{\lambda_w - \lambda_{pw(D_c)}}{\lambda_{rw} - \lambda_{pw(D_c)}}\right)\right]\frac{M_p}{M_{yt}} \le \frac{M_p}{M_{yt}}$$

<div align="right">Equation 2.133</div>

<div align="right">*AASHTO LRFD* Equation A6.2.2-5</div>

where λ_w is equal to the web slenderness $2D_c/t_w$ based on the elastic moment, λ_{rw} is equal to the web slenderness limit for a noncompact web section given in Equation 2.105, and $\lambda_{pw(Dc)}$ is the limit slenderness ratio for a compact web corresponding to $2D_c/t_w$ given as follows:

$$\lambda_{pw(D_c)} = \lambda_{pw(D_{cp})}\left(\frac{D_c}{D_{cp}}\right) \le \lambda_{rw}$$

<div align="right">Equation 2.134</div>

<div align="right">*AASHTO LRFD* Equation A6.2.2-6</div>

D_{cp} is the depth of the web in compression at the plastic moment, and $\lambda_{pw(Dcp)}$ is the limiting slenderness ratio for a compact web corresponding to $2D_{cp}/t_w$ given by Equation 2.104.

Equations 2.132 and 2.133 define a linear transition in the maximum potential flexural resistance M_{max} of a noncompact web section between M_y and M_p as a function of the web slenderness. As $2D_c/t_w$ approaches the noncompact web section limit λ_{rw}, the web plastification factors approach values equal to the hybrid factor R_h, and therefore, M_{max} within the appropriate flexural resistance equations approaches a limiting value of R_hM_{yc} or R_hM_{yt}, as applicable. As $2D_{cp}/t_w$ approaches the compact web section limit $\lambda_{pw(Dcp)}$, the web plastification factors approach the cross-section shape factors (refer to Equations 2.130 and 2.131), and therefore, M_{max} within the appropriate flexural resistance equations approaches a limiting value of M_p. Equation 2.134 converts the web compactness limit defined in terms of D_{cp}, as given by Equation 2.103, to a value that can be used consistently in Equations 2.132 and 2.133 with the web slenderness λ_w, which is expressed in terms of D_c. The reason for the upper limit of λ_{rw} in Equation 2.134 was discussed previously (refer to Section 2.2.3.7.1.2 of this chapter).

Upper limits of M_p/M_{yc} and M_p/M_{yt} are placed on R_{pc} and R_{pt}, respectively, in Equations 2.132 and 2.133. These upper limits will limit the larger of the base resistances $R_{pc}M_{yc}$ or $R_{pc}M_{yt}$ to M_p for the rare case of an extremely monosymmetric section in which M_{yc} or M_{yt} is greater than M_p. However, the flange-proportioning limit given by Equation 2.60 will generally tend to prevent the use of such sections.

Flexural Resistance Based on the Compression Flange

As specified in *AASHTO LRFD* Article A6.3.1, the nominal flexural resistance based on the compression flange M_{nc} is to be taken as the lesser of the local buckling resistance (*AASHTO LRFD* Article A6.3.2) and the lateral-torsional buckling resistance (*AASHTO LRFD* Article A6.3.3). This current language assumes the member is considered to be prismatic between brace points or the flange lateral bending stress is zero. Otherwise, local buckling and lateral-torsional buckling should be checked separately according to Equation 2.126. The equations for the local and lateral-torsional buckling resistance are reviewed below. The reader is referred back to Figure 2.19, which illustrates the basic form of these equations as a function of the compression-flange slenderness and unbraced length, respectively.

Local Buckling Resistance

According to *AASHTO LRFD* Article A6.3.2, the flexural resistance based on compression flange local buckling M_{nc} is to be taken as follows:

- If $\lambda_f \leq \lambda_{pf}$, then

$$M_{nc} = R_{pc}M_{yc}$$

Equation 2.135

AASHTO LRFD Equation A6.3.2-1

- Otherwise:

$$M_{nc} = \left[1 - \left(1 - \frac{F_{yr}S_{xc}}{R_{pc}M_{yc}}\right)\left(\frac{\lambda_f - \lambda_{pf}}{\lambda_{rf} - \lambda_{pf}}\right)\right]R_{pc}M_{yc}$$

Equation 2.136

AASHTO LRFD Equation A6.3.2-2

where:

λ_f = slenderness ratio for the compression flange = $b_{fc}/2t_{fc}$

λ_{pf} = limiting slenderness ratio for a compact flange

= $0.38\sqrt{\dfrac{E}{F_{yc}}}$ *AASHTO LRFD* Equation A6.3.2-4

λ_{rf} = limiting slenderness ratio for a noncompact flange

= $0.95\sqrt{\dfrac{Ek_c}{F_{yr}}}$ *AASHTO LRFD* Equation A6.3.2-5

F_{yr} = compression-flange stress at the onset of nominal yielding within the cross-section, including residual stress effects, but not including compression-flange lateral bending, taken as the smaller of $0.7F_{yc}$, $R_hF_{yt}S_{xt}/S_{xc}$ and F_{yw}, but not less than $0.5F_{yc}$ (ksi)

k_c = flange local buckling coefficient taken as follows:

For built-up sections:

= $4/\sqrt{D/t_w}$ with $0.35 \leq k_c \leq 0.76$

For rolled sections:

= 0.76

R_h = hybrid factor determined as specified in *AASHTO LRFD* Article 6.10.1.10.1 (Equation 2.21)

R_{pc} = web plastification factor for the compression flange determined as specified in *AASHTO LRFD* Article A6.2.1 or A6.2.2, as applicable

S_{xc} = elastic section modulus about the major axis of the section to the compression flange taken as M_{yc}/F_{yc} (in.^{3})

S_{xt} = elastic section modulus about the major axis of the section to the tension flange taken as M_{yt}/F_{yt} (in.^{3})

λ_{pf} and λ_{rf} are Anchor Points 1 and 2, respectively, as shown on Figure 2.19. The derivation of these Anchor Points was discussed previously in the section on Fundamental Concepts. λ_{pf} defines the limiting slenderness ratio for a *compact flange*. A compact flange is able to achieve the maximum potential local buckling resistance (M_{max} in Figure 2.19) of $R_{pc}M_{yc}$, which is independent of the flange slenderness. Values of λ_{pf} for different grades of steel were given previously.

λ_{rf} defines the limiting slenderness ratio for a *noncompact flange*. The local buckling resistance of a noncompact flange is expressed in Equation 2.136 as a linear function of the flange slenderness, as illustrated in Figure 2.19, which represents the

inelastic local buckling resistance. λ_{rf} is the compression-flange slenderness at which the inelastic and elastic local buckling resistances are the same. The resistance at this point is assumed to be $R_b F_{yr} S_{xc}$. F_{yr} (and its associated limits), along with the derivation of the flange local buckling coefficient k_c, are discussed in more detail in the section on Fundamental Concepts (Section 2.2.3.1.1.2 and Section 2.2.3.1.1.3, respectively).

Compression flanges with a slenderness greater than λ_{rf} are termed *slender flanges* and their resistance is controlled by elastic local buckling. However, as pointed out previously, because $b_{fc}/2t_{fc}$ is limited to a practical maximum value of 12.0 in *AASHTO LRFD* Article 6.10.2.2, elastic flange local buckling typically does not control for specified minimum yield strengths of the compression flange F_{yc} up to and including 70 ksi, which is the limiting yield strength for the application of the provisions of Appendix A.

Lateral-Torsional Buckling Resistance

According to *AASHTO LRFD* Article A6.3.3, the flexural resistance based on lateral-torsional buckling M_{nc} is to be taken as follows:

- If $L_b \leq L_p$, then

$$M_{nc} = R_{pc} M_{yc} \qquad \text{Equation 2.137}$$

$$\textit{AASHTO LRFD Equation A6.3.3-1}$$

- If $L_p < L_b \leq L_r$, then

$$M_{nc} = C_b \left[1 - \left(1 - \frac{F_{yr} S_{xc}}{R_{pc} M_{yc}} \right) \left(\frac{L_b - L_p}{L_r - L_p} \right) \right] R_{pc} M_{yc} \leq R_{pc} M_{yc} \quad \text{Equation 2.138}$$

$$\textit{AASHTO LRFD Equation 6.3.3-2}$$

- If $L_b > L_r$, then

$$M_{nc} = F_{cr} S_{xc} \leq R_{pc} M_{yc} \qquad \text{Equation 2.139}$$

$$\textit{AASHTO LRFD Equation A6.3.3-3}$$

where:
L_b = unbraced length (in.)
L_p = limiting unbraced length to achieve the nominal flexural resistance M_{max}
   = $R_{pc} M_{yc}$ under uniform bending (in.)
   = $1.0 r_t \sqrt{\dfrac{E}{F_{yc}}}$ *AASHTO LRFD* Equation A6.3.3-4

L_r = limiting unbraced length to achieve the onset of nominal yielding in either flange under uniform bending with consideration of compression-flange residual stress effects (in.)

$$= 1.95 r_t \frac{E}{F_{yr}} \sqrt{\frac{J}{S_{xc} h}} \sqrt{1 + \sqrt{1 + 6.76 \left(\frac{F_{yr}}{E} \frac{S_{xc} h}{J} \right)^2}}$$

AASHTO LRFD Equation A6.3.3-5

C_b = moment gradient modifier (discussed below)

F_{cr} = elastic lateral-torsional buckling stress (ksi)

$$= \frac{C_b \pi^2 E}{(L_b / r_t)^2} \sqrt{1 + 0.078 \frac{J}{S_{xc} h} (L_b / r_t)^2}$$

AASHTO LRFD Equation A6.3.3-8

F_{yr} = compression-flange stress at the onset of nominal yielding within the cross-section, including residual stress effects, but not including compression-flange lateral bending, taken as the smaller of $0.7F_{yc}$, $R_h F_{yt} S_{xt} / S_{xc}$ and F_{yw}, but not less than $0.5F_{yc}$ (ksi)

J = St. Venant torsional constant (in.[4])

$$= \frac{D t_w^3}{3} + \frac{b_{fc} t_{fc}^3}{3} \left(1 - 0.63 \frac{t_{fc}}{b_{fc}} \right) + \frac{b_{ft} t_{ft}^3}{3} \left(1 - 0.63 \frac{t_{ft}}{b_{ft}} \right)$$

AASHTO LRFD Equation A6.3.3-9

R_h = hybrid factor determined as specified in *AASHTO LRFD* Article 6.10.1.10.1 (Equation 2.21)

R_{pc} = web plastification factor for the compression flange determined as specified in *AASHTO LRFD* Article A6.2.1 or A6.2.2, as applicable

S_{xc} = elastic section modulus about the major axis of the section to the compression flange taken as M_{yc}/F_{yc} (in.[3])

S_{xt} = elastic section modulus about the major axis of the section to the tension flange taken as M_{yt}/F_{yt} (in.[3])

h = depth between the centerline of the flanges (in.)

r_t = effective radius of gyration for lateral torsional buckling (in.)

$$= \frac{b_{fc}}{\sqrt{12 \left(1 + \frac{1}{3} \frac{D_c t_w}{b_{fc} t_{fc}} \right)}}$$ *AASHTO LRFD* Equation A6.3.3-10

Brace points defining the unbraced length L_b of the compression flange are considered to be points where lateral deflection of the girder flange and twisting of the entire cross-section are restrained. In the past, points of contraflexure have sometimes been considered to act as brace points. Since this practice can lead to significantly unconservative estimates of the lateral-torsional buckling resistance, the *AASHTO LRFD* Specifications do not imply that points of contraflexure should be considered as brace points. Instead, the effects of moment gradient are to be handled directly through the use of the moment gradient modifier C_b (discussed below).

L_p and L_r are Anchor Points 1 and 2, respectively, as shown on Figure 2.19. L_p defines the *compact unbraced length* limit. A member braced at or below the compact unbraced length limit is able to achieve the maximum potential lateral-torsional buckling resistance (M_{max} in Figure 2.19) of $R_{pc}M_{yc}$ under uniform bending, which is independent of the unbraced length. ***Note again that in many cases, it will not be economical to brace the girder at a distance equal to L_p or below in order to reach M_{max}, particularly under uniform bending conditions for which C_b is equal to 1.0.***

L_r defines the *noncompact unbraced length* limit. The lateral-torsional buckling resistance of a member braced at or below the noncompact unbraced length limit is expressed in Equation 2.138 as a linear function of the unbraced length, as illustrated in Figure 2.19, which represents the inelastic lateral-torsional buckling resistance. L_r is the unbraced length at which the inelastic and elastic lateral-torsional buckling resistances are the same. The resistance at this point is assumed to be $R_b F_{yr} S_{xc}$. F_{yr} (and its associated limits) is discussed in more detail in the section on Fundamental Concepts (Section 2.2.3.1.1.2).

Unbraced lengths greater than L_r are termed *slender unbraced lengths* and their resistance is controlled by elastic lateral-torsional buckling. As mentioned previously, lateral-torsional buckling in the elastic range is of primary importance for relatively slender girders braced at longer than normal intervals, which most typically occurs during a temporary construction condition. The equation for the elastic lateral-torsional buckling stress F_{cr}, given above, is the exact beam-theory solution for the elastic lateral-torsional buckling resistance of a doubly symmetric I-section under uniform bending (when load-height effects are not considered), when an effective radius of gyration r_t given by Equation 2.115 is introduced into Equation 2.22. The expression for r_t given in the specifications, as shown above, is a simplification of Equation 2.115 obtained by assuming that $D = h = d$. However, Equation 2.115 is still provided in the *AASHTO LRFD* Article C6.10.8.2.3 should the Engineer require a more precise calculation of the elastic lateral-torsional buckling stress. The web term $D_c t_w$ in both expressions for r_t accounts for the destabilizing effects of the flexural compression in the web on the lateral-torsional buckling resistance, and also extends the equation to cover singly symmetric I-section members. For composite I-sections in negative flexure, the equations for F_{cr} and L_r are somewhat conservative compared to rigorous beam-theory solutions since they neglect the restraint provided to the bottom (compression) flange by the lateral and torsional stiffness of the concrete deck.

Unlike the Main Provisions, which assume slender-web behavior, the equations for F_{cr} and L_r in Appendix A include the St. Venant torsional constant J, which is appropriate for stockier compact web and noncompact web sections that are generally not subject to significant web distortion. Setting J equal to zero in the above expression for F_{cr} results in the equation for F_{cr} given in the Main Provisions. The above expression for J provides an accurate approximation of the St. Venant torsional stiffness neglecting the effect of the web-to-flange fillets (*33*). *Note that for flanges with $b_f/2t_f$ greater than 7.5, the term in parentheses for that particular flange in the above equation for J may be taken equal to one.* More accurate values for J

for rolled W-sections, including the effect of the web-to-flange fillets, are tabulated in Reference 128a. As pointed out in *AASHTO LRFD* Article CA6.3.3, for the unusual case of a noncompact compact or noncompact web section with $I_{yc}/I_{yt} > 1.5$ and $D/b_{fc} < 2$, $D/b_{ft} < 2$ or $b_{ft}/t_{ft} < 10$, consideration should be given to using more exact beam-theory solutions for the elastic LTB resistance, or else J may be factored by 0.8 to account for the tendency of the above equation for F_{cr} to overestimate the LTB resistance in this case (*73a*).

The above LTB equations assume an effective length factor k for lateral-torsional buckling equal to 1.0. As discussed in the previous section on Fundamental Concepts, warping restraint exists from adjacent unbraced lengths that are less critically loaded than the unbraced length under consideration, which can result in a reduced effective length factor for lateral-torsional buckling. A reduced effective length factor can be used to modify L_b (i.e., kL_b) and to increase the elastic lateral-torsional buckling stress F_{cr} by a factor of $(1/k^2)$ (*23*). *AASHTO LRFD* Article C6.10.8.2.3 makes reference to a procedure (*18, 22, 23*) that can be used to calculate a reduced effective length factor for lateral torsional buckling in special circumstances (e.g., when it becomes necessary to reduce the amplification of first-order flange lateral bending stresses).

The effect of a variation in the major-axis bending moment along the length between brace points, or a moment gradient, is accounted for by applying the moment gradient modifier C_b to the base inelastic and elastic LTB equations. When the moment and corresponding flange compressive major-axis bending stress are constant along the unbraced length, C_b has a base value of 1.0. Under moment gradient conditions, C_b may be taken greater than 1.0, which effectively increases the LTB resistance with the increase capped at $M_{max} = R_{pc}M_{yc}$ (refer to the dashed curves in Figure 2.19). C_b may conservatively be taken equal to 1.0 in all cases, except for some rare cases involving no cross-bracing within the span. In Appendix A, C_b is specified as follows:

- For unbraced cantilevers and for members when $M_{mid}/M_2 > 1$ or $M_2 = 0$:

$$C_b = 1.0$$

<div align="right">Equation 2.140
AASHTO LRFD Equation A6.3.3-6</div>

- For all other cases:

$$C_b = 1.75 - 1.05\left(\frac{M_1}{M_2}\right) + 0.3\left(\frac{M_1}{M_2}\right)^2 \le 2.3$$

<div align="right">Equation 2.141
AASHTO LRFD Equation A6.3.3-7</div>

where:

M_2 =   except as noted below, largest major-axis bending moment at either end of the unbraced length causing compression in the flange under consideration, calculated from the critical moment envelope value (kip-in.). M_2 shall be due to the factored loads and

shall be taken as positive. If the moment is zero or causes tension in the flange under consideration at both ends of the unbraced length, M_2 shall be taken as zero.

M_0 =   moment at the brace point opposite to the one corresponding to M_2, calculated from the moment envelope value that produces the largest compression at this point in the flange under consideration, or the smallest tension if this point is never in compression (kip-in.). M_0 shall be due to the factored loads and shall be taken as positive when it causes compression and negative when it causes tension in the flange under consideration.

M_1 =   moment at the brace point opposite to the one corresponding to M_2, calculated as the intercept of the most critical assumed linear moment variation passing through M_2 and either M_{mid} or M_0, whichever produces the smaller value of C_b (ksi). M_1 may be determined as follows:

➢ When the variation in the moment along the entire length between brace points is concave in shape:

$$M_1 = M_0$$

Equation 2.142

AASHTO LRFD Equation A6.3.3-11

➢ Otherwise:

$$M_1 = 2M_{mid} - M_2 \geq M_0$$

Equation 2.143

AASHTO LRFD Equation A6.3.3-12

M_{mid} =   major-axis bending moment at the middle of the unbraced length, calculated from the moment envelope value that produces the largest compression at this point in the flange under consideration, or the smallest tension if the point is never in compression (kip-in.). M_{mid} shall be due to the factored loads and shall be taken as positive when it causes compression and negative when it causes tension in the flange under consideration.

The basic form of the equation for C_b given by Equation 2.141 has been retained from previous Specifications. However, the definition of the cases where C_b must be taken equal to 1.0, and the calculation of the moments M_1 and M_2 in Equation 2.141, have each been modified to remove ambiguities and to address specific cases where Equation 2.141 was previously unconservative. The reader is referred to the previous discussion of C_b under the heading of the Main Provisions for further information on these issues, and also for further information on the application of the C_b equation to various cases (refer also to the examples given in Figure 2.58).

In the Main Provisions, major-axis bending stresses are used to calculate C_b since dead and live load bending moments are applied to different sections in composite girders, which is significant when the nominal flexural resistance is not permitted to exceed the moment at first yield. In Appendix A, where the nominal flexural

resistance is permitted to exceed the moment at first yield for certain compact and noncompact web sections, the major-axis bending moments are used to calculate C_b since the effect of applying the bending moments to different sections is less critical in these cases.

It is convenient and always conservative to use the critical moment envelope values to calculate C_b, particularly since concurrent moment values at the brace points are not normally tracked in the analysis. It can be shown that the use of the critical moment envelope values for M_2, M_{mid} and M_o is always conservative since a more critical moment distribution along the unbraced length, in terms of computing C_b, cannot exist for all possible concurrent loadings.

As shown in Figure 2.19, under moment gradient conditions (i.e., C_b > 1.0), in addition to an increase in the base LTB resistance, the maximum potential LTB resistance $M_{max} = R_{pc}M_{yc}$ can be reached at larger unbraced lengths. The provisions of *AASHTO LRFD* Article D6.4.2 (Appendix D to Section 6) can be used to calculate the maximum unbraced lengths to achieve M_{max} under moment gradient conditions, and are recommended for use whenever C_b is greater than 1.0. The modifications to Anchor Points 1 and 2 to account for the effect of the moment gradient are given as follows in *AASHTO LRFD* Article D6.4.2:

➢ If $L_b \leq L_p$, then:

$$M_{nc} = R_{pc}M_{yc}$$

Equation 2.144

AASHTO LRFD Equation D6.4.2-1

➢ If $L_p < L_b \leq L_r$, then:

• If $L_b \leq L_p + \dfrac{\left(1 - \dfrac{1}{C_b}\right)}{\left(1 - \dfrac{F_{yr}S_{xc}}{R_{pc}M_{yc}}\right)}\left(L_r - L_p\right)$, then:

$$M_{nc} = R_{pc}M_{yc}$$

Equation 2.145

AASHTO LRFD Equation D6.4.2-2

• Otherwise:

$$M_{nc} = C_b\left[1 - \left(1 - \frac{F_{yr}S_{xc}}{R_{pc}M_{yc}}\right)\left(\frac{L_b - L_p}{L_r - L_p}\right)\right]R_{pc}M_{yc} \leq R_{pc}M_{yc}$$

Equation 2.146

AASHTO LRFD Equation D6.4.2-3

➢ If $L_b > L_r$, then:

- If $L_b \leq 1.95 r_t \dfrac{C_b S_{xc} E}{R_{pc} M_{yc}} \sqrt{\dfrac{J}{S_{xc} h}} \sqrt{1 + \sqrt{1 + 6.76 \left(\dfrac{R_{pc} M_{yc}}{C_b S_{xc} E} \dfrac{S_{xc} h}{J} \right)^2}}$, then:

$$M_{nc} = R_{pc} M_{yc}$$

Equation 2.147

AASHTO LRFD Equation D6.4.2-4

- Otherwise:

$$M_{nc} = F_{cr} S_{xc} \leq R_{pc} M_{yc}$$

Equation 2.148

AASHTO LRFD Equation D6.4.2-5

The base LTB equations in the Specifications assume that the member is prismatic within the unbraced length. For reasons discussed previously under the heading of the Main Provisions, *AASHTO LRFD* Article A6.3.3 permits the effect of the section transition on the LTB resistance to be ignored when the transition is located at a distance less than or equal to 20 percent of the unbraced length from the brace point with the smaller moment.   If there is more than one transition within the unbraced length, any transition within 20 percent of the unbraced length from the brace point with the smaller moment may be ignored and the LTB resistance based on the remaining sections may then be computed as described in the next paragraph.

For unbraced lengths containing a transition to a smaller section at a distance greater than 20 percent of the unbraced length from the brace point with the smaller moment, the flexural resistance based on lateral-torsional buckling may be taken as the smallest resistance within the unbraced length according to *AASHTO LRFD* Article A6.3.3 (note that the transition can either be in the compression or tension flange). The flexural resistance M_{nc} at each section within the unbraced length is then to be taken as this resistance multiplied by the ratio of S_{xc} at the section under consideration to S_{xc} at the section governing the lateral-torsional buckling resistance. In addition, the C_b factor must be taken equal to 1.0 and the unbraced length must not be modified by an effective length factor. Essentially, the nonprismatic member is being replaced with an equivalent prismatic member. The cross-section of the equivalent member that gives the correct LTB resistance is generally some weighted average of all the cross-sections along the unbraced length. If the cross-section that gives the smallest uniform bending resistance is used (i.e., calculated assuming C_b is equal to 1.0) and the calculated resistance based on that cross-section is not exceeded anywhere along the unbraced length, a conservative solution is obtained. A suggested procedure to obtain a more refined estimate of the LTB resistance for this case is given in Reference 23.

To avoid a significant reduction in the LTB resistance in such cases according to the above criteria, consider locating flange transitions within 20 percent of the unbraced length from the brace point with the smaller moment and ensure that the lateral moment of inertia of the flange (or flanges) of the smaller section is equal to or larger

than one-half the corresponding value(s) for the flange(s) of the larger section at the transition.

Finally, for unbraced lengths consisting of singly symmetric noncomposite I-sections subject to reverse curvature bending, the LTB resistance must be checked for both flanges, unless the top flange is considered to be continuously braced. Because the flanges of these sections are different sizes, the LTB resistance may be governed by compression in the smaller flange, even though the compressive stress may be smaller than the maximum compressive stress in the larger flange.

Flexural Resistance Based on Tension Flange Yielding

For composite sections in negative flexure and noncomposite sections, the nominal flexural resistance based on tension flange yielding M_{nt} is to be taken as (*AASHTO LRFD* Article A6.4):

$$M_{nt} = R_{pt}M_{yt}$$

Equation 2.149

AASHTO LRFD Equation A6.4-1

where:
R_{pt} =   web plastification factor for the tension flange determined as specified in *AASHTO LRFD* Article A6.2.1 or A6.2.2, as applicable

Equation 2.149 represents a linear transition in the flexural resistance between M_{yt} and M_p as a function of the web slenderness. As the web slenderness approaches the noncompact web section limit λ_{rw} given in Equation 2.105, Equation 2.149 approaches the nominal flexural resistance based on tension flange yielding given by Equation 2.125. Note that for sections in which M_{yt} is greater than M_{yc}, Equation 2.149 does not control and need not be checked.

2.2.3.7.1.3 Miscellaneous Flexural Members

2.2.3.7.1.3.1 General

AASHTO LRFD Article 6.12 provides provisions for determining the nominal flexural resistance of miscellaneous rolled or built-up noncomposite or composite members used primarily in trusses or frames, or in applications where members are subject to combined axial loads and flexure (refer to Sections 2.4.2.2.2 and 2.4.3.2.2 of this chapter). This section of the chapter reviews these provisions for select noncomposite members only. Discussions on the determination of the nominal flexural resistance of noncomposite box-shaped members (*AASHTO LRFD* Article 6.12.2.2.2), noncomposite circular tubes (*AASHTO LRFD* Article 6.12.2.2.3), and noncomposite rectangular bars and rounds are generally considered to be outside the scope of this Manual. The reader is referred to References 26 and 154 for additional information regarding the flexural resistance of these members.

The reader is also referred to *AASHTO LRFD* Article 6.12.2.3 and to References 26 and 154 for additional information on determining the nominal flexural resistance of miscellaneous composite flexural members (e.g. concrete encased shapes and

concrete filled tubes). *AASHTO LRFD* Article 6.12.3 covers the determination of the shear resistance of miscellaneous composite flexural members.

2.2.3.7.1.3.2 I- and H-Shaped Members Subject to Weak-Axis Flexure

As specified in *AASHTO LRFD* Article 6.12.2.2.1, the nominal flexural resistance of noncomposite I- and H-shaped members subject to flexure about an axis parallel with the web (i.e. weak-axis flexure) is to be determined as follows:

If $\lambda_f \leq \lambda_{pf}$, then:

$$M_n = M_p$$

Equation 2.149a

AASHTO LRFD Equation 6.12.2.2.1-1

If $\lambda_{pf} < \lambda_f \leq \lambda_{rf}$, then:

$$M_n = \left[1 - \left(1 - \frac{S_y}{Z_y} \right) \left(\frac{\lambda_f - \lambda_{pf}}{0.45\sqrt{\dfrac{E}{F_{yf}}}} \right) \right] F_{yf} Z_y$$

Equation 2.149b

AASHTO LRFD Equation 6.12.2.2.1-2

where:

λ_f = largest flange slenderness ratio
    = $b_f/2t_f$ *AASHTO LRFD* Equation 6.12.2.2.1-3

λ_{pf} = $0.38\sqrt{\dfrac{E}{F_{yf}}}$ Equation 2.149c

AASHTO LRFD Equation 6.12.2.2.1-4

λ_{rf} = $0.83\sqrt{\dfrac{E}{F_{yf}}}$ Equation 2.149d

AASHTO LRFD Equation 6.12.2.2.1-5

F_{yf} = specified minimum yield strength of the lower-strength flange (ksi)
M_p = plastic moment about the axis parallel with the web = $F_{yf}Z_y$ (kip-in.)
S_y = elastic section modulus about the axis parallel with the web (in.^{3})
Z_y = plastic section modulus about the axis parallel with the web (in.^{3})

For sections where the largest slenderness ratio λ_f of the two flanges is less than or equal to the compact flange slenderness limit λ_{pf} given by Equation 2.149c, the nominal flexural resistance is to be taken as the full plastic moment resistance M_p, which is equal to $1.5F_{yf}S_y$ for a doubly-symmetric I- or H-shaped member bent about its weak axis (i.e. $Z_y = 1.5S_y$). For a hybrid section, the lower-strength flange is used in determining λ_{pf} and in calculating M_p (the web contribution to M_p about the weak axis is small).

For sections where the largest slenderness ratio λ_f of the two flanges is greater than the compact flange slenderness limit λ_{pf}, but less than or equal to the noncompact flange slenderness limit λ_{rf} given by Equation 2.149d, the nominal flexural resistance is controlled by inelastic flange local buckling. Hence, the linear Equation 2.149b is used to determine the nominal flexural resistance. λ_{rf} is derived from the right-hand side of Equation 2.24 with the plate buckling coefficient k_c taken equal to 0.76. For a linear stress distribution across the flange width with the maximum compressive stress at the flange tip and zero stress at the web/flange juncture, the theoretical elastic flange local buckling coefficient k_c is 0.57 assuming simply-supported edge conditions and 1.61 assuming fixed edge conditions at the web/flange juncture (*18*). A k_c of 0.76 is felt to be a reasonable value due to the restraint offered to the flanges by the web and due to the fact that a portion of the flanges is in tension (*154*). The effect of residual stresses is neglected since k_c is relatively small compared to the potential theoretical value and because of the strain gradient across the flange width (154). The web load-shedding factor R_b is not included in Equation 2.149b since the web flexural stress is zero.

An elastic flange local buckling equation (for $\lambda_f > \lambda_{rf}$) is not included since Equation 2.149d gives a λ_{rf} value equal to 14.1 for F_{yf} = 100 ksi, and λ_f is limited to 12.0 for I-sections according to the flange proportioning limits specified in *AASHTO LRFD* Article 6.10.2.2 (see Equation 2.59).

Note that for I-sections subject to strong-axis flexure in combination with flange lateral bending due to torsion or weak-axis flexure, the one-third rule equations provided in the specifications (discussed previously) should be utilized in lieu of the preceding equations.

2.2.3.7.1.3.3 Tees and Double Angles Subject to Strong-Axis Flexure

AASHTO LRFD Article C6.12.2.2.4 refers to the provisions of the 2005 AISC LRFD Specification (*26*) to determine the nominal flexural resistance of noncomposite tees and double angles.

Section F9 of Reference 26 covers the nominal flexural resistance of tees and double angles loaded in the plane of symmetry (for flexure of these members about their weak-axis or y-axis, which is considered to be a rare case in bridge applications, the reader is referred to the commentary to Section F9 of Reference 26). The nominal flexural resistance is to be taken as the lowest value based on yielding, lateral torsional buckling or flange local buckling. For yielding, the nominal flexural resistance is given as:

$$M_n = M_p$$

Equation 2.149e

AISC LRFD Equation (F9-1)

where:

M_p =   plastic moment = $F_y Z_x$ (kip-in.)

For yielding, M_n is limited to $1.6M_y$ for stems in tension and to M_y for stems in compression, where M_y is equal to the yield moment of the cross-section based on the distance to the tip of the tee stem. The limit on M_n of $1.6M_y$ for cases where the stem is in tension is intended to indirectly control situations where significant yielding of the stem might occur at service load levels.

For lateral-torsional buckling, a simplified version of the elastic lateral-torsional buckling equation developed in Reference 74c (and discussed further in Reference 74d) is given as:

$$M_n = \frac{\pi\sqrt{EI_yGJ}}{L_b}\left[B + \sqrt{1+B^2}\right] \leq M_p$$

<div align="right">Equation 2.149f</div>

<div align="right">*AISC LRFD* Equation (F9-4)</div>

where:

$$B \quad = \quad \pm\,2.3\frac{d}{L_b}\sqrt{\frac{I_y}{J}}$$

<div align="right">Equation 2.149g</div>

<div align="right">*AISC LRFD* Equation (F9-5)</div>

d = total depth of the section (in.)
G = shear modulus of elasticity for steel = 11,200 ksi
I_y = moment of inertia of the cross-section about the y-axis (in.[4])
J = St. Venant torsional constant (in.[4]) (Refer to Section 2.2.3.1.2.1 of this chapter. More accurate values for rolled tee sections including the effect of the web-to-flange fillets are given in Reference 128a.)
L_b = unbraced length (in.)

The plus sign on the value of *B* in Equation 2.149g applies when the stem is in tension and the minus sign applies when the stem is in compression. If the tip of the stem is in compression anywhere along the unbraced length, a negative value of *B* must be used. Note that Equation 2.149f does not contain the moment gradient modifier C_b. As discussed in the commentary to Section F9 of Reference 26, the C_b factor specified for I-sections in Reference 26 is unconservative for tees with the stem in compression. Also, for reverse curvature bending, the portion with the stem in compression may govern the lateral-torsional buckling resistance even though the corresponding moments may be small in relation to the moments in the other portions of the unbraced length. The lateral-torsional buckling resistance for the case where the stem is in compression is substantially smaller than for the stem in tension. As a result, Reference 26 conservatively takes C_b equal to 1.0 for all cases. The commentary to Section E9 of Reference 26 also cautions that for cases where the stem is in tension, connection details should be designed to minimize end restraint moments that may cause the stem to be in flexural compression at the ends of the member.

For sections where the flange is in compression, the limit state of flange local buckling must also be checked. Where the flange slenderness $\lambda_f = b_f/2t_f$ does not exceed the slenderness limit for a compact flange $\lambda_{pf} = 0.38\sqrt{E/F_y}$, flange local

buckling does not control and need not be checked. Otherwise, the nominal flexural resistance based on flange local buckling should be taken as (*154*):

$$M_n = M_p - \left(M_p - 0.7F_y S_{xc}\right)\left(\frac{\lambda_f - \lambda_{pf}}{\lambda_{rf} - \lambda_{pf}}\right) \le M_p \qquad\qquad \text{Equation 2.149h}$$

where:

λ_{rf} = limiting slenderness for a noncompact flange

= $1.0\sqrt{\dfrac{E}{F_y}}$ Equation 2.149i

S_{xc} = elastic section modulus with respect to the compression flange (in.^{3})

As discussed in Reference 154, Equation 2.149h corrects an error in *AISC LRFD* Equation (F9-7) for the flange local buckling resistance, in which a discontinuity in the flexural resistance occurs as the flange slenderness λ_f approaches the compact flange slenderness limit λ_{pf}. *AISC LRFD* Equation (F9-7) approaches M_y instead of the intended value of M_p as the flange slenderness approaches λ_{pf}. Reference 26 also provides an elastic local buckling resistance equation for tee sections with slender flanges in compression (i.e. with $\lambda_f > \lambda_{rf}$). However, this equation is not shown here as none of the rolled tee sections in the AISC Manual shape property tables have slender flange elements, and in general, the limiting slenderness values at which elastic flange local buckling controls are larger than the limiting flange slenderness value of 12.0 for I-sections specified in *AASHTO LRFD* Article 6.10.2.2 (see Equation 2.59 – note that this flange slenderness limit is logically assumed to apply also to flanges of tee sections).

For local buckling when tee stems are loaded in flexural compression, the commentary to Section F9 of Reference 26 provides the following equation, which is indirectly derived from Equation 2.149f in the limit of zero unbraced length:

$$M_n = \frac{\pi E J \sqrt{G/E}}{4.6d} = 0.424\frac{EJ}{d} \le M_y \qquad\qquad \text{Equation 2.149j}$$

<div align="right">AISC LRFD Equation (C-F9-1)</div>

2.2.3.7.1.3.4 Channels Subject to Strong- and Weak-Axis Flexure

AASHTO LRFD Article C6.12.2.2.4 refers to the provisions of the 2005 AISC LRFD Specification (*26*) to determine the nominal flexural resistance of noncomposite channels.

Section F2 of Reference 26 covers the nominal flexural resistance of channels bent about their strong-axis. The nominal flexural resistance is to be taken as the lowest value based on yielding and lateral torsional buckling. For yielding, the nominal flexural resistance is given as:

$$M_n = M_p \qquad\qquad\qquad\qquad \text{Equation 2.149k}$$

where:

M_p = plastic moment = $F_y Z_x$ (kip-in.)

Z_x = plastic section modulus about the x-axis (in.^{3})

For lateral-torsional buckling, when the unbraced length L_b is less than or equal to $L_p = 1.76 r_y \sqrt{E/F_y}$, lateral-torsional buckling does not control and need not be checked.   Otherwise, the nominal flexural resistance based on lateral-torsional buckling is to be taken as follows:

For $L_p < L_b \le L_r$:

$$M_n = C_b \left[M_p - (M_p - 0.7 F_y S_x) \left(\frac{L_b - L_p}{L_r - L_p} \right) \right] \le M_p \qquad \text{Equation 2.149}\ell$$

For $L_b > L_r$:

$$M_n = F_{cr} S_x \le M_p \qquad \text{Equation 2.149m}$$

where:

F_{cr} = elastic lateral torsional buckling stress (ksi)

$$= \frac{C_b \pi^2 E}{\left(\frac{L_b}{r_t} \right)^2} \sqrt{1 + 0.078 \frac{Jc}{S_x h_o} \left(\frac{L_b}{r_{ts}} \right)^2} \qquad \text{Equation 2.149n}$$

$$L_r = 1.95 r_{ts} \frac{E}{0.7 F_y} \sqrt{\frac{Jc}{S_x h_o}} \sqrt{1 + \sqrt{1 + 6.76 \left(\frac{0.7 F_y}{E} \frac{S_x h_o}{Jc} \right)}} \qquad \text{Equation 2.149o}$$

$$c = \frac{h_o}{2} \sqrt{\frac{I_y}{C_w}} \qquad \text{Equation 2.149p}$$

C_b = moment gradient modifier (refer to Section 2.2.3.7.1.2 of this chapter)

C_w = warping torsional constant (in.^{6}). From Reference 28:

$$= \frac{t_f b^3 h_o^2}{12} \left(\frac{3 b t_f + 2 h_o t_w}{6 b t_f + h_o t_w} \right) \qquad \text{Equation 2.149q}$$

(Note: more accurate values for rolled channels based on the sloping flanges and web-to-flange fillets are tabulated in Reference 128a.)

b = distance between the toe of the flange and the centerline of the web (in.)

h_o = distance between flange centroids (in.)

I_y = moment of inertia of the cross-section about the y-axis (in.[4])

J = St. Venant torsional constant (in.[4]) (Refer to Section 2.2.3.1.2.1 of this chapter. More accurate values for rolled channel sections including the effect of the sloping flanges and web-to-flange fillets are given in Reference 128a.)

r_y = radius of gyration of the cross-section about the y-axis (in.)

r_{ts} = $\dfrac{\sqrt{I_y C_w}}{S_x}$ Equation 2.149s

AISC LRFD Equation (F2-7)

S_x = elastic section modulus about the x-axis (in.[3])

t_f = thickness of the flange (in.)

t_w = thickness of the web (in.)

The lateral-torsional buckling equations given above assume that the channels have compact flanges and webs. All the rolled channels given in the AISC Manual shape property tables have compact flanges and webs for $F_y \leq 65$ ksi. To qualify as compact, the flange slenderness $\lambda_f = b_f/2t_f$ of fabricated channels must not exceed the slenderness limit $\lambda_{pf} = 0.38\sqrt{E/F_y}$ and the web slenderness D/t_w of fabricated channels must not exceed $3.76\sqrt{E/F_y}$. The above equations also assume that the channel is restrained at the brace points such that twisting of the member does not occur at those points.

For flexure of channels about their weak-axis or y-axis, it is recommended that the resistance equations for weak-axis flexure of I-sections be used (refer to Section 2.2.3.7.1.3.2 above). Section F6 of Reference 26 places an additional limit of $1.6F_yS_y$ on the computed maximum flexural resistance of I-sections and channels bent about their weak-axis to indirectly prevent substantial yielding of the member at service load levels. It is recommended that this limit be applied to channels. For I-sections, the shape factor Z_y/S_y is nearly always less than 1.6 (only four rolled W-shapes have $Z_y/S_y > 1.6$), whereas for channel sections, Z_y/S_y is commonly greater than 1.6 (*154*).

2.2.3.7.1.3.5 Single Angles Subject to Flexure

Single angles are not typically intended to serve as flexural members in bridge construction. However, in practical applications, they may be subject to flexure about both principal axes due to the eccentricity of applied axial loads. The condition of flexure plus eccentric axial tension is primarily addressed through the use of the shear lag coefficient *U*, as discussed further in Section 2.4.2.2 of this chapter. The condition of flexure plus eccentric axial compression is handled primarily through the

use of an effective slenderness ratio $K\ell/r$, as discussed further in Section 2.4.3.2.1.4 of this chapter.   In certain unusual cases spelled out in Section 2.4.3.2.1.4, single angles subject to combined flexure and axial compression must instead be evaluated as beam-columns according to Section H2 of Reference 26 in lieu of using the effective slenderness ratio. In such cases, the nominal flexural resistance of the angle M_n should be determined according to the procedures given in Section F10 of Reference 26, which will not be discussed in detail here. For these unusual cases, the reader is referred instead to Section F10 of Reference 26 and the corresponding commentary for additional information on the determination of the nominal flexural resistance of single-angle members.

2.2.3.7.2 Shear

Fundamental issues related specifically to shear in I-sections were reviewed in a previous section of this chapter under Fundamental Concepts (Section 2.2.3.1.3). The specific *AASHTO LRFD* design requirements for shear will now be discussed here.

As specified in *AASHTO LRFD* Article 6.10.6.3, shear design provisions for I-section flexural members at the strength limit state are covered in *AASHTO LRFD* Article 6.10.9. A flowchart for the shear design of I-sections is given in *AASHTO LRFD* Figure C6.10.9.1-1. In the discussions below, the resistance factor for shear ϕ_v is to be taken as 1.0, as specified in *AASHTO LRFD* Article 6.5.4.2.

Webs must satisfy the following relationship at the strength limit state:

$$V_u \leq \phi_v V_n$$

<div align="right">Equation 2.150
AASHTO LRFD Equation 6.10.9.1-1</div>

where:
V_n = nominal shear resistance (kips)
V_u = shear in the web at the section under consideration due to the factored loads (kips)

The nominal shear resistance V_n depends on if the web is considered stiffened or unstiffened. As specified in *AASHTO LRFD* Article 6.10.9.1, interior web panels of nonhybrid and hybrid I-shaped members: 1) without a longitudinal stiffener and with a transverse stiffener spacing not exceeding 3D, or 2) with one or more longitudinal stiffeners and with a transverse stiffener spacing not exceeding 1.5D are considered stiffened. Otherwise, the panel is considered unstiffened. The spacing of transverse stiffeners for end panels of stiffened webs, with or without a longitudinal stiffener, must not exceed 1.5D. The design of web stiffeners for I-sections is covered in *AASHTO LRFD* Article 6.10.11 and discussed in Section 2.2.6 of this chapter.

2.2.3.7.2.1 Unstiffened Webs

The nominal shear resistance of nonhybrid and hybrid unstiffened webs is specified in *AASHTO LRFD* Article 6.10.9.2. The nominal shear resistance is limited to the

shear buckling (or shear yielding) resistance V_{cr}, which was derived in Section 2.2.3.1.3 of this chapter as follows:

$$V_n = V_{cr} = CV_p$$

<div align="right">Equation 2.151</div>
<div align="right">AASHTO LRFD Equation 6.10.9.2-1</div>

where:

V_p =   plastic shear force (kips) = $0.58F_{yw}Dt_w$

C =   ratio of the shear buckling resistance to the shear yield strength determined as follows (refer to *AASHTO LRFD* Article 6.10.9.3.2):

➢   If $\dfrac{D}{t_w} \leq 1.12\sqrt{\dfrac{Ek}{F_{yw}}}$, then:

$$C = 1.0$$

<div align="right">Equation 2.152</div>
<div align="right">AASHTO LRFD Equation 6.10.9.3.2-4</div>

➢   If $1.12\sqrt{\dfrac{Ek}{F_{yw}}} < \dfrac{D}{t_w} \leq 1.40\sqrt{\dfrac{Ek}{F_{yw}}}$, then:

$$C = \frac{1.12}{\dfrac{D}{t_w}}\sqrt{\frac{Ek}{F_{yw}}}$$

<div align="right">Equation 2.153</div>
<div align="right">AASHTO LRFD Equation 6.10.9.3.2-5</div>

➢   If $\dfrac{D}{t_w} > 1.40\sqrt{\dfrac{Ek}{F_{yw}}}$, then:

$$C = \frac{1.57}{\left(\dfrac{D}{t_w}\right)^2}\left(\frac{Ek}{F_{yw}}\right)$$

<div align="right">Equation 2.154</div>
<div align="right">AASHTO LRFD Equation 6.10.9.3.2-6</div>

That is, the consideration of post-buckling shear resistance due to tension-field action is not permitted for unstiffened webs. The derivation of Equations 2.152 through 2.154 for the constant *C* is discussed in Section 2.2.3.1.3. ***In calculating the appropriate value of C for an unstiffened web, the shear-buckling coefficient is to be taken as 5.0.*** When *C* is equal to 1.0, the nominal flexural resistance is controlled by shear yielding.

In determining whether or not transverse stiffeners are required at a particular section, the Engineer will first have to determine the nominal shear resistance of the web, assuming it is unstiffened, to determine if it is less than the shear in the web

due to the factored loads at that section. If so, transverse stiffeners are required. *Note that cross-frame/diaphragm connection plates can be considered to act as transverse stiffeners.*

2.2.3.7.2.2 Stiffened Webs

The nominal shear resistance of nonhybrid and hybrid stiffened webs is specified in *AASHTO LRFD* Article 6.10.9.3. Requirements for interior web panels are given in *AASHTO LRFD* Article 6.10.9.3.2 and requirements for end panels are given in *AASHTO LRFD* Article 6.10.9.3.3. The maximum shear in the panel due to the factored loads is to be used to determine the required stiffener spacing, which cannot exceed the maximum values stated previously. For web panels with longitudinal stiffeners, the total web depth *D* is to be used in determining the nominal shear resistance of the panel; that is, the influence of the longitudinal stiffener is conservatively neglected.

2.2.3.7.2.2.1 Interior Panels

Stiffened interior web panels of both nonhybrid and hybrid sections (37, 38, 38a) are capable of developing post buckling shear resistance due to tension-field action. For reasons discussed previously in Section 2.2.3.1.3 of this chapter, in order to develop the full post buckling resistance, the section along the entire panel must be proportioned to satisfy the following relationship (37):

$$\frac{2Dt_w}{\left(b_{fc}t_{fc} + b_{ft}t_{ft}\right)} \le 2.5 \qquad \text{Equation 2.155}$$

AASHTO LRFD Equation 6.10.9.3.2-1

If the above web-to-flange area ratio is satisfied everywhere within the panel, the nominal shear resistance of the panel may be taken as the full post buckling shear resistance, or the sum of the shear yield or shear buckling force (the first term in the following equation) and the post buckling tension-field force (the second term in the following equation):

$$V_n = V_p\left[C + \frac{0.87(1-C)}{\sqrt{1+\left(\frac{d_o}{D}\right)^2}}\right] \qquad \text{Equation 2.156}$$

AASHTO LRFD Equation 6.10.9.3.2-2

where d_o is the transverse stiffener spacing. The constant C in this case is to be calculated from the appropriate equation (i.e. Equation 2.152, 2.153 or 2.154) using the following shear-buckling coefficient:

$$k = 5 + \frac{5}{\left(\dfrac{d_o}{D}\right)^2}$$ Equation 2.157

AASHTO LRFD Equation 6.10.9.3.2-7

If Equation 2.155 is not satisfied, the total area of the flanges is small relative to the area of the web within the panel such that it is assumed that the full post buckling resistance cannot be developed. However, rather than limiting the nominal shear resistance to V_{cr} in such cases, the following conservative estimate of the available post buckling resistance is specified (28) (as discussed previously):

$$V_n = V_p \left[C + \frac{0.87(1-C)}{\sqrt{1 + \left(\dfrac{d_o}{D}\right)^2} + \dfrac{d_o}{D}} \right]$$ Equation 2.158

AASHTO LRFD Equation 6.10.9.3.2-8

2.2.3.7.2.2.2 End Panels

End panels of stiffened webs, or the panels immediately adjacent to the abutments, are not permitted to develop any post-buckling shear resistance. Instead, the shear resistance of these panels is limited to V_{cr} (Equation 2.151) in order to provide a sufficient anchor for the development of the tension field in the immediately adjacent interior panels. In this case, the shear buckling coefficient k used to compute the constant C is to be calculated based on the spacing from the support to the first transverse stiffener adjacent to the support.

EXAMPLE

Given the shears due to the factored dead plus live loads V_u for the Strength I load combination shown in Figure 2.59, which are for an interior girder, determine the required transverse stiffener spacing in Field Section 1. The web in Field Section 1 is ½" x 69". The example bridge is a three-span continuous bridge (the shears for half the bridge are shown in Figure 2.59. The bridge is symmetrical about the longitudinal centerline).
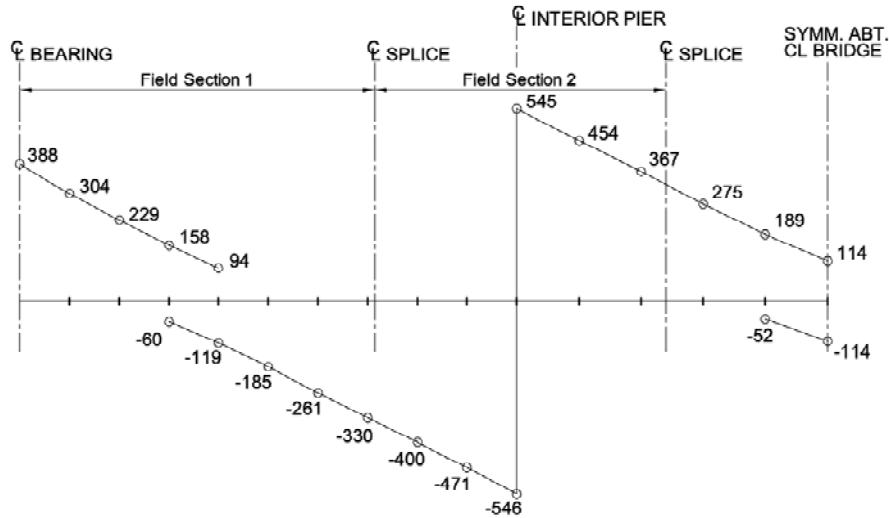
Figure 2.59 Example Problem Shears due to the Factored Loads – Strength I

First, to determine the regions where transverse stiffeners are required, calculate the nominal shear resistance of an unstiffened web. According to *AASHTO LRFD* Article 6.10.9.2, the nominal shear resistance of an unstiffened web is limited to the shear buckling resistance V_{cr} determined as:

$$V_n = V_{cr} = CV_p$$

AASHTO LRFD Equation 6.10.9.2-1

C is the ratio of the shear buckling resistance to the shear yield strength determined from *AASHTO LRFD* Equation 6.10.9.3.2-4, 6.10.9.3.2-5 or 6.10.9.3.2-6, as applicable, *with the shear buckling coefficient k taken equal to 5.0*.

Since,

$$1.40\sqrt{\frac{Ek}{F_{yw}}} = 1.40\sqrt{\frac{29,000(5.00)}{50}} = 75.4 < \frac{D}{t_w} = \frac{69.0}{0.5} = 138.0$$

$$C = \frac{1.57}{\left(\dfrac{D}{t_w}\right)^2}\left(\frac{Ek}{F_{yw}}\right)$$

AASHTO LRFD Equation 6.10.9.3.2-6

$$C = \frac{1.57}{(138.0)^2}\left(\frac{29,000(5.0)}{50}\right) = 0.239$$

V_p is the plastic shear force determined as follows:

$$V_p = 0.58F_{yw}Dt_w$$

AASHTO LRFD Equation 6.10.9.2-2

$$V_p = 0.58(50)(69.0)(0.5) = 1,001\,\text{kips}$$

Therefore,

$$V_n = V_{cr} = 0.239(1,001) = 239\,\text{kips}$$

$$\phi_v V_n = 1.0(239) = 239\,\text{kips}$$

Thus, transverse stiffeners are required in Field Section 1 wherever V_u exceeds $\phi_v V_n$ = 239 kips.

At the abutment, V_u is equal to 388 kips (Figure 2.59). Therefore, a transverse stiffener is required. According to *AASHTO LRFD* Article 6.10.9.3.3, the nominal shear resistance of a web end panel is limited to the shear buckling resistance V_{cr}. First, compute the shear buckling coefficient k. The transverse stiffener spacing for end panels is not to exceed $1.5D$ = 1.5(69.0) = 103.5 inches. Assume the spacing from the abutment to the first transverse stiffener is d_o = 7.25 feet = 87.0 inches.

$$k = 5 + \frac{5}{\left(\dfrac{87.0}{69.0}\right)^2} = 8.15$$

Since,

$$1.40\sqrt{\frac{Ek}{F_{yw}}} = 1.40\sqrt{\frac{29,000(8.15)}{50}} = 96.3 < \frac{D}{t_w} = \frac{69.0}{0.5} = 138.0$$

$$C = \frac{1.57}{(138.0)^2}\left(\frac{29,000(8.15)}{50}\right) = 0.390$$

$$V_p = 0.58(50)(69.0)(0.5) = 1,001\,\text{kips}$$

Therefore,

$$V_n = V_{cr} = 0.390(1,001) = 390\,\text{kips}$$

$$\phi_v V_n = 1.0(390) = 390\,\text{kips} > V_u = 388\,\text{kips} \quad \text{ok}$$

According to *AASHTO LRFD* Article 6.10.9.1, the transverse stiffener spacing for interior panels without a longitudinal stiffener is not to exceed $3D$ = 3(69.0) = 207.0 inches. For the first interior panel to the right of the end panel, assume a transverse stiffener spacing of d_o = 16.75 feet = 201.0 inches, which is the distance from the first transverse stiffener to the first intermediate cross-frame in Field Section 1 (assume that the cross-frame connection plate serves as a transverse stiffener). At the first transverse stiffener located d_o = 7.25 feet from the abutment, V_u is equal to

345 kips, which exceeds $\phi_v V_n$ = 239 kips for an unstiffened web. Therefore, an additional transverse stiffener is required.

For interior panels of both nonhybrid and hybrid members with the section along the entire panel proportioned such that:

$$\frac{2Dt_w}{\left(b_{fc}t_{fc} + b_{ft}t_{ft}\right)} \leq 2.5$$

AASHTO LRFD Equation 6.10.9.3.2-1

the nominal shear resistance is to be taken as the full post buckling shear resistance due to tension-field action, or:

$$V_n = V_p \left[C + \frac{0.87(1-C)}{\sqrt{1+\left(\dfrac{d_o}{D}\right)^2}} \right]$$

AASHTO LRFD Equation 6.10.9.3.2-2

Otherwise, the nominal shear resistance is to be taken as the post buckling shear resistance determined from *AASHTO LRFD* Equation 6.10.9.3.2-8.

For the interior web panel under consideration, the top-flange plate size is 1" x 16" and the bottom-flange plate size is 7/8" x 18". Therefore:

$$\frac{2(69.0)(0.5)}{\left[16(1.0) + 18(0.875)\right]} = 2.17 < 2.5$$

$$k = 5 + \frac{5}{\left(\dfrac{201.0}{69.0}\right)^2} = 5.59$$

Since, $\quad 1.40\sqrt{\dfrac{Ek}{F_{yw}}} = 1.40\sqrt{\dfrac{29,000(5.59)}{50}} = 79.7 < \dfrac{D}{t_w} = \dfrac{69.0}{0.5} = 138.0$

$$C = \frac{1.57}{\left(138.0\right)^2}\left(\frac{29,000(5.59)}{50}\right) = 0.267$$

$$V_p = 0.58(50)(69.0)(0.5) = 1,001\,\text{kips}$$

Therefore,

$$V_n = 1,001 \left[0.267 + \frac{0.87(1-0.267)}{\sqrt{1+\left(\frac{201.0}{69.0}\right)^2}} \right] = 475 \text{ kips}$$

$$\phi_v V_n = 1.0(475) = 475 \text{ kips} > V_u = 345 \text{ kips} \quad \text{ok}$$

V_u at the first intermediate cross-frame in Field Section 1 located 24.0 feet from the abutment is equal to 250 kips, which is greater than $\phi_v V_n = 239$ kips for an unstiffened web. Therefore, assume a transverse stiffener spacing of $d_o = 3D = 17.25$ feet = 207.0 inches from the cross frame to the next stiffener.

$$k = 5 + \frac{5}{\left(\frac{207.0}{69.0}\right)^2} = 5.56$$

Since,

$$1.40\sqrt{\frac{Ek}{F_{yw}}} = 1.40\sqrt{\frac{29,000(5.56)}{50}} = 79.5 < \frac{D}{t_w} = \frac{69.0}{0.5} = 138.0$$

$$C = \frac{1.57}{(138.0)^2} \left(\frac{29,000(5.56)}{50} \right) = 0.266$$

$$V_p = 1,001 \text{ kips}$$

Therefore,

$$V_n = 1,001 \left[0.266 + \frac{0.87(1-0.266)}{\sqrt{1+\left(\frac{207.0}{69.0}\right)^2}} \right] = 468 \text{ kips}$$

$$\phi_v V_n = 1.0(468) = 468 \text{ kips} > V_u = 250 \text{ kips} \quad \text{ok}$$

V_u at this stiffener is equal to 162 kips, which is less than $\phi_v V_n = 239$ kips for an unstiffened web. Therefore, no additional transverse stiffeners are required at the left end of Field Section 1.

At the right end of Field Section 1, V_u at the fourth intermediate cross-frame located 96.0 feet from the abutment is equal to 320 kips, which exceeds $\phi_v V_n = 239$ kips for an unstiffened web. Assume a transverse stiffener spacing of $d_o = 3D = 17.25$ feet = 207.0 inches to the left of this cross frame. For this panel, the top-flange plate size is 1" x 16" and the bottom-flange plate size is 1-3/8" x 18". Therefore:

$$\frac{2(69.0)(0.5)}{\left[16(1.0)+18(1.375)\right]} = 1.69 < 2.5$$

The nominal shear resistance may be taken as the full post buckling shear resistance due to tension-field action. As determined above for this stiffener spacing,

$$\phi_v V_n = 1.0(468) = 468 \text{ kips} > V_u = 320 \text{ kips} \qquad \text{ok}$$

V_u at this stiffener is equal to 233 kips, which is less than $\phi_v V_n$ = 239 kips for an unstiffened web. Therefore, no additional transverse stiffeners are required at the right end of Field Section 1.

72.   Barth, K.E., D.W. White, J.E. Righman, and L. Yang. (2005). "Evaluation of Web Compactness Limits for Singly and Doubly Symmetric Steel I-Girders." Journal of Constructional Steel Research, Elsevier, Vol. 61 (10).

73.   White, D.W. (2004). "Unified Flexural Resistance Equations for Stability Design of Steel I-Section Members - Overview." Structural Engineering, Mechanics and Materials Report No. 24a, School of Civil and Environmental Engineering, Georgia Institute of Technology, Atlanta, GA.

73a.   White, D.W., and S.-K Jung. (2003). "Simplified Lateral-Torsional Buckling Equations for Singly-Symmetric I-Section Members." Structural Engineering, Mechanics and Materials Report No. 24b, School of Civil and Environmental Engineering, Georgia Institute of Technology, Atlanta, GA.

74.   Carskaddan, P.S., and C. G. Schilling. 1974. "Lateral Buckling of Highway Bridge Girders." Research Laboratory Report 22-G-001 (019-3), United States Steel Corporation, Monroeville, PA.

74a.   NSBA. 2006. "Example 2A - Two-Span Continuous Straight Composite I-Girder." NSBA Steel Bridge Design Handbook, available from the National Steel Bridge Alliance (www.steelbridges.org), Chicago, IL.

74b.   NSBA. 2006. "Example 2B - Two-Span Continuous Straight Wide Flange Beam." NSBA Steel Bridge Design Handbook, available from the National Steel Bridge Alliance (www.steelbridges.org), Chicago, IL.

74c.   Kitipornchai, S., and N.S. Trahair. 1980. "Buckling Properties of Monosymmetric I-Beams." Journal of the Structural Division, American Society of Civil Engineers, New York, NY, Vol 109, No. ST5

74d.   Ellifritt, D.S., G. Wine, T. Sputo, and S. Samuel. 1992. "Flexural Strength of WT Sections." Engineering Journal, American Institute of Steel Construction, Chicago, IL, Vol. 29, No. 2, 2nd Qtr.

2.2.3.8 Design Considerations for Skewed Supports

Modern highway design must recognize vehicle speed and right-of-way cost. These factors have reversed the position of the bridge designer from determining the layout of a bridge, including the approaching roadway and span arrangement, to designing bridges for a predetermined space. This space may limit bridge depth, span arrangement and pier location. Additional constraints on the design include sight distances, setbacks, and other constraints such as environmental and aesthetic

factors. This plethora of constraining factors makes the design of bridges more challenging rather than limiting. Skewed supports are one of the most common factors introduced in modern bridge design. Spanning streams askance to the flow or highways not perpendicular to the bridge alignment frequently requires skewed supports when right supports are not practical.

Elimination of skews sometimes improves economy by reducing the length of support structures, but it usually involves increasing the span and often, increasing the girder depth, which tends to increase cost. When girder depth is limited, longer spans may not be practical. However, elimination of skew has the advantage of reducing the length of abutments and/or piers. Reduction of substructure cost should be balanced against any increase in superstructure cost. Minimizing the square footage of bridge deck is often not the most economical solution. Properly designed skewed steel I-girder bridges can be both economical and serviceable.

One of the most problematic skew arrangements is unparallel skewed supports. This arrangement leads to girders of different length and different stiffnesses, and subsequently, different vertical deflections. Hence, elimination of skew on one support while it remains on the other is not a desirable way to address skew. The integral behavior of multi-girder bridge superstructures with respect to transverse elements should be considered in the design. Analysis of these structures must acknowledge the restoring forces in the transverse members and their effect on the girders themselves. In multi-girder bridges with right supports and equal-stiffness girders, the action of these restoring forces is implicit within the wheel-load distribution factors. Bridges with parallel skews have equal length girders usually with equal stiffness. However, when the relative stiffness of points perpendicular to the girders attached by cross-frames or diaphragms is different, design of the girders as well as the cross-frames/diaphragms becomes more problematic.

Skew affects dead load as well as live load. However the specifications only address the effect of skew on live load. This is done by providing correction factors on the wheel-load distribution factors for bending moment and end-support shear in the obtuse corner (Tables 4.6.2.2.2e-1 and 4.6.2.2.3c-1, respectively); there is currently no provision addressing dead-load skew effects on skewed bridges. The correction for shear increases the shear in the obtuse corner caused by the skew. The above-mentioned tables implicitly demonstrate the effect of the cross-frames and the deck in distributing loads in multi-girder bridges. Hence, it is obvious that the cross-frames and deck are subject to larger loads in skewed bridges than in similar right bridges. The specifications leave it to the designer to determine if the cross-frames and deck reinforcing in skewed bridges are adequate.

The effect of skew is far from constant on all bridges. The significance of skew is increased with increasing skew with respect to the girder line; with increased deflections; and in simple spans. Skewed simple spans seem to be more problematic than continuous spans with similar span and skews.

Arrangement of cross-frames/diaphragms is challenging for sharply skewed girder bridges. As discussed in DM Volume 1, Chapter 2, Section 2.4.3.1.4.4.1, if the skew is 20 degrees or less and both supports have the same skew, it is usually desirable

to skew the cross-frames/diaphragms to be parallel with the supports. This arrangement permits the cross-frames/diaphragms to be attached to the girders at points of equal stiffness, thus reducing the relative deflection between cross-frame/diaphragm ends, and thus, the restoring forces in these members. The Specifications permit cross frames to be parallel to the skewed supports up to 20 degrees. Cross-frames/diaphragms with greater parallel skew angles have been used with no deleterious effect, but are currently forbidden by the Specifications.

For skews greater than 20 degrees, the cross-frames/diaphragms must be placed perpendicular to the girders. Typically, they are placed in a contiguous pattern with the cross-frames/diaphragms matched up on both sides of the interior girders, except near the bearings. This arrangement provides the greatest transverse stiffness. Thus, cross-frame/diaphragm forces are relatively large and the largest amount of load possible is transferred across the bridge. This results in the largest reduction of load in the longitudinal members, i.e., the girders. The bearings at oblique points receive increased load. Alternatively, the cross-frames/diaphragms can be staggered. This arrangement reduces the transverse stiffness because the flanges flex laterally and relieve some of the force in the cross-frames/diaphragms. There is a resultant increase in lateral bending moment in the flanges. Often, this lateral bending is not critical and the net result is a desirable reduction in cross-frame/diaphragm forces. Smaller cross-frame/diaphragm forces permit smaller cross-frame/diaphragm members and smaller, less expensive cross-frame/diaphragm connections.

The exterior girders always have cross-frames/diaphragms on one side, but since there are no opposing cross-frames/diaphragms on the other side, lateral flange bending is usually small in these girders, which often have critical vertical bending moments compared to the interior girders. Interior girders are generally subjected to larger lateral flange bending moments when a staggered cross frame arrangement is employed. Fortunately, these girders are usually loaded lighter than their exterior neighbors and thus, do not have to be sized up for lateral bending. In lieu of a refined analysis, Article C6.10.1 contains a suggested estimate of 10.0 ksi for the total *unfactored* lateral flange bending stress f_ℓ due to the use of discontinuous cross-frame/diaphragm lines in conjunction with a skew angle exceeding 20 degrees. It is further suggested that this value be proportioned to dead and live load in the same proportion as the unfactored major-axis dead and live load bending stresses. It is currently presumed that the same value of f_ℓ should be applied to interior and exterior girders, although the suggested value is likely to be conservative for exterior girders for the reason discussed previously. Therefore, lateral flange bending due to discontinuous cross-frame lines in conjunction with skew angles exceeding 20 degrees is preferably best handled by a direct structural analysis of the bridge superstructure.

At piers, it is usually not necessary to use a cross-frame/diaphragm line along a skewed pier. Nor is it necessary to have a cross-frame/diaphragm at each bearing. The specifications require that there be a perpendicular cross-frame/diaphragm at each bearing that is fixed laterally in order to transfer lateral loads into the bearing. Otherwise, lateral bending in the bottom flange near restrained bearings may be excessive. Some means must be provided to allow for jacking the girder to replace

bearings. At abutments (simple supports), a row of cross-frames/diaphragms is always required to support the free edge of the deck. As discussed previously in Volume 1, Chapter 2, the end rotation of the girders creates forces in these cross-frames/diaphragms, which in turn create end moments and shears in the girders. Usually the end moments are negative. Note that the larger the rotation and concomitant deflection of the girders, the larger the end moments. In certain cases, these end moments are important. Generally, they cannot be avoided altogether. However, by placing the deck at the ends of the bridge last, the tensile stresses in the deck can be minimized. The net components of the skewed end support cross-frame/diaphragm forces transverse to the girders result in a torque at the girder ends. The effect of these transverse forces may need to be considered in the design of the transverse deck reinforcement, particularly when the end cross-frame/diaphragm forces are large.

Differential girder deflections between adjacent girders at a cross-frame in skewed bridges results in twist of the girders. Twist makes girder erection and fit-up of the cross-frame connections more difficult as the dead load is applied. In order for the girder webs of straight skewed I-girder bridges to end up plumb with respect to an axis along the girder line at the bearings under either the steel or full dead load condition, the cross-frames/diaphragms must be detailed to introduce the necessary reverse twist into the girders under the no-load condition so that the girders will rotate back to a plumb position as the dead load is applied (See Article C6.7.2). The steel dead load condition refers to the erected steel. The full dead load condition refers to the condition after the full noncomposite dead load, including the concrete deck, is applied. The cross-frames/diaphragms are detailed to not be horizontal in the no-load condition; that is, they are detailed assuming the girder webs will be plumb and the top flanges will lie along a common plane after the dead load is applied. Hence, the girders must be reverse twisted to fit the cross frames into position, but this can usually be accomplished in straight I-girder bridges without inducing significant locked-in stresses in the girder flanges or the cross-frames/diaphragms. The reader is referred to Figure 1.6.1B of Reference 40 for an illustration of how this might be accomplished. The Engineer should be aware however that twisting the girders introduces torsional stresses into the girders, although they are typically small. Stresses induced in this manner are much more significant in curved girders.

The layover of the girders at the end supports in a straight skewed I-girder bridge, or relative lateral movement of the top and bottom flanges, can either be determined from a refined analysis, or approximated from the following equation (*75*):

$$\text{Layover} = \frac{\theta \cdot d}{\text{Tan } \alpha} \qquad \text{Equation 2.159a}$$

where:
α = skew angle of the end support measured with respect to the longitudinal axis of the girder (radians)

θ = girder end rotation due to the appropriate dead load about an axis transverse to the longitudinal axis of the girder (radians)

d   =   girder depth (in.)

Alternatively, the girders may be erected in the no-load condition (i.e. the condition where the girders are erected plumb under a theoretically zero-stress condition neglecting any stress due to the weight of the steel acting between points of temporary support), with the cross-frames/diaphragms detailed to fit theoretically stress-free. In this case, the girders will rotate out-of-plumb as the corresponding dead load is applied. Therefore, the Engineer should consider the effect of any potential errors in the horizontal roadway alignment under the full dead load condition resulting from the girder rotations. Also, it should be ensured that the rotation capacity of the bearings is sufficient to accommodate the twist or that the bearings are installed so that their rotation capacities are not exceeded.

For straight skewed I-girder bridges, Article 6.7.2 requires that the contract documents clearly state an intended erected position of the girders (i.e. either girder webs theoretically plumb or girder webs out-of-plumb) and the position under which that position is to be theoretically achieved (i.e. either the no-load condition, steel dead load condition or full dead load condition). The provisions of Article 2.5.2.6.1 related to bearing rotations for straight skewed I-girder bridges are also to be applied. These provisions are intended to ensure that the computed girder rotations at bearings for the accumulated factored loads corresponding to the Engineer's assumed construction sequence do not exceed the specified rotational capacity of the bearings.

It should be apparent that all of the issues relating to skewed bridges are related to deflection. The smaller the deflections, dead and live, the less critical are the above issues. Thus, deeper girders and lower design stresses are a skewed bridge's best friends.

75.   Ahmadi, A., R. Henney, and D. Thompson. 2005. "Lessons Learned from the Construction of a Sharply Skewed, Two-Span, Steel Multi-Girder Bridge." *Proceedings of the 22nd Annual International Bridge Conference*, Pittsburgh, PA, June 13-15.

2.2.3.9 Bearing Considerations

Traditionally, rocker bearings were used almost exclusively on girder bridges. These bearings permitted free longitudinal movement or else fully restrained such movement. Rocker bearings did not permit lateral movement. They did permit free rotation about a perpendicular axis; however, no rotation about any other axis was permitted. These bearings work quite well on bridges with supports perpendicular to the girder line. They have proven to be problematic on some skewed bridges.

Today the Engineer has a wide selection of bearing types from which to choose the proper bearing. Bearings are available that permit movement and rotation with respect to one, two, or three axes. As one might expect, the same capabilities can cause significant variation in the cost of the bearings. Hence, it is important to determine the expected forces and movements at the bearings to ensure that their

selection and design is compatible with the superstructure design in order that they function properly.

Relatively narrow bridges with perpendicular supports are simplest with respect to the design of bearings. Lateral movement is minimal. Lateral forces such as wind and stream forces are taken by the bearings. Longitudinal forces are also taken by the bearings. However. if the bridge is wide it will expand and contract laterally as well as longitudinally. Rocker bearings have pintels that forbid lateral movement, hence creating lateral forces on the bearings. If bearings at both ends of a span are fixed, load is resisted in part by arching against the fixed bearings. If the supports are piers, they most likely are not truly fixed longitudinally, but flex in proportion to the pier stiffness. Nonetheless, the arching effect creates significant longitudinal forces through the bearings to the piers. The bearings must be designed for these forces in addition to thermal and other longitudinal forces.

As discussed elsewhere, the girders of bridges with skewed supports also twist about the longitudinal axis of the girder, particularly during placement of the dead load. The bearings must be able to accommodate this rotation in some manner.

Bridges with skewed supports can create very large horizontal forces due to gravity, as well as thermal and lateral forces. Thermal forces are resisted by the longitudinally constrained bearings. Since the bearings are askance with respect to the girder lines, a torque is generated. The torque is resisted by lateral forces at the far support. These forces, in turn, cause lateral force at the fixed bearings. These forces have to be recognized in the design and usually mitigated in some manner. These forces increase with bridge width.

A similar phenomenon occurs when gravity load is applied. This is particularly critical on simple spans. As the bottom flange of the girder attempts to elongate, it is restrained by the fixed bearings, which are placed askance with respect to the girder lines. This again creates a torsion that may cause large horizontal forces. These large horizontal forces are evidenced by the failure of anchor bolts, concrete, and even bearings on skewed girder bridges. It is not uncommon for pot bearings on skewed supports to leak due to the large horizontal forces causing distortion of the pot.

The first means of reducing these forces is to free laterally some of the bearings under extreme outward girders. This may have some benefit, but frequently does not solve the problem satisfactorily. Orienting the guided bearings toward a single point is beneficial with regard to thermal forces. The concept is that the single point is fixed as the bridge temperature changes uniformly and the bridge expands along rays radiating from the fixed point. The best location of the fixed point is often at a central bearing. This will cause the bearings on that support line to be guided along the support line. Other supports will have bearings guided toward the fixed bearing. Combining this concept with free bearings on the extreme girders gives a good but not satisfactory design. Most Engineers want more than one bearing taking lateral load at a support in order to provide redundancy. Two or three bearings at each support can be fixed against horizontal translation and often do not substantially

affect performance of the bridge. Generally, the more constraint provided in the bearings, the larger the forces involved.

It is important to recognize that the horizontal forces from the bearings do not act at the neutral axis of the girders. As a result of this eccentricity, the vertical loads on the bearings are also affected, particularly due to thermal effects.

Often, the most economical choice is to not use a bearing. This option is rarely acceptable, but is sometimes employed when stringers rest on floor beams, and where integral abutments or piers are employed. When a bridge girder is restrained by an abutment or pier, the effect of that restraint needs to be considered in the analysis of the bridge. The moment to be resisted by the substructure is usually transferred by shear. Hence, adequate shear connection should be provided.

Elastomeric pads are perhaps the next least expensive bearing type. Often they are laminated to permit greater loads. They permit some girder rotation. They permit translation in horizontal directions.   These bearings can be restrained against translation by detailing of the anchor bolts. Unlike rockers, translation of elastomeric pads requires force. The force is a function of the bearing design and may be taken into account in design of both the superstructure and substructure. It is also possible to combine these bearings with a sliding faying surface to permit translation with the elastomer permitting rotation.

Pot bearings are commonly used in applications where elastomeric bearings are inadequate, such as where vertical or lateral loads are too large, or where required rotations exceed that possible with practical elastomeric bearings. Pot bearings often have a faying surface that permits translation. They may be guided to translate in only one direction or they may translate freely in both directions. If they are fixed against translation, they must resist translation through the pot. Typically, pot bearings are designed to resist 10 percent of the vertical design load. However, they can be designed to resist much larger lateral loads. It behooves the Engineer to properly compute the lateral loads. If the actual lateral load is greater than the design load, the pot may deform and fail by leakage.

Lubricated bronze bearings are another option for the Engineer. These bearings may be made with two lubricated faying surfaces. One is spherical to accommodate rotation. These bearings, when used as fixed bearings, have only a spherical lubricated surface. They have the disadvantage of being tight so that there is no play in fixed bearings for lateral movement.

Built-up rocker bearings are still employed for very large reactions. These bearings have little or no ability to accommodate any movement or rotation other than longitudinal translation and rotation about an axis transverse to the girder. They may be oriented in any fashion so that the translation and rotation are about any axis with respect to the girder.

Lateral restraint of the bearings of girder bridges can have significant effects on the girder moments and shears, and the restoring forces in the cross-frames/diaphragms. Close scrutiny of these restoring force effects is warranted.

Longitudinal restraint of supports at both ends of a span causes arching of the span's girders, reducing the observed girder positive moments while significantly increasing the thrust on the bearings. The bearings should be designed to reflect the large longitudinal forces. Generally, the girders should not be designed to take advantage of the reduced moments since the restraint may not always be present. For example, when bearings are replaced and the bridge must be jacked, the lateral forces on the bearing due to dead load are reduced. This is often evidenced by the bridge "jumping" on the jack when it is lifted, or when an inordinate amount of force is required to jack the bridge because the lateral force is binding the jack piston in the cylinder. However, bearing restraint can cause a substantial increase in cross-frame forces and should not be ignored, particularly on skewed bridges and very large girder spans. The girders may be designed to reflect the larger shears.

2.2.3.10 Cover Plates

In lieu of increasing the width and/or thickness of flange plates in order to increase the flexural resistance of welded beams, or in order to increase the flexural resistance of rolled beams, cover plates can be attached to one or both flanges. The design of cover plates is covered in *AASHTO LRFD* Article 6.10.12. Because of concerns about the fatigue resistance of cover-plated details, the use of cover plates has generally fallen into disfavor, except perhaps for rehabilitation purposes. Utilizing the moment redistribution provisions described in the next section of this chapter can help to eliminate the need for cover plates in straight continuous rolled-beam bridges.

As specified in *AASHTO LRFD* Article 6.10.12.1, the length of any cover plate L_{cp} in feet that is added to a member must satisfy the following:

$$L_{cp} \geq \frac{d}{6.0} + 3.0 \qquad\qquad \text{Equation 2.159}$$

AASHTO LRFD Equation 6.10.12.1-1

where *d* is the total depth of the steel section in inches. The maximum thickness of a single cover plate is not to be greater than two times the thickness of the flange to which it is attached. Multiple welded cover plates on a single flange are not permitted. Cover plates can either be wider or narrower than the flange to which they are attached, but where they are wider, welds are not to be wrapped around the ends of the cover plate. Transverse end welds may or may not be provided in this particular case, but if they are provided, they should be stopped short of the flange edges. Where transverse end welds are not provided in this case, the fatigue resistance at the cover-plate end is reduced from Category E to Category E′ (*AASHTO LRFD* Table 6.6.1.2.3-1). Cover plates may be tapered at their ends, but the width at the ends of the tapered plates must not be less than 3.0 inches. Tapering the cover plate ends does not significantly increase the fatigue resistance at welded ends. The stress concentration at the weld end that is transverse to the applied stress is not significantly altered by varying the shape of the cover-plate end (*64*).

As specified in *AASHTO LRFD* Article 6.10.12.2.1, the theoretical end or cutoff point of the cover plate is to be taken as the section where the major-axis bending stress f_{bu} or the moment M_u due to the factored loads is equal to the factored flexural resistance of the flange. The cover plate must then be extended a terminal distance beyond the theoretical end such that:

1) the stress range at the actual end of the cover plate (i.e. at the point located at the terminal distance beyond the theoretical end) satisfies the load-induced fatigue requirements specified in *AASHTO LRFD* Article 6.6.1.2 (see the previous section of this chapter on Fatigue Limit State Verifications), and

2) the longitudinal force in the cover plate due to the factored loads at the theoretical end can be developed by sufficient welds and/or bolts placed between the theoretical and actual ends.

As mentioned earlier, the fatigue resistance of cover-plated details is a significant consideration in locating the termination (i.e. the actual ends) of partial-length cover plates. Cover plates are typically attached to flanges using welds. The continuous longitudinal welds connecting the cover plate to the flange away from the cover-plate ends are fatigue detail Category B. Between the theoretical and actual ends of the cover plate, these welds must be adequate to develop the computed force in the cover plate at the theoretical end (*AASHTO LRFD* Article 6.10.12.2.2). The ends of the longitudinal welds and the toe of the transverse end weld (if provided) connecting partial-length welded cover plates to the flange provide comparable fatigue conditions.   These conditions result in a very low fatigue resistance. According to *AASHTO LRFD* Table 6.6.1.2.3-1, for base metal at the actual ends of partial-length welded cover plates narrower than the flange, with or without transverse end welds, or wider than the flange with transverse end welds, the nominal fatigue resistance is based on fatigue detail Category E (for flange thicknesses less than or equal to 0.8 inches) or Category E′ (for flange thicknesses greater than 0.8 inches).   As mentioned previously, where the cover plates are wider than the flange and transverse end welds are not provided, the nominal fatigue resistance is computed based on Category E′. For flanges more than 0.8 inches thick used in nonredundant load path structures subject to repetitive loadings that produce tension or stress reversal in the flange, partial-length welded cover plates are not to be used (*AASHTO LRFD* Article 6.10.12.1).

According to *AASHTO LRFD* Table 6.6.1.2.3-1, the nominal fatigue resistance at the ends of partial-length cover plates may be based on fatigue detail Category B if bolted slip-critical end connections are provided.   The bolts provided between the theoretical and actual ends of the cover plate must be sufficient to develop the force due to the factored loads in the cover plate at the theoretical end (*AASHTO LRFD* Article 6.10.12.2.3), and the continuous longitudinal welds connecting the cover plate to the flange must stop a distance of one bolt spacing before the first row of bolts in the end-bolted portion (*76*). The slip resistance of the bolts in the end-bolted portion is to be determined according to the provisions of *AASHTO LRFD* Article 6.13.2.8. As specified in *AASHTO LRFD* Article 6.10.12.2.3, the contract documents must indicate that end-bolted cover plates be installed in the following sequence:

1) drill holes,
2) clean faying surfaces,
3) install bolts, and
4) weld the cover plates.

If the cover plate is welded first to simplify fabrication, cutting oils used during the hole drilling process will reduce the slip coefficient and Category B stress levels will not be developed regardless of the surface preparation used (*76*).

76.   Wattar, F., P. Albrecht, and A.H. Sahli. 1985. "End-Bolted Cover Plates." *Journal of the Structural Division*, American Society of Civil Engineers, New York, NY, Vol. 3, No. 6, June.

2.2.3.11 Moment Redistribution

AASHTO LRFD Appendix B to Section 6 of the *AASHTO LRFD* Specifications provides optional provisions for the calculation of redistribution moments from the interior-pier sections of straight continuous-span I-girder bridges (meeting certain specified restrictions) at the service and/or strength limit states. These provisions replace the traditional flat ten-percent redistribution allowance given in previous *AASHTO* Standard Specifications (*157*) and, in general, provide simpler and more rational approaches for calculating the percentage of moment redistribution from interior-pier sections than the inelastic analysis procedures given in previous *AASHTO LRFD* Specifications. In the more simplified approach that is presented in *AASHTO LRFD* Appendix B (the Effective Plastic Moment Method), elastic moment envelopes are utilized and the direct use of any iterative inelastic analysis methods is not required. A more rigorous approach (the Refined Method) is also permitted to allow the Engineer to conduct a direct shakedown analysis, if desired, again utilizing the elastic moment envelope values.

Several restrictions are specified on the use of these approaches in order to ensure adequate ductility and robustness at interior-pier sections. Where these requirements are met, *the provisions may be applied to sections with compact, noncompact or slender webs*. Previous provisions were limited only to sections with compact webs, as defined in those earlier provisions. The provisions may also be applied to sections that are either composite or noncomposite in positive or negative flexure. As mentioned above, according to the provisions, the redistribution moments may be calculated using either a simplified effective plastic moment method that intrinsically accounts for the interior-pier section moment-rotation characteristics, or a more refined method in which a direct shakedown analysis is conducted to ensure the simultaneous satisfaction of continuity and moment-rotation relationships at all interior-pier sections from which moments are redistributed. Additional more detailed information on the development of these provisions may be found in References 77 through 80, which contain extensive references to other supporting research. Example applications of these provisions are demonstrated in References 74a and 74b.

Moment redistribution in straight continuous I-girder spans results from minor localized yielding at interior piers. However, in conventional elastic analysis and

design, moment and shear envelopes are typically determined by elastic analysis with no redistribution due to the effects of local yielding considered. As a result, cross-sections in regions adjacent to interior-pier sections are proportioned for a resistance equal or greater than that required by the elastic moment envelopes. Therefore, cover plates may be added to rolled beams in these regions to increase the flexural resistance, which introduces details that often have low fatigue resistance. In welded beams, multiple flange transitions are typically added in these regions according to the elastic moment demand, which can result in increased fabrication costs. Accounting for the redistribution of moments according to these optional provisions, where appropriate, can make it possible to eliminate such details by using prismatic sections along the entire length of the bridge or between field splices, which can provide fabrication economies and improve the overall fatigue resistance. This is made possible by removing restrictions on the flexural resistance in the regions adjacent to interior piers from which moments are redistributed by accounting for the strength and ductility of the pier sections directly within the procedures used to calculate the redistribution moments.

2.2.3.11.1 Restrictions

The following restrictions specified in *AASHTO LRFD* Article B6.2 must be satisfied in order to apply the optional provisions of *AASHTO LRFD* Appendix B to calculate the redistribution moments. Also, as discussed previously in the section of this chapter entitled Strength Limit State Verifications, when these restrictions are satisfied and when the appropriate value of θ_{RL} from *AASHTO LRFD* Article B6.6.2 (discussed below under the Refined Method) exceeds 0.009 radians at all adjacent interior-pier sections, the nominal flexural resistance M_n of composite sections in positive flexure in continuous spans need not be limited to $1.3R_hM_y$ (refer to Equation 2.97). Pier sections meeting the above requirements are assumed to have sufficient ductility and robustness such that the redistribution of moments to adjacent pier sections *caused by partial yielding within the positive flexure regions* is considered inconsequential.

The provisions of *AASHTO LRFD* Appendix B may be applied only to straight continuous-span I-section members whose bearing lines are not skewed more than 10 degrees from radial and along which there are no staggered cross-frames. Research to date has primarily focused only on straight non-skewed I-girder bridge superstructures without staggered cross-frames.

The cross-sections throughout the unbraced lengths immediately adjacent to interior-pier sections from which moments are redistributed must have a specified minimum yield strength not exceeding 70 ksi. The original development of these provisions considered only nonhybrid and hybrid girders with specified minimum yield strengths up to and including 70 ksi.

Because the effect of holes in the tension flange on potential net section fracture at cross-sections experiencing significant inelastic strains is not well understood, holes in the tension flange are not permitted over a distance of 2D on either side of the interior-pier sections from which moments are redistributed, where D is the web

depth. The distance of 2*D* approximately encompasses the zone of primary inelastic behavior at pier sections.

In addition, all of the following requirements must be met throughout the unbraced lengths immediately adjacent to interior-pier sections from which moments are redistributed. If the effective plastic moment approach (discussed below) is utilized to calculate the redistribution moments, the unbraced lengths immediately adjacent to *all* interior-pier sections of the continuous-span member must satisfy the following requirements. This restriction is due to the approximations involved in the development of the simplified effective plastic moment approach, and the fact that inelastic redistribution moments from one interior pier generally produce nonzero redistribution moments at all interior piers. If the refined method (also discussed below) is used to calculate the redistribution moments, the unbraced lengths immediately adjacent to all interior-pier sections are not required to satisfy the following requirements. However, moments may only be redistributed from interior-pier sections with adjacent unbraced lengths that do satisfy them.

In addition to the requirements given below, as specified in *AASHTO LRFD* Article B6.2.3, the steel I-section member must be prismatic within the unbraced length under consideration, as only prismatic members within unbraced lengths adjacent to interior piers were considered in the supporting research. Also, as specified in *AASHTO LRFD* Article B6.2.6, bearing stiffeners designed according to the provisions of *AASHTO LRFD* Article 6.10.11.2 (see later section of this chapter on Bearing Stiffener Design) must be provided at the interior-pier section under consideration (even on rolled beams). The bearing stiffeners help to ensure adequate robustness of the pier section as inelastic rotations occur.

2.2.3.11.1.1 Web Proportions

As specified in *AASHTO LRFD* Article B6.2.1, the web within the unbraced length under consideration must satisfy all the following requirements:

$$\frac{D}{t_w} \le 150 \qquad\qquad \text{Equation 2.160}$$

AASHTO LRFD Equation B6.2.1-1

$$\frac{2D_c}{t_w} \le 6.8\sqrt{\frac{E}{F_{yc}}} \qquad\qquad \text{Equation 2.161}$$

AASHTO LRFD Equation B6.2.1-2

$$D_{cp} \le 0.75D \qquad\qquad \text{Equation 2.162}$$

AASHTO LRFD Equation B6.2.1-3

where:
   D_c =   depth of the web in compression in the elastic range (in.). For composite sections, D_c is to be determined according to the provisions of *AASHTO LRFD* Article D6.3.1.

D_{cp} =   depth of the web in compression at the plastic moment determined as specified in *AASHTO LRFD* Article D6.3.2 (in.)

Equation 2.160 parallels the web-slenderness requirement given in *AASHTO LRFD* Article 6.10.2.1.1 and prevents the application of the provisions of *AASHTO LRFD* Appendix B to interior-pier sections with longitudinal web stiffeners. The moment-rotation characteristics of sections with longitudinal web stiffeners have not been studied in sufficient detail at this writing. Equations 2.161 and 2.162 are limits on the web slenderness $2D_c/t_w$ and depth of the web in compression at the plastic moment D_{cp} that were considered in the research conducted to date.

2.2.3.11.1.2 Compression Flange Proportions

As specified in *AASHTO LRFD* Article B6.2.2, compression flanges within the unbraced length under consideration must satisfy the following requirements:

$$\frac{b_{fc}}{2t_{fc}} \leq 0.38\sqrt{\frac{E}{F_{yc}}}$$

<div align="right">Equation 2.163</div>

<div align="right">*AASHTO LRFD* Equation B6.2.2-1</div>

$$b_{fc} \geq \frac{D}{4.25}$$

<div align="right">Equation 2.164</div>

<div align="right">*AASHTO LRFD* Equation B6.2.2-2</div>

Equation 2.163 conservatively ensures that all compression flanges within the unbraced length will be compact flanges (see the previous section of this chapter on Strength Limit State Verifications for the definition of a compact flange). Equation 2.164 corresponds to the largest aspect ratio D/b_{fc} considered in the supporting research. Larger values of this ratio reduce the strength and moment-rotation characteristics of I sections.

2.2.3.11.1.3 Lateral Bracing

As specified in *AASHTO LRFD* Article B6.2.4, the unbraced length L_b under consideration must satisfy:

$$L_b \leq \left[0.1 - 0.06\left(\frac{M_1}{M_2}\right)\right]\frac{r_t E}{F_{yc}}$$

<div align="right">Equation 2.165</div>

<div align="right">*AASHTO LRFD* Equation B6.2.4-1</div>

where:
  M_1 =   bending moment about the major-axis of the cross-section at the brace point with the lower moment due to the factored loads, taken as either the maximum or minimum moment envelope value, whichever produces the smallest permissible unbraced length (kip-in.)

M_2 =   bending moment about the major-axis of the cross-section at the brace point with the higher moment due to the factored loads, taken as the critical moment envelope value (kip-in.)

r_t =   effective radius of gyration for lateral torsional buckling within the unbraced length under consideration determined from *AASHTO LRFD* Equation A6.3.3-10 (in.)

The ratio of (M_1/M_2) is to be taken as negative when the moments cause reverse curvature bending. Equation 2.165 is similar to the compression-flange bracing requirement given for compact sections in previous *AASHTO LRFD* Specifications, but is written in terms of r_t rather than the radius of gyration of the entire steel section about the vertical axis r_y, which is felt by the specification writers to be more correct for handling composite sections in negative flexure. Since the negative-moment envelope is typically concave in shape near interior-pier sections, consideration of the moment at the mid-point of the unbraced length is not required for consideration of moment-gradient effects, as is required in general for the calculation of the moment-gradient modifier C_b in *AASHTO LRFD* Article A6.3.3. Using the ratio of the end moments (M_1/M_2) in Equation 2.165 is considered to be sufficient and conservative for considering the moment-gradient effects.

2.2.3.11.1.4 Shear

As specified in *AASHTO LRFD* Article B6.2.5, webs with or without transverse stiffeners within the unbraced length under consideration must satisfy the following requirement *at the strength limit state*:

$$V_u \leq \phi_v V_{cr}$$ Equation 2.166

AASHTO LRFD Equation B6.2.5-1

where:

ϕ_v =   resistance factor for shear specified in *AASHTO LRFD* Article 6.5.4.2 (= 1.0)

V_{cr} =   shear-buckling resistance determined from *AASHTO LRFD* Equation 6.10.9.2-1 for unstiffened webs and from *AASHTO LRFD* Equation 6.10.9.3.3-1 for stiffened webs (kips)

V_u =   shear due to the factored loads (kips)

Equation 2.166 limits the shear due to the factored loads within the unbraced length to the shear-buckling resistance to improve the moment-rotation characteristics of pier sections from which moments are redistributed. Therefore, the use of post-buckling shear resistance, or tension-field action, is not permitted within the vicinity of these pier sections.

2.2.3.11.2 Effective Plastic Moment Method

The redistribution moments at the service and/or strength limit states may be computed using a simplified effective plastic moment approach using an effective plastic moment that is based on a lower-bound estimate of the moment-rotation characteristics of interior-pier sections satisfying the restrictions of *AASHTO LRFD*

Article B6.2. At each limit state, the redistribution moments are computed according to the corresponding procedures given below, and are then added to the elastic moments due to the appropriate factored loads.

2.2.3.11.2.1 Service Limit State

Calculation of the redistribution moments at the service limit state using the effective plastic moment method is covered in *AASHTO LRFD* Article B6.3. As specified in *AASHTO LRFD* Article B6.3.1, load combination Service II (*AASHTO LRFD* Table 3.4.1-1) is to be applied in the calculations (see DM Volume 1, Chapter 5 for further discussion of the Service II load combination). In checking permanent deflections under the Service II load combination (see the previous section of this chapter on Service Limit State Verifications), localized yielding is permitted at interior-pier sections satisfying the restrictions of *AASHTO LRFD* Article B6.2, which results in a redistribution of the elastic moments. As discussed previously, when the effective plastic moment method is employed, these restrictions must be met at all interior-pier sections in the member. According to *AASHTO LRFD* Article B6.3.3.1, the redistribution moment M_{rd} at the interior-pier sections at the service limit state is to be taken as:

$$M_{rd} = |M_e| - M_{pe}$$

<div align="right">Equation 2.167</div>

<div align="right">*AASHTO LRFD* Equation B6.3.3.1-1</div>

where:
M_e = critical elastic moment envelope value at the interior-pier section due to the Service II loads (kip-in.)

M_{pe} = negative-flexure effective plastic moment for the service limit state determined as specified in *AASHTO LRFD* Article B6.5 (see below) (kip-in.)

Equation 2.167 is based on the concepts related to shakedown analysis of continuous-span girders under repeated applications of moving live loads (*79, 81*) utilizing an effective plastic moment M_{pe}. Shakedown has been determined to be the most appropriate limit state related to moment redistribution in continuous-span bridges (*82*). Flange lateral bending effects at interior piers under the Service II load combination were considered negligible by the specification writers due to the restrictions of *AASHTO LRFD* Article B6.2, and are therefore not included in Equation 2.167.

At the service limit state, unless the requirements of *AASHTO LRFD* Article B6.5.1 are satisfied to provide enhanced moment-rotation characteristics, the effective plastic moment M_{pe} at interior-pier sections satisfying the restrictions of *AASHTO LRFD* Article B6.2 is to be taken as (*AASHTO LRFD* Article B6.5.2):

$$M_{pe} = \left(2.90 - 2.3\frac{b_{fc}}{t_{fc}}\sqrt{\frac{F_{yc}}{E}} - 0.35\frac{D}{b_{fc}} + 0.39\frac{b_{fc}}{t_{fc}}\sqrt{\frac{F_{yc}}{E}}\frac{D}{b_{fc}} \right) M_n \leq M_n$$

<div align="right">Equation 2.168</div>

<div align="right">*AASHTO LRFD* Equation B6.5.2-1</div>

where:

M_n = nominal flexural resistance of the interior-pier section taken as the smaller of $F_{nc}S_{xc}$ and $F_{nt}S_{xt}$, with F_{nc} and F_{nt} determined as specified in *AASHTO LRFD* Article 6.10.8. For sections with compact or noncompact webs, M_n may be taken as the smaller of M_{nc} and M_{nt} determined as specified in *AASHTO LRFD* Appendix A (kip-in.)

For interior-pier sections satisfying the special requirements of *AASHTO LRFD* Article B6.5.1 to provide enhanced moment-rotation characteristics, namely:

1) where transverse web stiffeners spaced at D/2 or less are provided over a minimum distance of D/2 on each side of the interior-pier section, and
2) an ultracompact web satisfying the following requirement is provided:

$$\frac{2D_{cp}}{t_w} \le 2.3 \sqrt{\frac{E}{F_{yc}}}$$
Equation 2.169

AASHTO LRFD Equation B6.5.1-1

M_{pe} at the service limit state may instead be taken as follows:

$$M_{pe} = M_n$$
Equation 2.170

AASHTO LRFD Equation B6.5.1-2

Closely spaced transverse stiffeners adjacent to the interior-pier section help to restrain the local buckling distortions of the compression flange and web. A stocky ultracompact web also helps reduce web distortions and restrains flange local buckling distortions such that the moment-rotation characteristics of the pier section are enhanced relative to sections that only satisfy the restrictions of *AASHTO LRFD* Article B6.2 (*78*, *80*).

In both Equations 2.168 and 2.170, the influence of the web slenderness on M_{pe} for both noncompact web and slender web sections is captured through the inclusion of the term M_n. Equations 2.168 and 2.170 are based on an estimated upper-bound required plastic rotation of 0.009 radians at the pier sections at the service limit state that was determined by a direct inelastic analysis of various trial designs (*83*). The development of these equations is discussed in further detail in Reference 78.

According to *AASHTO LRFD* Article B6.3.3.1, the calculated pier-section redistribution moment M_{rd} must be greater than or equal to zero and less than or equal to $0.2|M_e|$. This requirement is intended to prevent the use of an interior-pier section in the design that is so small that it might violate the assumed upper-bound plastic rotation of 0.009 radians assumed in the development of the equations for M_{pe} at the service limit state. If the upper limit of $0.2|M_e|$ is violated, a larger section must be selected at the interior pier until this limit is satisfied.

The redistribution moments remain in the member after the live loads are removed and cause the member to shakedown or behave elastically under subsequent passages of heavy overload vehicles. The moments are held in equilibrium by the support reactions; hence, they must vary linearly between the supports. Therefore, as specified in *AASHTO LRFD* Article B6.3.3.2, the redistribution moments at all locations other than at interior piers are to be determined by connecting with straight lines the redistribution moments at adjacent interior-pier sections. The lines are to be extended to any points of zero redistribution moment at adjacent supports, including the abutments. A typical redistribution moment diagram for a three-span continuous member is illustrated in Figure 2.60. Note that the redistribution moments are positive at both interior-pier sections in this case.
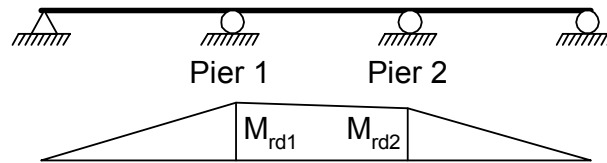
Figure 2.60   Typical Redistribution Moment Diagram for a Three-Span Continuous Bridge

At the service limit state, permanent deflections are controlled by limiting the flange stresses due to the Service II load combination according to the provisions of *AASHTO LRFD* Article 6.10.4.2 (refer to Equations 2.78 through 2.80). Also, except for composite sections in positive flexure in which the web satisfies the requirement of *AASHTO LRFD* Article 6.10.2.1.1 (i.e. $D/t_w \leq 150$), a web bend-buckling check is required (refer to Equation 2.81). *As specified in AASHTO LRFD Article B6.3.2.1, after the redistribution moments are calculated, the flange-stress limitations of AASHTO LRFD Article 6.10.4.2 (i.e. Equations 2.78 through 2.80, as applicable) are not to be checked within the regions extending in each adjacent span from interior-pier sections satisfying the restrictions of AASHTO LRFD Article B6.2 to the nearest flange transition or point of permanent-load contraflexure, whichever is closest.* These checks are not considered necessary in these regions because the redistribution moments cause the member to shakedown under repeated live loads and because the ductility and strength of the interior-pier sections has been considered within the calculation of those moments. *The web bend-buckling check (i.e. Equation 2.81) is still required in these regions however and should be based on the elastic moments prior to redistribution.*

At all other locations outside these regions, the provisions of *AASHTO LRFD* Article 6.10.4.2 (i.e. Equations 2.78 through 2,81, as applicable) *must* be checked after the redistribution moments are calculated (*AASHTO LRFD* Article B6.3.2.2). As discussed previously, the redistribution moments are added to the elastic moments due to the Service II loads before the checks are made. At composite sections, the stresses due to the locked-in redistribution moments tend to decrease with time due to creep in the concrete. These stresses are likely to be continually renewed however with the subsequent passages of similar heavy live loads. Therefore, at composite sections in positive flexure, the redistribution moments are to be added to

the DC$_2$ and DW (if present) moments and the corresponding flexural stresses in the steel section calculated using the long-term composite section (i.e. using a modular ratio of 3*n*), as specified in *AASHTO LRFD* Article B6.3.2.2.

As mentioned in *AASHTO LRFD* Article CB6.3.2.1, additional cambering of the girder steel to account for the small permanent deformations associated with localized yielding at the piers under the Service II loads and the corresponding redistribution of the pier-section moments is not recommended. Very small permanent deflections under an overload condition were observed during the testing of an actual full-scale bridge on a logging road that was designed to permit redistribution of negative moments (*84*).

2.2.3.11.2.2 Strength Limit State

Calculation of the redistribution moments at the strength limit state using the effective plastic moment method is covered in *AASHTO LRFD* Article B6.4. In checking the strength limit state, localized yielding is permitted at interior-pier sections satisfying the restrictions of *AASHTO LRFD* Article B6.2, which results in a redistribution of the elastic moments. As discussed previously, when the effective plastic moment method is employed, these restrictions must be met at all interior-pier sections in the member. According to *AASHTO LRFD* Article B6.4.2.1, the redistribution moment M_{rd} at the interior-pier sections at the strength limit state is to be taken as the *larger* of the following:

$$M_{rd} = \left|M_e\right| + \frac{1}{3}f_\ell S_{xc} - \phi_f M_{pe} \qquad \text{Equation 2.171}$$

AASHTO LRFD Equation B6.4.2.1-1

or

$$M_{rd} = \left|M_e\right| + \frac{1}{3}f_\ell S_{xt} - \phi_f M_{pe} \qquad \text{Equation 2.172}$$

AASHTO LRFD Equation B6.4.2.1-2

where:

ϕ_f = resistance factor for flexure specified in *AASHTO LRFD* Article 6.5.4.2 (= 1.0)

f_ℓ = lateral bending stress in the flange under consideration at the interior-pier section (ksi). For continuously braced flanges, f_ℓ is to be taken as zero.

M_e = critical elastic moment envelope value at the interior-pier section due to the factored loads (kip-in.)

M_{pe} = negative-flexure effective plastic moment for the strength limit state determined as specified in *AASHTO LRFD* Article B6.5 (see below) (kip-in.)

S_{xc} = elastic section modulus about the major-axis of the cross-section to the compression flange taken as M_{yc}/F_{yc} (in.^{3})

S_{xt} = elastic section modulus about the major-axis of the cross-section to the tension flange taken as M_{yt}/F_{yt} (in.^{3})

Flange lateral bending effects at interior piers are conservatively included in Equations 2.171 and 2.172 (according to the one-third rule – see Section 2.2.3.1.2.2 of this chapter under Fundamental Concepts) to account for the reduction in the flexural resistance at the interior-pier section due to these effects. In this case, at the strength limit state, flange lateral bending effects are primarily due to wind loads, which must be considered in certain strength load combinations (see DM Volume 1, Chapter 5).

At the strength limit state, unless the requirements of *AASHTO LRFD* Article B6.5.1 are satisfied to provide enhanced moment-rotation characteristics, the effective plastic moment M_{pe} at interior-pier sections satisfying the restrictions of *AASHTO LRFD* Article B6.2 is to be taken as (*AASHTO LRFD* Article B6.5.2):

$$M_{pe} = \left(2.63 - 2.3 \frac{b_{fc}}{t_{fc}} \sqrt{\frac{F_{yc}}{E}} - 0.35 \frac{D}{b_{fc}} + 0.39 \frac{b_{fc}}{t_{fc}} \sqrt{\frac{F_{yc}}{E}} \frac{D}{b_{fc}} \right) M_n \leq M_n \qquad \text{Equation 2.173}$$

AASHTO LRFD Equation B6.5.2-2

For interior-pier sections satisfying the special requirements of *AASHTO LRFD* Article B6.5.1 to provide enhanced moment-rotation characteristics, namely:

1) where transverse web stiffeners spaced at D/2 or less are provided over a minimum distance of D/2 on each side of the interior-pier section, and
2) an ultracompact web satisfying Equation 2.169 is provided, M_{pe} at the strength limit state may instead be taken as follows:

$$M_{pe} = \left(2.78 - 2.3 \frac{b_{fc}}{t_{fc}} \sqrt{\frac{F_{yc}}{E}} - 0.35 \frac{D}{b_{fc}} + 0.39 \frac{b_{fc}}{t_{fc}} \sqrt{\frac{F_{yc}}{E}} \frac{D}{b_{fc}} \right) M_n \leq M_n \qquad \text{Equation 2.174}$$

AASHTO LRFD Equation B6.5.1-3

In both Equations 2.173 and 2.174, the influence of the web slenderness on M_{pe} for both noncompact web and slender web sections is captured through the inclusion of the term M_n. Equations 2.173 and 2.174 are based on an estimated upper-bound required plastic rotation of 0.03 radians at the pier sections at the strength limit state that was determined by a direct inelastic analysis of various trial designs (*83*). The development of these equations is discussed in further detail in Reference 78.

According to *AASHTO LRFD* Article B6.4.2.1, the calculated pier-section redistribution moment M_{rd} must be greater than or equal to zero and less than or equal to $0.2|M_e|$. This requirement is intended to prevent the use of an interior-pier section in the design that is so small that it might violate the assumed upper-bound plastic rotation of 0.03 radians assumed in the development of the equations for M_{pe} at the strength limit state. If the upper limit of $0.2|M_e|$ is violated, a larger section must be selected at the interior pier until this limit is satisfied.

The redistribution moments at all locations other than at interior piers are to be determined in the same manner as discussed previously for the service limit state (*AASHTO LRFD* Article B6.4.2.2 – refer to Figure 2.60**)**.

As specified in AASHTO LRFD Article B6.4.1.1, after the redistribution moments are calculated, the strength limit state flexural resistance requirements (refer to the previous section of this chapter on Strength Limit State Verifications for Composite Sections in Negative Flexure and Noncomposite Sections) are not to be checked within the unbraced lengths immediately adjacent to interior-pier sections satisfying the restrictions of AASHTO LRFD Article B6.2. Again, these checks are not considered necessary in these regions because the redistribution moments cause the member to shakedown under repeated live loads and because the ductility and strength of the interior-pier sections has been considered within the calculation of the those moments.

At all other locations outside these regions, the strength limit state provisions of *AASHTO LRFD* Articles 6.10.7.1, 6.10.8.1 or A6.1, as applicable (refer to the previous section of this chapter on Strength Limit State Verifications), *must* be checked after the redistribution moments are calculated (*AASHTO LRFD* Article B6.4.1.2). The redistribution moments are added to the elastic moments due to the factored loads at the strength limit state before the checks are made. As discussed previously for the service limit state, at composite sections in positive flexure *where stress calculations are required at the strength limit state (e.g. at noncompact sections)*, the redistribution moments are to be added to the DC_2 and DW (if present) moments and the corresponding flexural stresses in the steel section calculated using the long-term composite section (i.e. using a modular ratio of 3n), as specified in *AASHTO LRFD* Article B6.4.1.2.

2.2.3.11.3 Refined Method

AASHTO LRFD Article B6.6 alternatively allows the use of a refined method to calculate the redistribution moments, in which a direct shakedown analysis is conducted to ensure the simultaneous satisfaction of rotational continuity and inelastic moment-rotation relationships at all interior-pier sections from which moments are redistributed. The refined method may be applied at the service and/or strength limit states, and utilizes the critical elastic moment envelope values due to the appropriate factored loads in the analysis. As specified in *AASHTO LRFD* Article B6.2, when the refined method is employed, all interior-pier sections are *not* required to satisfy the restrictions of *AASHTO LRFD* Article B6.2, but moments may not be redistributed from those particular sections and those sections must be assumed to remain elastic in the analysis. Also, those sections (and the corresponding portions of each span adjacent to those sections) must satisfy all applicable design requirements at the service and/or strength limit states after a final solution is obtained. As pointed out in *AASHTO LRFD* Article CB6.6.1, when the refined method is used, the calculated plastic rotations at the pier sections will typically be smaller than the upper-bound rotations assumed in the development of the effective plastic moment method (see above).

The refined method is similar in concept to the unified autostress method permitted in previous *AASHTO LRFD* Specifications and described in detail in Reference 85. In this method, at each pier from which moments are to be redistributed, continuity relationships are written relating the plastic rotations θ_p at all pier sections assumed to be undergoing yielding to the moment at the pier section under consideration. In this relationship, the pier-section moment is taken equal to the critical elastic moment envelope value at the pier section under consideration plus the sum of the redistribution moments at that pier due to any plastic rotations (and corresponding redistribution moments) occurring at all pier sections assumed to be undergoing yielding. Redistribution moments resulting from plastic rotations at one interior support generally produce nonzero redistribution moments at all interior supports. For example, assume for a three-span continuous bridge that moments are to be redistributed from both interior piers. The continuity relationship for Pier 1 can then be written as follows:

$$M_1 = \left|M_{e1}\right| - k_{\theta11}\theta_{p1} - k_{\theta12}\theta_{p2}$$

Equation 2.175

where:

M_1 = total continuity moment at Pier 1 (kip-in.)

M_{e1} = critical elastic moment envelope value at the Pier 1 due to the Service II loads or due to the factored loads at the strength limit state, as applicable (kip-in.)

$k_{\theta11}$, $k_{\theta12}$ = unit rotational stiffness constants at Pier 1 due to plastic rotations at Pier 1 and Pier 2, respectively (kip-in./radian)

θ_{p1}, θ_{p2} = plastic rotations at Pier 1 and Pier 2, respectively (radians)

A similar relationship would be written for Pier 2. The unit rotational stiffness constants are a function of the stiffness properties of the girder and are calculated in this particular case, for example, by applying a unit relative rotation at each pier in turn and calculating the resulting moment at Pier 1 using any appropriate indeterminate analysis approach. According to *AASHTO LRFD* Article B6.6.1, these coefficients are to be determined using the elastic stiffness properties of the short-term composite section assuming the concrete deck is effective over the entire span length, as the redistribution moments are assumed formed by short-term loads. For reasons discussed at some length in *AASHTO LRFD* Article CB6.6.1, the influence of any partial yielding in regions of positive flexure is neglected in developing the continuity relationships in the refined method.

At each location where yielding is assumed to occur, the total continuity moment and corresponding plastic rotation must fall on the moment-rotation curve for the cross-section at that location. The nominal moment-rotation curve taken from *AASHTO LRFD* Article B6.6.2 and shown below in Figure 2.61 may be used in the analysis when the restrictions of *AASHTO LRFD* Article B6.2 are satisfied. The development of this curve is discussed in References 78 and 80.
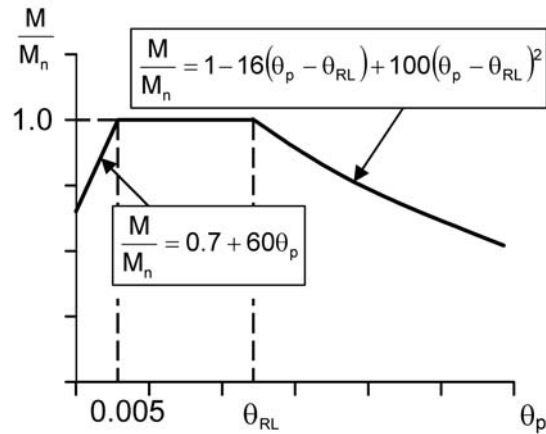
Figure 2.61   Nominal Moment-Rotation Curve for Interior-Pier Sections Satisfying *AASHTO LRFD* Article B6.2

where:

θ_p =   plastic rotation at the interior-pier section (radians)

θ_{RL} =   plastic rotation at which the interior-pier section moment nominally begins to decrease with increasing θ_p determined as shown below (radians)

M   =   bending moment about the major-axis of the cross-section due to the appropriate factored loads (kip-in.)

M_n =   nominal flexural resistance of the interior-pier section taken as the smaller of $F_{nc}S_{xc}$ and $F_{nt}S_{xt}$, with F_{nc} and F_{nt} determined as specified in *AASHTO LRFD* Article 6.10.8.   For sections with compact or noncompact webs, M_n may be taken as the smaller of M_{nc} and M_{nt} determined as specified in *AASHTO LRFD* Appendix A (kip-in.).   For load combinations that induce significant flange lateral bending, deduct the larger of $\frac{1}{3}f_\ell S_{xc}$ or $\frac{1}{3}f_\ell S_{xt}$ from the above values for M_n.

f_ℓ =   lateral bending stress in the flange under consideration at the interior-pier section (ksi).   For continuously braced flanges, f_ℓ is to be taken as zero.

For interior-pier sections satisfying the requirements of *AASHTO LRFD* Article B6.5.1 in order to provide enhanced moment-rotation characteristics, θ_{RL} is to be taken as follows:

$$\theta_{RL} = 0.137 - 0.143\frac{b_{fc}}{t_{fc}}\sqrt{\frac{F_{yc}}{E}} - 0.0216\frac{D}{b_{fc}} + 0.0241\frac{D}{b_{fc}}\frac{b_{fc}}{t_{fc}}\sqrt{\frac{F_{yc}}{E}} \qquad \text{Equation 2.176}$$

<div align="right">*AASHTO LRFD* Equation B6.6.2-1</div>

Otherwise, θ_{RL} is to be taken as:

$$\theta_{RL} = 0.128 - 0.143\frac{b_{fc}}{t_{fc}}\sqrt{\frac{F_{yc}}{E}} - 0.0216\frac{D}{b_{fc}} + 0.0241\frac{D}{b_{fc}}\frac{b_{fc}}{t_{fc}}\sqrt{\frac{F_{yc}}{E}} \qquad \text{Equation 2.177}$$

AASHTO LRFD Equation B6.6.2-2

As specified in *AASHTO LRFD* Article B6.6.1, the nominal moment-rotation curve in Figure 2.61 is to be multiplied by the resistance factor for flexure ϕ_f specified in *AASHTO LRFD* Article 6.5.4.2 in applying the refined method at the strength limit state. At the service limit state, the nominal moment-rotation curve is to be used. *AASHTO LRFD* Article B6.6.2 permits the use of other moment-rotation curves in lieu of the curve given in Figure 2.61, as long as all potential factors influencing the moment-rotation characteristics within the restrictions given by *AASHTO LRFD* Article B6.2 are considered.

Setting the appropriate continuity relationship equal to the selected moment-rotation relationship at each pier assumed to be undergoing plastic rotation results in a set of simultaneous equations that can be solved to yield the continuity moments and plastic rotations at those piers. In some cases, iteration may be required in order to arrive at a solution. Once the plastic rotations have been determined, the redistribution moments at the piers can be determined from the corresponding continuity relationship. For example, in the preceding three-span example, the redistribution moment at Pier 1 would be taken equal to the sum of the last two terms in Equation 2.175. The redistribution moments at all locations other than at interior piers can then be determined in the same manner as discussed previously for the service limit state (*AASHTO LRFD* Article B6.4.2.2 – refer to Figure 2.60).

AASHTO LRFD Article B6.6.1 states that sections adjacent to interior piers satisfy the requirements of *AASHTO LRFD* Article B6.3.2.1 at the service limit state and *AASHTO LRFD* Article B6.4.1.1 at the strength limit state after the redistribution moments are calculated. As specified in *AASHTO LRFD* Article B6.3.2.1, after the redistribution moments are calculated, the service limit state flange-stress limitations of *AASHTO LRFD* Article 6.10.4.2 (i.e. Equations 2.78 through 2.80, as applicable) are not to be checked within the regions extending in each adjacent span from interior-pier sections satisfying the restrictions of *AASHTO LRFD* Article B6.2 to the nearest flange transition or point of permanent-load contraflexure, whichever is closest. This is because the limit-state response is properly accounted for in Equation 2.175. The web bend-buckling check (Equation 2.81) is still required in these regions how ever and should be based on the elastic moments prior to redistribution. As specified in *AASHTO LRFD* Article B6.4.1.1, after the redistribution moments are calculated, the strength limit state flexural resistance requirements (refer to the previous section of this chapter on Strength Limit State Verifications for Composite Sections in Negative Flexure and Noncomposite Sections) are not to be checked within the unbraced lengths immediately adjacent to interior-pier sections satisfying the restrictions of *AASHTO LRFD* Article B6.2.

At all other locations outside these regions, the applicable provisions of *AASHTO LRFD* Articles 6.10.4.2, 6.10.7.1, 6.10.8.1 or A6.1 (refer to the previous sections of this chapter on the Service Limit State and Strength Limit State Verifications) *must* be checked after the redistribution moments are calculated (*AASHTO LRFD* Article

B6.6.1). The redistribution moments are added to the elastic moments due to the appropriate factored loads before the checks are made. As discussed previously, at composite sections in positive flexure where stress calculations are required at the service and/or strength limit states, the redistribution moments are to be added to the DC_2 and DW (if present) moments and the corresponding flexural stresses in the steel section calculated using the long-term composite section (i.e. using a modular ratio of $3n$), as specified in *AASHTO LRFD* Article B6.6.1.

77.   Barker, M.G., B.A. Hartnagel, C.G. Schilling, and B.E. Dishongh. 1997. "Inelastic Design and Experimental Testing of Compact and Noncompact Steel Girder Bridges." *Report 93-1*, Missouri Cooperative Highway Research Program.

78.   Barth, K.E., B.A. Hartnagel, D.W. White, and M.G. Barker. 2004. "Improved Simplified Inelastic Design of Steel I-Girder Bridges." *Journal of Bridge Engineering*, American Society of Civil Engineers, Reston, VA, Vol. 9, No. 3.

79.   Schilling, C.G., M.G. Barker, B.E. Dishongh, and B.A. Hartnagel. 1997. "Inelastic Design Procedures and Specifications." Final Report submitted to the American Iron and Steel Institute, Washington, D.C.

80.   White, D.W., J.A. Ramirez, and K.E. Barth. 1997. "Moment Rotation Relationships for Unified Autostress Design Procedures and Specifications." Final Report, Joint Transportation Research Program, Purdue University, West Lafayette, IN.

81.   ASCE. 1971. *Plastic Design in Steel – A Guide and Commentary*. 2nd Edition. ASCE Manual No. 41, American Society of Civil Engineers, New York, NY.

82.   Galambos, T.V., R.T. Leon, C.E. French, M.G. Barker, and B.E. Dishongh. 1993. "Inelastic Rating Procedures for Steel Beam and Girder Bridges." *NCHRP Report 352*, Transportation Research Board, National Research Council, Washington, D.C.

83.   Schilling, C.G. 1986. "Exploratory Autostress Girder Designs." Project 188 Report, American Iron and Steel Institute, Washington, D.C.

84.   Roeder, C.W., and L. Eltvik. 1985. "An Experimental Evaluation of Autostress Design." *Transportation Research Record 1044*, Transportation Research Board, National Research Council, Washington, D.C.

85.   Schilling, C.G. 1991. "Unified Autostress Method." *AISC Engineering Journal*, Vol. 28, No. 4.

2.2.4 Box Girders

Section 2.4.2 of DM Volume 1, Chapter 2 discussed important issues related to general bridge layout, including span optimization; the relationship of the substructure to the superstructure; the selection of girder spacing and deck overhangs; the determination of field section sizes; and the use of constant versus variable depth girders. Section 2.4.3.1.5 of DM Volume 1, Chapter 2 covered additional issues specific to the preliminary design of steel box-girder bridges. These issues included the selection of the type of girder (tub girder or closed box), and the layout of the framing plan -- including the internal and external cross-frame/diaphragm spacings and configurations. Issues related to the design of top-flange lateral bracing for tub girders, and related to the selection of bearing

arrangements and type of concrete deck, were also reviewed. The fundamental behavior of steel box-girder bridges, primarily related to their torsional resistance, was also discussed. This section of the Manual covers the proportioning of the flange and web plates for box girders, including the determination of initial sizes; the specific AASHTO LRFD design provisions for checking box girders for the service, fatigue and fracture, and strength limit states and for constructibility; and the proportioning of stiffeners for box flanges. But before covering these items, some important general considerations related to the design of box girders are reviewed in the following section.

2.2.4.1 General Considerations

The design of box sections for flexure and torsion (both straight and horizontally curved) is covered in *AASHTO LRFD* Article 6.11.

As specified in *AASHTO LRFD* Article 6.11.1, the provisions are limited to the design of single-cell box sections, where a cell is composed of two web plates and a bottom plate with the top flange composed of either single plate or two smaller flange plates that may be connected with a top-flange lateral bracing system. Other sections such as boxes formed with truss-type webs, with pipe flanges or with more than one web are not specifically addressed. As discussed in DM Volume 1, Chapter 2, Section 2.4.3.1.5.3, multi-cell single box sections are rarely employed in the U.S.

The provisions may be applied to tub girders, defined as open-top steel girders composed of a bottom flange plate, two inclined or vertical web plates, and an independent top flange attached to the top of each web. As specified in *AASHTO LRFD* Article 6.7.5.3, the common top flanges of straight individual tub girders must be connected with either a full- or partial-length lateral bracing system as necessary to ensure lateral stability of the top flanges and overall stability of the girders. A full-length lateral bracing system is required for horizontally curved tub girders.

The provisions may also be applied to closed-box girders. A closed-box girder is defined as a member having a closed cross-section composed of two vertical or inclined webs and top and bottom stiffened or unstiffened steel plate flanges. Under the provisions of *AASHTO LRFD* Article 6.11, and as discussed further below, the top flange of a closed-box girder used as a primary longitudinal flexural member must always be composite in the final constructed condition. There are few such composite closed-box girders built in the U.S. today due to the cost considerations related to the implementation of the necessary safety requirements for a welder to be inside a closed box. Closing the wide spacing between webs with a steel plate at the top of economical tub girders is also expensive. However, the provisions are applicable to composite or noncomposite closed boxes used as either integral pier caps, or to noncomposite closed boxes used as straddle beams. The flexural resistance of noncomposite closed-box sections used as compression or tension members is specified in *AASHTO LRFD* Article 6.12.2.2.2 and discussed further in Reference 154. The reader might note that two I-girders connected with top and bottom lateral bracing may be considered a box section for analysis. A composite deck may be thought of as replacing the top lateral bracing. Hence, a composite I-girder cross-section with one or more bay(s) of bottom lateral bracing may be more

accurately analyzed by treating each pair of I-girders as a box section. Since this is beyond the scope of the provisions, specific analysis and design issues related to this situation are not addressed herein. However, it should be noted, as discussed further in DM Volume 1, Chapter 2, Section 2.4.3.1.4.5, that the lateral bracing resists far higher loads than wind loads in such situations.

Finally, the provisions are also applicable to single box cross-sections (tub or closed-box). The steel box must be positioned in a central location with respect to the cross-section, and the center of gravity of the dead load should be as close to the shear center of the box as possible. *AASHTO LRFD* Article C6.11.1 indicates that the use of single box cross-sections provides torsional equilibrium with two bearings at some supports. Locating the center of gravity of the dead load near the shear center of single box cross-sections minimizes the torsion.

As indicated in *AASHTO LRFD* Article C6.11.1, the provisions are applicable to these sections when used in continuous, simple or tied-down spans up to approximately 350 feet in length. Further, the provisions may be applied to longer spans if a thorough evaluation, consistent with basic structural engineering fundamentals, is conducted. The article also refers to an alternative straight box-girder specification (*85a*) for further information on the design of long-span straight steel box-girder bridges. Reference 154 highlights the differences between this specification and the *AASHTO LRFD* Specification, which primarily relate to the calculation of the effective width for box flanges, the nominal flexural resistance of unstiffened and stiffened box flanges and web shear resistance.

The *AASHTO LRFD* provisions in Article 6.11 require that composite box sections used as primary longitudinal flexural members have a composite concrete deck throughout their length in the final constructed condition. *AASHTO LRFD* Article 6.10.1.5 specifies that the concrete deck be assumed effective over the entire span length in the analysis for loads applied to the composite section. Also, since torsional shear exists along the entire span in all types of composite box sections, shear connectors must be present along the entire span to resist the torsional shear and avoid possible debonding of the deck. Shear connectors must also be present in regions of negative flexure in continuous spans to be consistent with the prototype and model bridges that were studied in the original development of the live-load distribution factor for box sections (see Section 2.2.4.1.2 below); those bridges had shear connectors along their entire length (*85b*). As indicated in *AASHTO LRFD* Article C6.11.1, as of this writing (2006), the specifications do not apply to the use of composite concrete on the bottom flanges of box sections in order to stiffen the flanges in regions of negative flexure.

As specified in *AASHTO LRFD* Article 6.11.1.4, access holes in box sections for inspection should be located in the bottom flange in areas of low stress. The access holes should be large enough to provide easy access to the interior of the box (i.e. at least 18 inches by 36 inches). Access holes should be provided at each end of the bridge. The effect of access holes on stresses in the flange should be investigated to determine if reinforcement around the hole is required. Provision should be made for drainage and ventilation of the interior of box sections. Painting the interior of box sections a light color can facilitate inspections and in tub sections, can prevent

solar gain during construction and offer a level of protection to the steel while the tub is temporarily open during construction. As indicated in *AASHTO LRFD* Article C6.11.1.4, the paint quality need not match that normally used for exterior surfaces, particularly when provisions are made to drain and ventilate the interior of the box.

Although box sections have unique characteristics, many of the design requirements for box sections in flexure are identical to the requirements for I-sections in flexure. Thus, *AASHTO LRFD* Article 6.11 often refers to *AASHTO LRFD* Article 6.10 (i.e. the design provisions for I-sections in flexure).   This approach will also be followed in this section of the Manual. Only aspects unique to box sections in flexure are covered below; the reader will be referred to the appropriate sections of the Specifications (and Manual) dealing with the design of I-sections in flexure (and other related requirements), as necessary.

The design of shear connectors is covered in Section 2.2.5 of this chapter. The design of web stiffeners is covered in Section 2.2.6. Requirements specific to box girders are covered in each section. Bolted field splice design is covered in Section 2.3.4; requirements for bolted splice design specific to box girders are discussed in Sections 2.3.4.2.2.2.4 and 2.3.4.2.2.3.4.   Connection design and bracing member design is covered in general in Sections 2.3 and 2.4, respectively. The design of solid-plate diaphragms for box sections is discussed in Section 2.4.4.   Further information on practical tub-girder design may be found in Reference 85c.

2.2.4.1.1 Effective Width of Box Flanges

In the AASHTO LRFD Specification and in this Manual, a 'box flange' is defined as a flange that is connected to two webs. A box flange may be an unstiffened plate, a stiffened plate or a plate combined with reinforced concrete attached by shear connectors. Thus, unstiffened or stiffened bottom flanges of tub and closed-box sections and top flanges of closed-box sections are classified as box flanges under this definition.

When a box flange is particularly wide, the longitudinal stress in the flange near the webs may be significantly higher than at mid-width of the flange (i.e. a shear lag effect occurs) because the shear stiffness of the flange is less than the axial stiffness. As specified in AASHTO LRFD Article 6.11.1.1, box flanges in multiple- and single-box sections are to be considered fully effective for flexure (i.e. subject to a uniform longitudinal stress) if the width of the box flange does not exceed one-fifth of the effective span. The effective span is defined as the span length for simple spans, and as the distance between points of permanent load contraflexure or between a simple support and a point of permanent load contraflexure, as applicable, for continuous spans. If the flange width exceeds one-fifth of the effective span, only a width equal to one-fifth of the effective span is to be considered effective in resisting flexure. As indicated in AASHTO LRFD Article C6.11.1.1, the effective box-flange width, as defined above, is only to be used when determining the section properties used to calculate the flexural stresses on the section due to the factored loads. For calculating the nominal flexural resistance of a box flange, the full flange width is to be used.

The preceding effective width requirement is based on stress analyses of simple-span box-girder bridges to evaluate the effective width using a series of folded-plate equations (*85d*). Span-to-flange width ratios between 5.65 and 35.3 were included in the study. The effective flange width (as compared to the full flange width) ranged from 0.89 for the bridge with the smallest span-to-width ratio to 0.99 for the bridge with the largest span-to-width ratio. Based on those results, it was deemed reasonable to assume that a box flange is fully effective as long as the width of the flange does not exceed one-fifth of the span and, as stated in *AASHTO LRFD* Article C6.11.1.1, that the requirement can be extended to continuous spans by utilizing an effective span length in the requirement as defined above. *AASHTO LRFD* Article C6.11.1.1 indicates that for extremely wide box flanges, a special investigation of shear lag effects may be warranted.

2.2.4.1.2 Special Restrictions on the Use of the Live Load Distribution Factor for Multiple Box Sections

AASHTO LRFD Article 4.6.2.2.2b (Table 4.6.2.2.2b-1) provides the following distribution factor (in units of lanes) for determining the live load moment in multiple steel composite box-section members (in both interior and exterior girders):

$$\text{D.F.} = 0.05 + 0.85\,\frac{N_L}{N_b} + \frac{0.425}{N_L} \qquad \text{Equation 2.177a}$$

where:
N_b = number of box girders in the cross-section
N_L = number of design lanes as specified in *AASHTO LRFD* Article 3.6.1.1.1 (generally taken as the integer part of w/12.0 where w is the clear roadway width in feet between curbs or barriers)

The ratio of N_L/N_b must be between 0.5 and 1.5 to stay within the range of parameters considered in the development of the equation, and multiple presence factors specified in *AASHTO LRFD* Table 3.6.1.1.2-1 are not to be applied as the multiple presence factors given in previous editions of the Standard Specifications were considered in the development of the equation. The equation is deemed applicable to both simple and continuous spans according to *AASHTO LRFD* Article C4.6.2.2.2b. The equation was derived based on folded-plate theory, which was shown at the time to be valid to analyze the behavior of multiple box-section bridges based on analytical and model studies of simple-span bridges (*85b*). The theory was then used to determine the maximum live load per girder produced by critical combinations of load on 31 bridges having various numbers of box girders, numbers of traffic lanes and various spans. The study assumed an uncracked stiffness for the composite section with shear connectors provided along the entire span. The equation closely predicted the maximum live load per girder for both the interior and exterior girders in all the cases that were examined. The bridges considered in the development of Equation 2.177a had interior end diaphragms only; there were no intermediate internal diaphragms within the spans and no external diaphragms between boxes. As mentioned in *AASHTO LRFD* Article C4.6.2.2.2b, the provision of interior and/or exterior diaphragms within the span is expected to improve the

distribution characteristics of the bridge to some degree over that predicted by Equation 2.177a, which can be evaluated if desired using a more refined analysis approach meeting the requirements of *AASHTO LRFD* Article 4.4.

Equation 2.177a was implemented in the initial U.S. design provisions for straight box girders given in the 10th Edition of the AASHO Bridge Specifications (1969). To ensure that the equation was applied within the limitations and bridge characteristics of the research study upon which it was based, limits were placed on the cross-section as part of the specifications. Since refined analysis methods were not readily available or widely used at that time, designs outside the specified limits were rarely done. Bridge cross-section limitations were not included in the initial version of the AASHTO *Guide Specifications for Horizontally Curved Bridges* (1980). In lieu of distribution factors, rational analysis was required to distribute the loads in horizontally curved bridges. The Third Edition of the *AASHTO LRFD* Specifications unified the provisions for the design of straight and horizontally curved bridges into a single specification. In addition, with the more common availability and use of refined methods of analysis, the overall scope of the provisions was broadened to allow the consideration of a wider variety of box-girder bridge types and cross-sections that were outside of the initial specified limitations. However, since Equation 2.177a was also implemented in the *AASHTO LRFD* Specifications as an acceptable approximate analysis method for determining live load moments in straight bridges, it was necessary to continue the restrictions on its use. These restrictions are therefore specified in *AASHTO LRFD* Article 6.11.2.3 and are summarized as follows:

➢ The bridge cross-section must consist of two or more single-cell box sections;
➢ The bridge must not have any support skew;
➢ The bridge must be straight;
➢ The inclination of the webs with respect to a plane normal to the bottom flanges must not exceed 1 to 4.
➢ The width of the concrete deck overhang must not be greater than either 6 feet or 60 percent of the average distance *a* between the centers of the top flanges of adjacent box sections (Figure 2.62);
➢ The distance *a* center-to-center of flanges of adjacent boxes taken at midspan must not be greater than 120 percent nor less than 80 percent of the distance *w* center-to-center of flanges of each individual box (Figure 2.62);
➢ The distance *w* center-to center of flanges of each individual box must be the same;
➢ Where nonparallel box sections are used, in addition to the midspan requirement given above, the distance *a* center-to-center of flanges of adjacent boxes taken at the supports must not be greater than 135 percent nor less than 65 percent of the distance *w* center-to-center of flanges of each individual box (refer to Figure 2.21 in DM Volume 1, Chapter 2).
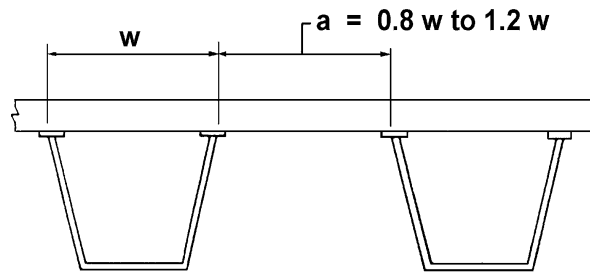
Figure 2.62 Center-to-Center Flange Distances

The development of Equation 2.177a was based on studies of bridges in which *a* and *w* (Figure 2.62) were equal. The requirements given by the sixth and eighth bullet items above are intended to allow some flexibility in bridge layout while generally maintaining the validity of the distribution factor equation. In cases where the spacing of the box girders varies along the span, *AASHTO LRFD* Article 4.6.2.2.2b permits the distribution factor to either be varied at selected locations along the span, or else a single distribution factor to be used based on a suitable value of N_L (calculated using the clear roadway width *w* at the section under consideration).

As specified in *AASHTO LRFD* Article 6.11.1.1, for multiple box sections in straight bridges satisfying the above restrictions *and* with fully effective box flanges (see Section 2.2.4.1.1 above), in addition to permitting the live load flexural moment in each box to be determined according to Equation 2.177a, the following approximations may also be applied:

➢ Shear due to St. Venant torsion may be neglected in the design of the girders, shear connectors and bolted splices;
➢ Transverse bending and longitudinal warping stresses due to cross-section distortion may be neglected in the design of all components (refer to DM Volume 1, Chapter 2, Section 2.4.3.1.5 for further description of these stresses and their effects); and
➢ The section of an exterior member assumed to resist horizontal factored wind loads may be taken as the bottom box flange acting as a web and 12 times the thickness of the web acting as flanges.

It was determined that when the preceding restrictions are satisfied, secondary bending stresses due to cross-section distortion and shear due to St. Venant torsion may be neglected if the box flange is fully effective (*85b*). Also, it was determined from the analytical studies described above that when bridges meeting the above restrictions were loaded to produce the maximum compression in the box flange near an intermediate support, the amount of twist in the girder was negligible (*85b*).

In addition, for multiple box sections in straight bridges satisfying the above restrictions and with fully effective box flanges:

➢ Sections in positive flexure may be considered compact sections at the strength limit state, if additional requirements specified in *AASHTO LRFD*

Article 6.11.6.2.2 are also satisfied (refer to Section 2.2.4.7.1.1 of this chapter).

Finally, as noted in *AASHTO LRFD* Article C6.11.9, when Equation 2.177a is employed to determine a live load distribution factor for moment, one-half of the resulting distribution factor should be used in the calculation of the live load vertical shear in each web of the box section.

The requirement that the center-to-center spacing *a* of flanges of adjacent box sections must be between 0.8 and 1.2 times the distance *w* center-to-center of flanges of each individual box is particularly inefficient. Often this requirement leads to unused box flange material and a need for longitudinal flange stiffeners. A more practical arrangement is often found to be narrow boxes with larger spacing between boxes than shown in Figure 2.62. Also, the load distribution rules for I-girders in the *AASHTO LRFD* provisions provide for improved assignment of live load to individual girders over previous specifications. Equation 2.177a was carried over from the *AASHTO* Standard Specifications and as such, does not provide for a similar improved assignment of live load to individual box girders to help offset the effects of the heavier HL-93 live load specified in the *AASHTO LRFD* provisions.

2.2.4.1.3 Bridges Outside the Special Restrictions Discussed in Section 2.2.4.1.2

Bridges not satisfying one or more of the special restrictions specified in *AASHTO LRFD* Article 6.11.2.3 for use of the live load distribution factor given by Equation 2.177a (discussed in the preceding section of this chapter) must be investigated using one of the available methods of refined structural analysis, or other acceptable methods of approximate structural analysis specified in *AASHTO LRFD* Articles 4.4 or 4.6.2.2.4. The additional torsional effects resulting from support skew are not comprehended by the specified live load distribution factor. Hence, a more refined analysis is required whenever one or more supports are skewed, even if the bridge satisfies the preceding cross-sectional limitations. ***Skewed supports are particularly problematic for box-girder bridges and special care should be taken in analyzing and detailing box girders with skewed supports in order to provide a successful bridge.*** A refined analysis is also recommended in *AASHTO LRFD* Article C6.11.2.3 if the straight portion of a bridge satisfies the preceding requirements, but also contains horizontally curved segments, as the effects of horizontal curvature generally extend beyond the curved segments. Torsion, unlike bending moment, is not mitigated over length   Refined analysis methods may be employed, even if the bridge satisfies all the preceding restrictions.

In addition, as specified in *AASHTO LRFD* Article 6.11.1.1, for all box sections that do not have fully effective box flanges, and/or for all the following sections:

➢ Single box sections in straight or horizontally curved bridges;
➢ Multiple box sections in straight bridges not satisfying the restrictions specified in *AASHTO LRFD* Article 6.11.2.3; or
➢ Multiple box section in horizontally curved bridges;

the following requirements must be satisfied:

➢ The effects of St. Venant torsional shear (in addition to flexural shear) must be considered in the design of the girders, shear connectors (see Section 2.2.5 of this chapter) and bolted splices (see Sections 2.3.4.2.2.2.4 and 2.3.4.2.2.3.4 of this chapter);

➢ Transverse bending stresses due to cross-section distortion must be considered when checking the girders for fatigue (see Section 2.2.4.6 of this chapter) and at the strength limit state. *Transverse bending stresses due to the factored loads must not exceed 20.0 ksi at the strength limit state*;

➢ Longitudinal warping stresses due to cross-section distortion must be considered for checking the girders for fatigue (see Section 2.2.4.6 of this chapter) and when checking bolted flange splices for slip and for fatigue (see Section 2.3.4.2.2.2.4 of this chapter). The effect of longitudinal warping stresses may be ignored in the design of all components at the strength limit state if the box flange(s) meets the requirements allowing it to be assumed fully effective. If these parameters are not met, longitudinal warping should usually be considered.

➢ Sections in positive flexure must be considered noncompact sections at the strength limit state (see Section 2.2.4.7.1.1 of this chapter).

Transverse (or through-thickness) bending stresses and longitudinal warping stresses due to cross-section distortion are best controlled with internal cross-frames or diaphragms (refer to DM Volume 1, Chapter 2, Section 2.4.3.1.5). As specified in *AASHTO LRFD* Article 6.11.1.1, these stresses are to be determined by the application of rational structural analysis in conjunction with strength-of-materials principles. The beam-on-elastic foundation (BEF) analogy (*85e*) is a well-established approach for estimating these stresses. The finite-element method is thought to be problematic and somewhat impractical for determining through-thickness bending stresses due to the mesh refinement required for the accurate calculation of these stresses. In the BEF method, the internal cross-bracing is considered analogous to intermediate elastic supports in the BEF. The resistance to distortion that is provided by the box cross-section is considered analogous to a continuous beam on an elastic foundation. The transverse bending stress is considered analogous to the deflection of the BEF, and the longitudinal warping stress is considered analogous to the moment in the BEF. Transverse stiffeners attached to web and box flanges should be considered effective when computing the flexural rigidities of the elements for resisting transverse bending.

Note that transverse through-thickness bending stresses are of particular concern for boxes subject to large torques; e.g. single box sections, sharply curved boxes and boxes resting on skewed supports. Longitudinal warping stresses are largest at the corners of the box section where critical details are often located and should be considered for fatigue (*85e*). However, tests have indicated that longitudinal warping stresses do not adversely affect the strength of boxes of proportions defined in the provisions. The application of the BEF analogy to compute cross-section distortional stresses is discussed further in Section 2.2.4.6.1.1.1 of this chapter.

85a.   FHWA. 1980. "Proposed Design Specifications for Steel Box Girder Bridges." *FHWA-TS-80-205*, Federal Highway Administration, Washington, D.C.

85b.   Johnston, S.B., and A.H. Mattock. 1967. "Lateral Distribution of Load in Composite Box Girder Bridges." *Highway Research Record*, No. 167, Bridges and Structures, Transportation Research Board, Washington, D.C.

85c.   Coletti, D., Z. Fan, W. Gatti, J. Holt, and J. Vogel. 2005. "Practical Steel Tub Girder Design." available from the National Steel Bridge Alliance, Chicago, IL, April.

85d.   Goldberg, J.E., and H.L. Leve. 1957. "Theory of Prismatic Folded Plate Structures." *IABSE*, Vol. 16, International Association for Bridge and Structural Engineers, Zurich, Switzerland.

85e.   Wright, R.N., and S.R. Abdel-Samad. 1968 "Analysis of Box Girders with Diaphragms." *Journal of the Structural Division*, American Society of Civil Engineers, New York, NY, Vol. 94, No. ST10, October.

2.2.4.2 Flange Sizing

2.2.4.2.1 Top Flanges of Tub Sections

As specified in *AASHTO LRFD* Article 6.11.2.2, top flanges of tub sections subject to tension or compression must satisfy the following requirements:

$$\frac{b_f}{2t_f} \leq 12.0 \qquad \text{Equation 2.177b}$$

AASHTO LRFD Equation 6.11.2.2-1

$$b_f \geq D/6 \qquad \text{Equation 2.177c}$$

AASHTO LRFD Equation 6.11.2.2-2

and:

$$t_f \geq 1.1t_w \qquad \text{Equation 2.177d}$$

AASHTO LRFD Equation 6.11.2.2-3

These same requirements are also specified for flanges of I-sections in *AASHTO LRFD* Article 6.10.2.2, and are discussed further in Section 2.2.3.2 of this chapter. For sections with inclined webs, *AASHTO LRFD* Article 6.11.2.1.1 requires that the distance along the web be used for checking all design requirements. Therefore, in checking Equation 2.177c for the case of an inclined web, D must be taken as $D/\cos\theta$, where θ is the angle of inclination of the web plate with respect to the vertical.

Recommendations regarding minimum flange width and thickness and flange transitions given in Section 2.2.3.2 should also be applied to top flanges of tub sections. The two top flanges of an individual tub section should be the same size at any given cross-section. In cases where lateral bracing members are bolted to the top flanges of a tub section (which is preferred), the width of the flanges should not be less than 16 inches to accommodate the connection of these members (larger widths may be required in some cases based on other criteria).

As discussed in *AASHTO LRFD* Article C6.11.3.2, in cases where a full-length top lateral bracing system is *not* employed within a straight tub section (refer to *AASHTO LRFD* Article 6.7.5.3 and DM Volume 1, Chapter 2, Section 2.4.3.1.5.6), *L* in the following guideline:

$$b_{fc} \geq \frac{L}{85}$$

Equation 2.177e

AASHTO LRFD Equation C6.10.3.4-1

where:
b_{fc} = minimum width of the compression flange within a girder shipping piece (in.)

should be taken as the larger of the distances along the field piece between panels of lateral bracing or between a panel of lateral bracing and the end of the piece. The preceding guideline, which is applicable primarily to I-sections, is intended to help ensure that a wide enough compression flange is provided so that field sections will be stable during normal handling and erection. *For cases where a full-length top lateral bracing system is provided, Equation 2.177e need not be considered for top flanges of tub sections.*

The sizes of top flanges of tub sections in regions of positive flexure are governed by constructibility verifications. The establishment of a reasonable preliminary design width and thickness for the flanges in these regions is primarily an educated guess based on experience, keeping the minimum width and thickness recommendations discussed in Section 2.2.3.2 of this chapter in mind. The final size of the top flanges and/or the spacing of the cross-frames/diaphragms in these regions will typically be controlled by either the calculated local buckling or lateral-torsional buckling resistance under the critical construction condition. The critical construction condition will most often be the combined major-axis and lateral bending stress in the outermost top flange of the tub due to the effect of the deck-casting sequence plus the deck overhang loads. Therefore, it is recommended that the final top-flange size and cross-frame/diaphragm spacing in these regions be determined based on this condition, and then subsequent design verifications be made at the strength, fatigue and service limit states, as applicable. The specific design verifications at the various limit states are discussed in greater detail in succeeding sections of this chapter.

The sizes of top flanges of tub sections in negative flexure are typically controlled by tension-flange yielding at the strength limit state once the flanges are continuously braced. Box girders must be composite throughout their entire length. The longitudinal deck reinforcement must be at least equal to one-percent of the total cross-sectional area of the deck as specified in *AASHTO LRFD* Article 6.10.1.7. This reinforcement is present for crack control. Typically, this reinforcement is included in the composite section and will permit a slight reduction in the size of the top flanges in compression. Initial trial flange sizes in these regions are based on experience. Depending on the span arrangement and other factors, the flanges in the negative moment regions near the piers of continuous spans may be wider than the flanges in regions of positive flexure. As discussed further in Section 2.2.3.2 of this chapter, width transitions should be made at the field splices. Changes in the top-flange width can lead to some

inconveniences with respect to deck forming, but these problems are relatively minor when compared to the overall economy of the structural steel design. Other limit state verifications, including web bend buckling at the service limit state and fatigue limit state checks of critical details (see below), may also prove critical in the design in regions of negative flexure in some cases.

Shear due to St. Venant torsion is typically neglected in the design of top flanges of tub sections. Before these flanges are continuously braced by the hardened concrete deck, the top lateral bracing resists the torsional shear. Once the flanges are continuously braced by the deck, the deck resists torsional shear along with the top lateral bracing. The torsional shear produces horizontal shear in the deck that should be considered when designing the deck reinforcing steel. Lateral bending stresses in the top flanges, from whatever source prior to hardening of the deck, must be considered in the design of the flanges. Once the flanges are continuously braced, lateral flange bending, local buckling and lateral-torsional buckling need not be considered.

In cases where the webs have slopes flatter than 1-to-4, the lateral force of the inclined web on the flanges should be evaluated for loads applied prior to hardening of the deck (see DM Volume 1, Chapter 2, Section 2.4.3.1.5.5.1).

2.2.4.2.2 Box Flanges

For box sections with inclined webs, the width of bottom box flanges is a function of the web depth and the slope of the web. Inclined webs are advantageous in reducing the width of bottom box flanges. As specified in *AASHTO LRFD* Article 6.11.2.1.1, the inclination of the web plates to a plane normal the bottom flange should not exceed 1-to-4. As discussed previously, where Equation 2.177a is used to determine the live load flexural moment in each box of a multiple-box section, the inclination of the web plates *must* not exceed 1-to-4. Therefore, in certain cases, there is some flexibility permitted in establishing the web slope. In general, a narrower box flange is more desirable. However, caution should be exercised in deviating too much from the well-established limit on the web slope. In tub sections, as the slope exceeds 1- to-4, lateral bending stresses in the discretely braced top flanges due to the transverse load resulting from the change in the horizontal component of the web dead load shear plus the change in the St. Venant torsional dead load shear per unit length along the member start to become more significant and need to be considered, as discussed above.

Recommendations regarding flange thickness transitions given in Section 2.2.3.2 of this chapter should also be considered for box flanges. Typically, a steel weight savings of 800 to 1,200 pounds justifies a flange butt splice in the top flanges of tub girders (which is based on the discussion and recommendations for I-sections given in Reference 40). For wider box flanges, there are additional issues involved. One fabricator has suggested that to warrant the introduction of a shop splice between 48-inch-wide straight box flanges 1½ and 2 inches in thickness composed of ASTM A 572 Grade 50 FCM (fracture-critical) material, at least 2,250 pounds of material must be saved. This number will vary depending on the width, thickness and grade of the plates being joined, whether the material is classified as FCM or non-FCM,

and whether the plates are straight or curved. Box flanges must be cut curved from large plates.   Thus, depending on the radius, it may be desirable to introduce additional shop splices in the flange to reduce waste. Therefore, it is recommended that fabricators who are likely bidders on the job be consulted with regard to the issue of shop splices in box flanges.

As indicated in *AASHTO LRFD* Article C6.11.2.2, box flanges should extend at least one inch beyond the outside of each web to allow for welding.   The Plans might provide for an option to permit the fabricator to increase this distance slightly to allow for greater welding access. Flange lips that are too wide may provide a place for birds to perch, which the box design might otherwise prevent.

The closed box presents special design considerations for closed-box sections. In positive flexure, the top flange is generally controlled by constructibility verifications (as discussed below in Section 2.2.4.4) if it is to be composite in the final condition. For closed-box sections in positive flexure or tub sections in negative flexure, the thickness of the noncomposite box flange is usually controlled by its local buckling resistance (see Section 2.2.4.7 below). It is recommended that the initial flange thickness in these cases be determined based on the local buckling resistance. Subsequent design verifications will then need to be made at the other limit states (as described in more detail in succeeding sections of this chapter).   When concrete is placed on a box flange, the deflection of the flange should be checked to ensure that the integrity of the box shape is maintained. The shear connection pattern needs to be determined to ensure proper attachment of the deck to the flange (see Section 2.2.5 of this chapter). The load path of the horizontal shear through the box flange should be checked.

Noncomposite box flanges in compression may be unstiffened or stiffened to prevent local buckling under combined uniform axial compression and St. Venant torsional shear (where considered). Lateral torsional buckling and flange lateral bending are not a consideration for box flanges. ***Unstiffened box flanges are preferred.*** However, an unstiffened box flange should not be so slender that its buckling resistance becomes impractical. Longitudinal flange stiffeners may be added to increase the compressive resistance of thin flanges. *The cost of these stiffeners is significant and they should be employed only after a thickness increase is evaluated.* A minimum thickness of ¾" is recommended for unstiffened box flanges for ease of handling and to minimize distortion and possible cupping of the flange during welding, with the maximum ratio of width to thickness of the flange recommended not to exceed around 120 (*85c*). A lesser thickness might be considered for a stiffened box flange; however, it is recommended that fabricators first be consulted before utilizing box flange thicknesses below ¾".

As discussed in *AASHTO LRFD* Article C6.11.11.2, the use of structural tees is recommended for longitudinal flange stiffeners; tees increase the lateral torsional buckling resistance of the stiffeners and provide a high ratio of out-of-plane stiffness to stiffener cross-sectional area.   Using less efficient flat bars as stiffeners is an undesirable alternative. Further discussion of the design of longitudinal flange stiffeners is provided in Section 2.2.4.8 below. If the inside of the box is to be painted, the cost of cleaning and painting the tee section(s) offsets some of the advantage of adding the stiffeners (*40*). The tee(s) must be spliced to ensure that the stiffeners are continuous at field section splices, which can complicate both the fabrication and field assembly. As

recommended in *AASHTO LRFD* Article C6.11.11.2, the stiffeners should also be continuous through internal diaphragms and consideration should be given to attaching the stiffeners to the internal diaphragms   Also, as the number of stiffeners is increased beyond one, the required moment of inertia of the stiffeners to achieve the desired buckling coefficient for the flange begins to increase dramatically and eventually becomes nearly impractical (as discussed further in Section 2.2.4.7.1.2.1 below). ***Therefore, where a stiffened box flange is necessary, only one longitudinal stiffener should be used in the majority of situations.*** The provisions allow the Engineer to balance the stiffness of the longitudinal stiffener with the flange local buckling resistance to provide an economical design; that is, simply providing the largest stiffener size to provide the largest permitted buckling coefficient is usually not the most economical solution.

The advantages of utilizing higher-strength high performance steel (HPS) for box flanges in compression are less evident as the local buckling resistance of box flanges (unstiffened or stiffened) is a function of Young's modulus rather than the yield strength of the steel.   Since the modulus is not increased with increasing yield strength, the compressive resistance of a plate of increased yield strength is not significantly changed.   Therefore, the increased strength of HPS cannot be utilized to advantage in most cases. For stiffened box flanges, the longitudinal flange stiffeners are primary load carrying members.   Therefore, as specified in *AASHTO LRFD* Article 6.11.11.2, the specified minimum yield strength of these stiffeners must not be less than the specified minimum yield strength of the box flange to which they are attached. Rolled structural tees are not available in HPS; therefore, when HPS is used for box flanges, tees must be fabricated from plates or from bars cut from plate.

Box flanges in tension are designed against nominal yielding under combined uniform axial tension and St. Venant torsional shear (where considered). Longitudinal stiffeners are not required structurally for box flanges in tension. However, they may assist in preventing any objectionable vibration and in maintaining the flatness of slender box flanges.

For closed-box and tub sections in regions of positive flexure, the controlling limit state for the design of bottom box flanges in tension depends on whether the section qualifies as a compact or noncompact section (see Section 2.2.4.7 below).   For a compact section, the design of the flange will typically be controlled by either the service or the fatigue limit state verifications under the appropriate load combination specified in *AASHTO LRFD* Table 3.4.1-1.   In such cases, it is recommended that the preliminary thickness for the flange be determined based on the relatively simple flange stress check at the service limit state (see Section 2.2.4.5 below). The thickness of the flange may have to be increased from this level in some cases due to stress-range limitations at the fatigue limit state at certain critical welded details (e.g. cross-frame/diaphragm connection plate welds to the flange or at the termination of longitudinal stiffener-to-flange welds near points of permanent load contraflexure – see Section 2.2.4.6 below). Design verifications on the flange at the strength limit state would be made last in this case. For a noncompact section, the design of the flange will typically be controlled by tension-flange yielding at the strength limit state (or perhaps by the fatigue limit state in some cases).   In all cases, the thickness of the flange may have to be increased adjacent to the termination of any longitudinal flange stiffeners near points of permanent load contraflexure to ensure that the unstiffened flange at the stiffener termination has adequate compressive resistance. Note that constructibility verifications will not typically

control the design of box flanges in these regions. For closed-box sections in regions of negative flexure, the controlling limit state for the design of the top box flange in tension will typically be tension-flange yielding at the strength limit state once the flanges are continuously braced.

2.2.4.3 Web Sizing

2.2.4.3.1 Web Depth

The first step in sizing the web plates of a steel box girder is to establish the web depth.   As for I-sections, the proper web depth is an extremely important consideration affecting the economy, constructibility and performance of steel-girder bridges.

Webs for box sections may either be inclined or vertical. As mentioned previously, AASHTO LRFD Article 6.11.2.1.1 indicates that the inclination of the web plates to a plane normal the bottom flange should not exceed 1-to-4. Further, as specified in AASHTO LRFD Article 6.11.2.3, where Equation 2.177a is used to determine the live load flexural moment in each box of a multiple-box section, the inclination of the web plates must not exceed 1-to-4. Webs attached to top flanges of tub sections must be attached at mid-width of the flanges. Should the flanges be attached to the webs at locations other than mid-width of the flanges, additional lateral bending effects are introduced in the flanges that would require special investigation.

In the absence of depth restrictions, the suggested minimum depths for steel I-girders in simple and continuous spans based on traditional maximum recommended span-to-depth ratios (AASHTO LRFD Table 2.5.2.6.3-1 – discussed further in Sections 2.2.3.3.1 and 2.2.3.5.1.1 of this chapter) may be used to establish a reasonable minimum vertical web depth for the design. In most cases, the optimum web depth will be greater than the minimum depth based on the traditional span-to-depth ratios. The optimum web depth can be established by preparing a series of designs with different web depths to arrive at an optimum cost-effective depth based on weight and/or cost.   However, it should always be kept in mind that the optimum web depth for a box section will typically be slightly less than the optimum web depth of an I-section for the same span because of the inherent torsional stiffness of a box section. The web depth obviously dictates the flange sizes for a given design. Therefore, establishing a sound optimum depth for box sections is particularly important because the size of box flanges can typically be varied less over the bridge length. Also, boxes that are overly shallow may potentially be subject to larger torsional shears. Box-girder web depths should not be less than about 5 feet to facilitate fabrication and inspection.

It is interesting to note that the two webs of a box are stressed roughly equally. This means that there will be only one critical location of the live load to produce the maximum moment in the box, whereas there are two critical positions of the live load for two I-girders.   The result is that the total live load moment resisted by two I girders is greater than the live load moment that must be applied to a box girder supporting the same width of deck. This occurrence is of particular interest when comparing an exterior box girder to an exterior I-girder and the adjacent interior

girder. Typically, the exterior I-girder is critical and all girders are often made the same size. The result of comparing a box girder design to an I-girder design is often that the total required moment capacity of the box girder design is less than that required for the I-girder design. This is particularly true when four I-girders are compared to two boxes.

The reader is referred to Sections 2.2.3.3.1 and 2.2.3.5.1.1 of this chapter for further information regarding the selection of an appropriate web depth. Refer also to Section 2.2.3.3.1 for suggestions on how to apply the suggested minimum depths to variable web depth members.

2.2.4.3.2 Web Thickness

Cross-section proportion limits for webs of box sections are specified in AASHTO LRFD Article 6.11.2.1. As specified in AASHTO LRFD Article 6.11.2.1.2, for webs without longitudinal stiffeners, the webs must be proportioned such that:

$$\frac{D}{t_w} \leq 150 \qquad \text{Equation 2.177f}$$

AASHTO LRFD Equation 6.11.2.1.2-1

where D is the web depth and t_w is the web thickness.

For webs that do not satisfy Equation 2.177f, longitudinal web stiffeners are required. As specified in *AASHTO LRFD* Article 6.11.2.1.3, for webs with longitudinal stiffeners, the webs must be proportioned such that:

$$\frac{D}{t_w} \leq 300 \qquad \text{Equation 2.177g}$$

AASHTO LRFD Equation 6.11.2.1.3-1

Further information regarding each of these web slenderness limits is given in Section 2.2.3.3.2 of this chapter.

Note again that for sections with inclined webs, *AASHTO LRFD* Article 6.11.2.1.1 requires that the distance along the web be used for checking all design requirements. Therefore, in checking Equations 2.177f and 2.177g for the case of an inclined web, D must be taken as $D/\cos\theta$, where θ is the angle of inclination of the web plate with respect to the vertical.

As discussed later on, computation of the shear must also take into account the slope of the web; that is, the vertical shear determined from the analysis must be divided by cos θ. Torsional shear must also be included if it is computed separately from the vertical bending shear.

Additional guidelines for I-sections provided in Section 2.2.3.3.2 of this chapter regarding minimum web thickness, change in web thickness along the girder, and determining the trade-off between adding more stiffeners versus increasing the

thickness of web material should be considered applicable to webs of box sections as well.

2.2.4.3.3 Variable Web Depth Members

As discussed in preceding sections of this chapter and in DM Volume 1, Chapter 2, Section 2.4.3.1.3, clearance requirements, a poor span arrangement, economics and/or aesthetics may lead to a variable web depth. As discussed in *AASHTO LRFD* Article C6.11.1, to simplify the analysis and fabrication of variable web depth box-section members with inclined webs, the inclination of the webs should remain constant. Of course, the width of the top of the box is normally kept constant. This will require that the width of the bottom flange vary along the length of the girder where the web depth varies. Webs with a uniform slope form a surface called a developable surface. This simply means that the web is from a truncated cone and can be formed to a circular shape without heat-bending the plate.

The vertical profile also must be built into the web. Several bridge detailers have computer software that can establish the necessary cutting patterns.

The design of variable web depth members is covered in *AASHTO LRFD* Article 6.10.1.4. The provisions of *AASHTO LRFD* Article 6.10.1.4 are discussed in Section 2.2.3.3.3 of this chapter. The reader is referred to that section, and also to DM Volume 1, Chapter 2, Section 2.4.3.1.3, for further information on variable web depth members.

2.2.4.4 Constructibility Verifications

Although not identified as a formal limit state, the AASHTO LRFD Specifications provide significant emphasis on constructibility and specify it as a primary objective of bridge design in AASHTO LRFD Article 1.3.1. General requirements for constructibility are specified in AASHTO LRFD Article 2.5.3; the reader is referred to the first paragraph of Section 2.2.3.4 of this chapter where these requirements are discussed in more detail.

For steel structures, AASHTO LRFD Article 6.5.1 requires that the bridge be investigated for each stage that may be critical during construction, handling, transportation and erection. Modern steel-bridge designs are typically more slender in the past due to the increased usage of higher-strength steels and limit-states design approaches (with a smaller factor of safety on dead load than traditional working stress design), and the advent of composite construction. In composite construction, the steel girders must be strong enough to carry the full noncomposite dead loads.   For tub sections with a wide bottom flange relative to the smaller top flanges, typically more than half the web depth is in compression in regions of positive flexure during construction. Thus, investigation of critical construction stages is important, particularly during deck placement of continuous-span bridges when the girders are subjected to negative bending.

For steel box-section flexural members, the provisions for design for constructibility are given in AASHTO LRFD Article 6.11.3. These provisions essentially refer back

to the design provisions for constructibility given in AASHTO LRFD Article 6.10.3 for steel I-section flexural members, with a few exceptions as discussed below. The design provisions for constructibility are intended to provide adequate strength and stability of the main load-carrying members during construction, to properly account for dead-load deflections, and to control the slip in load-resisting bolted connections at each critical construction stage to ensure that the proper geometry of the structure is maintained. As stated in AASHTO LRFD Article 6.10.3.1, nominal yielding or reliance on post-buckling resistance is not permitted for main load-carrying members during critical stages of construction. An exception is permitted for the localized yielding of the web that may occur in hybrid members.

All design checks for strength are to be made using the appropriate factored loads specified in AASHTO LRFD Articles 3.4.1 and 3.4.2. The applicable strength load combinations for these design checks include Strength I, Strength III and Strength IV (see DM Volume 1, Chapter 5 for additional information on these load combinations). Note that although the Strength IV load combination will typically only control where the dead-to-live load force effect ratio exceeds about 7.0 for the bridge in its final condition, this load combination can control for critical construction stages and should be considered in all constructibility design checks for strength. When considering construction loads, or dead loads and temporary loads that act on the structure only during construction, the provisions of AASHTO LRFD Article 3.4.2 apply for determining the appropriate load factor to be applied to these loads in each strength combination. For the calculation of deflections, all load factors are to be taken as 1.0. Slip of bolted connections is to be checked using the appropriate factored loads, with the slip resistance of the connection to be determined as specified in AASHTO LRFD Article 6.13.2.8 (see Section 2.3.2.4.1.1 of this chapter).

As specified in AASHTO LRFD Article 6.10.3.4, girder sections in positive flexure that are composite in the final condition, but noncomposite during construction, are to be investigated during the various stages of the deck placement. For the outermost flange of fascia tub girders, the effects of the forces resulting from the deck overhang loads must also be considered. Design checks are to be made for flexure (AASHTO LRFD Article 6.11.3.2) and shear (AASHTO LRFD Article 6.11.3.3), as appropriate, to ensure adequate strength. Checks on the concrete deck stresses during the deck placement must also be made (AASHTO LRFD Article 6.10.3.2.4). See Sections 2.2.3.4.1 and 2.2.3.4.2 of the chapter for detailed discussions on deck placement analysis and deck overhang loads, respectively, for I-girder bridges; these discussions are also applicable to box-girder bridges. Example calculations are given for the following: 1) the calculation of the major-axis bending moments and stresses, vertical deflections, vertical support reactions and critical concrete deck tensile stress for an assumed deck placement sequence, and 2) the calculation of the flange lateral bending stresses due to the deck overhang loads, including the amplification of the first-order lateral bending stresses according to the provisions of AASHTO LRFD Article 6.10.1.6. The specific girder design verifications that must be made for flexure and shear based on these calculated effects are discussed in Section 2.2.4.4.1 below.

Wind-load effects on the noncomposite structure prior to casting of the deck are an important consideration. As specified in AASHTO LRFD Article 4.6.2.7.3, the need

for temporary wind bracing to control lateral bending and lateral deflections during construction must be investigated. Since box girders are torsionally stiff and tub girders must always be provided with at least some degree of top lateral bracing, wind load generally has less effect on box girders than on I-girders during construction. Potential uplift at bearings is also an important consideration and must be investigated at each critical construction stage according to AASHTO LRFD Article 6.10.3.1. Should concentrated loads not be applied to the web through a deck or deck system, and bearing stiffeners also not be provided at such locations, the web must satisfy the provisions of AASHTO LRFD Article D6.5 (Appendix D to Section 6) to prevent web crippling and web local yielding.

AASHTO LRFD Article 6.10.3.5 refers to the provisions of AASHTO LRFD Article 6.7.2, which state that vertical camber must be specified to account for the dead-load deflections. The deflections due to the steel weight, concrete weight, future wearing surface or other loads not applied at the time of construction are reported separately. When staged construction is specified, i.e. when the superstructure is built in separate longitudinal units with a longitudinal joint, the sequence of the load application must be recognized in determining the stresses and the required cambers. This requires analysis of the planned construction stages.

The geometry of individual box sections must be maintained throughout all stages of construction as specified in AASHTO LRFD Article 6.11.3.1. Eccentric loads that may occur during construction should be considered. The need for temporary or permanent intermediate internal and/or external cross-frames/diaphragms, top lateral bracing, or other means must be investigated to ensure that deformations of the box are controlled.   Important considerations in investigating the need for these members are discussed in DM Volume 1, Chapter 2, Sections 2.4.3.1.5.5 and 2.4.3.1.5.6. As indicated in AASHTO LRFD Article C6.11.3.1, temporary cross-frames/diaphragms that are not part of the original design should be removed because the structural behavior of the box section, including the load distribution, may be affected if these members are left in place. As discussed further in DM Volume 1, Chapter 2, Section 2.4.3.1.5.5.2, released temporary members may have large built-up forces in them after the deck has hardened, which may introduce restoring forces into the bridge upon removal.

AASHTO LRFD Article C6.11.3.1 suggests that for painted box sections, an allowance be made in the dead load for the weight of the paint. An allowance of three percent of the steel weight has been found to be a reasonable allowance.

Further information regarding the construction of composite steel box-girder bridges may be found in Reference 85f.

2.2.4.4.1 Design Verifications for Flexure and Shear

To ensure the goal of providing adequate strength and stability of box-section flexural members during construction, without permitting nominal yielding (except for localized web yielding in hybrid sections) or relying on post-buckling resistance, the requirements of *AASHTO LRFD* Articles 6.11.3.2 (Flexure) and 6.10.3.3 (Shear) must be satisfied at each critical construction stage. The required check on the

concrete deck tensile stress during construction specified in *AASHTO LRFD* Article 6.10.3.2.4, which is also applicable to box girders, is discussed in Section 2.2.3.4.3.2 of this chapter and will not be repeated here.

2.2.4.4.1.1 Flexure

2.2.4.4.1.1.1 Top Flanges of Tub Sections

As specified in *AASHTO LRFD* Article 6.11.3.2, for critical stages of construction, the constructibility design provisions of *AASHTO LRFD* Articles 6.10.3.2.1 through 6.10.3.2.3 for flexure of I-sections are to be applied to the top flanges of tub sections. A single exception is that the provisions of *AASHTO LRFD* Article A6.3.3 (Appendix A to Section 6) are *not* to be applied in determining the lateral torsional buckling resistance of top flanges of tub sections with compact or noncompact webs (see Section 2.2.3.7.1.2 of this chapter for definitions of compact web and noncompact web sections). For I-sections in straight bridges with compact or noncompact webs, *AASHTO LRFD* Article A6.3.3 permits the lateral torsional buckling resistance of the compression flange to be determined including the beneficial contribution of the St. Venant torsional constant *J*. In some cases, the lateral torsional buckling resistance, so computed, may exceed the yield moment resistance, which is not permitted for noncomposite box sections.

The equations of *AASHTO LRFD* Articles 6.10.3.2.1 through 6.10.3.2.3, along with an example application of their use, are discussed in detail in Section 2.2.3.4.3.2 of this chapter and are not repeated here. Essentially, a single top flange of a tub section is considered equivalent to the top flange of an I-section in applying the equations; therefore, it is recommended that the checks using these equations be made for half of the tub section. In calculating the lateral torsonal buckling resistance of the flanges, *AASHTO LRFD* Article 6.11.3.2 conservatively suggests that the unbraced length be taken as the distance between interior cross-frames/diaphragms.   Further discussion on brace points for top flanges of tub sections subject to compression is provided in DM Volume 1, Chapter 2, Section 2.4.3.1.5.6.

The equations of *AASHTO LRFD* Articles 6.10.3.2.1 and 6.10.3.2.2 (i.e. Equations 2.71, 2.72 and 2.74) allow for the direct consideration of flange lateral bending in discretely braced top flanges of tub sections due to various sources, if deemed significant.   The distinction between discretely braced and continuously braced flanges is discussed in Section 2.2.3.4.3.2 of this chapter; a distinction is made because for a continuously braced flange, lateral flange bending effects need not be considered. If the flanges are discretely braced and lateral flange bending effects are deemed insignificant or incidental, the flange lateral bending term f_ℓ is set equal to zero in the appropriate equations. Potential sources of lateral flange bending include curvature, wind loads and eccentric concrete deck overhang loads acting on the outermost flanges of fascia girders. Additional potential sources of significant lateral bending in discretely braced top flanges occur in tub girders with inclined webs and with web slopes exceeding 1 to 4, in tub girders where the unbraced length of the top flange exceeds 30 feet, and in tub girders with Warren Truss top lateral bracing configurations, as discussed in DM Volume 1, Chapter 2, Sections

2.4.3.1.5.5.1 and 2.4.3.1.5.6. For loads applied during construction on top flanges that are continuously braced, the equation given in *AASHTO LRFD* Article 6.10.3.2.3 (i.e. Equation 2.75) applies. In checking all these equations, the effects of St. Venant torsional shear in the top flanges are neglected.

At sections with slender webs where discretely braced top flanges of tub sections are subject to compression, web bend-buckling must also be checked according to the provisions of *AASHTO LRFD* Equation 6.10.3.2.1-3 (i.e. Equation 2.73). In computing the web bend-buckling resistance F_{crw} from Equation 6.10.1.9.1-1 (i.e. Equation 2.11 – refer to Section 2.2.2.4 of this chapter) for sections with inclined webs, the web depth D and the depth of the web in compression D_c should each be measured along the web slope; that is, divided by $\cos\theta$, where θ is the angle of inclination of the web plate with respect to the vertical. For sections with compact or noncompact webs, web bend-buckling is not a consideration, and therefore, need not be checked for those sections. Again, Section 2.2.3.7.1.2 of this chapter discusses the distinction between compact, noncompact and slender web sections. A slender web section is defined as a section that does *not* satisfy the web-slenderness requirement given by *AASHTO LRFD* Equation 6.10.6.2.3-1 (i.e. Equation 2.13 – see also Table 2.3). Note that to determine the categorization of the web, the properties of the noncomposite section are to be used. Because the compression-flange stress is limited to F_{crw} during construction according to Equation 2.73, the web load-shedding factor R_b (see Section 2.2.2.5 of this chapter) is always taken equal to 1.0 when computing the nominal flexural resistance of the compression flange for the constructibility checks. Thus, the R_b factor is not included in Equations 2.71 and 2.72 for checking of the compression flange. Options to consider should the web bend-buckling resistance be exceed under the construction condition under consideration are given at the end of *AASHTO LRFD* Article C6.10.3.2.1 and are reiterated in Section 2.2.2.4 of this chapter.

2.2.4.4.1.1.2 Box Flanges

As specified in *AASHTO LRFD* Article 6.11.3.2, noncomposite box flanges in compression must satisfy the following requirements for critical stages of construction:

$$f_{bu} \leq \phi_f F_{nc}$$

<div align="right">Equation 2.177h</div>

and:

<div align="right">*AASHTO LRFD* Equation 6.11.3.2-1</div>

$$f_{bu} \leq \phi_f F_{crw}$$

<div align="right">Equation 2.177i</div>

<div align="right">*AASHTO LRFD* Equation 6.11.3.2-2</div>

where:

ϕ_f =   resistance factor for flexure specified in *AASHTO LRFD* Article 6.5.4.2 (= 1.0)

f_{bu} = longitudinal flange stress due to the factored loads at the section under consideration calculated without consideration of longitudinal warping (ksi)

F_{crw} = nominal web bend-buckling resistance determined as specified in *AASHTO LRFD* Article 6.10.1.9 (Equation 2.11) (ksi)

F_{nc} = nominal flexural resistance of box flanges in compression determined as specified in *AASHTO LRFD* Article 6.11.8.2 (see Section 2.2.4.7 below) (ksi). In computing F_{nc} for constructibility, the web load-shedding factor R_b is to be taken equal to 1.0.

Equation 2.177h is a check for local buckling of the flange during critical stages of construction. *Note that lateral flange bending and lateral-torsional buckling are not a consideration for box flanges*. Equation 2.177i ensures that theoretical web bend-buckling will not occur during construction at section where noncomposite box flanges are subject to compression. This check only need be made for sections with slender webs. The web bend-buckling check is discussed in more detail at the end of the preceding section of this chapter.

Noncomposite box flanges in tension and continuously braced box flanges in tension or compression must satisfy the following requirement for each critical stage of construction:

$$f_{bu} \leq \phi_f R_h F_{yf} \Delta \qquad \text{Equation 2.177j}$$

AASHTO LRFD Equation 6.11.3.2-3

where:

$$\Delta = \sqrt{1 - 3\left(\frac{f_v}{F_{yf}}\right)^2} \qquad \text{Equation 2.177k}$$

AASHTO LRFD Equation 6.11.3.2-4

f_v = St. Venant torsional shear stress in the flange due to the factored loads at the section under consideration not to exceed the factored torsional shear resistance of the flange F_{vr} given by Equation 2.177ee (see below) (ksi)

$$= \frac{T}{2A_o t_f} \qquad \text{Equation 2.177}\ell$$

AASHTO LRFD Equation 6.11.3.2-5

A_o = enclosed area within the box section (in.^{2})

R_h = hybrid factor determined as specified in *AASHTO LRFD* Article 6.10.1.10.1 (Equation 2.21)

t_f = thickness of the flange under consideration (in.)

T = internal torque due to the factored loads (kip-in.)

Equation 2.177j is a yielding check based on the von Mises yield criterion (*85g*), which is used to consider the effect of the St. Venant torsional shear in combination with flexure.   The enclosed area A_o in Equations 2.177ℓ is to be computed for the

noncomposite box section. If top lateral bracing in a tub section is attached to the webs, A_o is to be reduced to reflect the actual location of the bracing (*AASHTO LRFD* Article 6.7.5.3).

In checking Equations 2.177h and 2.177j, the effects of longitudinal warping stresses in the flanges due to cross-section distortion are not considered. However, the effects of these distortion related stresses must be considered in certain cases when checking bolt slip in flange splices for the construction condition, as discussed further in Section 2.3.4.2.2.2.4 of this chapter. Also, in checking these equations, the torque *T* should comprehend the critical torque induced in the girder during the deck-placement sequence.

In closed-box sections, noncomposite box flanges on top of the box receive the weight of the wet concrete and other loads during construction before the deck hardens. Therefore, the flange must be designed as a noncomposite box flange for those loads. As specified in *AASHTO LRFD* Article 6.11.3.2, the maximum vertical deflection of the noncomposite box flange due to the unfactored permanent loads, including the self-weight of the flange, and any unfactored construction loads must not exceed 1/360 times the transverse span between webs. Through-thickness bending stresses in the flange due to the factored permanent loads and factored construction loads must not exceed 20.0 ksi. The flange may be considered to act as a simple span between webs in making these checks. Transverse and/or longitudinal stiffening of the box flange may be necessary to control the flange stresses and deflections under these loads.

2.2.4.4.1.2 Shear

AASHTO LRFD Article 6.11.3.3 refers back to the shear requirement specified in *AASHTO LRFD* Article 6.10.3.3. This requirement states that for critical stages of construction, the shear in interior panels of stiffened webs due to the factored permanent loads and factored construction loads applied to the noncomposite section V_u must not exceed the shear-buckling resistance V_{cr} (refer to Equation 2.76 and Section 2.2.3.4.3.3 of this chapter). The use of tension-field action (i.e. post-buckling shear resistance) per Equation 2.53 or 2.55 is not permitted during construction.

In checking Equation 2.76, the provisions of *AASHTO LRFD* Article 6.11.9, as applicable, are to be applied. That is, for box sections with inclined webs, the web must be designed for the total vertical shear in the plane of the web V_{ui} taken equal to V_u divided by $\cos\theta$, where θ is the angle of inclination of the web plate with respect to the vertical (see *AASHTO LRFD* Equation 6.11.9-1). Also, in computing the shear-buckling resistance V_{cr} for the case of inclined webs from *AASHTO LRFD* Equation 6.10.9.3.3-1 (i.e. Equation 2.51), the web depth *D* must be taken as the depth of the web measured along the slope or $D/\cos\theta$. Finally, for all box sections discussed in Section 2.2.4.1.3 of this chapter, V_u is to be taken as the sum of the flexural and St. Venant torsional shears in checking this requirement. In cases where there is significant St. Venant torsional shear, the dead load shear in one web is greater than the flexural dead load shear by the amount of the torsional shear and less than the flexural shear by the same amount in the other web at the same cross-

section. For practicality, both webs are generally detailed as if they had the same critical shear. Shears in the web due to warping torsion and due to cross-section distortion may be ignored in making this check for typical box sections, as indicated in *AASHTO LRFD* Article C6.11.9.

85f.   United States Steel. 1978. *Steel/Concrete Composite Box-Girder Bridges: A Construction Manual*. available from the National Steel Bridge Alliance, Chicago, IL, December.

85g.   Boresi, A.P., M. Sidebottom, F.B. Seely, and J.O. Smith. 1978. Advanced Mechanics of Materials. 3rd ed. John Wiley and Sons, New York, NY.

2.2.4.5 Service Limit State Verifications

The service limit state restricts stress and deformation of the steel, and also attempts to control concrete crack widths under regular service conditions (*AASHTO LRFD* Article 1.3.2.2). *AASHTO LRFD* Article 6.5.2 specifies that the provisions of *AASHTO LRFD* Article 2.5.2.6 apply to steel structures. These provisions deal primarily with the control of elastic live load deflections and recommend span-to-depth ratios. The recommended span-to-depth ratios tend to limit not only live load deflections, but also affect dead load deformations. For box-section flexural members, permanent deformations are also addressed. The intent of these provisions is to prevent objectionable permanent deformations of the steel that would impair rideability. The level of live load used in this check is expected to occur relatively infrequently during the life of the bridge. *AASHTO LRFD* Article 6.11.4 deals with the specific service limit state checks that are to be made for box-section members, as discussed in more detail below.

2.2.4.5.1 Elastic Deformations

Regarding the control of elastic deformations under normal service conditions, AASHTO LRFD Article 6.11.4 refers back to AASHTO LRFD Article 6.10.4.1, which further refers back to the applicable provisions of AASHTO LRFD Article 2.5.2.6 dealing with live-load deflection criteria and the criteria for span-to-depth ratios. It is noted that both of these criteria are optional. Typically, the Engineer may defer to the Owner's instruction on these issues. As discussed previously, working stress design is an amalgam of stress level, deflection and stiffness criteria. Strength is not considered directly. LRFD separates the limit states and includes strength limit state checks, as well as service limit state checks related to deflection, stiffness and stress level.

The application to box sections of the suggested minimum depths based on traditional maximum recommended span-to-depth ratios, as given in AASHTO LRFD Article 2.5.2.6.3, was discussed previously in Section 2.2.4.3.1 of this chapter. The optional live load deflection criteria suggested in AASHTO LRFD Article 2.5.2.6.2 to control elastic live-load deformations at the service limit state are discussed in detail in Section 2.2.3.5.1.2 of this chapter. These criteria may be considered equally applicable to box girders.

2.2.4.5.2 Permanent Deformations

To control permanent deformations under repeated severe traffic loadings, checks are to be made on the flange stresses and for potential web bend-buckling under the Service II load combination (see DM Volume 1, Chapter 5 for additional information on the Service II load combination). The standard design Service II loading is specified as 1.0*DC* + 1.0*DW* + 1.3(*LL*+*IM*), where *DC* represents the component dead loads, *DW* represents the wearing surface and utility loads and (*LL*+*IM*) represents the design live load plus the dynamic load allowance placed in multiple lanes. As will be discussed later on in this chapter, checks are also made to prevent slip in bolted connections under the Service II loading (note that the relationship of the Service II load combination to the Overload given in the AASHTO *Standard Specifications* was discussed previously in Section 2.2.3.5.2 of this chapter). Owners sometimes require these checks to be applied to a design permit load. Since the live load is known in these cases, a reduction in the live load factor from 1.3 to 1.0 is often found desirable. Further, the typical assumption related to the live load distribution factor is that multiple lanes are to be loaded with the permit load. This conservative assumption tends to lend credence to the reduction of the live load factor to 1.0.

Under certain conditions, *AASHTO LRFD* Article 6.10.4.2.1 permits flexural stresses due to the Service II loads applied to the composite section to be computed assuming the concrete deck is effective for both positive and negative flexure for the permanent deflection design checks. To employ this method, shear connectors must be provided along the entire length of the girder (which is required for box sections as specified in *AASHTO LRFD* Article 6.11.10), and minimum longitudinal deck reinforcement equal to one percent of the total cross-sectional deck area must be placed wherever the calculated tensile stress in the concrete deck due to either load combination Service II or the factored construction loads exceeds the factored modulus of rupture (*AASHTO LRFD* Article 6.10.1.7). Under these conditions, the crack size is believed controlled such that the concrete deck is considered effective in tension at the service limit state. *When the above conditions are satisfied, the Engineer is encouraged to consider the concrete deck to be fully effective in calculating all Service II flexural stresses, as field tests show that this assumption better reflects the actual behavior*. An example illustrating the check of the tensile stresses in the deck and the placement of the longitudinal deck reinforcement under the Service II load combination is provided in Section 2.2.3.5.2 of this chapter.

2.2.4.5.2.1 Flange Stress Check

According to *AASHTO LRFD* Article 6.11.4, flange stresses due to the Service II loads are limited as specified in *AASHTO LRFD* Article 6.10.4.2.2 to control permanent deflections in the steel girder at the service limit state, with the following exceptions: 1) the f_ℓ term in *AASHTO LRFD* Equation 6.10.4.2.2-2 is to be taken as zero, and 2) *AASHTO LRFD* Equation 6.10.4.2.2-3 does not apply. Therefore, the specified stress checks reduce to the following:

For the top and bottom steel flange:

$$f_f \leq 0.95 R_h F_{yf} \qquad\qquad \text{Equation 2.177m}$$

where:

f_f =   flange stress at the section under consideration due to the Service II Loads calculated without consideration of flange lateral bending (ksi). f_f is always taken as positive in this equation.

R_h =   hybrid factor determined as specified in *AASHTO LRFD* Article 6.10.1.10.1 (Equation 2.21)

The genesis of the base stress limit given by Equation 2.177m is discussed further in Section 2.2.3.5.2.1 of this chapter. In the *AASHTO LRFD* Specifications, the hybrid factor R_h has been conservatively added to the stress limit in Equation 2.177m to account for the increase in flange stress caused by early web yielding in hybrid sections. A resistance factor ϕ is not included because the check is considered to be a serviceability check for which the resistance factor is implicitly taken equal to 1.0. Note that at sections where access holes are present in the box flange, f_f should be computed using section properties calculated assuming the area of the access hole is subtracted from the box-flange area.

The f_ℓ term not considered in the stress check for both flanges because flange lateral bending is not a consideration for box flanges and because top flanges (which must be composite in the final constructed condition) are continuously braced at the service limit state. *AASHTO LRFD* Equation 6.10.4.2.2-3, which applies to both steel flanges of noncomposite sections, does not apply -- again because box sections must be composite at the service limit state.

Longitudinal warping stresses due to cross-section distortion and St. Venant torsional shear stresses need not be considered in checking Equation 2.177m. As indicated in *AASHTO LRFD* Article C6.11.4, the effect of these stresses on the overall permanent deflections at the service limit state is considered to be insignificant. The effect of longitudinal warping stresses must be considered, however, in certain cases when checking slip of the connections in bolted noncomposite box flange splices at the service limit state, as discussed further in Section 2.3.4.2.2.2.4 of this chapter.

As indicated in *AASHTO LRFD* Article C6.11.4, under the load combinations specified in *AASHTO LRFD* Table 3.4.1-1, Equation 2.177 need only be checked for compact sections in positive flexure (see Section 2.2.4.7.1.1 of this chapter regarding the definition of a compact section in positive flexure). For all sections in negative flexure and for noncompact sections in positive flexure, Equation 2.177m does not control and need not be checked. However, web bend buckling must always be considered for these latter cross-sections, as discussed in the next section of this chapter.

AASHTO LRFD Article 6.10.4.2.2 optionally permits moment redistribution at the service limit state for continuous-span members in straight I-girder bridges that satisfy specific limitations spelled out in *AASHTO LRFD* Article B6.2 (in Appendix B to *AASHTO LRFD* Section 6 – see also Section 2.2.3.11 of this chapter). According

to *AASHTO LRFD* Article 6.11.4, the applicability of these moment redistribution procedures to box sections has not yet been demonstrated; therefore, the optional Appendix B provisions are not to be applied to box sections at the service limit state.

One final requirement in *AASHTO LRFD* Article 6.10.4.2.2 relates to the rare case of compact composite sections in positive flexure utilized in shored construction. In this case, longitudinal compressive stresses in the concrete deck due to the Service II loads are limited to $0.6f'_c$ to ensure linear behavior of the concrete. As discussed in *AASHTO LRFD* Article C6.10.1.1.1a, the use of shored construction is not common and is not recommended for use in highway bridge design (see also Section 2.2.1.2 of this chapter).

2.2.4.5.2.2 Web Bend Buckling Check

As specified in *AASHTO LRFD* Article 6.11.4, except for composite section in positive flexure in which the web satisfies the requirement of *AASHTO LRFD* Article 6.11.2.1.2 (i.e. $D/t_w \leq 150$ – no longitudinal web stiffeners), all sections must also satisfy the following requirement at the service limit state:

$$f_c \leq F_{crw} \qquad \text{Equation 2.177n}$$

$$\textit{AASHTO LRFD Equation 6.10.4.2.2-4}$$

where:
f_c =   compression-flange stress due to the Service II loads calculated without consideration of flange lateral bending (ksi)
F_{crw} =   nominal bend-buckling resistance for webs determined as specified in AASHTO LRFD Article 6.10.1.9 (Equation 2.11) (ksi)

Again, the resistance factor is implicitly assumed equal to 1.0 because this is a serviceability check. At sections where access holes are present in the box flange, f_c should be computed using section properties calculated assuming the area of the access hole is subtracted from the box-flange area.

In computing the web bend-buckling resistance F_{crw} from Equation 6.10.1.9.1-1 (i.e. Equation 2.11 – refer to Section 2.2.2.4 of this chapter) for sections with inclined webs, the web depth D and the depth of the web in compression D_c should each be measured along the web slope; that is, the vertical web depth in each case must be divided by $\cos\theta$, where θ is the angle of inclination of the web plate with respect to the vertical.

A web bend buckling check is specified at the service limit state to control deformations, including transverse displacements of the web. Regions in negative flexure are particularly susceptible to web bend buckling in composite girders at the service limit state, especially when the concrete deck is effective in tension as permitted for composite sections in *AASHTO LRFD* Article 6.10.4.2.1. When the concrete deck is considered effective in tension, usually the neutral axis is above half of the web depth so more than half of the web is in compression increasing the susceptibility of the web to bend buckling. As a result, this case may govern the web

thickness of the girder in these regions. Because an explicit web bend buckling check is specified, the web load-shedding factor R_b is not included in Equation 2.177m.

The reader is referred to Section 2.2.2.4 of this chapter for further discussion on the particulars of this check. Example calculations illustrating this check are also given for a web of a composite I-section without longitudinal stiffeners subject to negative flexure (in which the concrete deck is assumed to be effective in tension), and for a web of a composite I-section with longitudinal stiffeners subject to positive flexure. Similar checks would be made for a box-section web.

2.2.4.6 Fatigue and Fracture Limit State Verifications

The fatigue limit state is taken as restrictions on the stress range resulting from the passage of a single design truck in a critical path on the deck for an expected number of stress range cycles. It is believed that by limiting stresses so calculated to the level specified for each detail that fatigue crack growth will be adequately controlled to prevent fracture during the design life of the bridge (*AASHTO LRFD* Article 1.3.2.3). The fracture limit state is dealt with by a set of specified material toughness requirements intended to ensure that the steel has the ability to absorb expected energy levels without brittle fracture at minimum specified service temperatures.

For steel structures, *AASHTO LRFD* Article 6.5.3 requires components and details to be investigated for fatigue as specified in *AASHTO LRFD* Article 6.6.   The investigations are to be made for the Fatigue load combination specified in *AASHTO LRFD* Table 3.4.1-1 using the fatigue live load given in *AASHTO LRFD* Article 3.6.1.4. The Fatigue load combination and fatigue live load are discussed in DM Volume 1, Chapter 5. Fracture toughness requirements are to be in conformance with *AASHTO LRFD* Article 6.6.2.   In addition, a special fatigue requirement for webs is specified in *AASHTO LRFD* Article 6.10.5.3 and is to be applied to box-section webs as well, as discussed in Section 2.2.4.6.1.1 below. Requirements for fatigue design of shear connectors and for bolts subject to tensile fatigue are covered in later sections of this chapter.

2.2.4.6.1 Fatigue Limit State

The design of box sections for the fatigue limit state is covered in *AASHTO LRFD* Article 6.11.5. In the *AASHTO LRFD* Specifications, the fatigue design life is given to be 75 years. Definitions for fatigue, fatigue life and fatigue design life are given in Section 2.2.3.6.1 of this chapter. As discussed previously, load-induced fatigue (*AASHTO LRFD* Article 6.6.1.2) is defined as fatigue effects due to in-plane stresses for which components and details are explicitly designed. Load-induced fatigue is dealt with using specific design verifications for flexure and shear. Distortion-induced fatigue (*AASHTO LRFD* Article 6.6.1.3) is defined as fatigue due to stresses resulting from load paths not quantified in the analysis, since by strength of materials principles, all stress is distortion induced. The more inclusive the analysis, the fewer vagrant load paths exist.   Distortion-induced fatigue is typically controlled by preclusion of details that have been found to have induced fatigue cracks in the past.

An example of such a situation is the termination of cross-frame connection plate welds on girder webs. This detail was found to cause cracking in the webs at the terminus of the connection plate-to-web fillet welds. This has been treated in the specifications by requiring the connection plates to be attached to the flanges by welding or bolting (*AASHTO LRFD* Article 6.6.1.3). Note that if the cross-frame forces are computed from an analysis, such a load path must be created regardless to transfer these forces into the flanges. Although classified as distortion-induced fatigue details, the connection-plate attachments to the web and flanges must be checked for load-induced fatigue.

A helpful flowchart detailing the design checks to be made at the fatigue and fracture limit state (discussed below) is provided in Appendix C to Section 6 of the *AASHTO LRFD* Specifications – Figure C6.4.3-1.

2.2.4.6.1.1 Load-Induced Fatigue

2.2.4.6.1.1.1 Flexure

For load-induced fatigue considerations, each detail must satisfy the following design verification for flexure given in *AASHTO LRFD* Article 6.6.1.2.2:

$$\gamma(\Delta f) \le (\Delta F)_n \qquad\qquad \text{Equation 2.177o}$$

AASHTO LRFD Equation 6.6.1.2.2-1

where γ is the load factor specified in *AASHTO LRFD* Table 3.4.1-1 for the Fatigue load combination set at 0.75, and (Δf) is the stress range due to the passage of the HS20 (72 kip) fatigue design load specified in *AASHTO LRFD* Article 3.6.1.4 placed in the critical transverse position. The dynamic load allowance is specified to be 15 percent for the fatigue limit state (*AASHTO LRFD* Article 3.6.2.1). $(\Delta F)n$ is the nominal fatigue resistance determined as specified in *AASHTO LRFD* Article 6.6.1.2.5. The reader is referred to the extensive discussion given in Section 2.2.3.6.1.1 of this chapter regarding load-induced fatigue in general, and the calculation of the nominal fatigue resistance for various fatigue detail categories in particular.

As specified in *AASHTO LRFD* Article 6.6.1.2.1, Equation 2.177o need only be applied to details that are subject to a net applied tensile stress. That is, in regions where the unfactored permanent loads produce compression, fatigue need only be considered at a particular detail if the compressive stress at that detail is less than twice the maximum tensile live load stress caused by the factored fatigue design truck (i.e. 0.75 times the HS20 truck or a 54-kip truck). According to the specification, two times the factored fatigue design truck (or a 108-kip truck) represents the heaviest truck expected to cross the bridge over its assumed 75-year fatigue design life. The effect of any future wearing surface may be ignored when making this check.

It is worthwhile to note that a box girder typically is designed to carry live load contributed from a wider portion of the deck than is typically assigned to a single I-

girder. This means that the total design live load for a box girder consists of more lanes than for an I-girder. A box girder is also designed to carry more dead load than a single I-girder. Since the fatigue load consists of only one lane loaded at a time, load-induced fatigue is usually much less critical in box girder design than in I-girder design.

Fatigue of the base metal at the net section of access holes should be checked. The fatigue resistance at the net section of large access holes is not currently quantified in the specification; however, it is noted that the base metal at the net section of open bolt holes has been shown to satisfy fatigue Category D (85h). This assumes a stress concentration, or ratio of the elastic tensile stress adjacent to the hole to the average stress on the net area, of 3.0. A less severe fatigue category might be considered if the proper stress concentration at the edges of the access hole is evaluated through a refined analysis. Reinforcement of the hole may be necessary to satisfy this condition.

As discussed previously, under certain conditions, *AASHTO LRFD* Article 6.6.1.2.1 permits live load stresses and stress ranges for the fatigue limit state checks to be computed using the short-term composite section assuming the concrete deck is effective for both positive and negative flexure. As specified in *AASHTO LRFD* Article 6.10.1.7, those conditions are: shear connectors must be provided along the entire length of the girder (which is required for box sections as specified in *AASHTO LRFD* Article 6.11.10); and that minimum longitudinal reinforcement equal to one percent of the total deck cross-sectional area be placed wherever the computed tensile stress in the deck due to either the factored construction loads or load combination Service II exceeds the factored lower-bound modulus of rupture of the concrete. Under these conditions, the crack size is believed controlled such that full-depth cracks will not occur. Where cracks do occur, the stress in the longitudinal reinforcement will increase until it reaches equilibrium with the concrete and the crack will be arrested. Experience has shown that under these conditions, the small number of cracks that occur do not coalesce. Field tests show that the concrete provides adequate tensile stiffness at service load levels so that strength of materials assumptions using the concrete in tension yield correct stresses. Using the short-term composite section to compute the factored fatigue load stresses due to both positive and negative flexure results in a significant reduction in the computed stress range at and near the top flange. The stress range at or near the bottom flange is unaffected because the increase in stiffness is essentially offset by the increase in the distance from the n-composite neutral axis to the flange.

The reader is referred to Section 2.2.3.6.1.1 of this chapter for example calculations illustrating checks for load-induced fatigue of the base metal at cross-frame connection plate welds to flanges and at stud shear connection welds to the top flange. Although the checks are made for an I-section in these examples, similar procedures would be followed to make these checks for a box section. Note that in each example, where the unfactored permanent loads produce compression at top-flange details, checks are made to determine if those details are subject to a net applied tensile stress under the conditions specified in *AASHTO LRFD* Article 6.6.1.2.1.

For cases where the fatigue-load moments and shears are determined from a line-girder analysis, a live load distribution factor for one lane loaded is required. Equation 2.177a was not originally developed for the case of one lane loaded. In fact, when NL is equal to 1.0 and the number of box girders in the cross-section Nb exceeds two, the ratio of NL/Nb is less than 0.5, which is outside the range of this ratio that was considered in the original development of Equation 2.177a. For the case of Nb equal to two and NL equal to one, Equation 2.177a gives a distribution factor of 0.9 lanes. As additional boxes are added to the cross-section, the distribution factor is not anticipated to drop much below this value. As mentioned previously, each individual box carries a wider portion of the deck than an individual I-girder and thus, the total design live load for a box girder consists of more lanes than for an I-girder. Boxes are also more torsionally stiff than I-girders. Thus, in lieu of a refined analysis, it is suggested that a distribution factor between 0.9 and 1.0 lanes conservatively be used for the case of one lane loaded on a multiple-box section.

Cross-Section Distortional Stresses

As specified in *AASHTO LRFD* Article 6.11.5, both longitudinal warping stresses and transverse bending stresses due to cross-section distortion must be considered at the fatigue limit state for all box sections that do not have fully effective box flanges, and/or for all the following sections:

- ➤ Single box sections in straight or horizontally curved bridges;
- ➤ Multiple box sections in straight bridges not satisfying the restrictions specified in *AASHTO LRFD* Article 6.11.2.3; or
- ➤ Multiple box section in horizontally curved bridges;

Skewed box-girder bridges are comprehended in the above list. As discussed earlier, skewed supports create significant torque in box sections regardless of whether the bridge is straight or curved.

When box sections are subject to torsion, the cross-section becomes distorted giving rise to secondary bending stresses. Horizontal curvature produces torque when the curvature causes load to be applied eccentric to the shear center at the supports. At increasing distances from the supports into simple spans, the torque decreases. The phenomenon is less evident in continuous spans where the interaction between spans is complex. In straight girders, torque is produced by applying load eccentric to the shear center. If loads are applied through the shear center; for example, applied equally to the top and bottom flanges along the entire length of a symmetric straight box, there is no torque created. Skewed supports create such an unsymmetrical loading condition however. If there are two bearings, the reactions in the two bearings are significantly different, creating torque in the box. If there is one bearing, torque is created by diaphragms connecting adjacent boxes. It is easily seen that loading the opposite side of a box produces reversal of these secondary distortional bending stresses. Therefore, in the cases listed above, distortional stresses must be considered when checking fatigue. Although the stresses might be thought of as "distortion-induced", they are calculable and are treated herein as load-induced. Transverse bending stresses are typically most critical for cases where the

St. Venant torques are significant, e.g. boxes resting on skewed supports, single box sections and sharply curved boxes.

For the above cases, *AASHTO LRFD* Article 6.11.5 requires that the stress range due to longitudinal warping be considered in checking the fatigue resistance of the base metal at all details on the box section according to Equation 2.177o; the longitudinal warping stresses are generally assumed to be additive to the longitudinal major-axis bending stresses. This assumption is conservative since the critical longitudinal warping stresses are usually produced by eccentric live loads, whereas the critical major-axis bending stresses are produced by more centrally located (i.e. different) live load positions

For the above cases, *AASHTO LRFD* Article 6.11.5 also requires that the transverse bending stress range be investigated in the base metal adjacent to flange-to-web fillet welds and adjacent to the termination of fillet welds connecting transverse elements to webs and box flanges. This investigation is separate from the fatigue check for longitudinal stress ranges in the box. The condition at welded transverse elements is usually the critical case for transverse bending. A stress concentration occurs at the termination of these welds as a result of the transverse bending. The *AASHTO LRFD* Specification does not specifically address the fatigue resistance of this detail. *AASHTO LRFD* Article C6.11.5 indicates that the fatigue resistance of the base metal adjacent to the welds for this case may be perhaps as low as fatigue Category E. A means of reducing the criticalness of these details is to attach all transverse web stiffeners to the top and bottom flanges. Attachment of the transverse stiffeners to the flanges reduces the sharp through-thickness bending within the unstiffened portions of the web adjacent to the termination of the stiffener-to-web welds, which is typically the most critical region. *AASHTO LRFD* Article 6.6.1.3.1 already requires attachment of cross-frame connection plates to the top and bottom flanges. This provision was found necessary in order to transfer load from the cross-frames directly to the flanges rather than through the web via transverse bending. The same logic applies to all transverse stiffener termini when transverse bending exists in the web. The same check must then be made in the box flange at the terminus of the stiffener-to-flange fillet weld.

As specified in *AASHTO LRFD* Article 6.7.4.3, at the termination of fillet welds connecting cross-frame connection plates to box flanges subjected to calculated torque, the need for a transverse member within the internal cross-frames to resist the transverse bending stress range in the box flange at those locations must be considered (*intended to apply to the above cases only*). These members would typically be provided adjacent to the box flanges. These members, which are part of the internal cross-bracing, can significantly reduce the transverse bending stress range and help ensure integrity of the cross-section. To better control the distortion of box flanges, transverse cross-frame members next to box flanges must be attached to the flange. If a longitudinal flange stiffener(s) is present, the transverse members must be bolted to the longitudinal stiffener(s) and not welded to the box flange. This detail avoids the use of more discontinuous fillet welds. Where the transverse bracing members are welded directly to the box flange, the stress range due to transverse bending should also be considered in checking the fatigue resistance of the base metal adjacent to the termination of these welds. Where the

transverse bracing members are connected to longitudinal flange stiffeners, the box flange can be considered stiffened when computing the transverse bending stresses (see below). The moment of inertia of these transverse bracing members is not to be less than the moment of inertia of the largest transverse connection plate for the internal cross-frame under consideration taken about the edge in contact with the web [note that the current (2006) language in *AASHTO LRFD* Article 6.7.4.3 regarding the sizing of these members is in error]. In these cases, the transverse connection plates must still be attached to both flanges as required in *AASHTO LRFD* Article 6.6.1.3.1.

As in the case of longitudinal warping, the largest transverse bending stress range is caused by positioning the live load on one side and then on the opposite side of the box. This implies that either the vehicle moves sideways on the deck or two trucks traverse the bridge in separate transverse positions, with one vehicle leading the other. To account for the unlikely event of this occurring over millions of cycles, *AASHTO LRFD* Article 6.11.5 applies a factor of 0.75 to the computed range of distortionally-induced stresses, but in no case is the stress range to be less than the calculated stress range due to the load positioned in one lane. This factor is in addition to and distinct from the load factor of 0.75 specified for the Fatigue load combination in *AASHTO LRFD* Table 3.4.1-1. No allowance is made for the fact that two vehicles are required to cause the largest stress cycle. For cases the nominal fatigue resistance is calculated based on a finite life (refer to Section 2.2.3.6.1.1.1 of this chapter), the Engineer may consider a reduction in the number of stress cycles (i.e. less than the design number) when computing the fatigue resistance since two cycles are required to cause a single cycle of stress.

Consideration might be given to ignoring the distortional stresses in certain cases if it can be demonstrated that the torques are of comparable magnitude to the torques for cases where research has shown that these stresses are small enough to be neglected (*85b*); e.g. a straight bridge of similar proportion satisfying the restrictions discussed above in Section 2.2.4.1.2; or if the torques are deemed small enough in the judgment of the Owner and the Engineer. In such cases, however, it is strongly recommended that all web stiffeners be attached to both flanges in order to enhance fatigue performance.

BEF Analogy

The beam on elastic foundation (BEF) analogy for determining distortional stresses in box girders is based on the work reported in Reference 85e and sponsored by the American Iron and Steel Institute. The approach is described in detail in Reference 85i, which forms the basis for the following discussion.

Consider the deflection δ_1 due to the uniform torsional load with no cross-frames/diaphragms present, as shown in Figure 2.63.
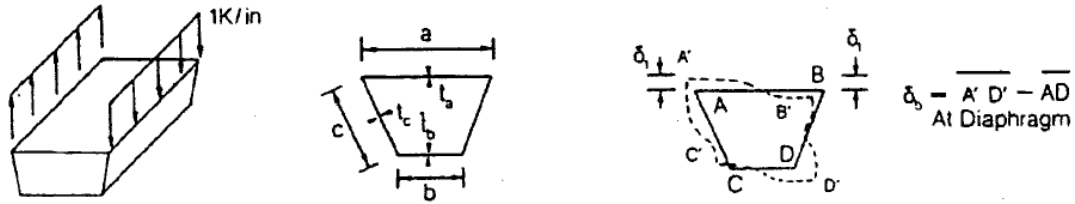
Figure 2.63 Box Under Uniform Torsional Loading

δ_1 is the reciprocal of the torsional stiffness of the box and is analogous to the reciprocal of the foundation modulus in the BEF problem. δ_1 (in units of in^2/kip) is computed as follows:

$$\delta_1 = \frac{ab}{24(a+b)}\left\{\frac{c}{D_c}\left[\frac{2ab}{a+b} - v(2a+b)\right] + \frac{a^2}{D_a}\left[\frac{b}{a+b} - v\right]\right\}$$
Equation 2.177p

where:

a, b, c = dimensions of box section as shown in Figure 2.63 (in.).

v   = compatibility shear at the center of the bottom flange for unit loads applied at the top corners of a box section of unit length (Figure 2.63)

$$= \frac{\dfrac{1}{D_c}\left[(2a+b)abc\right] + \dfrac{1}{D_a}\left[ba^3\right]}{(a+b)\left\{\dfrac{a^3}{D_a} + \dfrac{2c(a^2+ab+b^2)}{D_c} + \dfrac{b^3}{D_b}\right\}}$$
Equation 2.177q

D_a, D_b, D_c = transverse flexural rigidities of an unstiffened plate (kip-in.^{2}/in.)

D_a $= \dfrac{Et_a^3}{12(1-\mu^2)}$ Equation 2.177r

D_b $= \dfrac{Et_b^3}{12(1-\mu^2)}$ Equation 2.177s

D_c $= \dfrac{Et_c^3}{12(1-\mu^2)}$ Equation 2.177t

t_a, t_b, t_c = thickness of top flange, bottom flange and web, respectively (Figure 2.63) (in.)

μ = Poisson's ratio (= 0.2 for concrete – see *AASHTO LRFD* Article 5.4.2.5; 0.3 for steel)

The center of the bottom flange was chosen as the location for computing the compatibility shear because the transverse bending moment and thrust are zero at this point (*85e*).

When transverse stiffeners are present on either the flanges or the webs, they should be considered in calculating the transverse flexural rigidities for resisting transverse bending. The rigidity *D* of the stiffened plate is computed as:

$$D = \frac{EI_s}{d}$$ Equation 2.177u

where:

d   =   stiffener spacing (in.)

I_s =   moment of inertia of the stiffened plate for transverse bending (based on the effective width of the plate defined by Equation 2.177v below) including the transverse stiffener (in.[4])

The stiffness of the transverse stiffener is assumed distributed evenly along the stiffened plate.

The effective width of plate d_o acting with the stiffener can be determined from the following semi-empirical relationship (*85e*) as:

$$d_o = \frac{d \tanh\left(5.6\frac{d}{h}\right)}{\frac{5.6d}{h}\left(1 - \mu^2\right)}$$ Equation 2.177v

where:

h   =   length of web or box-flange element, as applicable (i.e. dimension "b" or "c" as shown in Figure 2.63 (in.)

The BEF stiffness parameter β (in units of in.[-1]) is a measure of the torsional stiffness of the beam and is analogous to the beam-foundation parameter in the BEF problem. β is calculated as follows:

$$\beta \approx \left(\frac{1}{EI\delta_1}\right)^{\frac{1}{4}}$$ Equation 2.177w

where:

I   =   moment of inertia of the box section (in.[4])

The cross-frames/diaphragms in the box girder restrict the box distortion and are analogous to the supports in the BEF. The cross-frames/diaphragms are incorporated in the solution by the dimensionless ratio *q* of the cross-frame/diaphragm stiffness to the box stiffness per unit length, which is defined as follows:

$$q = \left[\frac{E_b A_b}{L_b \ell \delta_1}\right]\delta_b^2$$ Equation 2.177x

where:

A_b =   cross-sectional area of one cross-frame/diaphragm bracing member (in.[2])

E_b = Young's modulus of the cross-frame/diaphragm material (ksi)

ℓ = cross-frame/diaphragm spacing (in.)

L_b = length of the cross-frame/diaphragm bracing member (in.)

δ_b = deformation of the bracing member due to the applied torque (Figure 2.63) (in.^{2}/kip)

$\quad\quad$ = $\dfrac{2(1+a/b)}{\sqrt{1+\left[\dfrac{a+b}{2h}\right]^2}}\,\delta_1$ $\quad\quad\quad\quad$ Equation 2.177y

h = vertical web depth of the box section (in.)

Equation 2.177y assumes that the cross-bracing member is effective in both compression and tension. If the bracing slenderness is large and the member is only considered effective in tension, then A_b in Equation 2.177y should be taken as one-half the area of one brace.

The distortional stresses in the box-section can be determined analogously by solving the BEF problem. The moment in the BEF is analogous to the distortional longitudinal warping stress σ_{dw}. The deflection of the BEF is analogous to the distortional transverse bending stress σ_t. The reactions in the BEF are analogous to the forces in the cross-bracing F_b. Solutions to the BEF problem for these three components are presented in graphical form in Figure 2.64 through Figure 2.73 below. These figures each give a BEF factor (or "C" value), which is then used in the appropriate corresponding equation given below (i.e. Equation 2.177z, 2.177aa or 2.177dd) to calculate the distortion-related stresses (and stress ranges) or forces (and force ranges). The graphs give relationships for the distortional stresses at either the cross-bracing or at midpanel between the cross-braces, and also for the cross-bracing force, under either a uniform torque per unit length m, or a concentrated torque T (or a range of m or T). Relationships are given for the concentrated torque T (or range of torque T) applied at either midpanel or at the cross-bracing. Given the box geometry, the value of β from Equation 2.177w, the loading, the cross-bracing stiffness ratio q from Equation 2.177x and the spacing of the cross-bracing ℓ, the appropriate value of "C" can be obtained from the graphs for use in the following equations.   Since only two loading positions are considered in the graphs for T, it may be necessary in some cases to interpolate between the appropriate graphs for each position. The principle of superposition applies for more than one torque.

The distortional longitudinal warping stress σ_{dw} at any point on the cross-section is obtained as follows:

$$\sigma_{dw} = \frac{C_w y}{I\beta a}\left(m\ell \ \ \text{or} \ \ T\right) \quad\quad\quad\quad \text{Equation 2.177z}$$

where:

$\quad$ C_w = BEF factor for distortional longitudinal warping stress obtained from Figure 2.64, Figure 2.65 or Figure 2.66, as applicable

y　　=　　distance along the transverse vertical axis of the box from the neutral axis to the point under consideration (in.)

All other terms are as defined previously. The range of longitudinal warping stress is obtained by substituting the range of m or T, as applicable, in Equation 2.177z.

The distortional transverse bending stresses σ_t in the web or box flange at the top or bottom corners of the box section are obtained as follows:

$$\sigma_t = C_t F_d \beta \frac{1}{2a} (m\ell \ \text{ or } \ T) \qquad\qquad \text{Equation 2.177aa}$$

where:

C_t　　=　　BEF factor for distortional transverse bending stress obtained from Figure 2.67, Figure 2.68, Figure 2.69 or Figure 2.70, as applicable

F_d　　=　　transverse bending stress in the web or box flange, as applicable, due to the applied torque (in.$^{-1}$)

　　　=　　$\dfrac{bv}{2S}$ for the bottom corner of the box　　　　Equation 2.177bb

　　　=　　$\dfrac{a}{2S}\left(\dfrac{b}{a+b} - v\right)$ for the top corner of the box　　Equation 2.177cc

S　　=　　section modulus per unit length of the web or box flange, as applicable, for transverse bending (in.^{3}/in.). For a stiffened plate, the section modulus per unit length should be based on the effective width of the plate defined by Equation 2.177v and include the transverse stiffener

All other terms are as defined previously. The critical transverse bending stress may be in either the web or the adjacent box flange(s). The range of transverse bending stress is obtained by substituting the range of m or T, as applicable, in Equation 2.177aa.

The axial force in the cross-bracing due to distortional forces applied to the box F_b is obtained as follows:

$$F_b = C_b \left[\frac{\sqrt{1 + \left(\dfrac{a+b}{2h}\right)^2}}{2\left(1+\dfrac{a}{b}\right)} \right] \frac{(m\ell \ \text{ or } \ T)}{a} \qquad\qquad \text{Equation 2.177dd}$$

where:

C_b　　=　　BEF factor distortional cross-bracing force determined from Figure 2.71 or Figure 2.72, as applicable

h　　=　　vertical web depth of the box section (in.)

Again, all other terms are as defined previously. The range of axial force is obtained by substituting the range of m or T, as applicable, in Equation 2.177dd. Note that Figure 2.73 shows the effect of β on the influence line for cross-bracing forces when the cross-bracing is rigid.
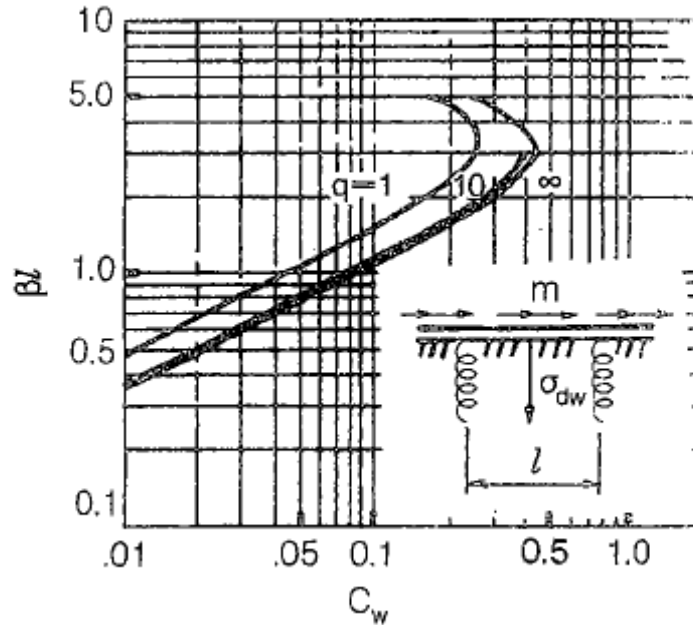
Figure 2.64 BEF Factor C_w for Distortional Longitudinal Warping Stress at Midpanel due to a Uniform Torque m
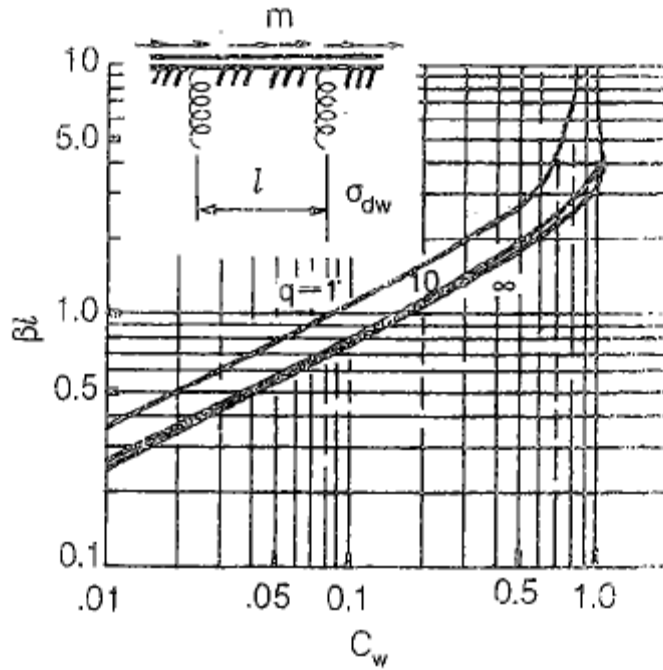
Figure 2.65 BEF Factor C_w for Distortional Longitudinal Warping Stress at Cross-Bracing due to a Uniform Torque m
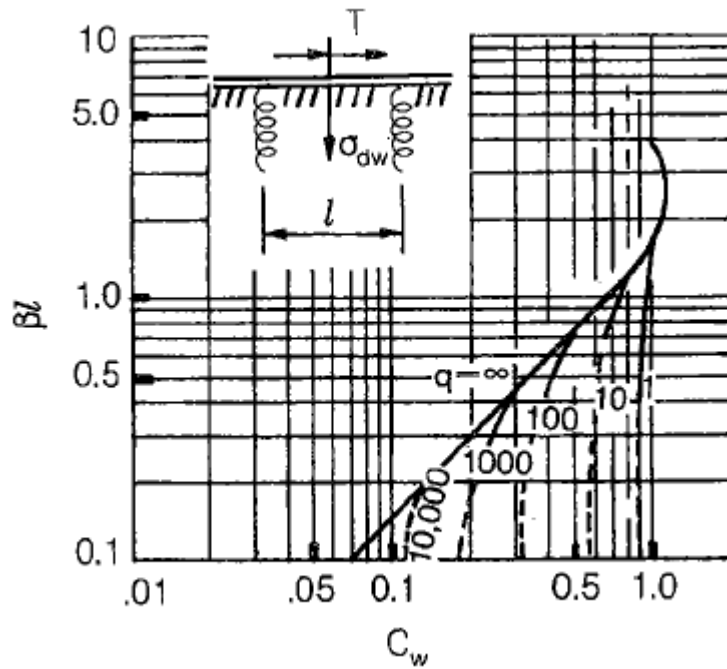
Figure 2.66 BEF Factor C_w for Distortional Longitudinal Warping Stress at Midpanel due to a Concentrated Torque T at Midpanel
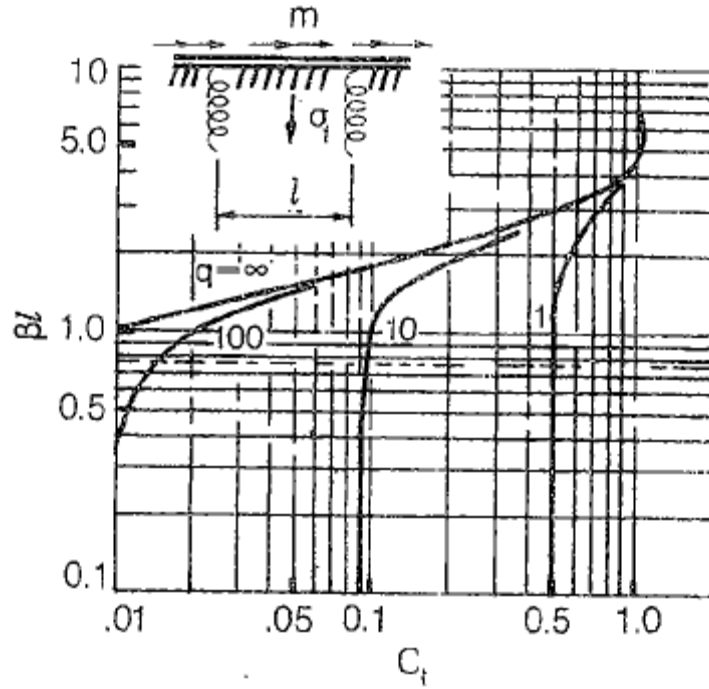
Figure 2.67 BEF Factor C_t for Distortional Transverse Bending Stress at Midpanel due to a Uniform Torque m
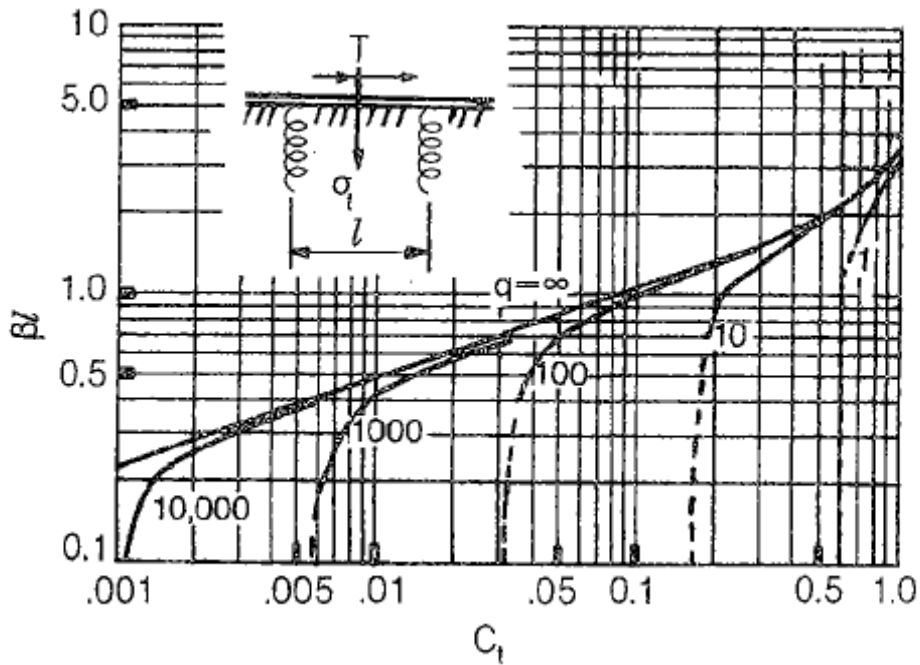
Figure 2.68 BEF Factor C_t for Distortional Transverse Bending Stress at Midpanel due to a Concentrated Torque T at Midpanel
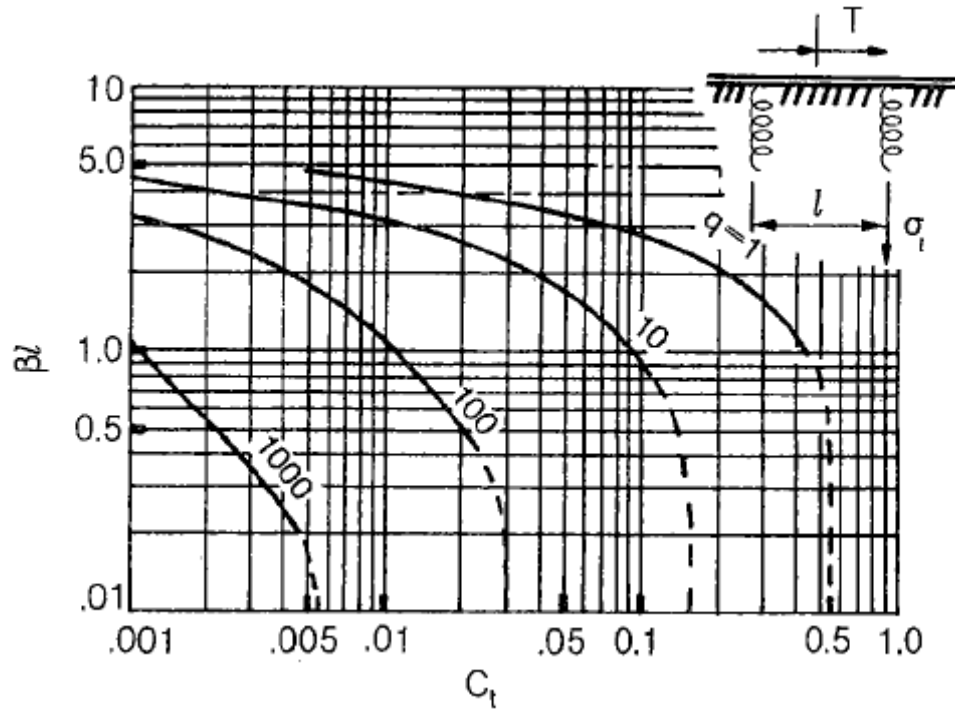
Figure 2.69 BEF Factor C_t for Distortional Transverse Bending Stress at Cross-Bracing due to a Concentrated Torque T at Midpanel
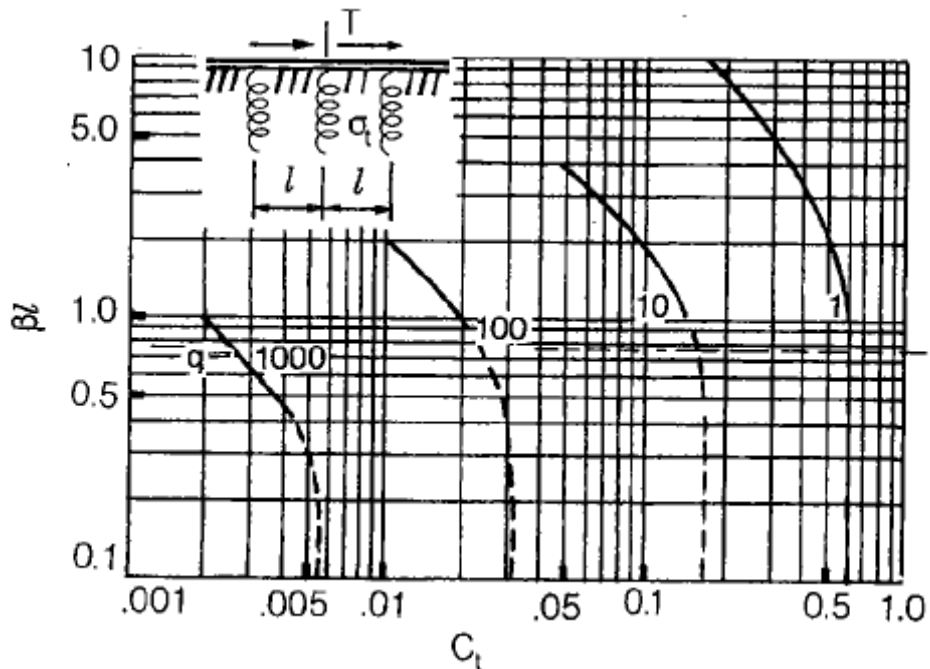
Figure 2.70 BEF Factor C_t for Distortional Transverse Bending Stress at Cross-Bracing due to a Concentrated Torque T at Cross-Bracing
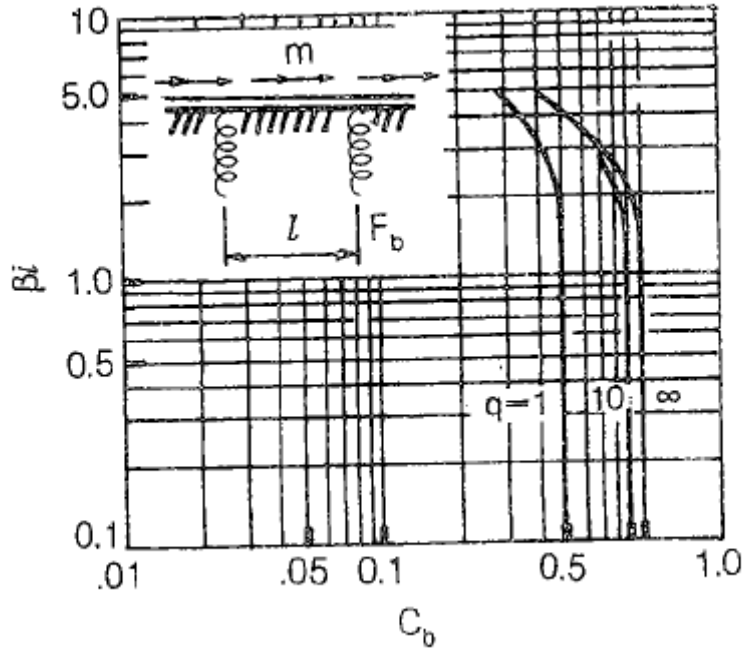
Figure 2.71 BEF Factor C_b for Distortional Axial Cross-Bracing Force due to a Uniform Torque m
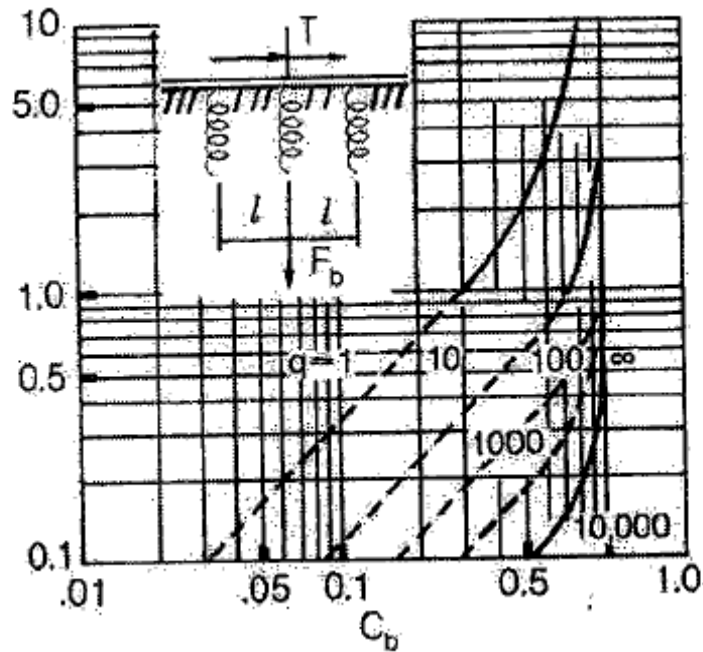
Figure 2.72 BEF Factor C_b for Distortional Axial Cross-Bracing Force due to a Concentrated Torque T at Cross-Bracing

2.347
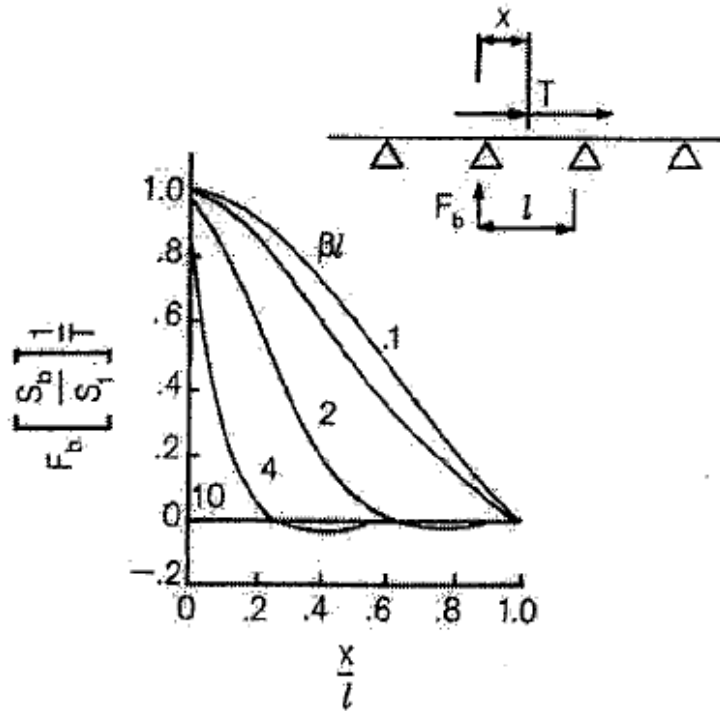
**Figure 2.73 Influence Line for Distortional Axial Cross-Bracing Force for a
Rigid Cross-Brace due to a Concentrated Torque *T***

EXAMPLE

Check the distortional transverse bending stress range for fatigue at the termination
of the fillet welds connecting the transverse stiffeners to the web of the following
composite tub girder cross-section, which is part of a straight multiple tub-girder
bridge resting on skewed supports.
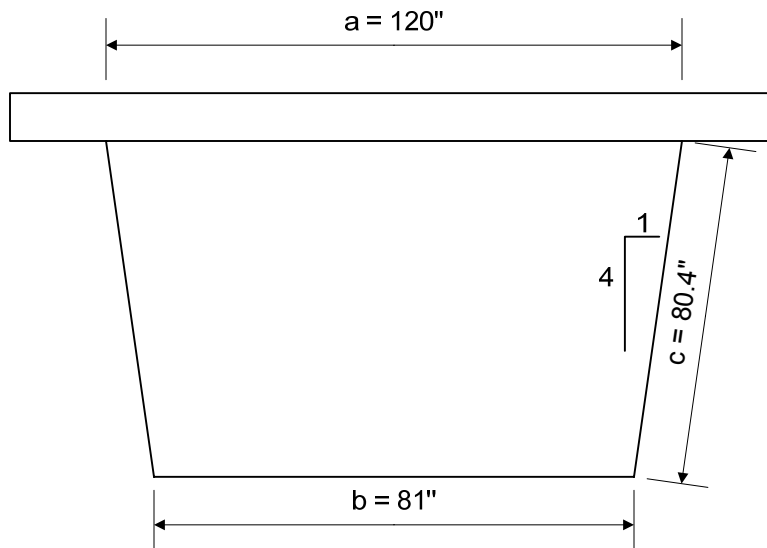
Since the bridge is resting on skewed supports, the restrictions specified in *AASHTO LRFD* Article 6.11.2.3 are not satisfied and distortional stresses must be considered for fatigue. It is assumed that the distortional longitudinal warping stress range has been considered separately and is negligible for this example.

The thicknesses of the cross-section components are as follows:

Slab (structural):	t_a	=	9.5 in.
Web	t_c	=	0.5625 in.
Bottom flange	t_b	=	1.5 in.

The vertical web depth is 78.0 inches. The moment of inertia of the composite tub cross-section is I = 836,080 in.[4] The transverse stiffener plates are ½" x 5.5" bars on one side of the web. The transverse stiffener spacing d adjacent to the section is 62.0 in. The cross-frame spacing ℓ adjacent to the section is 18.0 feet = 216.0 in. The bottom box flange is unstiffened both longitudinally and transversely.

The unfactored torques at this section due to the fatigue load specified in *AASHTO LRFD* Article 3.6.1.4 (i.e. a 72-kip HS20 truck with a constant rear-axle spacing of 30 feet) placed in a single lane, including the 15 percent dynamic load allowance, are as follows:

$+T_{LL+IM} =$ +370 kip-ft
$-T_{LL+IM} =$ -315 kip-ft

Therefore, the total range of torque is $370 + |-315| = 685 \, kip - ft$. From the results of a refined analysis of the superstructure (which is recommended for tub girders resting on skewed supports), this critical range is produced by placing the fatigue truck in two different transverse positions on opposite sides of the tub section (representing two trucks crossing the bridge in separate lanes with one vehicle leading the other), and is larger than the range produced by a single passage of the fatigue load in this case. Therefore, to account for the fact that two separate positions of the truck are required to cause the critical range of torque, a factor of 0.75 is applied to this range, as specified in *AASHTO LRFD* Article 6.11.5. In addition, the load factor of 0.75 specified for the Fatigue load combination in *AASHTO LRFD* Table 3.4.1-1 must also be applied.   Therefore:

$$T_{range} = 685 \, kip - ft * 0.75 * 0.75 = 385.3 \, kip - ft = 4,624 \, kip - in.$$

Calculate the transverse flexural rigidities D_a and D_b of the concrete deck and unstiffened bottom box flange, respectively. The modulus of elasticity E_c of the concrete is 3,834 ksi.   The Poisson's ratio μ for the concrete is taken as 0.2 for the concrete and 0.3 for the steel. Therefore, from Equations 2.177r and 2.177s:

$$D_a = \frac{Et_a^3}{12(1-\mu^2)} = \frac{3,834(9.5)^3}{12(1-0.2^2)} = 285,345 \, k - in.^2 / in.$$

$$D_b = \frac{Et_b^3}{12(1-\mu^2)} = \frac{29{,}000(1.5)^3}{12(1-0.3^2)} = 8{,}963 \text{ k} - \text{in.}^2 / \text{in.}$$

Calculate the transverse flexural rigidity D_c of the stiffened webs. Since the web is stiffened, D_c will be computed from 2.177u; that is, the transverse stiffeners will be considered effective in resisting the transverse bending. First, calculate the effective width of the web plate d_o acting with the transverse stiffener from Equation 2.177v (refer also to the figure below). For the web plate, $h = c = 78/\cos 14° = 80.4$ in.

$$d_o = \frac{d \tanh\left(5.6\dfrac{d}{h}\right)}{\dfrac{5.6d}{h}(1-\mu^2)} = \frac{62.0 \tanh\left[5.6\left(\dfrac{62.0}{80.4}\right)\right]}{\dfrac{5.6(62.0)}{80.4}(1-0.3^2)} = 15.8 \text{ in.}$$
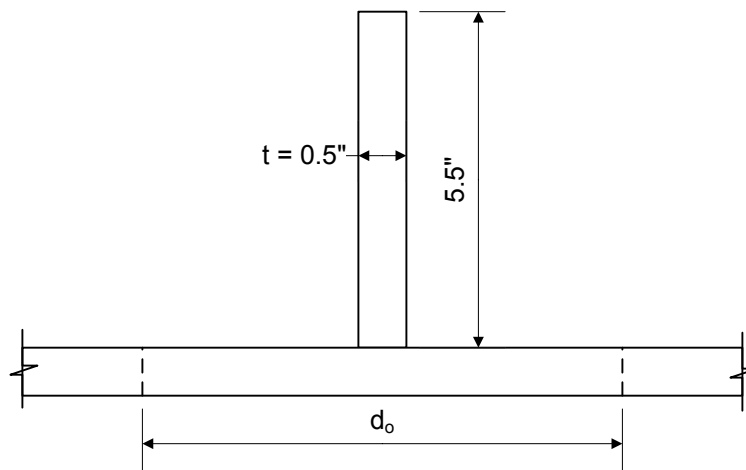
Compute the location of the neutral axis of the effective section from the outer web face.

Area of the stiffener =	5.5 * 0.5	=	2.75 in.^{2}
Area of effective web =	15.8 * 0.5625 =		8.89 in.^{2}
			11.64 in.^{2}

$$\text{N.A.} = \frac{2.75(0.5625 + 5.5/2) + 8.89(0.5625/2)}{11.64} = 1.0 \text{ in.}$$

Calculate the moment of inertia I_s of the effective stiffened web plate for transverse bending, including the transverse stiffener:

$$I_s = \frac{1}{12}(5.5)^3 + 2.75(5.5/2 + 0.5625 - 1.0)^2 + 8.89(0.5625/2 - 1.0)^2 + \frac{1}{12}(15.8)(0.5625)^3 = 33.40 \text{ in.}^4$$

From Equation 2.177u:

$$D_c = \frac{EI_s}{d} = \frac{29{,}000(33.40)}{62.0} = 15{,}623 \text{ kip} - \text{in.}^2 \,/\, \text{in.}$$

Compute the compatibility shear v at the center of the bottom box flange according to Equation 2.177q:

$$v = \frac{\dfrac{1}{D_c}\left[(2a+b)abc\right]+\dfrac{1}{D_a}\left[ba^3\right]}{(a+b)\left\{\dfrac{a^3}{D_a}+\dfrac{2c\left(a^2+ab+b^2\right)}{D_c}+\dfrac{b^3}{D_b}\right\}}$$

$$v = \frac{\dfrac{1}{15{,}623}\left[(2*120+81)(120*81*80.4)\right]+\dfrac{1}{285{,}345}\left(81*120^3\right)}{(120+81)\left\{\dfrac{120^3}{285{,}345}+\dfrac{2*80.4\left(120^2+120*81+81^2\right)}{15{,}623}+\dfrac{81^3}{8.963}\right\}} = 0.22$$

Calculate the box distortion per kip per inch of load δ_1 assuming no cross-bracing is present from Equation 2.177p:

$$\delta_1 = \frac{ab}{24(a+b)}\left\{\frac{c}{D_c}\left[\frac{2ab}{a+b}-v(2a+b)\right]+\frac{a^2}{D_a}\left[\frac{b}{a+b}-v\right]\right\}$$

$$\delta_1 = \frac{120*81}{24(120+81)}\left\{\frac{80.4}{12{,}381}\left[\frac{2*120*81}{120+81}-0.223(2*120+81)\right]+\frac{120^2}{285{,}345}\left(\frac{81}{120+81}-0.223\right)\right\} = 0.347 \text{ in.}^2 \,/\, \text{kip}$$

Compute the BEF stiffness parameter β from Equation 2.177w:

$$\beta = \left(\frac{1}{EI\delta_1}\right)^{\frac{1}{4}} = \left(\frac{1}{29{,}000 * 836{,}050 * 0.347}\right)^{\frac{1}{4}} = 0.00330 \text{ in.}^{-1}$$

$$\beta\ell = 0.00330(216.0) = 0.713$$

The transverse bending stress range at the top and bottom corners of the tub section may be computed from Equation 2.177aa as follows:

$$\sigma_t = C_t F_d \beta \frac{1}{2a} T_{range}$$

It will be assumed for this example that the transverse stiffeners are attached to the top and bottom flanges of the tub, which is recommended for these cases. Transverse stiffeners attached to the top and bottom flanges reduce the sharp through-thickness bending that would otherwise occur due to cross-section distortion

in the unstiffened portions of the web at the termination of the stiffener-to-web welds. Connection plates are required to be attached to the flanges for this reason.

First compute the section modulus S per unit length of the stiffened web (including the transverse stiffener). In the following equation, y is the distance from the neutral axis to the extreme fiber of the section consisting of the transverse stiffener and the effective portion of the web plate and d is the transverse stiffener spacing.

$$S = \frac{I_s}{yd} = \frac{26.47}{(5.5 + 0.5625 - 1.0)(62.0)} = 0.084 \text{ in.}^3 / \text{in.}$$

The calculated section modulus must at least equal or exceed the calculated section modulus per unit length of the unstiffened web, which is the lower bound. Compute the section modulus S per unit length of the unstiffened portions of the web, which by inspection is more critical than the unstiffened bottom box flange:

$$S = \frac{1}{6}(1)(0.5625)^2 = 0.053 \text{ in.}^3 / \text{in.}$$

For the bottom corner of the box, the transverse bending stress in the web due to the applied torque F_d is computed from Equation 2.177bb as follows:

$$F_d = \frac{bv}{2S}$$

- For the stiffened portions of the web:

$$F_d = \frac{81(0.223)}{2(0.084)} = 108 \text{ in.}^{-1}$$

For the top corner of the box, the transverse bending stress in the web due to the applied torque F_d is computed from Equation 2.177cc as follows:

$$F_d = \frac{a}{2S}\left(\frac{b}{a+b} - v\right)$$

- For the stiffened portions of the web:

$$F_d = \frac{120}{2(0.084)}\left(\frac{81}{120 + 81} - 0.223\right) = 129 \text{ in.}^{-1}$$
$$\text{(controls)}$$

Obtain the BEF factor C_t for distortional transverse bending stress. The transverse stiffener will be assumed at mid-panel with the torques conservatively assumed applied at mid-panel. This is the most critical case if one visualizes the analogous deflection of a beam on an elastic foundation. Therefore, C_t will be obtained from the graph given in Figure 2.68. If desired, greater precision could be obtained for an actual condition different than that assumed by interpolating between the appropriate

graphs. First, calculate the deformation of the internal bracing member δ_b due to the applied torque from Equation 2.177y:

$$\delta_b = \frac{2(1 + a/b)}{\sqrt{1 + \left[\dfrac{a+b}{2h}\right]^2}} \delta_1$$

$$\delta_b = \frac{2(1 + 120/81)}{\sqrt{1 + \left[\dfrac{120 + 81}{2(78.0)}\right]^2}} (0.347) = 1.056 \text{ in.}^2 \text{ / kip}$$

Calculate the cross-bracing stiffness ratio q from Equation 2.177x. Assume an internal K-brace with the area of one diagonal Ab equal to 6.94 in.2 and the length of the diagonal Lb equal to 87.9 in. Assume the bracing member has been designed to be effective in compression; therefore, the full area may be used for Ab.

$$q = \left[\frac{E_b A_b}{L_b \ell \delta_1}\right] \delta_b^2$$

$$q = \left[\frac{29{,}000(6.94)}{87.9(216.0)(0.347)}\right](1.056)^2 = 34.1$$

From the graph in Figure 2.68, for q = 34.1 and $\beta\ell$ = 0.713 (as computed previously), C_t is approximately equal to 0.15. Therefore, from Equation 2.177aa:

$$\sigma_t = 0.15(129)(0.00330)\left(\frac{1}{2(120)}\right)(4{,}624) = 1.23 \text{ ksi}$$

A stress concentration occurs at the termination of the transverse stiffener welds to the top flange as a result of the transverse bending. The fatigue resistance of this detail when subject to transverse bending is not currently quantified. As recommended in *AASHTO LRFD* Article C6.11.5, assume fatigue detail Category E for computing the nominal fatigue resistance. Assume the number of stress cycles per truck passage in this region *n* is equal to 1.0. From separate calculations, the single-lane average daily truck traffic *(ADTT)SL* is computed to be 1,600 trucks/day (refer to Section 2.2.3.6.1.1.1 of this chapter). According to *AASHTO LRFD* Table C6.6.1.2.5-1 (Table 2.11), since the *(ADTT)SL* does not exceed the 75-year *(ADTT)SL* equivalent to infinite life of 3,545 trucks/day for a Category E detail with *n* equal to 1.0, the nominal fatigue resistance *(ΔF)n* is computed from Equation 2.83 based on finite life as follows:

$$(\Delta F)_n = \left(\frac{A}{N}\right)^{\frac{1}{3}}$$

The detail category constant *A* for a Category E detail is taken as 11.0 x 10^8 ksi^3 from *AASHTO LRFD* Table 6.6.1.2.5-1 (Table 2.10). The number of stress cycles *N* is computed from Equation 2.88 as follows:

$$N = (365)(75)n(ADTT)_{SL}$$
AASHTO LRFD Equation 6.6.1.2.5-2

$$N = (365)(75)(1.0)(1,600) = 43.8 \times 10^6 \text{ cycles}$$

Therefore:

$$(\Delta F)_n = \left(\frac{11.0 \times 10^8}{43.8 \times 10^6} \right)^{\frac{1}{3}} = 2.93 \text{ ksi} > \sigma_t = 1.23 \text{ ksi} \quad \text{ok}$$

If necessary, the transverse bending stress could be reduced by decreasing the cross-frame spacing and/or increasing the thickness of the web plate.

2.2.4.6.1.1.2 Shear

AASHTO LRFD Article 6.11.5 refers back to the shear requirement specified in *AASHTO LRFD* Article 6.10.5.3. According to this requirement, the shear in the web due to the unfactored permanent load plus *two times* the factored fatigue design truck (i.e. the 54-kip truck plus the 15 percent dynamic load allowance) V_u must not exceed the shear-buckling resistance V_{cr} (refer to Equation 2.91 and Section 2.2.3.6.1.1.2 of this chapter). For the cases described in Section 2.2.4.1.3 of this chapter, the critical shear case includes torsional shear plus flexural shear. Proper determination of this value considers coincident flexure and torsion. Conservatively, critical torsion and critical flexural shears can be added. This requirement has been introduced to prevent shear buckling of the web under the heaviest truck expected to cross the bridge over its assumed 75-year fatigue design life. The intent of this provision is to prevent significant flexing of the web under repeated live load. The member is thus assumed able to resist an infinite number of smaller loadings without introducing fatigue cracks around the perimeter of the web panel.

In checking Equation 2.91, the provisions of *AASHTO LRFD* Article 6.11.9, as applicable, are to be applied. Inclined webs must be designed for the component of the vertical shear in the plane of the web V_{ui} taken equal to V_u divided by $\cos\theta$, where θ is the angle of inclination of the web plate with respect to the vertical (see *AASHTO LRFD* Equation 6.11.9-1). Also, in computing the shear-buckling resistance V_{cr} for the case of inclined webs from *AASHTO LRFD* Equation 6.10.9.3.3-1 (i.e. Equation 2.51), the web depth *D* must be taken as the depth of the web measured along the slope or $D/\cos\theta$. As discussed above, for all box sections in the bridges discussed in Section 2.2.4.1.3 of this chapter, V_u is to be taken as the sum of the flexural and St. Venant torsional shears in checking this requirement. In these cases (for which the St. Venant torsional shears must be considered), the dead and live load shears in one web are greater than in the other web at the same cross-section since the torsional shear is of opposite sign in the two webs. For practical reasons, however, both webs are usually detailed for the critical shear.

Shears in the web due to warping torsion and cross-section distortion may be ignored in all cases in making this check.

A check for bend-buckling of the web under this condition is not required for reasons discussed previously in Section 2.2.2.4 of this chapter.

2.2.4.6.1.2 Distortion-Induced Fatigue

The *AASHTO LRFD* Specifications define distortion-induced fatigue as fatigue due to secondary stresses not normally quantified in the typical analysis and design of a bridge. Out-of-plane distortions generated by forces resulting from three-dimensional interaction of bridge members result in localized secondary stresses, which can be significant in magnitude and generally are not explicitly considered in the design process. For a bridge detail and/or weldment to be susceptible to distortion-induced fatigue, there must be an unstiffened gap, constraints at boundaries of the unstiffened gap and out-of-plane distortion. Because the secondary stresses that develop in the web gap are difficult to estimate and the fatigue resistance of various details under these conditions has been difficult to quantify, the design approach taken is to avoid such details and to provide rigid load paths to preclude the development of significant secondary stresses. *AASHTO LRFD* Article 6.6.1.3 requires that sufficient load paths be provided by attaching transverse members to components that are attached to the longitudinal member by either welding or bolting.

AASHTO LRFD Article 6.6.1.3.1 deals with the detailing of transverse connection plates to prevent distortion-induced fatigue. Transverse connection plates (or transverse stiffeners serving as connection plates) attached to cross-frames or diaphragms are to be bolted or welded to both the compression and tension flanges of the cross-section in order to eliminate any web gaps. At locations where larger out-of-plane forces may develop, it is recommended in *AASHTO LRFD* Article 6.6.1.3.1 that in the absence of better information, that the welded or bolted connection in straight, nonskewed bridges be designed for a minimum of a 20.0 kip lateral force to ensure that the connection is not undersized. For straight, skewed bridges and horizontally curved bridges, it is recommended in *AASHTO LRFD* Article C6.6.1.3.1 that the force be determined by analysis.

The attachment of internal cross-frame connection plates to box flanges is discussed in *AASHTO LRFD* Article C6.6.1.3.1. In the fabrication of tub sections, webs are often joined to top flanges and cross-frame connection plates and transverse stiffeners are installed, and then the assemblies are attached to the common box flange. To accomplish this efficiently, the connection plates must be detailed to allow the weld connecting the flange and web to clear the bottom of the connection plates and stiffeners. Otherwise, continuity of the web-to-flange weld is interrupted. The subsequent attachment of the connection plates to the box flange, as required in *AASHTO LRFD* Article 6.6.1.3.1, is accomplished with an additional piece welded to the flange and connection plate. A similar detail may also be necessary for any intermediate transverse stiffeners that are to be attached to the box flange. These details are shown in Reference 40. Details on tub girders have a significant effect on cost. The Engineer is encouraged to consult with fabricators likely to build a project

regarding the preferred details for fabricating the tub sections. It may be desirable to provide alternate details for the connection plates on the design plans.

AASHTO LRFD Article 6.6.1.3.2 deals with the detailing lateral bracing connection plates. Although not required, it is desirable to attach lateral bracing connection plates to the top flanges rather than to the web. Generally, fabricators prefer the connection plates to be attached by bolting. Properly tensioned bolts provide improved fatigue resistance (Category B) and eliminate expensive radiused transitions at the ends of each welded connection plate needed to improve the fatigue category from Category E to Category C. Forces in the lateral bracing create a load path through the connection plate and through the web to the top flanges. This circuitous load creates potentially fatigue prone details that must be considered. In such cases, the connections to the web must be made according to the requirements of *AASHTO LRFD* Article 6.6.1.3.2 to prevent potential problems resulting from "distortion-induced fatigue" (refer to the Section 2.2.3.6.1.2 of this chapter for further discussion regarding these connections). Load-induced fatigue is usually not critical for top lateral bracing in tub sections since the concrete deck is much stiffer and resists more of the load than does the bracing; thus, the live-load forces in the bracing are usually relatively small. However, since the concrete deck resists the majority of the torsional shear in such cases, it is recommended that the transverse reinforcement in the deck be checked for torsional shear. Further information regarding the design and detailing of top lateral bracing in tub girders may be found in DM Volume 1, Chapter 2, Section 2.4.3.1.5.6.

2.2.4.6.2 Fracture Limit State

Fracture is defined as a tensile mode in which the metal of an element breaks into two parts. By definition, any force in the fractured element is redistributed into the remaining structure. The ability of the structure to absorb this energy without further damage and carry some additional load is called structural redundancy. Fracture can either be a ductile, brittle or a combination of the two modes. Section 2.2.3.6.2 of this chapter discusses the distinction between ductile and brittle fracture, the concept of fracture toughness, the definition of fracture-critical members (FCMs) and the Charpy V-Notch impact test. This Charpy V-Notch test is used to determine the fracture toughness, which is a material property much like the properties of yield or ultimate stress. Required minimum Charpy V-Notch values at various temperatures are specified for the various bridge steels. The specified values depend on the location of the application and the type of application of the particular element. Elements used in nonfracture-critical applications have less severe requirements than elements used in fracture-critical applications. A fracture-critical element is defined as an element that should it fracture, would release energy into the structure that the structure could not safely absorb without further damage. For this reason, further precautions are taken in the fabrication of fracture-critical members (FCMs). These members must be fabricated in accordance with the fracture control plan given in Reference 70. As specified in *AASHTO LRFD* Article 6.6.2, the Engineer must identify all FCMs in the bridge and clearly delineate their location on the contract plans.

These provisions came into being several decades ago after there were some fractures of steel bridge members that could be traced to low toughness material. Since they have been applied to U.S. bridge construction, there have been no such failures. Recent failures of steel bridges associated with tensile stress, such as the Hoan Bridge in Milwaukee, have been traced to inadequate detailing that did not provide an adequate load path. There have been far more sudden collapses of bridges associated with stability failures, particularly during construction, than due to fracture.

Nonetheless, redundant bridges are desirable. However, when a less redundant design is found desirable, it can be built under the current provisions. The economics often dictate non-redundant bridges. Single-box cross sections are often economical and are considered non-redundant.

Generally, the *AASHTO LRFD* Specification specifies capacity of individual elements or members. However, *AASHTO LRFD* Article 1.3.4 Redundancy addresses the entire structure. This article recommends either multi-load-path structures or continuous ones in order to provide redundancy. The article goes on to identify bridges that are thought to collapse if one main element should fail. Such bridges are to be called out on the Plans as "failure-critical". The member(s) that cause the structure to be failure-critical are to be identified as "fracture-critical". Another term often used to define such a structure is one susceptible to "progressive collapse. A load modifier η_R is provided that suggests a factor of 1.05 be applied for members in non-redundant structures. However, there are no instructions as to how to make the proper analysis or the level of live load that the bridge should be able to carry in its damaged condition. Load factors to be applied to the analysis of the damaged structure are also lacking. Three types of redundancy are identified in Section 2.2.3.6.2 of this chapter; multiple load path redundancy, statical redundancy and internal member redundancy. The type of redundancy that must be demonstrated in identifying FCMs is often dependent on the Owner who can accept an analysis as demonstration of adequate redundancy. Specification of FCMs is often satisfactory. The most conservative and often uneconomical choice is multiple load path redundant structures. Specific redundancy considerations related to composite steel bridges are discussed further in DM Volume 1, Chapter 2, Section 2.4.3.1.6.

Bridges utilizing single box sections and widely spaced multiple-box girders provide efficient designs that reduce steel quantities and fabrication cost savings. These savings usually more than offset the costs associated with FCM fabrication and stringent material requirements related to fracture-critical components in these structures.

AASHTO LRFD Article 6.11.5 specifies that box flanges in tension in single-box cross sections are to be considered FCMs, unless by analysis the bridge can be shown to support the dead load and the live load after sustaining a fracture of the flange and both webs at any point along the girder. If the bridge cannot be shown to be redundant, it does not mean that it cannot be built within the specification. It simply means that the elements leading to the non-redundant condition must be designated FCMs.

Another way to address the issue is with multiple load paths. The tension flanges in the negative moment regions of a single-box bridge may be shown to be redundant via the multiple longitudinal reinforcement provided in the composite deck. There must be adequate shear connection of the deck to permit the section to remain structurally intact. In cross-sections comprised of two box girders, the bottom flanges in positive moment regions are to be considered fracture-critical components according to *AASHTO LRFD* Article 6.11.5 unless adequate strength and stability of the hypothetically damaged structure can be verified by refined analysis. Where cross-sections contain more than two box sections, none of the components of the box sections are to be considered fracture critical according to this article.

The use of refined analyses to demonstrate redundancy, or to confirm that part of the hypothetically damaged structure is not fracture critical, is permitted according to *AASHTO LRFD* Article 6.6.2. The loading cases to be considered, the location of the potential cracks, the degree of the dynamic effects to be included, the software to be used and the degree of refinement of the model should be agreed upon by the Engineer and the Owner, as these items have not yet been codified. As discussed in *AASHTO LRFD* Article C6.6.2, relief from the full factored loads in the applicable strength limit state load combinations should be considered. Consideration should also be given to the number of loaded design lanes versus the number of striped traffic lanes in the analysis.

Material for nonfracture-critical members and components sustaining tensile force effects is also subject to Charpy V-Notch testing to demonstrate adequate fracture toughness, as specified in AASHTO LRFD Article 6.6.2. Components and connections requiring such testing must be so designated on the contract plans. The reader is referred to the last paragraph of Section 2.2.3.6.2 of this chapter for further information on the specific requirements.

85h.   Brown, J.D., D.J. Lubitz, Y.C. Cekov, and K.H. Frank. 2007. "Evaluation of Influence of Hole Making Upon the Performance of Structural Steel Plates and Connections." Report No. FHWA/TX-07/0-4624-1, University of Texas at Austin, Austin, TX, January.

85i.   Heins, C.P., and D.H. Hall. 1981. "Designers Guide to Steel Box Girder Bridges." *Booklet No. 3500*, Bethlehem Steel Corporation, Bethlehem, PA, February.

2.2.4.7 Strength Limit State Verifications

The strength limit state is taken to ensure that each element of a bridge has adequate capacity and global and local stability to resist the actions of the factored loads. The load factors are developed to account for the maximum expected permitted load that is bridge is expected to experience over its design life (*AASHTO LRFD* Article 1.3.2.4). Overall structural integrity is assumed maintained at the strength limit state even though structural damage and distress may be expected to occur.

AASHTO LRFD Article 6.5.4 states that for steel structures, the strength load combinations specified in *AASHTO LRFD* Table 3.4.1-1 in combination with the resistance factors specified in *AASHTO LRFD* Article 6.5.4.2 are to be used to check

the strength limit state. *AASHTO LRFD* Article 6.11.6 provides a "roadmap" to direct the Engineer to the appropriate articles giving the specific strength limit state checks that are to be made for box-section flexural members in regions of positive or negative flexure, as discussed in more detail below.

2.2.4.7.1 Flexure

In subsequent discussions, the resistance factor for flexure ϕ_f is to be taken as 1.0, as specified in *AASHTO LRFD* Article 6.5.4.2.

As specified in *AASHTO LRFD* Article 6.11.6.2.1, if there are holes in the tension flange of a flexural member at the section under consideration, that flange must satisfy the requirement specified in *AASHTO LRFD* Article 6.10.1.8 (i.e. Equation 2.92 – refer to Section 2.2.3.7.1 of this chapter). Where an access hole is provided in a box flange in tension, the hole should be deducted in determining the *gross area* of the flange for checking this requirement, as specified in *AASHTO LRFD* Article 6.8.1. Thus, yielding is effectively being checked on the net area of the flange at the hole through the use of Equation 2.92. Equation 2.92 was not specifically developed for the case at hand; i.e. large access holes in the flange. At the edges of a round unreinforced hole, the theoretical stress concentration factor is approximately 3.0. Therefore, the material adjacent to either side of the hole will yield first. At bolt holes, which are relatively small in width in relation to the width of the flange, the section will continue to resist load as the yielding spreads across the plate due to strain hardening at those sections. If Equation 2.92 is satisfied, yielding across the gross section will theoretically be achieved prior to fracture on the net section and each fiber of the cross-section can be assumed to be at the yield stress. Access holes are much larger relative to the width of the flange and there has been no research to determine whether sufficient strain hardening exists to permit development of the yield stress across the entire net section. Therefore, it is recommended here that until further research is conducted, the tensile stress f_t on the adjusted gross area of the box flange due to the factored loads at the strength limit state at access holes conservatively be limited to $0.33F_{yt}$ in lieu of using Equation 2.92.

As will be discussed below, at compact sections in positive flexure, the nominal flexural resistance is permitted to exceed the moment at first yield at the strength limit state. However, pending further research, the specification currently requires that Equation 2.92 be checked at sections where there are holes in the tension flange. Hence, holes are effectively prevented at or near points of maximum moment where significant yielding of the web may occur.

The flexural design provisions in the *AASHTO LRFD* Specifications assume zero or low levels of axial force in the member. Section 2.2.3.7.1 of this chapter discusses steps that can be taken to evaluate whether or not an axial force needs to be considered in the design of a flexural member. For cases where the axial force is deemed significant, note specifically that the reader is referred to Reference 154 for a more in-depth discussion regarding the design of composite steel bridge girders subjected to combined axial compression and flexure, such as might occur in a cable-stayed system with a composite box-girder deck system. A combination of flexural and thermal loads can also produce this situation; this is particularly true when there are stiff restraints against thermal movement.

For box flanges, the effect of the St. Venant torsional shear stress f_v in the flange must be considered for sections in bridges outside the special restrictions discussed in Section 2.2.4.1.2 of this chapter (see Section 2.2.4.1.3). For sections in bridges meeting the special restrictions, f_v may be taken equal to zero. In cases where f_v is judged to be insignificant or incidental, or is not to be considered, all terms related to f_v are simply set equal to zero in the appropriate equations given below. The equations then reduce to the equations given in the *AASHTO* Standard Specifications (*157*) for determining the nominal flexural resistance of straight box sections in the absence of St. Venant torsion. Again, the Engineer should consider torque when the supports are skewed.

f_v is determined by dividing the St. Venant torsional shear flow given by *AASHTO LRFD* Equation C6.11.1.1-1 (see Equation 2.6 in DM Volume 1, Chapter 2) by the thickness of the box flange (see for example Equation 2.177qq below). For such cases, the nominal flexural resistance of the box flange is based on the von Mises yield criterion (*85g*), which is used to consider the effect of the St. Venant torsional shear in combination with flexure (see for example Equations 2.177rr and 2.177ss below). Maximum bending moments and torques are typically not produced by concurrent loads. However, the coincident flexure and torsion due to moving loads to produce the critical von Mises stress is too complex to treat in a practical manner; therefore, maximum envelope values may be used to make all design checks. The Specification is currently silent regarding the inclusion of the elastic shear flow in the box flange due to flexure (i.e. $f = VQ/I$). As pointed out in Reference 154, consideration of the flexural shear stress in the flange may be prudent in cases there the thickness of the box flange is equal to or only slightly larger than the thickness of the web. In such cases, the shear flow in the box flange will be essentially the same as the shear flow in the web at the web-flange junctures.

As discussed in *AASHTO LRFD* Article C6.11.1.1, for torques applied to the noncomposite section, the enclosed area A_o used in computing the shear flow is to be computed for the noncomposite box section. If top lateral bracing in a tub section is attached to the webs, A_o is to be reduced to reflect the actual location of the bracing (*AASHTO LRFD* Article 6.7.5.3). Because shear connectors are required along the entire length of box sections as specified in *AASHTO LRFD* Article 6.11.10, the concrete deck is considered effective in resisting torsion along the entire span. Thus, for torques applied to the composite section in regions of positive or negative flexure, A_o is to be computed for the composite section using the depth from the bottom flange to the mid-thickness of the concrete deck. The depth may be conservatively determined by neglecting the thickness of the concrete deck haunch or by using a lower bound estimate of the actual thickness of the haunch, if desired.

The torsion acting on the composite section introduces horizontal shear in the concrete deck that should be considered in the design of the deck transverse reinforcement. *For tub sections, the deck should be assumed to resist all the torsional shear acting on top of the composite box section.* If top flange lateral bracing is present, it may be modified to an equivalent plate for the analysis. For closed-box sections, the torsional shear in the concrete deck can be determined by multiplying the torsional shear acting on top of the composite box section by the ratio of the thickness of the transformed concrete deck to the total thickness of the top flange plus the transformed deck, as suggested in *AASHTO LRFD* Article C6.11.10. Consideration may be given to adjusting the thickness of the deck for the difference in the Poisson's ratio of the concrete ($\mu = 0.2$) and the steel

($\mu = 0.3$). Adequate shear connection must be provided to ensure that the two materials act in concert.

As specified in *AASHTO LRFD* Article 6.11.1.1, in cases where the St. Venant torsional shears must be considered, the St. Venant torsional shear stress f_v in box flanges due to the factored loads at the strength limit state must not exceed the factored torsional shear resistance of the flange F_{vr} given as follows:

$$F_{vr} = 0.75\phi_v \frac{F_{yf}}{\sqrt{3}}$$

Equation 2.177ee

AASHTO LRFD Equation 6.11.1.1-1

where:

ϕ_v =   resistance factor for shear specified in *AASHTO LRFD* Article 6.5.4.2 (= 1.0)

The 1993 AASHTO Guide Specifications for horizontally curved bridges permitted levels of f_v up to the shear yield stress $F_{yf}/\sqrt{3}$, which can result in a significant reduction in the nominal flexural resistance of a box flange. Therefore, a lower limit on f_v is specified in the *AASHTO LRFD* Specifications according to Equation 2.177ee. It is unlikely, however, that such a level of torsional shear stress will actually be experienced in practical box-girder designs.

Note that in the following, to calculate the web load-shedding factor R_b (see Section 2.2.2.5 of this chapter – Equation 2.19) and the hybrid factor R_h (see Section 2.2.2.6 of this chapter – Equation 2.21) for a tub section, where applicable, one-half of the effective box flange width should be used in conjunction with one top flange and a single web (refer to *AASHTO LRFD* Article C6.11.8.2.2). For a closed-box section, one-half of the effective top and bottom box flange width should be used in conjunction with a single web. The effective box flange width is defined in *AASHTO* LRFD Article 6.11.1.1 (see also Section 2.2.4.1.1 of this chapter).

2.2.4.7.1.1 Sections in Positive Flexure

Fundamental issues related specifically to the behavior of composite sections subject to positive flexure were reviewed in a previous section of this chapter under Fundamental Concepts (Section 2.2.3.1.1.4). The majority of that discussion applies equally to I- and box-sections, with some exceptions as described below. The *AASHTO LRFD* design requirements for these sections, as related specifically to the design of these sections in box girders, will be discussed here.

Compact sections are defined as composite sections *in straight girders* without skew subject to positive flexure that satisfy specific steel grade, web slenderness, ductility and other cross-sectional requirements such that the nominal flexural resistance is permitted to exceed the moment at first yield at the strength limit state. Sections in horizontally curved bridges, or sections not meeting one or more of these

requirements, are termed noncompact sections. The design requirements for each
of these types of sections are discussed below.

2.2.4.7.1.1.1 Compact Sections

AASHTO LRFD Article 6.11.6.2.2 defines the specific requirements that must be met
in order for a composite section in positive flexure in a *straight* box-girder bridge to
qualify as compact. These requirements are restated as follows:

- ➢ The specified minimum yield strength of the flanges and web do not exceed
  70.0 ksi;
- ➢ The web must satisfy the requirement of *AASHTO LRFD* Article 6.11.2.1.2
  (i.e. $D/t_w \leq 150$ or no longitudinal web stiffeners, with D measured along the
  web slope for box sections with inclined webs);
- ➢ The section must be part of a bridge that satisfies the requirements of
  AASHTO LRFD Article 6.11.2.3 such that the effects of shear due to St.
  Venant torsion and cross-sectional distortion stresses need not be considered
  (see Section 2.2.4.1.2 of this chapter);
- ➢ Box flanges must be fully effective as specified in *AASHTO LRFD* Article
  6.11.1.1 (see Section 2.2.4.1.1 of this chapter); and
- ➢ The section must satisfy the following web slenderness limit:

$$\frac{2D_{cp}}{t_w} \leq 3.76\sqrt{\frac{E}{F_{yc}}}$$

Equation 2.177ff

AASHTO LRFD Equation 6.11.6.2.2-1

where:

D_{cp} =   depth of the web in compression at the plastic moment determined
as specified in *AASHTO LRFD* Article D6.3.2 (see Section
2.2.2.3.2 of this chapter) (in.). D_{cp} should be measured along the
web slope for box sections with inclined webs.

The reasoning behind the first, second and fifth requirements listed above was
discussed previously (see Section 2.2.3.1.1.4 under Fundamental Concepts). As
indicated by the third and fourth requirements above, if the section is not part of a
bridge that satisfies the restrictions specified in *AASHTO LRFD* Article 6.11.2.3 or if
any box flanges in the section are not fully effective as defined in *AASHTO LRFD*
Article 6.11.1.1, the section must be designed as a noncompact section. The ability
of such sections to develop a nominal flexural resistance greater than the moment at
first yield in the presence of potentially significant St. Venant torsional shear and
cross-sectional distortion stresses has not been demonstrated. The same concern
and conclusion holds true for sections that are part of a horizontally curved bridge
and/or a bridge with skewed supports.

The nominal flexural resistance of compact sections is given in AASHTO LRFD
Article 6.11.7.1. As specified in AASHTO LRFD Article 6.11.7.1.1, at the strength
limit state, these sections must satisfy the following requirement:

$$M_u \leq \phi_f M_n$$
<div align="right">Equation 2.177gg</div>
<div align="right">*AASHTO LRFD* Equation 6.11.7.1.1-1</div>

where:

M_n = nominal flexural resistance of the section determined as specified in *AASHTO LRFD* Article 6.11.7.1.2 (see below) (kip-in.)

M_u = bending moment about the major-axis of the cross-section due to the factored loads at the section under consideration (kip-in.)

Equation 2.177gg is expressed in terms of moment because for these types of sections, the major-axis bending moment is physically a more meaningful quantity than the elastically computed flange bending stress. Also, the nominal flexural resistance of these sections is generally greater than the yield moment with respect to the tension flange M_{yt}. If desired, the equation could be considered in a stress format by dividing both sides of the equation by S_{xt}.

Lateral bending does not need to be considered in the top (compression) flanges of tub sections at the strength limit state because the flanges are continuously supported by the concrete deck. As discussed previously, flange lateral bending is not a consideration for box flanges.

With one exception, *AASHTO LRFD* Article 6.11.7.1.2 refers back to the provisions of *AASHTO LRFD* Article 6.10.7.1.2 for the calculation of the nominal flexural resistance M_n of compact composite sections in positive flexure as follows:

If $D_p \leq 0.1 D_t$, then:

$$M_n = M_p$$
<div align="right">Equation 2.177hh</div>

<div align="right">*AASHTO LRFD* Equation 6.10.7.1.2-1</div>

Otherwise:

$$M_n = M_p \left(1.07 - 0.7 \frac{D_p}{D_t} \right)$$
<div align="right">Equation 2.177ii</div>

<div align="right">*AASHTO LRFD* Equation 6.10.7.1.2-2</div>

where:

D_p = vertical distance from the top of the concrete deck to the neutral axis of the composite section at the plastic moment (in.)

D_t = total vertical depth of the composite section (in.)

M_p = plastic moment of the composite section determined as specified in *AASHTO LRFD* Article D6.2 (see Section 2.2.2.1 of this chapter) (kip-in.)

For sections in continuous spans, the nominal flexural resistance is also given by Equation 2.177hh or 2.177ii, as applicable, but it is not to exceed the following:

$$M_n = 1.3R_hM_y \qquad\qquad \text{Equation 2.177jj}$$

where:
M_y = yield moment determined as specified in *AASHTO LRFD* Article D6.2 (see Section 2.2.2.2 of this chapter) (kip-in.)
R_h = hybrid factor determined as specified in *AASHTO LRFD* Article 6.10.1.10.1 (see Equation 2.21)

The reason for the limitation given by Equation 2.177jj is discussed at some length in Section 2.2.3.1.1.4 under Fundamental Concepts. It should be noted that the factor of 1.3 in the preceding equation was established based on engineering judgment. Also, the preceding equations do not account for any transverse redistribution of load through the bracing members as yielding occurs at positive moment sections. St. Venant torsion and cross-sectional distortion stresses need not be considered for compact sections.

The single exception alluded to above is that *Equation 2.177jj must always be enforced for compact box sections in positive flexure in continuous spans*. For compact I-sections in continuous spans, the nominal flexural resistance need not be subject to the limitation given by Equation 2.177jj when certain specific conditions in the span under consideration and at all adjacent interior-pier sections are met (as spelled out in *AASHTO LRFD* Article 6.10.7.1.2). These conditions are not presently applicable to box sections.

In addition, compact composite sections in positive flexure must satisfy the ductility requirement specified in *AASHTO LRFD* Article 6.10.7.3 as follows:

$$D_p \leq 0.42D_t \qquad\qquad \text{Equation 2.177kk}$$

AASHTO LRFD Equation 6.10.7.3-1

to prevent premature crushing of the concrete deck. This requirement is equivalent to the maximum reinforcement requirement for concrete structures specified in *AASHTO LRFD* Article 5.7.3.3.1. The thickness of the concrete deck haunch over the girder may be conservatively neglected in the calculation of D_t. Otherwise, a lower-bound estimate of this thickness should be used.

2.2.4.7.1.1.2 Noncompact Sections

The nominal flexural resistance of noncompact composite sections in positive flexure is given in *AASHTO LRFD* Article 6.11.7.2. As specified in *AASHTO LRFD* Article 6.11.7.2.1, at the strength limit state, compression flanges of these sections must satisfy the following:

$$f_{bu} \leq \phi_f F_{nc} \qquad\qquad \text{Equation 2.177}\ell\ell$$

AASHTO LRFD Equation 6.11.7.2.1-1

where:

f_{bu} = longitudinal flange stress at the section under consideration calculated without consideration of flange lateral bending or longitudinal warping, as applicable (ksi). f_{bu} is always taken as positive.

F_{nc} = nominal flexural resistance of the compression flange determined as specified in *AASHTO LRFD* Article 6.11.7.2.2 (ksi)

The tension flange must satisfy:

$$f_{bu} \le \phi_f F_{nt}$$ Equation 2.177mm

AASHTO LRFD Equation 6.11.7.2.1-2

where:

F_{nt} = nominal flexural resistance of the tension flange determined as specified in *AASHTO LRFD* Article 6.11.7.2.2 (ksi)

The stress format is more appropriate in members for which the maximum resistance is always less than or equal to the yield moment in major-axis bending. Flange lateral bending is not considered for compression flanges in Equation 2.177$\ell\ell$ because at the strength limit state, the flanges are continuously supported by the concrete deck. Lateral bending is also not a consideration for the tension flange in Equation 2.177mm because the tension flange is always a box flange in this case (and lateral bending is not a consideration for box flanges). As discussed previously, longitudinal warping stresses are typically ignored at the strength limit state, as permitted in *AASHTO LRFD* Article 6.11.1.1. St. Venant torsion and cross-sectional distortion stresses must be considered, however, for noncompact sections.

As specified in *AASHTO LRFD* Article 6.11.7.2.2, the nominal flexural resistance of the compression flanges of noncompact composite tub sections in positive flexure F_{nc} is taken as:

$$F_{nc} = R_b R_h F_{yc}$$ Equation 2.177nn

AASHTO LRFD Equation 6.11.7.2.2-1

where:

R_b = web load-shedding factor determined as specified in *AASHTO LRFD* Article 6.10.1.10.2 (Equation 2.19)

R_h = hybrid factor determined as specified in *AASHTO LRFD* Article 6.10.1.10.1 (Equation 2.21)

Local and lateral-torsional buckling of the tub top flanges is not a concern because the flanges are continuously braced; therefore, the nominal flexural resistance is based on nominal yielding. St. Venant torsional shears are also typically neglected in tub-girder top flanges.

The nominal flexural resistance of the compression flange of noncompact composite closed-box sections in positive flexure F_{nc} is to be taken as:

$$F_{nc} = R_b R_h F_{yc} \Delta \qquad\qquad \text{Equation 2.177oo}$$

AASHTO LRFD Equation 6.11.7.2.2-2

where:

$$\Delta = \sqrt{1 - 3\left(\frac{f_v}{F_{yc}}\right)^2} \qquad\qquad \text{Equation 2.177pp}$$

AASHTO LRFD Equation 6.11.7.2.2-3

f_v =   St. Venant torsional shear stress in the flange due to the factored loads at the section under consideration not to exceed the factored torsional shear resistance of the flange F_{vr} given by Equation 2.177ee (ksi)

$$= \frac{T}{2A_o t_{fc}} \qquad\qquad \text{Equation 2.177qq}$$

AASHTO LRFD Equation 6.11.7.2.2-4

A_o =   enclosed area within the box section (in.^{2})
t_{fc} =   thickness of the compression flange (in.)
T =   internal torque due to the factored loads (kip-in.)

Local buckling of the top box flange is not a concern because the flange is continuously braced at the strength limit state; therefore, the nominal flexural resistance is based on nominal yielding.

The nominal flexural resistance of the tension flange of noncompact composite closed-box and tub sections in positive flexure F_{nt} is based on nominal yielding and is to be taken as:

$$F_{nt} = R_h F_{yt} \Delta \qquad\qquad \text{Equation 2.177rr}$$

AASHTO LRFD Equation 6.11.7.2.2-5

where:

$$\Delta = \sqrt{1 - 3\left(\frac{f_v}{F_{yt}}\right)^2} \qquad\qquad \text{Equation 2.177ss}$$

AASHTO LRFD Equation 6.11.7.2.2-6

f_v =   St. Venant torsional shear stress in the flange due to the factored loads at the section under consideration not to exceed the factored torsional shear resistance of the flange F_{vr} given by Equation 2.177ee (ksi)

$$= \frac{T}{2A_o t_{ft}}$$

Equation 2.177tt

AASHTO LRFD Equation 6.11.7.2.2-7

t_{ft} = thickness of the tension flange (in.)

Load shedding of the web compressive stresses to the tension flange as a result of bend buckling of the web is considered insignificant; therefore, the R_b factor is not included in Equation 2.177rr.

In addition, noncompact composite sections in positive flexure must satisfy the ductility requirement specified in *AASHTO LRFD* Article 6.10.7.3 (Equation 2.177kk) to ensure a ductile failure, and to prevent premature crushing of the deck for sections that may utilize up to 100-ksi steel and/or that are utilized in shored construction. Should shored construction be used, the maximum longitudinal compressive stress in the deck is also limited to $0.6f'_c$ at the strength limit state to ensure linear behavior of the concrete according to *AASHTO LRFD* Article 6.11.7.2.1. As discussed in *AASHTO LRFD* Article C6.10.1.1.1a, the use of shored construction is not recommended (see also Section 2.2.1.2 of this chapter).

Note that the terms F_{nc} and F_{nt} as used throughout the specification identify resistance stresses rather than resistance moments. Moments are applied to different sections in a composite girder and cannot be added at elastic stress levels. Hence, in such cases, the resistance moment does not exist as a single number, but is represented by a stress that is compared to an accumulated stress caused by the total of the factored loads. F_{nc} and F_{nt} represent a measure of the limiting resistance at the strength limit state.

EXAMPLE

Check the composite tub section shown below (note: top lateral bracing not shown), which is in a region of positive flexure in the end span of a straight continuous-span bridge, for the Strength I load combination (see DM Volume 1, Chapter 5 for more information on the Strength I load combination). The girder is homogeneous with the flanges and web having a yield strength of 50 ksi. The 28-day compressive strength f'_c of the concrete deck is 4.5 ksi. The modular ratio n = 8. The load modifier η is assumed to be 1.0. Assume unshored construction.
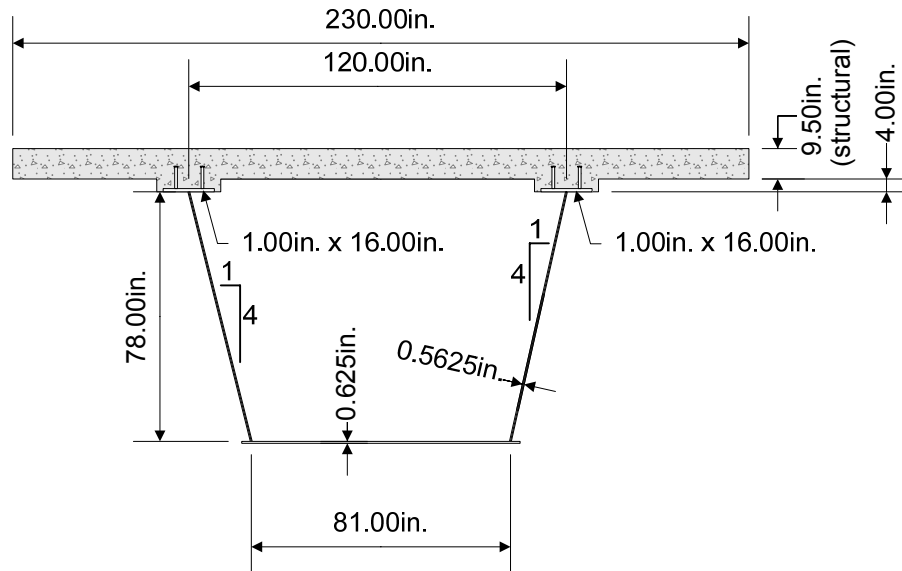
Assume the following unfactored bending moments:

M_{DC1} = +7,365 kip-ft
M_{DC2} = +1,219 kip-ft
M_{DW} =   +995 kip-ft
M_{LL+IM} = +6,748 kip-ft

The applicable elastic section properties for the strength limit state check (neglecting the longitudinal reinforcement) are as follows:

Steel girder:

I   =   185,356 in.^{4}
S_{top} =   4,333 in.^{3}
S_{bot} =   5,030 in.^{3}
N.A. is 36.85 in. from the bottom of the bottom flange

3n composite section:

I   =   339,167 in.^{4}
S_{top} =   13,126 in.^{3}
S_{bot} =   6,306 in.^{3}
N.A. is 53.79 in. from the bottom of the bottom flange

n composite section:

I   =   463,544 in.^{4}
S_{top} =   37,504 in.^{3}
S_{bot} =   6,891 in.^{3}
N.A. is 67.27 in. from the bottom of the bottom flange

The section properties include the longitudinal component of the top-flange lateral bracing area (as recommended in *AASHTO LRFD* Article C6.11.1.1); a single top-flange bracing member with a cross-sectional area A of 8.0 in.^{2} placed at an angle of 30 degrees from tangent to the girder is assumed. The bracing members are assumed bolted to the top flanges. Therefore, the additional cross-sectional area included with the top-flange areas in calculating the section properties is computed from Equation 2.3b as A_d = 8.0cos30° = 6.93 in.^{2} The section properties also include the 1-inch-wide bottom-flange lips (measured from the centerline of the webs) that are provided for web-to-flange welding access. The area of the *inclined* webs is used in computing all section properties. The moment of inertia of *each* inclined web I_{ow} with respect to a horizontal axis at mid-depth of the web is taken from Equation 2.3a as:

$$I_{ow} = I_w \left(\frac{S^2}{S^2 + 1} \right)$$

where:

I_w = moment of inertia of each inclined web with respect to an axis normal to the web (in.^{4})

S = web slope with respect to the horizontal (= 4.0 in this case)

Since the bottom box-flange width does not exceed one-fifth of the distance from the abutment to the point of permanent load contraflexure, the flange is considered fully effective and shear lag effects need not be considered in calculating the section properties for the determination of the flexural stresses (*AASHTO LRFD* Article 6.11.1.1). Therefore, the longitudinal bending stress may be assumed uniform across the full flange width.

Calculate the plastic moment M_p for the composite section. The equations given in *AASHTO LRFD* Table D6.1-1 (Table 2.1) for I-sections will be utilized to calculate M_p for one-half of the composite box section. The longitudinal reinforcement will be conservatively neglected. The longitudinal component of the top-flange lateral bracing area will be included. The web depth D will be taken as the depth measured along the web slope.

$$P_t = F_{yt} b_t t_t = 50(83.0 \, / \, 2)(0.625) = 1{,}297 \text{ kips}$$

$$P_w = F_{yw} D t_w = 50(78.0 \, / \cos 14°)(0.5625) = 2{,}261 \text{ kips}$$

$$P_c = F_{yc} b_c t_c + F_y A_d = 50(16.0)(1.0) + 50(6.93) = 1{,}147 \text{ kips}$$

$$P_s = 0.85 f'_c b_s t_s = 0.85(4.5)(230.0 \, / \, 2)(9.5) = 4{,}179 \text{ kips}$$

Since $P_t + P_w + P_c$ = 4,705 kips > P_s = 4,179 kips, the PNA is in the top flange. Therefore, use Case II in AASHTO LRFD Table D6.1-1 (Table 2.1):

$$\bar{y} = \frac{t_c}{2} \left[\frac{P_w + P_t - P_s}{P_c} + 1 \right]$$

$$\overline{y} = \frac{1.0}{2}\left[\frac{2{,}261 + 1{,}297 - 4{,}179}{1{,}147} + 1\right] = 0.229 \text{ in. from the top of the top flange}$$

Check equilibrium by calculating and comparing the total plastic forces acting on the compression and tension sides of the plastic neutral axis:

Compression side:

$$4{,}179 + 50(16.0)(0.229) + 50(6.93)(0.229/1.0) = 4{,}442 \text{ kips}$$

Tension side:

$$50(16.0)(1.0 - 0.229) + 50(6.93)[(1.0 - 0.229)/1.0] + 2{,}261 + 1{,}297 = 4{,}442 \text{ kips} \quad \text{ok}$$

Calculate the distances from the PNA for the centroid of each element:

$$d_s = \frac{9.5}{2} + 4.0 + 0.229 - 1.0 = 7.98 \text{ in.}$$

$$d_w = 1.0 + \frac{78.0}{2} - 0.229 = 39.77 \text{ in.}$$

$$d_t = 1.0 + 78.0 + \frac{0.625}{2} - 0.229 = 79.08 \text{ in.}$$

$$M_p = \frac{P_c}{2t_c}\left[\overline{y}^2 + (t_c - \overline{y})^2\right] + \left[P_s d_s + P_w d_w + P_t d_t\right]$$

$$M_p = \frac{1{,}147}{2(1.0)}\left[(0.229)^2 + (1.0 - 0.229)^2\right] +$$

$$\left[4{,}179(7.98) + 2{,}261(39.77) + 1{,}297(79.08)\right] = 226{,}206 \text{ kip} - \text{in.}$$

M_p = 18,851 kip-ft for ½ the box = 37,702 kip-ft for the whole box

Calculate the yield moment M_y for the composite section using the equations given in *AASHTO LRFD* Article D6.2.2 (see Section 2.2.2.2 of this chapter). For a composite section in positive flexure, M_{yt}, or the yield moment calculated for the tension flange, typically controls. From Equation 2.5:

$$F_{yf} = \frac{M_{D1}}{S_{nc}} + \frac{M_{D2}}{S_{LT}} + \frac{M_{AD}}{S_{ST}}$$

AASHTO LRFD Equation D6.2.2-1

$$50 = 1.0\left[\frac{1.25(7{,}365)(12)}{5{,}030} + \frac{1.25(1{,}219)(12) + 1.50(995)(12)}{6{,}306} + \frac{M_{AD}}{6{,}891}\right]$$

$$M_{AD} = 153,649 \text{ kip-in.} = 12,804 \text{ kip-ft}$$

From Equation 2.6:

$$M_y = M_{D1} + M_{D2} + M_{AD}$$

AASHTO LRFD Equation D6.2.2-2

$$M_y = 1.0[1.25(7,365) + 1.25(1,219) + 1.50(995) + 12,804] = 25,027 \text{ kip} - \text{ft}$$

Since the section is in a straight bridge, determine if the section qualifies as a compact section. According to *AASHTO LRFD* Article 6.11.6.2.2, composite sections in positive flexure in straight bridges qualify as compact when: 1) the specified minimum yield strengths of the flanges do not exceed 70 ksi (ok); 2) the web satisfies the requirement of *AASHTO LRFD* Article 6.11.2.1.2 such that longitudinal stiffeners are not required; i.e. $D/t_w \leq 150$ ($D/t_w = (78.0/\cos 14°)/0.5625 = 142.9 < 150$ ok); 3) the section is part of a bridge that satisfies the requirements of *AASHTO LRFD* Article 6.11.2.3 (see Section 2.2.4.1.2 of this chapter – it will be assumed for this portion of the example that all these requirements are satisfied); 4) the box flange is fully effective as specified in *AASHTO LRFD* Article 6.11.1.1 (see Section 2.2.4.1.1 of this chapter – ok); and 5) the section satisfies the web-slenderness limit given by Equation 2.177ff (earlier computations indicated that the plastic neutral axis of the composite section is located in the top flange. Therefore, according to AASHTO LRFD Article D6.3.2, D_{cp} is taken equal to zero for this case, and thus, Equation 2.177ff is considered to be automatically satisfied). Therefore, the section qualifies as a compact section.

Compact composite sections in positive flexure must satisfy the ductility requirement given by Equation 2.177kk to protect the concrete deck from premature crushing. At this section:

$$D_p = 9.5 + 4.0 - 1.0 + 0.229 = 12.73 \text{ in.}$$

$$D_t = 0.625 + 78.0 + 4.0 + 9.5 = 92.13 \text{ in.}$$

$$0.42D_t = 0.42(92.13) = 38.69 \text{ in.} > 12.73 \text{ in.} \quad \text{ok}$$

For Strength I:

$$M_u = 1.0[1.25(7,365 + 1,219) + 1.50(995) + 1.75(6,748)] = 24,032 \text{ kip} - \text{ft}$$

As specified in *AASHTO LRFD* Article 6.11.7.1.2, the nominal flexural resistance of compact composite box sections in positive flexure is to be determined according to the provisions of *AASHTO LRFD* Article 6.10.7.1.2. St. Venant torsion and cross-sectional distortion stresses need not be considered for compact sections.

$$0.1D_t = 0.1(92.13) = 9.21 \text{ in.} < D_p = 12.73 \text{ in.}$$

Therefore,

$$M_n = M_p\left(1.07 - 0.7\frac{D_p}{D_t}\right)$$

AASHTO LRFD Equation 6.10.7.1.2-2

$$M_n = 37,702\left[1.07 - 0.7\left(\frac{12.73}{92.13}\right)\right] = 36,695 \text{ kip} - \text{ft}$$

However, in a continuous span, the nominal flexural resistance of the section must be limited to the following according to *AASHTO LRFD* Article 6.11.7.1.2:

$$M_n = 1.3R_hM_y$$

AASHTO LRFD Equation 6.10.7.1.2-3

For a homogeneous girder, the hybrid factor R_h is equal to 1.0. Therefore:

$$M_n = 1.3(1.0)(25,027) = 32,535 \text{ kip} - \text{ft} \quad \text{(governs)}$$

$$\therefore \quad M_n = 32,535 \text{ kip} - \text{ft}$$

The factored flexural resistance is computed as:

$$M_r = \phi_f M_n$$

AASHTO LRFD Equation 6.11.7.1.1-1

$$M_r = 1.0(32,535) = 32,535 \text{ kip} - \text{ft} > M_u = 24,032 \text{ kip} - \text{ft} \quad \text{ok}$$

The section has significant excess flexural resistance at the strength limit state. Other limit-state criteria (e.g. service limit state or fatigue limit state criteria) must of course be checked and constructibility verifications must also be made, as discussed previously. Service or fatigue limit state criteria are likely to control the design of the section in this case. ***Because other limit-state criteria will likely control in this instance, treating these sections conservatively as noncompact sections (as illustrated below) at the strength limit state simplifies the calculations, in general, and should not result in a significant loss of economy in most cases***.

Now, assume that this same section is from a multiple box-section bridge that does *not* satisfy one or more of the special restrictions specified in *AASHTO LRFD* Article 6.11.2.3. Therefore, the section must be treated as a noncompact section, and the effects of St. Venant torsional shear and cross-sectional distortion stresses must be considered at the strength limit state (see Section 2.2.4.1.3 of this chapter).

Assume the following unfactored torques:

T_{DC1} =   +330 kip-ft

T_{DC2} = +65 kip-ft
T_{DW} = +54 kip-ft
T_{LL+IM} = +546 kip-ft

It is assumed that all the deck weight is applied to the girder top flanges in the analysis for this example. Thus, the DC_1 torque does not include the torque due to the weight of deck overhang acting on the boxes. The torque shown results primarily from the application of unequal deck weight loads to the girder top flanges.

Check the flexural resistance of the bottom box flange in tension. First, compute the flexural stress in the bottom flange due to the factored loads (ignoring the effect of longitudinal warping). For the Strength I load combination:

$$f_{bu} = 1.0 \left[\frac{1.25(7,365)}{5,030} + \frac{1.25(1,219)}{6,306} + \frac{1.5(995)}{6,306} + \frac{1.75(6,748)}{6,891} \right] 12 = 48.27 \text{ ksi}$$

Calculate the St. Venant torsional shear stress due to the factored loads f_v in the bottom flange. For the DC_1 torque, which is applied to the noncomposite section, the enclosed area A_o is computed for the noncomposite box section. The vertical depth between the mid-thickness of the flanges is used. It is also assumed that the top lateral bracing is connected to the top flanges so that a reduction in A_o is not required. Therefore:

$$A_o = \frac{(120 + 81)}{2} * (78.0 + 0.3125 + 0.5) * \frac{1 \text{ ft}^2}{144 \text{ in.}^2} = 55.0 \text{ ft}^2$$

$$f_v = \frac{T}{2A_o t_{fc}}$$

AASHTO LRFD Equation 6.11.8.2.2-6

$$f_v = \frac{1.0(1.25)(330)}{2(55.0)(0.625)} * \frac{1}{12 \text{ in.}/\text{ft}} = 0.500 \text{ ksi}$$

For the torques applied to the composite section, calculate A_o for the composite section from the mid-thickness of the bottom flange to the mid-thickness of the concrete deck (considering the deck haunch):

$$A_o = \frac{(120 + 81)}{2} * (78.0 + 0.3125 + 4.0 + \frac{9.5}{2}) * \frac{1 \text{ ft}^2}{144 \text{ in.}^2} = 60.8 \text{ ft}^2$$

$$f_v = \frac{1.0|1.25(65) + 1.5(54) + 1.75(546)|}{2(60.8)(0.625)} * \frac{1}{12 \text{ in.}/\text{ft}} = 1.23 \text{ ksi}$$

$$f_{v \text{ total}} = 0.500 + 1.23 = 1.73 \text{ ksi}$$

Check that $f_{v\ total}$ does not exceed the factored torsional shear resistance of the flange F_{vr}:

$$F_{vr} = 0.75\phi_v \frac{F_{yf}}{\sqrt{3}}$$

AASHTO LRFD Equation 6.11.1.1-1

$$F_{vr} = 0.75(1.0)\frac{50}{\sqrt{3}} = 21.65 \text{ ksi} > f_{v\ total} = 1.73 \text{ ksi} \quad \text{ok}$$

Calculate the nominal flexural tensile resistance of the bottom flange according to the provisions of *AASHTO LRFD* Article 6.11.7.2.2. The nominal flexural resistance F_{nt} of the tension flange of noncompact tub sections in positive flexure is to be taken as:

$$F_{nt} = R_h F_{yt} \Delta$$

AASHTO LRFD Equation 6.11.7.2.2-5

$$\Delta = \sqrt{1 - 3\left(\frac{f_v}{F_{yc}}\right)^2}$$

AASHTO LRFD Equation 6.11.7.2.2-6

$$\Delta = \sqrt{1 - 3\left(\frac{1.73}{50}\right)^2} = 0.998$$

$$F_{nt} = 1.0(50)(0.998) = 49.90 \text{ ksi}$$

The factored flexural resistance F_r is computed as:

$$F_r = \phi_f F_{nt} = 1.0(49.90) = 49.90 \text{ ksi} > f_{bu} = 48.27 \text{ ksi} \quad \text{ok}$$

Check the flexural resistance of the top flanges in compression. First, compute the flexural stress in the top flanges due to the factored loads (ignoring the effect of longitudinal warping). For the Strength I load combination:

$$f_{bu} = 1.0\left[\frac{1.25(7,365)}{4,333} + \frac{1.25(1,219)}{13,126} + \frac{1.5(995)}{13,126} + \frac{1.75(6,748)}{37,504}\right]12 = -32.03 \text{ ksi}$$

St. Venant torsional shears are typically neglected in continuously braced top flanges of tub sections.

Calculate the nominal flexural compressive resistance of the top flanges according to the provisions of *AASHTO LRFD* Article 6.11.7.2.2. The nominal flexural resistance

2.374

F_{nc} of the compression flanges of noncompact tub sections in positive flexure is to be taken as:

$$F_{nc} = R_b R_h F_{yc}$$

AASHTO LRFD Equation 6.11.7.2.2-1

As specified in *AASHTO LRFD* Article 6.10.1.10.2, R_b is to be taken as 1.0 at the strength limit state when the section is composite and is in positive flexure and the web slenderness D/t_w does not exceed 150 (i.e. when there are no longitudinal web stiffeners present). Therefore:

$$F_{nc} = 1.0(1.0)(50) = 50.00 \text{ ksi}$$

The factored flexural resistance F_r is computed as:

$$F_r = \phi_f F_{nc} = 1.0(50.00) = 50.00 \text{ ksi} > |f_{bu}| = 32.03 \text{ ksi} \quad \text{ok}$$

As specified in *AASHTO LRFD* Article 6.11.6.2.2, noncompact sections in positive flexure must also satisfy the ductility requirement given by Equation 2.177kk to ensure a ductile failure of the section. This requirement was previously checked and found to be satisfactory.

Regarding the cross-sectional distortion stresses, the longitudinal warping stresses due to cross-section distortion will be ignored at the strength limit state, as permitted in *AASHTO LRFD* Article 6.11.1.1.   It is assumed that the internal cross-frames are spaced so that the longitudinal warping stresses do not exceed 10 percent of the major-axis bending stresses at the strength limit state, as recommended in *AASHTO LRFD* Article C6.7.4.3 (with the spacing not to exceed 30.0 feet). The transverse bending stresses due to cross-section distortion are limited to 20.0 ksi at the strength limit state according to *AASHTO LRFD* Article 6.11.1.1.   Although not explicitly checked in this example, both the longitudinal warping and transverse bending stresses at the strength limit state can be computed using the BEF analogy, as discussed previously in Section 2.2.4.6.1.1.1 of this chapter. Specifically, Equations 2.177z and 2.177aa may be applied at the strength limit state to compute these stresses. The distortional stresses must be considered at the fatigue limit state in this case (refer to Section 2.2.4.6.1.1.1 of this chapter).

2.2.4.7.1.2 Sections in Negative Flexure

As specified in *AASHTO LRFD* Article 6.11.6.2.3, for closed-box and tub sections subject to negative flexure at the strength limit state, the provisions of *AASHTO LRFD* Article 6.11.8 are to be applied. The provisions of *AASHTO LRFD* Article 6.11.8 limit the nominal flexural resistance to always be less than or equal to the moment at first yield *for all types of box girder bridges.* Therefore, the nominal flexural resistance for these sections is always expressed in terms of the elastically computed flange stress.

Further, according to *AASHTO LRFD* Article 6.11.6.2.3, the optional provisions of *AASHTO LRFD* Appendices A and B to Section 6 are *not* to be applied to box sections. These optional appendices, which are described in more detail in Section 2.2.3.7.1.2 of this chapter, apply only to the design of I-section flexural members. Their applicability to the design of box-section flexural members has not yet been demonstrated.

As specified in *AASHTO LRFD* Article 6.11.8.1.1, for box sections subject to negative flexure, box flanges in compression (i.e. bottom flanges) must satisfy the following requirement at the strength limit state:

$$f_{bu} \leq \phi_f F_{nc}$$
Equation 2.177uu

AASHTO LRFD Equation 6.11.8.1.1-1

where:
f_{bu} = longitudinal flange stress due to the factored loads at the section under consideration calculated without consideration of longitudinal warping (ksi)

F_{nc} = nominal flexural resistance of the box flange in compression determined as specified in *AASHTO LRFD* Article 6.11.8.2 (ksi)

Equation 2.177uu is intended to ensure that box flanges in compression have sufficient local buckling resistance. Flange lateral bending and lateral-torsional buckling are not a consideration for box flanges. As mentioned previously, longitudinal warping stresses are typically ignored at the strength limit state, as permitted in *AASHTO LRFD* Article 6.11.1.1.

In general, bottom box flanges at interior-pier sections are subject to a complex stress state. The flanges are subject to biaxial bending due to major-axis bending of the box section and due to major-axis bending of the internal diaphragm over the bearing sole plate. Bending of the internal diaphragm over the bearing sole plate may be particularly significant for boxes supported on single bearings. The flange is also subject to shear stresses due to the vertical shear in the internal diaphragm, and in cases where it must be considered as discussed previously, the St. Venant torsional shear. Thus, for cases where the bending of the internal diaphragm and/or the flange shear stresses are deemed significant, *AASHTO LRFD* Article C6.11.8.1.1 suggests that the following equation be used to check the combined stress state in the box flange at interior-pier sections at the strength limit state. The equation represents the general form of the Huber-von Mises-Hencky yield criterion for combined stress (*85j*):

$$\sqrt{f_{bu}^2 - f_{bu}f_{by} + f_{by}^2 + 3(f_d + f_v)^2} \leq \phi_f R_b R_h F_{yc}$$
Equation 2.177v-v

AASHTO LRFD Equation C6.11.8.1.1-1

where:

f_{by} = stress in the box flange due to the factored loads caused by the major-axis bending of the internal diaphragm over the bearing sole plate (ksi)

f_d = shear stress in the box flange caused by the internal diaphragm vertical shear due to the factored loads (ksi)

= $\dfrac{VQ}{It_{fc}}$

Equation 2.177xx

AASHTO LRFD Equation C6.11.8.1.1-2

f_v = St. Venant torsional shear stress in the box flange due to the factored loads (ksi)

I = moment of inertia of the effective internal diaphragm section (discussed below) (in.^{4})

Q = first moment of one-half the effective box-flange area about the neutral axis of the effective internal diaphragm section (discussed below) (in.^{3})

R_b = web load-shedding factor determined as specified in *AASHTO LRFD* Article 6.10.1.10.2 (Equation 2.19)

R_h = hybrid factor determined as specified in *AASHTO LRFD* Article 6.10.1.10.1 (Equation 2.21)

V = factored vertical shear in the internal diaphragm due to flexure plus St. Venant torsion (kips)

f_{bu} and f_{by} are to be taken as signed quantities in Equation 2.177v-v. As indicated in *AASHTO LRFD* Article C6.11.8.1.1, for a box supported on two bearings, f_{by} in Equation 2.177v-v is typically relatively small and may be neglected in making this check.   For boxes resting on single bearings, f_{by} should be considered and may be computed using the effective section discussed in the next paragraph.

In calculating f_d from Equation 2.177xx, and also f_{by}, a portion of the box flange may be considered effective with the internal diaphragm. *AASHTO LRFD* Article C6.11.8.1.1 currently suggests that a flange width equal to 18 times its thickness may be considered effective with the internal diaphragm, which is similar to the portion of the web or diaphragm that is considered part of the effective column section for the design of bearing stiffeners (see Section 2.2.6.2.4.1 of this chapter). This assumes that most of the shear lag effects in the flange beyond the concentrated reaction(s) have been attenuated.   It is suggested that a more conservative value of 6 times the thickness be used instead. The assumption of 18 times the thickness that is made when the web is considered part of the column section for the design of bearing stiffeners is for buckling where shear lag effects have been mitigated.

Further, whenever an access hole is provided within the internal diaphragm for inspection purposes, the effect of the hole should be considered in computing the section properties of the effective diaphragm section. The application of Equations 2.177v-v and 2.177xx is demonstrated in the example given below.

As specified in *AASHTO LRFD* Article 6.11.8.1.2, for box sections subject to negative flexure, continuously braced flanges in tension (i.e. top flanges) must satisfy the following requirement at the strength limit state:

$$f_{bu} \leq \phi_f F_{nt}$$ Equation 2.177yy

AASHTO LRFD Equation 6.11.8.1.2-1

where:
   F_{nt} =   nominal flexural resistance of the flange in tension determined as specified in *AASHTO LRFD* Article 6.11.8.3 (ksi)

For continuously braced top flanges of tub sections, lateral flange bending stresses and St. Venant torsional shears need not be considered. The torsional shear must be considered in the continuously braced top flange of a closed-box section however.

2.2.4.7.1.2.1 Flexural Resistance of Box Flanges in Compression

General

In the AASHTO LRFD Specifications, the nominal flexural resistance of box flanges in compression F_{nc} is based on local buckling of the flange under combined uniform axial compression and shear (lateral-torsional buckling is not a consideration for box flanges). In general, the resistance is defined for three distinct regions based on the flange slenderness. For unstiffened flanges, the slenderness is based on the full flange width between webs b_{fc}. For longitudinally stiffened flanges, the slenderness is based on the larger of the width of the flange between longitudinal flange stiffeners or the distance from a web to the nearest longitudinal flange stiffener w. The local buckling resistance of longitudinally stiffened flanges is dependent on the rigidity of the longitudinal stiffener(s).

As for the compression-flange local buckling and lateral-torsional buckling resistance curves for I-section members, the local buckling resistance curves for box flanges are fitted to two anchor points (Figure 2.74).
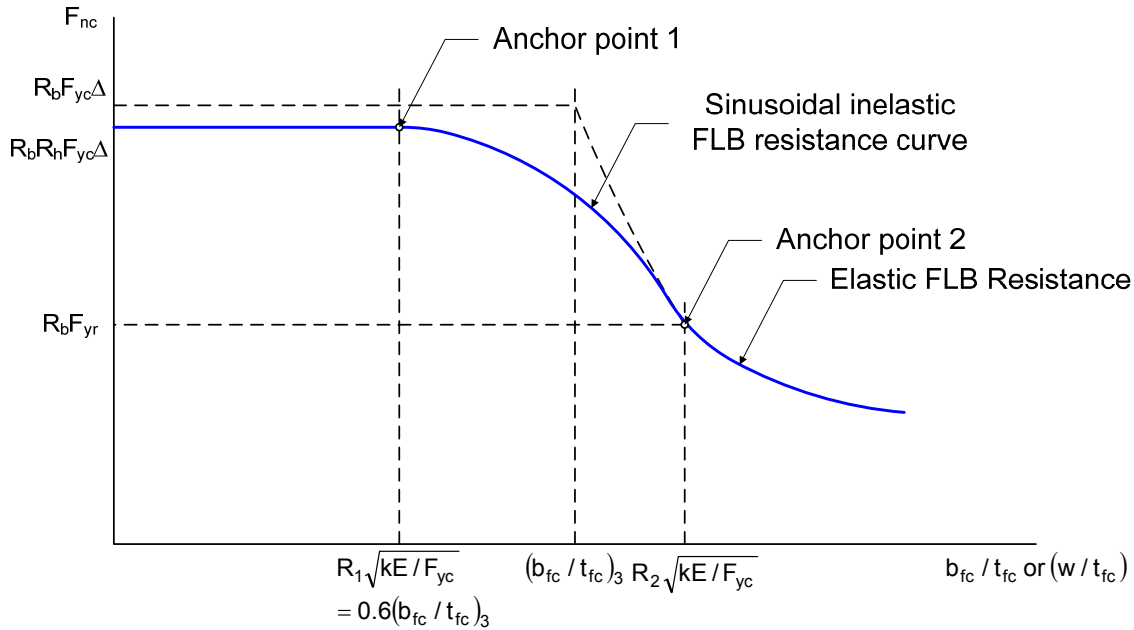
Figure 2.74 Local Buckling Resistance Curves for Box Flanges in Compression

These anchor points are discussed in more detail below. Note that the inelastic local buckling resistance of the box flange is represented by a sinusoidal function rather than by a linear interpolation between the two anchor points, as is the case for I-section members. The equations are based on the tacit assumptions that the flange panel is of infinite length and that the panel is subjected to a uniform stress field over its full width and length. Since the moment gradient in negative moment regions increases rather sharply near interior supports, the true stress usually decreases over the panel length from a maximum at one end of the panel. Further the panel is not of infinite length. So the true strength of actual box flanges in negative flexure is greater than implied. Still it is advisable to use the critical stress in the panel to make the following checks.

At access holes in box flanges subject to compression, it is recommended that the nominal flexural resistance of the remaining flange on each side of the hole be determined according to the provisions of *AASHTO LRFD* Article 6.10.8.2.2, with λ_f taken as the projecting width of the flange on that side of the hole divided by the flange thickness (refer to Section 2.2.3.7.1.2.1 of this chapter). The equations in *AASHTO LRFD* Article 6.10.8.2.2 are the local buckling resistance equations for I-girder compression flanges, with the flange width based on the projecting width of the flange on the side of the hole under consideration.

Unstiffened Flanges

According to AASHTO LRFD Article 6.11.8.2.1, the nominal flexural resistance of box flanges in compression without flange longitudinal stiffeners (i.e. unstiffened

flanges) is to be determined as specified in AASHTO LRFD Article 6.11.8.2.2. AASHTO LRFD Article 6.11.8.2.2 defines the nominal local buckling resistance of the flanges as follows:

If $\lambda_f \le R_1 \sqrt{\dfrac{kE}{F_{yc}}}$, then:

$$F_{nc} = R_b R_h F_{yc} \Delta \qquad\qquad \text{Equation 2.177zz}$$

AASHTO LRFD Equation 6.11.8.2.2-1

If $R_1 \sqrt{\dfrac{kE}{F_{yc}}} < \lambda_f \le R_2 \sqrt{\dfrac{kE}{F_{yc}}}$, then:

$$F_{nc} = R_b R_h F_{yc} \left[\Delta - \left(\Delta - \frac{F_{yr}}{R_h F_{yc}} \right) \left\{ 1 - \sin\left[\frac{\pi}{2} \left(\frac{R_2 - \dfrac{b_{fc}}{t_{fc}} \sqrt{\dfrac{F_{yc}}{kE}}}{R_2 - R_1} \right) \right] \right\} \right] \qquad \text{Equation 2.177A}$$

AASHTO LRFD Equation 6.11.8.2.2-2

If $\lambda_f > R_2 \sqrt{\dfrac{kE}{F_{yc}}}$, then:

$$F_{nc} = \frac{0.9 E R_b k}{\left(\dfrac{b_{fc}}{t_{fc}} \right)^2} - \frac{R_b f_v^2 k}{0.9 E k_s^2} \left(\frac{b_{fc}}{t_{fc}} \right)^2 \qquad \text{Equation 2.177B}$$

AASHTO LRFD Equation 6.11.8.2.2-3

where:
λ_f =   slenderness ratio for the compression flange

        = $\dfrac{b_{fc}}{t_{fc}}$ Equation 2.177C

AASHTO LRFD Equation 6.11.8.2.2-4

Δ = $\sqrt{1 - 3\left(\dfrac{f_v}{F_{yc}} \right)^2}$ Equation 2.177D

AASHTO LRFD Equation 6.11.8.2.2-5

b_{fc} =   compression-flange width between webs (in.)
f_v =   St. Venant torsional shear stress in the flange due to the factored loads at the section under consideration not to exceed the factored

torsional shear resistance of the flange F_{vr} given by Equation 2.177ee (ksi)

$$= \frac{T}{2A_o t_{fc}}$$ Equation 2.177E

AASHTO LRFD Equation 6.11.8.2.2-6

A_o = enclosed area within the box section (in.)

F_{yr} = smaller of the compression-flange yield stress at the onset of nominal yielding, with consideration of residual stress effects, or the specified minimum yield strength of the web (ksi)

$$= (\Delta - 0.4)F_{yc} \le F_{yw}$$ Equation 2.177F

AASHTO LRFD Equation 6.11.8.2.2-7

k = plate-buckling coefficient for uniform normal stress

= 4.0

k_s = plate-buckling coefficient for shear stress

= 5.34

R_1 = constant which when multiplied by $\sqrt{kE/F_{yc}}$ yields the slenderness ratio equal to 0.6 times the slenderness ratio for which F_{nc} from Equation 2.177B is equal to $R_b F_{yc}\Delta$

$$= \frac{0.57}{\sqrt{\frac{1}{2}\left[\Delta + \sqrt{\Delta^2 + 4\left(\frac{f_v}{F_{yc}}\right)^2\left(\frac{k}{k_s}\right)^2}\right]}}$$ Equation 2.177G

AASHTO LRFD Equation 6.11.8.2.2-8

R_2 = constant which when multiplied by $\sqrt{kE/F_{yc}}$ yields the slenderness ratio for which F_{nc} from Equation 2.177B is equal to $R_b F_{yr}$

$$= \frac{1.23}{\sqrt{\frac{1}{1.2}\left[\frac{F_{yr}}{F_{yc}} + \sqrt{\left(\frac{F_{yr}}{F_{yc}}\right)^2 + 4\left(\frac{f_v}{F_{yc}}\right)^2\left(\frac{k}{k_s}\right)^2}\right]}}$$ Equation 2.177H

AASHTO LRFD Equation 6.11.8.2.2-9

R_b = web load-shedding factor determined as specified in *AASHTO LRFD* Article 6.10.1.10.2 (Equation 2.19)

R_h = hybrid factor determined as specified in *AASHTO LRFD* Article 6.10.1.10.1 (Equation 2.21)

t_{fc} = thickness of the compression flange (in.)

T = internal torque due to the factored loads (kip-in.)

Referring to Figure 2.74, Anchor Point 1 is based on the constant R_1 given by Equation 2.177G. The anchor point $R_1\sqrt{kE/F_{yc}}$ is equal to 0.6 times the flange

slenderness $(b_{fc}/t_{fc})_3$ at which the elastic flange local buckling stress given by Equation 2.177B is equal to $R_b F_{yc}\Delta$. For the case of f_v equal to zero and thus Δ equal to 1.0, R_1 is equal to 0.57 and the limiting Anchor Point 1 value of b_{fc}/t_{fc} for F_{yc} = 50 ksi and k = 4.0 is 27.5. Anchor Point 2 is based on the constant R_2 given by Equation 2.177H. The anchor point $R_2\sqrt{kE/F_{yc}}$ is equal the flange slenderness at which the elastic flange local buckling stress given by Equation 2.177B is equal to $R_b F_{yr}$, where F_{yr} is given by Equation 2.177F. For the cases of f_v equal to zero and thus Δ equal to 1.0, R_2 is equal to 1.23 and the limiting Anchor Point 2 value of b_{fc}/t_{fc} for F_{yc} = 50 ksi and k =4.0 is 59.2.

For stocky box flange plates with a flange slenderness less than or equal to $R_1\sqrt{kE/F_{yc}}$, full yielding of the plate can be achieved as defined by the von Mises yield criterion for combined normal and shear stress (*85g*) (refer to Equation 2.177zz). For slender plates with a flange slenderness greater than or equal to $R_2\sqrt{kE/F_{yc}}$, the resistance is governed by elastic buckling. In this region, a non-linear interaction curve is used to relate the theoretical elastic Euler buckling equations for an infinitely long plate under a uniform normal stress and under shear stress resulting in Equation 2.177B (*7, 18, 85k*). The specified plate-buckling coefficient for uniform normal stress k = 4.0 and the specified shear-buckling coefficient k_s = 5.34 both assume simply supported boundary conditions at the edges of the flanges (*7*). For intermediate values of flange slenderness in-between the two limiting anchor points, the resistance is defined by a transition region reflecting the fact that partial yielding due to residual stresses and initial imperfections do not permit the attainment of the elastic buckling stress. As mentioned previously, the resistance was arbitrarily defined in this region as a sine curve (Equation 2.177A) in the original *AASHTO* box-girder design specifications. This assumption has been retained in the *AASHTO LRFD* Specifications. A residual stress level of $0.4F_{yc}$ was assumed in the original derivation of Equation 2.177A (*85k*).

Longitudinally Stiffened Flanges

When an unstiffened box flange becomes too slender, the nominal flexural resistance of the flange in compression will likely decrease to an impractical level. Longitudinal stiffeners can then be added to the flange to increase the nominal flexural resistance.

As specified in *AASHTO LRFD* Article 6.11.8.2.3, the nominal flexural resistance of a longitudinally stiffened box flange in compression F_{nc} is determined using the same basic equations specified for unstiffened box flanges in compression given in *AASHTO LRFD* Article 6.11.8.2.2 (see above), with the following substitutions:

The width w is to be substituted for b_{fc};
The plate-buckling coefficient for uniform normal stress k is to be taken as:

If n = 1, then:

$$k = \left(\frac{8I_s}{wt_{fc}^3} \right)^{\frac{1}{3}}$$ Equation 2.177I

AASHTO LRFD Equation 6.11.8.2.3-1

If n = 2, then:

$$k = \left(\frac{0.894I_s}{wt_{fc}^3} \right)^{\frac{1}{3}}$$ Equation 2.177J

AASHTO LRFD Equation 6.11.8.2.3-2

with $1.0 \le k \le 4.0$

The plate-buckling coefficient for shear stress k_s is to be taken as:

$$k_s = \frac{5.34 + 2.84 \left(\dfrac{I_s}{wt_{fc}^3} \right)^{\frac{1}{3}}}{(n+1)^2} \le 5.34$$ Equation 2.177K

AASHTO LRFD Equation 6.11.8.2.3-3

where:
  I_s = moment of inertia of a single longitudinal flange stiffener about an axis parallel to the flange and taken at the base of the stiffener (in.[4])
  n = number of equally spaced longitudinal flange stiffeners
  w = larger of the width of the flange between the longitudinal flange stiffeners or the distance from a web to the nearest longitudinal flange stiffener (in.)

The longitudinal flange stiffeners must satisfy the provisions of *AASHTO LRFD* Article 6.11.11.2 (the design of the longitudinal flange stiffeners is discussed further in Section 2.2.4.8 of this chapter – see below). Note as mentioned in *AASHTO LRFD* Article C6.11.1.1, the longitudinal flange stiffeners should be included in the box-section properties since they contribute to the flexural stiffness and strength of the section.

The values of *k* and k_s for a longitudinally stiffened flange are typically smaller than the prescribed values for an unstiffened flange due to the finite flexibility of the longitudinal stiffeners. The shear-buckling coefficient for the stiffened plate k_s given by Equation 2.177K is taken from Reference 85k. The plate-buckling coefficient for uniform stress *k* is related to the stiffness of the longitudinal flange stiffeners I_s and the number of stiffeners *n* according to Equations 2.177I and 2.177J. Equations 2.177I and 2.177J are derived directly from *AASHTO LRFD* Equation 6.11.11.2-2 by algebraic manipulation (see Equation 2.177S below). Therefore, Equation 2.177S is automatically satisfied by the value of I_s that is assumed in determining the *k* value from Equation 2.177I or 2.177J, as applicable, for that value of *k*.   In lieu of

assuming a value of I_s to determine k, another option is to assume a value of k and then determine the minimum required value of the longitudinal flange stiffener moment of inertia I_ℓ from Equation 2.177S that will provide the assumed value of k (as a minimum). Note that k can take any value between 1.0 and 4.0 according to *AASHTO LRFD* Article 6.11.8.2.3, but a value of k ranging from 2.0 to 4.0 should generally be assumed.

As discussed in *AASHTO LRFD* Article C6.11.8.2.3, k will be at or near a value of 4.0 if the longitudinal flange stiffeners are very rigid and plate buckling will therefore be forced to occur between the stiffeners. For lower values of k, the stiffeners are less rigid and the nominal flexural resistance of the flange will be reduced. *Therefore, using Equations 2.177I and 2.177J, or alternatively Equation 2.177S, the Engineer should attempt to efficiently balance the required stiffener size against the required flange resistance in order to provide an economical design. Selecting a k value of 4.0 to provide the largest longitudinal stiffener(s), or selecting a longitudinal stiffener(s) to provide the largest permitted k value of 4.0, may not always provide the most economical solution.* Also, as discussed previously, as the number of longitudinal stiffeners n increases beyond one, the required moment of inertia to achieve a desired k value begins to increase dramatically and eventually becomes impractical. Therefore, equations for k are only provided for values of n up to and including two. **For boxes of typical proportions, where longitudinal flange stiffeners are required, it is strongly recommended that the number of longitudinal flange stiffeners not exceed one**. This issue is discussed further in Section 2.2.4.8 of this chapter.

2.2.4.7.1.2.2 Tension-Flange Flexural Resistance

For sections in negative flexure, the nominal flexural resistance of the tension flange(s) is controlled by yielding. According to *AASHTO LRFD* Article 6.11.8.3, the nominal flexural resistance of the tension flanges of tub sections F_{nt} is to be taken as:

$$F_{nt} = R_h F_{yt}$$
<div align="right">Equation 2.177L</div>

<div align="right">*AASHTO LRFD* Equation 6.11.8.3-1</div>

where:

R_h =   hybrid factor determined as specified in *AASHTO LRFD* Article 6.10.1.10.1 (Equation 2.21)

The nominal flexural resistance of the tension flange of closed-box sections F_{nt} is to be taken as:

$$F_{nt} = R_h F_{yt} \Delta$$
<div align="right">Equation 2.177M</div>

<div align="right">*AASHTO LRFD* Equation 6.11.7.2.2-5</div>

where:

$$\Delta \quad = \quad \sqrt{1-3\left(\frac{f_v}{F_{yt}}\right)^2} \qquad \qquad \text{Equation 2.177N}$$

AASHTO LRFD Equation 6.11.7.2.2-6

f_v =   St. Venant torsional shear stress in the flange due to the factored loads at the section under consideration not to exceed the factored torsional shear resistance of the flange F_{vr} given by Equation 2.177ee (ksi)

$$= \quad \frac{T}{2A_o t_{ft}} \qquad \qquad \text{Equation 2.177O}$$

AASHTO LRFD Equation 6.11.7.2.2-7

A_o =   enclosed area within the box section (in.^{2})
t_{ft} =   thickness of the tension flange (in.)
T =   internal torque due to the factored loads (kip-in.)

EXAMPLE

Check the composite tub section shown below (note: longitudinal reinforcement and top lateral bracing not shown), which is at the interior pier of an exterior girder in a straight continuous-span bridge, for the Strength I load combination (see DM Volume 1, Chapter 5 for more information on the Strength I load combination). The girder is homogeneous with the flanges and web having a yield strength of 50 ksi. The load modifier η is assumed to be 1.0. Assume unshored construction and that the tub girder is supported on two bearings at the pier.

It is also assumed that the section is from a multiple box-section bridge that does *not* satisfy one or more of the special restrictions specified in *AASHTO LRFD* Article 6.11.2.3 (refer also to Section 2.2.4.1.2 of this chapter). Therefore, the effects of St. Venant torsional shear and cross-sectional distortion stresses must be considered at the strength limit state (see Section 2.2.4.1.3 of this chapter). Had the bridge met the special restrictions, all terms related to the St. Venant torsional shear stress f_v would simply be set equal to zero in the following resistance equations (assuming the box flange is also fully effective as confirmed below). Cross-sectional distortion stresses would also not need to be considered.
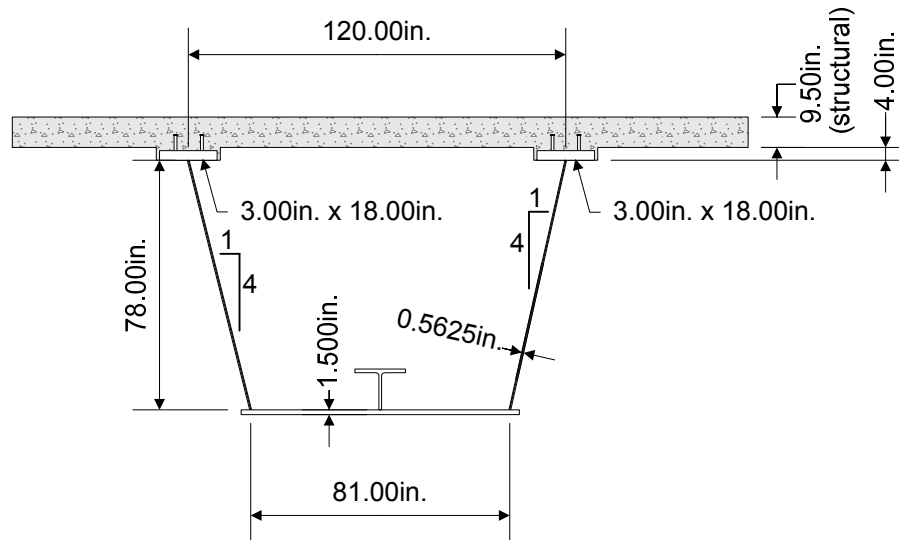
The area of the longitudinal deck reinforcement is 20.0 in.^{2} assumed placed at the neutral axis of the deck. The applicable elastic section properties for the strength limit state check are as follows:

Steel girder:

I	=	438,966 in.^{4}
S_{top}	=	10,047 in.^{3}
S_{bot}	=	11,311 in.^{3}

N.A. is 38.81 in. from the bottom of the bottom flange

Steel girder plus longitudinal reinforcement:

I	=	484,714 in.^{4}
S_{top}	=	11,837 in.^{3}
S_{bot}	=	11,666 in.^{3}

N.A. is 41.55 in. from the bottom of the bottom flange

The section properties include the longitudinal component of the top-flange lateral bracing area (as recommended in *AASHTO LRFD* Article C6.11.1.1); a single top-flange bracing member with a cross-sectional area *A* of 8.0 in.^{2} placed at an angle of 30 degrees from tangent to the girder is assumed. The bracing members are assumed bolted to the top flanges. Therefore, the additional cross-sectional area included with the top-flange areas in calculating the section properties is computed from Equation 2.3b as A_d = 8.0cos30° = 6.93 in.^{2} The section properties also include the single longitudinal flange stiffener (size given in the example at the end of Section 2.2.4.8 of this chapter) and the 1-inch-wide bottom-flange lips (measured from the centerline of the webs) that are provided for web-to-flange welding access. The area of the *inclined* webs is used in computing all section properties. The moment of inertia of *each* inclined web I_{ow} with respect to a horizontal axis at mid-depth of the web is taken from Equation 2.3a as:

$$I_{ow} = I_w \left(\frac{S^2}{S^2 + 1} \right)$$

where:

I_w = moment of inertia of each inclined web with respect to an axis normal to the web (in.^{4})

S = web slope with respect to the horizontal (= 4.0 in this case)

Since the bottom box-flange width does not exceed one-fifth of the distance between the points of permanent load contraflexure on either side of the pier section, the flange is considered fully effective and shear lag effects need not be considered in calculating the section properties for the determination of the flexural stresses (*AASHTO LRFD* Article 6.11.1.1). Therefore, the longitudinal bending stress may be assumed uniform across the full flange width.

Assume the following unfactored bending moments:

M_{DC1} = -17,007 kip-ft
M_{DC2} = -2,712 kip-ft
M_{DW} = -2,220 kip-ft
M_{LL+IM} = -9,444 kip-ft

Assume the following unfactored torques. Since the section is at an interior support, positive and negative torques exist at the section for each load case. Only the maximum and minimum values of the HL-93 live load plus impact torques are given:

T_{DC1} = +26/-3 kip-ft
T_{DC2} = +246/-190 kip-ft
T_{DW} = +201/-156 kip-ft
T_{LL+IM} = +854/-966 kip-ft

It is assumed that all the deck weight is applied to the girder top flanges in the analysis for this example. Thus, the DC_1 torque does not include the torque due to the weight of deck overhang acting on the boxes. The torque shown results primarily from the application of unequal deck weight loads to the girder top flanges.

Check the flexural resistance of the bottom box flange in compression. First, compute the flexural stress in the bottom flange due to the factored loads (ignoring the effect of longitudinal warping). For the Strength I load combination:

$$f_{bu} = 1.0 \left[\frac{1.25(-17,007)}{11,311} + \frac{1.25(-2,712)}{11,666} + \frac{1.5(-2,220)}{11,666} + \frac{1.75(-9,444)}{11,666} \right] 12 = -46.47 \text{ ksi}$$

Calculate the St. Venant torsional shear stress due to the factored loads f_v in the bottom flange. For the DC_1 torque, which is applied to the noncomposite section, the enclosed area A_o is computed for the noncomposite box section. The vertical depth between the mid-thickness of the flanges is used. It is also assumed that the top

lateral bracing is connected to the top flanges so that a reduction in A_o is not required. Therefore:

$$A_o = \frac{(120+81)}{2} * (78.0+1.5+0.75) * \frac{1 \text{ ft}^2}{144 \text{ in.}^2} = 56.0 \text{ ft}^2$$

$$f_v = \frac{T}{2A_o t_{fc}}$$

AASHTO LRFD Equation 6.11.8.2.2-6

$$f_v = \frac{1.0(1.25)(26)}{2(56.0)(1.5)} * \frac{1}{12 \text{ in.} / \text{ft}} = 0.016 \text{ ksi}$$

For the torques applied to the composite section, calculate A_o for the composite section from the mid-thickness of the bottom flange to the mid-thickness of the concrete deck (considering the deck haunch):

$$A_o = \frac{(120+81)}{2} * (78.0+0.75+4.0+\frac{9.5}{2}) * \frac{1 \text{ ft}^2}{144 \text{ in.}^2} = 61.1 \text{ ft}^2$$

The negative torque case controls. Therefore:

$$f_v = \frac{1.0|1.25(-190)+1.5(-156)+1.75(-966)|}{2(61.1)(1.5)} * \frac{1}{12 \text{ in.} / \text{ft}} = 0.983 \text{ ksi}$$

$$f_{v \text{ total}} = 0.016 + 0.983 = 0.999 \text{ ksi}$$

Note that although the critical torques acting on the non-composite and composite box sections act in opposite directions in this case, the shear flows are conservatively added together to since a future wearing surface is included in the negative torque applied to the composite section. Check that $f_{v \text{ total}}$ does not exceed the factored torsional shear resistance of the flange F_{vr}:

$$F_{vr} = 0.75\phi_v \frac{F_{yf}}{\sqrt{3}}$$

AASHTO LRFD Equation 6.11.1.1-1

$$F_{vr} = 0.75(1.0)\frac{50}{\sqrt{3}} = 21.65 \text{ ksi} > f_{v \text{ total}} = 0.999 \text{ ksi} \quad \text{ok}$$

Calculate the nominal flexural compressive resistance F_{nc} of the longitudinally stiffened bottom flange according to the provisions of *AASHTO LRFD* Article 6.11.8.2.3. For a longitudinally stiffened flange, the resistance is to be determined with the spacing w, taken as the larger of the width of the flange between the

longitudinal flange stiffeners or the distance from a web to the nearest longitudinal flange stiffener, substituted for the flange width b_{fc}. Therefore, in this case:

$$w = \frac{(81.0 - 0.5625)}{2} = 40.2 \text{ in.}$$

$$\lambda_f = \frac{w}{t_{fc}} = \frac{40.2}{1.5} = 26.8$$

$$\Delta = \sqrt{1 - 3\left(\frac{f_v}{F_{yc}}\right)^2}$$

AASHTO LRFD Equation 6.11.8.2.2-5

$$\Delta = \sqrt{1 - 3\left(\frac{0.999}{50}\right)^2} \cong 1.0$$

To determine which equation to use, first calculate R_1:

$$R_1 = \frac{0.57}{\sqrt{\frac{1}{2}\left[\Delta + \sqrt{\Delta^2 + 4\left(\frac{f_v}{F_{yc}}\right)^2 \left(\frac{k}{k_s}\right)^2}\right]}}$$

AASHTO LRFD Equation 6.11.8.2.2-8

For longitudinally stiffened flanges, k from Equation 2.177I or 2.177J, as applicable, and k_s from Equation 2.177K are be used in place of $k = 4.0$ and $k_s = 5.34$ (for unstiffened flanges), respectively. Since the longitudinal stiffener size is unknown at this point, instead of assuming a stiffener size, reasonable values of k and k_s will instead be assumed. The size of the longitudinal stiffener required to provide the assumed value of k (as a minimum) will be computed in a later example given at the end of Section 2.2.4.8 of this chapter.   The resulting stiffener size will then be used to compute the actual values of k and k_s in the same example using Equations 2.177I and 2.177K, respectively.   The factored flexural resistance will then be checked using the actual values of k and k_s to determine if there is a significant change in the resistance from what is computed below.

A value of k below the maximum permitted value of 4.0 will result in a smaller nominal flexural resistance, but will also result in a significantly smaller longitudinal flange stiffener than might otherwise be required.   Assume $k = 2.0$. Assume $k_s = 2.5$. Upon substituting these values and the previously computed values of Δ and f_v into the preceding equation, the denominator of the equation is approximately equal to 1.0. Therefore, $R_1 = 0.57$.

$$R_1 \sqrt{\frac{kE}{F_{yc}}} = 0.57\sqrt{\frac{2.0(29,000)}{50}} = 19.4$$

Calculate R_2:

$$R_2 = \frac{1.23}{\sqrt{\frac{1}{1.2}\left[\frac{F_{yr}}{F_{yc}} + \sqrt{\left(\frac{F_{yr}}{F_{yc}}\right)^2 + 4\left(\frac{f_v}{F_{yc}}\right)^2\left(\frac{k}{k_s}\right)^2}\right]}}$$

AASHTO LRFD Equation 6.11.8.2.2-9

$$F_{yr} = (\Delta - 0.4)F_{yc} \leq F_{yw}$$

AASHTO LRFD Equation 6.11.8.2.2-7

$$F_{yr} = (1.0 - 0.4)50 = 30.0 \text{ ksi}$$

Upon substituting F_{yr} and the previously computed values of k, k_s, Δ and f_v into the preceding equation, the denominator of the equation is again approximately equal to 1.0. Therefore, R_2 = 1.23.

$$R_2\sqrt{\frac{kE}{F_{yc}}} = 1.23\sqrt{\frac{2.0(29,000)}{50}} = 41.9$$

Since $19.4 < \lambda_f = 26.8 < 41.9$, then:

$$F_{nc} = R_b R_h F_{yc}\left[\Delta - \left(\Delta - \frac{F_{yr}}{R_h F_{yc}}\right)\left\{1 - \sin\left[\frac{\pi}{2}\left(\frac{R_2 - \frac{w}{t_{fc}}\sqrt{\frac{F_{yc}}{kE}}}{R_2 - R_1}\right)\right]\right\}\right]$$

AASHTO LRFD Equation 6.11.8.2.2-2

For a homogeneous girder, the hybrid factor R_h is equal to 1.0. Calculate the web load-shedding factor R_b. First, determine if R_b is indeed less than 1.0 by checking Equation 2.13 (refer to Section 2.2.2.5 of this chapter). For composite sections in negative flexure, the elastic depth of the web in compression D_c at the strength limit state is to conservatively be computed for the section consisting of the steel girder plus the longitudinal reinforcement (*AASHTO LRFD* Article D6.3.1). Also, for box sections with inclined webs, D_c must be measured along the web slope. Therefore:

$$\frac{2D_c}{t_w} = \frac{2(41.55 - 1.5)/\cos 14°}{0.5625} = \frac{2(41.28)}{0.5625} = 146.8$$

$$\frac{2D_c}{t_w} > \lambda_{rw} = 5.7\sqrt{\frac{E}{F_{yc}}} = 5.7\sqrt{\frac{29,000}{50}} = 137.3$$

AASHTO LRFD Equation 6.10.6.2.3-1

Therefore, the section is a slender-web section subject to web bend-buckling at elastic stress levels at the strength limit state and R_b is less than 1.0. Calculate R_b from Equation 2.19:

$$R_b = 1 - \left(\frac{a_{wc}}{1200 + 300a_{wc}}\right)\left(\frac{2D_c}{t_w} - \lambda_{rw}\right) \le 1.0$$

AASHTO LRFD Equation 6.10.1.10.2-3

where:

$$a_{wc} = \frac{2D_c t_w}{b_{fc} t_{fc}}$$

AASHTO LRFD Equation 6.10.1.10.2-5

As indicated in *AASHTO LRFD* Article C6.11.8.2.2, in calculating R_b for a tub section, one-half of the effective box flange width is to be used in conjunction with one top flange and a single web. Thus:

$$a_{wc} = \frac{2(41.28)(0.5625)}{((81.0 - 0.5625)/2)(1.5)} = 0.770$$

$$R_b = 1 - \left(\frac{0.770}{1200 + 300(0.770)}\right)(146.8 - 137.3) = 0.995$$

Therefore:

$$F_{nc} = (0.995)(1.0)(50)\left[1.0 - \left(1.0 - \frac{30.0}{1.0(50)}\right)\left\{1 - \sin\left[\frac{\pi}{2}\left(\frac{1.23 - \frac{40.2}{1.5}\sqrt{\frac{50}{2.0(29,000)}}}{1.23 - 0.57}\right)\right]\right\}\right] = 47.16 \text{ ksi}$$

The factored flexural resistance F_r is computed as:

$$F_r = \phi_f F_{nc} = 1.0(47.16) = 47.16 \text{ ksi} > \left|f_{bu}\right| = 46.47 \text{ ksi} \quad \text{ok}$$

The bottom flange at the interior pier acting in combination with the internal diaphragm is subject to bending in two directions plus the torsional and diaphragm shear (ignoring any through-thickness bending of the flange plate under its own self weight). *AASHTO LRFD* Article C6.11.8.1.1 suggests the use of Equation 2.177v-v for checking this combined stress state in the box flange at the strength limit state as follows (with f_{bu} and f_{by} taken as signed quantities):

$$\sqrt{f_{bu}^2 - f_{bu}f_{by} + f_{by}^2 + 3(f_d + f_v)^2} \le \phi_f R_b R_h F_{yc}$$

AASHTO LRFD Equation C6.11.8.1.1-1

For a box supported on two bearings, as is the case in this example, the bottom-flange stress f_{by} due to major-axis bending of the diaphragm over the bearing sole plate is typically relatively small and will be neglected. Therefore, f_{by} will be taken equal to zero in the preceding equation for this example (note: for a box supported on a single bearing, the reader is referred to Design Example 3). From previous calculations, the St. Venant torsional shear stress f_v due to the factored loads at the strength limit state was computed to be 0.999 ksi.

The shear stress in the bottom flange due to the internal diaphragm vertical shear f_d may be computed from Equation 2.177xx as follows:

$$f_d = \frac{VQ}{I t_{fc}}$$

AASHTO LRFD Equation C6.11.8.1.1-2

As suggested in the discussion above, a bottom flange width equal to 6 times its thickness (in lieu of the value of 18 times its thickness suggested in *AASHTO LRFD* Article C6.11.8.1.1) will be assumed effective with the internal diaphragm; i.e. 6 * 1.5 in. = 9.0 in. The internal diaphragm is 78 inches deep and 1.0 in. thick with a 36-inch deep access hole centered in the middle of the diaphragm. The diaphragm has a 1" x 12" top flange. Calculate the section properties of the effective section at the bearing stiffener adjacent to the critical web.

Component	A	d	Ad	Ad^2	I_o	I
Top Flange 1" x 12"	12.00	39.50	474.0	18,723	1.00	18,724
Web 1" x 78"	78.00				39,546	39,546
Bot. Flange 1-1/2" x 9"	13.50	39.75	-536.6	21,331	2.53	21,334
	103.50		-62.6			79,604

$$-0.605(62.6) = \quad -37.87$$
$$I_{NA} = \quad \overline{79,566} \text{ in.}^4$$

$$d_s = \frac{-62.6}{103.50} = -0.605 \text{ in.}$$

$$d_{TOP\ OF\ STEEL} = 40.00 + 0.605 = 40.61 \text{ in.} \qquad d_{BOT\ OF\ STEEL} = 40.50 - 0.605 = 39.90 \text{ in.}$$

$$S_{TOP\ OF\ STEEL} = \frac{79,566}{40.61} = 1,959 \text{ in.}^3 \qquad S_{BOT\ OF\ FLANGE} = \frac{79,566}{39.90} = 1,994 \text{ in.}^3$$

The first moment Q of one-half the effective box-flange area about the neutral axis of the effective internal diaphragm section is computed as:

$$Q = \frac{1}{2}(9.0)(1.5)(39.90 - 0.75) = 264.3 \text{ in.}^3$$

The factored vertical shear V in the internal diaphragm due to flexure plus St. Venant torsion on the critical side is given as 1,411 kips (the calculation of the internal diaphragm shear is discussed further in the example given in Section 2.4.4 of this chapter). Thus:

$$f_d = \frac{1{,}411(264.3)}{79{,}566(1.5)} = 3.12 \text{ ksi}$$

Calculate the section properties of the effective section through the center of the access hole. There is significant shear lag around the access hole and plane sections through the hole do not remain plane. Although the material above the hole is effective in bending (and shear), it will be conservatively ignored in the calculation of the section properties of the section composed of the bottom flange and the diaphragm below the hole:

Component	A	d	Ad	Ad^2	I_o	I
Web – below hole	21.00	28.50	-598.5	17,057	771.8	17,829
Bot. Flange 1-1/2" x 9"	13.50	39.75	-536.6	21,331	2.53	21,334
	34.50		-1,135			39,163
				$-32.90(1{,}135) =$		$-37{,}342$
				$I_{NA} =$		1,821 in.⁴

$$d_s = \frac{-1{,}135}{34.50} = -32.90 \text{ in.}$$

$$d_{BOT\,OF\,HOLE} = 22.50 - 7.60 = 14.90 \text{ in.}$$

$$S_{BOT\,OF\,HOLE} = \frac{1{,}821}{14.90} = 122 \text{ in.}^3$$

$$d_{BOT\,OF\,FLANGE} = 40.50 - 32.90 = 7.60 \text{ in.}$$

$$S_{BOT\,OF\,FLANGE} = \frac{1{,}821}{7.60} = 108 \text{ in.}^3$$

The first moment Q of one-half the effective box-flange area about the neutral axis of the effective internal diaphragm section is computed as:

$$Q = \frac{1}{2}(9.0)(1.5)(7.60 - 0.75) = 46.2 \text{ in.}^3$$

The total factored bearing reaction on the critical side under the Strength I load combination is computed as $R_u = 1{,}255$ kips (refer to the example given in Section 2.4.4 of this chapter). Therefore, the total factored vertical diaphragm shear at the section through the access hole is:

$$V = 1{,}411 \text{ kips} - 1{,}255 \text{ kips} = 156 \text{ kips}$$

$$f_d = \frac{156(46.2)}{1{,}821(1.5)} = 2.64 \text{ ksi}$$

The shear stress in the flange at the bearing stiffener is critical.

$$\sqrt{(-46.47)^2 - (-46.47)(0) + (0)^2 + 3(3.12 + 0.999)^2} = 46.78 \text{ ksi}$$

$$\phi_f R_b R_h F_{yc} = 1.0(0.995)(1.0)(50) = 49.75 \text{ ksi} > 46.78 \text{ ksi} \quad \text{ok}$$

Confirm the preceding calculation using the following alternative form of the Huber-von Mises-Hencky yield criterion (85j):

$$\sqrt{\sigma_1^2 - \sigma_1\sigma_2 + \sigma_2^2} \le \phi_f R_b R_h F_{yc}$$

where:

σ_1, σ_2 =   maximum and minimum principal stresses in the bottom flange (ksi)

$$= \left(\frac{f_{bu} + f_{by}}{2}\right) \pm \sqrt{\left(\frac{f_{bu} - f_{by}}{2}\right)^2 + (f_d + f_v)^2}$$

$$\sigma_{1,2} = \left(\frac{-46.47 + 0}{2}\right) \pm \sqrt{\left(\frac{-46.47 - 0}{2}\right)^2 + (3.12 + 0.999)^2} = -46.68, \; 0.21 \text{ ksi}$$

$$\sqrt{(-46.68)^2 - [(-46.68)(0.21)] + (0.21)^2} = 46.78 \text{ ksi} < \phi_f R_b R_h F_{yc} = 49.75 \text{ ksi} \quad \text{ok}$$

Check the flexural resistance of the top flanges of the tub section in tension. First, compute the flexural stress in the top flanges due to the factored loads (ignoring the effect of longitudinal warping). For the Strength I load combination:

$$f_{bu} = 1.0\left[\frac{1.25(-17{,}007)}{10{,}047} + \frac{1.25(-2{,}712)}{11{,}837} + \frac{1.5(-2{,}220)}{11{,}837} + \frac{1.75(-9{,}444)}{11{,}837}\right]12 = 48.96 \text{ ksi}$$

According to *AASHTO LRFD* Article 6.11.8.3, the nominal flexural resistance F_{nt} of the tension flanges of tub sections F_{nt} in regions of negative flexure is to be taken as:

$$F_{nt} = R_h F_{yt}$$

AASHTO LRFD Equation 6.11.8.3-1

$$F_{nt} = 1.0(50) = 50 \text{ ksi}$$

The factored flexural resistance F_r is computed as:

$$F_r = \phi_f F_{nt} = 1.0(50) = 50.00 \text{ ksi} \; > f_{bu} = 48.96 \text{ ksi} \quad \text{ok}$$

Regarding the cross-sectional distortion stresses, refer to the discussion at the end of the example given in Section 2.2.4.7.1.1 of this chapter.

2.2.4.7.2 Shear

Fundamental issues related specifically to shear were reviewed in a previous section of this chapter under Fundamental Concepts (Section 2.2.3.1.3). The majority of that discussion applies equally to I- and box-sections, with some exceptions as described below.

As specified in *AASHTO LRFD* Article 6.11.6.3, shear design provisions for box-section flexural members at the strength limit state are covered in *AASHTO LRFD* Article 6.11.9. For determining the factored shear resistance *of a single web* of a box section, *AASHTO LRFD* Article 6.11.9 essentially refers back to the provisions

of *AASHTO LRFD* Article 6.10.9 for I-sections (again, with a few exceptions as noted below). A flowchart for basic shear design is given in *AASHTO LRFD* Article C6.10.9.1-1. Note that in the discussions below, the resistance factor for shear ϕ_v is to be taken as 1.0, as specified in *AASHTO LRFD* Article 6.5.4.2.

Webs must satisfy the following relationship at the strength limit state:

$$V_u \leq \phi_v V_n \qquad \text{Equation 2.177P}$$

AASHTO LRFD Equation 6.10.9.1-1

where:
  V_n =   nominal shear resistance (kips)
  V_u =   shear in the web at the section under consideration due to the factored loads (kips)

For box sections with inclined webs, the web must be designed for the component of the vertical shear in the plane of the web according to *AASHTO LRFD* Article 6.11.9. That is, each web must be designed for a shear V_{ui} due to the factored loads taken as follows:

$$V_{ui} = \frac{V_u}{\cos \theta} \qquad \text{Equation 2.177Q}$$

AASHTO LRFD Equation 6.11.9-1

where:
  V_u =   vertical shear due to the factored loads on one inclined web (kips)
  θ =   angle of inclination of the web plate to the vertical (degrees)

Box-section webs are usually detailed to be of equal height. However, if the deck is superelevated, the box is typically rotated to match the deck slope, which simplifies fabrication by maintaining symmetry of the box sections. However, rotating the box increases the inclination angle of the web over what it would have been if the box were not rotated. In such cases, consideration should be given to adjusting the vertical shear in that web accordingly.

Also, according to *AASHTO LRFD* Article 6.11.9, for all box sections discussed in Section 2.2.4.1.3 of this chapter, V_u is to be taken as the sum of the flexural and St. Venant torsional shears. In these cases (for which the St. Venant torsional shears must be considered), the total shear in one web is greater than in the other web at the same cross-section since the torsional shear is of opposite sign in the two webs. For practical reasons, however, both webs may be designed for the critical shear. Shears in the web due to warping torsion and due to cross-section distortion may be ignored in all cases, as indicated in *AASHTO LRFD* Article C6.11.9.

The nominal shear resistance V_n depends on if the web is considered stiffened or unstiffened. As specified in *AASHTO LRFD* Article 6.10.9.1, interior web panels of nonhybrid and hybrid members: 1) without a longitudinal stiffener and with a

transverse stiffener spacing not exceeding 3*D*, or 2) with one or more longitudinal stiffeners and with a transverse stiffener spacing not exceeding 1.5*D* are considered stiffened. Otherwise, the panel is considered unstiffened. The spacing of transverse stiffeners for end panels of stiffened webs, with or without a longitudinal stiffener must not exceed 1.5*D*. The design of web stiffeners for box sections is covered in *AASHTO LRFD* Article 6.11.11.1 and discussed in Section 2.2.6 of this chapter.

2.2.4.7.2.1 Unstiffened Webs

The nominal shear resistance of nonhybrid and hybrid unstiffened webs is specified in *AASHTO LRFD* Article 6.10.9.2. The nominal shear resistance is limited to the shear buckling (or shear yielding) resistance V_{cr}, which was derived in Section 2.2.3.1.3 of this chapter and is given by Equation 2.151. Consideration of post-buckling shear resistance due to tension-field action is not permitted for unstiffened webs.

The shear buckling coefficient k is to be taken as 5.0 in calculating the appropriate value of the constant C for an unstiffened web (from Equation 2.152, 2.153 or 2.154, as applicable). When C is equal to 1.0, the nominal flexural resistance is controlled by shear yielding. In calculating the constant *C* and the plastic shear force V_p for use in Equation 2.151 for the case of inclined webs, *D* is to be taken as the depth of the web plate measured along the slope or $D/\cos\theta$ (AASHTO LRFD Article 6.11.9).

In determining whether or not transverse stiffeners are required at a particular section, the Engineer will first have to determine the nominal shear resistance of the web, assuming it is unstiffened, to determine if it is less than the shear in the web due to the factored loads at that section. If so, transverse stiffeners are required. The reader is referred to the example at the end of Section 2.2.3.7.2 of this chapter for an illustration of this calculation (for a box section with inclined webs, the adjustments discussed above would need to be made to this example). *Note that cross-frame/diaphragm connection plates can be considered to act as transverse stiffeners*.

2.2.4.7.2.2 Stiffened Webs

The nominal shear resistance of nonhybrid and hybrid stiffened webs is specified in *AASHTO LRFD* Article 6.10.9.3. Requirements for interior web panels are given in *AASHTO LRFD* Article 6.10.9.3.2 and requirements for end panels are given in *AASHTO LRFD* Article 6.10.9.3.3.   The maximum shear in the panel due to the factored loads is to be used to determine the required stiffener spacing, which cannot exceed the maximum values stated previously.   For web panels with longitudinal stiffeners, the total web depth *D* is to be used in determining the nominal shear resistance of the panel (i.e. the influence of the longitudinal stiffener is conservatively neglected). Again, in calculating the nominal shear resistance V_n of a box section for the case of inclined webs, *D* is to be taken as the depth of the web plate measured along the slope or $D/\cos\theta$ (AASHTO LRFD Article 6.11.9) in all equations.

2.2.4.7.2.2.1 Interior Panels

Stiffened interior web panels of both nonhybrid and hybrid sections are capable of developing post-buckling shear resistance due to tension-field action. As discussed previously in Section 2.2.3.1.3 of this chapter, in order to develop the full post-buckling resistance, the section along the entire panel must be proportioned to satisfy the relationship given by Equation 2.155. As specified in *AASHTO LRFD* Article 6.11.9, for box flanges, b_{fc} or b_{ft} in Equation 2.155, as applicable, is to be taken as one-half the effective flange width between webs, but not to exceed $18t_f$ where t_f is the thickness of the box flange. The effective flange width is determined as specified in *AASHTO LRFD* Article 6.11.1.1 (see Section 2.2.4.1.1 of this chapter).

If the web-to-flange area ratio given by Equation 2.155 is satisfied everywhere within the panel, the nominal shear resistance may be taken as the full post-buckling shear resistance given by Equation 2.156. If Equation 2.155 is not satisfied, the total area of the flanges is small relative to the area of the web within the panel such that it is assumed that the full post-buckling resistance cannot be developed. In such cases, V_n is to be based on the available post-buckling resistance given by Equation 2.158 in lieu of limiting V_n to V_{cr}. The calculation of the constant C for use in Equation 2.156 or 2.158, as applicable, is to be based on the shear buckling coefficient k given by Equation 2.157, which is a function of the transverse stiffener spacing d_o.

2.2.4.7.2.2.2 End Panels

End panels of stiffened webs, or the panels immediately adjacent to the abutments, are not permitted to develop any post-buckling shear resistance.   The shear resistance of these panels is instead limited to V_{cr} (Equation 2.151) in order to provide a sufficient anchor for the development of the tension field in the immediately adjacent interior panels.   The shear buckling coefficient k used to compute the constant C in this case is to be calculated based on the spacing from the support to the first transverse stiffener adjacent to the support.

The reader is again referred to the example at the end of Section 2.2.3.7.2 of this chapter for an illustration of the calculation of the required transverse stiffener spacing for both interior and end panels (note that for a box section with inclined webs, the adjustments discussed above would need to be made to this example).

85j.   Ugural, A.C., and S.K. Fenster. 1978. *Advanced Strength and Applied Elasticity*. Elsevier-North Holland Publishing Co., Inc., New York, NY.
85k.   Culver, C.G. 1972. "Design Recommendations for Curved Highway Bridges." *Final Report for PennDOT Research Project 68-32*, Civil Engineering Department, Carnegie-Mellon University, Pittsburgh, PA, June.

2.2.4.8 Flange Stiffener Design

The design of longitudinal compression-flange stiffeners for box sections is covered in *AASHTO LRFD* Article 6.11.11.2.   Longitudinal compression-flange stiffeners on

box sections are to be equally spaced across the flange width. Since the stiffeners are primary load carrying members, the specified minimum yield strength of the stiffeners must not be less than the specified minimum yield strength of the box flange to which they are attached. Also, as discussed previously, the stiffeners should be included in the section properties of the closed-box or tub section where they are used.

Structural tees are preferred for use as longitudinal flange stiffeners because tees increase the lateral torsional buckling resistance of the stiffeners, and also provide a high ratio of out-of-plane stiffness to stiffener cross-sectional area. As mentioned previously, structural tees are not available in grades of steel exceeding 50 ksi. In cases where higher strength tee sections are required (e.g. tees on Grade HPS 70W steel flanges), the tees must be fabricated from plates or bars cut from plate.

As indicated in *AASHTO LRFD* Article C6.11.11.2, longitudinal flange stiffeners should be continuous through internal diaphragms (cut-outs can be provided in the diaphragm to accommodate the stiffeners). Consideration should be given to attaching the longitudinal flange stiffeners to the internal diaphragms; tees can conveniently attached to the diaphragms with a pair of clip angles, as illustrated in Figure 2.75:
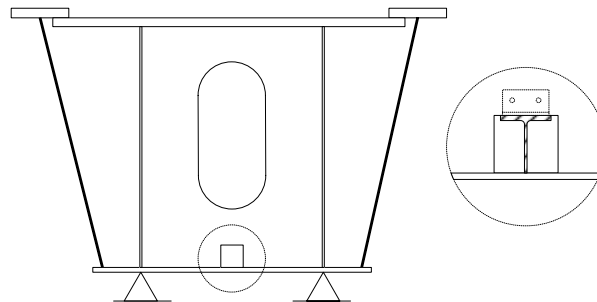
Figure 2.75 Longitudinal Flange Stiffener Detail at Internal Diaphragm

Longitudinal flange stiffeners are best discontinued at field splice locations at the free edge of the flange where the flange stress is zero, particularly when the span balance is such that the box flange on the other side of the field splice does not require stiffening. In such cases, the compressive resistance of the unstiffened box flange on the other side of the splice must always be checked (see Section 2.2.4.7.1.2.1 of this chapter under Unstiffened Flanges) to determine if the flange is satisfactory without a stiffener or is a slight increase in the flange thickness will suffice without providing a stiffener. Figure 2.132 illustrates a suggested box-flange bolted splice detail to accommodate a termination of the stiffener at the free edge of the flange.   When the stiffener is terminated as such, fatigue of the base metal at the stiffener-to-flange weld termination need not be checked in regions subject to a net applied tensile stress (as defined in *AASHTO LRFD* Article 6.6.1.2.1) because the flange stress is zero at the termination. Should it become necessary to terminate the stiffener beyond the field splice in a region subject to a net applied tensile stress (or should the stiffener be terminated *before* the field splice in such a region), the termination becomes more difficult and the base metal at the termination of the

stiffener-to-flange weld must be checked for fatigue according to the stiffener terminus detail (usually a low Category E or E′ detail unless an appropriate transition radius is provided at the termination – refer to *AASHTO LRFD* Table 6.6.1.2.3-1). Possible options to consider regarding termination of the stiffener in such cases are discussed in Section 2.3.4.2.2.2.4 of this chapter.

2.2.4.8.1 Projecting Width

As specified in *AASHTO LRFD* Article 6.11.11.2, the projecting width b_ℓ of a longitudinal flange stiffener element must satisfy the following requirement:

$$b_\ell \leq 0.48 t_s \sqrt{\frac{E}{F_{yc}}} \qquad \text{Equation 2.177R}$$

AASHTO LRFD Equation 6.11.11.2-1

where:
t_s = thickness of the projecting longitudinal stiffener element (in.)

For structural tees, b_ℓ is to be taken as one-half the width of the flange. Equation 2.177R is intended to prevent local buckling of the projecting elements of the longitudinal stiffener.

2.2.4.8.2 Moment of Inertia

As specified in *AASHTO LRFD* Article 6.11.11.2, the moment of inertia I_ℓ of *each* longitudinal flange stiffener about an axis parallel to the flange and *taken at the base of the stiffener* must satisfy the following:

$$I_\ell \geq \psi w t_{fc}^3 \qquad \text{Equation 2.177S}$$

AASHTO LRFD Equation 6.11.11.2-2

where:
ψ = $0.125k^3$ for *n* = 1
     = $1.120k^3$ for *n* = 2
k =   plate-buckling coefficient for uniform normal stress ($1.0 \leq k \leq 4.0$)
n =   number of equally spaced longitudinal flange stiffeners
w =   larger of the width of the flange between longitudinal flange stiffeners or the distance from a web to the nearest longitudinal flange stiffener (in.)

Equation 2.177S is a simplified approximate expression that yields values of the elastic critical stress for a longitudinally stiffened box flange close to those obtained using the exact but more complex equations of elastic stability (*7*). The simplified expression assumes that the box flange and the stiffeners are infinitely long and ignores the effect of any transverse bracing or stiffening. As a result, when *n*

exceeds one, the required moment of inertia from Equation 2.177S begins to increase dramatically. When *n* exceeds 2, for which the value of ψ for application in Equation 2.177S is equal to $0.07k^3n^4$, the required moment of inertia becomes nearly impractical. For the rare situation where an exceptionally wide box flange is required and *n* may need to exceed 2, *AASHTO LRFD* Article C6.11.11.2 suggests that transverse flange stiffeners be considered to reduce to size of the longitudinal stiffeners to a more practical value. The design of a box flange with longitudinal and transverse flange stiffeners is discussed in more detail in Section 2.2.4.8.3 below.

Equation 2.177S provides the minimum *required* moment of inertia I_ℓ. As discussed previously, when an *actual* assumed longitudinal flange stiffener moment of inertia I_s is used in determining the plate-buckling coefficient *k* from Equation 2.177I or 2.177J, as applicable, Equation 2.177S is automatically satisfied for that value of *k* since Equations 2.177I and 2.177J are simply algebraic manipulations of Equation 2.177S. As an alternative to using Equations 2.177I or 2.177J, however, the Engineer can assume a value of *k* ranging from 1.0 to 4.0 (although a *k* value ranging from 2.0 to 4.0 typically should be assumed), as demonstrated in the preceding example, and then determine the minimum required moment of inertia for each longitudinal stiffener to provide that assumed value of k (as a minimum) from Equation 2.177S, as demonstrated in the example below.

2.2.4.8.3 Transversely and Longitudinally Stiffened Box Flanges

As mentioned in the preceding section, in rare cases where an exceptionally wide box flange is needed and the number of longitudinal flange stiffeners *n* may need to exceed 2, the use of transverse flange stiffeners should be considered to reduce the required size of the longitudinal flange stiffeners to a more practical value. The required size of the longitudinal stiffeners is based on an infinite length of panel. This assumption becomes significantly conservative when more than two longitudinal stiffeners are used. Also, for cases where *n* is equal to 2 and a plate-buckling coefficient *k* greater than about 2.5 is required, the use of transverse flange stiffeners can help to reduce the required size of the longitudinal flange stiffeners over that given by Equation 2.177S. The use of transverse stiffeners reduces the length of the panel from infinity to the spacing of the transverse stiffeners. Equations for the design of transversely and longitudinally stiffened box flanges at the strength limit state are provided in *AASHTO LRFD* Article C6.11.11.2 and are reviewed below. These equations are based on classical plate-buckling equations (*7*) and have been carried over from the AASHTO Standard Specifications (*157*).

As indicated in *AASHTO LRFD* Article C6.11.11.2, for the exceptional case where transverse flange stiffeners are deemed necessary, the plate-buckling coefficient *k* for uniform normal stress to be used in determining the nominal compressive resistance of the flange (from Equation 2.177zz, 2.177A or 2.177B, as applicable) at the strength limit state may be taken as follows:

$$k = \frac{\left[1 + (a/b_{fc})^2\right]^2 + 87.3}{(n+1)^2(a/b_{fc})^2\left[1 + 0.1(n+1)\right]} \le 4.0 \qquad \text{Equation 2.177T}$$

AASHTO LRFD Equation C6.11.11.2-3

where:

a   =   longitudinal spacing of the transverse flange stiffeners (in.) $\leq 3b_{fc}$

Further, in determining the required moment of inertia of the longitudinal flange stiffeners I_ℓ from Equation 2.177S when transverse stiffeners are present, the constant ψ is to be taken as 8.0. The number of longitudinal flange stiffeners n preferably should not exceed 5 when transverse flange stiffeners are provided. When n does not exceed 5, transverse flange stiffeners spaced at a distance not exceeding $4w$ (see the preceding section for the definition of w) will provide a k of approximately 4.0 according to Equation 2.177T.

When the k value from Equation 2.177T is used to determine the nominal flexural resistance of the flange, the moment of inertia I_t of each transverse flange stiffener *about an axis through its centroid* and parallel to its bottom edge must satisfy the following:

$$I_t \geq 0.1(n+1)^3 w^3 \frac{f_s}{E} \frac{A_f}{a} \qquad \text{Equation 2.177U}$$

AASHTO LRFD Equation C6.11.11.2-4

where:

A_f =   area of the box flange including the longitudinal flange stiffeners (in.^{2})

f_s =   largest of the longitudinal flange stresses due to the factored loads in the panels on either side of the transverse flange stiffener under consideration (ksi)

In addition, the specified minimum yield strength of the transverse flange stiffeners should not be less than the specified minimum yield strength of the box flange according to *AASHTO LRFD* Article C6.11.11.2.

Transverse flange stiffeners can take one of two forms; either individual tees can serve as transverse flange stiffeners, or a bottom strut provided within the internal cross-bracing of the box satisfying the requirements of *AASHTO LRFD* Article 6.7.4.3 can serve as a transverse flange stiffener if the strut also satisfies the stiffness requirement given by Equation 2.177U. Regardless of which form is used, the transverse flange stiffeners should be attached to the longitudinal flange stiffeners by bolting, with the connection to each longitudinal flange stiffener designed to resist the following vertical force F_s at the strength limit state:

$$F_s = \frac{\phi_f F_{ys} S_s}{nb_{fc}} \qquad \text{Equation 2.177V}$$

AASHTO LRFD Equation C6.11.11.2-1

where:

ϕ_f =   resistance factor for flexure determined as specified in *AASHTO LRFD* Article 6.5.4.2 (= 1.0)

F_{ys} =   specified minimum yield strength of the transverse flange stiffener (ksi)

S_s =   section modulus of the transverse flange stiffener (ksi)

Individual tees serving as transverse flange stiffeners should also be attached to the webs of the box section. As indicated in *AASHTO LRFD* Article C6.11.11.2, the connection of the transverse flange stiffeners to each web should be designed to resist the following vertical force F_w at the strength limit state:

$$F_w = \frac{\phi_f F_{ys} S_s}{2b_{fc}}$$

Equation 2.177W

AASHTO LRFD Equation C6.11.11.2-2

Should a bottom strut be provided within the internal cross-bracing of the box to control distortion of the box flange and reduce the transverse bending stress ranges in the flange for fatigue, as discussed previously in Section 2.2.4.6.1.1.1 of this chapter, the bottom strut and its connections need *not* satisfy the requirements of Equations 2.177U, 2.177V and 2.177W, *unless* the strut is also intended to serve as a transverse flange stiffener at the strength limit state and the *k* value from Equation 2.177T is utilized in the design of the box flange.

EXAMPLE

Design the longitudinal flange stiffener for the box section shown in the preceding example (refer to the end of Section 2.2.4.7.1.2 of this chapter), which is at the interior pier of an exterior girder in a straight continuous-span bridge.

In the preceding example, a value of the plate-buckling coefficient *k* for uniform normal stress was assumed in order to design the box flange (i.e. *k* = 2.0 was assumed). Determine the minimum required moment of inertia I_ℓ of the longitudinal flange stiffener from Equation 2.177S necessary to provide this assumed value of *k* as follows:

$$I_\ell = \psi w t_{fc}^3$$

AASHTO LRFD Equation 6.11.11.2-2

For a single longitudinal flange stiffener (i.e. *n* = 1):

$$\psi = 0.125k^3 = 0.125(2.0)^3 = 1.0$$

Therefore:

$$I_\ell = 1.0(40.5)(1.5)^3 = 136.7 \text{ in.}^4$$

Try a WT8 x 28.5 rolled structural tee for the longitudinal stiffener. From the AISC Manual shape property tables:

b_f = 7.12 in.
t_s = 0.715 in.
I_x = 48.7 in.^{4}
A = 8.38 in.^{2}
N.A. is 6.275 in. from the tip of the tee stem

Check the projecting width of the tee flange according to Equation 2.177R:

$$b_\ell \leq 0.48t_s \sqrt{\frac{E}{F_{yc}}}$$

<div align="right">Equation 2.177R</div>

<div align="right">*AASHTO LRFD* Equation 6.11.11.2-1</div>

$$0.48(0.715)\sqrt{\frac{29{,}000}{50}} = 8.27 \text{ in.} > b_\ell = \frac{b_f}{2} = \frac{7.12}{2} = 3.56 \text{ in.} \quad \text{ok}$$

Calculate the actual moment of inertia I_s of the longitudinal flange stiffener *about the base of the stiffener*:

$$I_s = 48.7 + 8.38(6.275)^2 = 378.7 \text{ in.}^4 > I_\ell = 136.7 \text{ in.}^4 \quad \text{ok}$$

Note that substituting the calculated value of I_s into Equation 2.177I as follows gives:

$$k = \left(\frac{8I_s}{wt_{fc}^3} \right)^{\frac{1}{3}}$$

<div align="right">*AASHTO LRFD* Equation 6.11.8.2.3-1</div>

$$k = \left(\frac{8(378.7)}{40.5(1.5)^3} \right)^{\frac{1}{3}} = 2.8 \quad (1.0 \leq k \leq 4.0 \quad \text{ok})$$

versus the assumed value of *k* = 2.0.

In the preceding example, a value of the plate shear-buckling coefficient for shear stress k_s was also assumed in order to design the box flange (i.e. k_s = 2.5 was assumed). Using Equation 2.177K and the calculated value of I_s, determine the actual value of k_s as follows:

$$k_s = \frac{5.34 + 2.84\left(\dfrac{I_s}{wt_{fc}^3} \right)^{\frac{1}{3}}}{(n+1)^2} \leq 5.34$$

AASHTO LRFD Equation 6.11.8.2.3-3

$$k_s = \frac{5.34 + 2.84\left(\dfrac{378.7}{40.5(1.5)^3}\right)^{\frac{1}{3}}}{(1+1)^2} = 2.33 < 5.34 \quad \text{ok}$$

versus the assumed value of k_s = 2.5.

Repeating the calculations from the preceding example for k = 2.8 and k_s = 2.33 (calculations not shown) results in a final factored flexural resistance F_r for the box flange of 49.19 ksi (versus F_r = 47.02 ksi calculated previously for k = 2.0 and k_s = 2.5), which is still satisfactory. Use a single WT8 x 28.5 longitudinal flange stiffener.

2.2.5 Shear Connector Design

2.2.5.1 General

As discussed previously, in composite construction, the composite action between the deck and steel girders is ensured by the use of welded mechanical shear connectors between the girder and the deck (Figure 2.1). The primary function of the shear connectors is to transfer the horizontal shear between the deck and the girder forcing the steel girder and concrete deck to act together as a structural unit by preventing slip along the concrete-steel interface. Shear connectors also help control deck cracking in regions of negative flexure in regions where the deck is subject to tensile stress and also has longitudinal reinforcement present. In the *AASHTO LRFD* Specifications, the design of shear connectors is covered in *AASHTO LRFD* Article 6.10.10.

The shear connectors must be capable of resisting both horizontal and vertical movement between the concrete deck and the steel, and allow compaction of the concrete around them so that their entire surfaces are in contact with the concrete. Typically, stud shear connectors are used, but channel shear connectors are also permitted and may be designed according to the provisions of *AASHTO LRFD* Article 6.10.10. As specified in *AASHTO LRFD* Article 6.10.10.1.1, the ratio of the height to the diameter of a stud shear connector must be greater than or equal to 4.0 (Figure 2.76). The stud height includes the head, but the stud diameter is measured at the shaft rather than the head. Channel shear connectors must have fillet welds no smaller than 0.1875 in. placed along the heel and toe of the channel.

$$\frac{\text{Height}}{\text{Diameter}} \geq 4.0$$
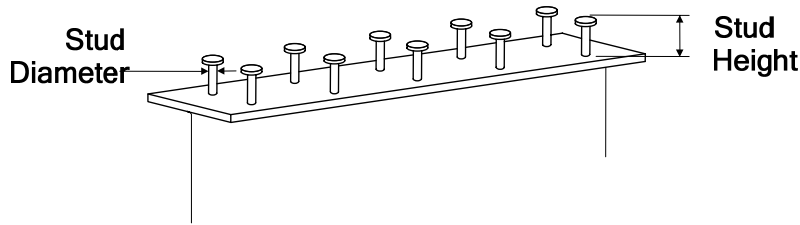
Figure 2.76 Layout of Shear Connectors

Transverse Spacing ≥ 4.0 x (Stud Diameter)

Clear Distance ≥ 1.0 Inch
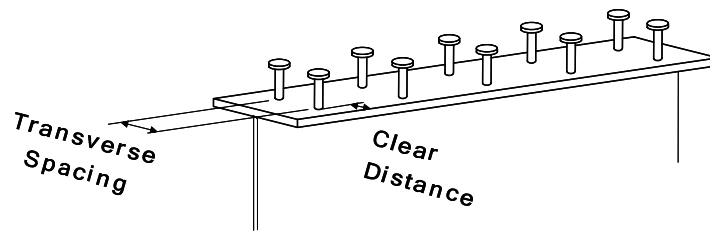
Figure 2.77 Layout of Shear Connectors

As specified in AASHTO LRFD Article 6.10.10.1.3, stud shear connectors are to be spaced no closer than 4.0 stud diameters center-to-center transversely across the top flange(s) of I-sections and tub-girder sections (Figure 2.77). As also illustrated in Figure 2.77, the clear distance between the edge of the top flange and the edge of the nearest shear connector is not to be less than 1.0 in. For closed-box sections, shear connectors should be uniformly distributed across the width of the top (box) flange to ensure composite action of the entire flange with the concrete. As specified in *AASHTO LRFD* Article 6.11.10, the maximum transverse spacing s_t between shear connectors on composite box flanges of closed-box sections must satisfy the following requirement to help prevent local buckling of the flange plate between connectors when subject to compression:

$$\frac{s_t}{t_f}\sqrt{\frac{F_{yf}}{kE}} \leq R_1 \qquad \text{Equation 2.178}$$

AASHTO LRFD Equation 6.11.10-1

where:
  k   =   plate-buckling coefficient for uniform normal stress on box flanges determined as specified in *AASHTO LRFD* Article 6.11.8.2

   R_1 =   limiting slenderness ratio for the box flange determined from
            AASHTO LRFD Equation 6.11.8.2.2-8

As specified in *AASHTO LRFD* Article 6.10.10.1.4, the clear depth of concrete cover over the tops of shear connectors must not be less than 2.0 in., and the shear connectors should penetrate at least 2.0 in. into the concrete deck (Figure 2.78). Otherwise, the deck haunch should be appropriately reinforced to contain the studs and develop their load in the deck.

Cover ≥ 2.0 Inches

Penetration ≥ 2.0 Inches
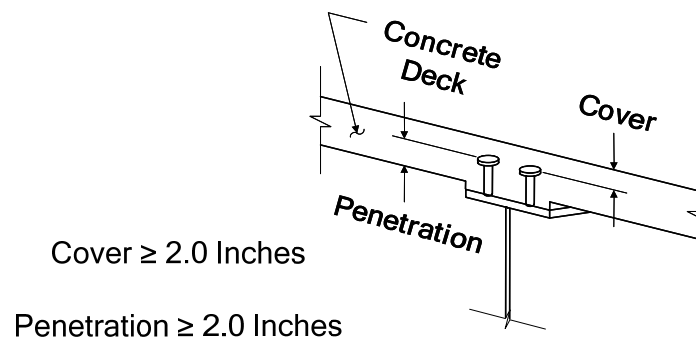
Figure 2.78 Height Requirements

Shear connectors may be spaced at regular or variable intervals longitudinally along the girder. The longitudinal center-to-center spacing of shear connectors is referred to as the pitch. As specified in *AASHTO LRFD* Article 6.10.10.1.2, the pitch must not exceed 24.0 in. and must not be less than six stud diameters (Figure 2.79). As described in more detail below, the pitch of the shear connectors is typically determined first to satisfy the fatigue limit state, as specified in *AASHTO LRFD* Article 6.10.10.2 and 6.10.10.3 (as applicable). The resulting number of shear connectors is then checked to ensure that it is not less than the number required to satisfy the strength limit state, as specified in *AASHTO LRFD* Article 6.10.10.4.

Pitch ≤ 24 Inches

Pitch ≥ 6 x (Stud Diameter)
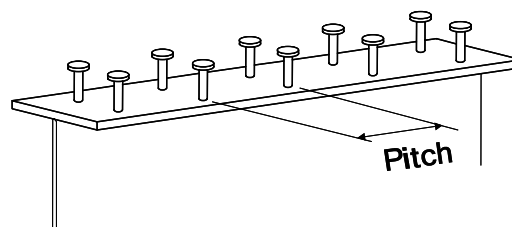
Figure 2.79 Pitch

As specified in *AASHTO LRFD* Article 6.10.10.1, simple span composite bridges are to have shear connectors provided throughout the length of the span. Straight

continuous composite I-girder bridges are to normally be provided with shear connectors throughout the length of the bridge, again to help control cracking in regions of negative flexure, but it is not required. However, if the longitudinal reinforcement in the deck in regions of negative flexure is considered in determining the composite I-section properties in these regions, then shear connectors must also be provided in these regions. Should shear connectors not be provided in these regions, the longitudinal reinforcement cannot be considered in the computation of the composite I-section properties. In addition, if shear connectors are omitted in regions of negative flexure in straight I-girder bridges, additional connectors must be placed in the region of the points of permanent load contraflexure according to the provisions of *AASHTO LRFD* Article 6.10.10.3, and the longitudinal deck reinforcement must be extended into the positive flexure region beyond the additional connectors a distance not less than the development length specified in Section 5 of the *AASHTO LRFD* Specifications (*AASHTO LRFD* Article 6.10.1.7). Because of the torsional shear that exists along the entire span of horizontally curved continuous bridges and all types of composite box-girder bridges, shear connectors are required throughout the entire length of each girder in these structures (*AASHTO LRFD* Articles 6.10.10.1 and 6.11.10).

2.2.5.2 Fatigue

At the fatigue limit state, the required pitch of the shear connectors is based on the horizontal fatigue live load shear range between the deck and top flange of the girder (see the section of this chapter on Fatigue Limit State Verifications for further discussion on the fatigue live load). In straight girders, if torsion is ignored, the shear range is due only to major-axis bending. However, in certain cases, skew can introduce significant torsion. Curvature and other conditions can also introduce torsion. In certain types of box sections, St. Venant torsional shears are significant and must be considered in the design of the shear connectors. The shear connector design provisions in the *AASHTO LRFD* Specifications allow for flexural and torsional components of the shear to be considered in these cases and to be added vectorially, as discussed in more detail below.

2.2.5.2.1 Pitch

According to *AASHTO LRFD* Article 6.10.10.1.2, the pitch *p* of the shear connectors at the fatigue limit state must satisfy the following:

$$p \leq \frac{nZ_r}{V_{sr}}$$

Equation 2.179

AASHTO LRFD Equation 6.10.10.1.2-1

where:

n   =   number of shear connectors in a cross-section
V_{sr} =   horizontal fatigue shear range per unit length determined as shown below (kips/in.)

Z_r =   shear fatigue resistance of an individual shear connector determined as specified in *AASHTO LRFD* Article 6.10.10.2 (discussed later) (kips)

The horizontal fatigue shear range per unit length V_{sr} is determined as follows:

$$V_{sr} = \sqrt{(V_{fat})^2 + (F_{fat})^2}$$

Equation 2.180
AASHTO LRFD Equation 6.10.10.1.2-2

where:
    V_{fat} =   longitudinal fatigue shear range per unit length determined as shown below (kips/in.)
    F_{fat} =   radial fatigue shear range per unit length determined as shown below (kips/in.)

That is, the horizontal shear range is taken as the vectorial sum of the longitudinal and radial fatigue shear ranges.

The longitudinal fatigue shear range per unit length V_{fat} is determined as follows:

$$V_{fat} = \frac{V_f Q}{I}$$

Equation 2.181
AASHTO LRFD Equation 6.10.10.1.2-3

where:
    I =   moment of inertia of the short-term composite section (in.^{4})
    Q =   first moment of the transformed short-term area of the concrete deck about the neutral axis of the short-term composite section (in.^{3})
    V_f =   vertical shear force under the Fatigue load combination specified in Table 3.4.1-1, with the fatigue live load taken as specified in Article 3.6.1.4 (kips)

As discussed in a previous section of this chapter on Fatigue Limit State Verifications, the fatigue live load is specified to be a single HS20 truck, weighing 72 kips, with a constant rear-axle spacing of 30 feet (*AASHTO LRFD* Article 3.6.1.4.1). Then, a load factor of 0.75 is to be applied to the fatigue live load, as specified for the Fatigue load combination in *AASHTO LRFD* Table 3.4.1-1, which results in a factored fatigue design live load weighing 54 kips. A dynamic load allowance (impact factor) of 1.15 is to be applied to the factored load (*AASHTO LRFD* Article 3.6.2). V_f in Equation 2.181 is to be taken equal to the vertical shear force due to the *factored* fatigue design live load, including the appropriate dynamic load allowance.

As specified in *AASHTO LRFD* Article 6.11.10, for all single box sections, horizontally curved box sections, and multiple box sections in bridges not satisfying the limitations of *AASHTO LRFD* Article 6.11.2.3, or with box flanges that are not fully effective according to the provisions of *AASHTO LRFD* Article 6.11.1.1, shear connectors are to be designed for the sum of the flexural and St. Venant torsional

shears. In such cases, for which the St. Venant torsional shears are considered to be more significant, V_f is to be computed by summing the maximum flexural and torsional shears in the web subject to additive shears. The maximum flexural and torsional shears are used, although they are typically not produced by concurrent loads, because the interaction between flexure and torsion due to moving live loads is too complex to treat in a practical manner. The shear range and resulting pitch should be computed using one-half the moment of inertia I of the box. The top flange over the web opposite to the web subject to additive flexural and torsional shears, or the other half of the flange for a closed-box section, should contain an equal number of shear connectors.

The parameters Q and I in Equation 2.181 should be determined assuming that the concrete deck within the effective flange width is fully effective, *including in regions of negative flexure*. In fact, this *must* be done to develop the shear force in the concrete deck if the deck is considered to be effective in tension for negative flexure when computing the range of longitudinal stress for checking fatigue, as permitted in *AASHTO LRFD* Article 6.6.1.2.1 (see the previous section of this chapter on Fatigue Limit State Verifications). V_{fat} is produced by placing the factored fatigue live load immediately to the left and right of the point under consideration. With the load in these positions, positive moments are produced over significant portions of the girder length. As a result, it is reasonable to assume that the concrete deck within the effective width is fully effective along the entire span in determining the stiffness used in the analysis to determine the shear range. In addition, the horizontal shear force in the deck is typically assumed to be effective along the entire span in the analysis. In order to satisfy this assumption, the shear force in the deck should be developed along the entire span. However, as mentioned in *AASHTO LRFD* Article C6.10.10.1.2, in negative flexure regions *of straight girders only*, Q and I are permitted to be determined using only the longitudinal reinforcement within the effective flange width in line with previous Specifications, unless the concrete is considered effective in tension in determining stress ranges for checking fatigue as permitted in *AASHTO LRFD* Article 6.6.1.2.1. When only the longitudinal reinforcement is considered, it must be ensured that the pitch of the shear connectors in these regions does not exceed the permitted maximum pitch of 24.0 in.

The radial fatigue shear range per unit length F_{fat} is to be taken as the *larger* of either of the following:

$$F_{fat1} = \frac{A_{bot}\sigma_{flg}\ell}{wR}$$ Equation 2.182

AASHTO LRFD Equation 6.10.10.1.2-4

or:

$$F_{fat2} = \frac{F_{rc}}{w}$$ Equation 2.183

AASHTO LRFD Equation 6.10.10.1.2-5

where:

σ_{flg}	=	range of longitudinal fatigue stress in the bottom flange without consideration of flange lateral bending (ksi)
A_{bot}	=	area of the bottom flange (in.^{2})
F_{rc}	=	net-range of cross-frame/diaphragm force at the top flange (kips)
ℓ	=	distance between brace points (ft)
R	=	minimum girder radius within the panel (ft)
w	=	effective length of concrete deck (in.) taken as 48.0 in., except at end supports where *w* may be taken as 24.0 in.

As mentioned previously, the radial fatigue shear range is provided to allow the radial component of the shear due to torsional effects (e.g. resulting from curvature and/or support skew) to be considered in the design of the shear connectors. Equations 2.182 and 2.183 ensure that a load path is provided through the shear connectors to satisfy equilibrium at a transverse section through the girders, deck and cross-frame/diaphragm in such cases. *F_{fat}* is typically determined by positioning the live load to produce the largest positive and negative major-axis bending moments in the span. Hence, vectorial addition of the longitudinal and radial components of the shear range in Equation 2.180 is conservative because longitudinal and radial shears are not produced by concurrent loads.

Equation 2.182 is for computing the radial shear range due to the effects of any horizontal curvature between brace points. In this case, the shear range is taken as the radial component of the maximum longitudinal range of force in the bottom flange between brace points, which is used as a measure of the major-axis bending moment. As specified in *AASHTO LRFD* Article 6.10.10.1.2, *the radial shear range from Equation 2.182 may be taken equal to zero for straight spans or segments*. Also, for box sections in horizontally curved spans or segments, *F_{fat1}* may be ignored, as permitted in *AASHTO LRFD* Article 6.11.10, because of the inherent conservatism in the shear connector design requirements for box sections.

The radial shear range from Equation 2.183 will typically control in cases where discontinuous cross-frame/diaphragm lines are used in conjunction with skew angles exceeding 20° in either a straight or horizontally curved bridge. *For all other cases, AASHTO LRFD Article 6.10.10.1.2 permits the radial shear range from Equation 2.183 to be taken equal to zero*. Equations 2.182 and 2.183 will yield approximately the same value if the span or segment is curved and there are no other sources of torsion in the region under consideration. *F_{rc}* in Equation 2.183 represents the resultant range of horizontal force due to the factored fatigue load (plus impact) from all cross-frames/diaphragms at the point under consideration that is resisted by the shear connectors. As indicated in *AASHTO LRFD* Article C6.10.10.1.2, *F_{rc}* may be taken equal to 25.0 kips for an exterior girder, which is typically the critical girder, in lieu of determining the value from a refined analysis. Also, the factor of 0.75 recommended for application to the computed stress range in cross-frame/diaphragm members in *AASHTO LRFD* Article C6.6.1.2.1 is not to be applied in computing *F_{rc}*.

In both Equations 2.182 and 2.183, the radial shear range is distributed over an assumed length of flange *w* equal to 48.0 in., which is considered representative of

the effective length of the deck assumed acting with the flange in the transverse direction. At end supports, the value of *w* is halved.

For composite box flanges in closed-box sections, V_{sr} is to be determined as the vector sum of the longitudinal fatigue shear range given by Equation 2.181 and the torsional fatigue shear range in the concrete deck, in lieu of using Equation 2.180 (*AASHTO LRFD* Article 6.11.10). According to *AASHTO LRFD* Article C6.11.10, the torsional shear range resisted by the concrete deck can be determined by multiplying the torsional shear range acting on the top of the box section by the ratio of the thickness of the transformed concrete deck to the total thickness of the top flange plus the transformed concrete deck.

2.2.5.2.2 Fatigue Resistance

The fatigue resistance of an individual stud shear connector Z_r to be used in Equation 179 for determining the shear connector pitch is to be taken as follows (*86*) (*AASHTO LRFD* Article 6.10.10.2):

$$Z_r = \alpha d^2 \geq \frac{5.5d^2}{2}$$ Equation 2.184

AASHTO LRFD Equation 6.10.10.2-1

where:
  α = constant = $34.5 - 4.28 \log N$
  d = diameter of the stud (in.)
  N = number of stress cycles specified in *AASHTO LRFD* Article 6.6.1.2.5 (refer to Equation 2.88)

The term αd^2 in Equation 2.184 represents the nominal fatigue resistance of the stud shear connector in the finite-life region. The term $5.5d^2$ represents the constant-amplitude fatigue threshold resistance in the infinite-life region, with the factor of ½ applied to allow the effective stress range (i.e. the factored fatigue design live load plus impact) to be used to check the fatigue resistance in both regions (see the previous section of this chapter on Fatigue Limit State Verifications). An equation for the fatigue resistance of channel shear connectors is currently not provided in the specifications.

The nominal fatigue resistance of the base metal adjacent to stud shear connector welds is calculated based on fatigue detail Category C (*AASHTO LRFD* Table 6.6.1.2.3-1). The nominal fatigue resistance of top flanges with welded studs attached and subject to a net applied tensile stress should be checked according to the load-induced fatigue provisions of *AASHTO LRFD* Article 6.6.1.2 for this detail category (see the example given in the previous section of this chapter on Fatigue Limit State Verifications).

2.2.5.2.3 Special Requirements at Points of Permanent Load Contraflexure

In straight continuous composite I-girder bridges, *AASHTO LRFD* Article 6.10.10.1 permits the elimination of shear connectors in the negative moment regions between permanent-load contraflexure points. Where shear connectors are eliminated, the member must be considered noncomposite. Thus, since there are no shear connectors within the regions between points of permanent-load contraflexure in this case, the member must be considered noncomposite when subjected to positive or negative flexure within these regions. *AASHTO LRFD* Article 6.10.10.3 requires that for this case, additional shear connectors be provided in the region of points of permanent load contraflexure. According to *AASHTO LRFD* Article 6.10.10.3, the number of additional connectors n_{ac} that must be provided is to be taken as:

$$n_{ac} = \frac{A_s f_{sr}}{Z_r}$$

<div align="right">Equation 2.185</div>

<div align="right">*AASHTO LRFD* Equation 6.10.10.3-1</div>

where:
A_s =   total area of longitudinal reinforcement over the interior support within the effective concrete deck width (in.^{2})

f_{sr} =   stress range in the longitudinal reinforcement over the interior support under the Fatigue load combination specified in *AASHTO LRFD* Table 3.4.1-1 with the fatigue live load taken as specified in *AASHTO LRFD* Article 3.6.1.4 (ksi)

Z_r =   fatigue shear resistance of an individual shear connector determined as specified in *AASHTO LRFD* Article 6.10.10.2 (kips)

This requirement is apparently intended to use the clump of shear connectors to develop the fatigue force in the longitudinal reinforcement due to the negative factored fatigue live load moment over the interior support, and is not related to girder shear in the normal sense. The additional connectors are to be placed within a distance equal to one-third of the effective concrete deck width on each side of the point of permanent load contraflexure (i.e. preferably centered about the point within the specified distance), with field splices placed so as not to interfere with the connectors.

Strength-of-materials principles demand that the shear force between the reinforcing steel and the steel girder be sufficient to develop the force in the reinforcing bars. The reinforcing bars must extend far enough past the clump of shear connectors that the force in the bars may be developed. Strength-of-materials also demands sufficient additional connectors be provided to transfer the force in the concrete deck, at both the fatigue and strength limit states, back into the steel girder in the regions of points of permanent load contraflexure since there are no shear connectors beyond those points. The current provision appears to violate those principles.

Discontinuing the shear connectors in these regions effectively causes the deck slab to act as a partial-length cover plate, which has two potential problematic effects.

First, the slab is likely to crack near the point at which it is no longer acting compositely with the steel girder. Second, the shear connectors at the discontinuity may be overloaded much as the welds at the termination of a partial length cover plate, particularly if sufficient shear connectors are not provided to transfer the appropriate deck forces back into the girder. If the reinforcing steel is in tension, the deck is also in tension. If the deck is in compression, the reinforcing steel is also in compression at the same cross-section. This conundrum can be avoided by simply continuing the shear connectors through the entire span. Most of the permanent load is not affected by the shear connectors and none of it affects the fatigue design of the shear connectors. Hence, the points of permanent load contraflexure should not be related to shear connector design for fatigue. As discussed previously, over most of the region of negative moment due to permanent load, the live load to obtain the maximum shear range produces positive moment, not negative moment. This fact can be demonstrated by examining influence lines for shear and moment on a two-span continuous beam.

EXAMPLE

Determine the required pitch of the stud shear connectors to satisfy the fatigue limit state for the exterior girder of a straight three-span continuous I-girder bridge (140 ft – 175 ft – 140 ft) with no skew. Shear connectors will be provided throughout the entire length of the bridge. Therefore, the longitudinal deck reinforcement may be considered as part of the composite section in regions of negative flexure. The average daily truck traffic in a single lane $(ADTT)_{SL}$ will be assumed equal to 1,600 trucks/day.

First, determine the required stud proportions. The structural thickness of the concrete deck is 9.0 in. The deck haunch thickness from the top of the web to the bottom of the deck is 3.5 in. The minimum top-flange thickness along the girder is 7/8". Terminating the studs at approximately the mid-thickness of the concrete deck will place them well within the limits for cover and penetration specified in *AASHTO LRFD* Article 6.10.10.1.4 and will also clear the reinforcing steel. Therefore,

$$\frac{9.0}{2} + (3.5 - 0.875) = 7.125 \text{ in.}$$

Use 7/8″ x 7″ studs. Check that the ratio of the height to the diameter is not less than 4.0, as required in *AASHTO LRFD* Article 6.10.10.1.1.

$$\frac{h}{d} = \frac{7.0}{0.875} = 8.0 > 4.0 \qquad \text{ok}$$

As specified in *AASHTO LRFD* Article 6.10.10.1.2, the pitch, p, of the shear connectors must satisfy the following:

$$p \leq \frac{nZ_r}{V_{sr}}$$

AASHTO LRFD Equation 6.10.10.1.2-1

V_{sr} is to be computed as follows:

$$V_{sr} = \sqrt{\left(V_{fat}\right)^2 + \left(F_{fat}\right)^2}$$

AASHTO LRFD Equation 6.10.10.1.2-2

Since the bridge in this example is straight and does not have skewed supports, the radial fatigue shear range per unit length F_{fat} will be taken equal to zero, as permitted in *AASHTO LRFD* Article 6.10.10.1.2. Therefore, in this case, V_{sr} is equal to V_{fat}. V_{fat} is computed as:

$$V_{fat} = \frac{V_f Q}{I}$$

AASHTO LRFD Equation 6.10.10.1.2-3

Since the minimum required one-percent longitudinal reinforcement is assumed provided in the deck according to the provisions of *AASHTO LRD* Article 6.10.1.7 and shear connectors will be provided along the entire length of the bridge, the concrete deck will be assumed effective in tension for negative flexure when computing longitudinal stress ranges for separate load-induced fatigue computations. Therefore, the cross-section parameters I and Q must be determined using the short-term area of the concrete deck (within the effective flange width) along the entire girder. A sample calculation of Q for the transformed short-term area of the concrete deck about the neutral axis of the short-term composite section at the interior-pier section is given below. The effective width of the deck over the interior pier is 100.5 in. The modular ratio n is equal to 8. The distance from the neutral axis of the short-term composite section to the mid-thickness of the deck is 22.03 in. Therefore:

$$Q = (9.0 \times 100.5 / 8.0)(22.03) = 2{,}491 \text{ in.}^3$$

Calculated values of Q and I at tenth points along the entire girder are given in the table below (only one-half of the girder is shown since the girder is symmetrical about the longitudinal centerline of the center span).

The fatigue resistance of an individual stud shear connector Z_r is given in *AASHTO LRFD* Article 6.10.10.2 as:

$$Z_r = \alpha d^2 \geq \frac{5.5 d^2}{2}$$

AASHTO LRFD Equation 6.10.10.2-1

$$\alpha = 34.5 - 4.28 \text{ Log N}$$

AASHTO LRFD Equation 6.10.10.2-2

$$N = (365)(75) n (ADTT)_{SL}$$

AASHTO LRFD Equation 6.6.1.2.5-2

For continuous spans with span lengths greater than 40.0 feet, the number of stress cycles per truck passage n is equal to 1.0 at sections away from the pier and 1.5 at sections near the pier (*AASHTO LRFD* Table 6.6.1.2.5-2). Sections 'near the pier'

are defined as sections within a distance of one-tenth the span on each side of the interior support. Therefore,

$$N = (365)(75)1.0(1,600) = 43,800,000 \text{ cycles} \quad \text{(away from the pier)}$$

$$\alpha = 34.5 - 4.28 \, \text{Log}(43,800,000) = 1.79 < \frac{5.5}{2} = 2.75$$

$$N = (365)(75)1.5(1,600) = 65,700,000 \text{ cycles} \quad \text{(near the pier)}$$

$$\alpha = 34.5 - 4.28 \, \text{Log}(65,700,000) = 1.04 < \frac{5.5}{2} = 2.75$$

$$\therefore \quad \text{use } Z_r = \frac{5.5(0.875)^2}{2} = 2.11 \, \text{kips} \quad \text{(at all locations)}$$

The number of shear connectors in a cross-section n will be assumed equal to three (3). Requirements for the transverse spacing of shear connectors across the top flange are given in *AASHTO LRFD* Article 6.10.10.1.3.

The vertical shear force range V_f is determined for the factored fatigue load (factored by the 0.75 load factor specified for the Fatigue load combination), including the specified dynamic load allowance of 15 percent. Calculated values of V_f from the analysis at tenth-point locations along the girder are shown in the table below (again, the girder is symmetrical about the longitudinal centerline of the center span).

Based on *AASHTO LRFD* Equations 6.10.10.1.2-1, 6.10.10.1.2-2 and 6.10.10.1.2-3 (recall that F_{fat} in *AASHTO LRFD* Equation 6.10.10.1.2-2 is taken equal to zero), the table below summarizes the required stud pitch along the girder to satisfy the fatigue limit state. As specified in *AASHTO LRFD* Article 6.10.10.1.2, the pitch must not be less than six stud diameters = 6(0.875) = 5.25 inches or more than 24.0 inches.

Required Stud Shear Connector Pitch – Fatigue Limit State

Length (ft)	V_f (kips)	Q (in^3)	I (in^4)	V_{sr} (kips/in)	p (in/row)
0.0	42.8	1,766	128,081	0.590	10.7
14.0	37.5	1,766	128,081	0.517	12.2
28.0	32.3	1,766	128,081	0.445	14.2
42.0	31.5	1,766	128,081	0.434	14.6
56.0	32.3	2,104	161,518	0.421	15.0
70.0	32.3	2,104	161,518	0.421	15.0
84.0	33.8	2,104	161,518	0.440	14.4
98.0	36.0	2,104	161,518	0.469	13.5
112.0	37.5	1,985	148,862	0.500	12.7
126.0	39.8	2,491	220,760	0.449	14.1
140.0	45.0	2,491	220,760	0.508	12.5
157.5	42.0	1,985	148,862	0.560	11.3
175.0	38.3	1,985	148,862	0.511	12.4
192.5	35.3	2,018	151,530	0.470	13.5
210.0	34.5	2,018	151,530	0.459	13.8
227.5	34.5	2,018	151,530	0.463	13.7

2.2.5.3 Strength

The resulting number of shear connectors determined to satisfy the fatigue limit state must then be checked against the number required to satisfy the strength limit state. According to *AASHTO LRFD* Article 6.10.10.4.1, the factored shear resistance Q_r of a single shear connector at the strength limit state is to be taken as:

$$Q_r = \phi_{sc} Q_n \qquad \text{Equation 2.186}$$

AASHTO LRFD Equation 6.10.10.4.1-1

where:

ϕ_{sc} =   resistance factor for shear connectors determined as specified in *AASHTO LRFD* Article 6.5.4.2 (= 0.85)

Q_n =   nominal shear resistance of a single shear connector determined as specified in *AASHTO LRFD* Article 6.10.10.4.3 (kips)

As specified in *AASHTO LRFD* Article 6.10.10.4.3, the nominal shear resistance Q_n of one stud shear connector embedded in a concrete deck is to be taken as (*87*):

$$Q_n = 0.5 A_{sc} \sqrt{f_c' E_c} \leq A_{sc} F_u \qquad \text{Equation 2.187}$$

AASHTO LRFD Equation 6.10.10.4.3-1

where:

A_{sc} =   cross-sectional area of a stud shear connector (in.^{2})

E_c = modulus of elasticity of the deck concrete determined as specified in Article 5.4.2.4 (ksi)

F_u = specified minimum tensile strength of a stud shear connector determined as specified in *AASHTO LRFD* Article 6.4.4 (ksi)

For one channel shear connector embedded in a concrete deck, the nominal shear resistance Q_n is to be taken as:

$$Q_n = 0.3(t_f + 0.5t_w)L_c\sqrt{f_c'E_c} \qquad \text{Equation 2.188}$$

AASHTO LRFD Equation 6.10.10.4.3-2

where:

t_f = flange thickness of the channel shear connector (in.)
t_w = web thickness of the channel shear connector (in.)
L_c = length of the channel shear connector (in.)

Equation 2.188 was modified from the original equation developed in Reference 88 to extend its use to both lightweight and normal weight concrete.

At the strength limit state, the minimum number of required shear connectors *n* for a given region is computed according to the following equation:

$$n = \frac{P}{Q_r} \qquad \text{Equation 2.189}$$

AASHTO LRFD Equation 6.10.10.4.1-2

where:

P = total nominal shear force determined as specified in *AASHTO LRFD* Article 6.10.10.4.2 (see below) (kips)

Q_r = factored shear resistance of one shear connector determined from Equation 2.186 (kips)

As will be discussed below, the regions are defined off the point of maximum live load plus impact moment, which is used because it applies to the composite section and is easier to locate than a maximum of the sum of all the moments acting on the composite section.

In certain cases, the neutral axis of composite girders will lie within the concrete deck at the strength limit state; e.g., at the plastic moment for composite sections in positive flexure (refer to Cases III through VII only in Table 2.1). The portion of the concrete deck below the neutral axis in tension is assumed ineffective and the compressive force in the deck is assumed resisted by the portion of the deck above the neutral axis. Only this upper portion of the deck in compression creates the load on the shear connectors in this case. Currently, the specification provisions for the design of shear connectors at the strength limit state do not address this issue and there is no known research related to this particular issue as of this writing (2006).

In Reference 87, it is assumed that the shear force is applied to the stud as a uniform load w_1 over the entire height h of the shear connector, with the shear connector assumed to resist the load as a cantilever beam. Assuming the same shear force is now resisted over a reduced height ℓ, the uniform load would have to be increased to $w_2 = w_1(h/\ell)$. The moment at the base of the shear connector in each case, assuming the shear connector to act as a cantilever beam, would then be computed as follows:

$$M_1 = \frac{w_1 h^2}{2}$$ Equation 2.190

$$M_2 = w_2 \ell \left(h - \frac{\ell}{2} \right) = w_1 \frac{h}{\ell} \left(h\ell - \frac{\ell^2}{2} \right)$$ Equation 2.191

Performing the necessary algebraic manipulations and simplifying leads to the following:

$$R = \frac{M_2}{M_1} = \left(2 - \frac{\ell}{h} \right)$$ Equation 2.192

Thus, based on the preceding assumptions, for the case where the shear connector is resisting the shear force over a reduced height ℓ, the factored shear resistance of the stud shear connector Q_r would need to be conservatively reduced by the factor $(1/R)$. This is simply one suggested approach for considering this issue in the design of the shear connectors at the strength limit state in such cases.

2.2.5.3.1 Nominal Shear Force

According to *AASHTO LRFD* Article 6.10.10.4.2, for simple spans and for continuous spans that are noncomposite for negative flexure in the final condition, the total nominal shear force P between the point of maximum positive design live load plus impact moment and each adjacent point of zero moment is to be taken as:

$$P = \sqrt{P_p^2 + F_p^2}$$ Equation 2.193

AASHTO LRFD Equation 6.10.10.4.2-1

where:
   P_p =   total longitudinal force in the concrete deck at the point of
                 maximum positive live load plus impact moment (see below) (kips)
   F_p =   total radial force in the concrete deck at the point of maximum
                 positive live load plus impact moment (see below) (kips)

P_p is taken as the lesser of the following:

$$P_{1p} = 0.85f_c'b_st_s \qquad \text{Equation 2.194}$$

or: *AASHTO LRFD* Equation 6.10.10.4.2-2

$$P_{2p} = F_{yw}Dt_w + F_{yt}b_{ft}t_{ft} + F_{yc}b_{fc}t_{fc} \qquad \text{Equation 2.195}$$

AASHTO LRFD Equation 6.10.10.4.2-3

where:
  b_s = effective width of the concrete deck (in.)
  t_s = thickness of the concrete deck (in.)

F_p is taken as follows:

$$F_p = P_p \frac{L_p}{R} \qquad \text{Equation 2.196}$$

AASHTO LRFD Equation 6.10.10.4.2-4

where:
  L_p = arc length between an end of the girder and an adjacent point of maximum positive live load plus impact moment (ft)
  R = minimum girder radius over the length L_p (ft)

F_p is provided in Equation 2.193 to account for the radial effect of curvature, and is required for curved spans or segments to bring the smallest of the longitudinal forces in either the deck or the girder (from Equation 2.194 or Equation 2.195) into equilibrium. The resulting longitudinal force P_p in Equation 2.196 is assumed to be constant over the length L_p when computing the radial component F_p. Note that for straight spans or segments, F_p may be taken equal to zero.

For continuous spans that are composite for negative flexure in the final condition, the total nominal shear force P between the point of maximum positive design live load plus impact moment and an adjacent end of the member is to be determined from Equation 2.193. The total nominal shear force P between the point of maximum positive design live load plus impact moment and the centerline of an adjacent interior support is to be taken as:

$$P = \sqrt{P_T^2 + F_T^2} \qquad \text{Equation 2.197}$$

AASHTO LRFD Equation 6.10.10.4.2-5

where:
  P_T = total longitudinal force in the concrete deck between the point of maximum positive live load plus impact moment and the centerline of an adjacent interior support (see below) (kips)

F_T =   total radial force in the concrete deck between the point of maximum positive live load plus impact moment and the centerline of an adjacent interior support (see below) (kips)

P_T is taken as follows:

$$P_T = P_p + P_n$$ Equation 2.198

AASHTO LRFD Equation 6.10.10.4.2-6

where:
P_n =   total longitudinal force in the concrete deck over an interior support (see below) (kips)

P_n is taken as the lesser of the following:

$$P_{1n} = F_{yw}Dt_w + F_{yt}b_{ft}t_{ft} + F_{yc}b_{fc}t_{fc}$$ Equation 2.199

or: *AASHTO LRFD* Equation 6.10.10.4.2-7

$$P_{2n} = 0.45f_c'b_st_s$$ Equation 2.200

AASHTO LRFD Equation 6.10.10.4.2-8

The number of shear connectors required between points of maximum positive design live load plus impact moment and the centerline of an adjacent interior support (for continuous spans that are composite for negative flexure in the final condition) is computed from the sum of the critical forces at the maximum positive and negative moment locations according to Equation 2.198. The sum of the critical forces at the maximum moment locations is conservatively used in order to provide adequate shear resistance for any live load position. Many shear connectors in this region resist reversing forces in the concrete deck depending on the live load position since there is no one point where the moment always changes sign. In this region, sufficient shear connectors are necessary to transfer the ultimate tensile force in the longitudinal reinforcement from the concrete deck to the steel section. The tension force given by Equation 2.200 is a conservative approximation to account for the combined contribution of the longitudinal reinforcement and the concrete deck that remains effective in tension based on its modulus of rupture. The Engineer may substitute a more precise value for this force, if desired.

F_T is taken as follows:

$$F_T = P_T \frac{L_n}{R}$$ Equation 2.201

AASHTO LRFD Equation 6.10.10.4.2-9

where:

L_n =   arc length between the point of maximum positive live load plus impact moment and the centerline of an adjacent interior support (ft)

R =   minimum girder radius over the length L_n (ft)

F_T may be taken equal to zero for straight spans or segments.

According to *AASHTO LRFD* Article 6.11.10, for box sections, the cross-sectional area of the steel box under consideration and the effective area of the concrete deck associated with that box are to be used to calculate the longitudinal force in Equations 2.194, 2.195, 2.199 and 2.200. Also, for composite box flanges in closed-box sections at the strength limit state, in addition to satisfying the provisions of *AASHTO LRFD* Article 6.10.10.4, the vector sum of the longitudinal and torsional shears due to the factored loads in the concrete deck per connector are not to exceed Q_r from Equation 2.186. The torsional shear in the concrete deck can be determined by multiplying the torsional shear acting on the top of the composite box section by the ratio of the thickness of the transformed concrete deck to the total thickness of the top flange plus the transformed deck. The deck should include adequate transverse reinforcement to resist this torsional shear.

EXAMPLE

Check the number of stud shear connectors that were determined to satisfy the fatigue limit state in the preceding example against the number required to satisfy the strength limit state. The preceding example determined the required pitch of the shear connectors to satisfy the fatigue limit state for the exterior girder of a straight three-span continuous I-girder bridge (140 ft – 175 ft – 140 ft) with no skew. Shear connectors are provided throughout the entire length of the bridge so the girder is assumed composite in regions of negative flexure in the final condition. As determined in the preceding example, 7/8" x 7" studs are to be used (3 studs per row). The specified minimum 28-day compressive strength f'_c of the concrete deck is 4.0 ksi.

According to *AASHTO LRFD* Article 6.10.10.4.1, the factored shear resistance of a single shear connector Q_r at the strength limit state is to be taken as:

$$Q_r = \phi_{sc} Q_n$$

AASHTO LRFD Equation 6.10.10.4.1-1

As specified in *AASHTO LRFD* Article 6.10.10.4.3, the nominal shear resistance of one stud shear connector embedded in a concrete deck is to be taken as:

$$Q_n = 0.5 A_{sc} \sqrt{f'_c E_c} \le A_{sc} F_u$$

AASHTO LRFD Equation 6.10.10.4.3-1

The modulus of elasticity of the deck concrete E_c is determined as follows:

$$E_c = 33,000 w_c^{1.5} \sqrt{f_c'}$$

AASHTO LRFD Equation 5.4.2.4-1

A unit weight w_c of 0.145 kcf will be assumed for the normal weight concrete. Therefore:

$$E_c = 33,000(0.145)^{1.5} \sqrt{4.0} = 3,644 \text{ ksi}$$

The specified minimum tensile strength of a stud shear connector F_u is taken as 60.0 ksi, as specified in Article 6.4.4. Thus:

$$A_{sc} = \frac{\pi}{4}(0.875)^2 = 0.60 \text{ in.}^2$$

$$A_{sc}F_u = (0.60)(60.0) = 36.00 \text{ kips}$$

$$Q_n = 0.5(0.60)\sqrt{4.0(3,644)} = 36.22 \text{ kips} > 36.00 \text{ kips}$$

$$\therefore \quad Q_n = 36.00 \text{ kips}$$

$$Q_r = 0.85(36.00) = 30.60 \text{ kips}$$

At the strength limit state, the minimum number of shear connectors, n, over the region under consideration is to be taken as:

$$n = \frac{P}{Q_r}$$

AASHTO LRFD Equation 6.10.10.4.1-2

where *P* is the total nominal shear force determined as specified in *AASHTO LRFD* Article 6.10.10.4.2. According to *AASHTO LRFD* Article 6.10.10.4.2, for continuous spans that are composite for negative flexure in the final condition, the total nominal shear force *P* between the point of maximum positive design live load plus impact moment and an adjacent end of the member is to be determined as:

$$P = \sqrt{P_p^2 + F_p^2}$$

AASHTO LRFD Equation 6.10.10.4.2-1

where P_p is the total shear force in the concrete deck at the point of maximum positive live load plus impact moment taken as the lesser of:

$$P_{1p} = 0.85 f_c' b_s t_s$$

AASHTO LRFD Equation 6.10.10.4.2-2

where b_s and t_s are the effective width and thickness of the concrete deck, respectively, (assumed to be equal to 100 inches and 9.0 inches in this region for this example), or:

$$P_{2p} = F_{yw}Dt_w + F_{yt}b_{ft}t_{ft} + F_{yc}b_{fc}t_{fc}$$

AASHTO LRFD Equation 6.10.10.4.2-3

$$P_{1p} = 0.85(4.0)(100.0)(9.0) = 3{,}060 \text{ kips}$$

For the steel section yielding the smallest force in this region (top flange = 1" x 16"; web = ½" x 69"; bottom flange = 7/8" x 18"):

$$P_{2p} = (50.0)(69.0)(0.5) + (50.0)(18.0)(0.875) + (50.0)(16.0)(1.0) = 3{,}313 \text{ kips}$$

Since the girder is straight, the radial force F_p is taken equal to zero.

$$\therefore P = P_p = P_{1p} = 3{,}060 \text{ kips}$$

$$n = \frac{P}{Q_r} = \frac{3{,}060}{30.60} = 100 \text{ studs}$$

Compute the required pitch, p, in this region at the strength limit state with 3 studs per row. The point of maximum positive live load plus impact moment in Span 1 is located 60.2 feet from the abutment. Therefore:

$$\text{No. of rows} = \frac{100}{3} = 34 \text{ rows}$$

$$p = \frac{60.2(12)}{(34-1)} = 21.9 \text{ in.}$$

The total nominal shear force P between the point of maximum positive design live load plus impact moment and the centerline of an adjacent interior support is to be determined as:

$$P = \sqrt{P_T^2 + F_T^2}$$

AASHTO LRFD Equation 6.10.10.4.2-5

where P_T is the total longitudinal force in the concrete deck between the point of maximum positive live load plus impact moment and the centerline of the adjacent interior support taken as:

$$P_T = P_p + P_n$$

AASHTO LRFD Equation 6.10.10.4.2-6

P_n is the total longitudinal shear force in the concrete deck over an interior support taken as the lesser of:

$$P_{1n} = F_{yw}Dt_w + F_{yt}b_{ft}t_{ft} + F_{yc}b_{fc}t_{fc}$$

AASHTO LRFD Equation 6.10.10.4.2-7

$$\text{or:} \quad P_{2n} = 0.45f_c'b_st_s$$

AASHTO LRFD Equation 6.10.10.4.2-8

For the steel section (top flange = 1" x 16"; web = ½" x 69"; bottom flange = 1-3/8"" x 18") and effective concrete deck yielding the smallest forces in this region:

$$P_{1n} = (50.0)(69.0)(0.5) + (50.0)(18.0)(1.375) + (50.0)(16.0)(1.0) = 3{,}763 \text{ kips}$$

$$P_{2n} = 0.45(4.0)(100.0)(9.0) = 1{,}620 \text{ kips}$$

$$\therefore P_n = 1{,}620 \text{ kips}$$

Since the girder is straight, the radial force F_T is taken equal to zero.

$$\therefore P = P_T = P_p + P_n = 3{,}060 + 1{,}620 = 4{,}680 \text{ kips}$$

$$n = \frac{P}{Q_r} = \frac{4{,}680}{30.60} = 153 \text{ studs}$$

Compute the required pitch, p, in this region at the strength limit state with 3 studs per row. The distance between the point of maximum positive live load plus impact moment in Span 1 and the adjacent interior support is (140.0 - 60.2) = 79.8 feet. Therefore:

$$\text{No. of rows} = \frac{153}{3} = 51 \text{ rows}$$

$$p = \frac{79.8(12)}{(51-1)} = 19.2 \text{ in.}$$

The distance between the point of maximum positive live load plus impact moment in Span 2 and each of the adjacent interior supports is 87.5 feet. Using calculations similar to the above:

$$P_p = 3{,}060 \text{ kips}$$
$$P_n = 1{,}620 \text{ kips}$$
$$P = 4{,}680 \text{ kips}$$
$$n = 153 \text{ studs}$$

No. of rows = 51 rows
p = 21.0 in.

The final recommended pitches are governed by the fatigue limit state and are shown below. The effective width of the concrete deck is larger for the interior girders, which in conjunction with different fatigue shear ranges, may result in slightly different recommended pitches. However, for practical purposes, unless the differences are deemed significant, it is recommended that the same pitches be used on all the girders.
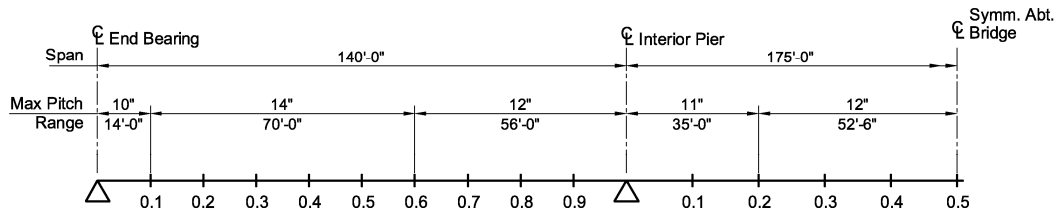
86.   Slutter, R.G., and J.W. Fisher. 1966. "Fatigue Strength of Shear Connectors." *Highway Research Record No. 147*, Highway Research Board, Washington, D.C.

87.   Ollgaard, J.G., R.G. Slutter, and J.W. Fisher. 1971. "Shear Strength of Stud Connectors in Lightweight and Normal Weight Concrete." *AISC Engineering Journal*, American Institute of Steel Construction, Chicago, IL, Vol. 8 No. 2, April.

88.   Slutter, R.G., and G.C. Driscoll, Jr. 1965. "Flexural Strength of Steel-Concrete Composite Beams." Journal of the Structural Division. American Society of Civil Engineers, New York, NY, Vol. 91, No. ST2, April.

2.2.6 Web Stiffener Design

Web stiffener design is covered in *AASHTO LRFD* Article 6.10.11.   The design of transverse stiffeners, bearing stiffeners and longitudinal stiffeners will be discussed in each of the following sections.

2.2.6.1 Transverse Stiffeners

2.2.6.1.1 General

The design of transverse web stiffeners is covered in *AASHTO LRFD* Article 6.10.11.1.   Transverse stiffeners are used to increase the shear resistance of a girder and are aligned vertically on the web. Transverse stiffeners are to consist of plate or angles welded or bolted to either one or both sides of the web (Figure 2.80). The term connection plate is given to a transverse stiffener to which a cross-frame or diaphragm is connected.   A connection plate can serve as a transverse stiffener for shear design calculations.

Figure 2.80 Transverse Web Stiffeners

As specified in *AASHTO LRFD* Article 6.10.11.1.1, stiffeners used as connection plates must be attached to both flanges. According to *AASHTO LRFD* Article 6.6.1.3.1, attachment of the connection plate to the flanges must be made by welding or bolting. The connection to the compression flange is typically welded. The connection to the tension flange is either welded or bolted through a tab plate that has been welded to the connection plate. Engineers have used the bolted tab plates to raise the nominal fatigue resistance of the flange base metal at the attachment detail from Category C′ to Category B. This should only be considered at connection plates where fatigue is a significant issue. However, as discussed in an example given in the previous section of this chapter on Fatigue Limit State Verifications, the bolted tab plate is significantly more expensive to furnish and install than a welded connection. Also, the fatigue category of the base metal at the termination of the weld attaching the connection plate to the web is of the same fatigue category as the base metal at the weld to the tension flange. In most cases, the live load stress range at these two adjacent locations is not significantly different. Therefore, an adjustment of the location of a problem connection plate to eliminate the need for a bolted tab connection should be considered.

Stiffeners in straight girders not used as connection plates are to be tight fit or attached at the compression flange, but need not be in bearing with the tension flange. Generally, attachment of such stiffeners to the compression flange is accomplished by welding. Also, these stiffeners are generally either tight fit or cut short of the tension flange. A tight fit can help straighten the flange tilt without the application of heat (*40*). According to AASHTO LRFD Article 6.10.11.1.1, single-sided stiffeners on horizontally curved girders should be attached to both flanges to help retain the cross-sectional shape of the girder when subjected to torsion and to avoid high localized bending within the web, particularly near the top flange due to the torsional restraint of the concrete deck. For the same reason, it is required that pairs of transverse stiffeners on horizontally curved girders be tight fit or attached to both flanges.

In the fabrication of tub sections, webs are often joined to top flanges and the connection plates and transverse stiffeners (not serving as connection plates) are installed, and then these assemblies are attached to a common box flange. The details in this case must allow the welding head to clear the bottom of the connection plates and stiffeners so the webs can be welded continuously to the box flange inside the tub section. A detail must also be provided to permit the subsequent attachment of the connection plates to the box flange (and any other transverse stiffeners that are to be attached to the box flange). Figures 3.5.A and 3.5.B in Reference 40 show suggested connection details for this particular situation. Figure 3.5.D in Reference 40 shows a suggested connection detail for cases where the box flange is welded to the webs prior to attaching the connection plates and stiffeners.

As discussed in the earlier section of this chapter on Fatigue Limit State Verifications, the distance between the end of the web-to-stiffener weld and the near edge of the adjacent web-to-flange or longitudinal stiffener-to-web weld is not to be less than $4t_w$ or more than the lesser of $6t_w$ and 4.0 in. (Figure 2.46).

Reference 40 recommends that stiffeners and connection plates be detailed to be normal to the girder flanges unless unusual conditions require them to be detailed otherwise. Also, a minimum spacing of 8 inches or 1-1/2 times the stiffener plate width should be provided between stiffeners or connection plates for welding access.

2.2.6.1.2 Proportions

As specified in *AASHTO LRFD* Article 6.10.11.1.2, the width b_t of each projecting transverse stiffener element (Figure 2.81) must satisfy the following requirements:

$$b_t \geq 2.0 + \frac{D}{30}$$
<div align="right">Equation 2.202</div>

<div align="right">*ASHTO LRFD* Equation 6.10.11.1.2-1</div>

and:

$$16t_p \geq b_t \geq b_f/4$$
<div align="right">Equation 2.203</div>

<div align="right">*AASHTO LRFD* Equation 6.10.11.1.2-2</div>

where:
   b_f =   for I-sections, full width of the widest compression flange within the field section under consideration; for tub sections, full width of the widest top flange within the field section under consideration; for closed box sections, the limit of $b_f/4$ does not apply (in.)
   t_p =   thickness of the projecting stiffener element (in.)
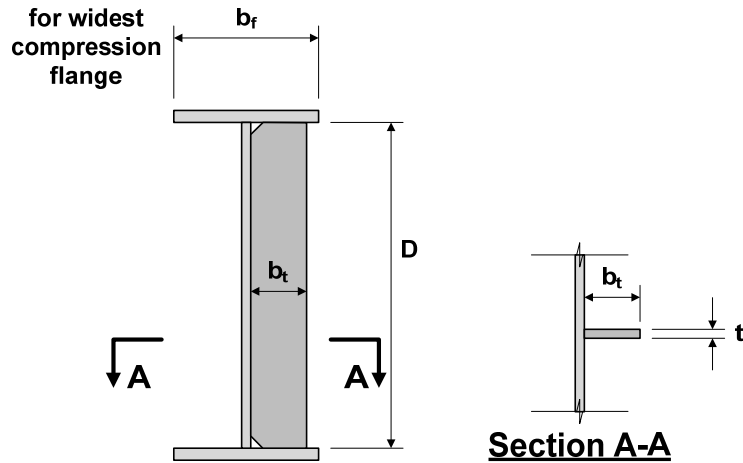
Figure 2.81 Projecting Width of Transverse Stiffeners

Equation 2.202 (*89*) tends to control relative to Equation 2.203 for I-girders with large ratios of D/b_f. In Equation 2.203, the full width of the widest compression flange within the field section under consideration is used for b_f to allow for the use of the same minimum stiffener width throughout the entire field section, if desired, and to help restrain the widest compression flange. Since the bottom flange of tub sections is restrained by a web along both edges, the widest top flange is used for b_f in Equation 2.203. Since the web restrains the edges of both flanges of a closed box section, the limit of $b_f/4$ does not apply.

Welded stiffeners and connection plates are commonly made up of less expensive flat bar stock. Flat bars are generally produced in whole-inch width increments and 1/8-in. thickness increments. ***Fabricators prefer a ½-inch minimum thickness for stiffeners and connection plates (40).***

2.2.6.1.3 Moment of Inertia

For the web to adequately develop the shear-buckling resistance, or the combined shear-buckling and postbuckling tension-field resistance, the transverse stiffener must have sufficient rigidity to maintain a vertical line of near zero lateral deflection of the web along the line of the stiffener. Therefore, the bending rigidity (or moment of inertia) is the dominant parameter governing the performance of transverse stiffeners.

As specified in *AASHTO LRFD* Article 6.10.11.1.3, for transverse stiffeners adjacent to web panels in which neither panel supports shear forces larger than the shear-buckling resistance (i.e. $V_n = V_{cr}$ from Equation 2.151), the moment of inertia of the transverse stiffener I_t must satisfy the *smaller* of the following (i.e. Equation 2.204 or 2.205):

$$I_t \geq bt_w^3 J \hspace{3cm} \text{Equation 2.204}$$

and:

$$I_t \geq \frac{D^4 \rho_t^{1.3}}{40}\left(\frac{F_{yw}}{E}\right)^{1.5} \qquad \text{Equation 2.205}$$

where:

b	=	the smaller of d_o and D (in.)
d_o	=	the smaller of the adjacent panel widths (in.)
I_t	=	moment of inertia of the transverse stiffener taken about the edge in contact with the web for single stiffeners and about the mid-thickness of the web for stiffener pairs (in.^{4})
J	=	stiffener bending rigidity parameter taken as follows:

$$J = \frac{2.5}{(d_o/D)^2} - 2.0 \geq 0.5 \qquad \text{Equation 2.206}$$

ρ_t	=	the larger of F_{yw}/F_{crs} and 1.0
F_{crs}	=	local buckling stress for the stiffener (ksi) taken as follows:

$$F_{crs} = \frac{0.31E}{\left(\dfrac{b_t}{t_p}\right)^2} \leq F_{ys} \qquad \text{Equation 2.207}$$

F_{ys}	=	specified minimum yield strength of the stiffener (ksi)

If the shear force in one of both panels is such that the web postbuckling or tension-field resistance is required (i.e. V_n from Equation 2.156 or 2.158), the moment of inertia of the transverse stiffener need only satisfy Equation 2.205.

For single-sided stiffeners, a significant portion of the web is implicitly assumed to contribute to the bending rigidity so that the neutral axis of the stiffener is assumed located close to the edge in contact with the web. Therefore, for this case, the moment of inertia is taken about this edge and the contribution of the web to the moment of inertia about the neutral axis is neglected for simplicity.

The smaller moment of inertia from Equation 2.204 or 2.205 is considered sufficient to develop the shear-buckling resistance of the web $V_{cr} = CV_p$ *(90)* when a larger shear resistance is not required in either panel adjacent to the stiffener. For members with $D/t_w = 1.12\sqrt{Ek/F_{yw}}$, which is the D/t_w value at (or below) which C is

equal to 1.0 and V_{cr} is equal to the plastic (or shear-yield) resistance V_p (refer to Equation 2.152), Equations 2.204 and 2.205 give approximately the same value of the I_t required to develop V_{cr}. For members with $D/t_w > 1.12\sqrt{Ek/F_{yw}}$, Equation 2.204 gives the smaller value of the I_t to develop the elastic or inelastic value of the shear-buckling resistance V_{cr}, and for members with $D/t_w < 1.12\sqrt{Ek/F_{yw}}$, Equation 2.205 gives the smaller value of the I_t required to develop $V_{cr} = V_p$. For the latter case, Equation 2.204 requires excessively large stiffener sizes since this equation is based on developing the elastic shear-buckling resistance of the web. Reference 91 gives inelastic buckling solutions, which show that such large stiffeners are not required as D/t_w is reduced below the limit of $1.12\sqrt{Ek/F_{yw}}$. Recent research based on refined finite-element studies has also confirmed this fact (*90*).

For ratios of (d_o/D) less than or equal to 1.0, much larger values of I_t are required to develop the shear-buckling resistance (*91*), which is represented by Equation 2.204. For ratios of (d_o/D) greater than 1.0, the term b in Equation 2.204 (which replaces the term d_o used in this equation in previous Specifications), along with Equation 2.206, provide a reasonably constant value of the required I_t to develop the shear-buckling resistance.

To develop the web postbuckling or tension-field resistance in one or both panels adjacent to the stiffener, the stiffener must generally have a larger I_t than defined by Equation 2.204 (*90*). In such cases, Equation 2.205 provides the larger required I_t necessary to maintain a line of near zero lateral deflection within the postbuckled web at the stiffener location. As discussed in Reference 90, Equation 2.205 provides an accurate to slightly conservative required stiffener size relative to refined finite-element solutions for straight and horizontally curved I-girders at all values of D/t_w permitted by the AASHTO LRFD Specifications. Although the required stiffener rigidity is insensitive to the parameter (d_o/D) according to Equation 2.205, the equation provides an approximate upper bound to the results from a comparable equation proposed in Reference 90 for all values of (d_o/D). The term ρ_t in Equation 2.205 accounts for the effect of potential local buckling of stiffeners having a relatively large width-to-thickness ration b_t/t_p, and also for the effect of potential early yielding in stiffeners with F_{ys} less than or equal to F_{yw}.

Equation 2.205 is intended to provide a required I_t that will allow the development of a factored shear resistance at or near the postbuckling tension-field shear resistance $\phi_v V_n$ in the adjacent web panel(s). However, in cases where V_u is smaller than $\phi_v V_n$, this value of I_t is not required. *The required value of I_t may be particularly large for deeper girders*. Hence, the following correction to this requirement is being proposed to AASHTO to handle such cases. In the following, I_{t1} is the required moment of inertia according to Equation 2.204 and I_{t2} is the required moment of inertia according to Equation 2.205. For transverse stiffeners adjacent to web panels in which the shear due to the factored loads V_u in one or both panels exceeds the factored shear buckling resistance $\phi_v V_{cr}$:

- If $I_{t2} > I_{t1}$:

$$I_t \geq I_{t1} + \left(I_{t2} - I_{t1}\right)\left(\frac{V_u - \phi_v V_{cr}}{\phi_v V_n - \phi_v V_{cr}}\right)$$

Equation 2.207a

- Otherwise:

$$I_t \geq I_{t2}$$

Equation 2.207b

In the above, V_u is the largest shear in the adjacent web panels due to the factored loads, V_{cr} is the smallest shear buckling resistance of the adjacent web panels and V_n is the smallest tension-field shear resistance of the adjacent web panels.

Previous Specifications included an area requirement for transverse stiffeners adjacent to panels subject to postbuckling tension-field action, which has since been removed. Multiple experimental and refined finite-element based research studies have shown that transverse stiffeners are loaded primarily in lateral bending by the postbuckled web panels, and not by axial forces associated with postbuckling tension-field action, even for web panels with D/t_w up to 300. Therefore, the stiffener moment of inertia has a much stronger correlation with the stiffener performance than the stiffener area. In addition, the research described in Reference 90 indicated that panels designed for shear postbuckling resistance using one-sided stiffeners and two-sided stiffeners based on the traditional area requirement had significantly different values of shear resistance. In fact, in some cases (primarily cases with two-sided stiffeners as D/t_w increased beyond $1.12\sqrt{Ek/F_{yw}}$), the area requirement provided a stiffener size that was insufficient to hold the postbuckled web in position at the stiffener location. Equation 2.205 recognizes the fact that one- and two-sided stiffeners, sized such that they have the same value of I_t, provide essentially the same shear resistance for a given stiffener spacing (*90*, *92-95*).

Transverse stiffeners used in panels with longitudinal web stiffeners must also satisfy the following relationship:

$$I_t \geq \left(\frac{b_t}{b_\ell}\right)\left(\frac{D}{3d_o}\right)I_\ell$$

Equation 2.208

AASHTO LRFD Equation 6.10.11.1.3-5

where:
    b_ℓ =   projecting width of the longitudinal stiffener (in.)
    b_t =   projecting width of the transverse stiffener (in.)
    I_ℓ =   moment of inertia of the longitudinal stiffener determined as
        specified in *AASHTO LRFD* Article 6.10.11.3.3 (in.[4])

Lateral loads along the length of a longitudinal stiffener are transferred to the adjacent transverse stiffeners as concentrated reactions at the stiffener intersections (*10*). Equation 2.208 provides a relationship between the moments of inertia of the transverse and longitudinal stiffeners to ensure that the transverse stiffeners do not fail under these concentrated reactions. The relationship applies whether the stiffeners are on the same or opposite side of the web.

EXAMPLE

Size the transverse stiffeners for Field Section 1 of the exterior girder of a three-span continuous I-girder bridge (refer to Figure 2.59). The web in Field Section 1 is ½" x 69". The top flange in Field Section 1 is 16 inches wide. The same size stiffeners will be used within the field section for practical purposes. Grade 50W steel will be used for the stiffeners (i.e. F_{ys} = 50.0 ksi), and for the flanges and web of the girder. All stiffeners are on one side of the web.

Determine the initial trail stiffener proportions. Size the stiffener width b_t to be greater than or equal to $b_f/4$ as required in *AASHTO LRFD* Equation 6.10.11.1.2-2. For I-sections, b_f is to be taken as the full width of the widest compression flange within the field section under consideration.

$$b_t \geq \frac{16.0}{4} = 4.0 \text{ in.}$$

AASHTO LRFD Equation 6.10.11.1.2-2

Again, stiffeners and connection plates are commonly made up of less expensive flat bar stock, which is generally produced in whole-inch width increments and 1/8-in. thickness increments. Therefore:

Use b_t = 6.0 in. > 4.0 in.   ok

Check that:

$$b_t \geq 2.0 + \frac{D}{30}$$

AASHTO LRFD Equation 6.10.11.1.2-1

$$2.0 + \frac{69.0}{30} = 4.3 \text{ in.} < 6.0 \text{ in.}$$ ok

Try a stiffener thickness t_p of 0.625 inches, which satisfies the preferred minimum thickness of ½ inch for stiffeners given in Reference 40.

Check that:
$$16t_p \geq b_t$$

AASHTO LRFD Equation 6.10.11.1.2-2

$$16(0.625) = 10.0 \text{ in.} > 6.0 \text{ in.}$$ ok

According to the shear calculations in the previous example accompanying Figure 2.59, for the majority of the web panels in Field Section 1, the shear is larger than the shear buckling resistance. Therefore, most of the web panels in this field section must develop the postbuckling or tension-field shear resistance. To adequately develop the tension-field shear resistance within these web panels, the transverse stiffeners (and any connection plates serving as transverse stiffeners) adjacent to these panels must satisfy the following single moment of inertia requirement:

$$I_t \geq \frac{D^4 \rho_t^{1.3}}{40} \left(\frac{F_{yw}}{E} \right)^{1.5}$$

AASHTO LRFD Equation 6.10.11.1.3-2

Since it desired to use the same size stiffeners within this field section, this requirement will be applied to all stiffeners and connection plates within the field section.

The local buckling stress F_{crs} for the stiffener is calculated as follows:

$$F_{crs} = \frac{0.31E}{\left(\dfrac{b_t}{t_p} \right)^2} \leq F_{ys}$$

AASHTO LRFD Equation 6.10.11.1.3-4

$$F_{crs} = \frac{0.31(29,000)}{\left(\dfrac{6.0}{0.625} \right)^2} = 97.5 \text{ ksi} > F_{ys} = 50 \text{ ksi}$$

$$\therefore F_{crs} = 50 \text{ ksi}$$

The term ρ_t is equal to the larger of F_{yw}/F_{crs} (i.e. 50 ksi/50 ksi = 1.0) and 1.0. Therefore, in this case, ρ_t is equal to 1.0.

$$I_t \geq \frac{(69.0)^4 (1.0)^{1.3}}{40} \left(\frac{50}{29,000} \right)^{1.5} = 40.57 \text{ in}^4$$

For single-sided stiffeners, the moment of inertia of the stiffener is to be taken about the edge in contact with the web. Therefore:

$$I_t = \frac{1}{3}(0.625)(6.0)^3 = 45.00 \text{ in.}^4 > 40.57 \text{ in.}^4 \quad \text{ok}$$

Use 5/8" x 6" stiffeners. Since the girder is not particularly deep, a reasonable required moment of inertia was obtained from Equation 2.205 and it was not deemed necessary to apply the correction given by Equation 2.207a in this example.

2.2.6.2 Bearing Stiffeners

2.2.6.2.1 General

The design of bearing stiffeners is covered in *AASHTO LRFD* Article 6.10.11.2. Bearing stiffeners, which are aligned vertically on the web, are designed as columns to resist the reactions at bearing locations and at other locations subjected to

concentrated loads where the loads are not transmitted through a deck or deck system (Figure 2.82).

Figure 2.82 Bearing Stiffener

As specified in *AASHTO LRFD* Article 6.10.11.2.1, bearing stiffeners must be placed on the webs of built-up sections at all bearing locations. At bearing locations on rolled shapes and at other locations on built-up sections or rolled shapes subjected to concentrated loads, where the loads are not transmitted through a deck or deck system, either bearing stiffeners must be provided or else the web must satisfy the provisions of Article D6.5 (Appendix D to Section 6). According to the provisions of *AASHTO LRFD* Article D6.5 (discussed in more detail below), webs without bearing stiffeners at the indicated locations are to be investigated for the limit states of web local yielding and web crippling. The section must either be modified to comply with these requirements, or else bearing stiffeners must be placed on the web at the locations under consideration. The Engineer should be especially aware of these provisions when concentrated loads (not transmitted through a deck or deck system) are applied during a temporary construction situation; e.g., when girders are incrementally launched over supports.

Bearing stiffeners must consist of one or more plates or angles welded or bolted to both sides of the web, with the connections to the web designed to transmit the full bearing force due to the factored loads. The stiffeners must extend the full depth of the web and as closely as practical to the outer edges of the flanges.

According to *AASHTO LRFD* Article 6.11.11.1, when inclined webs are used in box sections, the bearing stiffeners should be attached to either an internal or external diaphragm rather than to the webs so that the bearing stiffeners are perpendicular to the sole plate. In such cases, at expansion bearings, thermal movements of the bridge may cause the diaphragm to be eccentric with respect to the bearings. The effect of this eccentricity on the design of the bearing stiffeners and diaphragms should be recognized. Eccentricity effects can be recognized by designing the bearing stiffener assembly as a beam-column according to the provisions of *AASHTO LRFD* Articles 6.10.11.2 and 6.9.2.2.

Connection of the bearing stiffener to the flange through which it receives its load can either be made by finish-to-bear plus a fillet weld on each side of the stiffener plate (note that fillet welds are not necessary if a cross-frame/diaphragm is not connected to the stiffener plate), or by a full penetration groove weld. Finish-to-bear means allowing the fabricator the option of grinding or milling. *It is strongly recommended that the finish-to-bear option (with or without fillet welds as applicable) always be specified as this approach dramatically reduces the deformations of the flange induced by a full penetration groove weld, and also costs significantly less than a full penetration groove weld.*

Reference 40 recommends that permission be granted for the bearing stiffeners (and bearing diaphragms in box sections) to be detailed either vertical or normal to the girder top flange at the fabricator's option. Reference 40 further indicates that most fabricators prefer the bearing stiffeners to be detailed normal. Also, in cases where multiple bearing stiffeners are used at a given location, a minimum spacing of 8 inches or 1-1/2 times the stiffener plate width should be provided between the stiffener plates for welding access.

2.2.6.2.2 Projecting Width

As specified in *AASHTO LRFD* Article 6.10.11.2.2, the projecting width b_t of each bearing stiffener element (Figure 2.83) must satisfy the following requirement in order to prevent local buckling of the bearing stiffener plates:

$$b_t \leq 0.48t_p\sqrt{\frac{E}{F_{ys}}}$$

<div align="right">Equation 2.209</div>

<div align="right">*AASHTO LRFD* Equation 6.10.11.2.2-1</div>

where:

F_{ys} =   specified minimum yield strength of the stiffener (ksi)
t_p =   thickness of the projecting stiffener element (in.)
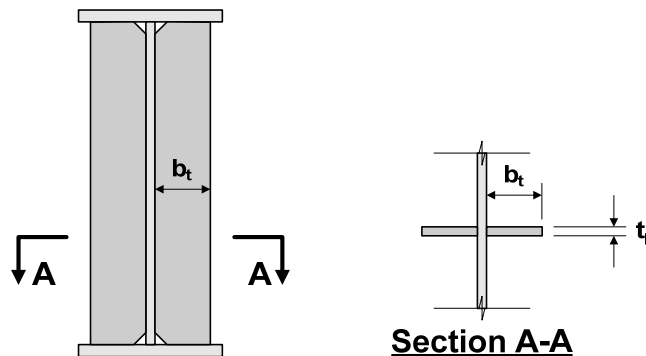
Figure 2.83 Projecting Width of Bearing Stiffener

2.2.6.2.3 Bearing Resistance

Bearing stiffeners must be clipped to clear the web-to-flange fillet welds and to bring the stiffener plates tight against the flange through which they receive their load. As a result, the area of the plates in direct bearing on the flange is less than the gross area of the plates. As specified in *AASHTO LRFD* Article 6.10.11.2.3, the factored bearing resistance of the fitted ends of bearing stiffeners is to be taken as:

$$\left(R_{sb}\right)_r = \phi_b \left(R_{sb}\right)_n$$ Equation 2.210

AASHTO LRFD Equation 6.10.11.2.3-1

where:

ϕ_b =   resistance factor for bearing on milled surfaces specified in *AASHTO LRFD* Article 6.5.4.2 (= 1.0)

$(R_{sb})_n$ =   nominal bearing resistance for the fitted ends of bearing stiffeners (kips)

=   1.4 $A_{pn}F_{ys}$ *AASHTO LRFD* Equation 6.10.11.2.3-2

A_{pn} =   area of the projecting elements of the stiffener outside of the web-to-flange fillet welds but not beyond the edge of the flange (in.^{2})

F_{ys} =   specified minimum yield strength of the stiffener (ksi)

In the *AISC LRFD* Specification (*26*), the nominal bearing resistance for the fitted ends of bearing stiffeners is given by Equation (J7-1) as $R_n = 1.8F_yA_{pb}$, where A_{pb} is equal to the projected bearing area. The specified nominal bearing resistance is twice the *AISC ASD* (Allowable Stress Design) value of $R_n = 0.9F_yA_{pb}$. Applying the specified *AISC* resistance factor of 0.75 to the nominal *AISC LRFD* nominal bearing resistance gives a factored bearing resistance of *1.35F_yA_{pb}*. Since the *AASHTO LRFD* resistance factors for connection elements are generally 0.05 higher than the *AISC LRFD* resistance factors, the nominal bearing resistance for the fitted ends of bearing stiffeners in the *AASHTO LRFD* Specification was raised to *0.8 * 1.8F_yA_{pb} = 1.4F_yA_{pb}*, which is then used in conjunction with a specified *AASHTO LRFD* resistance factor for bearing on milled surfaces of ϕ_b = 1.0.

2.2.6.2.4 Axial Resistance

As mentioned previously, bearing stiffeners are designed as columns. As specified in *AASHTO LRFD* Article 6.10.11.2.4a, the factored axial resistance of the stiffeners P_r is to be determined as specified in AASHTO LRFD Article 6.9.2.1 using the specified minimum yield strength of the stiffener plates F_{ys} in order to account for the effect of any early yielding of lower strength stiffener plates. The factored resistance of components in axial compression is given in *AASHTO LRFD* Article 6.9.2.1 as:

$$P_r = \phi_c P_n$$ Equation 2.211

AASHTO LRFD Equation 6.9.2.1-1

where:

ϕ_c = resistance factor for axial compression specified in *AASHTO LRFD* Article 6.5.4.2 (= 0.90)

P_n = nominal compressive resistance specified in *AASHTO LRFD* Article 6.9.4.1 (kips)

For bearing stiffeners, the nominal compressive resistance P_n is to be computed as (refer to *AASHTO LRFD* Article 6.9.4.1):

➢ If $\lambda \le 2.25$, then:

$$P_n = 0.66^\lambda F_{ys} A_s \qquad \text{Equation 2.212}$$

AASHTO LRFD Equation 6.9.4.1-1

➢ If $\lambda > 2.25$, then:

$$P_n = \frac{0.88 F_{ys} A_s}{\lambda} \qquad \text{Equation 2.213}$$

AASHTO LRFD Equation 6.9.4.1-2

where:

λ = $\left(\dfrac{K\ell}{r_s \pi}\right)^2 \dfrac{F_{ys}}{E}$ *AASHTO LRFD* Equation 6.9.4.1-3

A_s = effective column section of the bearing stiffeners (see below) (in.^{2})

F_{ys} = specified minimum yield strength of the stiffener (ksi)

$K\ell$ = effective length of the effective column taken as 0.75D, where D is the web depth (refer to *AASHTO LRFD* Article 6.10.11.2.4a) (in.)

r_s = radius gyration of the effective column about the plane of buckling computed about the mid-thickness of the web (refer to *AASHTO LRFD* Article 6.10.11.2.4a) (in.)

The reduced effective length $K\ell = 0.75D$ of the effective column is a result of the end restraint against column buckling provided by the flanges. Note that the width-to-thickness requirements of *AASHTO LRFD* Article 6.9.4.2 are not enforced in bearing stiffener design because the stiffener projecting width requirement specified in AASHTO LRFD Article 6.10.11.2.2 (i.e. Equation 2.209) is typically more severe.

2.2.6.2.4.1 Effective Column Section

The effective column section of the bearing stiffeners is defined in *AASHTO LRFD* Article 6.10.11.2.4b. For stiffeners bolted to the web, the effective column section is to consist of only the stiffener elements. For stiffeners welded to the web, a portion of the web is to be included as part of the effective column section, with some exceptions noted below. For stiffeners consisting of two plates welded to the web, the effective column section is to consist of the two stiffener plates, plus a centrally

located strip of web extending not more than $9t_w$ on each side of the stiffeners (Figure 2.84).
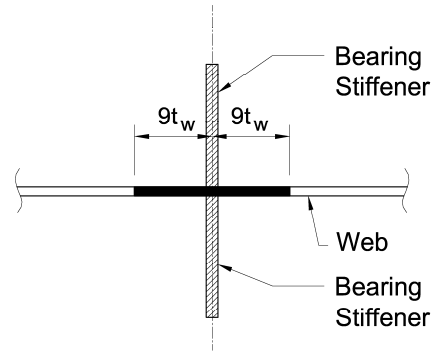
Figure 2.84 Effective Column Section for Welded Bearing Stiffener Design (One Pair of Stiffeners)

If more than one pair of stiffeners is used, the effective column section is to consist of all the stiffener plates, plus a centrally located strip of web extending not more than $9t_w$ on each side of the outer projecting elements of the group. In either case, the strip of web is not to be included in the effective section at interior supports of continuous-span hybrid members for which the specified minimum yield strength of the web is less than 70 percent of the specified minimum yield strength of the higher strength flange due to the amount of web yielding that may be expected due to the longitudinal flexural stress. The preceding exception does not apply at the end supports of hybrid members. For unusual cases in which F_{ys} is larger than F_{yw}, the yielding of the lower strength web is to be accounted for by reducing the width of the web strip included in the effective section by the ratio of F_{yw}/F_{ys}.

For bearing stiffeners attached to diaphragms in box sections, the preceding requirements regarding the effective section are to be applied to the diaphragm rather than the web, as specified in *AASHTO LRFD* Article 6.11.1.1.

EXAMPLE

Design a pair of welded bearing stiffeners at the end support of a three-span continuous I-girder bridge. The girder flanges and web are Grade 50W steel, and Grade 50W steel will also be used for the stiffeners (i.e. F_{ys} = 50.0 ksi).

The unfactored bearing reactions at the end support are as follows:

R_{DC1} = 87 kips
R_{DC2} = 13 kips
R_{DW} = 13 kips
R_{LL+IM} = 139 kips

Assemble the bearing reactions due to the factored loads at the end support. The Strength I load combination controls (see DM Volume 1, Chapter 5 for additional information on the Strength I load combination). Therefore:

$$R_u = 1.0[1.25(87 + 13) + 1.5(13) + 1.75(139)] = 388 \text{ kips}$$

The width b_t of each projecting stiffener element must satisfy:

$$b_t \le 0.48t_p\sqrt{\frac{E}{F_{ys}}}$$

AASHTO LRFD Equation 6.10.11.2.2-1

Welded bearing stiffeners are also commonly made up of less expensive flat bar stock, which is generally produced in whole-inch width increments and 1/8-in. thickness increments. Try two 7.0-inch-wide bars welded to each side of the web. Rearranging *AASHTO LRFD* Equation 6.10.11.2.2-1 gives:

$$\left(t_p\right)_{min.} = \frac{b_t}{0.48\sqrt{\dfrac{E}{F_{ys}}}}$$

$$\left(t_p\right)_{min.} = \frac{7.0}{0.48\sqrt{\dfrac{29{,}000}{50.0}}} = 0.61 \text{ in.}$$

Try a stiffener thickness t_p of 0.625 inches, which satisfies the preferred minimum thickness of ½ inch for stiffeners given in Reference 40.

According to *AASHTO LRFD* Article 6.10.11.2.3, the factored bearing resistance for the fitted ends of bearing stiffeners is to be taken as:

$$\left(R_{sb}\right)_r = \phi_b\left(R_{sb}\right)_n$$

AASHTO LRFD Equation 6.10.11.2.3-1

where *(R$_{sb}$)$_n$* is equal to the nominal bearing resistance for the fitted end of bearing stiffeners taken as:

$$\left(R_{sb}\right)_n = 1.4A_{pn}F_{ys}$$

AASHTO LRFD Equation 6.10.11.2.3-2

A_{pn} is the area of the projecting elements of the stiffener outside of the web-to-flange fillet welds but not beyond the edge of the flange. Assume for this example that the clip provided at the base of the stiffeners to clear the web-to-flange fillet welds is 1.5 inches in length. The resistance factor for bearing on milled surfaces ϕ_b = 1.0. Therefore:

$$A_{pn} = 2(7.0 - 1.5)(0.625) = 6.88 \text{ in.}^2$$

$$(R_{sb})_n = 1.4(6.88)(50.0) = 482 \text{ kips}$$

$$(R_{sb})_r = (1.0)(482) = 482 \text{ kips} > R_u = 388 \text{ kips} \quad \text{ok}$$

For computing the axial resistance of bearing stiffeners that are welded to the web, *AASHTO LRFD* Article 6.10.11.2.4b states that a portion of the web is to be included as part of the effective column section. For stiffeners consisting of two plates welded to the web, the effective column section is to consist of the two stiffener elements, plus a centrally located strip of web extending not more than $9t_w$ on each side of the stiffeners, as shown in Figure 2.84.

As specified in *AASHTO LRFD* Article 6.10.11.2.4a, the radius of gyration of the effective column section is to be computed about the mid-thickness of the web and the effective length is to be taken as 0.75D, where D is the web depth. The area of the effective column section is computed as:

$$A_s = 2[(7.0)(0.625) + 9(0.5)(0.5)] = 13.25 \text{ in.}^2$$

The moment of inertia of the effective column section (conservatively neglecting the web strip) is computed as:

$$I_s = \frac{0.625(7.0 + 0.5 + 7.0)^3}{12} = 158.8 \text{ in.}^4$$

The radius of gyration of the effective column section is therefore computed as:

$$r_s = \sqrt{\frac{I_s}{A_s}} = \sqrt{\frac{158.8}{13.25}} = 3.46 \text{ in.}$$

The effective length of the effective column section is computed as:

$$K\ell = 0.75D = 0.75(69.0) = 51.75 \text{ in.}$$

Check the limiting slenderness ratio of 120 specified for main members in compression in *AASHTO LRFD* Article 6.9.3:

$$\frac{K\ell}{r_s} = \frac{51.75}{3.46} = 15.0 < 120 \quad \text{ok}$$

As specified in *AASHTO LRFD* Article 6.10.11.2.4a, calculate the factored axial resistance P_r of the effective column section according to the provisions of *AASHTO LRFD* Article 6.9.2.1

$$P_r = \phi_c P_n$$

AASHTO LRFD Equation 6.9.2.1-1

where P_n is equal to the nominal compressive resistance determined as specified in *AASHTO LRFD* Article 6.9.4.1, and ϕ_c is equal to the resistance factor for axial compression = 0.90.

Calculate λ:

$$\lambda = \left(\frac{K\ell}{r_s \pi} \right)^2 \frac{F_{ys}}{E}$$

AASHTO LRFD Equation 6.9.4.1-3

$$\lambda = \left(\frac{51.75}{3.46\pi} \right)^2 \frac{50}{29,000} = 0.039$$

Since $\lambda < 2.25$, then:

$$P_n = 0.66^\lambda F_{ys} A_s$$

AASHTO LRFD Equation 6.9.4.1-1

$$P_n = 0.66^{0.039}(50.0)(13.25) = 652 \text{ kips}$$

$$P_r = 0.9(652) = 587 \text{ kips} > R_u = 388 \text{ kips} \qquad \text{ok}$$

Use 5/8" x 7" bearing stiffeners (one pair).

2.2.6.2.5 Concentrated Loads Applied to Webs Without Bearing Stiffeners

As mentioned previously, at bearing locations on rolled shapes and at other locations on built-up sections or rolled shapes subjected to concentrated loads, where the loads are not transmitted through a deck or deck system, either bearing stiffeners must be provided or else the web must be investigated for the limit states of web local yielding and web crippling as discussed below (refer to *AASHTO* LRFD Article D6.5 – Appendix D to Section 6).

The equations given in *AASHTO LRFD* Article D6.5 are essentially identical to the equations given in the *AISC LRFD* Specification (*26*). As noted in *AASHTO LRFD* Article CD6.5.1, the limit state of sidesway web buckling given in the *AISC LRFD* Specification is not included because it governs only for: 1) members subjected to concentrated loads applied directly to the steel section, 2) members for which the compression flange is braced at the load point, 3) members for which the tension flange is unbraced at the load point, and 4) members for which the ratio of D/t_w to L_b/b_{ft} is less than or equal to 1.7. The preceding conditions do not commonly occur in bridge construction.

2.2.6.2.5.1 Web Local Yielding

The limit state of web local yielding is covered in *AASHTO LRFD* Article D6.5.2, and is intended to prevent localized yielding of the web due to a high compressive or tensile stress caused by a concentrated load or bearing reaction. In order to satisfy this limit state without providing bearing stiffeners, webs subject to compressive or tensile concentrated loads must satisfy the following:

$$R_u \leq \phi_b R_n \qquad \text{Equation 2.214}$$
AASHTO LRFD Equation D6.5.2-1

where:

ϕ_b = resistance factor for bearing specified in *AASHTO LRFD* Article 6.5.4.2 (= 1.0)

R_u = factored concentrated load or bearing reaction (kips)

R_n = nominal resistance to the concentrated loading (kips) taken as follows:

➤ For interior-pier reactions and for concentrated loads applied at a distance from the end of the member that is greater than *d*:

$$R_n = (5k + N)F_{yw}t_w \qquad \text{Equation 2.215}$$
AASHTO LRFD Equation D6.5.2-2

➤ Otherwise:

$$R_n = (2.5k + N)F_{yw}t_w \qquad \text{Equation 2.216}$$
AASHTO LRFD Equation D6.5.2-3

where:

d = depth of the steel section (in.)

k = distance from the outer face of the flange resisting the concentrated load or bearing reaction to the toe of the fillet (in.). For a rolled shape, k is published in the available tables giving dimensions for the shapes. For a built-up section, k may be taken as the distance from the outer face of the flange to the web toe of the web-to-flange fillet weld.

N = length of bearing (in.). N must be greater than or equal to k at end bearing locations.

The preceding equations are largely based on the work described in References 96 and 97. The concentrated load acting on a rolled shape or a built-up section is assumed critical at the toe of the fillet, located a distance *k* from the outer face of the flange resisting the concentrated load or bearing reaction (Figure 2.85). For interior concentrated loads or interior-pier reactions, the load is assumed to distribute along the web at a slope of 2.5 to 1 and over a distance of (5*k* + *N*) according to Equation 2.215 (see also Figure 2.85). An interior concentrated load is assumed to be a load applied at a distance from the end of the member greater than the depth of the steel section *d*. For end concentrated loads or end reactions, the load is assumed to

distribute along the web at the same slope over a distance of $(2.5k + N)$ according to Equation 2.216 (Figure 2.85).
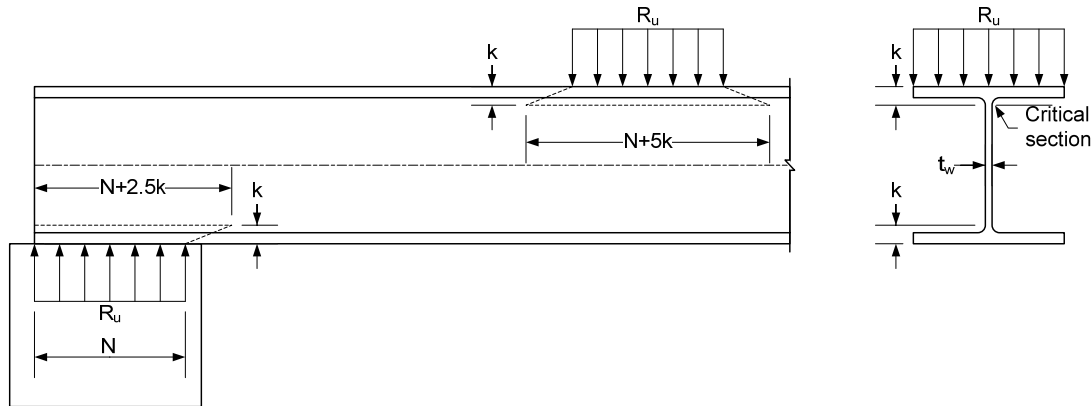
Figure 2.85 Local Web Yielding – Bearing Length and k

2.2.6.2.5.2 Web Crippling

The limit state of web crippling is covered in *AASHTO LRFD* Article D6.5.3, and is intended to prevent local instability or crippling of the web due to a high compressive stress caused by a concentrated load or bearing reaction. In order to satisfy this limit state without providing bearing stiffeners, webs subject to compressive concentrated loads must satisfy the following:

$$R_u \leq \phi_w R_n \qquad \text{Equation 2.217}$$
AASHTO LRFD Equation D6.5.3-1

where:

ϕ_w	=	resistance factor for web crippling specified in *AASHTO LRFD* Article 6.5.4.2 (= 0.80)
R_u	=	factored concentrated load or bearing reaction (kips)
R_n	=	nominal resistance to the concentrated loading (kips) taken as follows:

➤ For interior-pier reactions and for concentrated loads applied at a distance from the end of the member that is greater than or equal to $d/2$:

$$R_n = 0.8 t_w^2 \left[1 + 3\left(\frac{N}{d}\right)\left(\frac{t_w}{t_f}\right)^{1.5} \right] \sqrt{\frac{E F_{yw} t_f}{t_w}} \qquad \text{Equation 2.218}$$
AASHTO LRFD Equation D6.5.3-2

➤ Otherwise:

      ○ If $N/d \leq 0.2$, then:

$$R_n = 0.4t_w^2 \left[1 + 3\left(\frac{N}{d}\right)\left(\frac{t_w}{t_f}\right)^{1.5} \right] \sqrt{\frac{EF_{yw}t_f}{t_w}} \qquad \text{Equation 2.219}$$

AASHTO LRFD Equation D6.5.3-3

o   If N/d > 0.2, then:

$$R_n = 0.4t_w^2 \left[1 + \left(\frac{4N}{d} - 0.2\right)\left(\frac{t_w}{t_f}\right)^{1.5} \right] \sqrt{\frac{EF_{yw}t_f}{t_w}} \qquad \text{Equation 2.220}$$

AASHTO LRFD Equation D6.5.3-4

where:
  d =   depth of the steel section (in.)
  N =   length of bearing (in.). *N* must be greater than or equal to k at end bearing locations.
  t_f =   thickness of the flange resisting the concentrated load or bearing reaction (in.)

Equations 2.218 and 2.219 are based on research described in Reference 98. Equation 2.220 was developed after additional testing to better represent the effect of longer bearing lengths at the ends of members (*99*).

2.2.6.3 Longitudinal Stiffeners

2.2.6.3.1 General

The design of longitudinal web stiffeners is covered in *AASHTO LRFD* Article 6.10.11.3. Longitudinal stiffeners are aligned horizontally on the web along the length of the girder and divide the web panel into smaller sub-panels (Figure 2.86). In the *AASHTO LRFD* Specifications, longitudinal stiffeners are required whenever the web slenderness D/t_w exceeds 150, and are used to provide additional bend-buckling resistance to the webs of deeper girders.

Figure 2.86 Longitudinal Web Stiffeners

Longitudinal stiffeners, where required, are to consist of a plate welded to one side of the web or a bolted angle. As for welded transverse stiffeners and bearing stiffeners, welded longitudinal stiffeners are also commonly made up of less expensive flat bar stock, which is generally produced in whole-inch width increments and 1/8-in. thickness increments.

As specified in *AASHTO LRFD* Article 6.10.11.3.1, longitudinal stiffeners are to be located vertically on the web such that adequate web bend-buckling resistance is provided for constructibility and at the service limit state; i.e., the stiffeners must be located such that Equation 2.73 is satisfied when checking constructibility and Equation 2.81 is satisfied at the service limit state (see Section 2.2.2.4 of this chapter on Web Bend Buckling Resistance regarding the calculation of the web bend buckling resistance F_{crw} for a web with longitudinal stiffeners). It also must be verified that the section has adequate nominal flexural resistance at the strength limit state with the longitudinal stiffener in the selected position (see Sections 2.2.3.7 and 2.2.4.7 of this chapter on Strength Limit State Verifications).

For composite sections in positive flexure, the depth of the web in compression D_c in the elastic range changes relative to the vertical position of longitudinal stiffener after the concrete deck has been placed. As discussed in Section 2.2.2.3.1 of this chapter on the Depth of the Web in Compression in the Elastic Range, D_c for composite sections is a function of the dead-to-live load stress ratio because the dead and live loads are applied to different sections in a composite girder. For composite sections in positive flexure in particular, the dead load stress has a significant effect on the location of the elastic neutral axis. The noncomposite dead load stresses acting on the steel section alone cause the neutral axis to be lower than it would if all loads were applied to the composite section. This effect increases with increasing span length. After the deck has hardened and dead and live loads are applied to the composite section, the neutral axis moves higher on the web and D_c changes relative to the vertical position of the longitudinal stiffener, which is

usually located a fixed distance from the compression flange in these regions. As a result, the computed web bend-buckling resistance is different before and after placement of the deck and is dependent on the loading. Therefore, several trial locations of the stiffener on the web may be necessary in these regions in order to determine a location of the stiffener to satisfy Equation 2.73 when checking constructibility, Equation 2.81 at the service limit state and all applicable strength limit state criteria. The reader is referred to Section 2.2.2.4 of this chapter on Web Bend Buckling Resistance for additional information on this topic, and for an example calculation illustrating the process of locating a longitudinal web stiffener on the web of a composite girder in a region of positive flexure. It should be noted that *AASHTO LRFD* Article C6.10.11.3.1 provides the following equation for determining an initial trial location of a longitudinal stiffener in regions of positive flexure:

$$\frac{d_s}{D_c} = \frac{1}{1 + 1.5\sqrt{\dfrac{f_{DC1} + f_{DC2} + f_{DW} + f_{LL+IM}}{f_{DC1}}}} \qquad \text{Equation 2.221}$$

AASHTO LRFD Equation C6.10.11.3.1-1

where:

d_s = distance from the centerline of a plate longitudinal stiffener, or the gage line of an angle longitudinal stiffener, to the inner surface or leg of a compression-flange element (in.)

D_c = depth of the web of the noncomposite steel section in compression in the elastic range (in.)

f_{xx} = compression-flange stresses at the strength limit state caused by the different factored loads acting on their respective sections at the section with the maximum compressive flexural stress (ksi). Flange lateral bending is to be disregarded.

However, it is further noted that the stiffener may need to be moved vertically up or down from this initial trial location in order to satisfy all the specified limit-state criteria.

At composite sections in negative flexure and noncomposite sections, it is recommended that the longitudinal stiffener initially be located at $0.4D_c$ from the inner surface of the compression flange. For composite sections in negative flexure, D_c would be conservatively calculated for the section consisting of the steel girder plus the longitudinal reinforcement. For noncomposite sections, D_c would be based on the section consisting of the steel girder alone. Based on theoretical and experimental studies on noncomposite girders, the optimum location of a single longitudinal stiffener is $0.4D_c$ for bending and $0.5D$ for shear. Tests have also shown that longitudinal stiffeners located at $0.4D_c$ on these sections can effectively control lateral web deflections due to bending (*10*). Because shear is always accompanied by moment and because a properly proportioned longitudinal stiffener will also reduce lateral web deflections due to shear, the distance of $0.4D_c$ is recommended. For these sections, the stiffener may need to be moved vertically up or down from this initial trial location, especially for cases where the concrete deck is assumed effective in tension in regions of negative flexure at the service limit state as

permitted in *AASHTO LRFD* Article 6.10.4.2.1. In this case, D_c at the service limit state must be calculated based on the accumulated stresses using Equation 2.7 (as specified in *AASHTO LRFD* Article D6.3.1).

Because D_c may vary along the span, it is suggested that the longitudinal stiffener be located based on D_c computed at the section with the largest compressive flexural stress. Other sections must also be examined to ensure they satisfy the specified limit states since the stiffener cannot be at its optimum location at other sections along the girder length with a lower stress and a different value of D_c.

In some cases, particularly in regions of stress reversal, it may be necessary or desirable to use two longitudinal stiffeners on the web. The use of two longitudinal stiffeners on the web is discussed in greater detail in Section 2.2.2.4 of this chapter.

It is preferred that longitudinal stiffeners be placed on the opposite side of the web from transverse stiffeners. At bearing stiffeners and connection plates where the longitudinal stiffener and transverse web element must intersect, a decision must be made as to which element to interrupt. According to *AASHTO LRFD* Article 6.10.11.3.1, wherever practical, longitudinal stiffeners are to extend uninterrupted over their specified length, unless otherwise permitted in the contract documents, since longitudinal stiffeners are designed as continuous members to improve the web bend buckling resistance. In such cases, the interrupted transverse elements must be fitted and attached to both sides of the longitudinal stiffener with connections sufficient to develop the flexural and axial resistance of the transverse element. If the longitudinal stiffener is interrupted instead, it should be similarly attached to all transverse elements. All interruptions must be carefully designed with respect to fatigue, especially if the longitudinal stiffener is not attached to the transverse web elements, as a punitive Category E or E′ detail may exist at the termination points of each longitudinal stiffener-to-web weld. Copes should always be provided to avoid intersecting welds. If an interrupted longitudinal stiffener is attached to a transverse web element, Equation 2.84 may apply in checking fatigue (refer to Figure 2.45).   Reference 65 provides suggested longitudinal stiffener end details (and other related fatigue details).   Should longitudinal stiffeners be discontinued at bolted field splices, consideration should be given to taking the stiffener to the free edge of the web where the normal stress is zero to avoid the fatigue-sensitive details at the termination of the stiffener-to-web welds. This would require splitting of the web splice plates.

Longitudinal stiffeners are subject to the same flexural strain as the web at their vertical position on the web. As a result, the stiffeners must have sufficient strength and rigidity to resist bend buckling of the web (at the appropriate limit state) and to transmit the stresses in the stiffener and an effective portion of the web as a equivalent column (*10*).   Therefore, as specified in *AASHTO LRFD* Article 6.10.11.3.1, the flexural stress in the longitudinal stiffener due to the factored loads f_s must satisfy the following at the strength limit state and when checking constructibility:

$$f_s \leq \phi_f R_h F_{ys} \qquad\qquad \text{Equation 2.222}$$

AASHTO LRFD Equation 6.10.11.3.1-1

where:

ϕ_f =   resistance factor for flexure specified in *AASHTO LRFD* Article 6.5.4.2 (= 1.0)

F_{ys} =   specified minimum yield strength of the longitudinal stiffener (ksi)

R_h =   hybrid factor determined as specified in *AASHTO LRFD* Article 6.10.1.10.1

The hybrid factor R_h is included in Equation 2.222 to account for the influence of local web yielding on the longitudinal stiffener stress in hybrid sections. The appropriate corresponding value of R_h should be applied for the strength limit state and constructibility checks (see Section 2.2.2.6 of this chapter on the Hybrid Factor).

2.2.6.3.2 Projecting Width

As specified in *AASHTO LRFD* Article 6.10.11.3.2, the projecting width b_ℓ of the longitudinal stiffener must satisfy the following requirement in order to prevent local buckling of the stiffener plate:

$$b_\ell \leq 0.48 t_s \sqrt{\frac{E}{F_{ys}}} \qquad \text{Equation 2.223}$$

AASHTO LRFD Equation 6.10.11.3.2-1

where:

F_{ys} =   specified minimum yield strength of the stiffener (ksi)

t_s =   thickness of the longitudinal stiffener (in.)

2.2.6.3.3 Moment of Inertia

As specified in *AASHTO LRFD* Article 6.10.11.3.3, to ensure that a longitudinal stiffener will have adequate rigidity to maintain a horizontal line of near zero lateral deflection in the web to resist bend buckling of the web (at the appropriate limit state), the moment of inertia of the stiffener acting in combination with an adjacent strip of web must satisfy the following requirement (*18*):

$$I_\ell \geq D t_w^3 \left[2.4 \left(\frac{d_o}{D} \right)^2 - 0.13 \right] \beta \qquad \text{Equation 2.224}$$

AASHTO LRFD Equation 6.10.11.3.3-1

where:

d_o =   transverse stiffener spacing (in.)

I_ℓ =   moment of inertia of the longitudinal stiffener including an effective width of the web equal to $18t_w$ taken about the neutral axis of the combined section (in.[4]). If F_{yw} is smaller than F_{ys}, the strip of web

included in the effective section must be reduced by the ratio of F_{yw}/F_{ys}.

β =   curvature correction factor for longitudinal stiffener rigidity calculated as follows (equal to 1.0 for longitudinal stiffeners on straight webs):

➢ For cases where the longitudinal stiffener is on the side of the web away from the center of curvature

$$\beta = \frac{Z}{6} + 1$$ Equation 2.225

AASHTO LRFD Equation 6.10.11.3.3-3

➢ For cases where the longitudinal stiffener is on the side of the web toward the center of curvature

$$\beta = \frac{Z}{12} + 1$$ Equation 2.226

AASHTO LRFD Equation 6.10.11.3.3-4

where:
    Z   =   curvature parameter taken as follows:

$$Z = \frac{0.95d_o^2}{Rt_w} \leq 10$$ Equation 2.227

AASHTO LRFD Equation 6.10.11.3.3-5

where:
    R   =   minimum girder radius in the panel (in.)

As suggested in Reference 10, the moment of inertia (and radius of gyration – see below) of the longitudinal stiffener is taken about the neutral axis of an equivalent column cross-section consisting of the stiffener and an adjacent strip of web with a width of 18t_w. For a web having a lower yield strength than the yield strength of the longitudinal stiffener, the web strip that contributes to the effective column section is reduced by F_{yw}/F_{ys} in computing the moment of inertia of the longitudinal stiffener. Previous specifications required that the moment of inertia (and radius of gyration) of the stiffener be taken about the edge in contact with the web plate.

Longitudinal stiffeners on horizontally curved webs require greater rigidity than on straight webs because of the tendency of curved webs to bow. This is reflected by including the factor β in Equation 2.224, which is a simplification of a requirement for longitudinal stiffeners on curved webs given in Reference 100. For longitudinal stiffeners on straight webs, β is taken equal to 1.0.

2.2.6.3.4 Radius of Gyration

As specified in *AASHTO LRFD* Article 6.10.11.3.3, to ensure that the longitudinal stiffener acting in combination with an adjacent strip of web as an effective column section can withstand the axial compressive stress without lateral buckling, the radius of gyration of the effective column section must satisfy the following requirement:

$$r \geq \frac{0.16 d_o \sqrt{\dfrac{F_{ys}}{E}}}{\sqrt{1 - 0.6 \dfrac{F_{yc}}{R_h F_{ys}}}} \qquad \text{Equation 2.228}$$

AASHTO LRFD Equation 6.10.11.3.3-2

where:

d_o	=	transverse stiffener spacing (in.)
r	=	radius of gyration of the longitudinal stiffener including an effective width of the web equal to $18 t_w$ taken about the neutral axis of the combined section (in.)
F_{ys}	=	specified minimum yield strength of the longitudinal stiffener (ksi)
R_h	=	hybrid factor determined as specified in *AASHTO LRFD* Article 6.10.1.10.1

Equation 2.228 is a modification of the original requirement given in Reference 10 that accounts for the possibility of different specified minimum yield strengths for the longitudinal stiffener and compression flange. The hybrid factor R_h is also included in the equation to approximate the influence of a lower yield strength web in a hybrid section. For a section with F_{yc}/F_{ys} greater than one, a significantly larger radius of gyration is required than in previous Specifications because in this case, the longitudinal stiffener is subjected to larger stresses than in an equivalent homogeneous section. Equation 2.228 is valid as long as Equation 2.222 is satisfied to prevent full nominal yielding of the longitudinal stiffener at the strength limit state.

89. Ketchum, M.S. 1920. *The Design of Highway Bridges of Steel, Timber and Concrete.* McGraw-Hill Book Company, New York, NY.
90. Kim, Y.D., S.K. Jung, and D.W. White. 2004. "Transverse Stiffener Requirements in Straight and Horizontally Curved Steel I-Girders." Structural Engineering Report No. 36, School of Civil and Environmental Engineering, Georgia Institute of Technology, Atlanta, GA.
91. Bleich, F. 1952. *Buckling Strength of Metal Structures.* McGraw-Hill, New York, NY.
92. Horne, M.R., and W.R. Grayson. 1983. "Parametric Finite Element Study of Transverse Stiffeners for Webs in Shear." Instability and Plastic Collapse of Steel Structures, Proceedings of the Michael R. Horne Conference, L.J. Morris (ed.), Granada Publishing, London, England.
93. Rahal, K.N., and J.E. Harding. 1990. "Transversely Stiffened Girder Webs Subjected to Shear Loading – Part 1: Behaviour." *Proceedings of the Institution of Civil Engineers*, Part 2, 89, March.

94.	Stanway, G.S., J.C. Chapman, and P.J. Dowling. 1996. "A Design Model for Intermediate Web Stiffeners." *Proceedings of the Institution of Civil Engineers, Structures and Buildings*, 116, February.

95.	Lee, S.C., C.H. Yoo, and D.Y. Yoon. 2003. "New Design Rule for Intermediate Transverse Stiffeners Attached on Web Panels." *Journal of Structural Engineering*, American Society of Civil Engineers, Reston, VA, 129(12).

96.	Johnston, B.G., and G.G. Kubo. 1941. "Web Crippling at Seat Angle Supports." Fritz Engineering Laboratory, Report No. 192A2, Lehigh University, Bethlehem, PA.

97.	Graham, J.D., A.N. Sherbourne, R.N. Khabbaz, and C.D. Jensen. 1959. *Welded Interior Beam-to-Column Connections*. American Institute of Steel Construction, New York, NY.

98.	Roberts, T.M. 1981. "Slender Plate Girders Subjected to Edge Loading." *Proceedings, Institution of Civil Engineers*, Part 2, 71, London.

99.	Elgaaly, M., and R. Salkar. 1991. "Web Crippling Under Edge Loading." *Proceedings of the AISC National Steel Construction Conference*, Washington, D.C.

100.	Hanshin Expressway Public Corporation and Steel Structure Study Subcommittee. 1988. "Guidelines for the Design of Horizontally Curved Girder Bridges (Draft)." Hanshin Expressway Public Corporation, October.

2.3 Connection and Splice Design

2.3.1 General

Connection and splice design is covered in *AASHTO LRFD* Article 6.13. The design of bolted connections is covered in *AASHTO LRFD* Article 6.13.2. The design of welded connections is covered in *AASHTO LRFD* Article 6.13.3. The design of splices is covered in *AASHTO LRFD* Article 6.13.6. *AASHTO LRFD* Articles 6.13.4 and 6.13.5 deal with the topics of block shear rupture resistance and the design of connection elements (e.g. splice plates, gusset plates, brackets, etc.) in tension and shear, respectively. Each of these topics will be covered in detail in the following sections. *AASHTO LRFD* Article 6.13.7 deals with the design of rigid frame connections, which will not be covered in this Manual.

AASHTO LRFD Article 6.13.1 covers several general considerations related to connection and splice design. Where practical, connections should be made symmetrical about the axis of the members. Members, including bracing, should be connected so that their gravity axes will intersect at a point. Eccentric connections should be avoided, however, where this is not possible, the members and connections must be designed for the combined effects of the shear and moment due to the eccentricity. Bolted connections, except for connections on lacing and handrails, are to contain not less than two bolts.

Where connection angles are used at the ends of stringers, floorbeams and girders, two angles should be used and the thickness of the angles must not be less than 0.375 in. Bracket or shelf angles that may be used to furnish support during erection are not to be considered in determining the number of bolts required to transmit the end shear. Should timber stringers frame into steel floorbeams, shelf angles with stiffeners and with a thickness not less than 0.4375 in., are to be provided to support the total reaction.

End connections of stringers, floorbeams and girders should be connected with high-strength bolts. Where bolting is not practical, welded connections may be used, but they must be designed for the vertical loads and any bending moment resulting from restraint against end rotation.

With the important exception noted in the next paragraph, as specified in *AASHTO LRFD* Article 6.13.1, connections and splices for primary members (i.e. members designed to carry the internal forces determined from an analysis) are to be designed *at the strength limit state* for not less than the larger of:

➢ The average of the flexural moment-induced stress, shear or axial force due to the factored loads at the point of splice or connection and the factored flexural, shear or axial resistance of the member or element at the same point, or

➢ 75 percent of the factored flexural, shear or axial resistance of the member or element.

The important exception to the above requirement is stated as follows. ***Where cross-frames/diaphragms, lateral bracing, stringers or floorbeams for straight or horizontally curved members are included in the structural model used to determine force effects, or are designed for explicitly calculated force effects from the results of a separate investigation (e.g. an approximate wind load analysis), the end connections for those members are to be designed for the calculated factored member force effects. Otherwise, the end connections for these members are to be designed according to the 75 percent resistance provision given above.*** The preceding exception results from experience indicating that application of the 75 percent and average load provisions to the end connections of these members in which force effects have been determined by analysis has tended to result in large connections with large eccentricities and force concentrations. Therefore, it was felt by the specification writers that the above exception was justified to prevent the complications resulting from such large connections.

2.3.2 Bolted Connections

2.3.2.1 General

The design of bolted connections is covered in *AASHTO LRFD* Article 6.13.2. As specified in *AASHTO LRFD* Article 6.13.2.1, bolted steel parts must fit solidly together after the bolts are tightened. The bolted parts may be coated or uncoated. It must be specified in the contract documents that all joint surfaces, including surfaces adjacent to the bolt head and nut, be free of scale (except for tight mill scale), dirt or other foreign material. All material within the grip of the bolt must be steel.

As discussed in more detail below, high-strength bolts are installed to have a specified initial tension, which results in an initial precompression between the joined parts. At service load levels, the transfer of the loads between the joined parts may then occur entirely via friction with no bearing of the bolt shank against the side of the hole. Until the friction force is overcome, the shear resistance of the bolt and the bearing resistance of the bolt hole will not affect the ability to transfer the load across the shear plane between the joined parts.

In general, high-strength bolted connections designed according to the *AASHTO LRFD* Specification provisions will have a higher reliability than the connected parts because the resistance factors for the design of bolted connections were selected to provide a higher level of reliability than those chosen for member design. Also, the controlling strength limit state in the connected part, e.g. yielding or deflection, is typically reached well before the controlling strength limit state in the connection, e.g. the bolt shear resistance or the bearing resistance of the connected material.

The *AASHTO LRFD* Specifications recognize two types of high-strength bolted connections; slip-critical connections and bearing-type connections. The resistance of all high-strength bolted connections in transmitting shear across a shear plane between bolted steel parts is the same whether the connection is a slip-critical or

bearing-type connection. The slip-critical connection has an additional requirement that slip must not occur between the joined parts at service load levels.

2.3.2.1.1 Slip-Critical Connections

In high-strength bolted slip-critical connections subject to shear, the load is transferred between the joined parts by friction up to a level of force that is dependent upon the clamping force and the coefficient of friction of the faying surfaces. The coefficient of friction depends on the faying surface condition, with mill scale, paint or other surface treatments determining the value of the friction coefficient. Prior to joint slip, the bolts are not subject to shear nor are the joined parts subject to bearing stress. Once the load exceeds the frictional resistance between the faying surfaces, slip occurs; that is, the friction bond is broken and the two surfaces slip with respect to one another by a relatively large amount. A rupture failure does not occur. Therefore, the connection is able to continue resisting an even greater load through the shear resistance of the bolts and the bearing resistance against the connected material. Final failure of the connection will be by shear failure of the bolts, yielding or tear-out of the connected material or by an unacceptable deformation around the holes; the ultimate resistance of the connection is not related to the slip load. The slip and bearing resistances are computed separately for application at different load combinations (the calculation of the slip, shear and bearing resistances of bolted connections and the resistance of the connected material is discussed in more detail below). Because a high tensile force on the bolt is required to develop a significant resisting friction force, only bolts with a high tensile yield strength (i.e. A 325 and A 490 high-strength bolts) can be used in slip-critical connections.

As specified in AASHTO LRFD Article 6.13.2.1.1, slip-critical connections are to be proportioned to prevent slip under Load Combination Service II and to provide bearing, shear and tensile resistance under the applicable strength load combinations (see DM Volume 1, Chapter 5 for further information on the Service II and Strength load combinations). Slip is to be prevented under Load Combination Service II to control permanent deformations caused by slip in bolted joints that could adversely affect the serviceability of the structure. It is further assumed that under the strength load combinations, slip between the bolted parts occurs at the higher loads and that the bolts have gone into bearing against the connected material. Thus, the shear resistance of the bolts and bearing resistance of the bolt holes must be checked under the appropriate strength load combination. In addition, the resistance of the connected material must be checked at the strength limit state.

According to *AASHTO LRFD* Article 6.13.2.1.1, bolted joints subject to stress reversal, heavy impact loads, severe vibration or located where stress or strain due to joint slippage would be detrimental to the serviceability of the structure are to be designated as slip-critical (the reader is referred to this article for the specific list of joints that should be designated as slip-critical). Repeated loading may introduce fatigue concerns if slip occurs in these cases, particularly when oversize or slotted holes are used (see the section below on Holes).

The behavior of a bolted connection under fatigue loading is influenced by the type of load transfer in the connection. In tests of slip-critical lap joints subject to in-plane cyclic loading, crack initiation and growth typically occurred in the gross section in front of the first bolt hole of the connection (*101*). The cracks initiated on the faying surfaces. Failures that occur at the interface of metallic surfaces that are in contact and that slip a small amount relative to each other under an oscillating load are referred to as fretting failures. The point where fretting is initiated depends on the discontinuities of the mill scale, the clamping zone of the bolt and the frictional resistance of the faying surface. In bearing-type connections (see below) where the load is transmitted primarily by shear and bearing, the crack typically initiates instead at the edge of the bolt hole and grows in the region of the net section, with failure eventually occurring due to fracture of the net section. However, it was observed that slip-critical connections designed based on the gross section (i.e. stress ranges computed on the gross section) and bearing-type connections designed based on the net section (i.e. stress ranges computed on the net section) provide approximately the same nominal fatigue resistance.   It was determined that fatigue detail Category B (see the previous section of this chapter on Fatigue Limit State Verifications) provides a reasonable and conservative lower bound to the test data in both cases (*101*). Therefore, *AASHTO LRFD* Table 6.6.1.2.3-1 indicates that base metal at the gross section of high-strength bolted slip-critical connections and at the net section of high-strength bolted bearing-type connections subject to a net applied tensile stress (as defined in *AASHTO LRFD* Article 6.6.1.2.1) be designed for fatigue based on Category B. As discussed later, axially loaded joints subject to fatigue loading in direct tension (versus shear), in addition to prying action, are treated differently according to the provisions of *AASHTO LRFD* Article 6.13.2.10.3.

2.3.2.1.2 Bearing-Type Connections

In high-strength bolted bearing-type connections, the load is resisted by a combination of the shear resistance of the bolt, the bearing resistance of the connected material and an unknown amount of friction between the faying surfaces. The failure of a bearing-type connection will be by shear failure of the bolts, yielding or tear-out of the connected material or by an unacceptable deformation around the holes, with the final failure load independent of the clamping force provided by the bolts (*101*).

As specified in *AASHTO LRFD* Article 6.13.2.1.2, bearing-type connections are only to be permitted on bridges for joints subject to axial compression or joints on bracing members. Such connections are to be designed to provide the required factored resistance in shear and bearing at the strength limit state. Connections utilizing A 307 bolts are to be designed as bearing-type connections.

2.3.2.2 Bolts, Nuts and Washers

2.3.2.2.1 Bolts

2.3.2.2.1.1 Unfinished Bolts

Unfinished bolts, also referred to as common, machine, ordinary or rough bolts, are manufactured from low-carbon steel and are designated as ASTM A 307 bolts. There is no corresponding AASHTO material standard to ASTM A 307. Three grades – Grades A, B, and C – are covered in the ASTM standard. Grade A is the quality that is typically used for general structural applications. Grade A bolt heads and nuts are manufactured with a regular square shape. Grade B bolts are typically used for flanged joints in piping-systems with cast iron flanges. As indicated in *AASHTO LRFD* Article 6.4.3.1, the specified minimum tensile strength of these bolts (specifically Grades A and B) is 60 ksi. These bolts are typically tightened using long-handled manual wrenches and hardened steel washers are not generally used. Since these bolts do not have a specified proof load, they should only be used for connecting relatively light auxiliary components or members subject to light static loads or for temporary fit-up. These bolts should not be used in connections subject to slip or vibration because of the tendency of the nuts to loosen. ASTM A 307 Grade C bolts are nonheaded anchor bolts, either bent or straight, intended for structural anchorage purposes. The properties of ASTM A 307 Grade C bolts conform to the properties of ASTM A 36 material.

2.3.2.2.1.2 High-Strength Bolts

High-strength bolts are heavy hexagon-head bolts used with heavy semi-finished hexagon nuts. The threaded portion of high-strength bolts is shorter than for bolts used for nonstructural applications, which reduces the probability of having the threads present in the shear plane. High-strength bolts produce large and predictable tension when tightened. Initial tensioning of high-strength bolts results in more rigid joints and greater assurance against nut loosening in connections subject to slip or vibration.

High-strength bolts have replaced rivets as the primary means of making nonwelded structural connections. Initial experiments on high-strength bolted connections were first reported in Reference 102 in 1934. Follow-up research in 1938 (*103*) indicated that high-strength bolts had fatigue strengths equal to those of well-driven rivets as long as the bolts were sufficiently pretensioned. In 1947, the Research Council on Riveted and Bolted Structural Joints (currently known as the Research Council on Structural Connections or RCSC) was formed to carry out cooperative research into the behavior of various types of connections joined with rivets and bolts. The new Council began by using and extrapolating information from studies of riveted joints in order to evaluate the merits of high-strength bolts used in structural connections. This led to the publication by the Council in 1951 of the first edition of the "Specifications for Structural Joints Using A 325 Bolts", which permitted the replacement of rivets with bolts on a one-to-one basis. This specification assumed that friction transfer was necessary in all joints at service load conditions. The factor

of safety against slip was set at a high enough level to ensure fatigue resistance that was similar to or better than the fatigue resistance of riveted joints.

Additional research in 1956 (*104*) concluded that for high-strength bolts to be efficient and economical, the minimum initial bolt tension should be as high as practical. Therefore, by 1960, the minimum initial bolt tension was increased. Also, the bearing-type connection (i.e. a connection where the resistance of the connection is based on bearing of the bolt against the side of the hole and where high slip resistance at service loads is unnecessary) was recognized as an acceptable substitute for a riveted connection. It was further recognized that the so-called friction-type connection (now referred to as a slip-critical connection), in which the connection is designed on the basis of slip resistance at service loads, would only be necessary when stress reversals occur or when direct tension acts on the bolts. In 1960, the turn-of-the-nut installation method was also introduced as an alternative to the torque wrench (or calibrated wrench) method.   Furthermore, when the turn-of-the-nut method was used, only one washer located under the head of the element being turned was required, which further improved the economics of high-strength bolting. Previously, two washers were required in the connection. By 1962, the requirement for washers was eliminated, except for special circumstances (discussed below under Washers). In 1964, the higher strength ASTM A 490 bolt was introduced. The philosophy of the design of bearing-type and friction-type connections was revised in later versions of the RCSC Specifications in the mid to late 1980s. The reader is referred to the RCSC Specifications (*105*) and to Reference 101 (both documents are available for download from www.boltcouncil.org) for additional more detailed information on the historical background, research and recommendations that form the basis of the current *AASHTO LRFD* Specification provisions for the design of high-strength bolted connections.

As specified in *AASHTO LRFD* Article 6.4.3.1, ASTM A 325 bolts in diameters of 0.5 inch through 1 inch have a required minimum tensile strength of 120 ksi.   ASTM A 325 bolts in diameters of 1.125 inch through 1.5 inch have a required minimum tensile strength of 105 ksi. ASTM A 490 bolts in diameters of 0.5 inch to 1.5 inch have a required minimum tensile strength of 150 ksi. Both A 325 and A 490 bolts are available as Types 1 or 3 (Note: Type 2 bolts are no longer available). The A 325 Type 1 bolt is a medium-carbon steel bolt. The A 490 Type 1 bolt is an alloy steel bolt. Type 1 bolts are to be used with steels other than weathering steel and is the type furnished if not otherwise specified.   Type 1 bolts may be either mechanically or hot-dip galvanized. However, galvanizing of A 490 bolts (by either process) is not permitted due to the potential for hydrogen embrittlement (*105*). When galvanized A 325 bolts are used on weathering steel projects, only hot-dip galvanized bolts should be used as the relatively thin sacrificial coating on mechanically galvanized bolts will corrode too quickly in an uncoated weathering steel application. Galvanized bolts must be tension tested after galvanizing. The bolts, nuts and washers in any assembly must be galvanized using the same process. As discussed further in the section below on Nuts, galvanized nuts should be over-tapped to the minimum amount required for the assembly and lubricated with a lubricant containing a visible dye to allow for a visual check of the lubricant at the time of field installation. Type 3 bolts have an atmospheric corrosion resistance

and weathering characteristics comparable to weathering steels and are to be used only in weathering steel applications. A 325 and A 490 bolts (and the various bolt types) are distinguished by specific identifying marks described in Reference 105.

For high-strength bolts used in slip-critical connections, pretensioning of the bolt should be as high as possible without causing permanent deformation or failure of the bolt. As shown in Figure 2.87, the stress-strain or load-elongation behavior of bolt material in a direct-pull tension test has no well-defined yield point.
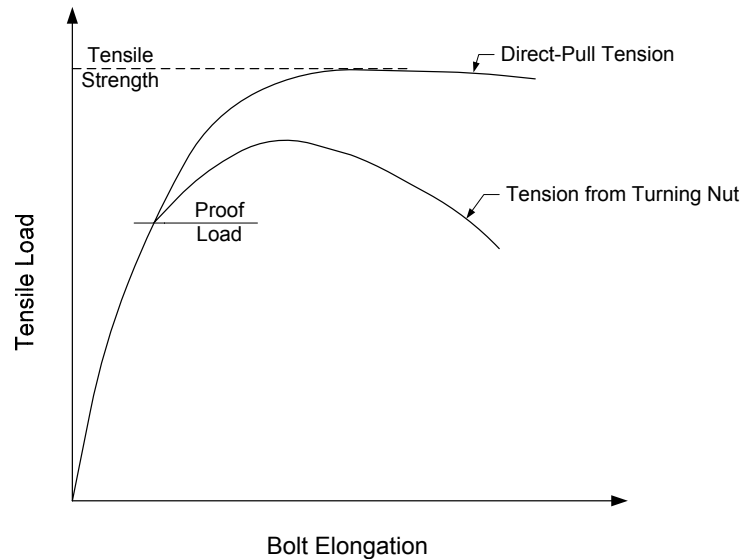
Figure 2.87 Typical Tensile Load-Elongation Curve for a High-Strength Bolt

Instead, a so-called proof load is used in lieu of directly specifying a yield stress. The proof load is obtained by multiplying the tensile stress area by a yield stress obtained by using either a 0.2% offset strain or a 0.5% extension under load. The tensile stress area is equal to the following:

$$\text{Tensile stress area} = 0.785 + \left(d - \frac{0.9743}{n} \right)^2 \quad \text{Equation 2.229}$$

where d is the bolt diameter and n is the number of threads per inch. For A 325 and A 490 bolts, the proof load stress is approximately a minimum of 70% and 80%, respectively, of the minimum tensile strength of the bolt, which is also established in a direct-pull tension test (Figure 2.87). In actual connections, the pretension in the bolt is established by turning the nut, which results in elongation of the bolt. Because of the torsional stresses in the bolt caused by tightening in this manner, the tensile strength and total elongation induced in the bolt by turning the nut are somewhat less than in a direct-pull tension test (*106, 107*). *AASHTO LRFD* Table 6.13.2.8-1 (Table 2.16) specifies the minimum required bolt tension for A 325 and A 490 bolts used in slip-critical connections, which is taken equal to 70% of the minimum tensile strength of the respective bolts. The minimum required bolt tension

is equal to the proof load for A 325 bolts and about 85 to 90% of the proof load for A 490 bolts.

Table 2.16 Minimum Required Bolt Tension

Bolt Diameter, in.	Required Tension-P_t (kips)	
	A 325	A 490
5/8	19	24
3/4	28	35
7/8	39	49
1	51	64
1-1/8	56	80
1-1/4	71	102
1-3/8	85	121
1-1/2	103	148

In order to obtain the minimum required bolt tension, four general methods of installing the bolts can be used: 1) turn-of-the-nut tightening, 2) calibrated wrench tightening, 3) installation of alternative fasteners, or 4) installation of load indicator devices.

The turn-of-the-nut method is the simplest and obtains the pretension by a specified rotation of the nut from the "snug tight" condition, which is defined as the point at which the turned element ceases to rotate freely and the impact wrench begins to impact. If ordinary spud wrenches are used, the "snug tight" position is signaled by the full effort of the worker. A sufficient number of bolts must initially be brought to the "snug tight" position to bring the connection components into full contact. All remaining bolts in the connection are then brought to the "snug tight" position. Once this phase is completed, all nuts in the joint are given an additional rotation depending on the bolt length and the type of connection. The additional rotation causes a specified strain in the bolt controlling the bolt elongation and obtaining bolt tension well beyond the specified proof load. In the plastic range, large changes in bolt strain cause small changes in bolt tension allowing high clamping forces to be consistently obtained under the additional specified rotation regardless of the variation of the initial "snug tightness".

Calibrated wrench tightening utilizes torque control to obtain the appropriate bolt tensions. Either manual torque wrenches or power wrenches adjusted to stall at a specified torque are used. To prevent large variations in bolt tensions, calibrated wrenches must be set to produce a bolt tension 5% in excess of the values prescribed in Table 2.16. Calibration must be repeated at least daily or whenever the wrench is used to tighten a different size bolt. A hardened washer must be used under the turned element (head or nut).

High-strength bolt installation utilizing alternative fasteners and load indicator devices is discussed in more detail below.

Regardless of the method used, the final tightening sequence should proceed in an orderly fashion from the most rigid part of the connection progressing systematically toward the less rigid areas or free edges. Additional more detailed information on high-strength bolt installation procedures and bolt inspection procedures (including required rotation capacity testing) may be found in References 105 and 108.

2.3.2.2.1.3 Alternative Fasteners

Alternative fasteners or fastener assemblies are permitted if approved by the Engineer and provided they satisfy the general provisions of *AASHTO LRFD* Article 6.4.3.4. Alternative fasteners are generally proprietary fasteners designed to automatically provide the required tension or indirectly indicate the bolt tension. Included in this category are so-called twist-off bolts (conforming to the requirements of ASTM F 1852) and lock-pin and collar fasteners.

2.3.2.2.1.4 Load Indicator Devices

Load indicating devices conforming to the requirements of ASTM F 959, or other alternate direct tension indicating devices approved by the Engineer, may be used according to *AASHTO LRFD* Article 6.4.3.5.   Load indicator devices conforming to ASTM F 959 are hardened washers with several formed arches that deform in a controlled manner when subjected to a compressive load. The washer is inserted between the turned element (head or nut) and the gripped material with the protrusions bearing against the underside of the element with a gap maintained by the protrusions. Tightening of the bolt flattens the protrusions and reduces the gap. The bolt tension is then determined by measuring the remaining gap with a feeler gage. For proper tension, the gap should be about 0.015 in. or less (*109*).   As specified in *AASHTO LRFD* Article 6.13.2.3.2, load indicator devices are not to be installed over oversize or slotted holes in an outer ply, unless a hardened washer or a structural plate washer is also provided.

2.3.2.2.1.5 Size of Bolts

AASHTO LRFD Article 6.13.2.5 gives some specific requirements regarding the size of bolts. Bolts are not to less than 0.625 in. in diameter. Bolts 0.625 in. in diameter are not to be used in primary members, except for 2.5-in. legs of angles and in flanges of sections whose dimensions require 0.625-in. bolts to satisfy other detailing provisions given in the Specifications. Structural shapes that do not permit the use of 0.625-in. bolts are to be limited to use in handrails.

The diameter of bolts in angles that serve as primary members is not to exceed one-fourth of the width of the leg in which the bolts are placed. Finally, angles whose size is *not* determined by a calculated demand may use the following bolt sizes: 1) 0.625-in. diameter bolts in 2.0-in. legs; 2) 0.75-in. diameter bolts in 2.5-in. legs; 3) 0.875-in. diameter bolts in 3.0-in. legs; and 4) 1.0-in. diameter bolts in 3.5-in. legs.

2.3.2.2.1.6 Spacing of Bolts

2.3.2.2.1.6.1 Minimum Spacing and Clear Distance

As specified in *AASHTO LRFD* Article 6.13.2.6.1, the minimum spacing between centers of bolts in standard holes is not to be less than 3.0d, where d is the diameter of the bolt (Figure 2.88).
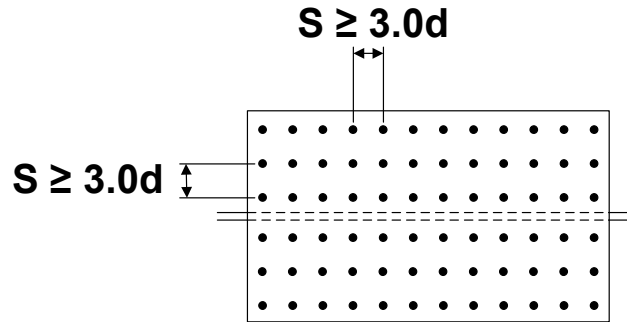
Figure 2.88 Minimum Spacing Between Centers of Bolts

When oversize or slotted holes are used, the minimum clear distance L_c between the edges of adjacent bolt holes in the direction of the force and transverse to the direction of the force is not to be less than 2.0d.

2.3.2.2.1.6.2 Maximum Spacing for Sealing Bolts

As specified in *AASHTO LRFD* Article 6.13.2.6.2, to seal against the penetration of moisture in joints, the spacing s of a single line of bolts adjacent to a free edge of an outside plate or shape must satisfy the following requirement (Figure 2.89a):

$$s \le (4.0 + 4.0t) \le 7.0 \text{ in.}$$

Equation 2.230
AASHTO LRFD Equation 6.13.2.6.2-1

where:
    t =   thickness of the thinner outside plate or shape (in.)

Where there is a second line of bolts uniformly staggered with the line adjacent to the free edge, at a gage less than 1.5 + 4.0t, the staggered spacing s in the two lines considered together must satisfy the following requirement (Figure 2.89b):

$$s \le 4.0 + 4.0t - \left(\frac{3.0g}{4.0}\right) \le 7.0 \text{ in.}$$

Equation 2.231

AASHTO LRFD Equation 6.13.2.6.2-2

where:
    g =   gage between bolts (in.)

$$S \leq (4.0+4.0t) \leq 7.0 \qquad\qquad S \leq 4.0+4.0t-(3.0g/4.0) \leq 7.0$$
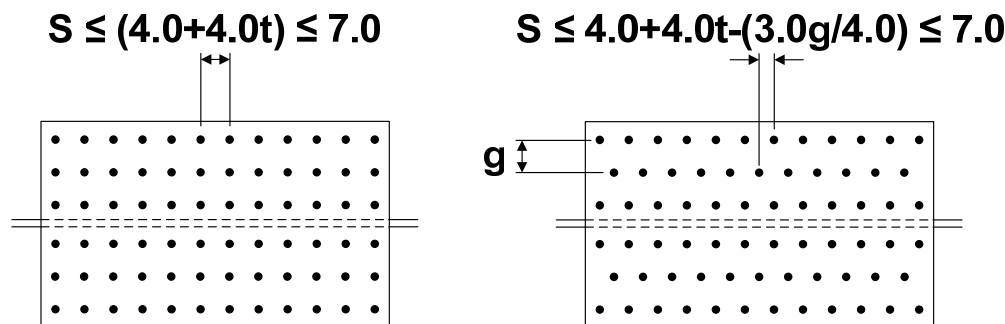
Figure 2.89 Maximum Spacing for Sealing Bolts

In uncoated weathering steel structures, it is critical that the bolt spacing be such that the connection joint is tight and moisture cannot enter between the plies of material. If sufficient moisture enters the joint, the resulting corrosion may cause prying, or pack-out, of the joint or bolt failure. Bolt spacing guidelines to insure proper tightness and stiffness of uncoated weathering steel bolted joints to avoid joint prying and corrosion pack-out are provided in Reference 110. The maximum spacing requirements for sealing bolts, given above, automatically satisfy these guidelines.

2.3.2.2.1.6.3 Maximum Pitch for Stitch Bolts

Stitch bolts are used to fasten together built-up compression or tension members where two or more plates or shapes are in contact (see Section 2.4.2.4 and Section 2.4.3.4 of this chapter). A maximum pitch of the bolts is specified to ensure that the parts act as a unit and to prevent buckling of compression members. The pitch is not to exceed the maximum pitch specified for sealing bolts (see above).

As specified in *AASHTO LRFD* Article 6.13.2.6.3, the pitch p of stitch bolts in compression members is not to exceed $12.0t$, and the gage g between adjacent lines of bolts is not to exceed $24.0t$. For two adjacent lines of staggered holes, the staggered pitch p of the stitch bolts must satisfy the following requirement:

$$p \leq 15.0t - \left(\frac{3.0g}{8.0}\right) \leq 12.0t \qquad\qquad \text{Equation 2.232}$$

AASHTO LRFD Equation 6.13.2.6.3-1

According to *AASHTO LRFD* Article 6.13.2.6.4, at the ends of compression members, the pitch p of the stitch bolts must not exceed $4.0d$ for a length equal to 1.5 times the maximum width of the member, where d is the diameter of the bolt. Beyond this length, p may be increased gradually over a length equal to 1.5 times the maximum width of the member until the maximum pitch given by either $12.0t$ or Equation 2.232, as applicable, is reached.

For tension members, the pitch p must not exceed twice the maximum pitch specified above for compression members, and the gage g between adjacent lines of bolts must not exceed $24.0t$.

2.3.2.2.1.6.4 Edge and End Distances

The edge distance of bolts is defined as the distance perpendicular to the line of force between the center of a hole and the edge of the component (Figure 2.90). The minimum edge distance is a function of the diameter of the bolt and the condition of the plate edge (i.e. sheared or rolled or gas cut). As specified in *AASHTO LRFD* Article 6.13.2.6.6, the minimum edge distance is to be taken specified in *AASHTO LRFD* Table 6.13.2.6.6-1 (Table 2.17):

Table 2.17 Minimum Edge Distances

Bolt Diameter	Sheared Edges	Rolled Edges of Plates or Shapes, or Gas Cut Edges
in.	in.	in.
5/8	1-1/8	7/8
3/4	1-1/4	1
7/8	1-1/2	1-1/8
1	1-3/4	1-1/4
1-1/8	2	1-1/2
1-1/4	2-1/4	1-5/8
1-3/8	2-3/8	1-3/4

The maximum edge distance is not to be more than the lesser of eight times the thickness of the thinnest outside plate and 5.0 in.
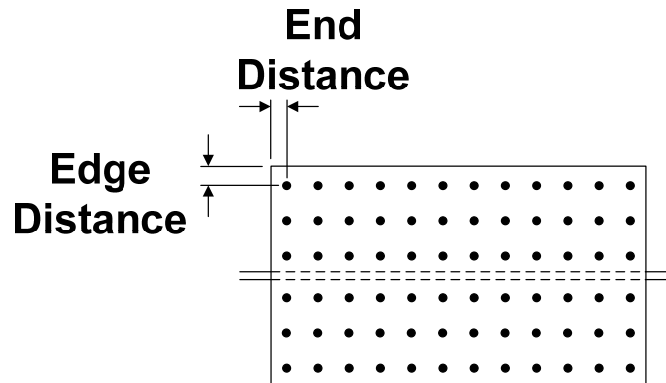
Figure 2.90 Edge and End Distance

The end distance of bolts is defined as the distance along the line of force between the center of a hole and the end of the component (Figure 2.90). As specified in *AASHTO LRFD* Article 6.13.2.6.5, the end distance for all types of holes is not to less than the appropriate minimum edge distance specified in Table 2.17. When oversize or slotted holes are used (see the section below on Holes), the minimum clear end distance, which is defined as the distance between the edge of the bolt hole and the end of the member, must not be less than the bolt diameter.

The maximum end distance is to be taken the same as the maximum edge distance, or the lesser of eight times the thickness of the thinnest outside plate and 5.0 in.

2.3.2.2.2 Nuts

Different grades of high-strength bolts are combined with various heavy hexagon-shaped nuts, which guarantee failure by bolt yielding rather than by stripping of the nut threads.

As specified in *AASHTO LRFD* Article 6.4.3.2, nuts for use with ASTM A 325 bolts must conform to the requirements of ASTM A 563 Grades DH, DH3, C, C3 and D. Nuts to be used with ASTM A 325 Type 3 bolts must be of Grade C3 or DH3. All plain nuts must have a minimum hardness of 89 HRB. Nuts to be galvanized must be heat-treated Grade DH nuts and must be lubricated with a lubricant containing a visible dye. To accommodate the relatively thick non-uniform zinc coatings on bolt threads during hot-dip galvanizing, the blank nut is typically hot-dip galvanized and then tapped over-size. This results in a reduction in the thread engagement and the resulting stripping strength. Only the stronger hardened nuts (Grade DH) have adequate strength to meet ASTM thread-strength requirements after over-tapping. Less over-tapping is usually required for mechanically galvanized nuts. Galvanizing increases the friction between the bolt and nut threads, as well as the variability of the torque-induced pretension (*111*). If the nuts are lubricated, a lower required torque and more consistent results are obtained. Therefore, the supplier must test a galvanized bolt, lubricated galvanized nut and a galvanized washer in an assembled steel joint prior to shipment to show that the galvanized nut with the lubricant provided can be rotated from the snug-tight condition well beyond the rotation required for pretensioned installation without stripping.

Nuts for use with ASTM A 490 bolts must conform to the requirements of ASTM A 563 Grades DH and DH3. Nuts to be used with ASTM A 490 Type 3 bolts must be of Grade DH3.

2.3.2.2.3 Washers

As specified in *AASHTO LRFD* Article 6.4.3.3, hardened steel washers must satisfy the requirements of ASTM F 436. *AASHTO LRFD* Article 6.13.2.3.2 spells out the conditions under which hardened washers are required in high-strength bolted connections. These conditions include the following:

➢ When the outer face of the bolted parts has a slope greater than 1:20 with respect to a plane normal to the bolt axis;
➢ When tightening is performed by the calibrated wrench method. The washer is to be used under the turned element;
➢ When ASTM A490 bolts are installed in material with a specified minimum yield strength less than 50 ksi regardless of the tightening method. This is to guard against galling and indenting the connected parts since A 490 bolts produce larger clamping forces than A 325 bolts;
➢ When oversize or short-slotted holes are used in an outer ply (see the section below on Holes). When ASTM A 490 bolts over 1.0 in. in diameter are used

in such cases, hardened washers with 0.3125 in. minimum thickness are to be used under both the head and the nut in lieu of standard thickness washers. Multiple hardened washers with a combined thickness greater than or equal to 0.3125 in. are not to be used;

➢ When long-slotted holes are used (see the section below on Holes). In such cases, structural plate washers or a continuous bar with standard holes not less than 0.3125 in. in thickness are to completely cover long-slotted holes. The hardened washer is then to be placed over the outer surface of the plate washer or bar.

Note that ASTM F 436 weathering steel washers should be used in conjunction with Type 3 high-strength bolts.

2.3.2.3 Holes

2.3.2.3.1 Size

The maximum permitted size of standard, oversize, short-slotted and long-slotted holes is given in *AASHTO LRFD* Table 6.13.2.4.2-1 (Table 2.18). In the table, *d* is the diameter of the bolt:

Table 2.18 Maximum Hole Sizes

Bolt Dia.	Standard	Oversize	Short Slot	Long Slot
d	Dia.	Dia.	Width × Length	Width × Length
in.	in.	in.	in.	in.
5/8	11/16	13/16	11/16 × 7/8	11/16 × 1-9/16
3/4	13/16	15/16	13/16 × 1	13/16 × 1-7/8
7/8	15/16	1-1/16	15/16 × 1-1/8	15/16 × 2-3/16
1	1-1/16	1-1/4	1-1/16 × 1-5/16	1-1/16 × 2-1/2
≥ 1-1/8	*d*+1/16	*d*+5/16	*d*+1/16 × *d*+3/8	*d*+1/16 × 2.5*d*

For design, an allowance is made for damage to the metal at the edge of the hole during the fabrication of the holes. It is assumed that the extent of the damage is limited to a radial distance of 1/32 in. around the hole (*28*). *Therefore, as specified in AASHTO LRFD Article 6.8.3, **for design calculations**, the width of standard bolt holes is to be taken as the nominal diameter of the bolt plus 0.125 in. (i.e. 1/8 in.). The width of oversize and slotted holes is to be taken as 0.0625 in. (i.e. 1/16 in.) greater than the hole size.*

2.3.2.3.2 Standard Holes

According to *AASHTO LRFD* Article 6.13.2.4.1a, standard holes (Table 2.18) are to be used for high-strength bolted connections, unless specified otherwise.

As specified in AASHTO LRFD Article 6.13.1, unless expressly permitted otherwise by the contract documents, standard holes are to be used in connections in horizontally curved bridges to ensure that the steel fits together in the field during erection. Curved girders depend on their connections to adjacent girders through bracing members for their stability. Therefore, cross-frames/diaphragms on curved girders should be firmly connected to the girders in order for the girders to remain stable during erection. Loosely connected cross-frames/diaphragms and oversize or slotted holes are not recommended for use in horizontally curved bridges as they may compromise the girder alignment and plumbness, as demonstrated in Reference 112, making cross-frame/diaphragm fit-up difficult.

2.3.2.3.3 Short-Slotted Holes

As specified in *AASHTO LRFD* Article 6.13.2.4.1c, short-slotted holes (Table 2.18) may be used in any or all plies of either slip-critical or bearing-type connections. In slip-critical connections, the slots may be used without regard to the direction of loading. However, in bearing-type connections, the length of the slot must be normal to the direction of the load.

2.3.2.3.4 Long-Slotted Holes

As specified in *AASHTO LRFD* Article 6.13.2.4.1d, long-slotted holes (Table 2.18) may be used only one ply of either slip-critical or bearing-type connections. As for short-slotted holes, in slip-critical connections, the slots may be used without regard to the direction of loading. However, in bearing-type connections, the length of the slot must be normal to the direction of the load.

2.3.2.4 Factored Resistance

2.3.2.4.1 Service Limit State

As specified in *AASHTO LRFD* Article 6.13.2.2, for slip-critical connections at the service limit state, the factored resistance R_r of a bolt at the Service II load combination is to be taken as:

$$R_r = R_n$$

Equation 2.233
AASHTO LRFD Equation 6.13.2.2-1

where:
R_n =   nominal slip resistance of the bolt specified in Article 6.13.2.8 (see below) (kips)

2.3.2.4.1.1 Slip Resistance of Bolts

The slip resistance of bolts is covered in *AASHTO LRFD* Article 6.13.2.8. The bolt pretension and surface condition of the faying surface (i.e. coefficient of friction) have the greatest effect on the slip-resistance of high-strength bolted connections.

As specified in *AASHTO LRFD* Article 6.13.2.8, the nominal slip resistance R_n of a bolt in a slip-critical connection (subject to shear) is to be taken as:

$$R_n = K_h K_s N_s P_t$$

Equation 2.234

AASHTO LRFD Equation 6.13.2.8-1

where:

N_s	=	number of slip planes per bolt
P_t	=	minimum required bolt tension specified in *AASHTO LRFD* Table 6.13.2.8-1 (Table 2.16) (kips)
K_h	=	hole size factor specified in *AASHTO LRFD* Table 6.13.2.8-2 (Table 2.19)
K_s	=	surface condition factor specified in *AASHTO LRFD* Table 6.13.2.8-3 (Table 2.20)

In a slip-critical connection subject to combined axial tension and shear, the tensile force reduces the contact pressure between the connected plates thereby reducing the slip resistance to the shear forces. The reduction in slip resistance is approximately proportional to the ratio of the applied tensile force to the bolt installation tension (*105*). Therefore, according to *AASHTO LRFD* Article 6.13.2.11, the nominal slip resistance of a bolt in a slip-critical connection subjected to combined axial tension and shear under service loads (i.e. under Load Combination Service II) must not exceed the nominal slip resistance given by Equation 2.234 times the following factor:

$$1 - \frac{T_u}{P_t}$$

Equation 2.235

AASHTO LRFD Equation 6.13.2.11-3

where:

T_u	=	tensile force due to the factored loads under Load Combination Service II (kips)
P_t	=	minimum required bolt tension specified in *AASHTO LRFD* Table 6.13.2.8-1 (Table 2.16)(kips)

The resistance to combined tension and shear once the connection slips and goes into bearing at the strength limit state is discussed later in this chapter under Combined Tensile and Shear Resistance of Bolts.

Since all locations must develop the slip resistance before a total joint slip can occur at that plane, the assumption is made that the slip resistance at each bolt is equal and additive with the slip resistance at the other bolts in the connection. It is also assumed that the full slip resistances must be mobilized at each slip plane before full joint slip can occur, although the forces at each slip plane do not necessarily develop simultaneously. Equation 2.234 is formulated for the case of a single slip plane. Therefore, the total slip resistance of a joint with multiple slip planes can be taken equal to the resistance of a single slip plane multiplied by the number of slip planes N_s.

For bolts in oversize or slotted holes, hole size factors K_h less than 1.0 are provided in *AASHTO LRFD* Table 6.13.2.8-2 (Table 2.19) because of the greater possibility of significant deformation occurring in joints with oversize or slotted holes. For long-slotted holes, even though the slip load is the same for bolts loaded transverse or parallel to the axis of the slot, the hole size factor for loading parallel to the axis has been reduced, based upon judgment, because of the greater consequences of slip in this case.

Table 2.19 Hole Size Factor, K_h

for standard holes	1.00
for oversize and short-slotted holes	0.85
for long-slotted holes with the slot perpendicular to the direction of the force	0.70
for long-slotted holes with the slot parallel to the direction of the force	0.60

The surface condition factor K_s is provided in *AASHTO LRFD* Table 6.13.2.8-3 (Table 2.20) and is a function of the class of the surface. Three different classes of surfaces are defined based on the mean value of slip coefficients from many tests of clean mill scale, blast-cleaned steel surfaces and galvanized and roughened surfaces. The classes of surfaces are described as follows:

- Class A Surface: unpainted clean mill scale and blast-cleaned surfaces with Class A coatings;
- Class B Surface: unpainted blast-cleaned surfaces and blast-cleaned surfaces with Class B coatings;
- Class C Surface: hot-dip galvanized surfaces roughened by wire brushing after galvanizing.

Table 2.20 Surface Condition Factor, K_s

for Class A surface conditions	0.33
for Class B surface conditions	0.50
for Class C surface conditions	0.33

It has been found that if tightly adherent mill scale is on the faying surface of a bolted connection on uncoated weathering steel, the connection slips into bearing at a lower shear stress than on a carbon steel with mill scale (*113*). *However, if the faying surface is blast-cleaned, slip-critical connections on uncoated weathering steel can be designed using a Class B surface condition (114).* Otherwise, a Class

A surface condition, which is appropriate for clean mill-scale surfaces, must be used. The slip resistance of bolted joints is not affected by the weathering of uncoated steel surfaces prior to erection, but any loose rust on the connection or faying surfaces must be removed. Pre-construction primers may be used for the cleaned bolted surfaces. Reference 113 indicates that the Class B surface condition can be maintained in such cases for up to one year prior to joint assembly.

Unpainted clean mill-scale faying surfaces and unpainted blast-cleaned faying surfaces must be protected from inadvertent paint overspray. *AASHTO LRFD* Article 6.13.2.8 requires that in uncoated joints, paint (including any inadvertent overspray) be excluded from areas closer than one bolt diameter but not less than 1.0 in. from the edge of any hole and all areas within the bolt pattern. Tests have demonstrated that for material with thickness in the range of 3/8 in. to ¾ in., the transfer of shear by friction between contact surfaces is concentrated in an annular ring around and close to the bolts (*115*).   Paint on the contact surfaces away from the edge of the bolt hole by not less than 1.0 in. nor the bolt diameter did not reduce the slip resistance.   For joints in thicker material, the minimum bolt pretension may not be adequate to completely flatten and pull the thick material into tight contact around every bolt in the pattern. Therefore, it is specified that all bolt areas within the pattern be kept free of paint, including any overspray.

Joints with painted faying surfaces must be blast-cleaned and coated with a paint that has been qualified by test as a Class A or Class B coating. A Class A coating will not reduce the slip coefficient below that provided by clean mill scale, and a Class B coating will not reduce the slip coefficient below that provided by blast-cleaned steel surfaces. A test method to determine the mean slip coefficient in order to qualify a particular coating for use according to the *AASHTO LRFD* Specifications is provided in Appendix A of Reference 105.   The method includes long-term creep test requirements to ensure that the creep deformations caused by the bolt clamping force and joint shear are such that the coating will provide satisfactory long-term performance under sustained loading (*116*).   Re-qualification of the coating is required if any essential variable is changed.   According to *AASHTO LRFD* Article 6.13.2.8, the contract documents must state that coated joints not be assembled before the coatings have cured the minimum time used in the qualifying test. Research has indicated that all curing of faying surface coatings ceases at the time the joints are assembled and tightened and that coatings that are not fully cured act as lubricants severely reducing the slip resistance of the joint (*117*).   The specification permits the use of faying-surface coatings with a slip resistance less than Class A, (i.e. K_s = 0.33) subject to the approval of the Engineer, provided that the mean slip coefficient is determined by the specified test procedure.

Galvanized faying surfaces must be hot-dip galvanized according to the procedures given in the ASTM A 123 Specification and then must be subsequently roughened by means of hand wire brushing. The mean slip coefficient for clean hot-dip galvanized surfaces is on the order of 0.19 compared to 0.33 for clean mill scale (*105*).   Research has indicated that the slip coefficient for galvanized surfaces can be significantly improved by hand wire brushing or light "brush-off" grit blasting (*111*). The treatment must be controlled in order to achieve visible scoring or roughening. Power wire brushing is not satisfactory because it may polish rather than roughen

the surface or remove the coating. Tests on surfaces that have been hand wire brushed after coating have indicated a mean slip coefficient of 0.35 (*101*).   The surface condition factor K_s for treated galvanized surfaces has been conservatively set at 0.33, which is the same as for Class A surfaces. A separate class (Class C) has been provided for galvanized surfaces to avoid potential confusion. Previous Specifications indicated a slip coefficient of 0.40 for galvanized surfaces, which assumed blast-cleaning of the surface after galvanizing; however, this is not the typical practice. Note that field experience and test results have indicated that galvanized surfaces may have a tendency to continue to slip under sustained loading illustrating a creep-type behavior (*101*). Relaxation of bolt tension may also occur where hot-dip galvanized coatings are used, particularly if there are many plies of thickly coated material in the joint. In such cases, this can either be allowed for in the design or else the bolts can be re-tightened after a period of settling-in subsequent to the initial tightening.

Since faying surfaces (that are not galvanized) are typically blast-cleaned as a minimum, a Class A surface condition should only be used to compute the slip resistance when Class A coatings are applied or when unpainted mill scale is left on the faying surface. Most commercially available primers will qualify as Class B coatings.

EXAMPLE

Calculate the factored slip resistance for a 7/8-in. diameter A325 high-strength bolt assuming a Class B surface condition for the faying surface, standard holes and two slip planes per bolt.

The nominal slip resistance per bolt R_n is computed as:

$$R_n = K_h K_s N_s P_t$$

AASHTO LRFD Equation 6.13.2.8-1

For standard holes: K_h =   1.0 (Table 2.19)
For a Class B surface: K_s =   0.50 (Table 2.20)
For two slip planes: N_s =   2
For a 7/8" A 325 bolt: P_t =   39 kips (Table 2.16)

Therefore: $R_n = 1.0(0.50)(2)(39) = 39.0 \text{ kips / bolt}$

Since:

$$R_r = R_n$$

AASHTO LRFD Equation 6.13.2.2-1

R_r = 39.0 kips/bolt

2.3.2.4.2 Strength Limit State

As specified in *AASHTO LRFD* Article 6.13.2.2, the factored resistance R_r of a bolt at the strength limit state (in a slip-critical or bearing-type connection) is to be taken as either:

$$R_r = \phi R_n \qquad \text{Equation 2.236}$$
$$\textit{AASHTO LRFD Equation 6.13.2.2-2}$$

or:

$$T_r = \phi T_n \qquad \text{Equation 2.237}$$
$$\textit{AASHTO LRFD Equation 6.13.2.2-3}$$

where:

ϕ = resistance factor for bolts specified in *AASHTO LRFD* Article 6.5.4.2

= ϕ_s for bolts in shear = 0.80 (for A 325 and A 490 bolts); 0.65 (for A 307 bolts)

= ϕ_t for bolts in tension = 0.80 (for A 325, A 490 and A 307 bolts)

= ϕ_{bb} for bolts bearing on connected material = 0.80

= ϕ_y for yielding in gross section for connected elements in tension = 0.95

= ϕ_u for fracture in net section for connected elements in tension = 0.80

= ϕ_v for connected elements in shear = 1.00

R_n = nominal resistance of the bolt, connected element or connected material (kips)

= for bolts in shear as specified in *AASHTO LRFD* Article 6.13.2.7 (see Section 2.3.2.4.2.1 below)

= for connected material in bearing joints as specified in *AASHTO LRFD* Article 6.13.2.9 (see Section 2.3.4.2.2 below)

= for connected elements in shear or tension as specified in *AASHTO LRFD* Article 6.13.5.2 (see Sections 2.3.4.2.3 and 2.3.4.2.4 below)

(Note: for connected elements in compression, refer to Section 2.3.2.4.2.7 of this chapter below.)

T_n = nominal resistance of the bolt (kips)

= for bolts in axial tension as specified in *AASHTO LRFD* Article 6.13.2.10 (see Section 2.3.4.2.5 below)

= for bolts in combined axial tension and shear as specified in *AASHTO LRFD* Article 6.13.2.11 (see Section 2.3.4.2.6 below)

2.3.2.4.2.1 Shear Resistance of Bolts

The shear resistance of bolts is covered in *AASHTO LRFD* Article 6.13.2.7. The shear failure of a bolt is illustrated in Figure 2.91.
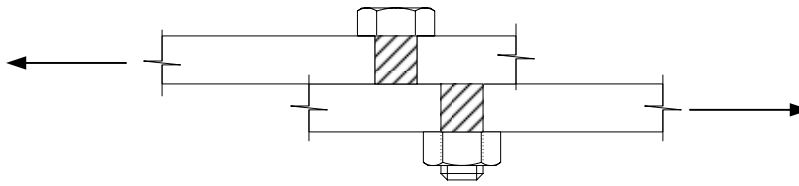
Figure 2.91 Shear Failure of a Bolt

As specified in *AASHTO LRFD* Article 6.13.2.7, the nominal shear resistance of a high-strength bolt (A 325 or A 490 bolt) or an A 307 bolt at the strength limit state in joints whose length between extreme fasteners measured parallel to the line of action of the force is less than 50.0 in. is to be taken as:

- Where threads are excluded from the shear plane:

$$R_n = 0.48 A_b F_{ub} N_s$$

Equation 2.238
AASHTO LRFD Equation 6.13.2.7-1

- Where threads are included in the shear plane:

$$R_n = 0.38 A_b F_{ub} N_s$$

Equation 2.239
AASHTO LRFD Equation 6.13.2.7-2

where:
A_b = area of the bolt corresponding to the nominal diameter (in.^{2})
F_{ub} = specified minimum tensile strength of the bolt specified in *AASHTO LRFD* Article 6.4.3 (ksi)
N_s = number of shear planes per bolt

For a bolt in a connection greater than 50.0 in. in length, the nominal shear resistance is to be taken as 0.80 times the value given by Equation 2.238 or 2.239, as applicable. The nominal shear resistance is based on the observation that the shear strength of a single high-strength bolt is about 0.60 times the tensile strength F_{ub} of the bolt (*101*). The shear resistance is not affected by the pretension in the bolts provided the connected material is in contact at the faying surfaces. In shear connections with more than two bolts in the line of force, the average bolt strength decreases as the joint length increases due to the nonuniform bolt shear force distribution caused by deformation of the connected material. For joints up to 50.0 in. in length, a single reduction factor of 0.80 is implicitly applied to the 0.60 multiplier rather than providing a function that reflects the decrease in average bolt strength with joint length (0.80 * 0.60 equals the 0.48 multiplier given in Equation 2.238). This was felt not to adversely affect the economy of very short joints. For bolts in joints longer than 50.0 in., the nominal shear resistance must be reduced by an additional 20 percent. *For bolted flange splices, note that the 50.0 in. length is to be measured between the extreme bolts on only one side of the connection.* The greater than 50.0 in. length reduction does *not* apply when the distribution of shear force is essentially uniform along the joint, such as in a bolted web splice (*105*).

When bolts are positioned so that they cross two planes of contact (i.e. N_s = 2), this is referred to as 'double shear'. Double shear is a symmetrical loading situation with regard to the shear planes and direction of shear transfer.   When there is a single plane of contact involved in the load transfer (i.e. N_s = 1), this is referred to as 'single shear', which is an unsymmetrical loading situation.

The average ratio of the nominal shear resistance for bolts with threads included in the shear plane to the nominal shear resistance for bolts with threads excluded from the shear plane is 0.83 with a standard deviation of 0.03 (*117*).   Therefore, a reduction factor of 0.80 is conservatively used to account for the nominal shear resistance when threads are included in the shear plane but calculated with the area corresponding to the nominal bolt diameter (0.48 * 0.80 equals the 0.38 multiplier given in Equation 2.239). In determining whether the threads are excluded from the shear planes, the thread length of the bolt is to be determined as two thread pitches greater than the specified thread length. If the threads of a bolt are included in a shear plane of a joint, the nominal shear resistance of the bolts in all shear planes of the joint is to conservatively be taken from Equation 2.239. That is, for bolts in double shear with a non-threaded shank in one shear plane and a threaded section in the other shear plane, the sharing of the load between the two dissimilar shear areas is uncertain. Also, knowledge about the specific bolt placement, which might result in both shear planes being in the threaded section, is not ordinarily available to the Engineer.

Since the threaded length of an A 307 bolt is not as predictable as that of a high-strength bolt, the nominal shear resistance of an A 307 bolt must always be based on Equation 2.239. Also, A 307 bolts with a long grip (i.e. the total thickness of the plies of a joint through which the bolt passes exclusive of any washers or load-indicating devices) tend to bend reducing their shear resistance.   Therefore, *AASHTO LRFD* Article 6.13.2.7 requires that when the grip length of an A 307 bolt exceeds 5.0 bolt diameters, the nominal shear resistance must be lowered 1.0 percent for each 1/16 in. of grip in excess of 5.0 bolt diameters.

EXAMPLE

Calculate the factored shear resistance for a 7/8-in. diameter A325 high-strength bolt in double shear assuming the threads are excluded from the shear planes. Assume the length between extreme fasteners measured parallel to the line of action of the force is less than 50 in. Therefore, the nominal shear resistance is taken as:

$$R_n = 0.48A_bF_{ub}N_s$$

AASHTO LRFD Equation 6.13.2.7-1

For a 7/8" A 325 bolt: A_b = $\dfrac{\pi(0.875)^2}{4} = 0.60 \text{ in}^2$

F_{ub} = 120 ksi (*AASHTO LRFD* Article 6.4.3.1)

For double shear: N_s = 2

Therefore: $R_n = 0.48(0.60)(120)(2) = 69.1\,\text{kips}/\text{bolt}$

Since: $R_r = \phi_s R_n$

AASHTO LRFD Equation 6.13.2.2-2

R_r = 0.80(69.1) = 55.3 kips/bolt

2.3.2.4.2.2 Bearing Resistance of Connected Material

The bearing resistance of the connected material in a bolted connection is covered in *AASHTO LRFD* Article 6.13.2.9. A bearing failure relates generally to either deformation of the bolt or deformation around a bolt hole, as illustrated in Figure 2.92a and Figure 2.92b, respectively.

(a)   (b)
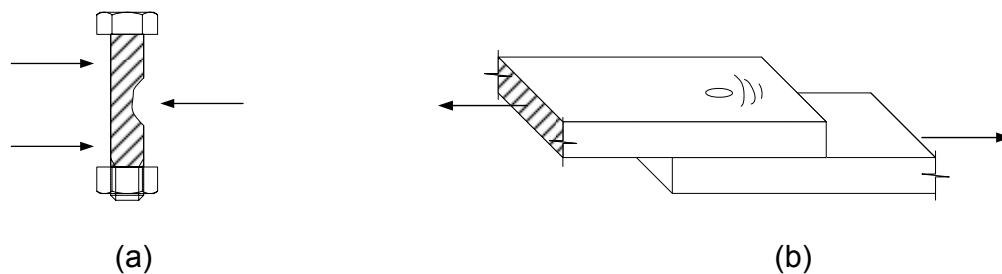
Figure 2.92 Bearing Failure of Bolt and Connected Material

After a major slip has occurred in a slip-critical connection, one or more bolts are in bearing against the side of the hole. The contact pressure between the bolt and connected material can be expressed as the bearing stress on the bolt or connected material. Tests have always shown that the bearing stress on the bolt is not critical (*101*). For simplicity, the bearing stress is assumed to be a uniform stress distribution equal to the load transmitted by the bolt divided by the bearing area taken as the bolt diameter times the thickness of the connected material. As specified in *AASHTO LRFD* Article 6.13.2.9, the effective thickness of connected material with countersunk holes is to be taken as the thickness of the connected material minus one-half the depth of the countersink.

The actual failure mode depends on the end distance or clear distance between bolts, the bolt diameter and the thickness of the connected material. Either the bolt will split out through the end of the plate because of insufficient end distance, or else excessive deformations are developed in the connected material adjacent to the bolt hole (Figure 2.92b) because of insufficient clear distance between the bolts.

The end distance required to prevent the plate from splitting out can be approximated by equating the maximum load R_n transmitted by the end bolt to the force corresponding to shear failure of the plate material of thickness t along the dotted Lines 1-1 and 2-2 shown in Figure 2.93. Although actual splitting would occur along the Lines 1-1 and 2-2 in Figure 2.93, the angle α will be assumed equal to zero in order to compute a lower-bound resistance and failure will be assumed to occur along the two solid lines instead.
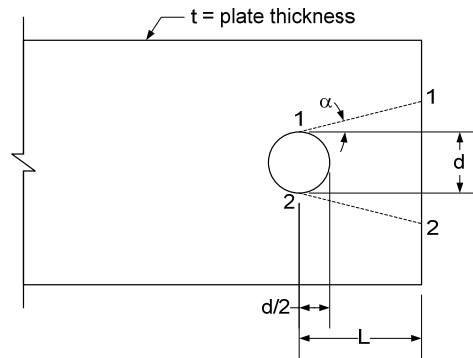
Figure 2.93 Bearing Resistance Related to End Distance

Therefore:

$$R_n = 2t(L - \frac{d}{2})\tau_u \qquad \text{Equation 2.240}$$

where τ_u is the ultimate shear resistance of the plate material. For commonly used steels, τ_u can be assumed approximately equal to $0.75F_u$, where F_u is the ultimate tensile strength of the plate material. Therefore, substituting $0.75F_u$ for τ_u and the clear distance L_c from the edge of the hole to the end of the plate in the direction of the force for $(L - d/2)$ in Equation 2.240 (to simplify the calculations for oversize and slotted holes) gives:

$$R_n = 1.5L_c tF_u \qquad \text{Equation 2.241}$$

Equation 2.241 can be used to determine the bearing resistance between bolt holes by substituting the clear distance between adjacent holes for the clear end distance. The same bearing resistance applied regardless of the bolt shear resistance or the presence or absence of bolt threads in the bearing area. An alternative equivalent relationship relating the bearing stress r_n to F_u as a function of the L/d ratio based conservatively on test results of finger-tight bolts (*101*) is given in *AASHTO LRFD* Article C6.13.2.9 as follows:

$$\frac{L}{d} \geq \frac{r_n}{F_u} \qquad \text{Equation 2.242}$$

AASHTO LRFD Equation C6.13.2.9-1

In order to limit deformations under the factored loads, Reference 101 further recommends that the ratio of r_n/F_u be limited to 3.0.   Substituting $r_n = R_n/dt$ in this ratio and rearranging gives an upper-bound bearing resistance of:

$$R_n = 3.0F_u dt \qquad \text{Equation 2.243}$$

Equations 2.241 and 2.243 are given as the bearing resistance equations in Reference 105 for cases where deformation at the bolt holes at service load is *not* a

design consideration for standard holes, oversize holes, short-slotted holes loaded in any direction and long-slotted holes parallel to the applied bearing force. In the *AASHTO LRFD* Specifications, the more conservative equations from Reference 105 when deformation at the bolt holes at service load *is* a design consideration for the preceding cases are instead specified as follows in *AASHTO LRFD* Article 6.13.2.9 (and are to be applied under the *factored* loads at the strength limit state):

$$R_n = 1.2L_c tF_u \le 2.4dtF_u \qquad \text{Equation 2.244}$$

AASHTO LRFD Equations C6.13.2.9-1 & 6.13.2.9-2

Equation 2.244 is derived based on tests that showed that the total elongation of a standard hole that is loaded to obtain the maximum recommended bearing resistance given by Equation 2.243 is on the order of the diameter of the bolt (*101*). Based on these tests, to prevent elongations exceeding 0.25 inches, a reduced limit on the bearing resistance of $2.4dtF_u$ is specified according to Equation 2.244.

For long-slotted holes perpendicular to the applied bearing force, the bending component of the deformation in the connected material becomes more critical (*105*). Therefore, for this case, the bearing resistance is further limited as follows:

$$R_n = L_c tF_u \le 2.0dtF_u \qquad \text{Equation 2.245}$$

AASHTO LRFD Equations C6.13.2.9-3 & 6.13.2.9-4

The design bearing resistance is expressed in terms of a single bolt, although it is really for the connected material adjacent to the bolt. Therefore, in calculating the nominal bearing resistance for the connected part, the total bearing resistance may be taken as the sum of the bearing resistances of the individual bolts (holes) parallel to the line of the applied force.

EXAMPLE

Calculate the total factored bearing resistance of the flange splice plate shown below subject to a tensile force *P*. The plate material is ASTM A 709 Grade 50W steel. From *AASHTO LRFD* Table 6.4.1-1, F_u for Grade 50W steel is 70 ksi. The bolts are 7/8-inch diameter A 325 bolts placed in standard holes.
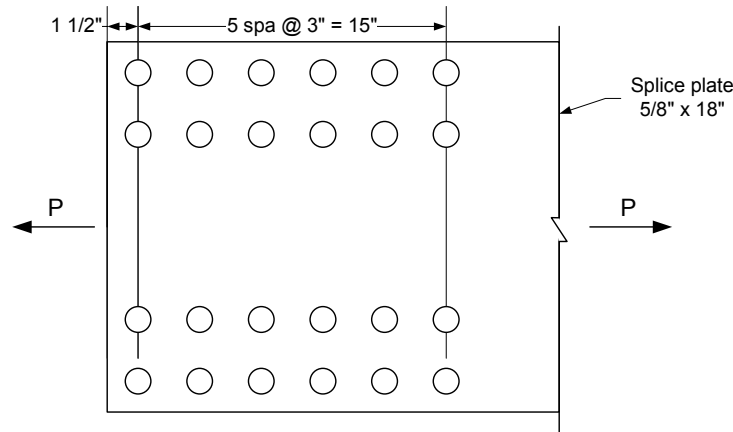
The bearing resistance of the connected part is calculated as the sum of the bearing resistances of the individual bolt holes parallel to the line of the applied force. As specified in *AASHTO LRFD* Article 6.8.3, for design calculations, the width of standard bolt holes is to be taken as the nominal diameter of the bolt plus 0.125 in. Therefore, the width of the holes is to be taken as (0.875 in. + 0.125 in. = 1.0 in.).

For standard holes, the nominal bearing resistance R_n parallel to the applied bearing force is to be taken as follows:

$$R_n = 1.2L_c tF_u \le 2.4dtF_u$$

AASHTO LRFD Equations C6.13.2.9-1 & 6.13.2.9-2

For the four bolts adjacent to the end of the splice plate, the end distance is 1.5 in. Therefore, the clear end distance L_c between the edge of the hole and the end of the splice plate is:

$$L_c = 1.5 - \frac{1.0}{2} = 1.0 \text{ in.}$$

Therefore:

$$R_n = 4(1.2L_c tF_u) = 4[1.2(1.0)(0.625)(70)] = 210.0 \text{ kips (governs)}$$

or: $\qquad R_n = 4(2.4dtF_u) = 4[2.4(0.875)(0.625)(70)] = 367.5 \text{ kips}$

For the other twenty bolts, the center-to-center distance between the bolts in the direction of the applied force is 3.0 in. Therefore, the clear distance L_c between the edges of the adjacent holes is:

$$L_c = 3.0 - 1.0 = 2.0 \text{ in.}$$

Therefore: $\qquad R_n = 20(1.2L_c tF_u) = 20[1.2(2.0)(0.625)(70)] = 2100.0 \text{ kips}$

or:

$$R_n = 20(2.4dtF_u) = 20[2.4(0.875)(0.625)(70)] = 1837.5 \text{ kips (governs)}$$

The total nominal bearing resistance of the splice plate is therefore:

$$R_n = 210.0 \text{ kips} + 1837.5 \text{ kips} = 2047.5 \text{ kips}$$

Since: $R_r = \phi_{bb}R_n$ *AASHTO LRFD* Equation 6.13.2.2-2

$$R_r = 0.80(2047.5) = 1638.0 \text{ kips}$$

2.3.2.4.2.3 Shear Resistance of a Connected Element

The shear resistance of a connected element (i.e. a splice plate, gusset plate, corner angle, bracket or connection plate) is covered in *AASHTO LRFD* Article 6.13.5.3. A shear failure of a connected element, which is closely related to a bearing failure, is illustrated in Figure 2.94.
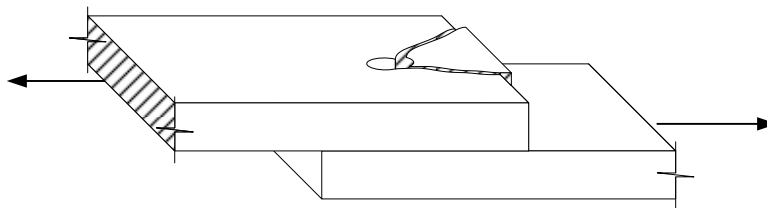
Figure 2.94 Shear Failure of a Connected Element

The nominal shear resistance of the connected element R_n is conservatively based on the shear yield stress (i.e. $F_y/\sqrt{3}$ = 0.58F_y) as follows:

$$R_n = 0.58A_gF_y \qquad\qquad\qquad \text{Equation 2.246}$$
$$\textit{AASHTO LRFD} \text{ Equation 6.13.5.3-2}$$

where:
- A_g = gross area of the connected element (in.^{2})
- F_y = specified minimum yield strength of the connected element (ksi)

The factored shear resistance of the connected element R_r is computed as follows:

$$R_r = \phi_v R_n \qquad\qquad\qquad \text{Equation 2.247}$$
$$\textit{AASHTO LRFD} \text{ Equation 6.13.5.3-1}$$

where:
- ϕ_v = resistance factor for shear specified in *AASHTO LRFD* Article 6.5.4.2 (= 1.0)

As will be discussed later, the shear resistance of the connected element is also important an important consideration in the design of certain welded connections.

2.3.2.4.2.4 Tensile Resistance of a Connected Element

The tensile resistance of a connected element (i.e. a splice plate, gusset plate, corner angle, bracket or connection plate) is covered in *AASHTO LRFD* Article 6.13.5.2. ***The factored tensile resistance of connected material R_r is to be taken as the smallest of the resistance based on yielding, net section fracture or block shear rupture, as described below***.

2.3.2.4.2.4.1 Yield Resistance

A connected element subject to tension must be checked for yielding on the gross section. A ductile steel loaded in axial tension can resist a force greater than the product of the yield strength times the gross area prior to fracture due to the effects of strain hardening. However, excessive elongation due to uncontrolled yielding of the gross area can limit the structural usefulness of the connected element so that it no longer serves its intended purpose. According to *AASHTO LRFD* Article 6.13.5.2, the factored yield resistance of a connected element in tension is to be computed from *AASHTO LRFD* Equation 6.8.2.1-1 as follows:

$$R_r = \phi_y F_y A_g \qquad \text{Equation 2.248}$$

<div align="right">

AASHTO LRFD Equation 6.8.2.1-1
</div>

where:

ϕ_y = resistance factor for yielding of tension members specified in *AASHTO LRFD* Article 6.5.4.2 (= 0.95)
F_y = specified minimum yield strength of the connected element (ksi)
A_g = gross cross-sectional area of the connected element (in.^{2})

2.3.2.4.2.4.2 Net Section Fracture Resistance

A connected element subject to tension must be checked for fracture on the net section. The connected element can fracture by failure of the net area at a load smaller than that required to yield the gross area depending on the ratio of net to gross area, the properties of the steel (i.e. the ratio of F_u/F_y) and the end connection geometry (Figure 2.95). Holes in a member cause stress concentrations at service loads, with the tensile stress adjacent to the hole typically about three times the average stress on the net area. As the load increases and the deformation continues, all fibers across the section will achieve or eventually exceed the yield strain. Failure occurs when the localized yielding results in a fracture through the net area.
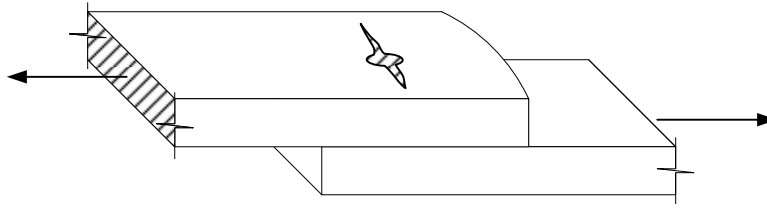
Figure 2.95 Tensile Failure of a Connected Element by Net Section Fracture

Typically, a higher margin of safety is used when considering the net section fracture resistance versus the yield resistance. According to *AASHTO LRFD* Article 6.13.5.2, the factored net section fracture resistance of a connected element in tension is to be computed from *AASHTO LRFD* Equation 6.8.2.1-2 as follows:

$$R_r = \phi_u F_u A_n U$$

<div align="right">Equation 2.249</div>
<div align="right">*AASHTO LRFD* Equation 6.8.2.1-2</div>

where:

ϕ_u = resistance factor for fracture of tension members specified in *AASHTO LRFD* Article 6.5.4.2 (= 0.80)

F_u = tensile strength of the connected element specified in *AASHTO LRFD* Table 6.4.1-1 (ksi)

A_n = net cross-sectional area of the connected element determined as specified in *AASHTO LRFD* Article 6.8.3 (in.^{2})

U = reduction factor to account for shear lag (see below)

As specified in *AASHTO LRFD* Article 6.8.3, the net area A_n of the connected element is to be taken as the product of the thickness of the material and its smallest net width.   The net width is to be determined for each chain of holes extending across the connected element along any transverse, diagonal or zigzag line.   For each chain, the net width is to be determined by subtracting from the total width the sum of all holes in the chain and adding the quantity $s^2/4g$ for each space between consecutive holes in the chain, where s is equal to the pitch of any two consecutive holes and g is the gage of the same two holes.   The development of the $s^2/4g$ rule is described in Reference 21.   When holes are staggered on *both* legs of an angle, the gage for holes in opposite adjacent legs is to be taken as the sum of the gages from the back of the angles less the thickness of the angle. As mentioned previously, in calculating A_n, the width of standard bolt holes is to be taken as the nominal diameter of the bolt plus 0.125 in. The width of oversize and slotted holes is to be taken as 0.0625 in. greater than the hole size. It is conservative to use the least net width in conjunction with the full tensile force to check the connected element. Assuming each bolt transfers an equal share of the load whenever the bolts are arranged symmetrically with respect to the centroidal axis of the connected element, a less conservative alternative is to check each possible chain with a tensile force obtained by subtracting the force removed by each bolt ahead of that chain from the full tensile force (see the example below).

According to AASHTO LRFD Article 6.13.5.2, for connection plates, splice plates and gusset plates only, A_n is not to be taken greater than 85 percent of the gross

area A_g of the plate in checking Equation 2.249. Because the length of these particular elements is small compared to the overall member length, inelastic deformation of the gross area is limited. Tests have shown that when holes are present in such short elements where general yielding on the gross section cannot occur, there will be at least a 15 percent reduction in tensile capacity from that obtained based on yielding of the gross section (*101*).

The reduction factor *U* in Equation 2.249 accounts for the effect of shear lag in connections. Shear lag is a consideration when the connection elements do not lie in a common plane and where the tensile force in the member is applied eccentrically or transmitted by connection to some but not all of the connection elements; e.g. an angle having a connection to only one leg. *As specified in AASHTO LRFD Article 6.13.5.2, for short connection elements such as connection plates, splice plates and gusset plates, where the elements of the cross-section essentially lie in a common plate, U is to be taken equal to 1.0.* For other cases involving bolted connections, *U* is to be determined as specified in *AASHTO LRFD* Article 6.8.2.2 (see Section 2.4.2.1 of this chapter under the design of Tension Members for additional information on the *U* factor). The *U* factor does not apply when checking yielding on the gross section because yielding will tend to equalize the non-uniform distribution of the tensile stresses resulting from shear lag.

EXAMPLE

Calculate the net section fracture resistance of the bolted flange splice plate shown below subject to a factored tensile force *T*. Assume that the flange has adequate net area and does not control the net section fracture resistance. Assume 7/8-inch diameter A 325 bolts placed in standard holes. Assume ASTM A 709 Grade 50W steel for the flange and splice plate.   From *AASHTO LRFD* Table 6.4.1-1, F_u for Grade 50W steel is 70 ksi.
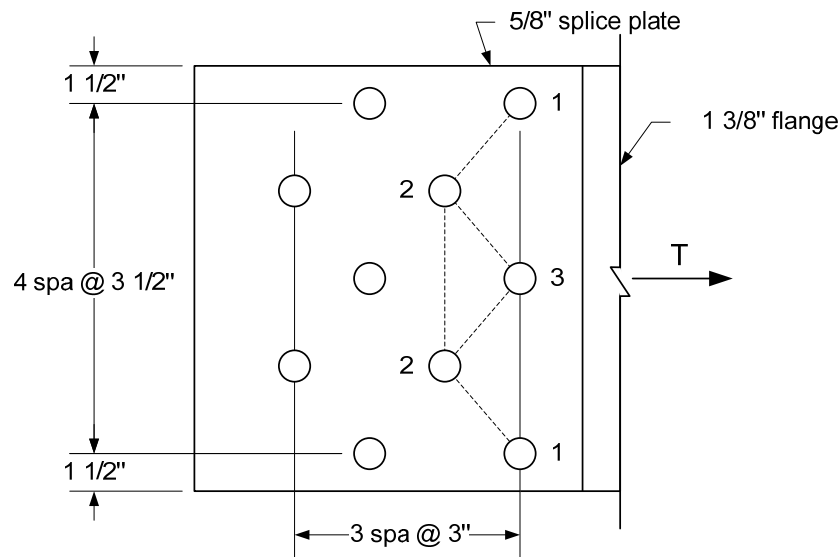
Calculate the deduction in width for one hole. For standard holes,

$$\text{Deduction} = \frac{7}{8} + \frac{1}{8} = 1.0 \text{ in.}$$

For chain 1-1: $\qquad\qquad A_n = [17.0 - 3(1.0)](0.625) = 8.75 \text{ in.}^2$

For chain 1-2-3-2-1: $\qquad A_n = \left[17.0 - 5(1.0) + 4\frac{(3.0)^2}{4(3.5)} \right](0.625) = 9.11 \text{ in.}^2$

For chain 1-2-2-1: $\qquad\quad A_n = \left[17.0 - 4(1.0) + 2\frac{(3.0)^2}{4(3.5))} \right](0.625) = 8.93 \text{ in.}^2$

The first two cases act in conjunction with the full tensile force T. The last case can be considered to act in conjunction with a reduced force of $0.9T$ since one bolt (at location 3) has transferred its share of the load prior to reaching chain 1-2-2-1. Therefore, A_n of 8.93 in^2 acting in conjunction with $0.9T$ is equivalent to A_n of $8.93/0.9 = 9.92$ in^2 acting in conjunction with T. As a result, chain 1-1 controls and the minimum A_n is equal to 8.75 in^2.

For splice plates, U is to be taken equal to 1.0 (*AASHTO LRFD* Article 6.13.5.2). Therefore:

$$R_r = \phi_u F_u A_n U \quad \textit{AASHTO LRFD} \text{ Equation 6.8.2.1-2}$$

$$R_r = 0.80(70)(8.75)(1.0) = 490 \text{ kips}$$

According to *AASHTO LRFD* Article 6.13.5.2, for splice plates subject to tension, A_n must not exceed $0.85A_g$.

$$0.85(17.0)(0.625) = 9.03 \text{ in}^2 > A_n = 8.75 \text{ in}^2 \quad \text{ok}$$

2.3.2.4.2.4.3 Block Shear Rupture Resistance

A connected element subject to tension must be checked for a tearing limit state known as block shear rupture. A block shear rupture failure for an angle in tension attached to a gusset plate is shown in Figure 2.96. In Figure 2.96, the tearing failure along the bolt holes occurs along section a-b-c. The tearing or shear rupture resistance on section a-b plus the tensile yield resistance on section b-c will result in the total block shear rupture resistance. Note that the failure path is defined by the centerlines of the bolt holes. Tests have shown that it is reasonable to add the resistance in tension yielding on one plane to the shear rupture resistance of the perpendicular plane (*118, 119*).
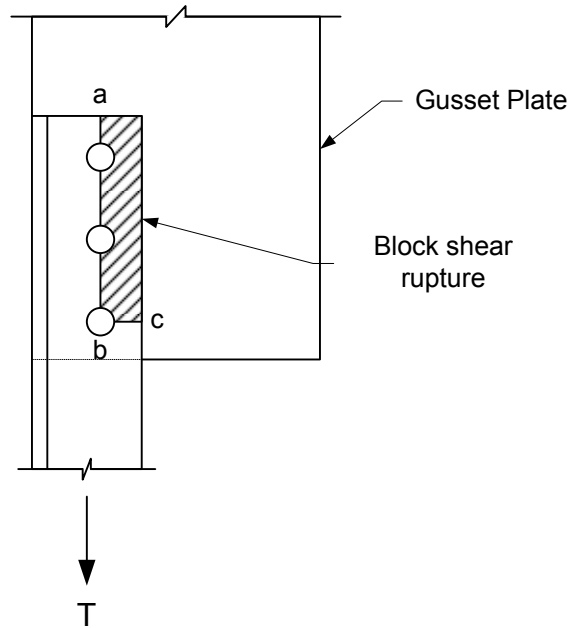
Figure 2.96 Tension Failure of a Connected Element by Block Shear Rupture

As specified in *AASHTO LRFD* Article 6.13.4, block shear rupture is to be checked for the web connection of coped beams and for all tension connections, including connection plates, splice plate and gusset plates. Tests on coped beams have indicated that a block shear failure can occur around the perimeter of the bolt holes (*120*). The connection is to be investigated by considering all possible failure planes in the connected elements, including those parallel and perpendicular to the applied forces, and determining the most critical set of planes. Planes parallel to the applied force are to be considered to resist only shear stresses and planes perpendicular to the applied force are to be considered to resist only tensile stresses. Block shear rupture is most likely to control in the design of bolted end connections to thin webs of girders (e.g. coped beams) and in the design of short compact bolted connections. It is unlikely to control in the design of bolted flange and web splices of typical proportions.

Two possible block shear resistances can be calculated: 1) fracture on the net area of the plane resisting the tensile stress A_{tn} based on the tensile strength of the connected material F_u, in conjunction with shear yielding on the gross area of the plane resisting the shear stress A_{vg} based on an assumed shear yield strength of the connected material of $0.58F_y$ (= $F_y/\sqrt{3}$), or 2) fracture on the net area of the plane resisting the shear stress A_{vn} based on a conservative assumption of the ultimate shear strength of the connected material of $0.58F_u$, in conjunction with yielding on the gross area of the plane resisting the tensile stress A_{tg} based on the yield strength of the connected material F_y. Because yielding cannot occur until after fracture has taken place, the governing block shear rupture resistance is the one having the greater ratio of fracture to yield resistance. As explained in Reference 28, instead of comparing the fracture and yield components within a single resistance equation, the fracture components within two separate resistance equations representing each of

the two possible modes of failure (i.e. shear yielding/tension fracture or shear fracture/tension yielding) are compared. That is, the resistance equation to use is based on the ratio of A_{tn} to A_{vn} as follows:

➢ If $A_{tn} \geq 0.58A_{vn}$, then:

$$R_r = \phi_{bs}\left(0.58F_y A_{vg} + F_u A_{tn}\right) \qquad \text{Equation 2.250}$$

$$\textit{AASHTO LRFD Equation 6.13.4-1}$$

➢ Otherwise:

$$R_r = \phi_{bs}\left(0.58F_u A_{vn} + F_y A_{tg}\right) \qquad \text{Equation 2.251}$$

$$\textit{AASHTO LRFD Equation 6.13.4-2}$$

where:

ϕ_{bs}	=	resistance factor for block shear specified in *AASHTO LRFD* Article 6.5.4.2 (= 0.80)
A_{vg}	=	gross area along the plane resisting shear stress (in.^{2})
A_{vn}	=	net area along the plane resisting shear stress (in.^{2})
A_{tg}	=	gross area along the plane resisting tension stress (in.^{2})
A_{tn}	=	net area along the plane resisting tension stress (in.^{2})
F_y	=	specified minimum yield strength of the connected material (ksi)
F_u	=	specified minimum tensile strength of the connected material specified in AASHTO LRFD Table 6.4.1-1 (ksi)

As specified in *AASHTO LRFD* Article 6.13.4, in determining the net area of cuts carrying tension stress, the effect of staggered holes adjacent to the cuts is to be determined as specified in *AASHTO LRFD* Article 6.8.3 (i.e. using the $s^2/4g$ correction). In determining the net area of cuts carrying shear stress, the full effective diameter of staggered holes centered within two hole diameters of the cut is to be deducted; holes further removed are to be disregarded.

EXAMPLE

Calculate the block shear rupture resistance for the outside and inside bolted flange splice plates and the smaller girder flange at the splice (shown below) subjected to a factored tensile force *T*. Assume 7/8-inch diameter A 325 bolts placed in standard holes. Assume ASTM A 709 Grade 50W steel for the splice plates and flange. From *AASHTO LRFD* Table 6.4.1-1, F_u for Grade 50W steel is 70 ksi.

Calculate the deduction in width for one hole. For standard holes,

$$\text{Deduction} = \frac{7}{8} + \frac{1}{8} = 1.0 \text{ in.}$$
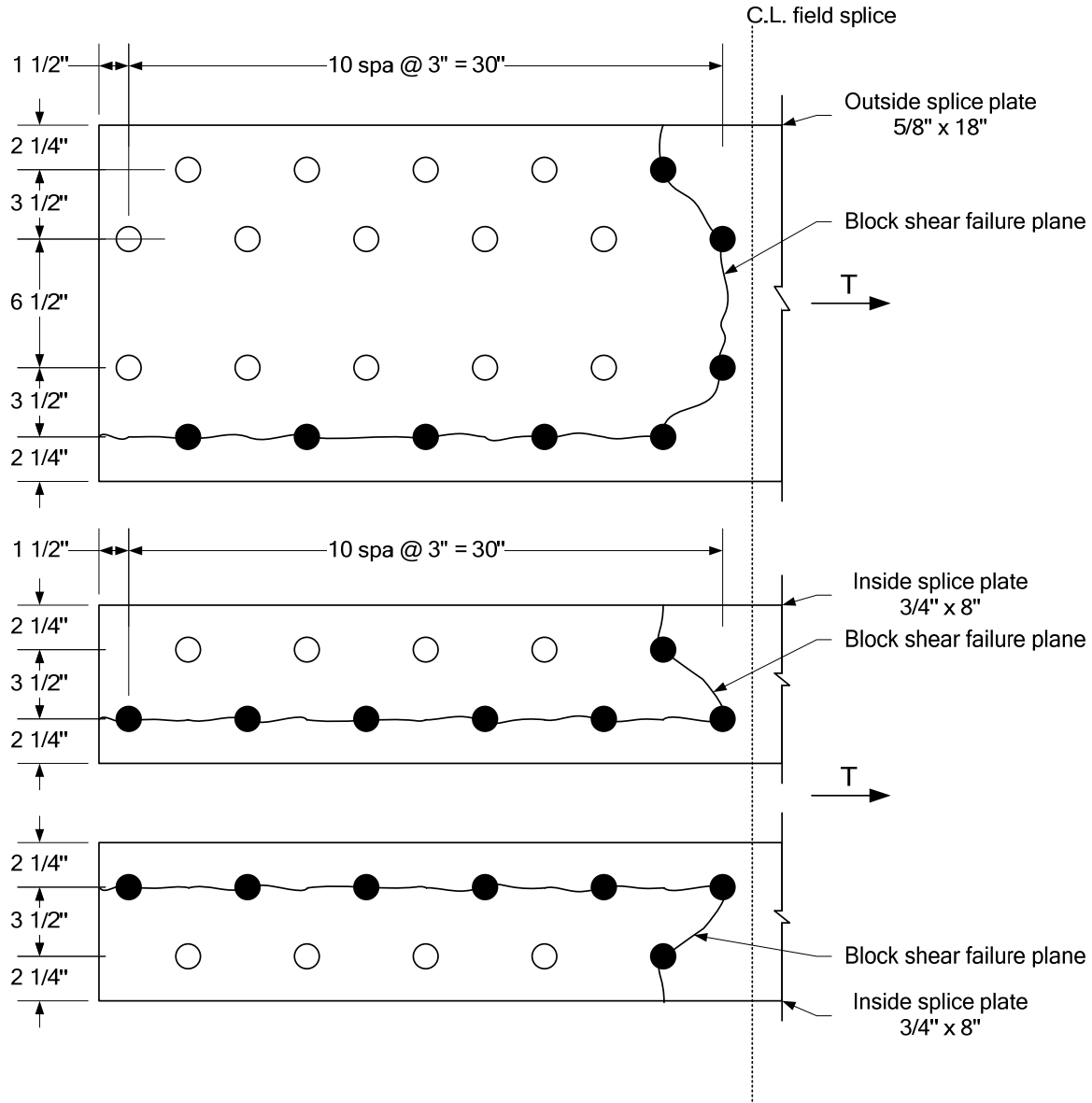
Check the outside splice plate. A_{tn} is the net area along the place resisting the tensile stress. The effect of the staggered holes must be considered in determining A_{tn}.

$$A_{tn} = \left[18.0 - 2.25 - 3.5(1.0) + 2\frac{(3.0)^2}{4(3.5)} \right](0.625) = 8.46 \text{ in.}^2$$

A_{vn} is the net area along the place resisting the shear stress. As specified in *AASHTO LRFD* Article 6.13.4, the full effective diameter of the staggered holes adjacent to the cut need not be deducted in determining A_{vn} in this case since these holes are centered more than two hole diameters from the cut. Therefore:

$$A_{vn} = \left[4(6.0) + 4.5 - 4.5(1.0) \right](0.625) = 15.00 \text{ in.}^2$$

$$A_{tn}/A_{vn} = 8.46/15.00 = 0.56 < 0.58$$

Therefore:

$$R_r = \phi_{bs}\left(0.58F_uA_{vn} + F_yA_{tg}\right)$$

AASHTO LRFD Equation 6.13.4-2

A_{tg} is the gross area along the plane resisting the tensile stress.

$$A_{tg} = [18.0 - 2.25](0.625) = 9.84 \text{ in.}^2$$

$$R_r = 0.80[0.58(70)(15.00) + 50(9.84)] = 880.8 \text{ kips}$$

Check the inside splice plates.

$$A_{tn} = 2\left[3.5 + 2.25 - 1.5(1.0) + \frac{(3.0)^2}{4(3.5)}\right](0.75) = 7.34 \text{ in.}^2$$

$$A_{vn} = 2[5(6.0) + 1.5 - 5.5(1.0)](0.75) = 39.00 \text{ in.}^2$$

$$A_{tn}/A_{vn} = 7.34/39.00 = 0.19 < 0.58$$

Therefore:

$$R_r = \phi_{bs}\left(0.58F_uA_{vn} + F_yA_{tg}\right)$$

AASHTO LRFD Equation 6.13.4-2

A_{tg} is the gross area along the plane resisting the tensile stress.

$$A_{tg} = 2[3.5 + 2.25](0.75) = 8.63 \text{ in.}^2$$

$$R_r = 0.80[0.58(70)(39.00) + 50(8.63)] = 1612 \text{ kips}$$

Failure Mode 1
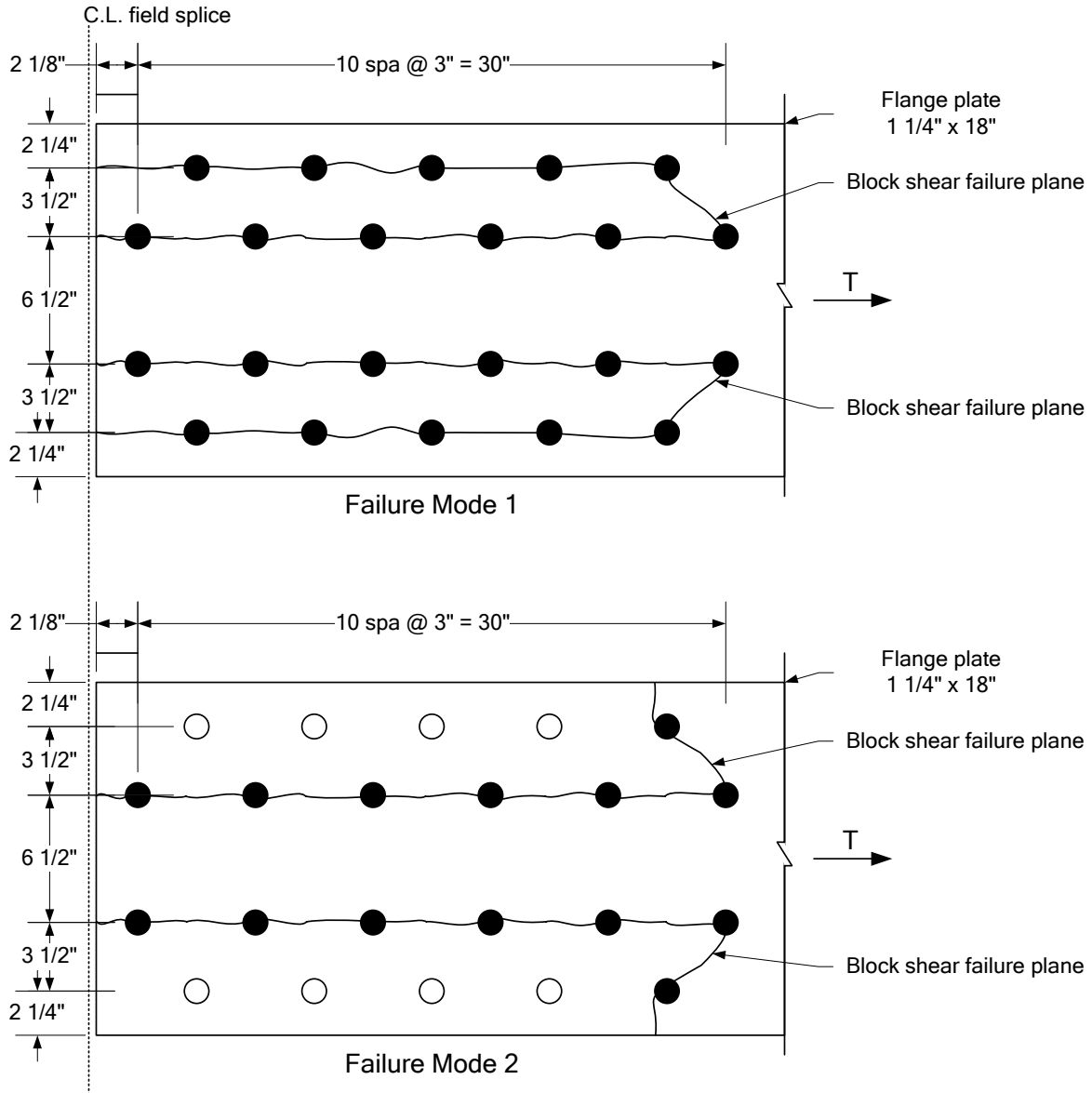
Failure Mode 2

Check the smaller girder flange at the splice. Two potential failure modes are investigated for the flange as shown in the preceding figure. For Failure Mode 1:

$$A_{tn} = 2\left[3.5 - 1.0 + \frac{(3.0)^2}{4(3.5)}\right](1.25) = 7.86 \text{ in.}^2$$

$$A_{vn} = 2[4(6.0) + 5.125 - 4.5(1.0)](1.25) + 2[5(6.0) + 2.125 - 5.5(1.0)](1.25) = 128.1 \text{ in.}^2$$

$$A_{tn}/A_{vn} = 7.86/128.1 = 0.06 < 0.58$$

Therefore:

$$R_r = \phi_{bs}\left(0.58F_u A_{vn} + F_y A_{tg}\right)$$

AASHTO LRFD Equation 6.13.4-2

A_{tg} is the gross area along the plane resisting the tensile stress.

$$A_{tg} = 2(3.5)(1.25) = 8.75 \text{ in.}^2$$

$$R_r = 0.80[0.58(70)(128.1) + 50(8.75)] = 4511 \text{ kips}$$

For Failure Mode 2:

$$A_{tn} = 2\left[3.5 + 2.25 - 1.5(1.0) + \frac{(3.0)^2}{4(3.5)}\right](1.25) = 12.23 \text{ in.}^2$$

$$A_{vn} = 2[5(6.0) + 2.125 - 5.5(1.0)](1.25) = 66.56 \text{ in.}^2$$

$$A_{tn}/A_{vn} = 12.23/66.56 = 0.18 < 0.58$$

Therefore:

$$R_r = \phi_{bs}\left(0.58F_u A_{vn} + F_y A_{tg}\right)$$

AASHTO LRFD Equation 6.13.4-2

A_{tg} is the gross area along the plane resisting the tensile stress.

$$A_{tg} = 2[3.5 + 2.25](1.25) = 14.38 \text{ in.}^2$$

$$R_r = 0.80[0.58(70)(66.56) + 50(14.38)] = 2737 \text{ kips (governs)}$$

As mentioned previously, the block shear rupture resistance will typically not control for bolted flange splices of typical proportion. Block shear rupture typically controls for short compact bolted connections and bolted end connections to thin webs of girders.

2.3.2.4.2.5 Tensile Resistance of Bolts

2.3.2.4.2.5.1 Nominal Tensile Resistance

The tensile resistance of bolts is covered in *AASHTO LRFD* Article 6.13.2.10. The tensile failure of a bolt is illustrated in Figure 2.97.

Figure 2.97 Tensile Failure of a Bolt

Axial tension occurring without simultaneous shear occurs in bolts for tension members such as hangers or other members whose line of action is perpendicular to the member to which it is fastened. The applied tensile force must be taken as the force due to externally applied loads plus any tension resulting from prying action produced by deformation of the connected parts (discussed further in the next section below).

As specified in *AASHTO LRFD* Article 6.13.2.10.1, high strength bolts subject to axial tension must be pretensioned to the level given in Table 2.16 regardless of whether the design is for a slip-critical or a bearing-type connection. According to AASHTO LRFD Article 6.13.2.10.2, the nominal tensile resistance of a bolt independent of any initial tightening force is to be taken as:

$$T_n = 0.76A_bF_{ub}$$
<div align="right">Equation 2.252</div>

<div align="right">*AASHTO LRFD* Equation 6.13.2.10.2-1</div>

where:

A_b = area of the bolt corresponding to the nominal diameter (in.^{2})

F_{ub} = specified minimum tensile strength of the bolt specified in *AASHTO LRFD* Article 6.4.3 (ksi)

The tensile resistance of a bolt is the product of the tensile strength of the bolt and the tensile stress area through the threaded portion of the bolt given by Equation 2.229. The tensile stress area is approximately 76 percent of the nominal cross-sectional area of the bolt for the usual sizes of structural bolt (105). Hence, the nominal tensile resistance per unit area (based on the nominal area of the bolt) is taken as 76 percent of the tensile strength of the bolt.

The specified nominal tensile resistance is approximately equal to the initial tightening force specified in Table 2.16. Thus, when a tensile force is applied to a high-strength bolt that has been properly pretensioned, the increase in the bolt tension is generally much smaller than the applied load. Consider a single high-strength bolt and a portion of two connected parts of thickness t subject to an externally applied tensile force P, as shown in Figure 2.98a. Prior to application of the external force, the bolt is installed with a pretension force T_b. As shown in Figure 2.98b, this causes the two parts to be initially compressed by an amount C_i. C_i must equal T_b for equilibrium. The external force P is then applied as shown in Figure 2.98c and for equilibrium, P plus C_f must equal T_f, where the subscript f refers to the final condition after the application of the force.
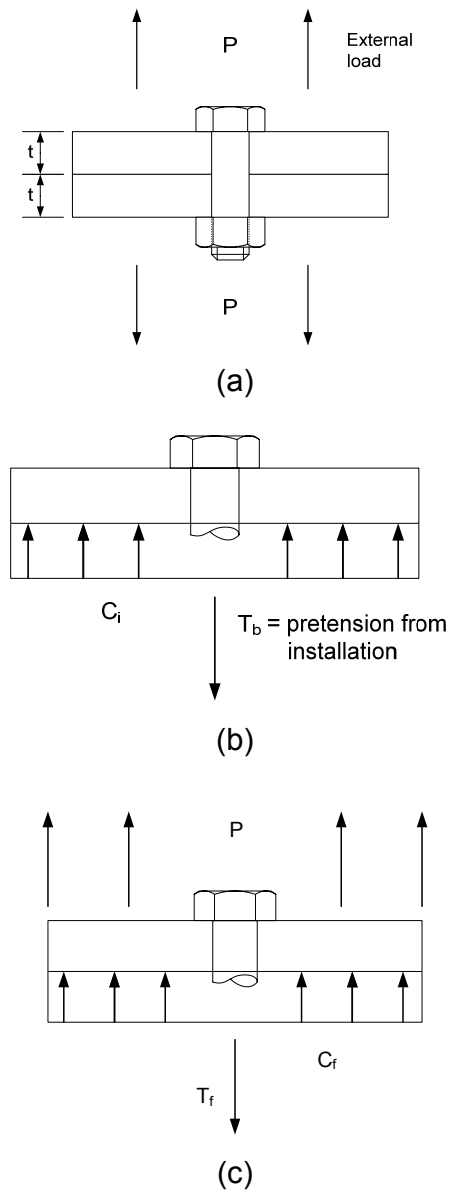
Figure 2.98 Pretensioning Effect on a Bolted Joint

As the tensile force is applied to the joint, the bolt elongates and the compressed plates simultaneously expand as the initial contact pressure is reduced. The applied force is offset by the increase in the bolt tension and the decrease in contact pressure. As illustrated in Reference 28, the increase in the bolt tension is a function of the relative stiffness of the bolt and connected plates, but it is typically minimal until the parts separate (*101*). At service load levels, there will be little increase in bolt force above the pretension load. After the parts separate, the bolt will act as a tension member with the applied force equaling the bolt tension. As a result, bolts in connections subject to axial tension are required to be fully pretensioned.

As mentioned above, pretensioning imposes a small axial elongation of the bolt. A joint subsequently loaded in tension, shear or combined tension and shear imposes significant deformations in the bolt prior to failure that override the small initial elongation and remove the pretensioning. Tests confirm that the initial pretension that would be sustained after the applied load is removed is essentially zero before the bolts fail in shear (*101*). Therefore, the tensile and shear resistances of the bolt are unaffected by the initial pretensioning of the bolt. Any residual torsion induced in the bolt during installation is also small and will be removed when the bolt is loaded to the point of plate separation. Hence, any effect of torsion on the tensile resistance of the bolt need not be considered (*101*).

EXAMPLE

Calculate the required number of 7/8-inch diameter A 325 high-strength bolts required to resist the applied tensile force due to the factored loads T_u of 250 kips acting on the hanger connection shown in the figure below. Assume that the connected parts are adequate and stiff enough to preclude any additional tensile force due to prying action.
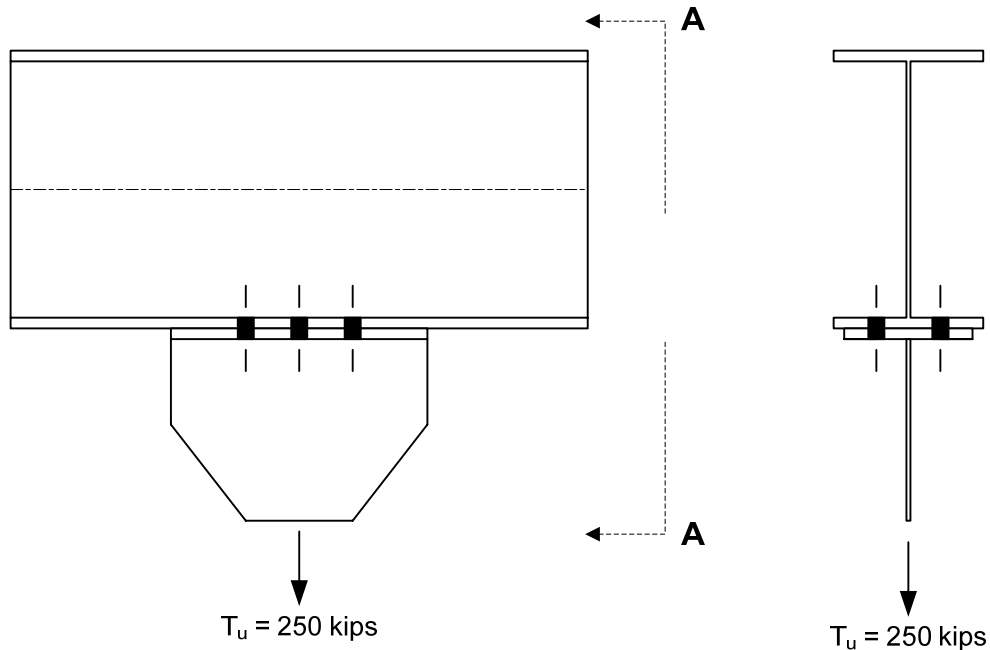
For a 7/8" A 325 bolt: $A_b = \dfrac{\pi(0.875)^2}{4} = 0.60 \text{ in}^2$

$F_{ub} =$ 120 ksi (*AASHTO LRFD* Article 6.4.3.1)

$$T_n = 0.76 A_b F_{ub}$$

AASHTO LRFD Equation 6.13.2.10.2-1

$$T_n = 0.76(0.60)(120) = 54.7 \text{ kips}$$

Since: $T_r = \phi_t T_n$

AASHTO LRFD Equation 6.13.2.2-3

$T_r = 0.80(54.7) = 43.8$ kips/bolt

$$n = \frac{T_u}{T_r} = \frac{250}{43.8} = 5.7 \text{ say 6 bolts}$$

Use 6 - 7/8" diameter A 325 bolts

2.3.2.4.2.5.2 Prying Action

The tensile load applied to a bolt may in certain cases be magnified by a prying action that can develop between the connected parts. As shown for the case of a hanger bracket in Figure 2.99, the tensile load on the web of the hanger deforms the flexible hanger flange and deflects it outward. Pressure develops at the outside edges of the flange resulting in a prying force *Q* at each edge, which increases the tensile load applied to each bolt. Therefore, as specified in *AASHTO LRFD* Article

6.13.2.10.1, any tension resulting from prying action must be added to the applied tensile force in checking bolts subject to axial tension.
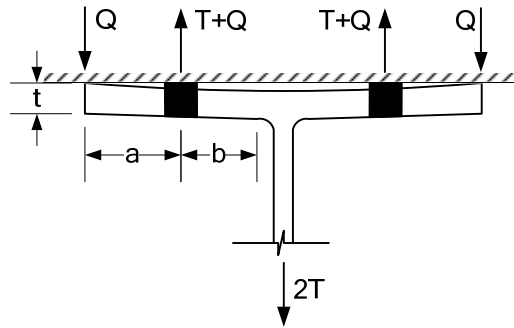
Figure 2.99 Prying Action

As a result of the effects of prying action, more than two lines of bolts in the flange is generally undesirable in hanger connections with flexible flanges because the inner lines of bolts tend to carry a substantially larger portion of the tensile load than the outer lines.   Unless the flanges are very heavy or are stiffened, the outer rows should be essentially discounted in such cases (*21*).   In situations where prying action is a consideration, the Engineer essentially has two choices: 1) use flanges that are heavy enough to prevent prying permitting the most effective use of the bolts, or 2) use lighter flanges and consider the prying effect and the resulting reduction in bolt effectiveness.

Tests reported in Reference 121 indicated that the increase in the bolt force prior to bolt line separation was not that significant. In a lighter T-stub hanger specimen (i.e. a piece of a W18 x 70), the prying force at the separation load was approximately 65 percent of the applied load. After separation when the bolt force was 33 percent greater than the initial bolt pretension, the prying force was approximately 40 percent of the applied load. Inelastic stretching of the bolts just prior to bolt fracture further reduced the prying effect down to about 30 percent of the applied load. In a heavier T-stub hanger specimen (i.e. a piece of a W36 x 300), the prying force right at the separation load was only about 5 percent of the applied load. At a bolt force 33 percent greater than the initial bolt pretension, the prying force was approximately zero and remained so until failure by bolt fracture. (Note: see the example below).

The following semi-empirical estimate of the approximate prying force Q_u due to the factored loads *prior to bolt line separation* was developed in Reference 121:

$$Q_u = \left[\frac{\dfrac{1}{2} - \dfrac{wt^4}{30ab^2 A_b}}{\dfrac{3a}{4b}\left(\dfrac{a}{4b}+1\right) + \dfrac{wt^4}{30ab^2 A_b}} \right] P_u \qquad \text{Equation 2.252}$$

where:

a	=	distance from the bolt line to the edge of the connected part subject to prying (in.). If $a \geq 1.25b$, $a = 1.25b$.
A_b	=	area of the bolt corresponding to the nominal diameter (in.^{2})
b	=	distance from the bolt line to the center of the fillet of the connected part subject to prying (in.)
P_u	=	direct tension per bolt due to the factored loads (kips)
t	=	thickness of the thinnest connected part (in.)
w	=	length of the connected part subject to prying tributary to each bolt (in.)

Any prying force computed from Equation 2.252 is assumed to act at a distance of $3a/4$ from the bolt line.

At loads that are slightly in excess of the bolt line separation load, the following semi-empirical equation applies (121):

$$Q_u = \left[\frac{\dfrac{1}{2} - \dfrac{wt^4}{30ab^2A_b}}{\dfrac{a}{b}\left(\dfrac{a}{3b}+1\right)+\dfrac{wt^4}{6ab^2A_b}}\right]P_u \qquad \text{Equation 2.253}$$

In this case, any prying force is assumed to act at the flange tips. When the numerator of Equation 2.252 or Equation 2.253 is less than or equal to zero, there is no prying.

In *AASHTO LRFD* Article 6.13.2.10.4, the following simplified semi-empirical equation is provided in place of Equation 2.253. Only a formula for the prying force following bolt line separation is provided since the increase in bolt tension is most significant following separation. This equation was based on a study evaluating the significance of several of the variables given in the more complex equations (*122*), and was found to usually provide a conservative estimate of the prying force for all bolt diameters (*123*).

$$Q_u = \left[\frac{3b}{8a} - \frac{t^3}{20}\right]P_u \qquad \text{Equation 2.254}$$

<div align="right">*AASHTO LRFD* Equation 6.13.2.10.4-1</div>

In the *AASHTO LRFD* Specification equation, *b* is defined slightly differently as the distance from the center of the bolt to the toe of the fillet of the connected part subject to prying. However, it is suggested here that the original definition of *b* from the center of the bolt line to the center of the fillet be retained for use in this equation for greater consistency with the original development (as illustrated in the example given below). All other terms are defined as above. If Equation 2.254 provides a zero or negative result, there is no prying.

Further information on prying action may be found in Reference 128a, and more recent research conducted to study the effects of prying action is discussed in Reference 101.

EXAMPLE

Calculate the prying force Q_u in the two T-stub hangers shown below using each of the three equations given above. Assume 7/8-inch diameter A 325 bolts. Assume in both cases that the hanger flange is thinner than the plate it is connected to.
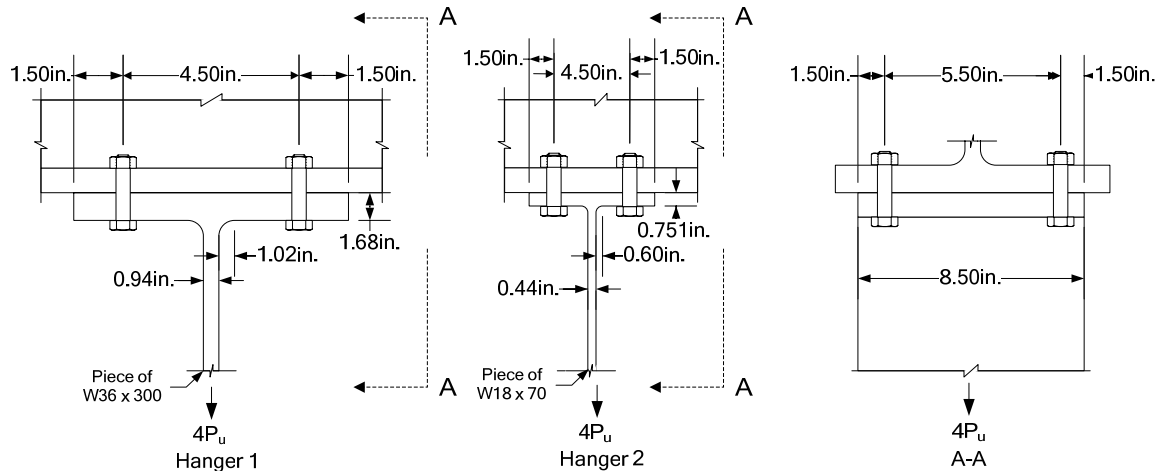
For a 7/8" A 325 bolt: $\quad A_b = \dfrac{\pi(0.875)^2}{4} = 0.60 \text{ in.}^2$

For Hanger #1 (piece of a W36 x 300):

a = 1.50 in.; b = 2.25 – (0.47 + 0.51) = 1.27 in.; w = 4.25 in.; t = 1.680 in.

Prior to bolt line separation (Equation 2.252):

$$Q_u = \left[\dfrac{\dfrac{1}{2} - \dfrac{wt^4}{30ab^2 A_b}}{\dfrac{3a}{4b}\left(\dfrac{a}{4b} + 1\right) + \dfrac{wt^4}{30ab^2 A_b}}\right] P_u$$

$$Q_u = \left[\dfrac{\dfrac{1}{2} - \dfrac{4.25(1.680)^4}{30(1.50)(1.27)^2(0.60)}}{\dfrac{3}{4}\left(\dfrac{1.50}{1.27}\right)\left(\dfrac{1.50}{4(1.27)} + 1\right) + \dfrac{4.25(1.680)^4}{30(1.50)(1.27)^2(0.60)}}\right] P_u$$

$$Q_u = \left[\dfrac{0.500 - 0.777}{1.147 + 0.777}\right] P_u \qquad \text{Since } 0.500 < 0.777 \quad \text{No prying}$$

Following bolt line separation (Equation 2.253):

$$Q_u = \left[\frac{\dfrac{1}{2} - \dfrac{wt^4}{30ab^2 A_b}}{\dfrac{a}{b}\left(\dfrac{a}{3b} + 1\right) + \dfrac{wt^4}{6ab^2 A_b}}\right] P_u$$

$$Q_u = \left[\frac{\dfrac{1}{2} - \dfrac{4.25(1.680)^4}{30(1.50)(1.27)^2(0.60)}}{\left(\dfrac{1.50}{1.27}\right)\left(\dfrac{1.50}{3(1.27)} + 1\right) + \dfrac{4.25(1.680)^4}{6(1.50)(1.27)^2(0.60)}}\right] P_u$$

$$Q_u = \left[\frac{0.500 - 0.777}{1.646 + 3.885}\right] P_u \qquad \text{Since } 0.500 < 0.777 \quad \text{No prying}$$

Following bolt line separation (Equation 2.254):

$$Q_u = \left[\frac{3b}{8a} - \frac{t^3}{20}\right] P_u \qquad \textit{AASHTO LRFD Equation 6.13.2.10.4-1}$$

$$Q_u = \left[\frac{3(1.27)}{8(1.50)} - \frac{(1.680)^3}{20}\right] P_u = 0.08 P_u \qquad \text{Since } Q_u \approx 0 \quad \text{No prying}$$

For Hanger #2 (piece of a W18 x 70):

a = 1.50 in.; b = 2.25 – (0.22 + 0.30) = 1.73 in.; w = 4.25 in.; t = 0.751 in.

Prior to bolt line separation (Equation 2.252):

$$Q_u = \left[\frac{\dfrac{1}{2} - \dfrac{4.25(0.751)^4}{30(1.50)(1.73)^2(0.60)}}{\dfrac{3}{4}\left(\dfrac{1.50}{1.73}\right)\left(\dfrac{1.50}{4(1.73)} + 1\right) + \dfrac{4.25(0.751)^4}{30(1.50)(1.73)^2(0.60)}}\right] P_u$$

$$Q_u = \left[\frac{0.500 - 0.017}{0.791 + 0.017}\right] P_u = 0.60 P_u$$

Following bolt line separation (Equation 2.253):

$$Q_u = \left[\frac{\dfrac{1}{2} - \dfrac{4.25(0.751)^4}{30(1.50)(1.73)^2(0.60)}}{\left(\dfrac{1.50}{1.73}\right)\left(\dfrac{1.50}{3(1.73)}+1\right) + \dfrac{4.25(0.751)^4}{6(1.50)(1.73)^2(0.60)}} \right] P_u$$

$$Q_u = \left[\frac{0.500 - 0.017}{1.118 + 0.084} \right] P_u = 0.40 P_u$$

Following bolt line separation (Equation 2.254):

$$Q_u = \left[\frac{3(1.73)}{8(1.50)} - \frac{(0.751)^3}{20} \right] P_u = 0.41 P_u$$

2.3.2.4.2.5.3 Bolt Tensile Fatigue

As specified in *AASHTO LRFD* Article 6.13.2.10.3, properly pretensioned high-strength bolts subject to fatigue in axial tension must satisfy *AASHTO LRFD* Equation 6.6.1.2.2-1 (Equation 2.90). The stress range (Δf) in the equation is to be taken as the stress range in the bolt due to the passage of the HS20 (72 kip) fatigue design load (plus the 15 percent dynamic load allowance) specified in *AASHTO LRFD* Article 3.6.1.4, plus any prying force resulting from the cyclic application of the fatigue load (the initial tension in the bolts is not to be included). The stress range is to be computed using the nominal diameter of the bolt. In calculating the nominal fatigue resistance ($\Delta F)_n$ from *AASHTO LRFD* Equation 6.6.1.2.5-1 (Equation 2.87), the detail category constant *A* and the constant-amplitude fatigue threshold ($\Delta F)_{TH}$ for A 325 and A 490 bolts in axial tension are to be taken directly from *AASHTO LRFD* Tables 6.6.1.2.5-1 and 6.6.1.2.5-3, respectively (see the previous section of this chapter on Fatigue Limit State Verifications).

Tests of various single-bolt assemblies and joints with bolts in tension subjected to repeated external loads that resulted in eventual failure of the pretensioned high-strength bolts indicated that properly tightened high-strength bolts are not adversely affected by repeated application of service-load tensile stress (*101*); that is, the nominal fatigue resistance of the bolts in such applications is relatively high. However, since a limited range of prying effects was investigated in these studies, the assumption is made that the connected material is sufficiently stiff that any prying force is a relatively small part of the applied tension. As of this writing (2006), *AASHTO LRFD* Article 6.13.2.10.3 limits the calculated prying force to 60 percent of the externally applied load when bolts are subject to tensile fatigue loading. It should be noted however that this limit has been reduced from 60 percent to 30 percent in Reference 105 based on the limited investigations of prying effects under fatigue loading, and a similar reduction is under consideration by AASHTO.

Since low carbon A 307 bolts are of lower strength and are not pretensioned, *AASHTO LRFD* Article 6.13.2.10.3 prohibits their use in connections subjected to fatigue loading.

2.3.2.4.2.6 Combined Tensile and Shear Resistance of Bolts

The resistance of bolts under combined axial tension and shear is covered in *AASHTO LRFD* Article 6.13.2.11. Examples of connections in which the bolts would be subject to combined tension and shear are shown in Figure 2.100.

(a)   (b)
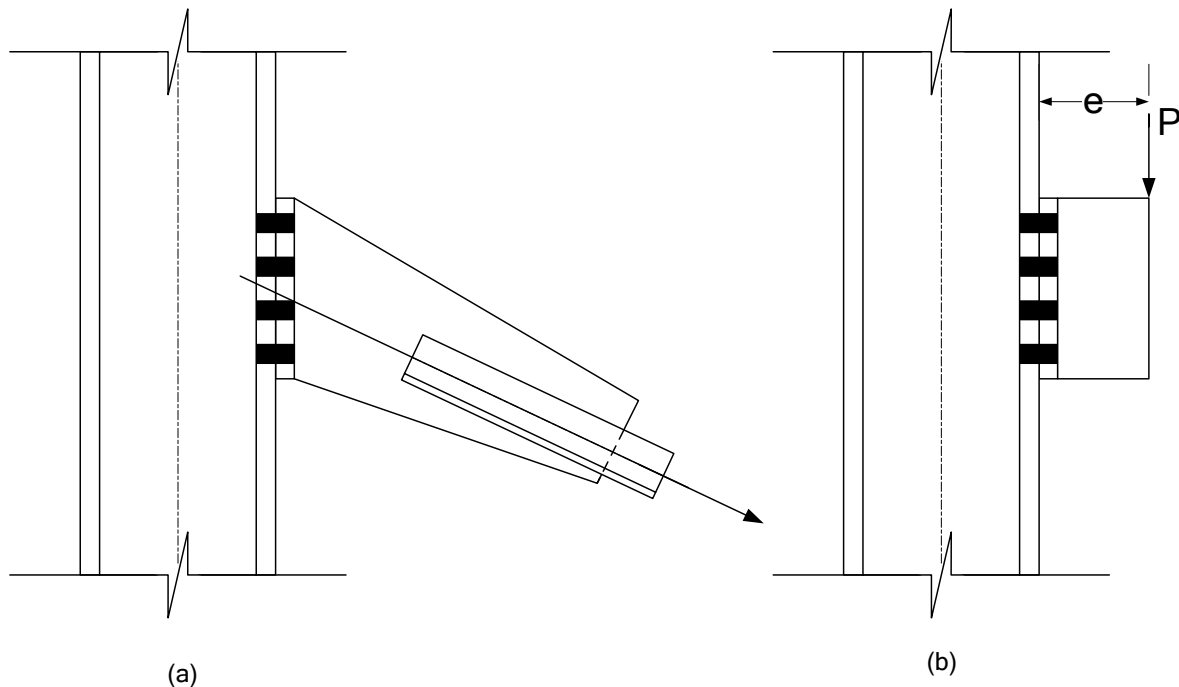
Figure 2.100 Connections Subject to Combined Tension and Shear

Once a bolt slips and goes into bearing, the bolt yields under the effects of combined tension and shear at a lower load than if only shear or tension were present. Tests on single high-strength bolts subject to various combinations of tension and shear in this condition were conducted at the University of Illinois (*124*). From these tests, it was determined that when both shear and tensile forces act on a high-strength bolt at the strength limit state, the interaction can be conveniently expressed by an elliptical interaction relationship as follows (*105*):

$$\left[\frac{T_u}{(R_r)_t}\right]^2 + \left[\frac{P_u}{(R_r)_s}\right]^2 \qquad \text{Equation 2.255}$$

where:
P_u =   shear force on the bolt due to the factored loads (kips)
T_u =   tensile force on the bolt due to the factored loads (kips)
$(R_r)_s$ =   factored resistance of the bolt in shear (kips)
$(R_r)_t$ =   factored resistance of the bolt in tension (kips)

Equation 2.255 accounts for the connection length effect on bolts loaded in shear, the ratio of the shear resistance to tensile resistance of threaded bolts, the ratio of root area to nominal body area of the bolt and the ratio of the tensile stress area to the nominal body area of the bolt. Equations for various cases based on Equation 2.255 can be found in Reference 125.

In *AASHTO LRFD* Article 6.13.2.11, a conservative simplification of the interaction relationship given by Equation 2.255 is used. In this article, the nominal tensile resistance T_n of a bolt subjected to combined shear and axial tension is to be taken as follows:

➢ If $\dfrac{P_u}{R_n} \leq 0.33$, then:

$$T_n = 0.76 A_b F_{ub} \qquad\qquad \text{Equation 2.256}$$

$$\textit{AASHTO LRFD}\ \text{Equation 6.13.2.11-1}$$

➢ Otherwise:

$$T_n = 0.76 A_b F_{ub} \sqrt{1 - \left(\frac{P_u}{\phi_s R_n}\right)^2} \qquad\qquad \text{Equation 2.257}$$

$$\textit{AASHTO LRFD}\ \text{Equation 6.13.2.11-2}$$

where:

ϕ_s	=	resistance factor for bolts in shear = 0.80
A_b	=	area of the bolt corresponding to the nominal diameter (in.^{2})
F_{ub}	=	specified minimum tensile strength of the bolt specified in Article 6.4.3 (ksi)
P_u	=	shear force on the bolt due to the factored loads (kips)
R_n	=	nominal shear resistance of the bolt determined as specified in Article 6.13.2.7 (kips)

In other words, no reduction in the nominal tensile resistance of the bolt is required when the shear force due to the factored loads does not exceed 33 percent of the nominal shear resistance of the bolt.

The nominal resistance of a bolt in a slip-critical connection subject to combined tension and shear under service loads (i.e. under Load Combination Service II) was discussed previously in Section 2.3.2.4.1.1 of this chapter.

In the bracket connection shown in Figure 2.100b, the eccentric load *P* results in a moment on the connection (Figure 2.101a) that produces both shear and tension in the upper bolts. The tension is largest on the top row of bolts (refer to Equation 2.235).
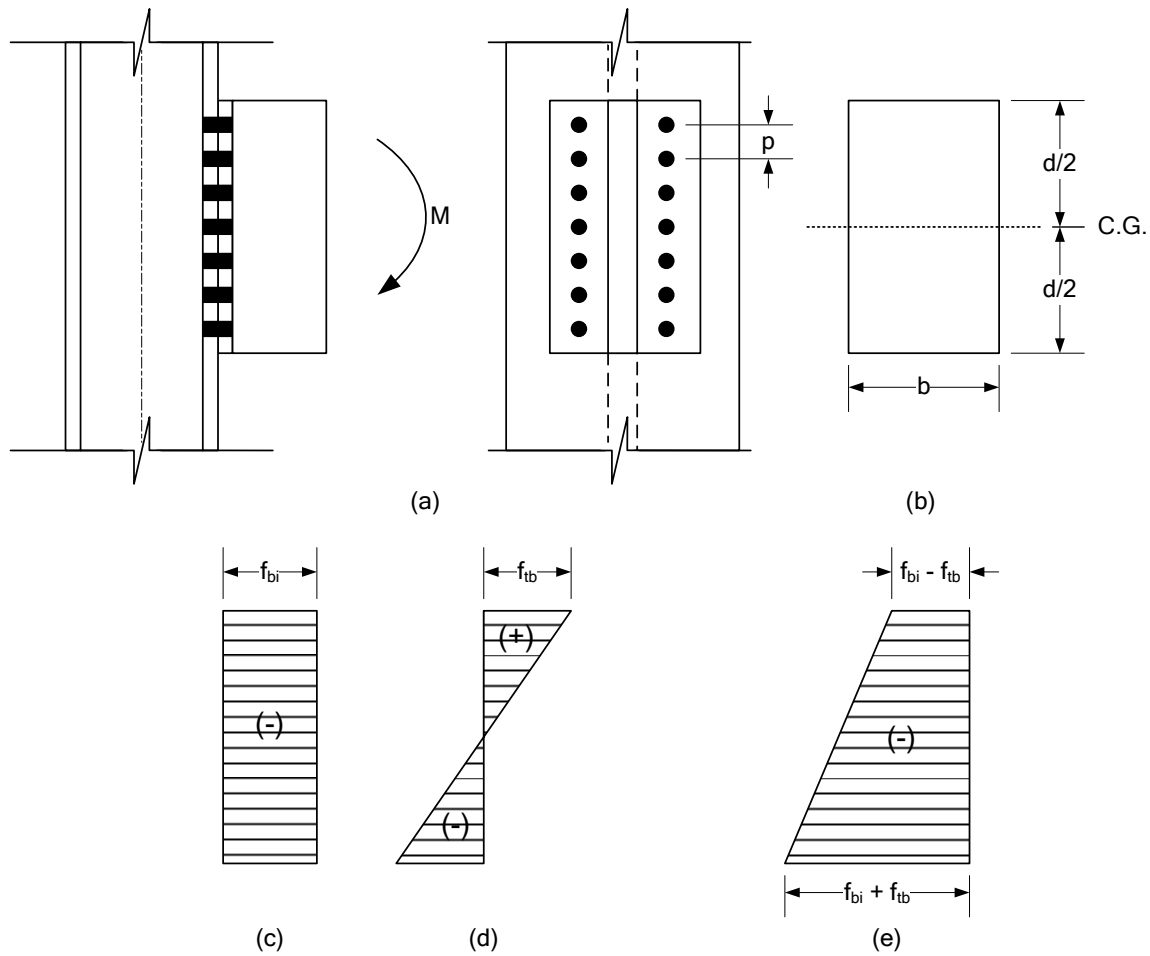
Figure 2.101 Tension and Shear from Eccentric Loading – Stresses on Contact Area

As shown in Figure 2.101b, the neutral axis under the bending moment M due to the factored loads occurs at the centroid of the rectangular contact area (i.e. at $d/2$). The initial pretension in the high-strength bolts introduces a precompression stress f_{bi} in the contact area of the joined plates (Figure 2.101c). Assuming this initial compression stress is uniform over the contact area bd, this stress can be computed as:

$$f_{bi} = \frac{\Sigma T_i}{bd}$$
Equation 2.258

where ΣT_i is the minimum required pretension from Table 2.16 times the number of bolts in the connection. The tensile stress at the top of the contact area f_{tb} due to the applied moment (Figure 2.101d) is computed as:

$$f_{tb} = \frac{Md/2}{I} = \frac{6M}{bd^2} \qquad \text{Equation 2.259}$$

As shown in Figure 2.101e, it should be checked that f_{tb} does not exceed f_{bi} in order to ensure that compression remains between the joined parts at the top of the connection. The tensile load T_u on the top bolt due to the factored loads is equal to f_{tb} times the bolt tributary area, or the width b times the bolt spacing p divided by the number of vertical rows of bolts n; i.e. $T_u = f_{tb}bp/n$. Substituting f_{tb} from Equation 2.259 gives:

$$T_u = \frac{6Mp}{nd^2} \qquad \text{Equation 2.260}$$

Assuming the top bolt is approximately $p/2$ from the top, T_u can be modified as follows (28):

$$T_u = \frac{6Mp}{nd^2}\left(\frac{d-p}{d}\right) \qquad \text{Equation 2.261}$$

For the typical case where all bolts in the connection are the same size, and where f_{bi} is not overcome by f_{tb}, it is shown in Reference 28 that T_u can also be computed from the following simplified formula:

$$T_u = \frac{My_b}{\sum y^2} \qquad \text{Equation 2.262}$$

where y_b is the vertical distance from the centroid of the connection to the extreme row of bolts, and y is the vertical distance from the centroid of the connection to each bolt. The same equations can be used to calculate T_u for use in Equation 2.235 at the service limit state (i.e. under the Service II Load Combination). The shear force P_u in each bolt due to the factored loads can be taken simply as the total load P divided by the number of bolts in the connection.

EXAMPLE

Check the bolts in the slip-critical bracket connection shown in Figure 2.100b at the strength limit state (i.e. assuming the bolts have slipped and gone into bearing). The number of vertical rows of bolt in the connection n is equal to two. The total force P due to the factored loads is 150 kips applied at an eccentricity e of 3 in. Assume 7/8-inch diameter A 325 bolts in standard holes with the threads *not* excluded from the shear plane. The vertical pitch between bolts p is 3 in. The end distance for the top and bottom bolts is 1.5 in. The bracket dimensions are b = 5.5 in. and d = 12 in. Assume that the connected parts are adequate and stiff enough to preclude any additional tensile force due to prying action.

From Table 2.16, the minimum required initial pretension for 7/8-inch diameter A 325 bolts is 39.0 kips. Therefore, from Equation 2.258, the initial precompression stress

f_{bi} on the contact area is equal to $(8)(39.0)/(5.5)(12) = 4.73$ ksi. From Equation 2.259, the tensile stress at the top of the bracket f_{tb} is equal to $6(150)(3)/(5.5)(12)^2 = 3.41$ ksi, which is less than f_{bi}. The pieces remain in compression (contact) at the top of the bracket.

For threads included in the shear plane, the nominal shear resistance of a bolt is computed from Equation 2.239 as follows:

$$R_n = 0.38 A_b F_{ub} N_s$$

AASHTO LRFD Equation 6.13.2.7-2

For a 7/8" A 325 bolt: $\quad A_b \quad = \quad \dfrac{\pi(0.875)^2}{4} = 0.60 \text{ in.}^2$

$\qquad\qquad\qquad\qquad F_{ub} = \quad 120$ ksi (*AASHTO LRFD* Article 6.4.3.1)

For single shear: $\qquad N_s \quad = \quad 1$

Therefore: $\qquad\qquad\qquad R_n = 0.38(0.60)(120)(1) = 27.4$ kips / bolt

The shear due to the factored loads P_u in each bolt is taken as P divided by the number of bolts. Therefore, $P_u = 150 /8 = 18.75$ kips. Since $P_u/R_n = 18.75/27.4 = 0.68 > 0.33$, the nominal tensile resistance of each bolt T_n under combined tension and shear is taken from Equation 2.257 as follows:

$$T_n = 0.76 A_b F_{ub} \sqrt{1 - \left(\frac{P_u}{\phi_s R_n}\right)^2}$$

AASHTO LRFD Equation 6.13.2.11-2

$$T_n = 0.76(0.60)(120)\sqrt{1 - \left(\frac{18.75}{(0.80)(27.4)}\right)^2} = 28.3 \text{ kips}$$

Since: $\qquad\qquad\qquad\qquad\qquad T_r = \phi_t T_n$

AASHTO LRFD Equation 6.13.2.2-3

$$T_r = 0.80(28.3) = 22.6 \text{ kips/bolt}$$

The tensile force in each bolt to the factored loads T_u may be computed from Equation 2.261 as follows:

$$T_u = \frac{6Mp}{nd^2}\left(\frac{d-p}{d}\right) \qquad\qquad \text{Equation 2.261}$$

$$T_u = \frac{6(150)(3)(3)}{2(12)^2}\left(\frac{12-3}{12}\right) = 21.1 \text{ kips} < T_r = 22.6 \text{ kips ok}$$

Alternatively, T_u may be computed from Equation 2.262 as follows:

$$T_u = \frac{My_b}{\Sigma y^2}$$ Equation 2.262

where y_b = 4.5 in. and $\Sigma y^2 = 4[(1.5)^2 + (4.5)^2] = 90$ in.^{2} Therefore:

$$T_u = \frac{150(3)(4.5)}{90} = 22.5 \text{ kips} < T_r = 22.6 \text{ kips ok}$$

2.3.2.4.2.7 Compressive Resistance of a Connected Element

As of this writing (2006), the compressive resistance of certain connected elements (e.g. gusset plates, corner angles, brackets or connection plates) is not specifically covered in the *AASHTO LRFD* Specifications.   The factored compressive resistance of flange splice plates is specified in *AASHTO LRFD* Article 6.13.6.1.4c and is discussed below in Section 2.3.4.2.2.2 of this chapter (refer to Equation 2.294). Local buckling of connection plates (serving as transverse stiffeners) adjacent to web panels subject to tension-field action at the strength limit state is considered in *AASHTO LRFD* Article 6.10.11.1 (refer to Equations 2.205 and 2.207).

Potential local buckling of connection plates at the strength limit state due to bending of the plates caused by the net factored lateral reactions at the cross-frames due to curvature and/or significant skew (in conjunction with the use of staggered cross-frames) is not currently covered. These net lateral reactions, resulting from either the lateral flange moments due to curvature or the lateral flange moments induced into the flanges from the cross-frames in the case of skew, are assumed applied where the cross-frame members are attached to the connection plates.

A suggested approach for checking this limit state for cases where these lateral reactions are deemed significant is to treat the connection plate as a fixed-end beam (or using another assumption perhaps deemed more appropriate based on the end conditions), loaded by the factored net lateral reactions at the appropriate locations (refer to the example at the end of Section 2.3.2.5 of this chapter for further discussion regarding the calculation of the factored lateral reactions at cross-frame member locations. For straight non-skewed bridges, the lateral force of 20.0 kips suggested in *AASHTO LRFD* Article 6.6.1.3.1 for the design of the connection of these plates to the flanges may conservatively be used for this check if desired). The maximum moment so computed should then be checked against the resistance factor for flexure ϕ_f from *AASHTO LRFD* Article 6.5.4.2 times the nominal local buckling resistance of the connection plate about an axis parallel with the web. The equations from *AASHTO LRFD* Article 6.12.2.2.1 giving the nominal local buckling resistance of I- and H-shaped members about an axis parallel with the web are appropriate to be applied to rectangular connection plates as follows:

If $\lambda_f \leq \lambda_{pf}$, then:

$$M_n = M_p$$ Equation 2.262a

AASHTO LRFD Equation 6.12.2.2.1-1

If $\lambda_{pf} < \lambda_f \leq \lambda_{rf}$, then:

$$M_n = \left[1 - \left(1 - \frac{S_y}{Z_y} \right) \left(\frac{\lambda_f - \lambda_{pf}}{0.45\sqrt{\dfrac{E}{F_{ys}}}} \right) \right] F_{ys} Z_y$$

Equation 2.262b

where:

λ_f =   slenderness ratio of the connection plate = b_t/t_t

λ_{pf} = $0.38\sqrt{\dfrac{E}{F_{ys}}}$

λ_{rf} = $0.83\sqrt{\dfrac{E}{F_{ys}}}$

F_{ys} =   specified minimum yield strength of the connection plate (ksi)

M_p =   plastic moment of the effective section (defined below) about the axis parallel with the web (kip-in.)

S_y =   elastic section modulus of the effective section (defined below) about the axis parallel with the web (in.^{3})

Z_y =   plastic section modulus of the effective section (defined below) about the axis parallel with the web (in.^{3})

In the above, λ_{rf} is derived from the right-hand side of Equation 2.24 with the plate buckling coefficient k_c taken equal to 0.76. For interior girders, S_y, M_p and Z_y may be calculated based on an effective rectangular section consisting of the connection plates on both side of the web. In this case, $M_p = 1.5F_{ys}S_y$ and $Z_y = 1.5S_y$. For exterior girders, S_y, M_p and Z_y may be calculated based on an effective section consisting of the connection plate plus a portion of the web. A portion of the web equal to $18t_w$ is suggested for inclusion with the connection plate in this case. In this case, all properties should be computed about the appropriate neutral axis of the effective tee section. Note that if F_{yw} is smaller than F_{ys}, the strip of web included in the effective section should be reduced by the ratio of F_{yw}/F_{ys}.

For determining and checking the compressive resistance of gusset plates for cross-frame and lateral-bracing members, it is recommended that the suggested procedures given in Reference 128a be followed and adapted to fit with the *AASHTO LRFD* Specifications. The design of gusset plates for truss members is covered in *AASHTO LRFD* Article 6.14.2.8.

2.3.2.5 Eccentric Shear

In Figure 2.102a, the force *P* is applied on a line of action that does not pass through the center of gravity of the bolt group. The resultant action may be represented as a

moment (torque) equal to P times the eccentricity e and a concentric force P acting on the connection, as shown in Figure 2.102b and Figure 2.102c.
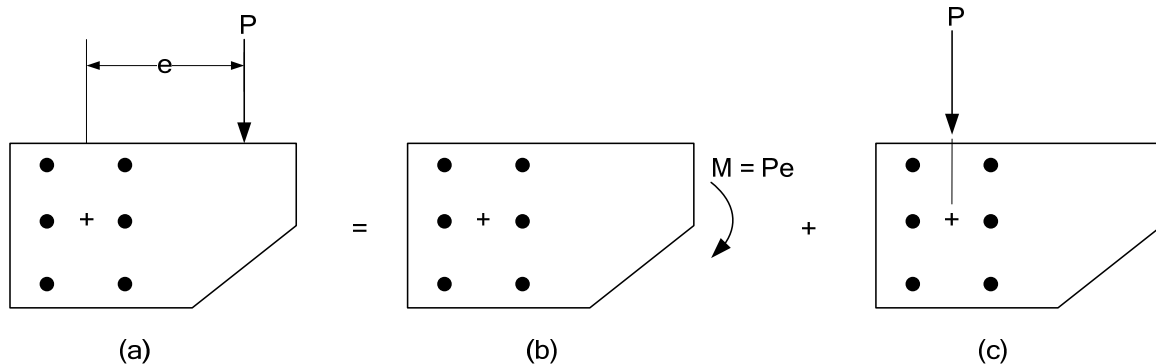
Figure 2.102 Eccentric Shear Connection

Since both the moment and concentric force cause shears on the bolt group, this particular situation is referred to as eccentric shear. As will be discussed later, a common example of a connection in a steel bridge subject to eccentric shear is a bolted web splice.

Bolt groups subject to eccentric shear have typically been analyzed using a traditional elastic vector analysis assuming no friction, that the bolts are elastic and that the plates are rigid ensuring a linear strain variation on the bolts (*101*). The concentric force P is assumed to stress the bolts uniformly and the stress due to the torsion is then superimposed vectorially. The torque has traditionally been treated using an adaptation of the theory of twisting of circular steel shafts, as discussed below. Reference 101 discusses an alternative ultimate strength approach in which the translation and rotation of the bolt group is reduced to a pure rotation about a point referred to as the instantaneous center of rotation. An empirical load-deformation relationship is used to relate the shear resistance of each bolt to its deformation (*126, 127*). However, it was felt by the *AASHTO LRFD* specification writers that the traditional elastic approach provides a more consistent factor of safety and is therefore recommended for use (refer to *AASHTO LRFD* Article C6.13.6.1.4b)

Consider the bolt group acted on by a torque M, as shown in Figure 2.103a. Assume the plate, which transmits the torque to the bolts, rotates about an axis through the centroid of the bolt group, and that the bolts all have different areas. It is assumed in this development that constraints on the members or connection do not force rotation about some point other than the centroid of the bolt group, which is typically the case in most practical connections.
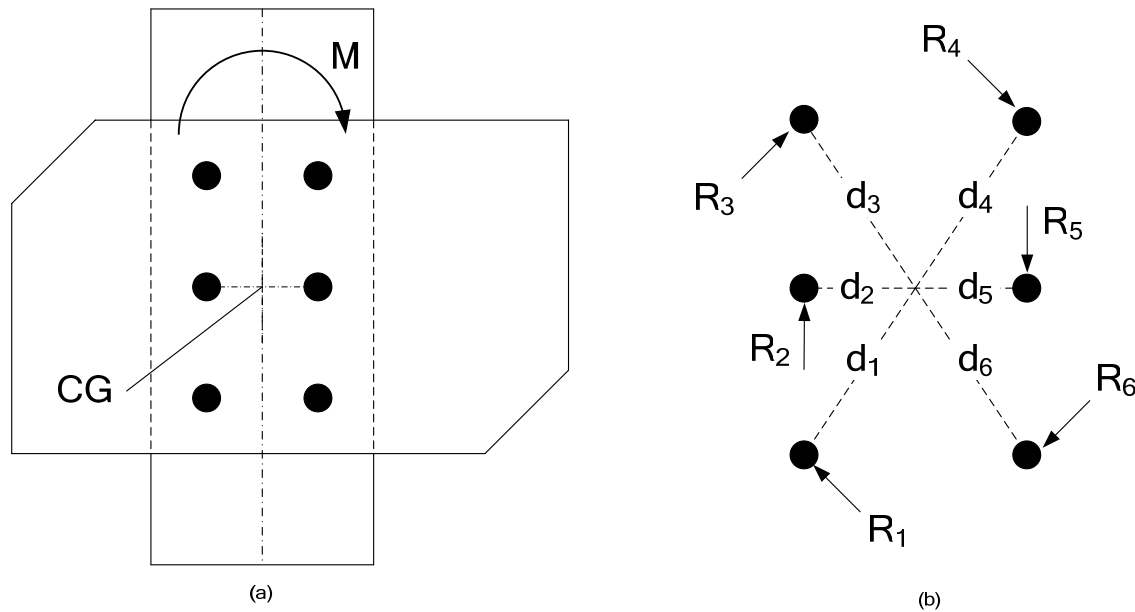
Figure 2.103 Analytical Model for Torque on Bolt Group

Neglecting friction between the plates, the torque on the bolt group is equal to (Figure 2.103b):

$$M = R_1 d_1 + R_2 d_2 + R_3 d_3 + ... + R_6 d_6 \qquad \text{Equation 2.263}$$

Assume that the shear stress in each bolt due to the torque acts normal to the radius drawn from the centroid and that the stresses vary linearly with the distance from the centroid. Thus, the bolt furthest removed from the centroid (say Bolt 6 in Figure 2.103b for the purposes of this discussion) is the one most heavily stressed. The shear force in Bolt 6 is equal to $R_6 = \tau_6 A_6$. The stresses in the other bolts are then proportional to the stress in Bolt 6. Therefore, the forces acting on the other bolts can be computed as:

$$R_1 = \frac{d_1 \tau_6}{d_6} A_1; R_2 = \frac{d_2 \tau_6}{d_6} A_2; R_3 = \frac{d_3 \tau_6}{d_6} A_3; R_4 = \frac{d_4 \tau_6}{d_6} A_4; R_5 = \frac{d_5 \tau_6}{d_6} A_5$$

Equation 2.264

Substituting the forces into Equation 2.263 gives:

$$M = \frac{\tau_6}{d_6} \sum_{i=1}^{n} d_i^2 A_i$$

Equation 2.265

where *n* is the total number of bolts in the connection (*n* = 6 in this case). Rearranging and substituting the polar moment of inertia I'_p for the term $\sum_{i=1}^{n} d_i^2 A_i$ gives the following equation for the stress in the most heavily stressed bolt in the group:

$$\tau_6 = \frac{Md_6}{I_p'}$$

Equation 2.266

which is analogous to the equation for the shear stress in a circular shaft subject to pure torsion (*21*).

In most cases, the bolts in the connection will be the same size. Therefore, it becomes convenient to factor the bolt cross-sectional area A out of I_p'. Therefore, letting $I_p' = A \sum_{i=1}^{n} d_i^2 = A I_p$ results in the following expression for the shear force in the most heavily stressed bolt:

$$R_6 = \frac{Md_6}{I_p}$$

Equation 2.267

Referring to Figure 2.104, since $d^2 = x^2 + y^2$:

$$I_p = \sum_{i=1}^{n} x_i^2 + \sum_{i=1}^{n} y_i^2$$

Equation 2.268

Note that *AASHTO LRFD* Article C6.13.6.1.4b provides the following alternative formula for computing the polar moment of inertia I_p about the centroid of the connection (*128*):

$$I_p = \frac{nm}{12}\left[s^2\left(n^2 - 1\right) + g^2\left(m^2 - 1\right)\right]$$

Equation 2.269

AASHTO LRFD Equation C6.13.6.1.4b-3

where:
m	=	number of vertical rows of bolts
n	=	number of bolts in one vertical row
s	=	vertical pitch of bolts (in.)
g	=	horizontal pitch of bolts (in.)

To facilitate combination with the direct shear in each bolt due to the concentric force P, it becomes convenient to use the x and y components of the bolt shears due to torsion. Referring again to Figure 2.104, $R_6 = R_y d_6 / x_6$ and $R_6 = R_x d_6 / y_6$. Substituting into Equation 2.267 gives:

$$R_x = \frac{My_6}{I_p}$$

Equation 2.270

$$R_y = \frac{Mx_6}{I_p}$$

Equation 2.271
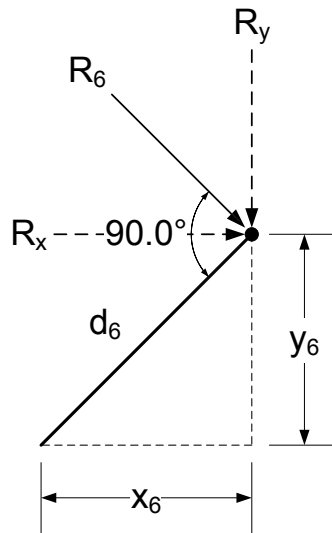
Figure 2.104 Horizontal and Vertical Components of Shear Force *R*

The direct shear force on a bolt in an eccentric shear connection due to the concentric force P can be computed as:

$$R_v = \frac{P}{n}$$ Equation 2.272

where *n* is again the total number of bolts in the connection. The total resultant force on the bolt is then computed from the vector sum of the direct shear force and the *x* and *y* components of the shear force due to torsion as follows:

$$R = \sqrt{(R_v + R_y)^2 + R_x^2}$$ Equation 2.273

In certain cases, additional horizontal components of shear force may act on a bolt group subject to eccentric shear (e.g. in bolted web splices for sections where the neutral axis is not as the middepth of the web, in cross-frame connections where the line of action of force in a diagonal member does not pass through the center of gravity of the corresponding bolt group). In such cases, the additional horizontal component would be appropriately combined with R_x in Equation 2.273 to determine the resultant bolt force.

EXAMPLE

A refined analysis of a three-span continuous straight skewed I-girder bridge with 4 girders in the cross-section yields the following unfactored cross-frame forces in the X-type cross-frames in the two bays between Girders 1 and 3 at a critical cross-section. Girder 1 is the exterior girder and Girders 2 and 3 are the two adjacent interior girders. All forces are in kips (positive is tension; negative is compression). A future wearing surface load (DW) is not specified in this example.
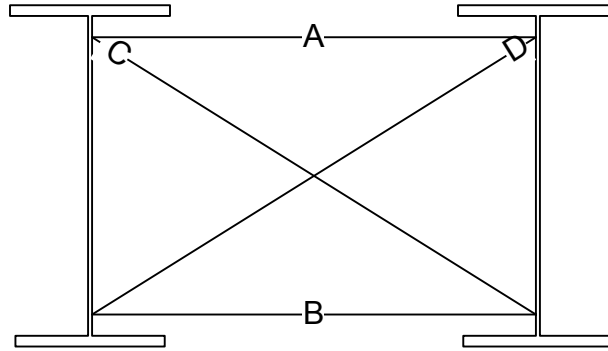
A. Cross-frame force top
B. Cross-frame force bottom
C. Cross-frame force left
D. Cross-frame force right

Girder 1	DC_1	DC_2	Total	+(LL+IM)	-(LL+IM)
Loc A	20	-7	13	1	-1
Loc B	-18	-5	-23	7	-12
Loc C	23	6	29	13	-8
Loc D	-24	-14	-38	13	-24
Girder 2	DC_1	DC_2	Total	+(LL+IM)	-(LL+IM)
Loc A	77	0	77	1	-6
Loc B	-72	-16	-88	12	-30
Loc C	41	0	41	9	-5
Loc D	-44	-12	-56	5	-26
Girder 3	DC_1	DC_2	Total	+(LL+IM)	-(LL+IM)
Loc A	57	-7	50	0	-5
Loc B	-52	-10	-62	6	-18
Loc C	-68	-24	-92	11	-39
Loc D	65	11	76	20	-6

The spans of the bridge are approximately 100 ft – 200 ft – 100 ft. The girder depth is 63 inches and the girder spacing is 8'-8". The cross-frame spacing adjacent to the critical cross-section is approximately 20 ft.

Design the high-strength bolted cross-frame gusset plate connection at the bottom flange of Girder 2. *AASHTO LRFD* Article 6.13.1 requires that the cross-frame connections be designed for the computed forces when the cross-frames are included in the structural model used to determine the force effects.

First, determine the proper resolution of the dead and live load plus impact forces at the connection in order to calculate the critical net force effect for the connection design. The horizontal forces may be resolved to ensure equilibrium based on a free-body diagram at the connection.   The figure below shows the unfactored computed dead and live load plus impact forces in the cross-frame members taken from the table above.

Dead Load (DC$_1$ + DC$_2$)
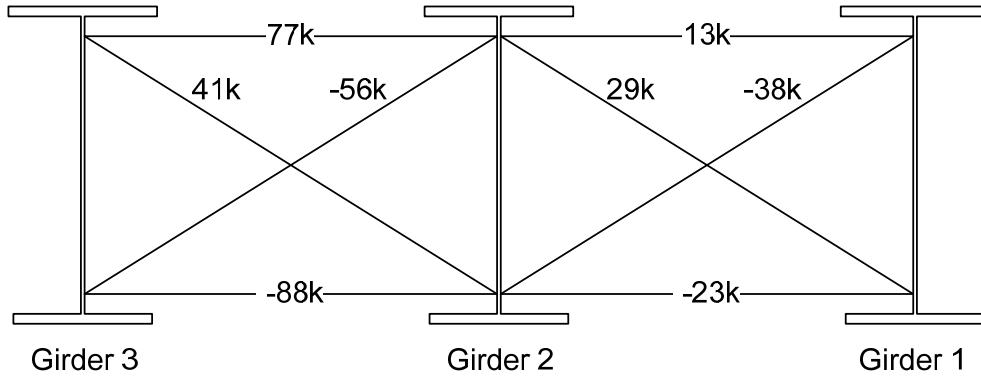
+ (LL + IM)
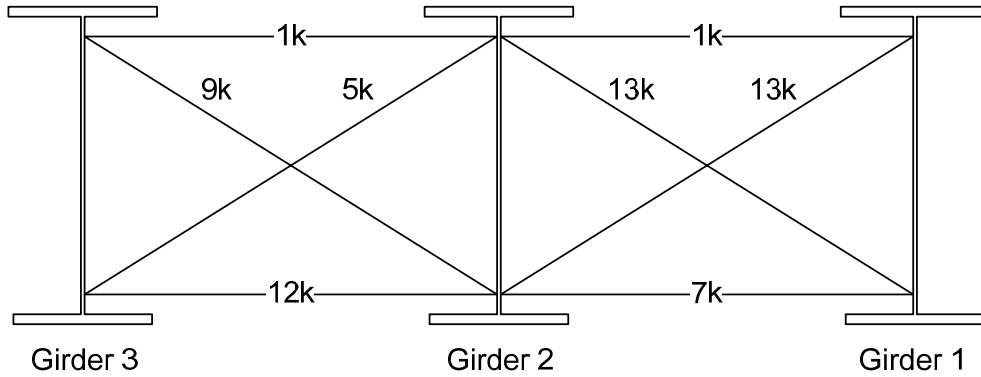
- (LL + IM)
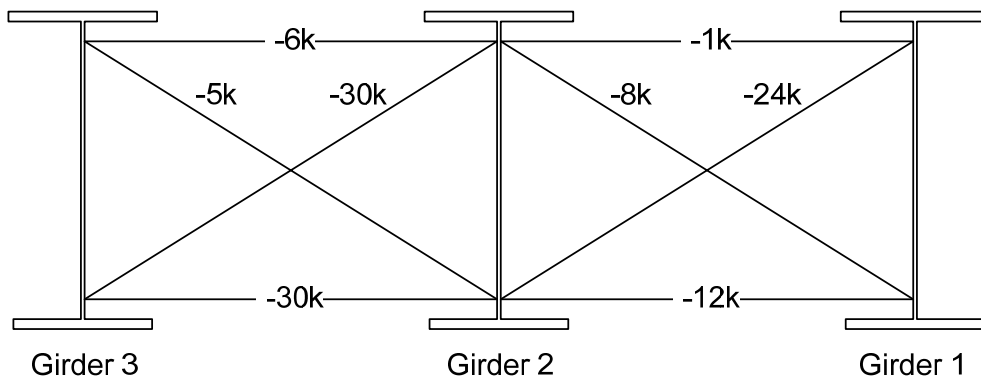
In this case, individual influence surfaces were created and loaded for each member to determine the critical live load forces. Hence, equilibrium may not be exact. However, a check of the forces will demonstrate that both dead and live loading satisfy statics at the bottom flange. The proper combination of live loads must be

used to obtain equilibrium. Since both maximum and minimum values are given for the live load forces, consideration of the proper combinations of the forces is necessary. Serendipitously, it is observed that although in this example, separate influence surfaces were loaded for each member, equilibrium can still be obtained by combination of the proper live load forces.

As discussed further below, if the lateral bending moment in the flange at the point is significant, the net horizontal force in the cross-frames at a connection is not zero without consideration of the lateral reaction at the point. A significant reaction always occurs when the cross-frames are staggered since there is no opposing cross-frame available directly on the opposite side of the girder. Note that the vertical components of the cross-frame forces are not in equilibrium since gravity loads are being transferred between the girders. The difference of the vertical loads from zero at the cross-frame is the net vertical load applied to or removed from the girder at that point.

The horizontal and vertical components of the diagonal forces will be determined from the cross-frame geometry.   The length of each diagonal is determined as:

$$\ell = \sqrt{(63)^2 + (104)^2} = 121.6 \text{ in.}$$

The horizontal component is:

$$\frac{104}{121.6} = 0.855$$

The vertical component is:

$$\frac{63}{121.6} = 0.518$$

Horizontal equilibrium at the bottom flange is checked because the resistance of the deck can be ignored. The deck carries the net of the horizontal forces at the top flange for the composite load cases. Since information regarding the lateral force in the deck is not provided, equilibrium can be only checked at the bottom flange. The resulting cross-frame forces can be applied at the top to determine the horizontal force resisted by the shear connectors.

Referring to the preceding figure, for horizontal equilibrium at the bottom flange of Girder 1:

For dead load (DC1 + DC2):

$$29(0.855) = 24.80 \text{ kips} - 23 \text{ kips} = 1.80 \text{ kips} \cong 0 \ \ \text{ok}$$

For live load, two cases are checked:

Live Load Case 1:

$$13(0.855) = 11.11 \,\text{kips} - 12 \,\text{kips} = -0.89 \,\text{kips} \cong 0 \quad \text{ok}$$

Live Load Case 2:

$$-8(0.855) = -6.84 \,\text{kips} + 7 \,\text{kips} = 0.16 \,\text{kips} \cong 0 \quad \text{ok}$$

Note that in each case at this location, the net horizontal force is approximately zero at the connection, as it must be since there is no offsetting force on the other side of Girder 1. The occurrence of near equilibrium for the two live load cases means that the live load pattern for the positive and negative forces in the two members (Members C and D) at this location was nearly the same. There are three reasons for the lack of perfect equilibrium in this case: 1) all forces are rounded off to integers, 2) the live load positions may be slightly different for the two members, and 3) the effect of small lateral bending moments in the bottom flange of Girder 1 at the cross-frame is ignored. It is significant that the Engineer can safely combine the two live load forces in each case with the dead load forces in the design of the member and the connection.   Otherwise, the sum of the maximum forces would conservatively have to be used. The top flange condition can safely be designed without checking equilibrium since it was confirmed at the bottom flange.

In cases where there is a significant cross slope or where there are large drops between adjacent girders (e.g. a bridge with skewed haunched girders) and the cross-frames are detailed as parallelograms to follow the cross slope or drops (which is generally preferred), the effect of the sloping cross-frame members may need to be considered in the analysis. In such cases, the vertical component of force in the bottom strut would need to be factored into the equilibrium calculation.

Horizontal equilibrium will now be confirmed at the bottom flange of Girder 2. At this location, the cross-frame forces on opposite sides of the girder are opposed to each other.   Hence, equilibrium is obtained by considering the forces on both sides simultaneously.   Referring to the figure below (note in the following that the vertical components of force at Girder 2 are also calculated and shown on the figure for completeness):

Dead Load (DC$_1$ + DC$_2$)

21.24k -19.68k

41k   -38k

35.06k ←   ← -32.49k

-88k — -23k

Total = -52.94k   Girder 2   Total = -55.49k

+ (LL + IM)

4.66k 6.73k

9k   13k

7.70k ←   → 11.12k

-12k — -7k

Total = 19.70k   Girder 2   Total = 18.12k

- (LL + IM)

-2.59k -12.43k

-5k   -24k

-4.28k →   ← -20.52k

-30k — -12k

Total = -34.28k   Girder 2   Total = -32.52k
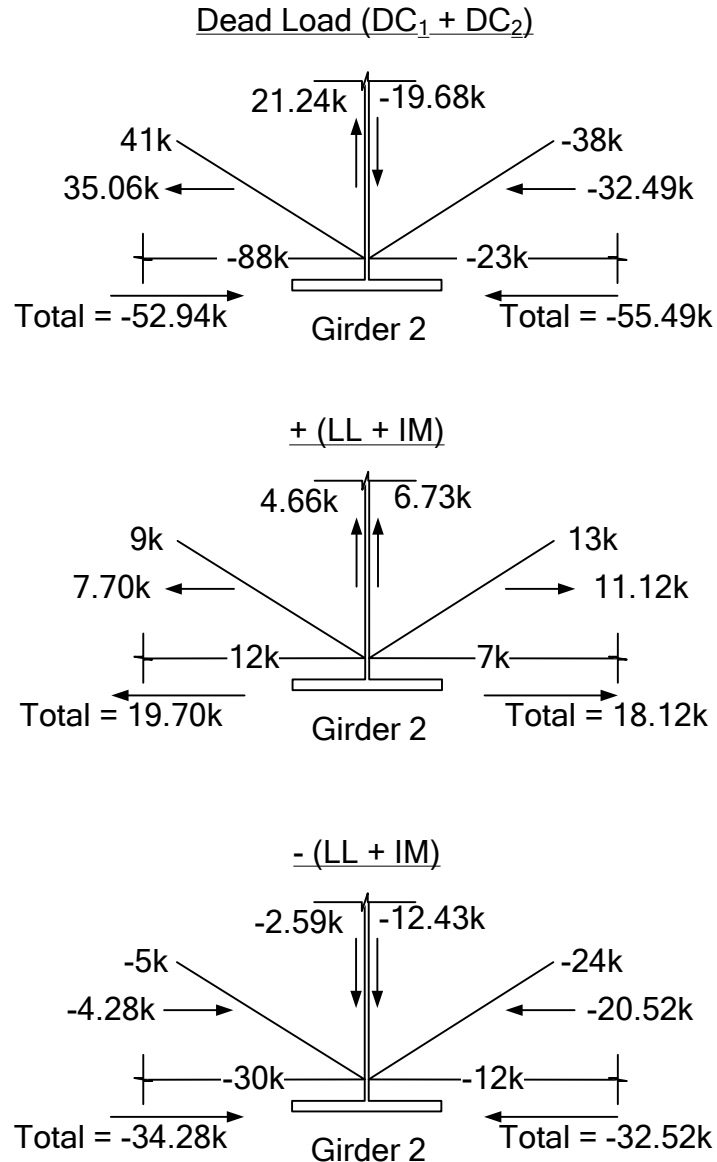
For dead load (DC$_1$ + DC$_2$):

      Horizontal: G1/G2   -38(0.855) = -32.49 kips – 23 kips = -55.49 kips

              G2/G3   41(0.855) = 35.06 kips – 88 kips = <u>-52.94 kips</u>

                                              Σ= -2.55 kips $\cong$ 0 ok

      Vertical: G1/G2 -38(0.518) = -19.68 kips

                 G2/G3 41(0.518) =   21.24 kips

For live load, two cases are checked:

      Live Load Case 1:

Horizontal:G1/G2   13(0.855) = 11.12 kips + 7 kips = 18.12 kips
   G2/G3   9(0.855) =   7.70 kips + 12 kips =   <u>19.70 kips</u>
                Σ =   1.58 kips $\cong$ 0 ok

Vertical: G1/G2 13(0.518) =   6.73 kips
    G2/G3 9(0.518) =   4.66 kips

Live Load Case 2:

Horizontal:G1/G2   -24(0.855) = -20.53 kips - 12 kips = -32.52 kips
   G2/G3   -5(0.855) =   -4.28 kips - 30 kips = <u>-34.28 kips</u>
               Σ = -1.76 kips $\cong$ 0 ok

Vertical: G1/G2 -24(0.518) =   -12.43 kips
    G2/G3 -5(0.518) = - 2.59 kips

Therefore, in this case, for the design of the connection at the bottom flange on the left-hand side of Girder 2, the horizontal component of the live load plus impact force of 9 kips in the diagonal should be combined with the force of 12 kips in the bottom strut (Live Load Case 1), and the horizontal component of the live load plus impact force of -5 kips in the diagonal should be combined with the force of -30 kips in the bottom strut (Live Load Case 2) in determining the total critical force effect. For the design of the connection at the bottom flange on the right-hand side of Girder 2, the horizontal component of the live load plus impact force of 13 kips in the diagonal should be combined with the force of 7 kips in the bottom strut (Live Load Case 1), and the horizontal component of the live load plus impact force of -24 kips in the diagonal should be combined with the force of -12 kips in the bottom strut (Live Load Case 2) in determining the total critical force effect.

The slight deviations from perfect equilibrium in the above results are again due to round-off, possible slight differences in the live load positions for determining the maximum effects in the diagonal and bottom-flange members, and the effect of the lateral reaction resulting from the lateral moment M_{lat} induced into the flanges from the cross-frames. In this particular case, the lateral flange moments from the analysis were found to be less than 5 kip-ft, so their effect is considered negligible. The cross-frames in this case were placed in contiguous lines normal to the girders. If the cross-frames had been placed in staggered lines, the lateral flange moments would be increased but the cross-frame forces would be lessened, with the magnitude of the differences being a function of the flange stiffness and relative cross-frame spacings. Had the lateral flange moments been deemed significant, the lateral reaction at the cross-frames for establishing equilibrium could be estimated as follows (derived from the equations for the interior reaction and moment in a three-span continuous beam loaded by equal concentrated loads P at the center of each span):

$$R = 1.14P$$

where:

$$P = \frac{3.33M_{lat}}{\ell}$$

and ℓ is the cross-frame spacing. The lateral reaction would act in the opposite direction at the top-flange connection.

In horizontally curved bridges, there is also a lateral reaction at the cross-frames resulting from the lateral flange moments due to curvature. This lateral reaction can be estimated as follows (derived from the equations for the interior reaction and moment in a three-span continuous beam loaded by a uniform load w in each span):

$$R = 1.1w\ell$$

where:

$$w = \frac{M}{RD}$$

and M is the major-axis bending moment in the girder at the cross-section under investigation, R is the girder radius and D is the web depth. Again, at the top-flange connection, the lateral reaction would act in the opposite direction.

Note that the above lateral reactions are only to be used as necessary to establish equilibrium (in an approximate fashion) for determining the proper combination of the forces at a particular joint. The lateral reactions do not influence the design of the cross-frame member end connections. However, the reactions so computed should be included when checking the cross-frame connection plate welds to the flange (and potential local buckling of the connection plates due to bending of the plates), as discussed at the end of this example. Such positive attachment of these plates to the flanges is required and avoids the transfer of the lateral loads through the web.

Calculate the factored cross-frame member forces at the strength limit state for the Strength I load combination (Note: the load modifier η is taken equal to 1.0). The minimum load factors γ_p from *AASHTO LRFD* Table 3.4.1-2 are considered for application to the permanent-load member forces whenever the corresponding sign of the forces is of opposite sign to the live load plus impact forces and a more critical load combination for the design of the bolted connection is produced (note: separate computations show that a more critical combination was not produced in this particular case. Thus, the maximum load factors are applied to the DC_1 and DC_2 loads). For the cross-frame on the right-hand side of Girder 2:

Horizontal force:

$DC_1 + DC_2$:	1.0[1.25(-55.49)]	=	-69.4 kips
Live Load Case 1:	1.0[1.75(18.12)]	=	<u>31.7 kips</u>
	Σ	=	-37.7 kips

$DC_1 + DC_2$:	1.0[1.25(-55.49)]	=	-69.4 kips
Live Load Case 2:	1.0[1.75(-32.52)]	=	<u>-56.9 kips</u>
	Σ	=	-126.3 kips

Vertical force:

$DC_1 + DC_2$:	1.0[1.25(-19.68)]	=-24.8 kips
Live Load Case 1:	1.0[1.75(6.73)]	= <u>11.8 kips</u>
	Σ	= -12.8 kips

$DC_1 + DC_2$:	1.0[1.25(-19.68)]	= -24.6 kips
Live Load Case 2:	1.0[1.75(-12.43)]	= <u>-21.8 kips</u>
	Σ	= -46.4 kips

For the cross-frame on the left-hand side of Girder 2:

Horizontal force:

$DC_1 + DC_2$:	1.0[1.25(-52.94)]	= -66.2 kips
Live Load Case 1:	1.0[1.75(19.70)]	= <u>34.5 kips</u>
	Σ	= -31.7 kips

$DC_1 + DC_2$:	1.0[1.25(-52.94)]	= -66.2 kips
Live Load Case 2:	1.0[1.75(-34.28)]	= <u>-60.0 kips</u>
	Σ	= -126.2 kips

Vertical force:

$DC_1 + DC_2$:	1.0[1.25(21.24)]	= 26.6 kips
Live Load Case 1:	1.0[1.75(4.66)]	= <u>8.2 kips</u>
	Σ	= 34.8 kips

$DC_1 + DC_2$:	1.0[1.25(21.24)]	= 26.6 kips
Live Load Case 2:	1.0[1.75(-2.59)]	= <u>-4.5 kips</u>
	Σ	= 22.1 kips

Assume the gusset-plate connection configuration and bolt pattern shown below. All bolts are 7/8-inch diameter A 325 high-strength bolts placed in standard holes. For this particular illustration, the working point (W.P. in the figure) has been selected as shown. The selection of efficient working points for cross-frame connections can be determined in consultation with a fabricator/detailer. As illustrated later, if there is enough space to place the working point closer to the center of the bolt group, it obviously is desirable. Depending on how the cross-frame is detailed, i.e. if the cross-frame is detailed as a rectangle rather than a parallelogram (which is not preferred), the space available for bolts beyond the working point may vary with the particular bridge cross slope. From separate calculations (similar to those shown below), the critical strength limit state load combination for the selected gusset-plate connection configuration is the horizontal force of –126.3 kips acting in combination with the vertical force of –46.4 kips (i.e. Dead Load plus Live Load Case 2) for the cross-frame on the right-hand side of Girder 2.

SECTION A-A
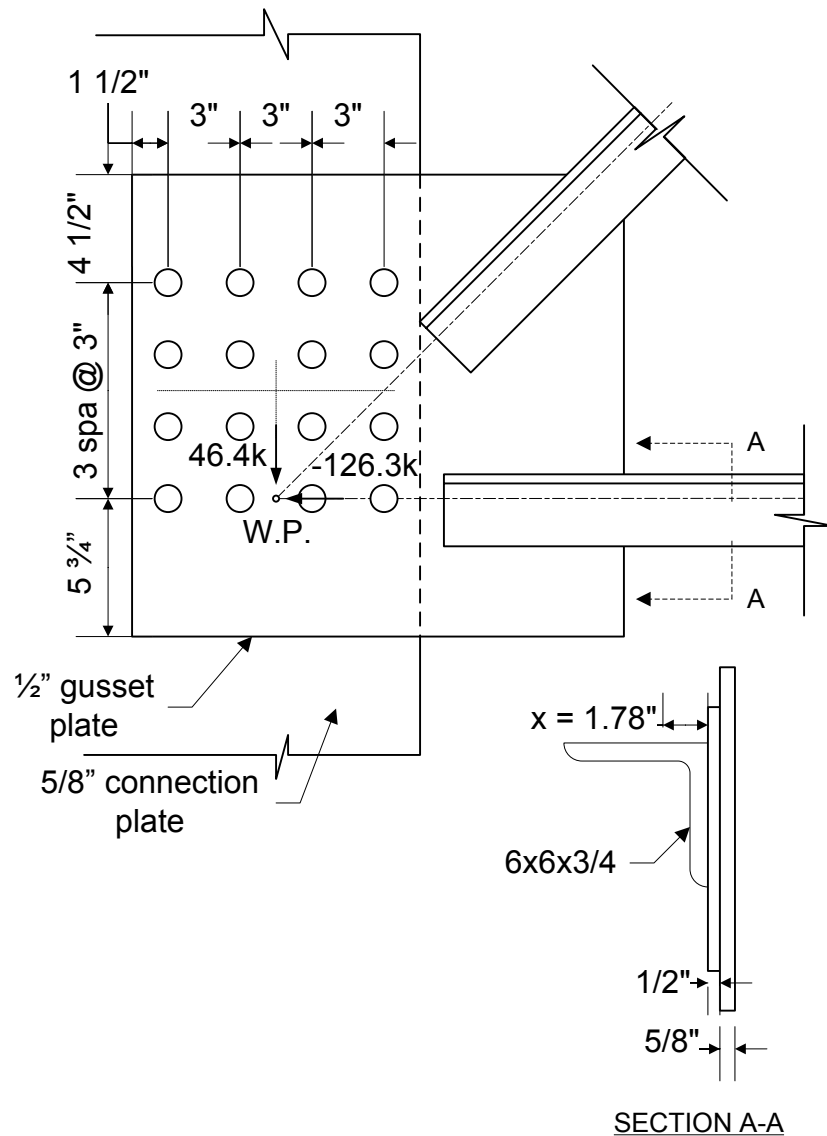
It is assumed that all bolt spacing and edge and end distance requirements are satisfied, and that the bearing resistance of the bolt holes at the strength limit state has been checked and is satisfactory. Check the bolts for shear at the strength limit state assuming the bolts in the connection have slipped and gone into bearing. The bolts are subject to eccentric shear to the in-plane eccentricity and to shear and tension due to the out-of-plane eccentricity. For the eccentric shear (in-plane eccentricity), the traditional elastic vector method is used for calculating the maximum resultant bolt force (refer to Section 2.3.2.5 of this chapter). The polar moment of inertia I_p of the bolts with respect to the centroid of the connection is computed as follows:

$$I_p = \frac{nm}{12}\left[s^2\left(n^2 - 1\right) + g^2(m^2 - 1)\right]$$

AASHTO LRFD Equation C6.13.6.1.4b-3

For the example connection (referring to the preceding figure), $n = 4$; $m = 4$, $s = 3.0$ in. and $g = 3.0$ in. Therefore:

$$I_p = \frac{4(4)}{12}\left[(3.0)^2\left(4^2 - 1\right) + (3.0)^2(4^2 - 1)\right] = 360.0 \text{ in.}^2$$

Determine the vertical bolt force R_v:

$$R_v = \frac{46.4}{16} = 2.90 \text{ kips / bolt}$$

Determine the horizontal bolt force R_h:

$$R_h = \frac{126.3}{16} = 7.89 \text{ kips / bolt}$$

Determine the vertical and horizontal components of the force on the extreme bolt due to the total moment on the connection M_{tot}:

$$M_{tot} = 126.3(4.5) - 46.4(0.0) = 568.4 \text{ kip} - \text{in.}$$

$$R_{M_v} = \frac{M_{tot}x}{I_p} = \frac{568.4(4.5)}{360.0} = 7.11 \text{ kips}$$

$$R_{M_h} = \frac{M_{tot}y}{I_p} = \frac{568.4(4.5)}{360.0} = 7.11 \text{ kips}$$

The resultant bolt force on the extreme bolt is:

$$R = \sqrt{\left(R_v + R_{M_v}\right)^2 + \left(R_h + R_{M_h}\right)^2} = \sqrt{(2.90 + 7.11)^2 + (7.89 + 7.11)^2} = 18.03 \text{ kips}$$

The factored shear resistance R_r for a 7/8-in. diameter A325 high-strength bolt in double shear assuming the threads are *excluded* from the shear planes was computed in an earlier example to be 55.3 kips/bolt (refer to Section 2.3.2.4.2.1 of this chapter). Therefore, for single shear, R_r is equal to 55.3/2 = 27.65 kips/bolt. Therefore:

$$R = 18.03 \text{ kips} < R_r = 27.65 \text{ kips} \quad \text{ok}$$

In addition to shear, the bolts are also subject to tension as a result of the out-of-plane eccentricity. By inspection, the 126.3 kip force controls this computation. Section 2.3.2.4.2.6 of this chapter discusses the design of bolts for combined shear and tension at the strength limit state. From Table 2.16, the minimum required initial pretension P_t for 7/8-inch diameter A 325 bolts is 39.0 kips. Therefore, from Equation 2.258 and referring to the preceding figure, the initial precompression stress f_{bi} on the contact area is equal to (16)(39.0)/(19.25)(12) = 2.70 ksi. Referring

to Section A-A in the preceding figure, the eccentricity to the center of the 5/8-inch-thick connection plate is conservatively computed as e = 1.78 + 0.5 + 0.625/2 = 2.59 in. (the eccentricity of the larger bottom chord member is used). From Equation 2.259, the tensile stress on the contact area f_{tb} is equal to $6(126.3)(2.59)/(19.25)(12)^2$ = 0.71 ksi, which is less than f_{bi}. Therefore, the pieces remain in compression (contact).

The nominal shear resistance of each bolt R_n is taken as the factored shear resistance R_r = 27.65 kips/bolt divided by the resistance factor ϕ_s for shear on a bolt equal to 0.80. Therefore, R_n = 27.65/0.8 = 34.56 kips/bolt. The shear due to the factored loads P_u in each bolt is taken as the maximum resultant force R computed above. Therefore, P_u = 18.03 kips. Since P_u/R_n = 18.03/34.56 = 0.52 > 0.33, the nominal tensile resistance of each bolt T_n under combined tension and shear is taken from Equation 2.257, which is a conservative simplification of an elliptical interaction relationship between bolt shear and tension, as follows:

$$T_n = 0.76A_bF_{ub}\sqrt{1-\left(\frac{P_u}{\phi_sR_n}\right)^2}$$

AASHTO LRFD Equation 6.13.2.11-2

For a 7/8" A 325 bolt: A_b = $\dfrac{\pi(0.875)^2}{4} = 0.60$ in.^{2}

F_{ub} =   120 ksi (*AASHTO LRFD* Article 6.4.3.1)

$$T_n = 0.76(0.60)(120)\sqrt{1-\left(\frac{18.03}{(0.80)(34.56)}\right)^2} = 41.5 \text{ kips}$$

Since: $T_r = \phi_t T_n$

AASHTO LRFD Equation 6.13.2.2-3

$T_r = 0.80(41.5) = 33.2$ kips/bolt

The tensile force in each bolt to the factored loads T_u may be computed from Equation 2.261 as follows:

$$T_u = \frac{6Mp}{nd^2}\left(\frac{d-p}{d}\right)$$

$$T_u = \frac{6(126.3)(2.59)(3)}{4(12)^2}\left(\frac{12-3}{12}\right) = 7.7 \text{ kips} < T_r = 33.2 \text{ kips   ok}$$

Alternatively, T_u may be computed from Equation 2.262 as follows:

$$T_u = \frac{My_b}{\sum y^2}$$

where y_b = 4.5 in. and $\Sigma y^2 = 8[(1.5)^2 + (4.5)^2] = 180.0$ in.^{2} Therefore:

$$T_u = \frac{126.3(2.59)(4.5)}{180.0} = 8.2 \text{ kips} < T_r = 22.6 \text{ kips ok}$$

Since the bolted connection is a slip-critical connection, *AASHTO LRFD* Article 6.13.2.1.1 also requires that the connection be proportioned to prevent slip under Load Combination Service II specified in *AASHTO LRFD* Table 3.4.1-1. Calculate the factored cross-frame member forces at the service limit state for the Service II load combination. Calculations are shown only for the critical load combination determined previously to be for the cross-frame on the right-hand side of Girder 2 (i.e. Dead Load plus Live Load Case 2):

Horizontal force:

$DC_1 + DC_2$:	1.0[1.0(-55.49)]	= -55.5 kips
Live Load Case 2:	1.0[1.3(-32.52)]	= <u>-42.3 kips</u>
	Σ	= -97.8 kips

Vertical force:

$DC_1 + DC_2$:	1.0[1.0(-19.68)]	= -19.7 kips
Live Load Case 2:	1.0[1.3(-12.43)]	= <u>-16.2 kips</u>
	Σ	= -35.9 kips

Determine the vertical bolt force R_v:

$$R_v = \frac{35.9}{16} = 2.24 \text{ kips / bolt}$$

Determine the horizontal bolt force R_h:

$$R_h = \frac{97.8}{16} = 6.11 \text{ kips / bolt}$$

Determine the vertical and horizontal components of the force on the extreme bolt due to the total moment on the connection M_{tot}:

$$M_{tot} = 97.8(4.5) - 35.9(0.0) = 440.1 \text{ kip} - \text{in.}$$

$$R_{M_v} = \frac{M_{tot} x}{I_p} = \frac{440.1(4.5)}{360.0} = 5.50 \text{ kips}$$

$$R_{M_h} = \frac{M_{tot} y}{I_p} = \frac{440.1(4.5)}{360.0} = 5.50 \text{ kips}$$

The resultant bolt force on the extreme bolt is:

$$R = \sqrt{\left(R_v + R_{M_v}\right)^2 + \left(R_h + R_{M_h}\right)^2} = \sqrt{(2.24 + 5.50)^2 + (6.11 + 5.50)^2} = 13.95 \text{ kips}$$

The factored slip resistance R_r for a 7/8-in. diameter A325 high-strength bolt assuming a Class B surface condition for the faying surface, standard holes and two slip planes per bolt was computed in an earlier example to be 39.0 kips/bolt (refer to Section 2.3.2.4.1.1 of this chapter). Therefore, for a single slip plane, R_r is equal to 39.0/2 = 19.50 kips/bolt. However, in the presence of tension (due to the out-of-plane eccentricity), the slip resistance must be reduced according to the following linear relationship between the applied tension and the minimum required initial pretension on the bolt (refer to Equation 2.235 in Section 2.3.2.4.1.1 of this chapter):

$$1 - \frac{T_u}{P_t}$$

AASHTO LRFD Equation 6.13.2.11-3

where T_u is equal to tensile force due to the factored loads under Load Combination Service II, and P_t is equal to the minimum required bolt tension specified in *AASHTO LRFD* Table 6.13.2.8-1 (specified as 39.0 kips for a 7/8-inch diameter A 325 bolt -- Table 2.16). Under the Service II load combination, T_u may be computed from Equation 2.262 as follows:

$$T_u = \frac{97.8(2.59)(4.5)}{180} = 6.3 \text{ kips}$$

Therefore, the slip resistance R_r modified for the effect of the tension is computed as:

$$R_r = 19.50\left(1 - \frac{6.3}{39.0}\right) = 16.35 \text{ kips}$$

$$R = 13.95 \text{ kips} < R_r = 16.35 \text{ kips} \quad \text{ok}$$

The slip resistance under the Service II load combination controls the design of the bolted connection in this case. Note that similar computations would need to be done if the cross-frame members had been bolted directly to the connection plate.

If it were possible, the moment on the connection could be reduced significantly in this particular case by moving the working point to the left. For example, if the working point could be moved 3 inches to the left along the bottom row of bolts, the total moment on the connection under the Service II load combination would be reduced from 440 kip-in. to:

$$M_{\text{tot}} = 97.8(4.5) - 35.9(3.0) = 332.4 \text{ kip} - \text{in.}$$

which may allow for an overall reduction in the number of bolts.

Assume that enough space is available to move the bottom row of bolts down (or move the bottom cross-frame member up) such that the working point can be located at the center of the bolt group. As slip controls, check the slip resistance of the bolts in the resulting reduced bolt pattern shown below (the critical Service II resultant cross-frame forces are shown in the figure).   Note that by going to this pattern, the size of the gusset plate is obviously reduced and the size of the connection plate is also reduced.
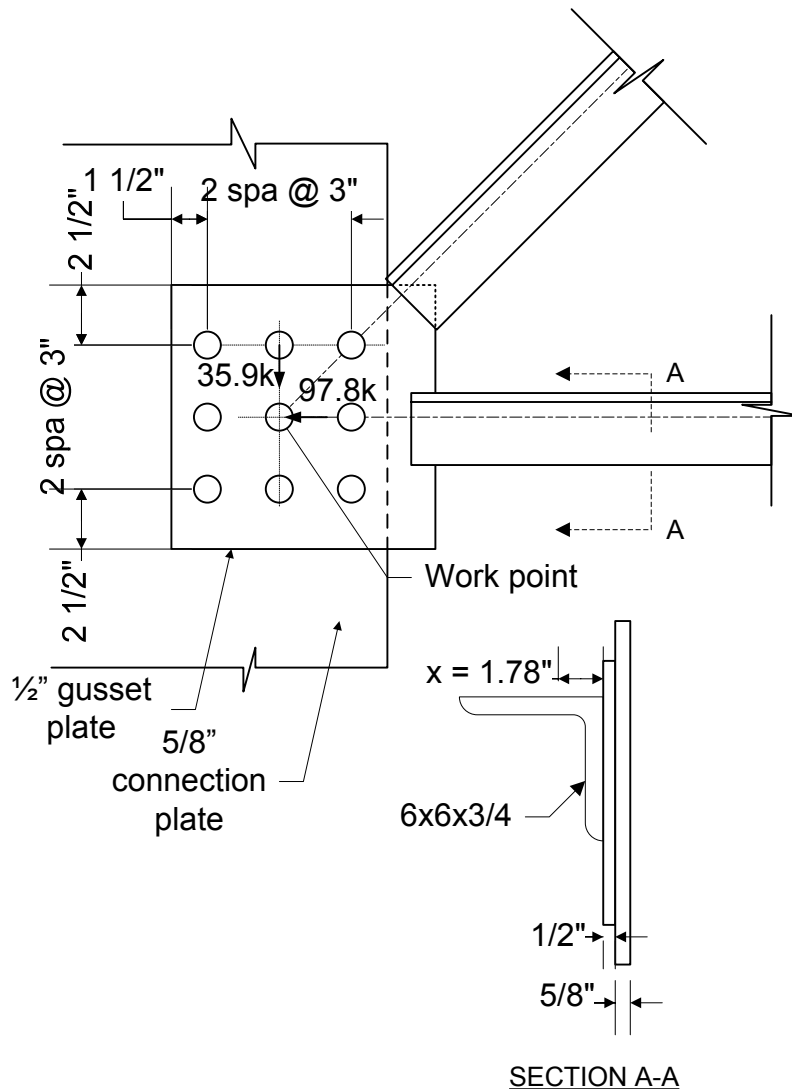
Determine the vertical bolt force R_v:

$$R_v = \frac{35.9}{9} = 3.99 \text{ kips / bolt}$$

Determine the horizontal bolt force R_h:

$$R_h = \frac{97.8}{9} = 10.87 \text{ kips / bolt}$$

The total moment on the connection M_{tot} is:

$$M_{tot} = 97.8(0.0) - 35.9(0.0) = 0.0 \text{ kip} - \text{in.}$$

The resultant bolt force on the extreme bolt is:

$$R = \sqrt{R_v^2 + R_h^2} = \sqrt{(3.99)^2 + (10.87)^2} = 11.58 \text{ kips}$$

To account for the tension on the bolts, y_b = 3.0 in. and $\Sigma y^2 = 3[(3.0)^2 + (3.0)^2] = 54.0$ in.^{2} T_u is therefore computed from Equation 2.262 as follows:

$$T_u = \frac{97.8(2.59)(3.0)}{54.0} = 14.07 \text{ kips}$$

Therefore, the slip resistance R_r modified for the effect of the tension is computed as:

$$R_r = 19.50\left(1 - \frac{14.07}{39.0}\right) = 12.47 \text{ kips}$$

$$R = 11.58 \text{ kips} < R_r = 12.47 \text{ kips} \quad \text{ok}$$

As this example clearly demonstrates, the location of the working point is a critical factor in determining the overall economy of the connection.

The shear, tensile and compressive resistances of the gusset plate should be checked according to the procedures discussed in Sections 2.3.2.4.2.3, 2.3.2.4.2.4 and 2.3.2.4.2.7 of this chapter, respectively.

The gusset plate is bolted to a connection plate that is fillet welded to the top and bottom flanges. The connection plate fillet welds to the flanges may be subject to eccentric loading from any significant net factored lateral reaction at the cross-frame locations resulting from lateral moment induced into the flanges from the cross-frames or due to curvature (as discussed previously). The lateral reactions subject these welds to combined shear and tension. Where deemed significant, the fillet welds should be checked for this condition at the strength limit state (note that for straight non-skewed bridges, the lateral force of 20.0 kips suggested in *AASHTO LRFD* Article 6.6.1.3.1 for the design of the connection of these plates to the flanges may conservatively be used in lieu of the factored lateral reactions to check the welds for this eccentric load condition, if desired). The reader is referred to the second example presented in Section 2.3.3.8.3.2 of this chapter for a suggested procedure to make this check. The moment on the welds may be estimated by treating the connection plate as a fixed-end beam (or using another assumption

perhaps deemed more appropriate based on the end conditions) loaded by the net factored lateral reactions at the appropriate locations. Potential local buckling of the connection plates due to bending of the plates caused by these net lateral reactions at the strength limit state should also be considered, as suggested in Section 2.3.2.4.2.7 of this chapter.

101. Kulak, G.L., J.W. Fisher, and J.H.A. Struik. 1987. *Guide to Design Criteria for Bolted and Riveted Joints.* 2nd Edition, John Wiley & Sons, New York, NY.

102. Batho, C., and E.H. Bateman. 1934. *Investigations on Bolts and Bolted Joints.* Second Report of the Steel Structures Research Committee, London; His Majesty's Stationary Office.

103. Wilson, W.M., and F.P. Thomas. 1938. "Fatigue Tests on Riveted Joints." *Bulletin 302*, University of Illinois, Engineering Experiment Station, Urbana, IL.

104. Munse, W. H. 1956. "Research on Bolted Connections." *Transactions*, American Society of Civil Engineers, New York, NY, No.121.

105. Research Council on Structural Connections. 2004. *Specification for Structural Joints Using ASTM A325 or A490 Bolts.* c/o American Institute of Steel Construction, Chicago, IL, June 30.

106. Rumpf, J.L., and J.W. Fisher. 1963. "Calibration of A 325 Bolts." *Journal of the Structural Division*, American Society of Civil Engineers, Vol. 89, No. ST6, December.

107. Sterling, G.H. et al. 1965. "Calibration Tests of A 490 High Strength Bolts." *Journal of the Structural Division*, American Society of Civil Engineers, Vol. 91, No. ST5, October.

108. AASHTO. 2004. *LRFD Bridge Construction Specifications and Interim Specifications.* Second Edition. American Association of State Highway and Transportation Officials, Washington, D.C.

109. Struik, J.H.A., A.O. Oyeledun, and J.W. Fisher. 1973. "Bolt Tension Control with a Direct Tension Indicator." *Engineering Journal,* American Institute of Steel Construction, Chicago, IL, Vol. 10, First Quarter.

110. Brockenbrough, R.L. 1983. "Considerations in the Design of Bolted Joints for Weathering Steel." *AISC Engineering Journal*, American Institute of Steel Construction, Chicago, IL, Vol. 20, 1st Qtr.

111. Birkemoe, P.C., and D.C. Herrschaft. 1970. "Bolted Galvanized Bridges: Engineering Acceptance Near." *Civil Engineering*, American Society of Civil Engineers, New York, NY, Vol. 40, No. 4, April.

112. Grubb, M.A., J.M. Yadlosky, and S.R. Duwadi 1996. "Construction Issues in Steel Curved-Girder Bridges." *Transportation Research Record No. 1544,* Transportation Research Board, National Research Council, Washington, D.C.

113. Yura, J.A., K.H. Frank, and L. Cayes. 1981. "Bolted Friction Connections with Weathering Steel." *Journal of the Structural Division*, American Society of Civil Engineers, Vol. 107, No. ST11, November.

114. Mathay, W.L. 1993. *Uncoated Weathering Steel Bridges.* Highway Structures Design Handbook, Volume 1, Chapter 9, available from the National Steel Bridge Alliance, Chicago, IL.

115. Polyzois, D., and K.H. Frank. 1986. "Effect of Overspray and Incomplete Masking of Faying Surfaces on the Slip Resistance of Bolted Connections."

AISC Engineering Journal, American Institute of Steel Construction, Chicago, IL, Vol. 23, 2nd Quarter.

116. Yura, J.A., and K.H. Frank. 1985. "Testing Method to Determine Slip Coefficient for Coatings Used in Bolted Joints." AISC Engineering Journal, American Institute of Steel Construction, Chicago, IL, Vol. 22, No. 3, Third Quarter.

117. Frank, K.H., and J.A. Yura. 1981. "An Experimental Study of Bolted Shear Connections." *FHWA/RD-81/148*, Federal Highway Administration, Washington, D.C., December.

118. Ricles, J.M., and J.A. Yura. 1983. "Strength of Double-Row Bolted Web Connections." *Journal of the Structural Division*, American Society of Civil Engineers, New York, NY, Vol. 109, No. ST1, January.

119. Hardash, S., and R. Bjorhovde. 1985. "New Design Criteria for Gusset Plates in Tension." *AISC Engineering Journal*, American Institute of Steel Construction, Chicago, IL, Vol. 22, 2nd Qtr.

120. Birkemoe, P.C., and M.I. Gilmour. 1978. "Behavior of Bearing Critical Double-Angle Beam Connections." *AISC Engineering Journal*, American Institute of Steel Construction, Chicago, IL, Vol. 15, No. 4, 4th Qtr.

121. Douty, R.T., and W. McGuire. 1965. "High-Strength Bolted Moment Connections." *Journal of the Structural Division*, American Society of Civil Engineers, New York, NY, Vol. 91, No. ST1, February.

122. ASCE. 1971. *Plastic Design in Steel – A Guide and Commentary.* 2nd ed. ASCE Manual No. 41, American Society of Civil Engineers, New York, NY.

123. Nair, R.S., P.C. Birkemoe, and W.H. Munse. 1974. "High-Strength Bolts Subjected to Tension and Prying." *Journal of the Structural Division*, American Society of Civil Engineers, New York, NY, Vol. 100, No. ST2, February.

124. Chesson, E., N.L. Faustino, and W.H. Munse. 1965. "High-Strength Bolts Subjected to Tension and Shear." *Journal of the Structural Division*, American Society of Civil Engineers, New York, NY, Vol. 91, No. ST5, October.

125. Research Council on Structural Connections. 1988. *Load and Resistance Factor Design Specification for Structural Joints Using ASTM A325 or A490 Bolts.* c/o American Institute of Steel Construction, Chicago, IL, June.

126. Fisher, J.W. 1965. "Behavior of Fasteners and Plates with Holes." *Journal of the Structural Division*, American Society of Civil Engineers, New York, NY, Vol. 91, No. ST6, December.

127. Crawford, S.F., and G.L. Kulak. 1971. "Eccentrically Loaded Bolted Connections." *Journal of the Structural Division*, American Society of Civil Engineers, New York, NY, Vol. 97, No. ST3, March.

128. AISC. 1963. *Manual of Steel Construction.* 6th ed. American Institute of Steel Construction, Chicago, IL.

128a. AISC. 2005. *Steel Construction Manual.* 13th ed. American Institute of Steel Construction, Chicago, IL, December.

2.3.3 Welded Connections

2.3.3.1 General

The design of welded connections is covered in *AASHTO LRFD* Article 6.13.3. Welding is the process of joining two pieces of material, usually metals, by heating the pieces to a suitable temperature such that the materials are soft enough to coalesce or fuse into one material. The pieces are held in position for welding and may or may not be pressed together depending on the process that is used. Also, the pieces may be joined directly to each other or they may be joined using filler material. Although there are some forty different welding processes, arc welding, in which electrical energy in the form of an electric arc is introduced to generate the heat necessary for welding, is the most commonly used process in the steel-bridge construction industry. The heat of the electric arc as the current passes through the system simultaneously melts a consumable electrode (deposited as filler material) and the parts of the material being joined, with the joint resulting from the cooling and solidification of the fused material. To protect the molten region from impurities, the zone to be welded is typically blanketed in an atmosphere supplied by a flux, which may be a fusible coating on the welding rod, a fusible powder spread over the line of the weld or a gas sprayed over the weld. To produce a weld of the desired quality, the properties of the electrode must be carefully controlled. Proper control of the current and voltage along with a skilled welder are also required in order to produce a quality weld.

Welding in its simplest form has been around for several thousand years, primarily in the form of forge welding in which pieces of metal were heated and hammered into the desired shapes. Brazing of metals was also done for many years. Significant advancements in welding technology did not occur, however, until the late 1800s. Resistance welding, which combines electrical energy with mechanical pressure (e.g. spot and seam welding primarily used for welding of light-gage steel plates and open-web steel joists), originated around 1877 (*129*). In the late 1880s and early 1890s, the metal arc process made its initial appearance in Russia and in the U.S. at about the same time using uncoated bare electrodes (*130*). Around the same time period, coated metal electrodes were introduced to eliminate many of the problems associated with the use of bare electrodes (*129*).   During World War I (1914-1918), welding techniques were primarily applied to repairing damaged ships. Right after the war, experimentation with electrodes and gases to shield the arc and weld area led to the development of gas metal arc welding and gas tungsten arc welding. In 1932, the use of granular flux to protect the weld was introduced, which along with the use of a continuously fed electrode led to the development of the commonly used submerged arc welding process in which the arc is buried under the granular flux (*130*). Research and advancements continue today with the increased usage of automated welding techniques and welding robotics.

The introduction of welding has led to significant advancements in steel-bridge design and fabrication. Welding is now used for the vast majority of shop connections. Welded connections are usually neater in appearance than bolted connections. Welded connections also allow the Engineer more freedom to be innovative and build-up cross-sections to transmit the loads in the most efficient

manner. Several factors influence the cost of welding, including but not limited to, the amount of weld material required, the costs of preparing the edges to be welded, the ratio of actual arc time to overall welding time and the amount of handling required. Shop welding is almost always less expensive than field welding. Reasons for this include the more ready availability of automatic welding machines and special jigs for holding the pieces in more favorable positions, a less hostile environment, the ability to more easily perform proper preheating of the joint and the ability to schedule a smooth continuous operation versus having to wait for cranes or special erection equipment to become available. More extensive information and discussion related to the variables influencing welding costs may be found in References 131 through 133.

The weldability of a steel is a measure of the ease of producing a crack-free and sound structural joint. The weldability of structural steel is primarily controlled by its carbon content. While carbon (C) is beneficial to the strength of the steel, it is detrimental to ductility. A high carbon content combined with the heat generated during welding may cause a brittle zone in which weld cracks may develop. A carbon content of about 0.20 percent results in a very weldable steel. Good weldability can be obtained with an upper limit on carbon content of about 0.25 percent. In certain steels, the addition of alloys to enhance the strength and/or corrosion resistance can increase the hardness of the steel.   Increased hardness results in an increased likelihood of brittle zones forming. Higher concentrations of carbon and other alloying elements such as manganese (Mn), chromium (Cr), silicon (Si), molybdenum (Mo), vanadium (V), copper (Cu) and nickel (Ni) tend to increase the hardness and decrease the weldability of the steel. Each of these alloying elements tends to influence the hardness and weldability of the steel to different magnitudes. Therefore, an approximate guide to the weldability of alloy steels against that of plain carbon steels is necessary. The most common standard used is the carbon equivalent (%CE) given as follows (*134*):

$$\%CE = \%C + \left(\frac{\%Mn + \%Si}{6} \right) + \left(\frac{\%Cr + \%Mo + \%V}{5} \right) + \left(\frac{\%Cu + \%Ni}{15} \right) \quad \text{Equation 2.274}$$

For %CE less than 14 percent, the steel is considered to have excellent weldability. For %CE between 14 and 45 percent, modest preheat and low hydrogen electrodes become necessary. For %CE greater than 45 percent, weld cracking is likely; therefore, larger preheats and low hydrogen electrodes are required. Weldability should be determined on the basis of actual rather than specified chemical compositions as compositions listed on actual mill certification reports are typically below the maximum alloy contents set by the specifications. Most of the bridge steels specified in the ASTM A 709 Specification can be welded without special precautions or procedures. However, special procedures should be followed to improve weldability and ensure high-quality welds when high-performance steels (HPS) are used (*135*).

2.3.3.2 Welding Processes

The following is a brief discussion of the processes that are used for arc welding carbon and low-alloy steels typically used in bridge construction. Note that the Engineer does not typically specify the welding process to be used or the exact filler metal (electrode/flux material) to be employed. These decisions are usually left with the fabricator. However, a basic understanding of the commonly used welding processes and corresponding AWS filler-metal designations is helpful. More extensive discussion of these processes and the decisions that go into selecting a particular process may be found in References 131 and 133. More detailed information on filler-metal designations may be found in References 133 and 136.

2.3.3.2.1 Shielded Metal Arc Welding (SMAW)

The shielded metal arc welding (SMAW) process is often referred to as 'stick electrode welding' or 'manual welding' and is one of the oldest, simplest and most popular welding processes. In this process, an electric arc is struck between a coated mild-steel or low-alloy electrode and the metals being joined. The electrode wire becomes the filler material and the coating is typically converted partly into a shielding gas, partly into slag and the rest is absorbed into the weld metal. The transfer of metal from the electrode to the piece being welded is accomplished by surface tension and molecular attraction, with no pressure applied. Depending on the combination of materials in the electrode coating, the coating may perform one or more of the following functions: 1) produce a gaseous shield to stabilize the arc and prevent atmospheric corrosion of the molten metal by excluding air, 2) introduce other material or alloying elements to the weld to refine the grain structure and other physical properties of the weld metal, and/or 3) produce a protective blanket of slag over the molten metal by introducing slag-producing fluxes, which retards cooling and protects the metal from oxygen and nitrogen in the air that may lead to embrittlement.

For bridges, the SMAW process is most commonly used for tack welding, repair welding, fabrication of miscellaneous components and for erection maintenance and repairs in the field. Because it is inherently slower and more costly than other welding processes, it is rarely used in the primary fabrication of bridges (*133*).

The electrodes for the SMAW process are classified on the basis of the mechanical properties of the deposited weld metal, the welding position of the electrode, the type of coating and the type of current required. For bridge welding purposes, all electrodes should be of low hydrogen type with coatings (i.e. lime materials) that are designed to be extremely low in moisture. Under the intensity of the arc, moisture will break down into its components hydrogen and oxygen. The hydrogen can then enter into the weld deposit and lead to heat-affected zone cracking (so-called delayed hydrogen cracking – discussed below) under certain conditions. Care must be taken to limit the exposure of the electrodes to the atmosphere where they can pick up moisture.

For the SMAW process, the filler metal is designated by AWS as EXXXX (or EXXXX-XX), where E stands for electrode and Xs immediately following the E

represent a number. The first two, or sometimes three, digits indicate the specified minimum tensile strength in ksi of the deposited weld metal. The next digit represents the welding position in which the electrode is capable of making satisfactory welds: '1' means all positions (i.e. flat, vertical, overhead and horizontal), '2' means flat and horizontal welding only and '3' means flat only (Figure 2.105). Since welds are not deposited by gravity, the welder is not limited to flat or horizontal welding positions. The welding position depends on the orientation of the connection and is a particularly critical factor for field welds where it may be impossible to weld in the flat or horizontal positions.

(a) FLAT

(b) HORIZONTAL

(c) VERTICAL

(d) OVERHEAD
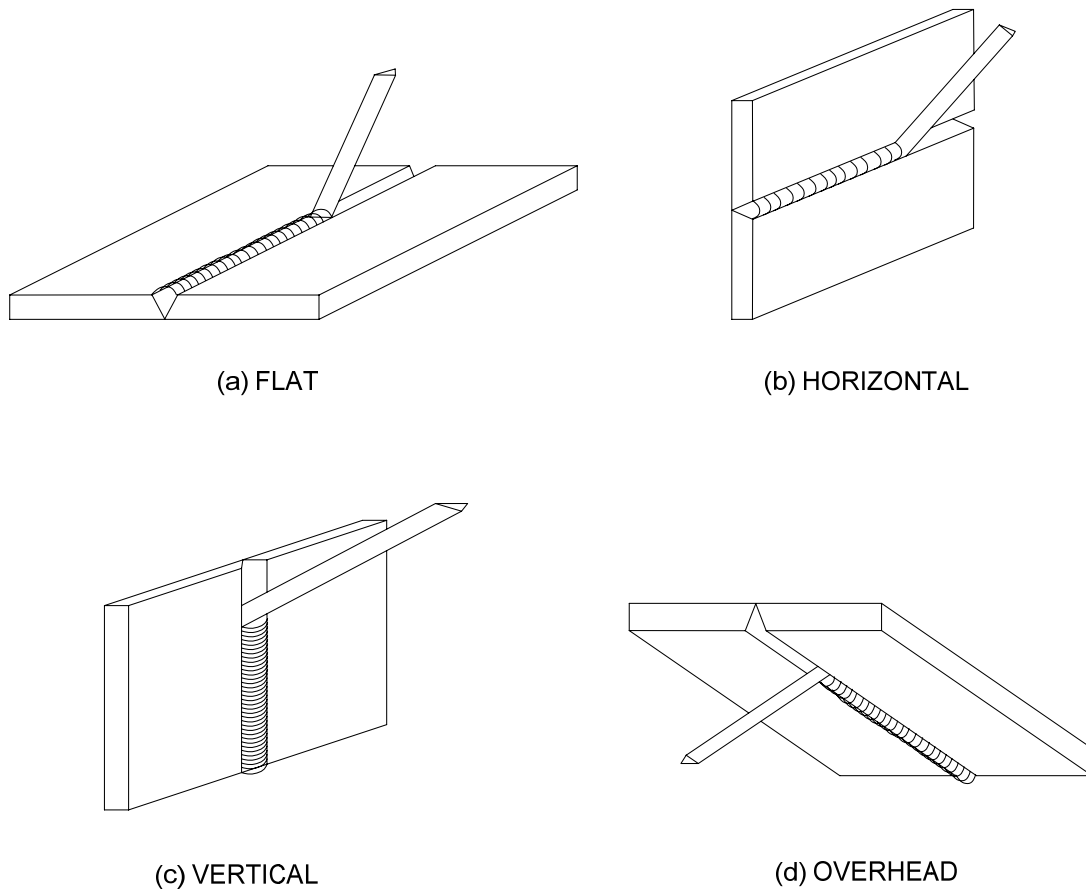
Figure 2.105 Welding Positions

The last digit in the filler-metal designation indicates the type of coating on the electrode in conjunction with the current to be used. The SMAW process can utilize either alternating current or direct current. Direct current is typically used for smaller diameter electrodes. Alternating current electrodes will operate under direct current, while the opposite is not necessarily true. Therefore, the designation 'E7018' indicates a mild-steel arc-welding electrode with a minimum tensile strength of 70 ksi. The electrode is an iron-powder low-hydrogen electrode that can be used in all positions as long as alternating current or direct current reverse-polarity is provided. The iron powder increases the rate at which the weld metal can be deposited.

The suffix '-XX' (shown in parentheses above) consists of a suffix letter and a number and is typically used to either identify low-alloy electrodes or to indicate the maximum level of diffusible hydrogen that may be present in the weld deposit. For example, for an 'E7018-H8' designation, the suffix '-H8' indicates that the deposit will contain a maximum diffusible hydrogen content of 8 milliliters per 100 grams. Most standard low hydrogen electrodes deposit maximum diffusible hydrogen levels of 16 milliliters per 100 grams. Lower levels of diffusible hydrogen are typically necessary when welding high-performance steels (HPS) (*135*).

Some electrodes carry a '-W' suffix indicating the presence of alloys necessary to give the electrode atmospheric corrosion resistance for weathering applications. For single pass fillet welds (1/4" and 5/16") on weathering steel, mild steel electrodes may be used since the admixture will inherit significant quantities of the corrosion resistant alloys contained in the base steel. Multiple pass fillet welds and multiple pass groove welds should be made with electrodes that contain the required alloy to provide the necessary corrosion resistance; normally nickel in levels from 1.0 to 4.0 percent.

2.3.3.2.2 Submerged Arc Welding (SAW)

The submerged arc welding (SAW) process is the commonly used in shop-fabrication operations typically using either fully automatic or semi-automatic equipment. In the SAW process, the filler metal is provided by a consumable bare metal mild-steel or low-alloy electrode (wire) that is continuously shielded by a fusible or molten flux (melted by the heat of the arc) surrounded by a remaining layer of granular unfused flux. The molten flux rises above the molten weld metal in the form of a slag, which freezes over the newly solidified weld metal to protect the weld metal against contamination from the atmosphere while it is still hot. After cooling, this layer of slag is easily peeled from the weld. The bare electrode is typically fed automatically from a coiled reel to the welding gun, head or heads, where it is then fed through the mound of flux. In a semi-automatic operation, the welder moves the gun, which is usually equipped with a flux-feeding device, along the joint. Since the arc is not visible, the term 'submerged arc' is given to the process. The granular flux may be laid through a nozzle concentric with the electrode or laid automatically ahead of the advancing electrode. The flux blankets the weld to prevent spatter, sparks or smoke. The flux may contain alloying material to refine the chemical composition of the weld. Because of the excellent insulating qualities of the flux, much higher welding currents can be used than in the SMAW process, which concentrates the heat to produce deep-penetration welds and allow for potential savings in filler material. Welding speeds are also much faster than the SMAW process, which minimizes heat input limiting heat distortion problems. Welds made by the SAW process typically have uniform high quality. Relatively thick joints can be welded in one pass with the SAW process. The process is routinely used for web-to-flange welds, flange splices, stiffener welds and long uninterrupted joints that lend themselves to automation.

The SAW process can be applied in a greater variety of ways than other arc welding processes. Parallel electrode welding is possible using two smaller diameter electrodes spaced a small distance apart to obtain very high current densities, and is

commonly used for fillet welding applications (*133*). Multiple electrode or tandem arc welding utilizing two larger diameter electrodes independently can also be used to create two-pass welds more efficiently or larger groove or fillet welds in the flat position. Because of the high energy levels in the SAW process, it is often possible to reduce preheats. Also, because of the deep penetration capabilities of the process, tack welds used to hold pieces together can usually be easily re-melted and therefore need not be made with preheat or made of the same quality level as the finished weld.

In the SAW process, the various combinations of mild steel or low allow granular flux and bare electrodes are selected to produce the specified properties in the weld metal. Choices are based on the welding procedure, the type of joint and composition of the base metal. Once a flux is selected and a classification test plate is welded, a flux-electrode combination can be established. Specimens are then extracted from the weld deposit to obtain the mechanical properties of the combination. The combinations are typically designated by AWS as FXXX-EXXX (or FXXX-EXX-XX). The first one, or sometimes two, numbers following the F represent the first, or the first two, digits of the lower end of the range of permitted tensile strengths for the resulting weld metal deposit (e.g. '7' for '70 ksi' or '10' for '100 ksi'). Note that other minimum required material properties are also specified in connection with each digit. The next digit is a letter, with 'A' indicating the deposit is tested in the as-welded condition and 'P' indicating testing in the postweld heat treated or stress-relieved condition (rarely done in bridge work). The last digit in the flux designation indicates the impact strength requirements for the resulting deposit (e.g. a '2' would mean that a Charpy V-notch impact strength of at least 20 ft-lbs is required at -20°F and a '6' would mean 20 ft-lbs is required at -60°F). The Xs following the letter E indicate the properties of the electrode. For mild steel electrodes, the second digit is a letter (L, M or H) referring to a low, medium or high level of manganese in the electrode. The next one, or two, digits indicate the nominal carbon content in hundredths of a percent (e.g.'12' for a nominal carbon content of 0.12%). In some cases, the electrode will be made of killed steel with silicone normally added and a K (for "killed") will also be included at the end of the designation. Therefore, a typical mild steel flux-electrode combination might be classified as 'F7A2-EM12'. Designations for low-alloy flux-electrode combinations (shown in parentheses above) are more complex and typically include the classification of a weld deposit composition as a suffix at the end (*133*, *134*).

2.3.3.2.3 Flux Cored Arc Welding (FCAW)

The flux cored arc welding (FCAW) process uses an arc between a continuous tubular filler metal electrode (mild steel or low alloy) and the weld pool. The wire is fed continuously from a coil through a gun-shaped device. Within the metal core of the electrode is a combination of materials that may include metal powder and flux. The core material provides the same function as the outside coating in SMAW and the granular flux in SAW. Although the process may be applied automatically or semi-automatically, bridge fabricators typically use the process semi-automatically for tack welding and miscellaneous fabrication. Production welds that are short, difficult to access, change direction, must be done in the vertical or overhead position or are part of a short production run will often be made with semi-automatic

FCAW (*133*). SAW is preferred for automatic welding because the smoke and intensity of the arc rays are less. Although the equipment is more expensive and complicated than for SMAW, most fabricators find the FCAW process to be more economical than SMAW. Because the electrode is continuous, the built-in starts and stops that are unavoidable with SMAW are eliminated. Also, increased amperages (current) may be used with FCAW.

Two separate categories of FCAW currently exist: 1) self-shielded flux core (FCAW-ss), and 2) gas-shielded flux core (FCAW-g). Self-shielded flux cored electrodes require no external shielding gas. Instead, shielding is provided by the flux ingredients contained within the tubular electrode. Thus, the process is ideally suited for field welding situations, particularly in windy conditions since no externally applied shielding gas is required. Gas-shielded varieties of flux cored electrodes utilize an externally applied shielded gas, usually carbon dioxide (CO_2) or an argon-CO_2 mixture. The shielding gas protects the weld deposit from the atmosphere, controls the arc and may help reduce spatter, controls undercutting and affects the penetration and speed of welding. Both processes are capable of producing high quality weld deposits with excellent mechanical properties.

For the FCAW process, the filler metal is typically designated by AWS as EXXT-X (or EXXTX-X). The T in the designation stands for tubular electrode. The first one, or sometimes two, numbers following the E represent the first, or the first two, digits of the tensile strength for the resulting weld metal deposit (e.g. '7' for '70 ksi' or '10' for '100 ksi'). A '1' in the position before the T indicates an all-position electrode, while a '0' would refer to an electrode designed for flat or horizontal welding only. The suffix (-X) indicates whether the electrode is self-shielded or gas-shielded, the level of impact properties required, whether the electrode can be used for single pass or multiple pass operation, the polarity to be used and the chemical composition of the weld deposit. For bridge applications, only electrodes capable of delivering weld deposits with good notch toughness are allowed. Therefore, the designation 'E71T-1' indicates a mild steel gas-shielded electrode that will deposit weld metal with a minimum tensile strength of 70 ksi that can be used in all positions. In the designations for low-alloy electrodes (shown in parentheses above), the suffix is instead a letter followed by a number (e.g. '-Ni1' indicating a nominal nickel content in the weld deposit of 1 percent).

2.3.3.2.4 Gas Metal Arc Welding (GMAW)

The gas metal arc welding (GMAW) process utilizes the same equipment as used in the FCAW process. The major difference in the two processes is that the GMAW process uses a solid wire or metal cored electrode, always utilizes an externally applied shielding gas and leaves no residual slag. Metal cored electrodes are tubular, as in the FCAW process, but the core contains metallic powders for excellent alloy control rather than slag forming materials. Originally, this process was used only with inert gas shielding; hence the term 'MIG' welding (metal inert gas welding) has been used for this process. The term 'solid wire and gas' has also been used for this process. Typically, the shielding gases now used are CO_2, which is classified as an active gas, or blends of argon with either CO_2 or oxygen or both (*133*).

For the GMAW process, the mild steel or low alloy filler metal is typically designated by AWS as ERXXS-X. The ER stands for electrode or rod. The S in the designation stands for solid electrode. For metal cored electrodes, the S is replaced with a C. The two, or sometimes three, digits following ER refer to the tensile strength of the weld metal deposit. The suffix (-X) indicates specific chemical composition and toughness requirements. For low-alloy electrodes, the suffix denotes the electrode composition.   Therefore, the designation 'ER70S-3' indicates a mild steel solid electrode that will deposit weld metal with a minimum tensile strength of 70 ksi.

2.3.3.2.5 Electroslag Welding (ESW)

The electroslag welding (ESW) process, which was originally developed in the U.S.S.R. in the early 1950s and introduced in the U.S in 1959 (*137*), is a process in which a molten slag simultaneously melts the filler metal and the surfaces of the parts to be joined. The molten weld pool, which is shielded by the molten slag, and the molten slag both extend along the full cross-section of the joint as the weld progresses. Electroslag welds are usually prepared in the vertical or near-vertical direction and utilize a starting sump and a runoff block to eliminate defects associated with the initiation and termination of the weld.

The ESW process is initiated by an electric arc between the electrode and the bottom of the joint. Powdered flux is then added and is subsequently melted by the heat of the arc. Once a layer of molten slag is established, the arc stops and the welding current passes from the electrode through the slag by electrical conduction. The necessary heat for fusion is provided by the passage of the current. Because of the larger heat input and slower cooling than in other welding processes, water-cooled copper shoes are generally used to contain the molten metal and slag. A consumable guide tube is often used that runs from the top to the bottom of the weld and is positioned with its tip above the bottom of the joint for weld initiation. The guide tube is then consumed as the weld progresses.

The ESW process can be used to weld sections several inches in thickness in a single pass, which results in significant savings in manpower, time and welding consumables. Sections being welded do not require machined edge preparation, and the combination of high heat input, welding speed and weld pool size eliminates the need for preheating. Post-weld distortion is also minimal as compared to other processes (*137*).

However, tighter control over welding parameters is required to produce sound electroslag welds. The ESW process as implemented in bridge fabrication throughout the early 1970s was unable to consistently produce defect-free welds. In early 1977, a back-channel girder on the I-79 Bridge over the Ohio River at Neville Island in Pittsburgh, PA fractured at an electroslag welded splice (*138*). The high incidence of weld defects on other bridges required major repairs, which further complicated subsequent inspection. In addition, examination of weld metal toughness revealed very low Charpy V-notch impact toughness values. As a result, the FHWA issued a moratorium in mid-February of 1977 on the use of electroslag

welds in tension and/or reversal stress loaded members used on Federal-aid projects (*139*).

After the moratorium was issued, FHWA-sponsored research has been aimed at improving the reliability and toughness of electroslag welds. This research has resulted in the development of the so-called Narrow-Gap Improved Electroslag Welding Process (NGI-ESW) (*137, 140-142*). This process utilizes a narrow gap between the parts being joined and a consumable plate guide tube in combination with reduced voltages and higher welding currents. The narrow-gap process has been shown to provide more consistent defect-free welds, improved fatigue performance, and improved impact toughness in the weld and heat-affected zones (*143*). As a result of this work, in March of 2000, the FHWA lifted the moratorium of the use of electroslag welds joining non-fracture critical tension and/or reversal stress members on Federal-aid projects in AASHTO Temperature Zones 1 and 2 in material up to 3 inches thick (*143*). NGI-ESW practices and procedures must be followed accordingly.

2.3.3.2.6 Stud Welding (SW)

The arc stud welding (SW) process is the most commonly used process to weld a stud shear connector to a flange. The process is essentially an automatic process in which the stud serves as the electrode and the arc is created from the end of the stud to the flange. The stud is contained in a gun that controls the timing of the process. A ceramic ferrule around the end of the stud in the gun shields and contains the molten metal. After the gun is placed into position and an arc is created, the gun drives the stud into the molten pool after a short instant of time. A small fillet around the end of the stud is created with full penetration across the shank of the stud. The weld is usually completed in less than one second.

2.3.3.3 Types of Welds

As shown in Figure 2.106, there are four basic types of welds – groove, fillet, slot and plug. Fillet welds represent the largest percentage of welds used in welded construction. Slot and plug welds are primarily used in lap joints (see below) in combination with fillet welds to assist in transmitting the shear when the size of the connection limits the length available for fillet or other edge welds. Slot and plug welds can also help prevent the overlapping parts from buckling. However, because of fatigue concerns, slot and plug welds are rarely used in bridge construction, and then, only to resist compression or shear stress; therefore, they are not covered any further here.

(a) GROOVE WELD   (b) FILLET WELDS

(c) SLOT WELD   (d) PLUG WELD
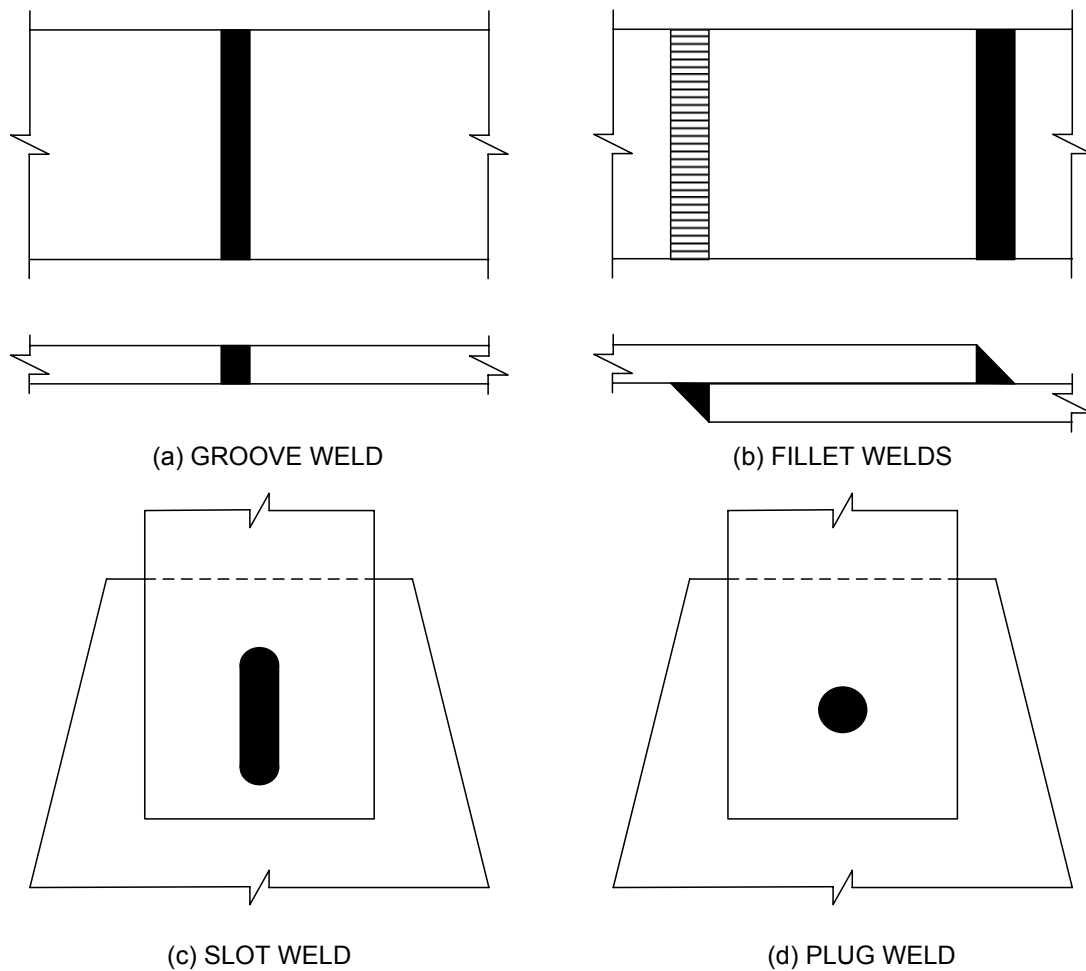
Figure 2.106 Types of Welds

2.3.3.3.1 Groove Welds

2.3.3.3.1.1 General

Groove welds are most often used to connect structural members that are aligned in the same plane (i.e. butt joints). They can also be used in tee and corner joints (see below). As shown in Figure 2.107, there are two basic subcategories of groove welds: complete penetration groove welds (CJP) and partial penetration groove welds (PJP).

Complete Joint
Penetration Groove Welds
(CJP)

Partial Joint Penetration
Groove Welds
(PJP)
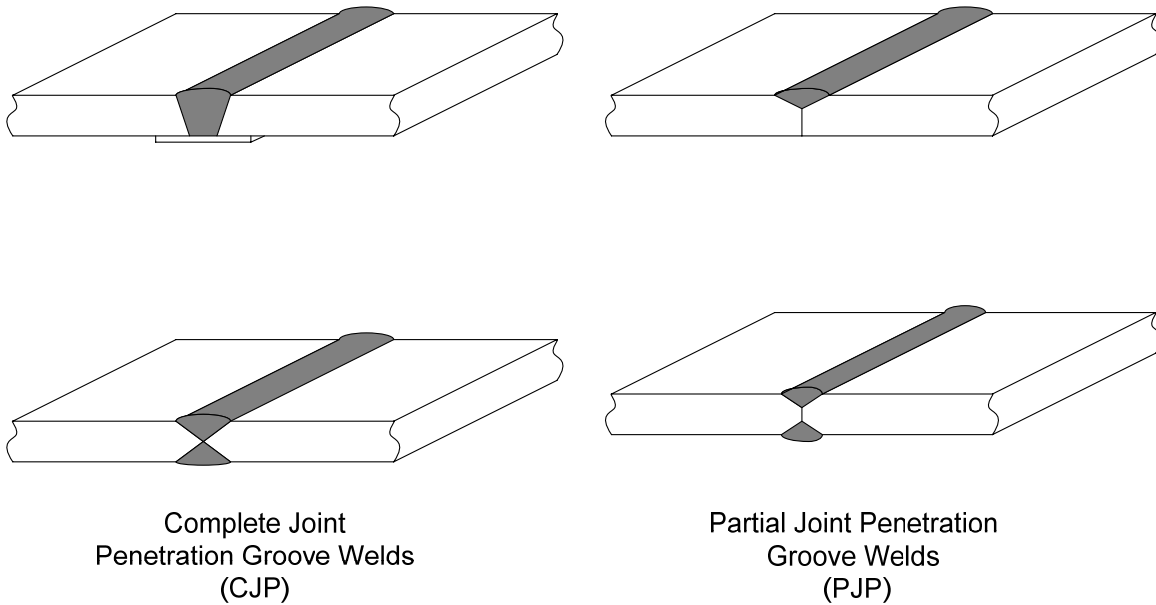
Figure 2.107 Subcategories of Groove Welds

CJP groove welds have the same resistance as the pieces joined and are intended to transmit the full load of the members that are joined. PJP groove welds do not extend completely through the thickness of the pieces being joined and are subject to special design requirements. PJP welds are sometimes used when stresses are low and there is no need to develop the complete strength of the base material.

Note that both types of welds may be single- or double-sided welds. Double-sided welds, which require access to both sides of the joint, may require less weld metal and result in less distortion and are of particular importance when joining thick members.

Basic groove weld nomenclature is shown in Figure 2.108.
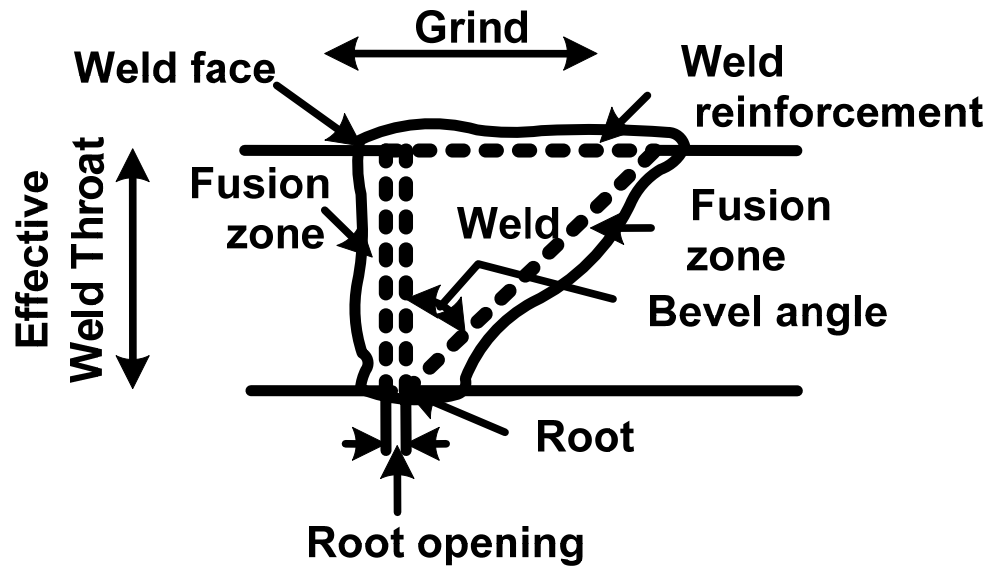
Figure 2.108 Groove Weld Nomenclature

2.3.3.3.1.2 Types

Groove welds are classified according to their particular shape. Most groove welds require a specific edge preparation and are named accordingly (Figure 2.109).

(a) SQUARE

(b) SINGLE-V

(c) DOUBLE-V

(d) SINGLE BEVEL

(e) DOUBLE BEVEL

(f) SINGLE-U

(g) DOUBLE-U

(h) SINGLE-J

(i) DOUBLE-J
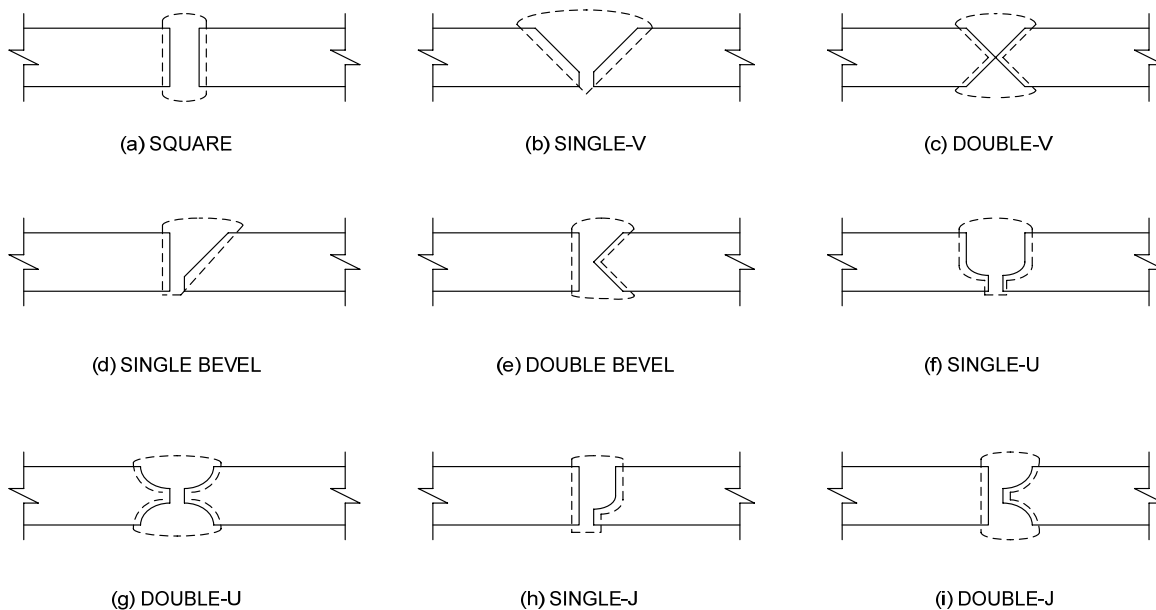
Figure 2.109 Types of Groove Welds

The square groove (Figure 2.109a) requires no edge preparation and is rarely used in bridge construction, except for thin sections. For the bevel groove (Figure 2.109d and Figure 2.109e), one plate is cut at a 90-degree angle and the second plate is

provided with a bevel cut. The V groove (Figure 2.109b and Figure 2.109c) is similar to the bevel groove, except that both plates are bevel cut. The J groove (Figure 2.109h and Figure 2.109i) resembles a bevel groove, except that the root has a radius instead of a straight cut. The U groove (Figure 2.109f and Figure 2.109g) is similar to two J grooves put together. In all grooves but the square groove, the small opening or separation of the pieces being joined is called the root opening, which is provided for electrode access to the base of the joint. Note that the smaller the root opening, the larger the angle of the bevel that must be provided. The selection of the proper groove weld is dependent on the cost of the edge preparations, the welding process used and the cost of making the weld. The decision as to which groove type to use is usually left to the fabricator/detailer, who will select the type of groove that will generate the required quality at a reasonable cost.

2.3.3.3.1.3 Effective Area

The resistance of welds is based on the effective area of the weld, which is taken as the effective length of the weld times the effective throat according to *AASHTO LRFD* Article 6.13.3.3. The effective throat is defined nominally as the shortest distance from the joint root to the face of the weld (neglecting any weld reinforcement), or the minimum width of the expected failure plane.

The effective length of a groove weld is the width of the part joined perpendicular to the direction of stress. By definition, the effective throat of a CJP groove weld is equal to the thickness of the thinner part joined (Figure 2.110a and Figure 2.110b), with no increase allowed for any weld reinforcement. To ensure fusion throughout the thickness of the part being joined, backing is usually required if the CJP weld is made from one side, and back gouging is usually required from the second side if the CJP weld is made from both sides. Otherwise, qualification testing is required to show that the full throat can be developed.

The effective throat of PJP groove welds is defined in Article 2.3 of Reference 136. The effective throat of PJP groove welds depends on the probable depth of fusion that will be achieved; that is, the depth of groove preparation and depth of penetration that can be achieved by the selected welding process and welding position. In certain cases, the effective throat may be specified to be 1/8 in. less than the depth of joint preparation; that is, it is assumed that the last 1/8 in. of the joint will not be fused (Figure 2.110c). Therefore, in such cases, the depth of joint preparation will have to be increased by 1/8 in. to offset the loss of penetration.

$t_e = T_1$

T_1 T_2

$T_1 < T_2$

(a)

$t_e = T$

T T

(b)

$t_e = D - 1/8"$
$45^o \leq a < 60^o$ (GMAW and FCAW vertical and overhead positions)

D t_e T

No Gap

(c) BEVEL- OR V-JOINT

$t_e = D$

$a \geq 60^o$

D t_e T

(d) BEVEL- OR V-JOINT
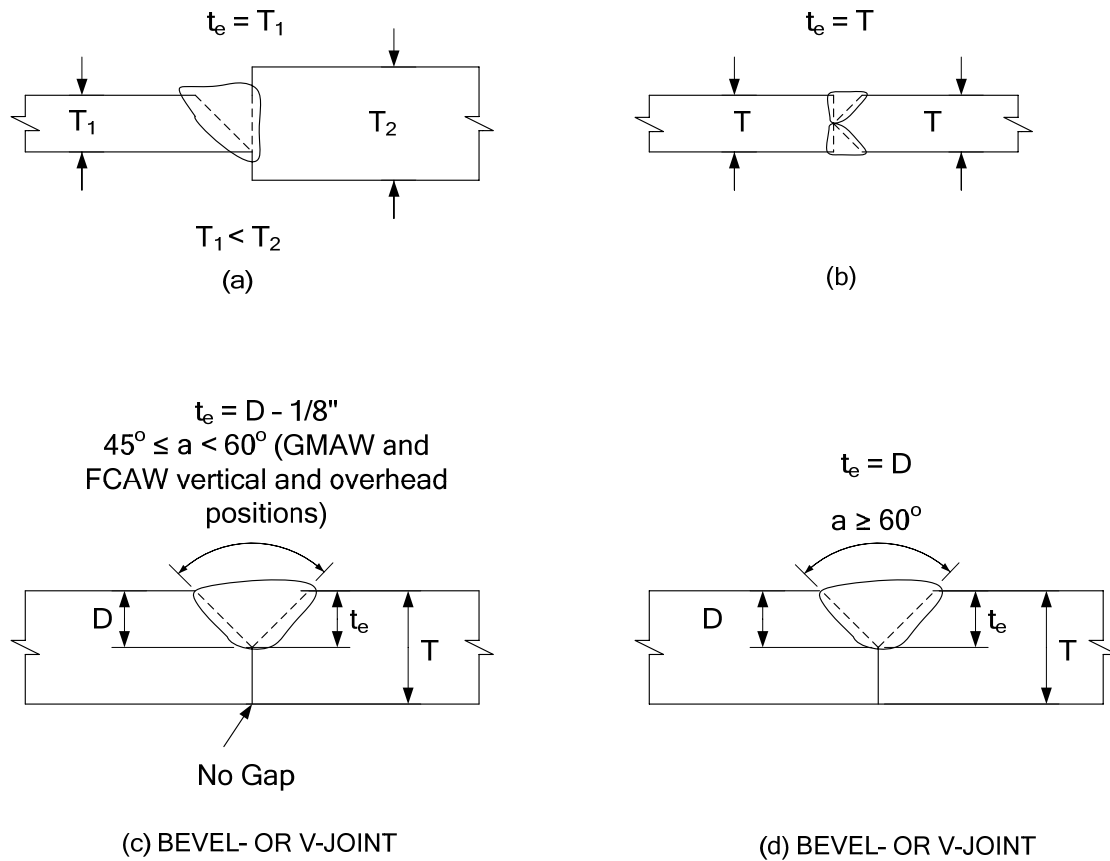
Figure 2.110 Effective Throat Dimensions for Groove Welds (SMAW, SAW, GMAW & FCAW)

The effective throat of a PJP weld is designated utilizing a capital 'E' and the required depth of penetration is designated by a capital 'S'. The Engineer will typically only specify the dimension for 'E'. The fabricator will then specify the appropriate 'S' dimension on the shop drawings based on the welding process and position that is selected. Both the 'E' and 'S' dimension are typically shown on the welding symbols (see below) on the shop drawings, with the effective throat shown in parentheses. Minimum effective throat thickness requirements for PJP welds are also given in Article 2.3 of Reference 136.

2.3.3.3.2 Fillet Welds

2.3.3.3.2.1 General

Fillet welds are the most widely used welds due to their ease of fabrication and overall economy. Fillet welds generally require less precision during fit-up and the edges of the joined pieces seldom need special preparation such as beveling or squaring. Fillet welds have a triangular cross-section and do not fully fuse the cross-sectional area of the parts they join, although full-strength connections can be developed with fillet welds.

Basic fillet weld nomenclature is shown in Figure 2.111. The size of a fillet weld is given as the leg size of the fillet. If the two legs are unequal, the nominal size of the weld is given by the shorter of the legs.
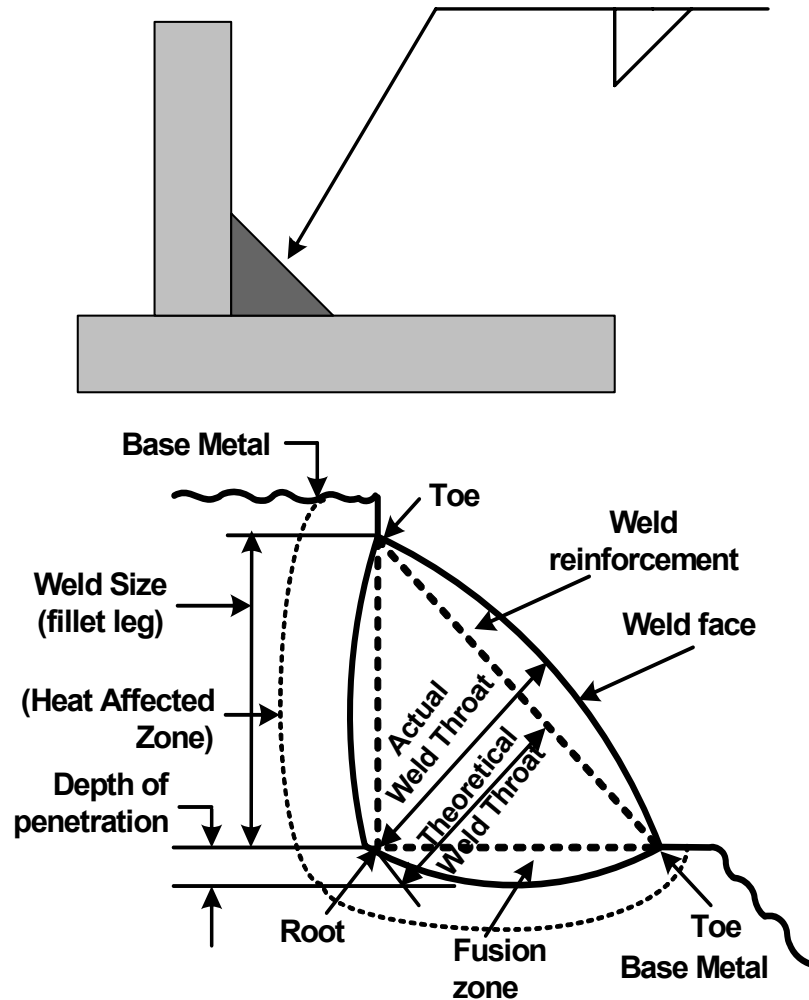
Figure 2.111 Fillet Weld Nomenclature

2.3.3.3.2.2 Effective Area

As for groove welds, the effective area of a fillet weld is taken equal to the effective length of the weld times the effective throat (*AASHTO LRFD* Article 6.13.3.3). The effective length is to be taken as the overall length of the full-size fillet. The effective throat is taken as defined below.

2.3.3.3.2.2.1 Effective Throat

The effective throat dimension of a fillet weld is nominally the shortest distance from the joint root to the weld face (neglecting any weld reinforcement), which for a typical fillet weld with equal legs of nominal size a is taken equal to $0.707a$ (Figure 2.112a).
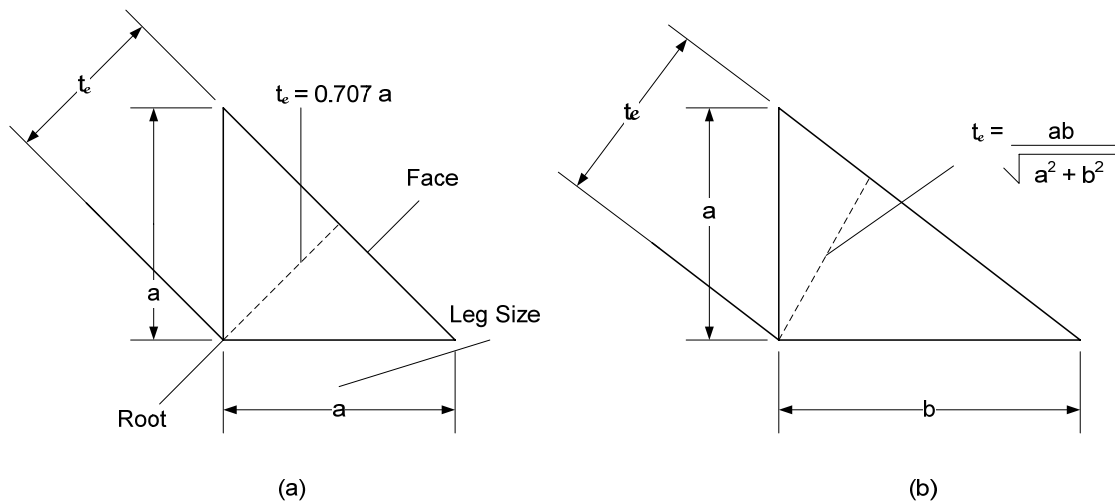
Figure 2.112 Effective Throat Dimensions for Fillet Welds

For the rare case of a fillet weld with unequal leg sizes, the effective throat would be computed as shown in Figure 2.112b.

2.3.3.3.2.2.2 Minimum Effective Length

When placing a fillet weld, the welder builds up the weld to the full dimension as near to the beginning of the weld as possible. However, there is always a slight tapering off of the weld where the weld starts and ends. Therefore, a minimum effective length of the weld is required. As specified in *AASHTO LRFD* Article 6.13.3.5, the minimum effective length of a fillet weld is to be taken as four times its leg size, but not less than 1.5 inches (Figure 2.113).
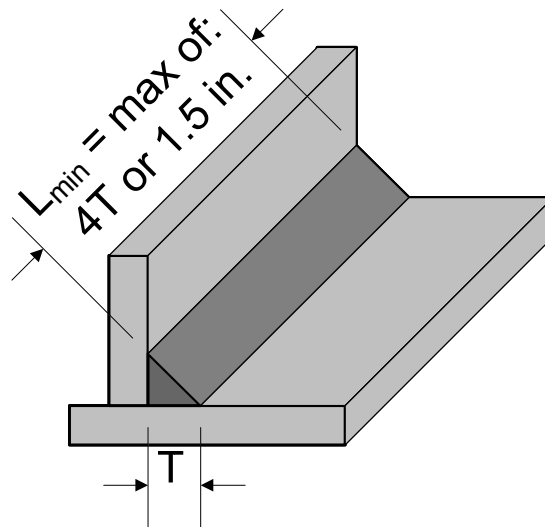
Figure 2.113 Minimum Effective Length of Fillet Welds

2.3.3.3.2.3 Maximum Thickness Requirements

As specified in *AASHTO LRFD* Article 6.13.3.4 and shown in Figure 2.114a and Figure 2.114b, maximum thickness (size) requirements for fillet welds *along edges of connected parts* depend on the thickness of the parts being connected (unless the weld is specifically designated on the contract documents to be built out to obtain full throat thickness).
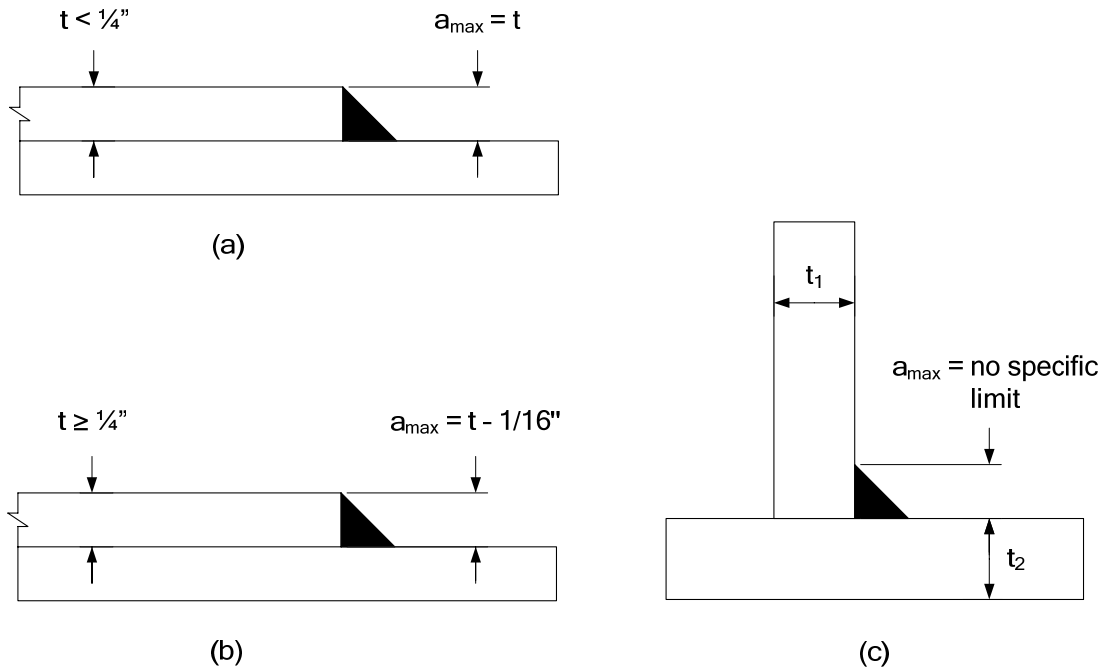
Figure 2.114 Maximum Size Requirements for Fillet Welds

Note that for the case shown in Figure 2.114c, no specific limit applies, except as limited by the resistance requirements for the base metal in some instances. The requirements prevent melting of the base metal where the fillet would meet the corner of the plate if the fillet were made the full plate thickness (*28*).

2.3.3.3.2.4 Minimum Thickness Requirements

The minimum thickness (size) of a fillet weld is not to be less than that required to transmit the required forces, nor the minimum thickness specified in *AASHTO LRFD* Table 6.13.3.4-1 (Table 2.21).

Table 2.21 Minimum Thickness Requirements for Fillet Welds

Base Metal Thickness of Thicker Part Joined (T)	Minimum Size of Fillet Weld
in.	in.
$T \le 3/4$	1/4
$3/4 < T$	5/16

The minimum weld size need not exceed the thickness of the *thinner* part joined. Note that the specified minimum weld sizes assume that the required preheats and interpass temperatures are provided (see below) (*133*). According to *AASHTO LRFD* Article 6.13.3.4, smaller welds than the minimum size welds may be approved by the Engineer if they are shown to be adequate for the applied stress and if the appropriate additional preheat is applied.

Minimum thickness requirements for fillet welds are based on preventing too rapid a rate of cooling in order to prevent a loss of ductility (i.e. the formation of a brittle microstructure) or a lack of fusion. The thicker the plate joined, the faster the heat is removed from the welding area. As a minimum, a weld of sufficient size is needed to prevent the thicker plate from removing heat at a faster rate than it is being supplied to cause the base metal to become molten. Thus, the minimum weld sizes implicitly imply a specified minimum heat input. In addition, restraint to weld metal shrinkage may result in weld cracking if the welds are too small.   Minimum weld sizes are frequently used for the case of longitudinal fillet welds that resist shear (e.g. girder flange-to-web welds).

Since the minimum size requirements for fillet welds imply a minimum level of heat input, the minimum size welds must be made in a single pass, as multiple passes to make the minimum size weld would not provide the assumed minimum level of heat input, essentially defeating the purpose of the requirement. The largest single pass fillet weld that can be made with the manual SMAW process is typically 5/16 in. (single-pass welds up to about ½ in. can be made with the SAW process).

2.3.3.3.2.5 End Returns

According to *AASHTO LRFD* Article 6.13.3.6, fillet welds that connect a part or member subject to a tensile force where the force is *not* parallel to the weld axis, or fillet welds that are *not* proportioned to withstand repeated stress, are not to be terminated at the corners of the part or member. Instead, in such cases, continuous full-size end returns are to be provided around the corner for a length equal to twice the weld size *a* where such returns can be made in the same plane. The end returns are to be indicated in the contract documents.

Also, as specified in *AASHTO LRFD* Article 6.13.3.6, fillet welds deposited on the opposite sides of a common plane of contact between two parts are to be interrupted at a corner common to both welds (e.g. double-sided fillet welds connecting transverse stiffeners, connection plates or bearing stiffeners to a flange).

2.3.3.3.2.6 Seal Welds

As specified in *AASHTO LRFD* Article 6.13.3.7, fillet welds to be used as seal welds are to be continuous and are to combine the functions of sealing and strength. Seal welds are to change section only as required by strength or by the minimum size requirements discussed previously.

2.3.3.3.3 Weld Symbols

Weld symbols are used to allow the Engineer to instruct the fabricator and detailer as to the type and size of weld required for a particular connection (and vice versa). A standard system of designating welds by symbols that communicate the desired weld size, location and type has been developed by the AWS (*144*). As specified in *AASHTO LRFD* Article 6.13.3.1, all welding symbols must conform to this system. As a minimum, the symbol consists of a reference line and an arrow, with the arrow pointing to the joint location, as shown in Figure 2.115. Symbols of the desired weld are drawn above or below the reference line.
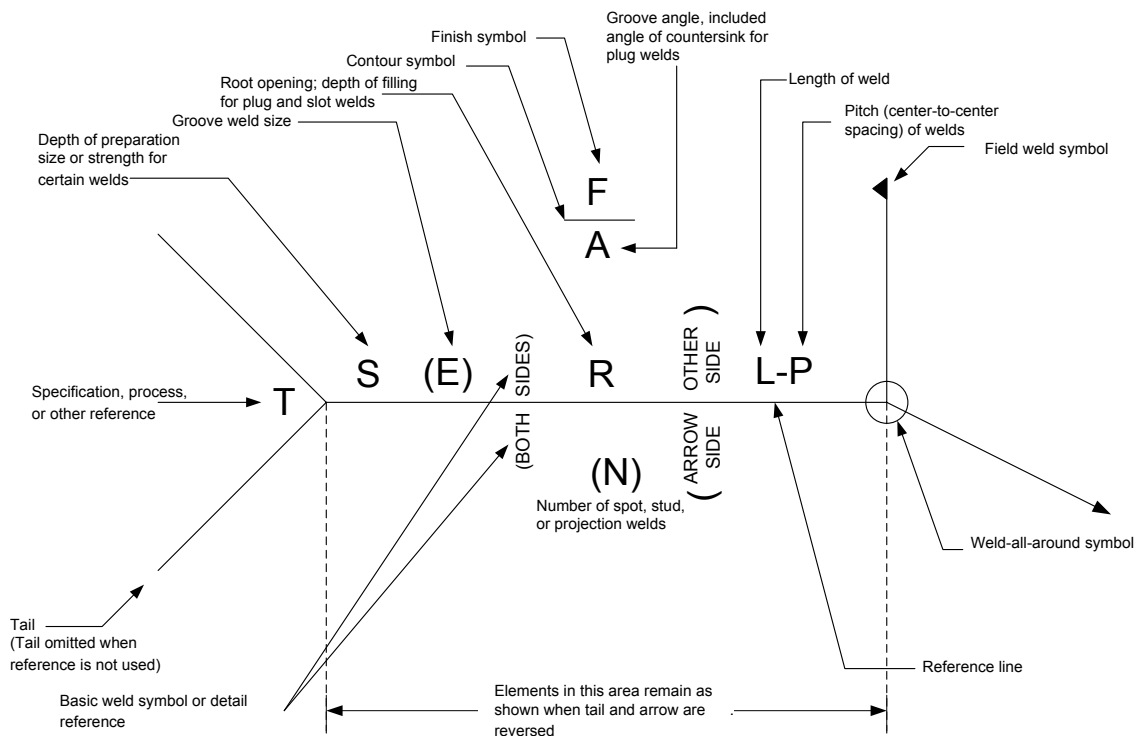
Figure 2.115 Weld Symbols

Examples illustrating the use of weld symbols for both fillet and groove welds are given in Figure 2.116.

<u>FILLET WELDS</u>

5/16

Fraction indicating leg shown
only on one weld when both
sides are the same.

SEAL WELD

Weld all around

<u>GROOVE WELDS</u>
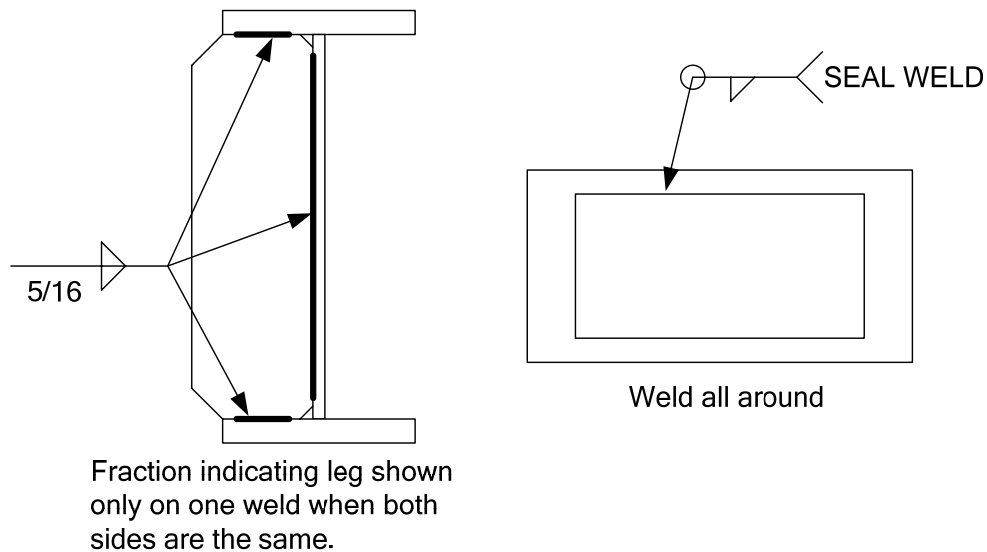
Square groove welded from
both sides.
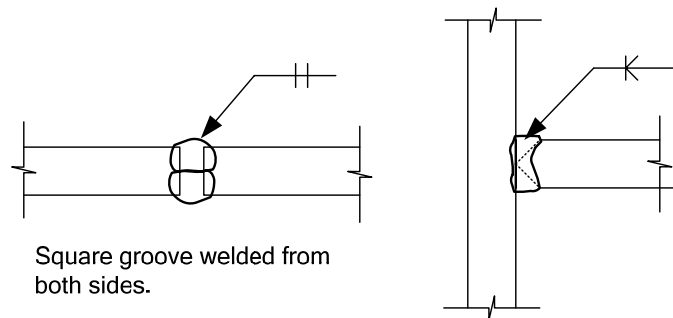
Figure 2.116 Examples of Use of Weld Symbols

If a particular welded connection is used in many different parts of the structure, it may only be necessary to show a typical detail utilizing the welding symbols. For special complex or confusing connections, additional sketches may be necessary to indicate what is required. Welding symbols should be used to communicate and not to confuse. The Engineer will typically use welding symbols to convey a minimum amount of information to the fabricator/detailer regarding the welded connection on the design drawings (e.g. type and size of weld, etc.). The fabricator/detailer will then provide welding symbols for the same connection, often conveying more detailed information about the connection, on the shop drawings for review and approval by the Engineer. Therefore, the Engineer should have a complete understanding of weld symbols. More detailed information on welding symbols may be found in References 136 and 144 and in most any structural steel textbook.

2.3.3.4 Types of Joints

2.3.3.4.1 General

As shown in Figure 2.117, there are five basic types of welded joints – butt, lap, tee, corner and edge joints. In practice, different variations and combinations of these joints may be used. Edge joints are more commonly used in sheet metal applications and will not be discussed further here.

(a) BUTT JOINT

(b) LAP JOINT

(c) TEE JOINT

(d) CORNER JOINT

(e) EDGE JOINT
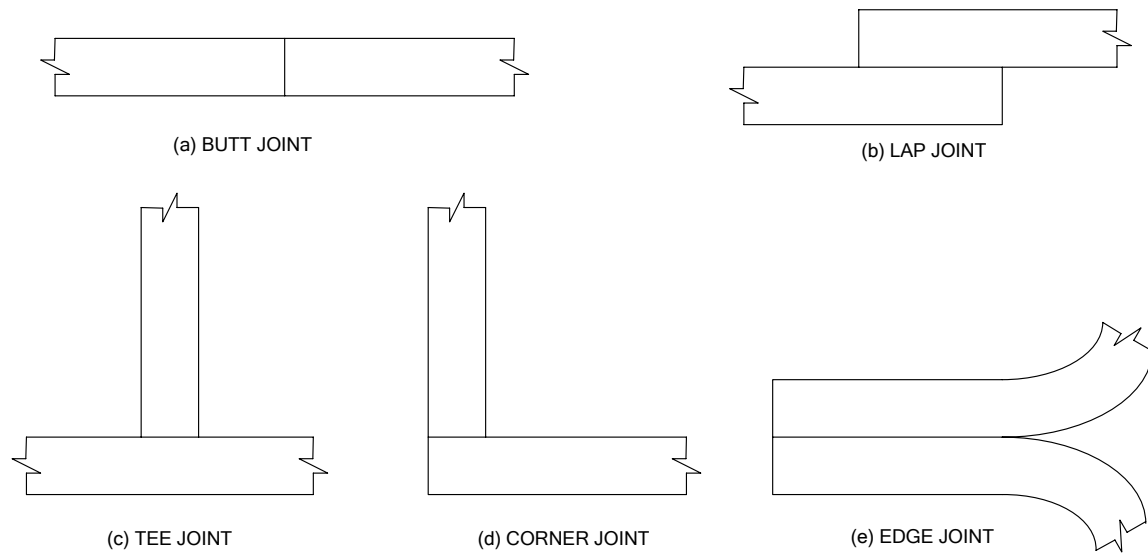
Figure 2.117 Types of Welded Joints

The joint type does not necessarily imply a specific type of weld. The selection of the weld type for certain types of joints (e.g. tee and corner joints) is usually dictated by the loading type and magnitude.

Butt joints are used to join the ends of flat plates together (e.g. girder flange and web shop splices). Butt joints in tension subject to fatigue loading are best made with complete penetration groove welds with the weld reinforcement removed. When subject to compression or shear only, partial penetration groove welds may be used providing adequate throats can be developed. The principal disadvantage of butt joints is that the connected edges typically require special preparation (i.e. beveling or grinding) and must be carefully aligned prior to welding.

Lap joints (e.g. cover plates and bracing member-to-gusset plate joints) do not require quite the preciseness in fabrication as other types of joints. The edges of the joined pieces are usually sheared or flame cut and do not require any special edge preparation. Lap joints utilize fillet welds.

Tee joints are used to fabricate built-up sections, or in general, any pieces framing in at right angles (e.g. plate girder web-to-flange connections, stiffener-to-web

connections, hangers, brackets).   For tee joints subject to longitudinal shear, continuous fillet welds or groove welds can be used to join the pieces; however, fillet welds are usually the most economical option when the fillet weld leg size is less than ¾ in. (*133*). As larger throats are required, partial penetration groove welds (perhaps with external fillet welds) are the most cost-effective option (*133*). Complete penetration groove welds are not recommended for use in tee joints because of the relatively high cost and resulting welding deformations. It should be noted that partial penetration groove welds are assigned a slightly lower fatigue category in this configuration (Category B′ vs. Category B), but this rarely controls.

Corner joints are typically used to form built-up non-composite rectangular closed box sections.   For corner joints, internal access to the box section has a major influence on the weld selection.   Article 3.1 of Reference 40 discusses suggested details for welding of corner joints in closed box configurations, including large boxes in which a person can safely work and boxes that are too small for a person to work safely inside. The suggested details primarily involve the use of fillet welds alone in all four corners of the box or a combination of fillet welds for one flange and partial penetration groove welds for the second flange. Combinations involving the use of fillet welds and complete penetration groove welds are included, but are generally not recommended due to the expense and the fact that backing bars must generally be left in place. For details where single fillet welds in all four corners, or double fillet welds for one flange in combination with partial penetration groove welds for the second flange, are recommended, the Engineer should evaluate the loading conditions (e.g. torsion) and ensure that sufficient internal diaphragms are provided to limit rotations at the corner joints.   Corner joints should also be carefully detailed to prevent the possibility of lamellar tearing, as discussed below.

2.3.3.5 Lamellar Tearing

Lamellar tearing is a separation in the base material caused by large thru-thickness strains induced by weld metal shrinkage (*145-148*). Strains due to applied loads are not a primary concern in causing lamellar tearing. Under conditions of high restraint, localized strains due to weld metal shrinkage may be many times higher than yield point strains. Lamellar tearing is primarily a concern in tee and corner joints where the degree of restraint is such that weld shrinkage strains imposed on the base metal in the thru-thickness direction cannot be accommodated because of limited ductility.

As a result of the hot-rolling operation during manufacture, steel exhibits different properties in the direction parallel to rolling, in the direction transverse to rolling and in the thru-thickness direction (Figure 2.118).

Z = Thru-Thickness Direction
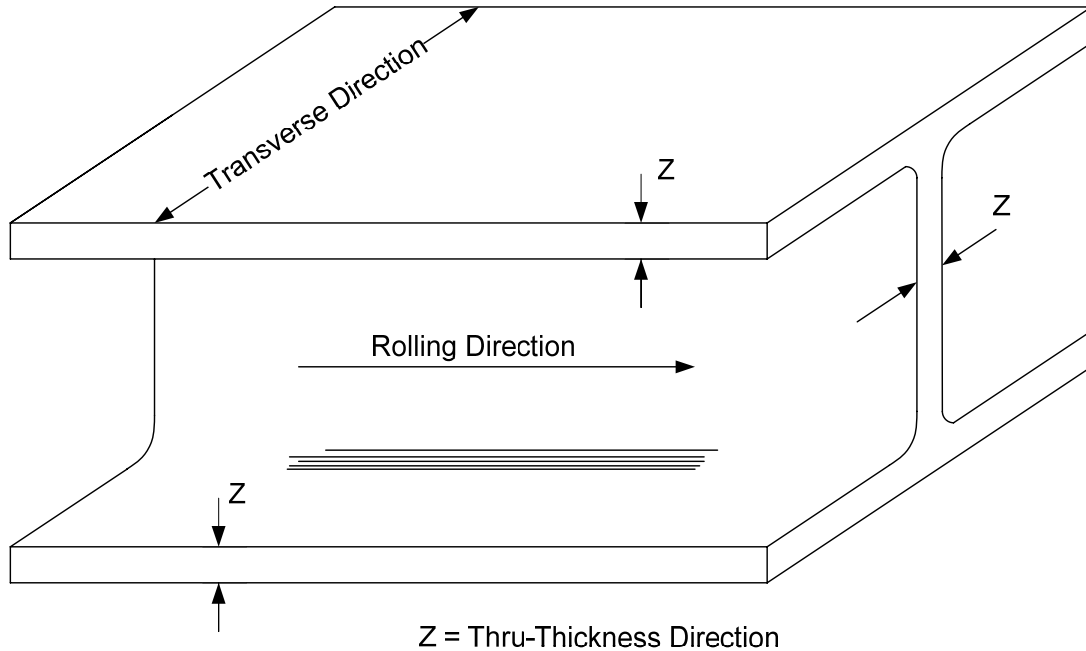
Figure 2.118 Rolling Direction Terminology

Steel loaded parallel or transverse to the rolling direction exhibits ductility to a greater extent than steel loaded in the thru-thickness direction. In the elastic range, the strength of steel in the thru-thickness direction is only slightly below the strength in the longitudinal or transverse direction, whereas steel loaded in the thru-thickness direction may have limited resistance to strains exceeding the yield point strains. Such strains may cause decohesion in the base metal and lead to a lamellar tear. Cooling of the weld to ambient temperature after the weld is completed increases strains so that terraces in the base metal resulting from decohesion link together by shearing failure to form a completed lamellar tear (*146*).

A lamellar tear occurs only in the base metal, and while the tear may originate close to the toe or root of a weld, often the tear will originate well outside the heat-affected zone and may not propagate to the surface. When weld metal is selected that will match closely the tensile strengths of typical structural steels, the weld yield points are typically significantly higher than the yield points of the base metal. Thus, when yield point strains occur in the connected material, the level of stress in the weld metal is well below its yield point. As a result, the total strain is forced to take place in the base metal.

All joints that stress the steel in the thru-thickness direction do not necessarily cause a problem. However, in a highly restrained joint, if weld shrinkage strains tend to pull the steel apart in the thru-thickness direction, the joint will exhibit a greater tendency to tear than when the shrinkage forces are oriented in the plane of the member. It can become a particularly significant concern in joints with large welds in thick material under high-restraint conditions (Figure 2.119).
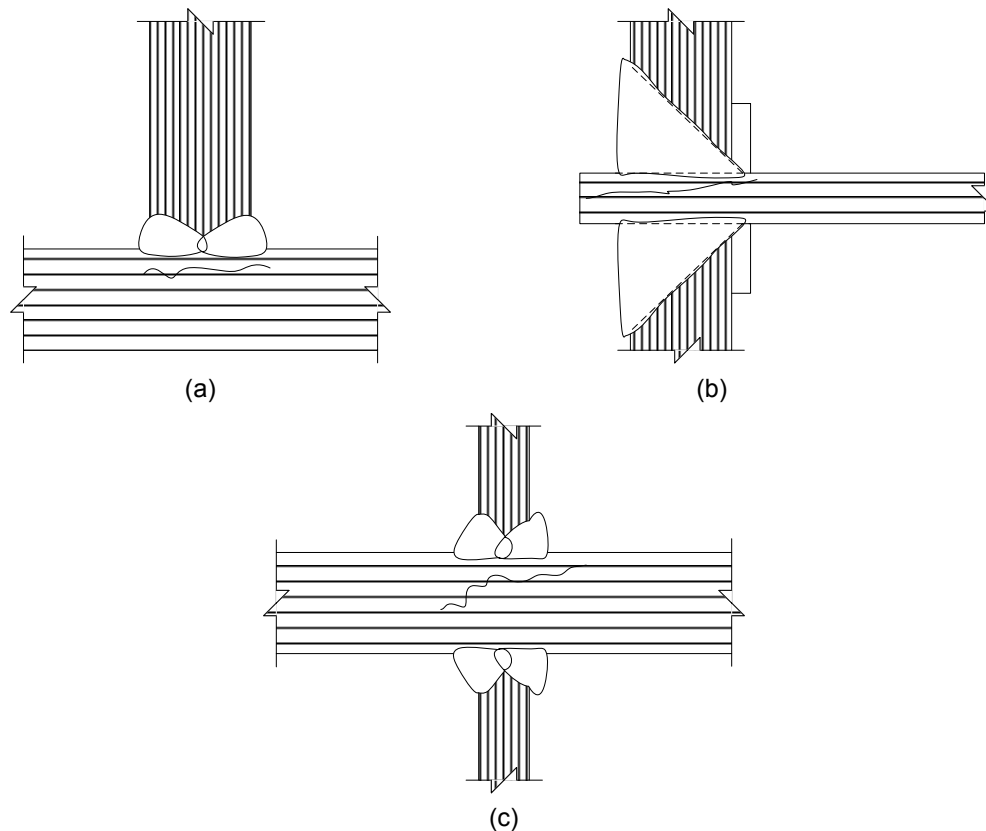
Figure 2.119 Joints Showing Typical Lamellar Tears

Lamellar tearing is not a concern in the design of bolted connections or low-restraint welded connections.

To avoid lamellar tearing, the concentration of strains should be minimized in localized areas. Shrinkage and residual stresses tend to increase with the volume of weld metal deposited (*146*). Therefore, in large volume multiple-pass groove welds, high restraint conditions resulting from initial weld passes force the strains from subsequent weld passes to be concentrated in highly localized areas. Thus, using complete penetration groove welds where they are not required can increase localized strains and contribute to lamellar tears in welded connections that load the base material in the thru-thickness direction.

Figure 2.120 illustrates some susceptible details where the weld shrinkage in the thru-thickness direction can increase the probability of lamellar tearing. The improved details (also shown in Figure 2.120) are such that the weld shrinkage occurs in the rolling direction so that the shrinkage pulls on the fibers longitudinally, or in their strongest orientation.

Susceptible detail | Improved detail

(a)

Susceptible detail | Improved detail

(b)

Susceptible detail | Improved detail

(c)
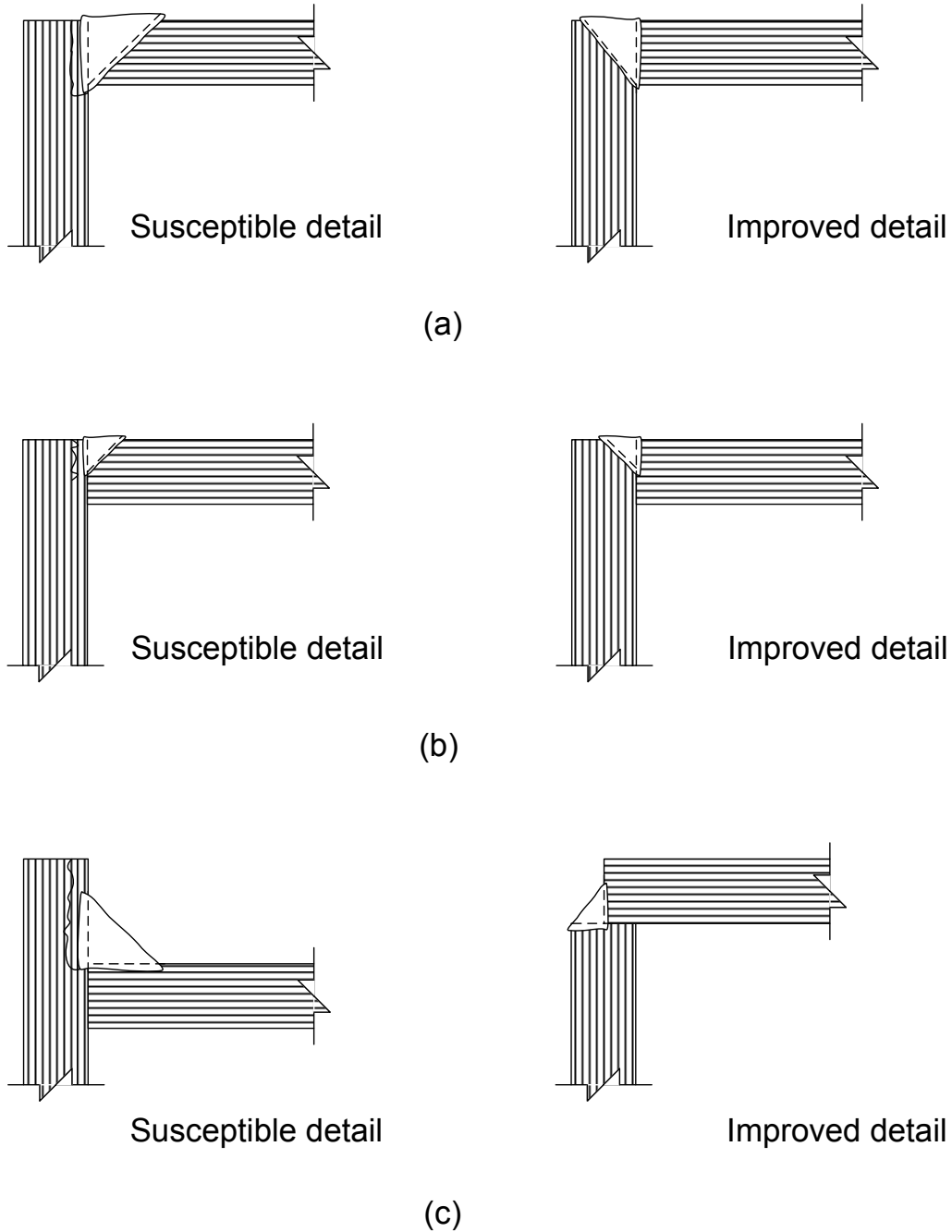
Figure 2.120 Detailing of Welded Connections to Reduce Susceptibility to Lamellar Tearing

2.3.3.6 Control of Distortion

Weld metal shrinkage can also result in distortion due to the non-uniform expansion and contraction of the weld metal and the adjacent base metal during the heating and cooling cycles of the welding process. As the weld metal cools and contracts, the resulting strains can cause distortion if the surrounding base material is free to move (Figure 2.121a). In heavily restrained materials, the strains induce stresses

that can potentially lead to cracking. Stresses that result from material shrinkage are inevitable in welding.   Distortions can be minimized, however, through efficient design and fabrication practices (*149*).
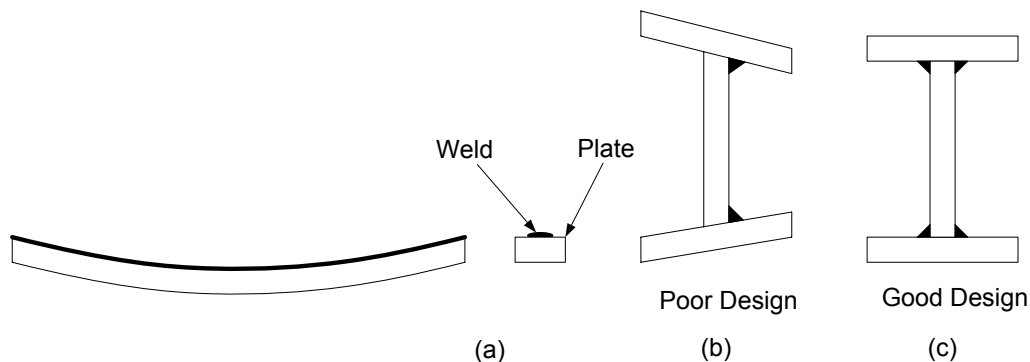
Figure 2.121 Welding Distortion

The Engineer can design welded assemblies to help minimize the amount of distortion.   Reducing the amount of weld metal will decrease the amount of distortion.   Therefore, the smallest acceptable weld size should be used.   Groove weld details with no greater root opening that necessary that require the minimum volume of weld metal per unit length are also beneficial. Symmetry in welding is also important in minimizing distortion. Consider using double-sided joints versus single-sided joints where practical. Balancing welds about the planes of symmetry of the cross-section can help the shrinkage forces from one set of welds counteract the shrinkage forces from the other set (Figure 2.121a and Figure 2.121b). Unbalanced welds removed from the neutral axis can cause longitudinal camber or sweep of the member.

The Fabricator can also use techniques to help minimize distortion. Using as few weld passes as possible can help limit the number of heating and cooling cycles and the concomitant accumulation of shrinkage stresses.   Overwelding should be avoided as it can result in more distortion than necessary. A well-planned welding sequence can help to balance the shrinkage forces. Parts to be welded may be pre-cambered prior to welding so that the parts will be drawn back into the proper alignment as weld shrinkage occurs. Clamps and jigs can be used to avoid rotation of the part and force the weld metal to stretch as it cools. Use of low heat input welding procedures that utilize high currents and high travel speeds can reduce the size of the heat affected zone and the amount of distortion.

To help minimize shrinkage and ensure adequate ductility, the AWS has established minimum preheat and minimum and maximum interpass temperatures (*136*). Preheat refers to the temperature of the steel immediately before the arc is struck on the steel.   Preheat slows the cooling rates in the heat affected zone to prevent hardening and potential heat affected zone cracking (discussed below). Conditions of higher restraint, enriched base metal chemistries and adverse fabrication conditions may require additional preheat beyond the minimum requirements. Interpass temperatures are measured after the welding (or the welding for each pass) has begun. The required minimum interpass temperature should be the same

as the minimum specified preheat. The minimum interpass temperature is the temperature below which welding should not be done unless additional heat is added to raise the temperature of the steel. Large weldments and long joints can fall below the minimum interpass temperature before starting the next pass necessitating the addition of more heat before welding can resume. The maximum interpass temperature is the temperature beyond which welding should not be performed. Small weldments and short joints can exceed the maximum interpass temperature, in which case welding must stop until the joint is cooled down to an acceptable level.

2.3.3.7 Weld Quality

2.3.3.7.1 Potential Defects in Welds

Discontinuities within a weld may result from a number of potential defects unless good welding techniques and practices are followed. Among the more common defects are incomplete fusion, inadequate joint preparation, porosity, undercutting, slag inclusions, and cracks.

As illustrated in Figure 2.122a, incomplete fusion results due to failure of the base metal and weld metal to fuse together properly. Potential causes of incomplete fusion include the use of welding equipment with insufficient current so that the base metal does not reach its melting point, too rapid a rate of welding and surfaces to be joined that are contaminated or coated with mill scale, slag, oxides or other foreign material.
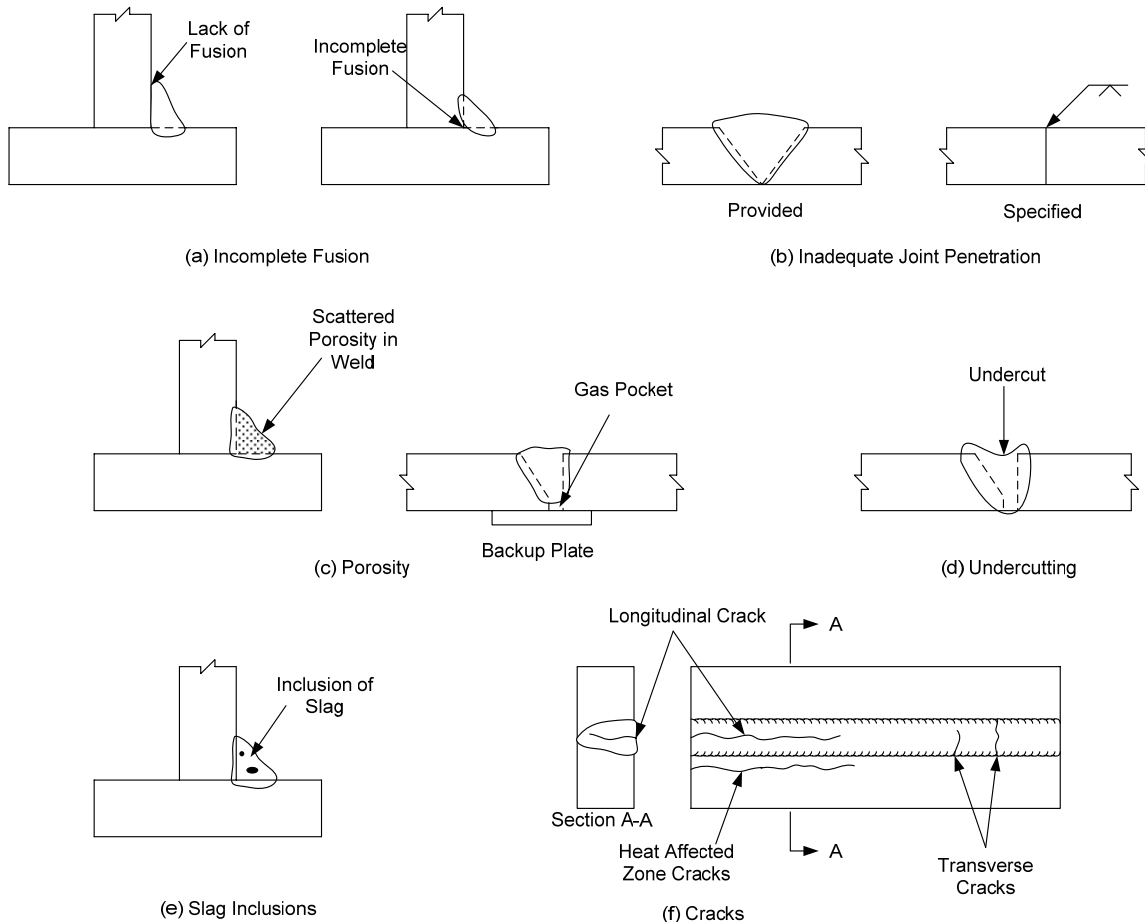
Figure 2.122 Potential Weld Defects

Incomplete joint penetration (Figure 2.122b) is associated primarily with groove welds and occurs when CJP groove welds are specified and the weld extends a shallower distance through the depth of the groove than specified. This defect can result from the use of insufficient welding current, too rapid a rate of welding, excessively large electrodes or the use of an improper groove design for the selected welding process. The use of the pre-qualified joints given by AWS in Reference 136, or joints that have a proven history of acceptable performance that can be used without again proving their adequacy by test, can help to minimize such defects. The specified combination of root opening, included angle, applicable thickness, etc. in a pre-qualified joint helps to ensure adequate fusion, welder access and joint penetration.   Specified tolerances may be applied to pre-qualified joints. When the actual joint detail fits within those tolerances, the joint is considered to be pre-qualified.   Otherwise,   the   joint   requires   qualification   by   test.   The fabricator/detailer will typically select the proper pre-qualified joint for a particular application and show it on the shop drawings.

Porosity in a weld occurs when voids or a number of small gas pockets are trapped in the weld during cooling (Figure 2.122c). The porosity may be scattered through the weld or concentrated as a large pocket at the root of a fillet weld or at the root of

a groove weld adjacent to a backup plate. Porosity typically results from using too long of an arc or an excessively high current.

Undercutting results when a groove is melted into the base material adjacent to a fillet weld toe or into the weld itself (Figure 2.122d) and is left unfilled by weld metal. This defect usually results from the use of excessive current or too long of an arc and can usually be corrected by depositing additional weld metal.

Slag inclusions result when the slag that forms during the welding process, which has a lower density than the molten weld metal and normally floats to the surface, is trapped within the weld due to too rapid a cooling of the joint (Figure 2.122e).   In multiple pass welds, the slag must be removed by the welder in-between each pass. Otherwise, slag inclusions may result. Overhead welds are particularly susceptible to slag inclusions.

Weld cracks, which are the most significant of the weld defects, result from internal shrinkage strains that occur as the weld metal cools. Weld cracks, as distinguished from weld failures that may occur due to underdesign, overload or fatigue, typically occur close to the time of fabrication. Hot cracks are cracks that occur at elevated temperatures and are usually related to solidification as cooling begins to occur. Hot cracks are usually caused by brittle states of various constituents (e.g. alloying elements) forming along grain boundaries and can usually be prevented by more uniform heating and slower cooling. Cold cracks are cracks that occur after the weld metal has cooled to ambient temperature and may be related to the effects of hydrogen, restraint to shrinkage and distortion and the formation of a brittle martensite microstructure. Cold cracking typically occurs in low-alloy steels and can be minimized through the use of low-hydrogen electrodes, use of the proper preheating and interpass temperatures, careful attention to welding sequences and procedures, use of the proper filler material, and in some cases, post weld heat treatment.

Weld cracks may be characterized as centerline (or longitudinal) cracks, heat affected zone cracks and transverse cracks (Figure 2.122f). Centerline cracking is a separation occurring in the center of a given weld bead. Heat affected zone cracking (also known as delayed or underbead cracking) is a separation occurring immediately adjacent to the weld bead in the base material. This region, termed the heat affected zone (HAZ), results from the thermal cycle experienced by this region during welding. This region is typically raised to a temperature above the transformation temperature of the steel, but below its melting point.   The final properties of this region depend on the cooling rate that it experiences. In base material with higher carbon and carbon equivalency levels, the HAZ is susceptible to increased hardness and reduced ductility upon cooling, which can increase the probability of HAZ cracking. Hydrogen on the steel, electrode, shielding material or in the atmosphere that is dissolved in the molten weld metal can also contribute to HAZ cracking in low-alloy steels that are subject to such cracking. Diffusion of the hydrogen through the weld metal toward any discontinuities in the HAZ occurs as the weld metal solidifies. As free hydrogen combines to form molecular hydrogen, a significant increase in internal pressure occurs within the HAZ. In susceptible steels, cracking can occur in the presence of this hydrogen in combination with the residual

stresses due to welding. Since the diffusion of the hydrogen through the weld metal takes time, such cracking may occur hours or even days after fabrication is completed; hence the term "delayed hydrogen cracking". Transverse cracking is a separation occurring within the weld metal perpendicular to the direction of travel. It is generally associated with weld metal that is high in strength that significantly overmatches the base metal, and is the least frequently encountered type of cracking. More detailed information on the causes of different types of weld cracks and potential corrective solutions may be found in Reference 133.

2.3.3.7.2 Inspection and Control

The success of welding in steel-bridge construction can be attributed to the inspection and control procedures that have been implemented to ensure the production of a sound quality weld.

Welding Procedure Specifications (WPS) are developed by welding engineers or technicians to communicate to the welders and inspectors the various parameters under which the welding is to be performed. The WPS is essentially the recipe for making a particular weld and should be made available to the welder and inspector near the point of welding for easy referral. The procedures are then tested to ensure their validity.   The supporting test data for a particular welding procedure is contained in a so-called Procedure Qualification Record (PQR). The tests typically include bend tests, transverse tension tests, all-weld-metal tension tests, Charpy impact tests and a marcoetch specimen. PQRs are typically filed in the fabrication office and are not made available to the welders. All welders should be pre-qualified; that is, they must pass an AWS Qualification Test prior to making a structural connection.

Welds must be inspected to ensure that they comply with the requirements of a given specification. Discontinuities are irregularities in the weld that may or may not be acceptable according to a given specification, whereas defects are discontinuities that are rejectable according to a given specification. A qualified welding inspector can utilize five primary non-destructive testing methods to locate and evaluate weld discontinuities. Each method has unique advantages and disadvantages. The methods are visual inspection (VT), penetrant testing (PT), magnetic particle inspection (MT), radiographic inspection (RT) and ultrasonic inspection (UT).

Visual inspection (VT) is the most powerful and simplest inspection method. Visual inspection commences well before welding begins by examining the materials to be welded, the alignment and fit-up of the parts, joint preparation and procedural data. During welding, visual inspection can ensure compliance with procedural requirements. Upon completion of welding, the size, appearance, bead profile and surface quality of the weld can be visually inspected.   Penetrant testing (PT) involves the application of a liquid dye penetrant to the weld, which is drawn to a surface discontinuity (i.e. porosity or a crack) by capillary action. A developer is then applied which absorbs the penetrant within the discontinuity and results in a stain indicating the presence of the discontinuity. This means of inspection is generally not specified for bridge fabrication since it is limited to the recognition of surface discontinuities, which can also be recognized by magnetic particle inspection.

Magnetic particle inspection (MT) involves the application of magnetic iron powders to the surface of the part. When a magnetic field is then applied, the change in magnetic flux that occurs in the presence of a discontinuity shows up as a different pattern within the powders. MT is most effective in locating surface discontinuities and those that are slightly subsurface. It is typically used to enhance visual inspection. Fillet welds and intermediate passes on large groove welds are often inspected using MT. Radiographic inspection (RT) utilizes X-rays or gamma rays that are passed through a groove weld to expose a photographic film on the opposite side of the joint producing a permanent record for future reference. Thin parts (e.g. porosity, slag and cracks) absorb less radiation than thick parts and therefore will appear darker on the radiograph, which is in effect a negative. RT is generally most effective in detecting porosity and slag inclusions and requires significant skill in order to properly interpret the radiograph.   Ultrasonic inspection (UT) utilizes high frequency sound waves that are transmitted through the materials. Discontinuity-free material will transmit the sound through the part in an uninterrupted fashion. A receiver hears the sound reflected off the back surface of the part being examined. A discontinuity between the transmitter and the back surface of the part will result in an intermediate signal being sent to the receiver.   The magnitude of the signal indicates the size of the discontinuity and the location of the discontinuity is indicated by the relationship of the signal with respect to the back surface. UT can be used to spot even small discontinuities and is generally most sensitive to cracks. UT is often used to inspect (and re-inspect) groove welds prior to code-mandated RT inspection. More detailed information on each of these inspection methods, including the relative advantages and disadvantages of each, may be found in References 131 and 133.

2.3.3.8 Factored Resistance

2.3.3.8.1 General

In addition to the requirements of the *AASHTO LRFD* Specifications discussed in the following, *AASHTO LRFD* Article 6.13.3.1 requires that all base metal, weld metal and weld design details conform to the requirements of Reference 136 (i.e. the *AASHTO/AWS D1.5M/D1.5 Bridge Welding Code*).

In the *AASHTO LRFD* Specifications, the factored resistance of a welded connection R_r at the strength limit state is based on either the factored resistance of the base metal or the product of the weld metal strength and the effective area of the weld that resists the load. The weld metal strength is the capacity of the weld metal itself, typically given in units of ksi. As discussed previously, the effective area of the weld that resists the load is the product of the effective length and the effective throat of the weld.

Weld metal strength may be classified as "matching", "undermatching" or "overmatching". Matching weld (filler) metal has the same or slightly higher specified minimum yield and tensile strength as compared to the specified minimum properties of the base metal. For example, matching weld metal for A 709 Grade 50 steel would be E70 filler material where the specified minimum weld/base metal properties for yield strength are 60/50 ksi and for tensile strength are 70/65 ksi. Although the weld metal has slightly higher properties than the base metal in this case, this is

considered to be a matching combination.   Note that according to Reference 135, matching consumables for A 709 Grade 50W base metal (as specified in Reference 136) are considered to be matching strength for hybrid designs where A 709 Grade HPS 70W base metal is joined to A 709 Grade 50W base metal.

As specified in *AASHTO LRFD* Article 6.13.3.1, matching weld metal must be used in groove and fillet welds, except that undermatching weld metal is permitted for fillet welds if the welding procedure and weld metal are selected to ensure the production of sound welds.   According to *AASHTO LRFD* Article C6.13.3.1, *the use of undermatched weld metal is strongly encouraged for fillet welds connecting steels with specified minimum yield strength greater than 50 ksi.* Lower strength weld metal will generally be more ductile than higher strength weld metal. Since the residual stresses in a welded connection are assumed to be on the order of the yield point of the weaker material in the connection (*133*), using lower strength weld metal will lower the level of residual stresses in the base metal at the connection reducing the cracking tendencies. Therefore, undermatched welds will be much less sensitive to delayed hydrogen cracking and are more likely to consistently produce sound welds. In such cases, the Engineer should indicate where undermatched welds are acceptable on the contract drawings.

Overmatching weld metal offers no significant advantages and increases the level of residual stresses and distortion at the connection. As mentioned above, higher yield strength weld metal is typically less ductile and more crack sensitive. Overmatching weld metal may also force the failure plane into the heat affected zone or fusion boundary, which is an undesirable condition (*133*).   Slight overmatching is acceptable in some cases. For example, in the process of adding alloys for improved atmospheric corrosion resistance, most filler metals for welding A 709 Grade 50W weathering steel will deposit weld metal with a specified minimum tensile strength of 80 ksi versus the specified minimum tensile strength of 70 ksi for the base metal. Since this combination performs well and there are limited alternatives, this slight overmatch is acceptable. Since some acceptable weld metals for weathering steel applications are classified as E70, basing the weld design calculations on E70 will give the fabricator the flexibility of using either E70 or E80 weld metal.

2.3.3.8.2 Groove Welds

2.3.3.8.2.1 Complete Penetration Groove Welds (CJP)

Groove welds of the same thickness as the connected parts are adequate to develop the factored resistance of the parts. Since matching weld metal is required for groove welds according to *AASHTO LRFD* Article 6.13.3.1, the weld metal will generally be slightly stronger than the base metal. Therefore, the factored resistance of the welded connection will most always be controlled by the resistance of the base metal.

The maximum forces in groove welds are usually tension or compression. According to *AASHTO LRFD* Article 6.13.3.2.2a, the factored resistance R_r of CJP groove-welded connections at the strength limit state subject to tension or compression

normal to the effective area of the weld or parallel to the axis of the weld (Figure 2.123) is to be taken as the corresponding factored resistance of the base metal. According to *AASHTO LRFD* Article 6.13.3.2.2b, the factored resistance R_r of CJP groove-welded connections at the strength limit state subject to shear on the effective area (Figure 2.123) is to be taken as the lesser of 60 percent of the factored resistance of the base metal *in tension* (assumed equal to the shear yield stress for the base metal) and the following:

$$R_r = 0.6\phi_{e1}F_{exx}$$ Equation 2.275

AASHTO LRFD Equation 6.13.3.2.2b-1

where:

ϕ_{e1} = resistance factor for shear on the effective area of CJP groove welds specified in *AASHTO LRFD* Article 6.5.4.2 (= 0.85)

F_{exx} = classification strength of the weld metal (ksi) (e.g. for E70 weld metal, F_{exx} = 70 ksi)

The factored resistance of connected elements (e.g. splice plates, gusset plates, brackets) in tension is specified in *AASHTO LRFD* Article 6.13.5.2 and was discussed previously in Section 2.3.2.4.2.4 of this chapter. In computing the net section fracture resistance of the connected element (Equation 2.249) for welded connections, the net area A_n is to be taken as the gross area less any access holes in the connection region (*AASHTO LRFD* Article C6.8.2.1).   The shear lag factor U for tension members connected by welds is discussed in Section 2.4.2.2.1 of this chapter under the design of Tension Members. As noted in *AASHTO LRFD* Article 6.13.5.2, U is to be taken equal to 1.0 for connection plates, splice plates and gusset plates. Also, as mentioned in *AASHTO LRFD* Article C6.13.4, block shear rupture should be checked around the periphery of welded connections subject to tension. The factored resistance of connected elements in compression is discussed above in Section 2.3.2.4.2.7 of this chapter.

Assuming that the connected elements have been designed accordingly (and that girder flanges and webs to be connected by groove welds have been designed for the appropriate strength limit state criteria), the Engineer need only indicate that a CJP groove weld is required at the appropriate location on the design drawings (using the acronym 'CJP'). Since the weld penetrates the full depth of the material and the weld length is equal to the width of the connected material (unless indicated otherwise), it is usually not necessary to specify the size or length of the weld. Also, as discussed previously, the fabricator/detailer will usually select the type of groove (often using a pre-qualified joint) that will generate the required quality weld at a reasonable cost, as well as the appropriate electrode/flux combination.
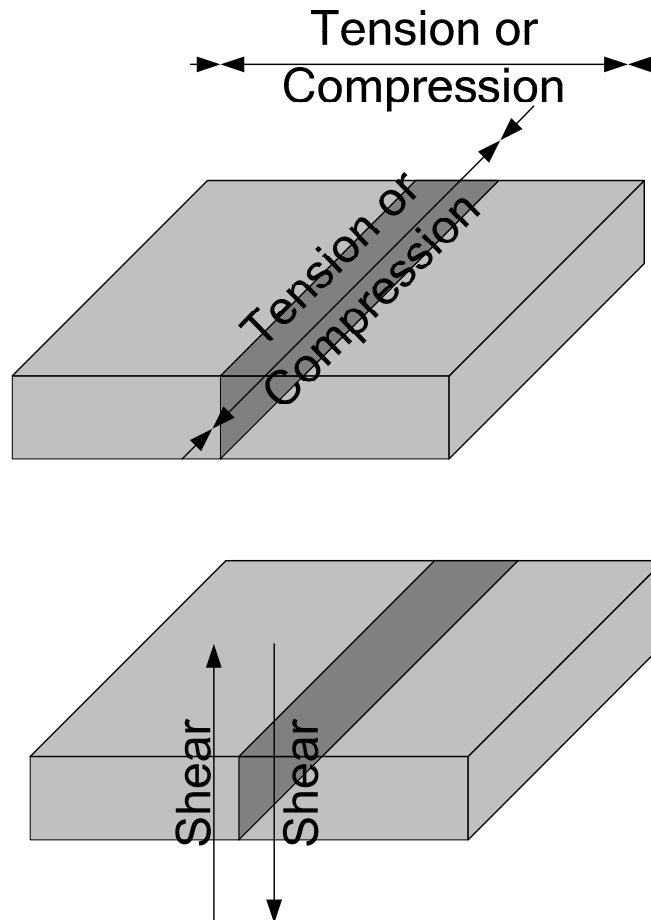
Figure 2.123 CJP Groove Weld Factored Resistance

2.3.3.8.2.2 Partial Penetration Groove Welds (PJP)

According to *AASHTO LRFD* Article 6.13.3.2.3a, the factored resistance R_r of PJP groove-welded connections at the strength limit state subject to compression normal to the effective area of the weld or tension or compression parallel to the axis of the weld (Figure 2.124) is to be taken as the corresponding factored resistance of the base metal. For PJP groove-welded connections subject to tension normal to the effective area of the weld (Figure 2.124), the factored resistance is to be taken as the lesser of the factored resistance of the base metal in tension and the following:

$$R_r = 0.6\phi_{e1}F_{exx} \qquad \text{Equation 2.276}$$

AASHTO LRFD Equation 6.13.3.2.3a-1

where:

ϕ_{e1} = resistance factor for tension normal to the effective area of PJP groove welds specified in *AASHTO LRFD* Article 6.5.4.2 (= 0.80)

F_{exx} = classification strength of the weld metal (ksi) (e.g. for E70 weld metal, F_{exx} = 70 ksi)

Note that PJP welds joining component elements of built-up members (e.g. girder flange-to-web welds) need not be designed for the tensile or compressive stress in those elements parallel to the axis of the welds. Recall that PJP groove welds are assigned a slightly lower fatigue category in this configuration (Category B′ vs. Category B – refer to *AASHTO LRFD* Table 6.6.1.2.3-1). Fillet welds will commonly suffice for these welds.

According to *AASHTO LRFD* Article 6.13.3.2.3b, the factored resistance R_r of PJP groove-welded connections at the strength limit state subject to shear parallel to the axis of the weld (Figure 2.124) is to be taken as the lesser of the factored shear resistance of the connected material and the following:

$$R_r = 0.6\phi_{e2}F_{exx}$$
<div align="right">Equation 2.277</div>

<div align="right">*AASHTO LRFD* Equation 6.13.3.2.3b-1</div>

where:
ϕ_{e2} = resistance factor for shear parallel to the axis of PJP groove welds specified in *AASHTO LRFD* Article 6.5.4.2 (= 0.80)

The factored resistance of connected material in shear is specified in *AASHTO LRFD* Article 6.13.5.3 and was discussed previously in Section 2.3.2.4.2.3 of this chapter.

As specified in *AASHTO LRFD* Article 6.6.1.2.4, transversely loaded partial penetration groove welds are not to be used, except for certain applications in orthotropic decks.

For tension or shear loads, the required resistance of the weld can be calculated as the force divided by the length of the weld. The result is then divided by the appropriate factored resistance of the connection (in units of ksi) to yield the required effective throat. Assume that this calculation determined the need for a one-inch effective throat size.   For a single-sided PJP groove weld, the effective throat (as defined previously) would have to be 1 in. As discussed previously, the actual depth of preparation of the production joint would be 1 in. or greater depending on the welding procedure and the included angle that are selected. A double-sided PJP groove weld would require two effective throats of 0.5 in. each. Another option would be PJP groove welds in combination with external fillet welds. If the plates to be joined are 1-in. thick, a CJP groove weld should be used to effectively transfer the stress since the effective throat of a CJP weld would equal the plate thickness, although a PJP/fillet weld combination may be capable of developing the necessary throat dimensions.

The Engineer would typically indicate a groove type (a bevel symbol is usually shown) and size (i.e. required effective throat) on the design drawings for a PJP groove weld. The fabricator/detailer would then select the desired groove type and

show the required depth of penetration as well as the appropriate electrode/flux combination on the shop drawings.
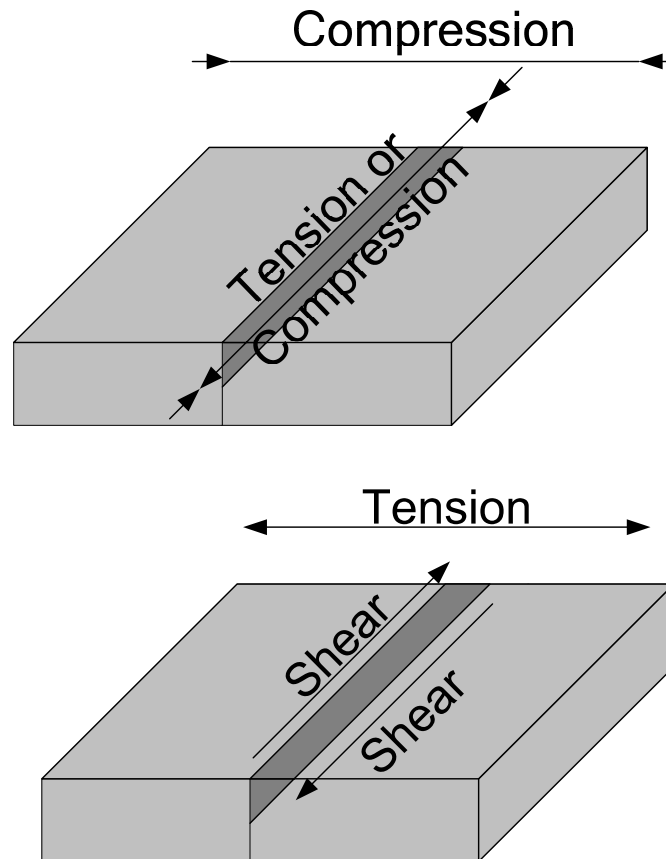
Figure 2.124 PJP Groove Weld Factored Resistance

2.3.3.8.3 Fillet Welds

For design purposes, fillet welds are assumed to transfer loads through shear on the effective area of the weld regardless of whether the shear transfer is parallel or perpendicular to the axis of the weld. The factored resistance is actually greater for shear transfer perpendicular to the weld, but there is less deformation capability. In both cases, although the weld fails in shear, the plane of rupture is not the same. In the *AASHTO LRFD* Specifications, the additional factored resistance of fillet welds loaded perpendicular to the axis of the weld is ignored and both loading situations are treated the same.

Figure 2.125a shows qualitatively a typical elastic shear stress distribution in the longitudinal fillet welds in a lap joint (i.e. for shear transfer parallel to the weld axis). The actual variation of shear stress from Point A to Point B depends on the ratio of the widths of the plates being joined and the length of the weld. Figure 2.125b shows a typical elastic shear distribution for fillet welds loaded perpendicular to the weld axis.
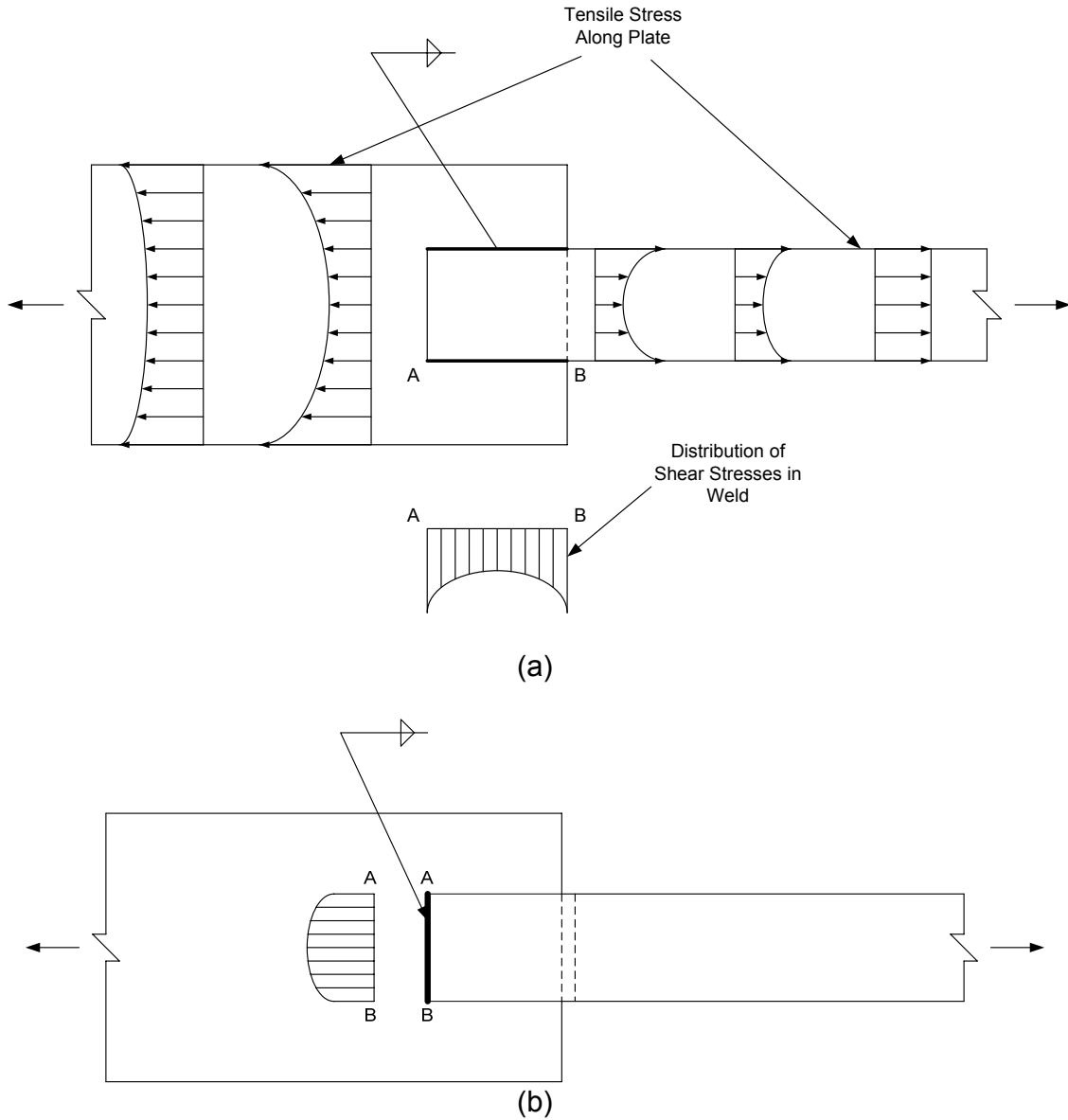
Figure 2.125 Typical Fillet Weld Shear Stress Distributions in a Lap Joint

Shear yielding is not critical in the welds because strain hardening occurs without significant overall deformation occurring in either case. Although the elastic shear stress distributions along the length of the weld are not uniform, the available ductility or plastic deformation capability permits lines of fillet weld loaded parallel or perpendicular to the weld to be assumed to resist the load equally along their lengths.

According to *AASHTO LRFD* Article 6.13.3.2.4a, the factored resistance R_r of fillet-welded connections at the strength limit state subject to tension or compression parallel to the axis of the weld (Figure 2.126) is to be taken as the corresponding factored resistance of the base metal. Note that fillet welds joining component elements of built-up members (e.g. girder flange-to-web welds) need not be

designed for the tensile or compressive stress in those elements parallel to the axis of the welds. According to *AASHTO LRFD* Article 6.13.3.2.4b, the factored resistance R_r of fillet-welded connections at the strength limit state subject to shear on the effective area (Figure 2.126) is to be taken as follows:

$$R_r = 0.6\phi_{e2}F_{exx}$$

Equation 2.278

AASHTO LRFD Equation 6.13.3.2.4b-1

where:

ϕ_{e2} = resistance factor for shear on the throat of the weld metal in fillet welds specified in *AASHTO LRFD* Article 6.5.4.2 (= 0.80)

F_{exx} = classification strength of the weld metal (ksi) (e.g. for E70 weld metal, F_{exx} = 70 ksi)

The welds must have typical weld profiles and may be matched or undermatched. The factored shear rupture resistance of the base metal (i.e. $R_r = \phi_u 0.6 F_u$) adjacent to the weld leg will seldom control since the effective area of the base metal at the weld leg is typically about 30 percent greater than the weld throat. Therefore, the specification does not require this resistance to be checked. In cases where overmatching weld metal is used, or where the weld throat has excessive convexity such that the resistance is governed by the weld leg, the shear rupture resistance should be checked to avoid overstressing of the base metal.

If a certain size fillet weld must be used in adjacent areas of a particular joint, it is desirable to use the same size weld to allow the same electrodes and welding equipment to be used for that joint and to simplify the inspection.
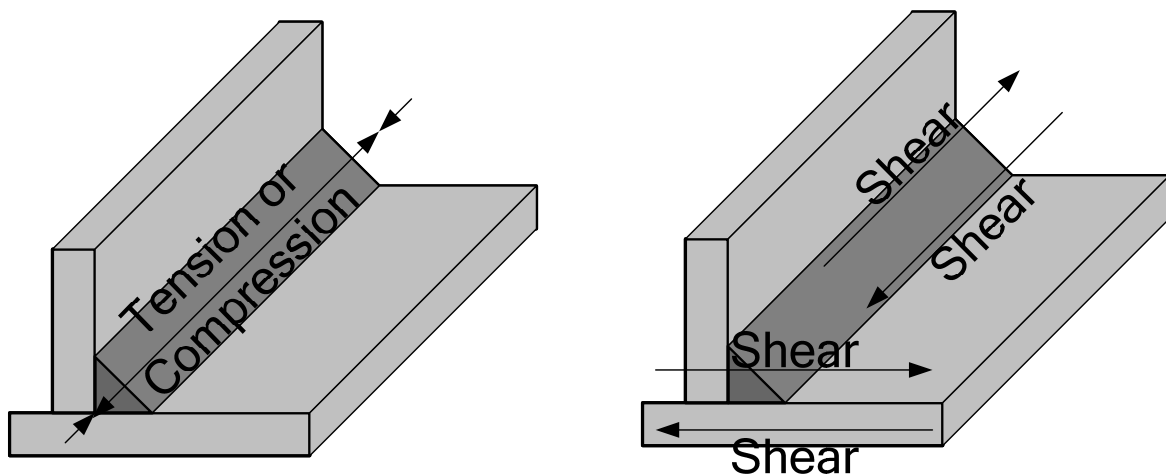
Figure 2.126 Fillet Weld Factored Resistance

Recall as discussed earlier that for fillet welds subject to a net applied tensile stress as defined in *AASHTO LRFD* Article 6.6.1.2.1 and with the welds normal or parallel

to the direction of applied stress, the range of shear stress on the weld throat due to the factored fatigue load is to be checked as a fatigue Category E detail to prevent fatigue cracking initiating in the weld metal at the weld root (*AASHTO LRFD* Table 6.6.1.2.3-1 -- refer also to the previous sections of this chapter on Fatigue Limit State Verifications - although consideration is being given to reinstating the previous Category F for this check or perhaps eliminating this check altogether). Note, however, that for the case of welds oriented normal to the direction of applied stress, the fatigue check for the base metal at the weld toe (a Category C or less detail) will typically control unless the weld is required to carry a relatively large shear through the throat. The check for shear on the weld throat may be significant in the design of fillet-welded gusset-plate connections for heavily loaded cross-frame or lateral bracing members, particularly when checked as a Category E detail.

EXAMPLE

Design the bearing stiffener-to-web fillet welds for the bearing stiffeners that were designed in a previous example (refer to Section 2.2.6.2 of this chapter). The maximum end reaction due to the factored loads R_u at the strength limit state is 388 kips. The girder web at the abutment is ½" x 69". The bearing stiffeners are 5/8" thick. The girder flanges and web and the stiffeners are ASTM A 709 Grade 50W steel with a specified minimum tensile strength F_u = 70 ksi (*AASHTO LRFD* Table 6.4.1-1). Assume E70 electrodes (i.e. matching weld metal) with a classification strength F_{exx} equal to 70 ksi.

According to *AASHTO LRFD* Table 6.13.3.4-1 (Table 2.21), the minimum size fillet weld is ¼ in. when the base metal thickness T of the thicker part joined is less than or equal to ¾ in. Therefore, try the minimum size fillet weld equal to ¼ in. The effective throat of a ¼ in. equal-leg fillet weld is equal to:

$$t_e = 0.707(0.25) = 0.177 \text{ in.}$$

According to *AASHTO LRFD* Article 6.13.3.2.4b, the factored resistance R_r of fillet-welded connections at the strength limit state subject to shear on the effective area is to be taken as:

$$R_r = 0.6\phi_{e2}F_{exx}$$

AASHTO LRFD Equation 6.13.3.2.4b-1

where ϕ_{e2} is equal to the resistance factor for shear on the throat of the weld metal in fillet welds specified in *AASHTO LRFD* Article 6.5.4.2 = 0.80. Therefore:

$$R_r = 0.6(0.80)(70) = 33.6 \text{ ksi}$$

The factored resistance of a ¼-in. fillet weld in shear in units of kips/inch at the strength limit state is computed as:

$$V_r = R_r t_e = 33.6(0.177) = 5.95 \text{ kips/in.}$$

Note that the governing factored shear rupture resistance of the base metal adjacent to the weld leg at the strength limit state is computed as:

$$V_r = \phi_u 0.6F_u t = 0.80(0.6)(70)(0.5) = 16.8 \text{ kips/in.}$$

and does not control. As mentioned previously, this will be the case in most situations unless overmatching weld metal is used, or where the weld throat has excessive convexity such that the resistance is controlled by the weld leg instead of the effective throat.

The total length of a single bearing stiffener-to-web weld, allowing 2.5 inches for clips at the top and bottom of the stiffeners to clear the flange-to-web welds, is:

$$L_w = 69.0 - 2(2.5) = 64.0 \text{ in.}$$

The total factored resistance of the four ¼-in. fillet welds connecting the stiffeners to the web (in kips) is therefore:

$$4(5.95)(64.0) = 1523 \text{ kips} > R_u = 388 \text{ kips} \quad \text{ok}$$

Since the stiffeners are located at an abutment, fatigue of the base metal adjacent to these welds and of the weld throat need not be checked. From *AASHTO LRFD* Table 6.6.1.2.3-1, the nominal fatigue resistance for base metal at the toe of stiffener-to-web welds is based on fatigue detail Category C′. Thus, when these welds are subject to a net applied tensile stress (as defined in *AASHTO LRFD* Article 6.6.1.2.1), the longitudinal stress range due to the factored fatigue load plus impact at the toe of the welds should be checked against the nominal fatigue resistance based on fatigue detail Category C′ (see the previous sections of this chapter on Fatigue Limit State Verifications for similar example calculations). Also, as discussed above, the range of shear stress on the weld throat due to the factored fatigue load is to be checked, but is not likely to control in this case regardless of the fatigue category that is specified for this check.

EXAMPLE

Design the flange-to-web fillet welds for the composite girder cross-section shown in Figure 2.3, which is in a region of positive flexure. The elastic section properties for this section are given in Section 2.2.1.4.1.2 of this chapter. The steel for the flanges and web is ASTM A 709 Grade 50W steel with a specified minimum tensile strength F_u = 70 ksi (*AASHTO LRFD* Table 6.4.1-1). Assume E70 electrodes (i.e. matching weld metal) with a classification strength F_{exx} equal to 70 ksi.

Flange-to-web welds are designed for the horizontal shear flow (i.e. *s = VQ/I*). The maximum unfactored vertical design shears acting on this section are as follows:

$$V_{DC1} = 87 \text{ kips}$$
$$V_{DC2} = 13 \text{ kips}$$

V_{DW} = 13 kips
V_{LL+IM} = 139 kips

For the steel section only:

$$I = 62,658 \text{ in.}^4$$

Top flange: $Q = 1(16)(39.13) = 626 \text{ in.}^3$
Bot. flange: $Q = 1.375(18)(31.06) = 769 \text{ in.}^3$

For the composite section ($n = 8$):

$$I = 161,518 \text{ in.}^4$$

Top flange: $Q = 1(16)(11.20)$ = 179 in.^3
Conc. deck: $Q = 9(100/8)(18.70)$ = $\underline{2,104 \text{ in.}^3}$
    $2,283 \text{ in.}^3$
Bot. flange: $Q = 1.375(18)(58.99) =$ $1,460 \text{ in.}^3$

Calculate the total shear flow at the top and bottom welds due to the factored loads at the strength limit state.

At the top welds:

$$s_u = \left[\frac{1.25(87)(626)}{62,658} + \frac{1.25(13)(2,283)}{161,518} + \frac{1.5(13)(2,283)}{161,518} + \frac{1.75(139)(2,283)}{161,518}\right] = 5.03 \text{ kips / in.}$$

At the bottom welds:

$$s_u = \left[\frac{1.25(87)(769)}{62,658} + \frac{1.25(13)(1,460)}{161,518} + \frac{1.5(13)(1,460)}{161,518} + \frac{1.75(139)(1,460)}{161,518}\right] = 3.86 \text{ kips / in.}$$

The shear flow at the top welds governs. For two welds, the shear flow at each weld is 5.03/2 = 2.52 kips/in.

According to *AASHTO LRFD* Article 6.13.3.2.4b, the factored resistance R_r of fillet-welded connections at the strength limit state subject to shear on the effective area is to be taken as:

$$R_r = 0.6\phi_{e2}F_{exx}$$

AASHTO LRFD Equation 6.13.3.2.4b-1

where ϕ_{e2} is equal to the resistance factor for shear on the throat of the weld metal in fillet welds specified in *AASHTO LRFD* Article 6.5.4.2 = 0.80. Therefore:

$$R_r = 0.6(0.80)(70) = 33.6 \text{ ksi}$$

Equating the factored resistance of a fillet weld in shear in units of kips/inch at the strength limit state to the shear flow due to the factored loads gives:

$$V_r = R_r t_e = 33.6(0.707a) = 2.52 \text{ kips/in.}$$

where t_e is the thickness of the effective throat and a is the leg size of the weld. Therefore:

$$a = 0.11 \text{ in.}$$

However, according to *AASHTO LRFD* Table 6.13.3.4-1 (Table 2.21), the minimum size fillet weld is 5/16 in. (0.3125 in.) when the base metal thickness *T* of the thicker part joined is greater than ¾ in. The top flange is 1" thick and the bottom flange is 1-3/8" thick (the web is ½" thick). Therefore, use the minimum size fillet weld equal to 5/16 in. for both the top and bottom flange welds. The minimum size weld will often control the size of flange-to-web welds.

As discussed above, for fillet welds subject to a net applied tensile stress as defined in *AASHTO LRFD* Article 6.6.1.2.1 and with the welds normal or parallel to the direction of applied stress, the range of shear stress on the throat of the weld due to the factored fatigue load is to be checked [currently checked as a fatigue Category E detail as of this writing (2006)]. Assume that the bottom-flange welds are subject to a net applied tensile stress according to the criterion given in *AASHTO LRFD* Article 6.6.1.2.1 (see the previous section of this chapter on Fatigue Limit State Verifications). The unfactored vertical shears due to the fatigue load specified in *AASHTO LRFD* Article 3.6.1.4 (i.e. a 72-kip HS20 truck with a constant rear-axle spacing of 30 ft) placed in a single lane, including the 15 percent dynamic load allowance, are as follows:

$+V_{LL+IM}$ = +51 kips
$-V_{LL+IM}$ = -6 kips

The range of horizontal shear flow at the bottom-flange welds caused by the factored fatigue load (i.e. factored by the 0.75 load factor specified for the Fatigue load combination) is:

$$s = \frac{0.75(51 + |-6|)(1,460)}{161,518} = 0.39 \text{ kips/in.}$$

The shear range at each weld is 0.39/2 = 0.20 kips/in. The shear stress range on the effective weld throat is computed as:

$$f_{vr} = \frac{0.20}{0.707(0.3125)} = 0.91 \text{ ksi}$$

It is assumed that the *(ADTT)*$_{SL}$ is such that the nominal fatigue resistance is governed by the constant-amplitude fatigue threshold. Therefore, $(\Delta F)_n = ½(\Delta F)_{TH}$ (see the previous sections of this chapter on Fatigue Limit State Verifications). For

Category E, the constant-amplitude fatigue threshold $(\Delta F)_{TH}$ = 4.5 ksi (*AASHTO LRFD* Table 6.6.1.2.5-3).   Thus, $(\Delta F)_n$ = ½(4.5) = 2.25 ksi > 0.91 ksi (ok).   This criterion is unlikely to control for typical flange-to-web welds regardless of the fatigue category that is specified for this check.

From *AASHTO LRFD* Table 6.6.1.2.3-1, the nominal fatigue resistance for base metal connected by continuous fillet-welded connections parallel to the direction of applied stress is based on fatigue detail Category B. Although not illustrated here, for flange-to-web welds subject to a net applied tensile stress, the longitudinal stress range due to the factored fatigue load plus impact should be checked against the nominal fatigue resistance based on fatigue detail Category B (see the previous sections of this chapter on Fatigue Limit State Verifications for similar example calculations).

2.3.3.8.3.1 Balanced Connections

In lap joints connecting members subject to in-plane axial stress, eccentricities usually result in the fillet-welded connections. Designing these welded connections to eliminate eccentric shear effects in the plane of the connection is referred to as balancing the welds. This is accomplished by specifying weld lengths such that the shear force resisted in the welds transfers the load between the members without creating an eccentric moment. *AASHTO LRFD* Article 6.13.1 recommends avoiding such eccentric connections. The Commentary to the AISC *LRFD Specification* (*26*) states the following: "…the fatigue life of eccentrically loaded welded angles has been shown to be very short (*149a*). Notches at the roots of fillet welds are harmful when alternating tensile stresses are normal to the axis of the weld, as could occur due to bending when axial cyclic loading is applied to angles with end welds not balanced about the neutral axis. Accordingly, balanced welds are required when such members are subjected to cyclic loading." This situation occurs most commonly in steel bridges when bracing or other members are welded to gusset plates. Referring to Section A-A in Figure 2.127 given below, eccentricities occur with respect to the axis perpendicular to the gusset (x-x axis), and with respect to the axis parallel to the gusset and perpendicular to the outstanding element of the bracing member (y-y axis). As a result of the latter eccentricity (i.e. with respect to the y-y axis), the connection should be checked for combined shear and tension due to bending, as discussed in the next section of this chapter (Section 2.3.3.8.3.2).

When the welds are not balanced, the effect of the eccentric shear effects in the plane of the connection, caused by the eccentricity with respect to the x-x axis, should also be considered in the design of the welded connection; i.e. the connection should be designed for combined shear and torsion, as discussed in the following section of this chapter. To balance the welds, consider a single-angle tension member fillet welded to a gusset plate, as shown in Figure 2.127. The tensile force T_u acts along the centroid of the member and is resisted by the forces F_1, F_2 and F_3 developed by the fillet welds. Note that a full-length end-weld is assumed. The force F_2 acts at the centroid of the transverse weld length, which is located at d/2 where d is the width of the connected angle leg. For simplicity, F_1 and F_3 are assumed to act at the edges of the angle rather than at the center of the effective weld throat.

SECTION A-A
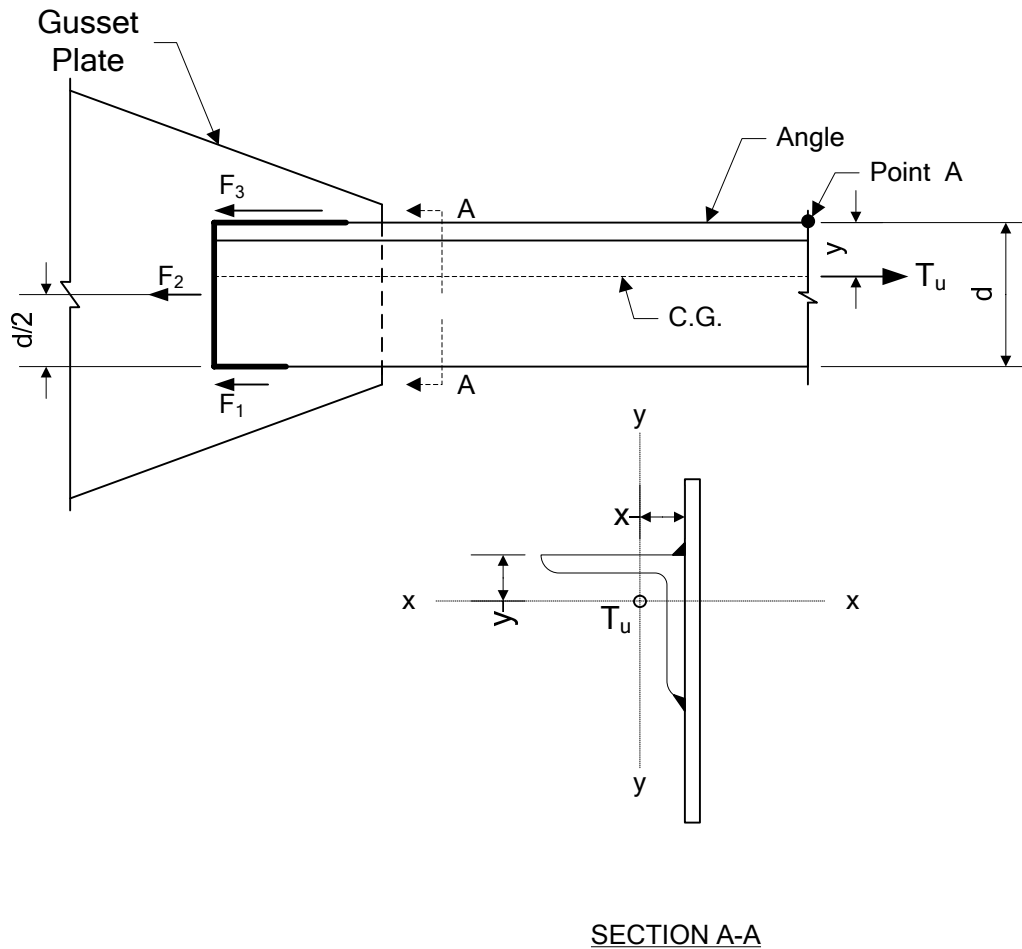
Figure 2.127 Balancing Welds on a Fillet Welded Connection

To eliminate the eccentric moment about the axis perpendicular to the gusset (x-x axis), the forces in the weld group must act along the axis of the angle. Taking moments about Point A (see Figure 2.127) gives:

$$\Sigma M_A = -F_1 d - F_2 (d/2) + T_u y = 0 \qquad \text{Equation 2.279}$$

Therefore:

$$F_1 = \frac{T_u y}{d} - \frac{F_2}{2} \qquad \text{Equation 2.280}$$

The force F_2 is equal to the factored resistance of the weld R_r from Equation 2.278 times the effective throat dimension t_e times the length of the end weld L_{w2}, or:

$$F_2 = R_r t_e L_{w2} \qquad \text{Equation 2.281}$$

Summing the forces in the horizontal direction gives:

$$\Sigma F_H = T_u - F_1 - F_2 - F_3 = 0 \qquad \text{Equation 2.282}$$

Substituting F_1 from Equation 2.280 into Equation 2.282 and solving for F_3 gives:

$$F_3 = T_u\left(1 - \frac{y}{d}\right) - \frac{F_2}{2} \qquad \text{Equation 2.283}$$

Therefore, the length of the welds can be determined such that they will balance the eccentricity of the load in the member as follows: 1) compute the force F_2 resisted by the end weld (if any) from Equation 2.281, 2) compute the force F_1 from Equation 2.280, 3) compute the force F_3 from horizontal equilibrium or using Equation 2.283, 4) compute the required lengths of weld lines 1 and 3 as $L_{w1} = F_1/R_r t_e$ and $L_{w3} = F_3/R_r t_e$, respectively. When there is no end weld, set F_2 equal to zero in the above equations. Should the end weld not be full-length, a different set of equations would need to developed.

A simpler alternative approach for balancing the welds *when there is no end weld* is to calculate the total length of weld L_w required to carry the load (i.e. $L_w = T_u/R_r t_e$), and then allocate that length to F_1 and F_3 in inverse proportion to the distance of each weld from the centroid of the member. This option leads to longer weld lines and perhaps a larger gusset plate.

Refer to the last example at the end of the next section of this chapter (Section 2.3.3.8.3.2), which illustrates the balancing of the welds on a fillet-welded cross-frame gusset plate connection for the in-plane eccentric shear effects. The example also considers the effects of the out-of-plane eccentric shear effects on the connection in the balancing of the welds.

2.3.3.8.3.2 Eccentric Shear

As indicated in *AASHTO LRFD* Article 6.13.1, eccentric connections should be avoided, but where they cannot be avoided, members and connections are to be designed for the combined effects of shear and moment due to the eccentricity. *AASHTO LRFD* Article C6.13.3.2.4b indicates that if fillet welds are subject to eccentric loads that produce a combination of shear and bending stresses, they are to be proportioned based on a direct vector addition of the shear forces on the weld. Eccentric shear can result, for example, when the loading of fillet welds is neither parallel to nor transverse to the axis of the welds. Basically, eccentric shear conditions occur when the welds are subject to pure torsion, a combination of shear and torsion or a combination of shear and bending.

As discussed previously for eccentric shear on bolted connections, the resistance of an eccentrically loaded fillet weld connection subject to a combination of shear and torsion can be conservatively determined using a traditional elastic vector analysis approach. The following assumptions are made in this approach: 1) assuming each segment of weld is of the same size, it is assumed that concentrically applied load (i.e. direct shear) is resisted equally by each weld segment, 2) any rotation caused by a torsional moment is assumed to occur about the centroid of the weld

configuration, 3) load on a weld segment caused by a torsional moment is assumed proportional to the distance of that segment from the centroid of the weld configuration, 4) the direction of the force on a weld segment caused by a torsional moment is assumed perpendicular to the radial distance of the segment from the centroid of the weld configuration, and 5) the resultant force is obtained by combining vectorially the components of the forces caused by direct shear and torsion. Also, for computing forces or stresses on the weld segments, the segment lines are assumed defined by the edges along which the fillets are placed, rather than to the center of the effective throats.

Consider the general case of an eccentrically loaded welded connection subject to combined shear and torsion shown in Figure 2.128.
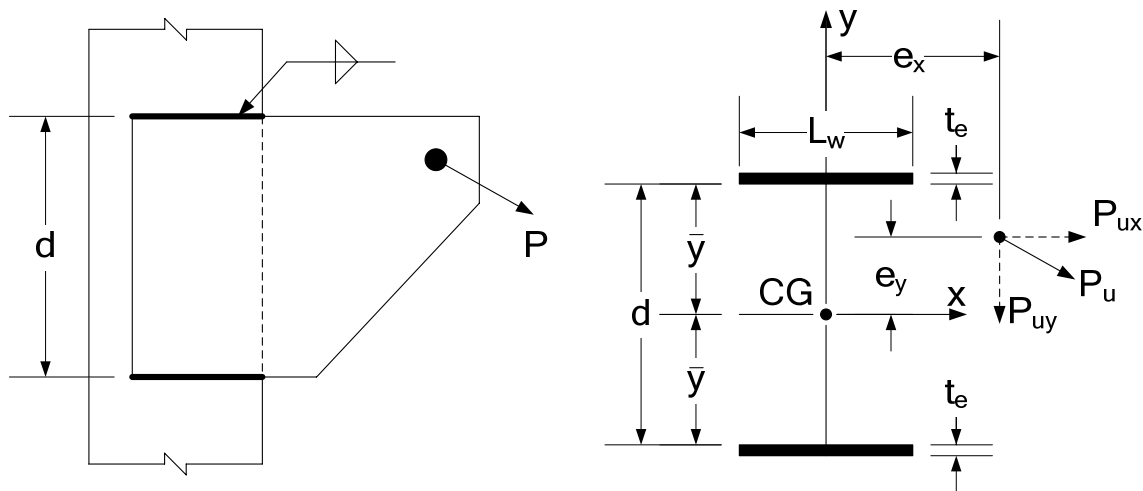
Figure 2.128 Eccentrically Loaded Fillet Welded Connection Subject to Combined Shear & Torsion

For this case, the components of stress in the weld segments caused by direct shear are determined as:

$$f_{vx} = \frac{P_{ux}}{A}$$
<div align="right">Equation 2.284</div>

$$f_{vy} = \frac{P_{uy}}{A}$$
<div align="right">Equation 2.285</div>

where A is the effective weld area taken as the thickness of the effective throat t_e times the total length L_w of the weld configuration.

The x- and y-components of stress due to the torsional moment can be computed as follows:

$$f_{Tx} = \frac{Ty}{I_p} = \frac{\left(P_{ux}e_y + P_{uy}e_x\right)y}{I_p}$$

Equation 2.286

$$f_{Ty} = \frac{Tx}{I_p} = \frac{\left(P_{ux}e_y + P_{uy}e_x\right)x}{I_p}$$

Equation 2.287

where I_p is the polar moment of inertia of the weld configuration about the centroid of the weld configuration calculated as follows:

$$I_p = \sum(I_x + I_y) + \sum A\left(\bar{x}^2 + \bar{y}^2\right)$$

Equation 2.288

where I_x and I_y are the moments of inertia of each weld segment about their own centroidal axes, A is the area of each weld segment and $\bar{x}$ and $\bar{y}$ are the distances from the centroid of the weld configuration to each individual weld segment. For the case shown in Figure 2.128:

$$I_p \cong \frac{t_e}{6}\left[12L_w\bar{y}^2 + L_w^3\right]$$

Equation 2.289

When the above stresses are multiplied by effective throat thickness t_e, the result is a component of force R in units of kips/inch.

It becomes convenient in these calculations to treat the welds as lines having length, but with an effective throat thickness (width) t_e equal to unity (Figure 2.129).
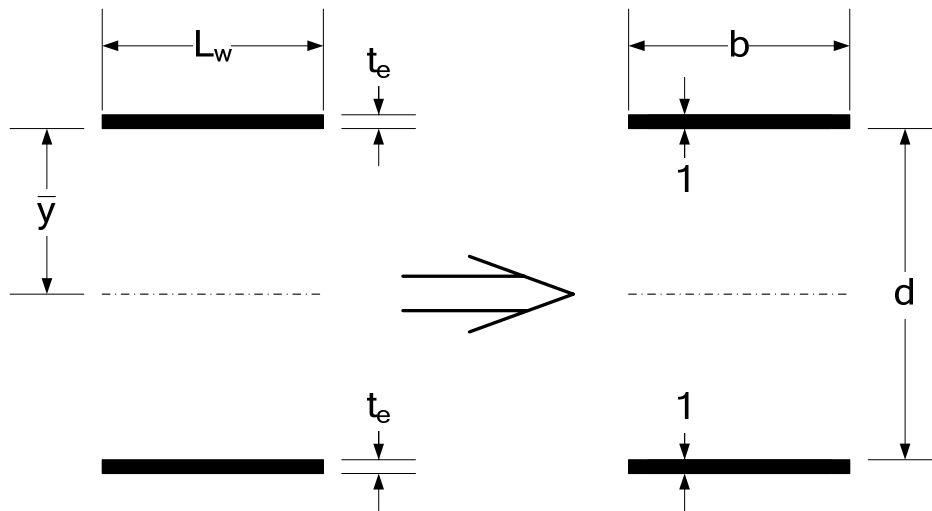
Figure 2.129 Weld Configuration Considered as Lines of Unit Thickness

For the above case, setting t_e equal to 1.0 and using the more general terms b and d as shown in Figure 2.129, Equation 2.289 can be written as follows:

$$I_p \cong \frac{1}{6}\left[12b\left(\frac{d}{2}\right)^2 + b^3\right] = \frac{b}{6}\left[3d^2 + b^2\right] \qquad \text{Equation 2.290}$$

Properties for other common weld line configurations are tabulated in Reference 28, or can be derived in a similar fashion by the Engineer.

A less conservative alternative approach to determine the resistance of a weld configuration subject to eccentric shear, in which an instantaneous center of rotation is located and the load-deformation relationship of a fillet weld is used, is provided in Reference 26.

The traditional elastic vector analysis method can also be used for the case where the applied load is eccentric to the plane of the weld configuration subjecting the configuration to combined shear and bending moment (Figure 2.130).
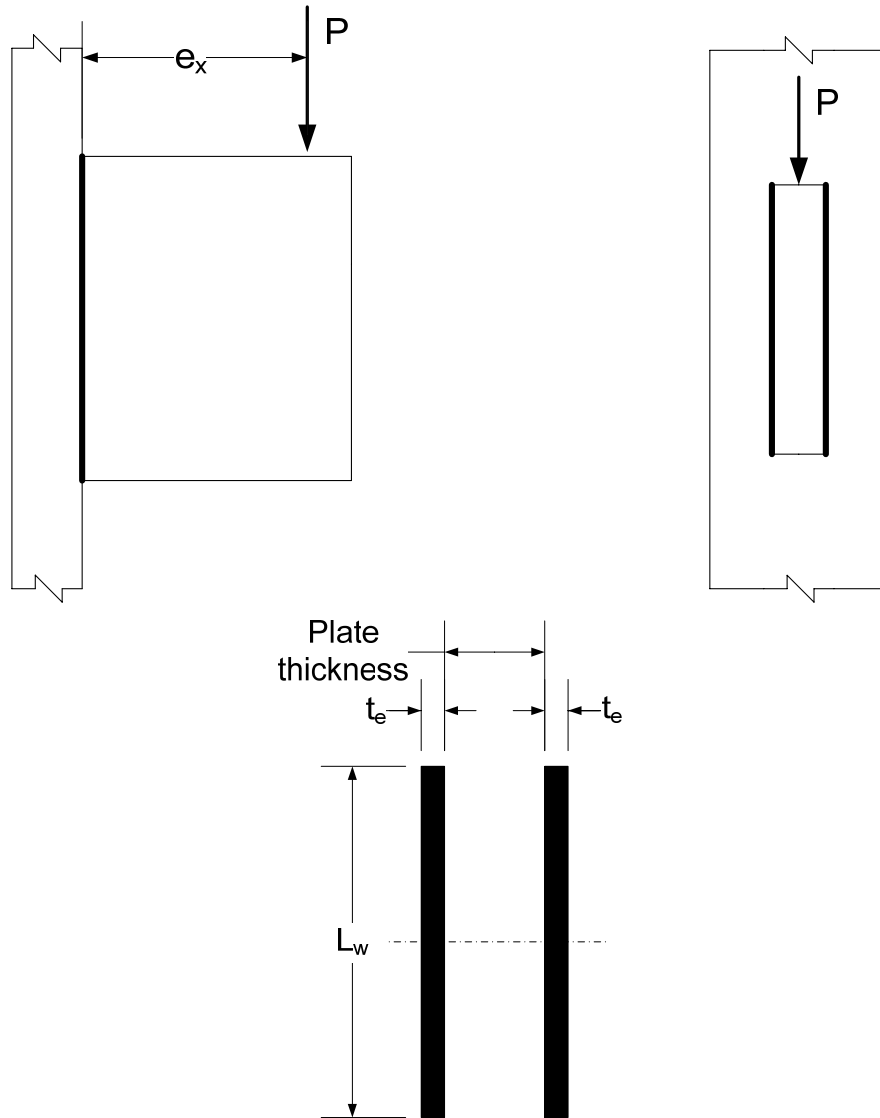
Figure 2.130 Eccentrically Loaded Fillet Welded Connection Subject to Combined Shear & Bending

In essence, the weld configuration is loaded in shear and tension. The compression force from the bending is typically assumed carried by direct compression of the pieces being welded rather than through the welds. The weld segments are again treated as lines with a thickness of unity. The procedure is conservative and relatively easy to apply as demonstrated in the second example to follow.

EXAMPLE

Using the elastic vector analysis method, design the fillet welds for the eccentrically loaded bracket shown in the figure below, which is subject to combined shear and torsion, for the strength limit state. The fatigue limit state is not checked in this example. Assume E70 electrodes.
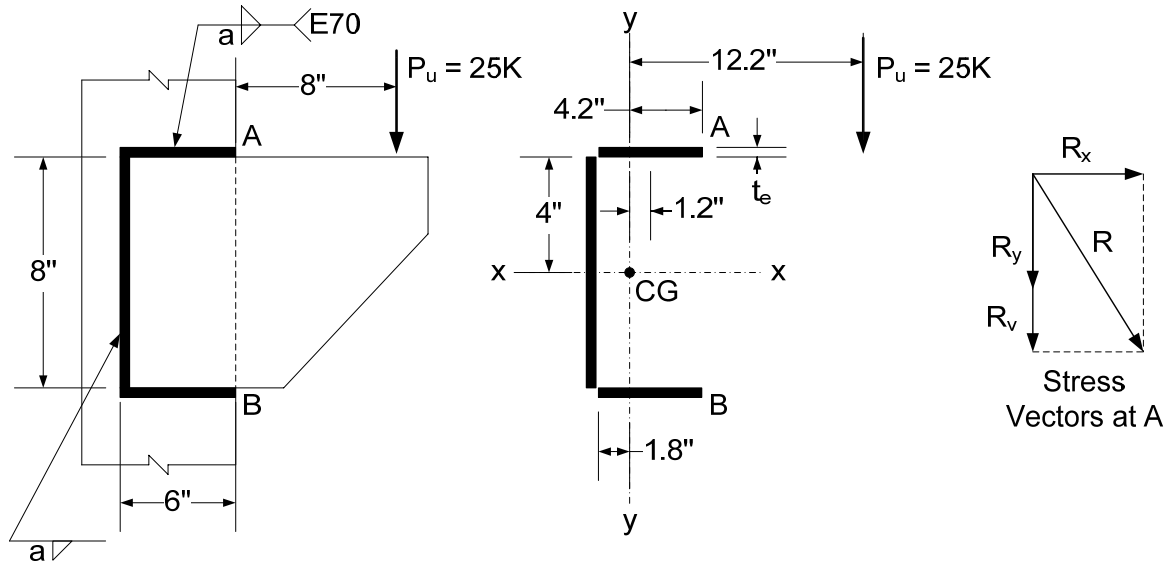
Reference 28 provides the following formulas for computing the location of the centroid (from the vertical weld) and polar moment of inertia of the above weld configuration treating the welds as lines:

$$\overline{x} = \frac{b^2}{2b + d}$$

Therefore:

$$\overline{x} = \frac{6^2}{2(6) + 8} = 1.8 \text{ in.}$$

$$I_p = \frac{8b^3 + 6bd^2 + d^3}{12} - \frac{b^4}{2b + d}$$

Therefore:

$$I_p = \frac{8(6)^3 + 6(6)(8)^2 + 8^3}{12} - \frac{6^4}{2(6) + 8} = 314 \text{ in}^3$$

The maximum resultant force R on the weld configuration is at Points A and B. Compute the vertical force on the weld line configuration R_v due to the direct shear:

$$R_v = \frac{P_u}{L_w} = \frac{25}{2(6) + 8} = 1.25 \text{ kips / in.}$$

Referring to the above figure, compute the x- and y-components of force R_{Tx} and R_{Ty} due to the torsion acting on the weld line configuration:

2.576

$$R_{Tx} = \frac{Ty}{I_p} = \frac{25(12.2)4}{314} = 3.89 \text{ kips / in.}$$

$$R_{Ty} = \frac{Tx}{I_p} = \frac{25(12.2)4.2}{314} = 4.08 \text{ kips / in.}$$

Compute the resultant force R by taking the vector sum of the horizontal and vertical components of force:

$$R = \sqrt{(3.89)^2 + (1.25 + 4.08)^2} = 6.60 \text{ kips / in.}$$

According to *AASHTO LRFD* Article 6.13.3.2.4b, the factored resistance R_r of fillet-welded connections at the strength limit state subject to shear on the effective area is to be taken as:

$$R_r = 0.6\phi_{e2}F_{exx}$$

AASHTO LRFD Equation 6.13.3.2.4b-1

where ϕ_{e2} is equal to the resistance factor for shear on the throat of the weld metal in fillet welds specified in *AASHTO LRFD* Article 6.5.4.2 = 0.80. Therefore:

$$R_r = 0.6(0.80)(70) = 33.6 \text{ ksi}$$

Equating the factored resistance of a fillet weld in shear in units of kips/inch at the strength limit state to the resultant force R on the weld line configuration due to the factored loads gives:

$$V_r = R_r t_e = 33.6(0.707a) = 6.60 \text{ kips / in.}$$

where t_e is the thickness of the effective throat and a is the leg size of the weld. Therefore:

$$a = 0.28 \text{ in.} \quad \text{Use 5/16 in. fillet welds}$$

EXAMPLE

Using the elastic vector analysis method, design the fillet welds for the eccentrically loaded bracket shown in the figure below, which is subject to combined shear and bending (i.e. shear and tension), for the strength limit state. The fatigue limit state is not checked in this example. Assume E70 electrodes.

b) Assumed weld
cross-section

a) Bracket
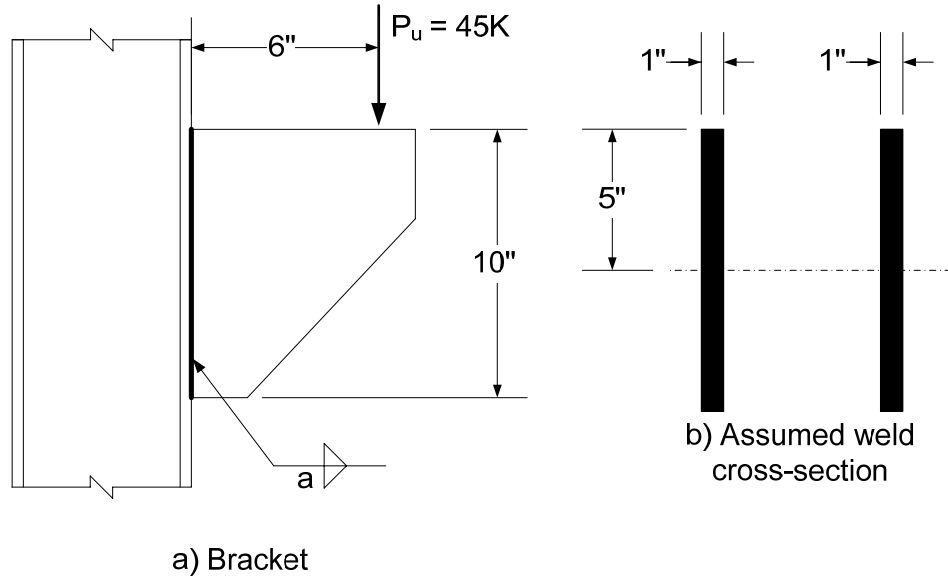
The welds are treated as lines with a thickness of one inch. The direct shear (vertical) component R_v is assumed carried equally by each weld segment. Therefore:

$$R_v = \frac{P_u}{L_w} = \frac{45}{2(10)} = 2.25 \text{ kips / in.}$$

The moment of inertia of the weld line segments is calculated as:

$$I = 2\left[\frac{(10)^3}{12}\right] = 166.7 \text{ in.}^3$$

Therefore, the tension (horizontal) component R_{mt} due to the moment (i.e. out of the paper referring to Figure b) is calculated as:

$$R_{mt} = \frac{45(6)(5)}{166.7} = 8.10 \text{ kips / in.}$$

Compute the resultant force R by taking the vector sum of the horizontal and vertical components of force:

$$R = \sqrt{(8.10)^2 + (2.25)^2} = 8.41 \text{ kips / in.}$$

According to *AASHTO LRFD* Article 6.13.3.2.4b, the factored resistance R_r of fillet-welded connections at the strength limit state subject to shear on the effective area is to be taken as:

$$R_r = 0.6\phi_{e2}F_{exx}$$

AASHTO LRFD Equation 6.13.3.2.4b-1

where ϕ_{e2} is equal to the resistance factor for shear on the throat of the weld metal in fillet welds specified in *AASHTO LRFD* Article 6.5.4.2 = 0.80. Therefore:

$$R_r = 0.6(0.80)(70) = 33.6 \text{ ksi}$$

Equating the factored resistance of a fillet weld in shear in units of kips/inch at the strength limit state to the resultant force *R* on the weld line configuration due to the factored loads gives:

$$V_r = R_r t_e = 33.6(0.707a) = 8.41 \text{ kips / in.}$$

where t_e is the thickness of the effective throat and *a* is the leg size of the weld. Therefore:

$$a = 0.35 \text{ in.} \quad \text{Use 3/8 in. fillet welds}$$

EXAMPLE

Design the fillet-welded gusset-plate connection for the cross-frame member shown in the figure below. This example addresses eccentricities with respect to two axes, as described in the preceding section of this chapter (Section 2.3.3.8.3.1). The potential eccentricity with respect to the axis perpendicular to the gusset (i.e. the x-x axis in Section A-A given below) can be balanced, but the eccentricity with respect to the axis parallel to the gusset (i.e. the y-y axis in Section A-A) cannot. The effect of this latter eccentricity is considered in the design of the welds.

Assume the connection is between the bottom chord of a cross-frame and its gusset. The cross-frame member is a single 6 x 6 x 3/4 angle (Area = 8.44 in^2). The steel is ASTM A 709 Grade 50 steel (from AASHTO LRFD Table 6.4.1-1, F_u = 65 ksi). The gusset is a 5/8-in.-thick plate.

L6x6x¾ (F_y = 50ksi)
A = 8.44 in.^{2}
$I_x = I_y$ = 28.2 in.^{4}
x = y = 1.78 in.

SECTION A-A
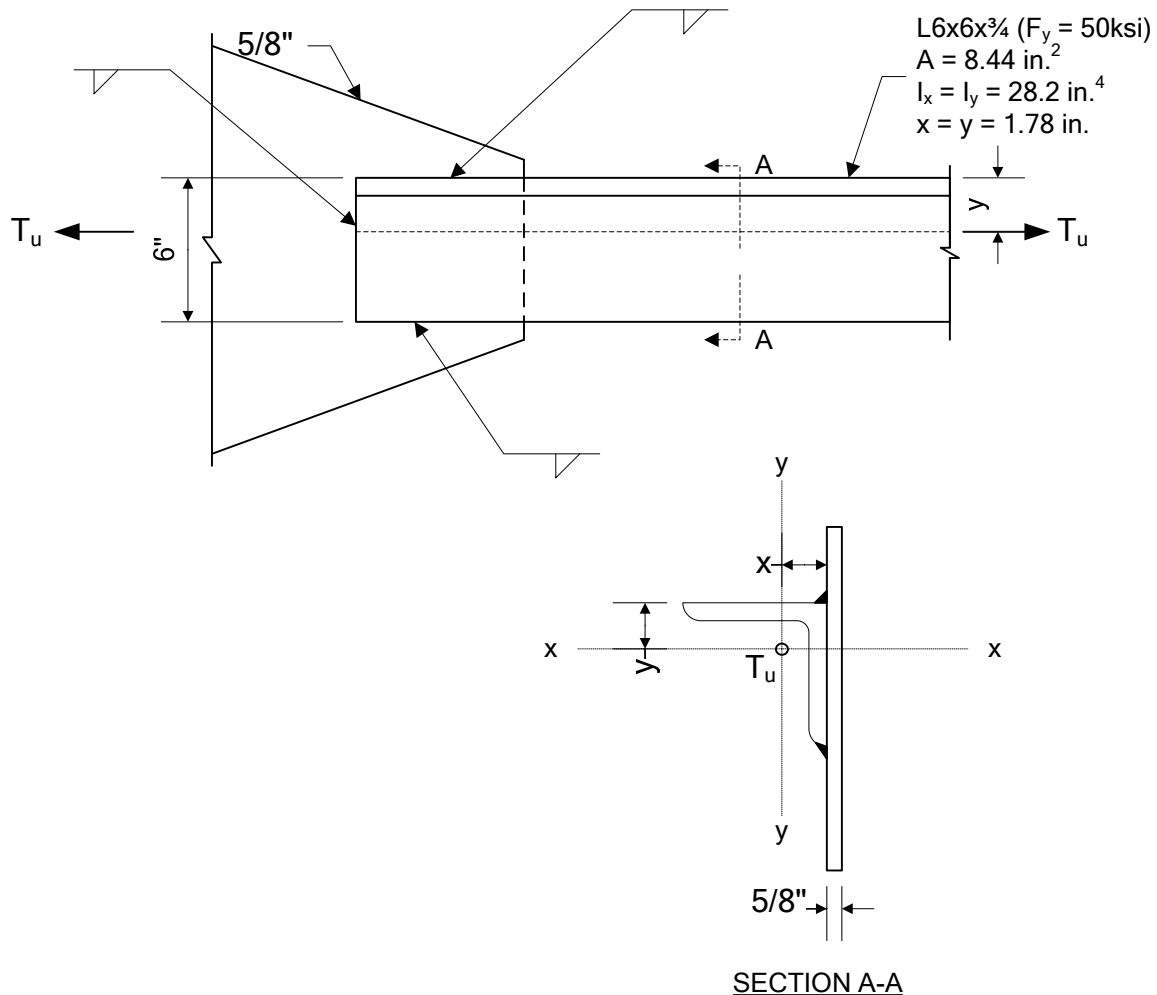
The cross-frame member is subject to a resultant tensile force due to the factored loads T_u at the strength limit state equal to 115.0 kips. At the fatigue limit state, the cross-frame member is subject to a net applied tensile stress according to the criteria specified in *AASHTO LRFD* Article 6.6.1.2.1 (see the previous section of this chapter on Fatigue Limit State Verifications), and the maximum resultant range of force due to the factored fatigue load plus impact is 13.0 kips. Since these forces were determined from a refined analysis in which the cross-frame members were included in the structural model, the end connections for the bracing member at the strength limit state are to be designed for the calculated force effects (refer to *AASHTO LRFD* Article 6.13.1). Otherwise, *AASHTO LRFD* Article 6.13.1 requires that the end connections be designed for 75 percent of the factored axial resistance of the member. No provision is made for consideration of fatigue in cases where cross-frame members have not been analyzed.

In addition to designing the welds, the fatigue of the base metal in the cross-frame member at the end of the longitudinal welds is checked in this example. From the analysis, it was found that the cross-frame member undergoes both tensile and compressive axial forces due to the design fatigue vehicle. The tensile and compression cases were caused by the fatigue vehicle traversing the bridge in

different transverse positions. In order to obtain one cycle of fatigue load (i.e. 13.0 kips), two vehicles -- one leading the other -- must traverse the bridge in different but critical transverse positions. To account in an approximate fashion for the probability of two vehicles being located in the critical relative position to cause the maximum range of force in the cross-frame member, *AASHTO LRFD* Article C6.6.1.2.1 recommends that one cycle of force be taken as 75 percent of the range of force in the member determined by the passage of the factored fatigue load in two different transverse positions, but not less than the range of force due to a single passage of the fatigue vehicle. Therefore, the maximum range of force in the cross-frame member for design will be taken as:

$$13.0 \times 0.75 = 9.75 \text{ kips}$$

The maximum range of axial stress in the cross-frame member is equal to 9.75 k/8.44 in^2= 1.16 ksi. Referring to Section A-A in the preceding figure, it can be seen that the force is applied eccentrically to the welds resulting in an additional stress range in the member at the weld terminations due to the range of moment about the vertical axis resulting from this eccentricity. The section modulus to the welds is equal to I_y/x = (28.2/1.78) = 15.84 in.^{3}. Therefore, the stress range in the base metal of the member at the weld terminations due to the eccentricity is 9.75(1.78)/15.84 = 1.09 ksi. The total stress in the base metal at the termination of the welds is therefore equal to 1.16 + 1.09 = 2.25 ksi. It is assumed that the $(ADTT)_{SL}$ is such that the nominal fatigue resistance is governed by the constant-amplitude fatigue threshold. Therefore, $(\Delta F)_n = \frac{1}{2}(\Delta F)_{TH}$ (see the previous section of this chapter on Fatigue Limit State Verifications). From *AASHTO LRFD* Table 6.6.1.2.3-1, the nominal fatigue resistance for base metal at the end of fillet-welded connections parallel to the direction of stress is based on fatigue detail Category E. For Category E, the constant-amplitude fatigue threshold $(\Delta F)_{TH}$ = 4.5 ksi (*AASHTO LRFD* Table 6.6.1.2.5-3). Thus, $(\Delta F)_n = \frac{1}{2}(4.5)$ = 2.25 ksi = 2.25 ksi (ok). Ratio = 1.00.

Assume E70 electrodes with a classification strength F_{exx} = 70 ksi. As discussed previously, this material provides a matching filler/base metal combination for Grade 50 steel. According to *AASHTO LRFD* Table 6.13.3.4-1 (Table 2.21), the minimum size fillet weld is ¼ in. when the base metal thickness T of the thicker part joined is less than or equal to ¾ in. Try a 5/16 in. fillet weld. The effective throat of a 5/16 in. equal-leg fillet weld is equal to:

$$t_e = 0.707(0.3125) = 0.221 \text{ in.}$$

According to *AASHTO LRFD* Article 6.13.3.2.4b, the factored resistance R_r of fillet-welded connections at the strength limit state subject to shear on the effective area is to be taken as:

$$R_r = 0.6\phi_{e2}F_{exx}$$

AASHTO LRFD Equation 6.13.3.2.4b-1

where ϕ_{e2} is equal to the resistance factor for shear on the throat of the weld metal in fillet welds specified in *AASHTO LRFD* Article 6.5.4.2 = 0.80. Therefore:

$$R_r = 0.6(0.80)(70) = 33.6 \text{ ksi}$$

The factored resistance of a 5/16-in. fillet weld in shear in units of kips/inch at the strength limit state is computed as:

$$V_r = R_r t_e = 33.6(0.221) = 7.42 \text{ kips / in.}$$

The required total length of weld L_w to satisfy the strength limit is therefore:

$$L_w = \frac{115.0}{7.42} = 15.50 \text{ in.}$$

Based on the current (2006) categorization of Category E for shear on the throat of a fillet weld and the total length of weld required for the strength limit state, the shear stress on the weld throat is checked as follows:

$$\frac{9.75}{15.50(0.221)} = 2.94 \text{ ksi} > (\Delta F)_n = 2.25 \text{ ksi}$$

<div align="right">NG</div>

As discussed in the previous section of this chapter on Fatigue Limit State Verifications, the fatigue category for shear on the throat of a fillet weld was Category F in previous AASHTO Specifications. Category F had a constant amplitude fatigue threshold of $(\Delta F)_{TH}$ of 8.0 ksi. Since the nominal fatigue resistance is assumed governed by the constant-amplitude fatigue threshold, $(\Delta F)_n = \frac{1}{2}(\Delta F)_{TH}$. Thus, assuming Category F, $(\Delta F)_n = \frac{1}{2}(8.0) = 4.0 \text{ ksi} > 2.94 \text{ ksi}$ ok. Consideration is currently being given to reinstating Fatigue Category F for shear on the throat of a fillet weld in the *AASHTO LRFD* Specifications (or perhaps eliminating this check altogether). Therefore, Category F will be assumed to apply in this example. As a result, the strength limit state controls the required length of the weld and the required total length of a 5/16-inch fillet weld is 15.50 in.

To balance the in-plane eccentric load, the length of the welds will be determined as described in the previous section of this chapter (Section 2.3.3.8.3.1). Both the strength and fatigue load effects will be balanced resulting in a weld configuration similar to that shown (in general) in the figure below:
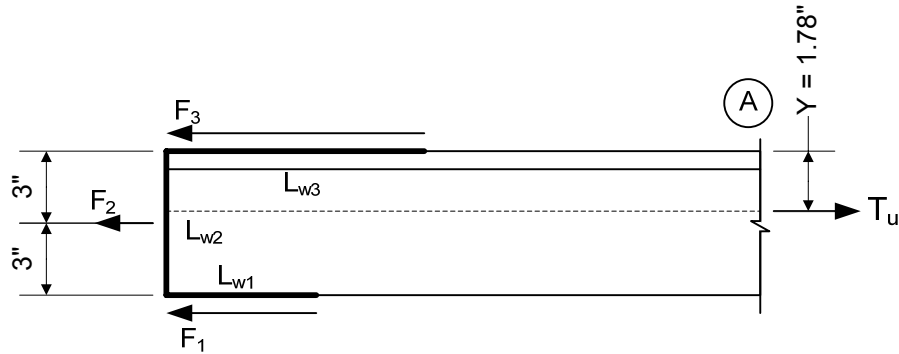
The force, F_2, in the end weld is computed from Equation 2.281:

$$F_2 = R_r t_e L_{w2}$$

As determined above, the strength limit state controls the required length of weld. At the strength limit state, R_r for each weld was computed previously to be 33.6 ksi.

$$F_2 = 33.6(0.221)(6) = 44.6 \text{ kips}$$

Calculate the force F_1 from Equation 2.280 as follows:

$$F_1 = \frac{T_u y}{d} - \frac{F_2}{2}$$

$$F_1 = \frac{115.0(1.78)}{6} - \frac{44.6}{2} = 11.8 \text{ kips}$$

$$L_{w1} = \frac{F_1}{R_r t_e} = \frac{11.8}{33.6(0.221)} = 1.59 \text{ in.}$$
(use 1¾")

As specified in AASHTO LRFD Article 6.13.3.5, the minimum effective length of a fillet weld is four times its leg size, but not less than 1.5 inches. In this case, the minimum effective length is taken equal to 4(0.3125) = 1.25 in. < 1.5 in. Therefore, the minimum effective length is 1.5 in. < 1.75 in. ok

Calculate the force F_3 from Equation 2.283 as follows:

$$F_3 = T_u\left(1 - \frac{y}{d}\right) - \frac{F_2}{2}$$

$$F_3 = 115.0(1 - \frac{1.78}{6}) - \frac{44.6}{2} = 58.6 \text{ kips}$$

$$L_{w3} = \frac{F_3}{R_r t_e} = \frac{58.6}{33.6(0.221)} = 7.89 \text{ in.}$$
(use 8")

Check equilibrium (referring to the preceding figure):

$$\Sigma F_H = 115.0 \text{ kips} - 11.8 \text{ kips} - 44.6 \text{ kips} - 58.6 \text{ kips} = 0 \quad \text{ok}$$

$$\Sigma M_A = -11.8(6) - 44.6(6/2) + 115.0(1.78) \cong 0 \quad \text{ok}$$

If there had been no end weld, the total length of weld L_w required to carry the load could simply be allocated to F_1 and F_3 in inverse proportion to the distance of each weld from the centroid of the member as follows:

$$L_{w1} = 15.50\left(\frac{1.78}{6}\right) = 4.60 \text{ in.}$$
(use 4¾")

$$L_{w3} = 15.50\left(\frac{6-1.78}{6}\right) = 10.90 \text{ in.}$$
(use 11")

The welds must also be designed for the moment about the y-y axis; i.e. the welds must be designed for the combined shear due to the horizontal load T_u and tension due to bending resulting from the eccentricity of this load with respect to a vertical axis passing through the centerline of the gusset. As a result, the lengths of the welds along the connected leg will have to be increased, but kept in balance due to the need to balance the eccentricity with respect to the x-x axis.   An iterative procedure is used to determine the proper lengths of the welds. The length of the end weld L_{w2} is constant (6 in.). The lengths of the welds along the angle are increased proportionally. By iteration (not shown), the following weld configuration was determined: L_{w1} = 3.75 in. and L_{w3} = 13.25 in. The longer weld must be near the heel of the angle (i.e. nearest the centroid of the single-angle):
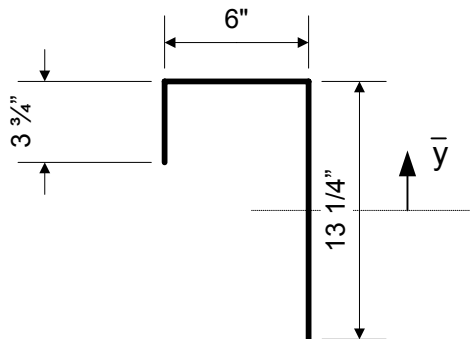
The effect on the weld of the moment about the y-y axis is determined by treating the welded connection as a bending element. The moment of inertia and section modulus of the weld configuration, treating the welds as lines with a thickness of one inch, is computed as follows:.

Weld Line	A	d	Ad	Ad^2	I$_o$	I
L$_{w1}$	3.75	4.75	17.81	84.61	4.39	89.00
L$_{w2}$	6.00	6.63	39.78	263.74		263.74
L$_{w3}$	13.25				193.85	193.85
	23.00		57.59			546.59

$$-2.50(57.59) = \quad -143.98$$

$$\bar{y} = \frac{57.59}{23.00} = 2.50 \text{ in.} \qquad\qquad I_{NA} = \quad 402.61 \quad \text{in.}^3$$

$$y_{TOP} = 6.63 - 2.50 = 4.13 \text{ in.} \qquad y_{BOT} = 6.63 + 2.50 = 9.13 \text{ in.}$$

$$S_{TOP} = \frac{402.61}{4.13} = 97.48 \text{ in.}^2 \qquad S_{BOT} = \frac{402.61}{9.13} = 44.10 \text{ in.}^2$$

At the strength limit state, the direct shear component R_v on the weld configuration is computed as:

$$R_v = \frac{T_u}{L_w} = \frac{115.0}{23.00} = 5.00 \text{ kips / in.}$$

The moment due to the eccentrically caused moment is calculated as:

$$M = 115.0(1.78 + \frac{0.625}{2}) = 240.6 \text{ kip} - \text{in.}$$

The resulting shear at the critical point in the weld pattern R_{Mt} due to the moment (i.e. out of the paper) is calculated as:

$$R_{Mt} = \frac{240.6}{44.10} = 5.46 \text{ kips / in.}$$

Since the two shear components are orthogonal with respect to each other, the resultant shear R is computed by taking their vector sum:

$$R = \sqrt{(5.00)^2 + (5.46)^2} = 7.40 \text{ kips / in.} < R_r = 7.42 \text{ kips / in.} \quad \text{ok}$$

Clearly, a longer weld on the toe side of the angle would reduce the stress in the weld on the heel side. However, If the weld pattern is not in balance with respect to the eccentricity of the applied load about the x-x axis and is not designed to account for the resulting in-plane eccentric shear effects, the welds may be overstressed, which would be particularly deleterious with respect to fatigue. Since consideration of the in-plane eccentric shear effects would require significant additional calculation, increasing the length of the weld on the heel side is not considered a viable avenue to pursue.

Check the balance of the revised weld configuration using the adjusted shear R_v = 5.00 kips/in. Calculate an adjusted R_r for balancing based on R_v as follows:

$$R_v = R_r t_e = R_r(0.221) = 5.00 \text{ kips / in.}$$

$$R_r = 22.62 \text{ ksi}$$

From Equation 2.281:

$$F_2 = R_r t_e L_{w2}$$

$$F_2 = 22.62(0.221)(6) = 30.0 \text{ kips}$$

Calculate the force F_1 from Equation 2.280 as follows:

$$F_1 = \frac{T_u y}{d} - \frac{F_2}{2}$$

$$F_1 = \frac{115.0(1.78)}{6} - \frac{30.0}{2} = 19.1 \text{ kips}$$

$$L_{w1} = \frac{F_1}{R_r t_e} = \frac{19.1}{22.62(0.221)} = 3.82 \text{ in.}$$

$$\cong \quad 3.75 \text{ in. assumed} \quad \text{ok}$$

$$\left(F_1\right)_{act.} = 22.62(0.221)(3.75) = 18.75 \text{ kips}$$

Calculate the force F_3 from Equation 2.283 as follows:

$$F_3 = T_u\left(1 - \frac{y}{d}\right) - \frac{F_2}{2}$$

$$F_3 = 115.0(1 - \frac{1.78}{6}) - \frac{30.0}{2} = 65.9 \text{ kips}$$

$$L_{w3} = \frac{F_3}{R_r t_e} = \frac{65.9}{22.62(0.221)} = 13.2 \text{ in.}$$

$$\cong \quad 13.25 \text{ in. assumed} \quad \text{ok}$$

$$\left(F_3\right)_{act.} = 22.62(0.221)(13.25) = 66.23 \text{ kips}$$

Check equilibrium (referring to the preceding figure):

$$\Sigma F_H = 115.0 \text{ kips} - 18.75 \text{ kips} - 30.0 \text{ kips} - 66.23 \text{ kips} = 0.02 \text{ kips} \cong 0 \quad \text{ok}$$

$$\Sigma M_A = -18.75(6) - 30.0(6/2) + 115.0(1.78) = 2.2 \text{ kip} - \text{in.} \cong 0 \quad \text{ok}$$

Hence, the pattern provides the lowest possible stress range for the length of weld used.

At the fatigue limit state, the direct shear (vertical) component R_v on the weld configuration is computed as:

$$R_v = \frac{9.75}{23.00} = 0.42 \text{ kips / in.}$$

The moment due to the eccentricity with respect to the y-y axis is calculated as:

$$M = 9.75(1.78 + \frac{0.625}{2}) = 20.40 \text{ kip} - \text{in.}$$

The tension (horizontal) component R_{Mt} due to the moment is calculated as:

$$R_{Mt} = \frac{20.40}{44.10} = 0.46 \text{ kips / in.}$$

Compute the resultant force R by taking the vector sum of the horizontal and vertical components of force:

$$R = \sqrt{(0.42)^2 + (0.46)^2} = 0.62 \text{ kips / in.}$$

Based on the current (2006) categorization of Category E for shear on the throat of a fillet weld, the permissible range of shear on the throat of the weld is computed as (assuming again the resistance is governed by the constant-amplitude fatigue threshold):

$$2.25(0.707)(0.3125) = 0.50 \text{ kips/in.} \ < \ R = 0.62 \text{ kips/in.} \quad \text{NG}$$

As discussed previously, since consideration is currently being given to reinstating Fatigue Category F for shear on the throat of a fillet weld in the *AASHTO LRFD* Specifications, the constant amplitude fatigue threshold of $(\Delta F)_{TH}$ of 8.0 ksi for Category F will be used in this check. Again, assuming that the nominal fatigue resistance is governed by the constant-amplitude fatigue threshold, $(\Delta F)_n = \frac{1}{2}(\Delta F)_{TH}$. Thus, $(\Delta F)_n = \frac{1}{2}(8.0) = 4.0$ ksi.

$$4.0(0.707)(0.3125) = 0.88 \text{ kips/in.} \ > \ R = 0.62 \text{ kips/in.} \quad \text{ok}$$

Check the balance of the revised weld configuration for fatigue using the shear $R_v = 0.42$ kips/in. computed above. Calculate R_r as follows:

$$R_v = R_r t_e = R_r (0.221) = 0.42 \text{ kips / in.}$$

$$R_r = 1.900 \text{ ksi}$$

From Equation 2.281:

$$F_2 = R_r t_e L_{w2}$$

$$F_2 = 1.900(0.221)(6) = 2.52 \text{ kips}$$

$$(F_1)_{act.} = 1.900(0.221)(3.75) = 1.57 \text{ kips}$$

$$(F_3)_{act.} = 1.900(0.221)(13.25) = 5.56 \text{ kips}$$

Check equilibrium:

$$\Sigma F_H = 9.75 \text{ kips} - 1.57 - 2.52 \text{ kips} - 5.56 \text{ kips} = 0.1 \text{ kips} \cong 0 \quad \text{ok}$$

$$\Sigma M_A = -1.57(6) - 2.52(6/2) + 9.75(1.78) = 0.38 \text{ kip} - \text{in.} \cong 0 \quad \text{ok}$$

Therefore, use the fillet welds as shown below for this connection:
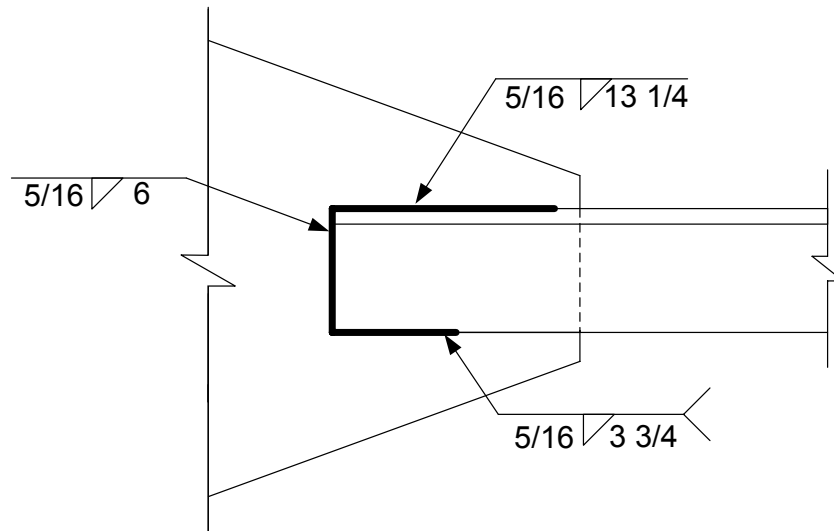
129. "100 Years of Metalworking – Welding, Brazing and Joining." *The Iron Age*, June 1955.
130. Miskoe, W.L. 1986. "The Centenary of Modern Welding, 1885-1985 – A Commemoration." *Welding Journal*, Volume 65, April.
131. AWS. 1987, 1991. *Welding Handbook*, 8th ed., Vol. 1, *Welding Technology*, 1987. Vol. 2, Welding Processes, 1991. American Welding Society, Miami, FL.
132. Blodgett, O.W. "How to Determine the Cost of Welding." *Bulletin G610*, The Lincoln Electric Company, Cleveland, OH (no date).
133. Miller, D.K., and J. Ogborn. 1994. "Welding of Steel Bridges." *Highway Structures Design Handbook*, available from the National Steel Bridge Alliance, Chicago, IL, Volume 1, Chapter 15.
134. Lincoln Electric Company. 1994. *The Procedure Handbook of Arc Welding*. Lincoln Electric Company, Cleveland, OH.
135. AASHTO. 2003. *Guide Specification for Highway Bridge Fabrication with HPS 70W (485W) Steel*. 2nd ed., American Association of State Highway and Transportation Officials, Washington, D.C., June.

136. AASHTO/AWS D1.5M/D1.5. 2002. *Bridge Welding Code.* American National Standard/American Association of State Highway and Transportation Officials/American Welding Society, available from the American Welding Society, Miami, FL.

137. Wood, W.E., and J.H. Devletian. 1987. "Improved Fracture Toughness and Fatigue Characteristics of Electroslag Welds."   FHWA Publication No. FHWA/RD-87/026, Federal Highway Administration, Washington, D.C., October.

138. Schwendeman, L.P., and A.W. Hedgren, Jr.   1978.   "Bolted Repair of Fractured I-79 Girder." Journal of the Structural Division, American Society of Civil Engineers, New York, NY, Vol. 104, No. ST10, October.

139. Lindberg, H.A.   1977.   *FHWA Notice N 5040.23*, Federal Highway Administration, Washington, D.C., February 16.

140. FHWA.   1995.   "Training Manual for Narrow-Gap Improved Electroslag Welding for Bridges." FHWA Report No. FHWA-SA-96-051, Federal Highway Administration, Washington, D.C., November.

141. FHWA.   1996.   "Technical Information Guide for Narrow-Gap Improved Electroslag Welding for Bridges." FHWA Administration Report No. FHWA-SA-96-053, Federal Highway Administration, Washington, D.C., January.

142. FHWA.   1996.   "Process Operational Guide for Narrow-Gap Improved Electroslag Welding for Bridges."   FHWA Report No. FHWA-SA-96-052, Federal Highway Administration, Washington, D.C., February.

143. Densmore, D.H.   2000.   *FHWA Memorandum: Narrow-Gap Electroslag Welding for Bridges*, Federal Highway Administration, Washington, D.C., March 20.

144. AWS. *Standard Symbols for Welding, Brazing and Nondestructive Examination*: ANSI/AWS A2.4. American Welding Society, Miami, FL, Latest Version.

145. Kaufman, E.J., A.W. Pense, and R.D. Stout. 1981. "An Evaluation of Factors Significant to Lamellar Tearing." *Welding Journal*. Research Supplement, Vol. 60, March.

146. AISC.   1973.   "Commentary on Highly Restrained Welded Connections." *Engineering Journal*, American Institute of Steel Construction, Chicago, IL, Vol. 10, No. 3, 3rd Quarter.

147. Thornton, C.H.   1973.   "Quality Control in Design and Supervision Can Eliminate Lamellar Tearing." *Engineering Journal*, American Institute of Steel Construction, Chicago, IL, Vol. 10, No. 4, 4th Quarter.

148. ASCE.   1982.   "Causes and Prevention of Lamellar Tearing." *Civil Engineering*, American Society of Civil Engineers, New York, NY, April.

149. Blodgett, O.W. 1960. "Shrinkage Control in Welding." *Civil Engineering*, American Society of Civil Engineers, New York, NY, November.

149a. Kloppel, K., and T. Seeger. 1964. "Dauerversuche Mit Einsohnittigen HV - Verbindurgen Aus ST37," *Der Stahlbau*, Vol. 33, No. 8, August, and Vol. 33, No. 11, November.

2.3.4 Splices

2.3.4.1 General

In *AASHTO LRFD* Article 6.2, a splice is defined as a group of bolted connections, or a welded connection, sufficient to transfer the moment, shear, axial force or torque between two structural elements joined at their ends to form a single, longer element.   In steel-bridge design, splices are typically used to connect girder sections together in the field; hence, the term field splices is often used.   The design of splices is covered in *AASHTO LRFD* Article 6.13.6. The design of bolted splices is covered in *AASHTO LRFD* Article 6.13.6.1 and the design of welded splices is covered in *AASHTO LRFD* Article 6.13.6.2.   Principles of bolted connection and welded connection design, discussed in the previous section of this chapter, are applied in the design of splices. The following discussion concentrates primarily on the specifics related to the design of field splices.   Discussions related to field section size and selecting field splice locations are contained in DM Volume 1, Chapter 2 (Section 2.4.3.1.2).

2.3.4.2 Bolted Splices

2.3.4.2.1 General

A schematic of a typical bolted splice is shown in Figure 2.131 (shown for an I-section).   Bolted splices generally include top flange splice plates, web splice plates and bottom flange splice plates.   In addition, if the plate thicknesses on one side of the joint are different than those on the other side, then filler plates are usually needed. For the flange splice plates, there is typically one plate on the outside of the flange and two smaller plates on the inside, one on each side of the web. For the web splice plates, there are two plates, one on each side of the web. High-strength bolts are typically used to connect the splice plates to the member in the final condition.
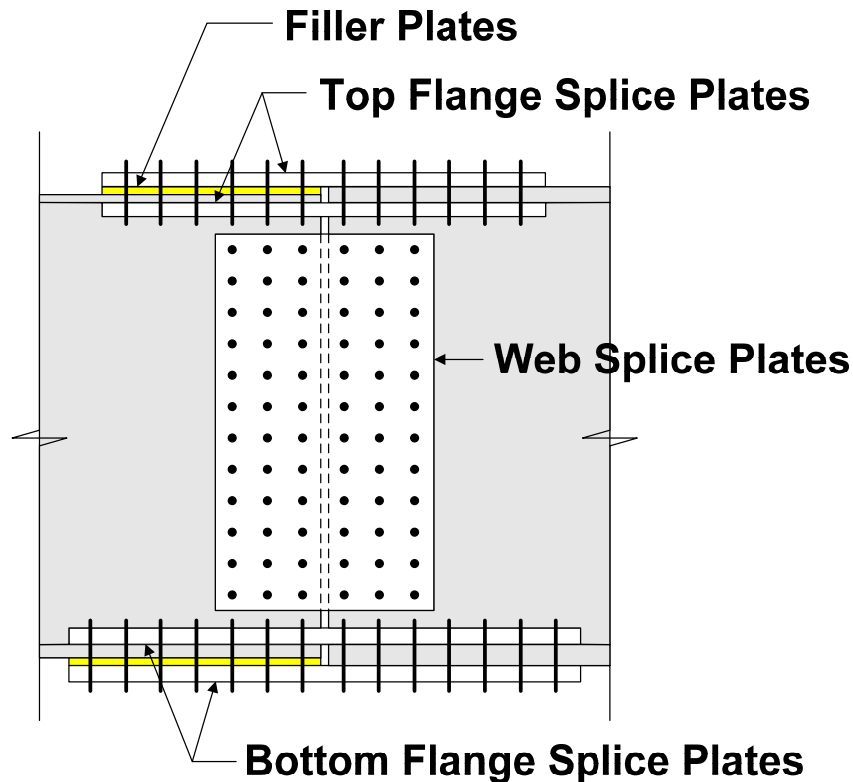
Figure 2.131 Typical Bolted Splice

As specified in AASHTO LRFD Article 6.13.6.1.1, at the strength limit state, bolted splices are to be designed to satisfy the requirements of *AASHTO LRFD* Article 6.13.1; that is, unless specified otherwise, the splices are to be designed for not less than the larger of: 1) the average of the flexural stress, shear or axial force due to the factored loads at the point of splice, or 2) 75 percent of the factored flexural, shear or axial resistance of the member. In addition, where a section changes at the splice, the smaller of the two connected sections is to be used in the design.

2.3.4.2.2 Flexural Members

2.3.4.2.2.1 General

The design of bolted splices for flexural members is discussed first, as these are the most common field splices utilized in steel-bridge construction.   General requirements for the design of bolted splices for flexural members are covered in *AASHTO LRFD* Article 6.13.6.1.4a and are reviewed below. A complete example bolted splice design for a flexural member is given below in Section 2.3.4.2.2.4.

Bolted splices in continuous spans should be made at or near points of permanent load contraflexure if possible, which helps to minimize the flange design forces (see below). *Splices located in areas of stress reversal near points of permanent load contraflexure are to be investigated for both positive and negative flexure in order to determine the governing condition.*

Web and flange splices are not to have less than two rows of bolts on each side of the joint to ensure proper alignment and stability of the girder during construction. Also, *oversize or slotted holes are not to be used in either the member or the splice plates at bolted splices*. This is also for improved geometry control during erection, and because a strength reduction (not recognized by the specifications) may occur when oversize or slotted holes are used in eccentrically loaded bolted web connections.

Bolted splice connections for flexural members are to be designed as slip-critical connections. Slip-critical bolted connections were previously discussed in Section 2.3.2.1.1 of this chapter. *As specified in AASHTO LRFD Article 6.13.2.1.1, slip-critical connections are to be proportioned to prevent slip under Load Combination Service II and to provide bearing, shear and tensile resistance at the strength limit state.* In addition, bolted connections for flange and web splices in flexural members are to be proportioned to prevent slip during the erection of the steel and during the casting of the concrete deck; once again for improved geometry control.

As discussed previously in the section of this chapter on Strength Limit State Verifications, the nominal flexural resistance of certain types of sections in straight bridges is permitted to exceed the moment at first yield at the strength limit state. Included are compact composite sections in positive flexure, and composite I-sections in negative flexure, or noncomposite I-sections, with compact or noncompact webs that are designed according to the optional provisions of Appendix A to Section 6. When these sections have holes in the tension flange, research to date has not fully documented that complete plastification of the cross-section can occur prior to fracture on the net section of the tension flange. Also, the provisions for the design of bolted splices do not consider the contribution of substantial web yielding, beyond the localized yielding of the web permitted in hybrid sections, to the flexural resistance of these sections. As a result, the factored flexural resistance of the tension flange at cross-sections with holes is limited to be less than or equal to the specified minimum yield stress of the tension flange at the strength limit state and when checking constructibility according to the provisions of *AASHTO LRFD* Article 6.10.1.8 (refer to Equation 2.92). *AASHTO LRFD* Article 6.13.6.1.4a states that the factored flexural resistance of the flanges at the point of splice at the strength limit state must satisfy the provisions of *AASHTO LRFD* Article 6.10.6.2, which in turn refers to AASHTO LRFD Article 6.10.1.8. Since this requirement will limit the stress in the tension flange at bolted splices to the yield stress of the tension flange, it effectively prevents bolted splices in the above types of sections from being located at or near points of maximum applied moment where significant yielding of the web is permitted at the strength limit state (e.g. near mid-span of straight composite simple-span bridges), as this would significantly limit the factored flexural resistance of the section at those points.

Although there are holes in the tension flange, for simplicity, *AASHTO LRFD* Article 6.13.6.1.4a states that flexural stresses due to the factored loads at the strength limit state and for checking slip of the bolted connections under the Service II load combination at the point of splice are to be determined using the properties of the gross section.

To determine the smaller section at the point of splice in a flexural member, it is suggested here in lieu of any other alternative rational criterion, that the smaller section be taken as the side of the splice that has the flange with the smallest nominal flexural resistance (see the design example in Section 2.3.4.2.2.4 below).

Finally, as discussed previously, the nominal fatigue resistance of base metal at the gross section adjacent to slip-critical bolted connections is based on fatigue detail Category B (*AASHTO LRFD* Table 6.6.1.2.3-1).   However, as mentioned in *AASHTO LRFD* Article C6.13.6.1.4a, fatigue will generally not control the design of the bolted splice plates for flexural members.   The areas of the flange and web splice plates typically equal or exceed the areas of the flanges and web to which they are attached, and the flanges and web are usually checked separately for either equivalent or more critical fatigue category details.   Therefore, fatigue of the splice plates will generally not need to be checked unless either of the preceding conditions is not satisfied.

2.3.4.2.2.2 Flange Splices

2.3.4.2.2.2.1 General

The design of bolted flange splices for flexural members is covered in *AASHTO LRFD* Article 6.13.6.1.4c and is discussed in detail below.   Where filler plates are required for flange splices, the provisions of *AASHTO LRFD* Article 6.13.6.1.5 apply (see also Section 2.3.4.2.5 of this chapter below).

2.3.4.2.2.2.2 Strength Limit State

At the strength limit state, bolted splice plates and their connections *on the controlling flange* are to be proportioned to provide a minimum design resistance (force) equal to the design stress F_{cf} times the smaller effective flange area A_e on either side of the splice. ***The controlling flange is defined as the top or bottom flange for the smaller section at the point of splice, whichever flange has the maximum ratio of the elastic flexural stress at its midthickness due to the factored loads to its factored flexural resistance.   The opposite flange is termed the noncontrolling flange.*** For splices located in regions of stress reversal, the splice must be checked independently for both positive and negative flexure.   For each condition, a different flange may qualify as the controlling flange.   For composite sections in positive flexure, the controlling flange is typically the bottom flange.   For sections in negative flexure, either flange may qualify as the controlling flange.   The design stress for the controlling flange F_{cf} is to be computed as follows:

$$F_{cf} = \frac{\left(\left| \dfrac{f_{cf}}{R_h} \right| + \alpha \phi_f F_{yf} \right)}{2} \geq 0.75 \alpha \phi_f F_{yf} \qquad \text{Equation 2.291}$$

AASHTO LRFD Equation 6.13.6.1.4c-1

where:

α	=	1.0, except that a lower value equal to F_n/F_{yf} may be used for flanges where F_n is less than F_{yf}
ϕ_f	=	resistance factor for flexure specified in *AASHTO LRFD* Article 6.5.4.2 (= 1.0)
f_{cf}	=	maximum flexural stress due to the factored loads at the midthickness of the controlling flange at the point of splice (ksi)
F_n	=	nominal flexural resistance of the flange (ksi)
F_{yf}	=	specified minimum yield strength of the flange (ksi)
R_h	=	hybrid factor determined as specified in *AASHTO LRFD* Article 6.10.1.10.1. For hybrid sections in which F_{cf} does not exceed the specified minimum yield strength of the web, R_h is to be taken as 1.0

Equation 2.291 is based on the general design requirements specified in *AASHTO LRFD* Article 6.13.1 and discussed above in Section 2.3.4.2.1 of this chapter. The 75 percent rule (i.e. the right-hand side of Equation 2.291), which normally governs in regions of lower moment or stress, is interpreted as providing a longitudinal stiffness at the splice that is consistent with the stiffness assumed at that point in the structural analysis. The average rule (i.e. the left-hand side of Equation 2.291), which normally governs in regions of higher moment or stress, is interpreted as providing adequate flexural resistance at the splice. The application of Equation 2.291 to provide a minimum design resistance for the controlling flange allows for possible unintended shifts in girder moment at the splice and for differences between the actual and predicted moment at the splice, which are certain to be more significant near points of permanent-load contraflexure.

Under previous specifications, bolted splices for flexural members were typically designed by treating the flanges and web of the girder as individual components and then proportioning a calculated minimum design *moment* to each component. However, for a singly-symmetric composite girder, the determination of the proportion of the total design moment carried by the web was not necessarily straightforward and many different approaches were used that did not always lead to consistent results. Also, the resistance of a composite section is different in positive and negative flexure and in regions of stress reversal, it was not always clear which flexural resistance (expressed in terms of moment) should be used to design the splice. Finally, for composite sections, dead and live load moments are applied to different sections and should not be directly summed when at elastic stress levels. Therefore, it becomes more convenient and more correct in a general sense to calculate the actions necessary to design the splice in terms of stress rather than moment.

The factor α is included in Equation 2.291 to allow for a reduction in the minimum design stress for cases where the nominal flexural resistance of the flange F_n is significantly below F_{yf}. An example is a bottom box flange in compression at the point of splice for which F_n is usually well below F_{yf}. As a result, it would be overly conservative to use F_{yf} in Equation 2.291 to determine the minimum design force for designing the splice as the box flange is not permitted to approach a stress level anywhere near F_{yf}. In such cases, α may be taken equal to F_n/F_{yf} (i.e. less than 1.0). For I-section flanges in compression, the reduction in F_n below F_{yf} is typically not as

large as for box flanges. Thus, for simplicity, a conservative value of 1.0 may be used for α in this case even though the specification would permit the use of a lower value. For tension flanges, α will typically always be taken equal to 1.0.

To calculate the minimum design force P_{cf} for the controlling flange, F_{cf} is multiplied by an effective flange area A_e. The *smaller* value of A_e on either side of the splice is to be used to compute the minimum flange design force to ensure the design force does not exceed the factored resistance of the smaller flange. For compression flanges, A_e is to be taken as the gross area of the flange. For tension flanges, A_e is to be calculated as follows:

$$A_e = \left(\frac{\phi_u F_u}{\phi_y F_{yt}} \right) A_n \leq A_g \qquad \text{Equation 2.292}$$

AASHTO LRFD Equation 6.13.6.1.4c-2

where:

ϕ_u	=	resistance factor for fracture of tension members specified in *AASHTO LRFD* Article 6.5.4.2 (= 0.80)
ϕ_y	=	resistance factor for yielding of tension members specified in *AASHTO LRFD* Article 6.5.4.2 (= 0.95)
A_n	=	net area of the tension flange determined as specified in *AASHTO LRFD* Article 6.8.3 (in.^{2})
A_g	=	gross area of the tension flange (in.^{2})
F_u	=	specified minimum tensile strength of the flange determined as specified in *AASHTO LRFD* Table 6.4.1-1
F_{yt}	=	specified minimum yield strength of the tension flange (ksi)

The calculation of the net area A_n at bolted connections was discussed previously in Section 2.3.2.4.2.4.2 of this chapter. For tension flanges, the use of A_e given by Equation 2.292 ensures that fracture on the net section of the flange will theoretically be prevented at the splice.

Bolted splice plates and their connections *on the noncontrolling flange* at the strength limit state are to be proportioned to provide a minimum design resistance (force) P_{ncf} equal to the design stress F_{ncf} times the smaller effective flange area A_e on either side of the splice. The design stress for the noncontrolling flange F_{ncf} is to be computed as follows:

$$F_{ncf} = R_{cf} \left| \frac{f_{ncf}}{R_h} \right| \geq 0.75 \alpha \phi_f F_{yf} \qquad \text{Equation 2.293}$$

AASHTO LRFD Equation 6.13.6.1.4c-3

where:

f_{ncf}	=	flexural stress due to the factored loads at the midthickness of the noncontrolling flange at the point of splice concurrent with f_{cf} (ksi)

R_{cf} = the absolute value of the ratio of F_{cf} to f_{cf} for the controlling flange

R_h = hybrid factor determined as specified in *AASHTO LRFD* Article 6.10.1.10.1. For hybrid sections in which F_{cf} does not exceed the specified minimum yield strength of the web, R_h is to be taken as 1.0

According to Equation 2.293, the flexural stress at the midthickness of the noncontrolling flange f_{ncf} concurrent with the stress in the controlling flange is being factored up in the same proportion as the flexural stress in the controlling flange f_{cf} (i.e. according to Equation 2.291) in order to satisfy the general design requirements of *AASHTO LRFD* Article 6.13.1. To satisfy the requirements of AASHTO LRFD Article 6.13.1, the factored-up stress in the noncontrolling flange must be equal to or greater than $0.75\alpha\phi_f F_{yf}$ as a minimum.

In both Equations 2.291 and 2.293, the flexural stress at the midthickness of the controlling and noncontrolling flange, respectively, is divided by the hybrid factor R_h instead of reducing F_{yf} by R_h. In actuality, yielding in the web of a hybrid section results in an increase in the flange stress and the flange is permitted to reach F_{yf} (see Section 2.2.2.6 of this chapter on the Hybrid Factor). When the minimum design stress for the controlling flange F_{cf} (Equation 2.291) is less than or equal to the specified minimum yield strength of the web F_{yw}, there is theoretically no yielding in the web and R_h is taken equal to 1.0. The web load-shedding factor R_b (see Section 2.2.2.5 of the chapter on the Web Load-Shedding Factor) is not included in either equation since the possibility of web bend-buckling, and the concomitant shedding of the web compressive stresses to the compression flange, is precluded by the presence of the web splice plates.

The calculated minimum design forces in the controlling and noncontrolling flanges are to be used to check the resistance of the flange splice plates (see next paragraph), and to check the shear resistance of the high-strength bolts (refer to Section 2.3.2.4.2.1 of this chapter) and the bearing resistance at the bolt holes (refer to Section 2.3.2.4.2.2 of this chapter) assuming the bolts have slipped and gone into bearing at the strength limit state. The bearing resistance is calculated as the sum of the bearing resistances of the individual bolt holes parallel to the line of the flange design force. When splicing two homogeneous sections of the same specified minimum yield strength, the bearing resistance of the thinner flange splice plate controls if the sum of the inner and outer splice-plate thicknesses is less than the thickness of the thinner flange at the point of splice; otherwise, the thinner flange plate controls. For all other cases, the comparison must be made between the sum of the inner and outer splice plate thicknesses times the specified minimum tensile strength F_u of the splice plates to the thickness of each flange times the corresponding F_u of each flange at the point of splice in order to determine which plate controls. Note that slip of the bolted connections is to be checked at the service limit state using a lower minimum design force (see the next section on the Service Limit State).

At the strength limit state, the minimum design force in flange splice plates subject to tension is not to exceed the factored resistance of the splice plates in tension specified in *AASHTO LRFD* Article 6.13.5.2; that is, the splice plates are to be

checked for yielding on the gross section, fracture on the net section and for block shear rupture (refer to Section 2.3.2.4.2.4 of this chapter). As mentioned previously, block shear rupture will not typically control the design of flange splice plates of typical proportion. Note also that according to *AASHTO LRFD* Article 6.13.5.2, for splice plates subject to tension, A_n must not exceed $0.85A_g$. For narrow splice plates on relatively narrow flanges requiring a relatively large number of bolts, it may be desirable to taper the splice plates at their ends in order to reduce the number of holes until the plates can be sufficiently unloaded to accomodate more holes across the width (refer to the example given in Section 2.3.2.4.2.4.2 of this chapter). The smallest value of A_e at the end of the taper should probably be used to conservatively compute the flange design forces in this case.

As specified in *AASHTO LRFD* Article 6.13.6.1.4c, for flange splice plates subject to compression at the strength limit state, the minimum design force must not exceed the factored resistance in compression given as:

$$R_r = \phi_c F_y A_s$$

<div align="right">Equation 2.294</div>

<div align="right">*AASHTO LRFD* Equation 6.13.6.1.4c-4</div>

where:

ϕ_c = resistance factor for compression specified in *AASHTO LRFD* Article 6.5.4.2 (= 0.90)

A_s = gross area of the splice plate (in.^{2})

F_y = specified minimum yield strength of the splice plate (ksi)

Equation 2.294 is a check for yielding on the gross section of the splice plates assuming an unbraced length of zero for the relatively short plates.

For a typical flange splice with inner and outer splice plates, an approach is needed to proportion the minimum design force to the inner and outer plates. According to *AASHTO LRFD* Article C6.13.6.1.4c, at the strength limit state, the minimum flange design force may be assumed equally divided to the inner and outer flange splice plates when the areas of the inner and outer plates do not differ by more than 10 percent. In this case, the shear resistance of the bolted connection should be checked for the total minimum flange design force assumed acting in double shear. Should the areas of the inner and outer plates differ by more than 10 percent, the minimum design force in each plate at the strength limit state should be determined by multiplying the total minimum flange design force by the ratio of the area of the splice plate under consideration to the total area of the inner and outer plates. In this case, the shear resistance of the bolted connection should be checked for the larger of the calculated splice-plate minimum design forces assumed acting on a single shear plane.

2.3.4.2.2.2.3 Service Limit State

At the service limit state, the slip resistance of the flange splice bolts (refer to Section 2.3.2.4.1.1 of this chapter) is to be checked under the Service II load combination

(see Volume 1, Chapter 5 for additional information on the Service II load combination). For this check, the minimum design force for the flange under consideration is to be taken as the Service II design stress F_s times the smaller gross flange area A_g on either side of the splice. The Service II design stress F_s is to be taken as:

$$F_s = \frac{f_s}{R_h}$$

Equation 2.295

AASHTO LRFD Equation 6.13.6.1.4c-5

where:
f_s =   maximum flexural stress due to Load Combination Service II at the midthickness of the flange under consideration for the smaller section at the point of splice (ksi)

R_h =   hybrid factor determined as specified in *AASHTO LRFD* Article 6.10.1.10.1. For hybrid sections in which f_s in the flange with the larger stress does not exceed the specified minimum yield strength of the web, R_h is to be taken equal to 1.0.

Since net section fracture is not a concern when checking for slip under this service limit state load combination, the smaller *gross* flange area on either side of the splice is to be used to compute the minimum design force. The smaller gross area on either side of the splice is used to ensure that the design force does not exceed the service limit state resistance of the smaller flange.

As discussed in *AASHTO LRFD* Article C6.13.6.1.4c, when checking the slip resistance of the bolts for a typical flange splice with inner and outer splice plates, the minimum design force at the service limit state should always be assumed divided equally to the two slip planes regardless of the ratio of the splice plate areas. Unless slip occurs on both planes, slip of the connection cannot occur. Therefore, in this case, the slip resistance of the bolted connection should always be checked for the total minimum flange design force assuming two slip planes (i.e. N_s = 2 in Equation 2.234).

A check of the flexural stresses in the flange splice plates under the Service II load combination to control permanent deformations in the plates is not currently required. However, such a check is recommended whenever the combined area of the inner and outer splice plates is less than the area of the smaller flange at the splice. It is recommended that the check be made in this instance by dividing the total minimum design force P_s (calculated from the design stress F_s obtained from Equation 2.295) equally to the inner and outer plates, dividing the resulting splice-plate minimum design forces by the gross area of the corresponding plate(s), and then checking that the resulting stresses do not exceed $0.95F_y$, where F_y is the specified minimum yield strength of the splice plate(s).

2.3.4.2.2.2.4 Box Sections

Additional requirements apply to the design of bolted flange splices for box sections in certain cases.

As specified in *AASHTO LRFD* Article 6.13.6.1.4c, for all single box sections, and for multiple box sections in bridges not satisfying the requirements of *AASHTO LRFD* Article 6.11.2.3, including horizontally curved bridges, or with box flanges that are not fully effective according to the provisions of *AASHTO LRFD* Article 6.11.1.1, longitudinal warping stresses due to cross-section distortion (see Section 2.2.4 of this chapter on Box Girders) are to be considered when checking the slip resistance of the bolts for constructibility and at the service limit state, and when checking fatigue of the splices. These stresses can potentially be significant under construction and service conditions in the box sections cited above, and therefore, should be considered in these cases when checking fatigue and when checking for slip of the bolts. The warping stresses under these conditions can be ignored when checking the top-flange splices after the flange is continuously braced. At the strength limit state, longitudinal warping stresses due to cross-section distortion may be ignored when checking both the top and bottom flange splices, as these stresses are typically limited at the strength limit state through the provision of sufficient internal cross bracing (*AASHTO LRFD* Article C6.7.4.3).

For the box sections cited in the preceding paragraph, St. Venant torsional shear must also be considered in the design of the bolted splices for box flanges at all limit states (note that according to *AASHTO LRFD* Article 6.2, a *box flange* is defined as a flange that is connected to two webs). The St. Venant torsional shear in the flange due to the factored loads can be determined by multiplying the shear flow given by *AASHTO LRFD* Equation C6.11.1.1-1 by the width of the box flange. The enclosed area of the box section A_o should be computed as discussed in *AASHTO LRFD* Article C6.11.1.1 for torques applied separately to the noncomposite and composite sections. The bolts for box-flange splices can be designed for the effects of the torsional shear using the traditional elastic vector method for eccentric shear (refer to Section 2.3.2.5 of this chapter). The direct shear on the flange bolts is caused by either the flange force due to the factored loads, or by the appropriate minimum flange design force, depending on the limit state under investigation. The moment on the bolt group is taken as the moment resulting from the eccentricity of the St. Venant torsional shear due to the factored loads, assumed applied at the centerline of the splice. Note that at the strength limit state, the torsional shear due to the factored loads need not be multiplied by the factor R_{cf} given in Equation 2.293 when computing the moment for the design of the splice (i.e. the torsional shear need not be factored-up). The box-flange splice plates in these cases should also be designed at the strength limit state for the combined effects of the appropriate flange force and the moment resulting from the eccentricity of the St. Venant torsional shear due to the factored loads.

St. Venant torsional shears are typically ignored in the design of the top flanges of tub sections once the flange is continuously braced and the section is closed, and therefore, need not be considered in the design of the splices for these flanges. The composite deck is assumed to resist all the torsional shear acting on the top of tub

sections once the section is closed.   For bolted flange splices in discretely braced top flanges of tub sections prior to hardening of the deck (i.e. during construction), flange lateral bending may need to be considered in the design of the splices, as discussed in the next section of this chapter.

If possible, longitudinal flange stiffeners on box flanges (see Section 2.2.4.8 of this chapter) are best discontinued at field splice locations at the free edge of the flange where the flange stress is zero. The compressive resistance of the unstiffened flange across the splice from the stiffener termination should be checked to determine if the flange is sufficient without a stiffener or if a slight increase in flange thickness will suffice. If the stiffener is terminated as such, fatigue of the base metal at the stiffener-to-flange weld termination need not be checked in regions subject to a net applied tensile stress (as defined in *AASHTO LRFD* Article 6.6.1.2.1). A suggested box-flange bolted splice detail to accommodate such a termination is shown in Figure 2.132.
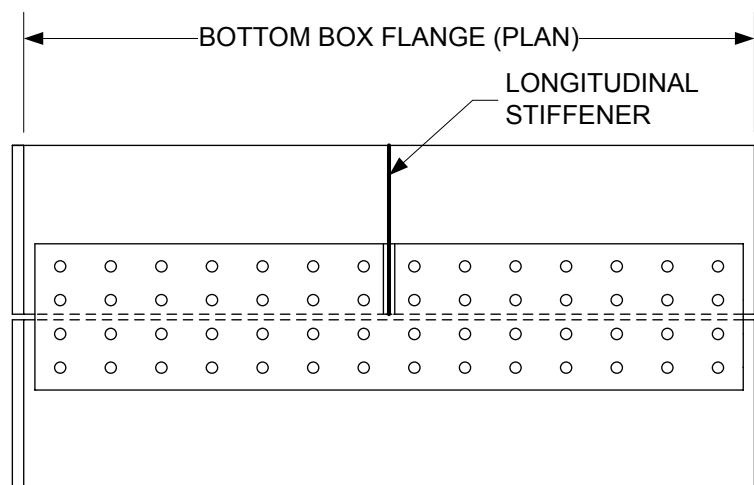
Figure 2.132 Suggested Box-Flange Bolted Splice Detail at Flange Stiffener Termination

Otherwise, termination of the longitudinal stiffener becomes difficult and a potential fatigue problem is created. In regions subject to a net applied tensile stress, the base metal at the termination of the stiffener-to-flange weld must normally be checked for fatigue according to the stiffener terminus detail. If a costly special transition radius is not provided in the stiffener at the weld termination, the fatigue category at the termination is either a low Category E or E′ detail depending on the detail thickness (refer to *AASHTO LRFD* Table 6.6.1.2.3-1). Should it become necessary to terminate the flange stiffener beyond the field splice and a Category E or E′ detail will not suffice, possible options to consider include thickening the flange in the region of the termination to eliminate the need for the stiffener, running the stiffener the full length of the span if the remaining length of unstiffened flange is reasonable (note that this option may help to stiffen a relatively thin tension flange. If a smaller tee section will suffice over the remaining length, it can be spliced onto the existing stiffener), and lastly, including an appropriate transition radius at the end of the stiffener to raise the fatigue detail category accordingly, which is the most costly

and least desirable option. The Engineer is advised to consult with a fabricator regarding the relative cost of each of these options. Splicing the flange stiffener across the field splice is recommended whenever it becomes necessary to run the stiffener beyond the splice.

2.3.4.2.2.2.5 Flange Lateral Bending

According to *AASHTO LRFD* Article 6.13.6.1.4c, in cases for straight girders where flange lateral bending is deemed significant, and for horizontally curved girders, the effects of flange lateral bending must be considered in the design of the bolted splices for discretely braced flanges of I-sections and for discretely braced top flanges of tub sections (a discretely braced flange was defined earlier in Section 2.2.3.4.3.2 of this chapter. Top flanges of I-sections and tub sections are typically discretely braced during the construction condition). Flange lateral bending may be ignored in the design of top-flange splices once the flange is continuously braced.

To account for the effects of flange lateral bending in the design of the flange splice bolts, the traditional elastic vector method for eccentric shear (refer to Section 2.3.2.5 of this chapter) may be used. The direct shear on the flange bolts is caused by either the flange force due to the factored loads, or by the appropriate minimum flange design force, depending on the limit state under investigation. The flange force is calculated without consideration of the flange lateral bending. The moment on the bolt group is taken as the calculated flange lateral bending moment due to the factored loads. Note that at the strength limit state, the flange lateral bending moment due to the factored loads need not be multiplied by the factor R_{cf} given in Equation 2.293 when computing the moment for the design of the splice (i.e. the flange lateral bending moment need not be factored-up).

Splice plates subject to flange lateral bending should also be designed at the strength limit state for the combined effects of the appropriate flange force and the flange lateral bending moment due to the factored loads.

2.3.4.2.2.3 Web Splices

2.3.4.2.2.3.1 General

The design of bolted web splices for flexural members is covered in *AASHTO LRFD* Article 6.13.6.1.4b. As illustrated in Figure 2.133, web splice plates and their connections for flexural members are to be designed in general for a design shear, the moment due to the eccentricity of the design shear at the point of splice, and the portion of the flexural moment assumed resisted by the web at the point of splice.
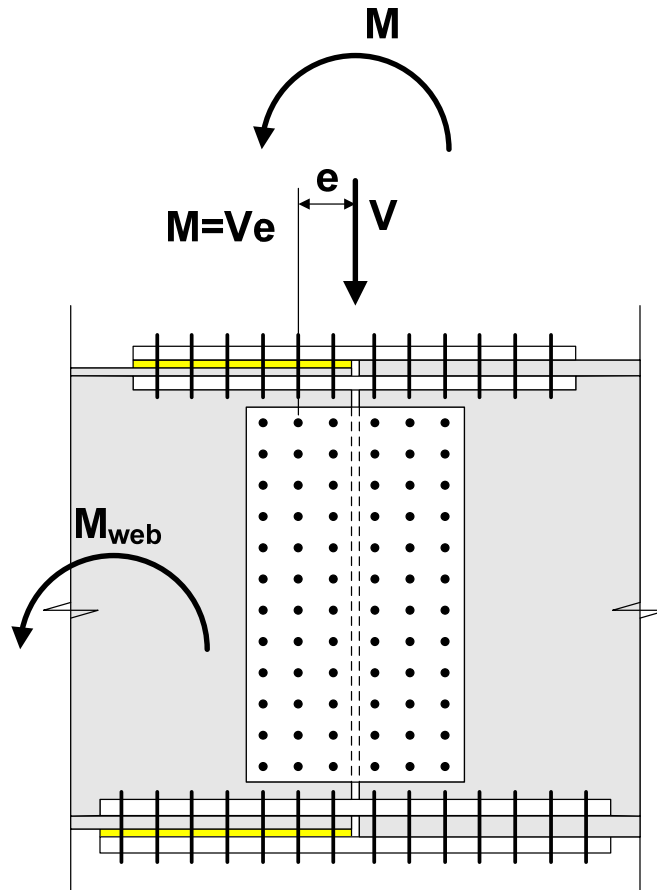
Figure 2.133 Design Actions for Bolted Web Splices for Flexural Members

The web moment is assumed applied at mid-depth of the web. Therefore, as discussed further below, at sections where the neutral axis is not at the mid-depth of the web, a horizontal force resultant must also be applied at the mid-depth of the web in order to establish equilibrium.

As specified in *AASHTO LRFD* Article 6.13.6.1.4b and illustrated in Figure 2.134, when computing the moment due to the eccentricity of the design shear at the point of splice, the correct eccentricity to use is the horizontal distance from the centerline of the splice to the centroid of the web bolt group on the side of the joint under consideration (*150*).
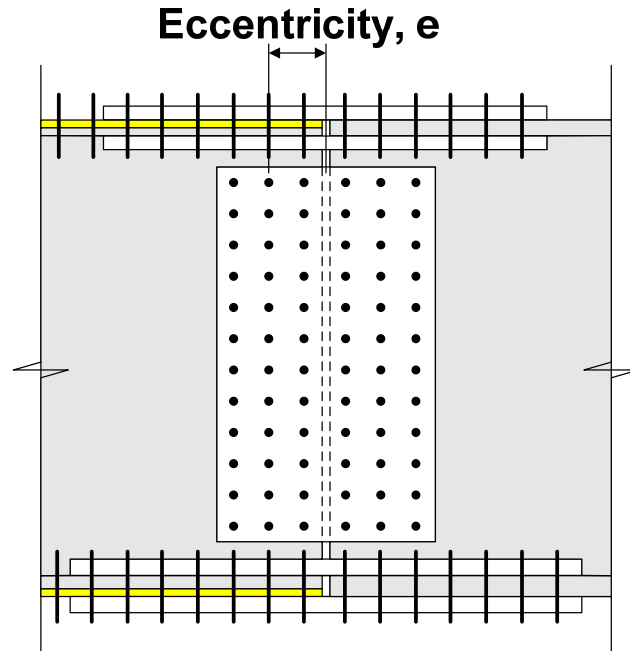
Eccentricity, e

Figure 2.134 Eccentricity of the Design Shear

Webs must be spliced symmetrically by plates on each side of the web. The splice plates must extend as near as practical for the full depth between flanges. Since the web splice is assumed to resist a portion of the flexural moment, maximizing the depth of the web splice plates also maximizes the flexural resistance of the web splice. However, it is important that the splice not impinge on bolt assembly clearances between the top/bottom row of web bolts and the adjacent flange splice bolts. Bolt assembly clearances are given in Reference 5.

If possible, longitudinal web stiffeners are best discontinued at field splice locations at the free edge of the web where the flexural stress in the web is zero, which will require splitting of the web splice plates. The issues related to this are similar to the issues related to the termination of longitudinal stiffeners on box flanges discussed previously (the reader is referred to the last paragraph of Section 2.3.4.2.2.2.4 of this chapter). As for the box-flange stiffener, splicing the longitudinal web stiffener across the field splice is recommended whenever it becomes necessary to run the stiffener beyond the splice.

2.3.4.2.2.3.2 Strength Limit State

At the strength limit state, bolted web splice plates and their connections for flexural members are to be proportioned for a minimum design shear V_{uw} equal to the following:

➤ If $V_u < 0.5\phi_v V_n$, then:

$$V_{uw} = 1.5 V_u$$

Equation 2.296

AASHTO LRFD Equation 6.13.6.1.4b-1

➢ Otherwise:

$$V_{uw} = \frac{(V_u + \phi_v V_n)}{2}$$ Equation 2.297

AASHTO LRFD Equation 6.13.6.1.4b-2

where:

ϕ_v	=	resistance factor for shear specified in *AASHTO LRFD* Article 6.5.4.2 (= 1.0)
V_u	=	shear due to the factored loads at the point of splice (kips)
V_n	=	nominal shear resistance determined as specified in *AASHTO LRFD* Articles 6.10.9.2 and 6.10.9.3 for unstiffened and stiffened webs, respectively (kips)

Equation 2.296 represents an exception to the general design requirements specified in *AASHTO LRFD* Article 6.13.1 and discussed above in Section 2.3.4.2.1 of this chapter. For cases where the shear due to the factored loads V_u is less than 50 percent of the factored shear resistance $V_r = \phi_v V_n$, the 75 percent rule is not applied. Instead, the increase in the shear is limited to 50 percent of V_u. This is done for several reasons. First, the opportunities for the shear V_u to change from its calculated value are less than for moment; that is, large unintended shifts in the shear at the splice are unlikely. Second, the maximum shear is usually not concurrent with the maximum moment at the splice, and therefore, the use of lower value of the design shear in these regions was felt by the specification writers to be reasonable. Lastly, a lower value of the design shear is more reasonable for rolled beams. Designing web splices for rolled beams for 75 percent of their factored shear resistance is unreasonable because the factored shear resistance of a rolled beam can be up to 4 to 5 times greater than V_u. For cases where V_u is greater than or equal to 50 percent of V_r, the average rule is retained for determining the design shear; that is, the minimum design shear is taken as the average of V_u and V_r. The web with the smallest nominal shear resistance on either side of the splice should be used to compute the minimum design shear to ensure that the shear resistance of that web is not exceeded.

Bolted web splices for flexural members are also to be designed at the strength limit state for a design moment M_{uv} due to the eccentricity of the design shear at the point of splice as follows:

$$M_{uv} = V_{uw}e$$ Equation 2.298

where:

e	=	eccentricity of the design shear at the point of splice (in.) (refer to Figure 2.134)
V_{uw}	=	design shear for the web splice determined from Equation 2.296 or 2.297, as applicable (kips)

As discussed previously, the determination of the proportion of the flexural moment resisted by the web at the point of splice is not necessarily straightforward, particularly for a singly symmetric composite girder. Many different approaches have been used, which have sometimes led to significant variations in the number of web bolts provided in different designs for similar splice geometries. To simplify the overall computations and eliminate any potential ambiguities, it is suggested In *AASHTO LRFD* Article C6.13.6.1.4b that the calculated portion of the flexural moment resisted by the web be applied at the mid-depth of the web. Therefore, at sections where the neutral axis is not at the mid-depth of the web (e.g. a singly symmetric composite girder), a horizontal force resultant must also be applied at the mid-depth of the web in order to establish equilibrium. In such cases, the horizontal force resultant may be assumed applied equally to all the web bolts. The following equations are provided to determine a design moment M_{uw} and a design horizontal force resultant H_{uw} to be applied at the mid-depth of the web:

$$M_{uw} = \frac{t_w D^2}{12} \left| R_h F_{cf} - R_{cf} f_{ncf} \right|$$

Equation 2.299

AASHTO LRFD Equation C6.13.6.1.4b-1

$$H_{uw} = \frac{t_w D}{2} \left(R_h F_{cf} + R_{cf} f_{ncf} \right)$$

Equation 2.300

AASHTO LRFD Equation C6.13.6.1.4b-2

where:
- D = web depth of the smaller section at the point of splice (in.)
- f_{ncf} = flexural stress due to the factored loads at the midthickness of the noncontrolling flange at the point of splice concurrent with f_{cf} (see below); positive for tension, negative for compression (ksi)
- F_{cf} = design stress for the controlling flange at the point of splice determined as specified in AASHTO LRFD Article 6.13.6.1.4c (Equation 2.291); positive for tension, negative for compression (ksi)
- R_{cf} = the absolute value of the ratio of F_{cf} to the maximum flexural stress f_{cf} due to the factored loads at the midthickness of the controlling flange at the point of splice
- R_h = hybrid factor determined as specified in AASHTO LRFD Article 6.10.1.10.1. For hybrid sections in which F_{cf} does not exceed the specified minimum yield strength of the web, R_h is taken equal to 1.0.
- t_w = web thickness of the smaller section at the point of splice (in.)

M_{uw} and H_{uw} from the preceding equations, applied together, yield a combined stress distribution equivalent to the unsymmetrical stress distribution in the web. For sections with equal compressive and tensile stresses at the top and bottom of the

web (i.e. where the neutral axis is located at the mid-depth of the web), H_{uw} will equal zero.

Note that M_{uw} and H_{uw} are conservatively computed using the flexural stresses at the midthickness of the flanges. By utilizing the stresses at the midthickness of the flanges, the same computed stresses are used for the design of the flange and web splices, which simplifies the calculations. The stresses at the inner fibers of the flanges may be used instead, if desired. In either case, for composite sections, the stresses due to the factored loads are to computed considering the application of the moments to the respective cross-sections supporting those loads. **_Note that all stresses in Equation 2.299 and 2.300 are to be taken as signed quantities._** Since the sign of M_{uw} corresponds to the sign of the flexural moment for the loading condition under consideration, absolute value signs are applied to the resulting difference of the stresses in Equation 2.299 for convenience. H_{uw} from Equation 2.300 is taken as a signed quantity; positive for tension, negative for compression.

In areas of stress reversal, M_{uw} and H_{uw} are to be computed independently for both positive and negative flexure in order to determine the governing condition. For a composite section subject to positive flexure at the strength limit state, the controlling flange is typically the bottom flange; thus, the top of the web is usually in compression and the neutral axis is usually near the top flange. To compute minimum design values of M_{uw} and H_{uw} for this case, the stress at the midthickness of the controlling (bottom) flange is assumed equal to its minimum flange design stress F_{cf} (from Equation 2.291) times the hybrid factor R_h (Figure 2.135). The stress f_{ncf} at the midthickness of the noncontrolling flange (the top flange in this case), which is taken as the flexural stress due to the factored loads concurrent with the maximum applied flexural stress f_{cf} at the midthickness of the controlling (bottom) flange, is assumed factored up by the ratio R_{cf}, which is taken as the absolute value of the ratio of F_{cf} to f_{cf}.

$$M_{uw} = \frac{t_w D^2}{12}\left|R_h F_{cf} - R_{cf} f_{ncf}\right| \qquad H_{uw} = \frac{t_w D}{2}\left(R_h F_{cf} + R_{cf} f_{ncf}\right)$$
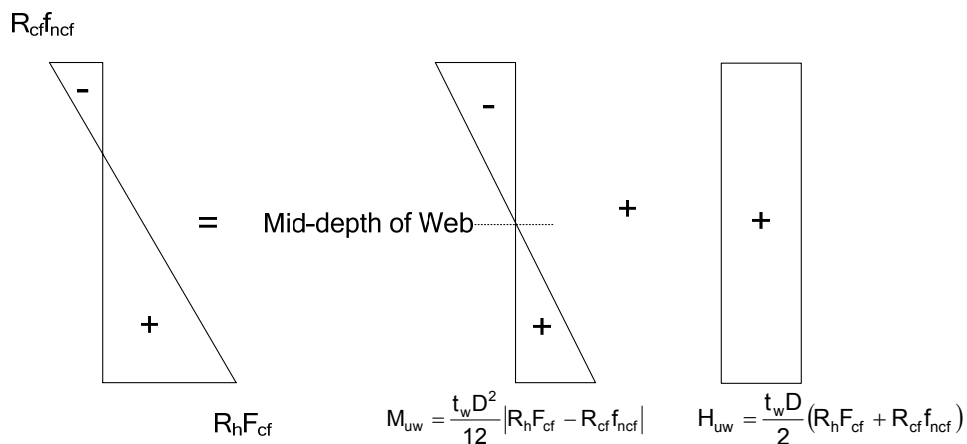
Figure 2.135 Assumed Flexural Stress Distribution in the Web at a Bolted Splice in a Composite Section Subject to Positive Flexure

Essentially, by factoring up the stress f_{ncf} by R_{cf}, the stresses in the web are being factored up in the same proportion as the flexural stress in the controlling flange so that the web splice is designed in a consistent fashion; that is, designed to also satisfy the general strength limit state design requirements specified in *AASHTO LRFD* Article 6.13.1. By integrating the resulting stress distribution over the depth of the web, Equation 2.299 is derived to determine the value of M_{uw} to be applied at the mid-depth of the web. H_{uw} in Equation 2.300 is then simply taken as the average of the factored up stresses at the midthickness of the top and bottom flange.

For the case of negative flexure at the strength limit state, the controlling flange can either be the top or bottom flange. The top of the web is usually in tension and the neutral axis is usually at or near the mid-depth of the web. To compute minimum design values of M_{uw} and H_{uw} for this case, the stress at the midthickness of the controlling flange is again assumed equal to its minimum flange design stress F_{cf} (from Equation 2.291) times the hybrid factor R_h. If the top flange is assumed to be the controlling flange (Figure 2.136), the stress f_{ncf} at the midthickness of the noncontrolling flange (the bottom flange in this case) is assumed factored up by the ratio R_{cf}, which would be taken as the absolute value of the ratio of F_{cf} to f_{cf} for the top flange. M_{uw} and H_{uw} would again then be computed from Equations 2.299 and 2.300, respectively.

$$M_{uw} = \frac{t_w D^2}{12}\left|R_h F_{cf} - R_{cf} f_{ncf}\right| \qquad H_{uw} = \frac{t_w D}{2}\left(R_h F_{cf} + R_{cf} f_{ncf}\right)$$
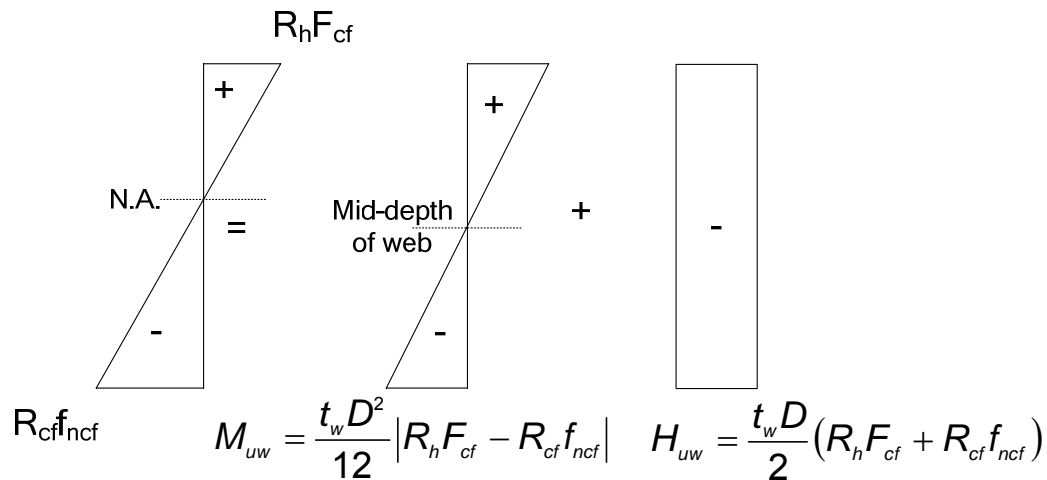
Figure 2.136 Assumed Flexural Stress Distribution in the Web at a Bolted Splice in a Section Subject to Negative Flexure

For splices not in areas of stress reversal, M_{uw} and H_{uw} need only be computed for the loading condition causing the maximum flexural stress in the controlling flange at the strength limit state; that is, only a single load condition need be checked.

AASHTO LRFD Article 6.13.6.1.4b permits an alternative approach for the design of web splices *for compact web sections at the strength limit state only* (see Section 2.2.3.1.1.1 of this chapter for the definition of a compact web section). In this approach, all the flexural moment is assumed resisted by the flange splices, provided the flanges are capable of resisting the design moment (*150, 151*). Should the flanges not be capable of resisting the entire design moment, the web splice is

assumed to resist any remaining flexural moment in addition to the design shear and the moment due to the eccentricity of the design shear. Note that when this alternate approach is used, the slip resistance of the bolts is still to be checked using conventional assumptions (i.e. that the web resists all of its portion of the flexural design moment at the service limit state – see the next section of this chapter on the Service Limit State).

The calculated minimum design actions in web given above (i.e. V_{uw}, M_{uv}, M_{uw} and H_{uw}) are to be used to check the resistance of the web splice plates (see below), and to check the shear resistance of the high-strength bolts (refer to Section 2.3.2.4.2.1 of this chapter) and the bearing resistance at the bolt holes (refer to Section 2.3.2.4.2.2 of this chapter – further discussion on checking the bearing resistance at the web bolt holes is also given below) assuming the bolts have slipped and gone into bearing at the strength limit state. Note that slip of the bolted connections is to be checked at the service limit state using lower minimum design actions (see the next section of this chapter on the Service Limit State).

Since the web splice bolts are subject to eccentric shear, the traditional elastic vector method is recommended for calculating the maximum resultant bolt force (refer to Section 2.3.2.5 of this chapter). In applying this method, to simplify the calculations and avoid possible errors, all actions are to be applied at the mid-depth of the web and the polar moment of inertia of the bolt group I_p should be computed about the centroid of the connection (Equation 2.269 is recommended for use). Shifting I_p to the neutral axis of the composite section (which is typically not at the mid-depth of the web) may cause the bolt forces to be underestimated unless the location of the neutral axis is determined from the summation of the stresses due to the appropriate loadings acting on the respective cross-sections supporting those loadings. Again, the design horizontal force resultant H_{uw} may be assumed applied equally as a horizontal shear force to all the web bolts. In determining the maximum resultant bolt force R in the outermost bolt, the horizontal shear force in bolt due to H_{uw} would be appropriately combined with the horizontal component of the bolt shear due to torsion R_x in Equation 2.273. The application of the recommended approach to calculate the maximum resultant bolt force in a web splice is demonstrated in the example given below in Section 2.3.4.2.2.4.

There are several options for checking the bearing resistance of the web at bolt holes. The resistance of an outermost hole, calculated using the clear edge distance, can conservatively be checked against the maximum resultant bolt force acting on the extreme bolt in the connection (see the left-hand side of Figure 2.137). Since the resultant force acts in the direction of an inclined distance that is larger than the clear edge distance, the check is conservative.
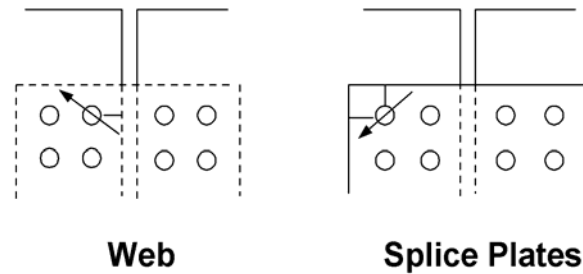
Figure 2.137 Critical Locations for Checking Bearing Resistance of Outermost Web Splice Bolt Holes

Alternatively, the bearing resistance can be calculated based on the inclined distance, or else the resultant bolt force can be resolved in the direction parallel to the edge distance. Regardless of which approach is used, should the bearing resistance be exceeded, it is strongly recommended that the edge distance be increased slightly in lieu of increasing the number of bolts or thickening the web, as this is clearly the simplest and most economical solution. In unusual cases where the bearing resistance of the web splice plate controls (i.e. where the sum of the web splice-plate thicknesses is less than the thickness of the thinner web at the splice), the smaller of the clear edge or end distance on the splice plates should be used to compute the bearing resistance of the outermost hole (see the right-hand side of Figure 2.137).

As specified in *AASHTO LRFD* Article 6.13.6.1.4b, at the strength limit state, the combined stress in the web splice plates due to M_{uv}, M_{uw} and H_{uw} must not exceed the specified minimum yield strength of the splice plates times the resistance factor ϕ_f specified in *AASHTO LRFD* Article 6.5.4.2 (= 1.0). In addition, the design shear V_{uw} must not exceed the lesser of the block shear rupture resistance specified in *AASHTO LRFD* Article 6.13.4 (refer to Section 2.3.2.4.2.4.3 of this chapter) or the factored shear resistance of the splice plates specified in *AASHTO LRFD* Article 6.13.5.3 (refer to Section 2.3.2.4.2.3 of this chapter). Note that because of the overall length of the connection, the block shear rupture resistance normally does not control for web splice plates of typical proportion. Also, a check of V_{uw} against the factored shear rupture resistance of the splice plates based on the net section of the plates (i.e. $R_r = \phi_u 0.6 F_u A_n U$) does not typically control and is not currently specified.

2.3.4.2.2.3.3 Service Limit State

At the service limit state, the slip resistance of the web splice bolts (refer to Section 2.3.2.4.1.1 of this chapter) is to be checked under the Service II load combination (see Volume 1, Chapter 5 for additional information on the Service II load combination). For this check, the design shear for the service limit state V_s is to simply be taken as the shear at the point of splice due to the factored loads under Load Combination Service II. The design moment M_{sv} at the service limit state due to the eccentricity of the design shear at the point of splice is to be taken as follows:

$$M_{sv} = V_s e \qquad \text{Equation 2.301}$$

where:
    e   =   eccentricity of the design shear at the point of splice (in.) (refer to Figure 2.133)

    V_s =   design shear for the web splice for the service limit state taken as the shear due to Load Combination Service II at the point of splice (kips)

According to *AASHTO LRFD* Article C6.13.6.1.4b, for checking slip of the web-splice bolts at the service limit state, the portion of the flexural moment resisted by the web (i.e. the design moment M_{sw}) and the design horizontal force resultant H_{sw} may be computed as follows:

$$M_{sw} = \frac{t_w D^2}{12} \left| f_s - f_{os} \right| \qquad\qquad \text{Equation 2.302}$$

$$H_{sw} = \frac{t_w D}{12} \left(f_s + f_{os} \right) \qquad\qquad \text{Equation 2.303}$$

where:
    D   =   web depth (in.)

    f_s =   maximum flexural stress due to Load Combination Service II at the midthickness of the flange under consideration for the smaller section at the point of splice; positive for tension, negative for compression (ksi)

    f_{os} =   flexural stress due to Load Combination Service II at the midthickness of the other flange at the point of splice concurrent with f_s in the flange under consideration; positive for tension, negative for compression (ksi)

    t_w =   web thickness (in.)

M_{sw} and *H_{sw}* are signed quantities in a similar fashion to *M_{uw}* and *H_{uw}* at the strength limit state. When checking for slip, it is not necessary to determine the controlling and noncontrolling flange; hence the terms *F_{cf}* and *R_{cf}* do not appear in Equations 2.302 and 2.303. As for the strength limit state, in areas of stress reversal, *M_{sw}* and *H_{sw}* must be computed independently for both positive and negative flexure to determine the governing condition. If the splice is not located in an area of stress reversal, *M_{sw}* and *H_{sw}* need only be computed for the loading condition causing the maximum flexural stress due to Load Combination Service II in the flange under consideration. The maximum resultant bolt force for checking the slip resistance of the web splice bolts should be determined using the traditional elastic vector method for eccentric shear, in a fashion similar to that described for the strength limit state in the previous section of this chapter.

A check of the combined stress due to *M_{sv}*, *M_{sw}* and *H_{sw}* in the web splice plates under the Service II load combination to control permanent deformations in the plates is not currently required. However, such a check is recommended for the unusual case where the combined area of the web splice plates is less than the area

of the smaller web at the splice. In this check, the maximum combined stress on the gross section of the web splice plates should not exceed $0.95F_y$, where F_y is the specified minimum yield strength of the splice plate(s).

2.3.4.2.2.3.4 Box Sections

Additional requirements apply to the design of bolted web splices for box sections in certain cases.

As specified in *AASHTO LRFD* Article 6.13.6.1.4b, for all single box sections, and for multiple box sections in bridges not satisfying the requirements of *AASHTO LRFD* Article 6.11.2.3, including horizontally curved bridges, or with box flanges that are not fully effective according to the provisions of *AASHTO LRFD* Article 6.11.1.1, the shear due to the factored loads is to be taken as the sum of the flexural and St. Venant torsional shears *in the web subjected to additive shears* in the design of bolted web splices at all limit states (see Section 2.2.4 of this chapter on Box Girders).

Also, for boxes with inclined webs, the web splice is to be designed at all limit states for the component of the vertical shear in the plane of the web by dividing the design shear by the cosine of the angle of inclination of the web plate to the vertical. When designing the web bolts for eccentric shear, this includes the direct shear on the bolts and the vertical component of the bolt shear due to torsion. Also, when computing the flexural stress in the web splice plates due to the sum of M_{uv} and M_{uw} (or M_{sv} and M_{sw} as applicable), the section modulus of the splice plates should reflect the slope of the web.

2.3.4.2.2.4 Example Splice Design

2.3.4.2.2.4.1 General

The following is a complete example design of a bolted field splice for the interior girder of an I-section flexural member. The splice is located 100 feet from the abutment (near the point of permanent load contraflexure) in the 140-foot end span of a three-span continuous bridge. The unbraced length adjacent to either side of the splice is 24'-0". The girder plate sizes on the left- and right-hand side of the point of splice are as follows:

Left Side: Top Flange   1" x 16"   Right Side: Top Flange   1" x 18"
            Web   ½" x 69"   Web   9/16" x 69"
            Bot. Flange   1-3/8" x 18"   Bot. Flange   1" x 20"

The section on the left-hand side of the splice is homogeneous utilizing ASTM A 709 Grade 50W steel for the flanges and web. The section on the right-hand side of the splice is a hybrid section utilizing ASTM A 709 Grade HPS 70W steel for the flanges and ASTM A 709 Grade 50W steel for the web.

The smaller section will be taken as the side of the splice that has the flange with the smallest nominal flexural resistance. Separate computations indicate that the left-

hand side of the splice qualifies as the smaller section according to this criterion. Thus, only the calculations for the left-hand side of the splice are shown below.

At the section on the left-hand side of the splice, the effective flange width of the concrete deck is 100 in. The structural slab thickness is 9.0 in. The modular ratio n is equal to 8. The deck haunch is 3.5 in. from the top of the web to the bottom of the deck. The area of the longitudinal deck reinforcement is 9.30 in.[2] and is assumed to be located at the centroid of the two layers of longitudinal reinforcement, or at 4.63 in. from the bottom of the deck. From separate calculations similar to those illustrated previously in this chapter, the elastic section properties of the gross section on the left-hand side of the splice are as follows:

	I (in.^{4})	S_{top} (in.^{3})	S_{bot} (in.^{3})	Neutral Axis* (in.)
Steel	62,658	1,581	1,973	31.75
Steel + Long. Reinforcement	80,757	2,341	2,189	36.89
3n Composite	117,341	4,863	2,483	47.25
n Composite	161,518	13,805	2,706	59.68

* Neutral axis is measured from the bottom of the steel

The unfactored moments and shears at the point of splice are as follows:

M_{DC1} = +248 kip-ft V_{DC1} = -82 kips
$M_{deck\ casting}$ = +1,300 kip-ft $V_{deck\ casting}$ = -82 kips
M_{DC2} = +50 kip-ft V_{DC2} = -12 kips
M_{DW} = +52 kip-ft V_{DW} = -11 kips
M_{+LL+IM} = +2,469 kip-ft V_{+LL+IM} = +19 kips
M_{-LL+IM} = -1,754 kip-ft V_{-LL+IM} = -112 kips

The DC$_2$ and DW moments are positive at the point of splice. However, these moments are relatively small since the splice is located near a point of permanent load contraflexure. By inspection, it is apparent that the flexural compressive stress is the concrete deck due to the sum of these moments is overcome by the tensile stress in the deck due to the negative live load moment plus impact (assuming all moments are appropriately factored). Therefore, as specified in *AASHTO LRFD* Article 6.10.1.1.1b, the flexural stresses due to the DC$_2$ and DW moments will be computed using the 3n composite section properties for combination with the positive live load plus impact flexural stress. For combination with the negative live load plus impact flexural stress, the stresses due to these moments will be computed using the section properties for the steel girder plus the longitudinal reinforcement.

Calculate the unfactored flexural stresses at the mid-thickness of the bottom flange:

$$f_{DC1} = \frac{248(12)(31.063)}{62,658} = +1.48 \text{ ksi}$$

$$f_{DC2} = \frac{50(12)(46.563)}{117,341} = +0.24 \text{ ksi} \ (3n)$$

$$f_{DC2} = \frac{50(12)(36.203)}{80,757} = +0.27 \text{ ksi} \ (\text{steel} + \text{re inf .})$$

$$f_{DW} = \frac{52(12)(46.563)}{117,341} = +0.25 \text{ ksi} \ (3n)$$

$$f_{DW} = \frac{52(12)(36.203)}{80,757} = +0.28 \text{ ksi} \ (\text{steel} + \text{re inf .})$$

$$f_{+LL+IM} = \frac{2,469(12)(58.993)}{161,518} = +10.82 \text{ ksi}$$

$$f_{-LL+IM} = \frac{-1,754(12)(36.203)}{80,757} = -9.44 \text{ ksi}$$

Calculate the unfactored flexural stresses at the mid-thickness of the top flange:

$$f_{DC1} = \frac{248(12)(39.125)}{62,658} = -1.86 \text{ ksi}$$

$$f_{DC2} = \frac{50(12)(23.625)}{117,341} = -0.12 \text{ ksi} \ (3n)$$

$$f_{DC2} = \frac{50(12)(33.985)}{80,757} = -0.25 \text{ ksi} \ (\text{steel} + \text{re inf .})$$

$$f_{DW} = \frac{52(12)(23.625)}{117,341} = -0.13 \text{ ksi} \ (3n)$$

$$f_{DW} = \frac{52(12)(33.985)}{80,757} = -0.26 \text{ ksi} \ (\text{steel} + \text{re inf .})$$

$$f_{+LL+IM} = \frac{2,469(12)(11.195)}{161,518} = -2.05 \text{ ksi}$$

$$f_{-LL+IM} = \frac{-1,754(12)(33.985)}{80,757} = +8.86 \text{ ksi}$$

Since the splice is located in an area of stress reversal, checks must be made for both the positive and negative flexure conditions. Compute the combined factored

flexural stresses at the midthickness of the bottom and top flanges at the strength limit state for each of these conditions using the appropriate load factors given in *AASHTO LRFD* Tables 3.4.1-1 and 3.4.1-2. The Strength I load combination is used. Note that the minimum load factors γ_p from *AASHTO LRFD* Table 3.4.1-2 are applied to the permanent loads when the corresponding stresses are of opposite sign to the live load plus impact stress.

Bottom Flange

    A. Dead Load + Positive Live Load:

$$f = 1.0[1.25(1.48 + 0.24) + 1.5(0.25) + 1.75(10.82)] = +21.46 \text{ ksi}$$

    B. Dead Load + Negative Live Load:

$$f = 1.0[0.90(1.48 + 0.27) + 0.65(0.28) + 1.75(-9.44)] = -14.76 \text{ ksi}$$

Top Flange

    A. Dead Load + Positive Live Load:

$$f = 1.0[1.25(-1.86 + -0.12) + 1.5(-0.13) + 1.75(-2.05)] = -6.26 \text{ ksi}$$

    B. Dead Load + Negative Live Load:

$$f = 1.0[0.90(-1.86 + -0.25) + 0.65(-0.26) + 1.75(+8.86)] = +13.44 \text{ ksi}$$

The controlling flange is defined as the top or bottom flange for the smaller section at a point of splice, whichever flange has the maximum ratio of the elastic flexural stress at its midthickness due to the factored loads to its factored flexural resistance. From separate calculations (see the previous section of this chapter on Strength Limit State Verifications), the factored flexural resistance F_r of each flange on the left-hand side of the splice and the ratio of f/F_r for each condition (positive and negative flexure) are as follows:

Bottom Flange

    A. Dead Load + Positive Live Load:

       F_r = 50 ksi; |f/F_r| = 0.43

    B. Dead Load + Negative Live Load:

       F_r = 49.8 ksi; |f/F_r| = 0.30

Top Flange

    A. Dead Load + Positive Live Load:

$$F_r = 50 \text{ ksi}; \quad |f/F_r| = 0.13$$

B. Dead Load + Negative Live Load:

$$F_r = 50 \text{ ksi}; \quad |f/F_r| = 0.27$$

Therefore, the bottom flange is the controlling flange for both the positive and negative flexure conditions.

Positive Flexure

For the case of positive flexure, the minimum design stress for the controlling (bottom) flange is computed as:

$$F_{cf} = \frac{\left(\left| \dfrac{f_{cf}}{R_h} \right| + \alpha \phi_f F_{yf} \right)}{2} \geq 0.75 \alpha \phi_f F_{yf}$$

AASHTO LRFD Equation 6.13.6.1.4c-1

The hybrid factor R_h is taken as 1.0 for homogeneous sections and α is taken equal to 1.0 for flanges in tension. f_{cf} is the maximum flexural stress due to the factored loads at the midthickness of the controlling flange at the point of splice = +21.46 ksi. Therefore:

$$\frac{\left| \dfrac{f_{cf}}{R_h} \right| + \alpha F_{yf}}{2} = \frac{\left| \dfrac{+21.46}{1.0} \right| + 1.0(50)}{2} = 35.73 \text{ ksi}$$

$$0.75 \alpha F_{yf} = 0.75(1.0)(50) = 37.50 \text{ ksi} \quad \text{(governs)}$$

The minimum design force for the controlling flange P_{cf} is taken equal to the design stress F_{cf} times the smaller effective flange area A_e on either side of the splice. The smaller effective bottom-flange area is on the right-hand side of the splice. For flanges subject to tension, A_e is computed as:

$$A_e = \left(\frac{\phi_u F_u}{\phi_y F_{yt}} \right) A_n \leq A_g$$

AASHTO LRFD Equation 6.13.6.1.4c-2

From *AASHTO LRFD* Table 6.4.1-1, F_u for ASTM A 709 Grade HPS 70W steel is 85 ksi. Assume the bottom flange splice will consist of 4 rows of 7/8-in. diameter A 325 high-strength bolts across the width of the flange. As specified in *AASHTO LRFD* Article 6.8.3, the width of standard bolt holes (which must be used for bolted splices in flexural members) for design is to be taken as the nominal diameter of the bolt plus 0.125 in. Therefore:

$$A_n = [20.0 - 4(0.875 + 0.125)](1.0) = 16.00 \text{ in.}^2$$

$$A_g = 20.0(1.0) = 20.00 \text{ in.}^2$$

$$A_e = \left(\frac{0.80(85)}{0.95(70)}\right)16.00 = 16.36 \text{ in.}^2 < 20.00 \text{ in.}^2$$

$$P_{cf} = F_{cf}A_e = 37.50(16.36) = 613.5 \text{ kips}$$

For the case of positive flexure, the minimum design stress for the noncontrolling (top) flange is computed as:

$$F_{ncf} = R_{cf}\left|\frac{f_{ncf}}{R_h}\right| \geq 0.75\alpha\phi_f F_{yf}$$

AASHTO LRFD Equation 6.13.6.1.4c-3

f$_{ncf}$ is the flexural stress due to the factored loads at the midthickness of the noncontrolling flange at the point of splice concurrent with *f$_{cf}$* and is equal to -6.26 ksi. The top flange is in compression and is continuously braced for this condition. Therefore, since *F$_{nc}$* = *F$_{yf}$*, α must be taken equal to 1.0.

$$R_{cf} = \left|\frac{F_{cf}}{f_{cf}}\right| = \left|\frac{37.50}{+21.46}\right| = 1.75$$

$$R_{cf}\left|\frac{f_{ncf}}{R_h}\right| = 1.75\left|\frac{-6.26}{1.0}\right| = 10.96 \text{ ksi}$$

$$0.75\alpha F_{yf} = 0.75(1.0)(50) = 37.50 \text{ ksi (governs)}$$

The minimum design force for the noncontrolling flange *P$_{ncf}$* is taken equal to the design stress *F$_{ncf}$* times the smaller effective flange area *A$_e$* on either side of the splice. The smaller effective top-flange area is on the left-hand side of the splice. For flanges subject to compression, *A$_e$* is taken equal to *A$_g$*.

$$A_e = A_g = 16(1.0) = 16.00 \text{ in.}^2$$

$$P_{ncf} = F_{ncf}A_e = 37.50(16.00) = 600.0 \text{ kips}$$

Negative Flexure

For the case of negative flexure, the controlling (bottom) flange is subject to compression. Although *F$_{nc}$* is slightly less than *F$_{yf}$* for this case, α will be conservatively taken equal to 1.0. *f$_{cf}$* = -14.76 ksi. Therefore:

$$\dfrac{\left|\dfrac{f_{cf}}{R_h}\right| + \alpha F_{yf}}{2} = \dfrac{\left|\dfrac{-14.76}{1.0}\right| + 1.0(50)}{2} = 32.38 \text{ ksi}$$

$$0.75\alpha F_{yf} = 0.75(1.0)(50) = 37.50 \text{ ksi} \quad \text{(governs)}$$

For flanges subject to compression, A_e is taken equal to A_g.

$$A_g = 20.0(1.0) = 20.00 \text{ in.}^2$$

$$P_{cf} = F_{cf}A_e = 37.50(20.00) = 750.0 \text{ kips}$$

For the case of negative flexure, the noncontrolling (top) flange is subject to tension; therefore, α is equal to 1.0. f_{ncf} = +13.44 ksi.

$$R_{cf} = \left|\dfrac{F_{cf}}{f_{cf}}\right| = \left|\dfrac{37.50}{-14.76}\right| = 2.54$$

$$R_{cf}\left|\dfrac{f_{ncf}}{R_h}\right| = 2.54\left|\dfrac{13.44}{1.0}\right| = 34.14 \text{ ksi}$$

$$0.75\alpha F_{yf} = 0.75(1.0)(50) = 37.50 \text{ ksi} \quad \text{(governs)}$$

Assume the top flange splice will consist of 4 rows of 7/8-in. diameter A 325 high-strength bolts across the width of the flange. Therefore:

$$A_n = [16.0 - 4(0.875 + 0.125)](1.0) = 12.00 \text{ in.}^2$$

$$A_g = 16.0(1.0) = 16.00 \text{ in.}^2$$

From *AASHTO LRFD* Table 6.4.1-1, F_u for ASTM A 709 Grade 50W steel is 70 ksi.

$$A_e = \left(\dfrac{0.80(70)}{0.95(50)}\right)12.00 = 14.15 \text{ in.}^2 < 16.00 \text{ in.}^2$$

$$P_{ncf} = F_{ncf}A_e = 37.50(14.15) = 530.6 \text{ kips}$$

A summary of the design forces for the bottom and top flange splices is as follows:

Bottom Flange: P_{cf} = 613.5 kips (tension)
P_{cf} = 750.0 kips (compression)

Top Flange: P_{ncf} = 600.0 kips (compression)
                       P_{ncf} = 530.6 kips (tension)

2.3.4.2.2.4.2 Flange Splice Design

Bottom Flange Splice

The width of the outside splice plate should be at least as wide as the width of the narrowest flange at the splice. Therefore, try a ½" x 18" outside splice plate with two 9/16" x 8" inside splice plates. Include a 3/8" x 18" filler plate on the outside. All plates are ASTM A 709 Grade 50W steel.
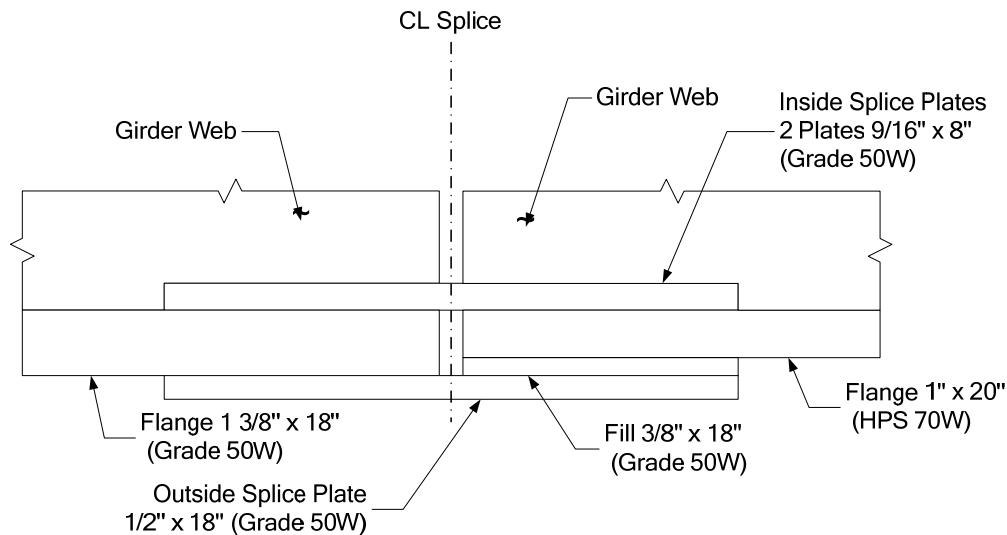
As specified in *AASHTO LRFD* Article C6.13.6.1.4c, at the strength limit state, the minimum flange design force may be assumed equally divided to the inner and outer flange splice plates when the areas of the inner and outer plates do not differ by more than 10 percent. In this case, the areas of the inner and outer plates are equal. Therefore, the design force will be equally divided to the inner and outer plates and the shear resistance of the bolted connection will be checked for the total minimum flange design force assumed acting in double shear. For checking the slip resistance of the bolts at the service limit state, the total Service II design force will be distributed equally to the two slip places, as slip of the connection cannot occur unless slip occurs on both planes.

As specified in *AASHTO LRFD* Article 6.13.5.2, the factored tensile resistance of splice plates R_r at the strength limit state is to be taken as the smallest of the resistance based on yielding, net section fracture or block shear rupture (refer to Section 2.3.2.4.2.4 of this chapter). The factored yield resistance of splice plates in tension is to be computed from *AASHTO LRFD* Equation 6.8.2.1-1 as follows:

$$R_r = \phi_y F_y A_g$$

AASHTO LRFD Equation 6.8.2.1-1

Outside plate:

$$R_r = 0.95(50)(18.0)(0.5) = 427.5 \text{ kips} > 613.5 / 2 = 306.8 \text{ kips} \quad \text{ok}$$

Inside plates:

$$R_r = 0.95(50)(2)(8.0)(0.5625) = 427.5 \text{ kips} > 613.5 / 2 = 306.8 \text{ kips} \quad \text{ok}$$

The factored net section fracture resistance of splice plates in tension is to be computed from *AASHTO LRFD* Equation 6.8.2.1-2 as follows:

$$R_r = \phi_u F_u A_n U$$

AASHTO LRFD Equation 6.8.2.1-2

where the reduction factor *U* to account for shear lag is to be taken as 1.0 for splice plates.

Outside plate:

$$R_r = 0.80(70)[18.0 - 4(0.875 + 0.125)](0.5)(1.0) = 392.0 \text{ kips} > 613.5 / 2 = 306.8 \text{ kips} \quad \text{ok}$$

Inside plates:

$$R_r = 0.80(70)[2(8.0) - 4(0.875 + 0.125)](0.5625)(1.0) = 378.0 \text{ kips} > 613.5 / 2 = 306.8 \text{ kips} \quad \text{ok}$$

Also, according to *AASHTO LRFD* Article 6.13.5.2, for splice plates subject to tension, A_n must not exceed $0.85A_g$.

Outside plate:

$$0.85(18.0)(0.5) = 7.65 \text{ in}^2 > A_n = [18.0 - 4(1.0)](0.5) = 7.00 \text{ in.}^2 \quad \text{ok}$$

Inside plates:

$$0.85(2)(8.0)(0.5625) = 7.65 \text{ in}^2 > A_n = [2(8.0) - 4(1.0)](0.5625) = 6.75 \text{ in.}^2 \quad \text{ok}$$

The block shear rupture resistance of the splice plates will be checked later.

As specified in *AASHTO LRFD* Article 6.13.6.1.4c, for flange splice plates subject to compression at the strength limit state, the minimum design force must not exceed the factored resistance in compression given as:

$$R_r = \phi_c F_y A_s$$

AASHTO LRFD Equation 6.13.6.1.4c-4

Outside plate:

$$R_r = 0.90(50)(18)(0.5) = 405.0 \text{ kips} > 750.0 / 2 = 375.0 \text{ kips ok}$$

Inside plates:

$$R_r = 0.90(50)(2)(8)(0.5625) = 405.0 \text{ kips} > 750.0 / 2 = 375.0 \text{ kips ok}$$

Determine the number of bolts for the bottom flange splice plates that are required to develop the governing minimum design force in the flange in shear at the strength limit state assuming the bolts in the connection have slipped and gone into bearing. A minimum of two rows of bolts must be provided to ensure proper alignment and stability of the girder during construction. The factored shear resistance R_r for a 7/8-in. diameter A325 high-strength bolt in double shear assuming the threads are *excluded* from the shear planes was computed in an earlier example to be 55.3 kips/bolt (refer to Section 2.3.2.4.2.1 of this chapter). Since the factored shear resistance of the bolts is based on the assumption that the threads are excluded from the shear planes, an appropriate note should be placed on the contract plans to ensure that the splice is detailed to exclude the bolt threads from the shear planes. It is assumed that the length between the extreme bolts (on one side of the connection) measured parallel to the line of action of the force will be less than 50.0 in. so that no reduction in the factored shear resistance is required (this will be checked later). Therefore, the minimum number of bolts required to develop the governing minimum design force in the flange in shear on the side of the splice without the filler plate is:

$$N = \frac{P}{R_r} = \frac{750.0}{55.3} = 13.6 \text{ bolts}$$

As discussed below in Section 2.3.4.2.5 of this chapter, filler plates 0.25 in. or greater in thickness in girder flange splices must be secured by additional bolts to ensure that shear planes are well defined and that no reduction in the factored shear resistance of the bolts results. As specified in *AASHTO LRFD* Article 6.13.6.1.5, this can be accomplished by either: 1) extending the fillers beyond the splice plate with the filler extension secured by enough additional bolts to distribute the total stress uniformly over the combined section of the member or filler, or 2) in lieu of extending and developing the fillers, reducing the factored shear resistance of the bolts by the following factor:

$$R = \left[\frac{(1+\gamma)}{(1+2\gamma)} \right]$$

AASHTO LRFD Equation 6.13.6.1.5-1

where the terms in the above equation are defined below in Section 2.3.4.2.5. In this example, the factored shear resistance of the bolts on the side of the splice with the filler plate will be reduced by the factor R.

$$A_f = 0.375(18.0) = 6.75 \text{ in.}^2$$
$$A_p = \text{flange area} = 1.0(20.0) = 20.0 \text{ in.}^2 \quad \text{or}$$
$$A_p = \text{splice plate area} = 2(0.5625)(8.0) + 0.5(18.0) = 18.0 \text{ in.}^2 \quad (\text{governs})$$

$$\gamma = \frac{6.75}{18.0} = 0.375$$

$$R = \frac{1 + 0.375}{1 + 2(0.375)} = 0.79$$

Therefore, the number of bolts required to develop the governing minimum design force in the flange in shear on the side of the splice with the filler plate is:

$$N = \frac{P}{R * R_r} = \frac{750.0}{0.79(55.3)} = 17.2 \text{ bolts}$$

For practical reasons, use the same number of bolts on either side of the splice. Therefore, a minimum of 18 bolts is required to provide the necessary factored shear resistance for the bottom flange splice under the controlling minimum design force.

AASHTO LRFD Article 6.13.6.1.4c requires that high-strength bolted connections for flange splices be designed to prevent slip at the service limit state under a Service II design force. In addition, *AASHTO LRFD* Article 6.13.6.1.4a requires that high-strength bolted splices for flexural members be proportioned to prevent slip during the erection of the steel (assuming an erection analysis is conducted) and during the casting of the concrete deck. For the service limit state check, the Service II design stress F_s is to be taken as:

$$F_s = \frac{f_s}{R_h}$$

AASHTO LRFD Equation 6.13.6.1.4c-5

where f_s is the maximum flexural stress due to Load Combination Service II at the midthickness of the flange under consideration for the smaller section at the point of splice. For the left-hand side of the splice, which is deemed the smaller section, the Service II stress in the bottom flange is computed as follows. It will be assumed that the conditions specified in AASHTO LRFD Article 6.10.4.2.1 are met such that flexural stresses caused by Service II loads applied to the composite section can be computed using the short-term or long-term composite section, as appropriate, assuming the concrete deck is effective for both positive and negative flexure.

    A. Dead Load + Positive Live Load:

$$f = \left[1.0(1.48 + 0.24 + 0.25) + 1.3(10.82)\right] = +16.04 \text{ ksi}\ \ (\text{governs})$$

B. Dead Load + Negative Live Load:

$$f = \left[1.0(1.48 + 0.24 + 0.25) + 1.3(-4.72)\right] = -4.17 \text{ ksi}$$

Therefore, f_s is equal to +16.04 ksi and F_s is equal to f_s/R_h = +16.04/1.0 = +16.04 ksi. The stress at the mid-thickness of the bottom flange due to the deck-casting sequence (the Strength IV load combination controls) is:

$$f = \frac{1.5(1,300)(12)(31.063)}{62,658} = +11.60 \text{ ksi} \qquad \frac{f}{R_h} = \frac{+11.60}{1.0} = +11.60 \text{ ksi}$$

which is less than F_s; therefore, the Service II design stress controls the slip resistance check. The design force P_s for the flange splice is taken as F_s times the smaller gross flange area on either side of the splice, or

$$P_s = F_s A_g = 16.04(1.0)(20.0) = 320.8 \text{ kips}$$

Determine the number of bolts for the bottom flange splice plates that are required to prevent slip under the design force P_s. The factored slip resistance R_r for a 7/8-in. diameter A325 high-strength bolt assuming a Class B surface condition for the faying surface, standard holes and two slip planes per bolt was computed in an earlier example to be 39.0 kips/bolt (refer to Section 2.3.2.4.1.1 of this chapter). As specified in *AASHTO LRFD* Article 6.13.6.1.5 (and discussed in Section 2.3.4.2.5 below), the factored slip resistance need not be adjusted for the effect of filler plates. Therefore, the minimum number of bolts required is:

$$N = \frac{P}{R_r} = \frac{320.8}{39.0} = 8.2 \text{ bolts}$$

which is less than the minimum number of bolts required to provide adequate factored shear resistance at the strength limit state (i.e. N = 18 bolts). Thus, use twenty (20) 7/8-in. diameter high-strength bolts on each side of the bottom flange splice (5 rows of bolts with 4 bolts per row -- no stagger).

In order to check the factored bearing resistance of the bolt holes and the block shear rupture resistance of the splice plates and the flange, the bolt spacings and bolt edge and end distances must first be established and checked (refer to the figure below).
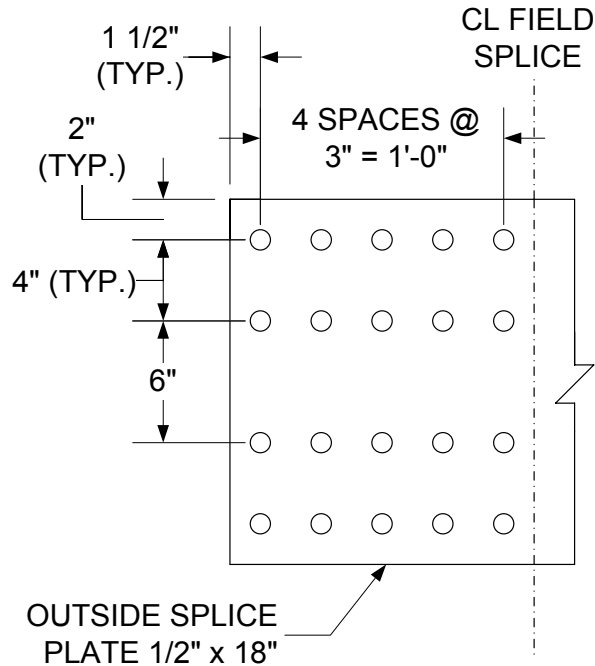
As specified in *AASHTO LRFD* Article 6.13.2.6.1, the minimum spacing between centers of bolts in standard holes is not to be less than 3.0d, where d is the diameter of the bolt. For 7/8-in. diameter bolts:

$$s_{min} = 3d = 3(0.875) = 2.63 \text{ in.} \quad \text{use } 3.0 \text{ in.}$$

Since the length between the extreme bolts (on one side of the connection) measured parallel to the line of action of the force is less than 50.0 in., no reduction in the factored shear resistance of the bolts is required, as originally assumed.

As specified in *AASHTO LRFD* Article 6.13.2.6.2, to seal against the penetration of moisture in joints, the spacing s of a single line of bolts adjacent to a free edge of an outside plate or shape (when the bolts are not staggered) must satisfy the following requirement:

$$s \le (4.0 + 4.0t) \le 7.0 \text{ in.}$$

AASHTO LRFD Equation 6.13.2.6.2-1

where t is the thickness of the thinner outside plate or shape. First check for sealing along the edges of the outer splice plate (which is the thinner plate) parallel to the direction of the applied force:

$$s_{max} = 4.0 + 4.0(0.5) = 6.0 \text{ in.} > 3.0 \text{ in.} \text{ ok}$$

Check for sealing along the free edge at the end of the splice plate:

$$s_{max} = 4.0 + 4.0(0.5) = 6.0 \text{ in.} = 6.0 \text{ in.} \text{ ok}$$

Note that the maximum pitch requirements for stitch bolts specified in *AASHTO LRFD* Article 6.13.2.6.3 apply only to the connection of plates in mechanically fastened built-up members and would not be applied here.

The edge distance of bolts is defined as the distance perpendicular to the line of force between the center of a hole and the edge of the component. In this example, the edge distance of 2.0 inches satisfies the minimum edge distance requirement of 1½ inches specified for 7/8-in. diameter bolts and sheared edges in *AASHTO LRFD* Table 6.13.2.6.6-1 (Table 2.17). This distance also satisfies the maximum edge distance requirement of 8.0t (not to exceed 5.0 in.) = 8.0(0.5) = 4.0 in. specified in *AASHTO LRFD* Article 6.13.2.6.6.

The end distance of bolts is defined as the distance along the line of force between the center of a hole and the end of the component. In this example, the end distance of 1½ inches satisfies the minimum end distance requirement of 1½ inches specified for 7/8-in. diameter bolts and sheared edges in *AASHTO LRFD* Table 6.13.2.6.6-1 (Table 2.17). The maximum end distance requirement of 8.0t (not to exceed 5.0 in.) = 8.0(0.5) = 4.0 in. specified in *AASHTO LRFD* Article 6.13.2.6.5 is also obviously satisfied. Although not specifically required, note that the distance from the corner bolts to the corner of the splice plate, equal to $\sqrt{(1.5)^2 + (2.0)^2} = 2.5$ in., also satisfies the maximum end distance requirement. If desired, the corners of the plate can be clipped to meet this requirement.

The bearing resistance of the connected material at the strength limit state is calculated as the sum of the bearing resistances of the individual bolts (holes) parallel to the line of the applied force (refer to Section 2.3.2.4.2.2 of this chapter). As specified in *AASHTO LRFD* Article 6.8.3, for design calculations, the width of standard bolt holes is to be taken as the nominal diameter of the bolt plus 0.125 in. Therefore, the width of the holes is taken as 0.875 in. + 0.125 in. = 1.0 in. Since in this case the sum of the inner and outer splice plate thicknesses times the specified minimum tensile strength F_u of the splice plates is less than the thickness of each flange times its corresponding F_u, the thinner outside splice plate controls the bearing resistance of the connection.

For standard holes, the nominal bearing resistance R_n parallel to the applied bearing force is taken as follows:

$$R_n = 1.2L_c t F_u \le 2.4 d t F_u$$
AASHTO LRFD Equations C6.13.2.9-1 & 6.13.2.9-2

For the four bolts adjacent to the end of the splice plate, the end distance is 1.5 in. Therefore, the clear end distance L_c between the edge of the hole and the end of the splice plate is:

$$L_c = 1.5 - \frac{1.0}{2} = 1.0 \text{ in.}$$

Therefore: $\quad R_n = 4(1.2L_c t F_u) = 4[1.2(1.0)(0.5)(70)] = 168.0$ kips (governs)

or: $\quad R_n = 4(2.4dtF_u) = 4[2.4(0.875)(0.5)(70)] = 294.0$ kips

For the other sixteen bolts, the center-to-center distance between the bolts in the direction of the applied force is 3.0 in. Therefore, the clear distance L_c between the edges of the adjacent holes is:

$$L_c = 3.0 - 1.0 = 2.0 \text{ in.}$$

Therefore: $\quad R_n = 16(1.2L_c tF_u) = 16[1.2(2.0)(0.5)(70)] = 1344.0$ kips

or:
$$R_n = 16(2.4dtF_u) = 16[2.4(0.875)(0.5)(70)] = 1176.0 \text{ kips (governs)}$$

The total nominal bearing resistance of the splice plate is therefore:

$$R_n = 168.0 \text{ kips} + 1176.0 \text{ kips} = 1344.0 \text{ kips}$$

Since: $\qquad\qquad\qquad\qquad R_r = \phi_{bb}R_n$
AASHTO LRFD Equation 6.13.2.2-2

$$R_r = 0.80(1344.0) = 1075.2 \text{ kips} > \frac{750.0}{2} = 375.0 \text{ kips} \text{ ok}$$

Check the block shear rupture resistance of the bottom flange splice plates and the bottom flange when subject to the minimum design force in tension at the strength limit state (refer to Section 2.3.2.4.2.4.3 of this chapter). Assume the potential block shear failure planes on the outside and inside splice plates shown below.
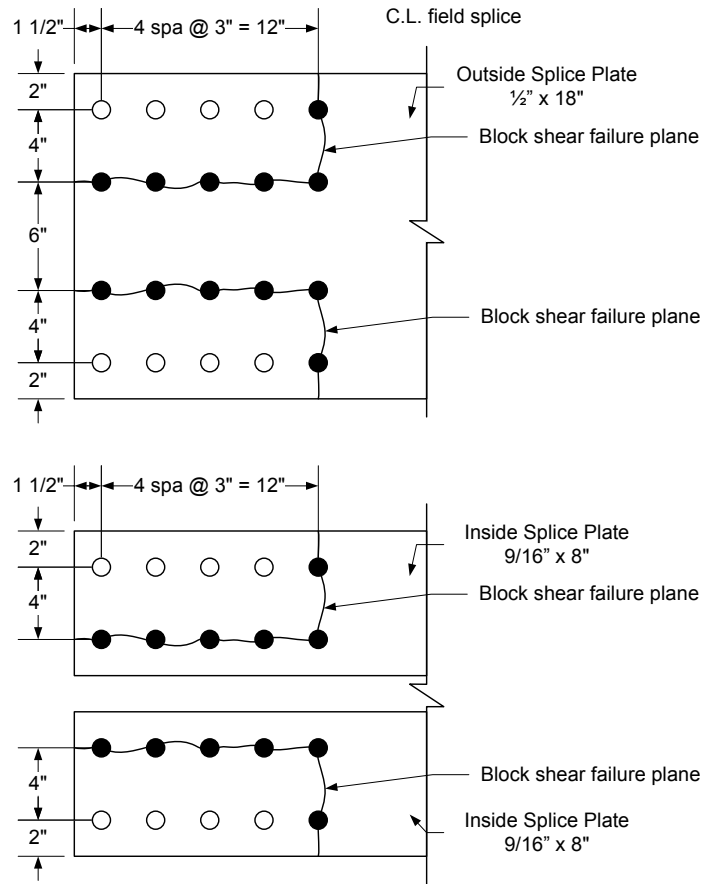
Check the outside splice plate. A_{tn} is the net area along the place resisting the tensile stress.

$$A_{tn} = 2[4.0 + 2.0 - 1.5(1.0)](0.5) = 4.50 \text{ in}^2$$

A_{vn} is the net area along the place resisting the shear stress.

$$A_{vn} = 2[4(3.0) + 1.5 - 4.5(1.0)](0.5) = 9.00 \text{ in}^2$$

$$A_{tn}/A_{vn} = 4.50/9.00 = 0.50 < 0.58$$

Therefore:

$$R_r = \phi_{bs}(0.58 F_u A_{vn} + F_y A_{tg})$$

AASHTO LRFD Equation 6.13.4-2

A_{tg} is the gross area along the plane resisting the tensile stress.

$$A_{tg} = 2[4.0 + 2.0](0.5) = 6.00 \text{ in}^2$$

$$R_r = 0.80[0.58(70)(9.00) + 50(6.00)] = 532.3 \text{ kips} > \frac{613.5}{2} = 306.8 \text{ kips   ok}$$

Check the inside splice plates.

$$A_{tn} = 2[4.0 + 2.0 - 1.5(1.0)](0.5625) = 5.06 \text{ in}^2$$

$$A_{vn} = 2[4(3.0) + 1.5 - 4.5(1.0)](0.5625) = 10.13 \text{ in}^2$$

$$A_{tn}/A_{vn} = 5.06/10.13 = 0.50 < 0.58$$

$$A_{tg} = 2[4.0 + 2.0](0.5625) = 6.75 \text{ in}^2$$

$$R_r = 0.80[0.58(70)(10.13) + 50(6.75)] = 599.0 \text{ kips} > \frac{613.5}{2} = 306.8 \text{ kips ok}$$

Check the critical girder flange at the splice. Since the areas and yield strengths of the flanges on each side of the splice differ, both sides would need to be checked. Only the calculations for the flange on the right-hand side of the splice, which is determined to be the critical flange, are shown below. Two potential failure modes are investigated for the flange as shown in the figure below.

Failure Mode 1
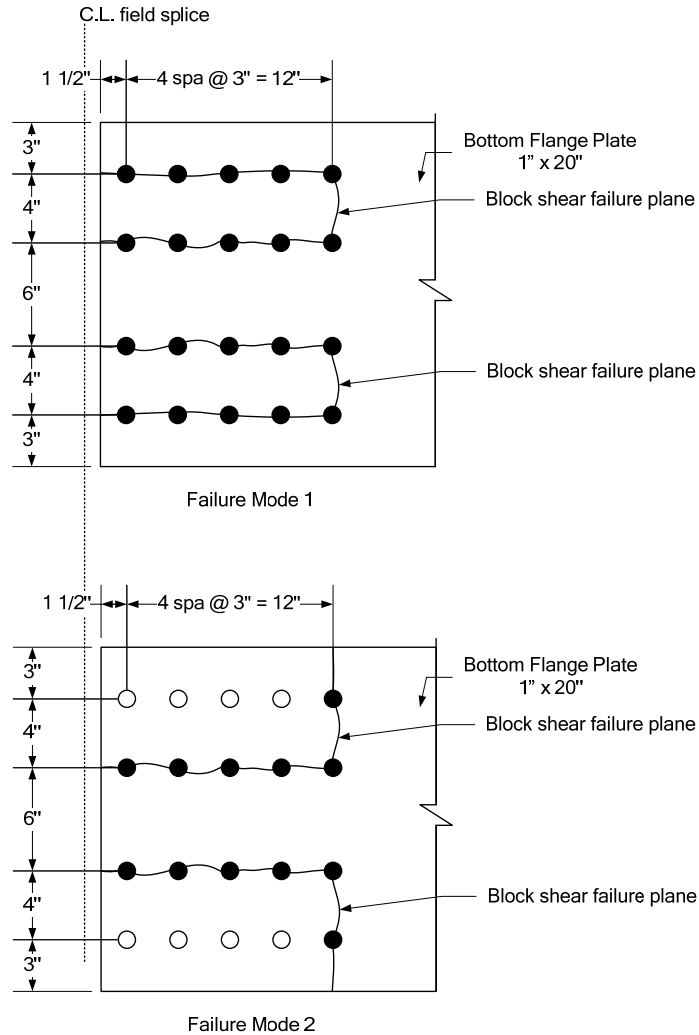
Failure Mode 2

For Failure Mode 1:

$$A_{tn} = 2[4.0 - 1.0](1.0) = 6.00 \text{ in}^2$$

$$A_{vn} = 4[4(3.0) + 1.5 - 4.5(1.0)](1.0) = 36.0 \text{ in}^2$$

$$A_{tn}/A_{vn} = 6.00/36.0 = 0.17 < 0.58$$

Therefore:

$$R_r = \phi_{bs}\left(0.58F_u A_{vn} + F_y A_{tg}\right)$$

AASHTO LRFD Equation 6.13.4-2

$$A_{tg} = 2(4.0)(1.0) = 8.00 \text{ in}^2$$

$$R_r = 0.80[0.58(85)(36.0) + 70(8.00)] = 1868 \text{ kips} > 613.5 \text{ kips ok}$$

For Failure Mode 2:

$$A_{tn} = 2[4.0 + 3.0 - 1.5(1.0)](1.0) = 11.00 \text{ in}^2$$

$$A_{vn} = 2[4(3.0) + 1.5 - 4.5(1.0)](1.0) = 18.00 \text{ in}^2$$

$$A_{tn}/A_{vn} = 11.00/18.00 = 0.61 > 0.58$$

Therefore:

$$R_r = \phi_{bs}\left(0.58F_y A_{vg} + F_u A_{tn}\right)$$

AASHTO LRFD Equation 6.13.4-1

A_{vg} is the gross area along the planes resisting the shear stress.

$$A_{vg} = 2[4(3.0) + 1.5](1.0) = 27.00 \text{ in}^2$$

$$R_r = 0.80[0.58(70)(27.00) + 85(11.00)] = 1625 \text{ kips} > 613.5 \text{ kips} \text{ ok}$$

Check for net section fracture of the critical bottom flange at the point of splice when subject to tension at the strength limit state according to the following requirement (refer to Section 2.2.3.7.1 of this chapter):

$$f_t \le 0.84\left(\frac{A_n}{A_g}\right)F_u \le F_{yt}$$

AASHTO LRFD Equation 6.10.1.8-1

The flange on the left-hand side of the splice is the critical flange for this particular check.

$$0.84\left(\frac{A_n}{A_g}\right)F_u = 0.84\left(\frac{19.25}{24.75}\right)70 = 45.7 \text{ ksi} < F_{yt} = 50 \text{ ksi}$$

From separate calculations, f_t in the bottom flange at the strength limit state (Strength I) is equal to +21.73 ksi for the section on the left-hand side of the splice, which is less than 45.7 ksi. Therefore, net section fracture of the bottom flange at the point of splice will not occur.

Since the combined area of the inside and outside flange splice plates is less than the area of the smaller flange at the splice, check the fatigue stresses in the base metal of the bottom flange splice plates adjacent to the slip-critical bolted connections. Also, check the flexural stresses in the splice plates at the service limit state under the Service II load combination. Although the area of the splice plates is less than the area of the flange in this case, design of the splice for the specified minimum design force is assumed to provide adequate stiffness and strength. By inspection, the bottom flange is subject to a net tensile stress. The moments at the

point of splice due to the factored fatigue load (factored by the 0.75 load factor specified for the Fatigue load combination) plus the 15 percent dynamic load allowance are:

M_{+LL+IM} = +721 kip-ft
M_{-LL+IM} = - 505 kip-ft

The maximum flange stresses rather than the stresses at the midthickness of the flange (acting on the gross section) will be conservatively used in the fatigue check. It will be assumed that the conditions spelled out in *AASHTO LRFD* Article 6.6.1.2.1 are met such that the fatigue live load stresses can be computed using the short-term composite section assuming the concrete deck is effective for both positive and negative flexure. Therefore, using the section properties of the smaller section at the point of splice:

$$f_{+LL+IM} = \frac{721(12)}{2,706} = 3.20 \text{ ksi} \qquad \text{(tension)}$$

$$f_{-LL+IM} = \frac{-505(12)}{2,706} = -2.24 \text{ ksi (compression)}$$

$$\gamma(\Delta f) = f_{+LL+IM} + |f_{-LL+IM}| = 3.20 + |-2.24| = 5.44 \text{ ksi}$$

For checking the base metal at the gross section of high-strength bolted slip-resistant connections, the fatigue detail category is Category B (*AASHTO LRFD* Table 6.6.1.2.3-1). From separate calculations, assuming an $(ADTT)_{SL}$ of 1600 trucks per day, the nominal fatigue resistance $(\Delta F)_n$ for a fatigue Category B detail is computed to be 8.00 ksi (see the earlier chapter on Fatigue Limit State Verifications). The range of flange force in the smaller bottom flange is computed from the stress range as follows:

$$\Delta P = 5.44(1.0)(20.0) = 108.8 \text{ kips}$$

The range of fatigue force and stress in the outside splice plate is computed as:

$$\Delta P = \frac{108.8}{2} = 54.4 \text{ kips}$$

$$\Delta f = \frac{54.4}{(0.5)(18.0)} = 6.04 \text{ ksi} < (\Delta F)_n = 8.00 \text{ ksi ok}$$

The range of fatigue force and stress in the inside splice plates is computed as:

$$\Delta P = \frac{108.8}{2} = 54.4 \text{ kips}$$

$$\Delta f = \frac{54.4}{2(0.5625)(8.0)} = 6.04 \text{ ksi} < (\Delta F)_n = 8.00 \text{ ksi ok}$$

At the service limit state, the stress in the splice plates under the Service II load combination will be checked against a limiting stress of $0.95F_y$, where F_y is the specified minimum yield strength of the splice plates (refer to Section 2.3.4.2.2.2.3 of this chapter). The minimum service limit state design force P_s for the splice was computed earlier to be 320.8 kips. As discussed previously in Section 2.3.4.2.2.2.3, the minimum design force at the service limit state should always be assumed divided equally to the two slip planes regardless of the ratio of the splice plate areas. Therefore, the force on the outside and inside splice plates will be taken as 320.8/2 = 160.4 kips. The resulting stress on the gross area of the outside splice plate is:

$$f = \frac{160.4}{(0.5)(18.0)} = 17.8 \text{ ksi} < 0.95(50) = 47.5 \text{ ksi} \text{ ok}$$

The stress on the gross area of the inside splice plates is:

$$f = \frac{160.4}{2(0.5625)(8.0)} = 17.8 \text{ ksi} < 0.95(50) = 47.5 \text{ ksi} \text{ ok}$$

Top Flange Splice

The width of the outside splice plate should be at least as wide as the width of the narrowest flange at the splice. Therefore, try a 7/16" x 16" outside splice plate with two 1/2" x 7" inside splice plates. A filler plate is not required. All plates are ASTM A 709 Grade 50W steel.
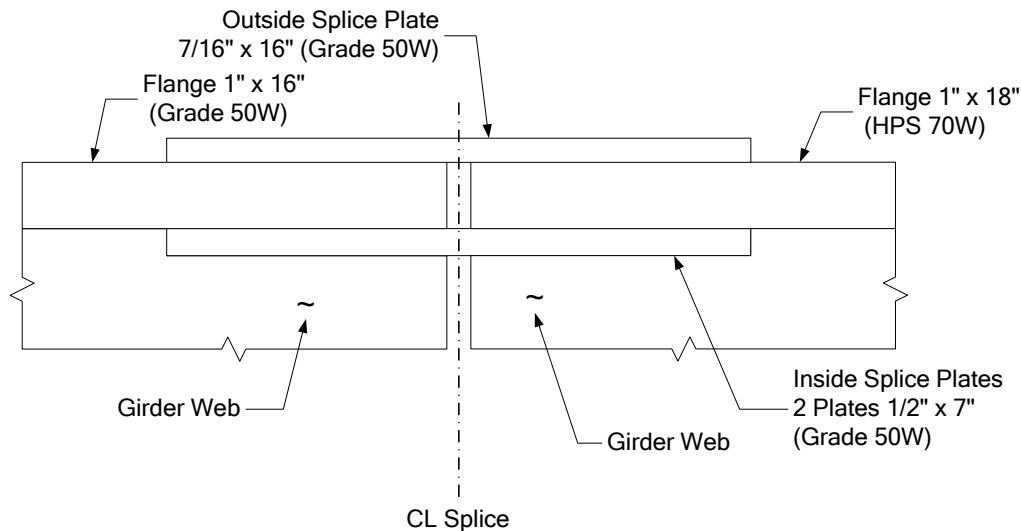
As the areas of the inner and outer plates are equal, the design force will be equally divided to the inner and outer plates and the shear resistance of the bolted connection at the strength limit state will be checked for the total minimum flange design force assumed acting in double shear.

The factored yield resistance of the splice plates in tension at the strength limit state is checked as follows:

Outside plate:

$$R_r = 0.95(50)(16.0)(0.4375) = 332.5 \text{ kips} > 530.6 / 2 = 265.3 \text{ kips} \quad \text{ok}$$

Inside plates:

$$R_r = 0.95(50)(2)(7.0)(0.5) = 332.5 \text{ kips} > 530.6 / 2 = 265.3 \text{ kips} \quad \text{ok}$$

The factored net section fracture resistance of the splice plates in tension at the strength limit state is checked as follows:

Outside plate:

$$R_r = 0.80(70)[16.0 - 4(0.875 + 0.125)](0.4375)(1.0) = 294.0 \text{ kips} > 530.6 / 2 = 265.3 \text{ kips} \quad \text{ok}$$

Inside plates:

$$R_r = 0.80(70)[2(7.0) - 4(0.875 + 0.125)](0.5)(1.0) = 280.0 \text{ kips} > 530.6 / 2 = 265.3 \text{ kips} \quad \text{ok}$$

Also, according to *AASHTO LRFD* Article 6.13.5.2, for splice plates subject to tension, A_n must not exceed $0.85A_g$.

Outside plate:

$$0.85(16.0)(0.4375) = 5.95 \text{ in}^2 > A_n = [16.0 - 4(1.0)](0.4375) = 5.25 \text{ in.}^2 \quad \text{ok}$$

Inside plates:

$$0.85(2)(7.0)(0.5) = 5.95 \text{ in}^2 > A_n = [2(7.0) - 4(1.0)](0.5) = 5.00 \text{ in.}^2 \quad \text{ok}$$

The block shear rupture resistance of the splice plates will be checked later.

The factored resistance of the splice plates in compression at the strength limit state is checked as follows:

Outside plate:

$$R_r = 0.90(50)(16)(0.4375) = 315.0 \text{ kips} > 600.0 / 2 = 300.0 \text{ kips} \quad \text{ok}$$

Inside plates:

$$R_r = 0.90(50)(2)(7.0)(0.5) = 332.5 \text{ kips} > 600.0 / 2 = 300.0 \text{ kips} \quad \text{ok}$$

The minimum number of bolts required to develop the governing minimum design force in the flange in shear at the strength limit state (in the absence of a filler plate) is:

$$N = \frac{P}{R_r} = \frac{600.0}{55.3} = 10.8 \text{ bolts} \quad \text{Use N = 12 bolts}$$

For the left-hand side of the splice, which is deemed the smaller section, the Service II stress in the top flange is computed as follows:

A. Dead Load + Positive Live Load:

$$f = \left[1.0(-1.86 + -0.12 + -0.13) + 1.3(-2.05)\right] = -4.78 \text{ ksi} \quad \text{(controls)}$$

B. Dead Load + Negative Live Load:

$$f = \left[1.0(-1.86 + -0.12 + -0.13) + 1.3(+4.43)\right] = +3.65 \text{ ksi}$$

Therefore, f_s is equal to -4.78 ksi and F_s is equal to f_s/R_h = -4.78/1.0 = -4.78 ksi. The stress at the mid-thickness of the top flange due to the deck-casting sequence (the Strength IV load combination controls) is:

$$f = \frac{1.5(1,300)(12)(39.125)}{62,658} = -14.61 \text{ ksi} \qquad \frac{f}{R_h} = \frac{-14.61}{1.0} = -14.61 \text{ ksi}$$

which is greater than F_s; therefore, the stress due to the deck-casting sequence controls the slip resistance check. The design force P_s for the flange splice is taken as this stress times the smaller gross flange area on either side of the splice, or

$$P_s = |-14.61|(1.0)(16.0) = 233.8 \text{ kips}$$

The minimum number of bolts required to provide adequate slip resistance under this design force is:

$$N = \frac{P}{R_r} = \frac{233.8}{39.0} = 6.0 \text{ bolts}$$

which is less than the minimum number of bolts required to provide adequate factored shear resistance at the strength limit state (i.e. N = 12 bolts). Thus, use twelve (12) 7/8-in. diameter high-strength bolts on each side of the top flange splice (3 rows of bolts with 4 bolts per row -- no stagger).

The bolt spacing and bolt edge and end distances shown in the figure below satisfy the appropriate requirements as illustrated earlier for the bottom flange splice.
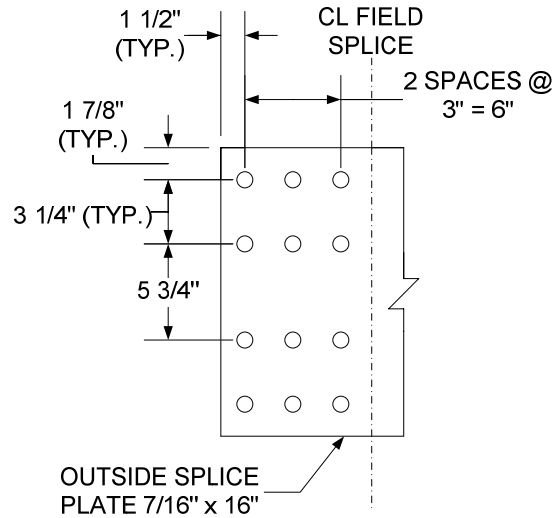
Check the bearing resistance at the bolt holes at the strength limit state. Since the sum of the inner and outer splice plate thicknesses times the specified minimum tensile strength F_u of the splice plates is less than the thickness of each flange times its corresponding F_u, the thinner outside splice plate controls the bearing resistance of the connection.

For the four bolts adjacent to the end of the splice plate, the end distance is 1.5 in. Therefore, the clear end distance L_c between the edge of the hole and the end of the splice plate is:

$$L_c = 1.5 - \frac{1.0}{2} = 1.0 \text{ in.}$$

Therefore:
$$R_n = 4(1.2L_c tF_u) = 4[1.2(1.0)(0.4375)(70)] = 147.0 \text{ kips (governs)}$$

or:
$$R_n = 4(2.4dtF_u) = 4[2.4(0.875)(0.4375)(70)] = 257.3 \text{ kips}$$

For the other eight bolts, the center-to-center distance between the bolts in the direction of the applied force is 3.0 in. Therefore, the clear distance L_c between the edges of the adjacent holes is:

$$L_c = 3.0 - 1.0 = 2.0 \text{ in.}$$

Therefore:
$$R_n = 8(1.2L_c tF_u) = 8[1.2(2.0)(0.4375)(70)] = 588.0 \text{ kips}$$

or:
$$R_n = 8(2.4dtF_u) = 8[2.4(0.875)(0.4375)(70)] = 514.5 \text{ kips (governs)}$$

The total nominal bearing resistance of the splice plate is therefore:

$$R_n = 147.0 \text{ kips} + 514.5 \text{ kips} = 661.5 \text{ kips}$$

$$R_r = 0.80(661.5) = 529.2 \text{ kips} > \frac{600.0}{2} = 300.0 \text{ kips} \text{ ok}$$

Check the block shear rupture resistance of the top flange splice plates and the top flange when subject to the minimum design force in tension at the strength limit state. Assume the same potential block shear failure planes on the outside and inside splice plates as shown previously for the bottom flange splice plates (refer to the previous figure).

Check the outside splice plate. A_{tn} is the net area along the place resisting the tensile stress.

$$A_{tn} = 2[3.25 + 1.875 - 1.5(1.0)](0.4375) = 3.17 \text{ in}^2$$

A_{vn} is the net area along the place resisting the shear stress.

$$A_{vn} = 2[2(3.0) + 1.5 - 2.5(1.0)](0.4375) = 4.38 \text{ in}^2$$

$$A_{tn}/A_{vn} = 3.17/4.38 = 0.72 > 0.58$$

Therefore:
$$R_r = \phi_{bs}\left(0.58F_y A_{vg} + F_u A_{tn}\right)$$

AASHTO LRFD Equation 6.13.4-1

A_{vg} is the gross area along the planes resisting the shear stress.

$$A_{vg} = 2[2(3.0) + 1.5](0.4375) = 6.56 \text{ in}^2$$

$$R_r = 0.80[0.58(50)(6.56) + 70(3.17)] = 329.7 \text{ kips} > \frac{530.6}{2} = 265.3 \text{ kips} \text{ ok}$$

Check the inside splice plates.

$$A_{tn} = 2[3.25 + 1.875 - 1.5(1.0)](0.5) = 3.63 \text{ in}^2$$

$$A_{vn} = 2[2(3.0) + 1.5 - 2.5(1.0)](0.5) = 5.00 \text{ in}^2$$

$$A_{tn}/A_{vn} = 3.63/5.00 = 0.73 > 0.58$$

$$A_{vg} = 2[2(3.0) + 1.5](0.5) = 7.50 \text{ in}^2$$

$$R_r = 0.80[0.58(50)(7.50) + 70(3.63)] = 377.3 \text{ kips} > \frac{530.6}{2} = 265.3 \text{ kips} \text{ ok}$$

Check the critical girder flange at the splice. Since the areas and yield strengths of the flanges on each side of the splice differ, both sides would need to be checked. Only the calculations for the flange on the left side of the splice, which is determined to be the critical flange, are shown below. The same two potential failure modes are investigated as for the bottom flange (refer to the previous figure).

For Failure Mode 1:

$$A_{tn} = 2[3.25 - 1.0](1.0) = 4.50 \text{ in}^2$$

$$A_{vn} = 4[2(3.0) + 1.5 - 2.5(1.0)](1.0) = 20.0 \text{ in}^2$$

$$A_{tn}/A_{vn} = 4.50/20.0 = 0.23 < 0.58$$

Therefore:

$$R_r = \phi_{bs}(0.58F_uA_{vn} + F_yA_{tg})$$

                                        AASHTO LRFD Equation 6.13.4-2

A_{tg} is the gross area along the plane resisting the tensile stress.

$$A_{tg} = 2(3.25)(1.0) = 6.50 \text{ in}^2$$

$$R_r = 0.80[0.58(70)(20.0) + 50(6.50)] = 909.6 \text{ kips} > 530.6 \text{ kips} \text{ ok}$$

For Failure Mode 2:

$$A_{tn} = 2[3.25 + 1.875 - 1.5(1.0)](1.0) = 7.25 \text{ in}^2$$

$$A_{vn} = 2[2(3.0) + 1.5 - 2.5(1.0)](1.0) = 10.00 \text{ in}^2$$

$$A_{tn}/A_{vn} = 7.25/10.00 = 0.73 > 0.58$$

Therefore:

$$R_r = \phi_{bs}(0.58F_yA_{vg} + F_uA_{tn})$$

                                        AASHTO LRFD Equation 6.13.4-1

A_{vg} is the gross area along the planes resisting the shear stress.

$$A_{vg} = 2[2(3.0) + 1.5](1.0) = 15.00 \text{ in}^2$$

$$R_r = 0.80[0.58(50)(15.00) + 70(7.25)] = 754.0 \text{ kips} > 530.6 \text{ kips} \text{ ok}$$

Check for net section fracture of the critical top flange at the point of splice when subject to tension at the strength limit state according to *AASHTO LRFD* Equation 6.10.1.8-1.

The flange on the left-hand side of the splice is the critical flange for this particular check.

$$0.84 \left(\frac{A_n}{A_g} \right) F_u = 0.84 \left(\frac{12.0}{16.0} \right) 70 = 44.1 \, \text{ksi} < F_{yt} = 50 \, \text{ksi}$$

From separate calculations, f_t in the top flange at the strength limit state (Strength I) is equal to +13.63 ksi for the section on the left-hand side of the splice, which is less than 44.1 ksi. Therefore, net section fracture of the top flange at the point of splice will not occur.

Since the combined area of the inside and outside flange splice plates is less than the area of the smaller flange at the splice, check the fatigue stresses in the base metal of the top flange splice plates adjacent to the slip-critical bolted connections. Also, check the flexural stresses in the splice plates at the service limit state under the Service II load combination.

The factored fatigue live load plus impact moments were given earlier. The maximum flange stresses rather than the stresses at the midthickness of the flange (acting on the gross section) will be conservatively used in the fatigue check. It will again be assumed that the conditions spelled out in *AASHTO LRFD* Article 6.6.1.2.1 are met such that the fatigue live load stresses can be computed using the short-term composite section assuming the concrete deck is effective for both positive and negative flexure. First, determine if the top flange splice plate is subject to a net tensile stress under the unfactored permanent loads plus twice the factored fatigue load plus impact, as specified in *AASHTO LRFD* Article 6.6.1.2.1. The future wearing surface will be conservatively neglected in this calculation.

$$f_{DC1} = \frac{248(12)}{1,581} = -1.88 \, \text{ksi}$$

$$f_{DC2} = \frac{50(12)}{4,863} = -0.12 \, \text{ksi}$$

$$f_{-LL+IM} = \frac{2(-505)(12)}{13,805} = +0.88 \, \text{ksi}$$

Since |-1.88 + -0.12| = 2.00 ksi > 0.88 ksi, the top flange splice plate is not subject to a net tensile stress under the specified load combination and fatigue need not be checked.

At the service limit state, the stress in the splice plates under the Service II load combination will be checked against a limiting stress of $0.95F_y$, where F_y is the specified minimum yield strength of the splice plates. The minimum service limit state design force P_s for the splice is equal to F_s (computed earlier) times the gross

area of the smaller flange at the point of splice =|-4.78|(1.0)(16.0) = 76.5 kips. As discussed previously in Section 2.3.4.2.2.2.3, the minimum design force at the service limit state should always be assumed divided equally to the two slip planes regardless of the ratio of the splice plate areas. Therefore, the force on the outside and inside splice plates will be taken as 76.5/2 = 38.3 kips. The resulting stress on the gross area of the outside splice plate is:

$$f = \frac{38.3}{(0.4375)(16.0)} = 5.5 \text{ ksi} < 0.95(50) = 47.5 \text{ ksi ok}$$

The stress on the gross area of the inside splice plates is:

$$f = \frac{38.3}{2(0.5)(7.0)} = 5.5 \text{ ksi} < 0.95(50) = 47.5 \text{ ksi ok}$$

2.3.4.2.2.4.3 Web Splice Design

The web splice will be designed based on the conservative assumption that the maximum moment and shear at the splice will occur under the same loading condition.

Determine the design shear in the web V_{uw} at the point of splice at the strength limit state. Compute the maximum shear at the splice due to the factored loads V_u at the strength limit state using the appropriate load factors given in *AASHTO LRFD* Tables 3.4.1-1 and 3.4.1-2. The Strength I load combination is used. Note that the minimum load factors γ_p from *AASHTO LRFD* Table 3.4.1-2 are applied to the permanent load shears when the corresponding shears are of opposite sign to the live load plus impact shear.

   A. Dead Load + Negative Live Load Shear:

$$V_u = 1.0\left[1.25(-82 + -12) + 1.5(-11) + 1.75(-112)\right] = -330 \text{ kips (governs)}$$

   B. Dead Load + Positive Live Load Shear:

$$V_u = 1.0\left[0.90(-82 + -12) + 0.65(-0.11) + 1.75(+19)\right] = -58.5 \text{ kips}$$

Calculate the factored shear resistance of the web $V_r = \phi_v V_n$ adjacent to the splice. From separate calculations, the smallest nominal shear resistance is for the web on the left-hand side of the splice. The transverse stiffener spacing adjacent to the splice on the left-hand side is d_o = 17'-3" = 207 in., which is equal to the maximum permitted spacing of $3D$ = 3(69.0) = 207 in. As discussed previously in Section 2.2.3.7.2.2 of this chapter, in order for a stiffened panel to develop the full post-buckling shear resistance, the section along the panel must satisfy the following relationship:

$$\frac{2Dt_w}{\left(b_{fc}t_{fc} + b_{ft}t_{ft}\right)} \le 2.5$$

<p align="right">AASHTO LRFD Equation 6.10.9.3.2-1</p>

$$\frac{2(69.0)(0.5)}{\left[16(1.0) + 18(1.375)\right]} = 1.69 < 2.5$$

Therefore:

$$V_n = V_p \left[C + \frac{0.87(1-C)}{\sqrt{1 + \left(\dfrac{d_o}{D}\right)^2}} \right]$$

<p align="right">AASHTO LRFD Equation 6.10.9.3.2-2</p>

$$k = 5 + \frac{5}{\left(\dfrac{d_o}{D}\right)^2}$$

<p align="right">AASHTO LRFD Equation 6.10.9.3.2-7</p>

$$k = 5 + \frac{5}{\left(\dfrac{207.0}{69.0}\right)^2} = 5.56$$

Since,

$$1.40\sqrt{\frac{Ek}{F_{yw}}} = 1.40\sqrt{\frac{29,000(5.56)}{50}} = 79.5 < \frac{D}{t_w} = \frac{69.0}{0.5} = 138.0$$

$$C = \frac{1.57}{\left(\dfrac{D}{t_w}\right)^2}\left(\frac{Ek}{F_{yw}}\right)$$

<p align="right">AASHTO LRFD Equation 6.10.9.3.2-6</p>

$$C = \frac{1.57}{(138.0)^2}\left(\frac{29,000(5.56)}{50}\right) = 0.266$$

$$V_p = 0.58F_{yw}Dt_w$$

<p align="right">AASHTO LRFD Equation 6.10.9.3.2-3</p>

$$V_p = 0.58(50)(69.0)(0.5) = 1,001\,\text{kips}$$

Therefore,
$$V_n = 1{,}001 \left[0.266 + \frac{0.87(1 - 0.266)}{\sqrt{1 + \left(\dfrac{207.0}{69.0}\right)^2}} \right] = 468 \text{ kips}$$

$$V_r = \phi_v V_n = 1.0(468) = 468 \text{ kips} > |V_u| = 330 \text{ kips}$$

As specified in *AASHTO LRFD* Article 6.13.6.1.4b, the equation to use to compute the design shear V_{uw} depends on the value of V_u with respect to $V_r = \phi_v V_n$ as follows:

$$0.5\phi_v V_n = 0.5(468) = 234 \text{ kips}$$
$$|V_u| = 330 \text{ kips} > 234 \text{ kips}$$

Therefore:
$$V_{uw} = \frac{(V_u + \phi_v V_n)}{2}$$

AASHTO LRFD Equation 6.13.6.1.4b-2

$$V_{uw} = \frac{\left(|-330| + 468\right)}{2} = 399 \text{ kips}$$

Two vertical rows of bolts with 14 bolts per row will be investigated. According to *AASHTO LRFD* Article 6.13.6.1.4a, a minimum of two rows of bolts is required on each side of the joint to ensure proper alignment and stability of the girder during construction. The bolts are spaced horizontally and vertically as shown below.

2 Spa at 3" = 6"
(12 Bolts Total)

Outside Splice Plate
7/16" x 16"
(Grade 50W)

Flange Plate
1" x 18"
(Grade HPS 70W)

Flange Plate
1" x 16"
(Grade 50W)

5 ¼"

Inside Splice Plates
½" x 7"
(Grade 50W)

3"   3"

4 ½"

Web Plate
½" x 69"
(Grade 50W)

13 Spa of 4 ½"
= 58 ½"

Web Plate
9/16" x 69"
(Grade 50W)

Web Splice Plates
3/8" x 63"
(Grade 50W)

Inside Splice Plates
9/16" x 8"
(Grade 50W)

5 ¼"

Flange Plate
1 3/8" x 18"
(Grade 50W)

4 Spa at 3" = 12"
(20 Bolts Total)

Fill Plate
3/8" x 18"
(Grade 50W)

Flange Plate
1" x 20"
(Grade HPS 70W)

Outside Splice Plate
½" x 18"
(Grade 50W)

All Bolts –
7/8" Dia. (ASTM A325)
H.S. Bolts

The outermost bolts are located 5¼" inches from the flanges to provide clearance for assembly (see Reference 5 for bolt assembly clearances). The web is spliced symmetrically by plates with a thickness not less than one-half the web thickness. Assume 3/8" x 63" splice plates on each side of the web. The splice plates are ASTM A 709 Grade 50W steel. As permitted in *AASHTO LRFD* Article 6.13.6.1.5 (and discussed below), a fill plate is not included since the difference in thickness of the web plates on either side of the splice does not exceed 0.0625 in. (i.e. 1/16 in.). Although not illustrated here, the number of bolts in the web splice could be decreased by spacing a group of bolts closer to the mid-depth of the web (where the flexural stress is relatively low) at the maximum spacing specified for sealing

(*AASHTO LRFD* Article 6.13.2.6.2), and by spacing the remaining two groups of bolts near the top and bottom of the web at a closer spacing.

Calculate the design moment M_{uv} due to the eccentricity of the design shear at the point of splice at the strength limit state as follows:

$$M_{uv} = V_{uw}e$$

Referring to the preceding figure, the correct eccentricity to use is the horizontal distance from the centerline of the splice to the centroid of the web bolt group on the side of the joint under consideration as follows:

$$e = \left(2.25 + \frac{3.0}{2}\right)\frac{1}{12} = 0.3125 \text{ ft}$$

$$M_{uv} = 399.0(0.3125) = 124.7 \text{ kip} - \text{ft}$$

Determine the portion of the flexural moment to be resisted by the web M_{uw} and the horizontal design force resultant H_{uw} in the web at the strength limit state. Use the equations provided in *AASHTO LRFD* Article C6.13.6.1.4b. Again, since the splice is located in an area of stress reversal, checks must be made for both the positive and negative flexure conditions.

Positive Flexure

For the case of positive flexure, the controlling flange was previously determined to be the bottom flange. The maximum flexural stress due to the factored loads at the midthickness of the controlling flange f_{cf}, and the minimum design stress for the controlling flange F_{cf}, were previously computed for this loading condition to be:

$$f_{cf} = +21.46 \text{ ksi}$$
$$F_{cf} = +37.50 \text{ ksi}$$

For the same loading condition, the concurrent flexural stress at the mid-thickness of the noncontrolling (top) flange was previously computed to be:

$$f_{ncf} = -6.26 \text{ ksi}$$

The portion of the flexural moment assumed to be resisted by the web is computed as:

$$M_{uw} = \frac{t_w D^2}{12}\left|R_h F_{cf} - R_{cf} f_{ncf}\right|$$

AASHTO LRFD Equation C6.13.6.1.4b-1

where the hybrid factor R_h is taken as 1.0 for a homogeneous section and ratio R_{cf} is computed as follows:

$$R_{cf} = \left| \frac{F_{cf}}{f_{cf}} \right| = \left| \frac{+37.50}{+21.46} \right| = 1.75$$

Therefore:

$$M_{uw} = \frac{0.5(69.0)^2}{12} \left| 1.0(+37.50) - 1.75(-6.26) \right| = 9{,}612 \text{ kip} - \text{in.} = 801.0 \text{ kip} - \text{ft}$$

The design horizontal force resultant for this loading condition is computed as:

$$H_{uw} = \frac{t_w D}{2} \left(R_h F_{cf} + R_{cf} f_{ncf} \right)$$

AASHTO LRFD Equation C6.13.6.1.4b-2

$$H_{uw} = \frac{0.5(69.0)}{2} \left[1.0(+37.50) + 1.75(-6.26) \right] = +457.9 \text{ kips}$$

Note that all stresses in the above equations are to be taken as signed quantities. Since the sign of M_{uw} corresponds to the sign of the flexural moment for the loading condition under consideration, absolute value signs are applied to the resulting difference of the stresses for convenience. H_{uw} is always taken as a signed quantity; positive for tension, negative for compression. Check the above computed values of M_{uw} and H_{uw}. For the web, the section modulus $S = (0.5)(69.0)^2/6 = 396.8$ in.^{3} and the area $A = 0.5(69.0) = 34.5$ in.^{2}. Therefore:

$$f_{bot} = \frac{801.0(12)}{396.8} + \frac{457.9}{34.5} = 37.50 \text{ ksi} = R_h F_{cf} \quad \text{ok}$$

$$f_{top} = -\frac{801.0(12)}{396.8} + \frac{457.9}{34.5} = -10.95 \text{ ksi} = R_{cf} f_{ncf} = 1.75(-6.26) \quad \text{ok}$$

The use of $R_h F_{cf}$ and the application of the factor R_{cf} to f_{ncf} in essence is factoring up the stresses in the web by the same amount as the stresses in the controlling flange so that the web splice is designed in a consistent fashion at the strength limit state.

The total moment on the web splice for this condition is equal to the sum of M_{uv} and M_{uw}:

$$M_{tot} = M_{uv} + M_{uw} = 124.7 + 801.0 = 925.7 \text{ kip} - \text{ft}$$

Negative Flexure

For the case of negative flexure, the controlling flange was also previously determined to be the bottom flange. The maximum flexural stress due to the factored loads at the midthickness of the controlling flange f_{cf}, and the minimum design stress for the controlling flange F_{cf}, were previously computed for this loading condition to be:

$$f_{cf} = -14.76 \text{ ksi}$$
$$F_{cf} = -37.50 \text{ ksi}$$

For the same loading condition, the concurrent flexural stress at the mid-thickness of the noncontrolling (top) flange was previously computed to be:

$$f_{ncf} = +13.44 \text{ ksi}$$

The ratio R_{cf} is computed as follows:

$$R_{cf} = \left|\frac{F_{cf}}{f_{cf}}\right| = \left|\frac{-37.50}{-14.76}\right| = 2.54$$

Therefore:

$$M_{uw} = \frac{0.5(69.0)^2}{12}\left|1.0(-37.50) - 2.54(+13.44)\right| = 14{,}211 \text{ kip} - \text{in.} = 1{,}184 \text{ kip} - \text{ft}$$

The design horizontal force resultant for this loading condition is computed as:

$$H_{uw} = \frac{0.5(69.0)}{2}\left[1.0(-37.50) + 2.54(+13.44)\right] = -58.0 \text{ kips}$$

Check the above computed values of M_{uw} and H_{uw}:

$$f_{bot} = -\frac{1{,}184(12)}{396.8} - \frac{58.0}{34.5} = -37.50 \text{ ksi} = R_h F_{cf} \quad \text{ok}$$

$$f_{top} = \frac{1{,}184(12)}{396.8} - \frac{58.0}{34.5} = +34.13 \text{ ksi} = R_{cf} f_{ncf} = 2.54(+13.44) \quad \text{ok}$$

The total moment on the web splice for this condition is equal to the sum of M_{uv} and M_{uw}:

$$M_{tot} = M_{uv} + M_{uw} = 124.7 + 1{,}184 = 1{,}309 \text{ kip} - \text{ft}$$

Check the web-splice bolts for shear at the strength limit state assuming the bolts in the connection have slipped and gone into bearing. The web-splice bolts are to be designed for the effects of the design shear, the moment due to the eccentric design shear, and the flexural moment and horizontal design force resultant in the web, which are all assumed applied at the mid-depth of the web. The traditional elastic vector method is used for calculating the maximum resultant bolt force (refer to Section 2.3.2.5 of this chapter). The polar moment of inertia I_p of the bolts with respect to the centroid of the connection is computed as follows:

$$I_p = \frac{nm}{12}\left[s^2\left(n^2 - 1\right) + g^2(m^2 - 1)\right]$$

AASHTO LRFD Equation C6.13.6.1.4b-3

For the example web splice (referring to the preceding figure), $n = 14$; $m = 2$, $s = 4.5$ in.; and $g = 3.0$ in. Therefore:

$$I_p = \frac{14(2)}{12}\left[(4.5)^2\left(14^2 - 1\right) + (3.0)^2\left(2^2 - 1\right)\right] = 9{,}277 \text{ in.}^2$$

Determine the vertical bolt force R_v due to the design shear V_{uw} assuming two vertical rows with 14 bolts per row for a total number of bolts N_b equal to 28:

$$R_v = \frac{V_{uw}}{N_b} = \frac{399}{28} = 14.25 \text{ kips / bolt}$$

Positive Flexure

Determine the bolt force due to the horizontal design force resultant H_{uw}:

$$R_h = \frac{H_{uw}}{N_b} = \frac{457.9}{28} = 16.35 \text{ kips / bolt}$$

Determine the vertical and horizontal components of the force on the extreme bolt due to the total moment on the web splice M_{tot}:

$$R_{M_v} = \frac{M_{tot}\, x}{I_p} = \frac{925.7(12)(3.0/2)}{9{,}277} = 1.80 \text{ kips}$$

$$R_{M_h} = \frac{M_{tot}\, y}{I_p} = \frac{925.7(12)(29.25)}{9{,}277} = 35.02 \text{ kips}$$

The resultant bolt force on the extreme bolt is:

$$R = \sqrt{\left(R_v + R_{M_v}\right)^2 + \left(R_h + R_{M_h}\right)^2} = \sqrt{(14.25 + 1.80)^2 + (16.35 + 35.02)^2} = 53.82 \text{ kips}$$

Negative Flexure

Determine the bolt force due to the horizontal design force resultant H_{uw}:

$$R_h = \frac{H_{uw}}{N_b} = \frac{|-58.0|}{28} = 2.07 \text{ kips / bolt}$$

Determine the vertical and horizontal components of the force on the extreme bolt due to the total moment on the web splice M_{tot}:

$$R_{M_v} = \frac{M_{tot}\, x}{I_p} = \frac{1{,}309(12)(3.0/2)}{9{,}277} = 2.54 \text{ kips}$$

$$R_{Mh} = \frac{M_{tot}\, y}{I_p} = \frac{1{,}309(12)(29.25)}{9{,}277} = 49.53 \text{ kips}$$

The resultant bolt force on the extreme bolt is:

$$R = \sqrt{\left(R_v + R_{Mv}\right)^2 + \left(R_h + R_{Mh}\right)^2} = \sqrt{(14.25 + 2.54)^2 + (2.07 + 49.53)^2} = 54.26 \text{ kips} \ \ (\text{governs})$$

The factored shear resistance R_r for a 7/8-in. diameter A325 high-strength bolt in double shear assuming the threads are *excluded* from the shear planes was computed in an earlier example to be 55.3 kips/bolt (refer to Section 2.3.2.4.2.1 of this chapter). Note that the greater than 50.0 in. length reduction does *not* apply when computing the factored shear resistance of the bolts in a web splice since the distribution of shear force is essentially uniform along the joint. Therefore:

$$R = 54.26 \text{ kips} < R_r = 55.3 \text{ kips} \quad \text{ok}$$

AASHTO LRFD Article 6.13.6.1.4b requires that high-strength bolted connections for web splices be designed to prevent slip at the service limit state under the maximum resultant bolt force due to Load Combination Service II. In addition, *AASHTO LRFD* Article 6.13.6.1.4a requires that high-strength bolted splices for flexural members be proportioned to prevent slip during the erection of the steel (assuming an erection analysis is conducted) and during the casting of the concrete deck. As a minimum, for checking slip of the bolts, the design shear V_s is to be taken as the shear at the point of splice due to Load Combination Service II. The Service II shears at the point of splice for the positive and negative flexure conditions are computed as follows:

   A. Dead Load + Negative Live Load Shear:

$$V_s = \left[1.0(-82 + -12 + -11) + 1.3(-112)\right] = -251 \text{ kips} \ \ (\text{governs})$$

   B. Dead Load + Positive Live Load Shear:

$$V_s = \left[1.0(-82 + -12 + -0.11) + 1.3(+19)\right] = -80.3 \text{ kips}$$

The factored shear due to the deck-casting sequence (the Strength IV load combination controls) is computed as:

$$V = 1.5(-82) = -123 \text{ kips}$$

which is less than the governing value of V_s. Therefore, the design shear for checking slip of the web bolts will be taken as V_s.

Calculate the design moment M_{sv} due to the eccentricity of the design shear at the point of splice at the service limit state as follows:

$$M_{sv} = V_s e$$

$$M_{sv} = |-251.0|(0.3125) = 78.44 \text{ kip} - \text{ft}$$

Determine the portion of the flexural moment to be resisted by the web M_{sw} and the horizontal design force resultant H_{sw} in the web at the service limit state. The maximum Service II flexural stress at the midthickness of the bottom flange f_s was computed previously to be +16.04 ksi due to the positive flexure load condition. The flexural stress in the other (top) flange at the point of splice f_{os} concurrent with f_s in the bottom flange for this load condition is –4.78 ksi. The portion of the flexural moment assumed to be resisted by the web is computed as:

$$M_{sw} = \frac{t_w D^2}{12} |f_s - f_{os}|$$

$$M_{sw} = \frac{0.5(69.0)^2}{12} |+16.04 - (-4.78)| = 4{,}130 \text{ kip} - \text{in.} = 344.2 \text{ kip} - \text{ft}$$

The design horizontal force resultant for this loading condition is computed as:

$$H_{sw} = \frac{t_w D}{12} (f_s + f_{os})$$

$$H_{uw} = \frac{0.5(69.0)}{2} [+16.04 + (-4.78)] = +194.2 \text{ kips}$$

Check the above computed values of M_{sw} and H_{sw}:

$$f_{bot} = \frac{344.2(12)}{396.8} + \frac{194.2}{34.5} = 16.04 \text{ ksi} = f_s \quad \text{ok}$$

$$f_{top} = -\frac{344.2(12)}{396.8} + \frac{194.2}{34.5} = -4.78 \text{ ksi} = f_{os} \quad \text{ok}$$

The total moment on the web splice for this condition is equal to the sum of M_{sv} and M_{sw}:

$$M_{tot} = M_{sv} + M_{sw} = 78.44 + 344.2 = 422.6 \text{ kip} - \text{ft}$$

In this case, the loading condition causing the maximum Service II flexural stress in the top flange is the same loading condition (i.e. the positive flexure condition). Therefore, slip of the web bolts only needs to be checked for the one load condition.

The traditional elastic vector method is again used for calculating the maximum resultant bolt force. Determine the vertical bolt force R_v due to the design shear V_s assuming two vertical rows with 14 bolts per row for a total number of bolts N_b equal to 28:

$$R_v = \frac{V_s}{N_b} = \frac{|-251|}{28} = 8.96 \text{ kips / bolt}$$

Determine the bolt force due to the horizontal design force resultant H_{sw}:

$$R_h = \frac{H_{sw}}{N_b} = \frac{194.2}{28} = 6.94 \text{ kips / bolt}$$

Determine the vertical and horizontal components of the force on the extreme bolt due to the total moment on the web splice M_{tot}:

$$R_{M_v} = \frac{M_{tot}x}{I_p} = \frac{422.6(12)(3.0/2)}{9,277} = 0.82 \text{ kips}$$

$$R_{M_h} = \frac{M_{tot}y}{I_p} = \frac{422.6(12)(29.25)}{9,277} = 15.99 \text{ kips}$$

The resultant bolt force on the extreme bolt is:

$$R = \sqrt{\left(R_v + R_{M_v}\right)^2 + \left(R_h + R_{M_h}\right)^2} = \sqrt{\left(8.96 + 0.82\right)^2 + \left(6.94 + 15.99\right)^2} = 24.93 \text{ kips}$$

The factored slip resistance R_r for a 7/8-in. diameter A325 high-strength bolt assuming a Class B surface condition for the faying surface, standard holes and two slip planes per bolt was computed in an earlier example to be 39.0 kips/bolt (refer to Section 2.3.2.4.1.1 of this chapter). Therefore:

$$R = 24.93 \text{ kips} < R_r = 39.0 \text{ kips} \quad \text{ok}$$

Check the bolt spacings and bolt edge and end distances for the web splice (refer to the preceding figure).

As specified in *AASHTO LRFD* Article 6.13.2.6.1, the minimum spacing between centers of bolts in standard holes is not to be less than $3.0d$, where d is the diameter of the bolt. For 7/8-in. diameter bolts:

$$s_{min} = 3d = 3(0.875) = 2.63 \text{ in.} < 3.0 \text{ in.} \quad \text{ok}$$

As specified in *AASHTO LRFD* Article 6.13.2.6.2, to seal against the penetration of moisture in joints, the spacing s of a single line of bolts adjacent to a free edge of an outside plate or shape (when the bolts are not staggered) must satisfy the following requirement:

$$s \le \left(4.0 + 4.0t\right) \le 7.0 \text{ in.}$$

AASHTO LRFD Equation 6.13.2.6.2-1

where t is the thickness of the thinner outside plate or shape. Check for sealing along the vertical edges of the web splice plates:

$$s_{max} = 4.0 + 4.0(0.375) = 5.5 \text{ in.} > 4.5 \text{ in. ok}$$

The edge distance of bolts is defined as the distance perpendicular to the line of force between the center of a hole and the edge of the component. In this example, the edge distance from the center of the vertical line of holes in the web plate to the edge of the field piece of 2-1/8 inches satisfies the minimum edge distance requirement of 1½ inches specified for 7/8-in. diameter bolts and sheared edges in *AASHTO LRFD* Table 6.13.2.6.6-1 (Table 2.17). This distance also satisfies the maximum edge distance requirement of 8.0t (not to exceed 5.0 in.) = 8.0(0.375) = 3.0 in. specified in *AASHTO LRFD* Article 6.13.2.6.6. The edge distance for the outermost vertical row of holes on the web splice plates is set at 2 inches.

The end distance of bolts is defined as the distance along the line of force between the center of a hole and the end of the component. In this example, the end distance of 2¼ inches at the top and bottom of the web splice plates satisfies the minimum end distance requirement of 1½ inches specified for 7/8-in. diameter bolts and sheared edges in *AASHTO LRFD* Table 6.13.2.6.6-1 (Table 2.17). The maximum end distance requirement of 8.0t (not to exceed 5.0 in.) = 8.0(0.375) = 3.0 in. specified in *AASHTO LRFD* Article 6.13.2.6.5 is also satisfied. Although not specifically required, note that the distance from the corner bolts to the corner of the web splice plate, equal to $\sqrt{(2.0)^2 + (2.25)^2} = 3.0 \text{ in.}$, also satisfies the maximum end distance requirement.

Check the bearing resistance at the web-splice bolt holes at the strength limit state. Since in this case the thickness of the thinner web at the point of splice times its specified minimum tensile strength F_u is less than the sum of the web splice-plate thicknesses times the corresponding F_u of the splice plates and the thickness of the thicker web at the point of splice times its corresponding F_u, the thinner web (on the left-hand side) controls the bearing resistance of the connection. The resistance of an outermost hole, calculated using the clear edge distance (which is smaller than the clear vertical distance between the bolt holes), can conservatively be checked against the maximum resultant bolt force acting on the extreme bolt in the connection (refer to the left-hand side of Figure 2.137). Since the resultant force acts in the direction of an inclined distance that is larger than the clear edge distance, the check is conservative. Other options for checking the bearing resistance were discussed previously. Based on the edge distance from the center of the hole to the edge of the field piece of 2-1/8 inches, the clear edge distance is computed as:

$$L_c = 2.125 - \frac{1.0}{2} = 1.625 \text{ in.}$$

For standard holes, the nominal bearing resistance R_n parallel to the applied bearing force is taken as follows:

$$R_n = 1.2L_c tF_u \leq 2.4dtF_u$$

AASHTO LRFD Equations C6.13.2.9-1 & 6.13.2.9-2

$$R_n = 1.2L_c tF_u = 1.2(1.625)(0.5)(70) = 68.25 \text{ kips (governs)}$$

or: $$R_n = 2.4dtF_u = 2.4(0.875)(0.5)(70) = 73.50 \text{ kips}$$

$$R_r = \phi_{bb} R_n$$

AASHTO LRFD Equation 6.13.2.2-2

$$R_r = 0.80(68.25) = 54.60 \text{ kips} > R = 54.26 \text{ kips ok}$$

Had the bearing resistance been exceeded, the preferred option would be to increase the edge distance slightly in lieu of increasing the number of bolts or thickening the web.

Check the block shear rupture resistance of the web splice plates at the strength limit state. Because of the overall length of the connection, the block shear rupture resistance normally does not control for web splice plates of typical proportion, but the check is illustrated here for completeness. Assume the block shear failure plane on the web splice plates shown below:
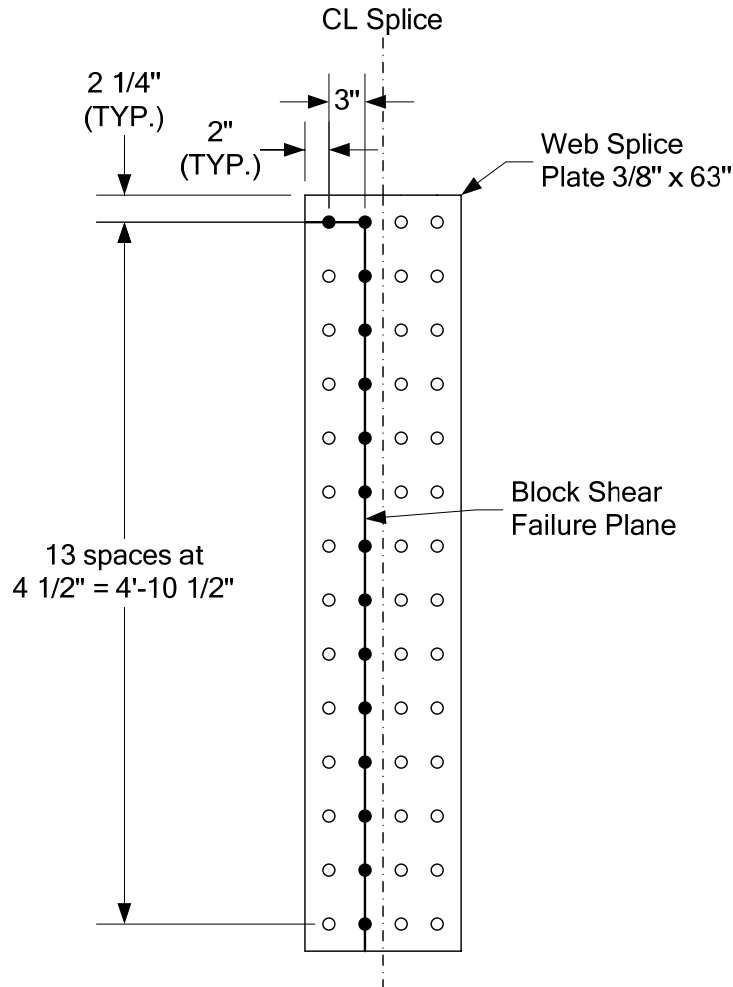
A_{tn} is the net area along the place resisting the tensile stress.

$$A_{tn} = 2[3.0 + 2.0 - 1.5(1.0)](0.375) = 2.63 \text{ in}^2$$

A_{vn} is the net area along the place resisting the shear stress.

$$A_{vn} = 2[63.0 - 2.25 - 13.5(1.0)](0.375) = 35.44 \text{ in}^2$$

$$A_{tn}/A_{vn} = 2.63/35.44 = 0.07 < 0.58$$

Therefore:

$$R_r = \phi_{bs}\left(0.58F_u A_{vn} + F_y A_{tg}\right)$$

AASHTO LRFD Equation 6.13.4-2

A_{tg} is the gross area along the plane resisting the tensile stress.

$$A_{tg} = 2[3.0 + 2.0](0.375) = 3.75 \text{ in}^2$$

$$R_r = 0.80[0.58(70)(35.44) + 50(3.75)] = 1{,}301 \text{ kips} > V_{uw} = 399 \text{ kips} \quad \text{ok}$$

Check for flexural yielding on the gross section of the web splice plates at the strength limit state.

$$A_{PL} = 2(0.375)(63.0) = 47.25 \text{ in.}^2$$

$$S_{PL} = \frac{2(0.375)(63.0)^2}{6} = 496.1 \text{ in.}^3$$

$$f_{PL} = \frac{M_{tot}}{S_{PL}} + \frac{H_{uw}}{A_{PL}}$$

For positive flexure:

$$f_{PL} = \frac{925.7(12)}{496.1} + \frac{457.9}{47.25} = 32.08 \text{ ksi} < \phi_f F_y = 1.0(50) = 50 \text{ ksi} \quad \text{ok}$$

For negative flexure:

$$f_{PL} = \frac{1{,}309(12)}{496.1} + \frac{|-58.0|}{47.25} = 32.89 \text{ ksi} < \phi_f F_y = 1.0(50) = 50 \text{ ksi} \quad \text{ok}$$

Check for shear yielding on the gross section of the web splice plates under the design shear V_{uw} at the strength limit state. As specified in *AASHTO LRFD* Article 6.13.5.3, the nominal shear resistance of a connected element R_n is conservatively based on the shear yield stress (i.e. $F_y/\sqrt{3} = 0.58F_y$) as follows (refer to Section 2.3.2.4.2.3 of this chapter):

$$R_n = 0.58A_g F_y$$
AASHTO LRFD Equation 6.13.5.3-2

$$R_n = 0.58(2)(0.375)(63.0)(50) = 1{,}370 \text{ kips}$$

The factored shear resistance of a connected element R_r is computed as follows:

$$R_r = \phi_v R_n$$
AASHTO LRFD Equation 6.13.5.3-1

$$R_r = 1.0(1{,}370) = 1{,}370 \text{ kips} > V_{uw} = 399 \text{ kips} \quad \text{ok}$$

Since the combined area of the web splice plates is greater than the area of the web on both sides of the splice, the fatigue stresses in the base metal of the web splice plates adjacent to the slip-critical bolted connections need not be checked. Also, the

flexural stresses in the splice plates at the service limit state under the Service II load combination need not be checked.

2.3.4.2.3 Tension Members

The design of bolted splices for tension members is covered in *AASHTO LRFD* Article 6.13.6.1.2. All bolted splices for tension members are to be designed using slip-critical connections (refer to Section 2.3.2.1.1 of this chapter), and are to satisfy the tensile resistance requirements for connected elements specified in *AASHTO LRFD* Article 6.13.5.2 (refer to Section 2.3.2.4.2.4 of this chapter). The splices are to be designed for the load as determined by the general requirements of *AASHTO LRFD* Article 6.13.1 for the smaller section at the point of splice (refer to Section 2.3.4.2.1 of this chapter).

2.3.4.2.4 Compression Members

The design of bolted splices for compression members is covered in *AASHTO LRFD* Article 6.13.6.1.2. Splices for compression members (e.g. arch members, truss chords and columns) may either be designed at the strength limit state as: 1) open joints (i.e. no contact between adjoining parts) with enough bolts provided in the splice to carry 100 percent of the load as determined by the general requirements of *AASHTO LRFD* Article 6.13.1 for the smaller section at the point of splice (refer to Section 2.3.4.2.1 of this chapter), or 2) milled joints in full contact bearing with the bolts designed to carry no less than 50 percent of the lower factored resistance of the sections spliced.   If the latter option is chosen, *AASHTO LRFD* Article 6.13.6.1.2 requires that the contract documents call for inspection of the joint during fabrication and erection. According to Reference 40, fabricators generally prefer the first option because it is less expensive and has the potential for fewer problems in the field.

The splices in these members are to be located as near as practicable to the panel points and usually on the side of the panel point where the smaller force effect occurs. The arrangement of all splice elements must make proper provision for all force effects in the component parts of the spliced members.

2.3.4.2.5 Fillers

The design of filler plates is covered in *AASHTO LRFD* Article 6.13.6.1.5. In bolted splices, filler plates are typically used when the thicknesses of the adjoining plates at the point of splice are different. Filler plates are frequently used on flange splices of flexural members (Figure 2.138). In such cases, it is often advantageous to transition one or more of the flange thicknesses down adjacent to the point of splice, if possible, so as to reduce the required size of the filler plate or eliminate the need for a filler plate altogether.
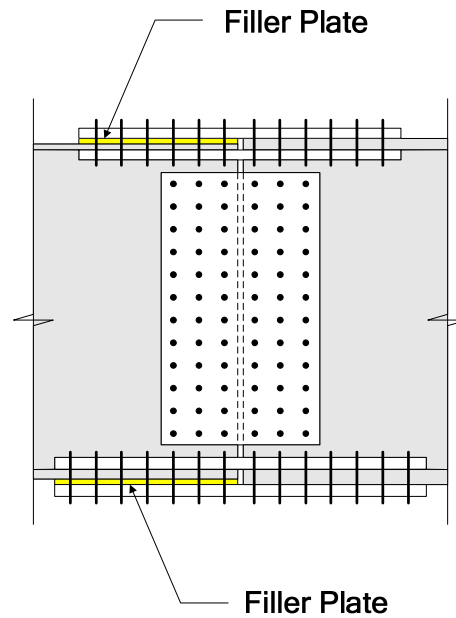
Figure 2.138 Filler Plates in Bolted Flange Splices

In axially loaded connections at the strength limit state, fillers must be secured by additional bolts to ensure that the fillers are an integral part of the connection; that is, to ensure that the shear planes are well-defined and that no reduction in the factored shear resistance of the bolts results.

AASHTO LRFD Article 6.13.6.1.5 provides two choices for developing fillers 0.25 in. or more in thickness in axially loaded bolted connections, which include girder flange splices. The choices are to either: 1) extend the fillers beyond the gusset or splice plate with the filler extension secured by enough additional bolts to distribute the total stress uniformly over the combined section of the member or filler, or 2) in lieu of extending and developing the fillers, reduce the factored shear resistance of the bolts (refer to Section 2.3.2.4.2.1 of this chapter) by the following factor:

$$R = \left[\frac{(1+\gamma)}{(1+2\gamma)} \right]$$
　　　　　　　　　　　　　　　　　　　Equation 2.304

AASHTO LRFD Equation 6.13.6.1.5-1

where:

γ　=　A_f / A_p

A_f　=　sum of the area of the fillers on the top and bottom of the connected plate (in.^{2})

A_p　=　smaller of either the connected plate area or the sum of the splice plate areas on the top and bottom of the connected plate (in.^{2})

Equation 2.304 was developed mathematically (*152*) and compared to the results from an experimental program on axially loaded bolted splice connections with undeveloped fillers (*153*). The reduction factor *R* accounts for the reduction in the nominal shear resistance of the bolts due to bending in the bolts and will likely result

in having to provide additional bolts in the connection to develop the filler(s). *Note that the reduction factor is only to be applied on the side of the connections with the filler(s).* Unlike the empirical reduction factor given in Reference 26, Equation 2.304 will typically be less than 1.0 for connections utilizing 0.25-in.-thick fillers in order to limit the deformation of the connection. Note that fillers 0.25-in. or more in thickness are not to consist of more than two plates, unless approved by the Engineer.

AASHTO LRFD Article 6.13.6.1.5 also requires that the specified minimum yield strength of fillers 0.25 in. or more in thickness not be less than the larger of 70 percent of the specified minimum yield strength of the connected plate and 36.0 ksi. To provide fully developed fillers that act integrally with the connected plate, the specified minimum yield strength of the fillers should theoretically be greater than or equal to the specified minimum yield strength of the connected plates times the factor $[1/(1+\gamma)]$, where γ is taken as defined above. However, this may not be practical or convenient in some cases due to thinner filler-plate material availability issues. Therefore, in some cases at the strength limit state, premature yielding of the fillers, bolt bending and increased deformation of the connection may occur. To control the potential for excessive deformation of the connection, the lower limit on the specified minimum yield strength of the fillers (given above) is specified. Although in some cases there may be an increased probability of larger deformations in the connection at the strength limit state, the connection bolts will still have adequate reserve shear resistance as long as the fillers are appropriately extended and developed, or in lieu of extending the fillers, additional bolts are added according to Equation 2.304. According to *AASHTO LRFD* Article C6.13.6.1.5, the effects of yielding of the fillers and connection deformation are not considered to be significant for connections with fillers less than 0.25 in. in thickness. Note that for connections involving the use of weathering steels, a weathering grade product should be specified for the filler-plate material.

At the service limit state, the resistance to slip between the filler and either connected part is comparable to the slip resistance that would exist between the connected parts if the filler were not present. Therefore, as specified in *AASHTO LRFD* Article 6.13.6.1.5, for slip-critical connections (refer to Section 2.3.2.1.1 of this chapter), the factored slip resistance of the bolts (refer to Section 2.3.2.4.1.1 of this chapter) under the Service II load combination is *not* to be adjusted for the effect of the fillers.

At bolted web splices where the thicknesses of the adjoining web plates differ by 0.0625 in. (1/16 in.) or less, *AASHTO LRFD* Article 6.13.6.1.5 permits the omission of filler plates.

2.3.4.3 Welded Splices

The design of welded splices is covered in *AASHTO LRFD* Article 6.13.6.2. Welded splices must also conform to the requirements given in the latest edition of Reference 136.

As a minimum, welded splices are to be designed according to the general design requirements given in *AASHTO LRFD* Article 6.13.1 for the smaller section at the

point of splice (refer to Section 2.3.4.2.1 of this chapter). Groove welds are typically used for the butt joints at welded splices (refer to Sections 2.3.3.3.1 and 2.3.3.8.2 of this chapter). According to *AASHTO* LRFD Article 6.13.6.2, complete penetration groove welds may be used to splice tension and compression members; the use of splice plates should be avoided. Fatigue should be checked at all welded splices subject to an applied net tensile stress (determined as specified in *AASHTO LRFD* Article 6.6.1.2.1) based on the appropriate fatigue detail category for the splice configuration given in *AASHTO LRFD* Table 6.6.1.2.3-1 (see the previous sections of this chapter on Fatigue Limit State Verifications).

As discussed previously in Section 2.2.3.2.1 of this chapter (Flange Width), changing flange widths at welded shop splices should be avoided if at all possible. Should it become necessary to splice material of different widths using welded butt joints, symmetric transitions must be used that conform to one of the details shown in *AASHTO LRFD* Figure 6.13.2.6.2-1.   The transition often starts at the butt splice. However, note that *AASHTO LRFD* Figure 6.13.2.6.2-1 shows a preferred detail in which the butt splice is located a minimum of 3.0 in. from the transition for greater ease in fitting the run-off tabs. At welded butt splices joining material of different thicknesses, the transition (including the weld) must be ground to a uniform slope between the offset surfaces of not more than 1 in 2.5 (and must be indicated as such in the contract documents).

Welded field splices are less commonly used. If used, they should be arranged to minimize overhead welding.

150. Sheikh-Ibrahim, F.I., and K.H. Frank. 1998. "The Ultimate Strength of Symmetric Beam Bolted Splices." AISC Engineering Journal, American Institute of Steel Construction, Chicago, IL, Vol. 35, No. 3, 3rd Quarter.
151. Sheikh-Ibrahim, F.I., and K.H. Frank. 2001. "The Ultimate Strength of Unsymmetric Beam Bolted Splices." AISC Engineering Journal, American Institute of Steel Construction, Chicago, IL, Vol. 38, No. 2, 2nd Quarter.
152. Sheikh-Ibrahim, F.I. 2002. "Design Method for Bolts in Bearing-Type Connections with Fillers." AISC Engineering Journal, American Institute of Steel Construction, Chicago, IL, Vol. 39, No. 4, 4th Quarter.
153. Yura, J.A., M.A. Hansen, and K.H. Frank. 1982. "Bolted Splice Connections with Undeveloped Fillers." Journal of the Structural Division. American Society of Civil Engineers, New York, NY, Vol. 108, No. ST12, December.

2.4 Bracing Member Design

2.4.1 General

As discussed at length in DM Volume 1, Chapter 2, bracing members (i.e. cross-frames/diaphragm and lateral bracing members) perform many important functions in steel I- and box-girder bridges. In addition to reviewing those functions, DM Volume 1, Chapter 2 discusses the process of selecting the type of bracing member (cross-frame or diaphragm), laying out the spacing of cross-frame/diaphragm members, the different possible configurations of cross-frame and lateral bracing members, and some suggestions on the detailing and preliminary sizing of these members. This section of the Manual reviews in more detail the *AASHTO LRFD* Specification provisions for the detailed design of the bracing members themselves. The discussion covers the design of tension members, compression members and solid-plate diaphragms. Design of the connections and connection elements (e.g. gusset plates) for bracing members (bolted or welded) is discussed in the preceding section of this chapter.

The minimum permitted thickness of steel must sometimes be considered in the design of bracing members and their connections. According to *AASHTO LRFD* Article 6.7.3, *structural steel, including bracing, cross-frames and all types of gusset plates must not be less than 0.3125 in. (5/16") in thickness*. Excluded from this requirement are webs of rolled shapes and closed ribs in orthotropic decks, which should not be less than 0.25 in. (1/4") in thickness, and also fillers and railings. *AASHTO LRFD* Article 6.7.3 further states that if the metal is exposed to severe corrosive influences, it must either be specially protected against corrosion or else sacrificial metal thickness must be specified.

As noted in Section 2.4.3.1.4.4.2 of DM Volume 1, Chapter 2, single angles, or when necessary, structural tees, are preferred for cross-frame and lateral bracing members. Double angles are more expensive to fabricate and painting the backs of the angles can cause difficulties.

2.4.2 Tension Members

2.4.2.1 General

The design of tension members is covered in *AASHTO LRFD* Article 6.10.8. Tension members may consist of a single structural shape or they may be built-up from several structural shapes. Built-up tension members generally consist of rolled or welded shapes connected by continuous plates with or without perforations or by tie plates with or without lacing bars on the open sides. Perforated plates are now more commonly used. The design of built-up tension members is covered in *AASHTO LRFD* Article 6.8.5 (see Section 2.4.2.4 below).

Although not classified as bracing members, tension members in bridges also include eyebars and pin-connected members. The design of eyebars is covered in *AASHTO LRFD* Article 6.8.6 and the design of pin-connected plates is covered in

AASHTO LRFD Article 6.8.7. Additional information on the design of these members may be found in References 21, 26 and 154. The design of eyebars and pin-connected plates is not covered in this Manual. As pointed out in Reference 21, eyebars and pin-connected plates were commonly used in the nineteenth century when Engineers were often concerned with minimizing secondary stresses. They were also often more economical and faster to erect than hand-riveted construction. Since there is greater knowledge and less concern in modern design about the minimization of secondary stresses, the use of these members in new construction has largely disappeared.

Although steel cables, strands and rods also qualify as tension members, they are not typically used as permanent bracing members and so they are not covered in this particular section of the Manual.

2.4.2.2 Factored Resistance

2.4.2.2.1 Axial Tension

As specified in *AASHTO LRFD* Article 6.8.1, members subject to axial tension at the strength limit state must be investigated for yield on the gross section of the member and fracture on the effective net section at the connection. In addition, the block shear rupture resistance of the member must be investigated at the end connections (refer to Section 2.3.2.4.2.4.3 of this chapter). According to *AASHTO LRFD* Article 6.8.2.1, the factored tensile resistance P_r of members subject to axial tension only at the strength limit state is to be taken as the lesser of the values given by the following two equations:

$$P_r = \phi_y P_{ny} = \phi_y F_y A_g \qquad \text{Equation 2.305}$$

AASHTO LRFD Equation 6.8.2.1-1

$$P_r = \phi_u P_{nu} = \phi_u F_u A_n U \qquad \text{Equation 2.306}$$

AASHTO LRFD Equation 6.8.2.1-2

where:
  ϕ_u = resistance factor for fracture of tension members specified in *AASHTO LRFD* Article 6.5.4.2 (= 0.80)
  ϕ_y = resistance factor for yielding of tension members specified in *AASHTO LRFD* Article 6.5.4.2 (= 0.95)
  A_g = gross cross-sectional area of the connected element (in.^{2})
  A_n = net cross-sectional area of the connected element determined as specified in *AASHTO LRFD* Article 6.8.3 (in.^{2})
  F_u = tensile strength of the connected element specified in *AASHTO LRFD* Table 6.4.1-1 (ksi)
  F_y = specified minimum yield strength of the connected element (ksi)
  P_{nu} = nominal tensile resistance for fracture on the net section (kips)
  P_{ny} = nominal tensile resistance for yielding on the gross section (kips)

U = reduction factor to account for shear lag (see below)

Equation 2.305 provides the factored tensile resistance for yielding on the gross section. As discussed previously, due to strain hardening, a ductile steel member loaded in axial tension can resist a force greater than the product of the yield strength times the gross area prior to fracture. However, the structural usefulness of the member may be limited due to excessive elongation resulting from uncontrolled yielding of the gross area. Equation 2.306 provides the factored tensile resistance for fracture on the effective net section. Depending on the ratio of net to gross area, the properties of the steel (i.e. the ratio of F_u/F_y) and the geometry of the end connection (captured by the shear lag factor U), a member subject to axial tension can fracture by failure of the net area at a load smaller than that required to yield the gross area. Therefore, both yielding and fracture are specified as limit states. Since the width of the member occupied by the net area at bolt holes is generally negligible relative to the overall width of the member, strain hardening is easily reached in the vicinity of the holes and yielding on the net area at bolt holes is not considered to be a significant limit state, except perhaps for built-up members of unusual proportions. A higher margin of safety is typically used when considering the net section fracture resistance versus the yield resistance, as reflected in the specified resistance factors.

The gross area A_g is to be determined considering all holes larger than those typically used for connectors, such as bolts. Holes that must typically be deducted when computing the gross area include access holes, pin holes and perforations. The calculation of the net area A_n was discussed previously at length under Section 2.3.2.4.2.4.2 of this chapter dealing with the computation of the net section fracture resistance of connected elements subject to tension. Rather than repeat this discussion here, the reader is referred to this section of the chapter for additional information. Note that for welded connections, A_n is to be taken as the gross area less any access holes within the connection region.

The effective net section is equal to A_n times the shear lag factor U. The U factor, which accounts for the shear lag effects associated with the end connection geometry, is specified in *AASHTO LRFD* Article 6.8.2.2. As discussed previously, shear lag is a consideration where the tensile force in the member is applied eccentrically or transmitted by connection to some but not all of the connection elements, e.g. an angle having a connection to only one leg, or when the connection elements do not lie in a common plane. Other examples include a rolled or built-up I-shape, tee or channel connected only through the flanges or only through the web. In such cases, the tensile force is not uniformly distributed over the net area and the critical net section may not be fully effective. Shear lag does not need to be considered when checking yielding on the gross section because the nonuniform tensile stresses over the cross-section tend to be equalized by the yielding. Research on the effects of shear lag in end connections of tension members is described in References 155 and 156.

As specified in *AASHTO LRFD* Article 6.8.2.2, if the tensile force is transmitted directly to every component plate of a member cross-section by bolts or welds, U is to be taken equal to 1.0. For members where the tensile load is transmitted to some

but not all of the component plates of a member cross-section by bolts or longitudinal (or longitudinal plus transverse) welds, Reference 26 permits U to be calculated by the following formula (*155*):

$$U = 1 - \frac{\bar{x}}{\ell}$$ Equation 2.307

where:

$\bar{x}$ = perpendicular distance from the connection plane or face of the member to the centroid of the member section resisting the connection force (in.) (Note: illustrative examples for different cases are given in the Article D3 of the Commentary to Reference 26)

ℓ = for bolted connections, distance parallel to the line of force between the first and last row of bolts in the line with the maximum number of bolts in the connection (for staggered bolts, use the out-to-out distance). For welded connections, the length of weld parallel to the force (in.)

In lieu of using Equation 2.307, *AASHTO LRFD* Article 6.8.2.2 instead specifies the following values of U for bolted connections in such members (Note: similar values are also permitted as alternative values for U in Reference 26. Reference 26 further states that if U is also calculated from Equation 2.307, the larger value may be used).

➢ For rolled I-shapes with flange widths b_f greater than or equal to 2/3 of the section depth d, or structural tees cut from such shapes, *connected to the flanges* with three or more bolts in the direction of the line of force:

$$U = 0.90$$

➢ For all other members having three or more bolts in the direction of the line of force:

$$U = 0.85$$

➢ For all other members having only two bolts in the direction of the line of force:

$$U = 0.75$$

AASHTO LRFD Article 6.8.2.2 also permits U to be alternatively determined by refined analysis or tests. It should be mentioned that Reference 26 specifies lower alternative values for single angles than those given above. That is, for single angles with four or more bolts in the direction of the line of force, U may be taken as 0.80. For single angles with two or three bolts in the direction of the line of force, U may be taken as 0.60. Reference 26 also specifies a lower alternative U factor of 0.70 for rolled I-shapes or tees *with the web connected* by four or more bolts in the direction of the line of force.

For the case of a tensile load transmitted by fillet welds to some but not all of the component plates of a member cross-section, *AASHTO LRFD* Article 6.8.2.2 states at this writing (2006) that the factored tensile resistance of the member (based on net section fracture) is simply to be taken as the factored resistance of the welds (see Section 2.3.3.8.3 of this chapter for the calculation of the factored resistance of fillet welds). This is in lieu of using Equation 2.306 in conjunction with Equation 2.307 to compute *U*.

It is noted that Reference 26 specifies that for all tension members, when the load is transmitted only by transverse welds to some but not all of the component plates (which is relatively rare in bridges), *U* is to be taken as 1.0 and A_n is to be taken as only the area of the directly connected component plates (which indirectly accounts for the shear lag effect by using the reduced area). Furthermore, for the case of lapped-plate tension members, where the load is transmitted by longitudinal welds only, Reference 26 specifies reduced values of *U* (i.e. less than 1.0) when ℓ is less than twice the distance *w* between the longitudinal welds (i.e. the plate width).

2.4.2.2.2 Combined Axial Tension and Flexure

As specified in *AASHTO LRFD* Article 6.8.2.3, a member or component subject to combined tension and flexure must satisfy the following two interaction relationships:

➤ If $\dfrac{P_u}{P_r} < 0.2$, then:

$$\frac{P_u}{2.0P_r} + \left(\frac{M_{ux}}{M_{rx}} + \frac{M_{uy}}{M_{ry}} \right) \leq 1.0 \qquad \text{Equation 2.308}$$

AASHTO LRFD Equation 6.8.2.3-1

➤ If $\dfrac{P_u}{P_r} \geq 0.2$, then:

$$\frac{P_u}{P_r} + \frac{8.0}{9.0} \left(\frac{M_{ux}}{M_{rx}} + \frac{M_{uy}}{M_{ry}} \right) \leq 1.0 \qquad \text{Equation 2.309}$$

AASHTO LRFD Equation 6.8.2.3-2

where:

M_{rx} = factored flexural resistance about the x-axis taken as ϕ_f times the nominal flexural resistance about the x-axis determined as specified in *AASHTO LRFD* Article 6.10, 6.11 or 6.12, as applicable (kip-in.)

M_{ry} = factored flexural resistance about the y-axis taken as ϕ_f times the nominal flexural resistance about the y-axis determined as specified in *AASHTO LRFD* Article 6.12, as applicable (kip-in.)

M_{ux} = moments about the x-axis due to the factored loads (kip-in.)

M_{uy} = moments about the y-axis due to the factored loads (kip-in.)

P_r = factored tensile resistance determined as specified in *AASHTO LRFD* Article 6.8.2.1 (see Equations 2.305 and 2.306 above) (kips)

P_u = axial force due to the factored loads (kips)

ϕ_f = resistance factor for flexure determined as specified in *AASHTO LRFD* Article 6.5.4.2 (= 1.0)

AASHTO LRFD Article 6.8.2.3 further specifies that a flange subject to a compressive stress under combined tension and flexure must be investigated for local buckling.

For prismatic members along the unbraced length, the largest value of P_u/P_r based on the axial tensile resistance limit states of yielding or net section fracture is to be used in Equations 2.308 or 2.309 as applicable. Also, the largest values of M_{ux}/M_{rx} and M_{uy}/M_{ry} based on the flexural resistance limit states of yielding, local buckling or lateral-torsional buckling are to be used. Strictly speaking, for a particular load combination, concurrent values of P_u, M_{ux}, and M_{uy} should be used in computing and determining the critical ratios to use. However, since concurrent actions are not typically tracked in the analysis, it is conservative and convenient to use the maximum envelope values for these actions in combining the ratios in these equations. For nonprismatic members, the reader is referred to Reference 154 for additional information regarding the proper application of the preceding equations to such members.

As indicated in *AASHTO LRFD* Article C6.8.2.3, for sections where the nominal flexural resistance about the x-axis is expressed in terms of stress (i.e. determined from the Main Provisions – refer to the previous section of this chapter on Strength Limit State Verifications), the factored flexural resistance about the x-axis M_{rx} in Equations 2.308 and 2.309 is to be taken as:

$$M_{rx} = \text{the smaller of } \phi_f F_{nc} S_{xc} \text{ and } \phi_f F_{nt} S_{xt} \qquad \text{Equation 2.310}$$

AASHTO LRFD Equation C6.8.2.3-1

where:

F_{nc} = nominal flexural resistance of the compression flange (ksi)

F_{nt} = nominal flexural resistance of the tension flange (ksi)

S_{xc} = elastic section modulus about the major axis of the section to the compression flange taken as M_{yc}/F_{yc} (in.^{3})

S_{xt} = elastic section modulus about the major axis of the section to the tension flange taken as M_{yt}/F_{yt} (in.^{3})

M_{yc} = yield moment with respect to the compression flange determined as specified in *AASHTO LRFD* Article D6.2 (kip-in.)

M_{yt} = yield moment with respect to the tension flange determined as specified in *AASHTO LRFD* Article D6.2 (kip-in.)

S_{xc} and S_{xt}, as defined above, are equivalent values that account for the combined effects of the loads acting on different sections in composite members. For sections where the nominal flexural resistance about the x-axis is determined according to the provisions of *AASHTO LRFD* Appendix A (see the previous section of this chapter

on Strength Limit State Verifications), the factored flexural resistance about the x-axis M_{rx} in Equations 2.308 and 2.309 is to be taken as:

$$M_{rx} = \text{the smaller of } \phi_f M_{nc} \text{ and } \phi_f M_{nt} \qquad \text{Equation 2.311}$$

AASHTO LRFD Equation C6.8.2.3-2

where:
   M_{nc} = nominal flexural resistance based on the compression flange (kip-in.)
   M_{nt} = nominal flexural resistance based on the tension flange (kip-in.)

In cases where the member is subject to flexure about the y-axis, the nominal flexural resistance about the y-axis for I-shaped members is determined according to the provisions of *AASHTO LRFD* Article 6.12.2.2.1 (See Section 2.2.3.7.1.3 of this chapter. This section also contains further information on determining the nominal flexural resistance of miscellaneous members such as tees, double angles, and channels.).   Otherwise, the y-axis terms are set to zero in Equations 2.308 and 2.309.

Although not currently specified in the *AASHTO LRFD* Specifications as of this writing (2006), Reference 26 specifies that unless tension members such as single angles, double angles and tees have their connections proportioned such that the shear-lag factor *U* is greater than or equal to 0.6, the members must be proportioned for the effects of the combined flexure and axial force due to the eccentricity of the loading. If *U* is greater than or equal to 0.6, the eccentricity due to the lack of connection of some of the component plates in these types of members may be neglected in determining their resistance.   In such cases, the effects of the eccentricity may be ignored when determining the factored resistance of the member at the strength limit state, but these effects should always be considered when checking a member subject to an eccentric net tensile force at the fatigue limit state.

EXAMPLE

Determine the factored tensile resistance P_r of the single-angle bracing member shown below. The steel is ASTM A 709 Grade 50S steel. All bolts are 7/8-inch diameter A 325 high-strength bolts placed in standard holes.   From *AASHTO LRFD* Table 6.4.1-1, F_u for Grade 50S steel is 65 ksi.

Detail A
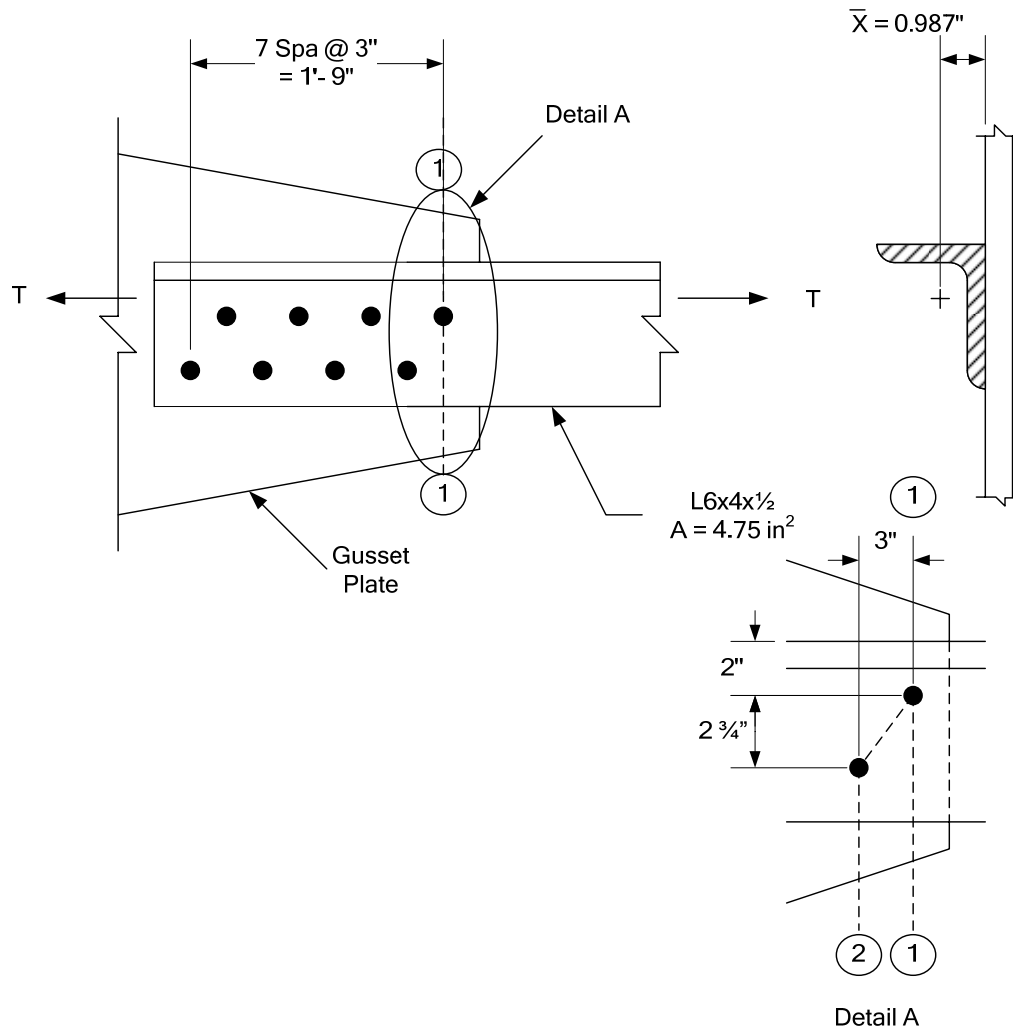
The factored tensile resistance for yielding on the gross section is calculated as:

$$P_r = \phi_y P_{ny} = \phi_y F_y A_g$$

AASHTO LRFD Equation 6.8.2.1-1

$$P_r = 0.95(50)(4.75) = 225.6 \text{ kips}$$

The factored tensile resistance for fracture on the effective net section is computed as:

$$P_r = \phi_u P_{nu} = \phi_u F_u A_n U$$

AASHTO LRFD Equation 6.8.2.1-2

Determine the net area A_n. Calculate the deduction in width for one hole. For standard holes,

$$\text{Deduction} = \frac{7}{8} + \frac{1}{8} = 1.0 \text{ in.}$$

For chain 1-1:

$$A_n = 4.75 - [1(1.0)](0.5) = 4.25 \text{ in.}^2$$

For chain 1-2 (Detail A):

$$A_n = 4.75 - [2(1.0)](0.5) + \left[\frac{(3.0)^2}{4(2.75)} \right](0.5) = 4.16 \text{ in.}^2 \quad \text{(governs)}$$

Both cases act in conjunction with the full tensile force *T*.

As specified in *AASHTO LRFD* Article 6.8.2.2, the shear-lag factor *U* for this case is equal to 0.85. Therefore:

$$P_r = 0.80(65)(4.16)(0.85) = 183.9 \text{ kips}$$

According to Reference 26, the shear-lag factor *U* for this case would be taken as 0.80 (for single angles with four or more bolts per line in the direction of the load), or else a larger value could be used if the *U* factor were calculated from Equation 2.307 as follows:

$$U = 1 - \frac{\bar{x}}{\ell} = 1 - \frac{0.987}{21} = 0.95$$

Calculate the factored block shear rupture resistance of the connection.

Block Shear Failure Plane
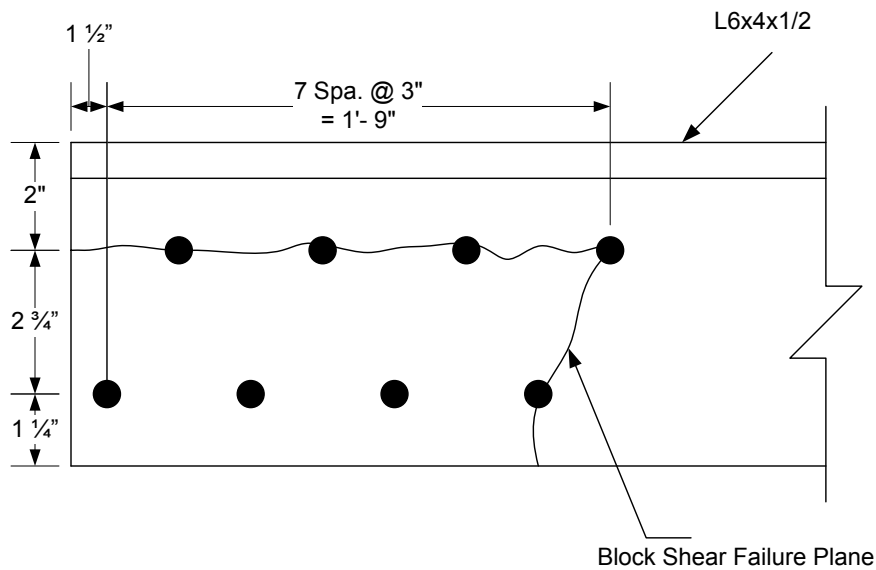
$$A_{tn} = \left[2.75 + 1.25 - 1.5(1.0) + \frac{(3.0)^2}{4(2.75)}\right](0.5) = 1.66 \text{ in.}^2$$

A_{vn} is the net area along the place resisting the shear stress. As specified in *AASHTO LRFD* Article 6.13.4, the full effective diameter of the staggered holes adjacent to the cut need not be deducted in determining A_{vn} in this case since these holes are centered more than two hole diameters from the cut. Therefore:

$$A_{vn} = [3(6.0) + 4.5 - 3.5(1.0)](0.5) = 9.50 \text{ in.}^2$$

$$A_{tn}/A_{vn} = 1.66/9.50 = 0.17 < 0.58$$

Therefore:
$$P_r = \phi_{bs}\left(0.58 F_u A_{vn} + F_y A_{tg}\right)$$
<div align="right">*AASHTO LRFD* Equation 6.13.4-2</div>

A_{tg} is the gross area along the plane resisting the tensile stress.

$$A_{tg} = [2.75 + 1.25](0.5) = 2.00 \text{ in.}^2$$

$$P_r = 0.80[0.58(65)(9.50) + 50(2.00)] = 366.5 \text{ kips}$$

Therefore, the factored tensile resistance of the member is governed by fracture on the effective net section; that is $P_r = 183.9$ kips.

Since the *U* factor exceeds 0.6, the effects of the combined flexure and axial force due to the eccentricity of the loading will be neglected in determining the factored tensile resistance of the member at the strength limit state in this case (refer to Reference 26).

2.4.2.3 Limiting Slenderness Ratios

AASHTO LRFD Article 6.8.4 specifies limiting slenderness ratios ℓ/r for tension members other than rods, eyebars, cables and plates, where ℓ is the unbraced length and r is the minimum radius of gyration for the cross-section. The slenderness limits are not intended to ensure the structural integrity of tension members, but to ensure a minimum degree of stiffness to reduce the potential for undesirable lateral movements or vibrations of the members. The resistance of tension members is not affected by out-of-straightness within reasonable tolerances as the applied tension tends to reduce the out-of-straightness, whereas out-of-straightness tends to be amplified by applied compression.

For primary tension members subject to stress reversals, the maximum ℓ/r is limited to 140. For primary tension members not subject to stress reversals, the maximum ℓ/r is limited to 200. In the *AASHTO LRFD* Specifications, a primary member is defined as a member designed to carry the internal forces determined from an

analysis. For secondary members (i.e. members in which stress is not normally evaluated in the analysis), the maximum ℓr is limited to 240. Note that for single angles, the radius of gyration about the z-axis typically produces the maximum ℓr.

2.4.2.4 Built-Up Members

Built-up tension members are covered in *AASHTO LRFD* Article 6.8.5. As mentioned previously, built-up tension members typically consist of rolled or welded shapes connected on the open sides by continuous plates with or without perforations. Tie plates (sometimes referred to as batten or stay plates) or end tie plates and lacing bars are also permitted on the open sides where special circumstances warrant, but are now less commonly used. Only the design requirements for perforated plates are covered in this Manual. Specific design requirements for tie plates and lacing bars may be found in References 26 and 157. Additional information on the design of laced and battered members may also be found in References 18, 21, and 28.

As specified in *AASHTO LRFD* Article 6.8.5.1, welded connections between the plates and shapes of built-up tension members must be continuous and bolted connections between the shapes and plates must satisfy the provisions of *AASHTO LRFD* Article 6.13.2, including the appropriate bolt spacing requirements (see in particular the maximum pitch requirements for stitch bolts - refer to Section 2.3.2.2.1.6.3 of this chapter).

Specific design requirements for perforated plates in built-up members (subject to tension or compression) are given in *AASHTO LRFD* Article 6.8.5.2 (*18*). These requirements are summarized as follows:

  ➢ The ratio of the length of the holes in the direction of stress to the width of the holes is not to exceed 2.0;
  ➢ The clear distance between the holes in the direction of stress is not to be less than the transverse distance between the nearest line of connection bolts or welds;
  ➢ The clear distance between the end of the plate and the first hole is not to be less than 1.25 times the transverse distance between the bolts or welds;
  ➢ The periphery of the holes is to have a minimum radius of 1.5 in.;
  ➢ The unsupported widths at the edges of the holes may be assumed to contribute to the net area of the member, and;
  ➢ Where the holes are staggered in opposite perforated plates, the net area of the member is to be considered the same as for a section having holes in the same transverse plane.

154.   White, D.W., 2006. "Structural Behavior of Steel." to be published as Chapter 6 of the NSBA *Steel Bridge Design Handbook*, available from the National Steel Bridge Alliance (www.steelbridges.org), Chicago, IL.
155.   Munse, W.H., and E. Chesson, Jr. 1963. "Riveted and Bolted Joints: Net Section Design." *Journal of the Structural Division.* American Society of Civil Engineers, New York, NY, Vol. 83, No. ST2, February.

156. Easterling, W.S., and L.G. Giroux. 1993. "Shear Lag Effects in Steel Tension Members." *AISC Engineering Journal*, American Institute of Steel Construction, Chicago, IL. Vol. 30, No. 3, 3rd Qtr.

157. AASHTO. 2002. *Standard Specifications for Highway Bridges and Interim Specifications*. 17th Ed., American Association of State Highway and Transportation Officials, Washington, D.C.

2.4.3 Compression Members

2.4.3.1 General

This section addresses the design of steel compression members, which are covered primarily in *AASHTO LRFD* Article 6.9. Compression members may consist of a single structural shape or may be built-up from plates or shapes. Common built-up compression members include back-to-back angles, "boxed" channels, and members connected by lacing (flat bars, angles, channels or other shapes), tie plates (also referred to as batten or stay plates) or perforated cover plates. The design of built-up compression members is covered in *AASHTO LRFD* Article 6.9.4.3 (see 2.4.3.4 below).

Compression members include solid-web arch ribs (refer to *AASHTO LRFD* Article 6.14.4 and Reference 154), and compression chords of half-through trusses (refer to *AASHTO LRFD* Article 6.14.2.9). However, these members are not addressed herein as this document is primarily concerned with the design of bracing members.

The design of composite columns (i.e. concrete filled steel tubes and concrete encased steel shapes) is covered in *AASHTO LRFD* Article 6.9.5. The *AASHTO LRFD* Specification provisions for composite columns as of this writing (2006) are based on the work of SSRC Task Group 20 and others (*158*, *159*). As discussed further in Reference 154, the 2005 AISC LRFD Specification (*26*) provides significantly revised provisions for the design of composite columns that provide improved accuracy in the prediction of the nominal compressive resistance of these members. This improved accuracy is reflected by a reduced value of the resistance factor (i.e. ϕ_c = 0.75 vs. 0.90). The design procedures for composite columns are not covered in this Manual. The reader is referred instead to Reference 154 for additional more detailed discussion related to the design of composite columns. Reference 154 also discusses the issue of composite steel bridge girders subjected to combined axial compression and flexure, such as might occur in a cable-stayed system with a composite I- or box-girder deck system. The subsequent discussion focuses on the design of noncomposite elements subject to axial compression or combined axial compression and flexure.

AASHTO LRFD Article 6.9 applies to prismatic members with at least one plane of symmetry and subject to either axial compression or combined axial compression and flexure about an axis of symmetry. The design of tapered compression members is not covered. The reader is referred to Reference 154 for assistance regarding the design of nonprismatic and/or tapered compression members.

2.4.3.2 Factored Resistance

2.4.3.2.1 Axial Compression

As specified in *AASHTO LRFD* Article 6.9.2.1, the factored resistance of components subject to axial compression is to be taken as:

$$P_r = \phi_c P_n$$

Equation 2.312

AASHTO LRFD Equation 6.9.2.1-1

where:

ϕ_c = resistance factor for axial compression specified in *AASHTO LRFD* Article 6.5.4.2 (= 0.90)

P_n = nominal compressive resistance based on the limit state of flexural buckling, torsional buckling or flexural-torsional buckling, whichever controls (kips)

The calculation of the nominal compressive resistance P_n for the limit states of flexural buckling, torsional buckling and flexural-torsional buckling is discussed below.

2.4.3.2.1.1 Flexural Buckling Resistance

For noncomposite members composed of nonslender elements that satisfy the width-to-thickness requirements for axial compression specified in *AASHTO LRFD* Equation 6.9.4.2 (discussed in Section 2.4.3.2.1.3.1 below), the nominal compressive resistance P_n based on flexural buckling is to be taken as follows according to the provisions of *AASHTO LRFD* Article 6.9.4.1:

If $\lambda \leq 2.25$, then:

$$P_n = 0.66^\lambda F_y A_s$$

Equation 2.313

AASHTO LRFD Equation 6.9.4.1-1

If $\lambda > 2.25$, then:

$$P_n = \frac{0.88 F_y A_s}{\lambda}$$

Equation 2.314

AASHTO LRFD Equation 6.9.4.1-2

where:

λ = $\left(\dfrac{K\ell}{r_s \pi}\right)^2 \dfrac{F_y}{E}$ *AASHTO LRFD* Equation 6.9.4.1-3

A_s = gross cross-sectional area (in.^{2})

F_y =   specified minimum yield strength of the member (ksi)

K   =   effective length factor in the plane of buckling specified in *AASHTO LRFD* Article 4.6.2.5

ℓ =   unbraced length (in.)

r_s =   governing radius of gyration (in.)

r_s is taken as the governing (smallest) radius of gyration about the axis normal to the plane of buckling. Should the member consist of one or more elements not satisfying the width-to-thickness requirements of *AASHTO LRFD* Article 6.9.4.2 (i.e. slender elements), the nominal compressive resistance must be reduced according to the procedures given in Reference 26 (and discussed in Section 2.4.3.2.1.3.2 below) to account for a slender element that may be subject to local buckling. Such elements do not carry their proportion of the load and potentially affect the buckling resistance of the member (refer to *AASHTO LRFD* Article C6.9.4.1).

Equations 2.313 represents the inelastic column flexural buckling resistance and Equation 2.314 represents the elastic column flexural buckling resistance. The equations are of essentially the same form as the equations presented in Reference 26. The term λ is equivalent to the expression P_o/P_e, where P_o is equal to the full yield or stub-column resistance (i.e. assuming a compression member with a small $K\ell$) for a homogenous prismatic steel member consisting of all non-slender elements calculated as follows:

$$P_o = P_y = F_y A_s \qquad \text{Equation 2.315}$$

P_e is critical elastic buckling load for flexural buckling about either the major or minor principal axis of a compression member calculated as:

$$P_e = F_e A_s = \frac{\pi^2 E}{\left(\dfrac{K\ell}{r_s}\right)^2} A_s \qquad \text{Equation 2.316}$$

Note that the term $\sqrt{\lambda} = \sqrt{P_o/P_e}$ is a normalized slenderness parameter that has been frequently used in the literature as the abscissa in plots showing normalized column resistance curves.

Column buckling theory originated from the work of Leonhard Euler in 1744 (*160*). Euler investigated the buckling strength of an initially straight, concentrically loaded, pinned-end member, in which all fibers are assumed to remain elastic until buckling instability occurs. Instability occurs at the load at which the lateral bending moment in the column (due to an infinitesimal lateral deflection) is large enough to cause infinite lateral deflection. The derivation of the critical Euler buckling stress, on which the critical stress F_e in Equation 2.316 is based, is discussed elsewhere (*21, 28, 91, 161*) and will not be repeated here.

Euler's theory pertains to columns with uniform stress over the cross-section and stresses below the elastic limit. These conditions never occur in bridges, but are approached in compression members with large slenderness ratios. Test results prove that typical columns are not as strong as predicted by Euler's theory.

In 1889, Considere (*162*) and Engesser (*163*) independently found that portions of steel columns were strained beyond the proportional limit prior to buckling. They postulated that a variable modulus of elasticity should be used to account for the fact that columns fail by inelastic rather than elastic buckling. Engesser proposed the Euler equation with the substitution of the tangent modulus for the elastic modulus. The tangent modulus is defined as the tangent to the stress-strain curve of a stub-column test at F_{cr}. Thus, Engesser modified the Euler buckling equation by inserting the tangent modulus of elasticity E_t at the stress F_{cr} as follows:

$$F_{cr} = \frac{\pi^2 E_t}{\left(\dfrac{K\ell}{r_s}\right)^2}$$

Equation 2.317

The basic assumptions with regard to material, shape and end conditions that were made in the determination of the basic column buckling strength of an ideal column given by Equation 2.317 were that the same compressive stress-strain properties exist throughout the section, all fibers remain elastic until buckling occurs, no twisting or distortion of the cross-section occurs during bending, small-deflection theory applies with shear neglected, determinate end conditions exist so that an equivalent pinned-end length can be established, no residual stresses are present in the member due to welding or cooling after rolling, and loading of the member occurs through the centroidal axis until the member begins to bend. The theory ignores the effect of residual stresses on the stiffness of the column. The portion of the section containing compressive residual stresses will yield first. This yielding will be evidenced by a non-linear appearance to the stress-strain curve. However, it will not have any influence on the moment of inertia of the section. Typically, compressive residual stresses exist at the critical exterior fibers of column sections. Hence, the tangent modulus does not accurately reflect the column strength of those sections with high residual stresses. It is noted that the above method is empirical in that it can only be found by test.

Engesser's tangent modulus theory still gave computed buckling loads lower than measured ultimate resistances. Therefore, in 1895, he revised his tangent modulus theory to incorporate the phenomenon of strain reversal; that is, to account for the fact that at the onset of bending, some fibers undergo increased strain at the lower tangent modulus while other fibers are unloaded at a higher modulus under the reduced strain. This led to the development of his double modulus theory, in which a combined reduced modulus was used to calculate the critical buckling load. The double modulus theory was generally accepted, but gave computed resistances somewhat higher than the test values. The double modulus theory only considered equilibrium positions near the ideal straight position and still did not address the effect of residual stresses on the column moment of inertia. Some attempts to address the column problem analytically were made in the 1960s by computing the

tangent modulus of a shape with the effect of residual stresses on the moment of inertia considered; however, strain reversal was not addressed.

An explanation of the true behavior of concentrically loaded columns was presented in 1946, when Shanley (*164*) reasoned that as the column bends beyond infinitesimal values of curvature upon reaching the buckling load, which includes the inelastic effects on the cross-section, it is still possible for the column to resist increasing axial compression if its initial bending is due to non-linear behavior. As bending occurs and the curvature increases to a finite value, strain reversal must again occur to develop a resisting moment to maintain equilibrium with the moment due to the external load times the lateral deflection. However, the load on the column will continue to increase above the buckling load in a non-linear fashion for small but finite values of curvature as long as the increment of load represented by the stress acting on the area of increasing strain exceeds the increment of load represented by the stress acting on the area of decreasing strain. For practical design, this increase in the load carrying capacity above the buckling load is neglected, but the true flexural buckling behavior of an ideal concentrically loaded column was now well understood.

Practically speaking, however, actual conditions do not generally correspond to the ideal conditions represented by the preceding assumptions. Test results typically include the effects of residual stresses, initial imperfections (i.e. out-of-straightness), unintended eccentricity of the load, end restraint and local buckling. As a result of these effects, the term *buckling* represents more of a transition between stable and unstable deflections of a compression member rather than an instantaneous (or bifurcation) type behavior.

Residual stresses are stresses that remain in an unloaded member after that member has been formed into a finished product by cold bending and/or cooling after rolling or welding. Residual stresses are also introduced by cutting operations and by the punching of holes during fabrication. However, residual stresses introduced by uneven cooling (*131*) are the most significant stresses. As shown in Figure 2.139, after hot rolling, the thicker flanges of rolled wide-flange or H-shaped sections cool more slowly than the web region. Also, the flange tips cool more rapidly than the region at the flange-to-web juncture. As a result, compressive residual stresses exist at the flange tips and at mid-depth of the web, or the regions that cool the fastest, while tensile residual stresses exist where the flanges and web are joined.
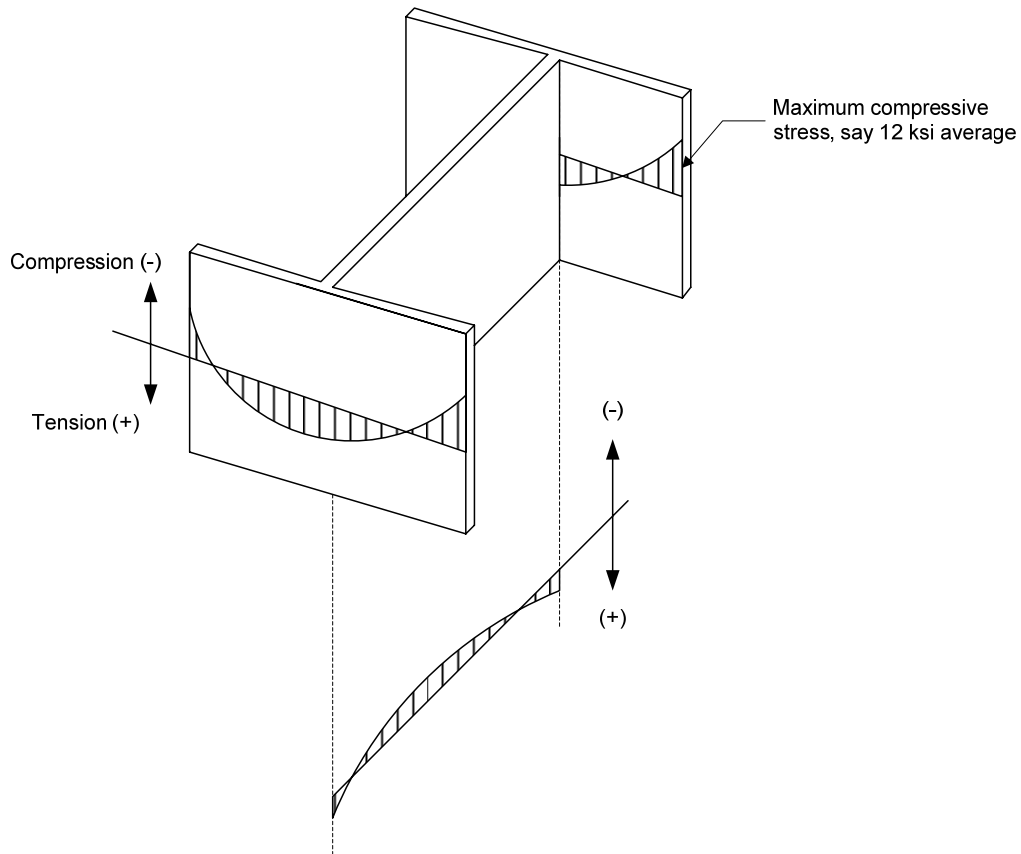
Figure 2.139 Typical Residual Stress Distribution for Rolled Shapes

Figure 2.139 shows a typical residual stress pattern for an unstraightened hot-rolled shape. The magnitude of these stresses varies based on the dimensions of the section. Residual stresses are essentially independent of yield strength (*165*) and have been measured as high as 20 ksi at the tips of rolled shapes (*28*). Residual stresses shown in this figure are due to differential cooling of the steel subsequent to rolling. This variable cooling causes the shapes to go out-of-straight and they must be straightened. Smaller shapes, such as angles and tees commonly used in bracing, are passed through a rotary straightener. This machine flexes the shape back and forth removing the residual stresses due to cooling. Generally, the final residual stresses are much less than those due to cooling. For example, when a smaller wide flange shape is flexed in the strong direction, as is done in a rotary straightener, the maximum residual stress is due to springback from the plastic moment M_p. The shape factor M_p/M_y is 1.12 so the residual stresses are not greater than 12 percent of the yield stress.

Figure 2.140 shows qualitatively the effect of residual stresses on the stress-strain curve for a rolled shape, plotted using the average stress versus the average compressive strain.
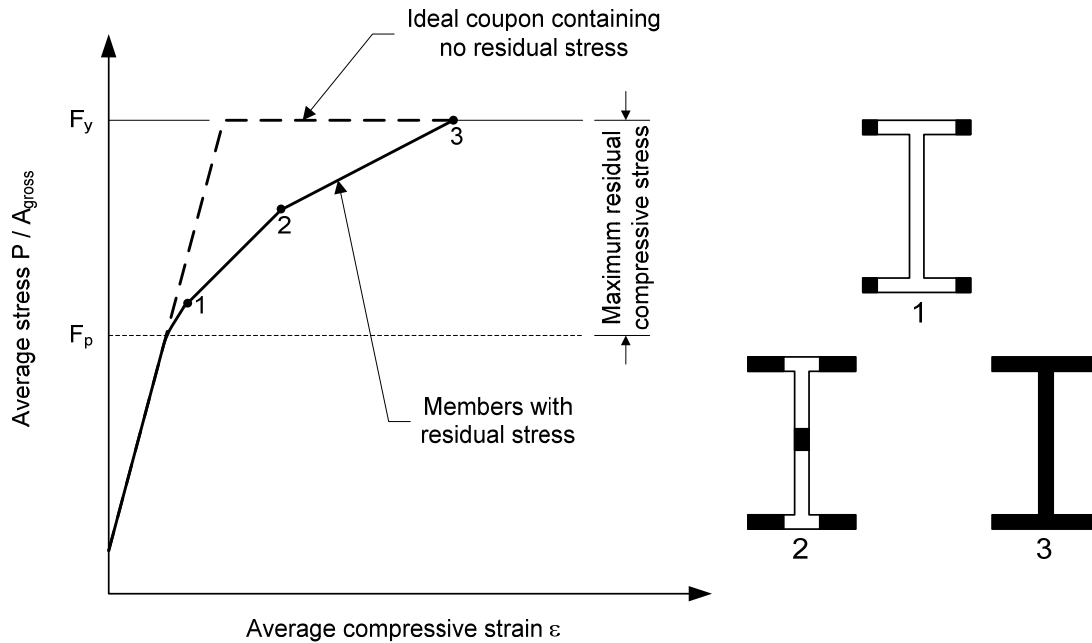
Figure 2.140 Residual Stress Effects on the Average Stress-Strain Curve for a Rolled Shape

The so-called secant formula was an early attempt to account for the effects of residual stresses, accidental eccentricities, and initial out-of-straightness. However, cooling residual stresses, more than initial imperfections or unintended eccentricity of load, have been shown to be the primary contributor to the non-linear portion of the average stress-strain curve for axially loaded compression members in tests (*166*). The tangent modulus theory based on inelastic buckling applies because the average stress-strain curve is non-linear when F_{cr} is reached, however, the tangent modulus on one fiber is not the same as on the adjacent fiber and all fibers cannot be assumed stressed to the same level due to the effect of the residual stresses.

In welded built-up shapes, the plates themselves have little or no initial residual stress due to cooling. Modern steel is rolled in wide plates and sheared to approximate widths for sale to fabricators. The fabrication process involves cutting the sheared plates into individual flange widths. This may be performed with a torch or with other means such as a laser. The local heat input of the cutting creates rather high local tensile stresses at the cut lines (Figure 2.141a). Welding causes high tensile residual stresses with a magnitude at or near the yield stress in the vicinity of the welds. The remainder of the section must balance the tensile force with compressive stresses. The resulting nonuniform cooling results in a residual stress pattern such as that shown in Figure 2.141b for the flange of a welded I-section. When the heat due to welding is large in comparison to the heat sink formed by the attached material, distortions in the plate may occur.

(a)

C = compression
T = tension

(b)
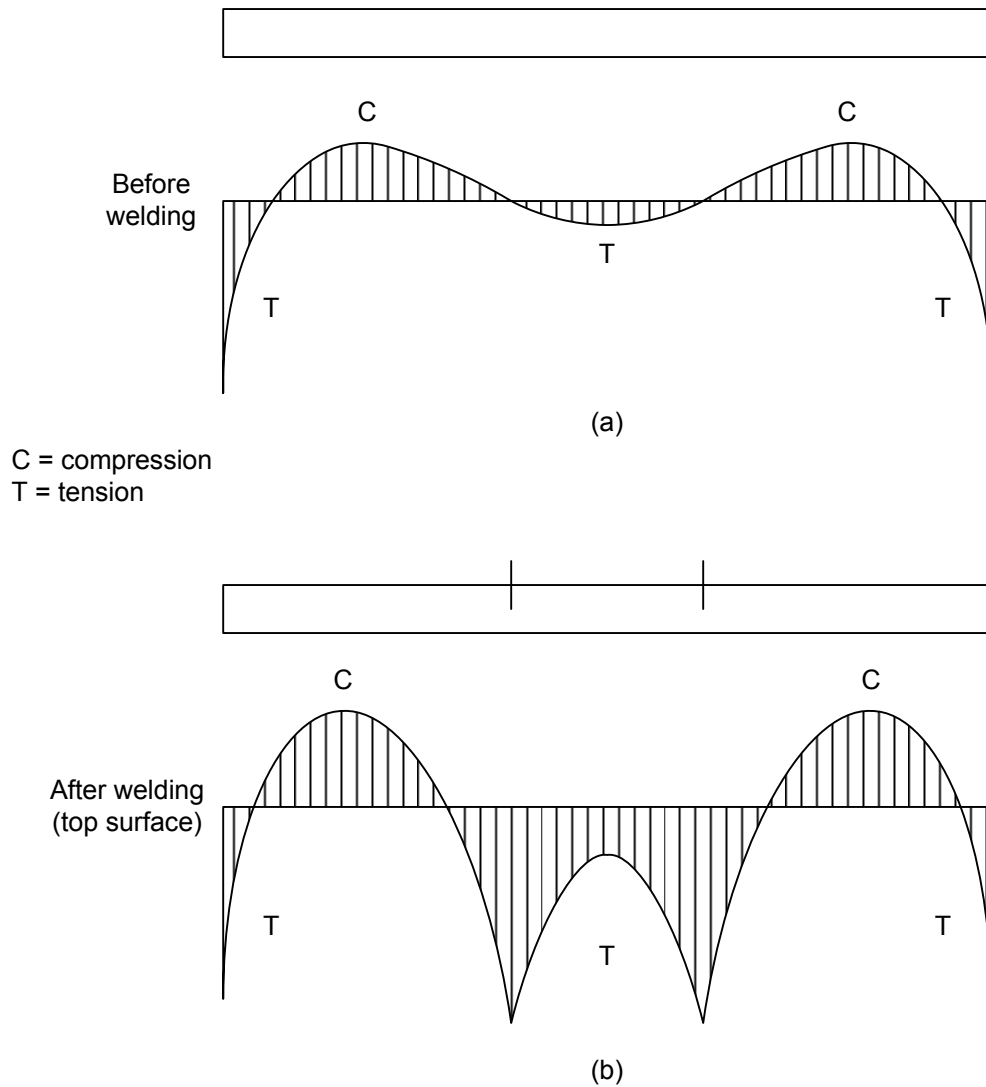
Figure 2.141 Typical Residual Stress Distribution in Welded Flange Plates

Residual stresses balance in tension and compression within a section. Hence, as a section is loaded in flexure, residual stresses have no effect on the ultimate strength of the section, but may cause it to deflect more than would be predicted ignoring residual stresses. Euler showed that a column fails in bending. Hence, the flexural strength of a column is not affected by residual stresses. The deleterious effect of residual stresses on columns is in their reduction in the bending stiffness *I* of the column.   The location of residual stresses in a cross-section, as well as their magnitude, affects the column strength of a section.   Shanley showed that the flexural strength of a column shape is greater than the tangent modulus strength because of strain reversal. When a part of the section yields prematurely due to residual stresses and the column commences to bend, the fibers on the outside of the bend go into tension increasing the strength. Shanley's discovery explains why the column strength of shapes with large residual stresses are not affected as much as tangent modulus theory would indicate.

Recognizing the overall importance of residual stresses and in an attempt to better fit the test results, various column strength design curves were developed for strong- and weak-axis buckling based on various assumed distributions of residual stress. In 1960, the AISC Allowable Stress Design (ASD) specification implemented the following SSRC parabolic equation initially proposed by Bleich (*91*) to define the transition region in column strength between elastic buckling and yielding:

$$F_{cr} = F_y \left[1 - \frac{F_y}{4\pi^2 E} \left(\frac{K\ell}{r_s} \right)^2 \right]$$

Equation 2.318

This equation was also implemented in earlier versions of the AASHTO Standard Specifications, including the Guide Specifications for horizontally curved girders. The effects of initial imperfections and unintended eccentricity of the load increase with increasing slenderness. In the AISC and AASHTO ASD Specification, these effects were accounted for via a variable factor of safety that increased with slenderness. Note that Equation 2.318 is a parabolic equation, whereas the Euler equation is a hyperbola. In the AISC Specification, where Equation 2.318 was tangent to the Euler hyperbola, it was terminated. However, AASHTO extended the parabolic equation beyond where AISC switched to the hyperbola. At these large slenderness values, the parabolic equation is very conservative.

In the transition to the AISC LRFD Specification, it was decided to provide a constant margin of safety for all columns and to instead account for the variation of resistance with slenderness through the calculation of the nominal axial resistance P_n. Bjorhovde's probability-based work examining the resistance of steel columns (*167, 168*) resulted in his recommendation of three column strength curves. The three curves represented a central strength for theoretical column strength based on measured residual stresses. The work assumed a mean out-of-straightness of 1/1470 based on measured out-of-straightness of unstraightened columns (*18*). The permitted out-of-straightness is L/1000 so the expected effect of out-of-straightness is much less than assumed in that study. The difference in strength reflected in the three groups was based on means of manufacture not including straightening. SSRC presented these curves. Column curve P1 represented the data band of highest resistance, included hot- and cold-formed heat-treated HSS columns. Column curve P3 represented the data band of lowest resistance, included welded built-up H-sections made from universal mill plates with a yield strength less than 50 ksi for major-axis buckling and a yield strength less than 60 ksi for minor-axis buckling, and heavy W-shapes with a yield strength less than 50 ksi. Column curve P2 included the largest group of columns. Additional information on the recommended use of curves P1 and P2 for a range of I-shaped steel-column sections subject to major- or minor-axis bending, and the reliability provided by each curve, may be found in Reference 18. Since welded built-up shapes are no longer manufactured from universal mill plates and the minimum yield strength of constructional steels used in new construction is typically 50 ksi or larger, curve P3 is no longer shown in Reference 18.

For a number of reasons, including simplicity, the decision was eventually made by the AISC Specification Committee to retain a single column curve. SSRC Column

curve P2 is closest to the AISC curve. A resistance factor ϕ_c of 0.85 was chosen in the First Edition of the AISC LRFD Specifications (1986). The development of the mathematical form of the equations representing this curve – i.e. Equations 2.313 and 2.314 – is discussed in References 169 and 170.   Reference 28 shows a reasonable comparison of the results from Equations 2.313 and 2.314 with physical column test data compiled by Hall (*171*). It should be noted that the 2005 AISC LRFD Specification (*26*) has increased ϕ_c for steel columns to 0.90 to reflect changes in industry manufacturing practice since the original calibration was performed.   The *AASHTO LRFD* value of ϕ_c, which is typically 0.05 higher than the AISC value, has not yet been increased accordingly as of this writing (2006).

2.4.3.2.1.1.1 Effective Length Factor

The effective length factor *K*, which is applied to the actual member unbraced length ℓ, accounts for the influence of end conditions.   *K* is used to compensate for translational and rotational boundary conditions.   It represents the ratio of the idealized pinned-end compression member length to the actual length of a member with other than pinned ends.

In many cases, some degree of end restraint exists causing an effective length factor other than 1.0. *AASHTO LRFD* Table C4.6.2.5-1 provides a table of theoretical *K* values taken from Reference 18 for idealized end conditions in which translational and/or rotational end conditions are either fully restrained or free. Because actual member end conditions are seldom perfectly fixed or perfectly unrestrained as represented by the ideal conditions, *AASHTO LRFD* Table C4.6.2.5-1 also provides recommended design values as suggested by the Structural Stability Research Council.   These simple modifications of the ideal values lead to either equal or somewhat higher *K* values.

In the absence of refined inelastic analysis, *AASHTO LRFD* Article 4.6.2.5 provides recommended *K* values in the braced plane of triangulated trusses, trusses and frames where lateral stability is provided. The recommended values are as follows:

  ➢ For bolted or welded end connections at both ends: *K* = 0.750
  ➢ For pinned connections at both ends: *K* = 0.875
  ➢ For single angles, regardless of end connection: *K* = 1.0

The recommended values for *K* do not account for any relative translation or rotation of the ends of the member.   These relative motions are not usually present in building columns.   They more closely resemble the actions found in transmission towers.   Caution should be exercised in applying these recommended values to cases with larger unbraced lengths where elastic buckling may control.

A conservative *K* value of 1.0 is suggested for single angles since these members are often loaded through only one leg and are subject to eccentric loading as well as twist. These effects may not be properly recognized in design. The recommended value of *K* = 1.0 for single angles also closely matches that provided in Reference 172 (the design of single-angle compression members is discussed in more detail in Section 2.4.3.2.1.4 below).

Reference 18 gives more specific recommendations of *K* values to use for in-plane buckling of various truss members. In some cases, the *K* values are higher than the recommended values given above. This reference also gives recommendations for buckling of truss members in the out-of-plane direction. Suggested *K* values for in-plane buckling of arch members are provided in *AASHTO LRFD* Article 4.5.3.2.2c. The reader is referred to Reference 154 for additional discussion of *K* values.

Where non-rigid rotational restraint exists, *K* may be determined from traditional alignment charts for sidesway-inhibited or sidesway-uninhibited cases that are provided in *AASHTO LRFD* Article C4.6.2.5. Closed-form equations are also provided. The assumptions made in the alignment charts and equations are discussed in detail in the commentary to Chapter C of the 2005 AISC LRFD Specification (*26*). Modifications are also presented there that extend the range of applicability of the alignment charts. The reader is urged to review these assumptions and modifications prior to using the alignment charts and/or equations.

2.4.3.2.1.2 Torsional and Flexural-Torsional Buckling Resistance

2.4.3.2.1.2.1 General

Torsional or flexural-torsional buckling may be critical in certain shapes. These forms of buckling are mentioned in *AASHTO LRFD* Article C6.9.4.1. Torsional buckling is usually found in doubly symmetric built-up sections such as the cruciform or doubly symmetric built-up sections with very thin walls. Singly symmetric compression members such as double angles, channels and tees, and non-symmetric compression members may be governed by flexural-torsional buckling rather than flexural buckling. The Engineer is referred to the 2005 AISC LRFD Specification (*26*) to obtain the appropriate torsional buckling and flexural-torsional buckling resistance equations to use for the design of these members. These equations are reviewed below. The equations, as written below, apply only to members composed of nonslender elements (for members composed of one or more slender elements, refer also to Section 2.4.3.2.1.3.2 below). *Note that according to Section E4 of Reference 26, flexural-torsional buckling does not need to be checked for single angles (see Section 2.4.3.2.1.4 of this chapter instead).*

The torsional and flexural-torsional buckling resistance equations given in Section E4 of Reference 26 (and summarized in the following) provide a critical stress for elastic buckling only. Except as noted herein (refer specifically to Section 2.4.3.2.1.2.4 below), to modify the equations for inelastic buckling, F_{cr} must be determined from one of the following equations taken from Section E3 of Reference 26, using the critical elastic torsional or flexural-torsional buckling stress F_e determined as described in the following sections:

If $\dfrac{K\ell}{r_s} \leq 4.71\sqrt{\dfrac{E}{F_y}}$ (or $F_e \geq 0.44F_y$), then:

$$F_{cr} = \left[0.658^{\frac{F_y}{F_e}} \right] F_y \qquad \qquad \text{Equation 2.319}$$

AISC LRFD Equation (E3-2)

If $\dfrac{K\ell}{r_s} > 4.71 \sqrt{\dfrac{E}{F_y}}$ (or $F_e < 0.44F_y$), then:

$$F_{cr} = 0.877F_e \qquad \qquad \text{Equation 2.320}$$

AISC LRFD Equation (E3-3)

The nominal compressive resistance P_n is then taken as:

$$P_n = F_{cr}A_s \qquad \qquad \text{Equation 2.321}$$

AISC LRFD Equation (E3-1)

Note that Equations 2.319 and 2.320 are equivalent to AASHTO LRFD Equations 6.9.4.1-1 and 6.9.4.1-2 (i.e. Equations 2.313 and 2.314), respectively, but are simply written in a different format in terms of the member slenderness ratio $K\ell/r_s$ rather than the slenderness parameter λ. As an aside, it is pointed out in Reference 154 that the immediately preceding form of the buckling equations can be used to conveniently calculate P_n when a refined buckling analysis is employed to assess the stability of trusses, frames or arches (in lieu of using an effective length factor approach). In this case, F_e in the equations would simply be taken as the axial load P_e in a given member, taken from the analysis at incipient elastic buckling of the structure or subassemblage, divided by A_s.

2.4.3.2.1.2.2 Torsional Buckling Resistance

The limit state of torsional buckling, or twisting about the shear center, applies only to concentrically loaded doubly symmetric and point symmetric (e.g. Z-shaped) compression members. For such members, the critical elastic torsional buckling stress F_e is computed as:

$$F_e = \left[\frac{\pi^2 E C_w}{(K_z\ell)^2} + GJ \right] \frac{1}{I_x + I_y} \qquad \qquad \text{Equation 2.322}$$

AISC LRFD Equation (E4-4)

where:

C_w = warping torsional constant for the cross-section (equal to zero for a cruciform section), in.[6] For a doubly symmetric I-section, C_w may be taken as $I_y h^2/4$, where h is the distance between flange centroids in lieu of a more precise analysis.

K_z = effective length factor for torsional buckling

G	=	shear modulus of elasticity for steel = 11,200 ksi
J	=	St. Venant torsional constant for the cross-section, in.^{4} (refer to Section 2.2.3.1.2.1 of this chapter)
I_x, I_y	=	moments of inertia about the major and minor principal axes of bending, respectively, in.^{4}

The effective length for torsional buckling $K_z\ell$ is the length between locations where the member is prevented from twisting and warping. Typically, $K_z\ell$ can conservatively be taken as 1.0ℓ. Reference 154 indicates that for a cantilever member fully restrained against twisting and warping at one end with the other end free, $K_z\ell$ is equal to 2ℓ. For a member with twisting and warping restrained at both ends, $K_z\ell$ is equal to 0.5ℓ.

Torsional buckling will rarely control (as opposed to flexural buckling), except possibly for built-up cruciform sections and/or built-up doubly symmetric sections with very thin walls. Torsional buckling does not need to be considered for doubly-symmetric I-section members that satisfy the proportioning limits specified in *AASHTO LRFD* Article 6.10.2, unless the effective length for torsional buckling is significantly larger than the effective length for weak-axis flexural buckling (*154*).

2.4.3.2.1.2.3 Flexural-Torsional Buckling Resistance - General

Concentrically loaded compression members composed of singly symmetric open cross-sections, *where the y-axis is defined in the subsequent discussion as the axis of symmetry of the cross-section*, can either fail by flexural buckling about the x-axis or by torsion combined with flexure about the y-axis. Unsymmetric open-section compression members, or members with no cross-section axis of symmetry, that are concentrically loaded fail by torsion combined with flexure about both the x- and y-axes. In all the preceding cases, the shear center and centroid of the cross-section do not coincide. As buckling occurs, the axial load has a lateral component resulting from the deflection of the member. The torsional moment of this lateral component of axial force acting about the shear center of the section causes twisting of the member. As discussed in Reference 18, the degree of interaction between the torsional and flexural deformations determines the amount of reduction of the buckling load in comparison to the flexural buckling load. As the distance between the centroid and shear center increases, the twisting tendency increases and the flexural-torsional buckling load decreases. Because of their relatively low torsional rigidity, flexural-torsional buckling may be a critical mode of failure for thin-walled singly-symmetric and unsymmetric open sections. Flexural-torsional buckling is not a consideration for closed sections.

Except as permitted alternatively in the next section for tees and double angles, for members composed of singly symmetric cross-sections where the y-axis is defined as the axis of symmetry of the cross-section, the critical elastic flexural-torsional buckling stress F_e may be computed as:

$$F_e = \left(\frac{F_{ey} + F_{ez}}{2H} \right) \left[1 - \sqrt{1 - \frac{4 F_{ey} F_{ez} H}{(F_{ey} + F_{ez})^2}} \right]$$

Equation 2.323

AISC LRFD Equation (E4-5)

where:

F_{ey} = $\dfrac{\pi^2 E}{\left(\dfrac{K_y \ell}{r_y} \right)^2}$

Equation 2.324

AISC LRFD Equation (E4-10)

F_{ez} = $\left(\dfrac{\pi^2 E C_w}{(K_z \ell)^2} + GJ \right) \dfrac{1}{A_s \bar{r}_o^2}$

Equation 2.325

AISC LRFD Equation (E4-11)

H = $1 - \dfrac{y_o^2}{\bar{r}_o^2}$

Equation 2.326

$\bar{r}_o$ =   polar radius of gyration about the shear center, in.

$\bar{r}_o^2$ = $y_o^2 + \dfrac{I_x + I_y}{A_s}$

Equation 2.327

K_y =   effective length factor for flexural buckling about the y-axis or the axis of symmetry of the cross-section

r_y =   radius of gyration about the y-axis, in.

y_o =   distance along the y-axis between the shear center and the centroid of the cross-section, in.

All other terms are as defined previously. *It should be emphasized again that the y-axis is defined as the axis of symmetry of the cross-section in the above equations. Therefore, for a single channel section, the y-axis would actually be taken as the x-axis of the cross-section (as shown in the AISC Manual shape property tables), in calculating the preceding values.* Note that the warping torsional constant C_w is to conservatively be taken as zero for tees and double angles if the above formulation is used for these members (C_w is typically small for these sections). For a single channel section, refer to Section 2.2.3.7.1.3.4 of this chapter regarding the computation of C_w.

The governing nominal compressive resistance is then determined by first substituting the smaller of F_e from Equation 2.323 (which is always smaller than F_{ey}) and the flexural buckling resistance about the x-axis F_{ex} (taken from Equation 2.329 below) into Equations 2.319 or 2.320, as applicable. The resulting F_{cr} is then substituted into Equation 2.321 to obtain P_n.

For unsymmetric members, or members with no cross-section axis of symmetry, the failure mode always involves torsion combined with flexure about both the x- and y-

axes (i.e. flexural buckling need not be considered). In this case, the critical elastic flexural-torsional buckling stress F_e may be computed as the smallest root of the following cubic equation:

$$\left(F_e - F_{ex}\right)\left(F_e - F_{ey}\right)\left(F_e - F_{ez}\right) - F_e^2\left(F_e - F_{ey}\right)\left(\frac{x_o}{\bar{r}_o}\right)^2 - F_e^2\left(F_e - F_{ex}\right)\left(\frac{y_o}{\bar{r}_o}\right)^2 = 0 \qquad \text{Equation 2.328}$$

AISC LRFD Equation (E4-6)

where:

$$F_{ex} \quad = \quad \frac{\pi^2 E}{\left(\dfrac{K_x \ell}{r_x}\right)^2} \qquad\qquad\qquad\qquad \text{Equation 2.329}$$

AISC LRFD Equation (E4-9)

$\bar{r}_o \quad = \quad$ polar radius of gyration about the shear center, in.

$$\bar{r}_o^2 \quad = \quad x_o^2 + y_o^2 + \frac{I_x + I_y}{A_s} \qquad\qquad \text{Equation 2.330}$$

AISC LRFD Equation (E4-7)

$K_x \quad = \quad$ effective length factor for flexural buckling about the x-axis
$r_x \quad = \quad$ radius of gyration about the x-axis, in.
$x_o \quad = \quad$ distance along the x-axis between the shear center and the centroid of the cross-section, in.

Again, all other terms are as defined previously. The nominal compressive resistance is determined by first substituting the resulting value of F_e into Equations 2.319 or 2.320, as applicable. The resulting F_{cr} is then substituted into Equation 2.321 to obtain P_n.

As discussed further in Reference 154, for singly-symmetric I-sections with equal flange widths (i.e. differing flange thicknesses), flexural-torsional buckling does not need to be considered as long as $0.67 \leq t_{f1}/t_{f2} \leq 1.5$, where t_{f1} and t_{f2} are the flange thicknesses, and $K_z\ell \leq K_y\ell$. However, it is recommended that flexural-torsional buckling always be checked for singly symmetric I- sections with differing flange widths that are loaded in axial compression. The warping torsional constant C_w for such sections (with equal flange thicknesses) may be computed as follows (*28*):

$$C_w = \frac{t_f h^2}{12}\left(\frac{b_1^3 b_2^3}{b_1^3 + b_2^3}\right) \qquad\qquad \text{Equation 2.330a}$$

where:
$b_1, b_2 \quad = \quad$ individual flange widths (in.)
$h \qquad = \quad$ distance between flange centroids (in.)

t_f =   flange thickness (in.). Use an average thickness if the flange thicknesses differ.

2.4.3.2.1.2.4 Flexural-Torsional Buckling Resistance – Tees and Double Angles

For tee-shaped and double-angle compression members only, *composed of all nonslender elements*, a simpler method is provided in Section E4 of Reference 26 for calculating the flexural-torsional buckling resistance. The method directly utilizes the flexural buckling resistance about the y-axis of symmetry (*173*). For these cases, the critical elastic flexural-torsional buckling stress ($F_{cr})_{ft}$ may be computed as:

$$\left(F_{cr}\right)_{ft} = \left(\frac{F_{cry} + F_{crz}}{2H}\right)\left[1 - \sqrt{1 - \frac{4F_{cry}F_{crz}H}{\left(F_{cry} + F_{crz}\right)^2}}\right]$$

Equation 2.331

AISC LRFD Equation (E4-2)

where:

F_{cry} =   critical stress for flexural buckling about the y-axis (the axis of symmetry) computed from Equation 2.319 or Equation 2.320, as applicable (ksi)

F_{crz} = $\dfrac{GJ}{A_s \bar{r}_o^2}$

Equation 2.332

AISC LRFD Equation (E4-3)

All other terms are as defined previously. In this case, the terms H and $\bar{r}_o^2$ would be computed from Equations 2.326 and 2.327, respectively. Equation 2.332 is equivalent to the torsional buckling resistance F_{ez} from Equation 2.325 with the warping constant C_w set equal to zero.

The governing nominal compressive resistance is then taken as the smaller of the buckling resistance due to torsion combined with flexure about the y-axis ($F_{cr})_{ft}$ from Equation 2.331 and the flexural buckling resistance about the x-axis F_{cr} determined from Equations 2.319 or 2.320, as applicable. The smaller value is then substituted into Equation 2.321 to obtain P_n.

Note that the commentary to Section E of the 2005 AISC LRFD Specification (*26*) indicates that flexural-torsional buckling need not be checked for tee-sections composed of all nonslender elements with $b_f/d \geq 0.5$, and with $t_f/t_w \geq 1.10$ for rolled tees or $t_f/t_w \geq 1.25$ for built-up tees. *This recommendation should be disregarded; flexural-torsional buckling of tee sections should always be explicitly checked.*

2.4.3.2.1.3 Slender vs. Nonslender Elements

2.4.3.2.1.3.1 Width-to-Thickness Ratio Limits for Axial Compression (Nonslender Elements)

AASHTO LRFD Article 6.9.4.2 specifies width-to-thickness ratio limits that enable cross-section elements (or components) subject to uniform axial compression to develop their full nominal yield strength before the onset of local buckling. Elements satisfying these particular limits are classified as non-slender elements. All the buckling resistance equations presented above apply as shown to compression members composed entirely of non-slender elements. Elements not satisfying these particular limits are classified as slender elements. *AASHTO LRFD* Article C6.9.4.1 refers to the 2005 AISC Specification (26) (in particular Section E7) for the procedures to calculate the nominal compressive resistance of compression members consisting of one or more slender elements, which are reviewed below. It is important to note that under uniform compression, cross-section elements are classified as either slender or non-slender in both the AASHTO and AISC Specifications. Compactness requirements apply only when determining the nominal resistance of flexural members for which compression flange and web elements may need to withstand larger inelastic strains in order to ensure that local buckling does not adversely affect the nominal flexural resistance.

In general, as specified in *AASHTO LRFD* Article 6.9.4.2, to qualify as a non-slender element, plates in members subject to uniform compression must satisfy the following requirement:

$$\frac{b}{t} \leq k\sqrt{\frac{E}{F_y}} \qquad \text{Equation 2.333}$$

AASHTO LRFD Equation 6.9.4.2-1

where:
  k   =   plate buckling coefficient specified in *AASHTO LRFD* Table
             6.9.4.2-1 (Table 2.22)
  b   =   width of plate as specified in *AASHTO LRFD* Table 6.9.4.2-1
             (Table 2.22)
  t   =   plate thickness (in.)

Table 2.22 Plate Buckling Coefficients an Width of Plates for Axial Compression

Plates Supported Along One Edge	k	b	
Flanges and Projecting Legs or Plates	0.56	Half-flange width of rolled I-sections	
		Full-flange width of channels	
		Distance between free edge and first line of bolts or welds in plates	
		Full width of an outstanding leg for pairs of angles in continuous contact	
Stems of Rolled Tees	0.75	Full depth of tee	
Other Projecting Elements	0.45	Full width of outstanding leg for single angle strut or double angle strut with separator	
		Full projecting width for others	
Plates Supported Along Two Edges	**k**	**b**	
Box Flanges and Cover Plates	1.40	Clear distance between webs minus inside corner radius on each side for box flanges	
		Distance between lines of welds or bolts for flange cover plates	
Webs and Other Plate Elements	1.49	Clear distance between flanges minus fillet radii for webs of rolled beams	
		Clear distance between edge supports for all others	
Perforated Cover Plates	1.86	Clear distance between edge supports	

More specifically, the half-width of flanges of built-up I-sections must satisfy the following requirements:

$$\frac{b}{t} \leq 0.64 \sqrt{\frac{k_c E}{F_y}} \qquad\qquad \text{Equation 2.334}$$

AASHTO LRFD Equation 6.9.4.2-2

and:

$$0.35 \leq k_c \leq 0.76 \qquad\qquad \text{Equation 2.335}$$

AASHTO LRFD Equation 6.9.4.2-3

where:

$$k_c \quad = \quad \frac{4}{\sqrt{\dfrac{D}{t_w}}} \qquad\qquad \text{Equation 2.336}$$

AASHTO LRFD Equation 6.9.4.2-4

b   =   half-width of flange (in.)

D   =   web depth (in.)

Equation 2.336 accounts for the effects of web-flange interaction on local buckling in built-up I-sections subject to axial compression, and its development is discussed further in Section 2.2.3.1.1.3 of this chapter. Since web-flange interaction effects are considered negligible in rolled sections, these sections are not required to satisfy Equations 2.334 and 2.335. Note however that the upper limit on k_c of 0.76 given in Equation 2.335 (which would apply to built-up I-sections with web slenderness ratios less than or equal to about 28) yields a *k* value of 0.56 (i.e. $0.64\sqrt{k_c} = 0.56$), which is equivalent to the value of *k* given for the half-flange width of rolled I-sections in Table 2.22 for use in Equation 2.333.   Although not explicitly stated in Table 2.22, presumably, the specified *k* values would also be applied in checking the half-flange width and stem of fabricated tee sections; *note that none of the rolled tee sections in the AISC Manual shape property tables have slender flanges*. The values of the plate buckling coefficient k_c assumed for all other cases listed in Table 2.22 can be calculated as $(k/0.64)^2$, where *k* is the tabulated plate buckling coefficient given in Table 2.22.

The last paragraph of *AASHTO LRFD* Article 6.9.4.2 states that for members designed for combined axial compression and flexure according to the equations of *AASHTO LRFD* Article 6.9.2.2 (see Section 2.4.3.2.2 below – Equations 2.361 and 2.362), F_y in Equations 2.333 and 2.334 may be replaced with the calculated compressive stress due to the factored axial load and concurrent bending moment. As discussed further in Reference 154, if this done, a linear axial force versus bending moment interaction curve should be used rather that the bilinear curve given by Equations 2.361 and 2.362. This is because the application of Equations 2.361 and 2.362 to members containing slender cross-section elements is based on calculating the nominal compressive resistance P_n by treating the member as a column subject to uniform axial compression. Reference 154 further recommends using Equations 2.361 and 2.362 in such cases as specified, in lieu of a linear interaction equation with a potentially larger value of P_n. The calculations are simpler and are anticipated to be of comparable accuracy. Also, in many cases, the calculated compressive stress due to the factored axial load and bending moment will be close to F_y so the overall effect of replacing F_y with the actual combined stress in checking the plate slenderness limits will be small.

2.4.3.2.1.3.2 Compression Members with Slender Elements

General

For compression members with one or more elements not satisfying the width-to-thickness limitations specified in *AASHTO LRFD* Article 6.9.4.2 (i.e. slender elements), potential local buckling of those elements may adversely affect the overall buckling resistance of the member. Therefore, the nominal compressive resistance P_n (based on flexural, torsional or flexural-torsional buckling, as applicable) must be reduced. Many of the rolled wide-flange sections given in the AISC Manual shape property tables (i.e. rolled W-sections with $d/b_f \geq 1.7$) have slender webs under uniform axial compression. The webs of welded I- and box girders are almost

always classified as slender for uniform axial compression. The stems of a large number of rolled tee sections and one or both legs of many rolled angle sections also classify as slender elements according to the preceding criteria.

In such cases, P_n is to be determined according to the provisions given in the 2005 AISC LRFD Specification Section E7 (*26*). According to those provisions, for the limit states of flexural, torsional or flexural-torsional buckling, P_n is to be calculated as follows:

$$P_n = F_{cr}A_s$$

Equation 2.337

AISC LRFD Equation (E7-1)

If $\dfrac{K\ell}{r_s} \le 4.71\sqrt{\dfrac{E}{QF_y}}$ (or $F_e \ge 0.44QF_y$), then:

$$F_{cr} = Q\left[0.658^{\frac{QF_y}{F_e}}\right]F_y$$

Equation 2.338

AISC LRFD Equation (E7-2)

If $\dfrac{K\ell}{r_s} > 4.71\sqrt{\dfrac{E}{QF_y}}$ (or $F_e < 0.44QF_y$), then:

$$F_{cr} = 0.877F_e$$

Equation 2.339

AISC LRFD Equation (E7-3)

where:
  F_e = elastic critical buckling stress (ksi) calculated as follows:

➤ Doubly symmetric sections: for torsional buckling, use F_e from Equation 2.322, and for flexural buckling, use:

$$F_e = \dfrac{\pi^2E}{\left(\dfrac{K\ell}{r_s}\right)^2}$$

Equation 2.340

AISC LRFD Equation (E3-4)

➤ Singly symmetric sections (including tees, channels and double angles): for flexural-torsional buckling, use F_e from Equation 2.323, and for flexural buckling, use F_e from Equation 2.340
➤ Unsymmetrical sections: use F_e from Equation 2.328, except for single angles, use F_e from Equation 2.340 (i.e. flexural buckling) using the appropriate effective slenderness ratio $K\ell/r$ in place of $K\ell/r_s$ (the effective slenderness ratio is discussed in Section 2.4.3.2.1.4 below)

Q   =   cross-section form factor

      =   1.0 for members with all nonslender elements

      = $Q_s Q_a$ for members with one or more slender elements (where Q_s and Q_a are defined below)

For compression members containing slender elements, the nominal compressive resistance is calculated by using a reduced equivalent yield capacity $P_o = QP_y$, where the cross-section form factor Q is less than or equal to 1.0. The AISC Specification has used this approach, as adopted from Reference 174, since 1969. Prior to 1969, a more conservative approach was used in which any portion of the plate width that exceeded the appropriate slenderness limit was disregarded.

In calculating Q, Section E7 of Reference 26 distinguishes between *unstiffened elements*, which refer to elements supported along only one longitudinal edge, and *stiffened elements*, which refer to elements supported along two longitudinal edges. Unstiffened elements are assumed to reach their limit of resistance when they attain their theoretical local buckling resistance. Stiffened elements take advantage of the post-buckling resistance that is available to a plate supported along two longitudinal edges. The post-buckling resistance is determined using an effective width approach. An effective width approach was adopted for both unstiffened and stiffened elements in Reference 175; however, subsequent editions of the AISC Specification did not adopt this approach primarily because the advantages of post-buckling resistance for unstiffened elements do not become significant unless the plate elements are very slender. Such dimensions are not commonly encountered in structures fabricated from hot-rolled plates. Other reasons for not adopting this approach are summarized in Reference 154.

For cross-sections composed of only unstiffened slender elements, Q is to be taken equal to Q_s (i.e. Q_a = 1.0). For cross-sections composed only of stiffened slender elements, Q is to be taken equal to Q_a (i.e. Q_s = 1.0). For cross-sections composed of both unstiffened and stiffened slender elements, Q is to be taken equal to $Q_s Q_a$.

Equations for Q_s and Q_a from Section E7 of Reference 26 are reproduced below. Further information regarding the development and application of these equations may be found in the commentary to Section E7 (*26*) and in References 28 and 154. Reference 154 also provides recommendations for the application of these equations to hybrid I-sections with slender web elements subject to axial compression.

Slender Unstiffened Elements, Q_s

For slender unstiffened elements, the form factor Q_s is equal to the ratio of the smallest local buckling resistance of all the unstiffened elements in the cross-section divided by F_y. In other words, for a compression member consisting entirely of unstiffened elements, the reduced equivalent yield strength of the member is taken as the average axial stress at which the most critical unstiffened element reaches its local buckling resistance (i.e. the elastic or inelastic local buckling resistance depending on the values of b/t, k_c and F_y). In the following, unless otherwise

specified, b is the width of the unstiffened compression element as defined in Table 2.22 and t is the thickness of the element. Only the equations for single angles and stems of tees are given below, as these are likely to be the most common equations utilized in steel-bridge design. Equations for flange, angles and plates projecting from rolled or built-up compression members may be found in Reference 26.

For single angles:

For $\dfrac{b}{t} \leq 0.45\sqrt{\dfrac{E}{F_y}}$:

$$Q_s = 1.0$$

Equation 2.341

AISC LRFD Equation (E7-10)

For $0.45\sqrt{\dfrac{E}{F_y}} < \dfrac{b}{t} \leq 0.91\sqrt{\dfrac{E}{F_y}}$:

$$Q_s = 1.34 - 0.76\left(\dfrac{b}{t}\right)\sqrt{\dfrac{F_y}{E}}$$

Equation 2.342

AISC LRFD Equation (E7-11)

For $\dfrac{b}{t} > 0.91\sqrt{\dfrac{E}{F_y}}$:

$$Q_s = \dfrac{0.53E}{F_y\left(\dfrac{b}{t}\right)^2}$$

Equation 2.343

AISC LRFD Equation (E7-12)

where b is the full width of the longest angle leg (in.)

For stems of tees:

For $\dfrac{d}{t} \leq 0.75\sqrt{\dfrac{E}{F_y}}$:

$$Q_s = 1.0$$

Equation 2.344

AISC LRFD Equation (E7-13)

For $0.75\sqrt{\dfrac{E}{F_y}} < \dfrac{d}{t} \leq 1.03\sqrt{\dfrac{E}{F_y}}$:

$$Q_s = 1.908 - 1.22\left(\frac{d}{t}\right)\sqrt{\frac{F_y}{E}}$$

<div align="right">Equation 2.345</div>

<div align="right">*AISC LRFD* Equation (E7-14)</div>

For $\dfrac{d}{t} > 1.03\sqrt{\dfrac{E}{F_y}}$:

$$Q_s = \frac{0.69E}{F_y\left(\dfrac{d}{t}\right)^2}$$

<div align="right">Equation 2.346</div>

<div align="right">*AISC LRFD* Equation (E7-15)</div>

where *d* is the full nominal depth of the tee (in.)

Slender Stiffened Elements, *Qₐ*

The reduction factor Q_a for slender stiffened elements is taken as:

$$Q_a = \frac{A_{eff}}{A}$$

<div align="right">Equation 2.347</div>

<div align="right">*AISC LRFD* Equation (E7-16)</div>

where:
- A = total cross-sectional area of the member (in.^{2})
- A_{eff} = summation of the effective areas of the cross-section based on the reduced effective width b_e (in.) = $A - \sum(b-b_e)t$

The reduced effective width b_e is the width of the rectangular stress blocks over which the maximum stress f at the longitudinal edges can be assumed to act uniformly to produce the same force at the actual stresses acting over the full width of the plate. The actual average stresses in the middle of the plate, averaged through the thickness, are smaller due to the post-buckling deformations (Figure 2.142).
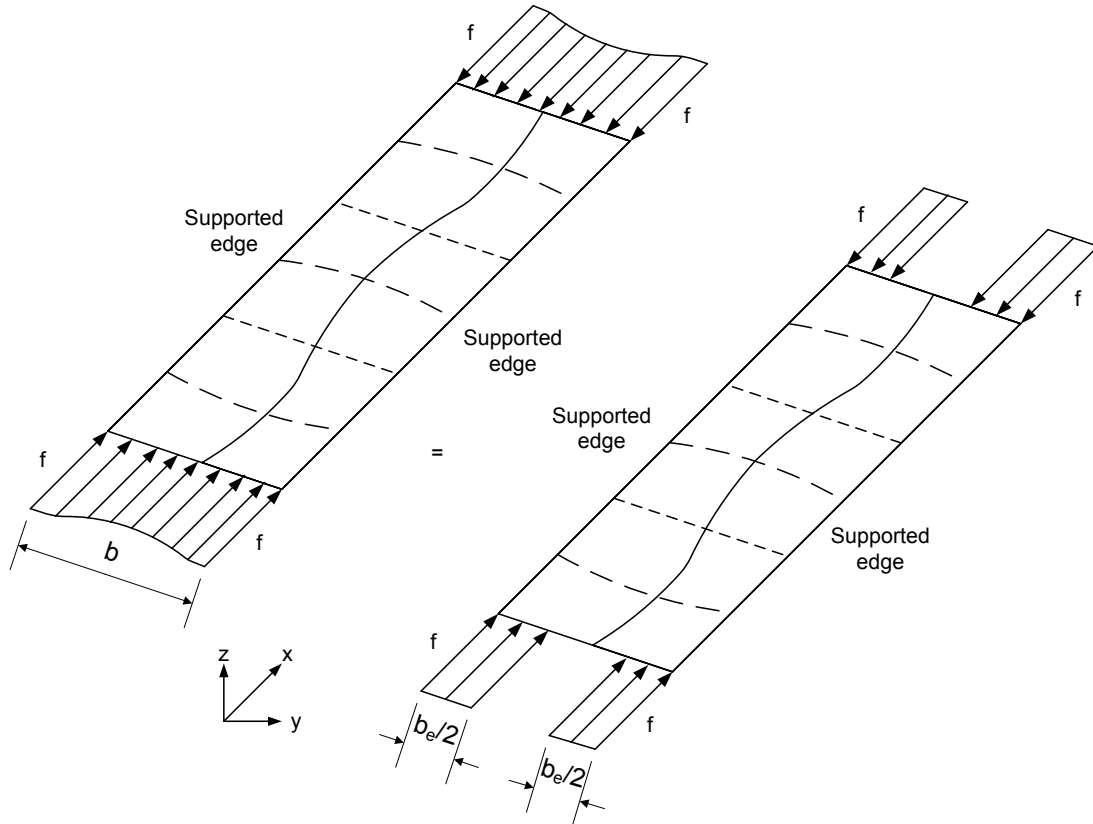
Figure 2.142 Average vs. Idealized Stress Distribution Across the Width of a Post-Buckled Stiffened Plate Element

b_e is determined as follows:

➢ For uniformly compressed slender stiffened elements with $\dfrac{b}{t} \geq 1.49\sqrt{\dfrac{E}{f}}$, except for flanges of square and rectangular sections of uniform thickness:

$$b_e = 1.92t\sqrt{\dfrac{E}{f}}\left[1 - \dfrac{0.34}{(b/t)}\sqrt{\dfrac{E}{f}}\right] \leq b \qquad \text{Equation 2.348}$$

AISC LRFD Equation (E7-17)

where *f* is taken as F_{cr} with F_{cr} calculated based on *Q* = 1.0.

➢ For flanges of square and rectangular slender-element sections of uniform thickness with $\dfrac{b}{t} \geq 1.40\sqrt{\dfrac{E}{f}}$:

$$b_e = 1.92t\sqrt{\frac{E}{f}}\left[1 - \frac{0.38}{(b/t)}\sqrt{\frac{E}{f}}\right] \le b \qquad \text{Equation 2.349}$$

AISC LRFD Equation (E7-18)

where *f* is taken as P_n/A_{eff}. Taking *f* as such requires an iterative solution. Section E7 of Reference 26 alternatively allows *f* to be conservatively taken equal to F_y.

It should be noted that Reference 154 recommends simply using $f = Q_sF_y$ in both Equations 2.348 and 2.349 in lieu of the values specified in Section E7, as this is felt to provide a more representative calculation of the true resistance in all cases (*175a*).

➢ For axially loaded circular sections:

$$\text{For } 0.11\frac{E}{F_y} < \frac{D}{t} < 0.45\frac{E}{F_y}:$$

$$Q = Q_a = \frac{0.038E}{F_y(D/t)} + \frac{2}{3} \qquad \text{Equation 2.350}$$

AISC LRFD Equation (E7-19)

2.4.3.2.1.4 Single-Angle Compression Members

Single angles are commonly used as compression members in cross-frames and lateral bracing for steel bridges. Since the angle is typically connected through one leg only, the member is subject to combined flexure (i.e. moments about both principal axes due to the eccentricities of the applied axial load) and axial compression and is usually restrained by differing amounts about its geometric x- and y-axes. As a result, the prediction of the nominal compressive resistance of these members is difficult. The AASHTO Specifications have been largely silent regarding the design of these members for these conditions. Prior to 2005, the AISC provided specific design provisions applicable to these members in an *LRFD Specification for Design of Single-Angle Members* (*176, 177*). These provisions essentially treated the angle as a beam-column and were somewhat complex and difficult to implement. Section E5 of the 2005 AISC Specification (*26*) provides significantly simplified provisions for the design of single-angle compression members satisfying certain conditions that are based on the ASCE 10-97 provisions for the design of single-angle members used in latticed transmission towers (*172*). Similar procedures are also employed in the Eurocode 3 standard (*178*) and in British Standard BS5950 (*179*).

In essence, the simplified provisions permit the effect of the eccentricities to be neglected when the members are evaluated as axially loaded compression members using an appropriate specified effective slenderness ratio $K\ell/r$ (see below), as long as the following conditions are satisfied:

> ➤ The end connections are to a single leg,
> ➤ The member is loaded at the ends in compression through the same leg,
> ➤ The end connections are welded or use a minimum of two bolts,
> ➤ The member is not subjected to any intermediate transverse loads, and
> ➤ When used as web members in trusses, all adjacent web members are attached to the same side of the gusset plate or chord.

The effective slenderness ratio indirectly accounts for the bending in the angles due to the eccentricity of the loading allowing the member to be proportioned as if it were a pinned-end concentrically loaded compression member. Thus, it may be proportioned using the effective slenderness ratio to check for flexural buckling only under axial compression using Equation 2.319 or 2.320, as applicable. Should the angle consist of any slender leg elements (i.e. elements not satisfying the applicable width-to-thickness requirements of *AASHTO LRFD* Article 6.9.4.2), the resulting nominal compressive resistance should be reduced according to the appropriate procedures discussed previously in Section 2.4.3.2.1.3 of this chapter. *Furthermore, according to Section E4 of Reference 26, when the effective slenderness ratio is used, single angles need not be checked for flexural-torsional buckling.*

The expressions for the effective slenderness ratio presume significant end rotational restraint about the y-axis, or the axis perpendicular to the connected leg and gusset plate (Figure 2.143).
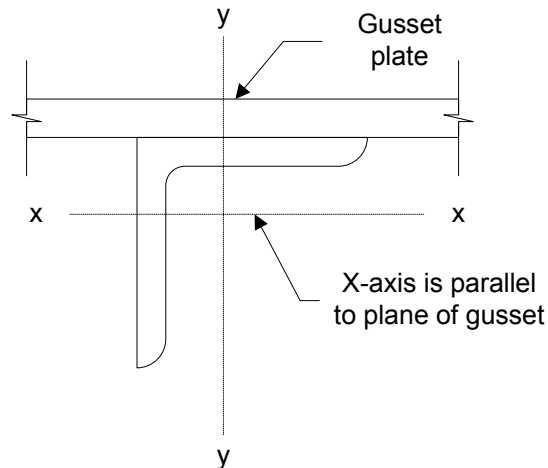
Figure 2.143 Single-Angle Geometric Axes Utilized in the Effective Slenderness Ratio Expressions

As a result, as shown in various tests (*180*, *181*, *182*), the angle tends to buckle primarily about the x-axis due to the eccentricity of the load about the x-axis coupled with the high degree of restraint about the y-axis (it should be noted that References 180 and 182 included tests of unequal-leg angles). Therefore, the radius of gyration in the effective slenderness ratio expressions is to be taken as r_x, or the radius of gyration for bending about the geometric x-axis (parallel to the connected leg), and not the minimum radius of gyration r_z about the minor principal axis of the angle.

When an angle has significant rotational restraint about the y-axis, the stress along the connected leg will be approximately uniform (*183*). As discussed in Reference 183, to achieve a uniform stress along the connected leg, the axial load should be applied along a line such that the ratio of the eccentricities e_z/e_w about the minor and major principal axes, respectively, is equal to the ratio of I_z/I_w.

Section E5 of Reference 26 provides two sets of equations for the effective slenderness ratio. One set of equations [Case (b) in Section E5] is based on the assumption of a higher degree of x-axis rotational restraint at the ends of the member than the other set [Case (a) in Section E5]. The Case (b) equations are essentially equivalent to equations employed in Reference 172 for equal-leg angles acting as web members in latticed transmission towers; the difference being that the equations in Reference 172 are in terms of r_z rather than r_x. In Section E5, the Case (b) equations, which assume additional end rotational restraint, are intended to apply only to single angles used as web members in box or space trusses. As indicated in the commentary to Section E5, the web members framing into the top chord of space trusses typically restrain twisting of the chord at the panel points providing significant x-axis restraint to the angles. The Case (a) equations are intended to apply to individual single-angle members and to single angles used as web members in planar trusses. The commentary to Section E5 suggests that simple single-angle diagonals in braced frames can be considered to have enough end restraint that the Case (a) equations apply. Lutz (*184*) compared the results from the Case (a) equations to test results for single-angle members in compression with essentially pinned-end conditions reported in References 185 and 186 and found an average value of P_n/P_{test} of 0.998 with a coefficient of variation of 0.109. Thus, based on this data and as recommended also in Reference 154, the Case (a) equations are considered applicable to individual single-angle compression members employed in bridge cross-frames and lateral bracing systems, and will be the only set of equations presented herein.

For equal-leg angles and unequal-leg angles connected through the longer leg that are individual members or that are web members of planar trusses satisfying the conditions outlined above, the effective slenderness ratio $K\ell/r$ is to be taken as follows:

When $0 \le \dfrac{\ell}{r_x} \le 80$:

$$\frac{K\ell}{r} = 72 + 0.75\,\frac{\ell}{r_x}$$

<div align="right">Equation 2.351</div>

<div align="right">*AISC LRFD* Equation (E5-1)</div>

When $\dfrac{\ell}{r_x} > 80$:

$$\frac{K\ell}{r} = 32 + 1.25\,\frac{\ell}{r_x}$$

<div align="right">Equation 2.352</div>

AISC LRFD Equation (E5-2)

The effective slenderness ratio from Equation 2.352 is limited to a maximum value 200 in the 2005 AISC LRFD Specification. However, as discussed below in Section 2.4.3.3 of this chapter, the maximum slenderness ratio $K\ell/r$ of compression members is limited to 120 for primary members and 140 for secondary members in *AASHTO LRFD* Article 6.9.3. *Therefore, the calculated effective slenderness ratio in all cases should be limited to either 120 or 140, as applicable.* ℓ is to be taken as the length of the member between the end-connection work points. It should be emphasized again that r_x as utilized in the above equations is the radius of gyration about the angle geometric axis parallel to the connected leg (Figure 2.142). *Therefore, for an unequal-leg angle connected through the longer leg, r_x should be taken as the smaller value about the angle geometric axes, which is typically listed as r_y in the AISC Manual shape property tables.* For unequal-leg angles connected through the shorter leg with the ratio of the leg widths less than 1.7:

When $0 \le \dfrac{\ell}{r_x} \le 80$:

$$\frac{K\ell}{r} = 72 + 0.75\frac{\ell}{r_x} + 4\left[\left(\frac{b_\ell}{b_s}\right)^2 - 1\right]$$

Equation 2.353

When $\dfrac{\ell}{r_x} > 80$:

$$\frac{K\ell}{r} = 32 + 1.25\frac{\ell}{r_x} + 4\left[\left(\frac{b_\ell}{b_s}\right) - 1\right] \ge 0.95\frac{\ell}{r_z}$$

Equation 2.354

where b_ℓ and b_s are the lengths of the longer and shorter legs, respectively. For the case of unequal-leg angles connected through the shorter leg, the limited available test data (*180, 182*) for this case give lower capacities for comparable ℓ/r_x values than equal-leg angles (*184*).   Stiffening the shorter leg rotationally tends to force the buckling axis of the angle away from the x-axis and closer to the z-axis of the angle (*184*).   Thus, the effective slenderness for this case is modified by adding an additional term along with a governing slenderness limit based on ℓ/r_z (for more slender unequal-leg angles) in Equations 2.353 and 2.354. The upper limit on b_ℓ/b_s of 1.7 is based on the limits of the available physical tests.

Comparisons of the results from the above equations to the results from similar criteria provided in the Eurocode 3 standard (*178*) and in British Standard BS5950 (*179*) are discussed in References 154 and 184.   In general, the European procedures produce much higher capacities than the AISC procedures for angles with smaller values of ℓ/r_x.   The capacities predicted utilizing the effective slenderness ratios from the applicable Equations 2.351 through 2.354 are below the

capacities predicted from the European procedures for the entire range of slenderness values.

As specified in Section E5 of Reference 26, single-angle compression members not meeting one or more of the conditions spelled out in the above bullet list, or with leg length ratios b_ℓ/b_s greater than 1.7, are to be evaluated for combined axial load and flexure as beam-columns according to Section H2 of Reference 26 (refer also to Section 2.4.3.2.2 below – specifically Equation 2.364). In computing P_n, the end restraint conditions should be evaluated in calculating the effective length $K\ell$ (with the in-plane effective length factor K taken equal to 1.0, as discussed previously in Section 2.4.3.2.1.1.1 of this chapter). As suggested in the commentary to Section E5, after the effective length factors about the geometric axes (i.e. x- and y-axes) have been computed, the procedures of Reference 187 can be used to obtain a minimum effective radius of gyration for the single-angle member in computing P_n. In determining whether the flexural-torsional buckling resistance of the angle needs to be considered in computing P_n for this case, it is recommended that Reference 177 be consulted. Also, it has been observed that the actual eccentricity in the angle is less than the distance from the centerline of the gusset if there is any restraint present about the x-axis (*188*). Reference 181 recommends reducing the eccentricity in this instance to $\bar{y} - t/2$, where t is the thickness of the angle, as long the angle is on one side of the chord or gusset plate. The nominal flexural resistance of the angle M_n for this case should be determined according to the procedures given in Section F10 of Reference 26.

Single-angle members are often employed in X-type configurations in cross-frames. Reference 172 suggests that for cases in these configurations where one diagonal is in tension with a force not less than 20 percent of the force in the diagonal compression member, that the crossover or intersection point may be considered as a brace point for out-of-plane buckling. A different approach is suggested in Reference 189 for equally loaded compression and tension diagonals in X-type configurations in which all connections are welded. This approach also assumes a significant level of restraint at the crossover point. While such approaches could potentially be utilized with the effective slenderness ratio approach discussed above, they have not yet received any validation. For example, should the members be connected with only a single bolt at the crossover point, which is a commonly used detail, the necessary rotational restraint about the y-axis assumed in the effective slenderness ratio equations may not be present at that point. It is suggested in Reference 154 that in the interim, the effective slenderness ratio equations given above may be conservatively applied to single-angle compression members used in X-type bracing configurations by using the full length of the diagonal between the connection work points for ℓ.

EXAMPLE

Determine the factored compressive resistance P_r at the strength limit state of a 5 x 5 x 7/16 single angle used as a bottom strut in an I-girder cross frame. The angle is 8.0 feet long and the steel for the angle is ASTM A 709 Grade 50W steel. The angle is subject to a compressive force due to the factored loads P_u under the Strength I

load combination of 62.0 kips. The angle meets all the conditions spelled out in the preceding bullet list. From the AISC Manual shape property tables, the cross-sectional area of the angle A_s is equal to 4.18 in.^{2}, and the radius of gyration about the x-axis r_x is equal to 1.55 in. Therefore:

$$\frac{\ell}{r_x} = \frac{8.0(12)}{1.55} = 61.9$$

For an equal-leg angle with $\ell / r_x < 80$, use the effective slenderness ratio calculated from Equation 2.357 as follows:

$$\frac{K\ell}{r} = 72 + 0.75 \frac{\ell}{r_x}$$

AISC LRFD Equation (E5-1)

$$\frac{K\ell}{r} = 72 + 0.75(61.9) = 118.4$$

The value of the effective slenderness ratio is less than the maximum permitted slenderness ratio of 120 for main compression members specified in *AASHTO LRFD* Article 6.9.3 and discussed in Section 2.4.3.3 below – ok (since the force in the angle is assumed to be determined from an analysis, the member is considered to be a main or primary member).

Check if the angle has any slender elements. As specified in *AASHTO LRFD* Article 6.9.4.2, to qualify as a nonslender element, plates in members subject to uniform compression must satisfy the following requirement:

$$\frac{b}{t} \le k \sqrt{\frac{E}{F_y}}$$

AASHTO LRFD Equation 6.9.4.2-1

From Table 2.22, for the outstanding leg of single angle struts, *k* in the preceding equation is taken equal to 0.45. Therefore:

$$0.45 \sqrt{\frac{29,000}{50}} = 10.8 < \frac{b}{t} = \frac{5}{0.4375} = 11.4$$

Therefore, the nominal compressive resistance of the angle must be reduced due to potential local buckling of the slender outstanding leg. Since *b/t* is less than $0.91\sqrt{E/F_y} = 21.9$, calculate the form factor Q_s for the slender unstiffened element from Equation 2.348 as follows:

$$Q_s = 1.34 - 0.76\left(\frac{b}{t}\right)\sqrt{\frac{F_y}{E}}$$

<div align="right">AISC LRFD Equation (E7-11)</div>

$$Q_s = 1.34 - 0.76(11.4)\sqrt{\frac{50}{29,000}} = 0.98$$

Since there are no stiffened elements, Q is taken equal to Q_s; therefore, $Q = 0.98$.

Since the effective slenderness ratio approach is used, the effect of all load eccentricities can be neglected and flexural-torsional buckling does not need to be considered.   Therefore,   since   the   effective   slenderness   ratio $\frac{K\ell}{r} > 4.71\sqrt{\frac{E}{QF_y}} = 114.6$, F_{cr} is computed based on flexural buckling from Equation 2.339 as follows:

$$F_{cr} = 0.877F_e$$

<div align="right">AISC LRFD Equation (E7-3)</div>

For single angles, the elastic critical buckling stress F_e is computed from Equation 2.340 as follows, with the effective slenderness ratio $K\ell/r$ substituted for $K\ell/r_s$:

$$F_e = \frac{\pi^2 E}{\left(\dfrac{K\ell}{r_s}\right)^2}$$

<div align="right">AISC LRFD Equation (E3-4)</div>

$$F_e = \frac{\pi^2(29,000)}{(118.4)^2} = 20.42 \text{ ksi}$$

Therefore:

$$F_{cr} = 0.877(20.42) = 17.91 \text{ ksi}$$

The nominal compressive resistance P_n is computed from Equation 2.337 as:

$$P_n = F_{cr}A_s$$

<div align="right">AISC LRFD Equation (E7-1)</div>

$$P_n = 17.91(4.18) = 74.9 \text{ kips}$$

The factored compressive resistance Pr is computed from Equation 2.312 as:

$$P_r = \phi_c P_n$$

<div align="right">*AASHTO LRFD* Equation 6.9.2.1-1</div>

where ϕ_c is the resistance factor for axial compression specified in *AASHTO LRFD* Article 6.5.4.2 = 0.90. Therefore:

$$P_r = 0.90(74.9) = 67.4 \text{ kips} > P_u = 62.0 \text{ kips} \quad \text{ok}$$

2.4.3.2.2 Combined Axial Compression and Flexure

2.4.3.2.2.1 General

For members subject to combined axial compression and flexure, often referred to as beam-columns, the resistance is typically defined by interaction equations that reduce to the compressive resistance in the limit of pure axial compression (with no flexure), or to the flexural resistance about the corresponding principal axis of the section in the limit of pure flexure about that axis (with no axial compression).

AASHTO LRFD Article 6.9.2.2 specifies the following bilinear relationship to define the resistance of members subject to combined axial compression and flexure:

If $\dfrac{P_u}{P_r} < 0.2$, then:

$$\frac{P_u}{2.0 P_r} + \left(\frac{M_{ux}}{M_{rx}} + \frac{M_{uy}}{M_{ry}} \right) \leq 1.0 \qquad \text{Equation 2.355}$$

<div align="right">*AASHTO LRFD* Equation 6.9.2.2-1</div>

If $\dfrac{P_u}{P_r} \geq 0.2$, then:

$$\frac{P_u}{P_r} + \frac{8.0}{9.0} \left(\frac{M_{ux}}{M_{rx}} + \frac{M_{uy}}{M_{ry}} \right) \leq 1.0 \qquad \text{Equation 2.356}$$

<div align="right">*AASHTO LRFD* Equation 6.9.2.2-2</div>

where:

M_{rx} = factored flexural resistance about the x-axis taken as ϕ_f times the nominal flexural resistance about the x-axis determined as specified in *AASHTO LRFD* Article 6.10, 6.11 or 6.12, as applicable (kip-in.)

M_{ry} = factored flexural resistance about the y-axis taken as ϕ_f times the nominal flexural resistance about the y-axis determined as specified in *AASHTO LRFD* Article 6.12, as applicable (kip-in.)

M_{ux} = the maximum second-order elastic moment along the member unbraced length taken about the x-axis of the cross-section (kip-in.)

M_{uy} = the maximum second-order elastic moment along the member unbraced length taken about the y-axis of the cross-section (kip-in.)

P_r = factored compressive resistance determined as specified in *AASHTO LRFD* Article 6.9.2.1 (see Equation 2.312 above) (kips)

P_u = axial compressive force due to the factored loads (kips)

ϕ_f = resistance factor for flexure determined as specified in *AASHTO LRFD* Article 6.5.4.2 (= 1.0)

The calculation of M_{rx} for use in Equations 2.355 and 2.356 was discussed previously in Section 2.4.2.2.2 of this chapter (refer to Equations 2.310 and 2.311). For cases where the member is subject to flexure about the y-axis, the nominal flexural resistance about the y-axis for I-shaped members is determined according to the provisions of *AASHTO LRFD* 6.12.2.2.1 (see Section 2.2.3.7.1.3 of this chapter. This section also contains further information on determining the nominal flexural resistance of miscellaneous members such as tees, double angles and channels).

For prismatic members along the unbraced length, the largest value of P_u/P_r based on the axial compressive resistance limit states of flexural buckling, torsional bucking or flexural-torsional buckling is to be used in Equations 2.355 or 2.356, as applicable. Also, the largest values of M_{ux}/M_{rx} and M_{uy}/M_{ry} based on the flexural resistance limit states of yielding, local buckling or lateral-torsional buckling are to be used. Strictly speaking, for a particular load combination, concurrent values of P_u, M_{ux} and M_{uy} should be used in computing and determining the critical ratios to use. However, since concurrent actions are not typically tracked in the analysis, it is conservative and convenient to use the maximum envelope values for these actions in combining the ratios in these equations. For nonprismatic members, the reader is referred to Reference 154 for additional information regarding the proper application of the preceding equations to such members.

As specified in *AASHTO LRFD* Article 6.9.2.2, the second-order elastic moments M_{ux} and M_{uy} may either be determined from a second-order elastic analysis that accounts for the magnification of moment caused by the factored axial load, or by an approximate single-step adjustment (i.e. moment magnification) applied to the first-order elastic moments obtained from the analysis. As specified in *AASHTO LRFD* Article 4.5.3.2.2b, the single-step adjustment or moment magnification may be determined as follows (where M_c is the approximate second-order elastic value of M_{ux} or M_{uy}, as applicable):

$$M_c = \delta_b M_{2b} + \delta_s M_{2s}$$ Equation 2.357

AASHTO LRFD Equation 4.5.3.2.2b-1

where:

δ_b = $\dfrac{C_m}{1 - \dfrac{P_u}{\phi_K P_e}} \geq 1.0$ Equation 2.358

AASHTO LRFD Equation 4.5.3.2.2b-3

$$\delta_s = \cfrac{1}{1-\cfrac{\Sigma P_u}{\phi_K \Sigma P_e}}$$ Equation 2.359

AASHTO LRFD Equation 4.5.3.2.2b-4

ϕ_K = stiffness reduction factor equal to 1.0 for steel members and 0.75 for concrete members

C_m = equivalent uniform moment factor. For members braced against sidesway and without transverse loading between supports in the plane of bending:

$$= 0.6 + 0.4\frac{M_{1b}}{M_{2b}}$$ Equation 2.360

AASHTO LRFD Equation 4.5.3.2.2b-6

where M_{1b} and M_{2b} are the smaller and larger moments, respectively, calculated from a first-order elastic analysis at the ends of that portion of the member unbraced in the plane of bending under consideration. M_{1b}/M_{2b} is positive when the member is bent in single curvature and negative when the member is bent in reverse curvature.

For all other cases:

$= 1.0$

M_{2b} = moment on the compression member about the axis under consideration due to factored loads that result in no appreciable sidesway calculated by first-order elastic analysis (kip-ft.). M_{2b} is always taken as positive.

M_{2s} = moment on the compression member about the axis under consideration due to factored loads that result in sidesway Δ greater than $\ell_u/1500$ calculated by first-order elastic analysis (kip-ft.). M_{2s} is always taken as positive.

P_e = Euler buckling load calculated based on the assumption of no sidesway, which is to be taken as follows for noncomposite members:

$$= \frac{\pi^2 EI}{(K\ell_u)^2}$$ Equation 2.361

AASHTO LRFD Equation 4.5.3.2.2b-5

P_u = factored axial load (kips)

I = moment of inertia of the member about the axis under consideration (in.[4])

K = effective length factor in the plane of bending determined as specified in *AASHTO LRFD* Article 4.6.2.5 (see also Section 2.4.3.2.1.1.1 above). For the calculation of δ_b, P_e is to be based on

the *K* factor for braced frames. For the calculation of δ_s, P_e is to be based on the *K* factor for unbraced frames.

ℓ_u =   unbraced length of the compression member (in.)

A stress-based form of the single-step adjustment is also given in *AASHTO LRFD* Article 4.5.3.2.2b as follows:

$$f_c = \delta_b f_{2b} + \delta_s f_{2s}$$ Equation 2.362

AASHTO LRFD Equation 4.5.3.2.2b-2

where f_{2b} and f_{2s} are the bending stresses corresponding to M_{2b} and M_{2s}, respectively.

δ_b is an amplifier to account for second-order effects due to displacements between brace points, and δ_s is an amplifier to account for second-order effects due to displacements of the braced points (or P-Δ effects). For members braced against sidesway, δ_s is to be taken as 1.0 unless analysis indicates that a lower value may be used. For members not braced against sidesway, δ_b is to be determined as for a braced member and δ_s is to be determined as for an unbraced member. As specified in *AASHTO LRFD* Article 4.5.3.2.2b, to calculate δ_s for the case where a group of compression members on one level comprise a bent, or where they are connected integrally to the same superstructure and collectively resist the sidesway of the structure, ΣP_u and ΣP_e are to be taken as the summations for all columns in the group. Also, for structures not braced against sidesway, the flexural members and foundation units framing into the compression member are to be designed for the sum of the end moments of the compression member at the joint.

The bilinear form of the interaction curve given by Equations 2.355 and 2.356 combines member strength and stability considerations into one single curve. Previous specifications utilized two curves; one that addressed stability or strength considerations and one that addressed yielding as a member cross-section check. The bilinear form is simpler to use and better represents the fact that beam-columns actually fail through a combination of inelastic bending and stability effects (*154*). As discussed further in Reference 154, Equations 2.355 and 2.356 were established based on curve fitting to results from a large number of rigorous beam-column solutions; primarily for noncomposite doubly symmetric I-section members composed of compact elements. The equations provide an excellent fit to solutions using a second-order moment magnification factor applied to first-order analysis results for doubly-symmetric I-sections subject to strong-axis bending with an ℓ/r ranging from 0 to 100. The equations are accurate to conservative for such shapes subject to weak-axis bending and become increasingly conservative in these cases when ℓ/r is less than about 40 due to the large shape factor (or ratio of M_p/M_y) and increasing convexity of the curve representing the fully plastic weak-axis bending resistance of these sections. The equations are moderately conservative for both axes when ℓ/r is greater than 120. For the no sidesway case, the equations also tend to be more conservative for beam-columns subject to reverse-curvature bending since they do not account for the influence of moment gradient on the shape

of the strength or resistance curve (*190*).   Additional information on the interaction behavior of doubly symmetric I-sections may be found in Reference 154 and in References 191 through 193.

2.4.3.2.2.2 Singly Symmetric Sections

Equations 2.355 and 2.356 are considered applicable to singly symmetric sections also.   Figure 2.144 qualitatively shows a series of resistance envelopes for a prismatic singly symmetric I-section member subject to combined flexure and axial load (*154*). The outer envelope represents the fully plastic axial force versus moment resistance envelope for a short (approximately zero length) singly symmetric I-section member composed of compact elements. The linear envelope immediately inside the outer envelope represents the first-yield axial force versus moment resistance envelope for the same member. Note that the envelopes are not symmetric and that a bulge exists in the upper right and lower left quadrants of the plot where the axial and flexural stresses on the larger flange are additive either in compression or in tension.
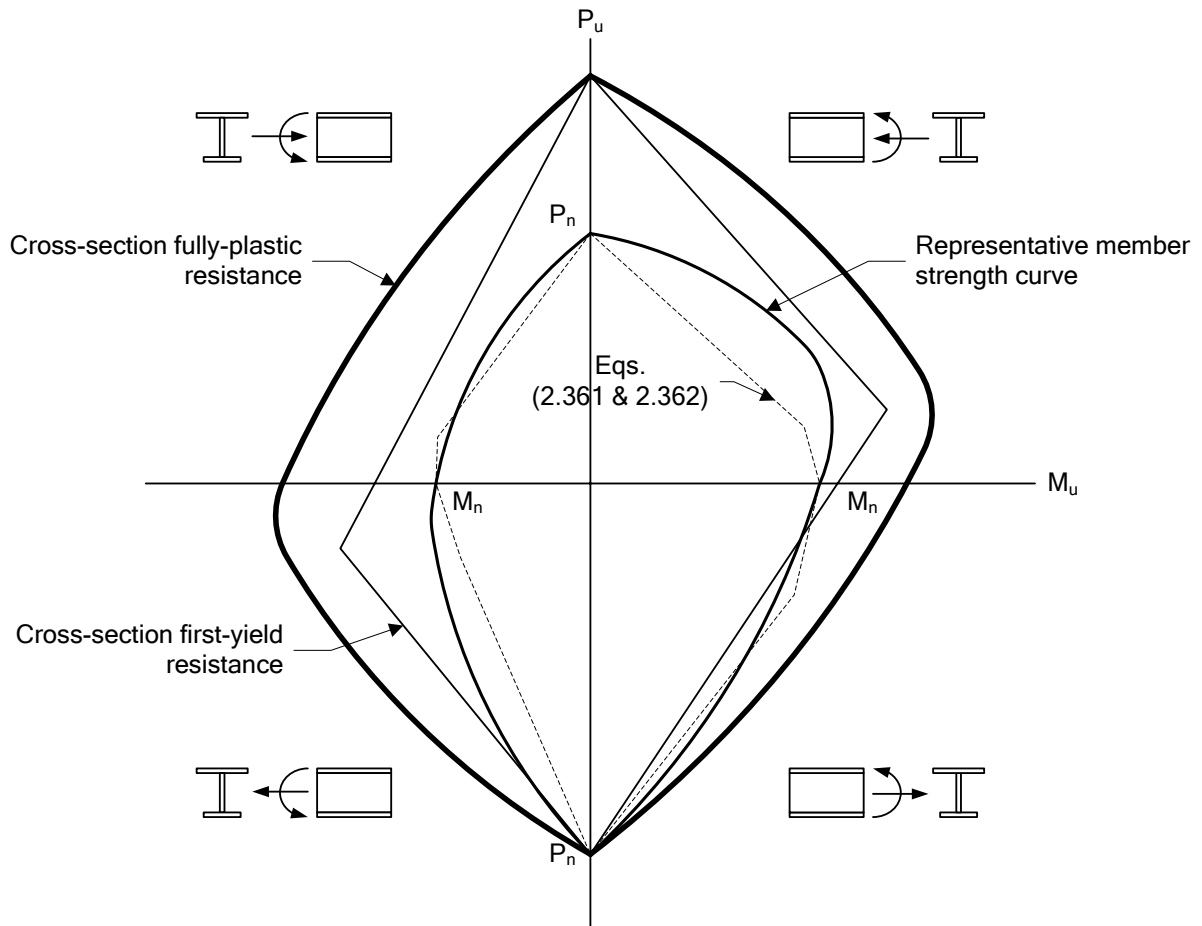
Figure 2.144 Axial Force versus Moment Resistance Envelopes for a Singly Symmetric I-Section Beam-Column

For a finite-length prismatic singly symmetric I-section beam-column braced at discrete points, the actual resistance may be influenced by a combination of yielding, local and overall stability, particularly when the member is composed of noncompact and/or slender elements. The darker solid curve in Figure 2.144 qualitatively shows a representative resistance envelope for such a member. The dashed lines in Figure 2.144 represent the interaction curves in each quadrant given by Equations 2.355 and 2.356.   In general, Equations 2.355 and 2.356 provide an accurate to conservative estimate of the resistance of these sections relative to available test results (*194*), particularly for sections where the smaller flange is subjected to additive flexural and axial stresses (i.e. sections falling in the upper left and lower right quadrants).   The level of conservatism increases for cases where the larger flange is subjected to additive flexural and axial stresses (i.e. sections falling in the upper right and lower left quadrants).

For tee and double-angle beam-columns of finite length, the behavior is similar to that illustrated in Figure 2.144. However, the non-symmetry of the interaction curves for these members is increased, particularly for members of intermediate and longer

lengths. This behavior is illustrated in Figure 2.145 for a simply supported WT18 x 67.5 tee-section beam-column that was analyzed in Reference 195. The section has a specified minimum yield strength of 50 ksi and an unbraced length L_b of 20 feet.
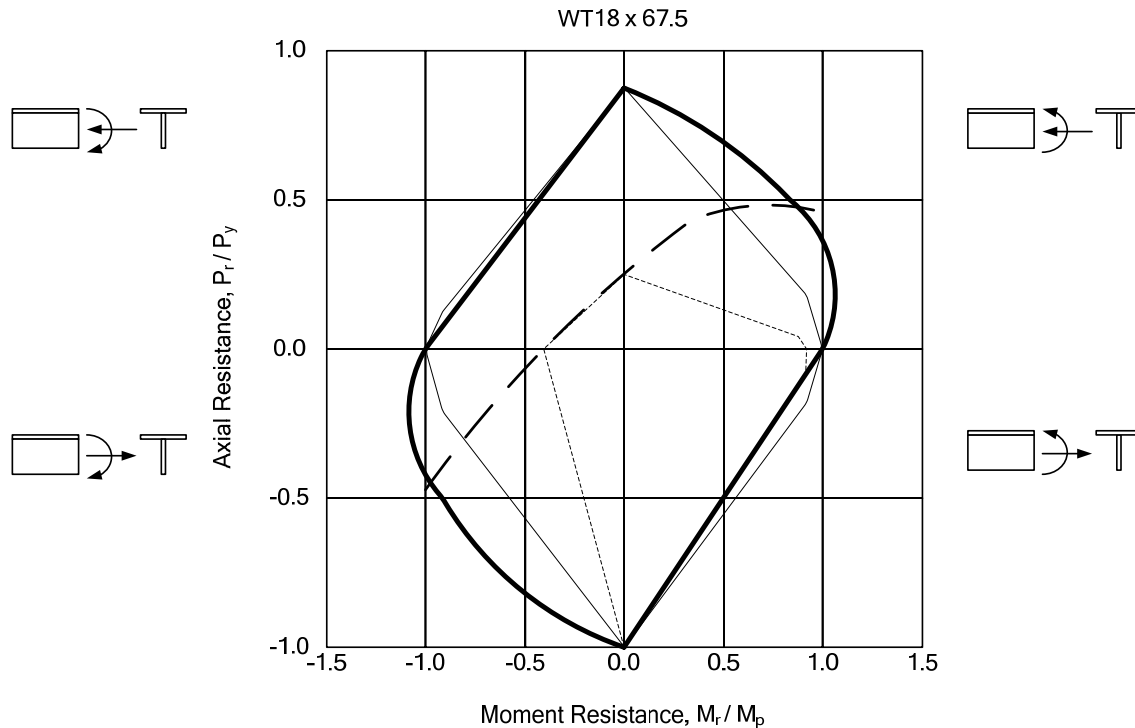
Figure 2.145 Axial Force versus Moment Resistance Envelopes for a WT18 x 67.5 Beam-Column; F_y = 50 ksi and L_b = 20 ft (*195*)

Note for this member that the bulge in the interaction curves is particularly large in the upper right and lower left quadrants. As a result, the actual resistance may be significantly underestimated in these regions when using Equations 2.355 and 2.356. In the upper left and lower right quadrants, where the stem of the tee is subject to additive axial and flexural tension or compression, Equations 2.355 and 2.356 provide a reasonably accurate estimate of the actual resistance.   Connections of tee sections used as bracing members are typically made to the flange of the tee. Therefore, the resulting moment due to the eccentricity of the connection typically places the member design in the upper right or lower left quadrant, and often in the vicinity of the largest bulge in the resistance envelope.

Reference 195 details a procedure that attempts to better capture the bulge in the upper right and lower left quadrants of the interaction curves for singly symmetric beam-columns with compact elements subject to uniform bending (the procedure is

also applicable to doubly symmetric I-section beam-columns as a special case). To accomplish this objective, separate formulations are used to determine the in-plane and out-of-plane nominal resistances of these beam-column members.

For the in-plane nominal resistance (i.e. in the plane of symmetry), which determines the available moment resistance of the member in the presence of an applied axial force P_u, the full plastic moment resistance envelope is calculated for a zero-length member in the presence of an axial force, using an adjusted yield strength when the axial force is compression that varies linearly from F_y at $P_u = 0$ to F_{cr} at $P_u = P_{cr}$. F_{cr} and P_{cr} are the in-plane column resistances of the member (i.e. for buckling about the x-axis) in terms of stress and load, respectively. For the sample WT18 x 67.5 member that was examined, this nominal in-plane resistance curve is represented by the heavy solid line shown in Figure 2.131. The thin solid line shown in represents the interaction curve for this same case determined using Equations 2.355 and 2.356 (i.e. setting P_r equal to $P_y = F_y A_s$ and M_r equal to M_p in both equations).

For the out-of-plane nominal resistance, which determines the available compressive resistance for a finite-length member braced at discrete points in the presence of an applied bending moment M_u, the elastic flexural-torsional buckling resistance P_e for a singly symmetric beam-column subject to equal end bending moments M_o about the x-axis is first computed from the following quadratic equation (*18*):

$$\left(P_{ey} - P_e\right)\left(\bar{r}_o^2 P_z - \bar{r}_o^2 P_e + \beta_x M_o\right) = \left(M_o + P_e y_o\right)^2 \qquad\qquad \text{Equation 2.363}$$

where P_{ey} and P_{ez} are equal to F_{ey} and F_{ez} from Equations 2.324 and 2.325, respectively, times the area A_s of the cross-section, $\bar{r}_o$ is determined from Equation 2.327, y_o is the distance along the y-axis between the shear center and the centroid of the cross-section, and β_x is a cross-section monosymmetry parameter (*18, 195*). The critical flexural-torsional buckling resistance is then computed from Equation 2.321, after substituting $F_e = P_e/A_s$ into Equation 2.319 or 2.320, as applicable. For the sample tee-shaped member, the nominal out-of-plane resistance curve based on this procedure is represented by the heavy dashed line shown in .

Finally, the thin dashed line shown in represents the interaction curve determined from Equations 2.355 and 2.356 for a finite-length member; i.e. considering lateral-torsional buckling of the tee section in the calculation of M_r.

While the suggested procedure appears to do a satisfactory job of capturing the available additional resistance for these members in the upper right and lower left quadrants, it should be emphasized that the, strictly speaking, the procedure is applicable only to singly symmetric sections composed of compact elements. For singly and doubly symmetric I-section members composed of compact elements, the approach is also satisfactory when the members are braced such that M_n is equal to M_p for P_u equal to zero. However, for longer unbraced lengths in the limit of P_u equal to zero, the approach predicts a lateral-torsional buckling (LTB) resistance equal to the elastic critical LTB moment, which is overly optimistic for I-sections when the effective length $K\ell$ of the beam-column falls between the LTB anchor points L_p and

L_r (*154*). Reference 154 suggests capping the nominal flexural resistance at the applicable inelastic LTB resistance in such cases, which assumes the inelastic LTB resistance is unaffected by the presence of the axial load.

Section H2 of Reference 26 suggests the following interaction equation for unsymmetric beam-columns:

$$\left| \frac{f_a}{F_a} + \frac{f_{bw}}{F_{bw}} + \frac{f_{bz}}{F_{bz}} \right| \leq 1.0 \qquad \qquad \text{Equation 2.364}$$

<div align="right">AISC LRFD Equation (H2-1)</div>

where:

f_a = axial stress due to the factored loads (ksi)

f_{bw} = flexural stress about the major principal axis due to the factored loads (ksi)

f_{bz} = flexural stress about the minor principal axis due to the factored loads (ksi)

F_a = factored axial tensile or compressive resistance, as applicable (ksi)

F_{bw} = factored flexural resistance about the major principal axis = M_r/S_w where S_w is the section modulus about the major principal axis to the point under consideration (ksi)

F_{bz} = factored flexural resistance about the minor principal axis = M_r/S_z where S_z is the section modulus about the minor principal axis to the point under consideration (ksi)

This equation is intended to capture some of the bulge in the upper right and lower left quadrants by allowing the Engineer to consider the sign of the axial and flexural stresses, which are additive on one side of the cross-section and subtractive on the other side. However, Equation 2.364 results in an anomaly for a flange subject to axial compression in combination with tension due to flexure about the major principal axis where $\left| f_a/F_a \right| < \left| f_{bw}/F_{bw} \right|$. In this case, if the unbraced length of the flange is increased, F_a is reduced leading to a larger value of the subtractive term f_a/F_a and a *smaller* value for the unity check (*194*). Also, since Equation 2.364 is expressed in terms of stresses and must be checked at all points on the cross-section, there will always be a point on the cross-section where the axial and flexural stress effects are additive, which will govern the resistance. Therefore, Equation 2.370 will always be more restrictive than if Equations 2.355 and 2.356 are employed.

Reference 194 discusses a potential solution to the anomalous behavior of Equation 2.364 based on a set of straight-line interaction curves expressed in terms of forces and moments, as shown below in Figure 2.146 and suggested by Sherman in correspondence with AISC TC4 (*196*). Such curves may provide an improved solution in the critical quadrants, at least for tee-section members. However, the curves provide no particular advantage and are more restrictive for short singly symmetric I-sections with compact elements.

$M_{rc,\,top}$ = governing nominal flexural resistance from flange local buckling or lateral-torsional buckling for flexure causing compression in the top flange (kip-in.)

$M_{rt,top}$ = governing nominal flexural resistance based on tension flange yielding for flexure causing tension in the top flange (kip-in.)

$M_{rc,\,bot}$ = governing nominal flexural resistance from flange local buckling or lateral-torsional buckling for flexure causing compression in the bottom flange (kip-in.)

$M_{rt,\,bot}$ = governing nominal flexural resistance based on tension flange yielding for flexure causing tension in the bottom flange (kip-in.)

P_{rc} = nominal compressive resistance of the member (kips)
P_{rt} = nominal tensile resistance of the member (kips)

**Figure 2.146 Interaction Curves for Singly Symmetric Beam Columns
Suggested in Reference 196**

It is recommended here that until further developments in this area are advanced, that Equations 2.355 and 2.356 be conservatively applied to singly symmetric beam-columns, as illustrated in the following example. Should a case occur where significant additional resistance is required for these members, particularly for members subject to the conditions governed by the upper right and lower left quadrants of the above interaction curves, the Engineer may wish to consider

application of one or more of the above approaches to arrive at a reasonable solution.

EXAMPLE

Check the suitability of a WT12 x 47 rolled structural tee for use as a top-flange diagonal lateral bracing member for a tub girder. Top-flange bracing for tub sections is to be designed for constructibility only for the forces due to the factored loads before the concrete deck has hardened (*AASHTO LRFD* Article 6.7.5.3). A refined analysis of the tub for the steel weight plus an assumed deck-casting sequence yields a governing factored compressive force in the bracing member P_u due to the torque, flexure of the tub and the effects of top-flange lateral bending due to the deck overhang bracket forces of -169.5 kips (the Strength IV load combination controls – see DM Volume 1, Chapter 5 for further information on the Strength IV load combination). The steel for the tee is ASTM A709 Grade 50S steel.

Assume the stem of the tee section is pointed down with the flange of the tee bolted to the bottom of the tub top flanges, which is the preferred method of connection. The width w of the tub section at the top between the centerlines of the flanges is 120 inches and the top flange width is 16 inches. Therefore, the clear distance between the top flanges is 120 in. – 16 in. = 104 inches. The spacing between the internal cross-frames is 16 feet = 192 inches. Thus, the length ℓ of the bracing member is computed as:

$$\ell = \sqrt{104^2 + 192^2} = 218.4 \text{ in.}$$

From the AISC Manual shape property tables:

A_s = 13.8 in.^{2} (> $0.03w$ = 0.03(120) = 3.6 in.^{2} – see *AASHTO LRFD* Equation C6.7.5.3-1)
d = 12.155 in.
t_w = 0.515 in.
b_f = 9.065 in.
t_f = 0.875 in.
I_x = 186 in.^{4}
S_x = 20.3 in.^{3}
r_x = 3.67 in.
$\bar{y}$ = 2.99 in.
I_y = 54.5 in.^{4}
r_y = 1.98 in.
J = 2.62 in.^{4}
$\bar{r}_o$ = 4.89 in.
H = 0.727

Calculate the factored compressive resistance P_r. First, check if the tee section has any slender elements. As specified in *AASHTO LRFD* Article 6.9.4.2, to qualify as a nonslender element, plates in members subject to uniform compression must satisfy the following requirement:

$$\frac{b}{t} \leq k\sqrt{\frac{E}{F_y}}$$

AASHTO LRFD Equation 6.9.4.2-1

As discussed previously, none of the rolled tee sections in the AISC Manual shape property tables have slender flanges. From Table 2.22, for the stem of rolled tees, *k* in the preceding equation is taken equal to 0.75. Therefore:

$$0.75\sqrt{\frac{29,000}{50}} = 18.06 < \frac{d}{t_w} = \frac{12.155}{0.515} = 23.60$$

Therefore, the nominal compressive resistance of the tee must be reduced due to potential local buckling of the stem. Since d/t_w is less than $1.03\sqrt{E/F_y} = 24.81$, calculate the form factor Q_s for the slender unstiffened element from Equation 2.351 as follows:

$$Q_s = 1.908 - 1.22\left(\frac{d}{t}\right)\sqrt{\frac{F_y}{E}}$$

AISC LRFD Equation (E7-14)

$$Q_s = 1.908 - 1.22(23.60)\sqrt{\frac{50}{29,000}} = 0.712$$

Since there are no stiffened elements, Q is taken equal to Q_s; therefore, $Q = 0.712$.

Tee sections loaded in compression can either fail by flexural buckling about the x-axis or by torsion combined with flexure about the y-axis (where the y-axis is defined as the axis of symmetry of the tee section). Since Q is less than 1.0, the critical elastic flexural-torsional buckling stress F_e *must* be computed as:

$$F_e = \left(\frac{F_{ey} + F_{ez}}{2H}\right)\left[1 - \sqrt{1 - \frac{4F_{ey}F_{ez}H}{\left(F_{ey} + F_{ez}\right)^2}}\right]$$

AISC LRFD Equation (E4-5)

That is, the alternate Equation 2.331 for tees and double angles cannot be used to compute F_e in this case.

$$F_{ey} = \frac{\pi^2 E}{\left(\dfrac{K_y\ell}{r_y}\right)^2}$$

AISC LRFD Equation (E4-10)

AASHTO LRFD Article 4.6.2.5 allows K to be taken as 0.750 for members with bolted or welded connections at both ends. Assume K_y = 0.750. However, since only the tub flanges are providing restraint for buckling about the x-axis, K_x will conservatively be taken equal to 1.0. The slenderness ratios about each axis in this case are therefore:

$$\frac{K_y \ell}{r_y} = \frac{0.750(218.4)}{1.98} = 82.7$$

$$\frac{K_x \ell}{r_x} = \frac{1.0(218.4)}{3.67} = 59.5$$

The maximum slenderness ratio $K_y \ell / r_y$ in this case is less than the maximum permitted slenderness ratio of 120 for main compression members specified in *AASHTO LRFD* Article 6.9.3 and discussed in Section 2.4.3.3 below – ok (since the forces in the tee were determined from an analysis, the member is considered to be a main or primary member).

$$F_{ey} = \frac{\pi^2(29,000)}{\left(\dfrac{0.750(218.4)}{1.98}\right)^2} = 41.8 \text{ ksi}$$

$$F_{ez} = \left(\frac{\pi^2 E C_w}{(K_z \ell)^2} + GJ\right)\frac{1}{A_s \bar{r}_o^2}$$

AISC LRFD Equation (E4-11)

Since C_w is taken equal to zero for tee sections, F_{ez} simplifies to the following:

$$F_{ez} = \frac{GJ}{A_s \bar{r}_o^2} = \frac{11,200(2.62)}{13.8(4.89)^2} = 88.9 \text{ ksi}$$

Therefore:

$$F_e = \left(\frac{41.8 + 88.9}{2(0.727)}\right)\left[1 - \sqrt{1 - \frac{4(41.8)(88.9)(0.727)}{(41.8 + 88.9)^2}}\right] = 35.4 \text{ ksi}$$

$$F_{ex} = \frac{\pi^2 E}{\left(\dfrac{K_x \ell}{r_x}\right)^2}$$

AISC LRFD Equation (E4-9)

$$F_{ex} = \frac{\pi^2(29{,}000)}{\left(\dfrac{1.0(218.4)}{3.67}\right)^2} = 80.8 \text{ ksi}$$

Since F_e is less than F_{ex}, flexural-torsional buckling controls. Since Q is less than 1.0, F_{cr} is then determined by substituting the governing value of F_e into Equations 2.338 or 2.339, as applicable. The resulting F_{cr} is then substituted into Equation 2.337 to obtain P_n. Since the governing F_e is greater than $0.44QF_y = 0.44(0.712)(50) = 15.7$ ksi:

$$F_{cr} = Q\left[0.658^{\frac{QF_y}{F_e}}\right]F_y$$

AISC LRFD Equation (E7-2)

$$F_{cr} = 0.712\left[0.658^{\frac{0.712(50)}{35.4}}\right]50 = 23.4 \text{ ksi}$$

$$P_n = F_{cr}A_s$$

AISC LRFD Equation (E7-1)

$$P_n = 23.4(13.8) = 322.9 \text{ kips}$$

$$P_r = \phi_c P_n$$

AASHTO LRFD Equation 6.9.2.1-1

$$P_r = 0.90(322.9) = 290.6 \text{ kips}$$

Since the tee flange is bolted to the top flanges of the tub, the tee is also subject to a uniform bending moment about the major principal axis (x-axis) due to the eccentricity of the connection at each end of the member. Assuming a top-flange thickness of 1.0 inch, the first-order moment $(M_{ux})_1$ due to the eccentricity is computed as:

$$(M_{ux})_1 = |P_u|(y + \frac{1.0}{2}) = |-169.5|(2.99 + 0.5) = 591.6 \text{ kip} - \text{in.}$$

As specified in *AASHTO LRFD* Article 4.5.3.2.2b, the single-step adjustment or moment magnification method may be used to determine the second-order elastic moment as follows (where M_c is the approximate second-order elastic value of M_{ux} and M_{2b} is the first-order elastic moment $(M_{ux})_1$):

$$M_c = (M_{ux})_2 = \delta_b M_{2b} + \delta_s M_{2s}$$

AASHTO LRFD Equation 4.5.3.2.2b-1

Assume the tub section is braced sufficiently to prevent appreciable sidesway at the ends of the bracing member.   Therefore, $\delta_s = 0$.   The amplification factor δ_b is computed as follows:

$$\delta_b = \frac{C_m}{1 - \dfrac{P_u}{\phi_K P_e}} \geq 1.0$$

AASHTO LRFD Equation 4.5.3.2.2b-3

C_m is the equivalent uniform moment factor, which for members braced against sidesway and without transverse loading (other than the self weight of the member) between supports in the plane of bending, is to be taken as:

$$C_m = 0.6 + 0.4 \frac{M_{1b}}{M_{2b}}$$

AASHTO LRFD Equation 4.5.3.2.2b-6

The tee section is bent in single curvature by equal moments at the end of the member due to the eccentricity. For single curvature, the ratio of the end moments $M_{1b}/M_{2b} = 1.0$ is to be taken as positive. Therefore, from the preceding equation, $C_m = 1.0$.

P_e is the Euler buckling load calculated based on the assumption of no sidesway, which is to be taken as follows for noncomposite members:

$$P_e = \frac{\pi^2 EI}{(K\ell_u)^2}$$

AASHTO LRFD Equation 4.5.3.2.2b-5

Where K is the effective length factor in the plane of bending and ℓ_u is the unbraced length. Since bending is about the x-axis, K is equal to $K_x = 1.0$ and I is equal to $I_x = 186$ in.[4]. Therefore:

$$P_e = \frac{\pi^2(29{,}000)(186)}{(1.0 * 218.4)^2} = 1{,}116 \text{ kips}$$

$$\delta_b = \frac{1.0}{1 - \dfrac{|-169.5|}{1.0(1{,}116)}} = 1.18$$

Thus:

$$M_c = (M_{ux})_2 = 1.18(591.6) = 698.1 \text{ kip} - \text{in.}$$

Calculate the factored flexural resistance M_r of the tee-section member about the strong axis. Referring to Section 2.2.3.7.1.3.3 of this chapter, the nominal flexural resistance M_n is to be taken as the lowest value based on yielding, lateral torsional buckling or flange local buckling. For yielding, the nominal flexural resistance is given as:

$$M_n = M_p$$

AISC LRFD Equation (F9-1)

where $M_p = F_y Z_x$. The plastic section modulus Z_x for the tee section neglecting the effect of the web-to-flange fillets is computed by first locating the plastic neutral axis (assumed to be a distance $\bar{y}$ from the top of the flange) as follows:

$$\text{Depth of stem} = (12.155 - 0.875) = 11.28 \text{ in.}$$
$$\bar{y}(9.065) = 9.065(0.875 - \bar{y}) + (11.28)(0.515)$$
$$\bar{y} = 0.758 \text{ in.}$$

Then, taking moments of the cross-sectional areas about the plastic neutral axis yields:

$$Z_x = \frac{9.065(0.758)^2}{2} + \frac{9.065(0.875 - 0.758)^2}{2} + 0.515(11.28)\left[(0.875 - 0.758) + \frac{(11.28)}{2}\right] = 36.1 \text{ in.}^3$$

$$M_p = (50)(36.1) = 1,805 \text{ kip} - \text{in.}$$

M_n for yielding is limited to $1.6M_y$ for stems in tension and to M_y for stems in compression. Determine if the tip of the stem is in compression or tension:

$$f_{tip} = \frac{-169.5}{13.8} + \frac{591.6}{20.3} = 16.9 \text{ ksi} \quad (\text{tension})$$

Therefore:

$$1.6M_y = 1.6F_y S_x = 1.6(50)(20.3) = 1,624 \text{ kip} - \text{in.} < M_p$$

$$\therefore M_n = 1,624 \text{ kip} - \text{in.} \quad (\text{for yielding})$$

For lateral-torsional buckling:

$$M_n = \frac{\pi\sqrt{EI_y GJ}}{L_b}\left[B + \sqrt{1 + B^2}\right] \leq M_p$$

AISC LRFD Equation (F9-4)

where:

$$B = \pm 2.3 \frac{d}{L_b}\sqrt{\frac{I_y}{J}}$$

<div align="right">AISC LRFD Equation (F9-5)</div>

The plus sign on the value of *B* applies when the stem is in tension. Therefore:

$$B = +2.3\frac{12.155}{218.4}\sqrt{\frac{54.5}{2.62}} = +0.584$$

$$M_n = \frac{\pi\sqrt{29{,}000(54.5)(11{,}200)(2.62)}}{218.4}\left[0.584 + \sqrt{1+0.584^2}\right] = 5{,}396 \text{ kip}-\text{in.} > M_p$$

$$\therefore M_n = M_p = 1{,}805 \text{ kip}-\text{in.} \quad \text{(lateral-torsional buckling)}$$

Since the flange is in compression, the limit state of flange local buckling must also be considered. The flange slenderness $\lambda_f = b_f/2t_f = 9.065/2(0.875) = 5.2$ does not exceed the slenderness limit for a compact flange $\lambda_{pf} = 0.38\sqrt{E/F_y} = 9.2$. Therefore, flange local buckling does not control and need not be checked.

Thus, the nominal flexural resistance M_n of the tee section is controlled by yielding and is equal to 1,624 kip-in. The factored flexural resistance M_r is equal to:

$$M_r = \phi_f M_n = 1.0(1{,}624) = 1{,}624 \text{ kip}-\text{in.}$$

As recommended above, the beam-column resistance for the singly symmetric tee-section member will conservatively be checked using Equations 2.355 and 2.356. Since $P_u/P_r = |-169.5|/290.6 = 0.58 > 0.2$, Equation 2.356 controls as follows:

$$\frac{P_u}{P_r} + \frac{8.0}{9.0}\frac{M_{ux}}{M_{rx}} \leq 1.0$$

<div align="right">AASHTO LRFD Equation 6.9.2.2-2</div>

$$\frac{|-169.5|}{290.6} + \frac{8.0}{9.0}\frac{698.1}{1{,}624} = 0.97 < 1.0 \quad \text{ok}$$

Separate calculations (similar to the above) show that if a timber were used to brace the member at mid-length in the vertical plane during construction, and upward movement of the tee section was prevented at the brace point, the unbraced length with respect to flexural buckling about the x-axis would be reduced to 218.4/2 = 109.2 in. and a smaller WT8 x 38.5 could potentially be used.

2.4.3.3 Limiting Slenderness Ratios

AASHTO LRFD Article 6.9.3 specifies limiting slenderness ratios *Kℓ/r* for compression members, where *K* is the effective length factor determined as

specified in *AASHTO LRFD* Article 4.6.2.5 (see Section 2.4.3.2.1.1.1 above), ℓ is the unbraced length and *r* is the minimum radius of gyration for the cross-section. In computing the maximum slenderness *for checking the appropriate limiting ratio only as given below*, *AASHTO LRFD* Article 6.9.3 permits the radius of gyration to be computed on a notional section that neglects part of the area of a component provided that the resistance of the component based on the actual area and radius of gyration exceeds the factored loads, and the resistance of the notional component based on the reduced area and corresponding radius of gyration also exceeds the factored loads.

For primary compression members, the maximum $K\ell/r$ is limited to 120. In the *AASHTO LRFD* Specification, a primary member is defined as a member designed to carry the internal forces determined from an analysis. For compression members used as secondary members (i.e. members in which stress is not normally evaluated in the analysis), the maximum $K\ell/r$ is limited to 140. Note that for single angles where the effective slenderness ratio approach (discussed in Section 2.4.3.2.1.4 above) is used to design the angle, the effective slenderness ratio should be checked against the appropriate limiting value.

2.4.3.4 Built-Up Members

Built-up compression members are covered in *AASHTO LRFD* Article 6.9.4.3. As mentioned previously, built-up compression members typically consist of two or more shapes. Included in this category are back-to-back angles connected by intermittent bolted or welded filler plates, boxed channels, and flange components (i.e. two rolled shapes or plates) spaced widely apart and connected by lacing (flat bars, angles, channels or other shapes), tie plates (also referred to as batten or stay plates) or perforated cover plates.

To utilize the full calculated factored compressive resistance of a built-up member (determined as discussed below), each component of the member must satisfy the corresponding width-to-thickness requirement for axial compression specified in *AASHTO LRFD* Equation 6.9.4.2 (see Section 2.4.3.2.1.3.1 above). Should the member consist of one or more elements not satisfying the width-to-thickness requirements of *AASHTO LRFD* Article 6.9.4.2 (i.e. slender elements), the nominal compressive resistance of the member must be reduced according to the procedures given in Reference 26 (and discussed further in Section 2.4.3.2.1.3.2 above) to account for the fact that the slender elements might potentially undergo local buckling, which may adversely affect the overall buckling resistance of the member.

In many instances, the axial resistance of built-up columns used as compression members is also affected by any relative deformation between the shapes that produces shear forces in the connectors between the individual shapes. Shear in a compression member can result due to lateral loads, end eccentricity of the axial load, and/or by the slope of the member with respect to the line of thrust of the axial load caused by bending during buckling or any unintended initial curvature. Shear has an insignificant effect on reducing the compressive resistance of sections with solid webs (*28*), and on box-section members built-up using perforated cover plates.

However, the effect of shear on the compressive resistance for all other types of built-up compression members should not be neglected.

As discussed further in References 18, 21 and 28, the shear effect can be accounted for by an adjustment to the effective length of the member. *AASHTO LRFD* Article 6.9.4.3 specifies the following modified slenderness ratio $(K\ell r)_m$ for built-up members composed of two or more shapes where the buckling mode involves relative deformation that produces shear forces in connectors between the individual shapes. This modified ratio applies when the intermediate connectors between the shapes are welded or fully-tensioned bolted (*197*):

$$\left(\frac{K\ell}{r}\right)_m = \sqrt{\left(\frac{K\ell}{r}\right)_o^2 + 0.82\left(\frac{\alpha^2}{1+\alpha^2}\right)\left(\frac{a}{r_{ib}}\right)^2} \qquad \text{Equation 2.365}$$

AASHTO LRFD Equation 6.9.4.3.1-1

where:

$(K\ell/r)_o$ = slenderness ratio of the built-up member (with shear deformation neglected) acting as a unit in the buckling direction being considered

α = separation ratio = $h/2r_{ib}$

a = distance (center-to-center) between connectors (in.)

r_{ib} = radius of gyration of an individual component shape relative to its centroidal axis parallel to the member axis of buckling (in.)

h = distance between centroids of individual component shapes perpendicular to the member axis of buckling (in.)

For example, for a built-up double-angle or double-channel compression member interconnected at intervals along its length in the plane defined by the y-axis of the cross-section, $(K\ell r)_m$ would be used in place of $(K\ell r)_y$ for flexural buckling about the y-axis to account for the effect of the shear displacements between the shapes. Flexural buckling about the x-axis would be checked in conventional fashion, as shear effects would have no effect on buckling about the x-axis. For the case of the singly-symmetric back-to-back double-angle member, F_{ey} calculated from Equation 2.324 -- using the modified $(K\ell r)_m$ in place of $(K\ell r)_y$ -- would be used in the flexural-torsional buckling Equation 2.323 or 2.331, as applicable. The nominal compressive resistance in this case would then be computed as the smaller value based on either flexural buckling about the x-axis or flexural-torsional buckling, which involves torsion of the member in combination with flexure about the y-axis.

As discussed in Reference 154, Equation 2.365 is a refinement of an equation originally derived in Reference 91 for battened columns neglecting the influence of the strain energy developed due to localized bending of the batten plates and assuming zero shearing deformation of the end tie plates. Reference 197 summarizes the theoretical derivation of Equation 2.365 and illustrates that the equation gives accurate to slightly conservative predictions compared to

experimental test data for built-up double-angle compression members. However, since the derivation of the equation is general in nature, Reference 197 suggests that the equation is also applicable to built-up compression members utilizing widely spaced components.

AASHTO LRFD Article C6.9.4.3.1 gives the following alternate equation for $(K\ell/r)_m$ assumed applicable to compression members, for which shear-force effects are a concern, that are built-up using other types of intermediate connectors, including those members on existing structures that are interconnected with rivets:

$$\left(\frac{K\ell}{r}\right)_m = \sqrt{\left(\frac{K\ell}{r}\right)_o^2 + \left(\frac{a}{r_i}\right)^2}$$ Equation 2.366

AASHTO LRFD Article C6.9.4.3.1-1

where:
   r_i =   minimum radius of gyration of an individual component shape (in.)

Equation 2.366 is based on the equation given in Section E6 of Reference 26 for application to built-up compression members in which the intermediate connectors are snug-tight bolted. The equation is empirically based on test results, as discussed further in Reference 198.

In addition, *AASHTO LRFD* Article 6.9.4.3.1 specifies that for built-up compression members composed of two or more shapes interconnected at intervals, the slenderness ratio of each component shape between connecting fasteners or welds (i.e. the maximum value of a/r_{ib} for each shape) must not exceed 75 percent of the governing slenderness ratio of the built-up member. Also, lacing members and/or tie plates are to be spaced such that the slenderness ratio of each component shape between the lacing and/or tie-plate connection points does not exceed 75 percent of the governing slenderness ratio of the built-up member. In each case, the least radius of gyration is to be used in computing the slenderness ratio of each component shape between the connectors or connection points. Formulas giving approximate radii of gyration for various potential configurations of built-up members are provided in Table A1 of Reference 28. This requirement is intended to mitigate the possibility of so-called compound buckling, or the interaction between global buckling of the built-up member and local buckling of the individual components between intermediate connectors or lacing and/or tie-plate connection points (*199*).

As mentioned in *AASHTO LRFD* Article C6.9.4.3.1, the connectors in built-up compression members must be designed to resist the shear forces that develop in the buckled member, but no additional guidance is offered. Reference 154 suggests that the additional transverse shear force due to stability effects (given by Equation 2.367 below) might be used to design the connectors. Along the length of the member between the end connections, the maximum longitudinal spacing or pitch of bolts must satisfy the spacing requirements for stitch bolts specified in *AASHTO LRFD* Article 6.13.2.6.3 (see also Section 2.3.2.2.1.6.3 of this chapter). These maximum pitch requirements are intended to ensure that the individual

components of the member act as a unit to transfer the required forces without buckling of the member. Note that the maximum pitch must also not exceed the maximum pitch for sealing specified in *AASHTO LRFD* Article 6.13.2.6.2 (see Section 2.3.2.2.1.6.2 of this chapter). Reference 26 suggests that the specified maximum pitch requirements might also be applied to the spacing of intermittent welds used to connect built-up compression members.

As indicated in the commentary to Section E6 of Reference 26, in the case of both of the preceding equations, the ends of the member must be connected rigidly by welding or full-tension bolting, or by the use of end tie plates. Section E6 of Reference 26 suggests designing bolted end connections of built-up compression members for the full compressive load as a bearing-type connection, with the bolts fully pretensioned and a Class A or B faying surface provided. The Class A or B surface is not recommended to develop slip resistance in the bolts, but to help prevent relative moment between the components at the end as the member takes a curved shape [the shear is highest at the ends of the member where the slope of the buckled member is the greatest (*91*)]. At the ends of built-up compression members, bolts must also satisfy the maximum pitch requirements specified for the ends of these members in *AASHTO LRFD* Article 6.13.2.6.4 (see Section 2.3.2.2.1.6.3 of this chapter).

Perforated cover plates are more likely to be used for built-up members in new bridge construction than laced or battened compression members. Specific design requirements for perforated cover plates used in built-up compression or tension members are given in *AASHTO LRFD* Article 6.8.5.2 (see Section 2.4.2.4 of this chapter for a summary of these requirements). In addition, for built-up compression members utilizing perforated cover plates, *AASHTO LRFD* Article 6.9.4.3.2 specifies that the perforated plates must be designed for the sum of the shear force due to the factored loads (i.e. shear due to self weight of the member plus any additional applied force), and an additional transverse shear force *V* (kips) due to stability effects, assumed divided equally to each plane containing a perforated plate, taken as:

$$V = \frac{P_r}{100}\left(\frac{100}{(\ell/r)+10} + \frac{8.8(\ell/r)F_y}{E}\right)$$

Equation 2.367

AASHTO LRFD Equation 6.9.4.3.2-1

where:
P_r = factored compressive resistance determined as specified in *AASHTO LRFD* Article 6.9.2.1 or 6.9.2.2 (kips)
ℓ = member length (in.)
r = radius of gyration about an axis perpendicular to the plane of the perforated plate (in.)

The preceding equation is carried over from the Standard Specifications (*157*), and should also be applied to any built-up compression member design in which lacing might be used. Specific design requirements for lacing bars and tie or batten plates, which are not covered in this Manual, may be found in References 26 and 157.

Additional information on the design of laced and battened compression members may also be found in References 18, 21 and 28. Reference 200 provides an approach for determining the section properties of latticed built-up members, including the moment of inertia and torsional constant.

158. SSRC Task Group 20. 1979. "A Specification for the Design of Steel Concrete Composite Columns." *AISC Engineering Journal*, American Institute of Steel Construction, Chicago, IL., Vol. 16, 4th Qtr.
159. Galambos, T.V., and J. Chapuis. 1980. *LRFD Criteria for Composite Columns and Beam Columns*. Revised draft. Washington University Department of Civil Engineering, St. Louis, MO, December.
160. Euler, L. 1744. *De Curvis Elasiticis, Additamentum I, Methodus Inveniendi Lineas Curvas Maximi Minimive Proprietate Gaudentes*. Lausanne and Geneva; and "Sur le Forces des Colonnes," *Memories de l'Academie Royale des Sciences et Belles Lettres*, Vol. 13, Berlin, 1759; English translation of the letter by J.A. Van den Broek, "Euler's Classic Paper 'On the Strength of Columns'," *American Journal of Physics*, Volume 15, January/February, 1947.
161. Johnston, B.G. 1983. "Column Buckling Theory: Historic Highlights." *Journal of Structural Engineering*, American Society of Civil Engineers, New York, NY, Vol. 109, No. 9, September.
162. Considere, A. 1891. "Resistance des pieces comprimees." *Congres International des Procedes de Construction*, Paris.
163. Engesser, F. 1889. "Ueber die Knickfestigkeit gerader Stabe." *Zeitschrift des Architekten-und Ingenieur- Vereins zu Hannover*, Volume 35; and "Die Knickfestigkeit gerader Stabe." *Zentralblatt der Bauverwaltung*, Berlin, December 5, 1891.
164. Shanley, F.R. 1946. "The Column Paradox." *Journal of the Aeronautical Sciences*, Volume 13, No. 12, December.
165. Yang, C.H., L.S. Beedle, and B.G. Johnston. 1952. "Residual Stress and the Yield Strength of Steel Beams." *Welding Journal*, April.
166. Huber, A.W., and L.S. Beedle. 1954. "Residual Stress and the Compressive Strength of Steel." *Welding Journal*, December.
167. Bjorhovde, R. 1972. "Deterministic and Probabilistic Approaches to the Strength of Steel Columns." Ph.D. Dissertation, Lehigh University, Bethlehem, PA, May.
168. Bjorhovde, R. 1978. "The Safety of Steel Columns." *Journal of the Structural Division*, American Society of Civil Engineers, New York, NY, Vol. 104, No. ST9, September.
169. Tide, R.H.R. 1985. "Reasonable Column Design Equations." *Proceedings of the Annual Technical Session and Meeting*, Cleveland, OH, April 16-17, Structural Stability Research Council, University of Missouri, Rolla, MO.
170. Tide, R.H.R. 2001. "A Technical Note: Derivation of the LRFD Column Design Equations." *Engineering Journal,* American Institute of Steel Construction, Chicago, IL, Vol. 38, No. 3, 3rd Qtr.
171. Hall, D.H. 1981. "Proposed Steel Column Strength Criteria." *Journal of the Structural Division*, American Society of Civil Engineers, New York, NY, Vol. 107, No. ST4, April.
172. ASCE. 2000. *Design of Latticed Steel Transmission Structures*, ASCE 10-97, American Society of Civil Engineers, Reston, VA.

173. Galambos, T.V. 1991. "Design of Axially Loaded Compressed Angles." *Proceedings of the Annual Technical Session and Meeting*, Chicago, IL, Structural Stability Research Council, University of Missouri, Rolla, MO.

174. AISI. 1969. *Specification for the Design of Cold-Formed Steel Structural Members*. American Iron and Steel Institute, Washington, DC.

175. AISI. 2001. *North American Specification for the Design of Cold-Formed Steel Structural Members*. American Iron and Steel Institute, Washington, DC.

175a. White, D.W., Shafer, B.W., and S.-C. Kim. 2006. "Implications of the AISC (2005) Q-Factor Equations for Rectangular Box and I-Section Members." Structural Mechanics and Materials Report, Georgia Institute of Technology, Atlanta, GA.

176. AISC. 1993. *Specification for Load and Resistance Factor Design of Single-Angle Members.* American Institute of Steel Construction, Chicago, IL.

177. AISC. 2000. *Load and Resistance Factor Design Specification for Single-Angle Members.* American Institute of Steel Construction, Chicago, IL, November 10.

178. CEN. 1993. *Eurocode 3: Design of Steel Structures, Part 1.1 – General Rules and Rules for Buildings*, ENV 1992-1-1, European Committee for Standardization, Brussels, Belgium.

179. BSI. 1990. "BS5950: Part 1: 1990, Structural Use of Steelwork in Buildings, Part 1, Code of Practice for Design in Simple and Continuous Construction: Hot Rolled Sections." British Standards Institution, London.

180. Usami, T., and T.V. Galambos. 1971. "Eccentrically Loaded Single-Angle Columns." International Association for Bridge and Structural Engineering, Zurich, Switzerland.

181. Woolcock, S.T., and S. Kitipornchai. 1986. "Design of Single-Angle Web Struts in Trusses." *Journal of Structural Engineering*, American Society of Civil Engineers, New York, NY, Vol. 112, No. ST6, June.

182. Mengelkoch, N.S., and J.A. Yura. 2002. "Single-Angle Compression Members Loaded Through One Leg." *Proceedings of the Annual Technical Session and Meeting*, Structural Stability Research Council, University of Missouri, Rolla, MO.

183. Lutz, L.A. 1996. "A Closer Examination of the Axial Capacity of Eccentrically Loaded Single Angle Struts." *Engineering Journal*, American Institute of Steel Construction, Chicago, IL, Vol. 33, No. 2, 2nd Qtr.

184. Lutz, L.A. 2006. "Evaluating Single Angle Compression Struts Using an Effective Slenderness Approach." *Engineering Journal*, American Institute of Steel Construction, Chicago, IL, submitted for publication.

185. Foehl, P.J. 1948. "Direct Method of Designing Single Angle Struts in Welded Trusses." *Design Book for Welding*, Lincoln Electric Company, Cleveland, OH, November.

186. Trahair, N.S., T. Usami, and T.V. Galambos. 1969. "Eccentrically Loaded Single-Angle Columns." *Research Report No. 11*, Civil and Environmental Engineering Department, Washington University, St. Louis, MO.

187. Lutz, L.A. 1992. "Critical Slenderness of Compression Members with Effective Lengths about Non-Principal Axes." *Proceedings of the Annual Technical Session and Meeting*, Pittsburgh, PA, Structural Stability Research Council, University of Missouri, Rolla, MO.

188. Lutz, L.A. 1998. "Toward a Simplified Approach for the Design of Web Members in Trusses." *Proceedings of the Annual Technical Session and Meeting*, Structural Stability Research Council, University of Missouri, Rolla, MO.

189. El-Tayem, A., and S.C. Goel. 1986. "Effective Length Factor for the Design of X-Bracing Systems." *Engineering Journal*, American Institute of Steel Construction, Chicago, IL, Vol. 23, No. 1, 1st Qtr.

190. Clarke, M.J., and R.Q. Bridge. 1992. "The Inclusion of Imperfections in the Design of Beam-Columns." *Proceedings of the Annual Technical Session and Meeting*, Pittsburgh, PA, Structural Stability Research Council, University of Missouri, Rolla, MO.

191. Liew, J.Y.R., D.W. White, and W.F. Chen. 1992. "Beam-Columns." *Constructional Steel Design, An International Guide*, Chapter 2.5, P.J. Dowling, J.E. Harding and R. Bjorhovde (ed.), Elsevier, Essex, England.

192. ASCE. 1997. *Effective Length and Notional Load Approaches for Assessing Frame Stability: Implications for American Steel Design*. American Society of Civil Engineers Structural Engineering Institute's Task Committee on Effective Length under the Technical Committee on Load and Resistance Factor Design.

193. Maleck, A.E., and D.W. White. 2003. "Alternative Approaches for Elastic Analysis and Design of Steel Frames, I: Overview." *Journal of Structural Engineering*, American Society of Civil Engineers, Reston, VA, Vol. 130, No. 8.

194. White, D.W., and Y.-D. Kim. 2006. "A Prototype Application of the AISC (2005) Stability Analysis and Design Provisions to Metal Building Structural Systems." Report to Metal Building Manufacturers Association, School of Civil and Environmental Engineering, Georgia Institute of Technology, Atlanta, GA, January.

195. Galambos, T.V. 2001. "Strength of Singly Symmetric I-Shaped Beam-Columns." *Engineering Journal*, American Institute of Steel Construction, Vol. 38, No. 2, 2nd Qtr.

196. Sherman, D. 2005. Communication to AISC TC4, June.

197. Aslani, F., and S.C. Goel. 1991. "An Analytical Criteria for Buckling Strength of Built-Up Compression Members." *Engineering Journal*, American Institute of Steel Construction, Chicago, IL, Vol. 28, No. 4, 4th Qtr.

198. Zandonini, R. 1985. "Stability of Compact Built-Up Struts: Experimental Investigation and Numerical Simulation." *Construczione Metalliche*, Milan, Italy, No. 4.

199. Duan, L., M. Reno, and C.M. Uang. 2002. "Effect of Compound Buckling on Compression Strength of Built-Up Members." *Engineering Journal*, American Institute of Steel Construction, Chicago, IL, Vol. 39, No. 1, 1st Qtr.

200. Duan, L., M. Reno, and L. Lynch. 2000. "Section Properties for Latticed Members of San-Francisco-Oakland Bay Bridges." *Journal of Bridge Engineering*, American Society of Civil Engineers, Reston, VA, Vol. 4, No. 2, May.

2.4.4 Solid-Plate Diaphragms

Solid-plate diaphragms are most commonly used as internal and external diaphragms in steel box-girder bridges at supports or as internal diaphragms in steel box-section integral bent caps. Solid-plate diaphragms are rarely used in steel I-girder bridges, unless needed as special jacking diaphragms to accommodate bearing replacement.

As specified in *AASHTO LRFD* Article 6.7.4.3, either solid-plate diaphragms or cross-frames must be provided within box sections at each support to resist displacement, transverse rotation and cross-section distortion. The diaphragms or

cross-frames must be designed to resist torsional moments and transmit lateral forces from the box to the bearings. As mentioned previously, solid-plate diaphragms are almost universally employed for this function. Where internal plate diaphragms provide continuity or resist torsional forces, they are to be connected to the webs and flanges of the box section according to *AASHTO LRFD* Article 6.7.4.3. The connections should be adequate to transmit the bending and torsional shears due to the factored loads between the box and the diaphragm.

For cross-sections consisting of two or more boxes, external diaphragms or cross-frames must also be used between the boxes at end supports according to *AASHTO LRFD* Article 6.7.4.3. Again, solid-plate diaphragms are commonly used. Unlike internal diaphragms, which usually do not have flanges, external diaphragms typically have top and bottom flanges. External diaphragms act to restrain the rotation of the boxes at the end supports, particularly before the deck hardens. The external diaphragm also acts with the internal diaphragm to support the deck and the wheel loads coming onto the bridge at the end supports. Thus, the diaphragms must be designed for these loads. End moments should be considered in the design of external diaphragms and their connections to the girders. As indicated in DM Volume 1, Chapter 2, Section 2.4.3.1.5.5.2, where single bearings are used, the distance that the deck and its supporting members span is effectively the distance between bearings, and not the distance between flanges. This causes deck stresses roughly double those that would occur if the deck were supported rigidly by the webs of the boxes. The demand on the diaphragm spanning between the boxes is also affected.

As specified in *AASHTO LRFD* Article 6.7.4.3, the need for external cross-bracing between girder lines *at interior supports* should be evaluated, including consideration of torsional stability, particularly during erection. This is especially true when the box girder has only one bearing per support.

If excessive rotations of the box sections are anticipated when the deck is placed, additional bracing between boxes may be desirable in-between supports. These intermediate external bracing members (which are typically *not* solid-plate diaphragms) are often removed after the deck hardens (issues to be considered when removing these members are discussed further in DM Volume 1, Chapter 2, Section 2.4.3.1.5.5.2). Note that *AASHTO LRFD* Article 6.7.4.3 requires that an interior cross-frame/diaphragm be used in-line with each exterior cross-frame/diaphragm to balance the forces from the external bracing.

In reinforced concrete design, beams deeper than about one-fourth of their span are classified as deep beams. For deep beams, ordinary beam theory does not apply, meaning that shear deformations should be considered and principal stresses should be evaluated. Thus, as indicated in *AASHTO LRFD* Article C6.7.4.3, consideration should be given to evaluating the principal stresses in all internal support diaphragms, and in external support diaphragms with aspect ratios (ratios of length to depth) less than 4.0 (external support diaphragms with aspect ratios greater than or equal to 4.0 may be designed as ordinary I-section flexural members). In these cases, the combined principal stresses in the diaphragm can be

evaluated at the strength limit state using the following general form of the Huber-von Mises-Hencky yield criterion (*85i*):

$$\sqrt{\sigma_1^2 - \sigma_1\sigma_2 + \sigma_2^2} \le \phi_f F_y \qquad \text{Equation 2.368}$$

where:

ϕ =   resistance factor for flexure specified in *AASHTO LRFD* Article 6.5.4.2 (= 1.0)

σ_1, σ_2 =   critical maximum and minimum principal stresses in the diaphragm (ksi)

$$= \quad \left(\frac{f_{by} + f_{bz}}{2}\right) \pm \sqrt{\left(\frac{f_{by} - f_{bz}}{2}\right)^2 + f_d^2} \qquad \text{Equation 2.369}$$

f_{by} =   for internal diaphragms, stress in the diaphragm due to the factored loads caused by major-axis bending of the diaphragm over the bearing sole plate (ksi). For external diaphragms, stress in the diaphragm due to the factored loads caused by major-axis bending of the diaphragm (ksi)

f_{bz} =   stress in the diaphragm due to the factored loads caused by bending of the diaphragm about its longitudinal axis (ksi)

f_d =   shear stress in the diaphragm caused by the total vertical shear in the diaphragm due to the factored loads (ksi)

F_y =   specified minimum yield strength of the diaphragm (ksi)

f_{by} and *f_{bz}* are to be taken as signed quantities in Equations 2.368 and 2.369. The term *f_{bz}* is neglected in most all cases. For a box section supported on a single bearing, *f_{by}* may be particularly significant. In calculating *f_{by}*, a width of the bottom box flange equal to 18 times its thickness may be considered effective with the diaphragm in resisting bending, which is similar to the portion of the web or diaphragm that is considered part of the effective column section for the design of bearing stiffeners (see Section 2.2.6.2.4.1 of this chapter). More than one loading condition may need to be investigated in order to determine the critical principal stresses in the diaphragm. Should the diaphragm web have a different yield strength than the box flange (for the case of internal diaphragms) or the diaphragm flanges (for the case of external diaphragms), consideration should be given to including the hybrid factor R_h on the right-hand side of Equation 2.368 (see Section 2.2.2.6 of this chapter – Equation 2.21).

It is recommended that post bend-buckling resistance not be considered in the design of these critical diaphragm members. Therefore, when considering bending of the diaphragm, the diaphragm web should also satisfy the following:

$$\frac{2D_c}{t_w} \le \lambda_{rw} = 5.7\sqrt{\frac{E}{F_y}} \qquad \text{Equation 2.370}$$

AASHTO LRFD Equation 6.10.1.10.2-2

where:

D_c =   elastic depth of the diaphragm web in compression (in.)

Satisfaction of Equation 2.370 ensures that theoretical bend buckling of the diaphragm web will not occur. Thus, the web load-shedding factor R_b (see Section 2.2.2.5 of this chapter) is implicitly taken equal to 1.0 in Equation 2.368.

The factored shear resistance of the diaphragm should also be checked at the strength limit state as follows:

$$V \le \phi_v V_n$$
<div align="right">Equation 2.371</div>

where:

ϕ_v =   resistance factor for shear specified in *AASHTO LRFD* Article 6.5.4.2 (= 1.0)

V =   total vertical shear in the diaphragm due to the factored loads (kips)

V_n =   nominal shear resistance of the diaphragm (kips)

It is recommended that post-buckling shear resistance due to tension-field action also not be considered in the design of these critical diaphragm members. Therefore, the nominal shear resistance V_n should be limited to the shear buckling (or shear yielding) resistance V_{cr} given as follows:

$$V_n = V_{cr} = CV_p$$
<div align="right">Equation 2.372</div>

<div align="right">*AASHTO LRFD* Equation 6.10.9.2-1</div>

where:

V_p =   plastic shear force (kips) = $0.58F_y Dt_w$

C =   ratio of the shear buckling resistance to the shear yield strength determined from Equation 2.152, 2.153 or 2.154, as applicable (refer to Section 2.2.3.7.2.1 of this chapter)

D =   vertical depth of the diaphragm (in.)

t_w =   thickness of the diaphragm (in.)

In calculating the constant C, the shear buckling coefficient k should be taken as 5.0 for unstiffened webs and determined using Equation 2.157 for stiffened webs. Bearing stiffeners on internal plate diaphragms can be considered to act as transverse stiffeners.

Inspection access through internal solid-plate diaphragms at interior supports is usually provided by means of access holes, with the holes at least 18 inches wide and three feet deep. For a section supported on a single bearing, the section through the access hole is especially critical and additional stiffening and/or reinforcement around the hole may be necessary. In such cases, the bearing is typically wider than the access hole so bearing stiffeners provided on each side of the hole can be considered to act as transverse stiffeners to increase the shear resistance of the diaphragm at the hole. If necessary, horizontal stiffeners above

and below the hole might be used to increase the flexural resistance of the diaphragm at the hole in lieu of thickening the diaphragm plate.

Because of the presence of access holes and complex details such as stiffening around the holes, and because of the number of load points and more complicated mechanism of load transfer, a more refined analysis of internal plate diaphragms at supports may be desirable to obtain more accurate estimates of the diaphragm flexural and shear stresses than obtained using the procedure demonstrated in the example given below. This is particularly true for box sections supported on single bearings where the section through the access hole is usually critical. Procedures are available for estimating the moment and shear resistance of steel beams with unreinforced and reinforced web openings (*201*).   However, these procedures were primarily developed for rolled I-section flexural members used in multistory buildings with smaller web openings used to pass utilities through the beams and not for deeper and shorter solid-plate diaphragms used in bridges, with relatively large access holes, that exhibit deep-beam behavior. Therefore, until further research is conducted, the procedure demonstrated in the example given below is recommended for estimating the combined flexural and shear resistance of solid-plate diaphragms with holes.
.
As specified in *AASHTO LRFD* Article 6.11.11.1, bearing stiffeners for box sections with inclined webs should be attached to either an internal or external diaphragm rather than to the webs so that the bearing stiffeners will be perpendicular to the sole plate. Where a single centered bearing is used and a centered access hole is also provided in an internal diaphragm, the diaphragm must be stout enough to transfer the load around any access hole and to resist the reaction. As mentioned previously, a refined analysis of the diaphragm is desirable is such situations. Stiffening around the hole may be required. Auxiliary bearing stiffeners might be provided to spread out the reaction. At expansion bearings, thermal movements of the bridge may cause the diaphragm to be eccentric with respect to the bearings. *AASHTO LRFD* Article 6.11.11.1 states that the bearing stiffeners and diaphragms should be designed for the resulting eccentricity. The effect of the eccentricity can be recognized by treating the effective bearing stiffener/diaphragm assembly as a beam-column according to the provisions of *AASHTO LRFD* Article 6.9.2.2 (see Section 2.4.3.2.2 of this chapter). The effective bearing assembly consists of the stiffeners plus the portion of the diaphragm web specified in *AASHTO LRFD* Article 6.10.11.2.4b assumed to act with the stiffeners as an effective column section.

Details on diaphragms should be appropriately investigated for the fatigue limit state (refer to earlier sections of this chapter on Fatigue Limit State Verifications). On diaphragms for which principal stresses are considered, fatigue-sensitive details should be investigated by considering the principal tensile stress range due to the factored fatigue live load (i.e. factored by the 0.75 load factor specified for the Fatigue load combination in *AASHTO LRFD* Table 3.4.1-1) that results from the diaphragm acting as a deep beam, which may preclude the use of certain fatigue-sensitive details on the diaphragm.   Note that the direction of the principal tensile stress may change for different positions of the live load. Details need only be checked for fatigue if they are subject to a net tensile stress according to the criterion specified in *AASHTO LRFD* Article 6.6.1.2.1.

EXAMPLE

Design the solid-plate internal diaphragm at the interior pier of an exterior tub girder in a straight continuous-span bridge for the strength limit state (see figure below). The tub girder is supported on two bearings at the pier and a single pair of bearing stiffeners is to be provided on the diaphragm over each bearing.   The bearing stiffeners are assumed spaced 60 inches apart.   An 18-inch wide by 36-inch deep access hole is provided in the center of the diaphragm. The girder is homogeneous with the flanges and web having a yield strength of 50 ksi.
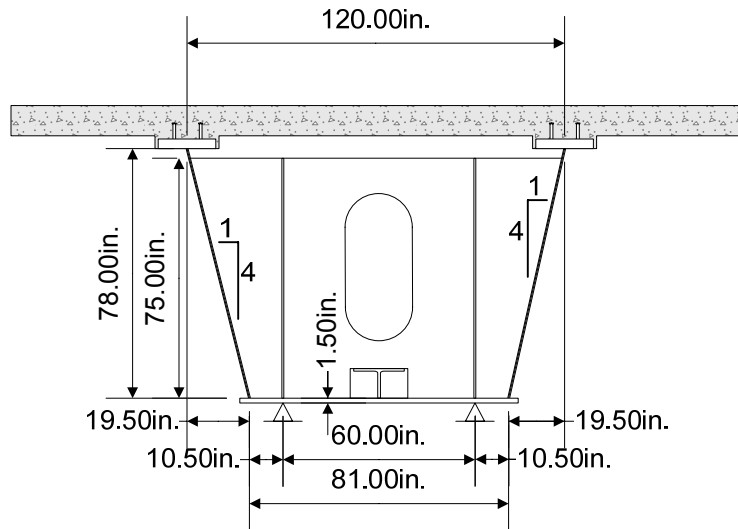
The load modifier η is assumed to be 1.0 and the Strength I load combination will be assumed to control.

It is assumed that the section is from a multiple box-section bridge that does *not* satisfy one or more of the special restrictions specified in *AASHTO LRFD* Article 6.11.2.3 (refer also to Section 2.2.4.1.2 of this chapter). Therefore, the effects of St. Venant torsional shear must be considered in the design of the girder and the diaphragm (see Section 2.2.4.1.3 of this chapter).

Assume the following total unfactored vertical shears in the critical web of the tub section. The critical web is considered to be the web subject to additive flexural and St. Venant torsional shears for each load case. Since the section is at an interior support, positive and negative shears exist at the section for each load case. Only the maximum and minimum values of the HL-93 live load plus impact shears are given:

$$V_{DC1} \quad = \quad +255/-254 \text{ kips}$$
$$V_{DC2} \quad = \quad +62/-58 \text{ kips}$$
$$V_{DW} \quad = \quad +50/-48 \text{ kips}$$
$$V_{LL+IM} \quad = \quad +183/-175 \text{ kips}$$

Compute the total maximum factored vertical shear in the diaphragm. The total unfactored vertical dead load shear in the diaphragm will be computed by summing the vertical dead load shears in the critical web of the tub section acting on each side of the interior-pier section

DC_1: $V = 255 + |-254| = 509 \text{ kips}$

DC_2: $V = 62 + |-58| = 120 \text{ kips}$

DW: $V = 50 + |-48| = 98 \text{ kips}$

Total unfactored dead load shear: = 727 kips

In this case, the HL-93 live load plus impact shear in the critical web at the interior pier is governed by two lanes loaded. Thus, the total unfactored vertical live load plus impact shear in the diaphragm will be computed by summing the vertical live load plus impact shears in the critical web of the tub section acting on each side of the interior-pier section, and then subtracting two times the rear-axle load of the HL-93 design truck plus impact (assumed positioned directly over the interior pier to maximize the live load shear at the pier section). The rear axle of the HL-93 design truck weighs 32.0 kips and the dynamic load allowance applied to the design truck at the strength limit state is 33 percent. Therefore:

LL+IM: $V = 183 + |-175| - 2(32.0)(1.33) = 273 \text{ kips}$

The total factored vertical shear in the diaphragm under the Strength I load combination is computed as:

$$V = 1.0[1.25(509 + 120) + 1.50(98) + 1.75(273)] = 1{,}411 \text{ kips}$$

Assume a ¾-inch-thick A 709 Grade 50 diaphragm plate (i.e. F_y = 50 ksi). The vertical depth of the plate is 75 inches. Check the factored shear resistance of the diaphragm. The nominal shear resistance V_n is computed from Equation 2.372 as follows:

$$V_n = V_{cr} = CV_p$$

AASHTO LRFD Equation 6.10.9.2-1

The plastic shear force V_p is computed as:

$$V_p = 0.58F_y Dt_w = 0.58(50)(75.0)(0.75) = 1{,}631 \text{ kips}$$

Calculate the constant *C*. The bearing stiffeners will be assumed to act as transverse stiffeners. The critical region for shear in this case is the region outside the bearing stiffeners adjacent to the critical web. Therefore, use the spacing from the mid-depth of the girder web to the first pair of bearing stiffeners; that is, d_o = 19.5/2 + 10.5 = 20.25 in. Therefore, the shear buckling coefficient *k* is computed from Equation 2.157 as:

$$k = 5 + \frac{5}{\left(\dfrac{d_o}{D}\right)^2}$$

AASHTO LRFD Equation 6.10.9.3.2-7

$$k = 5 + \frac{5}{\left(\dfrac{20.25}{75}\right)^2} = 73.59$$

Since:

$$1.12\sqrt{\frac{Ek}{F_y}} = 1.12\sqrt{\frac{29{,}000(73.59)}{50}} = 231.4 > \frac{D}{t_w} = \frac{75.0}{0.75} = 100.0$$

$$C = 1.0$$

AASHTO LRFD Equation 6.10.9.3.2-4

$$V_n = V_{cr} = (1.0)(1{,}631) = 1{,}631 \text{ kips}$$

$$V_r = \phi_v V_n = 1.0(1{,}631) = 1{,}631\,\text{kips} > V = 1{,}411 \text{ kips} \quad \text{ok}$$

$$\text{Ratio} = \frac{1{,}411}{1{,}631} = 0.87$$

An interior support diaphragm is subject to major-axis bending over the bearing sole plates in addition to shear. Therefore, evaluate the principal stresses. Compute the maximum total vertical shear stress f_d in the diaphragm at critical sections. First, separate out the flexural shear V_b due to major-axis bending of the tub section and the St. Venant torsional shear V_T from the total vertical diaphragm shear V. Referring to the example given at the end of Section 2.2.4.7.1.2 of this chapter, the factored torsional shear flow in the noncomposite tub section was computed as:

$$f = \frac{T}{2A_o} = \frac{1.0(1.25)(26)}{2(56.0)(12)} = 0.024 \text{ kips/in.}$$

Therefore:

$$V_T = 0.024(78.0/\cos 14°) = 0.024(80.4) = 1.93 \text{ kips}$$

The vertical component of V_T is computed as:

$$(V_T)_v = 1.93\left(\frac{78.0}{80.4}\right) = 1.87 \text{ kips}$$

The horizontal component of V_T is computed as:

$$\left(V_T\right)_h = 1.93\left(\frac{19.5}{80.4}\right) = 0.47 \text{ kips}$$

The total factored DC$_1$ vertical diaphragm shear acting on the non-composite section on the critical side is V_{DC1} = 1.0[1.25(509)] = 636.3 kips. Therefore, the flexural shear is:

$$V_b = 636.3 - 1.87 = 634.4 \text{ kips}$$

The total factored DC$_1$ vertical diaphragm shear acting on the non-composite section on the non-critical side is:

$$V_{DC_1} = 634.4 - 1.87 = 632.5 \text{ kips}$$

From the previous example, the factored torsional shear flow in the composite tub section was computed as:

$$f = \frac{T}{2A_o} = \frac{1.0\left|1.25(-190) + 1.5(-156) + 1.75(-966)\right|}{2(61.1)(12)} = 1.474 \text{ kips/in.}$$

Therefore:

$$V_T = 1.474\left(80.4\right) = 118.5 \text{ kips}$$

The vertical component of V_T is computed as:

$$\left(V_T\right)_v = 118.5\left(\frac{78.0}{80.4}\right) = 115.0 \text{ kips}$$

The horizontal component of V_T is computed as:

$$\left(V_T\right)_h = 118.5\left(\frac{19.5}{80.4}\right) = 28.74 \text{ kips}$$

The total factored vertical diaphragm shear acting on the composite section on the critical side is V_c = 1.0[1.25(120)+1.50(98)+1.75(273)] = 774.8 kips. Therefore, the flexural shear is:

$$V_b = 774.8 - 115.0 = 659.8 \text{ kips}$$

The total factored vertical diaphragm shear acting on the composite section on the non-critical side is:

$$V_c = 659.8 - 115.0 = 544.8 \text{ kips}$$

Therefore, on each side of the diaphragm, the total factored vertical shear due to flexure is:

$$\left(V_b\right)_{tot} = 634.4 + 659.8 = 1{,}294 \text{ kips}$$

The total factored vertical shear in the diaphragm on the critical side (including the vertical component of the torsional shear) is:

$$V_{tot} = 636.3 + 774.8 = 1{,}411 \text{ kips} \qquad \text{(as computed previously)}$$

The total factored vertical shear in the diaphragm on the non-critical side is:

$$V_{tot} = 632.5 + 544.8 = 1{,}177 \text{ kips}$$

The factored shear stress in the diaphragm due to St. Venant torsion $(f_d)_T$ is equal to:

$$\left(f_d\right)_T = \left(0.024/0.75 + 1.474/0.75\right) = 2.00 \text{ ksi}$$

Note that although the torques on the noncomposite and composite box sections act in different directions in this case, the DC_1 shear flow is small and the shear flow acting on the composite section includes the effect of an assumed future wearing surface. Therefore, for simplicity, the shear flows are conservatively assumed to act in the same direction and are added together in this example.

The average factored flexural shear stress in the diaphragm web (on the critical side) at the bearing stiffener due to major-axis bending $(f_d)_b$ is taken as:

$$\left(f_d\right)_b = \frac{1{,}294}{75.0(0.75)} = 23.00 \text{ ksi}$$

Therefore, the total factored shear stress f_d in the diaphragm web (on the critical side) at the bearing stiffener is equal to:

$$f_d = \left(f_d\right)_T + \left(f_d\right)_b = 2.00 + 23.00 = 25.00 \text{ ksi}$$

Calculate the shear stress at the section through the access hole. Assume the following unfactored bearing reactions:

Critical side: R_{DC1} = 509 kips
R_{DC2} = 25 kips
R_{DW} = 18 kips
R_{LL+IM} = 320 kips

The total factored reaction on the critical side under the Strength I load combination is computed as:

$$R_u = 1.0[1.25(509 + 25) + 1.50(18) + 1.75(320)] = 1{,}255 \text{ kips}$$

Non-critical side: R_{DC1} = 349 kips
R_{DC2} = 120 kips
R_{DW} = 98 kips
R_{LL+IM} = 277 kips

The total factored reaction on the non-critical side under the Strength I load combination is computed as:

$$R_u = 1.0[1.25(349 + 120) + 1.50(98) + 1.75(277)] = 1{,}218 \text{ kips}$$

Therefore, the total factored vertical diaphragm shear due to flexure at the section through the access hole is:

$$V = 1{,}294 \text{ kips} - 1{,}255 \text{ kips} = 39.0 \text{ kips}$$

The average factored flexural shear stress in the diaphragm web at the section through the access hole due to major-axis bending $(f_d)_b$ is taken as:

$$(f_d)_b = \frac{39.0}{(75.0 - 36.0)(0.75)} = 1.33 \text{ ksi}$$

Therefore, the total factored shear stress f_d in the diaphragm web at the section through the access hole is equal to:

$$f_d = (f_d)_T + (f_d)_b = 2.00 + 1.33 = 3.33 \text{ ksi}$$

Calculate the stress due to major-axis bending of the diaphragm over the bearing sole plate f_{by}. The stress f_{bz} is typically neglected.   Assume a strip of the bottom box flange equal to 18 times its thickness (i.e. 18 * 1.5 in. = 27.0 in.) acts with the diaphragm in resisting major-axis bending of the diaphragm. Calculate the section properties of the effective section at the bearing stiffener adjacent to the critical web:

Component	A	d	Ad	Ad^2	I_o	I
Web ¾" x 75"	56.25				26,367	26,367
Bot. Flange 1-1/2" x 27"	40.50	38.25	-1,549	59,254	7.59	59,262
	96.75		−1,549			85,629
				−16.01(1,549) =		−24,799
				I_{NA} =		60,830 in.⁴

$$d_s = \frac{-1{,}549}{96.75} = -16.01 \text{ in.}$$

$$d_{TOP\ OF\ STEEL} = 37.50 + 16.01 = 53.51 \text{ in.}$$

$$d_{BOT\ OF\ STEEL} = 39.00 - 16.01 = 22.99 \text{ in.}$$

$$S_{TOP\ OF\ STEEL} = \frac{60{,}830}{53.51} = 1{,}137 \text{ in.}^3$$

$$S_{BOT\ OF\ STEEL} = \frac{60{,}830}{22.99} = 2{,}646 \text{ in.}^3$$

Calculate the section properties of the effective section through the center of the access hole:

Component	A	d	Ad	Ad^2	I_o	I
Web – above hole	14.63	27.75	406.0	11,266	463.4	11,729
Web – below hole	14.63	27.75	406.0	11,266	463.4	11,729
Bot. Flange 1-1/2" x 27"	40.50	38.25	-1,549	59,254	7.59	59,262
	96.75		−1,549			87,720

$$-22.20(1,549) = \quad -34,388$$

$$I_{NA} = \quad 48,332 \quad \text{in.}^4$$

$$d_s = \frac{-1,549}{69.76} = -22.20 \text{ in.}$$

$$d_{TOP\ OF\ STEEL} = 37.50 + 22.20 = 59.70 \text{ in.} \qquad d_{BOT\ OF\ STEEL} = 39.00 - 22.20 = 16.80 \text{ in.}$$

$$S_{TOP\ OF\ STEEL} = \frac{48,332}{59.70} = 809.6 \text{ in.}^3 \qquad S_{BOT\ OF\ STEEL} = \frac{48,332}{16.80} = 2,877 \text{ in.}^3$$

Check Equation 2.370 to ensure that bend buckling of the diaphragm web does not occur (the section at the bearing stiffener is critical for this check):

$$\frac{2D_c}{t_w} = \frac{2(22.99 - 1.5)}{0.75} = 57.3 < \lambda_{rw} = 5.7\sqrt{\frac{29,000}{50}} = 137.3 \quad \text{ok}$$

Check the section at the bearing stiffener. Moments of the factored St. Venant torsional shears and flexural shears will be taken about a point lying on the neutral axis of the diaphragm at this section directly above the bearing. First, compute the moment in the diaphragm due to the factored St. Venant torsional shears. For simplicity, the torsional shear flows due to the dead and live loads (computed previously) will be assumed to act around the same perimeter (i.e. the perimeter of the diaphragm). The horizontal and vertical components of the torsional web shears (computed previously) acting at the mid-depth of the web will be considered.

Top:

$$M = (0.024 \text{ kips/in.} + 1.474 \text{ kips/in.})(10.5 \text{ in.} + 19.5 \text{ in.})(53.51 \text{ in.}) = -2,405 \text{ kip} - \text{in.}$$

Web:

$$M = (1.87 \text{ kips} + 115.0 \text{ kips})(10.5 \text{ in.} + 19.5 \text{ in.}/2) - (0.47 \text{ kips} + 28.74 \text{ kips})(16.01 \text{ in.}) = -1,899 \text{ kip} - \text{in.}$$

Bot.:

$$M = (0.024 \text{ kips/in.} + 1.474 \text{ kips/in.})(10.5 \text{ in.})(21.49 \text{ in.}) = -338.0 \text{ kip} - \text{in}$$

Total:

$$M = \left(-2,405\right) + \left(-1,899\right) + \left(-338.0\right) = -4,642 \text{ kip} - \text{in.}$$

The moment in the diaphragm due to the factored flexural shears is computed as:

$$M = 1,294 \text{ kips}\left[10.5 \text{ in.} + 19.5 \text{ in.}\Big/2. - \frac{19.5}{78.0}(16.01)\text{ in.}\right] = -21,024 \text{ kip} - \text{in}$$

The total factored moment in the diaphragm at the bearing stiffener is:

$$M = (-4,642) + (-21,024) = -25,666 \text{ kip} - \text{in.}$$

The maximum bending stress at the top of the diaphragm is:

$$f_{by} = \frac{|-25,666 \text{ kip} - \text{in.}|}{1,137 \text{ in.}^3} = +22.57 \text{ ksi}$$

From Equation 2.369:

$$\sigma_{1,2} = \left(\frac{f_{by} + f_{bz}}{2}\right) \pm \sqrt{\left(\frac{f_{by} - f_{bz}}{2}\right)^2 + f_d^2}$$

$$\sigma_{1,2} = \left(\frac{22.57 + 0}{2}\right) \pm \sqrt{\left(\frac{22.57 - 0}{2}\right)^2 + (25.00)^2} = 38.71, -16.14 \text{ ksi}$$

Checking the combined principal stresses according to Equation 2.368 gives:

$$\sqrt{\sigma_1^2 - \sigma_1\sigma_2 + \sigma_2^2} \le \phi_f F_y$$

$$\sqrt{(38.71)^2 - (38.71)(-16.14) + (-16.14)^2} = 48.82 \text{ ksi} < 1.0(50) = 50.00 \text{ ksi} \quad \text{ok}$$

$$\text{Ratio} = \frac{48.82}{50.00} = 0.98$$

Check the section through the center of the access hole. Moments of the factored St. Venant torsional shears and flexural shears will be taken about a point lying on the neutral axis of the diaphragm at this section. First, compute the moment in the diaphragm due to the factored St. Venant torsional shears.

Top:

$$M = (0.024 \text{ kips}/\text{in.} + 1.474 \text{ kips}/\text{in.})(120 \text{ in.}/2)(59.70 \text{ in.}) = -5,366 \text{ kip} - \text{in.}$$

Web:

$M = (1.87 \text{ kips} + 115.0 \text{ kips})(120 \text{ in.}/2 - 19.5 \text{ in.}/2) - (0.47 \text{ kips} + 28.74 \text{ kips})(22.20 \text{ in.}) = -5,224 \text{ kip} - \text{in.}$

Bot.:

$M = (0.024 \text{ kips}/\text{in.} + 1.474 \text{ kips}/\text{in.})(81 \text{ in.}/2)(15.30 \text{ in.}) = -928.2 \text{ kip} - \text{in}$

Total:

$$M = (-5,366) + (-5,224) + (-928.2) = -11,518 \text{ kip} - \text{in.}$$

The moment in the diaphragm due to the factored flexural shears is computed as:

$$M = 1,294 \text{ kips}\left[81 \text{ in.}/2 + 19.5\Big/2 \text{ in.} - \frac{19.5}{78.0}(22.20) \text{ in.} \right] = -57,842 \text{ kip} - \text{in}$$

The total moment factored in the diaphragm at the center of the access hole (considering also the moment due to the critical bearing reaction) is:

$$M = (-11,518) + (-57,842) + (1,255 \text{ kips})(60 \text{ in.}/2) = -31,710 \text{ kip} - \text{in.}$$

The maximum bending stress at the top of the diaphragm is:

$$f_{by} = \frac{|-31,710 \text{ kip} - \text{in.}|}{809.6 \text{ in.}^3} = +39.17 \text{ ksi}$$

From Equation 2.369:

$$\sigma_{1,2} = \left(\frac{f_{by} + f_{bz}}{2}\right) \pm \sqrt{\left(\frac{f_{by} - f_{bz}}{2}\right)^2 + f_d^2}$$

$$\sigma_{1,2} = \left(\frac{39.17 + 0}{2}\right) \pm \sqrt{\left(\frac{39.17 - 0}{2}\right)^2 + (3.33)^2} = 39.45, -0.28 \text{ ksi}$$

Checking the combined principal stresses according to Equation 2.368 gives:

$$\sqrt{\sigma_1^2 - \sigma_1\sigma_2 + \sigma_2^2} \leq \phi_f F_y$$

$$\sqrt{(39.45)^2 - (39.45)(-0.28) + (-0.28)^2} = 39.59 \text{ ksi} < 1.0(50) = 50.00 \text{ ksi} \quad \text{ok}$$

$$\text{Ratio} = \frac{39.59}{50.00} = 0.79$$

The section at the bearing stiffener controls. Use a ¾" x 75" diaphragm plate. Similar computations should be done at the fatigue limit state to obtain the principal tensile stress range due to the factored fatigue live load to check potential fatigue-sensitive diaphragm details subject to a net tensile stress.

Design the bearing stiffeners (refer to Section 2.2.6.2 of this chapter). ASTM A 709 Grade 50 steel will be assumed for the stiffeners (i.e. F_{ys} = 50 ksi). Assume that the bearings are fixed at the piers. Thus, there will be no thermal expansion causing eccentric loading on the bearing stiffeners. The width b_t of each projecting stiffener element must satisfy:

$$b_t \leq 0.48 t_p \sqrt{\frac{E}{F_{ys}}}$$

<div align="right">AASHTO LRFD Equation 6.10.11.2.2-1</div>

Welded bearing stiffeners are also commonly made up of less expensive flat bar stock, which is generally produced in whole-inch width increments and 1/8-in. thickness increments. Try two 10.5-inch-wide bars welded to each side of the diaphragm web. Rearranging *AASHTO LRFD* Equation 6.10.11.2.2-1 gives:

$$\left(t_p\right)_{min.} = \frac{b_t}{0.48\sqrt{\dfrac{E}{F_{ys}}}}$$

$$\left(t_p\right)_{min.} = \frac{10.5}{0.48\sqrt{\dfrac{29,000}{50}}} = 0.908 \text{ in.}$$

Try a stiffener thickness t_p of 1.0 inches, which satisfies the preferred minimum thickness of ½ inch for stiffeners given in Reference 40.

According to *AASHTO LRFD* Article 6.10.11.2.3, the factored bearing resistance for the fitted ends of bearing stiffeners is to be taken as:

$$\left(R_{sb}\right)_r = \phi_b \left(R_{sb}\right)_n$$

<div align="right">AASHTO LRFD Equation 6.10.11.2.3-1</div>

where $(R_{sb})_n$ is   equal to the nominal bearing resistance for the fitted end of bearing stiffeners taken as:

$$\left(R_{sb}\right)_n = 1.4 A_{pn} F_{ys}$$

<div align="right">AASHTO LRFD Equation 6.10.11.2.3-2</div>

A_{pn} is the area of the projecting elements of the stiffener outside of the web-to-flange fillet welds. Assume for this example that the clip provided at the base of the

stiffeners to clear the web-to-flange fillet welds is 1.5 inches in length. The resistance factor for bearing on milled surfaces ϕ_b = 1.0. Therefore:

$$A_{pn} = 2(10.5 - 1.5)(1.0) = 18.00 \text{ in.}^2$$

$$(R_{sb})_n = 1.4(18.00)(50.0) = 1{,}260 \text{ kips}$$

$$(R_{sb})_r = \phi_b (R_{sb})_n = 1.0(1{,}260) = 1{,}260 \text{ kips} > R_u = 1{,}255 \text{ kips} \quad \text{ok}$$

For computing the axial resistance of bearing stiffeners that are welded to the diaphragm web, *AASHTO LRFD* Article 6.10.11.2.4b states that a portion of the web is to be included as part of the effective column section. For stiffeners consisting of two plates welded to the web, the effective column section is to consist of the two stiffener elements, plus a centrally located strip of web extending not more than $9t_w$ on each side of the stiffeners, as shown in Figure 2.70.

As specified in *AASHTO LRFD* Article 6.10.11.2.4a, the radius of gyration of the effective column section is to be computed about the mid-thickness of the web and the effective length is to be taken as 0.75D, where D is the web depth. The area of the effective column section is computed as:

$$A_s = 2[(10.5)(1.0) + 9(0.75)(0.75)] = 31.13 \text{ in.}^2$$

The moment of inertia of the effective column section (conservatively neglecting the web strip) is computed as:

$$I_s = \frac{1.0(10.5 + 0.75 + 10.5)^3}{12} = 857.4 \text{ in.}^4$$

The radius of gyration of the effective column section is therefore computed as:

$$r_s = \sqrt{\frac{I_s}{A_s}} = \sqrt{\frac{857.4}{31.13}} = 5.25 \text{ in.}$$

The effective length of the effective column section is computed as:

$$K\ell = 0.75D = 0.75(75.0) = 56.25 \text{ in.}$$

Check the limiting slenderness ratio of 120 specified for main members in compression in *AASHTO LRFD* Article 6.9.3:

$$\frac{K\ell}{r_s} = \frac{56.25}{5.25} = 10.7 < 120 \quad \text{ok}$$

As specified in *AASHTO LRFD* Article 6.10.11.2.4a, calculate the factored axial resistance P_r of the effective column section according to the provisions of *AASHTO LRFD* Article 6.9.2.1

$$P_r = \phi_c P_n$$

AASHTO LRFD Equation 6.9.2.1-1

where P_n is equal to the nominal compressive resistance determined as specified in *AASHTO LRFD* Article 6.9.4.1, and ϕ_c is equal to the resistance factor for axial compression = 0.90.

Calculate λ:

$$\lambda = \left(\frac{K\ell}{r_s\pi}\right)^2 \frac{F_{ys}}{E}$$

AASHTO LRFD Equation 6.9.4.1-3

$$\lambda = \left(\frac{56.25}{5.25\pi}\right)^2 \frac{50}{29,000} = 0.020$$

Since $\lambda < 2.25$, then:

$$P_n = 0.66^\lambda F_{ys} A_s$$

AASHTO LRFD Equation 6.9.4.1-1

$$P_n = 0.66^{0.020}(50.0)(31.13) = 1,544 \text{ kips}$$

$$P_r = 0.9(1,544) = 1,390 \text{ kips} > R_u = 1,255 \text{ kips} \quad \text{ok}$$

Use 1" x 10-1/2" bearing stiffeners (one pair) over each bearing.

201. Darwin, D. 1990. *Steel and Composite Beams with Web Openings.* AISC Steel Design Guide Series No. 2, American Institute of Steel Construction, Chicago, IL.

Volume 3
Concrete Bridge Superstructure Design

Chapter 1
Construction of Concrete Bridges

1.1 Introduction

This topic introduces basic concepts for the construction of prestressed concrete superstructures from the perspective of key constructibility considerations. Different types of construction are discussed with respect to project circumstances. Applicable span ranges are offered as an initial guide to type selection.

1.1.1 Introduction and Constructibility

As seen in DM Volume 1, Chapter 2.5 previously, there is a wide variety of types of prestressed concrete bridge solutions for any possible application. The final choice depends upon taking into account many diverse considerations. Out of expediency and custom, these are often expressed and evaluated in terms of economics, costs and benefits or simply reduced solely to costs. Before any economic evaluations can be made, it is necessary to appreciate factors that influence costs.

For any solution, the two most significant influences are "Design" – in the sense of developing a bridge solution with structural efficiency and effective use of materials on the one hand - and "Construction" or "Constructibility" on the other. Constructibility is the efficient and effective use of available resources, means, methods, techniques, equipment, labor, material and time for construction of the bridge.

"Design" and "Constructibility" significantly influence each other and are not easily separated. As a practical, administrative and contractual matter, it is essential and prudent to separate them. A design must be sufficiently prepared before proceeding with construction. (This is very obviously the case with "Design-Bid-Build" projects and is no less essential for "Design-Build" projects.) Constructibility aspects become even more important when structures are increasingly more complex; such as segmental and cable-stay bridges where construction techniques, equipment, loads, intermediate steps, concrete age and so forth, directly affect the design and vice-versa. Hence, it is important to have an overall understanding or appreciation of construction (constructibility) prior to commencing a design.

This Chapter provides an overall view of construction to illustrate aspects that should be considered in terms of their influence upon design or choice of a bridge solution. The applications of prestressed concrete bridges summarized in DM Volume I, Chapter 2.5 are reintroduced, basically in increasing order of complexity, and particular aspects of their construction that influence design are explained.

Other important factors to consider are materials and components. Physical properties of materials, such as concrete strength, elasticity, creep and shrinkage, should be properly taken into account when performing calculations during "Design". Design parameters are reserved for Section 1.2 (below). Aspects of construction itself, such as curing concrete or components for post-tensioning are discussed in Chapter 1.

1.1.2 Bridge Layout

When selecting a preliminary bridge type or layout key considerations are; site-specific constraints, roadway geometric constraints, constructibility, access, shipping and handling, weight limits or permits, maintenance of traffic, use of special construction or erection equipment, construction costs and aesthetics.

1.1.2.1 Site Constraints

Bridge layout is controlled by site specific constraints. Spans are set according to features to be crossed. Span length may dictate the type of bridge construction. Site constraints include existing or new highways, rail, navigation channels or locations where it may or may not be possible to place piers and foundations for geotechnical reasons.

Roadway geometric constraints include horizontal alignments and lateral clearances, vertical profile and permanent or temporary clearance, the width of the superstructure and the width and skew of substructure. Horizontal curvature of a superstructure may dictate, for example, the maximum practical span for a straight precast girder in order to restrict the width of a deck slab overhang. A sharp curve may require precast girders of varying length within a deck. In turn, this might require more prestress (pre- or post-tensioning) in the longer girders in that deck. Alternatively, curvature may require the use of a completely different superstructure such as a continuous, trapezoidal section box designed to follow the radius. Figure 1.1 shows a typical layout of a straight girder bridge on a curved horizontal alignment.
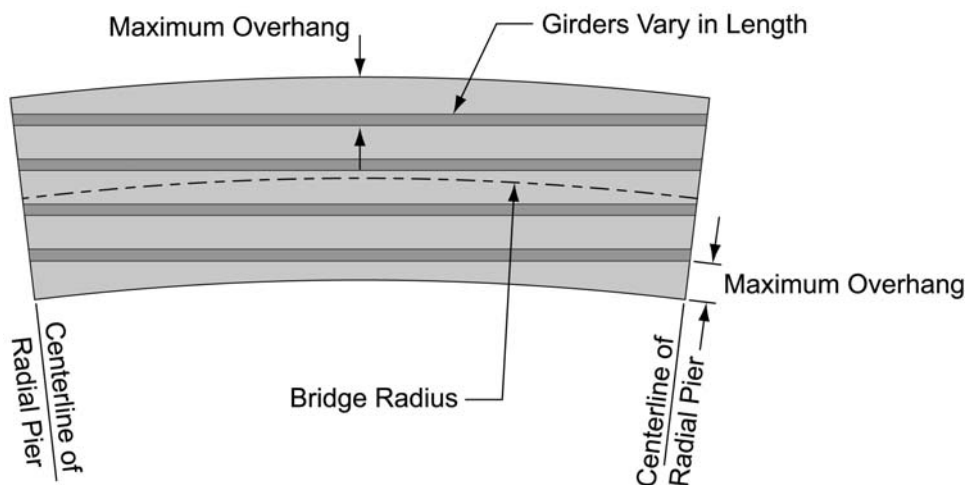
Figure 1.1 Typical Span of a Curved Girder Bridge

Vertical profile and clearance often restricts the depth of a superstructure. This in turn limits the maximum possible span length and may require more piers, more girders in a deck or both.

Skewed substructures require longer spans and deeper superstructure. In turn, this may require more girders, or more prestress force or both. Also, for girder bridges this requires special attention to details for diaphragms and setting of bridge bearings. Figure 1.2 shows two configurations of bearings of a girder bridge resting on skewed substructure caps. In Figure 1.2 (a) the bearing are placed parallel to the pier caps. This minimizes the width of the caps, but can lead to bearing instability and increased design requirements for the end of span diaphragms. Figure 1.2 (b) aligns the bearings along the axis of the girders.   In this case the bearing

performance is improved but the width of the pier cap must be increased to accommodate the bearing placement.
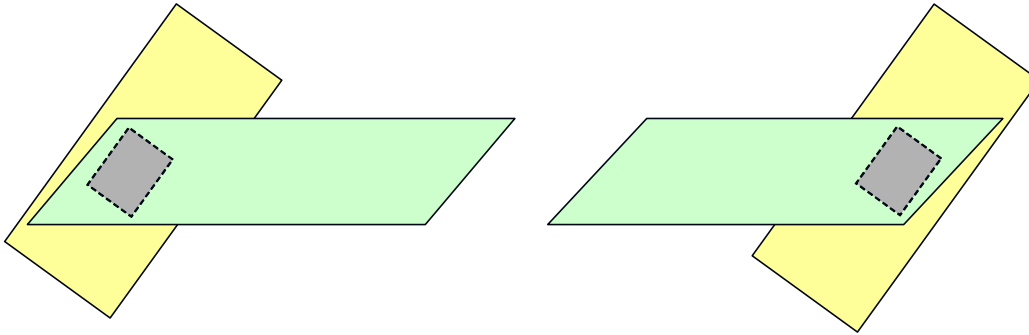
Figure 1.2(a) Bearings placed with pier caps.
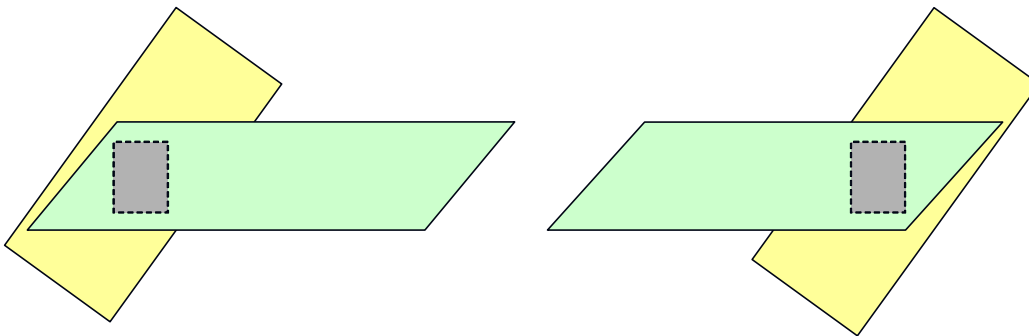
Figure 1.2(b) Bearings placed with girders.

Figure 1.2 Bearing Placements on Skewed Structures

1.1.2.2 Access

Constructibility considerations include accessibility to the site for delivery of materials, equipment and prefabricated components and the means of that delivery – whether by road, rail or water. The number, capacity and reach of cranes should be considered for lifting and placing precast components. Although it is the Contractor's responsibility to safely operate cranes from a barge or firm foundation, it is prudent to consider reasonable accessibility, clearances and possible crane locations during layout of the design. In general, the size of precast components, such as girders and segments, should be selected with access and delivery limitations in mind. The need to construction temporary access roads or dredge channels should be considered. In some cases, erection techniques such as overhead gantries, may avoid the need for special access or heavy cranes.

The shipping of prefabricated components, especially heavy precast girders or segments, may need special permits for weight limitations or routing. Intermediate handling and transfer from one mode to another, such as from road to water, requires intermediate crane facilities, possibly temporary storage and might bring

inadvertent delays. Shipping of long, slender girders requires appropriate precautions for lateral stability.

For many sites, the erection of precast components (girders or segments) or the delivery of supplies such as ready-mixed concrete often requires local traffic diversions or temporary road or lane closures with attendant traffic signs, safety and control measures. Such anticipated needs should be considered in the planning and layout of the bridge. In some cases, it might influence the location of permanent or temporary piers. In many, although by no means all cases, may be prudent to incorporate specifications or plans for possible "Maintenance of Traffic" in the final construction documents.

1.1.2.3 Special Construction Equipment

Aspects of "constructibility" such as the use of formwork, falsework, special equipment, launching gantries, trusses, form-travelers and the like are discussed within the context of the type and complexity of the bridge (below). In general, the greater a span, the more complex the type of construction needed (DM Volume I, Chapter 2.5). Figure 1.3 shows typical special falsework required for the construction of a three span, post-tensioned spliced girder bridge. Figure 1.4 shows a typical truss configuration for span-by-span construction.

Figure 1.3 Temporary Falsework for Spliced Girder Construction

Figure 1.4 Span-by-Span Construction using Erection Trusses

1.1.2.4 Span Length and Costs

For a particular type of bridge construction (for example, precast girders or cast-in-place boxes), increasing the span increases costs. As a result, as spans increase, it becomes more economical to switch to an alternative, usually more complex, type of construction more suited to the circumstances (Figure 1.5).
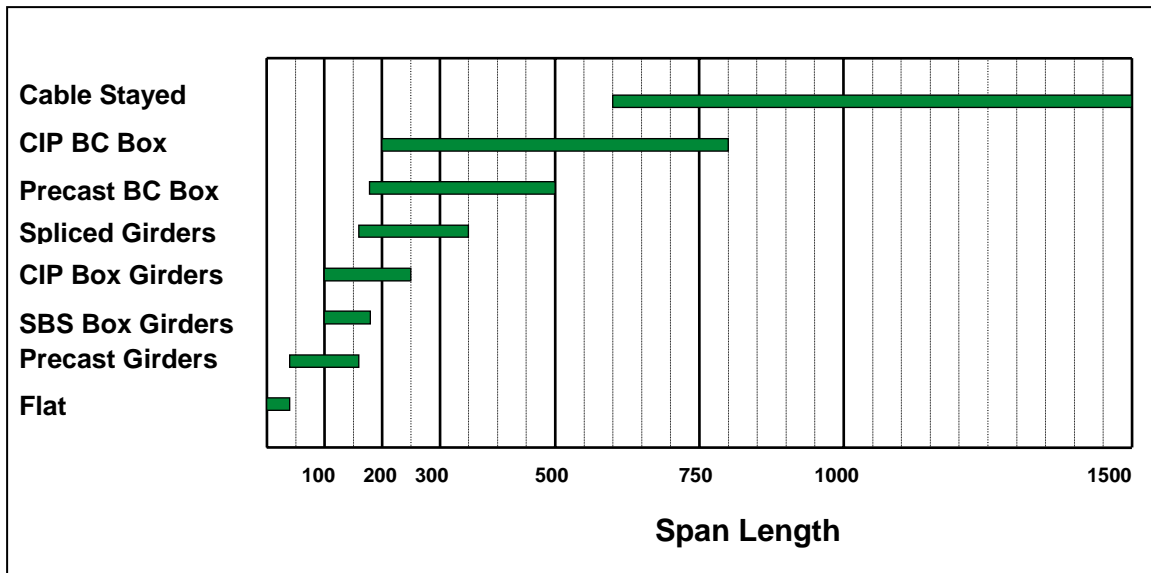
Figure 1.5 Bridge Types and Span Lengths

where:

CIP BC Box	= Cast-in-place, post-tensioned box girder superstructures built using the balanced cantilever method of construction,
Precast BC Box	= Precast, post-tensioned box girder superstructures built using the balanced cantilever method of construction,
CIP Box Girders	= Cast-in-place, post-tensioned box girder superstructures typically cast on falsework,
SBS Box Girders	= Precast, post-tensioned box girder superstructures built using the span-by-span method of construction.
PPC Girders	= Precast, prestressed concrete girder superstructures with cast-in-place deck slabs.

It should never be assumed that the comparison of bridge type and cost can be based solely upon span length. It is appropriate to optimize the span length within a given bridge type: for example, the choice of using different depth standard AASHTO I-girder with different span lengths and numbers of piers – or similarly, between the larger standard AASHTO girders and Bulb-T's. For the most commonly available types of precast girders, the range of applicable spans is illustrated in Figure 1.6. By making girders fully structurally continuous by the use of spliced joints and post-tensioning, it is possible to increase spans by 10 to 20% as indicated in Figure 1.7.
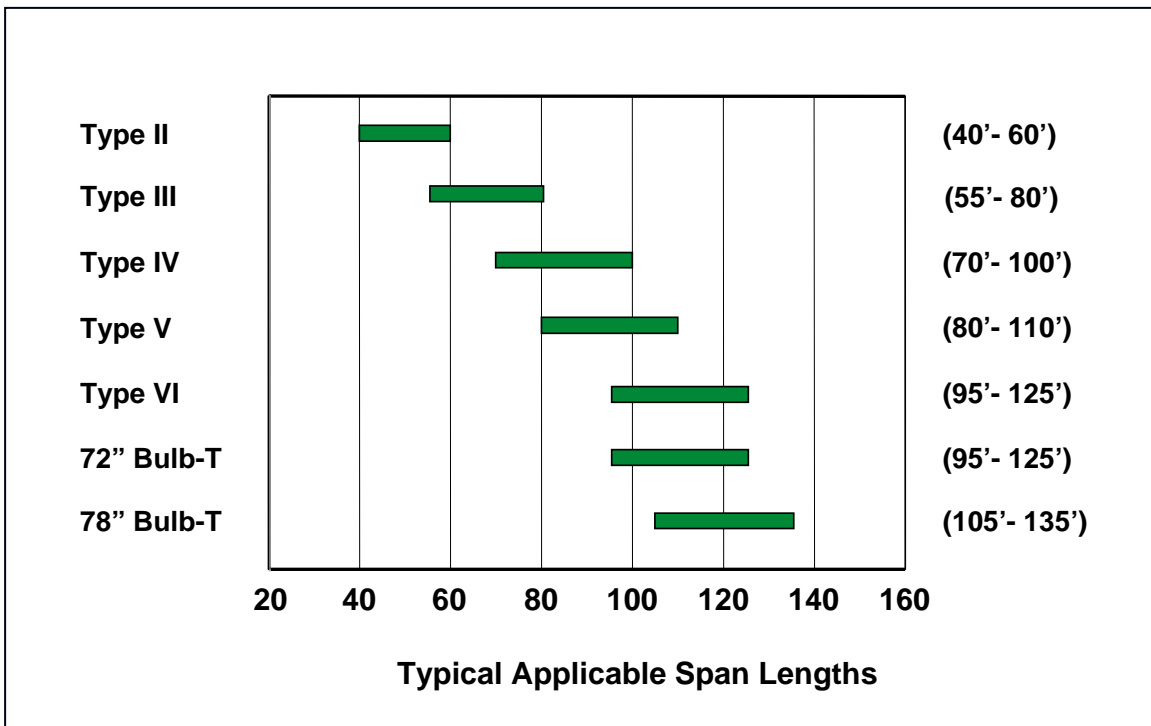
Figure 1.6 Precast Girder Types and Applicable Spans
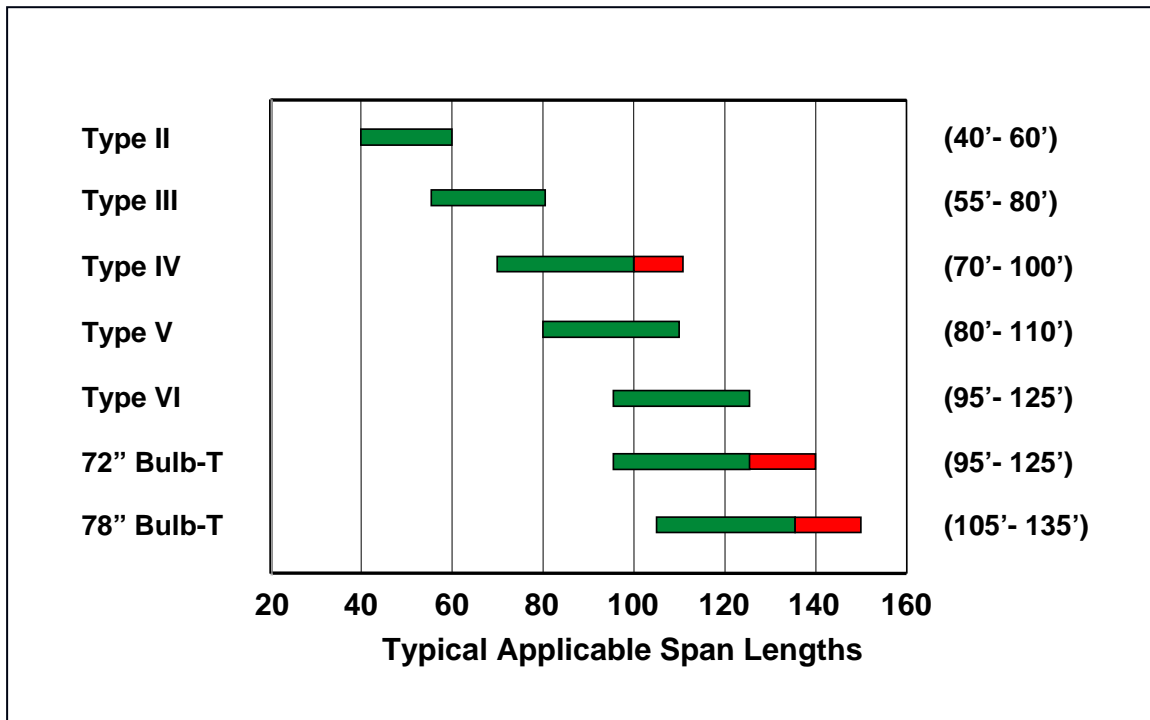
Figure 1.7 Increase in Span from Structural Continuity

For longer spans where the choice may lie, for instance, between precast or cast-in-place balanced cantilever, the span optimization exercise should consider the difference in construction techniques, schedules and times, in addition to the locations and numbers of piers for different span lengths.

It is less simple and sometimes can be misleading to compare span length and cost across different bridge types – for example; I-girders versus precast segmental. In such cases, a comprehensive examination of all viable, applicable scenarios should be made to obtain realistic construction costs, schedules and times.

In cases where significant lateral loads may need to be sustained by bridge piers, (e.g. for vessel impact) span lengths should be chosen to optimize the balance between permanent vertical loads and foundation size. It may be more cost effective to adopt a long span to take advantage of the large foundations required for the infrequent high lateral loads or to place piers in a lower vessel impact zone.

For preliminary layout and type selection purposes, comparison of bridge type and costs are usually based upon historical data or unit prices adjusted for inflation and region.

1.1.2.5 Aesthetics

Good aesthetics is not necessarily costly when incorporated in a design and selection of a bridge type at the outset. Some general principles are to adopt clean, uninterrupted lines to present a natural unobstructed feature for the eye to follow, aim for the shallowest superstructure, avoid the unresolved duality of a middle pier

or obstruction by as far as possible adopting an odd number of spans (i.e. 1, 3, 5), adopt and adapt slender and interesting pier shapes, adapt textures and colors to the local terrain and consider the entire structure within its local context. In general, bridges are large bold, intrusive and exist for a lifetime or more. Appearance is important. There is only one opportunity - it is worthwhile pursuing a pleasing but practical and cost effective engineering solution.

1.1.2.6 Optimization

Optimization of the preliminary concepts and alternative bridge types taking into account the various constraints, constructibility and engineering requirements outlined above will lead to a matrix of possible bridges and construction costs for selection, further development or refinement during final design. For preliminary design and cost-estimating purposes, it is usually sufficiently accurate to base estimates upon previous unit prices or contract history, suitably adjusted for inflation.

1.2 Materials and Components

This topic provides an overview of aspects of material properties and components and their influence upon construction that should be considered during design or addressed in specifications and procedures. It is intended only as an introduction. For more information for design purposes refer to DM Volume 3, Chapter 2, Section 2.2.

1.2.1 Concrete

For construction, concrete for bridges is either precast or cast-in-place. Concrete is produced in a batch plant at a precast production facility, on site or at a ready-mix concrete plant. Generally, concrete plants and precast production facilities are qualified or certified in an appropriate way to ensure quality. For the Owner and Designer, the essential qualities of concrete are strength and durability, assured by appropriate project specifications. For the Contractor, cost, equipment and schedule drive decisions to adopt precast or cast-in-place construction.

As regards bridge type selection, the advantages of using precast concrete must be weighed against those of using cast-in-place construction. For example, with a concrete deck slab on precast girders, it is a question not only of resources for delivery, placing, consolidating, finishing the slab but allowing time to cure before applying live load. By contrast, some types of construction, such as precast segmental - where once the segments have been erected the deck is complete - require no further time to mature before loading. Such considerations influence overall construction schedules and costs.

At the preliminary concept stage of a design, the types of concrete, materials and special requirements that may be desired not only for strength but also long term durability should be considered - for example, available resources of indigenous aggregates versus needs to import material. The benefits, costs and use of materials such as fly-ash, blast furnace slag, micro-silica and additives such as air entraining agents and high range water reducers to enhance durability should be considered in the preliminary design and appropriately incorporated in final project specifications, as necessary. In general, concrete mixes, specifications and use should be based upon those normally available for the project location.

Physical properties of concrete to consider in design are addressed in DM Volume 3, Chapter 2. For additional information on high performance concretes refer to "Guide Specification for High Performance Concrete for Bridges, EB233, Portland Cement Association, Skokie, IL."

1.2.2 Reinforcing Steel

The use of reinforcing steel is common and routine practice in the construction industry. Its quality and installation are addressed via normal construction specifications.

1.2.3 Prestressing Steel

Strand for prestressing is available in two nominal diameters of 0.5" or 0.6". The former size, 0.5" diameter is more widely used for the production of pretensioned girders, piles and similar components at precast concrete production factories. Both strand sizes are used in post-tensioning but the choice depends upon the particular supplier (manufacturer) of the post-tensioning system hardware, i.e. anchorages, wedges, wedge-plates and jacks. The use of a particular system depends upon the Contractor and his selection of a sub-contract supplier. It is for this important commercial reason that project specifications, plans and documents should allow for variations in the selection of a post-tensioning system. This is normally and routinely accommodated via an appropriate "Shop Drawing" submission and review process.

Bars for prestressing are most often used for relatively short permanent or temporary tendons. Temporary PT bars are frequently used to erect precast segments in order to secure, tightly close and compress match-cast joints until an applied epoxy seal has set.

Physical properties of prestressing steel to consider in design are addressed in DM Volume 3, Chapter 2.

1.2.4 Post-Tensioning Hardware

For strand tendons, post-tensioning hardware consists of and anchorage, wedges to grip each individual strand and a wedge-plate housing all the wedges that bears upon the anchorage. The anchorage itself is usually a high strength casting that comprises one or more (multi-plane) bearing plates and forms a cone-shape taper from the wedge plate to the post-tensioning duct (Figure 1.8). The cone connects with the post-tensioning duct. The duct itself is usually an approved plastic or steel material depending upon the type of tendon – whether internal (within the concrete) or external (exterior to the concrete) of the superstructure itself. Different sizes and types of anchorage devices are available from most suppliers according to the number of strands in the tendon
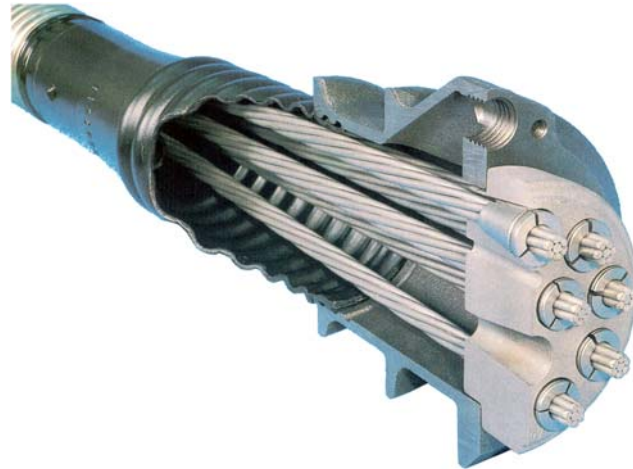
Figure 1.8 Post-Tensioning Anchor

Bar tendons are secured by a threaded anchor nut that bears against an anchor plate. The anchor plate may be a square or rectangular steel plate or a special embedded casting depending upon the system.

For more information on the installation and grouting of post-tensioning, refer to the "Post-Tensioning Tendon Installation and Grouting Manual" available from the Federal Highway Administration or the American Segmental Bridge Institute.

1.2.5 Loss of Prestress

In any application of prestress, losses arise from a variety of factors. The magnitude of the loss depends upon various circumstances – in particular the type of construction, i.e. whether precast or cast-in-place, the physical properties and maturity of the concrete at the time of application of the prestress and the history and sequence of permanent load applied to the concrete. The latter aspects especially influence creep which in turn, influences losses. Physical properties of concrete and prestressing steel that enter into calculation of internal forces and losses are addressed in DM Volume 3, Chapter 2.

For post-tensioned structures, tendons generally follow a profile. During installation and jacking of tendons, friction due to curvature and unintentional wobble of the ducts reduces the effective force along the length of the tendon. Also, when a jack is released, wedges are drawn into the wedge plate by a small amount, usually about 3/8", before they fully grip the strand. This induces a small additional loss. For more information on installation and calculation of post-tensioning losses, refer to the "Post-Tensioning Tendon Installation and Grouting Manual" available from the Federal Highway Administration or the American Segmental Bridge Institute.

1.2.6 Other Materials and Components

Various miscellaneous materials or components should be addressed in appropriate project specifications or plan notes. For example, occasionally in pre-tensioned girders strands in the web may be deflected upwards to a draped (depressed) profile. This requires embedding special hold-down devices in the bottom flange. A widely used alternative is to de-bond several strands in the bottom flange near the end of the girder using a suitable plastic shield (pipe) around each strand. These components must be of approved material and properly installed.

In post-tensioned construction, tendons pass through ducts and enter anchorages. Ducts may be made of plastic or metal. Anchorages require sealing and protection to prevent intrusion of deleterious elements. In addition, ducts are usually filled with a cementitious grout after installation and stressing of the tendons. All components and materials should be of approved materials and properly installed. For more information on installation, grouting and protection of post-tensioning, refer to the "Post-Tensioning Tendon Installation and Grouting Manual" available from the Federal Highway Administration or the American Segmental Bridge Institute.

1.3 Girder Precasting

This topic discusses various types of precast girders and sections used for prestressed concrete bridge superstructures normally available from the precast industry. Deck slab proportions and details are introduced. Typical activities involved in the manufacture of precast concrete girders, curing, storage and shipping are presented. The object is to provide a basic introduction to precast girders and production operations.

1.3.1 Typical Girder Types and Applications

1.3.1.1 General

To some extent, all of us are have some idea of concrete girder bridges as they have become a familiar feature of the Interstate landscape over the last few decades. This is a useful starting point for construction concepts, even though prestressed concrete girder bridges are by no means the only type of concrete bridge. The focus here is upon precast girder construction from the perspective of some of the more commonly available sections. The choice of a particular girder type and size depends very much upon the industrial availability of precast concrete components within a given region and on the availability of a particular production bed girder section and length. Storage capabilities at the yard or on site, transport, access and cranes also influence choice.

A typical concrete bridge deck may comprise several I-girders with a reinforced concrete deck slab (Figure 1.9). Span length depends upon the type and size of the girder section, the spacing between girders and the thickness of the deck slab. A deeper section beam will span a greater length. Also, for the same size of girder and overall width of deck, if more girders are provided (say five instead of four) so that the girders are closer together, then a greater span is possible.
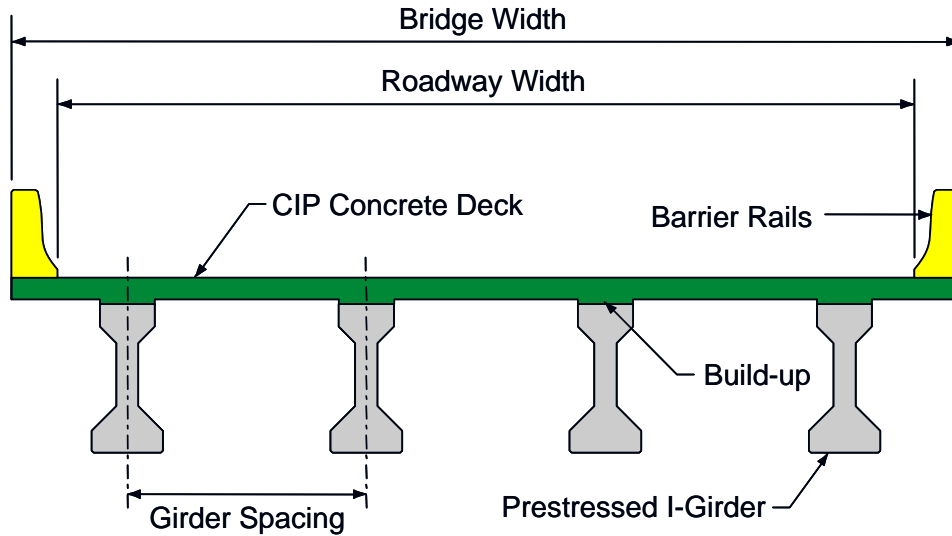
Figure 1.9 Typical Prestressed Concrete Girder Bridge Deck

Girders are usually spaced at 4 to 10 feet – possibly up to a maximum of 12 feet on center. The slab overhang is usually about 40% of the spacing but not more than 5 feet for most commercially available deck forming systems.

When girders are widely spaced, a deck slab must be thicker and heavier, than when girders are closely spaced. The minimum practical deck slab thickness (about 7") is governed by concrete cover, reinforcing bar diameters and construction tolerance. For this type of construction, deck slabs are rarely thicker than 8" or thereabouts. Usually, a slab is built-up over the girders to allow for camber. An economical bridge deck design strives for an overall balance between the thickness of the deck slab, girder spacing and span length.

1.3.1.2 AASHTO I-Girders

Standard AASHTO I-girder sections were developed in the 1950's. The most frequently used have been the Types II, III and IV for spans ranging from 40 to just over 100 feet (Figure 1.10). These particular sections have been widely adopted and the precast concrete industry is able to supply them in many areas.

Type II   Type III   Type IV
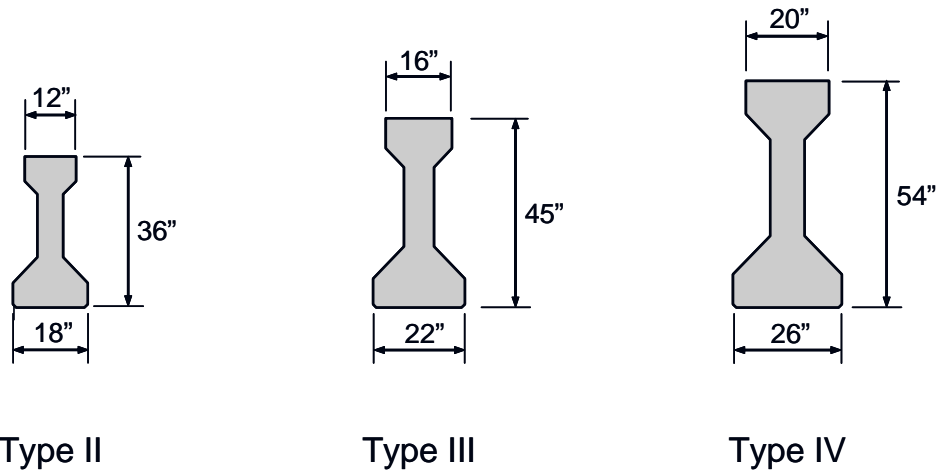
Figure 1.10 Standard AASHTO I-Girder Sections for Prestressed Bridges

At a shipping weight of 41 tons, a "Type IV" girder 100 feet long is about at the limit for convenient road transport and may require special routing or permits. Where transport by rail or water is feasible, or special road permits are possible, shipping lengths and weights can be greater and the use of a deeper, heavier, Type V or VI facilitate longer spans (Figure 1.11).

Several state departments of transportations have developed important variations on the basic AASHTO girder shapes. The designer should review state standards for the applicability of these shapes for a particular project.

Type V   Type VI
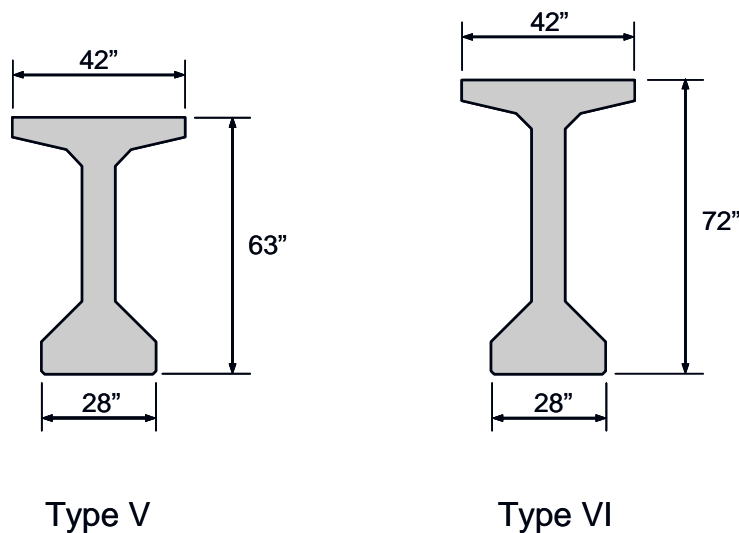
Figure 1.11 Larger AASHTO I-Girder Sections for Prestressed Bridges

1.3.1.3 Bulb-T Girders and U-Beams

In regions with a strong precast concrete industry, other types of sections have been developed to attain longer spans - for example, bulb-T girders (Figure 1.12) - or enhanced aesthetics – for example, U-beams (Figure 1.13).

Bulb-T girders facilitate simple spans up to about 135 feet, depending upon the depth of the girder section and spacing of the girders in the deck. U-beams are typically available in depths from 4 to 6 feet for simple spans up to about 125 feet. The wide top flanges of the bulb-t girders and the U-beam section provide increased lateral stability and can allow the development of very long girders. The Bow River Bridge near Calgary, Canada, for example, used 211' long, 9.2' deep precast, prestressed girders (Ref. HPC Bridge Views, Issue No. 22, FHWA-NCBC Publication, http://www.cement.org/bridges/br_newsletter.asp).

72" Bulb-T   78" Bulb-T
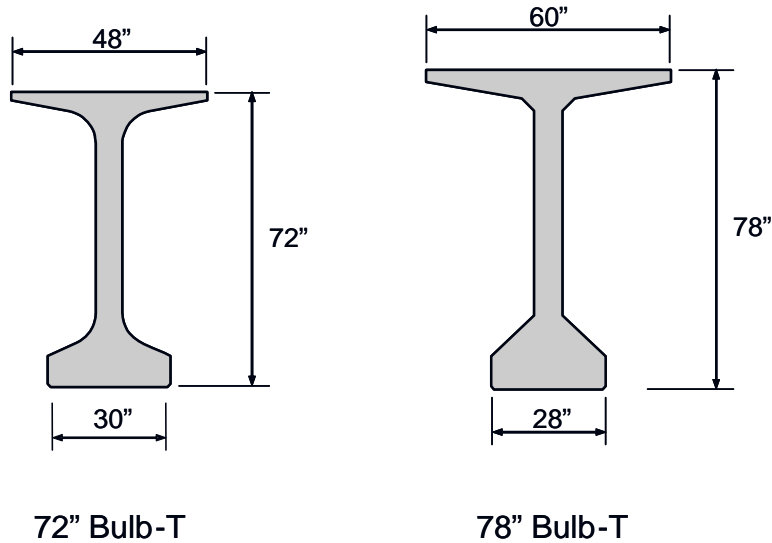
Figure 1.12 Bulb-T Girders

48 " U-Beam   U-Beam (54", 63", 72")
                                    (Florida)
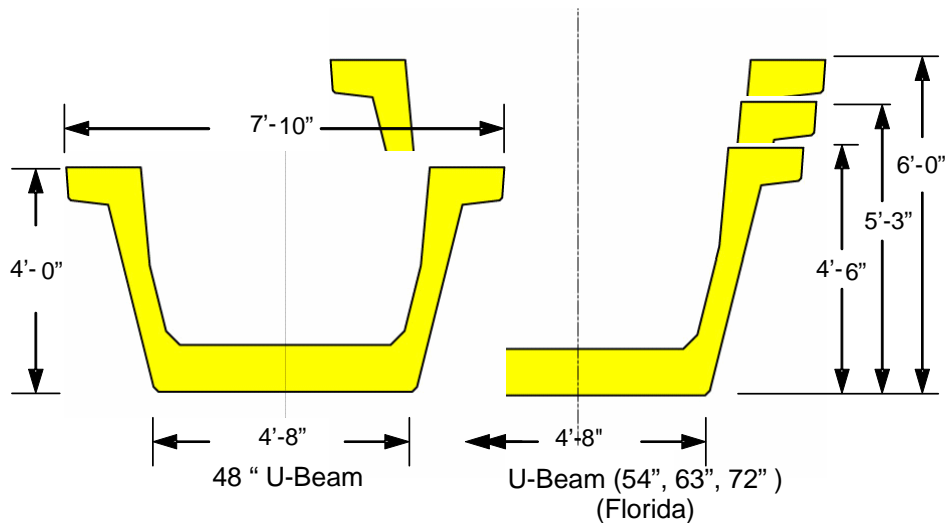
Figure 1.13 U-Beam Sections

1.3.1.4 Span Ranges

For preliminary purposes, Figure 1.6 may serve as a guide to girder selection. However, there is no prescription that requires a particular girder type be used for a particular span length.

When I-girders and bulb-T girders are made fully structurally continuous over interior piers by installing post-tensioning tendons through specially detailed cast-in-place spliced joints, it is possible to gain an extra 10 to 15% span length (Figure 1.7). This technique has been used for standard AASHTO girders, but in general, nowadays tends to be for larger scale projects. It is discussed further in below.

1.3.1.5 Planks, Inverted T's and Double-T Girders

At the other end of the scale, for small span structures, generally in the range of 20 to 35 feet, precast prestressed concrete planks, inverted T's and occasionally, double-T girders may prove useful (Figure 1.14).

Precast prestressed planks are placed side-by side and the joints between them are filled with a cast-in-place concrete. Transverse post-tensioning is usually necessary, either of strand or bar tendons installed through ducts in each plank, to make them function structurally as a deep slab. Special care is essential with design details, fabrication, erection and installation in order to align ducts transversely and properly seal them to protect the tendons from corrosion. This is discussed further in Section 1.4, below.

1'-4"

Precast Prestressed Plank
(Small spans; 20 – 30 ft)

1'-8"

Inverted T (20")
(Small spans; 25 - 35ft)   Double-Tees for Buildings, not Bridges
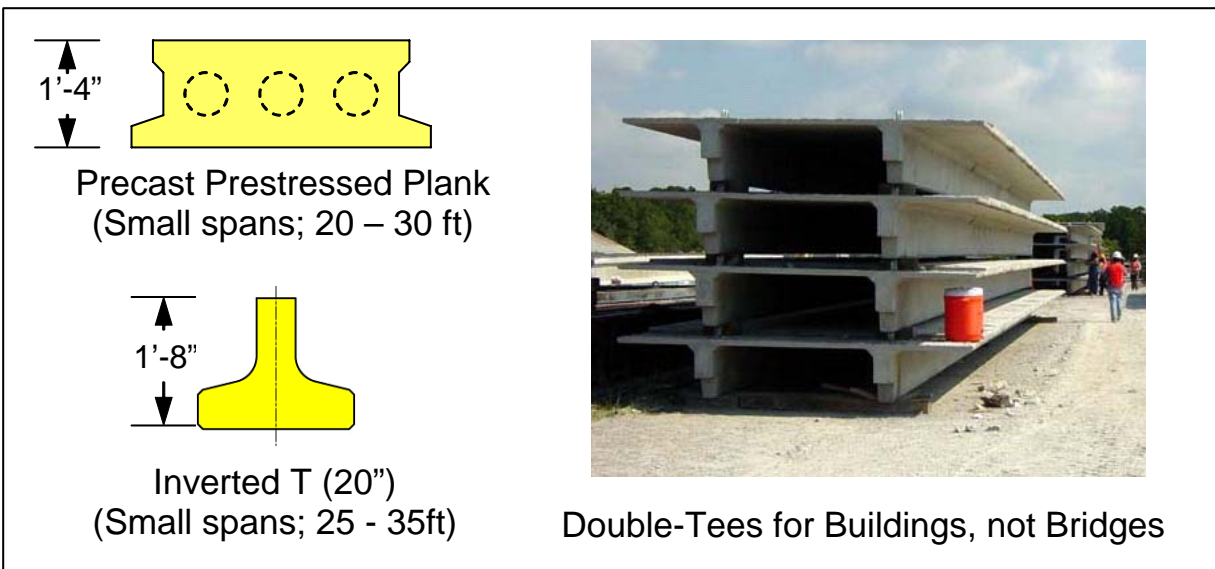
Figure 1.14 Other Miscellaneous Precast Concrete Sections

Inverted T-s beams are intended to be erected so that their bottom flanges are in contact. After placing transverse reinforcement, the spaces between them are

completely filled with cast-in-place concrete. In this manner, inverted T girders are both the primary structural member and permanent formwork.

Double-T girders are widely used by the building industry. However, for bridges, the top flange must be thickened to carry traffic loads or an additional reinforced concrete slab must be placed on site, using the thin top flange only as a form.

1.3.2 Precast Operations

Precast concrete components are normally produced in a factory using standardized fabrication processes. This offers efficiency, places fabrication off the critical path, provides economy and ensures good quality control.

Prestressed concrete girders are usually produced in a casting bed sufficiently long to make three or four girders in the same operation, using temporary intermediate bulkhead forms. Prestressing strands are laid in the bed from end to end at locations in the girder cross section according to design requirements (Figure 1.15).

Very often, portions of some strands near each end of each girder are de-bonded by shielding with plastic tubes to prevent contact with the concrete. The strands are tensioned to the required design force using a heavy duty stressing frame at each end of the bed (Figure 1.16)
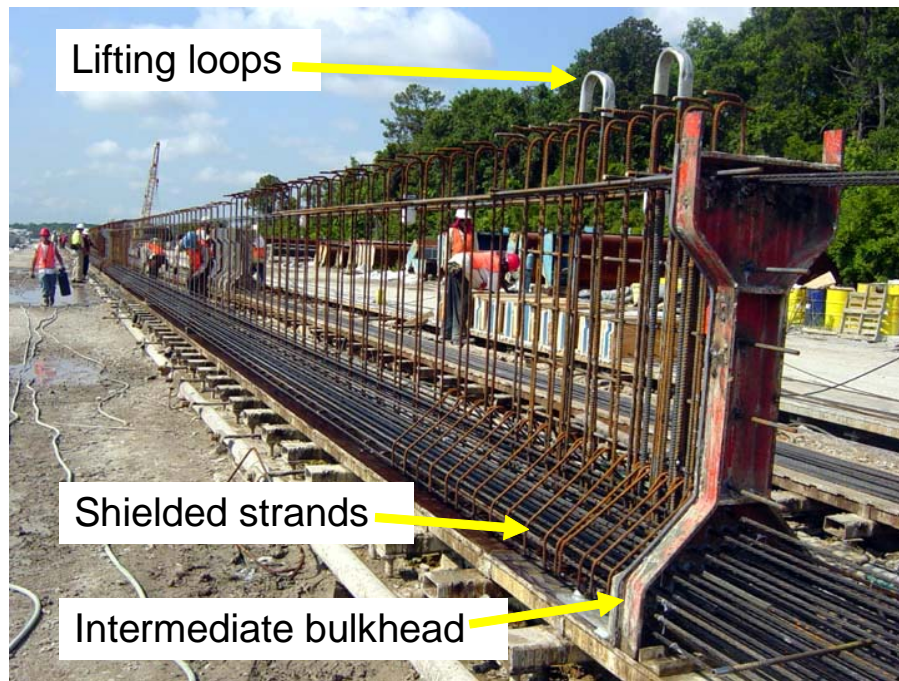
Figure 1.15 Precast I-Girder (Type IV) Fabrication

Figure 1.16 Stressing Frame and Side Forms

Mild steel web and flange reinforcement is placed at the necessary locations along each girder according to the design. Lifting devices, normally large loops of strand, are installed at each end. Web forms are installed on each side. Finally, when the bed is ready and everything has been checked, concrete is placed and consolidated (Figure 1.17).

Figure 1.17 Placing and Consolidating Concrete

1.3.3 Curing and Storage

Concrete is cured by different methods according to local conditions and procedures. These may involve steam curing, covering with wet burlap, fogging or application of curing compounds to exposed top surfaces. After a few days, when the concrete attains a required minimum strength determined by control cylinders, side forms are removed and strands are released by carefully cutting at the end of each girder, transferring their force to the girders. This is referred to as the "transfer" or "initial" condition. The corresponding concrete strength is the initial strength denoted by the symbol f'_{ci}.

Girders are then picked up and taken to a storage area in the casting yard (Figure 1.18). In storage, girders must be carefully supported on temporary blocks at the locations of the bearings or as otherwise approved by the Engineer. Because the prestressing effect is greater than self weight, most I-girders have a positive, upward, camber as seen in this figure. If girders are in storage for a long time, an initial camber can grow due to creep of the concrete under sustained stress. Camber growth can eat into the build-up allowed for in design above the top flange. In such cases, it may be necessary to adjust bearing elevations in the field prior to setting girders so that the deck slab can be built to the correct elevation.

Figure 1.18   Handling and Storage of Girders in Casting Yard

Occasionally while in storage, girders might develop a lateral bow, often referred to as "sweep". The cause can be orientation of the girder to direct radiant sunlight. Normally, such sweep is relatively small and inconsequential. However, if sweep grows or persistently exceeds a couple of inches in about 100 feet, the source should be more thoroughly examined. It might indicate a problem with the stressing operation that somehow applies more force to one side of the girder or perhaps a misalignment or lateral eccentricity of strands in the casting bed. Sweep and temporary support blocks should be checked during storage to make sure that girders are stable and not likely to topple over.

During the time in storage, girders are inspected and any defects remedied. Minor defects such as small, superficial air bubbles or "bug-holes" may need filling. More significant defects, such as cracks or spalls should be reported to the Engineer for further examination. In addition to dimensions, tolerances, material certifications, cylinder strengths and stressing forces, project specifications should contain other requirements and guidance to the acceptability of finished products and when such products are likely to be unacceptable and possibly subject to rejection. Such standards help not only the Owner, but also the Producer because they lead to early identification and rectification of potential production problems before components are shipped.

Refer to "Manual for Quality Control for Plants and Production of Structural Precast Concrete Products, Precast, MNL-116, Prestressed Concrete Institute, Chicago, IL" and "Manual for the Evaluation and Repair of Precast Concrete Bridge Products, MNL-137-06, Precast/Prestressed Concrete Institute, Chicago, IL, 2006,72pp" for further information related to curing and storing.

1.3.4 Shipping

Most precast concrete girders and components are conveniently shipped by road transport. However, longer and larger section girders may need heavy transporters and special permits (Figure 1.19). Sometimes, it may be more convenient to ship by rail or water, depending upon access to the production facility and job site, providing

that intermediate trans-shipment (i.e. off-loading, temporary storage and re-loading) costs are reasonable. Accessibility can control not only transport and girder size, but also the size of cranes capable of lifting and placing girders in the structure. Refer to "Bridge Design Manual, MNL-133-97, Precast/Prestressed Concrete Institute, Chicago, IL" for further information regarding transportation of precast, prestressed concrete members.

Transport for 95' U-Beam of 75 tons

Figure 1.19 Shipping

1.4 Construction of Adjacent Precast Girder Superstructures

Future Development

1.5 Construction of Precast Girder Superstructures with CIP Concrete Decks

The objective of this topic is to discuss the various types of precast girders and sections that are used in prestressed concrete bridges. Typical span ranges that are appropriate for the different types of girders, as well as precast operations, curing, and shipping will be discussed.

1.5.1 Site Access

The means of access to the site will determine the method of delivering precast concrete girders or components, whether by road, rail or water. It will also influence the type, size and capacity of cranes for lifting and placing girders. Accessibility for delivery and crane capacity will influence the choice of a precast concrete components or girders.

If a site is remote, say in rugged terrain where access is difficult, it would be appropriate to adopt the lightest possible section size for the necessary span. For small span structures, precast concrete planks and similar components can be sufficiently light-weight for lifting and placing by a single crane suitably located on a stable platform.

Occasionally, a crane may rest upon parts of the structure already completed and components may be delivered along a portion already built. This can be useful for building long, simple trestles across low lying wetlands or similar areas where delivery and erection cannot be made over the ground.

The use of a crane located at each pier or abutment to pick a girder at each end helps minimize crane size but requires two cranes. The larger sized, heavier girders typically require two medium to heavy-duty cranes. On land, cranes require firm temporary surfaces, support platforms or access (Figure 1.20). Also, at land sites, it may be necessary to construct special accesses or roads for delivery. All these rapidly drive up construction costs. In such cases, it may be cheaper to use shorter spans and smaller girders – even if it leads to additional piers.

Figure 1.20 Erection using Two Cranes

Large girders are often more suited to marine sites where water delivery is possible and heavier cranes can be conveniently placed on barges (Figure 1.21). Not only are costs of marine construction generally greater than on land, costs increase further and environmental controls must be considered, if temporary channels must be dredged.

Figure 1.21 Crane on Barge

As regards site access, in general, larger section girders are more suited to large-scale projects, on land or water, where access is not easy so higher delivery and

erection costs can be more readily absorbed. Smaller section girders (AASHTO Types II, III, IV and precast planks) are more suited to smaller scale projects.

1.5.2 Bearing Installation

For most concrete girder construction, bearings are usually simple neoprene pads. Occasionally, for large girders and spans, laminated neoprene bearings may be used. For short span, precast prestressed plank type structures where the deck effectively becomes a solid slab, a continuous neoprene strip may be placed under the ends of all the precast components.

For stability and to prevent walking or rolling, neoprene bearings should be set horizontal regardless of longitudinal grade. In turn, this requires the top of bearing seats or plinths should also be constructed horizontally.

When there is little or no longitudinal gradient, girders can usually be placed directly on the neoprene pad or bearing. The bearing design, i.e. plan dimensions, thickness, durometer hardness, laminations and elastic properties, should take into account the need to accommodate longitudinal gradient, initial camber and changes in rotation as the deck slab is cast.

When there is a significant longitudinal gradient, it may be accommodated by a suitable varying thickness of a durable mortar, cement-based or sand-filled epoxy grout placed atop the bearings (Figure 1.22). In some cases, it may be convenient and expedient to carefully place the girder while the mortar or grout is still wet but stiff, using the weight of the girder to automatically form the required variable thickness. In other cases, the mortar or grout may be dry-packed or injected under pressure while the girder is held on temporary blocks. In all cases, the initial camber and subsequent change in end rotation as the deck is constructed should be taken into account in the design of the bearings.
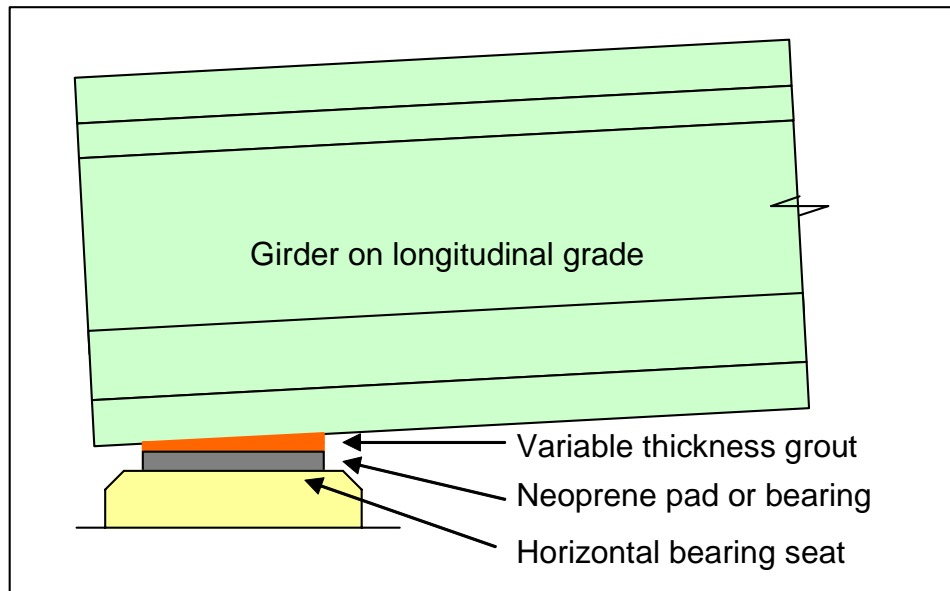
Figure 1.22 Neoprene Bearing Detail for Longitudinal Gradient

Care is required with skewed structures (Figure 1.23). Bearing pads should be oriented perpendicular to the in-plan axis of the girder and not parallel with the pier cap or abutment face, except perhaps for low skews up to about 10 degrees. For higher skews, if the pad is not perpendicular to the girder, the combination of camber, skewed-bearing and longitudinal gradient will cause uneven load distribution - concentrated more to one corner of the bearing. This may lead to undesirable consequences, such as local overstress of the bearing and temporary instability of the girder during erection. If this condition is unavoidable, then a suitable allowance should be made in the design, fabrication and installation of the bearings and measures should be taken to temporarily brace girders during erection.
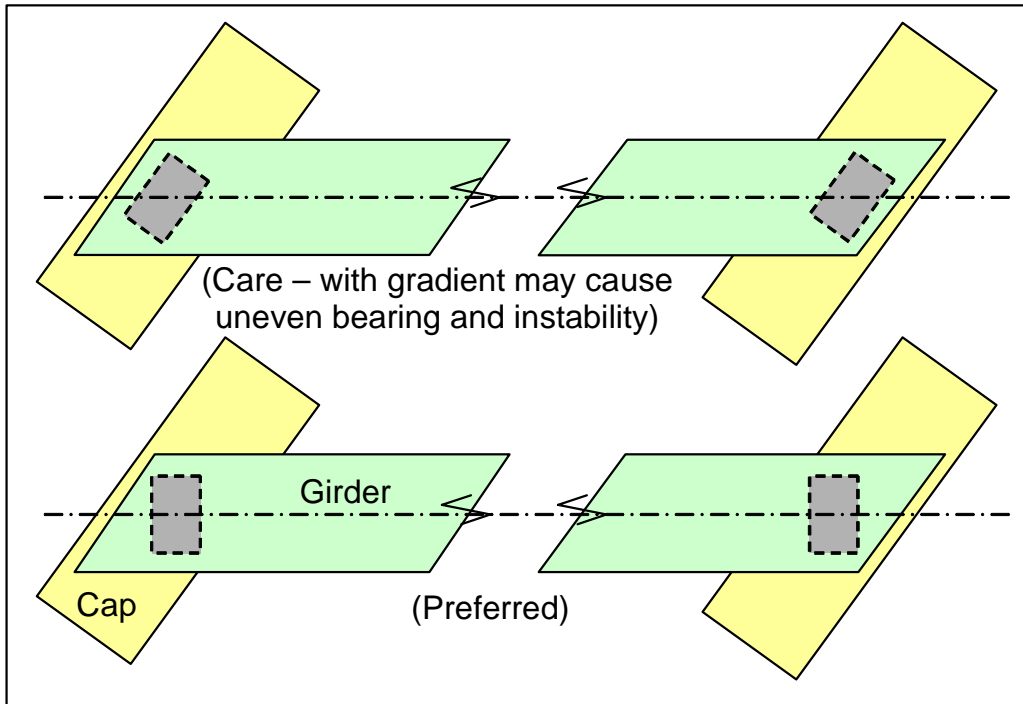
Figure 1.23 Bearing Orientation for High Skew

1.5.3 Girder Lifting and Placing (Lateral Stability)

Short span components and girders may be sufficiently light to be picked by a single crane. Long girders usually require simultaneous lifting by a crane at each end. Lifting attachments, such as loops of strand or other devices are usually cast into the component at the precasting yard. Structurally, lateral stability of most precast concrete sections is assured by the width of the compression flange. However, during lifting and placing, care must be exercised to keep a girder vertical – so as not to set it unevenly on bearings, uneven temporary supports or dunnage.

Tilt, along with excessive sweep, can lead to instability, especially with some long "top-heavy" sections. Temporary lateral bracing may be necessary when erecting some sections, particularly long girders, until permanent diaphragms have been installed. Temporary steel diaphragms have been used in some structures to provide construction stability until the deck slab has been cast (Figure 1.24). The cost of temporary intermediate steel diaphragm frames, their installation and removal should be considered in relation to the cost and benefits of alternative, permanent intermediate reinforced concrete diaphragms.

Long span beam, unstable.   Bracing by temporary steel frames.
                                   Alternative = concrete diaphragms
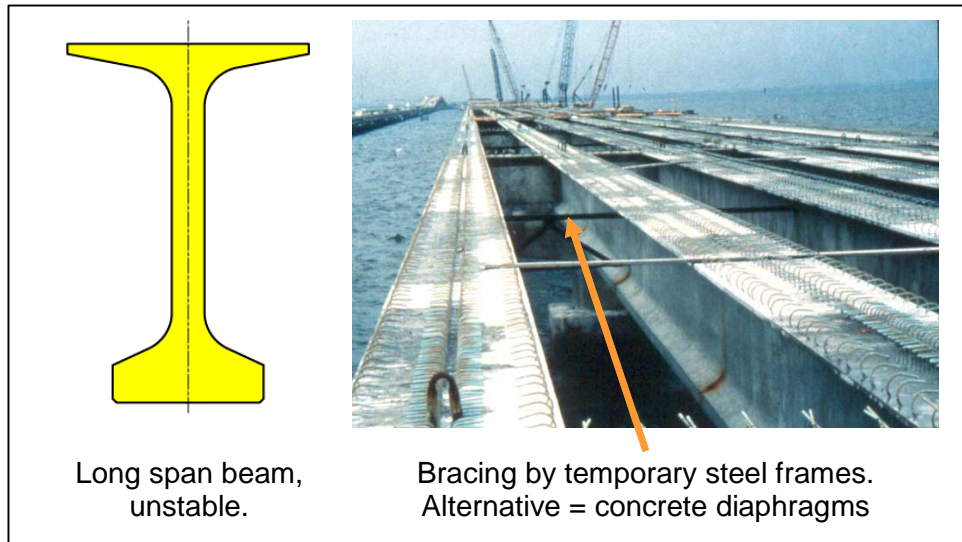
Figure 1.24 Temporary Bracing for Construction Stability

1.5.4 Deck Forming Systems

For many years, formwork for bridge deck slabs traditionally consisted of transverse timber joists supporting plywood soffit forms. Joists are suspended by hangers from the edges of the top flange of the girders. The lumber is temporary and is removed upon completion of the deck slab (Figure 1.25). Temporary lumber formwork remains an economical and preferred choice in some regions and maybe necessary in some cases for technical or environmental considerations.

Figure 1.25 Lumber Joists to Support Plywood Formwork

An increasing number of projects nowadays use permanent, "stay-in-place", metal forms. These are generally made of galvanized steel folded to a section of multiple trapezoidal shaped flutes (Figure 1.26). Typically, the minimum required slab depth is to the top of the metal flutes, so that the weight of the metal form and concrete filling the flutes must be added to the dead load of the slab. A disadvantage to this type of system is that the support angles might eventually corrode or come loose, being a risk to anything beneath the structure. Even though such instances are rare, the use of removable formwork may be preferred for certain spans.

Required min slab

Add weight of
Steel form and
Concrete flutes

Support angles
may corrode loose
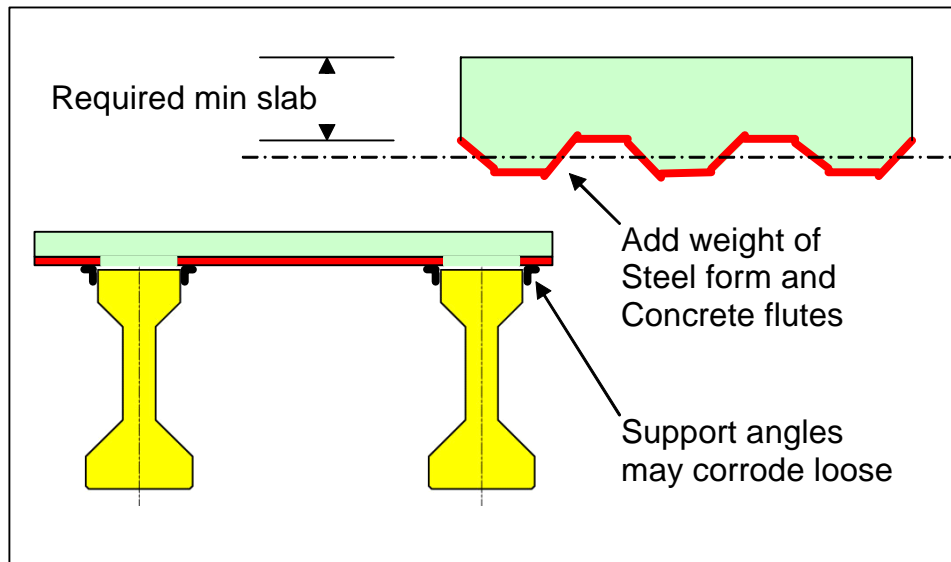
Figure 1.26 Stay-in-Place Metal Forms

Another alternative is to use permanent precast concrete panels as formwork. Usually these are designed to be about half the depth of the slab. They must be securely set upon on a stiff mortar bed or other firm material on the top edge of the girder flange. Care must be taken in the design, fabrication and construction to ensure that there is sufficient width of edge support and that the top flange does not crack or spall. Also, in order to ensure composite action between a girder and deck slab, reinforcement projects from the top of girders and a designed width of cast-in-place slab must be in direct contact with the top of the girder. So panels cannot extend more than a few inches onto the flange (Figure 1.27). Sometimes, precast concrete deck panels may comprise the full slab thickness; leaving a gap along the top of each girder for a cast-in-place joint to develop composite action.

Because concrete shrinks, different concretes of different maturity shrink by differing amounts, there is a tendency for shrinkage cracks to develop around the edges of precast deck panels. These cracks are aggravated by impact and stress from local wheel loads and so, as a deck ages, shrinkage and reflective stress cracks tend to propagate. Great care must be taken with design, detailing, fabrication, installation and casting of the deck slab and any concrete joints in order to minimize or eliminate such disadvantages.
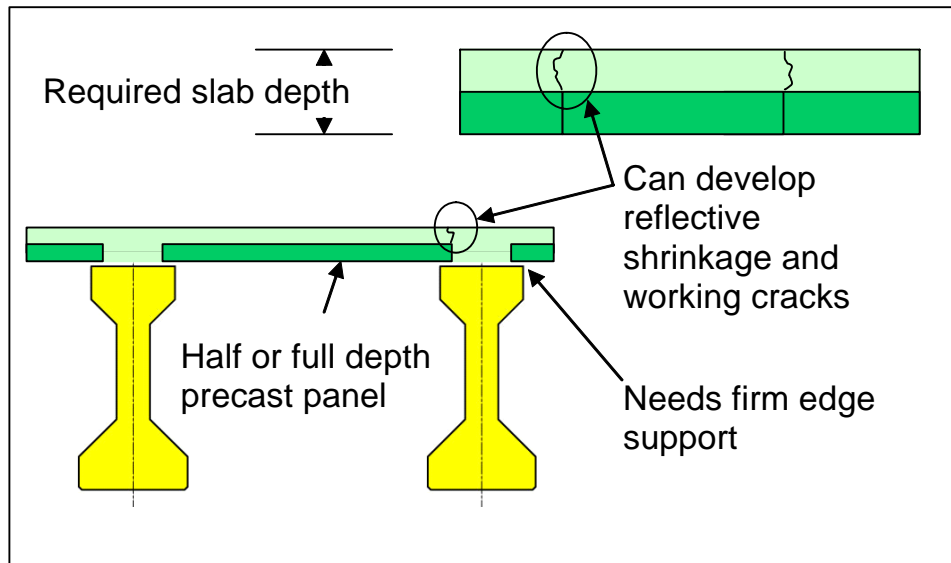
Figure 1.27 Precast Concrete Deck Slab Panels

In terms of on-site construction activity, the use of precast panels and stay-in-place metal forms is typically a little faster than lumber formwork, but time is not the only factor. Consideration should be given to the particular needs of the project, the site, environment, advantages, disadvantages, maintenance and relative costs of one system verses another. Figure 1.28 shows a lumber form system for widely spaced U-beams.

Figure 1.28 Lumber Form System for Widely Spaced U-Beams

1.5.5 Rebar Placement

Once the formwork is in place, reinforcing steel for the deck slab may be prepared. However, prior to installing rebar, it is usually practical to first install any hardware for expansion joint devices, anchor devices for lights, signs, barriers and similar

embedded items. Reinforcing is usually assembled and placed on the forms, using chairs of an approved (non-corrosive) material to provide the correct cover to the soffit. Chairs may be of different heights in order to support the top and bottom mat at the correct elevation (Figure 1.29).
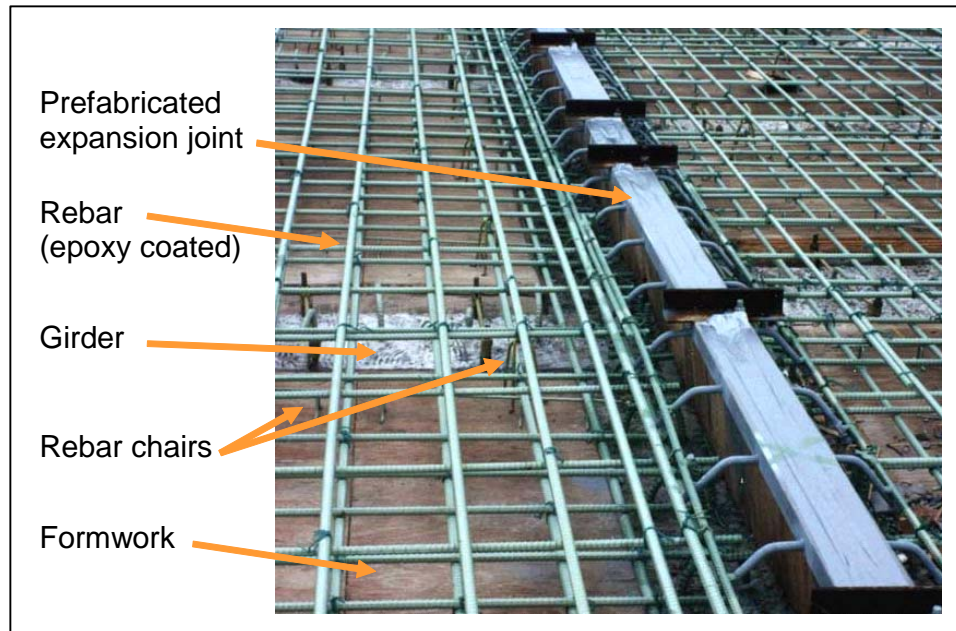
Figure 1.29 Installation of Deck Slab Reinforcing Steel

1.5.6 Deck Concreting

When the position and cleanliness of formwork, reinforcing steel and embedded items have been checked, concrete placement may commence. Concrete is placed by different techniques such as direct discharge from truck mixer where access is feasible, by chute, conveyor belt or pump (Figure 1.30).

Concrete is consolidated by vibrators and struck off to level by hand or by a mechanical screed. The mechanical screed rides on rails on each side of the deck that are adjusted to line and level to provide the correct surface geometry. After screeding, the surface is usually worked a little more by hand floats or additional passes of the screed, to attain the desired accuracy and finish. Nowadays, hand screeding and float finishing is rarely used – most decks are finished by machine.

| Pump discharge | Vibration and Screeding |
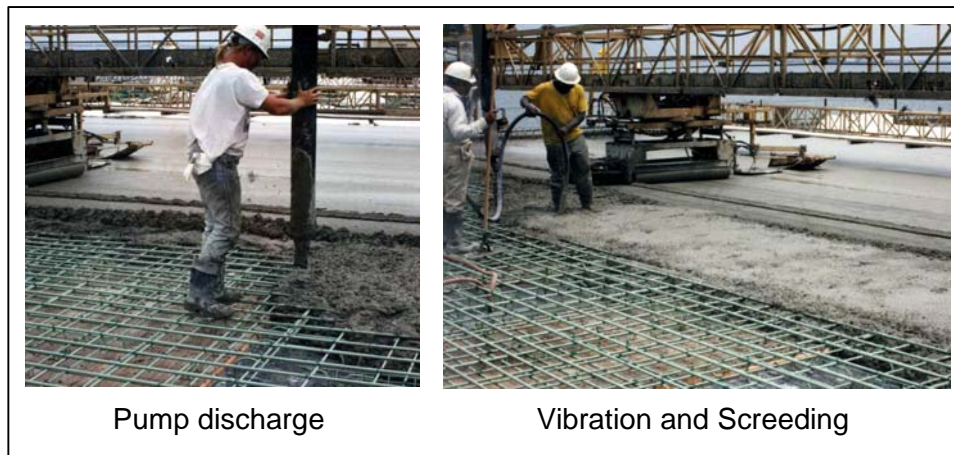
Figure 1.30 Placing, Consolidating and Screeding Concrete Slab

1.5.7 Deck Curing

In order to attain the required concrete strength, allow the heat of hydration to slowly dissipate and minimize undesirable effects of excessive shrinkage due to rapid water loss, deck slabs must be properly cured.

In most cases, a curing membrane is usually required for all exposed surfaces that have not been formed. Curing membranes are spray-applied compounds that form surface films to help minimize moisture loss.

Once the concrete has taken an initial set, curing blankets are placed to cover exposed surfaces. Curing blankets are usually a composite burlap-polyethylene sheet and may be quilted for added thermal protection. An alternative, often used in the past, is simply wet burlap. Polyethylene sheet is sometimes used. Curing blankets are normally kept wet for the curing period which may range from 3 days to over a week. In cold regions, it may be necessary to use steam or fog curing applied under covers or enclosures to help maintain air temperature at an acceptable level.

When deck slab concrete has attained a certain required minimum strength, formwork may be released and removed – this is not normally until the end of the curing period.

Project specifications should contain a requirement that decks not be used for traffic or storage of construction material for a minimum period, usually 14 days, after placing concrete. Likewise, a deck is not normally opened to traffic until the curing is complete and the concrete attains its specified 28-day strength.

If access from the deck is necessary for continued construction activity, then special procedures may be considered, such as a higher strength concrete, a mix designed for rapid hardening or special curing techniques such as steam or controlled heat and insulation, as appropriate or as necessary for the site.

1.6 Precast Girders Made Continuous by Reinforced Concrete Joints

This Section offers an account of structures built as simply-supported spans but where continuity of the deck slab alone or the full depth of structure is made using cast-in-place reinforced joints over interior piers.

The advantages and disadvantages of making a structure partially or fully continuous are:

Advantages:

- ➢ Reduce positive bending
- ➢ Reduce prestress demand
- ➢ Reduce structural depth
- ➢ Enhance overall structural redundancy
- ➢ Eliminate expansion joints for improved ride
- ➢ Eliminate expansion joint leakage
- ➢ Reduce overall maintenance needs

Disadvantages:

- ➢ Introduces negative bending over interior piers
- ➢ Requires significant longitudinal reinforcing (or Post-Tensioning)
- ➢ Requires special reinforcement details in the ends of girders to develop continuity
- ➢ Requires design study and construction control of sequence of casting the deck slab
- ➢ If casting sequence is not executed correctly, it might lead to cracking.

The primary advantages of continuity being the elimination of joints for improved traffic ride and reduced maintenance may often outweigh the disadvantages.

1.6.1 Partial Continuity of Deck Slabs Only ("Poor Boy" Joints):

In order to eliminate joints expansion, improve rideability, control deck drainage and reduce maintenance costs, continuous deck slabs were introduced. In such bridges, girders are designed, erected and the deck slab cast, as simply supported spans. However, the slab itself is made continuous over the gap between the ends of the girders (Figure 1.31 "Poor-Boy" Joint). Reinforcement is place in the slab over gap to tie together the rebar mats in the slabs over each span.

Section Thru Girder   **Side Elevation**
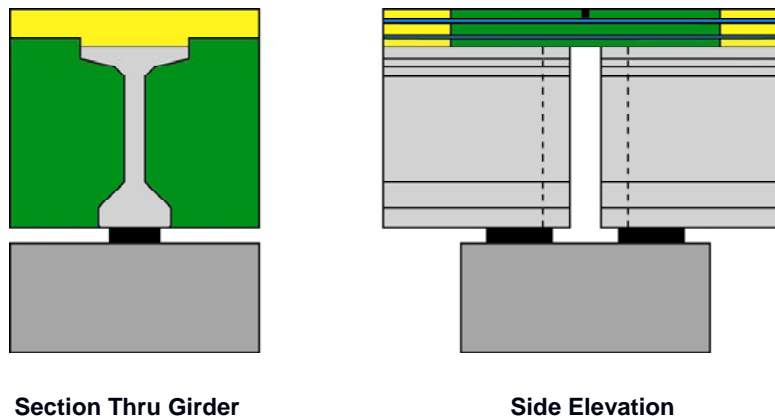
Figure 1.31 Deck Slab Continuity only

It is important that the ends of the girders themselves cannot come into direct contact (by inadvertent touching or deliberate blocking with hard material) as it will create leverage and attract negative dead load moments (from creep redistribution) and live load moments of similar magnitude to those in a fully continuous structure for which the deck and girders have not otherwise been designed. This detail is sometimes referred to as a "Poor-Boy" joint.

1.6.2 Full Continuity using Reinforced Concrete Joints:

An alternative to the above deck-slab-only joint is to make the joint between the ends of the girders structurally continuous for all loads applied after construction of the deck. This is achieved by extending longitudinal reinforcement from the ends of the girders into a full-depth cast-in-place reinforced joint, as shown in Figure 1.32. Full depth joints may be built as diaphragms.

Section Thru Girder   **Side Elevation**
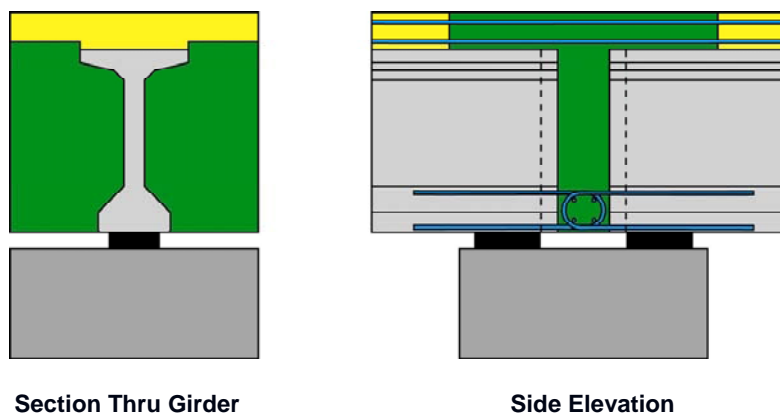
Figure 1.32 Full Depth Reinforced Concrete Joint

1.7 Construction of Precast Girder Superstructures made Continuous with Post-Tensioning

The objective of this topic is to present the basic concepts for the construction of superstructures of precast concrete girders, made continuous by means of spliced joints and longitudinal post-tensioning. Typical girder sections span lengths and post-tensioning layouts are described. Construction techniques using temporary supports, deck slab casting sequences and staged post-tensioning are discussed.

1.7.1 Introduction

The foregoing sections (1.4 and 1.5) addressed the construction of simply-supported precast concrete girder superstructures with cast-in-place deck slabs. This section deals with making such types of superstructures structurally continuous by the use of post-tensioning. The technique is often referred to as "spliced-girder construction" as it involves making small cast-in-place joints or "splices" to connect the ends of girders or portions of girders. Establishing structural continuity in this manner enables the length of otherwise simply-supported spans to be extended approximately 10 to 15% for the same girder size. In addition, if the section of girder over an interior pier is made deeper using a variable depth haunch, span length can be extended further. Consequently, this type of construction facilitates spans ranging from 140 to a practical limit of about 350 feet.

Post-tensioning tendons extend from one end of a continuous superstructure to the other. However, because of loss of post-tensioning force due to friction between the tendon and internal ducts during stressing and other effects, the longer the structure, the less effective the prestress – particularly in the mid-region of a continuous-span unit where it is usually needed most. For this reason, the design layout should seek an effective balance between overall superstructure length and structural prestress requirements.

Precast girders are pretensioned sufficiently to carry their own self weight and some portion, but not all, of the subsequent structural dead load of the cast-in-place composite deck slab. Additional structural capacity and overall continuity for both flexure and shear is achieved by installing longitudinal post-tensioning tendons through the girders and splice joints from one end of the continuous superstructure to the other. This usually requires four internal tendons per girder web.

Girder splice joints themselves may be located over piers or at intermediate points within spans in such a manner that the length and weight of precast concrete girders or portions thereof are convenient for delivery and erection. Cast-in-place splice joints over piers are an integral part of a transverse diaphragm.

Figure 1.33 4-Span Continuous Precast Spliced Girder Construction

At intermediate locations within a span, a transverse diaphragm may or may not be necessary. Mild steel reinforcing usually extends from the ends of the precast girders into the splice and is supplemented by additional rebar as necessary.

Figure 1.34 Construction of Haunched Spliced Girders

When precast girders are designed to span from pier to pier with splice joints at diaphragms over those piers, the erection of each individual girder is straightforward as for a simply-supported structure (Section 1.5 above). However, when splice joints are located within spans, temporary supports are necessary. Often this requires one or more temporary falsework towers, depending upon the locations of splice joints. Alternatively, in some cases, special devices may be used to suspend partial length girders from an already erected (cantilever) portion of the structure.

Ducts for post-tensioning are usually set to a draped profile, being in the bottom flange of the girders at mid-span and in the top over interior piers. At cast-in-place joints, the ends of ducts are spliced together. It is preferable that this be done using special couplers or connectors that provide a continuously sealed duct for enhanced durability. After casting the splice joints, longitudinal post-tensioning tendons are installed in each duct from one end of the continuous-span superstructure to the other. Usually the tendons must be tensioned in phases. For example, if there are four tendons per web, two of them may be tensioned before, and two after the deck slab has been cast and cured.

Since the final superstructure is structurally continuous over several spans, casting of the deck slab must proceed in a sequence of that applies most of the load to positive (mid-span) moment regions first - finishing with portions of slab at negative moment regions over the piers. This sequence, along with proper curing, is essential in order to eliminate or minimize potential transverse cracking of the deck slab.

Staged construction involving the sequential erection of precast girders, the use and removal of temporary supports, tendon installation and tensioning tendons in phases and the special casting sequence of the deck slab is essential in order to maintain stresses within acceptable limits and provide the required structural capacity. This "staged-construction" process is a very significant feature of this particular type of bridge. It must be properly taken into account during design and it must be faithfully executed during construction.

Attention to workable details is essential. The diameter of the tendon ducts must be limited to that which can be accommodated within the width of the web while leaving sufficient space for reinforcement, maximum aggregate size, fabrication tolerances and proper consolidation of concrete so as not to create local honeycomb voids or defects. This limitation on duct diameter automatically limits the size and number of strands that may be used to make up a tendon. In turn, this limits the maximum available tendon force, service stresses and strength capacity. Widening the web may relieve such limitations but only at the expense of additional weight. The use of vertically elongated (oval) ducts is not recommended because strands when tensioned bear against the duct walls and exterior web cover. This has caused local longitudinal cracks and web spalls. Similar problems have also been encountered even with circular ducts when crimped by rebar or badly aligned.

Splice-joints themselves need to be sufficiently long to facilitate alignment of tendon ducts from one precast girder to the next. A portion of duct may need to extend from the end of each girder in order to facilitate installation of a duct coupler to complete the splice.

At girder ends, webs typically flare to a width sufficient for anchor blocks to accommodate tendon anchorages and all necessary anchor-zone reinforcement. For all the above aspects, proper attention to design and detailing is essential for an efficient, practical and constructible solution.

The key aspects of spliced-girder construction are best illustrated with by the two following examples. In most other respects, such as formwork, placing and tying

reinforcement, pouring, curing and finishing concrete, the construction of precast girder superstructures made continuous with post-tensioning employs techniques common to simply-supported girder construction.

1.7.2 Installation of Bearings, Lifting and Placing Girders (lateral stability)

In general, spliced-girder construction utilizes relatively long, slender I-girders. Although some cross-sections have wide top flanges that help assist lateral stability, the installation of bearings and the lifting and placing of slender girders should always be done with care and attention to details and procedures (refer to Section 1.5 above). Temporary transverse bracing may be necessary to prevent toppling.

1.7.3 Typical Layout and Construction of 4-Span Continuous Unit

Structures of this type are typically made from precast girders with individual lengths of 100 to 150 feet or so depending upon the particular girder section. A completed four-span unit may be 400 to 600 feet long or thereabouts.

A four-span continuous superstructure is made by first erecting girders spanning from pier to pier as with a simply-supported structure. Temporary lateral cross bracing or the construction of permanent transverse diaphragms between parallel girders is installed to prevent lateral instability or toppling – especially if the girders are slender or top heavy.

Longitudinally, girders are pretensioned for their own self weight and to help carry some but by no means all of the weight of the cast-in-place slab. Longitudinal post-tensioning is necessary to provide the capacity for additional dead and live load. Tendons are installed to a profile that drapes from anchorages in the very ends of the continuous four-span unit, into the bottom flange in the positive moment (in-span) regions and up to the top over the interior piers (Figure 1.35).

When the spliced joints have been cast and cured, the first stage of post-tensioning – usually one half of the number of tendons – is stressed to impose a force solely upon the precast-girder section alone. This provides the section with the capacity to carry the load of the deck slab.

A feature of this particular erection technique is that each interior pier has a double row of bridge bearings – one under the end of each original precast girder. This creates a moment connection between the continuous superstructure and pier. The stiffness of the connection depends upon the vertical stiffness of the bearings and their lever arm (i.e. separation). This moment connection and stiffness of the substructure should be appropriately taken into account for structural analysis of loads applied after continuity has first been made and the first stage post-tensioning installed.

0.75 L   0.5 L   0.5 L   0.5 L   0.5 L   0.5 L   0.75 L

Approximate

DECK SLAB POURING SEQUENCE
(Typical example, may be changed to suit design or construction)

Cast-In-Place Splice
Joints at Diaphragm

Continuous P.T. Tendon
to Draped Profile

SECTION AT MIDSPAN   **SECTION AT PIER**   **END ANCHORS**
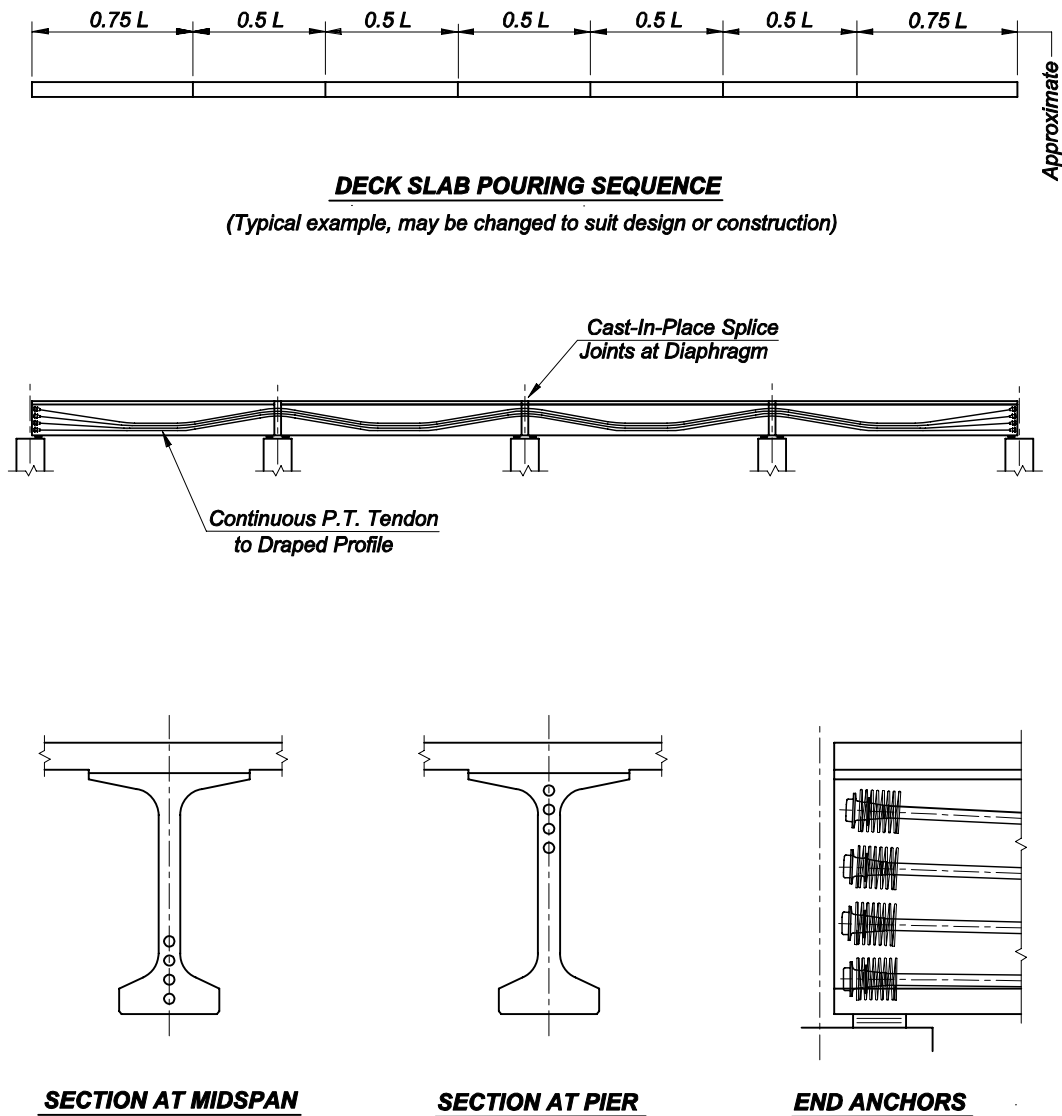
Figure 1.35 Post-Tensioning for 4-Span Spliced Girder

The next construction step is to form and install reinforcement for the deck slab. The slab is then cast in a pre-determined sequence – beginning with portions in positive moment regions and ending with those in negative moment regions over interior piers. The sequence in the figure is an example – a different sequence may be feasible and should be adapted according to the particular project.

When the deck slab has cured and gained sufficient strength, the remaining tendons are stressed. This second stage of post-tensioning applies prestress force to the composite section of the girder and the effective portion of the deck slab. The structure is now fully continuous for subsequent superimposed dead and live load. Finally, the superstructure is completed with the installation of traffic barriers, wearing surface and utilities as necessary.

1.7.4 Typical Layout and Construction of 3-Span Haunched Girder Unit

A girder deepened over the piers facilitates a longer main and side-spans in a typical three-span continuous unit (Figure 1.36).
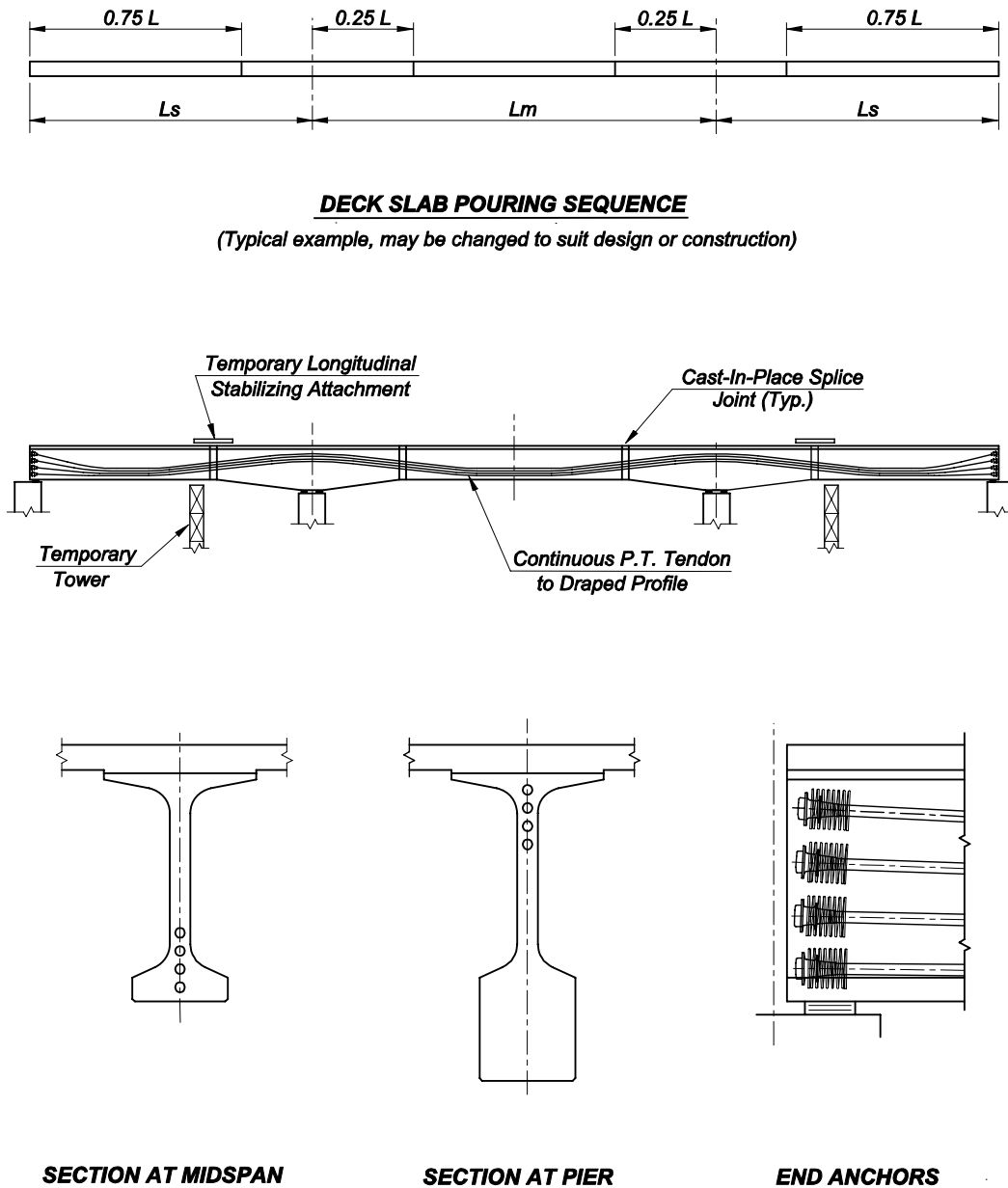
Figure 1.36 Post-Tensioning for 3-Span Haunched Girder Unit

This type is often used for the main-span unit of a bridge over a navigation channel or similar situation. It is limited by the length and weight of splice girder portions to be precast, delivered and erected. It is relatively efficient for main spans of 200 to 250 feet, but longer spans (up to 350 feet) require increasingly heavy and far less efficient components. As side spans usually range from about 60 to 75% of the main span, the total length of a three-span unit might range from about 500 to 750 feet.

(A) Erect Pre-tensioned Precast Girder

Temporary
Tower

(B) Stabilize and construct Splices in Side Spans

Temporary Stabilizing
Device and Forms

Cast-In-Place Splice
Joint (Typ.)

(C) Erect Main Span Girders, complete Splices and Install Post-Tensioning

Temporary Suspension
Device
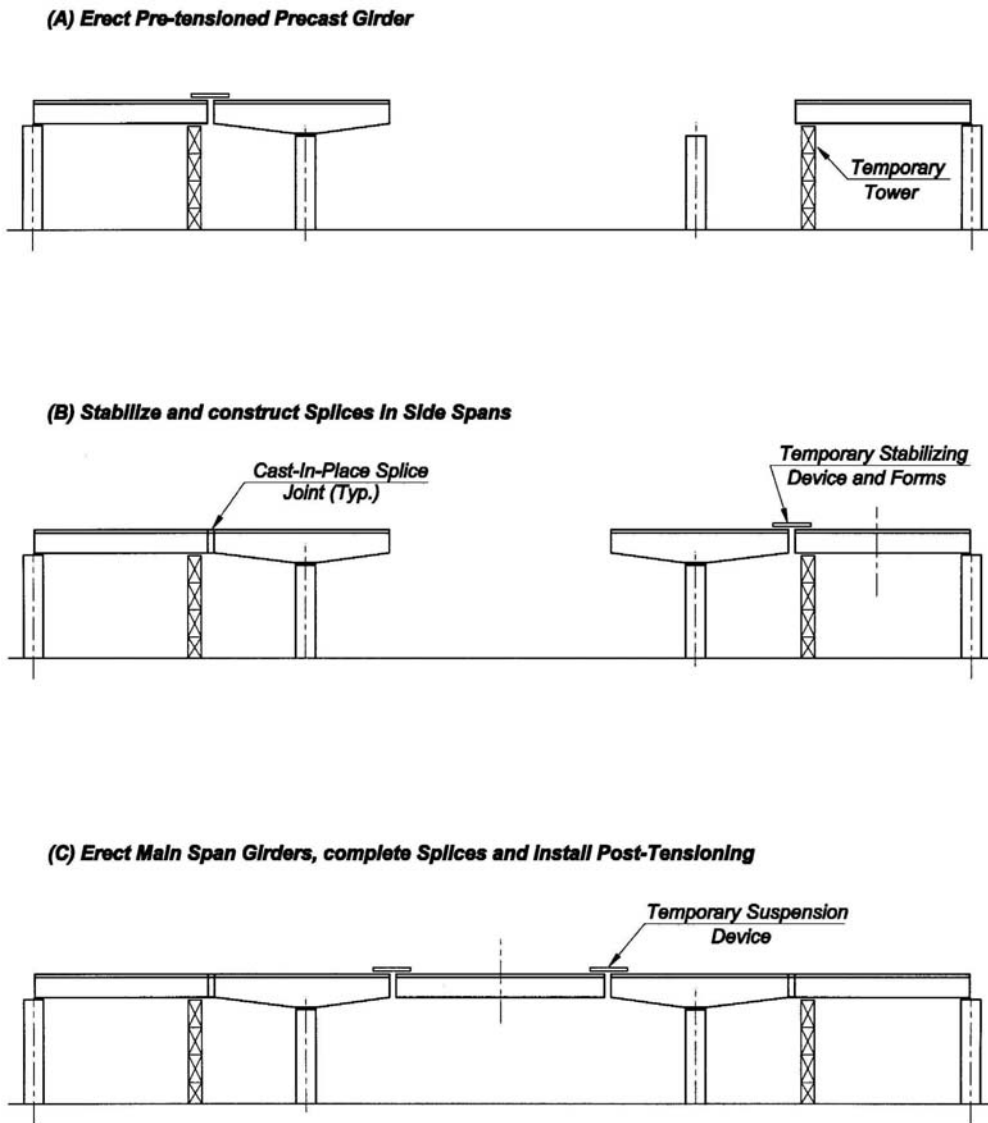
Figure 1.37 Erection of Precast Girders for 3-Span Unit

Longitudinal post-tensioning is essential because the precast girder portions themselves have insufficient pretensioning to carry little more than their own self weight. They cannot carry the weight of the deck slab or any live load without post-tensioning. Post-tensioning tendons follow a draped profile - being in the bottom flange of the girders in the positive moment (in-span) regions and in the top over the piers.

Longitudinally, erection proceeds in stages until all cast-in-place splices have been made connecting each precast girder continuously from one end of the three-span unit to the other. Post-tensioning is also installed in stages, before and after casting the deck slab. Typical construction stages are broadly illustrated in Figure 1.37.

Temporary supports and bracing are essential. Erection of the partial-length precast girders requires temporary towers or piers and devices to longitudinally stabilize the haunched cantilever portions over the main piers. Additional temporary lateral cross bracing or the construction of permanent transverse diaphragms between parallel girders is necessary to prevent lateral instability or toppling – especially for long slender girders.

Variations in the location of temporary towers, sequence of erecting girders, installing post-tensioning tendons and pouring the deck slab are possible. This type of construction requires an appropriate sequence be assumed for design. The assumed sequence should be shown on the plans.

After the precast girders have been erected and spliced to be continuous, the first stage (usually half) of the longitudinal post-tensioning is installed and stressed, acting on the precast section alone with no deck slab. This first-stage provides the precast section the capacity to carry the additional dead load of the deck slab itself.

Then, formwork and reinforcement for the deck slab is installed. The slab is cast in a specific sequence - beginning with the portions in positive moment regions and ending with those over the piers - as illustrated. Establishing and maintaining such a sequence is vital as variations significantly affect the capacity and performance of the final structure.

After the deck slab has cured and gained sufficient strength, the remaining tendons are stressed. This second stage post-tensioning applies prestress to the composite section of the girder and effective portions of the deck slab and makes the superstructure fully continuous for subsequent superimposed dead and live load. Traffic barriers, wearing surface and utilities are installed as necessary.

The following construction sequence is typical for the above example:

1. Construct pier and erect temporary tower in side-span
2. Place side span girder on pier and temporary tower (A)
3. Laterally install cross-braces or permanent diaphragms to stabilize girders
4. Erect haunched girder on main pier
5. Longitudinally stabilize haunched girder to side span girder (B)
6. Laterally install cross-braces or diaphragms to stabilize haunched girders
7. Make PT duct connections, install rebar, form and cast splice
8. Repeat above sequence for other side-span of unit
9. Erect main "drop-in" span girder with attachments to haunched girders (C)
10. Make PT duct connections, install rebar, form and cast splice
11. Install and tension first stage longitudinal PT tendons

12.   Complete any remaining permanent diaphragms
13.   Form deck slab, place reinforcement
14.   Cast deck slab in sequence, finish and cure as necessary
15.   Install and tension second (final) stage longitudinal PT tendons
16.   Grout tendons, seal and protect anchorages.

The above sequence is only an example. A different sequence may be necessary for a particular structure or to accommodate a Contractor's elected means and methods of construction.

Administratively, for any type of continuous structure built in stages, changes from an assumed construction sequence shown on the plans to one that accommodates a Contractor's elected means and methods, should be reviewed by the Engineer via a "Shop Drawing" process. Alternatively, if a change is sufficiently significant, a "Value Engineering Change Proposal" process may be more appropriate. For contract administration purposes, guidance should be offered on plans or in project specifications as to the structural nature of a change that would make it sufficiently significant to warrant the latter as opposed to the former. Final construction should be in accordance with agreed and approved procedures.

1.7.5 Tendon Grouting and Anchor Protection

After post-tensioning tendons have been installed and stressed, they must be properly grouted and anchorages sealed and protected to ensure long term durability.

With staged construction, it may also be necessary to take temporary measures to protect tendons if a long period is anticipated between the first and second stage of post-tensioning. Measures might require, for example, opening duct drains, sealing grout vents and installing temporary caps on anchorage devices. The use of corrosion prevention chemicals should be in accordance with established practice and specifications. Such measures are an alternative to grouting the first stage immediately after stressing as there can be a potential risk of cross-grouting between internal ducts. Grout blockage might prevent further tendon installation or might trap tendons yet to be stressed.

Along with concrete cover or enclosing structure and the duct material itself, completely filling a duct with grout is key to ensure protection of a post-tensioning tendon. Grout should be of an acceptable quality, mixed and injected carefully, under controlled conditions to fill the duct. Grout material should have "no-bleed" properties to reduce or eliminate air and moisture voids. Injection should continue until all slugs of air and moisture have been expelled and the grout at the outlet is of a consistency of that at the inlet. Injection should proceed from low points and intermediate vents may be needed along the profile of a tendon. Outlets should be inspected for complete filling. During construction, grouting should be done within a reasonable and short time frame as possible that minimizes risk to corrosive exposure of tendons after tensioning. At all times, appropriate quality control and records should be kept.

Anchorages should also be completely filled with grout during the grouting process. In addition, components and details should enhance sealing and protection of the tendon. Anchor devices may need permanent concrete cover blocks (pour-backs) and additional sealing with suitable materials such as epoxy or elastomeric coatings.

All grouting and protection requirements should be addressed via appropriate details and notes on plans and in project specifications. For comprehensive information on the installation, stressing, grouting and protection of post-tensioning tendons and anchorages, including recommendations for the location of grout injection ports, vents, laboratory and field tests, quality control and records, etc., refer to "Post-Tensioning Tendon Installation and Grouting Manual" available from the Federal Highway Administration. Additional information is available from the Post-Tensioning Institute.

1.7.6 Deck Forming Systems

Deck forming systems for superstructures of girders made continuous with post-tensioning, are the same as for any other type of girder construction – refer to Section 1.5, above.

1.7.7 Rebar Placement

Rebar placement for superstructures of girders made continuous with post-tensioning, are the same as for any other type of girder construction - refer to Section 1.5, above.

1.7.8 Deck Concreting and Curing

With the very important exception of the need to follow a predetermined sequence of placing deck concrete, superstructures of girders made continuous with post-tensioning are the same as for any other type of girder construction - refer to Section 1.5, above.

1.8 Construction of Cast-in-Place Post-Tensioned Superstructures

The objective of this topic is to present the basic concepts for the construction of post-tensioned concrete superstructures cast-in-place on falsework. Typical cross-sections, span lengths, post-tensioning layouts are described. Basic construction techniques such as falsework, casting, curing and post-tensioning are discussed.

1.8.1 Introduction

This section is concerned primarily with post-tensioned superstructures built cast-in-place (CIP) on falsework.

The history of the bridges built using cast-in-place concrete harks back to the introduction of reinforced concrete construction in general. The techniques remain the same. It requires the construction of formwork to contain and provide shape to the wet concrete and it requires the support of the formwork by falsework, centering or other temporary construction normally resting on the ground or prepared foundations, until the structure itself is self-supporting. For beam-type spans, reinforced concrete alone can only suffice for relatively short distances. Longer spans are possible using arched construction. The advent of post-tensioning in the 1950's facilitated lighter sections and longer span girders than reinforcement alone and brought new erection methods such as segmental construction (below). Despite such advances, tried and proven cast-in-place concrete construction techniques using formwork and falsework remain applicable for many situations and regions.

For straight structures, cast-in-place construction on falsework is a practical alternative to precast girder construction for spans up to about 250 feet. Beyond this, other techniques such as cantilever construction using form-travelers or precast segmental cantilever construction tend to become increasingly more appropriate and economical (below). For curved structures such as viaducts and ramps and for those where the width of the entire superstructure cross section changes significantly, cast-in place construction is often a solution. Cast-in-place superstructures may be simply-supported, but are usually continuous over a number of interior piers to take advantage of the benefits of redundancy and structural efficiency afforded by continuity.

1.8.2 Typical Superstructure Cross-Section

With the exception of short-span structures such as cast-in-place and voided slabs, superstructure cross sections are usually a single or multiple cell box, with a top slab, bottom slab and a number of webs. Transversely, the section may be reinforced with mild steel alone or post-tensioned with internal tendons. The choice, size and use of a particular cross section depend very much upon the longitudinal post-tensioning layout and vice-versa. Typical cross sections are illustrated in Figure 1.38 and Figure 1.39.
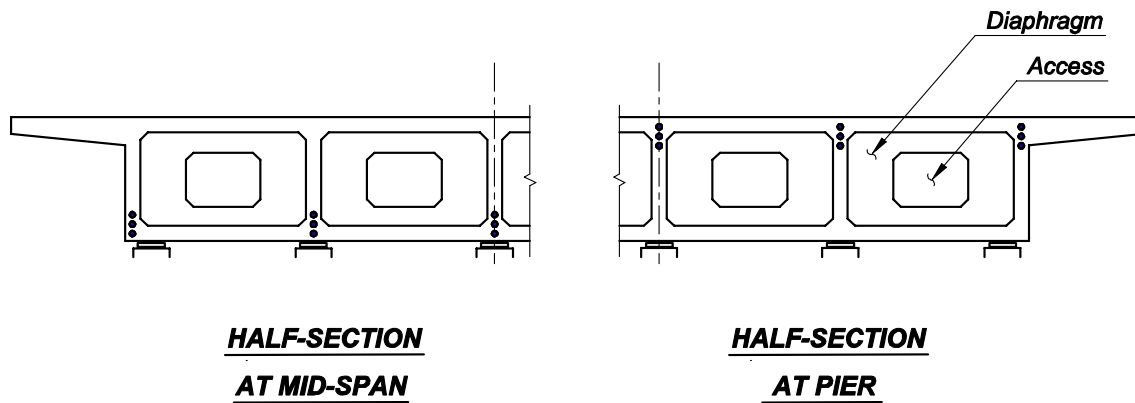
Figure 1.38 Typical Multi-Web, Multi-Cell, Cast-in-Place Box Section

A multi-web (multi-cell) box is shown in Figure 1.38. Such a section could be used for a structure of any width, simply by increasing the number of webs. It is easy to adapt such a superstructure to a variable width by varying the distance between webs. A longer span may be attained by increasing the depth over the piers.
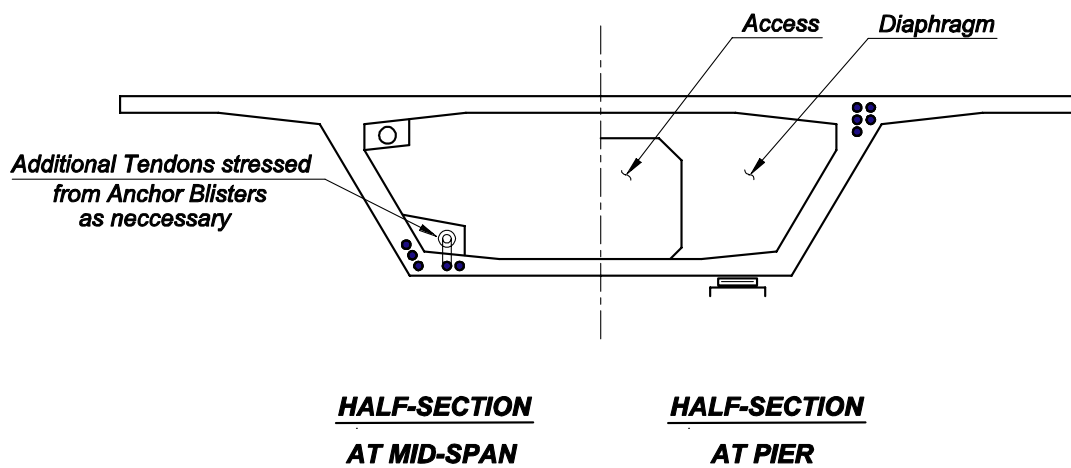
Figure 1.39 Two-Web, Single-Cell, Cast-in-Place Box Section

A two-web (single cell) box is shown in Figure 1.39. This type of section, usually of a constant depth, is suitable for continuous curved viaduct or ramp superstructures.

Typically, for continuous spans of constant depth, the depth of the superstructure is usually about L/18 to L/24 where L is the longest span. For a structure of variable depth, the depth at the pier is typically about L/20 of longest span and at mid-span perhaps as shallow as L/40.

The minimum thickness of top and bottom slabs is usually set by requirements to meet minimum concrete cover, allow for the size of reinforcing bars and to accommodate transverse and longitudinal post-tensioning ducts. For transverse post-tensioning, the edge thickness needs to be at least 9" in order to accommodate anchorages and hardware. Between webs, top slab thickness typically ranges from 7" to 9" with additional thickness at haunches and fillets. The bottom slab thickness

is similar. Occasionally, a bottom slab may be thickened to the inside or outside at interior supports of continuous spans for additional overall capacity.

1.8.3 Longitudinal Post-Tensioning Layout

Longitudinally, a cast-in-place section is prestressed using an arrangement of post-tensioning tendons usually internal to the webs. However, tendons may also be external and combinations of internal and external tendons have been used.

For simply supported superstructures, tendons within webs are usually draped - being in the bottom within the span and rising to an arrangement of anchors dispersed over the depth of the web at each end. Anchorages are contained in anchor blocks comprising a thickened portion of the web reinforced to restrain local bursting effects from the concentrated force. External tendons are similarly draped, passing through deviators within the span, riding just above the bottom slab within the box and rising to anchorages in diaphragms at the end expansion joints. In some cases, external tendons may pass into the bottom slab, becoming internal over the central (positive moment) portion of a span. This increases the effective lever arm and efficiency of the post-tensioning at mid-span compared to having external tendons higher up, above the top of the bottom slab.

For continuous superstructures, long tendons, may be anchored at the very ends of the superstructure and drape through interior spans; being low in the section in the positive (in-span) regions and high in sections over interior piers (Figure 1.40). Such long tendons are usually internal to webs, but the alternative use of external tendons and combinations of external and internal tendons is feasible. Depending upon the overall structural configuration and sequence of constructing spans, tendons may be arranged to begin or terminate at intermediate locations within spans or at other points along the structure, anchoring at diaphragms or anchor blisters as necessary.
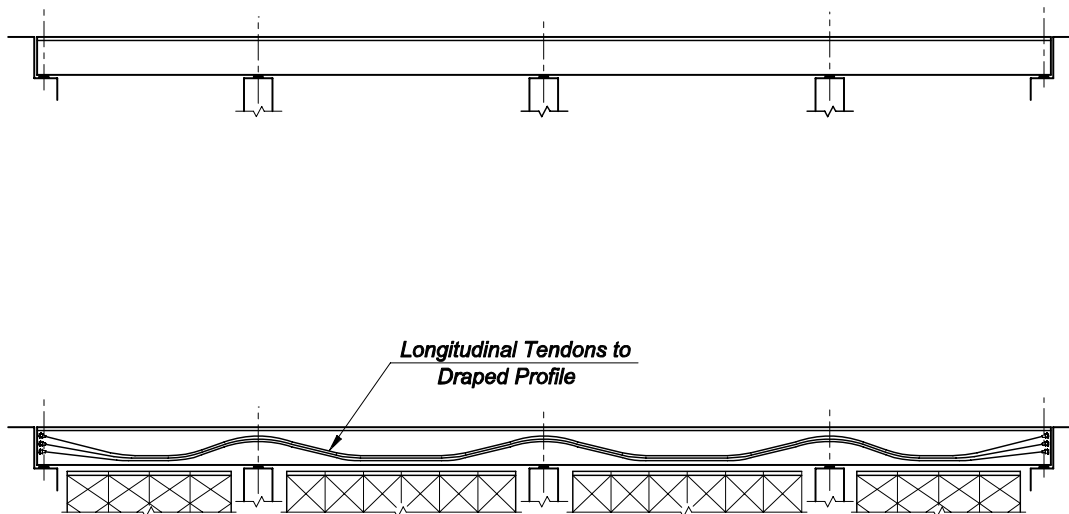
- **Provide Falsework throughout**
- **Construct Cast-In-Place Spans**
- **Install and stress Longitudinal Tendons**
- **Release Falsework**

Figure 1.40 Tendon Layout for 4-Span Bridge, CIP on Falsework

In a continuous superstructure, the use of a draped longitudinal profile will minimize, or in some cases eliminate, secondary forces and moments arising from the structural effects of redundant reactions at interior supports. Secondary moments directly reduce the primary prestressing moment (given by the prestress force at its eccentricity from the neutral axis) to a less effective moment. There are no secondary moments in a simply-supported structure.

The amount of longitudinal post-tensioning required at any cross-section depends upon the distribution of forces and internal stresses as a consequence of permanent and live loads. Usually, all spans of a continuous superstructure are cast-in-place before longitudinal post-tensioning is installed and stressed; making it self-supporting before falsework is removed. However, for the same continuous structure, if falsework is moved from one span to another (Figure 1.41) as soon as each individual span has been stressed before others have been built, the permanently induced forces and stresses are significantly different. For a continuous structure, a change from a structure designed to be cast entirely on falsework from end to end before post-tensioning to one built and tensioned sequentially one span after another, significantly changes the design, induces different secondary moments, and requires an appropriate change to the post-tensioning layout
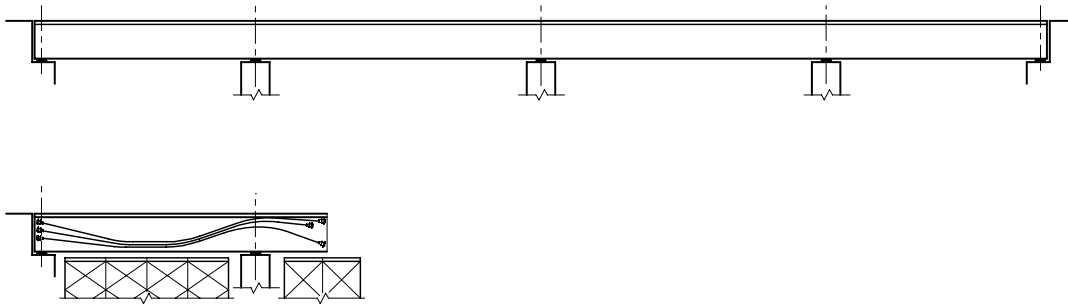
Stage 1 - Construct First Span, install and stress Tendons, release Falsework.
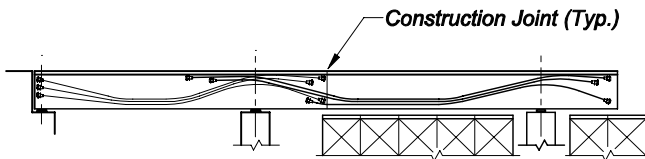
Construction Joint (Typ.)

Stage 2 - Construct Second Span, install and stress Second Span Tendons, release Falsework.
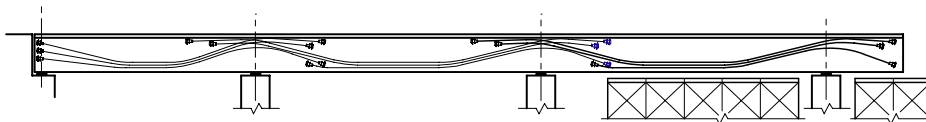
Stage 3 - Construct Third Span, install and stress Third Span Tendons, release Falsework.
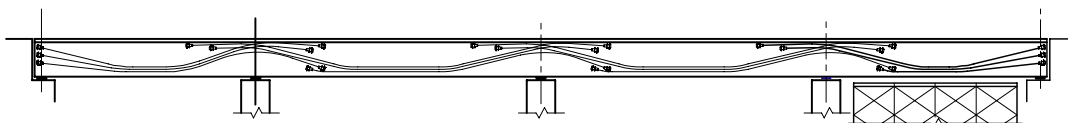
Stage 4 - Construct Fourth Span, install and stress Fourth Span Tendons, release Falsework.

Figure 1.41 Possible Tendon Layout for Sequentially Cast Spans

During construction, post-tensioning tendons suffer loss of stress due to friction in the ducts and elastic shortening. Friction can significantly reduce the effective prestress force on long internal tendons. By contrast, although external tendons lose force passing through deviators, overall losses tend to be less because of reduced duct contact friction. When stressing a group of tendons in sequence, elastic shortening causes greater loss in those stressed before others in that sequence. After stressing, further permanent loss of force occurs due to long term creep and shrinkage, depending upon the maturity of the concrete. For these reasons and because of possible changes for construction means and methods and that post-

tensioning systems vary from supplier to supplier, it is normal to require shop drawings and appropriate review by the Engineer prior to construction.

1.8.4 Falsework

Falsework is very often made from prefabricated modular shoring towers comprising well-braced interlocking frames in a square or rectangular arrangement of four legs. Each leg may have an individual capacity of up to about 100 kips (Figure 1.42). Multiple towers are located as necessary to support a temporary decking system for the superstructure formwork and work platform.

INSERT PHOTO OF SHORING TOWER FOR FALSEWORK

Figure 1.42 Shoring Tower for Falsework

Alternatively, the main vertical falsework supports may be built from temporary steel towers, heavy section lumber, precast concrete piles or similar members as convenient and available. Temporary steel girders or trusses purposefully fabricated for the application or assembled from prefabricated modular systems may offer viable alternatives where temporary foundations can be placed only in certain locations due to poor conditions or as may be needed to span a traffic diversion.

Figure 1.43 Side-Span Falsework for Cast-in-Place Box (Acosta Bridge)

Depending upon the nature of the site, availability of local materials and equipment, and costs of temporary construction, falsework may be provided for the superstructure to be cast-in-place over the full length of the bridge or it may be necessary to move falsework from span to span as each is constructed and made

self supporting. This is mainly a matter of construction efficiency, economics and the elected means and methods of construction. In general, as span lengths increase, it is more economical to consider other types of construction such as cast-in-place or precast balanced cantilever (below).

For falsework, guidance for design and construction is provided in two AASHTO publications:

"Guide Design Specifications for Bridge Temporary Works", 1995
"Construction Handbook for Bridge Temporary Works", 1995

Elevations of the falsework and formwork should be adjusted to compensate for any anticipated deflection of the falsework itself and for deflections of the superstructure itself arising from simply supported effects or construction in stages.

1.8.5 Superstructure Forming

Formwork for the superstructure may be made from lumber and plywood or prefabricated modular forming systems. Accuracy to line, level and thickness is essential to ensure the correct shape and size of concrete members. External surfaces are usually formed of a high quality, smooth and dense finished plywood, metal or any required aesthetic texture, as necessary. Internal surfaces should be within tolerance but are usually of a lesser quality finish and forming material.

Box girder sections are usually formed and cast in stages, commencing with the bottom slab, webs and finally the top slab; so formwork is arranged accordingly. Access to internal cells is usually necessary through diaphragms or manholes for future maintenance inspection and provides a convenient way through which internal formwork can be removed after casting. Purpose made, permanent, internal top slab soffit forms may remain in place provided that they have been accounted for in the design.

1.8.6 Rebar placement

For a casting a typical box section, rebar is installed in stages as necessary – i.e., bottom slab, webs and top slab. It is helpful if reinforcement is detailed accordingly, giving attention to the location of bar splices to meet structural requirements and also facilitate forming and casting. Reinforcement should be installed within construction tolerances.

All necessary post-tensioning ducts, anchorage components and anchorage reinforcement should be installed in conjunction with the reinforcement. It is preferable that reinforcement and post-tensioning be designed and detailed to be free of conflicts. However, this is not always evident in advance. Whenever a conflict is encountered between reinforcement and post-tensioning, in general, the reinforcement should be adjusted locally as necessary to maintain the desired post-tensioning alignment. In cases of doubt, a decision should be sought from the Engineer.

1.8.7 Superstructure Concreting

Typically a box section superstructure of any number of webs or size is cast in stages – i.e. bottom slab, webs, top slab – allowing the concrete to harden each time. Longitudinal construction joints are normally created a few inches above the bottom slab and at the top of the webs. This is mainly for convenience of construction. In order to ensure proper structural integrity and function, joints should be prepared, cleaned and roughened prior to the next pour. This is usually sufficient, however, construction keyways, if necessary, should be shown on the plans.

Concrete placement, consolidation, finishing and curing should be addressed in project specifications. Care should be exercised when placing and consolidating concrete around post-tensioning ducts so that they are not displaced or damaged. The top of the bottom slab is usually float finished to line and level by hand as access between webs restricts mechanical devices. When the bottom slab concrete has set and sufficient hardened the webs are formed. Web concrete is then placed and consolidated. Web forms may have to remain in place for a minimum period for curing. This may restrict progress installing top slab soffit forms and reinforcement and should be coordinated accordingly.

With a wide, single-cell (two-web) box, concrete for the top slab should be placed at the outer wings and center first, finishing by placing portions over the webs last. This should minimize any tendency for deflection of formwork to cause longitudinal separation or cracking of partially set concrete if placed otherwise. With multi-cell boxes and relatively closely spaced webs, this tendency is normally of little concern and concrete can be placed across the width from one side to the other as convenient. Finishing of a top slab may be done by hand or mechanical screed as used for slabs cast atop precast girders.

Longitudinally, vertical construction joints may be needed at various locations in a span or superstructure in order to keep the total volume of concrete placed within a work period to that which can be delivered, placed, consolidated and finished.

1.8.8 Superstructure Curing

Curing of concrete should be addressed in project specifications. With cast-in-place construction, it is necessary to attain a proper set and sufficient strength, prior to releasing forms before the next stage of casting and especially prior to imposing high local anchorage forces from post-tensioning or releasing falsework.

On site, curing is usually done using blankets, wet-burlap, moisture, fogging and application of suitable curing compounds. Steam curing for large pours is less practical than at a precast production facility or when using enclosed form-travelers, and is not normally used on site. Protection of pours from adverse weather and heating may be necessary in some situations. Monitoring of internal concrete temperature using thermocouples or other devices at suitable locations over the curing period can be helpful in some cases, particularly for thick members and large pours. It provides a record of curing and can help avoid potential difficulties from a

too rapid rise or fall from the heat of hydration. Curing and monitoring techniques should be addressed via appropriate specifications.

1.8.9 Post-Tensioning Operations

Post-tensioning operations for cast-in-place construction involve the same procedures and techniques as discussed previously.

For comprehensive information on the installation, stressing, grouting and protection of post-tensioning tendons and anchorages, including recommendations for the location of injection grout ports, vents, laboratory and field tests, quality control and records, etc., refer to "Post-Tensioning Tendon Installation and Grouting Manual" available from the Federal Highway Administration.

1.8.10 Tendon Grouting and Anchor Protection

After post-tensioning tendons have been installed and stressed, they must be properly grouted and anchorages sealed and protected to ensure long term durability (refer to above manual).

1.8.11 Staged Construction

Construction of a continuous cast-in-place superstructure in stages, for example, one span at a time, has been addressed in the discussion of longitudinal post-tensioning layout, above. In such situations, it is also necessary to calculate the amount of deflection of the structure as a consequence of the stages of construction and to make compensating adjustments (i.e. camber) to the elevations of the forms. Such deflections depend upon the sequence in which permanent load (self-weight) and prestress is applied and the material properties (elasticity, creep and shrinkage) of the concrete. The latter are influenced by the type of concrete, maturity and age at loading. In addition, corrections to elevations for setting forms are necessary for anticipated deflection of falsework itself.

This page intentionally left blank.

Volume 3
Concrete Bridge Superstructure Design

Chapter 2
Concrete Bridge Design

2.1 Introduction

The objective of this topic is to introduce the fundamentals of prestressed concrete design. Commonly used terms are defined and the mechanism of applying prestress to overcome applied loads is described in terms of general effects and illustrated by the incremental summation of internal stress necessary for basic design and analysis.

2.1.1 Concrete Behavior

Concrete is strong in compression but very weak in tension, as illustrated by the typical stress-strain curve in Figure 2.1.
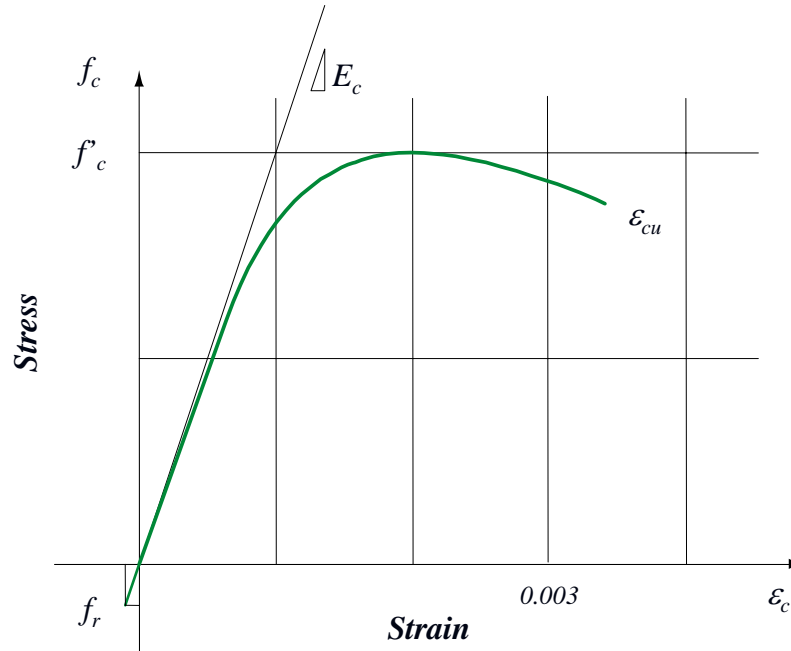
Figure 2.1 Stress-Strain Curve for Concrete

Tensile cracks develop at low load levels. The capacity of a plain concrete beam in flexure is limited by the flexural tensile strength or "modulus of rupture" given by:

Tensile cracks develop at low load levels. The capacity of a plain concrete beam in flexure is limited by the flexural tensile strength or "modulus of rupture". AASHTO LRFD Article 5.4.2.6 provides two different equations for the modulus of rupture depending on the usage of the value.

When used to calculate the cracking moment of a member in LRFD Articles 5.7.3.4 and 5.7.3.6.2 the modulus of rupture to be used is:

$$f_r = 0.24\sqrt{f'_c}$$

When used to calculate the cracking moment of a member in LRFD Article 5.7.3.3.2 the modulus of rupture to be used is:

$$f_r = 0.37\sqrt{f'_c}$$

The equations above are for normal-weight concretes with strengths up to 15.0 ksi. For sand-lightweight concrete and all-lightweight concrete single expressions are used:

$$f_r = 0.20\sqrt{f'_c} \qquad \text{(Sand-lightweight concrete)}$$

$$f_r = 0.17\sqrt{f'_c} \qquad \text{(All-lightweight concrete)}$$

Considering a concrete with a 28-day compressive strength (f'_c) of 5.5 ksi, the predicted modulus of rupture (f_r) would be 0.56 ksi, or about 10% of the compressive strength. This low tensile strength means that a plain concrete beam has very little flexural capacity (Figure 2.2) and fails easily under load.

The flexural capacity of concrete beams is improved by placing reinforcing steel to resist the tension that the concrete cannot carry (Figure 2.3). Under load, the concrete cracks as the tensile strength is exceeded. The reinforcing steel crossing the cracks resists the tensile stresses, providing internal equilibrium and increased load carrying capacity.
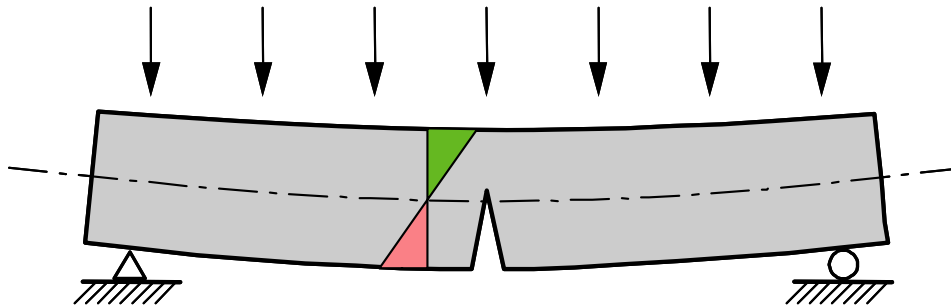
Figure 2.2 Plain, Unreinforced Concrete Beam in Flexure
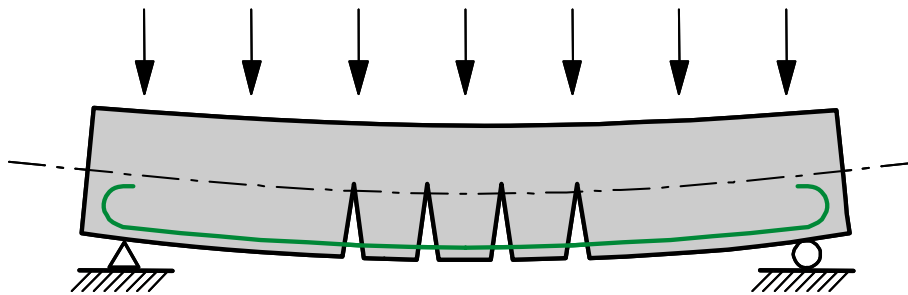
Figure 2.3 Reinforced Concrete Beam in Flexure

Reinforced concrete construction has been satisfactorily used for flat slab bridges and bridge beams with relatively short spans. Span length limitations for these bridges are approximately 25 to 30 feet. In longer span reinforced concrete bridges, the quantity of reinforcing steel and the dimensions of the concrete to effectively

resist loads increase significantly. The results are heavy members that are not cost effective.

Cracking in reinforced concrete bridges required to effectively engage the reinforcing steel can be undesirable. Although cracks can be controlled to be relatively narrow and well distributed, even small cracks afford pathways for corrosive agents to attack reinforcing steel. In addition, bridges in regions subjected to cyclical freeze-thaw action can experience undesired deterioration of the concrete, reducing long-term durability.

Introducing a means of pre-compressing the tensile zones of concrete to offset anticipated tensile stresses makes efficient use of the compressive strength of the concrete and reduces or eliminates cracking, producing more durable concrete bridges.

2.1.2 Prestressing

Prestressing is the introduction of a compression force into the concrete. Tension stress caused by load must first overcome compression induced by prestressing before it can crack the concrete. Prestressing is applied by means of high-strength steel strands tensioned so as to react against the concrete. The effect of prestressing is illustrated in Figure 2.4. Placing the prestressing low in the simple span beam induces compression in the tension zone creating an upward camber which opposes the deflection caused by load.
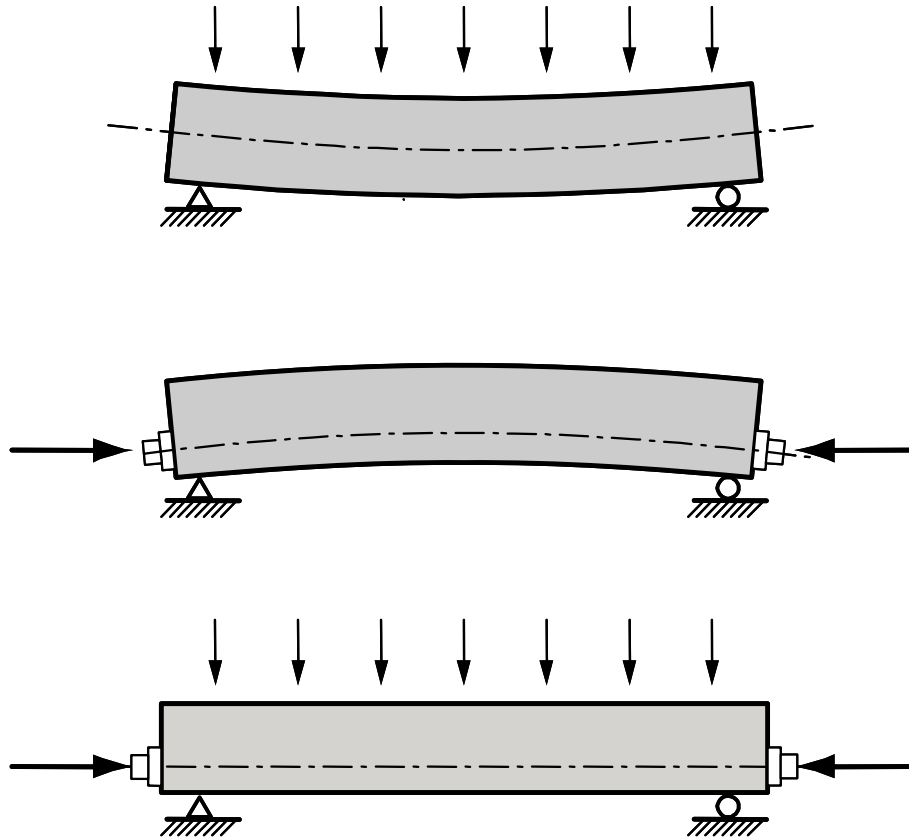
Figure 2.4 Effect of Prestressing in Simple-Span Beam

Design of prestressed concrete involves balancing the effects of loads and prestressing to eliminate or minimize tension, eliminate cracks, and optimize materials leading to structural efficiency and reduced construction cost.

Prestressing can be applied in two ways, by pre-tensioning or post-tensioning.

Pre-tensioning – In pre-tensioned members strands are installed along the length of a casting bed and tensioned against restraining bulkheads <u>before</u> the concrete is cast (Figure 2.5). After the concrete has been placed, allowed to harden and gain sufficient strength, the strands are released and their force transferred to the concrete member by bond.

Figure 2.5 Casting Bed for Pretensioned Girders

Post-tensioning – Post-tensioned construction involves installing and stressing strand or bar tendons only <u>after</u> the concrete has been placed, cured and hardened. Ducts are placed inside the concrete so that the tendons can be threaded through after the concrete hardens. Once in place, the tendons are tensioned by jacks and anchored against the hardened member using anchorage devices cast into the concrete.
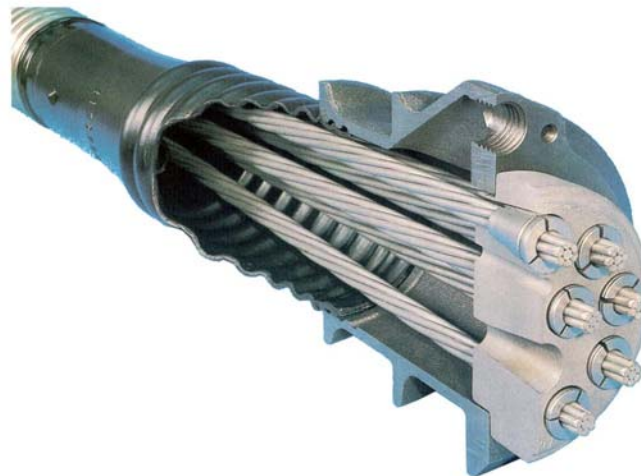
Figure 2.6 Post-Tensioning Anchor

Figure 2.6 illustrates a post-tensioning anchor for a tendon comprised of 9 strands. At the anchor, strands are gripped by hardened steel wedges housed in a wedge-plate. The wedge plate bears against an anchor plate or, in this figure a special steel casting that bears upon the concrete. Figure 2.7 shows a typical application of

post-tensioning tendons and jack during the erection of a precast concrete segmental balanced cantilever bridge.

Figure 2.7 Jacking of Post-Tensioning Tendon

2.1.3 Determination of Stressed under Affect of Prestressing

In order to appreciate the affect of prestressing, first consider the flexure of a simply-supported concrete beam section under the action of its own self weight as shown in Figure 2.8. Top and bottom stresses are determined according to normal beam theory. The top of the beam is in compression; the bottom is in tension. For plain concrete, the tensile stress will exceed the modulus of rupture – the beam will crack and fail.

$$f_t = \frac{M \cdot y_t}{I}$$

$$f_b = \frac{M \cdot y_b}{I}$$
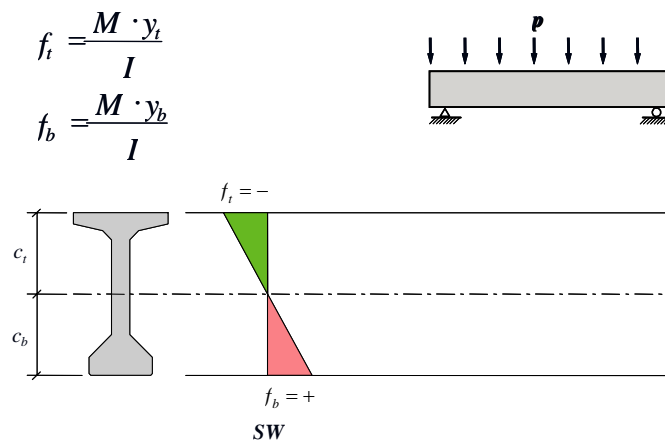
Figure 2.8 Self Weight Flexure Stress in Simply-Supported Beam

If a purely axial compression stress is applied (Figure 2.9), more compression is induced in the top and the tension in the bottom is reduced. However, the presence of the bottom tension means that the beam is incapable of carrying more applied load and it might still crack under its own weight.

$$f_t = f_b = f_{c_{axial}} = \frac{F_{ps}}{A_g}$$
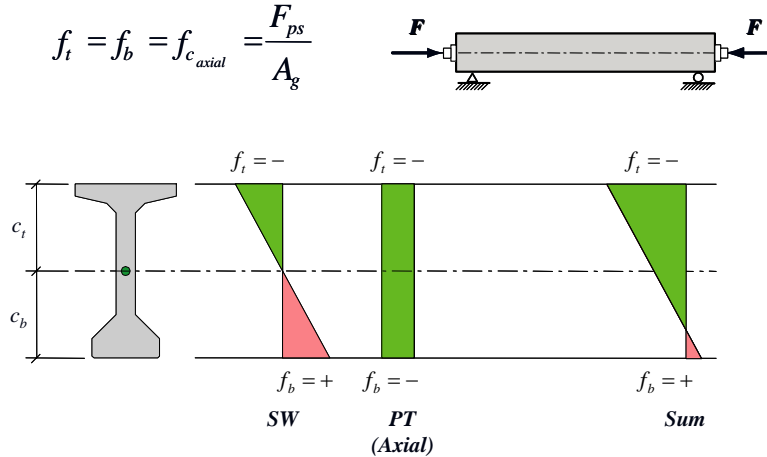
Figure 2.9 Self Weight Plus Axial Compression

Although pure axial compression helps, it is insufficient. What can be done?

The solution is to make the prestressing force eccentric (Figure 2.10). In this case, in addition to the self-weight stress and the axial prestress effect, the eccentricity causes an upward flexural moment that induces compression in the bottom of the beam and tension in the top.

$$f_t = \frac{Fe\ y_t}{I}$$

$$f_b = \frac{Fe \cdot y_b}{I}$$
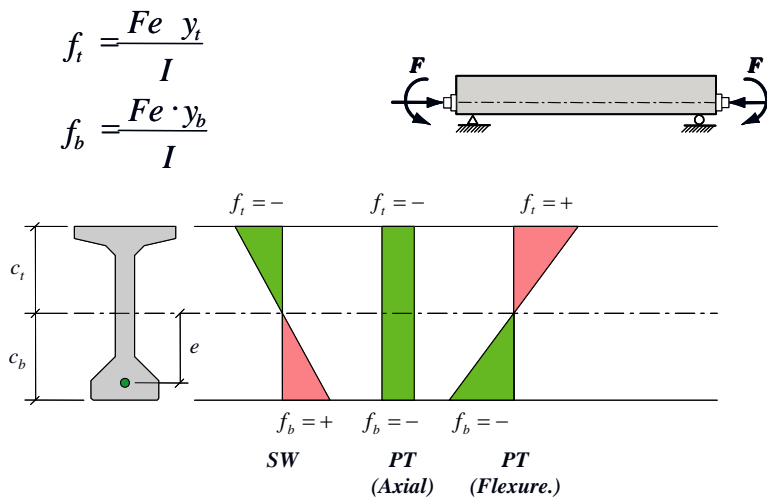
Figure 2.10 Self Weight, Axial and Eccentric Prestress Stresses

The summation of these three effects (i.e. self weight, axial and eccentric prestress) is shown in Figure 2.11. The result is compression stress throughout the depth of the

beam. Not only so, but there is more compression in the bottom than the top. Additional load applied to the beam from hereon must overcome the bottom compression and the tensile strength of the concrete itself, before the beam can crack. Eccentric prestress is the sought-for solution. Furthermore, this is structurally very efficient. It takes advantage of the fundamental properties of concrete (good in compression) and prestressing steel (good in tension) to optimize their use to the greatest extent; overcoming any disadvantages.
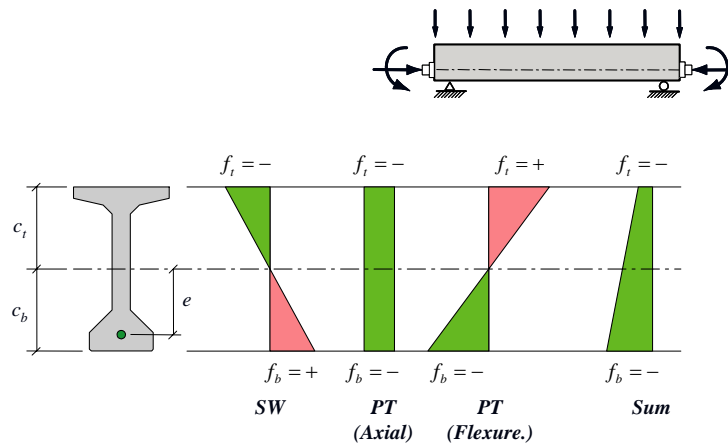
Figure 2.11 Summation of Self Weight, Axial and Eccentric Prestress Stresses

The incremental summation of stress illustrated above for midspan flexural stress in a simple beam can be applied at other locations along the beam not only for flexure, but also for web shear stress or principal tensile stress (Mohr's circle). In a prestressed concrete structure, the incremental summation of stress in the above manner is fundamental to determining the final state of stress – particularly if the section properties change during construction as is the case for composite behavior with a deck slab atop a precast girder. Incremental summation of stress is also necessary when post-tensioning is applied in stages as sections become composite or as a structure changes from simply-supported to continuous during construction.

2.1.4 Summary of Benefits of Prestressing

Prestressing minimizes or eliminates cracking. Compared to reinforced concrete structures, prestressing reduces the gross section size and girder depth, saving both concrete and weight. The weight reduction afforded by prestressing facilitates longer spans and greater structural efficiency than reinforced concrete alone. Pre-compression of otherwise tensile zones in the concrete prevents cracking and increases durability. Structural efficiency reduces construction costs and durability reduces maintenance costs.

2.2 Materials

2.2.1 Introduction

The objective of this topic is to explain the behavior and properties of the key materials used in the construction of prestressed concrete bridges and their influence upon the design.   Variations in material characteristics carry significant implications for design and must be properly estimated. This is especially true for time-dependent properties including concrete creep, concrete shrinkage, and relaxation of the prestressing steel.

2.2.2 Concrete

2.2.2.1 Compressive Strength

The fundamental property of concrete is its compressive strength, conventionally denoted by the symbol f'_c. It is determined at an age of 28 days by standardized compression tests of sample cylinders, 6 in. diameter by 12 in. long in accordance with ASTM C 42. Concrete matures and gains strength with age (Figure 2.12). Strength gain is rapid in the first days but then slows, eventually becoming only very gradual in the long term. An age of 28 days is the conventional time for defining the strength of concrete.
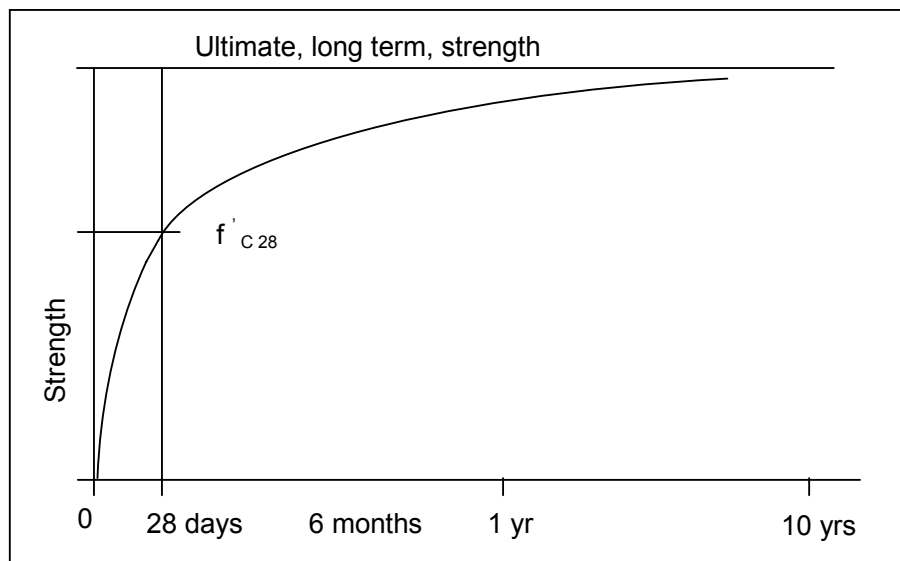
Figure 2.12 Gain of Concrete Strength with Time

Other properties, such as stress-strain relationship, tensile strength, shear strength, bond strength, creep and shrinkage, are often defined in terms of strength. Such relationships are empirical, having been established by experiment and experience.

Compressive strength is primarily governed by the strength of the cement paste, by the bond between the cement paste and aggregate particles, and by the strength of the aggregate itself. These are influenced by:

(a)   the ratio of water to cementitious material,
(b)   the ratio of cementitious material to aggregate,
(c)   the grading, surface texture, shape and strength of aggregate, and
(d)   the maximum size of aggregate.

In general, a lower water-cementitious ratio produces a higher strength. Consequently, in addition to compressive strength, concrete is further conventionally defined by the maximum "water-cementitious ratio" and/or "aggregate size".

Other mix factors, partially or wholly independent of water-cementitious ratio, that affect strength are:

(e)   the type and brand of cement,
(f)   the amount and type of admixture, such as air-entraining agent or super-plasticizer,
(g)   the type and amount of other pozzolanic materials, e.g. fly-ash and micro-silica, and
(h)   the mineral composition, gradation and shape of aggregate.

Factors such as the brand of cement and mineral composition of aggregate are clearly regionally dependant. A controlled percentage (4% to 8%) of well dispersed, microscopic air bubbles introduced by air-entraining agents enhances durability against freeze-thaw and improves workability for placement and consolidation. Super-plasticizers improve workability, facilitating reduced water content and enhanced strength. Cement replacement by a certain percentage of fly-ash and/or the use of micro-silica improves durability.

Concrete sets and gains strength as a consequence of a chemical reaction or hydration, between the cementitious material and water. This forms chemical bonds and gradual crystal growth in the cement matrix. Too much water will react prematurely with the cement, preventing the growth of bonds and crystals, resulting in a weak matrix. Too little water will result in an incomplete reaction, low strength and an unworkable mix. The mix must be correct. Also, to ensure complete hydration, not only must the mix be correct, but the concrete must be properly cured. The main purpose of curing is to prevent unnecessary moisture loss, especially in the first few days of the initial hydration and strength development. Hydration is an exothermic reaction, so heat builds up, particularly in the interior of a component. This heat must be gradually dissipated in a controlled manner. Curing processes involve covering the concrete, keeping covers and exposed surfaces damp to prevent moisture loss and allowing heat to slowly dissipate. Controlled steam or fog curing is also widely used, especially at precast concrete production yards, where

concrete mixes are designed for relatively rapid strength gain in the first few hours or days, to facilitate turnover.

Concrete mix design is clearly very important not only to the inherent strength of the structure, but also to long term performance and durability. For these reasons, project specifications should comprehensively address concrete mix requirements, production, handling, placing, consolidation, finish, curing and appropriate quality control.

Guidance as to the type or "Class of Concrete", for various applications is provided in *AASHTO LRFD* Article 5.4.2.1. Concrete mix characteristics, including strength, minimum cement content, maximum water cement ratio, range of air content and coarse aggregate per class of concrete, are given in *AASHTO LRFD* Table C5.4.2.1-1.

For example, for bridge construction, reinforced concrete for abutments, piers and deck slabs is typically "Class A" with a minimum compressive strength of 4.0 ksi. For prestressed concrete, "Class P" is required, normally in the range of 5.0 to 6.0 ksi. Occasionally, strengths as high as 8.0 and 10.0 ksi have been used for special cases.

For a given project and location, an appropriate 28-day concrete compressive strength should be established as one of the first steps in the design process.

2.2.2.2 Tensile Strength

The direct tensile strength of concrete should be determined by test (ASTM C 900 or ASTM C 496 (AASHTO T 198). *AASHTO LRFD* Article C5.4.2.7 states that for most regular concretes, the direct tensile strength may be estimated as:

$$f_r = 0.23\sqrt{f'_c}$$

2.2.2.3 Shear Strength (Diagonal Tension)

In a manner similar to flexural tensile strength, the shear, or diagonal tension, strength of concrete can also be expressed as a function of compressive strength. Although requirements are not specified in *AASHTO LRFD*, guidance is offered in the *AASHTO LRFD Guide Specification for Segmental Bridges*. Some authorities have adopted criteria to limit service cracking.

2.2.2.4 Modulus of Elasticity

The modulus of elasticity, E_c, is the ratio of normal stress to corresponding strain in compression or tension. For concrete, the stress-strain curve is non-linear (see Figure 2.12, above).

The modulus of elasticity is required for the calculation of deflections, axial shortening, buckling. As concrete is composed of different materials with different

characteristics, the elastic modulus is not easily formulated. However, from empirical results, the secant modulus is expressed with sufficient accuracy, as a function of density and strength by *AASHTO LRFD* Article 5.4.2.4:

$$E_c = 33,000 \ w_c^{1.5} \ \sqrt{f_c'}$$

AASHTO LRFD Equation 5.4.2.4-1

2.2.2.5 Poisson's Ratio

Poisson's Ratio is the ratio of lateral to axial strain. For concrete, *AASHTO LRFD* Article 5.4.2.5 prescribes a value of 0.20. Poisson's Ratio has little importance in the longitudinal analysis of concrete superstructures. It is an important characteristic in the analysis of complex details using finite element techniques or in predicting the degree of confinement developed in laterally reinforced concrete members.

2.2.2.6 Volume Changes

Volume changes in concrete arise from variations in temperature, shrinkage due to air-drying, and creep caused by sustained stress. These are influenced by environmental conditions such as temperature, humidity, and the maturity of the concrete, which is influenced by whether it is cast-in-place or precast, and by the time and duration of loading. Volume changes affect structural performance and must be properly accounted for when determining loss of prestress and long-term deflections.

AASHTO LRFD Article 5.4.2.2 defines the coefficient of thermal expansion. For normal weight concrete, the value is 0.000006 per ^{O}F. For lightweight concrete the coefficient of thermal expansion is 0.000005 per degree Fahrenheit.

2.2.2.7 Shrinkage

Shrinkage is primarily a result of sustained air-drying. Shrinkage occurs rapidly in the first few days but gradually slows over a long time, approaching, but never quite reaching, an ultimate limit (Figure 2.13).   The rate of shrinkage and shape of the shrinkage curve varies with the type of concrete, maturity, exposure and environment.
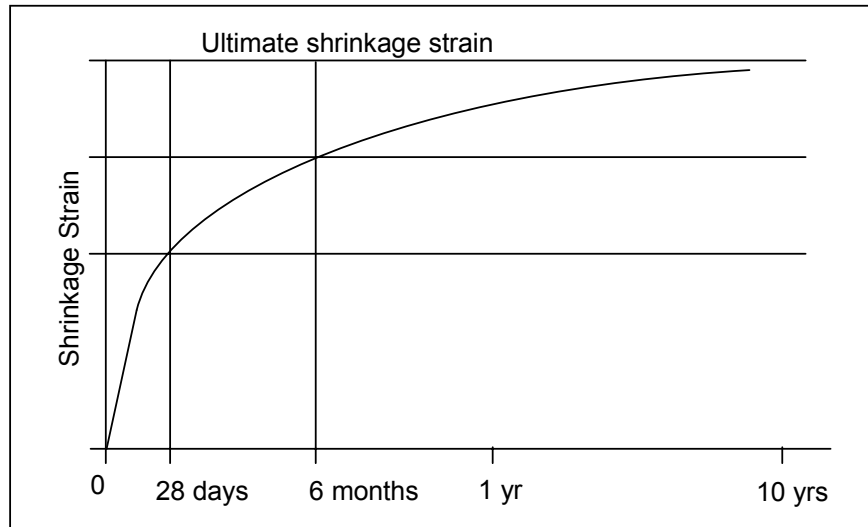
Figure 2.13 Shrinkage

2.2.2.8 Creep

Creep is the prolonged deformation of concrete under sustained stress. When loaded, concrete undergoes an initial "instantaneous" elastic strain which is a function of the modulus of elasticity at the time of loading. When the stress is sustained, a delayed strain occurs over time. If the stress is held indefinitely, the strain tends to an ultimate limit which is typically in the range of 2 to 2.5 times the instantaneous strain (Figure 2.14). If at some point the stress is released, there is an instantaneous recovery, proportional to the effective modulus of elasticity for the age of the concrete. A delayed recovery of strain follows. However, the recovery is never 100%, and a residual permanent strain remains.
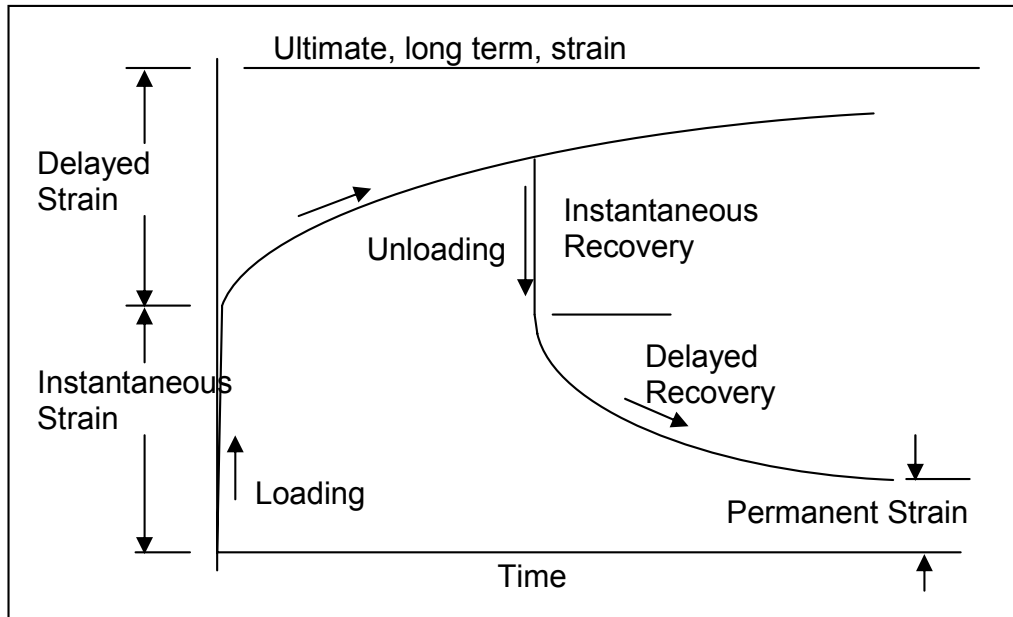
Figure 2.14 Creep; Response to Sustained Stress

AASHTO LRFD Article 5.4.2.3 offers basic formulae and guidance for shrinkage and creep. It also allows shrinkage and creep to be determined by the provisions of CEB-FIP (European Code) and ACI 209. The approach of each code takes into account the same key factors in similar, but slightly different, formulations. The key factors are:

➢ Maturity of concrete

➢ Strength of concrete

➢ Time and duration of sustained stress

➢ Exposed perimeter (volume to surface ratio)

➢ Average relative humidity

➢ Water-cementitious ratio

➢ Type of curing

Experience and comparison of results of different codes for different projects and locations might sometimes reveal different proportions of shrinkage and creep. Figure 2.15 (a) and (b), show relative values of creep and shrinkage predicted by four codes. These results are the average of values computed for four segmental and one bulb-t girder bridge. Though the individual components of creep and shrinkage predicted by the different codes may vary, the sums of the two volumetric changes are sufficiently close to warrant any of their use in design.
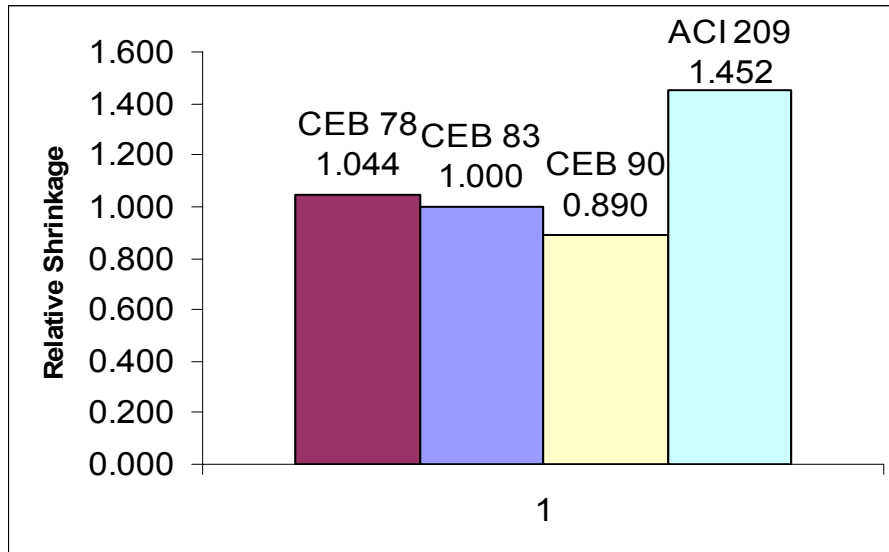
Figure 2.15(a) Relative Shrinkage by Different Codes
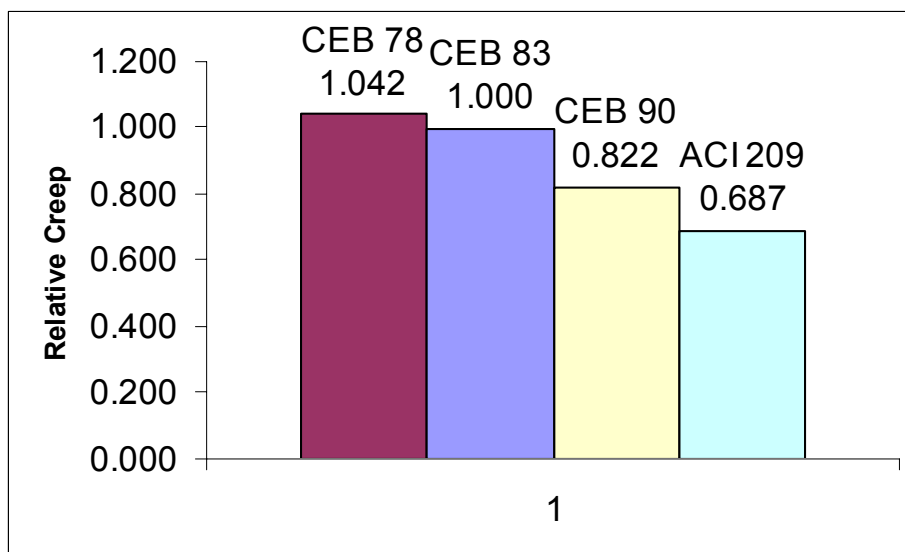
Figure 2.15(b) Relative Creep by Different Codes

2.2.3 Reinforcing Steel

Today, ordinary mild steel reinforcing typically has a yield strength of 60 ksi or greater, although *AASHTO LRFD* places a limit of 75 ksi for design calculations regardless of actual strength. The modulus of elasticity is assumed to be 29,000 ksi. (*AASHTO LRFD* Articles 5.4.3.1 and 5.4.3.2). Other types of mild reinforcing, such as stainless steel or stainless clad reinforcing, have also been used effectively. While producing increased resistance to corrosion, these steels originally did not have yield strengths or modulii of elasticity consistent with code requirements. Since

their introduction, producers of these types of reinforcing bars have altered their formulation to produce acceptable characteristics.

2.2.4 Prestressing Steel

Prestressing strand is very high strength steel with an ultimate strength (f_{pu}) much greater than the yield point (f_y) of ordinary mild steel reinforcing (Figure 2.16). Typical seven-wire prestressing strand (for pre- or post-tensioning) typically has an ultimate strength of 270 ksi, about 4.5 times the yield point of 60 ksi for mild steel reinforcing. Bars for post-tensioning typically have an ultimate strength of 150 or 160 ksi.
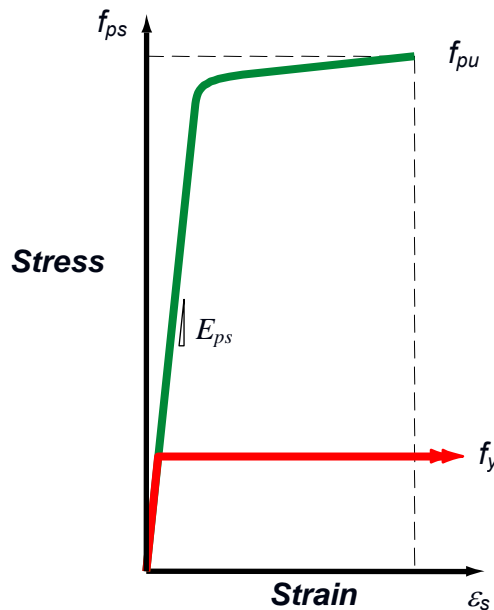
Figure 2.16 Stress-Strain Curves for Prestress Strand and Mild Steel

Unlike mild-steel, prestressing steel does not have a definite yield point, although its behavior is linear-elastic to $0.75f_{pu}$. Thereafter, it is non-linear but exhibits a significant strain to failure. The yield strength is taken as that point where the strain reaches 1% or the point where a line parallel to the initial modulus at a 0.2% offset meets the stress-strain curve. Both techniques give similar results. The modulus of elasticity for strand is usually assumed to be 28,500 ksi, for elongation calculations during stressing operations (*AASHTO LRFD* Article 5.4.4.2). This value is less than that for bars (i.e. 30,000 ksi) or that of an individual wire of a strand. The reason is attributed to the helically wound outer six wires being slightly longer than the central king wire resulting in a very slightly longer actual test gauge length than theoretical, which, along with the tightening or straightening effect of the outer wires under load leads to a slightly lower effective modulus.

Prestressing makes use of the full elastic range to impart a sustained force on the concrete. The stress in the steel at tensioning is typically $0.75f_{pu.}$ After initial and

long-term losses, which must be accounted for in the design, the final stress is usually in the range of 0.55 to $0.65f_{pu}$, depending upon application. This final stress level (typically at least 150 ksi for strand and 83 ksi for bar) is greater than the yield of mild steel (60 ksi) and is only possible by the availability of high strength steel.

Under sustained stress, prestressing steel creeps and relieves itself of stress in a process referred to as relaxation. Two types of strand are available: stress-relieved (normal relaxation) and low relaxation. The latter has undergone an additional treatment and has a final relaxation of about 3.5%, one quarter that of stress-relieved strand. Since losses are detrimental to prestressed concrete, low-relaxation strand has taken a greater market share over time and is the recommended strand at the present time.

The significant, almost an order of magnitude difference, between the modulus of elasticity of steel on the one hand and concrete on the other is the primary reason it is possible to make prestressed concrete function structurally.

2.2.5 Post-Tensioning Hardware

Various types and sizes of components are commercially available for post-tensioning. A typical anchor for a multi-strand tendon is shown in Figure 2.5 (above). For bridges, post-tensioning bars are most often used for temporary construction uses, for example for erecting precast segments, but also for permanent applications. Bar anchorages are either rectangular plates, usually for surface mounts, or special embedded components. Couplers are available for post-tensioning bars.

For more information on post-tensioning, including recommendations for the location of grout injection ports, vents, laboratory and field tests, quality control and records, etc., refer to "Post-Tensioning Tendon Installation and Grouting Manual" available from the Federal Highway Administration. Additional information is available from the Post-Tensioning Institute.

Figure 2.17 Post-tensioning Bar Anchors and Couplers

2.2.6 Loss of Prestress

2.2.6.1 Sources of Loss

Whether prestress is applied by pretensioning or post-tensioning, various losses of effective force occur as a natural response from the properties of the two materials; concrete and steel. The final effective prestress in influenced by:

- ➢ Relaxation (creep) of prestressing steel
- ➢ Elastic deformation of concrete
- ➢ Shrinkage of concrete
- ➢ Creep of concrete

Loss of prestress due to relaxation (creep) of prestressing steel depends upon the type of steel – whether normal or low-relaxation. Elastic deformation of concrete occurs initially at transfer of the prestress force and subsequently from the addition of structural loads and changes during construction. The modulus of elasticity of concrete depends primarily upon its strength – and this is influenced by many construction related factors, age, type of curing, type of cement, aggregate, environment and so on. Creep and shrinkage are affected by the same factors.

Additional loss of prestress arises in post-tensioning as a result of physical aspects of the post-tensioning system and ducts- these are:

➢ Wedge set (pull-in)

➢ Friction in the jack

➢ Friction in the anchorage

➢ Duct friction due to curvature

➢ Duct friction due to unintentional variation from profile (wobble)

For design purposes, it is normal to make assumptions on the basis of past experience or code guidance in order to reasonably estimate the final effective prestress force as a consequence of these losses and effects. For simply-supported structures and relatively straightforward two and three span continuous structures, estimates can be made by hand. For more complex structures involving multiple stages of construction and time-dependent changes, special structural analysis computer programs are commercially available to assist the tedious analysis process.

For initial member selection, sizing of a cross section and preliminary design purposes, in general, for pre-tensioned girders and cast-in-place post-tensioned construction, the final stress in the strands after all losses lies approximately in the range of 55 to 62% F_{pu}. For precast segmental construction, where concrete is loaded at a later age, final forces after losses, including those due to friction and wedge set, tend to be higher, approximately in the range of 60 to 65% F_{pu}. These are approximations. Final design should always properly account for loss of prestress according to recognized procedures.

2.2.6.2 Estimate of Loss of Prestress in Pretensioned Structures

According to *AASHTO LRFD*, prestress losses can be calculated using alternative procedures. The two main methods are:

➢ Approximate Method (*AASHTO LRFD* Article 5.9.5.3)
➢ Refined Method (*AASHTO LRFD* Article 5.9.5.4)

In order to enable a designer to determine a likely final prestressing force, the following summary of the approximate method is offered at this time. This basic process can then be adapted for other circumstances according to the type of construction.

The approximate method applies under the following circumstances:

➢ Precast components are of standard sections (AASHTO Type Girders and similar)
➢ Precast components are pre-tensioned (not post-tensioned)
➢ Concrete is normal weight (not light-weight or other special mix)
➢ Components are pretensioned with bars or strands of either normal or low relaxation properties
➢ The project is in a location of average exposure conditions and temperatures

These circumstances apply to the vast majority of precast concrete girder bridges – which makes it ideal for illustration and initial design purposes.

Losses by the "Approximate Method" are calculated for:

- ➢ Elastic shortening (instantaneous)
- ➢ Shrinkage
- ➢ Creep
- ➢ Relaxation of prestressing steel

The latter three are time dependant (long-term) losses influenced by the type of structure and environment.

Elastic shortening: this is the loss due to the initial elastic shortening (deformation) of the concrete as a result of the (instantaneous) release of pretensioned strands in the casting bed at the time of transfer. Usually, a component is relatively young; i.e. from a day to about a week old, and may have been cured by steam or moist curing. Elastic shortening loss is given by *AASHTO LRFD* Article 5.9.5.2.3, as:

$$\Delta f_{pE} = \frac{E_p}{E_c} f_{cg}$$

where:

f_{cg} = stress in the concrete at the centroid of the prestress at transfer
E_p = elastic modulus of strand
E_c = elastic modulus of concrete

In the casting bed the strands are tensioned against bulkheads. After casting and after the concrete has attained the required transfer strength, the strands are cut – transferring their force to the concrete by bond. As a result, the concrete shortens. This shortening affects the strands too; the equation follows directly from consideration of elastic conditions. If transformed section properties are used for stress analysis, then the initial elastic shortening loss should be taken as zero – as it is automatically accounted for within procedures for calculating transformed properties.

Long term, time dependant, loss can be estimated from *AASHTO LRFD* Article 5.9.5.3, as;

$$\Delta f_{pLT} = 10.0 \frac{f_{pi}A_{ps}}{A_g} \gamma_h \gamma_{st} + 12.0 \gamma_h \gamma_{st} + \Delta f_{pR}$$

where:

$$\gamma_h = 1.7 - 0.01H$$

$$\gamma_{st} = \frac{5}{\left(1 + f_c^`\right)}$$

and:

Δf_{pR} = 2.5 ksi for low relaxation strand or 10.0 ksi for stress relieved strand

H = Relative humidity for bridge location (percent)

The first term in the equation corresponds to loss due to creep, the second to shrinkage loss and the third to relaxation loss. According to calibrations and tests, this equation gives a conservative approximation to results from the refined method. For most practical cases with ordinary precast girder bridges, the approximate method is sufficient.

2.2.6.3 Estimating Loss of Prestress in Post-Tensioned Structures

If prestress is applied by post-tensioning (i.e. installing tendons in ducts and tensioning after the concrete has hardened) then there is no elastic shortening loss in the first tendon stressed – because the girder shortens while the tendon is jacked to load. However, when the second tendon passing through the same girder is stressed, the girder shortens elastically again. This shortening affects the first tendon, so it suffers an elastic shortening loss from the second tendon stressed. This process repeats as subsequent tendons are stressed. The final tendon stressed suffers no elastic shortening loss itself but affects all previous ones already stressed. Altogether, the total elastic shortening loss is the average of all individual tendon loss except for the last tendon – i.e. the quotient "(N-1)/2N" in equation 5.9.5.2.3b-1 of *AASHTO LRFD*.

Giving proper consideration to this phenomenon, loss from post-tensioning can be roughly estimated for preliminary design purposes in a similar manner using the above formulae. However, it is also necessary to consider losses from duct friction and wobble, anchor friction and wedge pull-in effects first; prior to making estimates for subsequent shrinkage, creep, and relaxation. In addition, for more complex structures, staged construction, intermediate post-tensioning steps and changes in statical scheme during construction, require more detailed consideration and accumulation of losses. These subjects are discussed in greater detail in following sections.

2.3 Design of Adjacent Precast, Pretensioned Girder Superstructures with Integral Decks (Precast Planks, Double Tees and Box Beams)

Future Development

2.4 Design of Precast, Pretensioned Girders

2.4.1 Preliminary Sizing (Typical Span Lengths and Girder Spacing)

For guidance on the preliminary selection of a girder type and size, refer to DM Volume 3 Sections 1.3 and 2.4.1.

Applicable simply-supported span ranges are shown in DM Volume 1, Chapter 2. Considerable overlap of span range for different sizes of girders offers flexible choice to best suit the circumstances of an individual project – such as site layout, geometric constraints, accessibility etc. (DM Section 1.1.2).

In general, a span is usually 16 to 24 times the depth of a girder – but it also depends upon girder spacing and stiffness (or thickness) and weight of the deck slab (DM Section 1.3.1). Girder spacing may range from 4 to 12 feet – but is more usually from 6 to 10 feet – and is chosen to suit the required overall width of the highway deck. Typical deck slab thickness ranges from 7 to 9 inches; 8 inch depth is quite common. A deck slab overhang is about 40% of the spacing but not usually more than 5 feet for most commercially available deck forming systems.

All precast girder sections developed over the years are able to accommodate a sufficient number of pre-tensioning strands to provide the necessary flexural capacity for the span range of each type of girder. Longitudinal pretensioning strands are most often 0.5" nominal diameter, although 0.6" dia. strand may be used in some cases. The number of strands can be varied, but must be arranged to a specific pattern and spacing within the section. The strand size and pattern depends upon the manufacturing facility and, in particular, the size and capacity of the stressing bulkheads. Before commencing a design, check with local industry as to availability.

The calculation process for starting a new design usually begins with a selected girder section and an initial estimate of the strand-layout, force and eccentricity.

2.4.2 Longitudinal Flexural Design (Service Limit State)

2.4.2.1 Service Limit States

The design of precast, prestressed concrete girders is typically governed by stress control at the Service Limit State. The girder must be verified under these service conditions from initial transfer through to final service conditions. After service conditions are satisfied, the Strength Limit State must then be verified to ensure overall capacity of a structure to safely resist factored design loads.

2.4.2.2 Applicable Loads and Bending Moments for Composite Construction

Construction of bridges using precast concrete girders with cast-in-place deck slabs comprises composite construction where loads and moments are applied first to a

non-composite girder section and then, after hardening of the deck slab, to the composite section.

The different loads and bending moments acting on the non-composite and composite section are summarized in Figure 2.18. This also illustrates that stresses are calculated separately, according to the section acting at the time of application of the load or moment. Final stresses are determined by accumulating the individual stresses (i.e. not by accumulating moments).
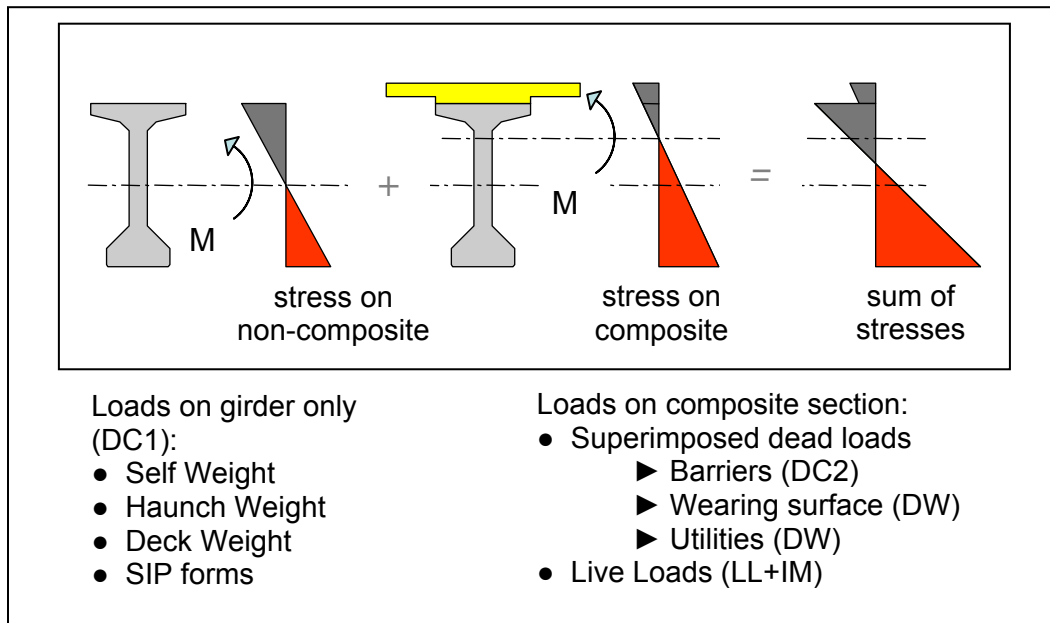
Figure 2.18 Loads and Stresses in Composite Construction

The fact that the load factor at the Service Limit State is 1.00 simplifies the essential incremental summation of stresses; particularly when stresses depend upon the change from non-composite to composite section properties.

For convenience, a designer may prefer to calculate the individual stress from each of the above applied load conditions at sections and elevations of interest along the girder before attempting to establish a necessary level of prestress. Calculation of stress depends upon the appropriate section properties; these are defined and determined as follows.

2.4.2.3 Composite and Transformed Section Properties

2.4.2.3.1 Non-Composite and Composite Properties

Prior to hardening of the deck slab, all load (i.e. self weight of girder and the weight of the deck slab, temporary or permanent forms) is applied only to the non-composite girder section alone and stresses are determined for the girder's section properties alone (or the properties using the transformed area of prestressing steel,

2.5.2.3.3, below). After the slab has been cast and hardened, subsequent loads are applied to the composite section of the slab and girder; so stresses are calculated using the non-composite section.

2.4.2.3.2 Effective Flange Widths

Composite section properties are determined for the effective flange widths in Figure 2.19 and Figure 2.20 according to *AASHTO LRFD* Article 4.6.2.6.

Tension

The least of:

- ¼ of effective span length

- 12t$_s$ plus the greater of the web thickness or ½ the width of the top flange

- The average girder spacing

AASHTO LRFD Article 4.6.2.6
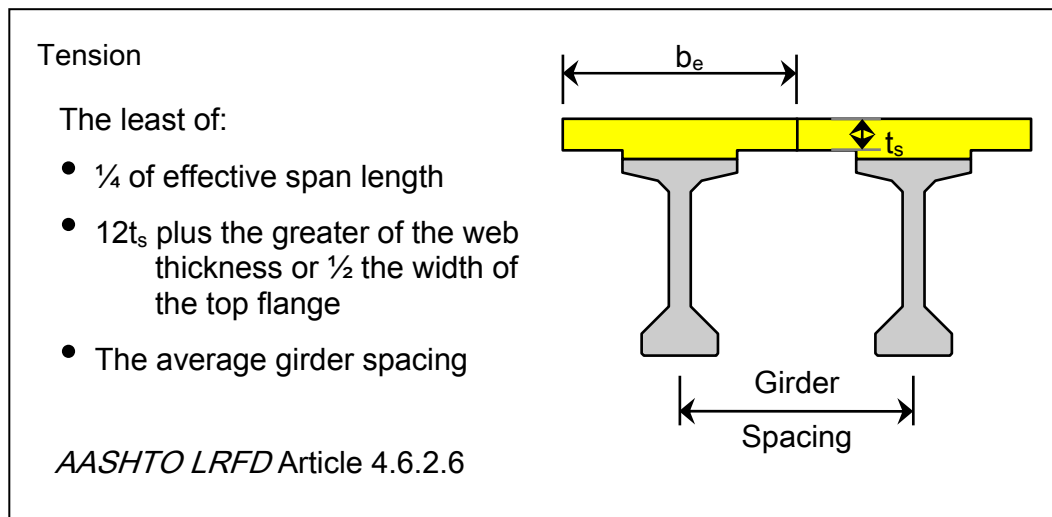
Figure 2.19 Effective Flange Width of Interior Girder

Effective Flange Width – Exterior

½ Interior Width and the least of:

- 1/8 of the effective span length

- 6t$_s$ plus the greater of ½ the web thickness or ¼ the width of the top flange

- Width of the overhang

AASHTO LRFD Article 4.6.2.6
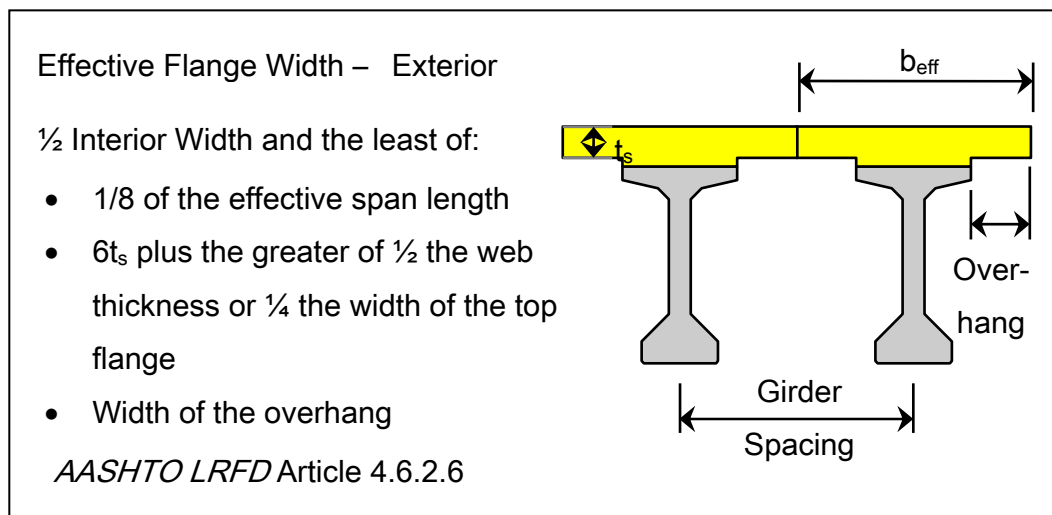
Figure 2.20 Effective Flange Width of Exterior Girder

The top slab is of a different concrete to the girder (different strength and maturity). It is necessary to transform the effective flange width to an equivalent width of girder concrete by multiplying the effective width of the slab by the modular ratio (n) of the modulus of elasticity for the slab concrete divided by that of the girder concrete.
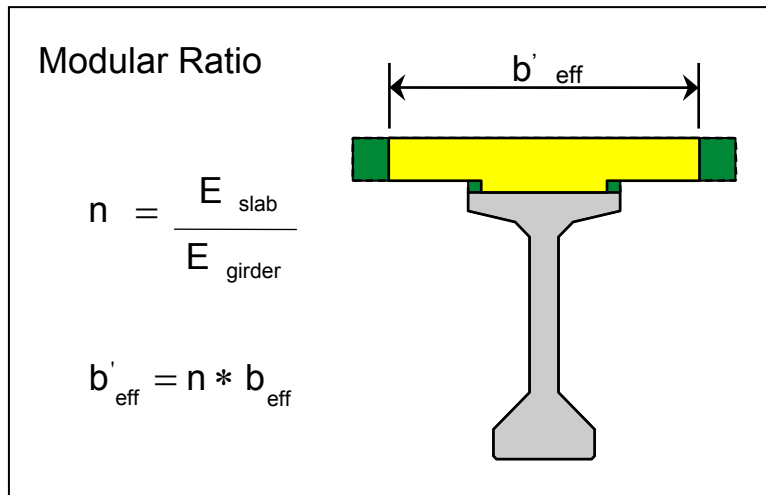
Figure 2.21 Modular ratio (n) of elasticity of slab to girder concrete

Gross composite section properties are calculated using formulae illustrated in Figure 2.22.
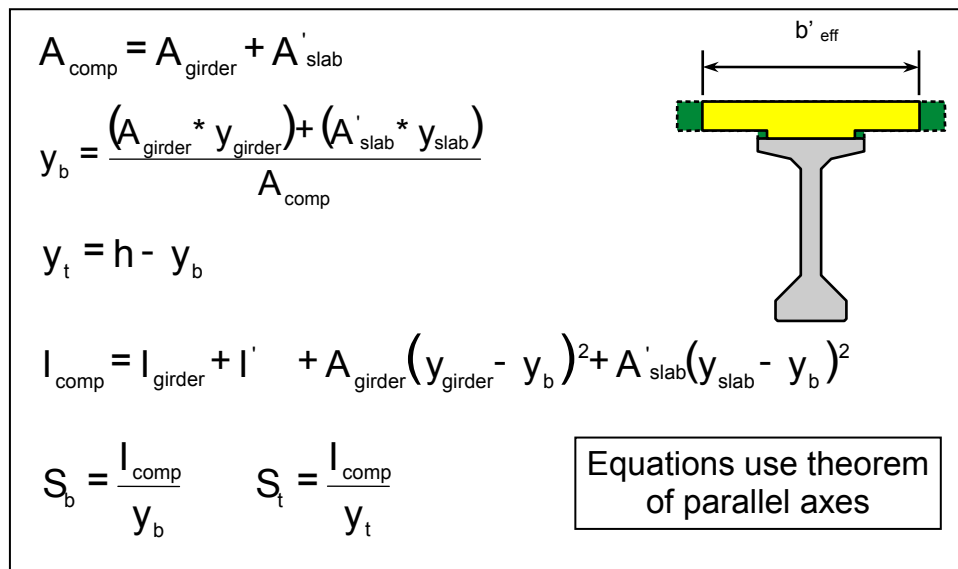
Figure 2.22 Calculation for Composite Section Properties

2.4.2.3.3 Transformation of Prestressing Steel

Some jurisdictions allow the transformation of the prestressing steel to an equivalent area of concrete section equal to $(n-1).A_{ps}$ (where n = modular ratio of elastic modulus of prestress steel to that of the girder concrete) located at the average eccentricity, e, when determining section properties for the girder alone. In which case, the above composite section properties are calculated using the transformed non-composite properties (Figure 2.23).
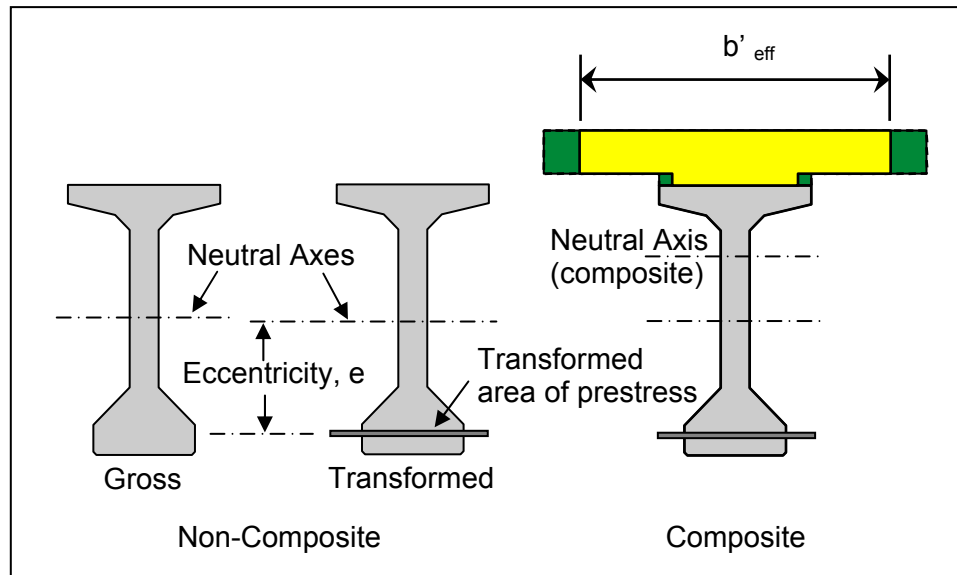
Figure 2.23 Transformed Area of Prestress

When using the transformed prestress area, in accordance with *AASHTO LRFD* Article C5.9.5.2.3a, elastic shortening loss Δf_{pES} should not be applied at transfer as it is automatically accounted for by using the transformed steel area.

2.4.2.3.4 Accumulation of Stress in Non-Composite and Composite Section

Calculation of stress is made by classical beam theory. Flexural stresses are determined at the top of the deck and at the top and bottom of the girder by dividing the applied moment by the applicable section modulus at each of these elevations. The resulting flexural stresses at the top and bottom of the girder are the actual stresses the girder experiences under the applied moment. However, the stress at the top of the slab is given as a stress in terms of girder concrete. To convert it to one of magnitude appropriate to the strength of the slab concrete, it is multiplied by the modular ratio of the elastic modulus of the slab to that of the beam.

Final stresses are determined by summation of all individual stresses applied to the non-composite and composite section in turn, from the time of transfer to final (long-term) service conditions after all loss of prestress due to elastic shortening, shrinkage, creep and relaxation of the prestressing steel has occurred. (For calculation of losses, see below).

2.4.2.4 Prestress Force and Eccentricity, Begin a Design

Calculation of the eccentricity of a group of prestressing strands from the neutral axis of the non-composite section is made using the technique illustrated in Figure 2.24.

$$e = \frac{\sum N_i e_i}{\sum N_i}$$

e = average eccentricity of strands from N.A.
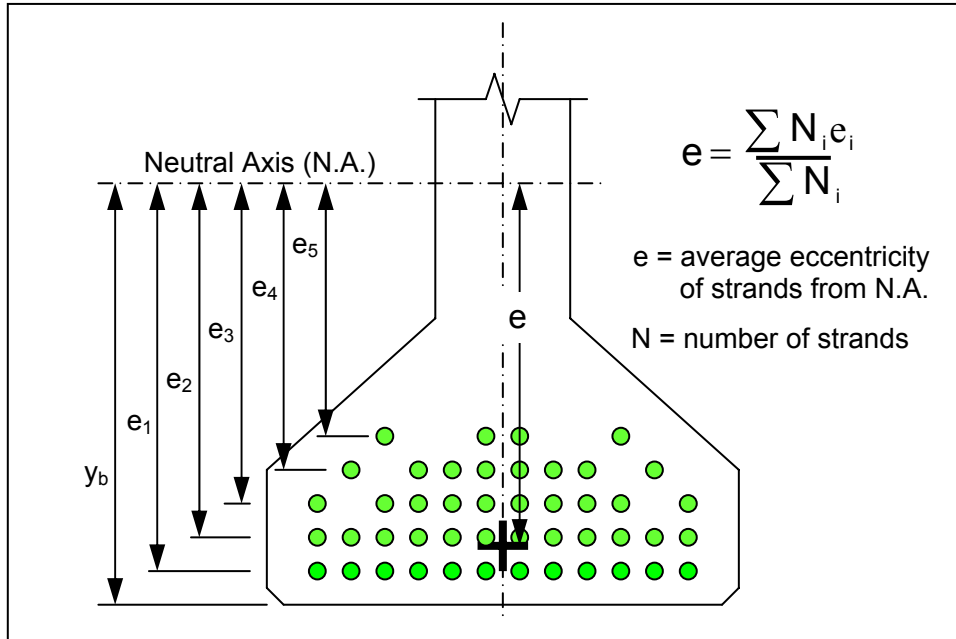
N = number of strands

Figure 2.24 Eccentricity of Prestress Strands

Strands are set out in the pattern of available bulkhead stressing locations. The prestressing force depends upon knowing the number of strands and their eccentricity at various sections along the girder. Key sections are midspan, at each end of the girder, and at locations where strands are deflected or the number is reduced by debonding with plastic shielding. The design process involves some iteration and repetitive calculation to arrive at the optimum solution. It is helpful to have a simple spreadsheet or program to facilitate calculation of strand eccentricity.

A new design generally begins by making an estimate of the required magnitude of the final prestress force and eccentricity at mid-span, after all losses, to satisfy final service conditions for the allowable bottom fiber tensile stress. This requires first knowing the bottom fiber tensile stress induced by all accumulated dead and live loads on the non-composite and composite section and the appropriate allowable tensile stress limit.

A convenient starting point for a new design is to assume that the final prestress after all losses is in the range of 55 to 60%f_{pu} – say, 58% f_{pu}. An assumed final prestress force at an assumed eccentricity is applied to the non-composite section (Figure 2.25). The effect of the self weight of the deck slab, forms and diaphragms are applied on the non-composite section and the stresses are added to those from the assumed final prestress (Figure 2.26).

Superimposed dead loads are applied to the composite section and the stresses at each elevation are added to the previous ones (Figure 2.27). Finally, service live load is applied to the composite section and the stresses are added to the previous ones giving the final conditions (Figure 2.28) for the assumed final prestress.
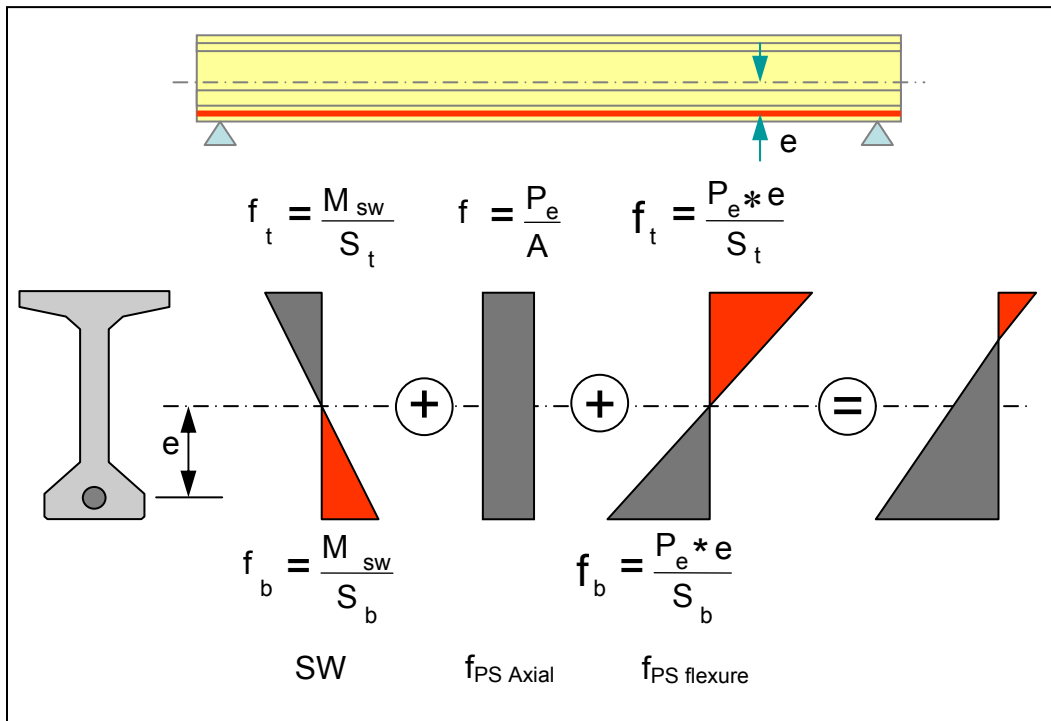
Figure 2.25 Non-Composite Section under an Assumed Final Prestress

$$f_t = \frac{M_{sw}}{S_t} \qquad f = \frac{P_e}{A} \qquad f_t = \frac{P_e * e}{S_t}$$

$$f_b = \frac{M_{sw}}{S_b} \qquad f_b = \frac{P_e * e}{S_b}$$

SW $\qquad$ $f_{PS\ Axial}$ $\qquad$ $f_{PS\ flexure}$

$$f_t = \frac{M_{SLAB}}{S_t}$$

$$f_b = \frac{M_{SLAB}}{S_b}$$

SW + PS $\qquad$ Slab, Forms, Diaphragms $\qquad$ DL_{nc} + PS
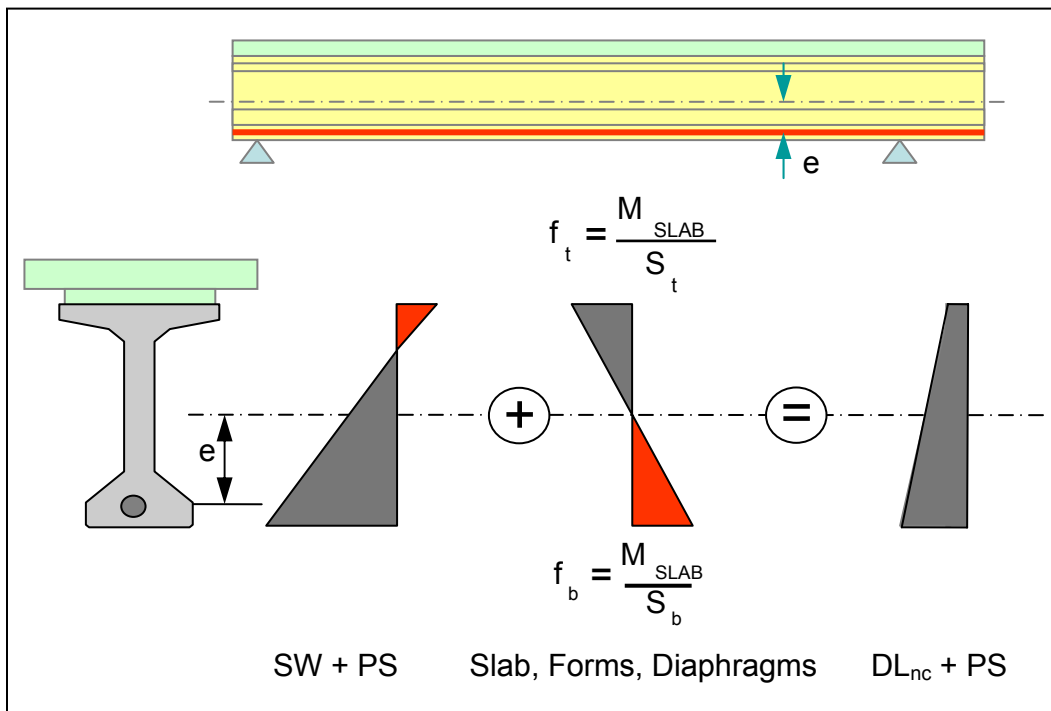
Figure 2.26 Loads of Slab, Forms and Diaphragms applied to Non-Composite
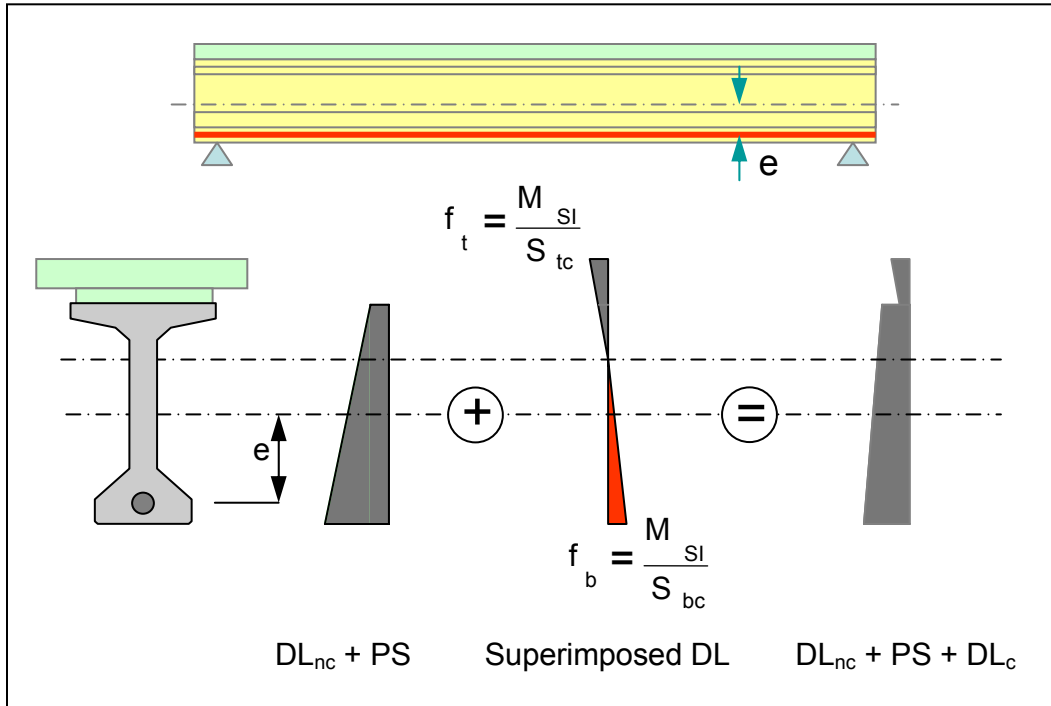
Figure 2.27 Application of Superimposed Dead Load on Composite Section
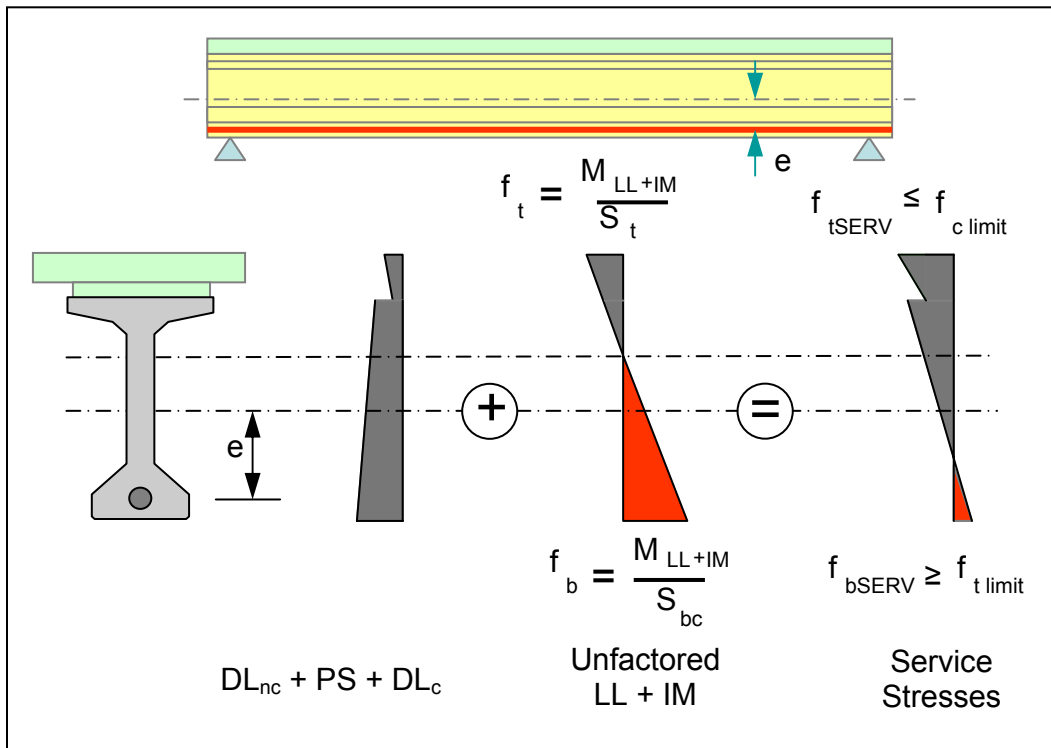
Figure 2.28 Application of Live Load on Composite Section

The assumed final force and eccentricity is adjusted until the bottom fiber tensile stress satisfies the allowable service limit tension. This gives a revised estimate of the required final prestress force, area of prestress, A_{ps}, number of strands and eccentricity at midspan.

The number of strands is laid out to the available bulkhead pattern and the actual eccentricity at midspan, e_m, is calculated (Figure 2.24). For beginning purposes, section properties may be based on gross sections with or without the transformed area of the prestressing steel, as appropriate.

Also, for the purpose of beginning a new design, the top fiber tension may be checked at this point for the initial condition at transfer assuming a transfer stress of 0.70 or $0.75f_{pu}$ for stress relieved or low relaxation strands, respectively. Appropriate checks are midspan, with the self weight bending moment of the girder acting, and at the ends where there is no self weight moment. The prestress force and eccentricity are revised, as necessary. This calculation is refined as iterations improve estimates for the actual number of strands and eccentricity at various sections.

2.4.2.5 Flexural Conditions that Control the Required Prestress Force

For a simply-supported precast pretensioned girder, two conditions generally control:

First - tensile stress in the bottom fiber at mid-span when the girder is in long term service carrying all dead and live loads after all loss of prestress force have occurred.

Second - tensile stress in the top fiber at transfer when the initial force in the strands is released from the stressing bulkheads and transferred to the newly cast section. This is particularly critical at the ends where there is little or no top fiber flexural compression from self weight to offset tensile stress from eccentric prestress force. For the same reason, it is also important over the mid-range of the span where both prestress force and eccentricity are usually at a maximum and induce significant top tension.

(Limits on tensile stress in concrete are given in *AASHTO LRFD* Article 5.9.4.)

The above two conditions occur not only at different times and maturity (strength) of the girder concrete, but apply to structurally different cross sections – the first applies to the non-composite girder section alone at initial transfer and the second to the girder section for most dead load and to the composite section of the deck slab plus girder for superimposed dead and live load.

The objective is to make sure that the final prestressing force is sufficiently large to avoid excessive tensile stress in the bottom fiber in service after all losses, yet not be too large so as to induce cracking in the top at transfer.

2.4.2.6 Incremental Summation of Stress and Final Prestress Strand Selection

The need and technique for an appropriate summation of stresses should be apparent from the foregoing Figures. Once the beginning estimate has been made for the final prestress force and eccentricity at midspan, detailed calculations may commence with the initial transfer conditions, through all intermediate steps, including prestress losses, to conclude with revised final stresses and the actual effective prestress force at each section and elevation of interest. If necessary, revisions are made and the process repeated to attain an optimum solution.

Although iteration may appear tedious, much of the information remains the same (for instance, accumulated applied load stresses). It leads to the required strand pattern and eccentricity after only a few iterations. This can be facilitated by a spreadsheet or computer program. The final controlling bottom fiber tensile limit conditions at midspan are shown in Figure 2.29.

$$f_b = -\frac{P_e}{A} - \frac{P_e * e}{S_b} + \frac{M_{SW}}{S_b} + \frac{M_{SLAB}}{S_b} + \frac{M_{SI}}{S_{bc}} + \frac{M_{L+I}}{S_{bc}} \leq f_{t\,limit}$$

$$f_b = -\frac{P_e}{A} - \frac{P_e * e}{S_b} + \sum f_b \leq f_{t\,limit}$$

Severe corrosion,

$$f_{t\,limit} = 0.0948\sqrt{f'_c}$$

$$P_e = \frac{\sum f_b - f_{t\,limit}}{\frac{1}{A} + \frac{e}{S_b}}$$

Less than moderate corrosion,

$$f_{t\,limit} = 0.19\sqrt{f'_c}$$

AASHTO LRFD Table 5.9.4.2.2-1
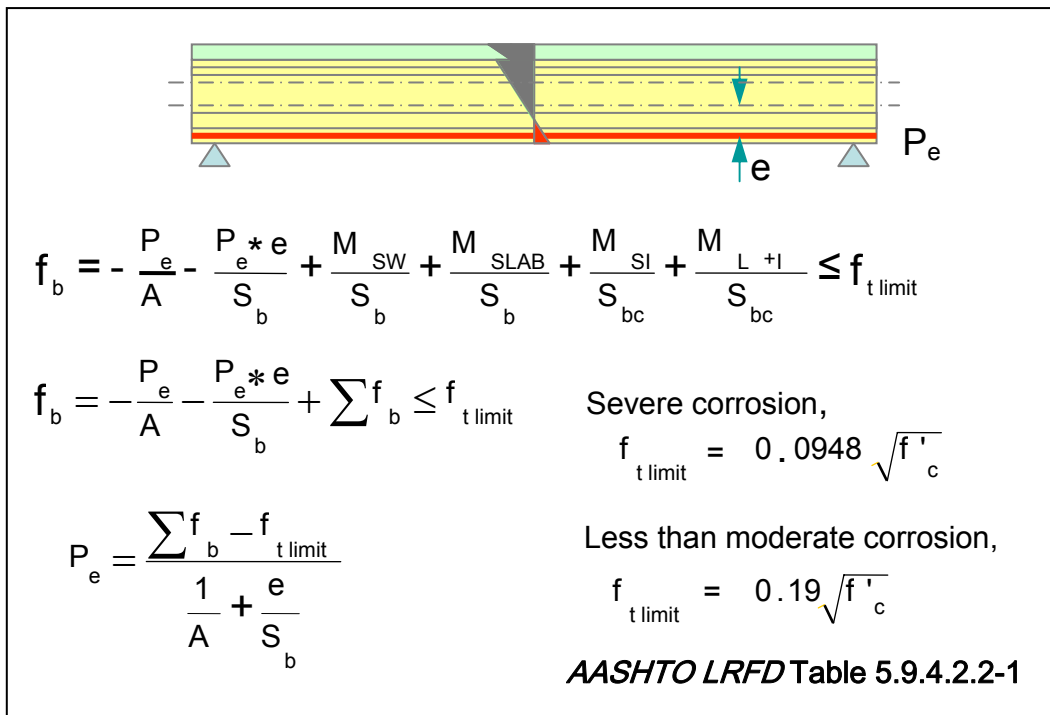
Figure 2.29 Final effective prestress force for bottom fiber tensile limit

The final bottom fiber service stress should be less than the allowable tensile stress – if not increase the prestress force (i.e. number of strands). If the final bottom fiber stress is significantly less than the allowable tensile limit then the number of strands might be decreased. It is a relatively simple task to adjust the magnitude of the final effective prestressing force and eccentricity until the bottom fiber tension is satisfied.

Because the two main variables are the assumed magnitude and eccentricity of the final prestress force, iteration involves only the first two terms of the equations in Figure 2.29. All other stresses in the summation remain unaffected. Summarizing,

the required final prestressing force, P_e, and thus the number of strands, may be determined from:

$$P_e = \frac{\sum f_b - f_{tAllow}}{\dfrac{1}{A} + \dfrac{e}{S_b}}$$

Where $\sum f_b$ = sum of stresses due to permanent gravity loads and the maximum live load in the bottom fiber, calculated and summed for the applicable section properties.

So far, the magnitude of the final prestress force has been set by the first of the controlling criteria, the bottom fiber tensile limit. It is now necessary to reconsider conditions at transfer; properly account for prestress loss at transfer, and if necessary, revise the prestress to satisfy second controlling condition – that of the initial top fiber tension (*AASHTO LRFD* Table 5.9.4.1.2-1).

Loss of prestress occurs due to shrinkage and creep of the concrete and relaxation of the prestressing steel during the time from transfer until the girder is erected and the deck slab cast. Further time dependant losses occur under permanent loads as the deck slab and girder continue to shrink and creep and the prestressing steel relaxes, until these effects gradually diminish, finally reaching a long-term level at which no further loss occurs.

When the calculated prestress loss is incorporated in the incremental summation process (above figures) it leads to the final stresses in Figure 2.30 at each section and elevation of interest. Compression stress in the top of the girder and deck slab should be checked against the maximum limit allowed for the service limit state (*AASHTO LRFD* Article 5.9.4).
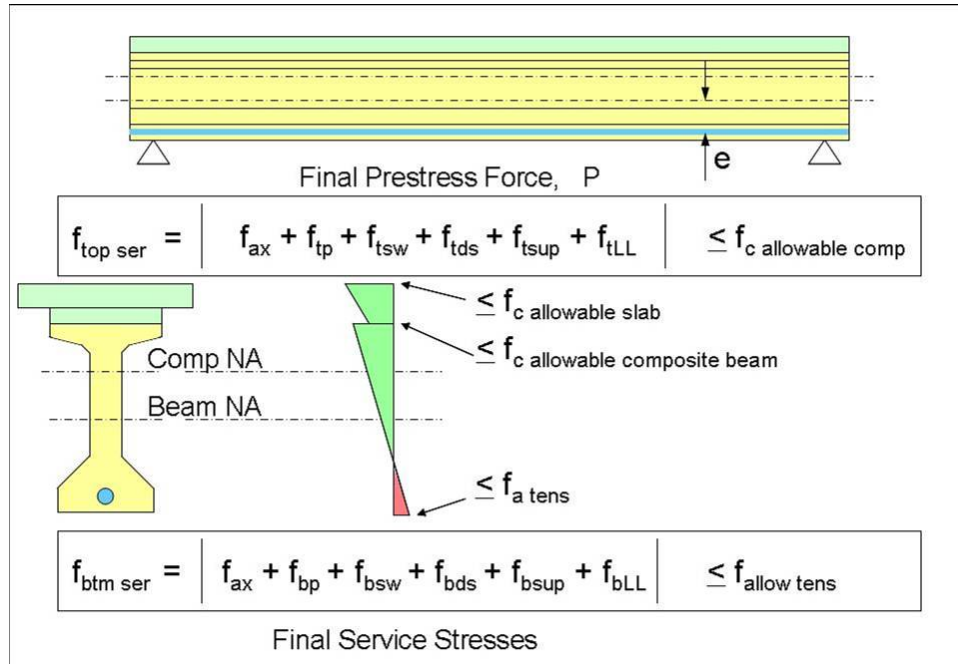
Figure 2.30 Final stresses in service after all prestress losses

The iterative calculation process is illustrated in the flowchart in Figure 2.31a, b, and c. However, before the calculation of prestress loss is considered, it is necessary to examine conditions at transfer and the use of de-bonded or deflected strands to improve the end conditions.
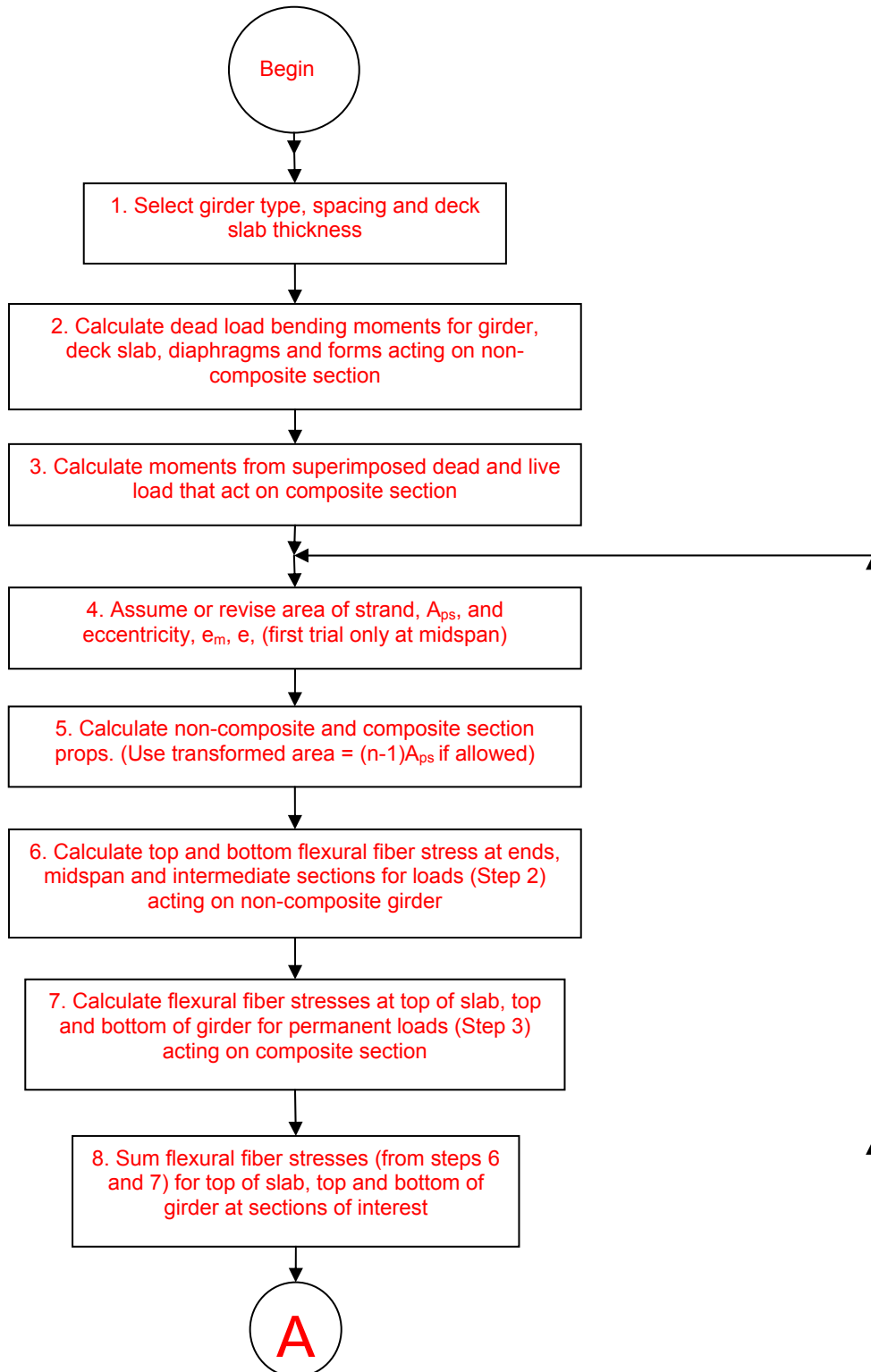
Figure 2.31(a) Flowchart for determination of prestress force and strand pattern, part (a)

A

9. Determine max bottom fiber tension stress at midspan from foregoing (Step 8)

10. Deduct allowable tensile stress to find residual tension

Using transformed A_{ps}?

Yes

No

11. Determine final prestress force, F', and av. eccentricity, e_m, to provide compression of same magnitude acting on non-composite section only

12. Determine or revise area, A_{ps}, number of strands (n_s) and pattern to provide e_m and F', (First time assume final effective stress, f_{pe}, is 55 to 60% f_{pu})

13. Estimate / revise initial prestress force at transfer (First time assume 0.75 to 0.80f_{pu} prior to transfer)

14. Calculate elastic shortening loss, Δf_{pES}, and determine initial force at transfer (F_{pt})

Revise

15. Calculate top fiber stress, $f_{ci\ top}$ at transfer due to initial force, F_{pt}, eccentricity e_m and self weight only

$f_{ci\ top} <$ Limit?

No

Yes

B

Figure 2.31(b) Flowchart for determination of prestress force and strand pattern, part (b)

B

16. Estimate number of strands (n_s), strand pattern and eccentricity, e, and initial force at transfer, F_{pt}, at end of girder (deflect or debond)

17. Calculate top fiber stress, $f_{ci\ top}$, at transfer at ends of girder

$f_{ci\ top} <$ Temporary Limit?

No

Yes

18. Calculate long term losses, Δf_{pLT}, and final effective prestress force, F' (use approximate method)

19. Calculate top and bottom fiber stress for final effect force F', and eccentricity, (e_m, e) applied to the non-composite section properties only

20. Sum results of Step 19 with fiber stresses for dead and live loads from Step 8

Tension and compression stresses < limits?

No

Yes

Revise

C

Proceed with calculations for Strength Limit State

Figure 2.31(c) Flowchart for determination of prestress force and strand pattern, part (c)

2.4.2.7 Stress at Other Locations of Interest

For flexure, at any given cross-section, e.g. mid-span, the final state of stress requires the summation of stress (not moment) from loads and prestress applied first to the non-composite section alone and then to the composite section. Stress is calculated at each elevation at each section of interest for each stage of construction through final conditions. Elevations of interest are usually; top and bottom of non-composite girder and then top of deck slab and top and bottom of girder for the composite section. Sections of interest are midspan, the girder ends, location of deflection points for deflected strands and locations of debonded strands.

In addition, stresses can be calculated or interpolated for intermediate elevations, such as, for example, the elevation of the prestress (for losses), and the neutral axes of the non-composite and composite sections, as necessary. The reason or interest for doing this is that, although not required by code, a designer may consider it prudent to check a residual flexural tensile stress or combine it with a shear stress to provide principal tensile stresses at, say, the elevation of the neutral axes or other location of interest. This is facilitated by keeping a detailed stress accumulation in a program or spreadsheet.

2.4.2.8 Conditions at Transfer

It is essential to check temporary stresses in the girder at transfer (Second controlling conditions). Under the initial release of the strand force in the casting bed, the only load is the self weight of the girder. At transfer, there is far more prestress than necessary just to support the girder itself. The result is that girder flexes upwards and the top experiences flexural tension.

$$f_t = \frac{M_{sw}}{S_t} \qquad f = \frac{P_i}{A} \qquad f_t = \frac{P_i{}^*}{S_t}$$

$$f_b = \frac{M_{sw}}{S_b} \qquad\qquad f_b = \frac{P_i{}^*e}{S_b}$$

SW $\qquad$ $f_{PS\ Axial}$ $\qquad$ $f_{PS\ flexure}$ $\qquad$ SW + PS
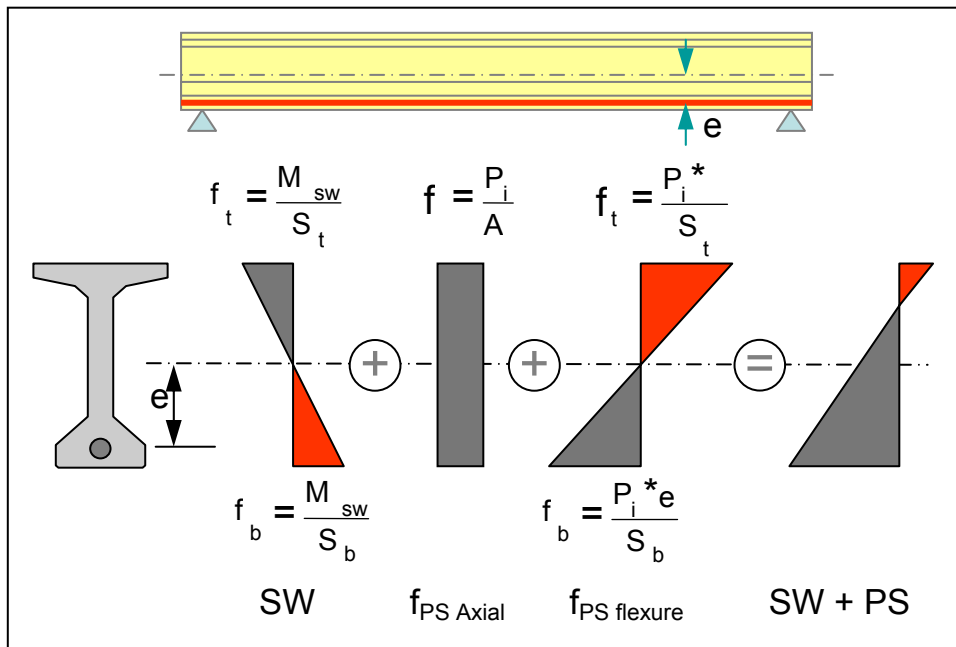
Figure 2.32 Girder self weight and prestress only at transfer

$$f_t = -\frac{P_i}{A} + \frac{P_i e}{S_t} - \frac{M_{SW}}{S_t} \le f_{t\,limit}$$

$$f_{t\,limit} = 0.0948\sqrt{f'_{ci}} \le 0.2\;ksi$$

If sufficient reinforcement is provided,

$$f_{t\,limit} = 0.24\sqrt{f'_{ci}}\;ksi$$

AASHTO LRFD Table 5.9.4.1.2-1

$$f_b = -\frac{P_i}{A} - \frac{P_i\,e}{S_t} + \frac{M_{SW}}{S_t} \le f_{b\,limit}$$

SW + PS

$$f_{b\,limit} = 0.6 f'_{ci}$$
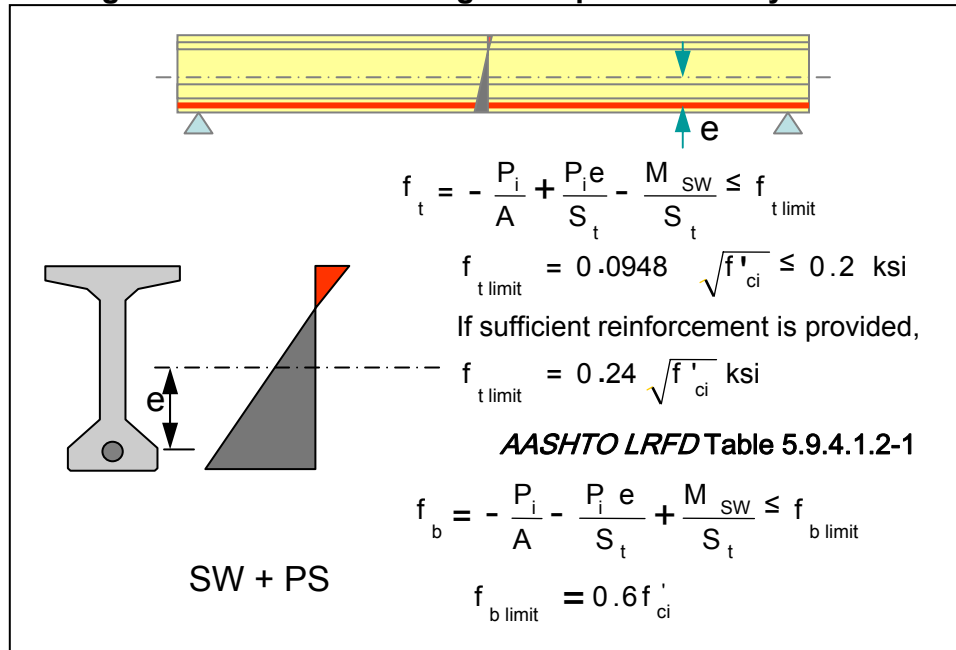
Figure 2.33 Stresses limits at transfer

Top tension can be significant, particularly at the ends where as the self weight moment and compression stress reduces to zero. If the net resultant of the line of prestress is below the kern (the "middle-third") of girder section, top tension is induced. If precautions are not taken to reduce the force and/or eccentricity, the top of the girder may crack. In addition, this tension can make local conditions worse, especially when combined with shear stress in the web or splitting effects from the local, concentrated transfer of prestress. For this reason, even though it is not required by *AASHTO LRFD*, sometimes it is prudent to check the principal tensile stress (Mohr's circle stress) from combined flexural and shear stress.

$$f_t = -\frac{P_i}{A} + \frac{P_i e}{S_t} - \frac{M_{sw}}{S_t} \cancelto{0}{} \leq f_{t\,limit}$$

AASHTO LRFD Table 5.9.4.1.2-1

At ends, PS only
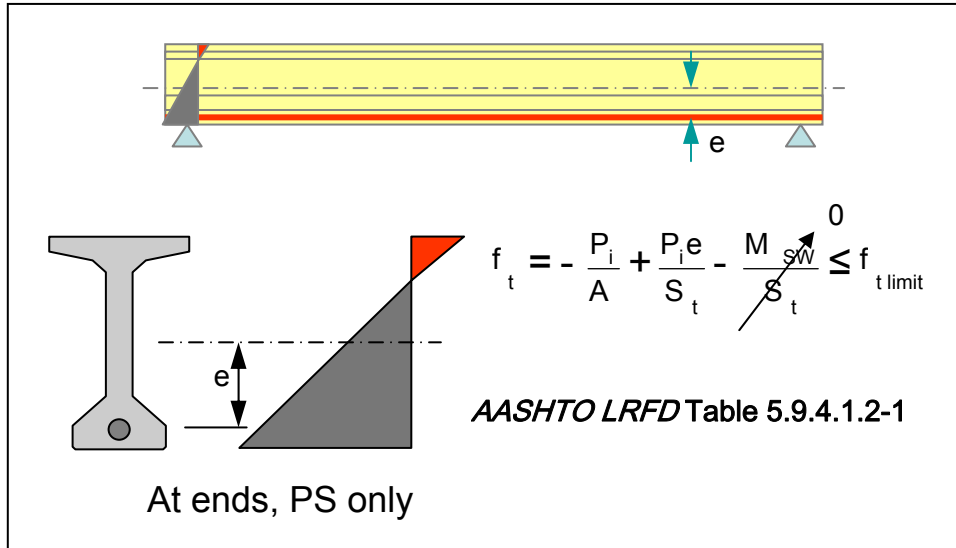
Figure 2.34 End conditions at transfer

2.4.2.8.1 De-bonded Strands

One method of reducing the effective prestress force is to de-bond a number of strands near the ends of the girder using shielding. This reduces the effective force and slightly changes the eccentricity. By shielding a number of strands by different lengths from each end, it is possible to reduce the prestress force in a few steps to best suit the necessary stress conditions both at transfer and under final service loads (Figure 2.35).
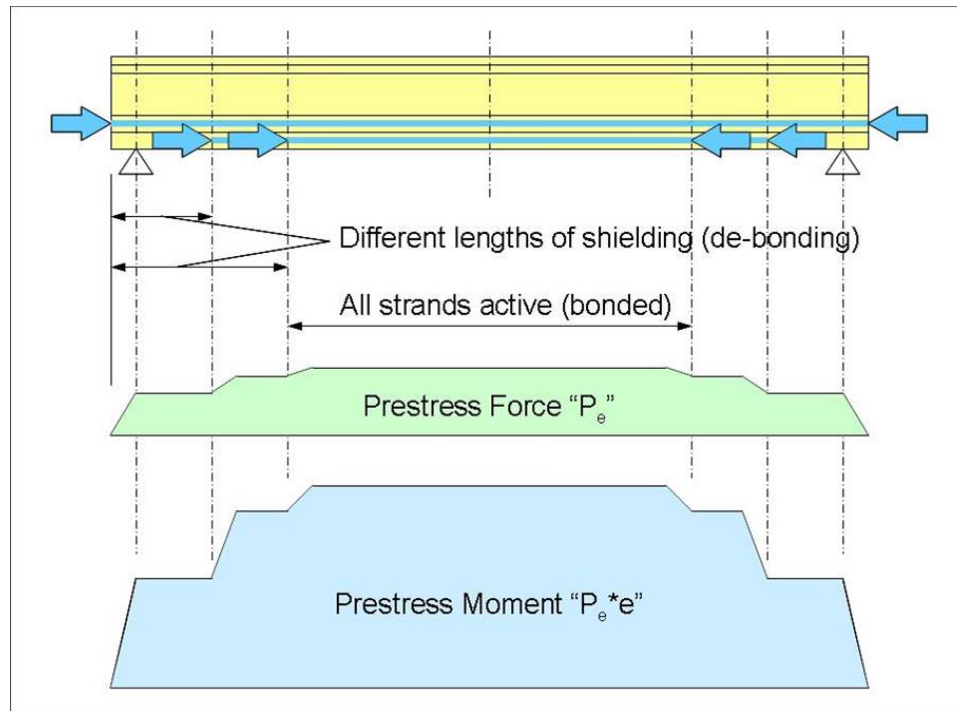
Figure 2.35 Reduction of Prestress Force by Shielding Strands (de-bonding).

The force does not immediate develop at each step because a short distance is needed to effectively transfer the force in each individual strand through bond with the concrete. This is referred to as the transfer length and is typically about 2'-6" for ½" strand. Shielding of strands reduces prestressing force but is usually not sufficient to eliminate top tensile stress altogether while at the same time, retaining sufficient prestress for bottom flexure and other local conditions near the ends of the girders. Consequently, if the top tensile stress exceeds $0.0948\sqrt{f'c}$, (*AASHTO LRFD* Table 5.9.4.1.2-1) it is necessary to provide local longitudinal mild steel reinforcement to carry the total estimated tensile force. Under no circumstances should the tensile stress exceed $0.24\sqrt{f'c}$ (*AASHTO LRFD* Table 5.9.4.1.2-1) – should it do so, then the prestressing force should be modified or a new girder section chosen.

2.4.2.8.2 Deflected Strands

An alternative to debonding is to deflect some of the pre-tensioning strands upwards in the web, from about the one-quarter to one-third points of the span to the ends of the girder. This significantly reduces the eccentricity but does not significantly change the force. It leads to a more ideal, axial prestress condition at the girder ends. Deflected strands can eliminate all top tension at the ends and enhance the shear capacity of the girder at the same time by virtue of the vertical component of the prestressing force. The technique is illustrated in Figure 2.36. It requires the use of special hold-down devices passing through the soffit form and special frames to elevate the deflected strands in the casting bed. As deflection forces can be quite large, care and attention to equipment and procedures is necessary.
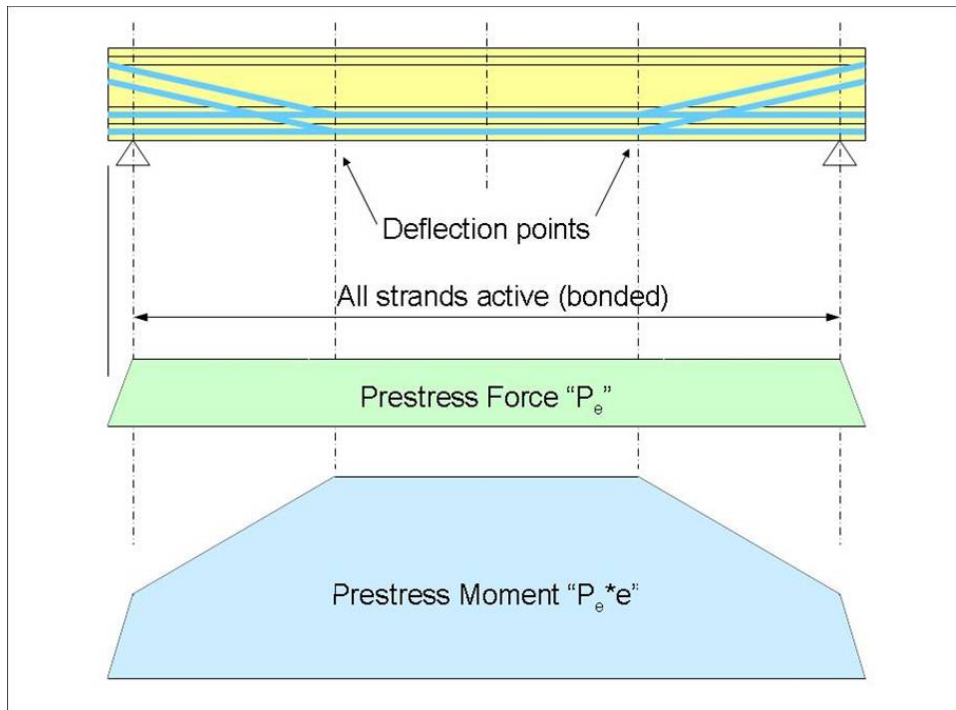
Figure 2.36 Deflected Pre-Tensioning Strands

2.4.2.9 Prestressing Losses

In pretensioned members, loss of prestress force is caused by elastic shortening, shrinkage of the girder and deck, creep of concrete and relaxation of prestressing steel. These losses occur at transfer, during the time the girder is in storage or on site until the deck is cast, and then in the long term after the deck has been cast. They are summarized in Table 2.1.

Table 2.1 Prestress Losses in Pre-Tensioned Girders

Prestress Loss (*AASHTO LRFD* Article 5.9.5.1)	At Transfer	Transfer to Deck Placement	Deck Placement to Final Time
Elastic Shortening	Δf_{pES}		
Shrinkage of Girder		Δf_{pSR}	Δf_{pSD}
Creep of Girder		Δf_{pCR}	Δf_{pCD}
Relaxation of Steel		Δf_{pR1}	Δf_{pR2}
Shrinkage of deck on Composite Section			Δf_{pSS}

Briefly summarizing, the terms for prestress loss (expressed in ksi) in the above table are:

Δf_{pES} = Elastic shortening under the initial prestress force at transfer.

Δf_{pSR} = Shrinkage of girder concrete between transfer and deck placement.

Δf_{pCR} = Creep of girder concrete between transfer and deck placement.

Δf_{pR1} = Relaxation of prestressing strands between transfer and deck placement.

Δf_{pR2} = Relaxation of prestressing strands in composite section after deck placement.

Δf_{pSD} = Shrinkage of girder concrete after deck placement to final time.

Δf_{pCD} = Creep of girder concrete after deck placement to final time.

Δf_{pSS} = Shrinkage of deck composite section.

In pretensioned girders, elastic shortening (Δf_{pES}) is an instantaneous loss that occurs when the strands are released in the casting bed and the initial force is transferred to the concrete. It is calculated according to *AASHTO LRFD* Article 5.9.5.2.3.

For pretensioned members, *AASHTO LRFD* Article 5.9.5.4 permits a refined estimate of time dependant prestress loss where each of the above terms (except elastic shortening) is evaluated discretely for various elements such as relevant material properties, structure proportions and environmental conditions; i.e. the long term prestress loss is given by:

$$\Delta f_{pLT} = (\Delta f_{pSR} + \Delta f_{pCR} + \Delta f_{pR1})_{initial} + (\Delta f_{pR2} + \Delta f_{pSD} + \Delta f_{pCD} - \Delta f_{pSS})_{final}$$

The various elements that influence these terms include;

➢ The strength of the concrete (f'_{ci}) at time of initial loading (transfer)

➢ The age of the concrete (t_i) when load is initially applied (transfer)

➢ The maturity of the concrete (t, days) between the time of loading for creep calculations, or the end of curing for shrinkage calculations, and the time being considered for analysis of creep or shrinkage effects.

➢ The volume to surface ratio of the component (V/S)

> ➢ The annual average ambient relative humidity (%)

> ➢ The modulus of elasticity of prestressing steel (E_p)

> ➢ The modulus of elasticity of concrete at transfer (E_{ci})

> ➢ The modulus of elasticity of concrete at transfer or load application (E_{ct})

> ➢ The modulus of elasticity of deck concrete (E_{cd})

> ➢ The type of prestressing strand, whether low relaxation or other

Along with composite and non-composite section properties, structural proportions and area of prestressing steel, the above elements are accounted for either directly in the various formulae in *AASHTO LRFD* Article 5.9.5.4 or indirectly via the creep coefficient $\Psi(t,t_i)$ defined in *AASHTO LRFD* Article 5.4.2.3.2. The latter is also used as a modifier for shrinkage effects with time on the basis that both creep and shrinkage have similar time development patterns – especially for modern concrete mixes with high range water reducing admixtures and relatively low water/cement ratios (Commentary, *AASHTO LRFD* Article C.5.4.2.3.2).

The various refined formulaic relationships in *AASHTO LRFD* Article 5.9.5.4 for each of the prestressing losses in the above table have been established algebraically or experimentally, and because of their complexity, will not be repeated here. Computation of losses using such complex formulae, applied at various elevations and sections along the girder, has really only been made feasible by the widespread use of computers and spreadsheets.

More empirical and approximate relationships used previously have been retained in *AASHTO LRFD* Article 5.9.5.3 for use in cases of standard precast, pretensioned girders, subject to normal loading and environmental conditions; providing that components are made from normal weight concrete, are either steam- or moist-cured, with prestressing of bars or strands and the site is of average exposure and temperatures.

For the approximate method, the total long term prestress loss (Δf_{pLT}) given by *AASHTO LRFD* Equation 5.9.5.3-1 contains three components for, respectively, creep of concrete, shrinkage of concrete and relaxation of steel – as compared to the seven terms for the refined estimate of *AASHTO LRFD* Article 5.9.5.4. The creep and shrinkage components depend upon the relative humidity (H) but not, in the approximate method, upon the volume to surface ratio (V/S). The latter is accounted for by the limitations placed on the use of the approximate method. Also, the shrinkage of the deck composite section (- Δf_{pSS}) is not accounted for in the approximate method – this is most probably because in the refined method, this term is taken with a negative sign indicating that for a simply supported beam, the effect actually increases the effective prestress force. Thus said, it depends upon the magnitude of the deck slab shrinkage relative to that of the girder and the strain

induced at the elevation of the strands. The approximate method conservatively disregards this effect.

In the approximate method, relaxation of prestressing steel (Δf_{pR}) is taken as a lump sum amount of 2.5 ksi for low relaxation strands, 10.0 ksi for normal strands or as given by the manufacturer – as compared to a formulation that also depends upon the stress in the strands at transfer (*AASHTO LRFD* Equation 5.9.5.4.2c-1) in the refined method.

AASHTO LRFD also permits the use of the CEB-FIP (European) model code or ACI 209 for estimates of creep and shrinkage in the absence of mix-specific data (*AASHTO LRFD* Article 5.4.2.3.1). For information, a comparison of results for different codes based upon a limited number of structures is offered in Figure 2.15, above. The results show an apparent difference between CEB-FIP and ACI 209 for individual calculation of creep or shrinkage; but the overall sum of both effects would seem similar. Such differences, perhaps not so pronounced, can be expected when using different codes. For construction of a major project, it is best to adopt a formulation for long term creep and shrinkage that is agreed between the different parties to the contract – for example, between the Designer on the one hand and the Contractor's Engineer on the other. This should help resolve or avoid otherwise potential differences in the calculation of intermediate staged construction conditions, deflections and camber.

2.4.2.10 Service Limit Verification (Flexure)

Once the loss prestressing force has been determined from the above effects, using either the refined or approximate method, the final prestressing force is known. It is a simple matter then to return to the summation of stress (shown above) and recalculate the final conditions. This process is repeated at as many sections of interest as necessary along the length of the girder. These should also include the locations at which shielding (debonding) of strands terminates.

If it is not possible to satisfy the allowable stress limits in the code – for both tension and compression at transfer and final conditions – then the prestressing force or and eccentricity should be revised or a new girder section chosen. Alternatively, using the same section, adding a girder line might solve the problem by reducing moments and forces on the critical member. Allowable stresses are given in *AASHTO LRFD* Article 5.9.4.

There are no specific rules in *AASHTO LRFD* that limit the shear stress or principal tensile (Mohr's circle) stress in the webs of prestressed concrete girders. If necessary, guidance is offered by reference to those parts of *AASHTO LRFD* Tables 5.9.5.4.1.2-1 and 3 that address principal stress conditions at the neutral axis of the web in segmental structures.

For the prestressing steel, the initial stress at transfer and final stress after all losses should not exceed the limits in *AASHTO LRFD* Table 5.9.3-1. To illustrate, consider for example: For Grade 270ksi, low relaxation strand at transfer the stress should not

exceed $0.75f_{pu}$ = 0.75*270 = 203ksi. After all losses, the stress should not exceed $0.80f_{py}$. If it is assumed that the yield stress is, say, 90% of the ultimate strength, then the final stress should be less than 0.80*0.90*270 = 194ksi. In general, for pretensioned girders, the final stress after losses is rarely greater than $0.65f_{pu}$ = 0.65*270 = 175ksi – so this latter condition is usually satisfied.

2.4.2.11 Deflection and Camber

2.4.2.11.1 Deflection

All girders deflect under load. The amount of deflection depends upon the magnitude of the load and flexural stiffness of the girder as represented by the product "EI" of the modulus of elasticity of the concrete, E, and the inertia of the section, I. A simply-supported girder deflects downward under the action of gravity loads and deflects upwrds as a result of internal prestress forces. For example, consider an axial prestress force, F, at an eccentricity, e_m, below the neutral axis. This creates a mostly constant negative moment, $M = -F.e_m$, that flexes the girder upward. At transfer in the casting bed, this upward prestress deflection is only partially countered by the self-weight deflection of the girder alone. The net effect at transfer is a residual upward deflection. The girder lifts off the bed, being supported at its ends. This is clearly noticeable in the Type 4 girders in storage at a casting yard in Figure 2.37.

Figure 2.37 Residual, upward deflection from prestress and self-weight

After erection, under the weight of the deck slab and forms, a girder will again deflect downward. Finally, after construction, a girder will continue to deflect due to creep under the total effect of all permanent loads (prestress and dead load).

2.4.2.11.2 Camber

To compensate for deflections it is necessary to determine the elevations to which the bearings should be set, those to which the deck should be cast and the variable depth of the haunch (build-up) over the girders to which the deck forms should be set at the time of construction so that deck elevations will be correct in the long-term configuration. Making such adjustments to compensate for deflections is referred to as "camber". It is basically the difference between the vertical profile to which the deck should be cast and the desired highway geometry vertical profile grade. Deriving correct "camber" requires calculation of deflections for various load conditions.

For a simply-supported structure, deflections are determined for:

a) The self weight of the girder at transfer (downward).
b) The prestress in girder at transfer (upward but greater than magnitude of (a))
c) The growth of the net deflection of the above due to creep during the time from transfer to casting the deck slab (upward).
d) The deflection of the girder under the weight of the wet concrete deck slab, diaphragms and deck forms (downward).
e) The recovery of deflection of the now composite section when forms are removed (usually slight and sometimes disregarded).
f) The deflection of the composite section under the weight of superimposed dead load.
g) The growth of deflection of the composite section due to creep under all sustained permanent effects from the time of casting the slab to final long-term conditions. This includes the creep of the non-composite girder itself due to the locked in forces at the time of casting the slab. This may also include the effect of the differential shrinkage of the deck slab relative to the girder, if it is significant.

Deflections may be calculated at intervals along the span. Some of the deflections may be relatively small and inconsequential as far as making adjustments in the field. However, it should be evident that there is an important need to calculate deflections in order to establish bearing and girder elevations and the depths of haunches (build-ups).

2.4.2.11.3 Calculation of Deflection

Calculation of deflection is based upon routine Euler-Bernoulli Beam Theory. Using Euler-Bernoulli beam behavior requires the following assumptions:

➢ The girder length is much greater than its width or depth
➢ Load is applied in the vertical plane and symmetric to the section
➢ Deflections are small
➢ Plane sections remain plane
➢ The material has linear-elastic behavior
➢ Materials are isotropic

Under these conditions, the classic Euler-Bernoulli equations for deflection and rotation of a portion of a beam given a constant value of EI, are given in Figure 2.38.

$$\frac{dV}{dx} = p$$

p = load

V = shear

$$\frac{dM}{dx} = V \qquad EI\frac{d^4w}{dx^4} = p$$

M = moment

ϕ = curvature

$$\frac{d\theta}{dx} = \phi = \frac{M}{EI} \qquad \text{(EI = constant)}$$

θ = rotation

w = deflection

$$\frac{dw}{dx} = \theta$$

Figure 2.38 Euler-Bernoulli Equations for Deflection and Rotation

Solution and application of the above equations is possible using different methods, such as rigorous mathematics, numerical integration, area-moment, slope-deflection, McCauley's method, virtual work (Castigliano) or other beam analysis methods, published design aids or stiffness solution by matrix inversion. The classical solution for a uniform load on a simply-supported beam is given in Figure 2.39.

$$V = -px + \frac{pL}{2} \qquad \Delta_{max} = \frac{5pL^4}{384EI}$$

$$M = -\frac{px^2}{2} + \frac{pLx}{2} \qquad \text{(EI = constant)}$$

$$\theta = -\frac{px^3}{6EI} + \frac{pLx^2}{4EI} + \frac{pL^3}{24EI} \qquad \begin{array}{l} p = \text{uniform load (k/ft)} \\ L = \text{Span} \end{array}$$

$$\Delta = -\frac{px^4}{24EI} + \frac{pLx^3}{12EI} - \frac{pL^3x}{24EI}$$
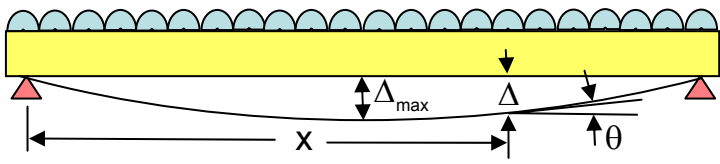
Figure 2.39 Deflection of a Beam under Uniform Load

In lieu of using rigorous classical methods, other techniques are available to the engineer for the computation of deflections of prestressed concrete girders. These techniques include: numerical integration, area-moment, slope-deflection, virtual work, published design aids, and computer based stiffness solutions.

Newmark's Method of Numerical Analysis (Figure 2.40) divides a girder into segments of convenient length. Bending moments are determined by statics, and curvatures are found along the girder by dividing the bending moment by the modulus of elasticity and the girder inertia (EI). The distributed curvatures are concentrated to nodes at the ends of the segments using concentration formulas (Figure 2.41). The concentrated curvatures are summed across the girder to give the slopes of the individual segments. The chord slopes are then multiplied by the segment length to give deflection increments, which in turn are summed to find girder deflections. This solution begins with a boundary condition of no rotation or deflection at the first node. Corrections may need to be applied in order to satisfy actual boundary conditions.
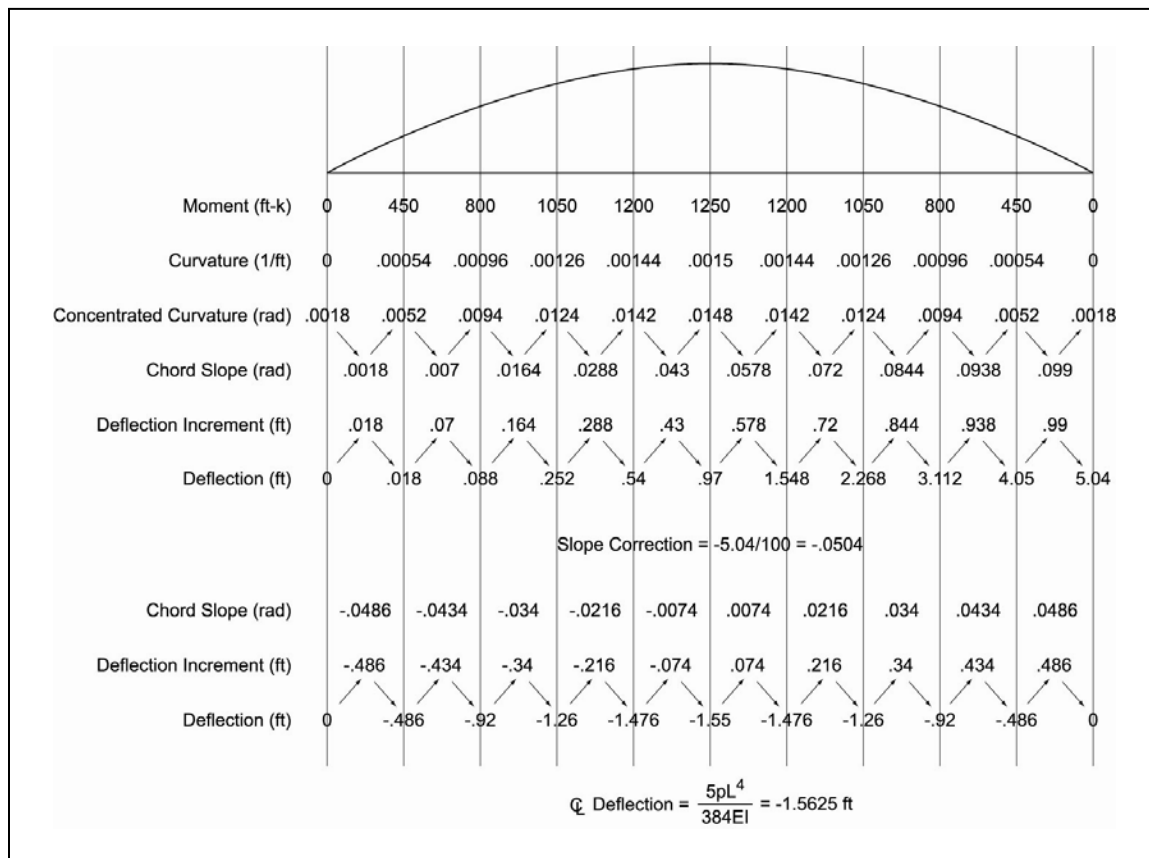
Figure 2.40 Numerical integration for slopes and deflections (Newmark)

For comparison, the maximum deflection for the simply-supported girder using numerical integration is found to be 1.55 feet units; whereas classical (rigorous) formulae gives 1.5625 feet units – i.e. sufficiently good agreement for practical purposes.

Using a greater number of intervals will improve the accuracy of the numerical integration. Alternatively, a refinement to improve the numerical accuracy is to use trapezoidal concentration formulae illustrated in Figure 2.41.

$$R1_{i-1} = \frac{L_{i-1}}{6}(2k_{i-1} + k_i)$$

$$R2_{i-1} = \frac{L_{i-1}}{6}(2k_i + k_{i-1})$$

$$R1_i = \frac{L_i}{6}(2k_i + k_{i+1})$$

$$R2_i = \frac{L_i}{6}(2k_{i+1} + k_i)$$

Concentrated Curvature at i = $R_i = R_{i-1} + R_i$
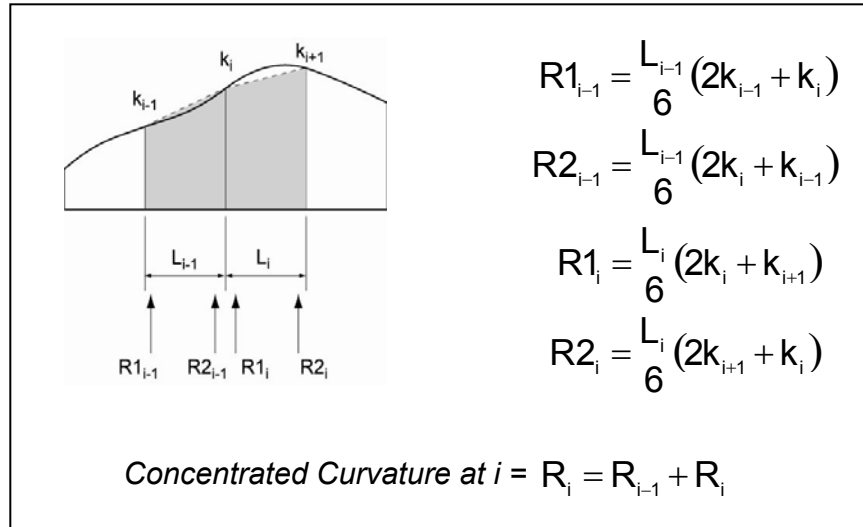
Figure 2.41 Trapezoidal concentration formulae for equivalent smooth curve

Numerical integration methods are readily adaptable to spreadsheet computation and may, in principle, be extended to spans of variable depth and continuous structures.

Many design aids are available for calculating deflections for the more commonplace types of load found in bridge applications; namely, uniformly distributed loads, partial distributed loads and point loads. Eight solutions for external load on a simply supported beam are provided in Figure 2.42(a) and (b).

In addition to applied (gravity) loads, the same approach is used to calculate upward girder deflections from the effects of prestress. A practical approach is to reduce prestress effects to a set of equivalent loads that can be applied "externally". Deflections are then calculated for these equivalent loads using any of the above methods. Figure 2.43 illustrates equivalent loads and deflections for the most commonly encountered prestress patterns.

(1) SIMPLE BEAM – UNIFORMLY DISTRIBUTED LOAD

$R = V$ .... $= \dfrac{w\ell}{2}$

V_x .... $= w\left(\dfrac{\ell}{2} - x\right)$

M_{MAX} (AT CENTER)......................... $= \dfrac{w\ell^2}{8}$

M_x .... $= \dfrac{wx}{2}(\ell - x)$

Δ_{MAX} (AT CENTER) .... $= \dfrac{5w\ell^4}{384\,EI}$

Δ_x .... $= \dfrac{wx}{24\,EI}(\ell^3 - 2\ell x^2 + x^3)$
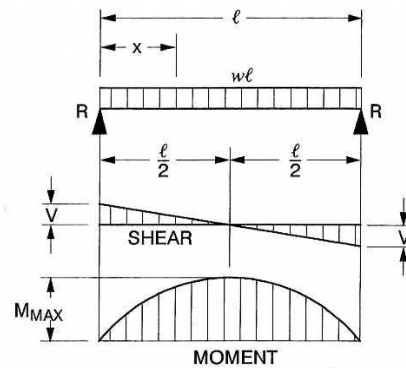
(2) SIMPLE BEAM – CONCENTRATED LOAD AT CENTER

$R = V$ .... $= \dfrac{P}{2}$

M_{MAX} (AT POINT OF LOAD) .... $= \dfrac{P\ell}{4}$

M_x $\left(\text{WHEN } x < \dfrac{\ell}{2}\right)$ .... $= \dfrac{Px}{2}$

Δ_{MAX} (AT POINT OF LOAD) .... $= \dfrac{P\ell^3}{48\,EI}$

Δ_x $\left(\text{WHEN } x < \dfrac{\ell}{2}\right)$ .... $= \dfrac{Px}{48\,EI}(3\ell^2 - 4x^2)$
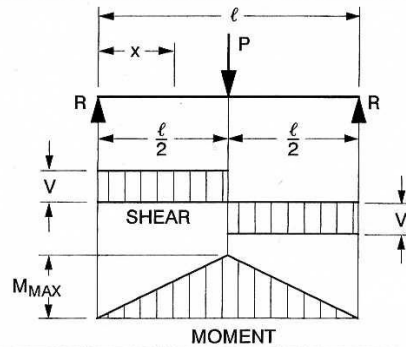
(3) SIMPLE BEAM – CONCENTRATED LOAD AT ANY POINT

$R_1 = V_1$ (MAX WHEN $a < b$) .... $= \dfrac{Pb}{\ell}$

$R_2 = V_2$ (MAX WHEN $a > b$) .... $= \dfrac{Pa}{\ell}$

M_{MAX} (AT POINT OF LOAD) .... $= \dfrac{Pab}{\ell}$

M_x (WHEN $x < a$) .... $= \dfrac{Pbx}{\ell}$

$\Delta_{MAX}\left(\text{AT } x = \sqrt{\dfrac{a(a + 2b)}{3}} \text{ WHEN } a > b\right)$ .. $= \dfrac{Pab\,(a + 2b)\,\sqrt{3a\,(a + 2b)}}{27\,EI\,\ell}$

Δ_a (AT POINT OF LOAD) .... $= \dfrac{Pa^2 b^2}{3\,EI\,\ell}$

Δ_x (WHEN $x < a$) .... $= \dfrac{Pbx}{6\,EI\,\ell}(\ell^2 - b^2 - x^2)$
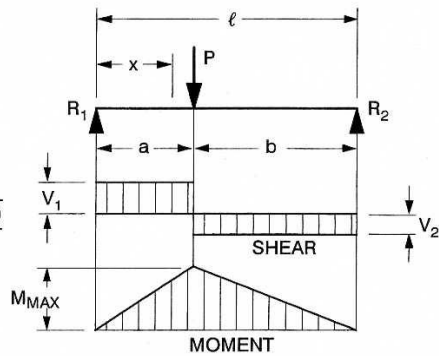
(4) SIMPLE BEAM – TWO EQUAL CONCENTRATED LOADS SYMMETRICALLY PLACED

$R = V$ .... $= P$

M_{MAX} (BETWEEN LOADS) .... $= Pa$

M_x (WHEN $x < a$) .... $= Px$

Δ_{MAX} (AT CENTER) .... $= \dfrac{Pa}{24\,EI}(3\ell^2 - 4a^2)$

Δ_x (WHEN $x < a$) .... $= \dfrac{Px}{6\,EI}(3\ell a - 3a^2 - x^2)$

Δ_x (WHEN $x > a$ AND $< (\ell - a)$) ...... $= \dfrac{Pa}{6\,EI}(3\ell x - 3x^2 - a^2)$
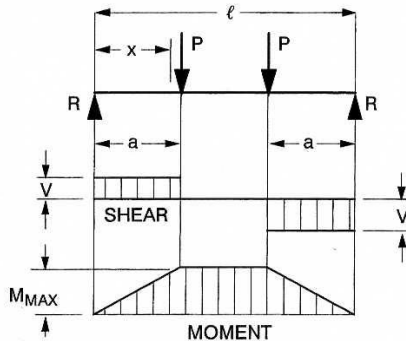
Figure 2.42(a) Deflection of simply-supported beam under external load

(5) SIMPLE BEAM – TWO UNEQUAL CONCENTRATED LOADS UNSYMMETRICALLY PLACED

$R_1 = V_1 \dots\dots = \dfrac{P_1(\ell-a)+P_2 b}{\ell}$

$R_2 = V_2 \dots\dots = \dfrac{P_1 a + P_2(\ell-b)}{\ell}$

V_x (WHEN $x > a$ AND $< (\ell-b)$) $\dots = R_1 - P_1$

M_1 (MAX WHEN $R_1 < P_1$) $\dots\dots = R_1 a$

M_2 (MAX WHEN $R_2 < P_2$) $\dots\dots = R_2 b$

M_x (WHEN $x < a$) $\dots\dots = R_1 x$

M_x (WHEN $x > a$ AND $< (\ell-b)$) $\dots = R_1 x - P_1(x-a)$
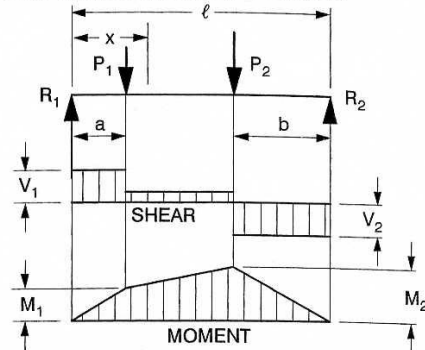
(6) SIMPLE BEAM – UNIFORM LOAD PARTIALLY DISTRIBUTED

$R_1 = V_1$ (MAX WHEN $a < c$) $\dots = \dfrac{wb}{2\ell}(2c+b)$

$R_2 = V_2$ (MAX WHEN $a > c$) $\dots = \dfrac{wb}{2\ell}(2a+b)$

V_x (WHEN $x > a$ AND $< (a+b)$) $\dots = R_1 - w(x-a)$

M_{MAX} $\left(\text{AT } x = a + \dfrac{R_1}{w}\right) \dots = R_1\left(a+\dfrac{R_1}{2w}\right)$

M_x (WHEN $x < a$) $\dots\dots = R_1 x$

M_x (WHEN $x > a$ AND $< (a+b)$) $\dots = R_1 x - \dfrac{w}{2}(x-a)^2$

M_x (WHEN $x > (a+b)$) $\dots\dots = R_2(\ell-x)$
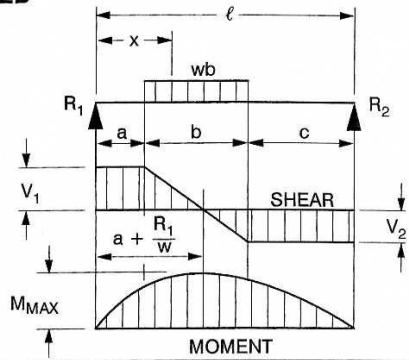
(7) SIMPLE BEAM – LOAD INCREASING UNIFORMLY TO ONE END (W IS TOTAL LOAD)

$R_1 = V_1 \dots\dots = \dfrac{W}{3}$

$R_2 = V_2$ MAX $\dots\dots = \dfrac{2W}{3}$

$V_x \dots\dots = \dfrac{W}{3} - \dfrac{Wx^2}{\ell^2}$

M_{MAX} $\left(\text{AT } x = \dfrac{\ell}{\sqrt 3} = .5774\ell\right) \dots = \dfrac{2W\ell}{9\sqrt 3} = .1283\,W\ell$

$M_x \dots\dots = \dfrac{Wx}{3\ell^2}(\ell^2 - x^2)$

Δ_{MAX} $\left(\text{AT } x = \ell\sqrt{1-\sqrt{\tfrac{8}{15}}} = .5193\,\ell\right) = .01304\dfrac{W\ell^3}{EI}$

$\Delta_x \dots\dots = \dfrac{Wx}{180\,EI\,\ell^2}(3x^4 - 10\ell^2 x^2 + 7\ell^4)$
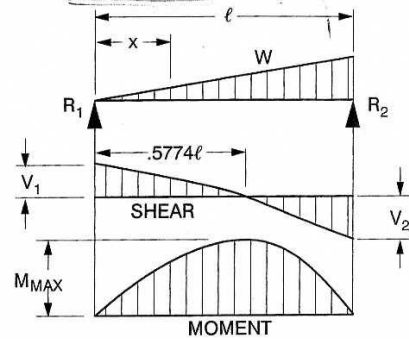
(8) SIMPLE BEAM – LOAD INCREASING UNIFORMLY TO CENTER (W IS TOTAL LOAD)

$R = V \dots\dots = \dfrac{W}{2}$

V_x $\left(\text{WHEN } x < \dfrac{\ell}{2}\right) \dots = \dfrac{W}{2\ell^2}(\ell^2 - 4x^2)$

M_{MAX} (AT CENTER) $\dots\dots = \dfrac{W\ell}{6}$

M_x $\left(\text{WHEN } x < \dfrac{\ell}{2}\right) \dots = Wx\left(\dfrac{1}{2} - \dfrac{2x^2}{3\ell^2}\right)$

Δ_{MAX} (AT CENTER) $\dots\dots = \dfrac{W\ell^3}{60\,EI}$

Δ_x $\left(\text{WHEN } x < \dfrac{\ell}{2}\right) \dots = \dfrac{Wx}{480\,EI\,\ell^2}(5\ell^2 - 4x^2)^2$
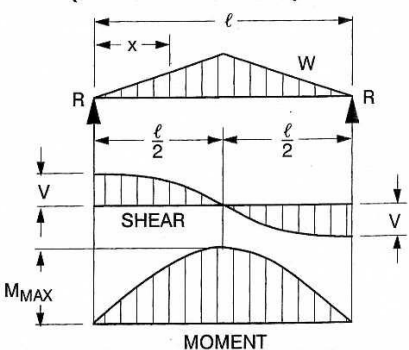
Figure 2.42 (b) Deflection of simply-supported beam under external load

PRESTRESS PATTERN	EQUIVALENT MOMENT OR LOAD	EQUIVALENT LOADING	CAMBER $+\uparrow$	END ROTATION $\angle\,+$	END ROTATION $+\,\angle$
(1)	$M = Pe$		$+\dfrac{M\ell^2}{16EI}$	$+\dfrac{M\ell}{3EI}$	$-\dfrac{M\ell}{6EI}$
(2)	$M = Pe$		$+\dfrac{M\ell^2}{16EI}$	$+\dfrac{M\ell}{6EI}$	$-\dfrac{M\ell}{3EI}$
(3)	$M = Pe$		$+\dfrac{M\ell^2}{8EI}$	$+\dfrac{M\ell}{2EI}$	$-\dfrac{M\ell}{2EI}$
(4)	$N = \dfrac{4Pe'}{\ell}$		$+\dfrac{N\ell^3}{48EI}$	$+\dfrac{N\ell^2}{16EI}$	$-\dfrac{N\ell^2}{16EI}$
(5)	$N = \dfrac{Pe'}{b\ell}$		$+\dfrac{b(3-4b^2)N\ell^3}{24EI}$	$+\dfrac{b(1-b)N\ell^2}{2EI}$	$-\dfrac{b(1-b)N\ell^2}{2EI}$
(6)	$w = \dfrac{8Pe'}{\ell^2}$		$+\dfrac{5w\ell^4}{384EI}$	$+\dfrac{w\ell^3}{24EI}$	$-\dfrac{w\ell^3}{24EI}$

Figure 2.43 Deflection of a girder under some common prestress patterns

2.4.2.11.4 Deck Slab Elevations and Height of Haunch (Build-Up)

After calculating girder deflections for each of the key conditions (a through g) in 2.5.11.2 above, the elevations to which the deck slab should be cast and the height of the haunch (build-up) should be set, can be calculated, as follows.

If the basic highway geometric elevation (allowing for superelevation) at a section of interest on a particular girder line is say PG, and the Owner specified minimum height of haunch is h $_{min}$, then the required elevation for the deck slab (on the vertical centerline of the girder) is given by:

Deck slab casting elevation   =   [PG + g + f - e] + h $_{min}$

The camber, C, i.e. the difference between the deck slab concrete elevation required at the time of casting the slab and the basic final highway geometric profile grade, is

Camber, C=   [g + f - e] + h $_{min}$

Where g, f and e are the numerical magnitudes of the deflections calculated above.

The required height of haunch (build-up), say, H, at a location along the girder is given by:

$$\text{Haunch,} \quad H \quad = \quad [g + f - e + d - (b - a + c)] + h \min$$

Where again, items a through g are taken as numerical magnitudes. The maximum height of the haunch is calculated at the ends of the girder (i.e. at the bearings). This then leads to setting elevations for the bearings.

Appropriate adjustments should be made to the above equations to allow for superelevation across the top flange width of the girder, as necessary, or for any other similar basic geometric requirements of the highway and structure.

It is important to recognize that the actual deflection of a girder (upwards) at the time of delivery can be significantly different from the theoretically calculated value (i.e. the theoretical value given by: (b –a + c)). This difference is likely for a number of reasons; for example, difference in material properties such as assumed and actual modulus of elasticity, creep and shrinkage properties, difference in stressing and release assumptions, curing and exposure of the girder while in storage, and so forth. Consequently, haunch heights should be shown along with corresponding deflections and the theoretical assumptions underlying the calculated deflections. A Contractor can then make appropriate adjustments for setting forms and deck slab casting elevations in the field.

2.4.3 Longitudinal Flexure Design (Strength Limit State)

2.4.3.1 Introduction

Figure 2.4 in DM Section 2.1.2 presented the goal of prestressing in offsetting flexural tension in girders produced by self weight and externally applied loads. DM Section 2.4.2 of this manual presented the methodology and requirements for selecting the number and location of prestressing strands to satisfy the Service Limit States for girder flexure. This section presents the approach by which the girders, now designed for flexural service conditions, are verified at the Strength Limit State. Figure 2.44 depicts a girder subjected to a loading beyond the flexural tension capacity of a simple span girder. As the flexural tension capacity is exceeded, the girder cracks leading to failure of the girder. To offset the inability of the concrete to resist significant tension, reinforcing bars are added in the tension regions. As load is applied the girder deflects, the reinforcing strains, and force, in accordance with Hooke's Law, is produced in the steel. This tensile force in the steel is counteracted by compression in the girder concrete. These balancing tensile and compressive forces multiplied by the lever arm between the centroids of action produce an internal bending moment resisting the moments caused by the applied loads. The bottom portion of Figure 2.44 shows the relationship of girder cross section, strains produced by loads, forces in the steel and concrete and the resisting moment.
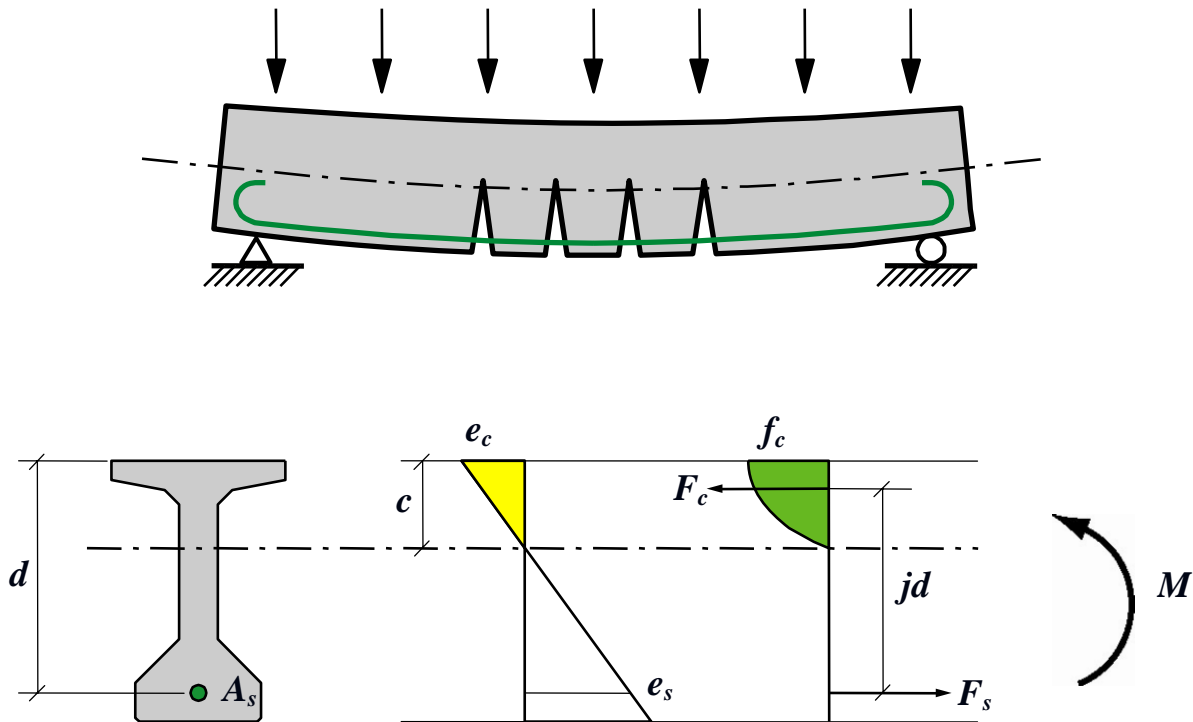
Figure 2.44 Ultimate Flexural Resistance in Girders

The internal resistance described above is fundamentally the same whether a girder is reinforced with mild reinforcing or prestressing strands. Results differ, however, as a result of material differences between mild reinforcing and prestressing steel, and the state of stress in the steel at the onset of loading. See Section 2.2 in this Volume for material characteristics. With regard to the state of stress at loading, there is no initial strain in the reinforcing steel of a reinforced concrete girder when first subjected to loading. Prestressed girders, however, have a significant stress as a result of the jacking operation. The strain produced by external loads at the Strength Limit State is in addition to the initial stresses.

2.4.3.2 Loads at Strength Limit State

Load factors for the Strength Limit State are addressed in DM Volume I, Chapter 5.

2.4.3.3 Strain Compatibility

The LRFD Bridge Design Specifications provides equations for determining the ultimate strength of typical prestressed girders with composite deck slabs. These equations, presented in detail below, were developed from the more generalized approach of considering strain compatibility between the materials at a cross section of a girder subjected to load. Figure 2.45 shows the relationships between strain, stress and force for this more generalized approach.
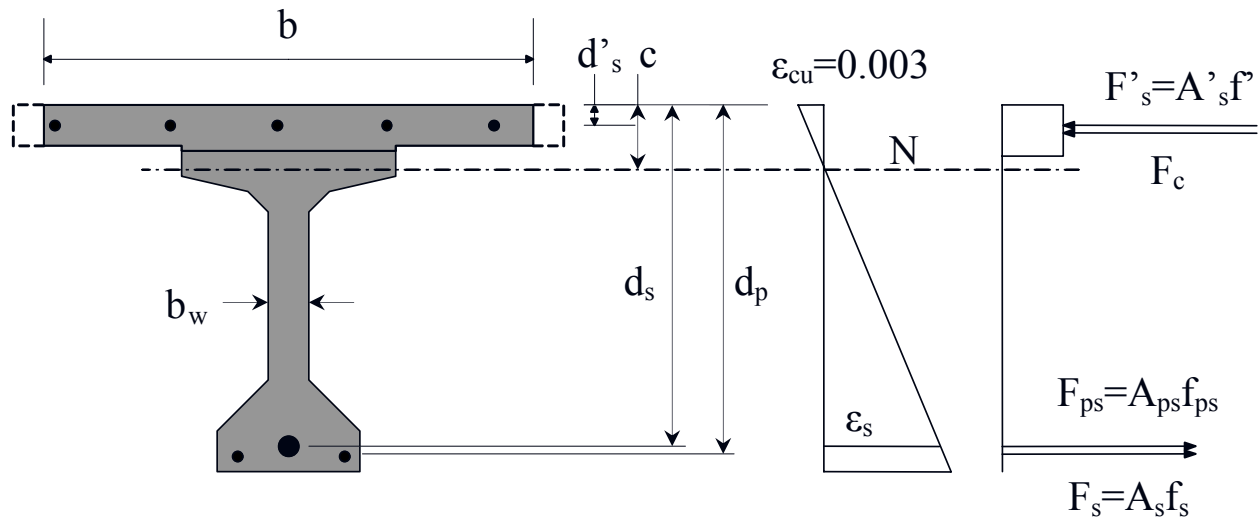
Figure 2.45 Strain Compatibility for a Composite Concrete Girder

where:

b	=	effective width of the slab
b_w	=	width of the web of the prestressed girder
c	=	distance to the neutral axis
d_s	=	distance from the extreme compression fiber to the centroid of mild tension reinforcing
d_p	=	distance from the extreme compression fiber to the centroid of prestressing steel
d'_s	=	distance from the extreme compression fiber to the centroid of mild compression reinforcing
ε_{cu}	=	ultimate strain in the concrete
ε_s	=	strain in a layer of reinforcing or prestressing steel
A_s	=	area of flexural tension reinforcing
A_{ps}	=	area of prestressing steel
A'_s	=	area of compression reinforcing
f_s	=	stress in the flexural tension reinforcing
f_{ps}	=	stress in the prestressing steel
f'_s	=	stress in the compression reinforcing
F_s	=	force in the flexural tension reinforcing
F_{ps}	=	force in the prestressing steel
F'_s	=	force in the compression reinforcing
F_c	=	force in the concrete

2.4.3.4 Code Equations

Application of strain compatibility in the AASHTO LRFD Bridge Design Specifications is based on assumptions that must be considered in order to know when its use is appropriate. These assumptions are:

- Plane sections remain plane during loading. The implication is that strains will be linearly distributed over the depth of the cross section and as a result can be found by simple geometry. The use of strain compatibility to justify members where behavior is contrary to this assumption, such as deep beams, should be avoided.

- The section is said to fail when the extreme concrete compression fiber reaches a strain of ε_{cu} = -0.003 (compression shown as negative). Another assumption is that plane faces remain plane or that the member will displace with linear strain over the cross-section.

- A couple of simplifications are to neglect the tensile strength of the concrete and to model the compressive stress-strain distribution to be rectangular or parabolic.

- The first step in applying the principals of strain compatibility by way of the AASHTO LRFD Bridge Design Specifications is in understanding the Whitney stress block or the equivalent rectangular stress block as it is sometimes called. The equation reads $a=\beta_1 c$. Which is a well-known approximation that the compressive stress can be modeled as a uniform stress with a depth a. The value β_1 is based on experimental studies by Whitney. The β_1 value varies linearly from 0.85 for concrete with a 28 day compressive strength of 4.0 ksi or less to 0.65 for concrete with a 28 day compressive strength of 8.0 ksi or more.
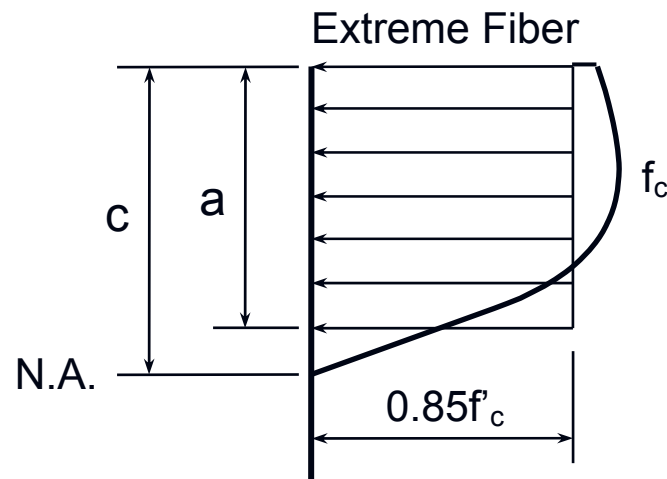
Figure 2.46 Stress Block Assumption

There are two commonly used methods of obtaining the stress in pretensioning steel:

The AASHTO equation which can be used for bonded and closely grouped strands, formula 5.7.3.1.1-1 states:

$$f_{ps} = f_{pu}(1 - k \cdot \frac{c}{d_p})$$

AASHTO LRFD Equation 5.7.3.1.1-1

This equation makes uses the ultimate strength of the steel and makes adjustments for the type of tendon and the ratio of depths of the neutral axis and the depth of the post-tensioning. Since it yields only one prestressing stress, this equation is only appropriate for post-tensioning in one area.

For bonded prestressing which is spread throughout a section the stress in the post-tensioning must be derived from the fundamentals of strain compatibility. Due to the nonlinear nature of steel after yielding, an assumption as to the depth of the neutral axis must be made. Using the neutral axis depth along with the assumption that the extreme compression fiber will be at a strain of -0.003, the linear nature of strain compatibility will reveal a strain at every elevation throughout the member at strength conditions. It is important to remember that unlike the reinforcing steel, the strain in the prestressing steel is not equal to the strain in the surrounding concrete. Allowance must be made for the difference in strain between the steel and the concrete when they are bonded together.   Once this strain is known, the pretensioning stress can be determined by using equations such as those in the PCI Design Handbook fifth edition in Design Aid 11.2.5.
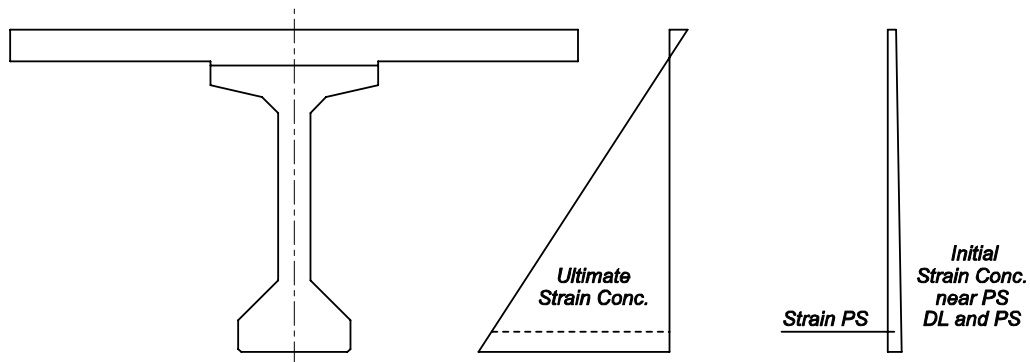
Figure 2.47 Total Strain in Prestressing at Strength Limit State

**MATERIAL PROPERTIES
PRESTRESSING STEEL**

Design Aid 11.2.5   Typical stress-strain curve, 7-wire low-relaxation prestressing strand

These curves can be approximated by the following equations:

250 ksi

$\varepsilon_{ps} \leq 0.0076 : f_{ps} = 28,500\varepsilon_{ps}$ (ksi)

$\varepsilon_{ps} > 0.0076 : f_{ps} = 250 - \dfrac{0.04}{\varepsilon_{ps} - 0.0064}$ (ksi)

270 ksi

$\varepsilon_{ps} \leq 0.0086 : f_{ps} = 28,500\varepsilon_{ps}$ (ksi)

$\varepsilon_{ps} > 0.0086 : f_{ps} = 270 - \dfrac{0.04}{\varepsilon_{ps} - 0.007}$ (ksi)
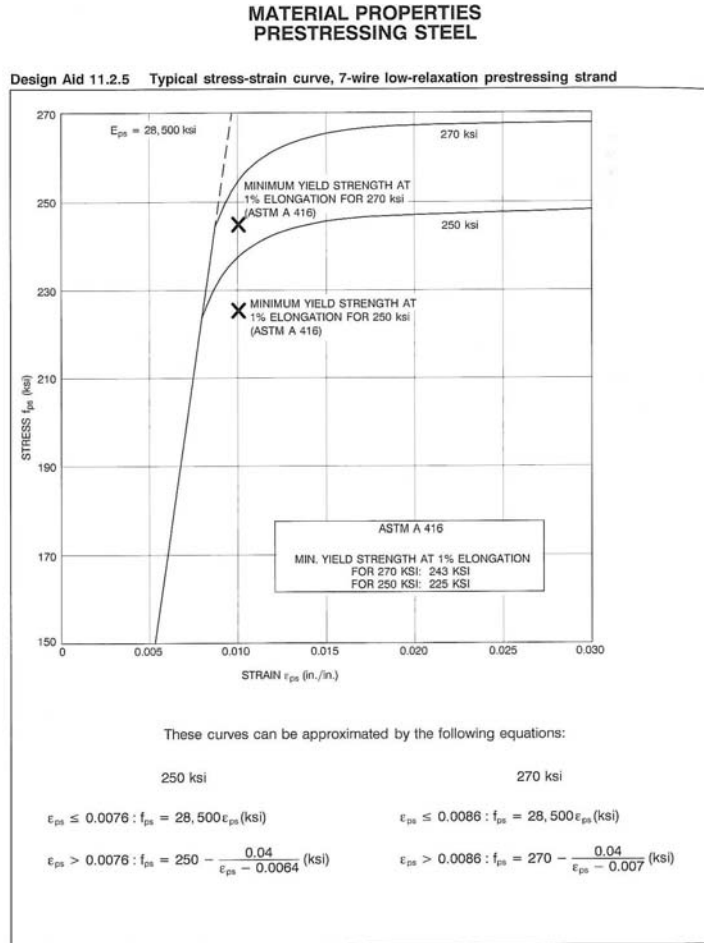
11–22   PCI Design Handbook/Fifth Edition

Figure 2.48 Material Properties of Prestressing Steel

The set of equations beginning with *AASHTO LRFD* Equation 5.7.3.1.1-2, involve the internal balance of forces. For example, the compressive force in a cross-section must be equal in magnitude to the tensile force in the same cross-section. Using this property and knowing the tensile force in the prestress and the mild reinforcing, the depth of the compressive stress block can be determined.

If the tension in concrete is neglected as small, then tensile forces come from two sources, the prestressing and the mild steel. For example, if it is assumed that the prestress comprises bonded and grouped tendons, then the total tensile force is given by:

$$F_T = A_{ps} \cdot f_{ps} + A_s \cdot f_y$$

Then *AASHTO LRFD* Equation 5.7.3.1.1-1 can be substituted into the above equation to reveal:

$$F_T = A_{ps} \cdot f_{pu} \cdot (1 - k \cdot \frac{c}{d_p}) + A_s \cdot f_y$$

Expanding this equation gives:

$$F_T = A_{ps} \cdot f_{pu} - k \cdot A_{ps} \cdot c \cdot \frac{f_{pu}}{d_p} + A_s \cdot f_y$$

Expressions for compressive forces are a little more complicated due to the changes in compressive area as the neutral axis deepens. The basic equation for the compressive force is:

$$F_C = 0.85 \cdot f'_c \cdot area_C + A'_s \cdot f'_s$$

At this point the *AASHTO LRFD* code makes a couple of simplifications:
- $f'_s = f'_y$
- For T-Section behavior, the section is treated as a true T with only one abrupt change in width.
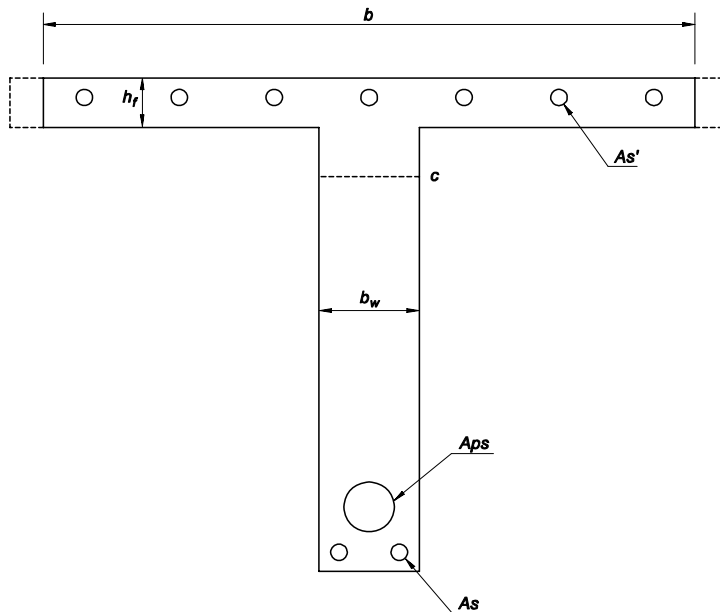
Figure 2.49 Schematic Drawing of T-Section

Using these simplifications, the T-Section compressive force could be written as:

$$F_C = 0.85 \cdot f'_c \cdot [a \cdot b - (a - h_f) \cdot (b - b_w)] + A'_s \cdot f'_y$$

By substituting $\beta_1 c$ for "a" this equation becomes:

$$F_C = 0.85 \cdot f'_c \cdot [\beta_1 \cdot c \cdot b - (\beta_1 \cdot c - h_f) \cdot (b - b_w)] + A'_s \cdot f'_y$$

Now expanding the terms in the brackets gives:

$$F_C = 0.85 \cdot f'_c \cdot [\beta_1 \cdot c \cdot b - \beta_1 \cdot c \cdot (b - b_w) + h_f \cdot (b - b_w)] + A'_s \cdot f'_y$$

The next step is to simplify this giving:

$$F_C = 0.85 \cdot f'_c \cdot [\beta_1 \cdot c \cdot b_w + (b - b_w) \cdot h_f] + A'_s \cdot f'_y$$

Expanding this by terms that are multiplied by $0.85f'_c\beta_1$ provides:

$$F_C = 0.85 \cdot f'_c \cdot \beta_1 \cdot c \cdot b_w + 0.85 \cdot f'_c \cdot (b - b_w) \cdot h_f + A'_s \cdot f'_y$$

All that remains is to set the compressive force, F_C, equal to the tensile force, F_T, and to solve for "c". Equating forces gives:

$$0.85 \cdot f'_c \cdot \beta_1 \cdot c \cdot b_w + 0.85 \cdot f'_c \cdot (b - b_w) \cdot h_f + A'_s \cdot f'_y = A_{ps} \cdot f_{pu} - k \cdot A_{ps} \cdot c \cdot \frac{f_{pu}}{d_p} + A_s \cdot f_y$$

Collecting together on the left side of this equation all terms containing the unknown quantity "c", gives:

$$0.85 \cdot f'_c \cdot \beta_1 \cdot c \cdot b_w + k \cdot A_{ps} \cdot c \cdot \frac{f_{pu}}{d_p} = A_{ps} \cdot f_{pu} + A_s \cdot f_y - A'_s \cdot f'_y - 0.85 \cdot f'_c \cdot (b - b_w)$$

From which it is found that:

$$c = \frac{A_{ps} \cdot f_{pu} + A_s \cdot f_y - A'_s \cdot f'_y - 0.85 \cdot f'_c \cdot (b - b_w) \cdot h_f}{0.85 \cdot f'_c \cdot \beta_1 \cdot b_w + k \cdot A_{ps} \cdot \frac{f_{pu}}{d_p}}$$

This expression appears to be very similar to *AASHTO LRFD* Equation 5.7.3.1.1-3. The only difference between the two equations is an extra β_1 value in the numerator. This factor is explained the *AASHTO LRFD* Commentary C5.7.3.2.2. It is an adjustment to account for the case when "c" is greater than h_f, but "a" is less than h_f. As stated in the code, the validity of this inclusion can be argued, but it is convenient and has little significant effect on the value of the nominal flexural resistance. A similar process can be applied to rectangular section behavior or to cases of unbonded tendons. As a final verification, the neutral axis must be compared to the

initial assumption. If the assumption is not correct, then a new assumption must be made and the process repeated.

2.4.3.5 Resistance Factors

The *AASHTO LRFD* Specifications relate the Resistance Factor (ϕ) for combined flexure/axial force loadings to whether a cross section is compression controlled or tension controlled. Article 5.7.2.1 offers the following definitions for these behaviors:

Sections are compression-controlled when the net tensile strain in the extreme tension steel is equal to or less than the compression-controlled strain limit at the time the concrete in compression reaches its assumed strain limit of 0.003. The compression-controlled strain limit is the net strain in the reinforcement at balanced strain conditions. For Grade 60 reinforcement, the compression-controlled strain limit may be set equal to 0.002.

Sections are tension-controlled when the net tensile strain in the extreme tension steel is equal to or greater than 0.005 just as the concrete in compression reaches its assumed strain limit of 0.003. Sections with net tensile strain in the extreme tension steel between the compression-controlled strain limit and 0.005 constitute a transition region between compression-controlled and tension controlled sections.

Using these definitions, *AASHTO LRFD* Article 5.5.4.2 provides the following Resistance Factors:

For tension-controlled prestressed concrete sections as defined in *AASHTO LRFD* Article 5.7.2.1, ϕ =1.00.

For compression-controlled sections with spirals, or ties, as defined in Article 5.7.2.1, except as specified in *AASHTO LRFD* Article 5.10.11.4.1b for Seismic Zones 3 and 4 at the extreme event limit state, ϕ =0.75.

2.4.3.6 Limits of Reinforcing

The minimum reinforcement limit is defined in *AASHTO LRFD* Article 5.7.3.3.2. The requirement is that the flexural capacity (ϕM_n) should be greater than 1.2 times the cracking moment or 1.33 times the controlling strength limit state. The cracking moment is defined by *AASHTO LRFD* Equation 5.7.3.3.2-1 as:

$$M_{cr} = S_c(f_r + f_{cpe}) - M_{dnc}(\frac{S_c}{S_{nc}} - 1) \le S_c f_r$$

where:
   f_{cpe} =   the compressive stress in concrete due to effective prestress
             forces only (after allowance for all prestress losses) at extreme
             fiber of section where tensile stress is caused by externally applied
             loads (ksi)

M_{dnc} = the total unfactored dead load moment acting on the monolithic or noncomposite section (kip-ft)

S_c = the section modulus for the extreme fiber of the composite section where tensile stress is caused by externally applied loads (in^3)

S_{nc} = the section modulus for the extreme fiber of the monolithic or noncomposite section where tensile stress is caused by externally applied loads (in.^{3})

Mathematically this works out to the extra moment that when added to the dead load and the prestressing will create a stress that will cause a crack in the member.

2.4.4 Longitudinal Shear Design (Service Limit State)

2.4.4.1 Shear Forces and Limit States

In simply supported precast pretensioned girders, shear force is at a maximum at or near supports and reduces to zero at midspan. The applied shear force is made up of a combination of dead load, superimposed dead load and live load. The contribution of live load is determined according to acceptable live load distribution techniques of *AASHTO LRFD* Article 4. The vertical component of prestress, (Vp), arising from deflected pretensioned strands (or draped post-tensioning) is taken as an unfactored contribution to the overall shear capacity. Load factors for the Strength Limit State are applied as discussed in DM Volume 1, Chapter 5.

AASHTO LRFD requires only that the Strength Limit State be satisfied in order to ensure overall capacity to safely resist factored shear forces. No limits are placed on shear stress or principal tensile stress at the Service Limit State as a means of ensuring resistance to cracking, enhancing durability or a providing a minimum level of maintainability. According to *AASHTO LRFD*, for pretensioned girders, performance under normal service level conditions is assumed to be satisfactory if the Strength Limit State alone is satisfied. The following comments on conditions at the service limit state are for information only.

2.4.4.2 Service Limit State

As there are no rules in *AASHTO LRFD* that limit the shear stress or principal tensile (Mohr's circle) stress in the webs of prestressed concrete girders, the need to check either shear or principal tensile stress at the Service Limit State is a matter entirely for the discretion of the Engineer.

Limits on the magnitude of purely "shear stress" itself cannot be defined in the context of a prestressed member where longitudinal axial compression, in addition to flexural tension or compression stress, is present at a section of interest. Rather, it is necessary to consider shear stress in the context of the associated principal tensile stress. The latter is the resultant tensile stress on a small element, usually taken as a portion of the web, subject to shear stress due to vertical shear force, longitudinal compression or tension and any concomittent vertical compression or tension – as illustrated in Figure 2.50. Stresses are determined according to classical beam

theory and Mohr's circle provides the magnitude and direction of the principal tensile stress.

Near the end of a plain or reinforced concrete beam, the direction of principal tension lies at 45° below the neutral axis. Under sufficient shear force, it gives rise to classical diagonal shear cracks rising at 45° from the soffit. The influence of longitudinal compressive prestress near the end of a girder is to reduce the angle of the diagonal shear crack – the higher the local axial prestress, the shallower the crack. The result is to lengthen the potential crack, prior to the onset of cracking. This increases the effective length of web that can potentially be mobilized to resist shear. In turn this increase the magnitude of shear force needed to induce cracking.
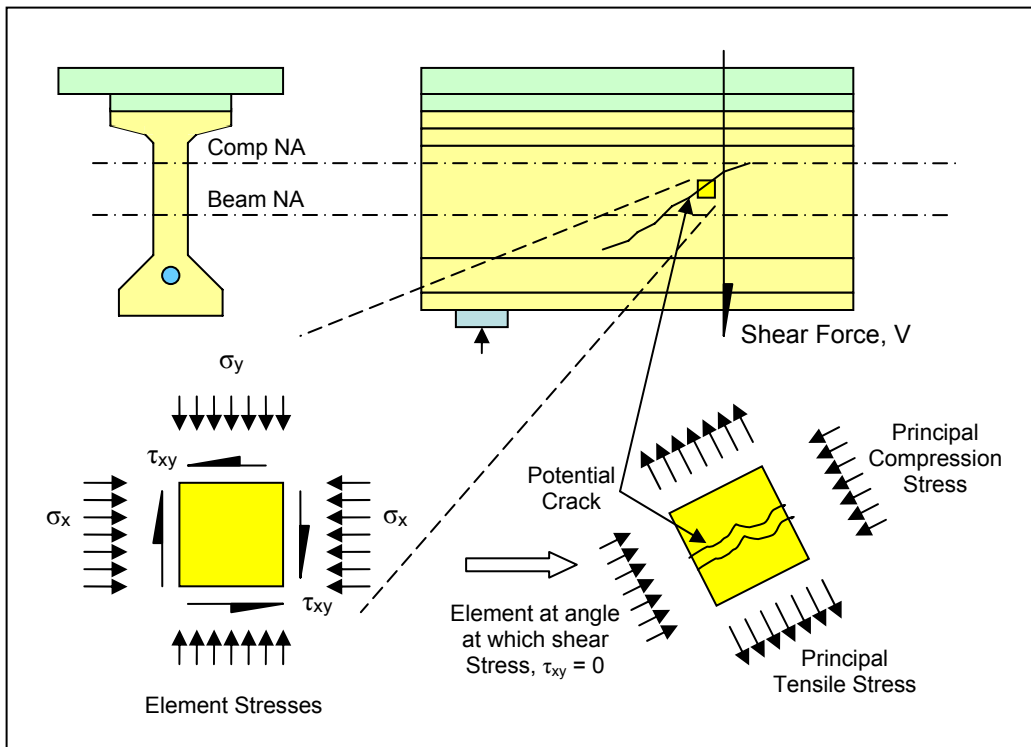
Figure 2.50 State of stress on an element in a web near the end of a beam
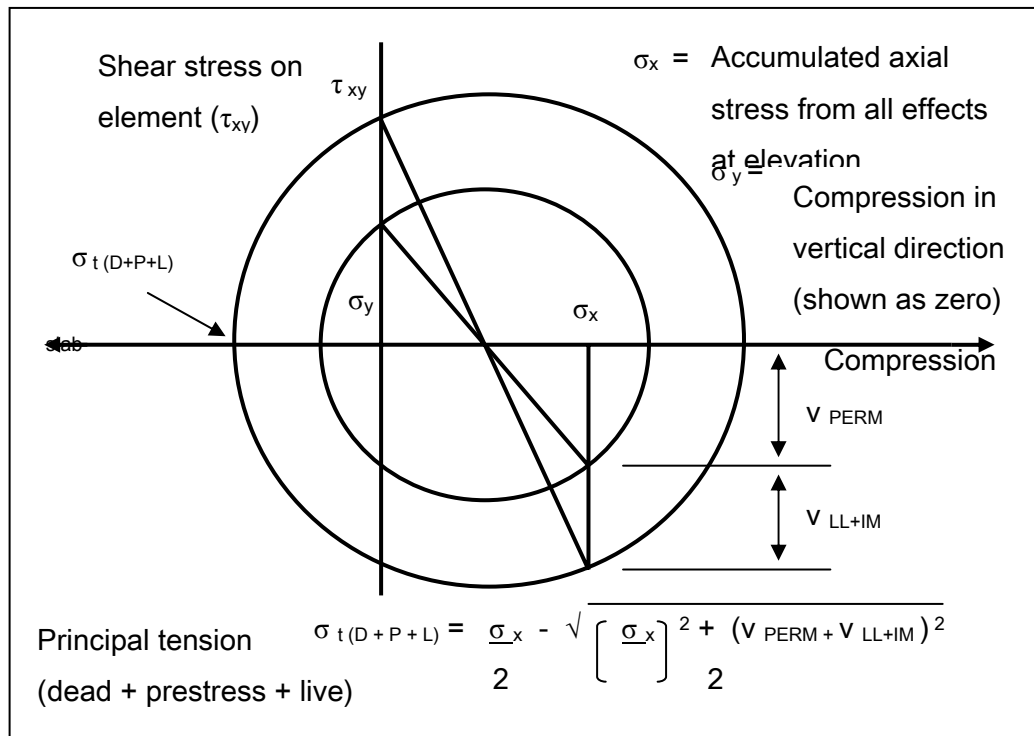
Figure 2.51 Mohr's Circle for Stress (Principal Tension)

In the end region of a typical prestressed I-girder the stress regime is complex as it is influenced by the prestress, the local bearing reaction, and the development length and de-bonding of the strands in addition to dead and live load moments and shear forces. All must be correctly accounted for in any attempt to determine either the flexural tensile stress in the bottom fiber or the principal tensile stress on an element within the depth of the girder. When the load on the girder is increased, near the support, cracks are generally initiated by the principal tension stress in the web as it reaches the cracking strength of the concrete. Further away from the bearing, cracks are generally initiated by flexural tension in the bottom fiber and propagate into the web, and curve over to follow the trajectory of the principal compression stress (being at right angles to the principal tensile stress).

This complexity in the end region of a pretensioned girder makes it difficult to define performance criteria for the Service Limit State. Limiting the magnitude of the shear stress itself cannot be used because shear capacity increases significantly with increasing axial prestress. The only possible means then is to limit the magnitude of the principal tensile stress. This would be in conjunction with existing limits for flexural tension stress per *AASHTO LRFD* Table 5.9.

Limits for principal tensile stress in a web at the elevation of the neutral axis of a segmental (box) girder in *AASHTO LRFD* Tables 5.9.5.4.1.2-1 and 3 were introduced in an endeavor to ensure a minimum web thickness for durability and avoid or minimize web cracking; albeit that this check is applied under much

simplified circumstances – namely, at the neutral axis where the longitudinal flexural stress is zero.

The designer of a pretensioned girder should exercise his judgment as to whether or not the service level stresses should be checked in the end regions of a girder to ensure satisfactory performance, durability or maintainability.

2.4.5 Longitudinal Shear Design (Strength Limit State)

2.4.5.1 *AASHTO LRFD* Shear Design

The *AASHTO LRFD* Specifications specifies two methods for shear design: the strut-and-tie model (*AASHTO LRFD* Article 5.6.3) and a more elaborate sectional model (*AASHTO LRFD* Article 5.8.3). These can be used for concrete members containing reinforcing steel and/or prestressing tendons. **Strut-and-tie** is used primarily for:

> ➢ Regions near discontinuities, such as regions adjacent to abrupt changes in cross-section, openings and dapped ends, deep beams and corbels, where the assumption that plane sections remain plane is not valid, or

> ➢ Components in which the distance from the point of zero shear to the face of the support is less than 2d, or components in which a load causing more than ½ of the shear at a support is closer than 2d from the face of the support.

Sectional Model – The sectional model is used in "flexural regions" where plane sections remain plane after loading. Flexural regions are defined in *AASHTO LRFD* as regions of members where the response of the section depends only upon the sectional force effects, moment, shear, axial load and torsion, and not upon how the force effects are introduced into the member.

2.4.5.2 Background

It is important to know the traditional approach to shear design, which is part of the AASHTO Standard Specifications. In the past, a variable-angle truss model has been used to predict shear strength. This type of approach incorporates diagonal compression struts to direct the applied loads to the supports. Longitudinal tension ties at the bottom, compression ties at the top, and vertical steel ties to connect the diagonals. The result is a system of members that resembles a truss, which can be solved using equilibrium.

In the traditional approach, the shear strength comes from the vertical stirrups and from an empirically-derived concrete strength. Prior to the formation of cracks, the vertical stirrups have no noticeable effect on strength. After cracking, however, the vertical stirrups that cross the crack are engaged and, therefore, contribute to the strength. The diagonal compression struts are assumed to have the same orientation as the cracks. Details of the development of the traditional equation for

shear strength will not be covered in this section since it will be discussed with other components of the shear resisting mechanism in the following section on MCFT. However, equilibrium of the truss model would lead to the following well-known expression for the vertical stirrup component of shear strength:

$$V_s = \frac{A_v f_y}{s} d_v \cot \theta$$

where:

A_v = area of transverse reinforcement within distance s (in^2)
f_y = minimum yield strength of reinforcing bars (ksi)
d_v = effective shear depth, taken as the distance between the resultants of the tensile and compressive forces due to flexure; it need not be taken less than the greater of $0.9d_e$ or $0.72h$, where d_e is the distance from the extreme compression fiber to the centroid of the tensile force in the tensile reinforcement, and where h is the overall depth of the member (in)
s = spacing of reinforcing bars (in)
θ = angle of inclination of diagonal compressive stresses (degrees)

The simple approach is to assume that the angle of crack is 45 degrees, simplifying the expression to the following:

$$V_s = \frac{A_v f_y d_v}{s}$$

The expression can be modified to take into account inclined stirrups if necessary.

The *AASHTO LRFD Standard Specifications* include an additional component of shear strength, V_c, loosely referred to as the "contribution of the concrete". The equation, not repeated here, was determined from experimental results. The total shear strength was then equal to

$$V_n = V_c + V_s$$

2.4.5.3 The Modified Compression Field Theory

In the *AASHTO LRFD Specifications*, shear design is based upon the MCFT, also known as the sectional model. The rationale was developed by Vecchio and Collins (1986 and 1988) and Collins and Mitchell (1991). It is based on the following rules of mechanics:

➢ Constitutive Laws (stress-strain)

➢ Equilibrium

➢ Strain Compatibility

Experimental tests have shown that a beam has more shear capacity than that provided by stirrup reinforcement, by an amount about equal to the cracking strength. The MCFT theoretically analyzes, based on the rules of mechanics listed above, the principal stresses in a beam, with the principal compression, f_2, being parallel to the cracks and the principal tension, f_1, being the average tension that the concrete can carry in between the cracks. The angle of orientation of the principal stresses is also derived from the theory.

2.4.5.3.1 Constitutive (Stress-Strain) Laws

The stress-strain behavior of concrete leads to relationships between the principal compressive strain, the principal compressive stress, and the principal tensile strain, and also between the principal tension stress and tensile strain. Experimental tests on concrete specimens containing bonded reinforcement show that, after concrete in tension cracks, tensile strains still exist, due to aggregate interlock. This strain drops gradually after cracking (Figure 2.52), and can be expressed as follows:

$$f_1 = \frac{f_{cr}}{1 + \sqrt{500\varepsilon_1}}$$

Equation 2.1

where:

f_1	=	average principal tensile
f_{cr}	=	cracking stress of concrete
ε_1	=	average principal tensile

The compressive strength of concrete, f'_c, is usually obtained from cylinder tests, in which uniaxial compression is applied to the specimen. However, in a beam element, stresses in two directions, i.e., biaxial stresses, exist. When tensile strains exist perpendicular to the compression, the compression strength decreases, known as "softening". A relationship between the compressive strain, the compression stress, and the tensile strain has been derived experimentally, giving the following expressions:

$$f_2 = f_{2\max}[2(\frac{\varepsilon_2}{\varepsilon'_c}) - (\frac{\varepsilon_2}{\varepsilon'_c})^2]$$

Equation 2.2

$$\frac{f_{2\max}}{f'_c} = \frac{1}{0.8 + 170\varepsilon_1} \leq 1.0$$

Equation 2.3

where:

f_2	=	principal compressive stress
f_{2max}	=	reduced peak compressive stress
ε_2	=	principal compressive strain
ε'_c	=	maximum strain corresponding to f'_c
f'_c	=	28-day compressive strength of the concrete

Substituting ε'_c = -0.002 and substituting the expression for f_{2max} from Equation 2.3 into
 Equation **2.2**, and solving for ε_2 leads to the following expression:

$$\varepsilon_2 = -0.002\left(1 - \sqrt{1 - \frac{f_2}{f'_c}(0.8 + 170\varepsilon_1)}\right)$$

Equation 2.4

2.4.5.3.2 Equilibrium of Vertical Section

The basic expression for shear strength that includes the contribution of the concrete and stirrup steel is found from equilibrium. A portion of a beam, cut vertically is shown in Figure 2.54. The compressive stress, f_2, is projected onto the dashed line, which has a length d(cosθ), while the tensile stress, f_1, is projected onto the solid line, which has a length d(sinθ). The stresses are then resolved into their vertical components and added together, giving:

$$V = f_2\left(b_w d \ \cos\theta\right)\sin\theta + f_1\left(b_w d \ \sin\theta\right)\cos\theta$$

where:

b_w	=	width of web
d	=	d_v

Which reduces to

$$f_1 + f_2 = \frac{v}{\sin\theta\cos\theta}$$

Equation 2.5

where: v = shear stress = $V/b_w d$

Equilibrium can also be taken from a portion that is cut from the bottom of the beam (Figure 2.55). Using the same procedure as above, the force in the stirrup steel is found to be:

$$A_v f_v = f_2\left(b_w s \sin\theta\right)\sin\theta - f_1\left(b_w s \cos\theta\right)\cos\theta$$

2.70

where: f_v = stress in the transverse reinforcement

which reduces to:

$$\left(f_2 \sin^2 \theta - f_1 \cos^2 \theta\right) b_w s = A_v f_v$$

Equation 2.6

Combining Equation 2.4 and Equation 2.5 and setting $f_v = f_y$, where f_y = yield strength of the reinforcement, gives:

$$V = f_1 b_w d \cot \theta + \frac{A_v f_y}{s} d \cot \theta$$

Equation 2.7

where the first part of the equation is referred to as the concrete contribution to the shear strength, V_c, and the second part is the steel reinforcement contribution, V_s:

$$V_n = \text{"}V_c\text{"} + \text{"}V_s\text{"}$$

2.4.5.3.3 Shear transfer at a crack

Because of aggregate interlock, concrete has the ability to transfer shear along a crack. Experimental tests show that this ability is limited by the crack width, w, and the maximum aggregate size, a_{max}. The crack width will be put in terms of the principal tensile strain later. In the final formulation, a_{max} is assumed. Crack slipping may be prevented if the following limit is placed on the shear stress along the crack:

$$v_{ci} \leq \frac{12\sqrt{f_c'}}{0.31 + 24w \big/ \left(a_{max} + 0.63\right)}$$

Equation 2.8

The shear stress along a crack can be related to the tensile stress by taking vertical equilibrium at a crack and also between cracks.

At a crack (Figure 2.56), the forces that counteract shear are the concrete shear along the crack, v_{ci}, and the stirrup reinforcement. Note that the concrete tension stress, f_1, discussed previously is not included because it is an average across the cracks; directly at a crack, the concrete does not carry tension. The number of bars engaged along the crack is essentially $d(\cot\theta)/s$, giving a force in the stirrups equal to $A_v f_y \dfrac{d\cot\theta}{s}$. Note that the stirrups are assumed to be yielding because the concrete has cracked and the stirrups are fully engaged. The concrete shear acts

along an inclined length of d/sinθ; taking the vertical component of this shear results in $v_{ci} \dfrac{b_w d}{\sin \theta} \sin \theta$. Adding the two components results in:

$$V = A_v f_y \frac{d \cot \theta}{s} + v_{ci} \frac{b_w d}{\sin \theta} \sin \theta$$

<div align="right">Equation 2.9</div>

Taking a section between two cracks (Figure 2.57), the forces that counteract shear are the tensile stress in the concrete and the stirrup reinforcement. The force in the stirrups is the same as derived above for a section between the cracks, except that the stirrups are not yielding, for $A_v f_v \dfrac{d \cot \theta}{s}$. The concrete tension acts along an inclined length of d/sinθ; taking the vertical component of this shear results in $f_1 \dfrac{b_w d}{\sin \theta} \cos \theta$. Adding the two components results in:

$$V = A_v f_v \frac{d \cot \theta}{s} + f_1 \frac{b_w d}{\sin \theta} \cos \theta$$

<div align="right">Equation 2.10</div>

Equating Equation 2.9 and Equation 2.10 gives:

$$f_1 \leq v_{ci} \tan \theta$$

<div align="right">Equation 2.11</div>

with the inequality added to set an upper limit for f_1 in order to prevent crack slipping, as defined by the parameter v_{ci}. Substituting Equation 2.8 for v_{ci} gives:

$$f_1 \leq \frac{12}{0.31 + 24w \big/ (a_{max} + 0.63)} \sqrt{f_c'} \tan \theta$$

<div align="right">Equation 2.12</div>

The equation above can be simplified by defining a new parameter β, with the upper limit imposed to limit crack slipping, as:

$$\beta \leq \frac{12}{0.31 + 24w \big/ (a_{max} + 0.63)} \theta$$

<div align="right">Equation 2.13</div>

The crack width w can be expressed in terms of the tensile strain as:

$$w = \varepsilon_1 s_{m\theta}$$

<div align="right">Equation 2.14</div>

where: $s_{m\theta}$ = mean crack spacing

In the final formulation, a crack spacing is assumed, so β becomes a function of the tensile strain, ε_1, and aggregate size. Substitution of β into Equation 2.12 results in:

$$\beta = \frac{f_1}{\sqrt{f_c'}} \cot\theta \text{ or, alternately, } \beta\sqrt{f_c'} = f_1 \cot\theta$$

<div align="right">Equation 2.15</div>

which can be substituted into Equation 2.7 to give the final expression:

$$V_n = \beta\sqrt{f_c'} b_w d + \frac{A_v f_y}{s} d \cot\theta$$

<div align="right">Equation 2.16</div>

Equation 2.14 is combined with Equation 2.1, and using $f_{cr} = 0.33\sqrt{f_c'}$ gives:

$$\beta = \frac{0.33\cot\theta}{1 + \sqrt{200\varepsilon_1}}$$

<div align="right">Equation 2.17</div>

To calculate β, a final expression is needed for the tensile strain ε_1. This can be found from strain compatibility.

2.4.5.3.4 Strain Compatibility

One assumption of the MCFT is that the angle of orientation of the principal stresses is equal to the angle of the principal strains. From the transformation equations for plane strain from mechanics, the principal strains are related to the longitudinal strain, ε_x, and θ in the formula:

$$\varepsilon_1 = \varepsilon_x + \left(\varepsilon_x - \varepsilon_2\right)\cot^2 \theta$$

<div align="right">Equation 2.18</div>

Combining this expression with Equation 2.4 and Equation 2.5, and considering f_1 in Equation 2.5 to be small in comparison to f_2, would give:

$$\varepsilon_1 = \varepsilon_x + \left[\varepsilon_x + 0.002\left(1 - \sqrt{1 - \frac{v}{f_c'}\frac{0.8 + 170\varepsilon_1}{\sin\theta\cos\theta}}\right)\right]\cot^2 \theta$$

<div align="right">Equation 2.19</div>

2.4.5.3.5 AASHTO LRFD Procedure

As seen above, the equations used in the MCFT contain many of the same variables; therefore, calculating the most efficient shear steel arrangement can be time consuming. First, the shear stress, v, is calculated. After estimating θ, ε_x and ε_1 are calculated. Then β can be found, from which the shear strength can be determined. The procedure can be repeated for different values of θ until the shear steel requirement is minimized. Alternately, one may use the *AASHTO LRFD* design aid tables, which were originally presented by Collins and Mitchell (1991). The procedure used in *AASHTO LRFD* is discussed as follows.

2.4.5.3.6 Basic Equations for Shear Strength

The equations for shear strength in *AASHTO LRFD* Article 5.8.3.3 are similar to those derived above, where the concrete contribution is:

$$V_c = 0.0316\beta\sqrt{f_c'}b_v d_v$$

<div align="right">Equation 2.20</div>

The constant of 0.0316 is added so that f'_c can be entered in ksi.

The strength from the steel stirrups is:

$$V_s = \frac{A_v f_y d_v\left(\cot\theta + \cot\alpha\right)\sin\alpha}{s}$$

<div align="right">Equation 2.21</div>

The angle α is added to include the case of inclined stirrups, where α is 90 degrees for vertical stirrups. The total shear strength, including the effect of prestressing, V_p, is:

$$V_n = V_c + V_s + V_p$$

Equation 2.22

To ensure that the concrete in the web does not crush prior to yield of the transverse reinforcement, the strength is limited by:

$$V_n = 0.25 f_c' b_v d_v + V_p$$

Equation 2.23

To use the method in *AASHTO LRFD*, the values for the shear stress, v_u, and the longitudinal strain, ε_x, are needed. The shear stress is calculated from:

$$v_u = \frac{V_u - \phi V_p}{\phi b_v d_v}$$

Equation 2.24

where:

v_u	=	average factored shear stress on the concrete
V_u	=	factored shear force at section
ϕ	=	resistance factor

The longitudinal strain, ε_x, caused by the applied loads and the prestressing, as shown in Figure 2.58, is found from one of three equations. If the section contains at least the minimum transverse reinforcement, the section has the capacity to redistribute shear stresses. Thus, the strain can be calculated at mid-height as follows:

$$\frac{\left(M_u / d_v\right) + 0.5 N_u + 0.5 \left(V_u - V_p\right) \cot \theta - A_{ps} f_{po}}{2 \left(E_s A_s + E_p A_{ps}\right)} \le 0.001$$

Equation 2.25

where:

M_u	=	factored moment at the section
N_u	=	applied factored axial force taken as positive if tensile
A_{ps}	=	area of prestressing steel
f_{po}	=	a parameter taken as modulus of elasticity of prestressing tendons multiplied by the locked-in difference in strain between the prestressing tendons and the surrounding concrete
E_s	=	modulus of elasticity of reinforcing bars
A_s	=	area of nonprestressed tension reinforcement
E_p	=	modulus of elasticity of prestressing tendons

If the section contains less than the minimum transverse reinforcement, the strain is calculated at the location of maximum tension in the web:

$$\varepsilon_x = \frac{\left(M_u/d_v\right) + 0.5N_u + 0.5\left(V_u - V_p\right)\cot\theta - A_{ps}f_{po}}{E_s A_s + E_p A_{ps}} \leq 0.002$$

Equation 2.26

If a negative value of ε_x results from either of the two equations above, there is compression at that location. The concrete stiffness will contribute and should be added in the denominator, for:

$$\varepsilon_x = \frac{\left(M_u/d_v\right) + 0.5N_u + 0.5\left(V_u - V_p\right)\cot\theta - A_{ps}f_{po}}{2\left(E_c A_c + E_s A_s + E_p A_{ps}\right)}$$

Equation 2.27

2.4.5.3.7 Longitudinal Reinforcement

Essentially, both transverse and longitudinal reinforcement contribute to shear strength. The horizontal component of the compression strut in the web has to be resisted by longitudinal tension reinforcement. The longitudinal reinforcement can be checked for adequacy with the following *AASHTO LRFD* Equation:

$$A_s f_y + A_{ps} f_{ps} \geq \frac{|M_u|}{d_v \phi_f} + 0.5\frac{N_u}{\phi_c} + \left(\left|\frac{V_u}{\phi_v} - V_p\right| - 0.5V_s\right)\cot\theta$$

Equation 2.28

where:
   f_{ps} =   average stress in prestressing steel at the time for which the nominal resistance of member is required

If this inequality is not met, either the transverse or the longitudinal reinforcement must be increased.

2.4.5.3.8 Procedure for Reinforcement Selection

Rather than presenting all of the equations that are needed to calculate β, *AASHTO LRFD* Tables 5.8.3.4.2-1 and 5.8.3.4.2-2 tabulate θ and β values for sections with and without the minimum amount of transverse reinforcement. This simplifies the procedure to just a few steps, which are outlined in a flow chart in *AASHTO LRFD* Article 5.8.3.4.2, and are summarized below:

1. Calculate factored load effects. Assume a value for θ.

2. Determine d_v. Calculate V_p. Check that b_v satisfies the requirement in Equation 2.23.

3. Calculate shear stress ratio v_u/f'_c.

4. Calculate the effective value of f_{po} if the section is within the transfer length of any strands. Otherwise, assume $f_{po}=0.7f_{pu}$.

5. Calculate ε_x using Equation 2.25, Equation 2.26, or Equation 2.27.

6. Determine θ, choosing the next-larger ε_x, from *AASHTO LRFD* Tables 5.8.3.4.2-1 and 5.8.3.4.2-2. Alternately, interpolate the tables to find θ, recalculate ε_x in Step 5, and reselect θ from the tables. Repeat until θ converges]. Select β from the tables.

7. Calculate V_c. Then calculate V_s required. The required stirrup spacing can then be found by assuming a bar size.

8. Check that the longitudinal reinforcement can resist the resulting tension using Equation 2.28.

9. If there is not enough longitudinal reinforcement, either provide more longitudinal reinforcement or more transverse reinforcement. If the designer chooses to provide more transverse reinforcement, the strength V_s should be recalculated, and Step 8 should be repeated to obtain the reduced requirement for longitudinal reinforcement.

2.4.5.4 Other Approaches to Strength Limit State Verification

Previous *AASHTO LRFD* and LFD methods for calculating shear strength capacity generally followed the basic principles contained in the above and, in particular, took account of the strength provided by the three key components namely; concrete, reinforcement and prestress, including not only the vertical component of prestress but also the magnitude of the axial prestress itself towards enhancing overall behavior. An alternative approach based upon the traditional shear and torsion design for plane sections, has been retained in the AASHTO Guide Specification for Segmental Bridges. It sets a limit on the overall capacity for shear and for the combination of both torsion and shear effects in relatively large boxes. The procedure is subject to certain constraints; for instance, that there are no significant discontinuities such as abrupt changes in cross section or openings, there are limits on the contribution from concentrated loads near supports and certain requirements for reinforcement detailing. The overall approach is more simple, yet appropriate to the circumstances of large box sections, than Modified Compression Field Theory. It is a conservative approach since the effective angle of the tension crack is implicitly assumed to be 45°, as for reinforced (non-prestressed) concrete. Slightly modified versions that take into account the beneficial change from the angle of a potential shear crack as a result of axial or longitudinal compression stress, have been studied and used occasionally for enhanced load rating under increased loads or permit conditions (e.g. FDOT LRFR).
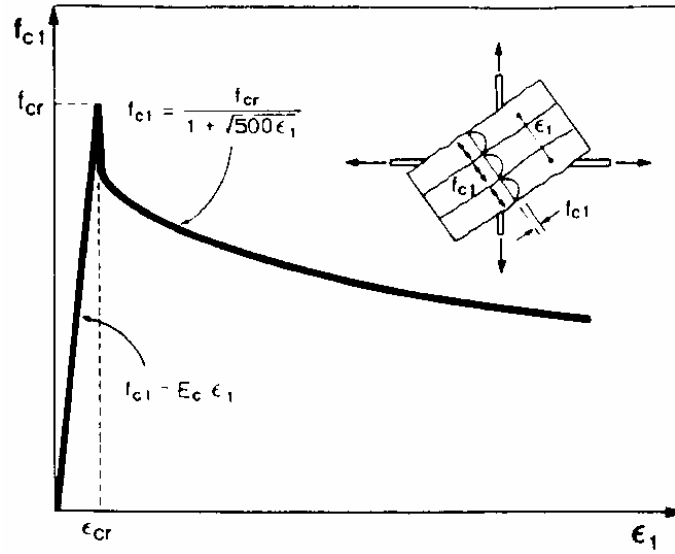
Figure 2.52 Average Stress-Strain Relationship for Cracked Concrete in Tension
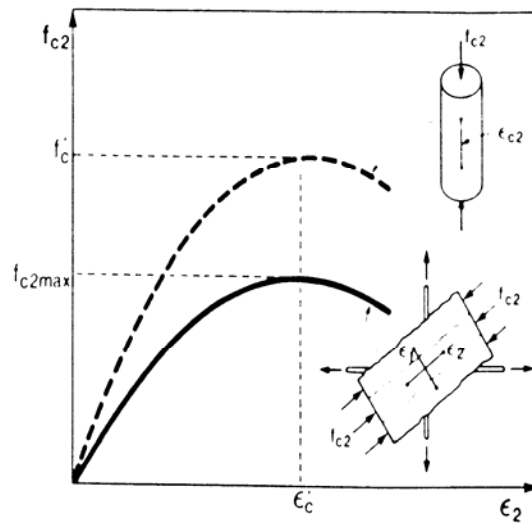
Figure 2.53 Average Stress-Strain Relationship for Concrete in Compression
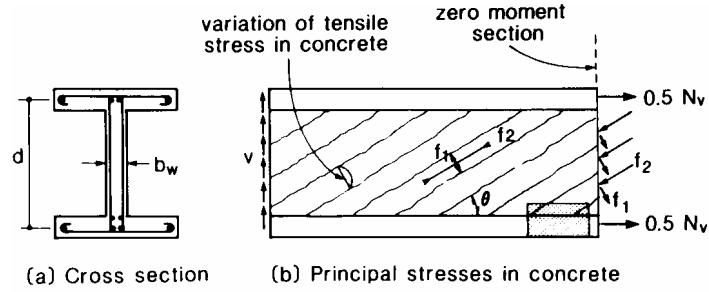
Figure 2.54 Equilibrium of Vertical Section of Diagonally Cracked Beam
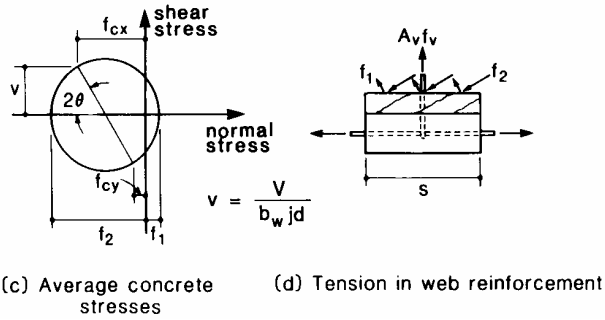
Figure 2.55 Equilibrium of Section of Diagonally Cracked Beam
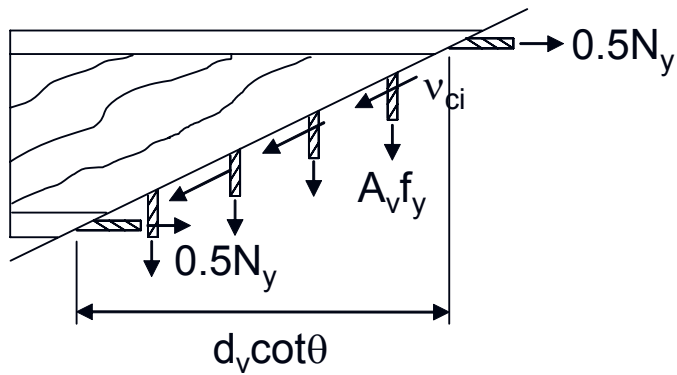
Figure 2.56 Stresses at a Crack
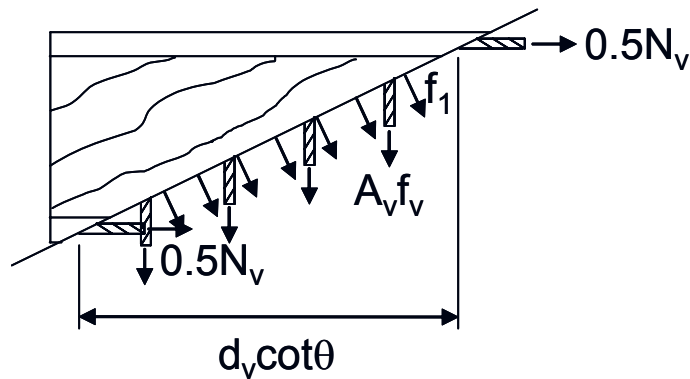
Figure 2.57 Average Stresses between Cracks
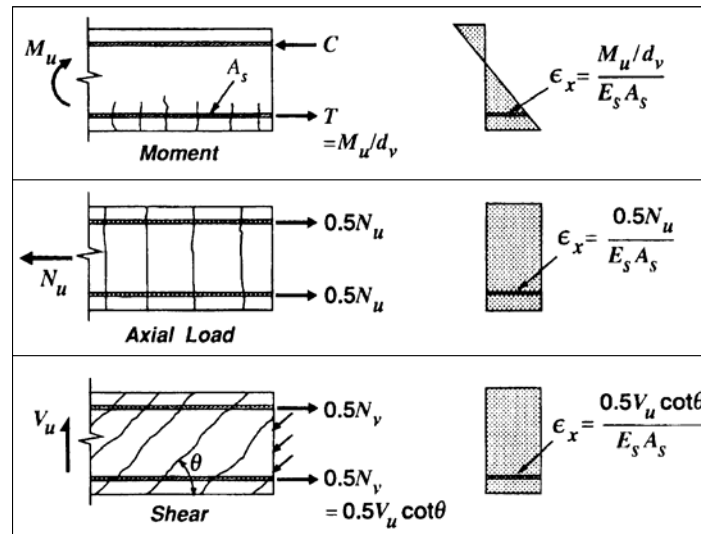
Figure 2.58 Longitudinal Strain in the Web Reinforcement

2.4.5.5 Interface Shear Design

2.4.5.5.1 The Interface

Interface shear occurs where shear is transferred across a plane that is made up of two components. *AASHTO LRFD* Article 5.8.4.1 states that interface shear transfer shall be considered at:

  ➢ An existing or potential crack
  ➢ An interface between dissimilar materials
  ➢ An interface between two concretes cast at different times
  ➢ The interface between different elements of the cross-section

In particular, for a composite girder, the girder and concrete slab are made up of two concretes that are cast at different times. Interface shear is, therefore, analyzed where the two components connect, i.e., at the interface of the top of the girder and the bottom of the slab.

2.4.5.5.2 Shear mechanism

The best way to understand the origin of interface shear is to compare the behavior of a non-composite beam with a composite beam. Consider first a "non-composite" beam (i.e. prior to the slab being cast). The loads that the beam must resist are from the self weight of the beam, the pretensioning effects, and the weight of the slab that will be placed on top of it (Figure 2.59).
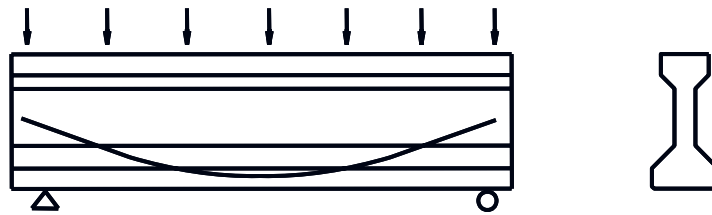
Figure 2.59 Non-composite Beam

Once the slab has been placed and cured, the beam must now resist effects from utilities, barriers, wearing surface, and live loads (Figure 2.60).
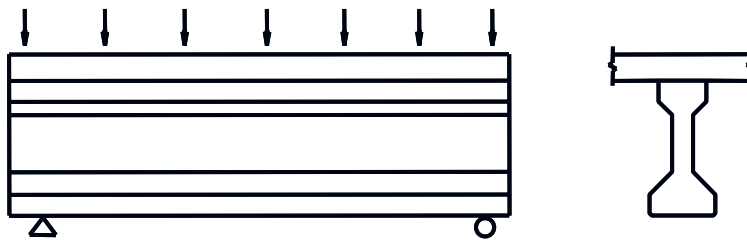
Figure 2.60 Deck Placed on Non-composite Beam

If the slab simply rests on the beam, and the beam and slab are not connected, the non-composite beam behaves somewhat independently from the slab if friction between the two is ignored. Each component carries separately a part of the load. Under vertical load causing positive moment, the lower surface of the deck will theoretically be in tension and elongate while the top surface of the girder will be in compression and shorten. With friction neglected, only vertical internal forces will act between the deck and the girder, and slip will occur between the two components (Figure 2.61).

Figure 2.61 Independent Behavior

Consider now the case where the beam has been made "composite", and the beam and slab are connected together structurally with some connectors (the design of which will be discussed later). In this case, the components will bend "together". The shear that must be designed for at the interface arises from the girder and slab trying to act "together", as shown by the arrows in Figure 2.62, even though they are cast at different times and from different concretes.
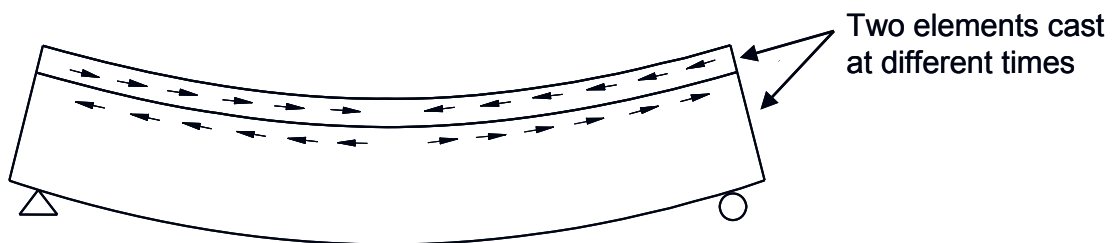
Figure 2.62 Composite Beam

A beam that is composite with a slab has much better resistance to bending than a plain beam (i.e., the moment of inertia is greatly increased). The result is weight and cost savings since shallower sections can be used.

The simplest way to calculate the magnitude of the horizontal shear is by using the *AASHTO LRFD* method, as found in *AASHTO LRFD* Article C5.8.4.1. The method gives an expression that relates the horizontal shear to the vertical shear, and it is based on equilibrium of a section of beam (Figure 2.63).

(a)

(b)
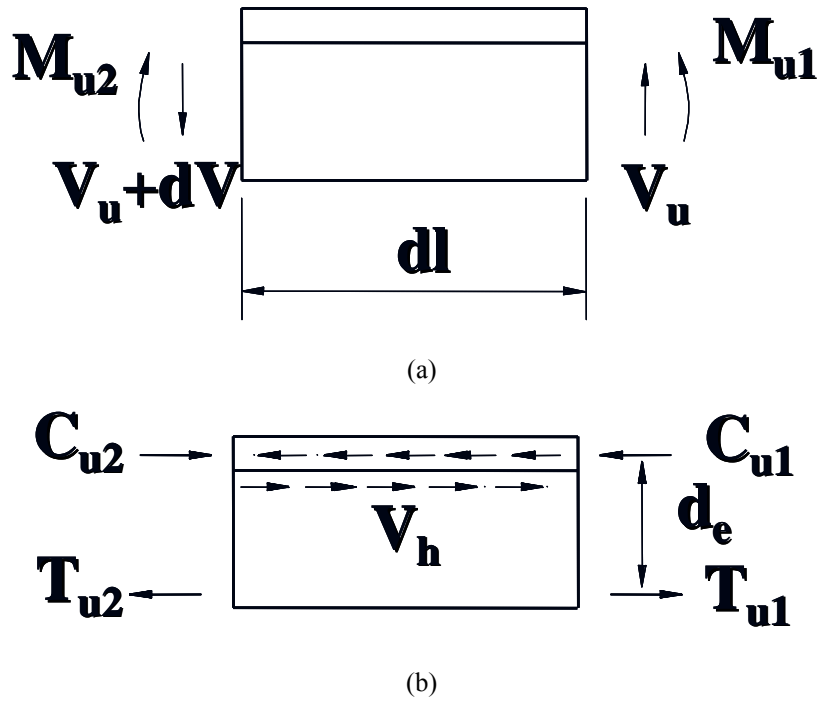
Figure 2.63 Relationship Between Horizontal and Vertical Shear

First understand that diagram (a) in Figure 2.63 is roughly equivalent to diagram (b). The pertinent variables in the diagrams are V_h, the horizontal shear per unit length of girder, V_u, the factored vertical shear, and d_e, the distance between the centroid of the steel in the tension side of the beam to the center of the compression blocks in the deck. For simplicity, d_e can be taken as the distance between the centroid of the tension steel and the midthickness of the deck.

Taking moments about the left-hand side of (a),

$$M_{u2} = M_{u1} + V_u dl$$

Equation 2.29

Equating moments on the left-hand side of (a) with the left-hand side of (b),

$$C_{u2} \approx \frac{M_{u2}}{d_e}$$

Equation 2.30

Substituting Equation 2.29 into Equation 2.30,

$$C_{u2} \approx \frac{M_{u1}}{d_e} + \frac{V_u dl}{d_e}$$

Equation 2.31

Equating moments on the right-hand side of (a) with the right-hand side of (b),

$$C_{u1} \approx \frac{M_{u1}}{d_e}$$

Equation 2.32

Equating the horizontal forces at the interface in (b),

$$V_h = C_{u2} - C_{u1}$$

Equation 2.33

Substituting Equation 2.31, Equation 2.32, and Equation 2.33,

$$V_h = \frac{V_u dl}{d_e}$$

Equation 2.34

For a unit length segment, Equation 2.34 reduces to

$$V_h = \frac{V_u}{d_e}$$

Equation 2.35

The result is a simple way to calculate the magnitude of horizontal shear by using the vertical shear. It is expressed as a force per length (i.e. kips/ft). For V_u, use only the loads that are applied to the composite section for Strength I Limit State:

$$V_u = 1.25V_{DC} + 1.5V_{DW} + 1.75V_{LL+IM}$$

Equation 2.36

2.4.5.5.3 Resistance

When connectors are used, the resistance to interface shear is calculated in three parts. The first is the cohesion component, c, between the interface, and the second is the connector strength component, $A_{vf}f_y$. A third contributor can be considered if the interface has a compressive force, P_c, normal to the shear plane. Recall from mechanics that the friction that is developed between two objects is proportional to the normal force.

Because the interface is rough, shear displacement will cause the discontinuity to widen. This opening will cause tension in the reinforcement crossing the discontinuity balanced by compressive stresses on the concrete discontinuity surfaces. The resistance of the face to shear is assumed to be a function of both cohesion and friction.

Reinforcement "ties" the beam and slab together, contributing to friction strength. Usually, mechanical shear connectors are used at the interface between the girder and slab. In a composite beam that is made up of a steel girder and a concrete slab, the most typical connectors that are used are shear studs that are welded onto the top flange that protrude into the slab. In a concrete girder, reinforcing bars (single or multiple leg stirrups) are typically cast into the top of the girder. The bars must be anchored in both the girder and the slab to develop the specified yield strength.

The interface shear resistance due to all of the above contributors is given in *AASHTO LRFD* Equation 5.8.4.1-1 as

$$V_n = cA_{cv} + \mu \left[A_{vf} f_y + P_c \right]$$

where:

V_n	=	nominal shear resistance (kip)
c	=	cohesion factor (ksi)
A_{cv}	=	area of concrete engaged in shear transfer (in^2)
μ	=	friction factor
A_{vf}	=	area of shear reinforcement crossing the shear plane (in^2)
f_y	=	yield strength of reinforcement (ksi)
P_c	=	permanent net compressive force normal to the shear plane; if force is tensile, P_c = 0.0 (kip)

Upper limits on the strength are given in *AASHTO LRFD* Equations 5.8.4.1-2 and 5.8.4.1-3 as

$$V_n \leq 0.2 f_c' A_{cv} \text{ , or}$$

$$V_n \leq 0.8 A_{cv}$$

where:

f_c'	=	specified 28-day compressive strength of the weaker concrete (ksi)

The values given in *AASHTO LRFD* Article 5.8.4.2 for the cohesion and friction factors are dependent upon how the two different concretes are placed (Table 2.2).

Table 2.2

	c	μ
For concrete placed monolithically	0.150 ksi	1.4 λ
For concrete placed against clean, hardened concrete with surface intentionally roughened to an amplitude of 0.25 in.	0.100 ksi	1.0 λ
For concrete placed against hardened concrete clean and free of laitance, but not intentionally roughened	0.075 ksi	0.6 λ

λ = 1.00 for normal weight concrete
= 0.85 for sand-lightweight concrete
= 0.75 for all-lightweight concrete

2.4.5.5.4 Reinforcement Required

For design, the required size and spacing of reinforcing steel must be determined. The horizontal shear (in units of force/length) is usually multiplied by the spacing of the reinforcement (in units of length) so that the resulting force can be equated to the expression for shear strength.

This amounts to "designing" a length of interface along the beam equal to the spacing of the reinforcement, such that $A_{cv} = b_v s$ (Figure 2.64).

where:
    b_v =   width of the interface (in)
    s =   spacing of interface shear reinforcement (in)
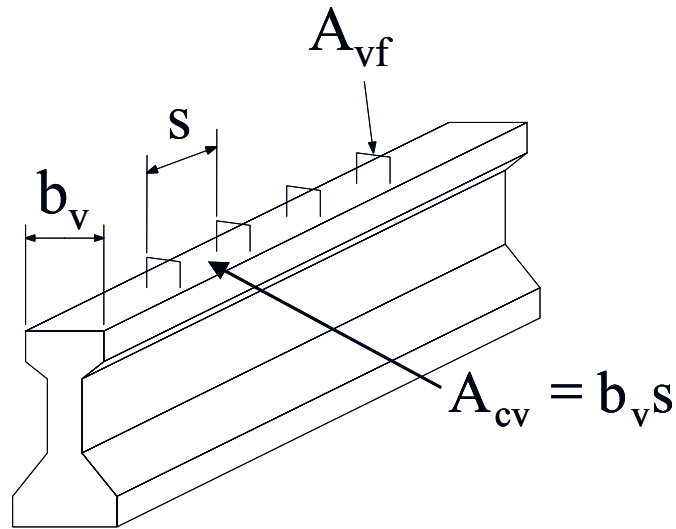
Figure 2.64 Reinforcement Required

The resulting equation is as follows:

$$\frac{V_h s}{\phi} \leq c(b_v s) + \mu(A_{vf} f_y + P_c)$$

Solving for the required spacing of reinforcement,

$$s = \frac{\mu(A_{vf} f_y + P_c)}{V_h/\phi - cb_v}$$

2.4.5.5.5 Minimum Requirements

The minimum cross-sectional area of reinforcement per unit length that must be provided, given in *AASHTO LRFD* Article 5.8.4.1, must satisfy

$$A_{vf} \geq \frac{0.05 b_v}{f_y}$$

The minimum requirement may be waived if

$$\frac{V_h}{A_{cv}} < 0.100 \ \text{ksi}$$

The longitudinal spacing of the reinforcement shall not exceed 24.0 inches. Also, if the contact surface width (i.e., the top flange beam width) is greater than 48 inches, at least four bars in each row must be used.

2.4.6 Anchor Zone Considerations for Pretensioned Girders

2.4.6.1 Anchor Zone in Pretensioned Girder – Description

Anchor zones in pretensioned girders are the area where the prestressing force in the steel is transferred to the concrete section. In this area where forces are being transferred and distributed there are several things to account for. The most basic is the transfer and development lengths where the concrete resists the prestressing force. In some cases the bond is intentionally prevented usually by means of an empty sheath surrounding a strand. In these cases the anchor zones may be staggered as each set of strands bonds with the concrete. Distribution of these forces, from the area in contact with the strands, to the section in general, causes some areas of tension around the anchorage zone generally located above the strands in a prestressed beam. Using strut and tie analysis these tension "ties" can be identified and properly reinforced. Another item of concern to anchor zones is that the concrete surrounding the prestressing steel be able to confine that force before it is spread out to the entire member. This can also be aided by carefully placed reinforcing.

2.4.6.2 Transfer and Development

According to *AASHTO LRFD* Article 5.11.4.1, transfer length for bonded strand may be estimated at 60 strand diameters. This distance of thirty inches for ½" diameter strands is assumed to be the length where the stress in the prestressing steel varies from 0 to the effective stress in the prestressing steel after losses (f_{pe}). Beyond this zone there is another component that along with the transfer length makes up the development length. This zone is known as the flexural bond length. As its name suggests, the flexural bond length is the area where the additional bond is acquired to allow the strands to reach stresses required by flexural strength conditions (f_{ps}). Unlike the linear stress change in the transfer length, the flexural bond length uses a parabolic stress change. The total development length (l_d) is defined in *AASHTO LRFD* Equation 5.11.4.2-1as:

$$l_d \geq k(f_{ps} - \tfrac{2}{3}f_{pe})d_b$$

where:
    k   =   1.6 for precast, prestressed beams,
    f_{ps} =   average stress in steel at nominal bending resistance (ksi),
    f_{pe} =   effective stress in steel after losses (ksi),
    d_b =   nominal strand diameter,
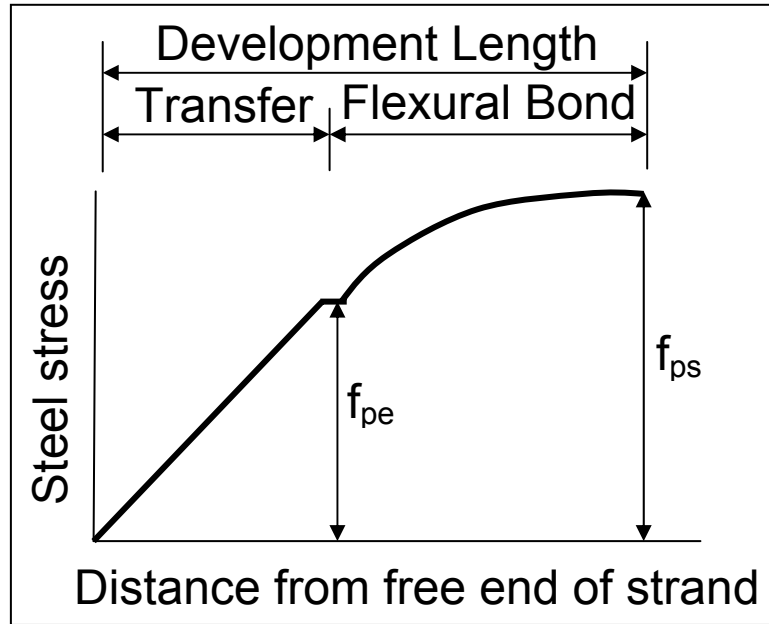
Figure 2.65 Development Length

2.4.6.3 Debonding

Even with the stress in the prestressing going to zero at the strand ends, often the strand pattern necessary to meet the flexural requirements at mid span can cause tension in the top of the beam near the beam end. There are two methods of reducing these prestressing moments at the beam ends; debonding and deflecting. Since the concrete does not restrain debonded strands, the stress in the strands goes to zero at release. By carefully choosing which strands to debond, the axial force from prestressing is lessened thereby reducing the prestressing moment causing tension in the top of the beam. Another way to reduce the prestressing moment is to reduce the eccentricity of the prestressing by deflecting. Deflecting prestressing steel also has the added beneficial effect of lifting up the beam where the strands are deviated. Unfortunately, deflecting strands has fallen out of favor with precasters and debonding is more the current standard of practice. Development length is affected by debonding in two ways. The first and most obvious is that the transfer length and the flexural bond length do not start until the strands are bonded to the concrete. The second and more subtle change is that the k factor in the development length calculation rises from 1.6 to 2.0 for debonded strands. There are also code requirements for how many strands can be debonded and which strands these are. *AASHTO LRFD* Article 5.11.4.3 states the following:

> ➢ No more that 25% of the total number of strands in any section may be debonded

> ➢ No more than 40% of the total number of strands in any row may be debonded

➢ No more than 40% of the debonded strands or 4 strands, whichever is larger shall have the debonding terminated at any section

➢ Debonded strands shall be symmetrical about the centerline of the section

➢ Debonded lengths of pairs of strands that are symmetrical about the centerline shall be equal

➢ The exterior strands on each horizontal row shall be fully bonded
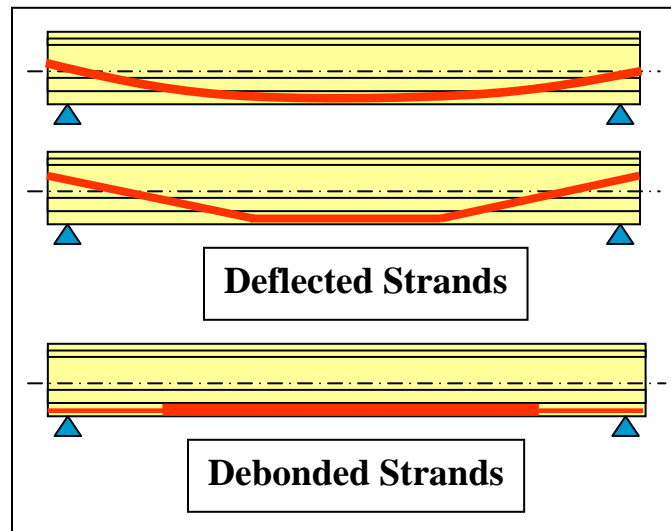
Figure 2.66 Typical Prestressing Steel Layouts

2.4.6.4 Analysis (Srut and Tie)

Strut and tie models like the one in Figure 2.67 can help to visualize the areas in tension and compression. The idea is to simplify a segment as though it were a truss. For anchorage zones in a pretensioned girder, the application of the force is known and the distribution of that force some distance away is known. Using some creativity and engineering judgment, a drawing of the force flow can be created which can then be turned into a strut and tie model. From the strut-and-tie model below, it can be seen that there are two major sections of tension that must be reinforced one perpendicular to the force of the prestressing modeled by T_1 and T_3 and one parallel to the force of prestressing modeled by T_2. In a beam the tension parallel to the prestressing force would be counter balanced by the dead load of the beam and checked at service level flexure. The tension perpendicular to the prestressing force is dealt with in the AASHTO code by the vertical reinforcement. The area of high compression must also be reinforced with confinement reinforcing.
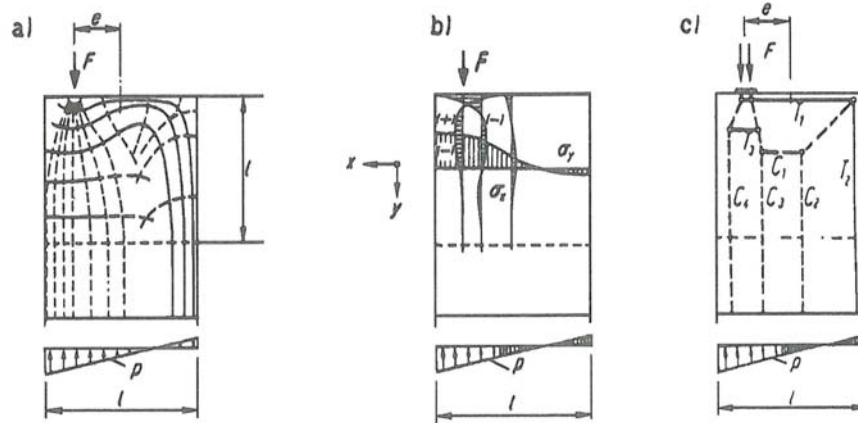
Figure C5.10.9.4.1-3 Strut-and-Tie Model for the Outer Regions of
the General Zone.

Figure 2.67 Development of Strut-and-Tie Model for Pretensioning

2.4.6.5 Confinement (Bursting) Reinforcement

The *AASHTO LRFD* Code gives guidance for reinforcing both the vertical tension above the anchorage zone and the confinement reinforcement. In *AASHTO LRFD* Article 5.10.10.1 the code specifies that the vertical reinforcement shall account for not less than 4% of the prestressing force. This steel should be located as close to the end of the beam as practical. However, all vertical reinforcement within h/4 of the end of the beam can be used. The bursting resistance (P_r) = $f_s A_s$. Where f_s is the stress in the steel not to be taken as greater than 20 ksi, and A_s is the area of all vertical reinforcement within h/4 of the end of the beam. The confinement steel is distributed along the beam for 1½d. The reinforcement should consist of bars not less than #3's at 6". These bars should enclose the strands.

2.4.6.6 Reinforcement Details

Most state departments of transportation have standard drawings of anchorage zones appropriate for use in their state. Using these standards will insure that local precasters are familiar with the reinforcing details.

2.5 Design of Precast Girders Made Continuous with Reinforced Concrete Joints

This topic extends the concept of simply supported prestressed concrete girder to applications where spans are made continuous by means of reinforced concrete joints connecting the superstructure of adjacent spans over interior piers. Consideration is given to accounting for the effect of the sequence of construction, statically indeterminate reactions and redistribution of moments due to creep.

Making a structure continuous by means of reinforced concrete joints requires that account be taken of the influence of the construction technique upon the design and the effects of redistribution of bending moments due to creep.

  ➢ Summarizing, the impacts of the construction sequence on the design are:
  ➢ The self-weight of the girder, forms and deck slab, along with pretensioning effects are applied on the non-composite section on the simply supported span.
  ➢ Subsequent loads are applied on a composite, continuous structure.
  ➢ It is necessary to evaluate the effects of redistribution due to creep for the effect of differential shrinkage of the deck slab.
  ➢ Reinforced spice joints should be designed and detailed for the resulting positive and negative moments.

An important aspect is to identify and evaluate the effects of creep redistribution (below).

2.5.1 Partial Continuity of Deck Slabs Only

Where only a deck slab is made continuous, continuity reinforcement is basically a nominal amount to control cracking. It is not structurally designed for a "particular load or effect" as such. Although theoretically, one could perform a rigorous analysis taking into account the distance between the adjacent bearings and their shear stiffness to develop or generate an opposing strut or tie force in the slab, the engineering effort is hardly worthwhile. Nominal rebar is usually sufficient; with #4 or #5 rebar lap-spliced with the deck slab longitudinal steel. In practice, as the spans expand and contract and work under traffic loads, a crack may form over the gap. In order to control the crack, a crack-inducer, such as a small saw cut or formed strip is installed in the top of the slab over the gap.

This detail enables a few spans of continuous slab between true expansion joints in lengths up to about 400 feet. This facilitates, for example, 4-span bridges over interstate highways with continuous decks from end to end, with expansion joints only at the abutments.

Section Thru Girder   **Side Elevation**
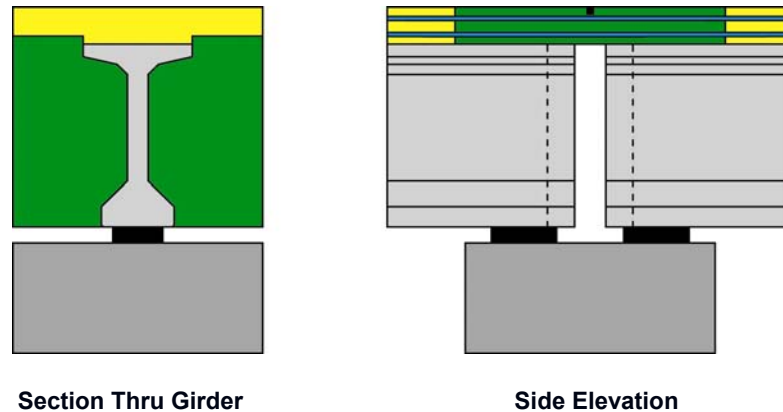
Figure 2.68 Partial Continuity of Deck Slab Only

2.5.2 Full Continuity using Reinforced Concrete Joints

An alternative to the above deck-slab-only joint is to make the joint between the ends of the girders structurally continuous for all loads applied after construction of the deck. This is achieved by extending longitudinal reinforcement from the ends of the girders into a full-depth cast-in-place reinforced joint, as shown in Figure 2.69.

Longitudinal reinforcement in the deck slab is designed to resist negative moments over the pier arising from subsequent superimposed dead load (barriers, utilities, surfacing, etc.) and live load. In addition, there is a certain amount of redistribution of structural dead load and prestress from the effect of long-term creep. This should be properly accounted for in any superstructure made structurally continuous in this manner. Similar considerations are essential where girders are made continuous using post-tensioning tendons (see 2.7).

Section Thru Girder   Side Elevation
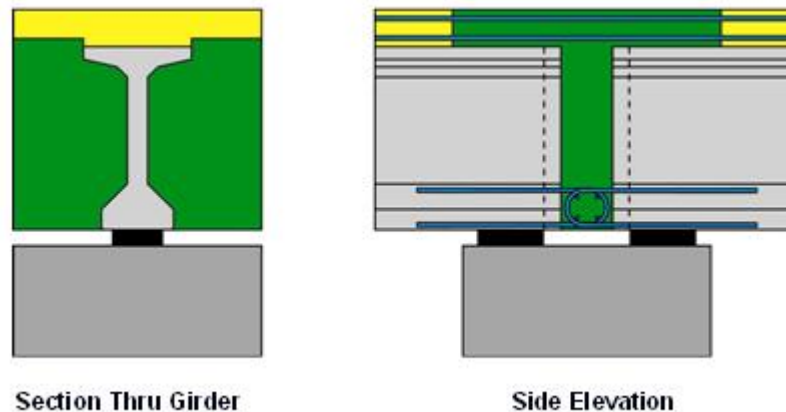
Figure 2.69 Full Depth Reinforced Concrete Joint

2.5.3 Longitudinal Analysis (Bending Moments and Forces)

2.5.3.1 Analysis Methods

Making any superstructure continuous over one or more interior supports, introduces a number of redundant or indeterminate reactions equal to the number of interior supports. Support reactions can no longer be determined from statical analysis alone. If the interior supports are "simple bearings" (e.g. pins or rollers) that provide vertical support but little or no longitudinal constraint, then reactions can be determined using any classical formulae for continuous beams given in most structural engineering text books or manuals.

When girders are first erected as simply supported beams with a bearing under the end of each girder but and then made fully continuous, *AASHTO LRFD* allows the designer to utilize formulae for continuous beams as a close approximation to actual conditions. More rigorous analysis may be used at the discretion of the designer. Such rigor might be appropriate if, for example, (a) the distance between the bearings under the ends of the girders (b) the vertical stiffness of the bearings and (c) the rotational stiffness of the pier cap and columns are sufficient to generate a local couple. This couple would be taken by the substructure in flexure and would appear in the superstructure as a difference in negative moment from that at the bearing on one side of the pier to that on the other.

Classical analysis methods for determining bending moments at interior supports in (statically indeterminate) continuous beams may be summarized in the following steps:

➤ Consider the effect on the simply-supported span
➤ Calculate the end rotations
➤ Calculate the continuity moments from the end rotations
➤ Superimpose the spans to give final moments

Reference should be made to engineering text books for the analysis of continuous beams. Various methods are available such as, slope-deflection, area-moment (flexibility) methods, moment distribution (Hardy-Cross), stiffness and matrix-methods. It is beyond the scope of this manual to address in detail methods of structural analysis statically indeterminate structures. For illustration, using the "Area-Moment Method", the above steps are expanded and summarized thus:

1. Reduce the structure to a statically determinate condition by removing redundant forces or constraints.
2. Develop the bending moment diagram, M, for this determinate condition.
3. Divide the ordinate of the bending moment, M, diagram by EI at each section to give the value of "M/EI". (This will facilitate analysis of both constant and variable depth structures.)
4. Divide the "M/EI" diagram into convenient geometrical areas and locate the centroid of each area.
5. Calculate the areas and moments of the areas of the "M/EI" diagram from each end of each simple span to determine rotations and displacements at each end respectively.
6. Apply unit redundant forces and moments to the structure and calculate the relevant bending moment diagrams.
7. Repeat steps 3, 4 and 5 for these diagrams to provide angular and linear displacements.
8. Equate the results of steps 5 and 7 to find values of actual redundant forces and moments.
9. Use these values to calculate the final bending moment diagram

The particular method of reducing a structure to a statically determinate condition is a matter of choice for the designer. The above is a general case. The designer may also utilize a suitable computer program. Most programs for the analysis of continuous beam or plane-frame structures are based on stiffness-matrix methods.

For the purpose of discussion, our illustration is simplified to superstructures of constant section – which is the case for the vast majority of precast girder bridges.

2.5.3.2 Continuity Effects

In continuous girders, significant continuity effects arise from (1) the construction process, i.e. the sequence of making continuity joints and casting the slab, (2) secondary moments from prestress (3) differential shrinkage of the deck slab relative to the girder (4) redistribution of moments due to creep. The latter may induce significant tensile stress in the bottom of the girders near the supports and reduce the effectiveness of prestress in the midspan region. An adjustment of the pre-tensioning force by magnitude and/or eccentricity may be needed. These topics are addressed in greater detail in the following.

2.5.3.2.1 Construction Sequence Effects

The effect of a different construction sequence when casting the deck slab and making the structure continuous is contrasted in Figure 2.70 and Figure 2.71 for the simplest case of a two span structure.

The first possibility, "A", (Figure 2.70) is to erect the girders and, while they rest on their own bearings as simply supported spans, the majority of the deck slab is cast, leaving a narrow closure gap (A.1). The reinforced concrete splice joint is then cast as a final closure operation (A.2). Disregarding the effect of the short distance between the bearings (as discussed above) the bending moment in each girder from the weight of the slab plus formwork (say, w per unit length) is that for a simply supported span, namely;

$$\text{Maximum positive moment,} \qquad M_{A\ pos} = \qquad + wL^2 / 8$$

Slab and Joint Construction Sequence - A

(A.1) Erect girders, cast deck slab cast on simple spans
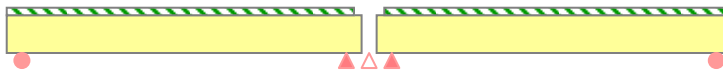
(A.2) Cast reinforced concrete splice joint
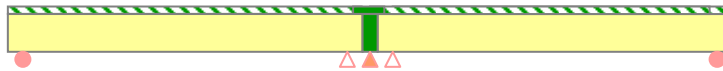
(A) Bending moment from deck slab weight "as-
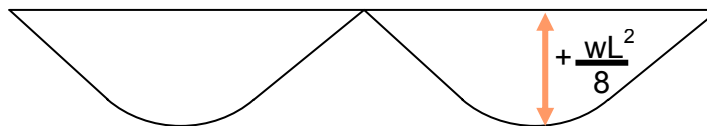
Figure 2.70 Construction Sequence Effects – Case (A)

An alternative possibility (B), (Figure 2.71) is to erect the girders, cast the splice joint and allow it to harden making the girders into to continuous spans. In order to generate negative moment capacity, this would require significant longitudinal reinforcement to connect the top of the girders. For the purpose of this illustration only, if it is assumed that such capacity is available, then when the deck slab is cast on the now continuous girders the bending moments due to the weight of the slab are significantly different, namely;

$$\text{Maximum positive moment, } M_{B\ pos} = \qquad + 9wL^2 / 128$$

$$\text{Maximum negative moment, } M_{B\ neg} = \qquad - wL^2 / 8$$

Slab and Joint Construction Sequence - B

(B.1) Erect girders, cast joint, allow to harden
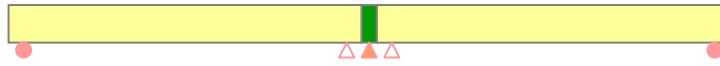
(B.2) Cast top slab on 2-span continuous unit
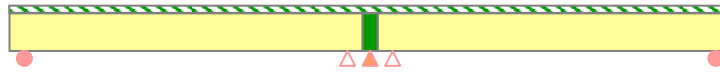
(B) Bending moments in girder from slab continuous

$$- \frac{wL^2}{8}$$

$$+ \frac{9\,wL^2}{128}$$
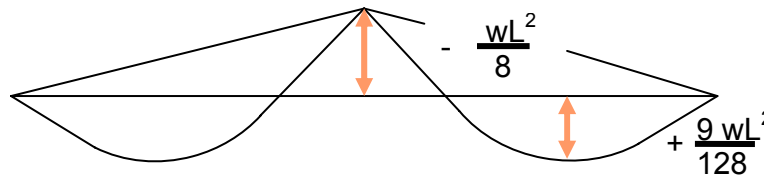
Figure 2.71 Construction Sequence Effects – Case (B)

These bending moments are those for a two-span girder as determined by any classical theory flexure under elastic conditions. It can be seen at a glance that the bending moments from the two construction sequences are significantly different. In reality, it is possible to generate significant negative moment capacity over the center support using mild steel reinforcement in the deck connection between the ends of the girders. (Alternatively, significant negative moment capacity can be achieved using post-tensioning (DM Section 2.7)

The most practical sequence of construction for a real 2-span case would be Case "A". This is further amplified below to illustrate the phases and considerations in.

In Phase 1, the pretensioned girders are erected. Since the flexural effect of the pretensioning is much greater than the moment of the girder self weight, the net camber is upward. A wide joint is left over the pier to accommodate overlap of longitudinal reinforcement. Deck slab forms and reinforcement are installed. In Phase 2, negative moment reinforcing in the slab extends over the pier and the deck slab is cast over most of each span. The girders deflect under the weight of the wet concrete, but the ends of the girders are free to rotate. In Phase 3, the closure joint reinforcement is completed and the joint is cast. Because this pour is small, there is negligible additional end rotation. The net camber is the sum of Phases 1 and 2 and is upward at this point. This is because the flexural effect of the pretensioning is greater than that of the girder and slab self weight combined simply because there must be sufficient to carry subsequent applied dead and live load. Permanent dead loads such as barriers, utilities, wearing surface and live load are applied to the 2-span continuous unit.

Phase 1:

Phase 2:

Phase 3:
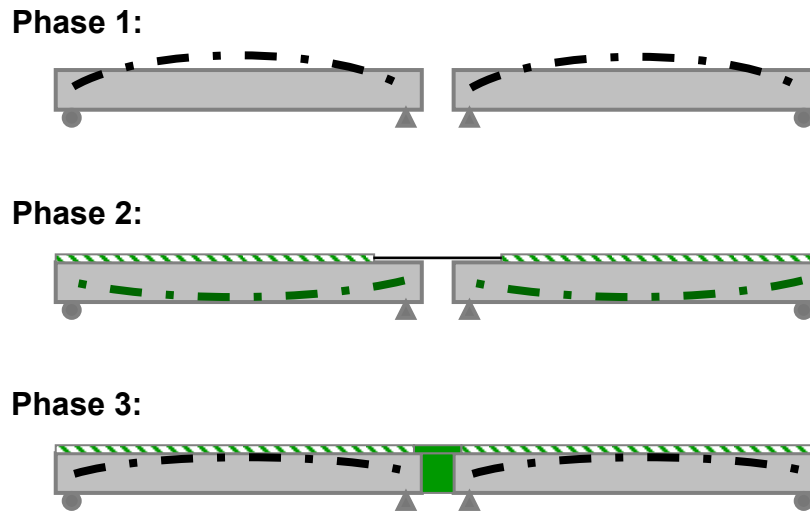
Figure 2.72 Practical Construction Sequence Considerations

The above 2-span examples serve to illustrate the importance of considering the construction sequence, the method of making continuity and of applying loads to a structure in one (simple span) configuration that becomes a different (continuous) structure at a later stage. The same principles extend to structures with a number of spans. In addition, effects from permanent dead load, prestress, creep and shrinkage occur at different times and stages of construction.

2.5.3.2.2 Secondary Prestress Reactions and Moments

Consider the case of 2-span girder continuous over a center support and prestressed with straight strands at a constant eccentricity applied from end to end of the two continuous spans – M_{ps}, is also the "Secondary Moment"

Two continuous spans, each = L ft

Prestress $M_p = - (F.e)$ ft k
for straight strands end to end

Unrestrained upward
deflection = $(F.e) L^2 / 2 E I$ ft

P

Apply load P at center so
that net deflection is zero

Unrestrained downward
deflection = $(P) L^3 / 6 E I$ ft

By equating deflections, we find: $P = 3 (F.e) / L$

And, at center support, $M_{sec} = 3 (F.e) / 2$

$R = P$ (down)
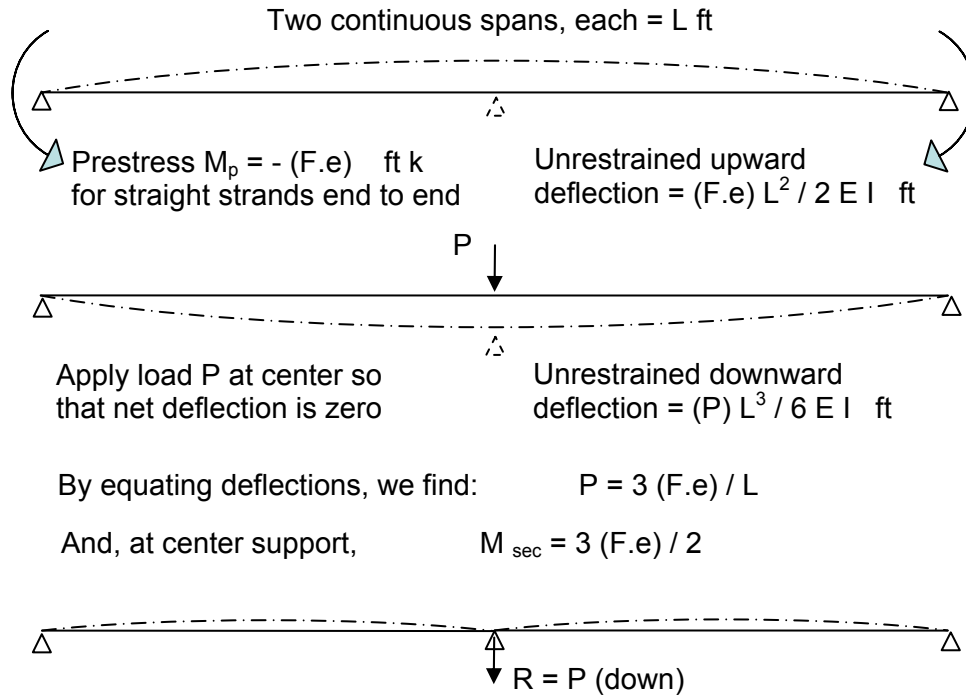
Figure 2.73 Secondary Reaction and Moment in Continuous Beam

This is statically indeterminate structure. We are interested in finding the magnitude of the reaction at the center support from the prestress effect alone. In order to do this, imagine that the support is removed and that a constant prestress moment, $M_p = (F.e)$, is applied to the simple span beam of length 2L.

The unrestrained upward deflection is determined by beam theory (e.g. area-moment or slope deflection). Then, applying the principle of compatibility, a downward load "P" is applied at the center to return the deflection to zero. By equating the deflections, the magnitude of the load P, in terms of the applied prestress, is found to be $P = 3(F.e)/L$. This is the "Secondary Reaction" (acting downward) at the center support induced by straight prestress.

The accompanying bending moment is the "Secondary Moment" due to prestress, and is found to be:

$$M_{sec} = 3(F.e) / 2$$

The net moment due to prestress at the center support is then

$$M_{net\ ps} = M_p - M_{sec} = (F.e) - 3(F.e)/2 = -(F.e)/2$$

The net effect is to induce a negative bending moment, i.e. one that creates tension in the top fiber over the center support. This net moment acts in the same sense as

that due to a uniform load applied to the two spans. Consequently, the secondary moment from the above condition adversely affects the capacity of the girder at the center support.

This has profound implications for prestress applied to continuous structures and for the effects of creep redistribution in structures built in one statical condition that is later changed to another – as is encountered in cases where simply supported pre-tensioned girders are made continuous over interior piers by reinforced concrete joints (below).

A similar redistribution of moments occurs for structures made continuous with post-tensioning; except that the redistribution is driven by the difference between the combination of pre- (if any) and post-tensioning effects and dead load (see DM Section 2.7). However, in post-tensioned structures, we shall see later that it is possible to reduce or eliminate secondary moments due to prestress by draping the tendon profile so that it is high up over the interior supports and low down within the span (DM Section 2.7).

2.5.3.2.3 Differential Shrinkage

Since a deck slab is of younger and usually lower strength concrete than a girder, there is a certain amount of differential shrinkage between the deck slab and the girder – both shrink but at different rates. The result of this effect is illustrated in Figure 2.74.
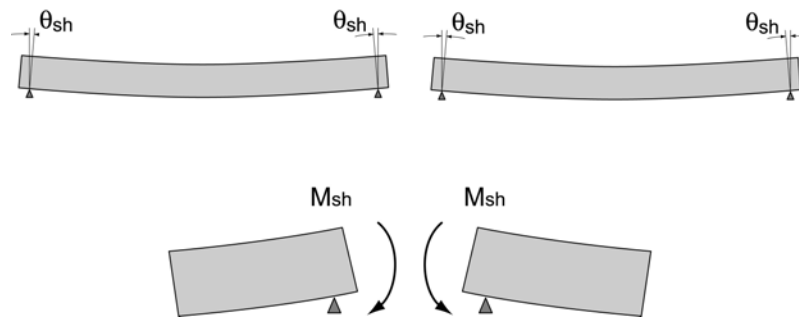
Figure 2.74 Differential Shrinkage

> ➢ Shrinkage of the deck relative to the girder results in a (uniform) positive moment that, if unrestrained, induces end rotations = $\theta_{shrinkage}$.
> ➢ However, since the structure is made continuous over the pier, the adjacent spans restrain the rotations and induce a moment = M_{sh} over the interior pier.

For the case of our two-span structure illustrated, this differential shrinkage effect is analogous to the above situation of secondary moments due to straight prestress at a constant eccentricity from end to end, but acting in the opposite sense. This can be

envisioned by imagining the differential shrinkage effect as equivalent to a prestress applied at the top of the girder from end to end of the two spans. The net effect is to induce a tensile stress in the bottom fiber of the girders at the interior pier. Calculation of the moment induced by this effect is addressed in detail below.

2.5.3.2.4 Redistribution of Moments Due to Creep

Since the girders are erected first in a statically determinate condition (simply-supported) that is later made continuous by means of a moment-resisting cast-in-place joint, a certain amount of redistribution of moments will occur due to creep. In this case, what was originally erected as two simply-supported spans, will tend to creep towards the condition that would have been the case had the entire superstructure structure, (i.e. girders, prestress and deck slab) been placed "instantaneously" as it were, in its final (2-span) continuous configuration. This creep redistribution effect also applies to the differential shrinkage between the slab and girder.

It should be noted that for any superimposed dead load (barriers, utilities, surfacing etc) applied to the completed, continuous structure in its final structural configuration, there is no redistribution of their moments due to creep. Creep will cause increasing deflection (deformation) under their load, but there will be no redistribution of moments or forces from this effect.

Summarizing, redistribution of moments due to creep applies to:

> ➢ Construction sequence effects
> ➢ Secondary reactions and moments due to prestress effects
> ➢ Differential shrinkage of the deck slab relative to the girder

Calculation of the effects is addressed in further detail in the following sections.

2.5.4 Creep Redistribution

2.5.4.1 Effect of Creep

Creep tends to make a structure, originally built in one condition (e.g. simply-supported) gradually act as if it had been built in its final condition, i.e. as a truly continuous structure from the outset. In the above two-span illustration, bending moment over the interior pier due to the self weight of the slab is initially zero in the "as-built" simply-supported condition, Case "A" in Figure 2.75. Gradually, creep redistributes the "as-built" moments.

In this illustration and considering only slab dead load, with time, creep induces a negative moment over the interior pier accompanied by a corresponding reduction in positive moments within each span. However, since creep is a function of the maturity of the concrete when loaded, the magnitude stress and duration of a particular load, 100% redistribution is never possible. That is to say, creep redistribution cannot attain the moments of Case "B" in Figure 2.75 which would be

the condition if the slab load was applied "instantaneously" to a continuous 2-span structure. The amount of redistribution is limited. For weight of the slab only, the final moments would be as illustrated in Figure 2.75.

(B) "instantaneous"

(A) "as-built"   (C) "creep redistributed" moments

$$\text{Final Moment Diagram, } M_C = (1 - e^{-\varphi})(M_B - M_A)$$

Where φ = "creep coefficient"
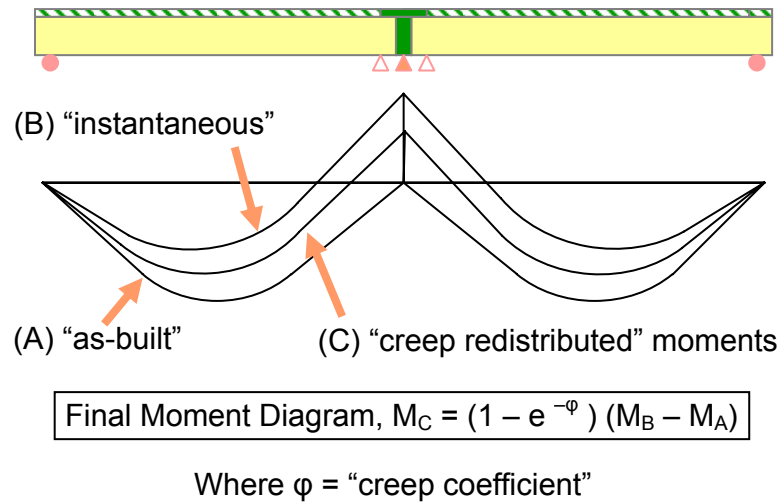
Figure 2.75 Creep Redistribution of Slab Weight in Continuous Spans

In this illustration, the final bending moments (M_C) due to the self weight of the slab only, after redistribution due to creep are given by the expression:

$$M_C = (1 - e^{-\varphi}).(M_B - M_A)$$

Where φ = "creep coefficient" which represents the ratio of the creep strain to the elastic strain from the time, in this illustration, that continuity is established.

In this 2-span illustration, moments from creep redistribution gradually generate tension in the top longitudinal reinforcement in the slab over the piers and reduce the flexural tensile stress in the bottom fiber. The latter reduction is a maximum at the interior pier, diminishing to zero across each span.

In an actual structure, the situation is more complex since creep happens under all changes of internal stress from the combination of permanent load and prestress applied at different stages of construction. However, creep redistribution of moments only occurs after the stage and time of construction that continuity is established – i.e. the change from a statically determinate (simple span) to a statically indeterminate (continuous) superstructure.

A thorough, classic, theoretical and practical treatment of creep redistribution in a continuous structure was originally developed by Mattock (1961) and later extended by Freyermuth (1969) under research projects for PCA. The approach takes into account:

> ➢ Effect of stresses in the composite section, of creep of the precast girder due to prestress.
> ➢ Effect of stresses in the composite section, of creep of the precast girder due to dead load moments.
> ➢ Restraint moments in continuous girder due to creep.
> ➢ Stresses in the composite member due to differential shrinkage (between the slab and precast girder).
> ➢ Restraint moments in a continuous girder due to differential shrinkage (between the slab and precast girder).

An important outcome of the development of the theory led directly to the above relatively simple equation for final moments (M_C) due creep redistribution given the definition of the creep coefficient, φ as the ratio of the final, long term, creep strain to the initial elastic strain. Mattock and Freyermuth pointed out a wide range of φ is possible from about 1.5 to 2.5. For most practical applications, a value of 2.0 would be reasonable. For the purpose of illustrating the calculations, a value of $\varphi = 2.0$ is used in the following example.

Consider the effects of creep in the spans shown in Figure 2.76. When erected the simple spans deflect under loads and the ends rotate elastically by an amount equal to $\theta_{elastic}$. Unrestrained, these end rotations would grow because of creep by an amount equal to θ_{creep}. However, after the closure joint is cast the adjacent spans constrain the rotations, inducing a moment over the support equal to M_{cr}.
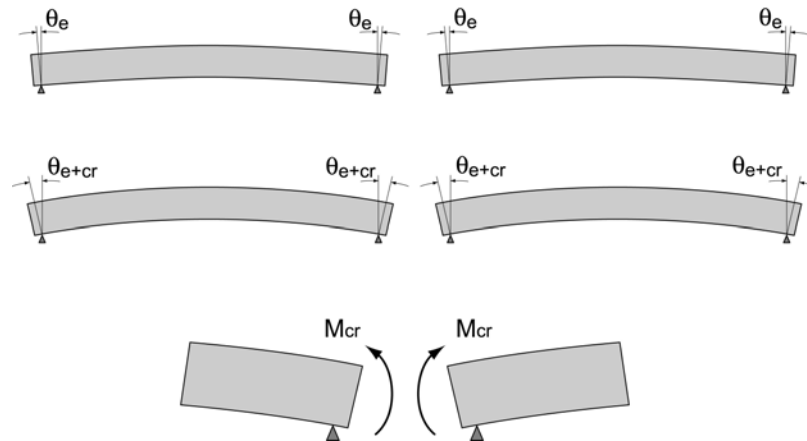
Figure 2.76 Creep Moments

2.5.4.2 Calculation of Creep Redistribution

For a continuous structure, redistribution of moments due to creep is determined using the "Rate of Creep Method" established by Mattock, as follows:

> ➢ Evaluate simple span rotations due to non-composite dead loads.

> ➤ Evaluate simple span rotations due to prestressing
> ➤ Solve for moments on the continuous structure
> ➤ Factor moments by "Rate of Creep" adjustment

The "Rate of Creep" is given by the formula:

$$M_{cr} = M_{sw+ps} (1 - e^{-\Phi})$$

where:

Φ	=	$\varepsilon_{cr} / \varepsilon_e$
ε_{cr}	=	creep strain after continuity is made (per unit stress)
ε_e	=	elastic strain per unit stress due to load
Φ	=	creep ratio (typically in the range of 1.5 to 2.5)

2.5.4.3 Illustration of Procedure

The process is illustrated by the following example. Consider a structure comprised of Type VI girders erected as two simple spans that are later made continuous, as illustrated in Figure 2.77. The simply supported, non-composite, span is 109'-0". After continuity has been made, the span for composite conditions is assumed to be 110'-0".

Non-Composite

Depth = 72 in
Area = 1085 in²
Inertia = 733,320 in⁴
y_{top} = 35.62 in
y_{bot} = 36.38 in

Composite

Depth = 79.5 in
Area = 1955 in²
Inertia = 1,384,254 in⁴
y_{top} = 27.96 in
y_{bot} = 51.54 in
Girder spacing = 9'-8"
Slab = 8"-1/2" = 7 1/2"
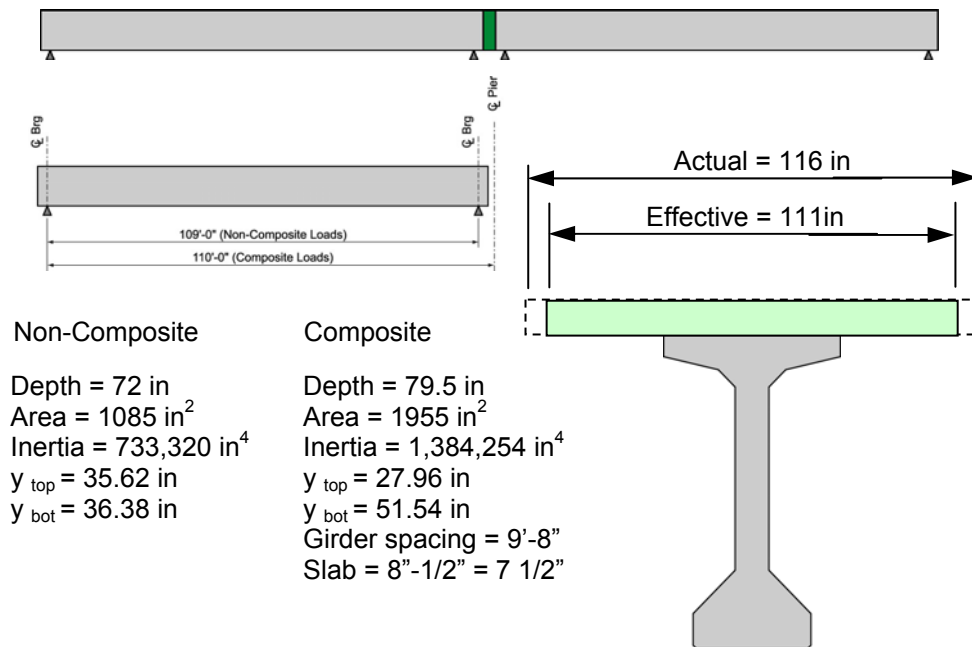
Figure 2.77 Two-Span Structure of Type VI Girders

The self weight load on the simply-supported, non-composite section span is:

Uniform self weight of girder	=	1.130 k/ft
Uniform load of slab	=	0.967 k/ft
Weight of haunch	=	0.175 k/ft

Total uniform load on non-comp (w)   =   2.272 k/ft

Using any classical elastic beam formulae, such as the area-moment theorem, the end rotation of the girder for a uniform load of w per unit length (Figure 2.78), is given by:

$$\theta_{sw} = \frac{w L^3}{24EI} = \frac{2.272\,(110.0^3)}{24\,EI}\ \text{radian}$$

Load = w kip / ft

Max Mt, $M_{sw} = \dfrac{w L^2}{8}$ ft kip

M_{sw}

End Rot $\theta_{sw} = \dfrac{w L^3}{24\,E\,I}$ radian

Deflection $\delta_{sw} = \dfrac{5\,w\,L^4}{384\,E\,I}$ ft

θ_{sw}

δ_{sw}
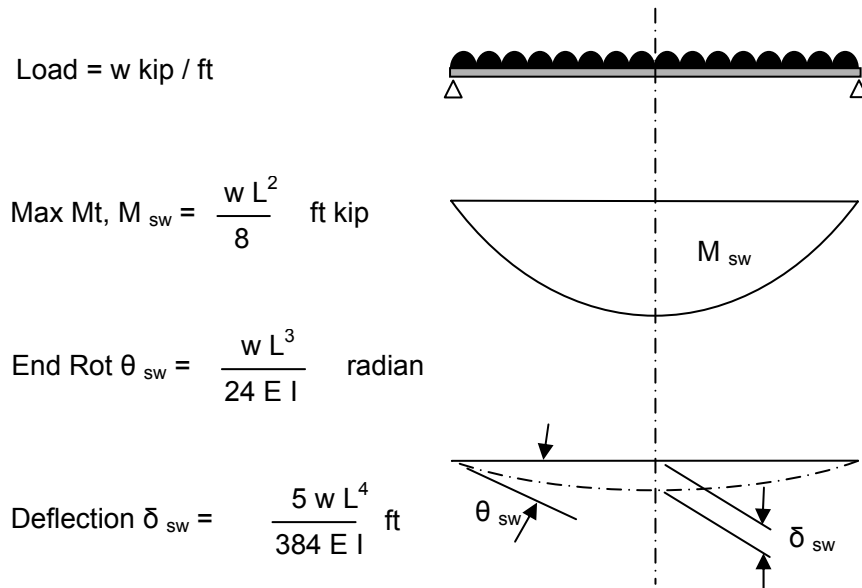
Figure 2.78 Simply-Supported Span under Uniform Load

Now apply a moment, M, at the closure of the 2-span girder to induce an equal and opposite end rotation to that of the simply supported girder under self weight (Figure 2.79).
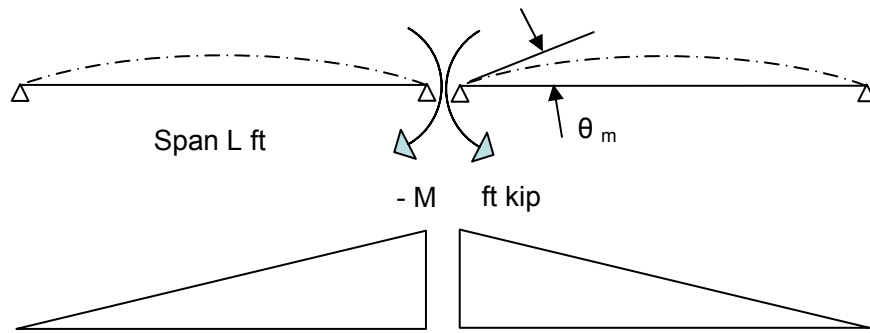
For Moment (- M) applied at closure, by area-moment =

End Rotation, $\theta_m = \dfrac{(-M)\,L}{3\,E\,I}$ radian

Figure 2.79 Continuity Moment, M

The end rotation due to a moment (-M) applied at one (closure joint) end of a simply supported beam is given by:

$$\theta_m = \frac{(-M_{sw})\,L}{3\,E\,I}$$

Equating θ_m to θ_{sw} provides the magnitude of the continuity moment (-M), thus:

$$End\ Rot\ \theta_{sw} = \frac{w\,L^3}{24\,E\,I} = (-)\,\theta_m = \frac{(-M_{sw})\,L}{3\,E\,I}$$

$$From\ which,\ M = -\frac{w\,L^2}{8}\ \ ft\ k$$

This is the negative bending moment over the central pier for a uniform load (w) applied to a continuous girder of two spans; as given by any elastic beam theory formula for bending moments in continuous beams. Substituting values for w (= 2.272k/ft) and L (= 110 ft) gives M = - 3,436 ft kip (Figure 2.80). In the 2-span case, the negative moment at the interior pier happens to be of the same magnitude as the simply-supported self weight moment at mid-span, but of opposite sign (assuming that the simple span and continuous span lengths are the same, which is approximately the case in our example).

Simple moment from w = self weight of beam,
slab and haunch - "as erected"

Continuous beam moment from self weight of beam, slab
and haunch - as if erected "instantaneously"
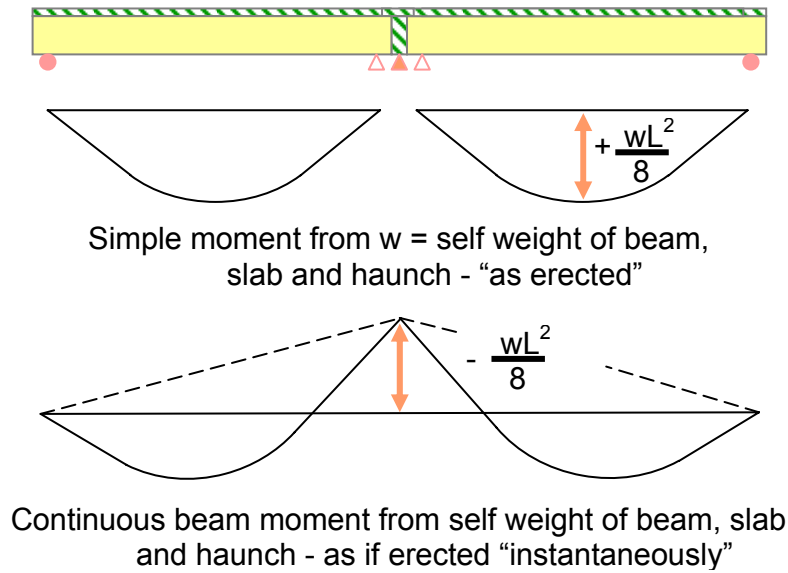
Figure 2.80 2-span, self weight continuity moment

Now, in a similar manner to the above, we can calculate the simple span end rotations due to prestressing and the moment necessary at the closure joint over the pier to provide an equal and opposite end rotation. In order to do this, we need to know the layout of the prestress – this is illustrated in Figure 2.81. In this case, the layout incorporates debonded (shielded) strands at the ends of the girder. The prestress force (F) and prestress moment (F.e) at each section of the girder is shown in Figure 2.82.
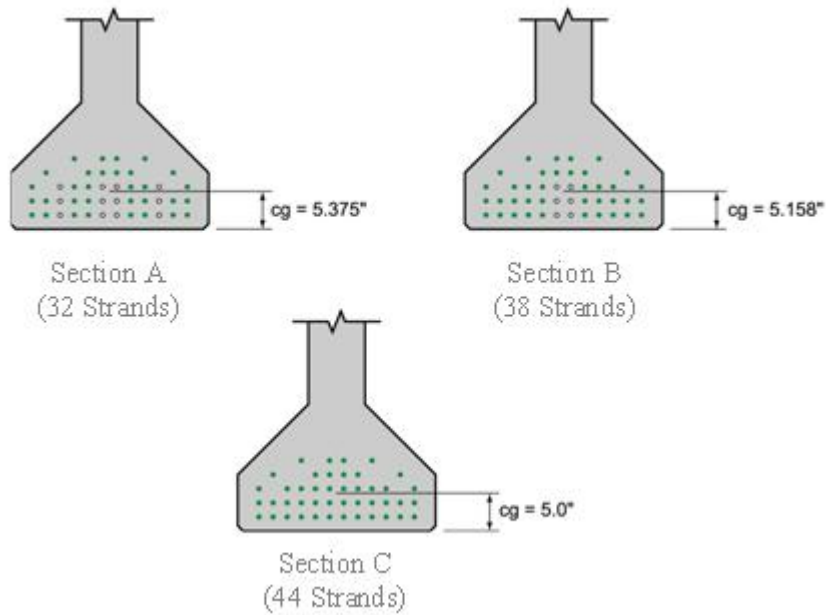
Figure 2.81 Prestressing Layout and Debonding
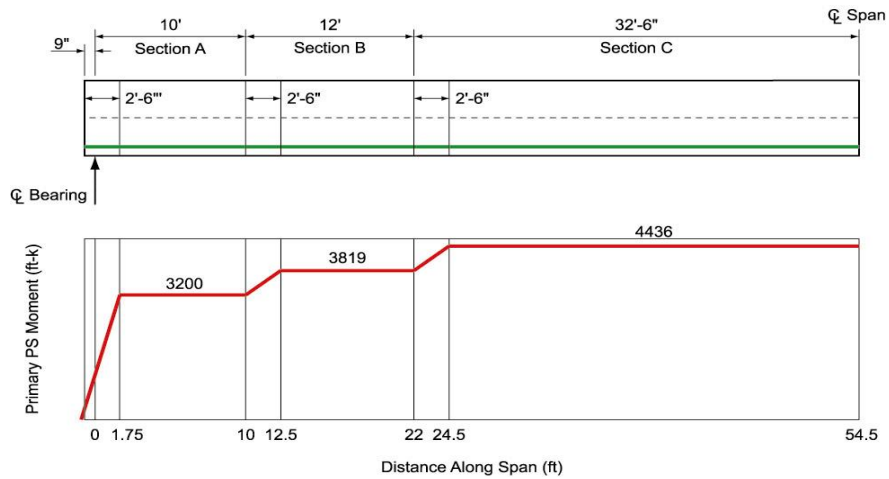
Figure 2.82 Prestress Moment for Simply-Supported Girder

The prestress moment varies along the girder due to deliberate debonding of strands to satisfy end conditions (i.e. to avoid excessive top tensile stress). As the prestress is symmetrical about mid-span, only half of the diagram is shown in the figure. Since it is symmetrical, the end rotation of the girder is calculated by applying the area-moment theorem in the manner described above, giving an end rotation of:

$$\text{End Rotation, } \theta_{ps} = -\left[\frac{1}{2}\right]\frac{\Sigma(F_e)}{E\,I}$$

In this case, the rotation, θ_{ps}, is negative (upwards) at the end of the girder. The continuity moment (M_{ps}) required at the closure joint is found by equating this end rotation to that for a moment of (M_{ps}) applied at the (closure joint) end of a simply supported beam (in the same manner but of opposite in sign to that in Figure 2.79. This gives;

$$\text{End Rotation, } -\theta_{ps}\quad\left[\frac{1}{2}\right]\frac{\Sigma(F.e)}{E\,I} = \theta_m = \frac{M_{ps}\,L}{3\,E\,I}$$

$$\text{From which, } M_{ps} = \left[\frac{3}{2}\right]\frac{\Sigma(F.e)}{L}$$

Inserting the summation of prestress area-moment $\Sigma(F.e) = 441,919$ ft k and the span length L of 110 ft. gives a (positive) continuity moment of, $M_{ps} = 6,026$ ft k.

The net continuity moment at the center pier of a 2-span unit is the sum of the continuity (fixity) moments from self weight and prestress, namely;

$$M_{sw+ps} = M_{sw} + M_{ps} = (-3,436 + 6,026) = 2,590 \text{ ft k}$$

This is the continuity moment that must be adjusted for creep. Applying the "Rate of Creep Method", the redistributed creep moment, M_{cr}, is given by:

$$M_{cr} = M_{sw+ps}\,(1 - e^{-\Phi})$$

If the creep ratio, Φ, is taken as 2.0, then the Creep Moment is;

$$M_{cr} = 2,590\,(0.8646) = 1,954 \text{ ft k}$$

2.5.4.4 Calculation of Moments Induced by Differential Shrinkage

Consider first a simply-supported span with a deck slab cast later and of different, less mature concrete than the precast girder. The slab tends to shrink relative to the girder but the girder also restrains that shrinkage. The net effect is to induce a bending moment, approximately constant, over the length of the span given by:

$$M_{sh} = \Delta\varepsilon_{sh}.\,E_d.\,A_d.\,(e')$$

Where:

$\Delta\varepsilon_{sh}$ = differential shrinkage strain of deck to girder

E_d =   Modulus of elasticity of deck slab
A_d =   area of deck slab (full area plus haunch)
e'   =   distance from centroid of slab to centroid of composite section

Now:

$$\Delta\varepsilon_{sh} = \varepsilon_{sh,s,\infty} - (\varepsilon_{sh,b,\infty} - \varepsilon_{sh,b,t}).$$

Where:

$\varepsilon_{sh,s,\infty}$ =   ultimate shrinkage of slab at time infinity
$\varepsilon_{sh,b,\infty}$ =   ultimate shrinkage of precast beam at time infinity
$\varepsilon_{sh,b,t}$ =   shrinkage of precast beam at time of casting deck slab

Shrinkage, according to *AASHTO LRFD* Article 5.4.2.3.3-1, is given by:

$$\varepsilon_{sh,s,\infty} = - k_{vs}.k_{hs}.k_f.k_{td}(0.48*10^{-3})$$

Where for the girder;

$k_{vs} = 1.45-0.13(V/S) = 0.877 < 1.0$; so for this case use 1.00

(Given V = 13,020 in^3/ft and S = 2,955 in^2/ft for the girder)

$k_{hs} = (2.00 - 0.14H) = 1.02$ taking H = 70% for relative humidity

$k_f = 5/(1+f'_{ci}) = 5/(1 + 4.8) = 0.862$

$k_{td} = t / (61-4(f'_{ci}) + t) = 1.0$ for t = infinity
Or k_{td} = 0.683 for t = 90 days

Inserting these in *AASHTO LRFD* Article 5.4.2.3.3-1 for the girder, we find;
$\varepsilon_{sh,b,\infty} = 0.000422$
$\varepsilon_{sh,b,t} = 0.000288$
(Assuming that the deck slab is cast when the girder is 90 days old)

Alternatively, for the slab:

$k_{vs} = 1.45-0.13(V/S) = 0.855 < 1.0$; so for this case use 1.00

(Given V = 10,440 in^3/ft and S = 2,280 in^2/ft for the slab)

$k_{hs} = (2.00 - 0.14H) = 1.02$ taking H = 70% for relative humidity

$k_f = 5/(1+f'_{ci}) = 5/(1 + 3.20) = 1.19$ (if f'$_c$ = 4.0 ksi for slab)

$k_{td} = t / (61-4(f'_{ci}) + t) = 1.0$ for t = infinity

Applying *AASHTO LRFD* Article 5.4.2.3.3-1 to the slab, we find for our example that at time infinity;

$$\varepsilon_{sh,s,\infty} = 0.000583$$

The modulus of elasticity for the slab is 3,834ksi.

$$\text{Giving } \Delta\varepsilon_{sh} = 0.000583 - (0.000422 - 0.000288) = 0.000449$$

This induces a constant positive moment of:

$$M_{ss} = 0.000449(3,834)(116*7.5)\,(72 - 51.54 + (7.5/2))$$

$$= +36,259 \text{ kip in} = +3,021 \text{ ft kip}$$

The end rotations due to this constant moment, using area-moment theory, are:

$$\text{End rotation, } \theta_{ss} = -\left[\frac{1}{2}\right] \int \frac{M(x)dx}{E\,I} = -\left[\frac{1}{2}\right] \frac{M_{ss}\,.\,L}{E\,I}$$

Applying a continuity moment, M_{cont}, at the end of a simply supported beam, the rotation at the point of application is given by:

$$\text{End rotation, } \theta_{cont} = \frac{M_{cont}\,.L}{3\,E\,I}$$

Applying compatibility and equating the rotations, we find that the continuity moment at the center support of a 2-span continuous girder induced as a result of shrinkage of the deck slab in the two spans <u>after</u> continuity has been established, is given by:

$$\text{Continuity Moment, } M_{cont} = \frac{-3\,M_{ss}}{2}$$

For the example, inserting the value of M_{ss} = 3021 ft kip, we find that the continuity moment M_{cont} = - 4,532 ft k. Note that this is a negative moment at the interior pier.

The final shrinkage moments are determined by applying the correction factor for shrinkage to the sum of the shrinkage driving moments (M_{ss}) and the shrinkage continuity moments (M cont), namely:

$$M_{sh} = M_{ss + cont} \left[\frac{(1 - e^{-\Phi})}{\Phi} \right]$$

For the example, inserting the value of M_{ss} = 3021 ft kip, we find that the continuity moment M_{cont} = - 4,532 ft k. Note that this is a negative moment at the interior pier.

The final shrinkage moments are determined by applying the correction factor for shrinkage to the sum of the shrinkage driving moments (M_{ss}) and the shrinkage continuity moments (M_{cont}), namely:

$$M_{sh} = M_{ss + cont} \left(\frac{1 - e^{-\varphi}}{\varphi 2} \right)$$

(The above correction factor is taken directly from the same work of Mattock (1961) and Freyermuth (1969) undertaken for PCA as for the formula for creep redistribution.)

In our example, if it is assumed that the creep ratio, φ = 2.0, then we find:

$$M_{sh} = (3,021 - 4,532)0.4323 = \text{-653 ft - kip}$$

The summation of final bending moments due to creep redistribution from differential shrinkage effects on the 2-span continuous girder is illustrated in Figure 2.83.

2.112

Differential Shrinkage

Simply-supported Moment

+ 1,306

Continuity

-1,959

Summation

- 653

+ 1,306
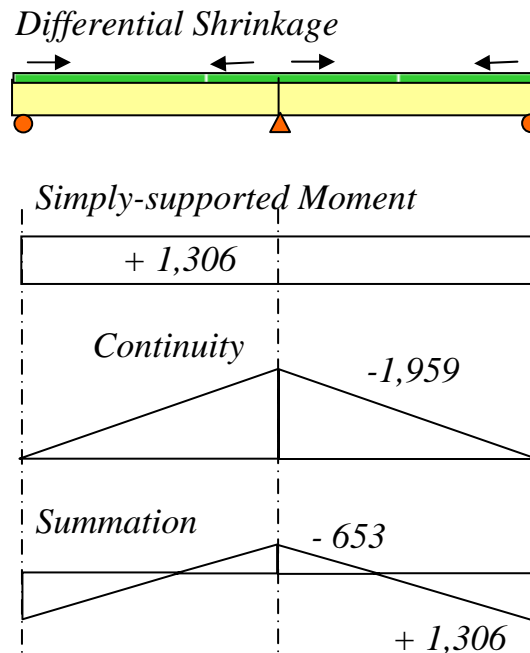
Figure 2.83 Redistributed Differential Shrinkage Moments

2.5.4.5 Effects of Permanent Loads applied to Final Continuous Structure

For the two-span continuous I-girder example above, bending moments from permanent superimposed dead load (i.e. barriers, utilities, surfacing) applied to the structure after it has been made continuous, are determined from routine formulae for continuous beams. As mentioned above, since these effects are applied to the continuous structure in its final structural configuration there is no redistribution of their moments due to creep. Creep will cause increasing deflection (deformation) under their load, but no redistribution.

Similarly, the effects of permanent superimposed dead load applied to any continuous superstructure after all structural continuity has been made, may be determined from classical beam theory for continuous beams, with no redistribution due to creep.

For the 2-span example; the moment at the center pier due to a superimposed dead load of 0.217 kip per ft is:

M supp dead = - 0.217*110^2 / 8   = -328 ft k

2.5.4.6 Effectiveness of Closure Joints

According to *AASHTO LRFD* Article 5.14.1.4.3, the joint at the pier may be considered fully effective if compression is induced in the bottom under the combination of superimposed dead load, settlement, creep, shrinkage, 50% live load

and thermal gradient, if applicable. Otherwise, the joint is considered only partially effective.

> ➢ For a fully effective joint, the structure is designed as continuous for all limit states for load applied after closure.

> ➢ For a partially effective joint, the structure is designed as continuous for strength and extreme limit states only.

If the resistance over the pier is less than the demand, then the positive resistance in the adjacent spans must be adjusted to accommodate redistribution.

For the 2-span example, over the center pier;

Superimposed permanent load (DW)	=	-328 ft k
Settlement (n/a)	=	0 ft k
Creep Moment	=	1,954 ft k
Differential Shrinkage Moment	=	-653 ft k
Live Load Moment (say)	=	0 ft k
Thermal Gradient (n/a this example)	=	0 ft k
Sum	=	973 ft k

The presence of live load on this 2-span structure would be to induce compression in the bottom fiber over the pier and therefore reduce the tensile demand. This is not a worst case rather zero live load is worse. So, absent live load, and assuming no settlement and no TG, the net moment at the center pier in this case is a positive moment inducing a tensile stress in the bottom fiber of the girders near the pier. Under this condition, the joint is partially effective; so the girder prestressing should be designed as for simply supported spans.

The magnitude of the positive moment at the pier is significant. The bottom of the closure joint should be appropriately reinforced. The amount of tensile reinforcement is determined as for a reinforced concrete (T) section under factored moments.

The factored demand moment, M_u, is:

$$M_u = 1.5(-328) + (1.0)(1,954) + (1.0)(-653) = 809 \text{ ft k}$$

The factored nominal resistance must be greater than the demand moment or 1.2 times the cracking moment, which for this example is 1,560 ft-kips. The nominal moment resistance is given by:

$$M_n = A_s f_y (d - a/2)$$

Using an average value of d of 79.5 inches, an effective top flange of 110 inches, a slab concrete strength of 4.0 ksi, and a capacity reduction factor (φ) of 1.0, 8 number 7 bars provides the needed capacity. The arrangement of the reinforcement in the section over the pier is illustrated in Figure 2.84.
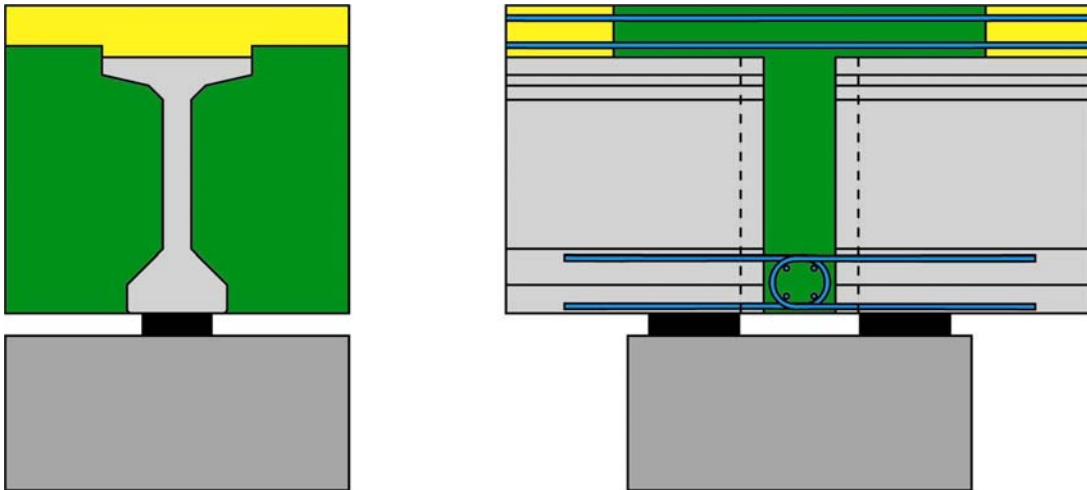
Figure 2.84 Bottom Reinforcement in Closure Joint at Pier

2.5.4.7 Creep Redistribution in Multiple Spans

Creep redistribution in superstructures of multiple spans is similar to that for the two-span example above. The final effects depend upon the sequence of casting deck slabs and making continuity. However, practical considerations may favor one sequence (Option B) over another (Option A) illustrated in Figure 2.85. Sequence of "Option A" will theoretically minimize redistribution effects but "Option B" is more practical for construction purposes, depending upon the size of the structure and amount of concrete to be placed in a given work day - and it will lead to similar, though not precisely the same, results.

Slab Pour and Closure Sequence
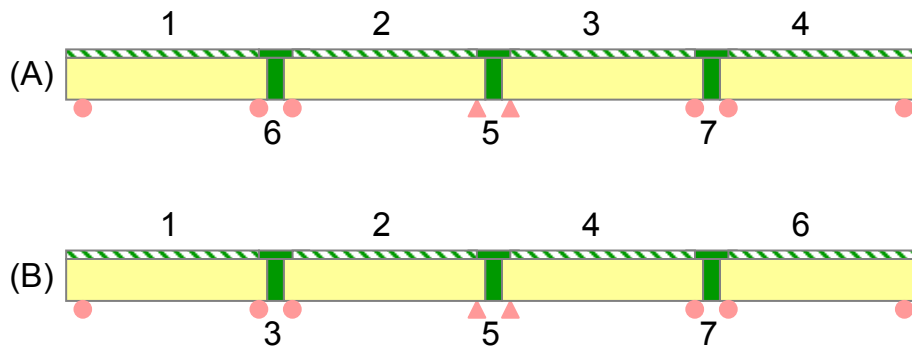
- Reinforced splice joints only (not post-tensioned)

- Option (A) may be "ideal" but option (B) is more practical for field operations and gives similar result

Figure 2.85 Multiple-Span Construction Continuity and Redistribution

For continuous structures, key points to remember are:

> ➢ The Designer should consider the sequence of casting the deck slab and closure joints and the effects it might have upon the girder and deck design.
> ➢ Required or preferred casting sequences should be shown on the plans or clearly addressed in construction specifications.
> ➢ Variations to facilitate alternative construction sequences may also be shown
> ➢ Requests from Contractors to vary the sequence from that shown on the plans should be reviewed by the Designer.

2.5.4.8 Creep Coefficient (φ)

The creep coefficient (φ) takes into account a variety of concrete properties and environmental conditions, in particular:

> ➢ Type of concrete, aggregate and cement
> ➢ Method of curing (steam*, blankets, fog, etc)
> ➢ Strength of concrete
> ➢ Maturity of the concrete from time of casting (i.e. strength gain)
> ➢ Notional thickness (ratio of volume to surface area, V/S)
> ➢ Humidity at the site

(* According to *AASHTO LRFD* Article 5.4.2.3.2, one day of steam curing may be considered the equivalent of one week under ordinary conditions. The formulae for creep and shrinkage development in *AASHTO LRFD* Articles 5.4.2.3.2 and 5.4.3.2.3 for precast girders already include an assumption that steam curing is used.)

The role of creep coefficient (φ) may be understood in the context of the development of strain. For a concrete loaded at time t_0, with a constant stress of σ_0, the total strain $\varepsilon_{total}(t, t_0)$ at time t, may be expressed in a general form as:

$$\varepsilon_{total}(t,t_0) = \sigma_0\left(\frac{1}{E_c(t_0)} + \frac{\varphi(t,t_0)}{E_{c2}}\right)$$

where:
t_0	=	age of concrete at time of loading
t	=	age of concrete at time of evaluation
σ_0	=	applied stress
$E_c(t_0)$	=	modulus of elasticity of concrete at age of loading
E_{c2}	=	modulus of elasticity of concrete at 28 days
$\varphi(t,t_0)$	=	age of area of deck slab (full area plus haunch)

The creep coefficient, $\varphi(t, t_0)$ represents the increase in strain over the time period from t_0 to a future point in time, t. It is expressed with respect to the modulus of elasticity for the concrete according to its strength at 28 days. The modulus of

elasticity at the time of loading, $E_c(t_0)$, is not necessarily the same as that at 28 days, depending upon the maturity of the concrete and time of loading. Within the brackets, the first term of the above expression represents the initial, elastic strain, under the stress at loading, σ_0.

Suppose it were possible to express the modulus of elasticity at the time of loading, $E_c(t_0)$, in terms of the 28 day modulus E_{c28}, then the above equation would lead to a slightly modified version – i.e:

$$\varepsilon_{total}(t,t_0) = \frac{\sigma_0}{E_{c28}}\left(\frac{1}{f_{28}} + \varphi(t,t_0)\right)$$

Where "f_{28}" is a function that relates $E_c(t_0)$ to E_{c28}. The term "$\varphi(t, t_0)$" would represent the development of the creep strain with time as ratio of that at time infinity (Figure 2.86). But, $\varphi(t,t_0)$ does not correspond to the term $\psi(t,t_i)$ of *AASHTO LRFD* (ACI 209). There is an anomaly and no direct link between *AASHTO LRFD* (ACI 209) and FIB (CEB-FIP) – see also Figure 2.87.

The development of the creep strain as a ratio may be expressed algebraically as a function:

$$\text{Ratio of creep strain} = (1 - e^{-\varphi})$$

According to Mattock (1961) and Freyermuth (1969) any reasonable formulation for the creep coefficient, φ with time, may be adopted based on the results of tests or previous data and the final (infinite time) creep ratio typically lies between 1.5 and 2.5.

The development of shrinkage strain follows a similar pattern with time. As discussed in 2.5.4.4 above, the effects of differential shrinkage are accounted for by applying a correction factor $= (1 - e^{-\varphi})/\varphi$ to the shrinkage driving and continuity moments.
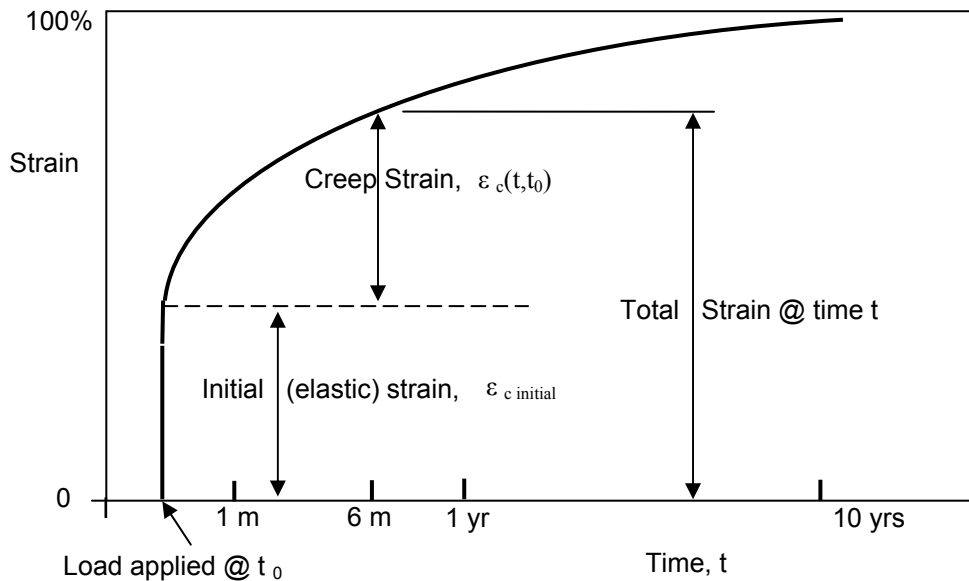
Figure 2.86 Development of Creep Strain with Time

In the absence of any information, *AASHTO LRFD* allows estimates for creep (and shrinkage) to be based on:

- ➢ *AASHTO LRFD* Articles 5.4.2.3.2 (Creep) and 5.4.2.3.3 (Shrinkage)
- ➢ The CEB-FIP (European) model code, or
- ➢ ACI 209

Terminology adopted by different codes for describing creep behavior is illustrated in greater detail in Figure 2.87. However, this does not mean that the codes are "equal". Rather the contrary; experience indicates a noticeable difference between FIB (CEB-FIP) and ACI 209 upon which *AASHTO LRFD* is based.

The manner in which creep and shrinkage are formulated in these codes indicates greater shrinkage by ACI 209 than FIB (CEB-FIP) but less creep. This divergence has been made more pronounced by the current (2006) formulation in *AASHTO LRFD* Articles 5.4.2.3.2 and 5.4.2.3.3 which are supposedly applicable to so called "high strength girders". Designers need to be aware of this aspect of the *AASHTO LRFD* formulation.

For other structures, such as precast or cast-in-place segmental, structures cast-in-place on falsework and particularly concrete cable-stayed structures, Designers and Contractor's Engineers need to be aware of the nuances and adopt the use of appropriate material properties and formulations for creep and shrinkage in accordance with experience.
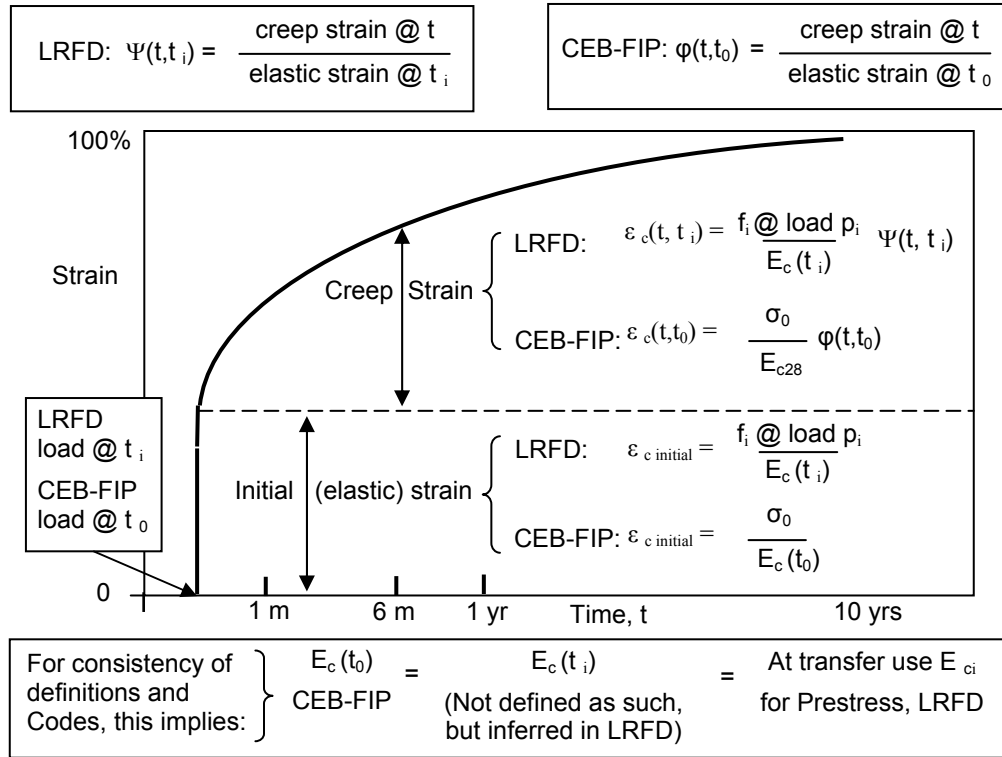
Figure 2.87 Terminology of CEB-FIP and *AASHTO LRFD*

With regard to the time, t_∞, at which the ultimate strain due to creep or shrinkage is attained, it is conventional to assume t = 4,000 days (or about 10 years).

AASHTO LRFD provisions apply for concrete strengths up to 15 ksi. Also, for shrinkage, in the absence of more accurate data, the shrinkage coefficients may be assumed to be 0.0002 after 28 days and 0.0005 after one year of drying.

2.5.5 Flexural Limit States

2.5.5.1 Differences between Continuous and Simply-Supported Structures

For prestressed girder superstructures made continuous with reinforced concrete joints, at flexural limits subtle differences arise compared to simply-supported superstructures. The most obvious are negative moments over interior supports from gravity loads such as self-weight, superimposed dead load and live load that create flexural tension in the top fiber and compression in the bottom fiber at interior supports. In addition, secondary effects from prestress induce further negative moment over the pier. Differential shrinkage of the slab relative to the girder tends to induce a positive moment (bottom fiber tension) over interior piers. As a result of the structure being built in a simply-supported condition and then changed to a continuous condition, there is a redistribution of structural moments due to long term creep. Creep tends to reduce negative moments at piers due to structural dead load

– but with a corresponding increase in positive moments within spans. Creep also redistributes secondary prestress and differential shrinkage effects.

Precast girders generally have straight strands in the bottom flange. Occasionally, some strands may be deflected to terminate high up in the webs at the ends. Deflected strands can minimize but not eliminate adverse secondary prestress moment effects at interior piers.

2.5.5.2 Structural Analysis

Calculation of bending moments, shear forces and reactions for continuous structures may be accomplished by various methods based on classical beam theory, such as: flexibility analysis, displacement (stiffness) analysis, area-moment theorem, moment-distribution, matrix methods, and so forth. Computer models are generally based on matrix (stiffness) methods.

2.5.5.3 Application of Vehicular Live Load

For negative moment and support reactions at interior piers, there is a particular nuance in the *AASHTO LRFD* Article 3.6.1.3.1, bullet point 3. Namely, that for negative moment between points of contra-flexure, 90% of two trucks spaced a minimum of 50ft apart along with 90% of the effect of the design lane load may be applied to induce a negative moment. For this purpose, the location of the points of contra-flexure corresponds to that determined by applying a uniform load on all continuous spans.

2.5.5.4 Service Limit State

At the Service Limit State, limiting flexural stresses for continuous structures are the same as for simply-supported structures (*AASHTO LRFD* Article 5.9.4); the difference being that these are now applied to the top or bottom fiber as the case may be. Stresses due to secondary moments should be calculated and added to other effects as necessary. In continuous structures, thermal gradient (TG), especially negative thermal gradient, can induce additional top tension over interior supports – presenting difficulties for some structures and load combinations.

For a composite section, determination of the final state of stress can only be successfully accomplished by accumulating stresses from each individual effect (load or prestress) at each elevation of interest at each cross-section of interest. (It is quite wrong to accumulate only moments or shear forces and apply the total to the final section.) Stress accumulation is made more tedious for continuous, composite girders, although the principle is merely an extension of that for simply-supported pre-tensioned girders (DM Section 2.4). To recap; stresses are first calculated and accumulated for the non-composite properties up to the time the slab has been cast and becomes effective. Thereafter, stresses are calculated and accumulated for the composite section properties comprising the non-composite section, the effective slab and, possibly, the transformed area of pre-tensioned strand.

Longitudinal stresses should be accumulated at least at the top of the deck slab, top of precast girder and bottom of precast girder. If there is an interest in needing to know final principal tensile stress at various elevations, then it is necessary to accumulate longitudinal and shear stresses at those elevations too. Such elevations would include the neutral axis of the non-composite and composite sections and perhaps top and bottom of web, as necessary. Given that the section properties (for flexure and shear) change with the construction process, meticulous accounting is necessary to track accumulated stress from initial to final long-term, in-service, conditions. Nowadays, this is greatly facilitated by spreadsheets.

2.5.5.5 Strength Limit State

In continuous prestressed structures, applying a load factor of 1.0, secondary moments due to prestress must be added to the load-demand when checking the Strength Limit State. Also, for a continuous composite structure, differential shrinkage effect of the deck slab tends to induce positive moment (bottom tension) at interior piers which undergoes redistribution due to creep. The magnitude of this effect depends upon the assumption made for the creep coefficient and the sequence and timing of construction activities. Since the effect is to assist toward carrying other gravity loads, care is needed not to overestimate the effects. With these exceptions, the calculation of the flexural capacity of a cross section itself is otherwise the same as for any prestressed girder and may be determined as outlined in *AASHTO LRFD* Article 5.7.3.

2.5.5.6 Contribution of Mild-Steel to Flexural Capacity

In superstructures of precast-girders made continuous by reinforced concrete joints, precast girders are usually provided with reinforcement in the form of L or U-bars, projecting into the splice from the ends of the girders at the bottom of the splice in addition to continuous (spliced) mild-steel reinforcement in the deck over the joint. Both sets of reinforcement may be counted toward flexural strength capacity, as necessary, at positive and negative moment regions.

2.5.5.7 Redistribution of Negative Moment at the Strength Limit

AASHTO LRFD Article 5.7.3.5 addresses this issue. If tensile steel (in this case deck slab rebar) in the negative moment region yields, which occurs when the net tensile strain (ε_t) exceeds 0.0075, the moment determined by elastic theory at the strength limit state is to be reduced by a percentage not greater than $1000\varepsilon_t$ or 20% at that section. In order to maintain equilibrium, positive moments should be adjusted to account for the change in negative moments. Positive moment capacity should be checked for the redistributed amounts.

2.5.6 Longitudinal Shear Design

2.5.6.1 Service Limit State

Design for shear at the Service Limit State is not a requirement of *AASHTO LRFD*. However, to be mindful of the need for durability, a Designer may choose to assure himself that the structure will not experience shear cracking at the service level. High shear forces can cause diagonal cracking in webs as the result of large principal tensile stresses. The magnitude of the effect can be determined by applying classical theory using Mohr's circle for stress. Limiting the principal tensile stress to 3 or 4√f'c (psi) at the elevation of the neutral axis has traditionally and conveniently been used to establish an approximate web thickness for durability and detailing purposes.

2.5.6.2 Strength Limit State

AASHTO LRFD shear design using Modified Compression Field Theory was covered in DM Section 2.4.5.3 for precast, pretensioned girders. Shear design for pre-tensioned girders made continuous by reinforced concrete joints is similar with few refinements.

In a simply-supported girder, or any statically determine structure, internal forces from the prestressing do not cause reactions at the supports. However, when girders are continuous, the structure is then statically indeterminate. Prestressing then causes small secondary reactions. This is sometimes called the "continuity effect" or "secondary effect". Secondary reactions induce corresponding shear forces and secondary moments. This directly modifies the summation of shear forces from all loads.

Secondary effects have been discussed above for prestressed girders made continuous with reinforced joints. Further elaboration of secondary effects is provided in DM Sections 2.6 (girders made continuous by post-tensioning) and 2.7 (structures cast-in-place on falsework).

Although common practice for simply-supported pretensioned girders is to use straight strands, they can be draped upwards at the ends, as discussed in DM Section 2.4.6.3. For pre-tensioned girders with deflected (draped) strands at the ends of the girders, the force in the strands can be resolved to provide a vertical component - typically opposing shear from dead and live loads. Essentially, the effect is a reduction in shear demand. However, *AASHTO LRFD* includes this effect as a component of strength rather than a reduction in demand. In this case, the vertical component of the effective prestressing force, V_p, is added to the strength of the concrete, V_c, and vertical reinforcement, V_s. The total shear strength is then

$$V_n = V_c + V_s + V_p$$

If V_p is in the same direction as the dead and live load demand, then V_p should be taken as negative in this equation for total shear strength. Whether positive or negative, if V_p is considered to be a component of "strength", then shear effects from prestressing should *not* be included as a load "demand." Care should be exercised to make sure that the deflected (draped) strands can develop sufficiently to contribute to the vertical component, Vp, at the section required.   Vertical

prestressing by means of post-tensioned bars placed in webs is not a practical option for precast, pre- and post-tensioned I-girders.

2.6 Design of Precast Girders made Continuous with Post-Tensioning

2.6.1 Introduction

The objective of this topic is to introduce the fundamentals of prestressed concrete design. Commonly used terms are defined and the mechanism of applying prestress to overcome applied loads is described in terms of general effects and illustrated by the incremental summation of internal stress necessary for basic design and analysis.

The concept of continuity introduced in DM Section 2.5 above, is extended to cases where full structural continuity is achieved by means of post-tensioning tendons installed in the girder webs, to a draped profile, passing through reinforced concrete spliced joints at the ends of the girders or between precast portions (segments) of girders. Precast girders or portions (segments) of girders are pre-tensioned with a sufficient number of strands to carry their own self weight and a portion of subsequent loads. Longitudinal post-tensioning tendons are installed on site to provide the additional capacity for permanent, transient and live loads. Post-tensioning tendons usually extend the full length of the superstructure spans comprising a continuous span unit between expansion joints. Tendons are anchored by post-tensioning anchors embedded in the expansion joint ends of the girders. At these locations, the web is widened to provide a suitable anchorage zone.

Post-tensioning tendons follow a gradually curving draped profile, being high up in the web over the piers and low down in the mid-span regions. This type of profile is preferred because it can minimize or even eliminate secondary reactions and moments from prestress. These invariably reduce the effectiveness of the prestressing system. However, if the net prestressing profile (combination of pretensioning and post-tensioning) leads to a final condition where there are no secondary effects, the profile is said to be "concordant". In general, it is easier to attain a concordant profile when all the prestress is provided by post-tensioning (as in cast-in-place construction on falsework, DM Section 2.7) rather than by the combination of straight (not-deflected) pre- and post-tensioning discussed in this section.

Key aspects of the structural system and design that differ from considerations for pretensioned I-girders are addressed. These include, for instance, the influence of the construction technique upon the design, the effects of redistribution of bending moments due to creep, additional prestress loss due to friction and anchor set in post-tensioning tendons and the treatment of anchor zones.

In addition to the advantages and disadvantages of continuity outlined in DM Section 2.5 above, longitudinal post-tensioning offers:

Additional advantages:

  ➢ Shallower overall structural depth

> Longer span applications
>> o Splices over piers – up to 140 feet
>> o Variable depth with splices in spans – up to 350 feet

Additional disadvantages:

> Requires thicker webs to accommodate post-tensioning ducts
> Requires closer inspection of ducts and anchors at precast yard
> Requires closer inspection of installation and grouting of tendons on site
> Friction loss especially in long, draped, tendons becomes significant

The method of construction is an integral feature of this type of bridge that must be properly considered in the design. Refer to DM Volume 3, Chapter 1, Section 1.7, for an account of construction techniques for two of the most often used applications, namely; a 4-Span Spliced I-Girder with spliced joints over interior piers and a 3-Span Haunched Girder Unit utilizing variable depth I-girder with spliced joints approximately at inflection points within the spans.

2.6.2 Longitudinal Analysis (Bending Moments and Shear Forces)

For any structure built in stages, longitudinal analysis must take into account both the sequence of construction, the maturity of the concrete and the times at which key activities occur. In particular, this includes, making closures that change the statical structural configuration from simple to continuous spans, adding a span onto previously erected continuous spans, the introduction or removal of temporary supports and/or construction equipment loads, the sequence of pouring deck slab concrete, and last, but not least, the sequence of installing and stressing post-tensioning tendons.

In all other respects, design follows the same processes described above for pre-tensioned girders, such as, for example; effective cross section, longitudinal pretensioning strands (for carrying all loads up to the time that additional capacity is provided by installing post-tensioning tendons), service and strength limit states for flexure and shear – such topics are not repeated. Likewise, methods of longitudinal structural analysis for continuous girders are not reiterated.

2.6.2.1 Continuity Effects

Continuity effects arise from the construction sequence (making continuity between spans), creep redistribution of permanent dead load and prestress secondary moments and differential shrinkage.

2.6.2.2 Construction Sequence Effects

There is no unique or standard nomenclature for either major or intermediate construction activities or steps. Common terms include "construction step", "construction phase" or "construction stage". The techniques are often referred to as "phased construction", "staged construction" or similar. On large projects, terms are

often nested; such as "Construction Phase X, Stage Y, Step Z". For illustration purposes, the term "construction step" is used.

A Designer has to assume sequences and times for key activities according to a likely construction schedule. Engineering judgment is necessary; there is no absolute right or wrong answer. For instance, if it is expected that differential shrinkage effects between the slab and girder (See 2.6) are likely to be significant, then it would be reasonable to assume a long time (say a year) between casting (t0) and erecting (t1) girders. On the other hand, if a project is on a speedy schedule where girders are made and delivered just ahead of superstructure construction, then a shorter time interval (say 28 days) would be appropriate.

For design purposes, it is usually sufficient to identify certain "key activities" as given in the two examples below. For an actual structure, it may be necessary to break down some of these into greater detail. For instance, casting the deck slab (activity 5, in the first example, 7 in the second example) may need breaking into several sub-activities for each of the anticipated deck slab pours, depending on the size of the structure and concrete delivery. Each activity then becomes a discrete "construction step". Clearly, a large project may require many such discrete "construction steps". The "key activities" in these examples are the significant points where a major event happens – new concrete is cast or loaded, or a change of structural continuity occurs - as such, they possibly indicate the fewest steps to consider.

Long term conditions after which all creep and shrinkage effects are assumed to have taken place (i.e. time t ∞) is conventionally taken as about 10 years or 4,000 days.

(Example 1)   4-Span Spliced I-Girder

For the purposes of design, "key activities" of the construction sequence that affect the design are summarized as:

- (1)   Fabricate, cast and pretension precast girders (say, at time t0)
- (2)   Erect all pretensioned girders (say, at time t1)
- (3)   Cast in place spliced joints over piers between ends of girders (time t2)
- (4)   Install first stage of post-tensioning (on non-composite section, time t3)
- (5)   Form and cast deck slab (in a specific sequence, time t4)
- (6)   Install second (final) stage of post-tensioning (on composite section, time t5)
- (7)   Apply superimposed dead load (barriers, surfacing, etc., time t6)
- (8)   End of Construction (EOC), open to traffic, (time t7)
- (9)   Allow creep and shrinkage to take place to long term service, (time t ∞)

(Example 2)   3-Span Variable-Depth Spliced I-Girder

For the purposes of design, "key activities" of the construction sequence that affect the design are summarized as:

(1) Fabricate, cast and pretension precast girders (could be at various times, say t0)
(2) Erect pretensioned girders in side-spans (time, t1)
(3) Erect pretensioned cantilever girders over main piers (time, t2)
(4) Cast in place spliced joints in side spans girders (time t3)
(5) Suspend main span girder on temporary hangers and cast splices (time t4)
(6) Install and stress first stage longitudinal PT from end to end (time t5)
(7) Form and cast deck slab (in a specific sequence, times could be various, say t6)
(8) Install and stress second stage longitudinal PT from end to end (time t7)
(9) Remove temporary support towers (time t8 - alternative might be after step 6)
(10) Apply superimposed dead load (barriers, surfacing, etc., time t9)
(11) End of Construction (EOC), open to traffic, (time t10)
(12) Allow creep and shrinkage to take place to long term service, (time t ∞)

In both examples, each construction step should be considered in design calculations.

Notice that up to a certain point, (step 2 of example 1; step 4 of example 2) the two structures are statically determinate. When the splice-joints are cast, both structures (strictly) become statically indeterminate - because the joints begin to carry continuity effects, albeit it slight, by virtue of rebar projecting from the girders into the joints even before post-tensioning.

In the first example (4-span structure), initial conditions have already been addressed for pretensioned girders. For instance, initial transfer of pretensioning in the casting yard and subsequent loss of prestress from creep, shrinkage and relaxation from the time of casting to erection. This also applies to the pre-tensioned components of the second example (3-span structure).

In both examples, changes due to creep and shrinkage occur in the intervals between each construction step. These cause loss of prestress (in both pretensioning and post-tensioning force) and redistribution of internal force due to creep arises from changes in the statical scheme and differential shrinkage of the deck slab (as addressed in 2.5 above.)

In the second example, the temporary support towers remain in place until the superstructure has been post-tensioned to be fully continuous for all subsequent loads, whereupon the towers may be removed. Depending upon the amount of post-tensioning and section capacities, this might conceivably occur after step 6, but more safely after step 8.
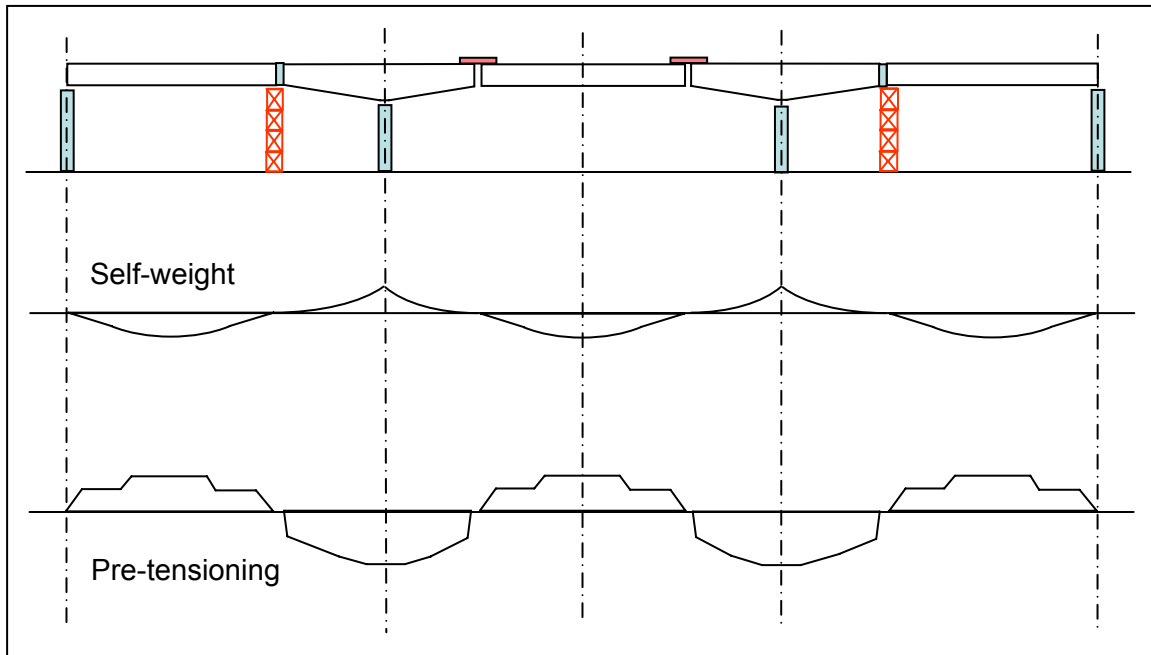
Figure 2.88 Spliced Girder Construction - Self Weight and Pretensioning Moments

The reaction of the support tower needs to be determined. Initially, the reaction is statically determinate and equal to a portion of load from the self-weight of the end-span girder (step 2). This reaction will change only slightly under steps 3 and 4. It will reduce under step 5 and will further (perhaps lifting off) under step 6. The amount of reduction will depend upon the relative stiffness of the superstructure and support towers.
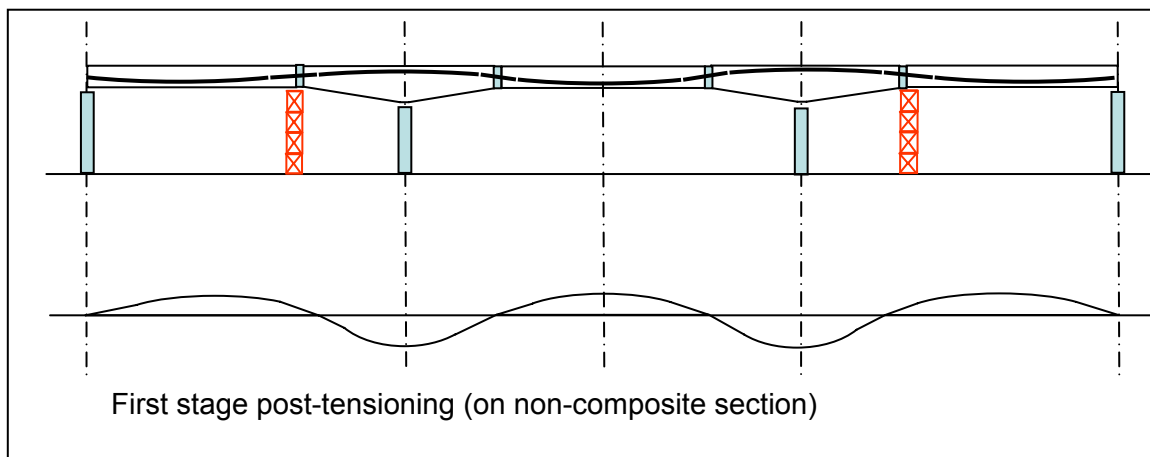
Figure 2.89 Spliced Girder Construction - Stage 1 PT Moments
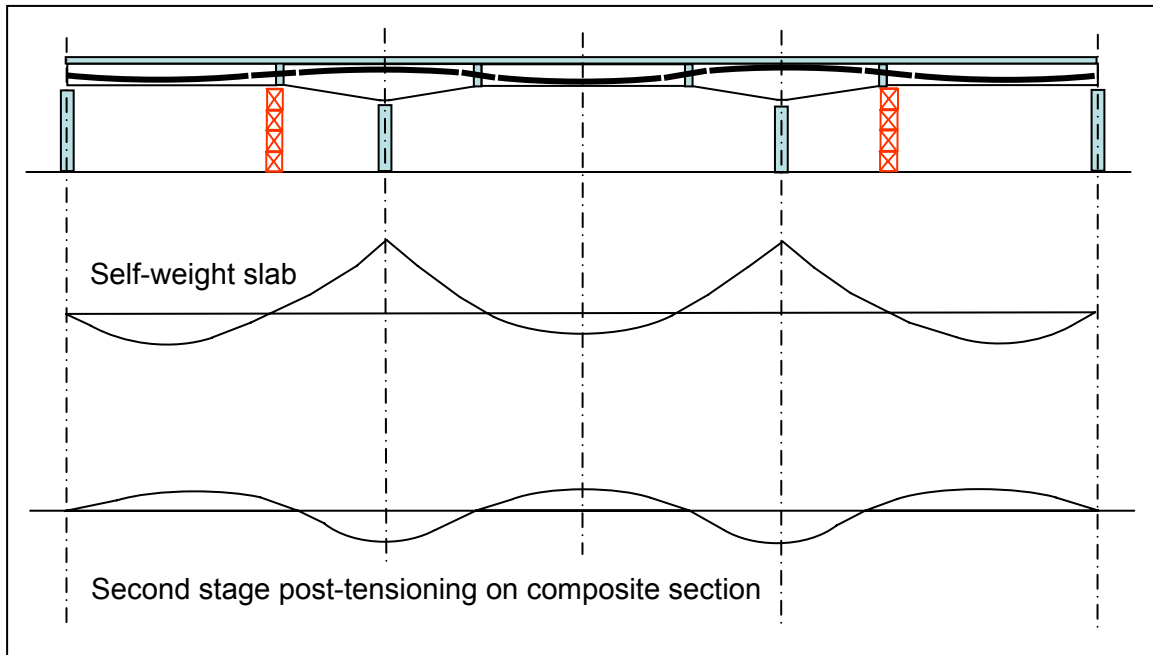
Figure 2.90 Spliced Girder Construction - Slab and Stage 2 PT Moments

The reaction will increase again under step 7 but will reduce (and might lift-off again) under step 8. If it does not lift off at step 8, then removal of the residual (upward) reaction of the support tower imposes an equal and opposite (downward) load on the now completed continuous 3-span structure. The important point here is that although use of the temporary tower began in a statically determinate condition, in this example, it is removed from a statically indeterminate structure. In such a circumstance, in order to determine the reaction, it is necessary to know or assume a vertical stiffness for the tower.

On the other hand, if lift-off occurs at step 6, and all subsequent loads can be carried safely by the superstructure and post-tensioning, then the maximum load on the tower occurs under steps 2 through 5. The latter might be, approximately, statically determinate, if the precast lengths and support locations can be carefully proportioned by the designer.

Obviously, safety is paramount for construction - so a Contractor should be given the opportunity to adjust proportions, support conditions and erection sequences for his elected means and methods of construction.
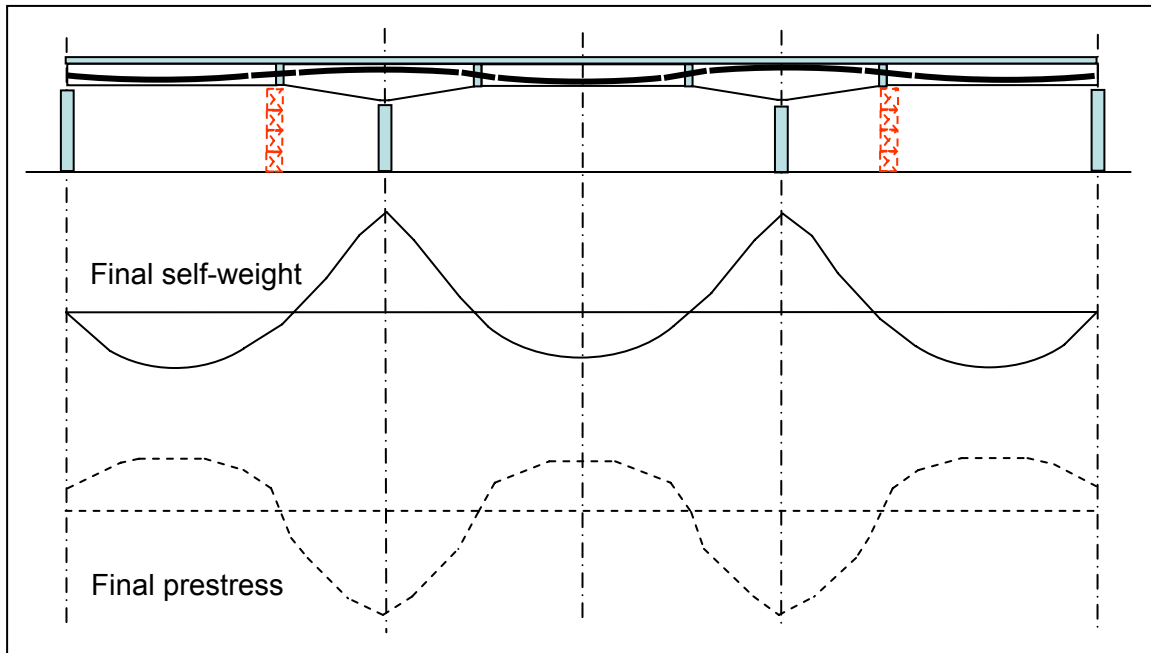
Figure 2.91 Spliced Girder Construction - Final Moments

Bending moments from permanent superimposed dead load (i.e. barriers, utilities, surfacing) applied to the structure after it has been made continuous, may be determined from standard formulae or any appropriate analysis for continuous beams. It should be noted that since these loads are applied to the continuous structure, there is no subsequent redistribution of their effects by creep. Creep will cause increasing deflection (deformation) under their load, but because the load is constant, there will be no redistribution of bending moment.

Summarizing for design purposes:

> ➢ Each construction step should be identified and considered in calculations.
> ➢ Each time a load is added or the structure changed, forces, moments and stresses must be calculated and accumulated at each cross-section of interest.
> ➢ Creep recommences for each new loading, structural system and stress regime.
> ➢ Differential shrinkage of the deck slab and creep redistribution should be included.
> ➢ Use of temporary supports and their residual loads should be accounted for.

2.6.2.3 Creep and Shrinkage – Redistribution Effects

A similar redistribution of moments occurs for structures made continuous with post-tensioning – except that the redistribution is driven by the difference between the combination of pre- (if any) and post-tensioning effects and dead load.

In post-tensioned spliced I-girder structures, similar losses are experienced as in pretensioned structures, but of a different order of magnitude due to differences in the maturity of concrete and the sequence and timing of construction and application of post-tensioning.

For instance, if a girder is pre-tensioned for its own self-weight (and possibly for a portion of the deck slab dead load) it experiences the same initial loss in the casting bed. It then experiences the same losses due to shrinkage, creep and steel relaxation from the time of transfer as for any pre-tensioned girder. Under its own self weight and pretensioning, these losses continue to increase while the girder is erected and splice joints are made, up to the time that the first stage of any post-tensioning is installed. This changes the internal stress regime in the girder. Losses are calculated for this new stress regime up to the time that the deck slab is cast and the non-composite girder section alone carries the additional weight of the (wet) deck slab and any formwork or stay-in-place forms. This again changes the stress regime so new losses are experienced up to the time when the next (and usually final) post-tensioning is installed. The final stage of post-tensioning acts upon the now composite section. But this again changes the internal stress regime so creep, shrinkage and relaxation loss are recalculated from this point onward.

However, in a post-tensioned girder, additional losses are experienced at the time of installation and stressing of the tendons. These losses arise from the effect of friction between the tendon and the duct and from the effect of seating of anchor wedges, at the time of stressing. It is necessary to determine the magnitude of this loss and to properly account for it in the design.

2.6.3 Additional Loss of Prestress in Post-Tensioned Structures

2.6.3.1 Introduction

As for pretensioned girders, post-tensioned girders are affected by instantaneous losses that occur at the time of stressing and also by long-term losses that occur over time due to changes in concrete and prestressing steel properties. Long-term losses due to creep, shrinkage, and relaxation for post-tensioned girders are similar to those discussed in Sec. xxx for pretensioned girders. However, instantaneous losses due to elastic shortening that were previously discussed are different for post-tensioning than for pretensioning. Also, post-tensioned members are affected by additional, unique instantaneous losses due to friction and anchorage set. Instantaneous losses will be discussed in the sections below, followed by an example on applying these losses to determine the stress variation along a tendon. Further, this information is used to calculate the amount of elongation that a tendon experiences when it is stressed.

2.6.3.2 Elastic Shortening Losses

Elastic shortening is a loss that occurs upon the application of prestress. As the prestress is transferred to the concrete, the girder will shorten. This causes the prestressed steel to also shorten, which causes the steel to lose stress. This loss

may occur to a strand whose force is being transferred to the girder or to a strand that has been stressed up to that point, depending on the method of stressing the strands. This is important when considering the difference between elastic shortening in a pretensioned versus a post-tensioned girder.

For a pretensioned girder, typically all of the force from the strands is transferred to the girder at once when the strands are cut from the bulkheads. The concrete will shorten, and there will be a loss in all of the prestressing strands. However, for a post-tensioned girder, the tendons are stressed in stages, with each one being stressed directly against the concrete via their anchors. As a tendon is stressed, the force in it increases, which causes the girder to shorten; this will continue as the tendon is gradually stressed to its specified amount. The force in the tendon is measured up to the very end of the stressing operation, with the measurements already accounting for loss in the tendon stress due to shortening of the girder. During stressing of this tendon, however, the shortening of the girder will cause a loss in any strands that have already been stressed. For instance, when the first tendon is stressed, it will have no elastic shortening loss. When the second tendon is stressed, it will have none, either, but its stressing will cause loss in the first tendon that was stressed. Stressing of the third tendon will cause a loss in only the first and second tendons, and so on. The tendon that is tensioned last will not suffer any elastic shortening losses, while the tendon that was tensioned first will suffer the most. The overall elastic shortening loss in a post-tensioned system is less than that of a similar pretensioned system. *AASHTO LRFD* Article 5.9.5.2.3b gives the following equation for elastic shortening losses in post-tensioned members:

$$\Delta f_{pES} = \frac{N-1}{2N} \frac{E_p}{E_{ci}} f_{cgp}$$

where:
- N = number of identical prestressing tendons
- E_p = modulus of elasticity of prestressing tendons (ksi)
- E_{ci} = modulus of elasticity of concrete at transfer (ksi)
- f_{cgp} = sum of concrete stresses at the center of gravity of prestressing tendons due to the prestressing force after jacking and the self-weight of the member at the sections of maximum moment (ksi)

This equation accounts for sequential post-tensioning and its effect on the elastic shortening of previously stressed tendons.

2.6.3.3 Friction Losses

Post-tensioning tendons are often placed inside ducts that have been positioned to achieve a specified tendon profile. The profile is often curved along portion(s) of its length. As the tendon is stressed, friction develops between the ducts and the strands, which produces a mechanical loss in the tendon stress, causing the stress to vary along its length. Friction losses are considered in two parts: wobble and curvature, as shown in Figure 2.92. The wobble, or "length", effect arises when the

duct is unintentionally misaligned, even though it is meant to be straight. This can occur when the ducts do not have adequate stiffness or when they are not properly supported and tied at sufficiently close intervals to prevent displacement or buoyancy during concrete placement. The curvature effect results from the tendon making contact with the duct wall at portions of intended curvature. The friction loss is calculated for the accumulated angle consumed along the three-dimensional tendon path.
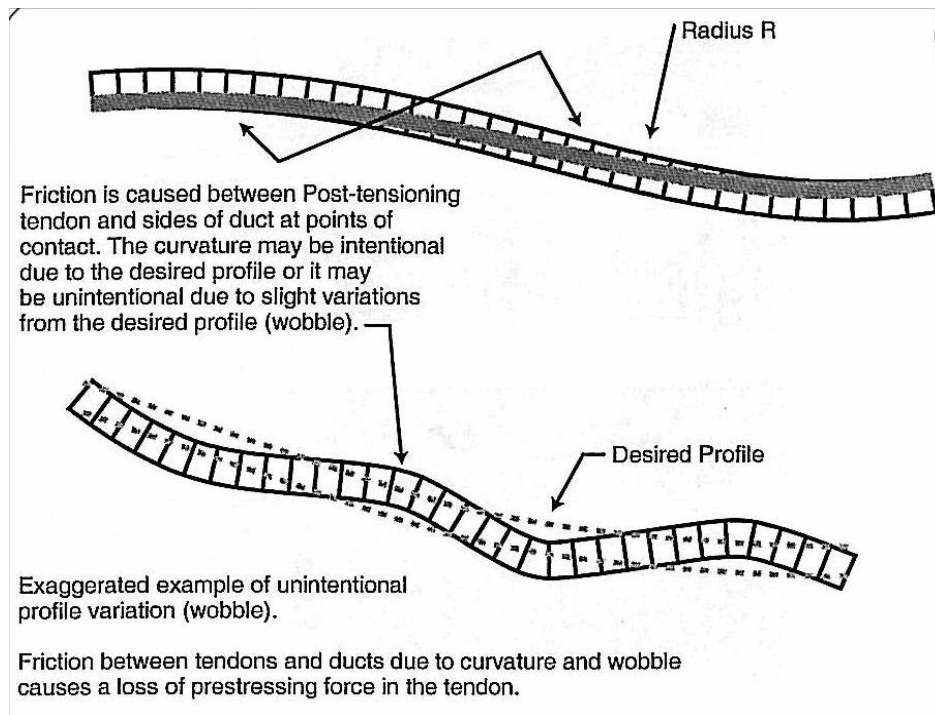

Figure 2.92 Friction Caused by Wobble and Duct Curvature

Loss due to friction may be calculated per *AASHTO LRFD* Article 5.9.5.2.2b, as follows:

$$\Delta f_{pF} = f_{pj}\left(1 - e^{-(Kx + \mu\alpha)}\right)$$

where:

f_{pj}	=	stress in the prestressing steel at jacking (ksi)
x	=	length of a prestressing tendon from the jacking end to any point under consideration (ft)
K	=	wobble friction coefficient (per ft of tendon)
μ	=	coefficient of friction
α	=	sum of the absolute values of angular change of prestressing steel path from jacking end, or from the nearest jacking end if tensioning is done equally at both ends, to the point under investigation (rad)

AASHTO LRFD Table 5.9.5.2.2b-1, repeated below, provides suggested wobble and friction coefficients.

Table 2.3 Wobble and Friction Coefficients (after *AASHTO LRFD*)

Type of Steel	Type of Duct	K	μ
Wire or strand	Rigid and semi-rigid galvanized metal sheathing	0.0002	0.15-0.25
	Polyethylene	0.0002	0.23
	Rigid steel pipe deviators for external tendons	0.0002	0.25
High-strength bars	Galvanized metal sheathing	0.0002	0.30

These equations are used to predict the elongation that a tendon will undergo during the stressing operation. Where large discrepancies occur between measured and calculated tendon elongations, in-place friction tests are required.

2.6.3.4 Anchorage Set Losses

Anchorage set, also known as wedge-set, is another instantaneous loss experienced by post-tensioning tendons. It occurs after the jack is released and when the prestressing is transferred to the anchorage. It is caused by the movement of the tendon prior to seating of the wedges or the anchorage gripping device. The friction wedges that ultimately hold the strands in place at the anchorage, shown in Figure 2.93 and Figure 2.94, slip slightly before the strands are firmly gripped. The magnitude of the minimum set depends on the prestressing system used. To ensure that the wedges will begin to grip immediately upon release of the jack, the wedges can be pre-seated by tapping with a steel pipe slid along the strand before installing the jack. Or, many commercial jacks have an internal power seating mechanism to ensure the wedges grip with minimal slip.

Anchorage set loss causes most of the difference between jacking stress and stress at transfer. A common value for anchor set is 0.25 to 0.375 inches, although values as low as 0.0625 inches are more appropriate for some anchorage devices, such as those for bar tendons. For short tendons, the elongations are small, so a typical anchorage set would be large in comparison. So, it is desirable to minimize the anchorage set for short tendons, such as by power wedge seating.
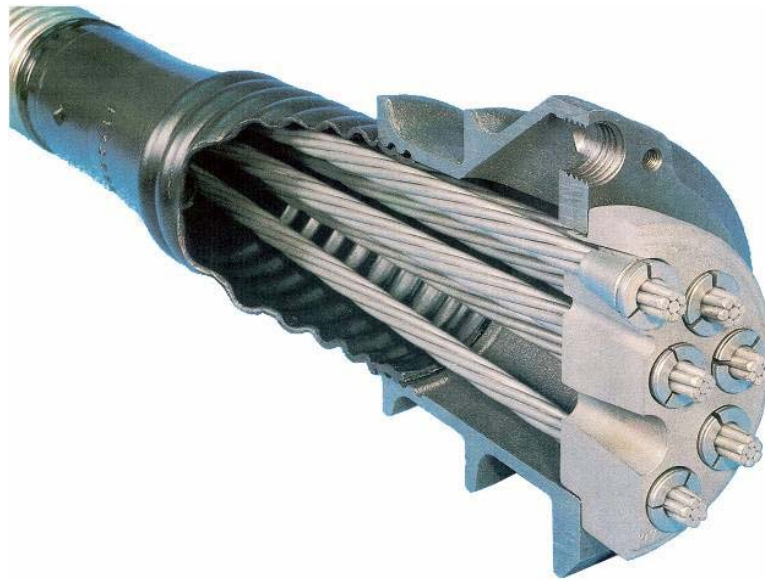
Figure 2.93 Cut-away of Post-tensioning Anchorage
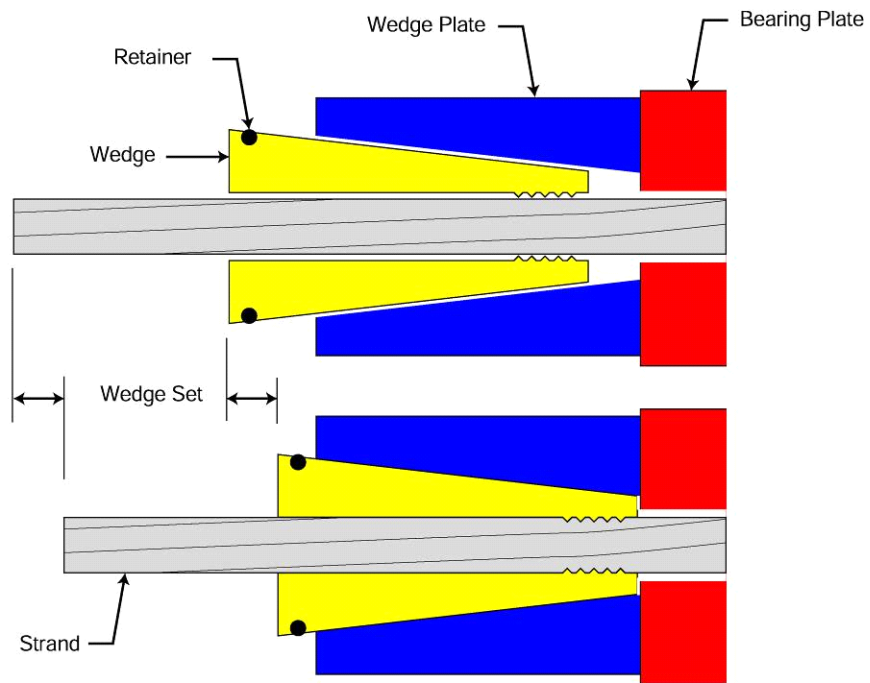
Figure 2.94 Gripping of Strands by Wedges

2.6.3.5 Tendon Elongations

Computation of elongations of prestressing strands is necessary to assure that the required forces are applied to the concrete. Elongations are proportional to the modulus of elasticity of the strands as represented by Hooke's Law:

$$\text{Elongation} = \Delta = \frac{FL}{A_{ps}E_s}$$

where:

F	=	Force applied to tendon
L	=	Length of tendon
A_{ps}	=	Area of strands
E_s	=	Modulus of elasticity of strands

The length, strand area and elasticity are constant for any strand or tendon. The force is constant along the length of the strands if the strands are straight and not affected by friction forces. A plot of the strand stress along the length shows that straight pretensioning strands have a very simple, constant stress diagram because of the lack of mechanical losses. The stress diagram shown in Figure 2.95 is for a straight tendon that has been locked off in the stressing buttresses at 202.5 ksi. Considering the basic relationship of Hooke's Law, we can arrange the terms to show that the modulus of elasticity times the elongation is equal to the stress in the strand times its length. This in turn is equal to the area below the stress diagram.
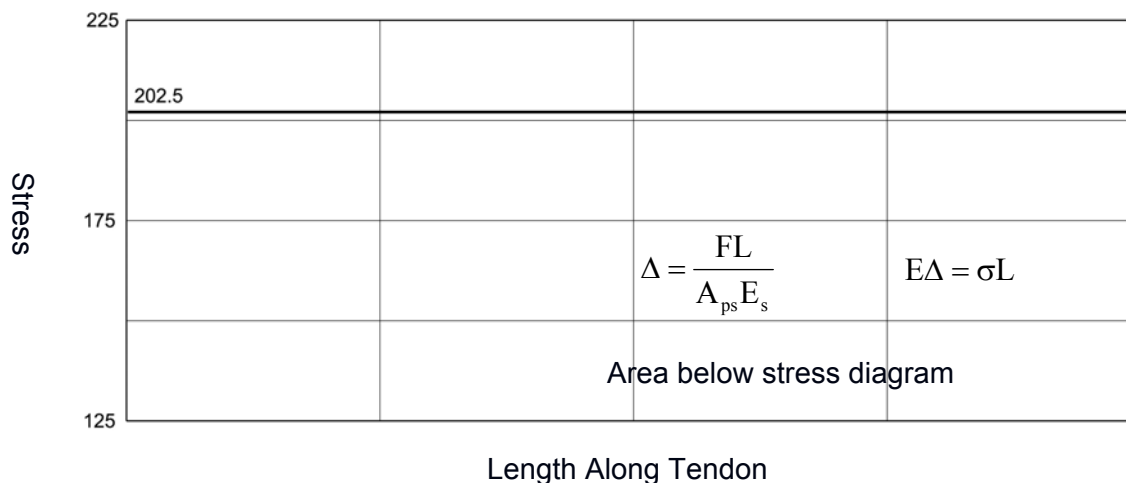
Figure 2.95 Stress Diagram of Straight Tendon

A post-tensioning tendon that deviates, or changes direction, along its length (Figure 2.96) experiences a loss in force at each of these locations. Stress changes due to friction are computed at major changes in tendon geometry. The diagram is developed with straight lines between these points (Figure 2.97). The elongation of

the tendon can be evaluated as previously shown by calculating the area below the stress diagram and dividing it by the modulus.
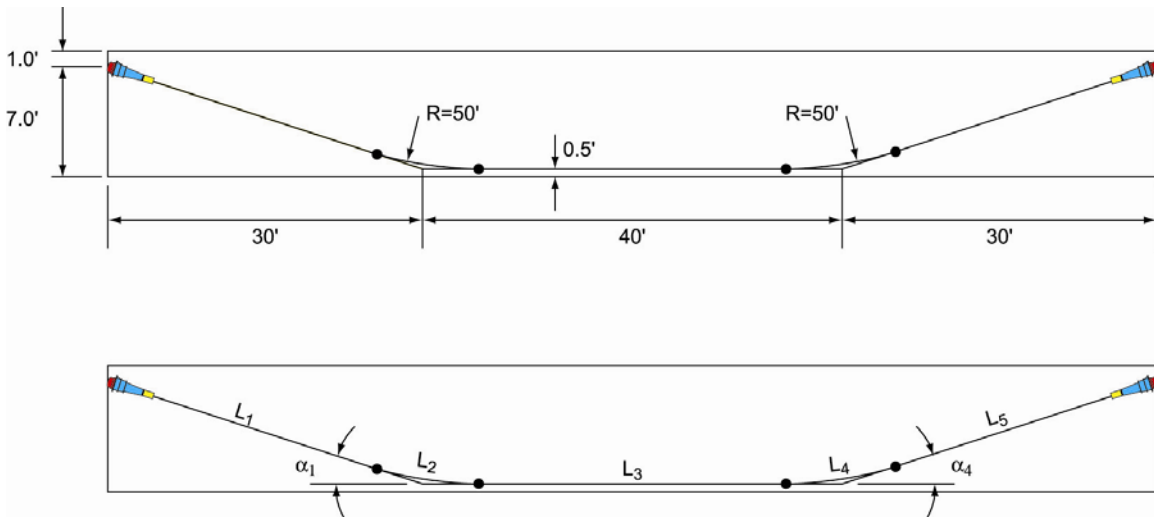
Figure 2.96 Example of Deviating Post-Tensioning Tendon
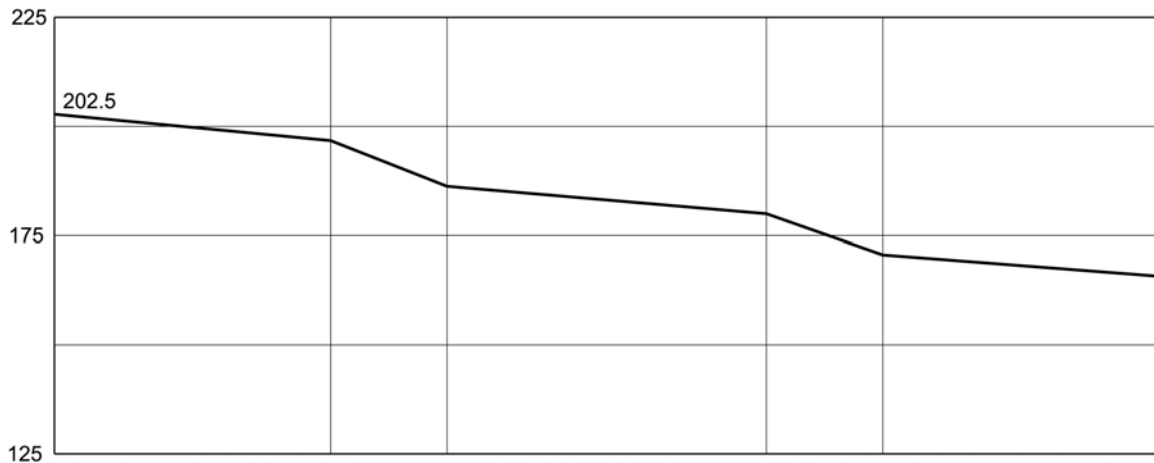
Figure 2.97 Stress Diagram of Deviating Tendon

2.6.3.6 Example for Tendon Stress and Elongation

As an example on how to calculate the elongation of a tendon, consider the tendon profile for the girder in Figure 2.98.
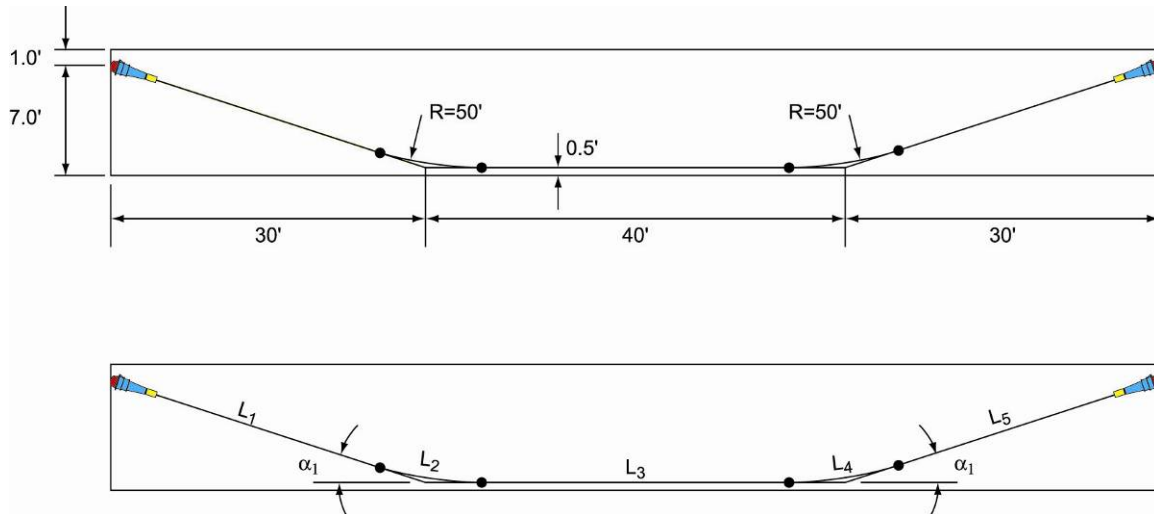
Figure 2.98 Tendon Profile

The geometry that is necessary for elongation computations is first calculated, namely the angle changes at the deviation points and the lengths of the straight and curved regions. The angle changes are as follows:

$$\alpha_1 = \alpha_4 = \tan^{-1}\left(\frac{6.5}{30}\right) = 12.225°$$

$$\alpha_1 = \alpha_4 = 0.21337 \text{ rad}$$

$$T = R\tan(\frac{\alpha}{2}) = 50\tan\left(\frac{12.225}{2}\right) = 5.355'$$

The lengths of the straight and curved regions are as follows:

$$L_1 = \sqrt{6.5^2 + 30^2} - T = 25.342'$$

$$L_2 = L_4 = R\alpha(\text{rad}) = 50 \times .21337 = 10.668'$$

$$L_3 = 40 - 2T = 29.29'$$

Next, the friction losses are calculated according to the formula

$$\%\Delta F_i = e^{-(Kl + \mu\alpha)}$$

Assuming a wobble coefficient K of 0.0002 and a friction coefficient μ of 0.25, the stresses are reduced to the following proportion along each of the six segments:

$$\%\Delta F_1 = \%\Delta F_5 = e^{-(.0015(25.342)+.25(0.0))} = 0.9627$$

2.138

$$\%\Delta F_2 = \%\Delta F_4 = e^{-(.0015(10.668)+.25(.21337))} = 0.9330$$

$$\%\Delta F_3 = e^{-(.0015(29.29)+.25(0.0))} = 0.9570$$

The stresses are calculated as follows:

Point	Segment	% Loss	Stress
1			202.50
2	1	.9627	194.95
3	2	.9330	181.89
4	3	.957	174.06
5	4	.9330	162.40
6	5	.9627	156.34

A plot of the stresses along the tendon is shown in Figure 2.99.
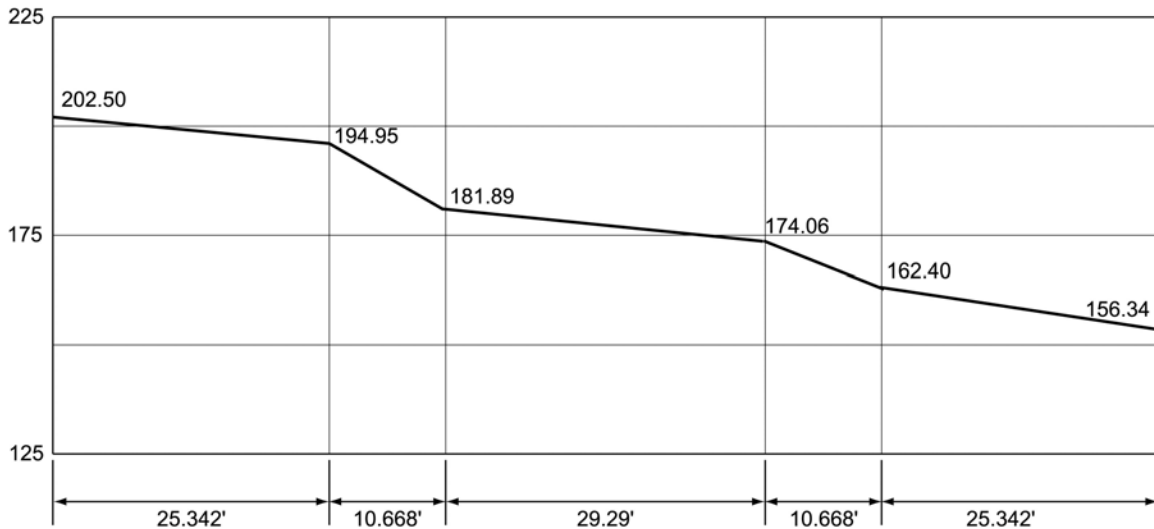
Figure 2.99 Stress Diagram after Friction Losses for Example Problem

By symmetry, the average stress in the tendon is 177.98 ksi. The length of the tendon is 101.31 ft, for an area under the stress diagram of 177.98 ksi * 101.31 ft.

Dividing by the modulus, the elongation becomes 177.98 ksi * 101.31 ft * 12 in/ft / 28500 ksi, or 7.59 inches.

If losses due to anchorage set occur, the diagram is modified by mirroring the stress function until the area difference from the original diagram is equal to the loss from the anchor set, which is equal to the modulus of elasticity times the anchor set. For example, if the anchor set is 0.375 inches, the area difference will be 0.375 inches * 28500 ksi / 12 in/ft, or 890.625 ksi-ft.

Mirroring the stress diagram until the area under the function is reduced by 890.625 ksi-ft gives the new stress diagram shown in Figure 2.100.
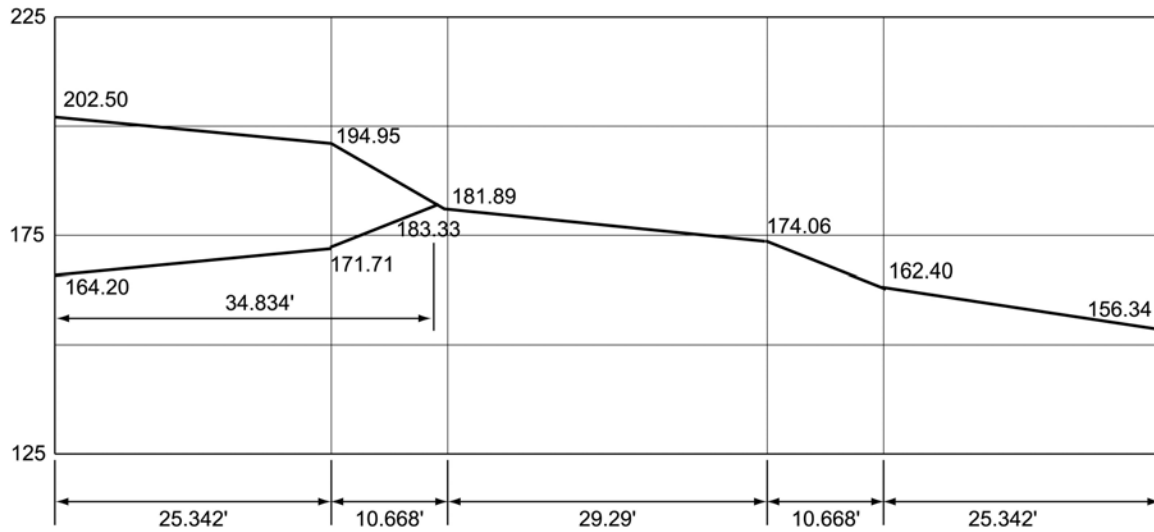
Figure 2.100 Stress Diagram after Anchorage Set for Example Problem

This final step requires iteration until the required reduction in area under the stress function is obtained. The result is to find the point at which the tendon experiences no further change in stress due to the anchorage set, i.e. beyond 34.834 ft from the left end.

2.6.4 Post-Tensioning Anchor Zones

2.6.4.1 General

Anchor zones for post-tensioning tendons are regions of complex stress as the localized, concentrated force from each anchorage, or group of anchorages, disperse over some distance to the full effective cross section, at which point stresses may determined by ordinary beam theory. The length over which the dispersal takes place from the anchorage devices to the full effective section is referred to as the "general zone". Immediately at the anchorages themselves, the post-tensioning force must be confined to prevent localized splitting of the concrete along the axis of the tendon. Very high transverse tensile stresses are set up as the concrete material responds by the Poisson-Ratio effect. The affect is the same as that of driving a wedge into the end of a log to split it. The localized splitting effect, or bursting force, ("T burst"), must be confined by local reinforcement around the anchorage in what is referred to as the "local-zone". Most commercially available

anchorage devices are supplied with a suitable spiral of reinforcement for this purpose. In the event that none is supplied, *AASHTO LRFD* (Article 5.10.9.7) offers guidance for designing suitable local-zone reinforcement.

It is the responsibility of the Engineer (designer), to design reinforcement and details for the effect of the dispersal of forces through the general zone (*AASHTO LRFD* Article 5.10.9.2.4). For this purpose, in *AASHTO LRFD* Article 5.10.9.3.1, three techniques are recognized:

> ➢ Equilibrium-based inelastic models, generally known as "strut-and-tie" models.
> ➢ Refined elastic stress analysis.
> ➢ Other approximate methods, where applicable.

In general, refined stress analysis and approximate methods have appropriate but limited application. By contrast, the "strut-and-tie" method is generally applicable to both routine and complex, three-dimensional shapes. The basic principles of this method are illustrated by considering the case at the end of a precast girder containing three anchorages stacked above each other and set at an angle following the draped profile of each tendon.
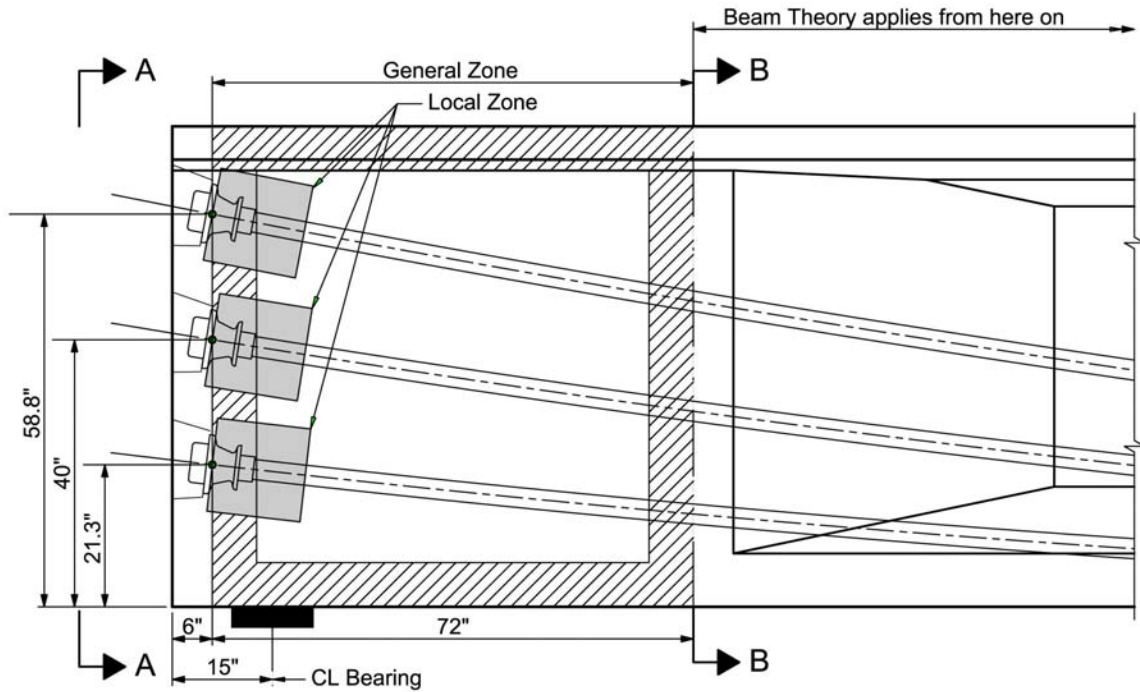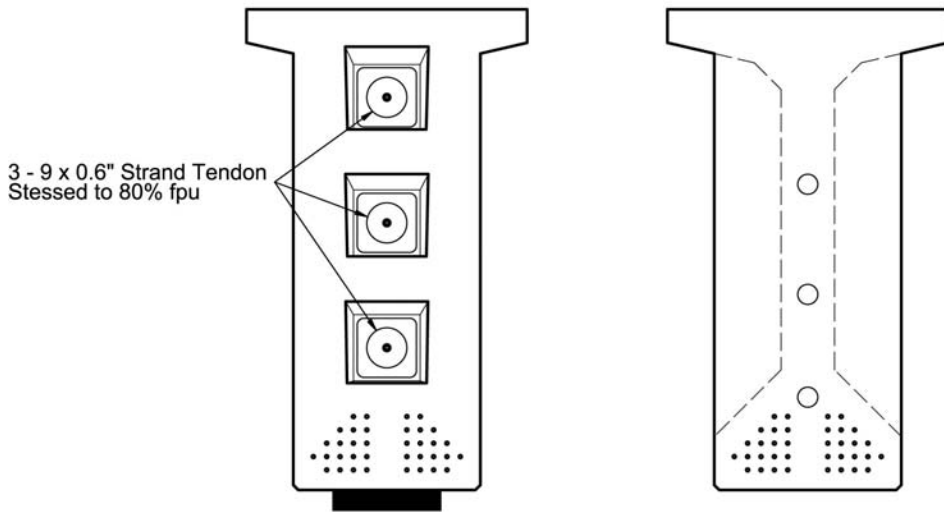
Figure 2.101 Anchor Zones for a Post-Tensioned Girder

2.6.4.2 Application of Strut-and-Tie to Case of Post-Tensioned I-Girder

When applying the strut-and-tie approach, various rudimentary questions arise:

1.   What is the magnitude of the anchor force to be used for design?
2.   Is there relief from the stressing sequence and forces after losses?
3.   What role does the bearing reaction play?
4.   Where is the location of the maximum bursting force, d_{burst}?
5.   Where is the end of the general zone at which beam theory applies?
6.   What is the size of the local zone?
7.   What is the size of the anchor plate?
8.   What is the effective cross-section at the end of the general zone?
9.   Where are nodes located at the end of the general zone?
10.   Where are nodes located relative to anchor plates?
11.   How to arrange struts and ties to simulate a credible, reliable, model?
12.   What is the effective width and thickness of each compression strut?
13.   What is the capacity of a strut (and limiting strain) in the concrete?
14.   What limiting concrete stress can be sustained by a node?
15.   What is the lateral bursting effect across the width of the end block?
16.   What is the strength of a tension tie?
17.   What other reinforcement might be needed, such as Corner Tension Ties?
18.   What are the results of the strut-and-tie approach?
19.   What should be the final disposition of reinforcement?
20.   Are there any other observations?

With reference to *AASHTO LRFD* Articles 5.10.9.3 and 4, by taking each of these questions in turn and applying them to our example, we find the following answers.

2.6.4.2.1 What is the Magnitude of the Anchor Force to be Used for Design?

The load factor for the applied anchor force is given by *AASHTO LRFD* Article 3.4.3.2 as 1.2. The force for design is taken as 1.2 times the maximum jacking force. Before losses due to wedge seating, the maximum jacking stress in the strand may be as high as 80%fpu. The factored jacking force is then:

Factored jacking force = 1.2 P_{jack} = 1.2*0.80*A_{ps}*f_{pu}

For example, using a tendon comprised of 9 * 0.6" dia. strands, with a specified tensile strength of 270 ksi, we find,

1.2 P_{jack} = 1.2*0.80*9*0.217 * 270 = 506 kips per tendon

2.6.4.2.2 Is There Relief From the Stressing Sequence and Forces After Losses?

In an actual structure, tendons would be stressed in sequence. Each one would experience wedge-seating loss at the anchor before the next tendon could be stressed. For 3/8" wedge set, a 9-strand tendon of this type might experience as much as 52 kips force loss. So that, after wedge seating the factored force of 506

kips could reduce to about 443 kips. This is a significant reduction. *AASHTO LRFD* Article 5.10.9.3 offers the possibility of relief of the required factored design forces by consideration of the stressing sequence – this would be appropriate.

It follows that the temporary condition between each stressing operation should be checked to ensure that the reinforcement and concrete strut capacities are satisfactory.

2.6.4.2.3 What Role Does the Bearing Reaction Play?

At the end of the girder, the reaction of the bearing itself helps to locally confine bursting forces and reduce the reinforcement demand. If it is not known if the deck slab will have been cast to add to the magnitude of the reaction, then conservatively, consider only a minimum reaction due to the self-weight of the girder. For strength limit design of the general zone, it is not appropriate to increase this reaction force above the anticipated minimum.

Under certain circumstances, the presence of a support reaction might be used to beneficially modify the location of the maximum bursting force, as considered below.

2.6.4.2.4 Where is the Location of the Maximum Bursting Force, d $_{burst}$?

The location of the maximum bursting force is needed in order to know were to locate reinforcement (according to *AASHTO LRFD* Article 5.10.9.3.2) in order to resist bursting forces and to facilitate construction of a suitable strut-and-tie model. The location of the maximum bursting force is given by *AASHTO LRFD* Article 5.10.9.6.3, equation 2, as:

$$d_{burst} = 0.5(h – 2e) + 5e \sin \alpha$$

where:
- h =   lateral dimension of the cross section in the direction considered.
- e =   eccentricity of tendon from the centroid (always taken positive).
- α =   inclination of tendon to axis; taken as negative if pointing away from the centroid.

For each of the three tendons in our illustration, in the vertical plane:

Top tendon:	h = 72 in, e = 22.8 in, α = 11.24°, d_{burst} = 35.4 in.
Middle tendon:	h = 72 in, e = 4.0 in, α = 9.46°, d_{burst} = 35.3 in.
Bottom tendon*:	h = 72 in, e = 14.7 in, α = -6.76° d_{burst} = 12.6 in.

    * Angle is negative since it is pointing away from the centroid.

This latter value (12.6 in) is very close to the anchorage. It is within the local zone (below) and might pose a difficulty in making a suitable strut-and-tie model. Can anything be done to improve the situation? There is. If the proximity of the support reaction, taken at its minimum value, (80 kips) is used to effectively modify the

direction of the local tendon force, the angle changes to a positive value of α = 2.27°. Choosing to remain conservative, it would be reasonable to take α = 0°, giving a revised value for the bottom anchor d $_{burst}$ = 21.3 in. Considering other needs (such as not to overlap anchor zones and struts except at nodes) we choose to locate the main vertical tension tie at 18 in from the anchor plate.

So much for the vertical plane – now consider the horizontal plane. In plan view, each tendon is at the center of the girder, so e = 0. Each is straight, so α = 0°. The width of the general zone is h = 28 in., these give d $_{burst}$ = 14.0 in. In this case, it turns out that the location of the maximum bursting effects is approximately at the end of the local zone found below. However, other considerations to do with the dispersal of forces and the need to avoid overlapping anchor zones and struts need taking into account when creating a strut-and-tie model. They are addressed in the following.

2.6.4.2.5 Where is the End of the General Zone at Which Beam Theory Applies?

According to *AASHTO LRFD* Article 5.10.9.1, the longitudinal extent of the anchor zone shall not be less than the greater of the transverse dimensions (i.e. the width of the anchor block or overall height) nor more than 1.5 times that dimension. At the end, the girder is widened to accommodate the anchorage zone. How much to widen a girder depends upon the particular type of girder, the size of the anchorages and available casting forms. For the purpose of this illustration, it is assumed that the end block would be as wide as the bottom flange. For a Type VI girder, this is 28 in. The girder height is 72 in. Consequently, we have:

Girder height, H (= 72 in. Type VI, say)   <   L general zone   <   1.5H (= 108 in.)

The dispersal of anchorage forces to general beam behavior in the discontinuous region of the girder end will not occur in a length less than the depth of the girder. Adopting this as the shortest length for the general zone usually leads to a conservative demand for reinforcement, particularly if tendons are on a slope or deviate appreciably.

2.6.4.2.6 What is the Size of the Local Zone?

The width and height of the local zone is given by *AASHTO LRFD* Article 5.10.9.7.1. At the design stage, the final supplier of the post-tensioning system is not known, so the transverse dimensions are taken as the greater of:

➢ The bearing plate size plus twice the minimum concrete cover, or
➢ The outer dimension of any confining reinforcement, plus the outer cover.

If the size of the anchor plate is "a" and the cover "c", then the transverse dimension of the local zone is equal to (a + 2c); see *AASHTO LRFD* Figure C.5.10.9.7.1-1. In our illustration, if the anchor plate size is 10in., cover 2in., the size of the local zone is 14in. The size of the bearing plate, "a", depends upon the limiting bearing resistance under the anchor plate given by *AASHTO LRFD* Equation 5.10.9.7.2

(below). Alternatively, if the manufacturer's recommended edge distance, "e", is known then the size of the local zone is 2e. The length of the local zone is then taken as either (a+2c) or (2e) respectively. The size of the anchor plate also depends upon the bearing resistance of the concrete beneath the plate; determined as follows.

2.6.4.2.7 What is the Size of the Anchor Plate?

The bearing resistance of an anchor plate is given by *AASHTO LRFD* Equation 5.10.9.7.2 as:

$$Pr = \Phi\, f_n\, A_b \qquad\qquad\qquad (5.10.9.7.2\text{-}1)$$

For which f_n is the lesser of:

$$f_n = 0.7 f'_{ci}\ \sqrt{(A / A_g)}\ ; \quad \text{or} \ \le 2.25 f'_{ci} \qquad (5.10.9.7.2\text{-}2 \text{ and } 3)$$

In this case, by *AASHTO LRFD* Article 5.5.4.2, for compression in anchorage zones, we find:

Φ = 0.80 for normal weight concrete (0.65 for lightweight aggregate concrete)
A = maximum area of the supporting surface that is similar to, but does not overlap, adjacent areas for anchorage devices
A_g = gross area of the anchor plate (including PT hole).

For our illustration, if it is assumed that the anchor plate is 10in. by 10in. then Ag = 100 in^2.

By scaling from a drawing or examination of the geometry, we find that if the anchor areas "A" are not to overlap, the maximum dimension is 18in. - so A = 324 in^2.

For precast girders subsequently post-tensioned after erection, the concrete strength at the time of stressing is usually the 28-day strength. Taking f'ci = 6.0 ksi, we find;

$$f_n = 0.7 * 6.0 * \sqrt{(324 / 100)} = 7.56 \text{ ksi.} \ \le \ 2.25(6.0) = 13.5 \text{ ksi}$$

Allowing for, say, a 4.5 in. dia. hole in the plate, the area of the bearing plate, A_b, = 84.0 in^2. Assuming that all other aspects of *AASHTO LRFD* Article 5.10.9.7.2 can be properly satisfied, this gives a bearing resistance of:

$$P_r = \phi\, f_n\, A_b = 0.80 * 7.56 * 84.0 \ = 508.6 \text{ kips (> 506.2 O.K.)}$$

This means that the minimum dimension of the anchor plate, "a", may be taken as 10 in. This also verifies that, if the cover is 2 in., the size and length of the local zone = 14 in.

Also, more importantly for our model, this enables us to determine where to locate nodes at the anchorages; namely at a/4 = 2.5 in. inwards from the bearing plate in each direction.

Also, important for starting our model, it infers that if two struts frame into the anchor, then the maximum thickness for each would be roughly half the anchor plate size (i.e. 5 inch)

2.6.4.2.8 What is the Effective Cross-Section at the End of the General Zone?

If some or all of the tendons are to be tensioned only after the deck slab has been cast, there may be a case for considering the effectiveness of the deck slab itself at the end of the general zone. In which case, guidance may be sought from Figure 4 of *AASHTO LRFD* Article 4.6.2.6.2. This shows normal forces dispersing at an angle of 30° to the longitudinal axis of the member into the slab. In which case, the width of slab to add to the width of the end block itself, at the end of the general zone, in our illustration would be:

$$2b_n = 2 * 72 * \tan 30° = 83 \text{ in.}$$

This would make the full effective top flange width:

$$2b_n + b_{n0} = 83 + 28 = 111 \text{ in.}$$

On the other hand, if the tendons are stressed before the deck slab is cast, then the effective section is that of the girder alone, with the widened end-block as shown in Figure 2.101. – Section BB. This is the section we will consider in this illustration. For simplicity, the small area of girder top flange is ignored in this case – making the section a rectangle. This simplifies the calculation of the effective longitudinal and shear stresses at various elevations in the section – the distribution of which is needed to locate nodes - as follows.

2.6.4.2.9 Where are Nodes Located at the End of the General Zone?

To answer this, consider a free-body diagram of the end of the girder cut at the end of the general zone and determine the forces acting. The factored jacking forces are resolved into horizontal and vertical components applied at the anchor locations. The bearing reaction is applied as an upward force on the free-body diagram. For these conditions, the bending moment, axial and shear force are determined at the location of the end of the general zone. Longitudinal fiber stresses and shear stresses are calculated by beam theory, using the appropriate section properties (in this case, the rectangular section BB in Figure 2.101).

Considering the vertical plane and using the magnitude of the longitudinal flexure and compression stresses and the effective width of the general zone (web), the height of the section is divided horizontally into portions so that the longitudinal force in each portion accumulates to half the magnitude of the longitudinal force from each anchorage. The reason for doing this is to facilitate the introduction of two local

nodes at each anchor, each of which will carry half the factored anchor force. For three tendons, division leads six separate stress-blocks at the end of the general zone (Section BB). Nodes at section BB are then located at the center of force (i.e. P1 through P6) of each individual stress block.

The intensity of the shear stress is determined at this location. For the rectangular section, this is a parabolic distribution from zero at the top to a maximum at mid-height to zero at the bottom. For analysis purposes, the vertical shear force is determined and proportionally allocated per node at this section (i.e. V1 through V6).

2.6.4.2.10 Where are Nodes Located Relative to Anchor Plates?

In the vertical plane of the member, two local nodes are placed at each anchor - each to carry half of the anchor force. In actual fact, the three-dimensional (out of plane) nature of the general zone must also be taken into account. In which case, in a three-dimensional model, four nodes would be located at a distance of (a/4) from each edge of the anchor plate and along the path of the tendon from the back of the plate. In our illustration, (a/4) = 10/4 = 2.5in. One quarter of factored anchor force would be applied at each node.

However, for the time being we are considering only the vertical plane. So for simplicity of analysis and because of the symmetrical nature of our illustration, in a side view of the vertical plane, two nodes are located at each anchor; each to carry half the force. We will consider the three dimensional nature of the lateral bursting effects later when we examine the dispersal of forces in the horizontal plane (plan view).

2.6.4.2.11 How to arrange struts and ties to simulate a credible, reliable, model?

In this respect, strut-and-tie analysis can be tedious and time consuming because the designer may need to try several different models before arriving at a satisfactory solution. Guidance is offered in *AASHTO LRFD* Article 5.10.9.4 and associated figures in the commentary.

An important consideration to help find a solution is to seek the simplest model that can be analyzed by statics alone. Models that contain redundant members and become statically indeterminate should not be used. On the contrary, it is preferable to seek models that would otherwise become mechanisms if the support from the mass of surrounding material was removed and they were truly pin-jointed. An example is that of *AASHTO LRFD* Figure C5.10.9.4.1-2(c) - the flow of force is evident and symmetry facilitates simplification, virtually to a mechanism. It should never be necessary, except perhaps as a check, to use a structural frame analysis program to analyze a strut-and-tie model.

Our illustration is chosen deliberately for a very common circumstance for the anchorages at the end of a precast post-tensioned girder. Three tendons in the web of a Type VI girder are draped to a longitudinal profile rising to the three anchor locations shown. The drape is gradual such that for practical purposes, in the

general anchorage zone, they may be considered straight, but inclined at an angle to the horizontal axis. The end of the girder rests on a bearing - so the bearing reaction should be considered when determining the strut and tie model. The arrangement constitutes a group of multiple anchors. Guidance for setting up the strut and tie model is sought from *AASHTO LRFD* Figures C5.10.9.4.2.1-2 and 3, as follows.

Choosing the length of the general zone as the depth of the girder, and considering all the forces acting at the end of that zone, it is found from beam theory that this section is in longitudinal compression with a lesser stress at the top fiber than the bottom. Being in compression, it means that the situation shown in *AASHTO LRFD* Figure C5.10.9.4.1-3 does not apply – because there is no longitudinal tensile force in the top of the girder. Also, because the tendons follow a gradually curved profile, there is a gradual distribution of the lateral tendon force (i.e. the force / radius of curvature, "P/R" effect) – there is no relatively sudden deviation of force in or near the general zone itself as shown in *AASHTO LRFD* Figure C5.10.9.4.1-2 (f) - so this does not apply.

Consequently, our problem reduces to the need to satisfy; "Small Eccentricity", "Multiple Anchors", a "Support Reaction" and "Inclined and (Straight) Tendons". In other words, we draw upon *AASHTO LRFD* Figures C5.10.9.4.1-2 (a), (c), (d) and (f) for our illustration.

In *AASHTO LRFD*, anchor force is shown to disperse at a rate of 1:2 (1 laterally for 2 longitudinally). If we were to apply this dispersal rate to our model, we would find that the anchor zones (represented by the area "A" = maximum area of the supporting surface that is similar to, but does not overlap, adjacent areas for anchorage devices) would rapidly come to overlap each other - which is not feasible – anchor zones should not overlap. Moreover, this would occur within the length of the local zone. The location of nodes in our model must be modified such that this does not happen.

After some trial and error examination of the geometry and allowing for an estimated depth of compression strut (initially about 5 inch), it is found that if the dispersal rate for regions between the anchors is taken as about 1:4, instead of 1:2, then a series of nodes can be placed just beyond the end of the local zone, so that no overlap of anchor zones occurs. Nevertheless, force from the upper half of the top anchor is allowed to disperse at a rate of 1:2 - because it is unrestrained by any adjacent anchor (Figure 2.102). Force dispersal from the lower half of the bottom anchor is restrained by the local bearing reaction. The actual dispersal depends upon the results of the final statical analysis in which the location of the bottom nodes (F and G of Figure 2.102) of the strut-and-tie model is adjusted so as to maintain equilibrium.
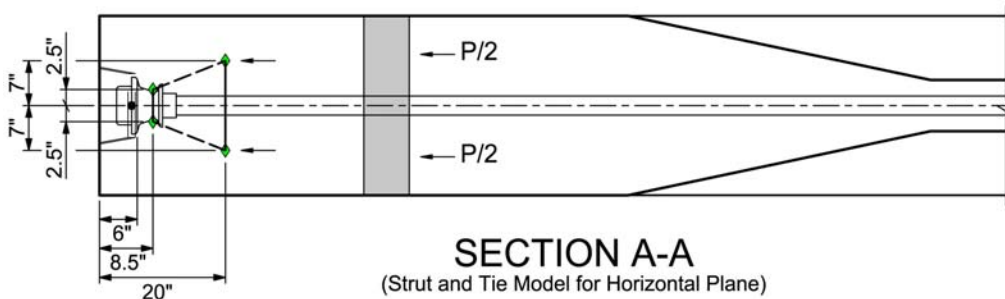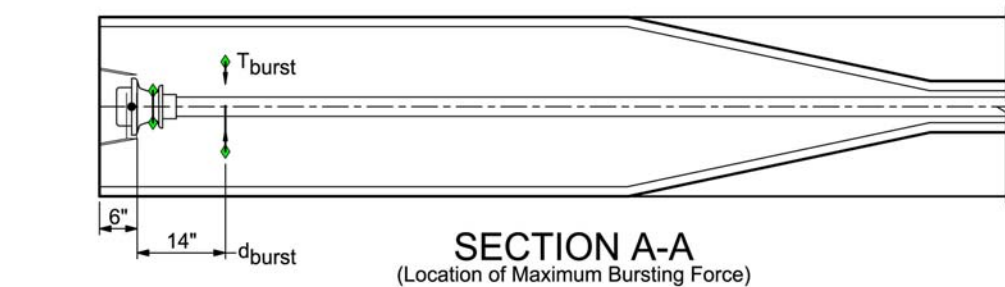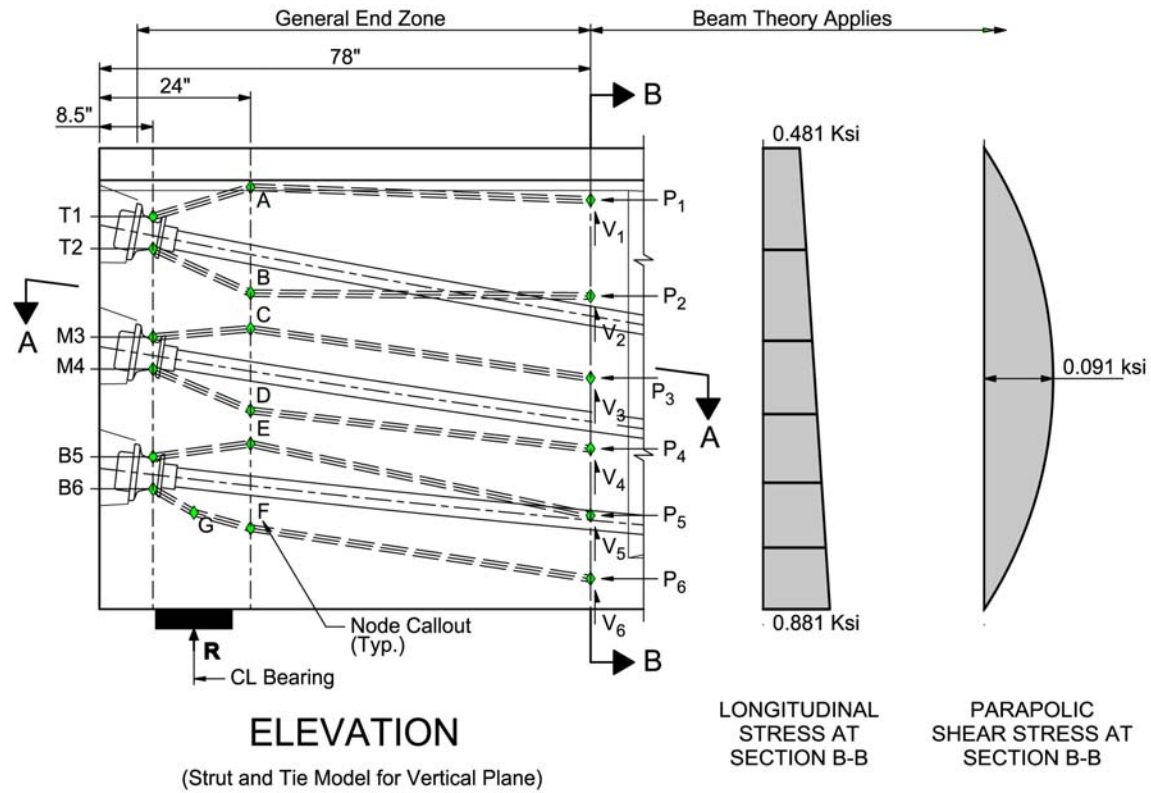
Figure 2.102 Strut and Tie Models for a Post-Tensioned Girder

A vertical tension tie is located at the point where the forces dispersed from the anchors must be restrained – just beyond the local zone (in this case, connecting nodes A through F at 18 in. from the anchor plates). Similarly, a vertical tie connects

all the nodes at the anchor face. For convenience and simplification of the analysis, the nodes at the anchor face and at the location where the forces dispersal is confined (nodes A through F) are aligned vertically. Analysis will reveal that these vertical "ties" actually behave as ties at some elevations (where dispersal of force from each anchor places them in tension) and as struts at others (i.e. between tendons, where they must resist the compression effect of the converging tendon paths).

Because the curvature of our tendon through the general zone is very slight (almost straight), longitudinal struts connect nodes A through F, directly with nodes at the end of the general zone located at the respective centers of force of the longitudinal stress distribution. These struts represent the effective inclined trajectory of the tendon forces and other loads including the bearing reaction, self weight and distributed lateral tendon force ("P/R"), as they transition from the anchorage to the section at the end of the general zone. At this section, the vertical components of each strut force are balanced by shear force determined by beam theory. (It follows that vertical web reinforcement as determined by normal beam theory for the final structure, can be used from this section onward for the rest of the girder.)

Note that the model is statically determinate. In fact, if an attempt were made to analyze it using a frame analysis program with all pin-jointed nodes, it would be unstable and the program would not run. Nevertheless, it serves to envision the flow of forces and to determine the magnitude of force in each strut and tie from the anchors to the end of the general zone.

2.6.4.2.12 What is the Effective Width and Thickness of Each Compression Strut?

An answer to this question is essential in order to be able to construct a credible strut-and-tie model in the first place – especially one in which struts do not overlap except where they meet at nodes of appropriate size. This can only be answered by knowing the limiting concrete stress a strut or node can sustain. This is given in terms of the strength of a compressive strut in *AASHTO LRFD* Article 5.6.3.3, Proportioning of Compressive Struts.

Unfortunately, before a model is analyzed, strut-forces and therefore required capacities and strut dimensions for the model, are not known. This is the quintessential dilemma for a designer. Where to begin? We have attained an idea of the size of the nodes at the anchorages (above) pointing to a possible minimum thickness for a strut of about 5 in (half the size of the minimum anchor plate size). This may be used to establish initial node and tie locations. Applying the forces to and analyzing this initial model provides an initial estimate of the corresponding maximum strut force and required capacity.

2.6.4.2.13 What is the capacity of a strut (and limiting strain) in the concrete?

The inclined struts in our model are not reinforced in the direction of compression, even though they are (will be) surrounded by orthogonally placed reinforcement. The

nominal resistance of an unreinforced compressive strut is given by *AASHTO LRFD* Article 5.6.3.3.1 as:

$$P_n = f_{cu} A_{cs}$$

The limiting compressive stress, f_{cu}, by *AASHTO LRFD* Article 5.6.6.3.3, is given as:

$$f_{cu} = f'_c / (0.8 + 170\varepsilon_1) < 0.85f'_c$$

in which:

$$\varepsilon_1 = \varepsilon_s + (\varepsilon_s + 0.002) \cot^2\alpha_s$$

where:

α_s	=	smallest angle between a compressive strut and adjoining tension tie
f'_c	=	specified compressive strength – in our case $f'_c = 6.0$ ksi.
ε_s	=	the tensile strain in the concrete in the direction of the tension tie.

In our example, f'c = 6.0 ksi, by examination of our initial model, α_s = 65.8°. Initially, ε_s is not known. However, if we make a reasonable assumption that when reinforcement is provided, it acts at its yield strength (say f_y = 60 ksi) and that the strain in the concrete is the same as that in the reinforcement, then εs = 60/28,000 = 0.002. Inserting these values gives:

$$\varepsilon_1 = 0.002 + (0.002 + 0.002) \cot^2 65.8 = 0.0028 \text{ in/in}$$

and

$$f_{cu} = 6.0 / (0.80 + 170*0.0028) = 4.70 \text{ ksi}$$

At this point we need to know the size of the strut, A_{cs}. Initially, when considering the local zones at the anchors and the location of the nodes (above), the anchor plate size was found to be 10 in. by 10 in. – implying that the minimum depth of a strut in the vertical plane terminating at an anchor zone would be about 5 in. Adjustment for strut inclination and the width of the strut perpendicular to the vertical plane have not yet been determined. For these we refer to the *AASHTO LRFD* Commentary C5.10.9.4.2 and 3, and Figure C5-10.9.4.2-1 in particular. The latter shows that the width of strut "w" is either constant or may widen, depending upon the details of the model. Applying this guidance, in the vertical direction, the width of the most critically loaded strut is 4.6 in (after also allowing for the inclination of the strut). The effective width in the horizontal direction (t') at the distance "a" from the anchor is 16.4 in. So we have:

$$P_n = f_{cu} . A_{cs} = 4.70 * 4.6 * 16.4 = 354.0 \text{ kip}$$

Applying the strength reduction factor, ϕ = 0.80 from *AASHTO LRFD* Article 5.5.4.2 for compression in anchorage zones, the reduced capacity is:

$$\phi \, P_n = 0.8 * 354 = 283 \text{ kip.}$$

Examination of our initial model reveals that the maximum compressive force in the worst loaded strut is 270 kips - in the strut framing into the lower half of the middle anchor. Now, we must check the proportions of the nodal regions and their limiting stresses.

2.6.4.2.14 What Limiting Concrete Stress can be Sustained by a Node?

For this we refer to *AASHTO LRFD* Article 5.6.3.5 - Proportioning of Node Regions.

For the support node (G) bounded by two compression struts and the bearing area, the compressive stress should not exceed $0.85 \, \phi \, f'_c$ – where by *AASHTO LRFD* Article 5.5.4.2, $\phi = 0.70$. This gives a limiting compression stress of:

$$f_{\text{limit}} = 0.85 * 0.70 * 6.0 = 3.57 \text{ ksi}$$

The smallest dimensional area at this node is estimated to have an area of at least 5.0 in by 16.43 in, subject to a maximum force of 225 kips, thereby imposing a stress of 2.74 ksi, which is less than 3.57 ksi and satisfactory.

Most other nodal regions in this model are bounded by a one directional tension tie and at least two compression struts, for which the limiting stress is $0.75 \, \phi \, f'_c$ – where again by *AASHTO LRFD* Article 5.5.4.2, $\phi = 0.70$. This gives a limiting compression stress of:

$$f_{\text{limit}} = 0.75 * 0.70 * 6.0 = 3.15 \text{ ksi}$$

The smallest dimensional area for the most highly loaded node, in this case node D, is again estimated to be 5.0 in by 16.43 in, subject to a maximum force of 270 kips, thereby imposing a stress of:

$$f = 270 / (5.0 * 16.43) = 3.29 \text{ ksi} > 3.15 \text{ ksi} \text{ which is not at first sight, satisfactory.}$$

However, upon closer examination of the internal forces at this node, we find that the force between nodes D and E is in fact compressive – only the residual tension is taken by the tie C to D. Consequently, a case can be made for allowing the higher stress level (3.57 ksi) as if it were bounded by three compressive struts – in which case it is satisfactory. If this were not the case, a solution would be to revise the node locations and more closely examine the available strut depth and width, or adopt a slightly higher strength of concrete.

Before considering the sizing of tension ties, we will consider the dispersal of forces across the width of the end block, perpendicular to the vertical plane or in plan view.

2.6.4.2.15 What is the Lateral Bursting Effect Across the Width of the End Block?

We have seen above that in plan view, the location of the maximum bursting force is estimated to be at 14.0 in from the anchor plate – which incidentally coincides with the end of the local zone, which is not quite at the chosen location of the vertical ties (18 in from the anchor plate). Using 14 in. and following the principle that the force disperses at approximately 1:2 we find that the dispersal is sufficient to engage the full width of the member (i.e. 28 in.). Considering the tension tie at this location and resolving forces from the anchorage nodes, the tensile force generated by from one tendon is:

$$T = (P/2) \tan \alpha$$

Where, in this case $\alpha = \tan^{-1} \{(7.0 - 2.5) / (14.0 - 2.5)\} = 21.3°$

$$\text{Thus, } T = 98.4 \text{ kips (per tendon).}$$

This is the total lateral tensile force to be resisted per tendon and can be satisfied by providing transverse reinforcement both above and below each tendon. The area of reinforcing steel required is determined as follows.

2.6.4.2.16 What is the Strength of a Tension Tie?

The strength and proportioning of tension ties is addressed by *AASHTO LRFD* Article 5.6.3.4. For our example, for a lateral force of 98.4 kips, the area of tensile steel (by *AASHTO LRFD* Article 5.6.4.3.2.1) required is:

$$A_{st} = 98.4 / (1.00 * 60.0) = 1.64 \text{ in}^2$$

Where the strength resistance factor, $\Phi = 1.00$ according to *AASHTO LRFD* Article 5.5.4.2. This area of reinforcement can be provided by 6 legs of #5 reinforcing bar, giving 1.86 in^2 - or 4 legs of #6 bar giving 1.76 in^2 (or similar, equivalent arrangement).

Before we consider rebar detailing, we will determine the reinforcement required in the vertical direction. From the results of our strut-and-tie model, we find that the maximum tensile force in this direction at the location of the end of the local zone is that between nodes A and B at the top anchor, and is 84.7 kips (which incidentally, only occurs if the top tendon is tensioned last in the sequence). This requires an area of reinforcement of:

$$A_{st} = 84.7 / (1.00 * 60.0) = 1.41 \text{ in}^2$$

The results also show that there is no tension, but compression, in the members in the vertical anchor face. The magnitude of the compression is well within the limits for the concrete between the anchors. However, none of this yet addresses or excludes corner tension.

2.6.4.2.17 What Other Reinforcement Might be Needed, Such as Corner Tension Ties?

It can be seen that our model does not yet contain any provision for tension ties around the top and bottom corners at the girder end. This stems from the fact that the anchorages are well centered and there is (theoretically) no net top or bottom tension. In practice, corner ties should always be provided. The minimum requirement would be to satisfy *AASHTO LRFD* Article 5.10.9.3.2 and to provide for 2 percent of the total factored tendon force.

The total factored tendon force in this case = 443 + 443 + 506 = 1392 kips – allowing for the reduction of force due to wedge set on two tendons but not the third as a result of sequential stressing. Applying the 2% results in a force of 28.0 kips - requiring 0.46 in^2 of reinforcement.

In this illustration, an alternative means to determine the size of the corner ties would be to modify the model. The reaction force and its node G would be removed or relocated. From the bottom corner an inclined strut would be inserted to connect with a relocated node G or node F. At the corner, the strut would be restrained by a vertical tie at the anchor face and horizontal tie connected to the bottom node at the end of the general zone. Nevertheless, a bearing, would have to be inserted somewhere – perhaps as a vertical tie to the top node A – to represent a lifting hook This alternative study would be appropriate if a girder had to be post-tensioned before erection.

2.6.4.2.18 What are the Results of the Strut-and-Tie Approach?

Results of the strut and-tie model are summarized as follows.

Vertical effects:

	Force	Stressing Sequence
Member AB	84.7 kip tension	(Mid, Btm, Top)
Member CD	53.9 kip tension	(Btm, Top, Mid)
Member EF	10.5 kip comp	(Btm, Mid, Top)
Between Top and Mid Anchor	50.8 kip compression	
Between Mid and Btm Anchor	47.4 kip compression	
Corner ties at anchor face	28.0 kip tension	

Reinforcement, max vertical tie;

$$A_{st} \text{ required} = 84.7 / 60.0 = 1.41 \text{ in}^2$$
$$= 0.71 \text{ in}^2 \text{ per face centered on tie (at 18 in. from anchor face)}$$

Corner ties;

$$A_{st} \text{ required} = 28.0 / 60.0 = 0.46 \text{ in}^2$$
$$= 0.23 \text{ in}^2 \text{ per face at top and bottom corners}$$

Transverse effects:

    Transverse force per tendon   = 98.4 kip tension

    Transverse reinforcement, A_{st} = 1.64 in^2 per tendon

                 (i.e. provide 0.76 in^2 both above and below each tendon.)

Location of bursting force:

Strut-and-Tie model locates bursting force d_{burst} = 18 in. from anchor face for various reasons to do with dispersal of forces and non-overlap of anchor zones (above).

2.6.4.2.19 What Should be the Final Disposition of Reinforcement?

Choosing not to use reinforcing bar diameters less than #4 rebar size and adopting a spacing of 6 in. for an anchor zone region, we find that the area of rebar provided centered on the vertical tie 18 in. from the anchor face will require:

    4 legs per face at 0.20 in^2 per leg provides 0.80 in^2 per face > 0.71 in^2 O.K.

This is provided by closed links around the perimeter of the section (Section BB Figure 2.103)

AASHTO LRFD Article 5.10.9.3.2 offers guidance for the distribution of bursting reinforcement – it should be located over a distance from the anchor face taken as the lesser of

$$2.5 \, d_{burst} = 2.5 * 18.0 = 45.0 \text{ in.}$$
$$1.5 * \text{width} = 1.5 * 28.0 = 42.0 \text{ in.}$$

However, being mindful of the range found for d_{burst} i.e. from 14.0 in for the transverse direction to a maximum of 35.4 in for the vertical direction for the two top anchors, we choose to distribute the reinforcement required for bursting effects in the vertical direction, over a distance of 48 in. from the anchor face – providing 9 closed links altogether. Since the primary purpose is to resist bursting forces in the vertical direction, including effects at corners of the cross section, these closed links should have continuous vertical legs with a splice in the top or bottom horizontal legs only. Also, in order to minimize congestion and allow for proper concrete placement and consolidation, these splices should be alternated from top to bottom.

By comparison and as a separate check, if the approximate method of *AASHTO LRFD* Article 5.10.9.6.3 is applied, taking the tendons as a group we find that d_{burst} = 35.7 in. and the required amount of reinforcement, A_{st} = 3.82 in^2. While the strut-and-tie model leads to a different location for the vertical tie resisting the bursting, the total area of reinforcement provided over the 48 in from the anchor face is in fact, 2 * 9 * 0.20 = 3.60 in^2 – which is a consistent result.

Lateral bursting effects, transverse to the girder require 1.64 in^2 per tendon – half of which would be provided above and below each tendon – centered on the lateral bursting location of d_{burst} = 14 in. from the anchor face. Since this will place some

lateral reinforcement within the local zone, there is a possibility of conflict with any local spiral from the PT supplier - and so some thought should be given to the need to minimize congestion.

This might be provided by 4 closed links of #4 reinforcing bar around the anchor zone of each tendon (and by the residual transverse top and bottom legs of the links provided for vertical effects). This results in a minimum provision of:

$$A_{st} \text{ provided} = 4 * 2 * 0.20 = 1.60 \text{ per tendon (O.K.)}$$

Alternatively, we choose to use 3 #5 rebar links per anchor to reduce congestion. Since these bars are to resist lateral forces, a closing splice should be located on one of the vertical faces and not on the horizontal legs in order to be able to properly develop the bars laterally.

Selection and disposition of reinforcement following the guidelines given in *AASHTO LRFD* leads to the final details shown in Figure 2.103. These details show reinforcement required for bursting effects determined and detailed as above. In this case, the final details are somewhat conservative, especially for bursting in the vertical direction and a refined distribution could probably be developed. However, additional area of web reinforcement for global beam shear force effect is not included, neither is any minor (temperature and shrinkage) distribution reinforcement, for example, across the anchor face.

2.6.4.2.20 Are There Any Other Observations?

In our illustration we chose to use an end-block of constant width for a length equal to the depth of the girder (Section BB in Figure 2.101). A valid alternative that would save a little weight would be to begin to taper the width of the end block before this location, at say 3 or 4 feet from the anchors. Since the location of the section of beam behavior (BB) cannot change (i.e. it remains at 6ft to 9 ft from the anchors (1.0 to 1.5 overall height) then new (smaller) section properties would have to be determined in order to facilitate recalculation of the longitudinal and shear stress dispersal. The centers of force and nodes would be re-located for a revised strut-and-tie model. Such a change would probably not significantly affect the total amount of reinforcement provided, but it has not been checked.

For lateral bursting, if the approximate method of *AASHTO LRFD* Article 5.10.9.6.3 is applied (which has its origin in the work of Guyon et al, circa 1960) we find that T = 73 kips per tendon - indicating an approximate level of correspondence between different approaches. For comparison, if the factor were to be increased from 0.25 to 0.35, as had been suggested at times (e.g. FDOT Criteria of 1983) then T = 113 kips per tendon – which is a little too conservative. In our illustration, "strut-and-tie" gives a more reasonable result of T = 98 kips.

In general, results in terms of the amount of reinforcement incorporated in the final detail, is in agreement with that required by the approximate method in this particular illustration.
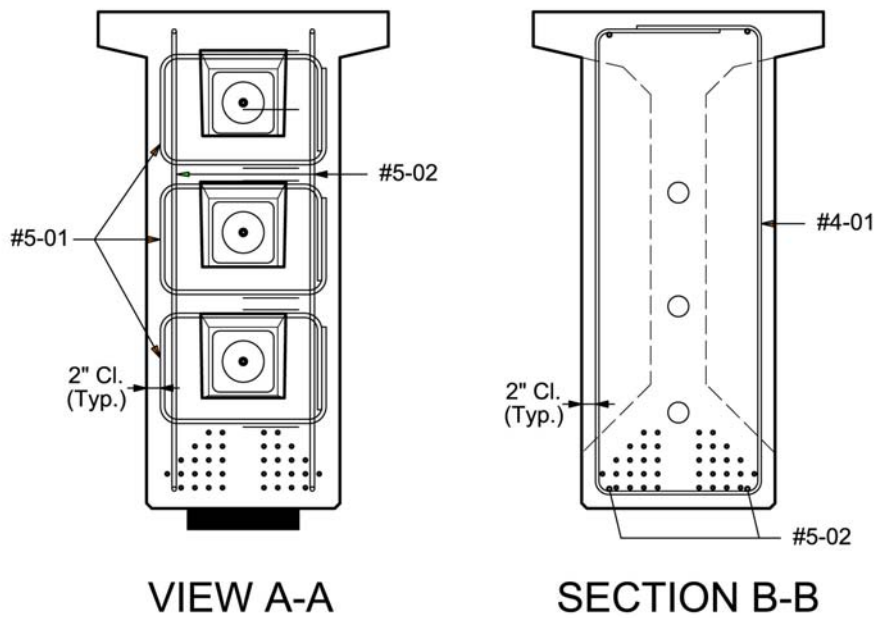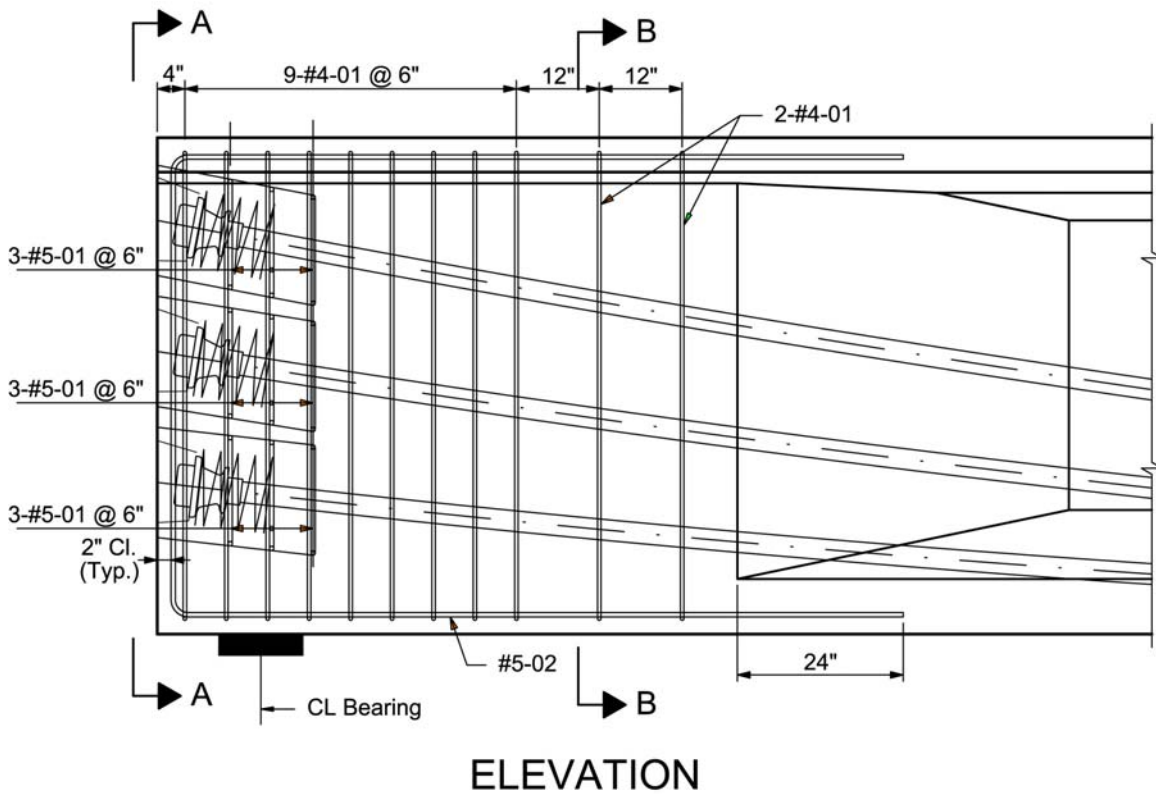
ELEVATION

VIEW A-A

SECTION B-B

Figure 2.103 Strut and Tie Models for a Post-Tensioned Girder

2.6.5 Flexural Limit States

2.6.5.1 Differences between Continuous and Simply-Supported Structures

For continuous prestressed superstructures, there are subtle differences in flexural limit states compared to simply-supported superstructures. The most obvious and significant difference are negative moments over interior supports. Negative moments from gravity loads such as self-weight, superimposed dead load and live load, create flexural tension in the top fiber and compression in the bottom fiber at support regions. In addition, depending upon the layout of post-tensioning, secondary moments from prestress can also induce negative moments. In continuous superstructures, creep redistribution tends to reduce negative moments due to dead loads and increase positive moments within spans.

The use of a draped post-tensioning layout where the tendons are low down in the section within a span and high up over the supports is purposefully intended to provide compressive stress where it is most needed - to offset permanent tensile stress from loads. It also minimizes the magnitude of adverse secondary moments from prestress.

2.6.5.2 Structural Analysis

Calculation of bending moments, shear forces and reactions for continuous structures may be accomplished by various methods based on classical beam theory, such as: flexibility analysis, displacement (stiffness) analysis, area-moment theorem, moment-distribution, matrix methods, and so forth. Computer models are generally based on matrix (stiffness) methods. For analysis purposes, post-tensioning forces may be applied as equivalent loads as discussed above.

2.6.5.3 Application of Vehicular Live Load

For negative moment and support reactions at interior piers, there is a particular nuance in the *AASHTO LRFD* Article 3.6.1.3.1, bullet point 3. Namely, that for negative moment between points of contra-flexure, 90% of two trucks spaced a minimum of 50ft apart along with 90% of the effect of the design lane load may be applied to induce a negative moment. For this purpose, the location of the points of contra-flexure corresponds to that determined by applying a uniform load on all continuous spans.

2.6.5.4 Service Limit State

At the Service Limit State, limiting flexural stresses for continuous structures are the same as for simply-supported structures (*AASHTO LRFD* Article 5.9.4); the only difference being that these are now applied to the top or bottom fiber as the case may be. Stresses due to secondary moments should be calculated and added to other effects as necessary. In continuous structures, thermal gradient (TG), especially negative thermal gradient, can induce additional top tension over interior supports – presenting difficulties for some structures and load combinations.

For a composite section, determination of the final state of stress can only be successfully accomplished by accumulating stresses from each individual effect (load or prestress) at each elevation of interest at each cross-section of interest (i.e. it is quite wrong to accumulate only moments or shear forces and apply the total only to the final section.) This accumulation is made more tedious for continuous, post-tensioned, composite girders, although the principle is only an extension of that for a simply-supported pre-tensioned girders and pre-tensioned girders made continuous using reinforced concrete joints. To cap; stresses are first calculated and accumulated for the non-composite properties up to the time the slab has been cast and becomes effective. Thereafter, stresses are calculated and accumulated for the composite section properties comprising the non-composite section, the effective slab and, possibly, the transformed area of pre-tensioned strand. For a post-tensioned structure, intermediate refinement of section properties may be necessary to allow for transformed areas of strands after they have been stressed and bonded. Post-tensioning added in stages would be transformed and incorporated with the concrete applicable at that stage.

Longitudinal stresses should be accumulated at least at the top of the cast-in-place deck slab, top of precast girder, bottom of precast girder. If there is an interest in needing to know final principal tensile stress at any elevation, then it is necessary to accumulate longitudinal and shear stresses at those elevations too. Such elevations would include those of the neutral axis of the non-composite and composite sections and others, possibly top and bottom of web, as necessary.

Given that the section properties (for flexure and shear) change throughout the construction process, meticulous accounting is necessary to keep track of accumulated stress from initial to final long-term, in-service, conditions. Nowadays, this is facilitated by spreadsheets.

2.6.5.5 Strength Limit State

In continuous prestressed structures, applying a load factor of 1.0, secondary moments due to prestress must be added to the load-demand (or deducted from the factored resistance) when checking the Strength Limit State. With this particular exception, the calculation of the flexural capacity of a cross section itself is otherwise the same as for any prestressed girder and may be determined as outlined in *AASHTO LRFD* Article 5.7.3.

2.6.5.6 Contribution of Mild-Steel to Flexural Capacity

In superstructures of precast-girders made continuous by post-tensioning, cast-in-place girders are usually provided with reinforcement in the form of L or U-bars, projecting into the splice from the ends of the girders at the bottom of the splice in addition to continuous (spliced) mild-steel reinforcement in the deck over the joint. Both sets of reinforcement may be counted toward flexural strength capacity, as necessary, at positive and negative moment regions.

2.6.5.7 Redistribution of Negative Moment at the Strength Limit

AASHTO LRFD Article 5.7.3.5 addresses this issue. If tensile steel (in this case prestress steel) in the negative moment region yields, which occurs when the net tensile strain (ε_t) exceeds 0.0075, the moment determined by elastic theory at the strength limit state is to be reduced by a percentage not greater than $1000\varepsilon_t$ or 20% at that section. In order to maintain equilibrium, positive moments should be adjusted to account for the change in negative moments. Positive moment capacity should be checked for the redistributed amounts.

2.6.6 Longitudinal Shear Design

2.6.6.1 Service Limit State

Design for shear at the Service Limit State is not a requirement of *AASHTO LRFD*. However, to be mindful of the need for durability, a Designer may choose to assure himself that the structure will not experience shear cracking at the service level. High shear forces can cause diagonal cracking in webs as the result of large principal tensile stresses. The magnitude of the effect can be determined by applying classical theory using Mohr's circle for stress. Limiting the principal tensile stress to 3 or $4\sqrt{f'c}$ (psi) at the elevation of the neutral axis has traditionally and conveniently been used to establish an approximate web thickness for durability and detailing purposes.

2.6.6.2 Strength Limit State

AASHTO LRFD shear design using Modified Compression Field Theory was covered in DM Section 2.4.5.3 for precast, pretensioned girders. Shear design for continuous, post-tensioned members is very similar with few refinements.

In a simply-supported girder, or any statically determine structure, internal forces from the prestressing do not cause reactions at the supports. However, when girders are continuous, the structure is then statically indeterminate. Prestressing then causes small secondary reactions due to the profile of the tendon. This is sometimes called the "continuity effect". The "secondary reactions" induce corresponding shear forces and secondary moments. This directly modifies the summation of shear forces from all loads. Secondary effects have been discussed in the context of prestressed girders made continuous with reinforced joints (DM Section 2.5). Further elaboration is provided in DM Section 2.7 for structures cast-in-place on falsework (below).

Although common practice for simply-supported pretensioned girders is to use straight strands, they can be draped upwards at the ends, as discussed in DM Section 2.4.6.3. Continuous or post-tensioned girders usually have draped prestressing at the ends of the girders and over the supports to counteract negative moments arising from dead and live loads. The force in the strands can be resolved to give a vertical component - typically being opposite the shear force from dead and live loads. Essentially, the effect is a reduction in shear demand. However,

AASHTO LRFD includes this effect as a component of strength rather than a reduction in demand.   In this case, the vertical component of the effective prestressing force, V_p, is added to the strength of the concrete, V_c, and vertical reinforcement, V_s. The total shear strength is then:

$$V_n = V_c + V_s + V_p$$

If V_p is in the same direction as the dead and live load demand, then V_p should be taken as negative in this equation for total shear strength. Whether positive or negative, if V_p is considered to be a component of "strength", then shear effects from prestressing should *not* be included as a load "demand."

Vertical prestressing by means of post-tensioned bars placed in webs is not a practical option for precast, pre- and post-tensioned I-girders.

2.7 Design of Cast-In-Place Post-Tensioned Superstructures

2.7.1 Introduction

This section is concerned primarily with post-tensioned superstructures built cast-in-place on falsework. This was the type of construction used when post-tensioning systems first became widely available in the 1950's. Different types of construction, cross sections, post-tensioning tendons, formwork, falsework and associated concrete placement, curing, finishing, tendon installation, stressing and grouting operations have already been introduced in DM Volume 3, Chapter 1, Section 1.8.

This section illustrates a few key aspects of design different or additional to those not already addressed in previous sections. For instance, loss of prestress force in pretensioned girders has already been addressed in DM Section 2.4. Additional losses due to friction and wedge set in post-tensioning systems have been addressed in DM Section 2.7. These same losses also occur in post-tensioned construction; so their calculation not repeated here.

2.7.1.1 Typical Superstructure Sections

The most common types of cross section are multiple cell (multiple webs) or single cell (two-web) boxes generically illustrated in Figure 2.104 and Figure 2.105, or similar variations. Variations include vertical or sloping outer webs, deck slabs with multiple T-section ribs, with or without bottom flanges, voided slabs or similar sections. The key feature is that the whole cross-section is "non-composite" and is subject to all loads and longitudinal post-tensioning force; i.e. there is no separately cast, "composite" deck-slab as considered in foregoing Sections 2.4, 2.5 and 2.6.
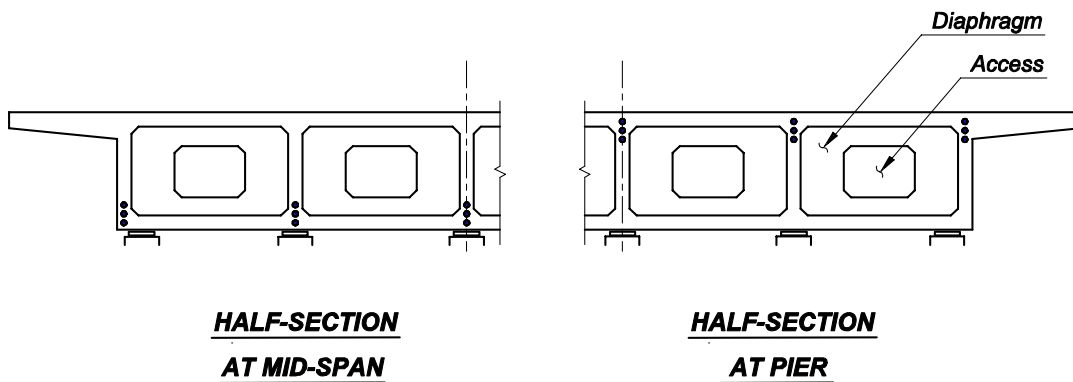

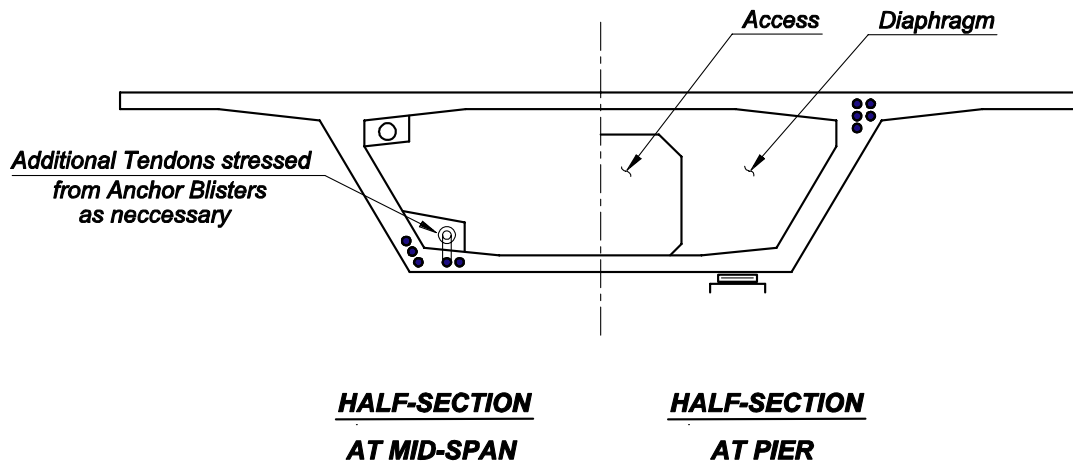**Figure 2.104 Typical Multi-Cell Cast-in-Place Superstructure**

HALF-SECTION   **HALF-SECTION**

AT MID-SPAN   **AT PIER**

Figure 2.105 Typical Single-Cell Box for Cast-in-Place Superstructure

2.7.1.2 Effective Cross Section and Preliminary Sizes

Although the whole cross-section contributes to dead load, it does not necessarily participate structurally in resisting loads and prestress. In some cases, only portions of the top and bottom slabs may be considered effective, depending upon various proportions. For design purposes, the effective width of slabs is given in *AASHTO LRFD* Article 4.6.2.6. (Reference may also be made to the AASHTO Guide Specification for Segmental Bridges.)

As regards the actual thickness to adopt for different portions of a cross-section, reference should be made to previous projects of a similar type and size. Attention should also be paid to practical thicknesses necessary to accommodate cover, reinforcement, longitudinal and transverse post-tensioning, construction tolerances for locations of such items, the maximum size of aggregate and clearance for effectively placing and consolidating concrete.

As a very general guide (not a hard and fast rule) the following are offered for estimating an initial concrete thickness:

➤ The thickness of the top edge of a slab needed to accommodate transverse post-tensioning anchors should usually not be less than 9 inches; to allow for the height of the anchor plate, local anchor reinforcement, top and bottom rebar and cover.

➤ The thickness of a top slab at the root of the cantilever wing should be about the edge thickness plus 0.5" to 0.75" for each foot of total overhang.

➤ The minimum thickness of a top or bottom slab between the webs of a box should usually not be less than about 8 inches.

➤ The total (sum of all) web thickness may be estimated at approximately 0.6 to 1.0 inches per foot of overall width.

> ➢ The minimum individual web width should be sufficient to accommodate post-tensioning ducts, rebar, cover, tolerances, maximum aggregate size and clearances.

> ➢ For a structure of constant depth, the overall structural depth is usually in the range of L/24 to L/18 – where L = span length.

> ➢ For a structure of variable depth, the overall depth at an interior pier is usually about L/20 and at mid-span, a minimum of L/40.

> ➢ In longer spans of box girders (usually over about 160 feet) the bottom slab may need to be thickened toward interior piers in order to accommodate negative moment conditions.

The above are approximate for initial guidance only. They are typical for most box structures with concrete strengths in the range of 5 to 8 ksi and spans up to about 400 feet. Local commercial conditions will govern the availability of concrete of a particular strength and size of aggregate. Local environmental conditions usually govern minimum cover requirements.

2.7.1.3 Construction Sequence

For a typical, box-type superstructure, the cross section is usually cast in phases beginning with the bottom slab, then the webs, then the top slab to facilitate convenient construction. The longitudinal length of a pour depends upon the rate of concrete delivery and placement within a given work period. This depends upon the overall size of the superstructure and scale of the project. Temporary transverse bulkheads may be necessary to divide the superstructure into workable lengths. As regards design, transverse construction joints can usually be located to accommodate construction needs.

Locations of potential longitudinal construction joints must be carefully considered. For instance, web reinforcement must be adequate not only for global loads in the web, but also for local interface shear effects when longitudinal construction joints are made, for instance, at the top and bottom of the webs. Shear friction calculations should consider the range of coefficient of friction (μ) between monolithic and jointed conditions. If necessary, restrictions on locations of such joints should be clearly shown on the plans.

With cast-in-place construction on falsework, it is usually assumed that all of superstructure is built and supported by the falsework until longitudinal post-tensioning is installed and stressed to make it self-supporting – at which point the falsework is removed. (Figure 2.106) This is equivalent to the case where the structure is "instantaneously" loaded with its own self weight and post-tensioning in its' final configuration. The camber required for setting the formwork using this technique is the opposite of the anticipated final, long-term, deflections under all dead and prestress loads.
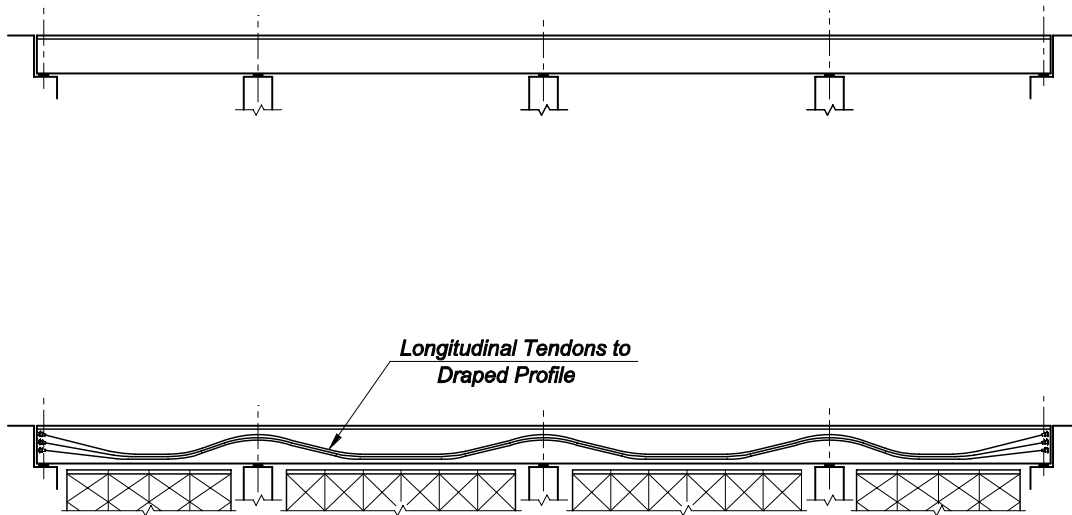
- *Provide Falsework throughout*
- *Construct Cast-In-Place Spans*
- *Install and stress Longitudinal Tendons*
- *Release Falsework*

Figure 2.106 Cast-in-Place on Falsework and Tendon Layout

With many continuous spans, construction might proceed in stages, with falsework supporting only one span - or a little more than one span – at a time. After the span has been post-tensioned, the falsework is released and re-cycled for a succeeding span. This requires detailed consideration of the layout of longitudinal tendons and their anchorages so as to properly overlap - with new ones picking up where previous ones terminate (Figure 2.107).

This technique also requires consideration of intermediate deflections and setting of formwork to an appropriate camber so that the final structure conforms as closely as possible to the desired profile after it has been constructed in stages (e.g. one span at a time). This camber is not the same as that where the entire structure is supported.
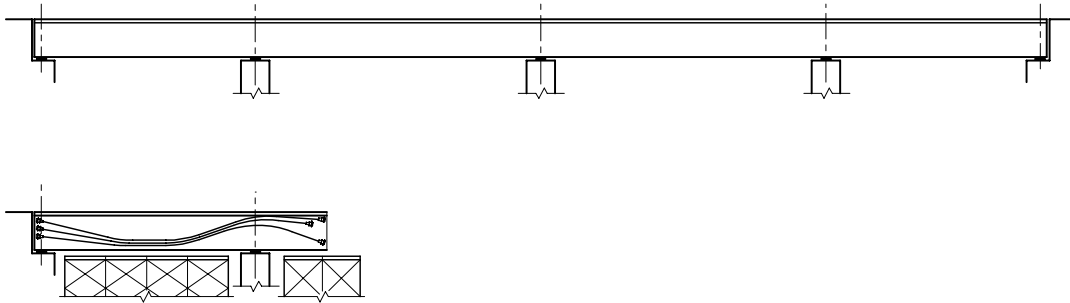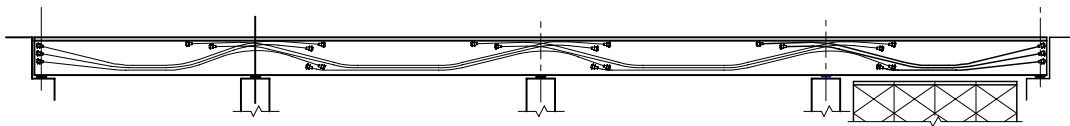
Stage 1 - Construct First Span, install and stress Tendons, release Falsework.
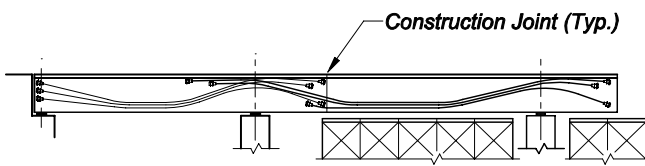
Stage 2 - Construct Second Span, install and stress Second Span Tendons, release Falsework.
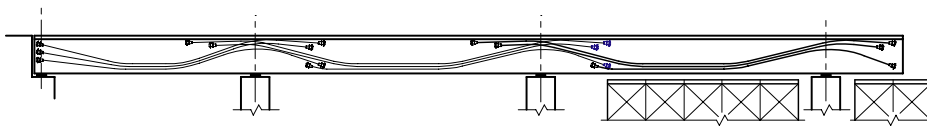
Stage 3 - Construct Third Span, install and stress Third Span Tendons, release Falsework.

Stage 4 - Construct Fourth Span, install and stress Fourth Span Tendons, release Falsework.

Figure 2.107 Spans Cast Sequentially on Falsework and Tendon Layout

2.7.2 Transverse Analysis and Design

In general, transverse design addresses the need for the deck slab to carry permanent structural dead and local wheel live loads and effectively transfer them to the webs in an appropriate manner - where they are then combined with global longitudinal conditions as necessary. Transverse analysis takes into account the transverse flexure of the multi-cell or single-cell box in acting like a frame to disperse

local effects. Torsional effects from eccentric live loads are considered and appropriately distributed to be combined with shear forces in the webs.

It is a matter of design preference whether to commence with transverse or longitudinal design. In actuality, both need to proceed together as the results of one influence the other and vice-versa. Since it is in the interests of any project to minimize weight, performing a transverse analysis usually leads to the minimum required thickness for slabs and webs. These are refined when combined with longitudinal design conditions (2.7.3 below).

Appropriate methods of structural analysis for transverse conditions include:

- Classical elastic theory for the flexure of plates or shells
- Equivalent strip (*AASHTO LRFD*)
- Influence surfaces for flexure (derived from classical theory)
- Influence surface combined with a transverse frame
- Three-dimensional finite element modeling using plates or shell elements

Each technique may have an application appropriate for one project yet not for another. The following are general comments and should not be considered mandatory in any way. In all circumstances, engineering knowledge and good judgment is required.

2.7.2.1 Classical Theory

Classical linear-elastic analysis theory for out of plane bending of plates in two directions has been previously developed (Westergard, Timoshenko, et al.). The theory is applicable for any surface, such as the top slab of a bridge deck, in flexure and supported by one or more fixed edges, such as a cantilever wing or the top of webs and diaphragms. Classical theory is laborious and not easily suited to practical application; except that it was used to develop influence surfaces.

2.7.2.2 Equivalent Strip

The approximate equivalent strip method of *AASHTO LRFD* Article 4.6.2.1 may be used to determine transverse effects in the deck slab of monolithic, multi-cell boxes (case (d) of Table 4.6.2.2.1-1) providing that the geometric proportions of the superstructure meet the requirements of this section.

Bending moments may be taken directly from *AASHTO LRFD* Table A4-1, basically if:
- There are at least 3 webs with not less than 14 ft between the centerlines of the outermost webs
- The overhang should be more than 21" but less than 0.625 times the web spacing (S) or 6.0 ft, whichever is the less.
- The maximum web spacing (S) should not exceed 15 ft.

Example: if it is assumed that the web spacing is 7ft 6in, and webs have a width of 10 in. then from Table A4.1, the maximum positive moment in the deck slab is M_{pos} = 5.44 kip-ft/ft. The corresponding maximum negative moment at the face of the web, by interpolation between the values given for the distance from the centerline of the web to the negative moment design section, is:

$$M_{neg} = 4.61 + (5.43 - 4.61)/3 = 4.88 \text{ kip-ft /ft.}$$

These are compared with those derived from influence surfaces (below), thus:

	Table A4-1	Influence Surface	Difference (%)
$M_{positive}$ =	5.44	5.24	3.8
$M_{negative}$ =	4.88	4.89	0.2

This close agreement lends credibility to both methods. The small variations may be accounted for by differences from reading influence charts, arithmetic, the size of wheel prints applied to the influence surfaces, and by differences in assumed edge support conditions.

2.7.2.3 Influence Surfaces

An influence surface is the two-dimensional, plate-bending equivalent of an influence line for flexure in a beam. Pucher and Homberg developed influence surfaces from classical theory for out of plane flexure of plates of constant and variable thickness for a variety of edge support conditions. Although now out of print and rarely found, their charts and tables offer the engineer a practical and straightforward application of classical theory.

Each influence surface is a contour of flexure, either in the transverse or longitudinal direction as the case may be, for the selected boundary conditions. The latter may be a fully fixed edge, an edge vertically supported but otherwise free to rotate, or an unsupported edge – or combination of these conditions. Influence surfaces have been developed for various locations of interest – such as maximum transverse and longitudinal flexure at midspan, transverse negative moment at a fixed edge and at one or two intermediate locations between midspan and the edge. All influence-surface bending moment results are calculated in terms of moment per unit length of slab in the direction considered.

Local loads – such as wheel loads - are applied as discrete patches of load in plan dimensions scaled proportionally to the span of the slab. The volume under the influence surface when summed up for each patch of load represents the magnitude of the bending moment for the orientation and location considered.

Where a multi-cell box has a constant thickness of deck slab and relatively closely spaced and thick webs such that the transverse "frame" is relatively stiff, flexural moments from a Pucher chart influence surface provide sufficiently conservative results for local design of the slab itself. A brief illustration is given for transverse

local slab positive flexure at mid-span and negative flexure at the supported edge in Figure 2.108 and Figure 2.109.

Single HL93 Tandem wheel prints at mid-depth of 8" slab

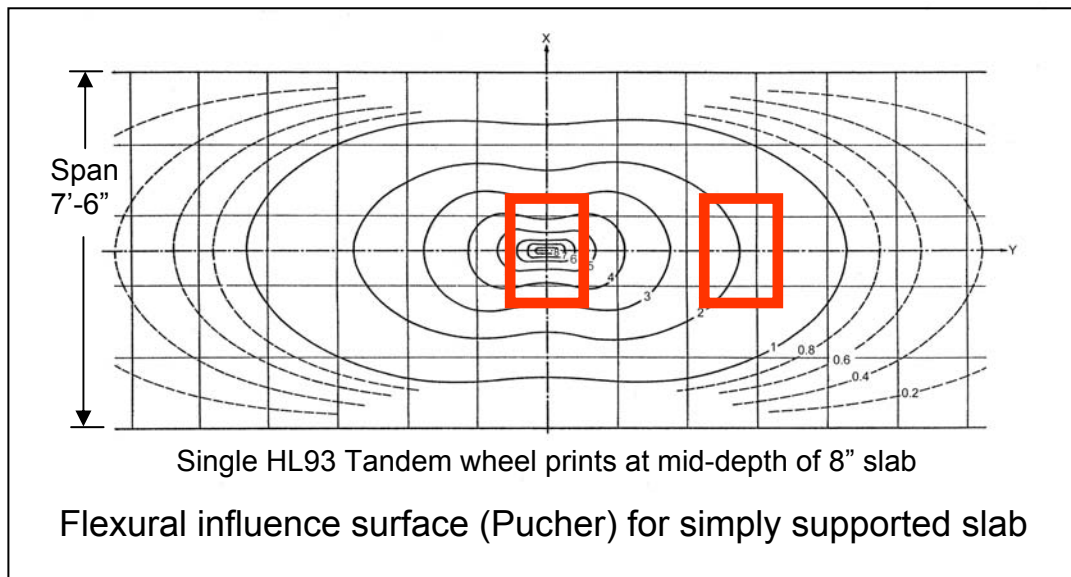Flexural influence surface (Pucher) for simply supported slab

Figure 2.108 Transverse Flexure at Midspan of Slab (Pucher)

Suppose we wish to determine the midspan transverse moment under the action of local wheel loads of the HL 93 Tandem with two axle loads of 25 kips each spaced 4 ft apart longitudinally on a top slab spanning between two stiff webs with a center to center of span of 7ft 6in. Assuming a web width of 10 in gives a clear span of 6ft 8in. Adopting a similar approach as the equivalent strip method by assuming a simply supported span, Figure 2.108 shows the Pucher chart influence surface for transverse flexure at midspan for a long plate strip with two supported but not restrained edges. Assuming a slab depth of 8 in, then wheel prints, 18" long by 28" wide, are plotted to scale.

By inspection of the influence line intensities we find that locating one wheel over the center of the chart will provide a maximum moment. The trailing wheel print is plotted to scale 4 feet distant longitudinally. From the intensity of the influence lines, it is clear that this wheel will contribute only a minor portion of the total. A parallel pair of wheels located 6 ft away transversely to represent the two other wheels of the one tandem, will clearly be off the chart. However, since a similar (second) tandem could be placed only 4 ft away, laterally, we find it could just be located on the edge of the chart – but its effect is negligible as regards the midspan moment. The total midspan moment is found by numerically reading the influence line values, integrating the volume under each wheel print and multiplying by the applied distributed wheel print pressure. In this case, we find:

Volume under wheel 1	=	2397 in^3 units
Volume under wheel 2	=	958 in^3 units
Total	=	3325 in^3 units

Since this is a "Pucher Chart", the influence surface values must be divided by a constant term (8π) incorporated in their original compilation. Inserting the wheel load of 12.5 kips, applying a dynamic allowance of IM = 1.33 and a multi-presence factor (1 lane) of 1.20, the positive bending moment at midspan is given by:

$$M_{midspan} = \frac{3{,}325 \times 12.5 \times 1.33 \times 1.20}{8\pi \times (18 \times 28)} = 5.24 \text{ ft-kip/ft}$$

This value is in close agreement with that found by using the equivalent strip method of *AASHTO LRFD* Table A4-1; namely 5.44 ft-kip/ ft.

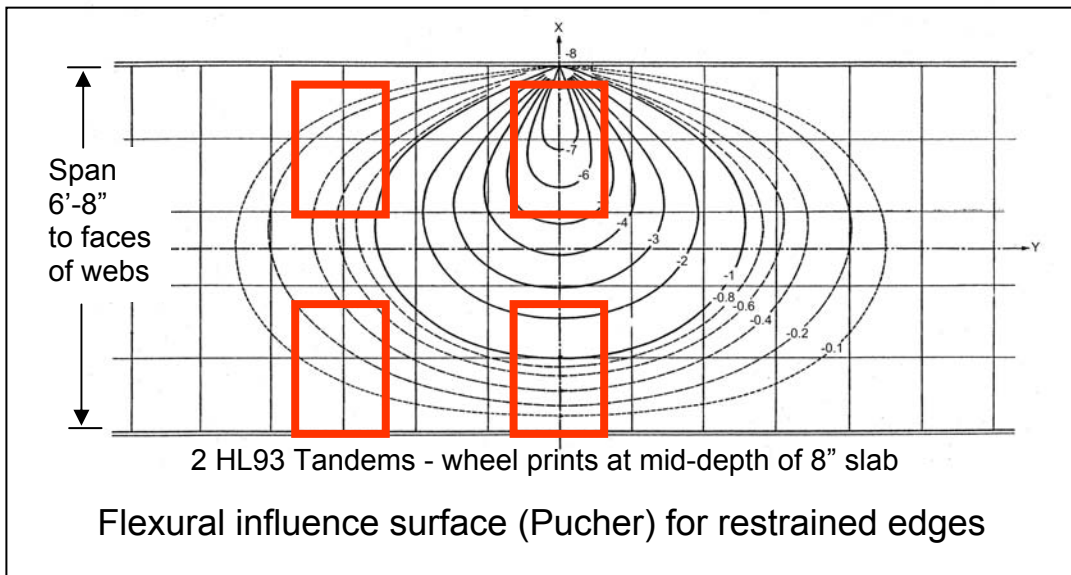A similar procedure is used to determine the negative moment at the "fixed" edge of the slab (Figure 2.109).

Flexural influence surface (Pucher) for restrained edges

Figure 2.109 Negative moment at fixed edge (Pucher)

The results are:

Volume under wheel 1	=	2747	in³ units
Volume under wheel 2	=	168	in³ units
Volume under wheel 3	=	677	in³ units
Volume under wheel 4	=	134	in³ units
Total	=	3726	in³ units

$$M_{fixed\ edge} = -\frac{3{,}726 \times 12.5 \times 1.33 \times 1.00}{8\pi \times (18 \times 28)} = -4.89 \text{ ft-kip/ft}$$

Notice that in this example, the adjacent wheel line from a similar tandem is located 4 ft away from the first tandem. In similar situations as in these two examples, it is

usually necessary to try several locations for wheel prints in order to determine the maximum effect.

Results from selected influence surfaces provide the main local flexural positive and negative moments in the transverse direction between webs and associated local longitudinal flexure of the slab under local wheel loads. Likewise, longitudinal conditions for negative flexure in a slab at a stiff transverse diaphragm can be found by selecting an appropriate chart.

Similar techniques using Homberg Charts for variable thickness slabs are used for slab flexure in a single-cell or multi-cell box with relatively widely spaced webs, or for a variable depth cantilever wing. In such cases, support edge fixity moments must be distributed around the transverse frame (below).

2.7.2.4 Influence Surface plus Distribution around Transverse Frame

For a single-cell box (or a multi-cell box with relatively wide spacing of webs) and therefore more flexible transverse frame, it is necessary to re-distribute local fixity moments in the top slab by frame action to the remainder of the cross section. This is similar to distribution of fixed-end moments around a plane-frame using moment distribution or other frame analysis technique.

The final, maximum redistributed live load moments, when combined with those of permanent effects (dead load and prestress) are those for which individual slab and web thicknesses should be designed and/or checked for transverse effects.

The effective length of bridge superstructure for transverse frame analysis should be a unit length (e.g. 1 foot) in order to provide results that correspond to those from associated influence surfaces. Application of transverse post-tensioning to the frame model should be so proportioned to give the correct force and moment per unit length of deck according to the longitudinal spacing of transverse tendons.

Use of a unit length (one foot) of transverse section as the frame model is correct for permanent loads (dead and prestress) but is conservative for local live load flexure transmitted to the webs. This is because local wheel loads cannot be placed closer together than the minimum axle spacing (say 4 feet). By the time local effects have dispersed through the thickness of the top slab and into the webs, a longer length of web may be mobilized than the assumed unit length. More rigorous account of this particular aspect is not normally considered – although it might be used for a more refined design or to improve load rating if such local conditions control.

This raises the question of what transverse conditions should be combined with global longitudinal conditions. For the time being it must suffice to observe that in general for large well-proportioned boxes, the maximum transverse conditions rarely, if ever, occur simultaneously with the maximum longitudinal conditions (see below).

Transverse analysis for a single cell box capable of carrying up to 3 lanes of live load is illustrated in the following example. Because the top slab varies in thickness, influence surface charts by Homberg are used.

Consider local wheel load effects for the HL 93 Tandem (Figure 2.110). Negative live load moment at the root of the cantilever wing at the face of the web is found by plotting to scale the wheel print of the tandem on the influence surface for slab with one fixed edge. The wheels are located relative to the traffic barrier. It usually takes a few attempts to locate the wheels so as to give the maximum effect. In this case, it is with the lead wheels 3 ft ahead and the trailing wheels 1 ft behind the point of maximum moment. Each wheel print is plotted with a surface contact area of 10in long by 20in wide. Given that the slab is relatively thick and the neutral axis of the slab is relatively deep, some additional dispersal of the wheel print is reasonable. In this case, it is chosen to disperse the wheel print at 45° to a depth of 4in making the effective wheel print 18in long by 28in wide. This is not completely to the depth of the neutral axis (slab varies from 9in to 17.8in deep) but facilitates a similar plan area for each wheel.
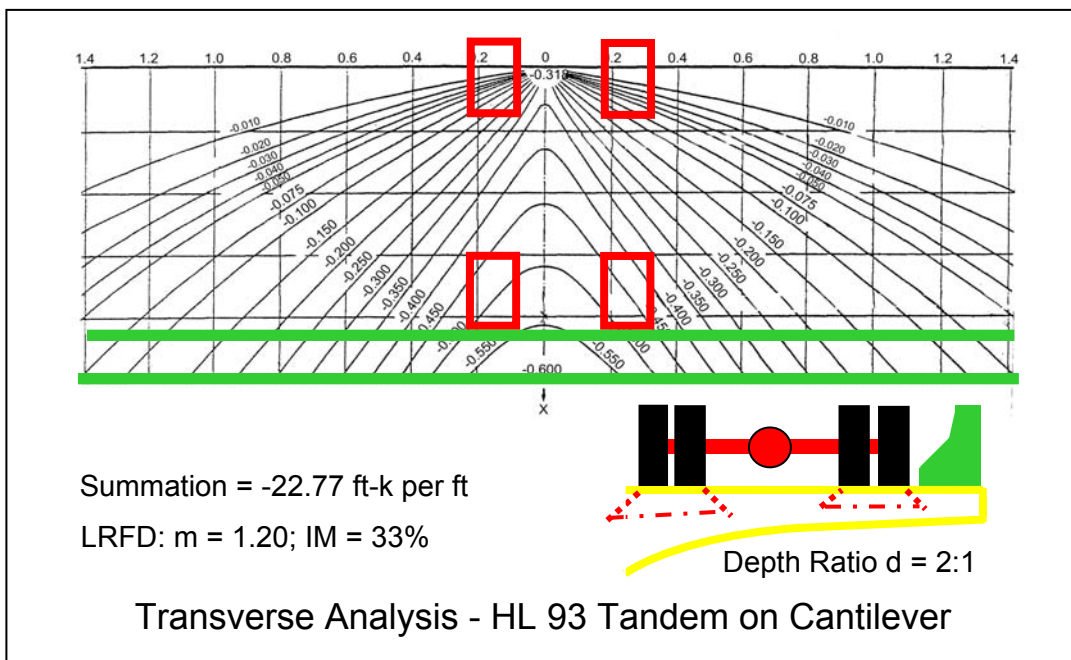

Figure 2.110 Moment in variable depth cantilever wing (Homberg)

The volume under the influence surface is calculated for each wheel print and multiplied by the applied load to give the total negative moment which, in this case, = -22.77 ft kip/ft. (There is no need to divide by (8π) since this has already been accounted for within the Homberg influence surface values.)

The negative fixity moment (-22.77 ft kip / ft) is applied to a transverse frame model of the section. This provides a final set of distributed moments given in Figure 2.111. In this example, the negative moments at the interior of the top slab and top of the

web sum to the applied fixity moment. (The fact that they are equal (-11.38) is a coincidental artifact of the relative stiffness of the top slab, webs and bottom slab of this particular box section – such equality would not normally be expected).
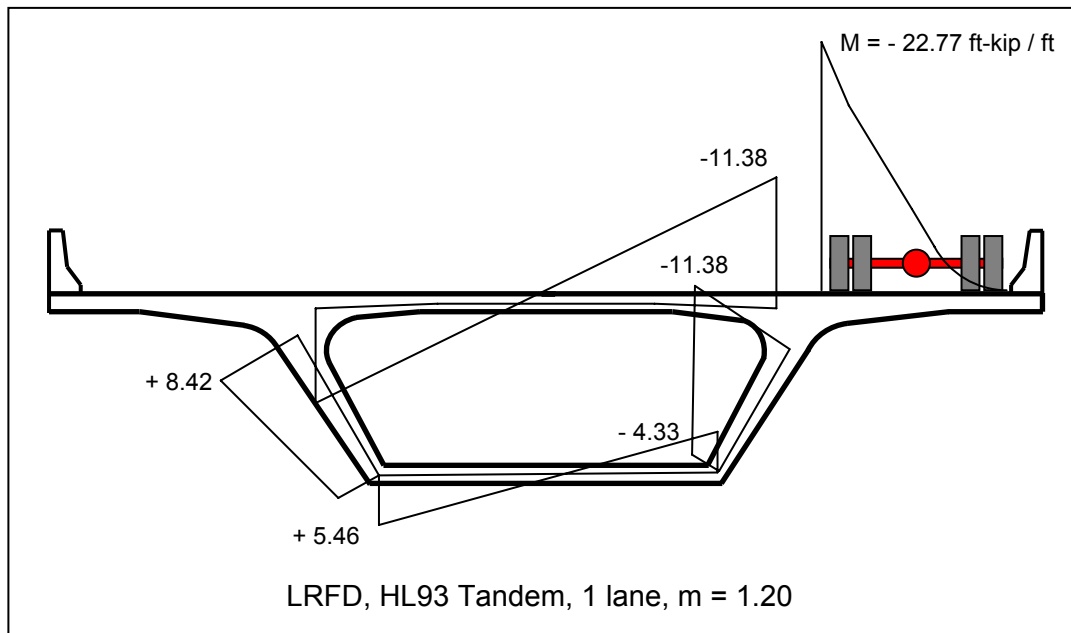

M = - 22.77 ft-kip / ft

-11.38

-11.38

+ 8.42

- 4.33

+ 5.46

LRFD, HL93 Tandem, 1 lane, m = 1.20

Figure 2.111 Cantilever moment distributed to frame

Distribution of moments around the box section can be made using any appropriate calculation method for indeterminate structures, such as; classical theory, flexibility methods, moment distribution or stiffness matrix analysis, etc. When using such techniques it is necessary to assume some support conditions – particularly with stiffness matrix methods used in structural analysis computer software – in order to avoid matrix instability (dividing by zero).

For stability, two vertical and one horizontal supports are needed. The vertical supports are placed at the bottom of the webs; the horizontal support may be at one of these. All supports should be unidirectional "pins" and otherwise free to rotate and translate. The frame is free to sway. Such a model will provide appropriate local transverse flexural moments around the frame for most conditions. An exception may be where a section could be prevented from swaying, as for instance, in proximity to a stiff transverse diaphragm. In the latter case, an additional horizontal support might be appropriate at the center of the top slab.

Continuing with the example, consider the case of the transverse fixity moment in the top slab between the webs due to the load of two HL93 Tandems, placed side by side. Figure 2.112 shows the influence surface (Homberg) for this case with the wheel loads applied.

LRFD: m = 1.00; IM = 33%
Summation:

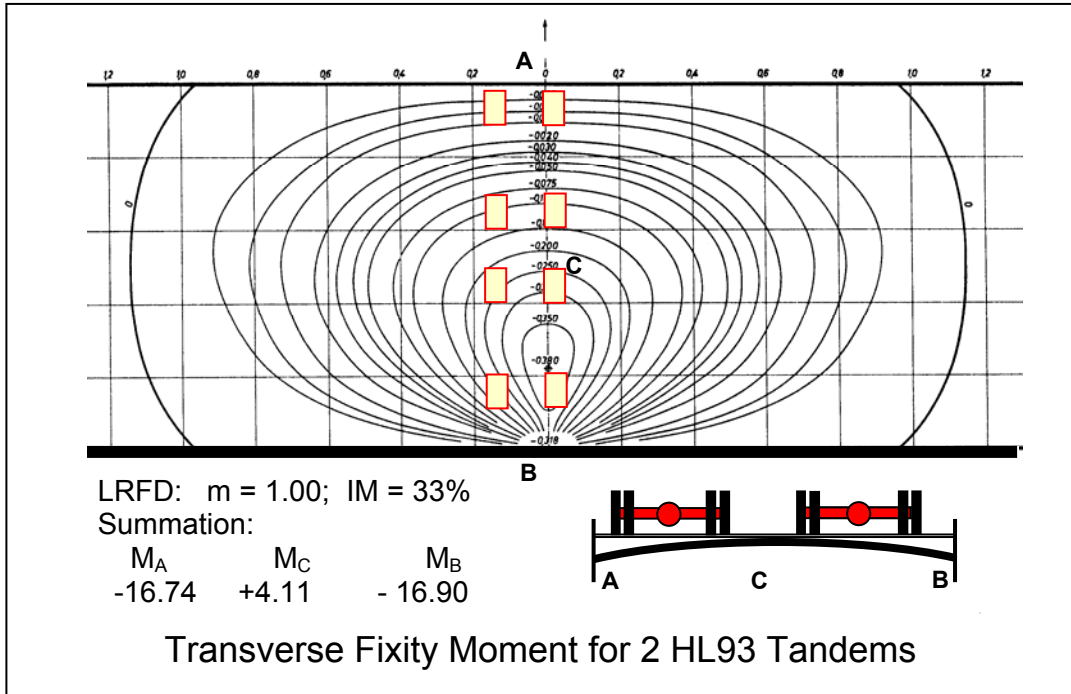| M_A	M_C	M_B
-16.74	+4.11	- 16.90

Transverse Fixity Moment for 2 HL93 Tandems

Figure 2.112 Influence surface for top slab with edges fully restrained

In Figure 2.113, the negative moment at Edge B is the maximum. The corresponding negative moment at Edge A is determined by applying the same load pattern to the chart turned by 180°. The corresponding positive moment (4.11 ft-k/ft) at midspan (C) is obtained for the same load pattern applied to a chart for positive moment within the span (this is not the maximum positive moment case – it occurs under a different wheel print pattern).
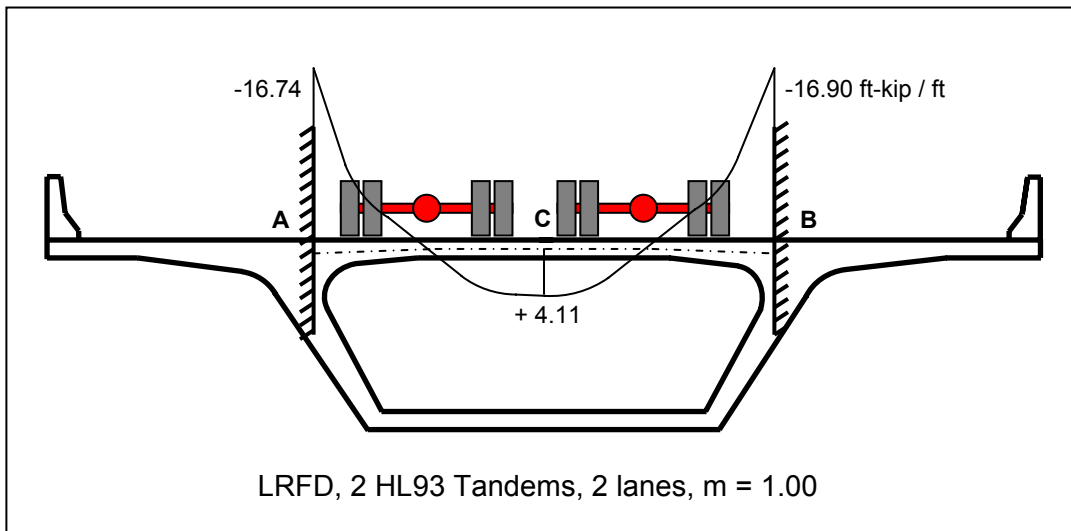

-16.74   -16.90 ft-kip / ft

+ 4.11

LRFD, 2 HL93 Tandems, 2 lanes, m = 1.00

Figure 2.113 Fixity moments at restrained edges

The slab fixity moments (-16.74 and -16.90 ft-k/ft) are then applied to and distributed around the transverse frame to give the final moments at locations of interest (Figure 2.114).
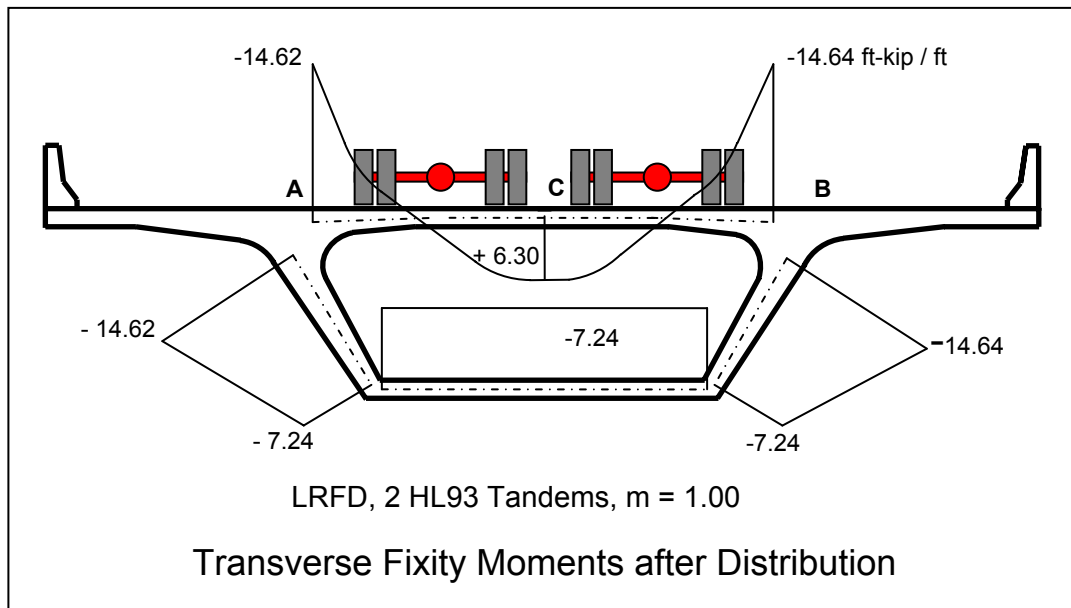

Figure 2.114 Moments after distribution to frame

It can be seen that after release and distribution around the transverse frame, the fixity moments are reduced by about 15% - inducing moments in the webs and bottom slab.

Figure 2.115 shows the frame moments from the combination of wheel loads on the cantilever wing and on the slab between the webs from the above two cases. These moments have been adjusted accordingly for multiple-presence factors for one, two and three live load lanes – namely 1.20, 1.00 and 0.85 respectively.
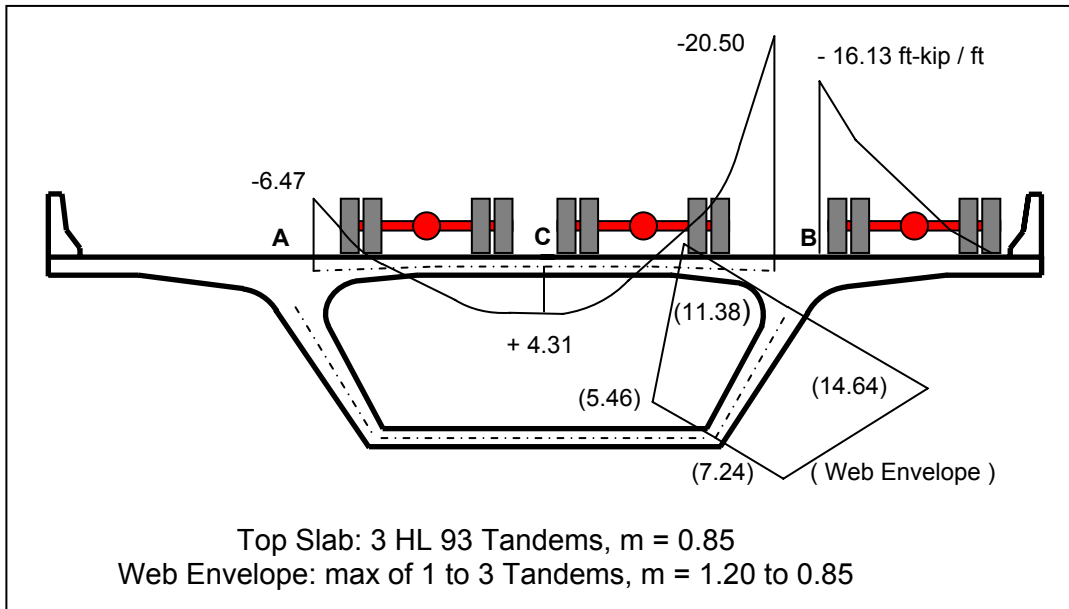
Figure 2.115 Combined results for up to three lanes of live load

The results for the web show the envelope of conditions in terms of the absolute maximum live load moments (ft-kips/ft) plotted on the tension side.

Note that for transverse frame distribution models of the above type, the "supports" are artificial. In reality there are no such "physical" supports. To be strictly correct, the final local support reactions should be resolved to equivalent shear forces in the webs and top and bottom slabs with corresponding longitudinal flange forces, taking account of the both the global transverse and longitudinal stiffness of the span. Although this can be done, it is not only tedious - because it must be done for each individual load case – but also, since most local effects are for particular locations of wheels on the section they rarely, if ever, correspond to live load conditions that result in the maximum global longitudinal effects. For instance; local transverse conditions may be at a maximum with only one or two lanes loaded, whereas maximum longitudinal effects may require three or more lanes of load. Also, local vehicle wheel loads usually govern transverse effects whereas longitudinal effects incorporate uniform live loading as well as the vehicle. In addition, if the frame model is only for a unit length of structure – local moment effects in the webs and bottom slab are overestimated – as the actual longitudinal dispersal of effects below the top of the webs is not taken into account.

For all the foregoing reasons, a transverse frame analysis is usually suitable and sufficient for all practical purposes for the distribution of wheel load moments around the frame of a large box. If a designer has need of more detail, the combination of local transverse frame and global longitudinal effects is more conveniently handled nowadays by means of three-dimensional finite models of all or portions of a superstructure.

2.7.2.5 Three Dimensional Finite (plate) Element Analysis:

Nowadays, rather sophisticated finite element models can be analyzed by relatively economical structural analysis computer programs. This may be the procedure of choice for a large or complex structure. Such models can provide not only transverse flexural results but also associated longitudinal local and global conditions.

The technique should be used with caution and the results should be carefully examined for consistency to ensure there are no modeling errors – such as wrong support conditions – and that all applied loads sum correctly, to the sum of reactions – and so forth. Reference to the above slab and frame analysis techniques is appropriate for checking the anticipated order of magnitude of local effects

The advantage of a finite element model is that it can provide both local and global results in combination; depending upon the proportions of the model, the size of a portion modeled and the size of the elements – all with appropriate boundary conditions.

The length of a model should ideally be sufficient to capture the maximum and minimum conditions – for instance, the negative conditions over an interior pier as well as positive conditions at midspan. Such a model might extend from the quarter point in one span to the corresponding quarter point in the next span or longer. Support conditions might include springs to model the effect of the structure continuing beyond these limits. Elements should be sufficiently small to provide local results of an order of accuracy commensurate with those from classical theory or influence surfaces. But, they should not be too small to make the model too big that there is an overwhelming amount of data from which to report, sift and check results.

2.7.3 Transverse Post-Tensioning of Deck Slab

For a large single-cell box (or a multi-cell box with wide web spacing) transverse mild-steel reinforcement alone is rarely sufficient. It is usually necessary to provide transverse post-tensioning, particularly for the top slab, in order to attain sufficient flexural capacity for service and strength conditions. Transverse post-tensioning is most frequently accomplished using tendons comprising 2 to 4 strands each, located at intervals of 2 to 4 ft along the structure (Figure 2.116). To minimize slab thickness and maximize efficiency, strands are placed side-by-side, usually in (plastic) ducts of approximately 1" by 3" oval section.
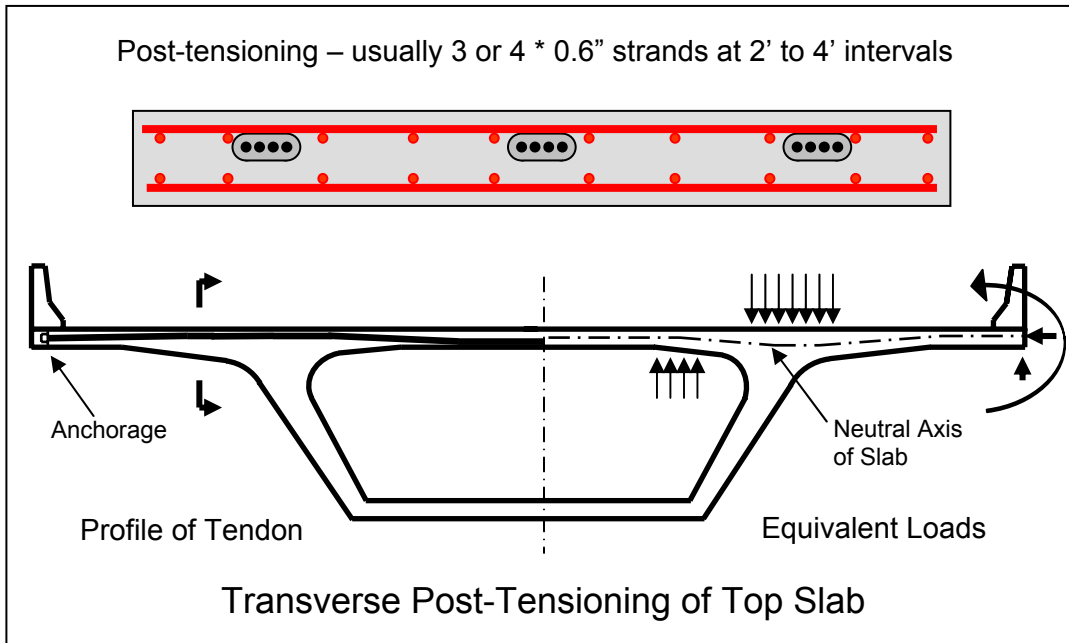
Figure 2.116 Transverse Post Tensioning of Slab (Single Cell Box)

The transverse tendon is set to a slight profile being as high up as possible over the webs, draping to the bottom in the central region between them and to the anchors set approximately at the mid-depth of the slab at the cantilever wing tips (below the traffic barriers, for example.) This type of profile is relatively efficient in that it minimizes secondary prestress moments.

At service level conditions, in the top slab prestress is normally provided to give either no tension or up to $0.19\sqrt{f'c}$ allowable tension depending upon local environmental conditions and criteria (*AASHTO LRFD* Table 5.9.4.2.2-1).

Analysis for the required magnitude of the post-tensioning force may be performed on a unit length transverse frame model using a frame analysis program, or by hand (e.g. moment distribution or flexibility methods) or by using a suitable 3-D finite element analysis model. For a transverse frame, post-tensioning may be applied in terms of equivalent loads as indicated in Figure 2.117. Equivalent loads include: the axial force applied at the anchorages (wing tips), the corresponding eccentric moment and vertical force, if any, at the same location and the distributed uniform force per unit length of curved contact portions ("F/R"). These equivalent load effects (i.e. F/R) are calculated according to the actual geometric (contact) profile of the tendon whereas the frame model geometry is defined by the neutral axes of the slabs and webs.

Some two-dimensional frame and 3-D finite element analysis computer programs have an internal facility to define tendons, determine equivalent prestressing loads, apply them and distribute them around the frame, given basic geometric and material property definitions.

Friction and wedge set losses for the tendon are estimated according to the actual profile (not the profile relative to the neutral axis) when determining the effective initial post-tensioning force to apply at each portion along the tendon.

The results of the transverse analysis for post-tensioning effects are combined with results for dead and live loads as necessary. Stresses and flexural capacity are checked at key locations such as the root of the cantilever, at the middle of the slab, at the deeper haunched sections over the inside web faces and at other locations as necessary.

2.7.4 Combination of Transverse Flexural and Longitudinal Shear Reinforcement for Webs

For large single cell (and multi-cell boxes with wide web spacing) it is necessary to combine the required transverse flexural reinforcement for the webs with that required for longitudinal shear.

As mentioned above, because of overall structural proportions and live load lanes, it is unlikely that the load condition giving the maximum of one effect (transverse flexure) is the also the condition that gives the maximum of the other (longitudinal shear and torsion). Also, for a large box, the local load pattern giving the maximum transverse flexural tension on the inside face of the web is mutually exclusive of that giving the maximum tension on the outside face of the web. In most cases, neither of these maxima occurs when then the load is applied to all lanes (refer to above example in Figure 2.111 through Figure 2.115) to generate the maximum longitudinal shear. Applying live load to all lanes, or a really eccentric fewer number of lanes, is usually required to generate a maximum global shear force in one or other of the webs.

So for relatively large single cell box sections it was proposed by J. Muller et al. and has been generally accepted that web reinforcement should satisfy the maximum of the following combinations:

$$A_w = A_f + (A_v/2)$$

$$A_w = (A_f/2) + A_v$$

$$A_w = 0.7(A_f + A_v)$$

where:
- A_w = total required area of web reinforcement
- A_f = area of web reinforcement required for transverse flexure
- A_v = area of web reinforcement required for the maximum longitudinal shear and torsion.

2.7.5 Longitudinal Analysis

2.7.5.1 Large Boxes - Section Properties for Analysis

For large single or double cell (two or three web) closed box sections of precast or cast-in-place construction, effective cross section properties may be determined by reference to *AASHTO LRFD* Article 4.6.2.6.2. This article of *AASHTO LRFD* is based upon investigations into the effects of shear lag in superstructures with relatively wide flange widths that were originally the basis of the German Code DIN 1075.

If reduced widths are used to determine effective section properties, the designer must always remember to use the full (gross) section for dead load – along with an allowance for any intermediate diaphragms, anchorage blisters or tendon deviators, and so forth. Take care not to rely upon a computer program that automatically generates self weight from (effective) section properties.

Given the proportions typically found on many single-cell trapezoidal cross sections, it is often - though not always - the case that for all practical purposes the full section may be effective. The designer should check for the proportions of the section and span lengths of his particular structure.

For illustration purposes, a set of gross and effective section properties for end and interior spans of 140 ft are:

	Gross Section	Effective End Mid.	Effective End Supp.	Effective Interior Mid.	Effective Interior Supp.
Area	58.23	56.31	49.39	54.78	46.27
Inertia	489.0	476.0	411.1	458.9	380.2
C top	2.479	2.529	2.629	2.532	2.672
C btm	5.521	5.471	5.371	5.468	5.328
S top	197.3	188.2	156.4	181.3	142.3
S btm	88.6	87.0	76.5	83.9	71.4

For this example, although there is a significant variation in inertia (I) of about 25% the reduced inertias apply only over a relatively short proportion of the span, (i.e. near the piers). Consequently, for longitudinal distribution of bending moments, there is only slightly less superstructure stiffness near the piers than for a structure of constant section. The result is a slight reduction (about 1%) in the negative moments over the piers with a corresponding increase in mid-span positive moments, in this example. So, depending upon structure geometry and situation, even a wide variation in effective section properties may result in only a small difference in bending moments.

For determining stresses, it is conservative to use the gross area for the prestress force effect, (i.e. P/A_g) but to use the effective (reduced) section properties for calculating flexural stress from applied loads and eccentric prestress (i.e. M/S_{eff} and $P.e/S_{eff}$). Applying this principle to the well proportioned section in this example, the worst effect of the change in stiffness and section properties makes a relatively small change in final permanent flexural stress; in this case, 0.035 ksi (which represents

an 8% change) at the bottom fiber of an interior pier - and other stress changes are less than this – compared to results where the same constant (gross) section was used. (These results are taken from an analysis of an actual six-span continuous structure after all time dependent losses). The same is not necessarily true of ill-proportioned sections; such as those with very wide flanges and narrow box-core sections.

A key observation here is that the procedures for calculating and applying appropriate section properties are neither exact nor prescriptive. A designer should always exercise a measure of engineering judgment for his particular project and span configuration.

An alternative way to analyze a box-type structure would be by three-dimensional finite element analysis using plates, space-frame members or similar with a sufficiently fine mesh to account for the global effects of shear lag. Providing that the model and applied loads are executed correctly, final stresses can be read directly from the element results.

Having determined the section properties, which may vary along a span, longitudinal moments, shear forces and reactions may be determined by classical analysis for continuous beams (area-moment theory, slope-deflection, moment distribution) or by using a continuous beam analysis computer program.

2.7.5.2 Application of Post-Tensioning Forces as Equivalent Loads

Loss of post-tensioning force from friction, wedge seating, elastic shortening, long-term creep and shrinkage are calculated for each section of interest along the superstructure using the same techniques as addressed in DM Section 2.6 above.

Force effects of draped post-tensioning may be applied to the continuous structure as a series of equivalent loads. In Figure 2.117, "P" is the effective force (usually taken after all losses) at any section of interest along the tendon. P varies along the tendon since it is reduced by friction loss. The vertical force that a tendon exerts on the concrete from the curve profile is $p = P/R$ per unit length; where R is the radius of curvature. (The instantaneous radius at any location is the second derivative of the geometric profile.)
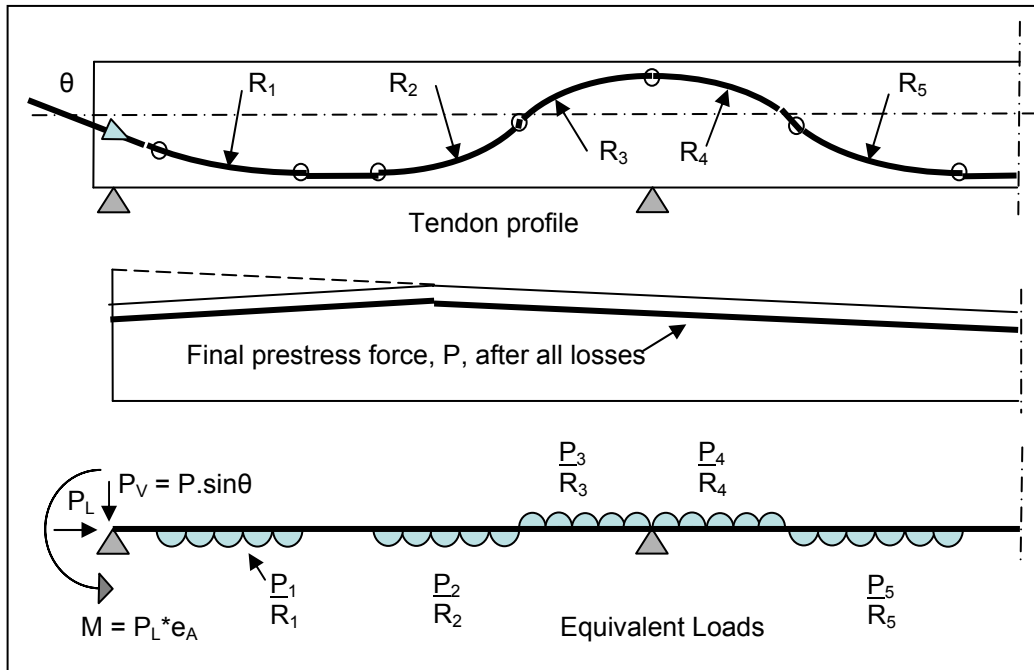
Figure 2.117 Equivalent loads represent post-tensioning effects

Numerically, for calculation purposes, it is usually convenient to divide a profile into portions over which the force and radius may be assumed to be constant and into portions that exert upward or downward effects. This leads to a set of equivalent loads of the type illustrated. This is repeated for each tendon, as necessary. A refinement would be to account for the actual eccentricity of a compacted bundle of strands within a duct and the true points of contact within of the tendon within the duct trajectory.

At an anchorage, there is both a longitudinal (horizontal or axial) component, P_L = $P.\cos\theta$ where "P" is the (final) prestress force applied at eccentricity (e_A) at the anchor from the neutral axis. This gives a moment of P_L*e_A and vertical component of force $P_V = P.\sin\theta$ if a tendon terminates at a longitudinal slope of θ.

The illustration shows a structure of constant depth. For a structure of variable depth, equivalent loads (e.g. "P/R") should be determined according to the absolute (global) geometric tendon profile and then applied to a model of the bridge whose nodes preferably vary in elevation to follow the profile of the neutral axis. For hand calculations, the latter may not be feasible and an approximation is made where all the nodes are at the same elevation. Regardless, the eccentricity of a tendon (e) is taken relative to the actual neutral axis at each cross-section of interest.

At a deviator, where a tendon may change direction rather sharply, in a matter of a few feet, the vertical force may be taken as the difference between the vertical components of force on one side of the deviator versus that on the other and approximated to an equivalent point load applied at the center of the deviator. (Deviators are used in situations where tendons often have a 3-D trajectory out of

the plane of a web. In which case, strictly, there would be both a lateral and longitudinal force difference to take into account too.)

After determining equivalent post-tensioning loads for each tendon, the structure is analyzed as a continuous beam subject to the various combinations of equivalent load making up one or all tendons to provide the resulting bending moments, shear forces and reactions. From these, it is possible to determine "Secondary Moments" due to prestress – as follows.

2.7.5.3 Secondary Moments from Prestressing

In a continuous structure, post-tensioning induces secondary reactions. The magnitude of these reactions depends upon the trajectory of the tendons and the resulting equivalent loads derived and applied to model their effects. A means to determine the secondary reactions is to apply the equivalent loads for each tendon profile to the (weightless) continuous structure and calculate the resulting reactions using classical beam theory or a continuous beam program.

If we were to do this for the 4-span structure in Figure 2.107, we would find non-zero reactions at each of the five supports (Figure 2.118). Some reactions would act upwards and some downwards – but the <u>sum</u> of all reactions would be zero. The bending moment diagram calculated from the resulting reactions alone (which is linear from pier to pier) gives the "Secondary Moment" (M_{sec}) due to prestress, at any section of interest. The primary bending moment due to prestress at any location is the effective prestress force at that location multiplied by its eccentricity (e) from the neutral axis of the member (i.e. $M_{primary} = P_{eff} * e$). This is readily obtained directly from the position of the tendon profile relative to the neutral axis.
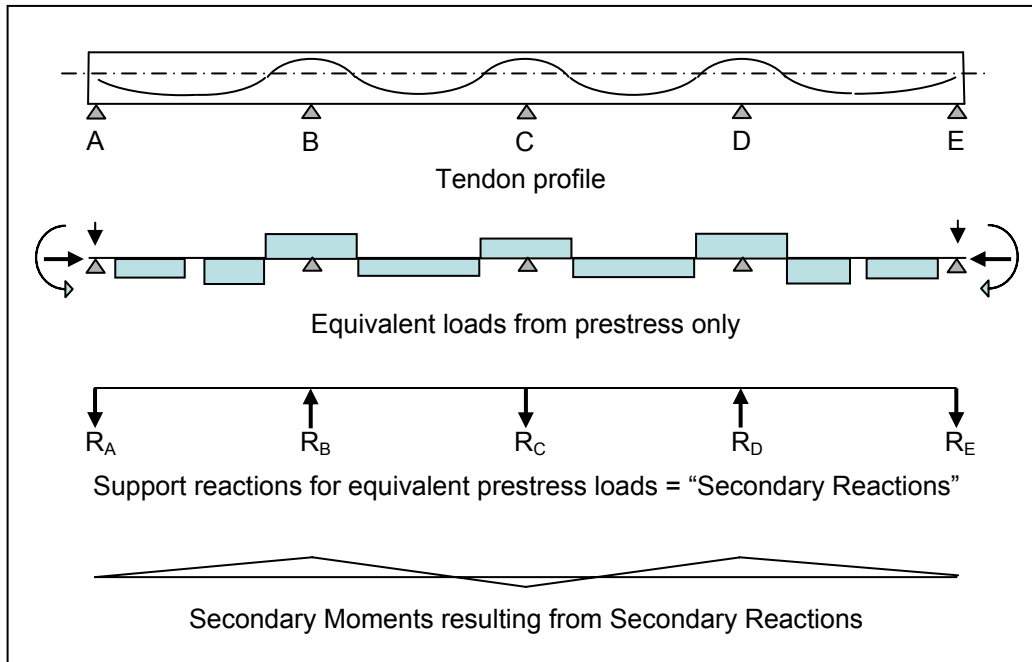
Figure 2.118 MSEC Secondary Moments from Prestress

If tendon profiles can be so arranged with a careful balance between upward and downward equivalent loads and eccentric moments at the anchors, so that each of the support reactions is zero, then there are no secondary reactions and no secondary moments. In such a case, the profile is said to be "concordant". Although theoretically possible, this is very difficult to achieve in practice, so secondary reactions and moments are encountered in most post-tensioned structures. Even so, secondary effects can be minimized – which is the chief reason for using draped tendon profiles in the first place.

In strength capacity calculations, a load factor, $\gamma_P = 1.0$, is applied to the moments and shear forces from secondary effects and the results are added algebraically to the factored moments and shears due to dead and live loads. In effect, for moments, 1.0 times the secondary moment, ("1.0*M sec") is deducted from the factored resistance ($M_r = \phi M_n$) at each section of interest (where ϕ = Resistance Factor). Secondary moments are considered under the term "EL" for accumulated locked-in construction effects per *AASHTO LRFD* Article 3.3.2 and Table 3.4.1-1.

2.7.5.4 Creep and Shrinkage Effects

For a superstructure cast entirely in place on falsework (Figure 2.107) that is removed only after installation of post-tensioning, (i.e. no staged construction) moments, shear forces and reactions are determined for the case where the self-weight and prestress is applied all at one time. For calculations and subsequent load combinations, the effects are determined separately, including secondary reactions and moments, using the above procedures.

After transfer, shrinkage and creep will cause a loss of post-tensioning force. This may be calculated in the same manner as discussed in DM Section 2.6 above. However, for a structure built entirely on falsework that is released after transfer, creep will cause an increase of the initial elastic deflection with time, but there will be no redistribution of bending moments or forces due to creep. The final long term deflections (Δ_∞) are given by:

$$\Delta_\infty = \Delta_i * (1 + \varphi)$$

where:

Δ_i =   Initial elastic deflection at transfer and release of falsework
φ =   creep coefficient (usually about 1.0 to 1.5: φ depends upon material properties and environmental characteristics, etc.)

For a structure built in stages, a separate analysis or model is needed for each stage – i.e. first a single span, then two-spans, then three spans and finally 4 spans where the additional cast-in-place span (namely span 2, then 3, then 4) and associated post-tensioning is added at different intervals of time and maturity of already cast concrete. The summation of the four stages represents the condition at the completion of construction. Not only will there be loss of prestress due to shrinkage and creep, but also, because of the staged construction, creep induced deflection will cause a redistribution of bending moments, shear forces and reactions. The final bending moments (M_∞) are given by:

$$M_\infty = M_{const} + (M_{inst} - M_{const})*(1 - e^{-\Phi})$$

where:

M_{const} =   moments at end of construction (e.g. after release of span 4)
M_{inst} =   moments as if the entire permanent structure had been cast on falsework, post-tensioned and released "instantaneously"

As can be seen, the form of the above equation for creep redistribution is the same as that discussed previously, because the driving effect (creep) is the same phenomena.

2.7.5.5 Torsional Effects of Eccentric Load

Under the action of eccentric (live) load, torsional effects are induced in single cell and multi-cell box superstructures. In a single cell (large) box section this sets up a torsional shear flow around the section in the direction of the applied torque. In a multi-cell box, the effect is to set up a torsional shear flow around each cell of the box section (Figure 2.119). At each of the inner webs the torsional shear flow from the cell on one side of the web acts in the opposite direction to the flow from the cell on the other side of the web. The sum of all the torsional shear flows equates to the global torque at the cross section considered. If the webs are of approximately equal thickness, then the resulting torsional shear flow stress (v_f) around the perimeter of the section is given by:

$$v_f = T / 2A_o.t$$

where:

T	=	torque
t	=	member thickness (web or slab)
A_o	=	area contained by the median line of the perimeter components

In practical terms, the torsional shear flow stress in the inner webs of a multi-cell box cancels out; leaving only a net effect in the outer webs and the top and bottom slabs. Torsional shear in the exterior web closest to the applied load adds to the shear force in that web, whereas it reduces the shear force in the opposite exterior web.
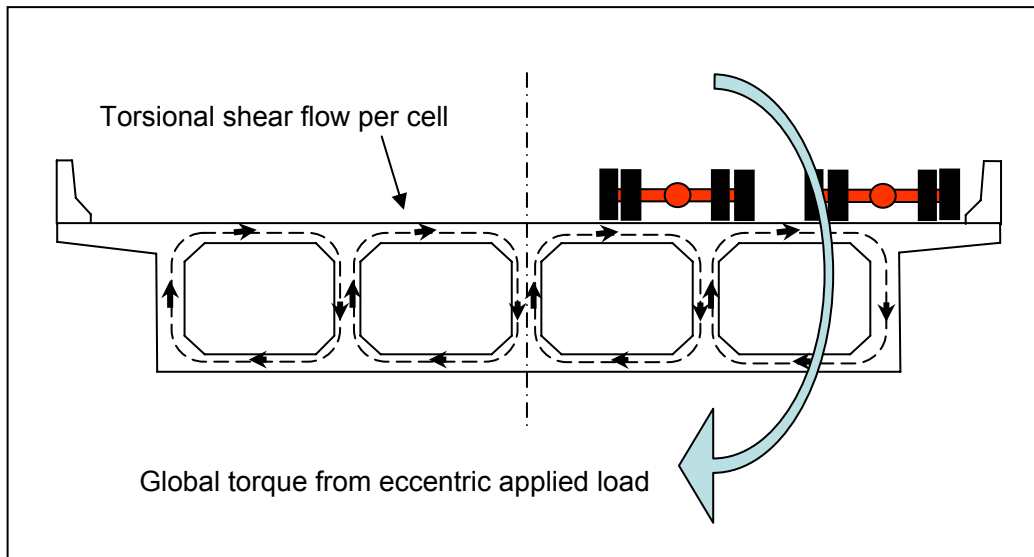

Torsional shear flow per cell

Global torque from eccentric applied load

Figure 2.119 Shear flow in multi-cell box

Torsion induces a slight deformation of the cross section, inducing transverse bending in the top and bottom flanges and webs – in the manner illustrated in Figure 2.120. Another way to envision this transverse action is to imagine the longitudinal girder lines attempting to deflect differently relative to each other as a result of carrying different proportions of the torsionally applied (eccentric) load – which can only be accommodated by a transverse flexure of the slabs and webs.
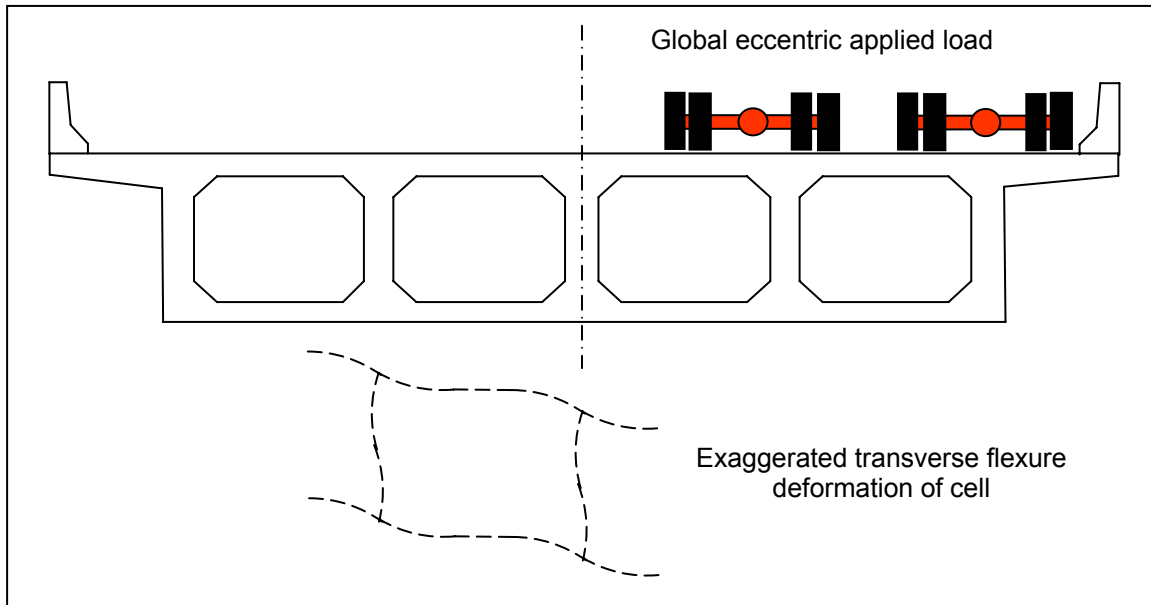
Figure 2.120 Transverse deformation of cells from eccentric load

This deformational effect is not as pronounced or significant for slab flexure as that of a deck slab supported by two, separate, stiff boxes of the type shown in *AASHTO LRFD* Commentary C9.7.2.4.

2.7.5.6 Cast-in-Place Multi-Cell Boxes

According to *AASHTO LRFD* Article 4.6.2, cast-in-place multi-cell concrete box girder bridge types may be designed as "whole-width" structures. In such closed sections, load sharing between "girders" is high and torsional loads are hard to estimate. Prestress should be evenly distributed between the girders and cell width-to-height ratios should be no more than about 2:1. The effects of the loss of area due to the presence of ducts prior to bonding (grouting) of tendons should be considered. After grouting, section properties may be taken on the gross or transformed section (*AASHTO LRFD* Article 5.9.1.4). In this respect, the transformed section is that where the prestressing steel is taken as an equivalent area of concrete given by the area of steel multiplied by the modular ratio of steel (E_s) to concrete (E_c). The minimum depth of a top slab should be 7 inches - to which would be added any necessary depth for grinding and grooving (*AASHTO LRFD* Article 9.7.1.1). The minimum depth of a bottom flange should be not less than 5.5 inch (*AASHTO LRFD* Article 5.14.1.5).

Live load effects may be determined using the approximate methods of analysis using the applicable cross section (d) of Table 4.6.2.2.1-1. By this method, a multi-cell box is treated as series of individual girders with section properties comprised of the web, the overhang of an exterior web and the associated top and bottom half-flanges between the web considered and the adjacent web. The procedure is closely

analogous to that for beam and slab decks, but the distribution factors are formulated differently.

Distribution factors for live load moment in an interior and exterior girder are taken according to Tables 4.6.2.2.2b-1 and 2d-1 respectively for the applicable section (d). If supports are skewed, distribution factors for moment may be reduced according to Table 4.6.2.2.2e-1.

Distribution factors for live load shear in interior and exterior girders are taken according to Tables 4.6.2.2.3a-1 and 3b-1 respectively for the applicable section (d). If the supports skewed, distribution factors for shear at the obtuse corner are reduced according to Table 4.6.2.2.3c-1.

Superstructures of multi-cell boxes may be of constant or varying cross-section. Variation may result from variation in thickness of flanges, variation in overall depth or change of overall width as may occur, for example, at gore areas. Longitudinal moments, shear forces and reactions may be determined by any classical analysis technique for continuous beams or by using a continuous beam analysis computer program. Post-tensioning forces may be applied to each "girder line" as equivalent loads calculated following the outline above.

Other appropriate methods of analysis include a three-dimensional finite element models using, say, plate elements or a space-frame or grillage. Such methods would be particularly appropriate for structures of variable width or other changing geometry.

2.7.5.7 Curved Structures

For structures curved in plan, *AASHTO LRFD* Article 4.6.1.2 permits a rational analysis of the entire superstructure including appropriate supporting elements such as bearings or integral connections to piers. This approach can be applied to both large single girder (torsionally stiff) box section superstructures and multi-cell concrete box girders.

For continuous concrete superstructures of these types, (unlike steel girders) there is usually little distortion or deformation of the cross section – especially if diaphragms are provided at interior piers. Rational analyses methods include classical theory based upon small deflections or modeling using finite-elements, space-frame or grillage techniques.

2.7.5.7.1 Spine-Beam Structure

A horizontally curved single girder torsionally stiff superstructure may be analyzed for global force effects as a curved spine beam (*AASHTO LRFD* Article 4.6.1.2.2). In the context of large (torsionally stiff) boxes, this should be taken to apply to closed-section boxes with either two or three webs (single or double cell respectively) and considered as a single, monolithic, cross-section.

The classical method of analysis for a spine beam is often referred to as the "M/R Method". This method is very tedious and too involved for a detailed treatment herein but the essential principles are summarized as follows. The horizontal curve effect increases the sectional weight per unit length and shifts the center of gravity of that weight slightly to the outside of the curve – the eccentricity (e_{sw}) is given by:

$$e_{sw} = \frac{\rho_y^2}{R}$$

Where:
ρ_y = radius of gyration about vertical axis at the centroid of the section
R = plan radius at centroid of box section

If it can be shown that if the values of bending moment (M) are known at all locations along a beam the distribution of torsional moment in the curved beam is equal to the distribution of shear on an equivalent straight beam subject to the distributed load (p) of magnitude:

$$p = \frac{M}{R} + m_T$$

Where m_T = the distributed (applied) local torque moment (ft kip per ft) and includes, in this case, that due to the self-weight eccentricity, given by = $w*e_{sw}$ where w is the self weight per unit length. Also, in general, m_T, should include eccentric effects due to permanent loads such as barriers at their effective net eccentricity. This means that for the "torque span" (which is the distance between points at which the curved beam is torsionally fixed) the bending and torsional moments can be determined by the following three steps:

(1) Straighten out the curved beam with its corresponding supports and determine the bending moments from each and every applied load (including equivalent prestress loads) by any method for indeterminate structures.

(2) Taking each torque span in turn, apply the distributed load (p) on a simply supported beam of span length equal to the torque span and calculate the distribution of shear force. The result is the distribution of torsional moment in the curved beam for that torque span.

(3) The algebraic difference between the end torsional moments for each torque span adjacent to a torsional support is the torsional moment reaction at that support.

If a support in the curved bridge is not torsionally fixed (e.g. a single bearing under the box) then the torque span should be the distance between the next torsionally fixed supports. For instance, if a three-span continuous spine beam girder has a single, central, bearing at the middle two piers and two (widely spaced) bearings at the abutments, then the torque span is the distance between the centerlines of the bearings at the abutments (i.e. the length of the three span bridge).

Absent classical analysis, a spine-beam structure may be approximated to a series of short, straight segments following the arc of the horizontal curve, supported by bearings or monolithic connections to piers as appropriate. This may be modeled as a space frame using a single superstructure member. A minimum of eight to ten straight segments per span is suggested.

For more details refer to "Simplified Method for the analysis of Torsional Moment as an Effect of Horizontally Curved Multi-span Continuous Bridge" by A. A. Witecki, ACI publication SP-23, pp 193-204, 1969. For an expansion and application of this method to a curved post-tensioned box structure incorporating the effects of creep redistribution, refer to "Curved Concrete Box Girder Bridges", Section 22, Structural Engineering Handbook, Gaylord, Gaylord and Stallmeyer, Fourth Edition, McGraw-Hill, 1997.

2.7.5.7.2 Multi-Cell Concrete Box Girders

According to *AASHTO LRFD* Article 4.6.1.2.3, horizontally curved cast-in-place multi-cell box girders may be designed as single spine beams with straight segments for central angles up to 34° within one span using the distribution factors from *AASHTO LRFD* formulae. Ten straight segments per span were used in parametric analyses that underlie the conclusion in *AASHTO LRFD* Commentary C4.6.1.2.3. This is considered reasonable for most cases; but for sharp radii, more straight segments may be needed per span.

2.7.5.8 Post-Tensioning Effects in Curved Structures

2.7.5.8.1 Tendons within Curved Webs

When curved webs contain (draped) post-tensioning tendons, a lateral force develops given by:

$$F_{lateral} = P/R \text{ per unit length}$$

where:
    $F_{lateral}$ =   lateral force acting on the web per unit of length
    P =   force in the tendon
    R =   radius of curvature of the web in plan view.

This lateral force effect will be at a maximum during stressing operations when the concrete itself might be young and not up to full strength. It can result in a tendon pulling through the side of the web – as happened on at least one occasion. This is easy to avoid by taking care to make sure that such ducts are regularly restrained by lateral ties. The effect is illustrated in *AASHTO LRFD* Figure C.5.10.4.3.1-2.

2.7.5.8.2 Internal Torsional Effects from Tendons

The above radial force effect in the horizontal direction also applies to tendons that lie mostly in the plane of the top or bottom slab. Because of their relatively large eccentricity from the shear center of the section, the horizontal effect induces torsion.

In the case of external tendons that pass over pier diaphragms and drape down to intermediate deviators at the bottom slab-web interface, there is a significant horizontal (lateral) as well as vertical force at each point of change in direction. In a straight bridge with a symmetrical section and symmetrical post-tensioning layout, these lateral effects cancel each other. However, this is not the case in a horizontally curved structure. The net lateral effects at their respective eccentricities from the shear center can induce significant (internal) torsional forces.

Consequently, care should be taken to minimize internal torsional effects as far as possible - first by attempting to modify or optimize the post-tensioning layout or system. But, no matter the modification, it is likely that residual torsional force effects of some magnitude will remain. Their effect should be appropriately added to other permanent torsional effects from gravity loads. Additional torsional reinforcement and possibly extra longitudinal post-tensioning may be needed to cater for these effects.

The magnitude of torsional force effects from post-tensioning may be calculated by determining the equivalent loads, applying them to a continuous girder and using classical theory (i.e. the "M/R Method" above) or by 3-dimension modeling.

2.7.6 Anchorages

Anchorages and end-zones for post-tensioning tendons for structures cast-in-place on falsework are designed and detailed in the same manner as for post-tensioned girders using strut-and-tie or other appropriate techniques.

2.7.7 Flexural Limit States

2.7.7.1 Differences between Continuous and Simply-Supported Structures

For continuous prestressed superstructures, there are subtle differences in flexural limit states compared to simply-supported superstructures. The most obvious and significant difference are negative moments over interior supports. Negative moments from gravity loads such as self-weight, superimposed dead load and live load, create flexural tension in the top fiber and compression in the bottom fiber at support regions. In addition, depending upon the layout of post-tensioning, secondary moments from prestress can also induce negative moments. In continuous superstructures, creep redistribution tends to reduce negative moments due to dead loads and increase positive moments within spans.

The use of a draped post-tensioning layout where the tendons are low down in the section within a span and high up over the supports is purposefully intended to provide compressive stress where it is most needed - to offset permanent tensile stress from loads. It also minimizes the magnitude of adverse secondary moments from prestress.

2.7.7.2 Structural Analysis

Calculation of bending moments, shear forces and reactions for continuous structures may be accomplished by various methods based on classical beam theory, such as: flexibility analysis, displacement (stiffness) analysis, area-moment theorem, moment-distribution, matrix methods, and so forth. Computer models are generally based on matrix (stiffness) methods. For analysis purposes, post-tensioning forces may be applied as equivalent loads as discussed above.

2.7.7.3 Application of Vehicular Live Load

For negative moment and support reactions at interior piers, there is a particular nuance in the *AASHTO LRFD* Article 3.6.1.3.1, bullet point 3. Namely, that for negative moment between points of contra-flexure, 90% of two trucks spaced a minimum of 50ft apart along with 90% of the effect of the design lane load may be applied to induce a negative moment. For this purpose, the location of the points of contra-flexure corresponds to that determined by applying a uniform load on all continuous spans.

2.7.7.4 Service Limit State

At the Service Limit State, limiting flexural stresses for continuous structures are the same as for simply-supported structures (*AASHTO LRFD* Article 5.9.4); the only difference being that these are now applied to the top or bottom fiber as the case may be. Stresses due to secondary moments should be calculated and added to other effects as necessary. In continuous structures, thermal gradient (TG), especially negative thermal gradient, can induce additional top tension over interior supports – presenting difficulties for some structures and load combinations.

2.7.7.5 Strength Limit State

In continuous prestressed structures, applying a load factor of 1.0, secondary moments due to prestress must be added to the load-demand (or deducted from the factored resistance) when checking the Strength Limit State. With this particular exception, the calculation of the flexural capacity of a cross section itself is otherwise the same as for any prestressed girder and may be determined as outlined in *AASHTO LRFD* Article 5.7.3.

For large single-cell box girders and multi-cell box girders, in support (negative moment) regions, it may be necessary to use formulae for flanged sections (*AASHTO LRFD* Article 5.7.3.2.2) as the compressive zone can extend higher than the thickness of the bottom slab, depending upon the proportions of the section,

lever-arm and tensile elements. If negative moment capacity is not quite sufficient, local thickening of the bottom slab may offer a solution. In many structures, particularly of the single-cell box type with a large available width, in positive moment (in-span) regions, the compressive zone may lie entirely within the depth of the top slab; thereby simplifying capacity calculation to that of a rectangular section (*AASHTO LRFD* Article 5.7.3.2.3).

2.7.7.6 Contribution of Mild-Steel to Flexural Capacity

In post-tensioned structures cast-in-place on falsework, continuous longitudinal mild-steel distribution reinforcement is usually provided for shrinkage, temperature and crack control. This reinforcement may be counted toward flexural strength capacity, if necessary, in both positive and negative moment regions.

2.7.7.7 Redistribution of Negative Moment at the Strength Limit

AASHTO LRFD Article 5.7.3.5 addresses this issue. If tensile steel (in this case prestress steel) in the negative moment region yields, which occurs when the net tensile strain (ε_t) exceeds 0.0075, the moment determined by elastic theory at the strength limit state is to be reduced by a percentage not greater than $1000\varepsilon_t$ or 20% at that section. In order to maintain equilibrium, positive moments should be adjusted to account for the change in negative moments. Positive moment capacity should be checked for the redistributed amounts.

2.7.8 Longitudinal Shear Design

2.7.8.1 Service Limit State

Design for shear at the Service Limit State is not a requirement of *AASHTO LRFD*. However, to be mindful of the need for durability, a Designer may choose to assure himself that the structure will not experience shear cracking at the service level. High shear forces can cause diagonal cracking in webs as the result of large principal tensile stresses. The magnitude of the effect can be determined by applying classical theory using Mohr's circle for stress. Limiting the principal tensile stress to 3 or $4\sqrt{f'_c}$ (psi) at the elevation of the neutral axis has traditionally and conveniently been used to establish an approximate web thickness for durability and detailing purposes.

Where torsional shear stress effects are significant relative to vertical shear stress, a convenient approach is to consider the combined magnitude of the torsion and vertical shear stress at the elevation of the neutral axis in the worst loaded web.

2.7.8.2 Strength Limit State

AASHTO LRFD shear design using Modified Compression Field Theory was covered in DM Section 2.4.5.3 for precast, pretensioned girders. Shear design for continuous, post-tensioned members is very similar with few refinements.

In a simply-supported girder, or any statically determine structure, internal forces from the prestressing do not cause reactions at the supports. However, when girders are continuous, the structure is then statically indeterminate. Prestressing then causes small secondary reactions due to the profile of the tendon. This is sometimes called the "continuity effect". The "secondary reactions" induce corresponding shear forces and secondary moments (as discussed above). This directly modifies the summation of shear forces from all loads.

Although common practice for simply-supported pretensioned girders is to use straight strands, they can be draped upwards at the ends, as discussed in DM Section 2.4.2.8.2. Continuous or post-tensioned girders usually have draped prestressing at the ends of the girders and over the supports to counteract negative moments arising from dead and live loads. The force in the strands can be resolved to give a vertical component - typically being opposite the shear force from dead and live loads. Essentially, the effect is a reduction in shear demand. However, *AASHTO LRFD* includes this effect as a component of strength rather than a reduction in demand. In this case, the vertical component of the effective prestressing force, V_p, is added to the strength of the concrete, V_c, and vertical reinforcement, V_s. The total shear strength is then

$$V_n = V_c + V_s + V_p$$

If V_p is in the same direction as the dead and live load demand, then V_p should be taken as negative in this equation for total shear strength. Whether positive or negative, if V_p is considered to be a component of "strength", then shear effects from prestressing should *not* be included as a load "demand."

For special cases, vertical prestressing can be placed in the webs for additional shear resistance. This is usually done using vertical post-tensioning bars. They compress the webs under service level conditions, which is beneficial for principal tension checks. For the strength limit state, the bars supplement the vertical reinforcing steel (rebar). Vertical prestressing is more appropriate for major structures, generally with superstructure depths of about 12-15 ft or greater.

This page intentionally left blank.